



AGRICULTURAL RESEARCH INSTITUTE  
**PUSA**





LONDON :  
HARRISON AND SONS, LTD., PRINTERS IN ORDINARY TO HIS MAJESTY,  
ST. MARTIN'S LANE.

# CONTENTS.

## SERIES A. VOL. CXIV.

No. 766 February 1, 1927.

	PAGE
An Investigation into the Nature and Occurrence of the Auroral Green Line $\lambda 5577 \text{ \AA}$ . By J. C. McLennan, F.R.S., J. H. McLeod, and W. C. McQuarrie. (Plates 1-5.)	1
An Analysis of the Electromagnetic Field into Moving Elements. By S. R. Milner. F.R.S. ....	23
Stark Patterns observed in Helium. By J. S. Foster. (Plates 6-8.) Communicated by A. S. Eve, F.R.S. ....	47
On the Mutual Potential Energy of a Plane Network of Doublets. By J. Topping. Communicated by Prof. S. Chapman, F.R.S. ....	67
On the Sparking Potentials of Discharge Tubes containing carefully Purified Elec- trodes. By J. Taylor. Communicated by O. W. Richardson, F.R.S. ....	73
Quasi-unimolecular Reactions. The decomposition of Diethyl Ether in the Gaseous State. By C. N. Hinshelwood. Communicated by H. Hartley, F.R.S. ....	84
The Nature and Artificial Production of the (so-called) Voiced and Unvoiced Con- sonants. By Sir Richard Paget. Communicated by Sir William Bragg, F.R.S.	98
Anodic Overvoltage Measurements with the Cathode Ray Oscillograph. By E. New- bery. (Plates 9 and 10.) Communicated by Sir Ernest Rutherford, F.R.S. ...	103
The Energy of the Struck String—Part I. By W. H. George and H. E. Beckett. (Plates 11 and 12.) Communicated by Sir William Bragg, F.R.S. ....	111

No. 767—March 1, 1927.

On Detonation of Gaseous Mixtures of Acetylene and of Pentane. By A. Egerton, F.R.S., and S. F. Gates. (Plates 13-16.) ....	137
On Detonation in Gaseous Mixtures at High Initial Pressures and Temperatures. By A. Egerton, F.R.S., and S. F. Gates. (Plates 17 and 18.) ....	152
Some Physical Properties of Icebergs and a Method for their Destruction. By H. T. Barnes, F.R.S. (Plates 19-22.) ....	161
Studies upon Catalytic Combustion.—Part V. By W. A. Bone, F.R.S., and A. Forshaw ....	169

	PAGE
The Theoretical Prediction of the Physical Properties of Many-Electron Atoms and Ions. Mole Refraction, Diamagnetic Susceptibility, and Extension in Space. By L. Pauling. Communicated by A. Sommerfeld, For. Mem. R.S. ....	181
The Effective Cross Section of the Oriented Hydrogen Atom. By R. G. J. Fraser. Communicated by H. M. Macdonald, F.R.S. ....	212
An X-Ray Investigation of Optically Anomalous Crystals of Racemic Potassium Chlorosulphoacetate. By W. G. Burgers. (Plate 23.) Communicated by Sir William Bragg, F.R.S. ....	222
The Electric Fields of South African Thunderstorms. By B. F. J. Schonland and J. Craib. (Plates 24 and 25.) Communicated by C. T. R. Wilson, F.R.S. ....	229
The Quantum Theory of the Emission and Absorption of Radiation. By P. A. M. Dirac. Communicated by N. Bohr, For. Mem. R.S. ....	243
The Photographic Action of $\beta$ -Rays. By C. D. Ellis and W. A. Wooster. Communicated by Sir Ernest Rutherford, P.R.S. ....	260
The Relative Intensities of the Groups in the Magnetic $\beta$ -Ray Spectra of Radium B and Radium C. By C. D. Ellis and W. A. Wooster. Communicated by Sir Ernest Rutherford, P.R.S. ....	276
Experiments to Test the Possibility of Transmutation by Electronic Bombardment. By M. W. Garrett. Communicated by F. A. Lindemann, F.R.S. ....	280
Bands in the Secondary Spectrum of Hydrogen. By H. S. Allen and I. Sandeman. Communicated by O. W. Richardson, F.R.S. ....	293
The Straggling of $\alpha$ Particles from Radium C. By G. H. Briggs. (Plate 26.) Communicated by Sir Ernest Rutherford, P.R.S. ....	313
The Decrease in Velocity of $\alpha$ Particles from Radium C. By G. H. Briggs. Communicated by Sir Ernest Rutherford, P.R.S. ....	341
The Thermal Conductivity of Carbon Dioxide. By H. Gregory and S. Marshall. Communicated by H. L. Callendar, F.R.S. ....	351

No. 768—April 1, 1927.

The Intensity of the Radiation from a Source of Electric Waves when the Electric Constants of the Medium in the Neighbourhood of the Source are different from the Electric Constants at a Distance from it. By H. M. Macdonald, F.R.S. ....	367
The Mechanism of a Thunderstorm. By G. C. Simpson, F.R.S. ....	376
The Initial Stages of Gaseous Explosions—Part I. Flame Speeds during the Initial "Uniform Movement." By W. A. Bone, F.R.S., R. P. Fraser and D. A. Winter. (Plates 27-29.) ....	402
The Initial Stages of Gaseous Explosions—Part II. An Examination of the supposed Law of Flame Speeds. By W. A. Bone, F.R.S., R. P. Fraser and D. A. Winter. (Plates 30-32.) ....	420

The Initial Stages of Gaseous Explosions—Part III. The Behaviour of an Equimolecular Methane-Oxygen Mixture when fired with Sparks of Varying Intensities. By W. A. Bone, F.R.S., R. P. Fraser and F. Witt. (Plates 33-35.) .....	412
The Structure of Certain Silicates. By W. L. Bragg, F.R.S., and J. West.....	450
The Constants of the Magnetic Dispersion of Light. By C. G. Darwin, F.R.S., and W. H. Watson.....	474
Periodic Orbits of the Second Genus near the Straight-Line Equilibrium Points in the Problem of three Bodies. By D. Buchanan. Communicated by J. S. Plaskett, F.R.S. ....	490
The Phenomena arising from the Addition of Hydrogen Peroxide to the Sol of Silicic Acid. By H. A. Fells and J. B. Firth. (Plate 36.) Communicated by F. S. Kipping, F.R.S. ....	517
Measurements of the Amount of Ozone in the Earth's Atmosphere and its Relation to other Geophysical Conditions—Part II. By G. M. B. Dobson, D. N. Harrison and J. Lawrence. Communicated by F. A. Lindemann, F.R.S. ....	521
An X-Ray Investigation of Certain Long-Chain Compounds. By A. Muller. (Plates 37-40.) Communicated by Sir William Bragg, F.R.S. ....	542
On the Capture of Electrons by Swiftly Moving Electrified Particles. By L. H. Thomas. Communicated by R. H. Fowler, F.R.S. ....	561
A Further Contribution to the Study of the Phenomena of Intertraction. By Sir Almroth E. Wright, F.R.S. (Plates 41 and 42.) .....	576
The Refractive Indices of Nicotine. By J. W. Gifford and T. M. Lowry, F.R.S.....	592
The Stability of an Infinitesimal System of Circular Vortices. By H. Levy and A. G. Forsythe. Communicated by S. Chapman, F.R.S. ....	594
The L-Emission Spectra of Lead and Bismuth. By C. E. Eddy and A. H. Turner. Communicated by Sir Ernest Rutherford, F.R.S.....	605
The Transverse Magneto-Resistance Effect in single Crystals of Iron. By W. L. Webster. Communicated by Sir Ernest Rutherford, F.R.S. ....	611

## No. 709—May 2, 1927.

Studies on the Mercury Band-Spectrum of Long Duration. By Lord Rayleigh, F.R.S. (Plates 43 and 44.) .....	620
Note on a Connection between the Visible and Ultra-Violet Bands of Hydrogen. By O. W. Richardson, F.R.S. ....	643
Absorption of Radiation in the Extreme Ultra-Violet by the Inert Gases. By C. Cuthbertson, F.R.S. (Plates 45 and 46) .....	650
On a Relation between the Refractive and Dispersive Constants of the Inert Gases. By C. Cuthbertson, F.R.S. ....	659

	PAGE
The Spectrum of Ionised Nitrogen (N II). By A. Fowler, F.R.S., and L. J. Freeman. (Plates 47 and 48.) .....	662
The Rigidity of Solid Unimolecular Films. By H. Mouquin and E. K. Rideal. Communicated by G. I. Taylor, F.R.S. ....	690
Doppler Effects and Intensities of Lines in Molecular Spectrum of Hydrogen Positive Rays. By M. C. Johnson. Communicated by S. W. J. Smith, F.R.S.....	697
The Quantum Theory of Dispersion. By P. A. M. Dirac. Communicated by R. H. Fowler, F.R.S. ....	710
The Analysis of Beams of Moving Charged Particles by a Magnetic Field. By W. A. Wooster. Communicated by Sir Ernest Rutherford, P.R.S. ....	729
 Index .....	 745

Minutes of Meetings of January 13, 20, 27; February 3, 10, 17, March 3, 10, 17, 24, 31.

# PROCEEDINGS OF THE ROYAL SOCIETY.

## SECTION A.—MATHEMATICAL AND PHYSICAL SCIENCES.

### *An Investigation into the Nature and Occurrence of the Auroral Green Line $\lambda$ 5577 Å.*

By Prof. J. C. McLENNAN, F.R.S., J. H. McLEOD, M.A., and W. C. McQUARRIE,  
M.A.

(Received January 3, 1927)

[PLATES I-5.]

#### I.—Introduction.

The wave-length at 5577 Å. which is the most prominent line in the spectrum of the auroral light, and which is the characteristic line of the spectrum of the light from the night sky, has been the subject of extensive research. Its wave-length has been measured very accurately by Babcock\* and has been found to be  $5577\cdot350 \pm 0\cdot005$  Å. In 1923 Prof. Vegard,† in Norway, put forward the view that the line had its origin in the luminescence of solid nitrogen suspended in a state of fine division in the upper atmosphere, but that view, in the light of a rigid investigation, has been found to be untenable. In 1925 McLennan and Shrum‡ announced that they had been able to obtain a green spectral line at  $\lambda$  5577 Å from the electrical discharge in a tube containing a mixture of helium and oxygen, and that its wave-length agreed with that found by Babcock for the line in the spectrum of the night sky. Later they obtained it quite strongly in a mixture of neon and oxygen, and in addition they found at a still later time that it could be observed faintly in the spectrum of the electrical discharge in low pressure oxygen presumably pure.

\* 'Astrophys. J.,' vol. 57, p. 209 (1923).

† 'Phil. Mag.,' vol. 46, p. 193 (1923).

‡ 'Roy. Soc. Proc.,' A, vol. 108, p. 501 (1925).

During the past year we have been engaged in a research to elucidate further the nature of this elusive radiation at  $\lambda 5577 \text{ \AA}$ , and to locate more definitely its origin and mode of occurrence.

Our efforts were directed at first to showing definitely that the line was obtainable with highly purified oxygen, and without the necessity of having any other gas or gases mixed with the oxygen. This we succeeded in doing. The best conditions for the production of the line in pure oxygen were also studied, variations being made in the pressure and in the strength of the electrical current passing through the gas. In dealing with the influence of extraneous gases a careful study was made of the modifications produced in the intensity of the green line obtained from oxygen when helium was mixed with it in various proportions. The enhancement of the line was also investigated, and from the results obtained it was possible to show that the three rare gases, helium, neon, and argon possessed the power in different degrees of enhancing the intensity of the green line  $\lambda 5577.35 \text{ \AA}$  when the oxygen from which the line was obtained was mixed with them. Finally the magnetic resolution or Zeeman effect of the green line was studied, and from the observations made some more or less definite conclusions were reached regarding the character of the line and its place in a spectral term scheme developed for oxygen.

## II.—*Apparatus.*

In the apparatus used in all the work, except that on the Zeeman effect, the discharge tube was one having a bore of 1.5 cm. and a length of 100 cm. In the earlier part of the work it was made of pyrex glass, but later on it was replaced by a tube made of fused silica. By means of sealed-in windows it was possible to observe the spectrum of the light issuing longitudinally from the tube at each end. As the electrodes were situated in side tubes attached to the main one it was practically the light of the positive column of the discharge that was always under observation. The tube is shown in diagram in fig. 1.

Every precaution was taken to insure the purity of the gases used. The helium was purified by passing it over charcoal cooled with liquid air. When argon was employed it was purified by the use of heated calcium turnings. Oxygen was obtained by heating a side tube containing potassium permanganate. In order to remove mercury vapour and carbon compounds, part of the discharge tube between each electrode and the long observation tube was surrounded by liquid air. For the purpose of measuring the gas pressure in the discharge tube at any time a McLeod gauge was attached to the system that included the purifying tubes and the discharge tube. The uncondensed discharge from

a 50,000-volt 3 K.V.A. transformer was used as the means of excitation, and currents as high as 165 milliamperes were used.

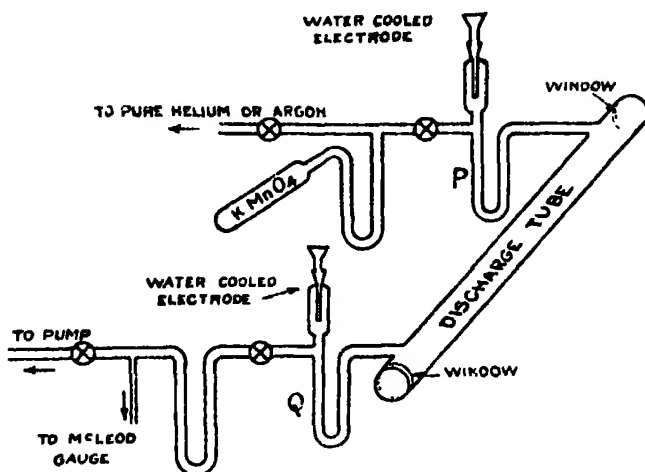


Fig. 1.

The spectrograms of the visible portions of the spectrum were taken with a Hilger constant deviation spectrograph, and a Hilger quartz spectrograph of type E<sub>31</sub> was used when the ultra-violet region of the spectrum was under observation.

### III.—Experiments with Pure Oxygen.

In commencing to make observations on the spectrum of oxygen in order to see if the spectral line  $\lambda = 5577.35$  Å originated in this element special care was taken to operate only on samples of the gas that had been subjected to a rigid purification. In using the tube shown in fig. 1 tap grease was eliminated as far as possible. Water vapour was removed with phosphorus pentoxide or with liquid air, and any carbon dioxide that was present by the use of liquid air. When making photographic exposures care was taken to keep the traps P and Q, fig. 1, surrounded with liquid air. By following this procedure spectra were obtained free from mercury lines or with them present only very faintly.

When using oxygen that was highly purified we found that the green line came out on every spectrogram taken, provided the length of exposure was not too short or the electrical current through the gas too small.

The intensity with which the green line appeared was noticed to vary greatly, and apparently depended on the pressure of the gas and on the strength of the current through the tube. Accordingly experiments were carried out to find the effect of both pressure and current.



*Effect of Pressure.*—To show the effect of pressure a series of spectrograms was taken. The time of exposure and the current in the tube was kept the same for all, but the gas pressure for different spectrograms was varied for 0.43 mm. to 7.0 mm. of mercury. In order to compare the intensity of the line on one spectrogram with that of the line on another it was necessary to have lines on each plate that were known to be of the same intensity. This was accomplished by taking on each plate a comparison spectrum of the light of a neon glow lamp with a constant duration of exposure. Subsequently the plates were run through a Moll microphotometer, and the deflections obtained with the oxygen lines were compared with that obtained with one of the neon spectral lines recorded on the same plate. Fig. 2 shows intensities of various

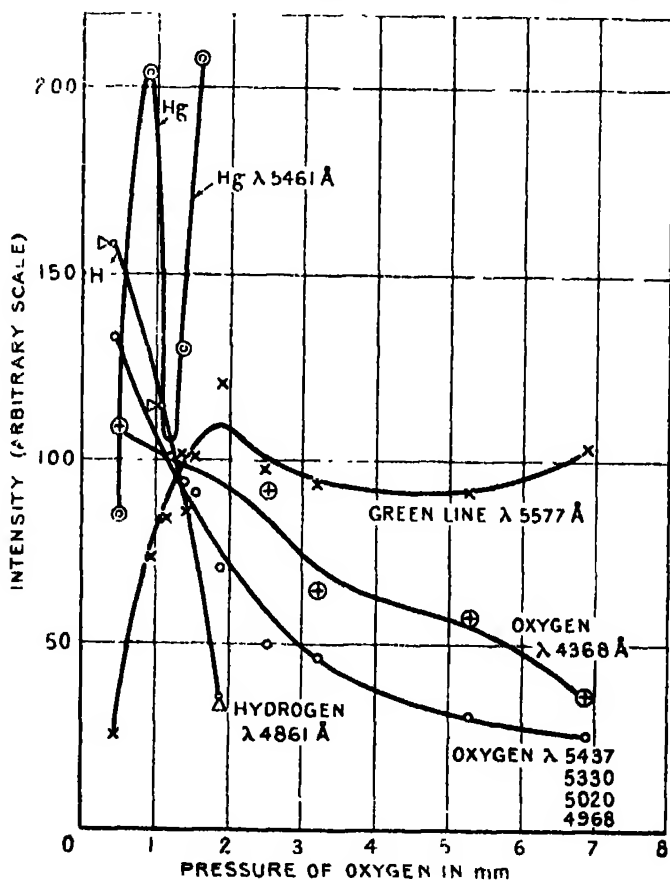


Fig. 2.

spectral lines as obtained from the microphotometer deflections, plotted against pressure of oxygen in the discharge tube. It is evident from the curve for the

green line  $\lambda$  5577.35 Å in fig. 2 that this line reached a maximum of intensity when the gas pressure was equivalent to 2 mm. of mercury. Plate 1, A, is a reproduction of a spectrogram showing the green line as it appeared in pure oxygen at this pressure. It was taken with a total exposure of 9 hours and a discharge current of 60 milliamperes. It will be seen that even with this long exposure the line, though clearly existent, did not come out on the spectrogram with any considerable intensity.

*Effect of current strength.*—The effect of using currents of different strengths on the intensity of the green line as obtained with oxygen was investigated in a manner similar to that just described for pressure changes, and it was found that the intensity of the line increased with the strength of the current used. The result obtained in one set of experiments in which currents as high as 165 milliamperes were used is given in Table I, and a curve representing them is given in fig. 3.

Table I.

Current (ma.).	Intensity.
90	38
120	51
165	100

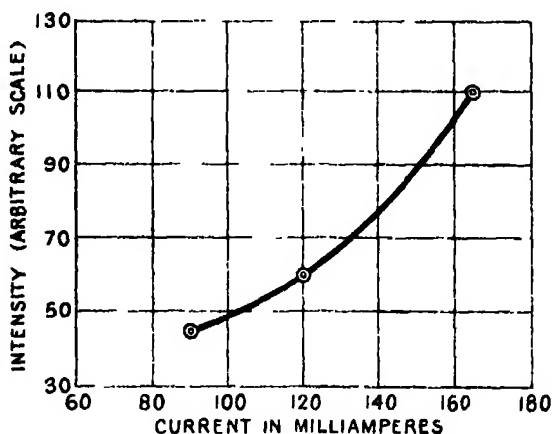


Fig. 3.

The fact that an investigation such as the above could be carried out, involving as it did the taking of more than a score of spectrograms each showing the green line in pure oxygen, is in itself very strong evidence that the line we were studying,  $\lambda$  5577.35 Å, had its origin in oxygen.

*Impurities.*—On quite a number of the plates taken while investigating the effects of pressure and current strength, two lines due to impurities were recorded, namely, the mercury line  $\lambda$  5461 Å and the hydrogen line  $H_{\beta}$ ,  $\lambda$  4861 Å. There is little reason for believing that mercury could be a possible source of the radiation of the line  $\lambda$  5577 Å and a glance at the intensity curve for the mercury line  $\lambda$  5461 Å shown in fig. 2 will suffice to confirm that view.

As hydrogen has often been considered to be a constituent of the upper atmosphere, and as we often had indications of its presence in our discharge tube, it was imperative that we should make a careful investigation to ascertain whether or not hydrogen could be the source of the green radiation.

As to this point we may again refer to fig. 2. The diagram, it will be seen, shows that the intensity of the hydrogen line dropped very rapidly as the pressure of the oxygen was increased, while that of the oxygen green line steadily rose. Moreover, at pressures above 2 mm. there was no trace whatever of the hydrogen line on any plates, and yet the intensity of the green line remained quite high even with the greatest pressures used.

To settle this point more definitely the discharge tube was exhausted as completely as possible, and all gas driven out of the electrodes. Pure hydrogen was then introduced into the discharge tube by diffusion through a heated palladium tube. When this gas was excited it gave only the spectrum of hydrogen, the secondary spectrum being especially strong. Not the slightest indication or trace of a line at  $\lambda$  5577 Å could be observed or photographed. The addition of helium enhanced somewhat the hydrogen spectrum, but still no line at  $\lambda$  5577 Å appeared on the plate. All the lines in the vicinity of  $\lambda$  5577 Å were identified as lines of the secondary spectrum of hydrogen. Plate 4, A, is an enlargement of part of a spectrogram taken with hydrogen and helium that shows there was no line just where the line  $\lambda$  5577.35 Å would have appeared if present. From these and similar experiments it appeared to us quite clear that the green line at  $\lambda$  5577 Å was not due in any way to the element hydrogen.

Numerous observations were made on the spectrum of the electrical discharge in various gases and on that of mixtures of gases in our discharge tubes, but in none of them was the line  $\lambda$  5577 Å obtained if oxygen was not included in the gaseous medium through which the discharge was passed. Only one conclusion is to be drawn therefore from our experiments, and that is that the green auroral line belongs definitely to some spectrum that is obtainable from oxygen.

IV.—*Experiments with Helium and Oxygen.*

As the best conditions for the production of the green line in pure oxygen had been found we turned our attention to its occurrence in the discharge in helium-oxygen mixtures. In agreement with the results obtained by McLennan and Shrum\* it was found that the presence of helium in excess enhanced the line at  $\lambda$  5577 Å. It remained to determine the effect of various proportions of helium and oxygen, and accordingly a set of spectrograms was taken of the electrical discharge in mixtures in which the partial pressure of the oxygen was always 2 mm., and the partial pressure of helium was varied from 15 mm. to 56 mm. of mercury. Plate 3 shows reproductions of these spectrograms. The accompanying curves are Moll microphotometric graphs of the plates. The partial pressures of helium used were as follows:—

<i>a</i>	..	..	..	15.0 mm.
<i>b</i>	..	..	..	20.5 „
<i>c</i>	..	..	..	26.5 „
<i>d</i>	..	..	..	30.5 „
<i>e</i>	..	..	..	35.5 „
<i>f</i>	..	..	..	45.0 „
<i>g</i>	..	..	..	56.0 „

From the curves it will be seen that the line at  $\lambda$  5577 Å came out most distinctly when the partial pressure of helium was between 15 mm. and 20 mm. of mercury.

Plate 4, B, shows a similar set of spectrograms taken with the partial pressure of oxygen at 5 mm. and with partial pressures of helium as follows:—

<i>a</i>	..	..	..	..	14 mm.
<i>b</i>	..	..	..	..	23 „
<i>c</i>	..	..	..	..	30 „
<i>d</i>	..	..	..	..	40 „

The microphotometer curves show that, with the partial pressure of oxygen at 5 mm. of mercury, the green line came out most clearly when the partial pressure of helium was about 30 mm. of mercury.

Plate 1, B, it may be added, shows a spectrogram of the discharge in a mixture of helium and oxygen in which the partial pressures of helium and of oxygen were respectively 17 mm. and 2 mm. The exposure had a total duration of 2 hours and the exciting current had a strength of 60 milliamperes.

\* *Loc. cit.*

V.—*The Wave-length of the Spectral Line at  $\lambda$  5577.35 Å.*

In the report of the work done by McLennan and Shrun\* on the auroral green line as obtained from oxygen-helium mixtures, it was shown that the wave-length of that radiation was  $5577.35 \pm 0.15$  Å. Later measurements by us agree with this result.

Plate 5 shows a reproduction of three spectrograms and their respective microphotometric graphs. They are intended to show the position of the spectral line  $\lambda$  5577.35 Å in relation to certain well-known lines of the iron arc spectrum. The upper spectrum and the microphotometric graph are those of the iron arc. The central one shows a portion of a spectrogram of pure oxygen with the spectrum of the iron arc superimposed on the lower part of it. The microphotometric graph was taken from the part of the plate on which both spectra were recorded. The lower spectrogram and graph are similar to those just described, except that the oxygen spectrum was obtained with a mixture of helium and oxygen in the discharge tube instead of with pure oxygen only. The curves and the spectrograms show the presence of the green line close to, but on the long wave-length side of, the iron spectral line  $\lambda$  5576.10 Å. From a consideration of the linear dispersion of these spectra which can be obtained from the wave-lengths of the iron lines it will be seen that the wave-length of the auroral green line, as obtained in the spectrum of pure oxygen or in that of oxygen in the presence of helium, is very close to 5577.35 Å.

VI.—*The Oxygen Band  $\lambda$  5630 Å.  $\lambda$  5553 Å.*

In 1924 the suggestion was made by R. d'E. Atkinson† and by Cario‡ that the auroral green line might be found to have its origin in the band spectrum of oxygen, and, in particular, might turn out to be the "null" line or some member, more or less prominent, of the negative band of the spectrum of molecular oxygen that falls in the region near  $\lambda$  5577 Å. Some support for this suggestion existed in the fact that Steubing§ had recorded a member of this band as existing at  $\lambda = 5577$  Å. It is clear, however, that the oxygen green line  $\lambda$  5577.35 Å cannot be the "null" line of the band, for it is quite readily obtained when the gas through which the discharge is passing is at an average temperature considerably higher than that prevailing in the room, and therefore

\* *Loc. cit.*

† 'Roy. Soc. Proc.,' A, vol. 106, p. 429 (1924).

‡ 'Naturwiss.,' vol. 12, p. 618 (1924).

§ 'Ann. d. Physik,' vol. 33, p. 555 (1910).

much too high for the band to have degenerated into a "null" line. In connection with the suggestion that the line  $\lambda$  5577·35 Å might prove to be a band component that could be described as prominent one recalls that the only member of the band that has been singled out by its prominence is  $\lambda$  5587·55 Å. This member Prof. Merton\* considers to be the leading component of the band as ordinarily observed. It is clear, however, that the band component  $\lambda$  5587·57 Å and the line  $\lambda$  5577·35 Å have had their wave-lengths determined with too great a precision to permit the possibility of any one considering that the two wave-lengths represent the same radiation. The line  $\lambda$  5577·35 Å can be obtained clearly and strongly without the slightest indication of the presence of any member of the negative band on the plates. The reproductions shown in Plate 3 and Plate 4, B, make it quite clear that the line  $\lambda$  5577·35 Å and the band  $\lambda$  5630 Å- $\lambda$  5553 Å have two entirely different and distinct origins. With pure oxygen at 2 mm. pressure the line  $\lambda$  5577·35 Å was obtained clearly, and without any sign of the members of the band. When helium was added to the oxygen the band members appeared faintly at first, but as the amount of helium added was increased there was a corresponding increase in the intensity of all the members of the band. With helium at the highest partial pressure used, the intensities of the band components were so strong that the line  $\lambda$  5577·35 Å was masked in great measure. Throughout the development of the intensities of the band members the identity of the line  $\lambda$  5577·35 Å was clearly evident even though it gradually came to be embedded in the band system. It should be stated here that measurements of precision were made recently by Holland† of the wave-lengths of the members of the "negative" oxygen bands in the visible region. Under "Bandengruppe II" he includes a component at  $\lambda$  5577·483 Å and one at  $\lambda$  5576·786 Å. As these negative bands of oxygen are rather complicated, and as their structures have not as yet been worked out, it is impossible to attach at present any special significance either to the component  $\lambda$  5577·483 Å or to the one  $\lambda$  5576·786 Å. But from our observations on the general behaviour of the band components when various pressures and current intensities were used, we think it is not likely that either of these components will be found to exhibit the fluctuations in intensity that constitute the feature that is so characteristic of the oxygen line  $\lambda$  5577·35 Å.

\* R. d'E. Atkinson, *loc. cit.*, p. 439.

† 'Z. f. wiss. Phot.,' vol. 23, p. 342 (1925).

VII.—*Neon and Oxygen.*

In the original announcement of the discovery of the line  $\lambda 5577.35 \text{ \AA}$  in the spectrum of oxygen, by McLennan and Shrum,\* brief mention was made of the fact that neon enhanced the line in the same manner as helium. A reproduction of a spectrogram made by Dr. Shrum with a neon oxygen mixture is shown in Plate 2, A. In taking this spectrum the partial pressure of the oxygen was between 1 mm. and 2 mm. and that of the neon between 20 mm. and 40 mm. of mercury, both pressures representing the state of affairs when the discharge tube was at room temperature and not under any electrical excitation. When the spectrogram was taken the tube was excited with an uncondensed discharge of 128 milliamperes from a 50,000-volt 3 K.V.A. transformer running under an overload. The actual time of exposure was between 1 and 1.5 hours. Though the actual intensity of the green line  $\lambda 5577.35 \text{ \AA}$  as shown in Plate 2, A, is less than that of the line in Plate 1, B, its intensity relative to such other oxygen lines as  $\lambda 5437 \text{ \AA}$  and  $\lambda 5333 \text{ \AA}$  is considerably greater. In the case of Plate 1, B, an Ilford panchromatic plate was used, while in the case of Plate 2, A, the spectrum was photographed on a Wratten and Wainwright panchromatic plate. It can be seen from the reproductions that in photographing the spectrum shown in Plate 1, B, the slit of the spectrograph was opened more widely than it was in taking the spectrum shown in Plate 2, A.

VIII.—*Discharge in Oxygen mixed with Argon.*

After it was found that the intensity of the green line  $\lambda 5577.35 \text{ \AA}$  was enhanced by helium or by neon, when either of these gases was added in excess to the oxygen, it seemed desirable to investigate whether argon would or would not produce a similar effect. For this purpose some commercial argon containing 20 per cent. of nitrogen was purified by passing it several times through a tube containing red-hot calcium. After being so treated it was admitted into the discharge tube, and on being examined spectroscopically when the discharge was passing it showed no indication of the presence of the well-known nitrogen bands or of the spectral lines of atomic nitrogen. This was taken as a proof that the argon was pure. A small amount of oxygen was then added by slightly heating some potassium permanganate contained in a side tube. When the spectrum of this mixture was examined, it was found that the green line came out with an intensity greater than that of any other line in the spectrum of oxygen in the visible region on the short wave-length side of  $\lambda 6158 \text{ \AA}$ .

\* *Loc. cit.*

Owing to its strong intensity the line was visible at quite low current values. The intensity increased as the current was strengthened, and finally attained a limiting value with a current of about 30 milliamperes. When the current was increased beyond this amount the intensity of the green line remained stationary, but the lines of the argon spectrum came out more and more strongly until at 65 milliamperes a majority of them had an intensity equal to or greater than that of the green line. A reproduction of the spectrum of the argon-oxygen mixture is shown in Plate 2, B. This spectrogram was taken with an exposure of only 45 minutes and with a discharge current of only 33 milliamperes. It will be seen that the line  $\lambda$  5577·35 Å as reproduced has an intensity about equal to that of the same line in the reproduction shown in Plate 1, B, which was obtained with a mixture of helium and oxygen with an exposure approximately three times as long and a current twice as great. The high value of the relative strength of the line  $\lambda$  5577·35 Å in the argon-oxygen spectrum can be gauged from the fact that, while the length of exposure was sufficient with the spectroscope slit width and current strength used to bring out the green line very clearly on the plate, it was only just sufficient for the lines  $\lambda$  5437 Å and  $\lambda$  5330 Å to be recorded. These lines, it may be added, and as Plate 1, A, shows, are ordinarily among the stronger lines in the spectrum of atomic oxygen.

It is interesting to find that the green line  $\lambda$  5577·35 Å can be obtained in the spectrum of a mixture of oxygen and argon with an intensity relatively great compared with that of many lines with which we are familiar in the spectrum of atomic oxygen. In this connection it will be recalled that while it is now generally accepted that a number of the bands that appear in the auroral spectrum originate in nitrogen, the green line, which is the strongest line in the auroral spectrum, is the only line in this spectrum that has as yet been assigned to oxygen. It may be that in the upper atmosphere the conditions are such as to intensify the line  $\lambda$  5577·35 Å still more than we have been able to do with argon, and to entirely suppress the spectral lines of oxygen that we ordinarily observe. It would have been interesting to investigate whether the green line could have been obtained with still greater intensity from oxygen when mixed with one or other of the heavy rare gases krypton, xenon and niton, but we have not as yet succeeded in obtaining the gases to enable us to carry out such experiments.

An observation that was made in our experiments with argon and oxygen, and also with the other gas mixtures used, as well as with pure oxygen, was that the green line was seldom visible on the first passage of the discharge through the tube. This possibly is not without significance for it has led us to conclude



that an appreciable time is needed for the electric forces to transform the oxygen into the state required for the emission of the radiation that gives rise to the green line.

*IX.—Comparative values of the enhancement of the green line by the different rare gases.*

In arranging the experiments in which the spectrograms shown in Plates 1, A, 1, B, 2, A, and 2, B, were photographed, care was taken to have the oxygen in the discharge tube at a partial pressure between 1 and 2 mm. of mercury, but in cases where oxygen was mixed with a rare gas the partial pressure of the latter gas was between 10 and 40 mm., but the exact pressure was always more or less fortuitously selected. Further, the value of the current-strength used as well as the duration of the exposure was more or less arbitrary for each mixture. Table II contains a summary of the data relating to this phase of the work. A microphotometric intensity curve for each spectrogram was traced with a Moll instrument, and from these curves approximate values were deduced for the intensities of the various spectral lines on the plates. Those corresponding to  $\lambda 5577.35 \text{ \AA}$  and  $\lambda 5437 \text{ \AA}$  are given in the table in columns (6) and (7). The plates were taken as occasion offered with long intervals of time intervening, and consequently it was not practicable to use the same slit width on the spectrograph. Neither was it practicable to use photographic plates of the same type and sensitivity.

Table II.

Gas mixture.	Partial pressures.		Current in tube.	Time of exposure.	Measurements of microphotometer.			Curves.
	Oxygen.	Inert gas.			Height of $\lambda 5577$ .	Height of $\lambda 5437$ .	Ratio $\lambda 5577$ to $\lambda 5437$ .	
(1)	(2)	(3)	(4)	(5)	(6)	(7)	(8)	(9)
Pure $O_2$	2 mm.	—	60 ma.	9 hrs.	9 mm.	49.2 mm.	0.18	1.00
$O_2 + He$	2 mm.	17 mm.	60 ma.	2 hrs.	15 mm.	50.0 mm.	0.30	1.67
$O_2 + Ne$	1-2 mm.	20-40 mm.	128 ma.	90 min.	5.5 mm.	7.8 mm.	0.70	3.89
$O_2 + A$	1 mm.	10 mm.	33 ma.	45 min.	39.8 mm.	2.6 mm.	15.3	85.00

Further, the adjustments of the slit on the Moll instrument were not the same when the intensity curves were traced for the various plates. Conse-

quently it is impossible to make direct comparison from the plates reproduced in Plates 1, A, 1, B, 2, A, and 2, B, of the intensity of the green line radiation obtained from pure oxygen with the intensities of the same radiation when obtained from oxygen mixed in turn with each of the three rare gases. The numbers show clearly, however, that the rare gases possess the power of enhancing the green line radiation in different degrees relative to that of the well-known oxygen line  $\lambda$  5437 Å. With the oxygen-helium mixture the ratio of the intensities of the two lines as the numbers in column (9) of the table show was represented by 1.67, if we take the ratio of their intensities when obtained with pure oxygen as unity. On the same scale the relative enhancement by neon was 3.89 while that by argon was 85. An estimate of the power possessed by argon of enhancing the intensity of the green line radiation regardless of any modifications that gas was capable of producing in the intensities of other oxygen lines can be gained from an inspection of the spectrogram taken with pure oxygen and of that obtained with the oxygen-argon mixture. By referring to the spectrograms so obtained and as reproduced in Plate 1, A, and Plate 2, B, it will be seen that in the case when pure oxygen was in the discharge tube a wider spectrograph slit was used than when the discharge tube contained the oxygen-argon mixture. Moreover, in the former case the exposure was one of 9 hours duration, while in the case of the latter it lasted only for 45 minutes. Again, with pure oxygen in the tube the discharge current was 60 milliamperes while with the oxygen-argon mixture it was only 33 milliamperes. Provided argon possessed no enhancing power all the factors mentioned above would have tended to make the green line appear stronger on the plate obtained with pure oxygen than on the one obtained with the oxygen-argon mixture. But a glance at the plates reproduced in Plate 1, A, and Plate 2, B, shows that the reverse occurred, for it is evident that the green line came out with considerably greater intensity on the plate obtained with the oxygen-argon mixture than it did on the one obtained with pure oxygen.

#### X. -*The Zeeman Effect.*

Prior to the discovery that argon possessed the power of enhancing to such a remarkable degree the intensity of the oxygen line  $\lambda$  5577.35 Å it was considered to be a hopeless task to attempt to make observations on the Zeeman effect with the line. Though it was obtainable with fair intensities by using mixtures of helium and oxygen or of neon and oxygen, the line was too feeble even when so obtained to admit of having its magnetically resolved components

either observed visually or recorded with reasonable exposures on even the most sensitive photographic plates.

Having demonstrated the increased enhancing power obtainable with argon we decided to make an attempt to resolve the line magnetically, for through a study of the Zeeman effect knowledge might be gained that would enable us to determine the energy levels in oxygen atoms between which the electronic transitions take place that give rise to the radiation  $\lambda 5577.35 \text{ \AA}$ .

*Apparatus.*—In this attempt to study the Zeeman effect a discharge tube was made of pyrex glass 30 cm. long and 1.5 cm. in diameter. The electrodes were sealed into side tubes attached to the main one. Commercial argon purified with red-hot calcium was admitted into the discharge tube until a pressure equal to about 7 mm. of mercury was obtained. A very small amount of oxygen was then added by slightly heating potassium permanganate contained in a side tube. Currents varying up to 70 milliamperes were sent through the gas mixture by means of a transformer capable of giving a maximum potential of 30,000 volts. Lateral observations of such discharges in the mixture showed the strong oxygen lines just barely visible. When the discharge was viewed along the tube, however, the lines were seen with considerable brilliance.

*Optical Arrangements.*—The choice of an optical instrument for studying the Zeeman effect was determined largely by the question of light economy. It was not found possible to produce the line in any but fairly wide tubes, so that the method of increasing the intrinsic brightness by use of a capillary was not available. For this reason a concave grating was not used, although it offered the advantage of requiring no auxiliary light analysis and of giving directly the relative intensity of the Zeeman components.

A 30-plate échelon grating with a resolving power greater than 300,000 was considered the most suitable instrument. Of the various arrangements the one giving the greatest light intensity was that in which the green line was isolated by a Hilger constant deviation spectrometer, and then allowed to pass through the échelon, the slit and edges of which were vertical. This method, therefore, was used.

*Structure of the oxygen line  $\lambda 5577.35 \text{ \AA}$ .*—In Babcock's paper on his investigation of the auroral green line in which he found its wave-length to be  $5577.35 \text{ \AA}$  he states that his observations led him to conclude that the width of the line was less than  $0.035 \text{ \AA}$ , and therefore approximately equal to the width of the finer arc lines of the iron spectrum when excited in a vacuum by a moderate electrical current. In so far as his observations went the line was single and without satellites.

Before proceeding to study the Zeeman effect with the line  $\lambda$  5577.35 Å of oxygen we examined it carefully and repeatedly with the échelon spectroscope under a variety of conditions of excitation, but in the absence of a magnetic field. We found it, too, always single, sharply defined and without satellites. Moreover, from the optical data and dimensions of the échelon grating we were able to show that the width of the line was less than 0.025 Å.

It follows then that all the physical characteristics of the radiation of the oxygen green line, in so far as we know them, and without exception, are such as to support our identification of it with the radiation that gives rise to the green line in the auroral spectrum.

*Magnetic Experiments.*—Three different methods of producing the magnetic field were tried in studying the Zeeman effect. First, a U-shaped iron-cored electromagnet with pierced pole pieces, through which the discharge tube passed, was used to produce an intense field parallel to the tube in the narrow gap between the pole pieces. Second, an electromagnet with large flat pole pieces was used to produce a transverse magnetic field across the tube. Finally, a solenoid, without iron core, wound on the discharge tube was used to produce a field parallel to the length of the tube, and of uniform intensity throughout that length.

With the first arrangement, in the attempt to photograph the transverse Zeeman effect, the light intensity was exceedingly poor. Conditions were made worse by a continuous spectrum which necessitated the use of a narrow slit for the spectrometer as well as for the échelon crossed with it. Long exposures extending over two days gave photographs which did not show any lines clearly. It was supposed that the échelon, on account of either temperature changes or vibration, had failed to stay in adjustment.

When the second method of producing the magnetic field was used a distinct, symmetrical broadening of the line took place. It was noticed, too, that the application of this type of magnetic field greatly enhanced the argon spectrum, but reduced the intensity of  $\lambda$  5577.35 Å and the other lines of the oxygen spectrum.

The solenoid was designed to secure good light intensity by allowing observation along the tube and at the same time to produce higher fields. It consisted of somewhat less than 200 feet of enamelled stranded aerial wire (equivalent gauge B. & S., No. 14) wound on the discharge tube. In order to produce sufficiently great fields it was necessary to have very high currents, and the wire was capable of carrying these only for very short periods of time. It was found that no serious overheating occurred in two seconds, and also that that time

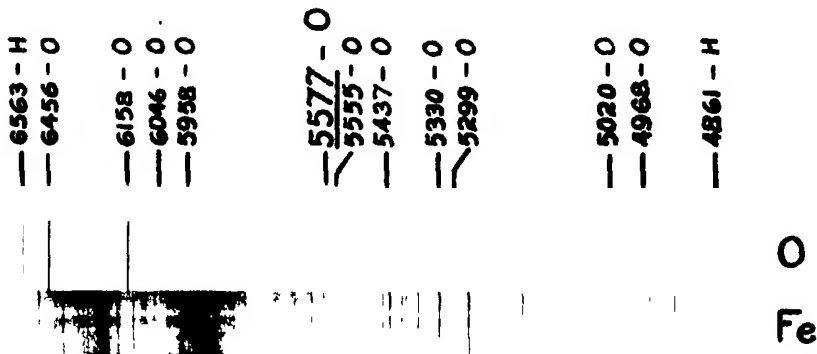
was sufficient to make visual observations on the Zeeman effect. After each observation the solenoid was cooled by pouring liquid air over it. To break the circuit in the required time a small fuse of calculated dimensions was used.

To make the resistance small, the leads were of copper 7 mm. in diameter, and all connections were made in mercury cups. About 6 feet of No. 12 advance wire was inserted in the circuit. This wire had a negative temperature coefficient, and so in a measure compensated for the rapid increase in the resistance of the copper wire of the solenoid due to rise in temperature.

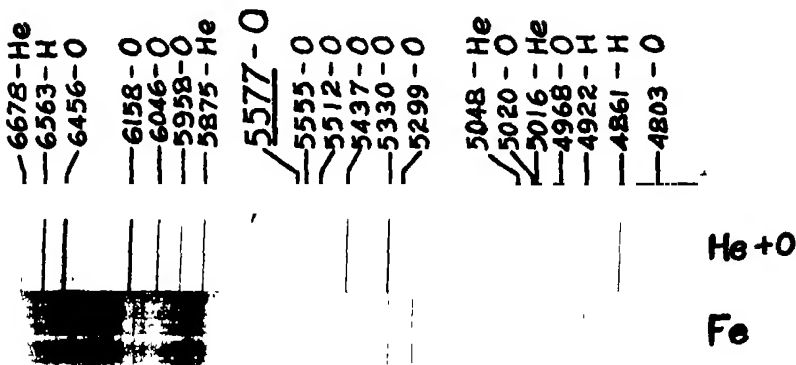
The total resistance of the circuit was about 0.70 ohms, and when 110 volts was applied to it the current in the coil was 160 amperes. As the number of turns in a centimetre length of the solenoid was 18.1 a simple calculation gave the strength of the field as 3,600 Gauss.

Visual observations of the green line in the field showed a beautifully clear doublet. The sharpness of the components would indicate that the resolution was complete, but one could not be absolutely certain that it was, so as the magnetic field was small.

The various orders of the green line showed faintly on either side of the central order in which most of the light was concentrated, and these orders were used to estimate the magnitude of the magnetic separation. The separation of two adjacent orders at this wave-length, calculated from the constants of the échelon, was equal to 0.495 Å. In two seconds time it was not possible to make measurements of the amount of separation, but two observers agreed in estimating that the separation was about one-fifth of the distance between adjacent orders of the échelon pattern. Therefore the estimated magnetic separation of the two components of the line was  $0.099 \pm 0.009$  Å. As no electronic jump, it may be stated, gives rise to singlet spectral lines with normal doublet Zeeman components we have taken this result of our observations to indicate that the line  $\lambda$  5577.35 Å can be resolved magnetically into a normal Zeeman triplet for, with a field of 3,600 Gauss, the normal separation of the outer components of such a triplet should in the case of a spectral line having the wave-length 5577.35 Å, be 0.105 Å. The fact that only two components were seen fits in with this conclusion, for the central component of a normal triplet being polarised parallel to the magnetic field could not be seen with longitudinal observation.

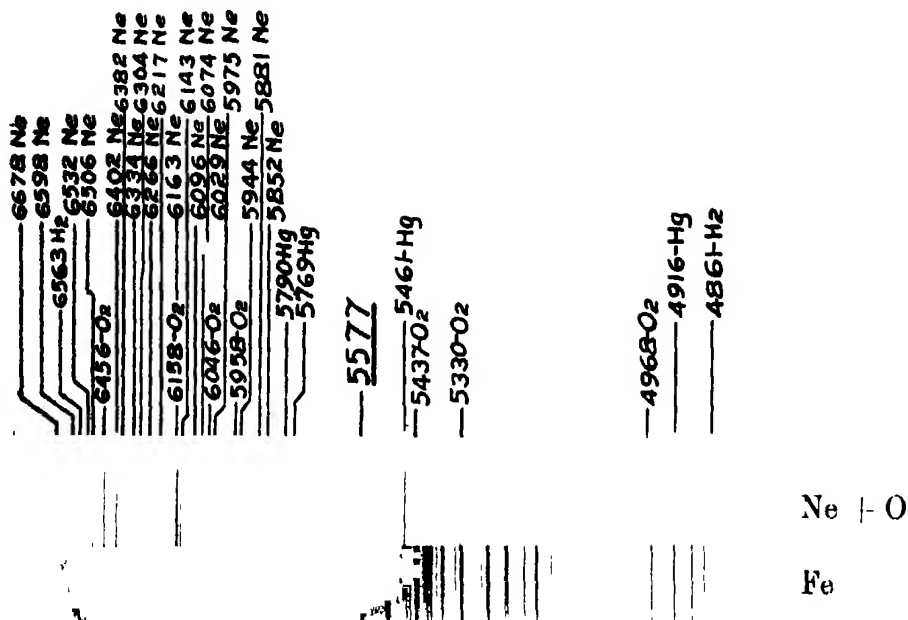


A. Pure Oxygen; pressure 2 mm, current 60 ma.; exposure 9 hours.

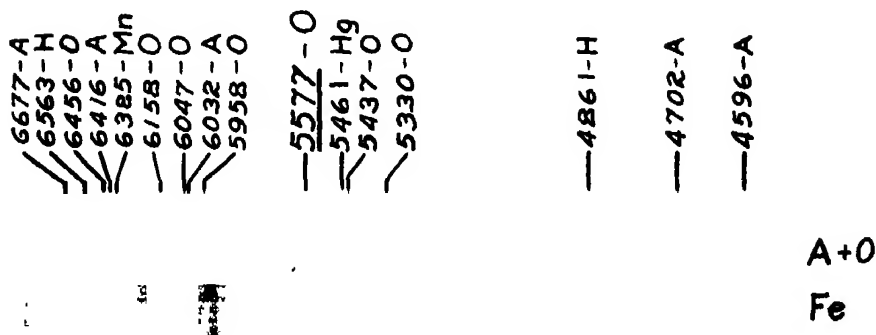


B. Helium-Oxygen mixture; pressure of helium 17 mm., of oxygen 2 mm.,  
current 60 ma.; exposure 2 hours.





A. Neon-Oxygen mixture; pressure of neon 20-40 mm., of oxygen 1-2 mm., current 128 ma.; exposure 1½ hours.



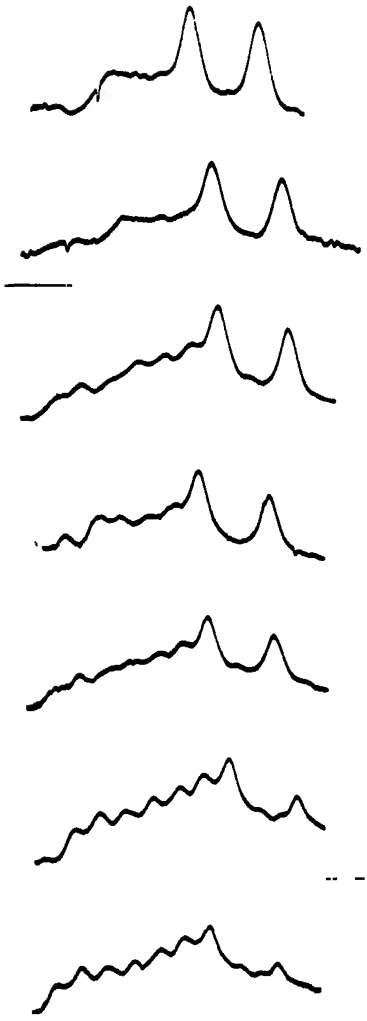
B. Argon-Oxygen mixture, pressure of argon 10 mm., of oxygen 1 mm., current 33 ma.; exposure ¼ hour.



O<sub>2</sub> 5577  
O<sub>2</sub> 5555  
O<sub>2</sub> 5512

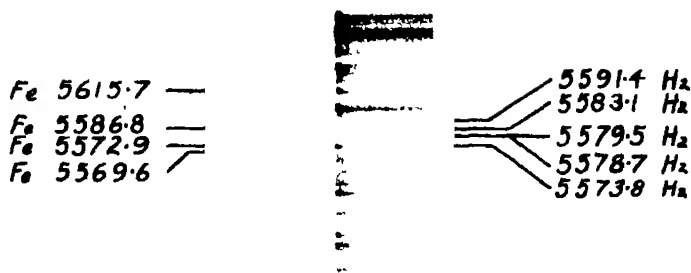
O<sub>2</sub> 5577  
O<sub>2</sub> 5555

Pressure of  
Helium (mm.).

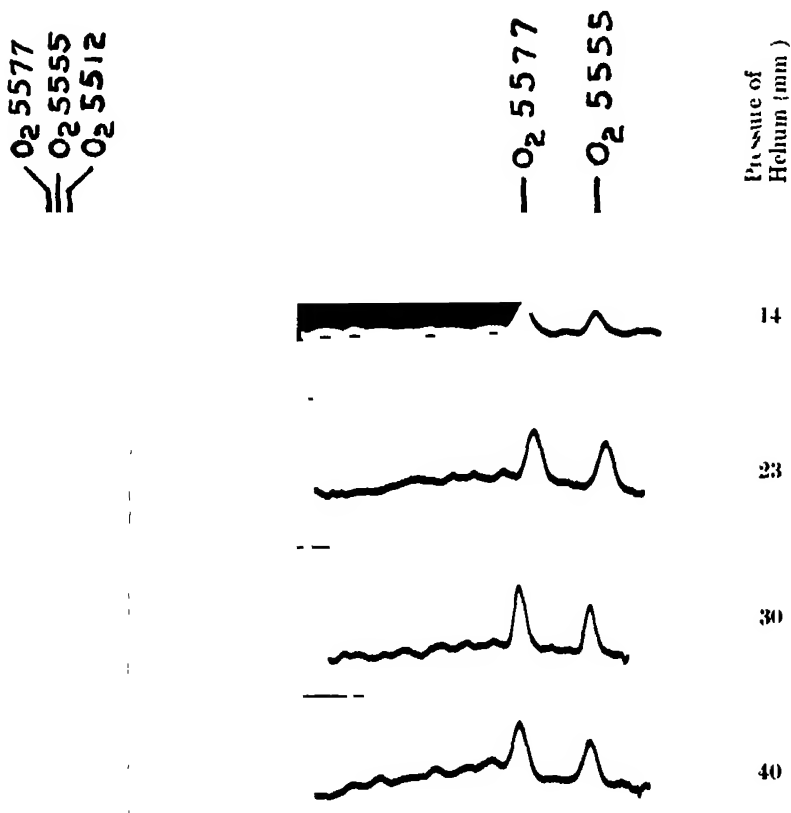


15.0  
20.5  
26.5  
30.5  
35.5  
45.0  
56.0

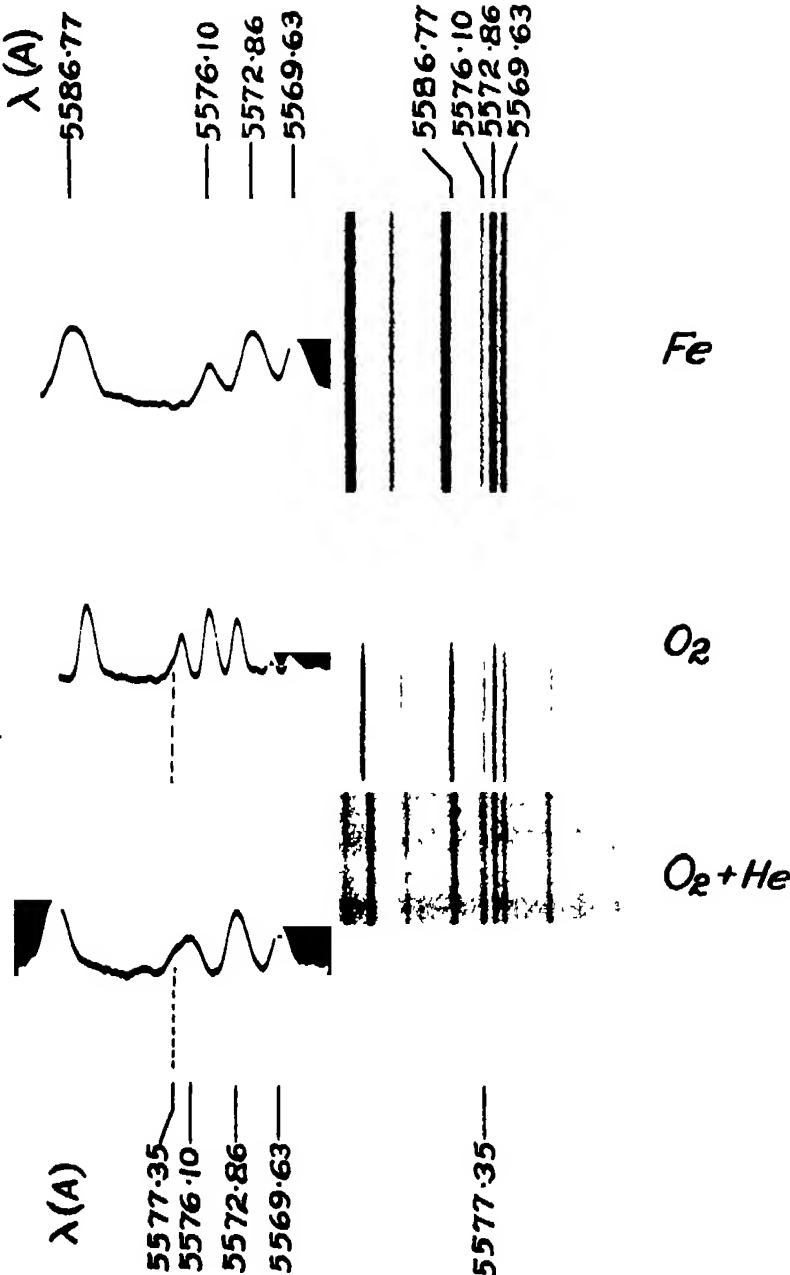
Helium-Oxygen mixture . pressure of oxygen 2 mm.



A Helium-Hydrogen mixture.



B. Helium-Oxygen mixture; pressure of oxygen 5 mm.



XI.—*Interpretation of Results.*

Through the work of Sommerfeld,\* Landé, Back† and others, the principles underlying the theoretical treatment of the Zeeman effect have become well established. It is now possible to predict with practical certainty the type of resolution that a spectral line will undergo in a magnetic field. It is only necessary to know the energy levels in the atomic edifice between which the electronic transitions takes place that gives rise to the radiation corresponding to the spectral line. Conversely, when a spectral line is shown to exhibit a certain type of Zeeman effect it is possible to define the atomic energy levels between which electronic transitions may occur that can give rise to the radiation corresponding to the spectral line. Our problem, therefore, is to determine the electronic transitions that can occur in an atomic system that will give rise to a singlet spectral line that is magnetically resolvable into a normal Zeeman triplet. In this connection we have made a study of the Zeeman effects of all types of singlet lines resulting from electronic transitions between energy levels representing atomic states defined by the spectral terms usually designated by the letters S, P, D, F and G. Assuming the spectral terms to have any multiplicity up to that of a sextet we find that the only electronic transitions within the range of terms indicated that can occur that will give normal magnetic triplets are the following:— $^1P \sim ^1S$ ;  $^1D \sim ^1P$ ;  $^1F \sim ^1D$ ;  $^1G \sim ^1D$ ;  $^1P \sim ^1\bar{P}$ ;  $^1D \sim ^1\bar{D}$ ;  $^1F \sim ^1\bar{F}$ ;  $^1G \sim ^1\bar{G}$ . Our conclusion then is that the green line  $\lambda 5577.35 \text{ \AA}$  must originate in a transition from one atomic state to another represented by one of the types included in this group.

Now it seems to be established from the results of the experiments described in this paper that the green line  $\lambda 5577.35 \text{ \AA}$  has its origin in oxygen, and the question that arises is: Are any of the types of electronic transitions given above possible with the spectral term schemes worked out up to the present for atomic oxygen?

In a paper published recently by McLennan, McLay and Grayson Smith‡ it was shown in detail by the use of the theory recently put forward by Pauli,§ Heisenberg|| and Hund¶ that it is possible to work out a complete spectral term scheme for the atom of any element. In this paper such a scheme was worked out for oxygen, and it was shown to include three groups of connected

\* 'Atombau und Spektrallinien,' 4th Ed.

† Back and Landé, 'Zeemaneffekt und Multiplettstruktur,' published 1925.

‡ 'Roy. Soc. Proc.,' A, vol. 112, p. 76 (1926).

§ 'Z. f. Physik,' vol. 31, p. 765 (1925).

|| 'Z. f. Physik,' vol. 32, p. 841 (1925).

¶ 'Z. f. Physik,' vol. 33, p. 345 (1925).

terms. These are given in Table III under the designations of A, B and C. Diagrams of the terms of each group with the terms arranged in the order of their magnitudes are shown in figs. 4, 5 and 6. Diagram A, it will be seen, consists of triplet and quintet terms and includes transitions corresponding to most of the well-known arc lines in the spectrum of oxygen. It will be seen that the spectral line  $\lambda 5577.35 \text{ \AA}$  finds no place in this scheme. Neither should one expect to find the green line appearing in it, for the scheme does not include any spectral terms of the singlet type. Such terms, however, are included in both of the schemes B and C where the terms are either of the singlet type or of triplet multiplicity. Moreover, the various types of terms  $^1S$ ,  $^1P$ ,  $^1D$ ,  $^1F$ , etc.,

Table III.

## Nitrogen.

$n_k$	$1_1$	$2_1$	$2_2$	$3_1$	$3_2$	$3_3$	Terms.
	2	2	3	—	—		$^4S_3$ $^2D_{33}$ $^2P_{12}$

## Oxygen.

A.							B.								
$n_k$	$1_1$	$2_1$	$2_2$	$3_1$	$3_2$	$3_3$	Terms.	$n_k$	$1_1$	$2_1$	$2_2$	$3_1$	$3_2$	$3_3$	Terms.
2	2	3	—	—	—		$^4S_2$	2	2	3	—	—	—		$^4D_{21}$
2	2	4	—	—	—		$^3P_{012}$	2	2	4	—	—	—		$^1D_2$
2	2	3	1	—	—		$^4S_3$ $^4S_1$	2	2	3	1	—	—		$^3D_{121}$ $^1D_2$
2	2	3	—	1	—		$^3P_{121}$ $^3P_{012}$	2	2	3	—	1	—		$^3F_{231}$ $^4D_{121}$ $^2P_{012}$
2	2	3	—	—	1		$^1D_{1214}$ $^3D_{123}$	2	2	3	—	—	1		$^1F_3$ $^1D_2$ $^1P_1$
								2	2	3			1		$^3G_{448}$ $^3F_{211}$ $^3D_{121}$
															$^3P_{012}$ $^3S_1$ $^1G_4$
															$^1F_3$ $^1D_2$ $^1P_1$ $^1S_0$

## C.

$n_k$	$1_1$	$2_1$	$2_2$	$3_1$	$3_2$	$3_3$	Terms.
2	2	3	—	—	—		$^2P_{12}$
2	2	4	—	—	—		$^1S_0$
2	2	3	1	—	—		$^2P_{012}$ $^1P_1$
2	2	3	—	1	—		$^2D_{113}$ $^2P_{012}$ $^3S_1$
							$^2D_1$ $^1P_1$ $^1S_0$
2	2	3	—	—	1		$^2F$ $^2D$ $^2P$
							$^2F$ $^1D$ $^1P$

are represented in both schemes, and electronic transitions of the types  $^1S \sim ^1P$ ;  $^1P \sim ^1D$ , etc., are provided for in both of them. Accordingly in each scheme

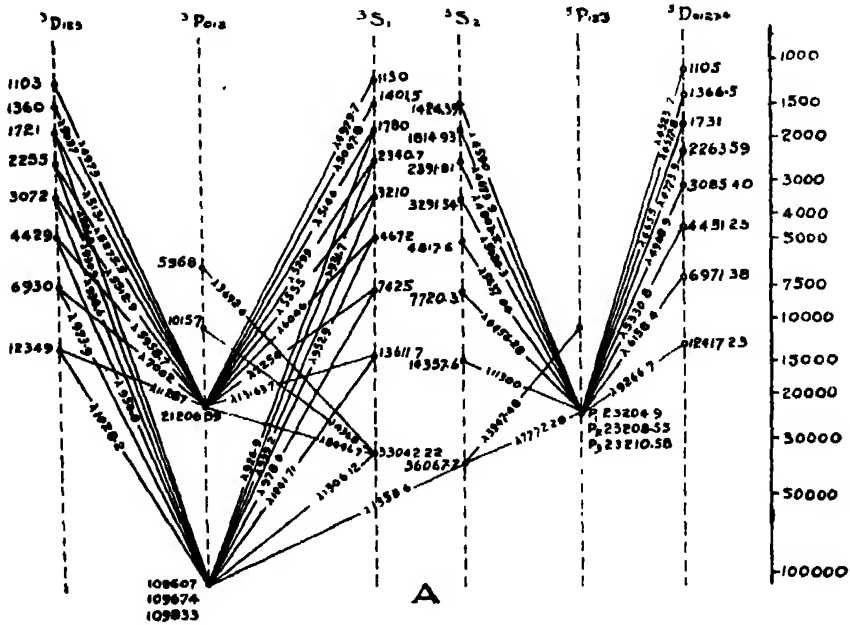
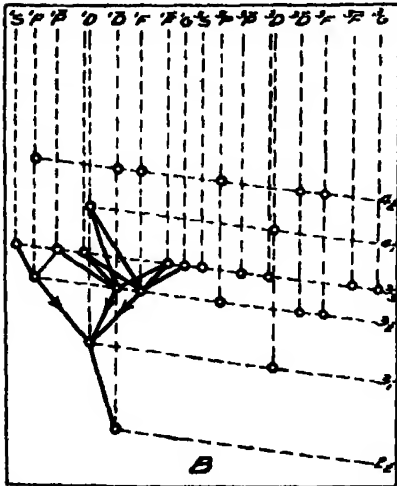
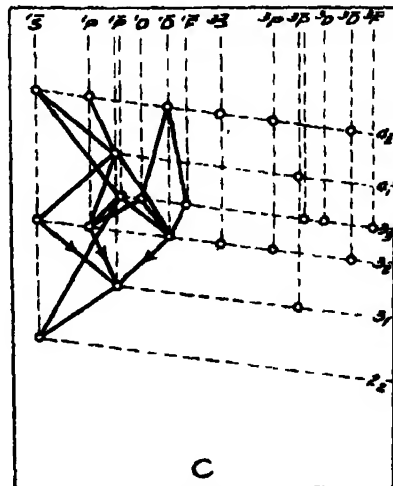


Fig. 4.



**FIG. 5.**



**Fig. 6.**

then we should expect to find a distinct spectrum for atomic oxygen that would include singlet spectral lines that could be resolved by a magnetic field into a

normal Zeeman triplet. There are a number of electronic transitions possible then under either scheme for the atom of oxygen that, in so far as resolution by a magnetic field is concerned, could give rise to radiation of the wave-length  $5577\cdot35\text{ \AA}$ .

Of all the electronic transitions that might possibly give rise to the radiation  $\lambda\ 5577\cdot35\text{ \AA}$  some are more probable than others. The three deepest energy levels of the oxygen atom give rise to the spectral terms  $^3P_{012}$ ,  $^1D_2$  and  $^1S_0$ . Of these  $^3P_{012}$  is the deepest term in the scheme A, and according to theory it should be deeper than  $^1D_2$ . Again,  $^1D_2$  is the deepest term in scheme B, and it again should be deeper than  $^1S_0$  which is the deepest term in scheme C.

When the oxygen atom is in its most stable state it gives rise to the spectral term  $^3P_{012}$ . When, however, it is in the state that gives rise to the spectral term  $^1D_2$  or in the one that gives rise to the spectral term  $^1S_0$  it is said to be in a metastable state, and when in either of such metastable states it is impossible for it to revert by the emission of radiation to the state that gives rise to the spectral term  $^3P_{012}$ . From the principles now generally accepted as underlying the analysis of spectra it would appear that the atoms of oxygen should be rendered capable of emitting radiations comprising the wave-lengths of scheme A more easily than they could be rendered capable of emitting those provided by the system of spectral terms given in scheme B. Similarly it would probably be more difficult to make the atoms of oxygen emit the wave-lengths provided by scheme C than to make them emit those embraced by scheme B.

If now we try to decide which of the schemes B or C the spectral line  $\lambda\ 5577\cdot35\text{ \AA}$  is most likely to originate in, we find two lines of argument may be followed that lead to entirely different results. On the one hand, practically all but a few of the known lines in the spectrum of atomic oxygen have been assigned to scheme A. Since this scheme of wave-lengths is the one most easily obtainable from oxygen atoms, one might naturally expect that with increased stimulation the atoms of oxygen would begin to emit radiation having the wave-lengths provided for by scheme B before those provided for by scheme C. As the wave-length  $\lambda\ 5577\cdot35\text{ \AA}$  is one of the few that we can obtain from atomic oxygen that does not fit into scheme A, it would be natural then to assign it to scheme B, the system next most easily obtainable.

On the other hand, it seems that the green line  $\lambda\ 5577\cdot35\text{ \AA}$  is the only line appearing in the spectrum of the aurora that has as yet been identified as belonging to oxygen. Again, in the spectrum of the light of the night sky the line  $\lambda\ 5577\cdot35\text{ \AA}$  is the only spectral line that has been recorded. Not a trace

of any of the well-known lines of atomic oxygen embraced by the scheme A has been observed in the photographs of this spectrum taken by any observer. This result, which is so remarkable that it merits very special consideration, might lead one to the view that when oxygen atoms are in the state to emit radiation of the wave-length  $\lambda$  5577.35 Å, they are in the state from which they are very unlikely to revert to the states that give rise to the spectral terms provided by scheme A, *i.e.*, to the states that give rise to the emission of the wave-lengths comprising the ordinary arc spectrum of oxygen.

As an application of the generally accepted empirical rules, regarding the structure of spectra, would lead one to the view that the reversion of oxygen atoms from the states represented by the term scheme C to the states represented by the term scheme A would be always less probable than for their reversion from the states given by the terms of scheme B to those provided by the terms of scheme A, one is led naturally by the line of argument set forth above to assign the radiation of wave-length  $\lambda$  5577.35 Å to the term system set forth in scheme C, *i.e.*, the one farthest removed from scheme A.

Under each of the schemes B and C electronic transitions to the lowest level would give the strongest lines in the spectrum corresponding to the scheme. One might, therefore, be inclined to think that the spectral line  $\lambda$  5577.35 Å would result from such a transition. When we remember, however, that the corresponding transitions in the known arc spectrum as represented by scheme A produce wave-lengths that fall far in the extreme ultra-violet region, it is highly improbable that any transition to the lowest term either in scheme B or scheme C can give rise to radiation falling in the visible spectral region at  $\lambda$  5577.35 Å does. It is more probable, therefore, that the green line radiation is produced by one or other of the electronic transitions to the level next higher than the lowest one. Such selected transitions are indicated in both the schemes B and C by arrowheads attached to the continuous lines that correspond to possible transitions for the production of the radiation  $\lambda = 5577.35$  Å.

But the whole question of the exact position of radiation of the wave-length 5577.35 Å in the spectral structure for atomic oxygen is as yet rather vague. It is clear that two new schemes of spectral terms are possible for atomic oxygen in addition to the ordinarily accepted one, and that under each of these new schemes ample provision is made for an electronic transition that could give rise to the radiation constituting the auroral green line. The immediate problem before us will be to find some way of stimulating the atoms of oxygen to emit not one only but a number of the wave-lengths that are possible ones under the two new schemes. With such wave-lengths available it should be



less difficult to locate the exact position of the wave-length 5577·35 Å in the spectral edifice of atomic oxygen.

We have seen that by adding the rare gases, helium, neon and argon, in turn to oxygen, it is possible to enhance more and more the intensity of the radiation  $\lambda$  5577·35 Å relative to that of the other types of radiation that up to the present time have been shown to be included in the spectrum of atomic oxygen. The question is, can any form of stimulation be devised that will result in the radiation from oxygen of wave-length 5577·35 Å being relatively so strong that with exposures of moderate duration this wave-length will be the only one recorded on spectrograms of oxygen so stimulated. There are indications that ozone may be a factor included in such stimulation.

## XII.—*Summary of Main Points.*

1. The green line  $\lambda$  5577·35 Å has been shown to occur in pure oxygen and with greatest intensity when the oxygen was at a pressure equivalent to 2 mm. of mercury.

2. With oxygen at 2 mm. pressure in a discharge tube the intensity of the line  $\lambda$  5577·35 Å was shown to increase with the strength of the current in the discharge tube.

3. It has been shown that the line is due to oxygen and not to any impurities that might be present in the discharge tube.

4. The green line appears with increased intensity in the spectrum of oxygen when mixed with one or other of the three rare gases, helium, neon and argon.

5. A very great increase in intensity, both absolute and in relation to other oxygen lines, was obtained when oxygen was mixed with argon.

6. The Zeeman effect of the green line from longitudinal observations gives a clear doublet with a separation equal to that of the outer components of a normal triplet.

7. Some considerations based on the properties of the oxygen green line  $\lambda$  5577·35 Å are presented in favour of the view that the line originates in an electronic transition between two singlet spectral terms that are included in one or other of two new schemes of singlet-triplet terms that have been shown to be possible for oxygen in addition to the ordinary well-known triplet-quintet scheme.

One of us, J. H. McLeod, is indebted to the National Research Council of Canada for the grant of a bursary that enabled him to participate in this work.

---

*An Analysis of the Electromagnetic Field into Moving Elements.*

By S. R. MILNER, D.Sc., F.R.S., Professor of Physics, The University, Sheffield.

(Received August 10, 1926.)

*Introduction and Summary.*—In Maxwell's equations of the electromagnetic field,

$$\left. \begin{aligned} \frac{\partial \mathbf{e}}{\partial t} &= \text{curl } \mathbf{h} & (a) \\ \frac{\partial \mathbf{h}}{\partial t} &= -\text{curl } \mathbf{e} & (b) \\ \text{div } \mathbf{e} &= 0, \quad \text{div } \mathbf{h} = 0 & (c, d) \end{aligned} \right\} \quad (1)$$

the properties of the field, in regions containing no charges, are described in terms of two vectors,  $\mathbf{e}$  and  $\mathbf{h}$ , which in the general case may have arbitrary magnitudes and directions at any given point of space and time. Although  $\mathbf{e}$  and  $\mathbf{h}$  are the quantities most closely related to experiment, they are not the only ones in terms of which the field can be described. The description can in fact be given in terms of any definite functions of  $\mathbf{e}$  and  $\mathbf{h}$  by making the appropriate substitutions in (1). The equations obtained by such a transformation cannot of course describe properties of the field which are not ultimately implied in Maxwell's equations; they may nevertheless lend themselves more readily to determining what these properties are.

It is shown in this paper that this is the case with a certain transformation in which, instead of in terms of  $\mathbf{e}$  and  $\mathbf{h}$ , vectors making an arbitrary angle with each other, the equations are expressed in terms of two vectors,  $\mathbf{R}$  and  $\mathbf{u}$ , at right angles to each other, and of a scalar function of position,  $\alpha$ . The equations obtained reveal that the most general electromagnetic field in regions not containing charges can be represented by a vector  $\mathbf{R}$  of invariant magnitude, the lines of which at each point are in motion at right angles to themselves with a definite velocity  $u$  relatively to the observer. They show further that small moving elements of the field can be constructed which can be regarded as keeping their identities permanently as they move. The movement of these elements takes place under the action of a simple form of stress in accordance with the fundamental laws of dynamics. In addition to their translatory motions and independent of them, the elements exhibit in the general case co-ordinated rotational movements. By their translatory and rotary movements, and the changes of shape which result from them, they fix definitely the local time rates

of change of the field. In fact every property of the field can be specified directly in terms of these moving and rotating elements. A field element is a space section constructed in a natural way from the four dimensional entity which constitutes the field in space-time. Considered in space-time as a four dimensional element, it appears as an element of *action*, and it is a result of the analysis that the general electromagnetic field can always be divided in a natural way into such elementary units of action. The properties which characterise them are of a kind which suggests and is consistent with the possibility that both field elements and the corresponding elements of action may have a finite magnitude in the field.

These results were obtained originally by translating into terms of space and time properties of the four dimensional electromagnetic tubes which have been derived in a previous paper.\* It is proposed here to develop them directly from the fundamental equations without referring to four dimensional theory except occasionally.

*Equations in terms of p, q, α.*—Consider two vectors, *p* and *q*, defined by the relations

$$\left. \begin{aligned} \mathbf{p} &= \mathbf{e} \cos \alpha + \mathbf{h} \sin \alpha \\ \mathbf{q} &= -\mathbf{e} \sin \alpha + \mathbf{h} \cos \alpha \end{aligned} \right\} \quad (2)$$

where  $\alpha$  is an arbitrary angle. Solved for *e* and *h* these equations give

$$\left. \begin{aligned} \mathbf{e} &= \mathbf{p} \cos \alpha - \mathbf{q} \sin \alpha \\ \mathbf{h} &= \mathbf{p} \sin \alpha + \mathbf{q} \cos \alpha \end{aligned} \right\} \quad (3)$$

and substituting these values in (1) we get, after a little reduction†

$$\left. \begin{aligned} \frac{\partial \mathbf{p}}{\partial t} - \text{curl } \mathbf{q} - \mathbf{q} \frac{\partial \alpha}{\partial t} + [\mathbf{p} \nabla \alpha] &= 0 & (a) \\ \frac{\partial \mathbf{q}}{\partial t} + \text{curl } \mathbf{p} + \mathbf{p} \frac{\partial \alpha}{\partial t} + [\mathbf{q} \nabla \alpha] &= 0 & (b) \\ \text{div } \mathbf{p} - (\mathbf{q} \nabla \alpha) &= 0 & (c) \\ \text{div } \mathbf{q} + (\mathbf{p} \nabla \alpha) &= 0 & (d) \end{aligned} \right\} \quad (4)$$

\* Milner, 'Phil. Mag.', vol. 44, p. 705 (1922).

† Making use of the identities

$$\begin{aligned} \text{curl } \mathbf{a}\phi &= \phi \text{ curl } \mathbf{a} - [\mathbf{a} \nabla \phi], \\ \text{div } \mathbf{a}\phi &= \phi \text{ div } \mathbf{a} + (\mathbf{a} \nabla \phi), \end{aligned}$$

where  $\phi$  is a scalar quantity. Equation (4a) corresponds not to (1a) but to (1a)  $\cos \alpha$  + (1b)  $\sin \alpha$ , (4b) to  $-(1a) \sin \alpha$  + (1b)  $\cos \alpha$ . In (4) and the later vector formulae, scalar products are denoted by round, and vector products by square brackets. Heaviside-Lorentz units are used throughout, with  $c = 1$ .

These equations are of a more general type than Maxwell's, since in addition to the six independent variables formed by the components of  $\mathbf{p}$  and  $\mathbf{q}$  they contain a seventh in the arbitrary scalar quantity  $\alpha$ , whereas there are only six independent variables in Maxwell's equations. We can, consequently, while still retaining the full generality of the electromagnetic equations, choose  $\alpha$  so that  $\mathbf{p}$  and  $\mathbf{q}$  satisfy any given single condition. We shall choose the condition that  $\mathbf{p}$  and  $\mathbf{q}$  shall be permanently at right angles to each other, and add to (4) the equation

$$(\mathbf{p}\mathbf{q}) = 0. \quad (4e)$$

By (2) the condition for this is found to be

$$\tan 2\alpha = \frac{2(\mathbf{e}\mathbf{h})}{\mathbf{e}^2 - \mathbf{h}^2}. \quad (5)$$

When  $\alpha = 0$ ,  $(\mathbf{e}\mathbf{h}) = 0$ , and the electric and magnetic forces of the field are perpendicular. In this case equations (4) reduce to Maxwell's form,  $\mathbf{p}$  being identical with  $\mathbf{e}$  and  $\mathbf{q}$  with  $\mathbf{h}$ . In the general case  $\alpha$  forms a parameter which measures the departure of the electric and magnetic forces from orthogonality. On the other hand,  $\alpha$  cannot be expressed in terms of  $\mathbf{p}$  and  $\mathbf{q}$ , since these are always orthogonal;  $\mathbf{p}$  and  $\mathbf{q}$ , in fact, represent five independent variables,  $\alpha$  is the sixth.

By means of (3) the dynamical properties of the field can be expressed in terms of  $\mathbf{p}$  and  $\mathbf{q}$ . We find at once

$$\left. \begin{aligned} W &= \frac{1}{2}(\mathbf{e}^2 + \mathbf{h}^2) = \frac{1}{2}(\mathbf{p}^2 + \mathbf{q}^2) & (a) \\ G &= [\mathbf{e}\mathbf{h}] = [\mathbf{p}\mathbf{q}] & (b) \\ \Pi_n &= \frac{1}{2}(\mathbf{e}^2 + \mathbf{h}^2)\mathbf{n} - (\mathbf{e}\mathbf{n})\mathbf{e} - (\mathbf{h}\mathbf{n})\mathbf{h} \\ &= \frac{1}{2}(\mathbf{p}^2 + \mathbf{q}^2)\mathbf{n} - (\mathbf{p}\mathbf{n})\mathbf{p} - (\mathbf{q}\mathbf{n})\mathbf{q} & (c) \end{aligned} \right\} \quad (6)$$

$W$  is here the energy density,  $G$  the momentum density, and  $\Pi_n$  the vector force outwards due to Maxwell's stress across a unit plane whose normal is  $\mathbf{n}$ . It is noteworthy that each of these quantities is given in terms of the new variables by precisely the same relations as in terms of  $\mathbf{e}$  and  $\mathbf{h}$ . Since, however,  $\mathbf{p}$  and  $\mathbf{q}$  are orthogonal an important simplification can be made in connection with the stress system. If we make successively in (6c) (1)  $\mathbf{n} \parallel \mathbf{p}$ , (2)  $\mathbf{n} \parallel \mathbf{q}$ , (3)  $\mathbf{n} \perp \mathbf{p}$  and  $\mathbf{q}$ , we see that the stress consists of a principal tension,

$$\Pi_1 = -\frac{1}{2}(\mathbf{p}^2 - \mathbf{q}^2) \quad (7a)$$

along the direction of  $\mathbf{p}$ , an equal pressure

$$\Pi_2 = +\frac{1}{2}(\mathbf{p}^2 - \mathbf{q}^2) \quad (7b)$$

along  $\mathbf{q}$ , and a pressure

$$\Pi_3 = +\frac{1}{2}(\mathbf{p}^2 + \mathbf{q}^2) \quad (7c)$$

along the third of three perpendicular directions, that of  $[pq]$ . Like  $\mathbf{e}$  and  $\mathbf{h}$ ,  $\mathbf{p}$  and  $\mathbf{q}$  define  $\Pi_n$ , but unlike  $\mathbf{e}$  and  $\mathbf{h}$ ,  $\mathbf{p}$  and  $\mathbf{q}$  are completely determined when the three principal stresses of Maxwell's system are given. We have, in fact, from (7)

$$\left. \begin{aligned} p &= (\Pi_3 - \Pi_1)^{\frac{1}{2}} \text{ along } \Pi_1 & (a) \\ q &= (\Pi_3 - \Pi_2)^{\frac{1}{2}} \text{ along } \Pi_2 & (b) \end{aligned} \right\} \quad (8)$$

*Equations on Special Axes.*—The perpendicular directions of the principal axes of Maxwell's stress system mark out naturally a special co-ordinate system in the field, the use of which produces considerable simplifications, without affecting the generality of the results in any essential way.\* For simplicity we shall henceforward employ this special co-ordinate system, and understand by  $Ox$ ,  $Oy$ ,  $Oz$  axes drawn, at any point in the field taken as origin, in the directions of  $\mathbf{p}$ ,  $\mathbf{q}$  and  $[pq]$  respectively. With this understanding we have at the origin

$$p_x = p, \quad q_y = q, \quad p_y = p_z = q_x = q_z = 0,$$

and equations (4), when written in full and simplified by omitting zero terms, become

$$\left. \begin{aligned} \frac{\partial p_x}{\partial t} - \frac{\partial q_x}{\partial y} + \frac{\partial q_y}{\partial z} &= 0 & (a) \\ \frac{\partial q_y}{\partial t} + \frac{\partial p_x}{\partial z} - \frac{\partial p_z}{\partial x} &= 0 & (b) \\ \frac{\partial p_y}{\partial t} - \frac{\partial q_x}{\partial z} + \frac{\partial q_z}{\partial x} - q \frac{\partial x}{\partial t} - p \frac{\partial x}{\partial z} &= 0 & (c) \\ \frac{\partial q_z}{\partial t} + \frac{\partial p_z}{\partial y} - \frac{\partial p_y}{\partial z} + p \frac{\partial x}{\partial t} + q \frac{\partial x}{\partial z} &= 0 & (d) \\ \frac{\partial p_z}{\partial t} - \frac{\partial q_y}{\partial x} + \frac{\partial q_x}{\partial y} + p \frac{\partial x}{\partial y} &= 0 & (e) \\ \frac{\partial q_z}{\partial t} + \frac{\partial p_y}{\partial x} - \frac{\partial p_x}{\partial y} - q \frac{\partial x}{\partial x} &= 0 & (f) \\ \frac{\partial p_x}{\partial x} + \frac{\partial p_y}{\partial y} + \frac{\partial p_z}{\partial z} - q \frac{\partial x}{\partial y} &= 0 & (g) \\ \frac{\partial q_x}{\partial x} + \frac{\partial q_y}{\partial y} + \frac{\partial q_z}{\partial z} + p \frac{\partial x}{\partial x} &= 0 & (h) \end{aligned} \right\} \quad (9)$$

\* The only limitation produced is that the equations obtained should not be differentiated to the second order without consideration, since they contain without showing them zero quantities of which the differential coefficients are not zero.

*Equations in terms of R, u, α.*—Consider now in place of **p** and **q** two vectors **R** and **u**, also mutually perpendicular, which are defined thus :

$$\mathbf{R} = (p^2 - q^2)^{\frac{1}{2}}, \quad (10a)$$

and coincides everywhere in direction with **p** ;

$$u = q/p, \quad (10b)$$

and is everywhere perpendicular to **p** and **q**.

At the origin **R** acts along *Ox*, **u** along *Oz*. The relations (9) may be expressed in terms of **R** and **u**, but instead of their Cartesian components it will be convenient to use as variables the magnitudes of **R** and **u** and the infinitesimal angles  $d\theta_{xy}$ ,  $d\theta_{yz}$ ,  $d\theta_{zx}$  through which, at a point of space or time near the origin, their directions have rotated from the fixed axes *Ox*, *Oy*, *Oz*.

To do this we substitute in (9) the values

$$\left. \begin{aligned} p &= \frac{R}{(1 - u^2)^{\frac{1}{2}}}, & dp_x &= dp = \frac{dR}{(1 - u^2)^{\frac{1}{2}}} + \frac{Ru du}{(1 - u^2)^{\frac{3}{2}}} \\ q &= \frac{Ru}{(1 - u^2)^{\frac{1}{2}}}, & dq_y &= dq = \frac{u dR}{(1 - u^2)^{\frac{1}{2}}} + \frac{R du}{(1 - u^2)^{\frac{3}{2}}} \end{aligned} \right\} \quad (11)$$

obtained from (10) and

$$\left. \begin{aligned} dp_y &= p d\theta_{xy} = \frac{R}{(1 - u^2)^{\frac{1}{2}}} d\theta_{xy}, & dp_z &= p d\theta_{xz} = -\frac{R}{(1 - u^2)^{\frac{1}{2}}} d\theta_{xz} \\ dq_x &= q d\theta_{yx} = -\frac{Ru}{(1 - u^2)^{\frac{1}{2}}} d\theta_{xy}, & dq_z &= q d\theta_{yz} = \frac{Ru}{(1 - u^2)^{\frac{1}{2}}} d\theta_{yz} \end{aligned} \right\}$$

which follow by simple geometry from a consideration of the rotation in the planes of *xy*, *yz*, *zx* of the perpendicular lines representing **p** and **q**.

The result of the substitution is to give, after some algebraical reduction, the following set of eight equations\* which are completely equivalent to the fundamental electromagnetic equations (1).

\* Although the sets (12) and (9) are equivalent, the single equations do not correspond exactly to each other. Two equations of (9) have been combined algebraically in some cases with the object of giving a more symmetrical form to the set.

$$\left. \begin{aligned}
 & \frac{1}{R} \frac{\partial R}{\partial x} + \frac{\partial \theta_{xy}}{\partial y} - \frac{1}{1-u^2} \left( \frac{\partial \theta_{xz}}{\partial z} + u \frac{\partial \theta_{xz}}{\partial t} \right) = 0 & (a) \\
 & \frac{1}{R} \frac{\partial R}{\partial y} - \frac{\partial \theta_{xy}}{\partial x} - \frac{u}{1-u^2} \left( \frac{\partial \theta_{yz}}{\partial t} + u \frac{\partial \theta_{yz}}{\partial z} \right) = 0 & (b) \\
 & \frac{1}{R} \left( \frac{\partial R}{\partial z} + u \frac{\partial R}{\partial t} \right) + \frac{1}{1-u^2} \left( \frac{\partial u}{\partial t} + u \frac{\partial u}{\partial z} \right) + \frac{\partial \theta_{xz}}{\partial x} = 0 & (c) \\
 & \frac{1}{R} \left( \frac{\partial R}{\partial t} + u \frac{\partial R}{\partial z} \right) + \frac{1}{1-u^2} \left( \frac{\partial u}{\partial z} + u \frac{\partial u}{\partial t} \right) - u \frac{\partial \theta_{yz}}{\partial y} = 0 & (d) \\
 & \frac{\partial \alpha}{\partial x} + \frac{1}{1-u^2} \frac{\partial u}{\partial y} + \frac{u}{1-u^2} \left( \frac{\partial \theta_{yz}}{\partial z} + u \frac{\partial \theta_{yz}}{\partial t} \right) = 0 & (e) \\
 & \frac{\partial \alpha}{\partial y} - \frac{1}{1-u^2} \frac{\partial u}{\partial x} - \frac{1}{1-u^2} \left( \frac{\partial \theta_{xz}}{\partial t} + u \frac{\partial \theta_{xz}}{\partial z} \right) = 0 & (f) \\
 & \left( \frac{\partial \alpha}{\partial z} + u \frac{\partial \alpha}{\partial t} \right) - \left( \frac{\partial \theta_{xy}}{\partial t} + u \frac{\partial \theta_{xy}}{\partial z} \right) - u \frac{\partial \theta_{yz}}{\partial x} = 0 & (g) \\
 & \left( \frac{\partial \alpha}{\partial t} + u \frac{\partial \alpha}{\partial z} \right) - \left( \frac{\partial \theta_{xy}}{\partial z} + u \frac{\partial \theta_{xy}}{\partial t} \right) - \frac{\partial \theta_{xz}}{\partial y} = 0 & (h)
 \end{aligned} \right\}, \quad (12)$$

*Transformation equations of new field variables.*—Light is thrown on the meaning of (12) by examining the transformation equations of the variables in it. These may be readily determined from the transformation equations for  $e$  and  $h$ , and the equations which define the variables in terms of  $e$  and  $h$ . For the present purpose it is only necessary to consider the transformation due to a velocity of the observer along the special axis  $Oz$ . The effect of transformations along other axes is considered at a later stage (p. 44). We have if  $e_x', h_x'$ , etc., represent the component electric and magnetic forces as observed in a co-ordinate system  $S'$ , ( $x'y'z't'$ ), which moves along the axis of  $z$  with velocity  $v$  relative to the system  $S$ , ( $xyzt$ ),

$$\left. \begin{aligned}
 e_x' &= \frac{e_x - v h_y}{(1-v^2)^{\frac{1}{2}}}, & h_x' &= \frac{h_x + v e_y}{(1-v^2)^{\frac{1}{2}}} \\
 e_y' &= \frac{e_y + v h_x}{(1-v^2)^{\frac{1}{2}}}, & h_y' &= \frac{h_y - v e_x}{(1-v^2)^{\frac{1}{2}}} \\
 e_z' &= e_z, & h_z' &= h_z.
 \end{aligned} \right\} \quad (13)$$

We find at once from (2) that  $p$  and  $q$  transform in the same way as do  $e$  and  $h$ , and that  $R$  ( $= (p^2 - q^2)^{\frac{1}{2}}$ ) is invariant, as is also  $\alpha$  by (5). The transformation of  $u$  is given by

$$u' = \frac{q_y'}{p_x'} = \frac{q_y - v p_x}{(1-v^2)^{\frac{1}{2}} / (1-v^2)^{\frac{1}{2}}} = \frac{p_x - v q_y}{1 - q_y v} = \frac{u - v}{1 - uv}. \quad (14a)$$

Similarly

$$d\theta_{xz}' = \frac{dp_z'}{p_z'} = \frac{dp_z}{p_z} \cdot \frac{(1-v^2)^{\frac{1}{2}}}{\left(1-v\frac{q_x}{p_x}\right)} = \frac{(1-v^2)^{\frac{1}{2}}}{1-uv} d\theta_{xz}, \quad (14b)$$

$$u' d\theta_{yz}' = \frac{dq_z'}{p_z'} = \frac{(1-v^2)^{\frac{1}{2}}}{1-uv} \cdot u d\theta_{yz}, \quad (14c)$$

and

$$\begin{aligned} d\theta_{xy}' &= \frac{dp_y'}{p_y'} = \frac{dp_y \left(1 + v \frac{\partial q_x}{\partial p_y}\right)}{(1-v^2)^{\frac{1}{2}}} \bigg/ \frac{p_x \left(1 - v \frac{q_x}{p_x}\right)}{(1-v^2)^{\frac{1}{2}}} \\ &= \frac{1 + v \frac{\partial q_x}{\partial p_y}}{1 - v \frac{q_x}{p_x}} d\theta_{xy}, \end{aligned}$$

but since  $p$  and  $q$  are perpendicular we have here

$$\frac{\partial q_x}{\partial p_y} = -\frac{q_y}{p_x} = -u,$$

so that

$$d\theta_{xy}' = d\theta_{xy}. \quad (14d)$$

In order to transform (12) from  $S$  to  $S'$  we substitute in it the following values for the undashed variables, obtained by solving (14) :

$$\left. \begin{aligned} u &= \frac{u' + v}{1 + u'v}, & du &= \frac{1-v^2}{(1+u'v)^2} du', \\ d\theta_{xz} &= \frac{(1-v^2)^{\frac{1}{2}}}{1+u'v} d\theta_{xz}', & u d\theta_{yz} &= \frac{(1-v^2)^{\frac{1}{2}}}{1+u'v} \cdot u' d\theta_{yz}', \end{aligned} \right\} \quad (15)$$

and also the values of the differential operators, obtained at once from the Lorentz transformation,

$$\left. \begin{aligned} \frac{\partial}{\partial z} &= \frac{1}{(1-v^2)^{\frac{1}{2}}} \left( \frac{\partial}{\partial z'} - v \frac{\partial}{\partial t'} \right), \\ \frac{\partial}{\partial t} &= \frac{1}{(1-v^2)^{\frac{1}{2}}} \left( \frac{\partial}{\partial t'} - v \frac{\partial}{\partial z'} \right); \end{aligned} \right\} \quad (16)$$

all other variables and operators are invariant.

On making these substitutions each equation of (12) is found to be invariant in form. This indeed is only to be expected as the equations are derived from the fundamental ones (1) which are also invariant in form. There is, however, this difference between (12) and (1), that, whereas no simple physical ideas can be attached to the transformation equations of  $e$  and  $h$ , those for the variables in (12) have in every case a straightforward geometrical meaning. Thus when



the phenomena are expressed in a co-ordinate system  $S'$  which is moving relatively to  $S$  with a velocity  $v$  in the direction  $Oz$ , the vector  $u$  transforms precisely as would a velocity parallel to  $Oz$ ;  $d\theta_{xx}$  precisely in the way in which a small angle in the plane of  $zx$ , which in  $S$  is moving with the velocity  $u$ , transforms;  $d\theta_{xy}$  is invariant, as a small angle in the plane  $xy$  moving along  $Oz$  with velocity  $u$  (or with any velocity) would be;  $ud\theta_{yz}$  transforms in the same way as a small component velocity along  $Oy$ , present in a body moving with the velocity  $u$  along  $Oz$ , would transform. Every other variable in (12) (except  $z$  and  $t$ ) is invariant. Now these transformations are exactly those which would apply to a vector the curved "lines of force" of which at the origin lie in the direction  $Oz$ , and which in the system  $S$  are moving everywhere in a direction perpendicular to their lengths with velocity  $u$ .

The equations thus lead directly to a view of the field as constituted of moving lines of the vector  $R$ , a conception which, contained as it is in the fundamental equations, is by no means suggested by them in their usual form. A little consideration shows that this conception of the field is not merely a possible one, but is one which must necessarily be adopted when the variables are expressed in terms of  $R$ ,  $u$ , etc. Their transformation equations are the only means we have of determining the meaning of the variables. If  $u$  and  $ud\theta_{yz}$  transform like velocities, they must be velocities, just as  $d\theta_{xx}$  and  $d\theta_{xy}$  are the angles which their transformation equations show them to be. It is unnecessary to give a proof that the transformation equations (14) have the meanings described except in the case of  $d\theta_{xx}$ , for the corresponding formulæ are given in numerous text-books. The proof for  $d\theta_{xx}$  is as follows:

Let a pair of lines, one being the line  $Ox$ , form an angle  $d\theta_{xx}^\circ$  when viewed by  $A^\circ$ , an observer at rest in relation to them. To an observer  $A$  moving with velocity  $-u$  along  $Oz$  relatively to  $A^\circ$  the angle will appear as a moving angle of magnitude

$$d\theta_{xx} = d\theta_{xx}^\circ (1 - u^2)^{\frac{1}{2}},$$

in consequence of the Lorentz contraction. Let  $A'$  move relatively to  $A$  with velocity  $+v$  along  $Oz$ , and therefore relatively to  $A^\circ$  with velocity  $\frac{v-u}{1-uv}$ .

He will observe the angle as

$$\begin{aligned} d\theta_{xx}' &= d\theta_{xx}^\circ \left\{ 1 - \left( \frac{v-u}{1-uv} \right)^2 \right\}^{\frac{1}{2}} \\ &= d\theta_{xx}^\circ \frac{(1-u^2)^{\frac{1}{2}}(1-v^2)^{\frac{1}{2}}}{1-uv}. \end{aligned}$$

Eliminating  $d\theta_{xx}^\circ$  between these equations we obtain (14b).

Since  $d\theta_{xz}$  and  $d\theta_{yz}$  have the transformation equations of angles it might perhaps be expected that  $d\theta_{yz}$  would transform like an angle also, but it does not. The reason is really pointed out by the equations themselves, for in the picture of the field derived from them, there is not in the  $y$  direction a moving physical line as there is along  $Ox$ . Consider two neighbouring points of the field which differ by  $d\theta_{yz}$ . One is a point of a line of  $R$  moving with velocity  $u$  along  $Oz$ , the other a point of another  $R$  line moving with velocity  $u + du$  along a line making an angle with  $Oz$  whose component in the plane of  $yz$  is  $d\theta_{yz}$ . All that an observer can appreciate concerning these points is their velocities, and the  $y$  component of their velocity of separation  $du_y = -u d\theta_{yz}$  must behave on transformation like a transverse velocity, as the equation derived for it shows that it does.

*An alternative interpretation.*—There is another transformation, quite different from that of Lorentz, to which the set of equations (12) is invariant. If we substitute in it throughout  $y$  for  $x$ ,  $x$  for  $y$ ,  $1/u$  for  $u$ ,  $-dx$  for  $dx$ , the component equations are transformed in such a way that the set as a whole is reproduced unaltered. This shows that an alternative picture of the field is possible, in which a vector  $R$  is directed along  $Oy$  and is in motion with the velocity  $1/u$  (or more generally  $c^2/u$ ) in the direction  $Oz$ . To every property of the moving lines which can be proved for the first picture a corresponding property is equally true of the second. We shall not here, however, consider this alternative picture further, beyond observing that it represents a different method of section into space and time of the four dimensional entity which must be regarded as the fundamental reality of the field.

*Electromagnetic Field Tubes and Elements.*—The properties of the field may be expressed in terms of tubes of  $R$  constructed in the same way as are Faraday tubes; small elements of these cut off by transverse sections everywhere perpendicular to  $R$  will be called "field elements." Let  $OG$ , fig. 1, be such an

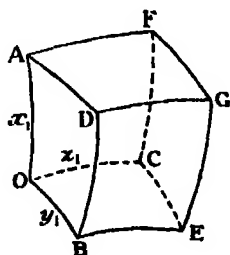


FIG. 1.

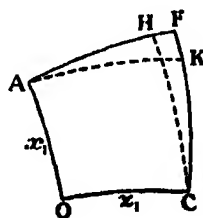


FIG. 2.

element, infinitesimal in size and approximately rectangular in shape. OA is a curved line of force of  $R$  of length  $x_1$  passing through the origin; OC a line of length  $z_1$  at each point coinciding in direction with  $u$ , OB one of length  $y_1$  at each point perpendicular to  $R$  and  $u$ . The remaining edges are drawn in a similar way, parallel to  $R$ ,  $u$  and  $[uR]$  respectively at each point of the field through which they pass.\*

A number of geometrical relations may readily be deduced between the variations in the lengths of the sides of a field element and those of the angles  $d\theta$ . Thus in the face OF, fig. 2, drawing CH, AK parallel to OA, OC, we have

$$\angle HCF = z_1 \frac{\partial \theta_{xz}}{\partial z}, \quad HF = x_1 \frac{\partial z_1}{\partial x}; \quad \angle KAF = x_1 \frac{\partial \theta_{xz}}{\partial x}, \quad FK = z_1 \frac{\partial x_1}{\partial z},$$

whence

$$\frac{\partial \theta_{xz}}{\partial z} = \frac{1}{z_1} \frac{\partial z_1}{\partial x}, \quad \frac{\partial \theta_{xz}}{\partial x} = \frac{1}{x_1} \frac{\partial x_1}{\partial z}. \quad (17a)$$

Similarly by considering other faces

$$\frac{\partial \theta_{xy}}{\partial y} = \frac{1}{y_1} \frac{\partial y_1}{\partial x}, \quad \frac{\partial \theta_{yz}}{\partial x} = \frac{1}{x_1} \frac{\partial x_1}{\partial y}, \quad (17b)$$

$$\frac{\partial \theta_{yz}}{\partial z} = \frac{1}{z_1} \frac{\partial z_1}{\partial y}, \quad \frac{\partial \theta_{xy}}{\partial y} = \frac{1}{y_1} \frac{\partial y_1}{\partial z}. \quad (17c)$$

Further in equations (12) instead of the time rates of increase of variables at a point fixed in space, use those appropriate to the moving element. If  $\partial/\partial t$  represents the former for any property of the field, and  $\delta/\delta t$  the local time rate of increase of the property in the moving element (both measured in the same space-time system of a given observer), we have the ordinary hydrodynamical relation between them

$$\frac{\delta}{\delta t} = \frac{\partial}{\partial t} + u \frac{\partial}{\partial z}. \quad (18)$$

*Field equations in terms of moving elements.*—On using (17) and (18), (12) may be written

\* An element so described will not in general be closed, due to twist (*cf. loc. cit.*, p. 713), but this will not affect any use here made of it.

$$\left. \begin{aligned}
 u \frac{\delta \theta_{xz}}{\delta t} &= (1-u^2) \left\{ \frac{1}{R} \frac{\partial R}{\partial x} + \frac{1}{y_1} \frac{\partial y_1}{\partial x} + \frac{1}{z_1} \frac{\partial z_1}{\partial x} \right\} & (a) \\
 u \frac{\delta \theta_{yz}}{\delta t} &= (1-u^2) \left\{ \frac{1}{R} \frac{\partial R}{\partial y} + \frac{1}{x_1} \frac{\partial x_1}{\partial y} \right\} & (b) \\
 (1-u^2) \frac{1}{R} \frac{\delta R}{\delta t} &= \frac{u(1-u^2)}{R} \frac{\partial R}{\partial z} + \frac{u}{x_1} \frac{\partial x_1}{\partial z} - \frac{u}{y_1} \frac{\partial y_1}{\partial z} - \frac{\partial u}{\partial z} & (c) \\
 \frac{\delta u}{\delta t} &= -\frac{1-u^2}{R} \frac{\partial R}{\partial z} - \frac{1}{x_1} \frac{\partial x_1}{\partial z} + \frac{u^2}{y_1} \frac{\partial y_1}{\partial z} + u \frac{\partial u}{\partial z} & (d) \\
 u^2 \frac{\delta \theta_{yz}}{\delta t} &= -(1-u^2) \left\{ \frac{\partial \alpha}{\partial x} + \frac{u}{z_1} \frac{\partial z_1}{\partial y} \right\} - \frac{\partial u}{\partial y} & (e) \\
 \frac{\delta \theta_{xz}}{\delta t} &= (1-u^2) \frac{\partial \alpha}{\partial y} - \frac{\partial u}{\partial x} & (f) \\
 (1-u^2) \frac{\delta \theta_{xy}}{\delta t} &= (1-u^2) \left\{ u \frac{\partial \theta_{xy}}{\partial z} + \frac{\partial \alpha}{\partial z} \right\} - u \frac{\partial \theta_{yz}}{\partial x} + u \frac{\partial \theta_{xz}}{\partial y} & (g) \\
 (1-u^2) \frac{\delta \alpha}{\delta t} &= (1-u^2) \left\{ \frac{\partial \theta_{xy}}{\partial z} + u \frac{\partial \alpha}{\partial z} \right\} - u^2 \frac{\partial \theta_{yz}}{\partial x} + \frac{\partial \theta_{xz}}{\partial y} & (h)
 \end{aligned} \right\} \quad (19)$$

The primary field properties which characterise the moving element are six in number, its  $R$ ,  $u$ ,  $\alpha$ ,  $\theta_{xy}$ ,  $\theta_{yz}$ ,  $\theta_{xz}$ . The time rate of increase of each of these is given by the equations of (19) in terms of the original size and shape of the element and the space derivatives of its  $R$ ,  $u$ , and  $\alpha$ .\*

To express the variation of the properties of the element itself the rates of alteration of its size and shape are also required. These may be deduced as follows:—

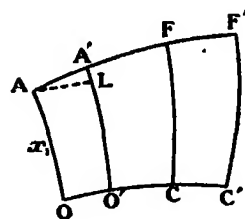


FIG. 3.

Let  $OACF$ , fig. 3, represent the  $xz$  face of the element at  $t = 0$ ,  $O'A'C'F'$  the displaced face at  $t = \delta t$ . Drawing  $AL$  parallel to  $OO'$  we have  $OO' = u\delta t$ ,  $CC' = \left(u + z_1 \frac{\partial u}{\partial z}\right) \delta t$ ,  $CC' - OO' = O'C' - OC = \frac{\delta z_1}{\delta t} \delta t$ ;  $A'L = \frac{\delta x_1}{\delta t} \delta t$ ,  $AA' = u \delta t$ ,  $\angle A'AL = x_1 \frac{\partial \theta_{xz}}{\partial x}$ . From these relations, supplemented by similar ones for the  $yz$  face and by (17 a, c), the following expressions for the rates of

\* Terms like  $\frac{\partial \theta_{xy}}{\partial z}$  mean that the element is twisted (in this case about the axis of  $z$ ), they may be included with terms like  $\frac{1}{x_1} \frac{\partial x_1}{\partial y}$  in the word "shape."

increase of the three edges of the element  $x_1 y_1 z_1$  may be readily obtained.

$$\left. \begin{aligned} \frac{\delta x_1}{\delta t} &= u \frac{\partial x_1}{\partial z} \\ \frac{\delta y_1}{\delta t} &= u \frac{\partial y_1}{\partial z} \\ \frac{\delta z_1}{\delta t} &= z_1 \frac{\partial u}{\partial z} \end{aligned} \right\} \quad (20)$$

*Laws of Motion of Field Elements.*—By means of (19) and (20) the time rate of increase of any property of the moving field element can be determined directly. We shall apply them to calculate the rates of increase of the element's total momentum and energy.

By (6) and (10) we have for the momentum and energy densities

$$G = \frac{R^2 u}{1 - u^2},$$

$$W = \frac{1}{2} \frac{R^2 (1 + u^2)}{1 - u^2},$$

and consequently

$$g = \frac{R^2 u}{1 - u^2} x_1 y_1 z_1$$

for the momentum of the element and

$$w = \frac{1}{2} \frac{R^2 (1 + u^2)}{1 - u^2} x_1 y_1 z_1$$

for its energy.

The following equations can be deduced from the first four equations of (19), on using (20),

$$\left. \begin{aligned} \frac{\delta g_x}{\delta t} &= \frac{R^2 u}{1 - u^2} x_1 y_1 z_1 \frac{\delta \theta_{xz}}{\delta t} = + \frac{x_1}{y_1 z_1} \frac{\partial}{\partial x} \left( \frac{1}{2} R^2 y_1^2 z_1^2 \right) & (a) \\ \frac{\delta g_y}{\delta t} &= \frac{R^2 u}{1 - u^2} x_1 y_1 z_1 \frac{\delta \theta_{xy}}{\delta t} = - \frac{y_1 z_1}{x_1} \frac{\partial}{\partial y} \left( \frac{1}{2} R^2 x_1^2 \right) & (b) \\ \frac{\delta g_z}{\delta t} &= \frac{\delta}{\delta t} \left( \frac{R^2 u}{1 - u^2} x_1 y_1 z_1 \right) = - \frac{y_1 z_1}{x_1} \frac{\partial}{\partial z} \left( \frac{1}{2} R^2 x_1^2 \right) & (c) \\ \frac{\delta w}{\delta t} &= \frac{\delta}{\delta t} \left( \frac{1}{2} \frac{R^2 (1 + u^2)}{1 - u^2} x_1 y_1 z_1 \right) = - z_1 \frac{\partial}{\partial z} \left( \frac{1}{2} R^2 x_1 y_1 u \right). & (d) \end{aligned} \right\} \quad (21)$$

The left hand and central expressions of (21) represent the time rates of increase of the components of the momentum, and that of the energy, of the element. It can be shown that the right hand sides stand respectively for the  $x$ ,  $y$ ,  $z$  components of the resultant force, and for the resultant activity, on the moving element of a stress system, consisting of a tension  $-P = -\frac{1}{2}R^2$  along the  $R$  direction of the element and an equal pressure  $+P$  in all directions perpendicular to  $R$ , which accompanies the element in its motion.

To do this, let us express the forces due to this stress on the various faces of the element  $OG$  (see fig. 1). On the three faces  $OE$ ,  $OF$ ,  $OD$ , containing the origin, the respective forces are  $-Py_1z_1$  along  $Ox$ ,  $+Pz_1x_1$  along  $Oy$ ,  $+Px_1y_1$  along  $Oz$ . On the three opposite faces the corresponding forces are

$$+\left\{Py_1z_1+x_1\frac{\partial}{\partial x}(Py_1z_1)\right\}, -\left\{Pz_1x_1+y_1\frac{\partial}{\partial y}(Pz_1x_1)\right\}, -\left\{Px_1y_1+z_1\frac{\partial}{\partial z}(Px_1y_1)\right\},$$

but as a result of the curvature of the lines these act in directions rotated from  $Ox$ ,  $Oy$ ,  $Oz$  by the component angles

$$x_1\frac{\partial\theta_{xy}}{\partial x}, x_1\frac{\partial\theta_{xz}}{\partial x}; y_1\frac{\partial\theta_{rx}}{\partial y}, y_1\frac{\partial\theta_{yz}}{\partial y}; z_1\frac{\partial\theta_{zx}}{\partial z}, z_1\frac{\partial\theta_{zy}}{\partial z},$$

respectively. The terms of the  $x$ ,  $y$ ,  $z$  components of the resultant force can readily be picked out, giving

$$\left. \begin{aligned} F_x &= +x_1\frac{\partial}{\partial x}(Py_1z_1) - Pz_1x_1 \cdot y_1\frac{\partial\theta_{xz}}{\partial y} - Px_1y_1 \cdot z_1\frac{\partial\theta_{zx}}{\partial z} & (a) \\ F_y &= -y_1\frac{\partial}{\partial y}(Pz_1x_1) + Py_1z_1 \cdot x_1\frac{\partial\theta_{xy}}{\partial x} - Px_1y_1 \cdot z_1\frac{\partial\theta_{yz}}{\partial z} & (b) \\ F_z &= -z_1\frac{\partial}{\partial z}(Px_1y_1) + Py_1z_1 \cdot x_1\frac{\partial\theta_{xz}}{\partial x} - Pz_1x_1 \cdot y_1\frac{\partial\theta_{yz}}{\partial y} & (c) \end{aligned} \right\}. \quad (22)$$

In consequence of the geometrical relations (17) these are identical with the right hand sides of (21a, b, c) respectively if we write  $P = \frac{1}{2}R^2$ .

The rate at which work is done on the element by the moving stress is obtained from the activity of the stress over the two faces  $OD$  and  $CG$ , which are perpendicular to the velocity  $u$ , for on all the remaining faces the stress itself is perpendicular to  $u$ . The activity of the stress on the first face is  $Px_1y_1u$ , and consequently  $-z_1\frac{\partial}{\partial z}(Px_1y_1u)$  is the net rate at which work is done on the element.

Putting  $P = \frac{1}{2}R^2$ , this is identical with the right hand side of (21d).

The stress system

$$P_n = \frac{1}{2}R^2n - (Rn) R \quad (23)$$

moving with the element is simpler than the system  $\Pi_n$  (6c) in that the principal tension and pressures are here all equal, whereas in (6c)  $\Pi_3$  is different from  $\Pi_1$  and  $\Pi_2$ . Maxwell's stress system  $\Pi_n$  expresses the flow of momentum in the field past an arbitrarily fixed plane, but it does not, and cannot, account for the flow of energy past such a plane, the reason being that the stress is formulated as fixed in space, and it is therefore dynamically incapable of doing work. Cunningham\* was the first to point out that in the electromagnetic field a moving stress is required to account simultaneously for both momentum and energy changes, and he has determined the necessary velocity of its motion. The conception of moving elements derived here is in general agreement with his results.

The four equations of (21), which express the facts that the rates of increase of the momentum and the energy of each element are equal respectively to the resultant force and to the activity of the moving stress upon it, and which may be written symbolically

$$\left. \begin{aligned} \frac{\delta \mathbf{g}}{\delta t} &= \int \mathbf{P}_n d\mathbf{S} \\ \frac{\delta w}{\delta t} &= \int \mathbf{P}_n \mathbf{u} d\mathbf{S} \end{aligned} \right\} \quad (24)$$

(where  $\mathbf{S}$  is the surface of the element and  $\mathbf{u}$  the velocity at each point of it) are derived from and are equivalent to the first four of the equations (12). We may say that one half of the fundamental equations of the electromagnetic field, when transformed so as to express the laws of motion of field elements, are found to be identical with the fundamental equations of mechanics.

*Flux of R in field tubes.*—The conception of field tubes would not have a great physical significance unless a property of constant flux can be associated with them. The point can, of course, be examined by equations (19) and we find at once from (a) that

$$\frac{1}{Ry_1z_1} \frac{\partial}{\partial x} (Ry_1z_1) = \frac{u}{1-u^2} \frac{\delta \theta_n}{\delta t}, \quad (25)$$

which shows that the flux of  $R$  over the section of the tube is not constant along its length.

It is to be observed, however, that the true criterion of the objective existence of a moving entity is not to be sought for, when we take account of the teachings of relativity theory, in the properties of the tube as appreciated by a fixed

\* E. Cunningham, 'Roy. Soc. Proc.' A, vol. 83, p. 110.

observer. It is on the constancy or otherwise of the "proper" flux, or the flux as it would be perceived by an observer who is at rest relatively to an element of the tube, that any conclusion as to its physical reality must be based.

*Proper relations characterising field elements.*—The proper relations which characterise an element can be determined by transforming (12) with the velocity  $v = u$  along the  $z$  axis. In consequence of the nature of the transformation equations it comes to the same thing if we write in either (12) or (19)  $u = 0$  (but not of course  $du = 0$ ) everywhere except in the term  $u d\theta_{yz}$ . This term represents, as has already been mentioned, a single quantity, the infinitesimal transverse velocity  $-du_y$ , and it must be retained as such in the transformed equations. The result of the transformation is to give the following set of proper equations. In what follows all proper relations, which hold only in the space-time measure of an observer to whom the element appears to be at rest, are marked with a star.

$$\left. \begin{aligned}
 & \frac{1}{R} \frac{\partial R}{\partial x} + \frac{1}{y_1} \frac{\partial y_1}{\partial x} + \frac{1}{z_1} \frac{\partial z_1}{\partial x} = 0 & (a) \\
 & \frac{1}{R} \frac{\partial R}{\partial y} + \frac{1}{x_1} \frac{\partial x_1}{\partial y} + \frac{\partial u_y}{\partial t} = 0 & (b) \\
 & \frac{1}{R} \frac{\partial R}{\partial z} + \frac{1}{x_1} \frac{\partial x_1}{\partial z} + \frac{\partial u_z}{\partial t} = 0 & (c) \\
 & \frac{1}{R} \frac{\partial R}{\partial t} + \frac{\partial u_y}{\partial y} + \frac{\partial u_z}{\partial z} = 0 & (d) \\
 & \frac{\partial x}{\partial x} + \frac{\partial u_z}{\partial y} - \frac{\partial u_y}{\partial z} = 0 & (e) \\
 & \frac{\partial x}{\partial y} - \frac{\partial u_z}{\partial x} - \frac{\partial \theta_{yz}}{\partial t} = 0 & (f) \\
 & \frac{\partial x}{\partial z} - \frac{\partial \theta_{xz}}{\partial t} + \frac{\partial u_x}{\partial x} = 0 & (g) \\
 & \frac{\partial x}{\partial t} - \frac{\partial \theta_{xy}}{\partial z} - \frac{\partial \theta_{xz}}{\partial y} = 0 & (h)
 \end{aligned} \right\} \quad (26^*)$$

We get from (a)

$$\frac{1}{R y_1 z_1} \frac{\partial}{\partial x} (R y_1 z_1) = 0, \quad (27^*)$$

which shows that the proper flux is constant along the tube. Hence the tubes fulfil a requirement for objective reality, which we have seen is more fundamental than would be that of the constancy of the actual flux. To a fixed observer who sees the tubes in different parts of the field moving with various velocities



in different directions, the want of constancy of the directly observed flux is what should be expected, since the moving sections of the real four dimensional entities undergo the Lorentz contraction, while  $R$  itself remains invariant.

*General conditions for permanent existence of moving tubes.*—When a field of force in general is representable by a system of moving tubes, certain conditions must be satisfied if each tube is to retain a permanent existence as an individual during its movement. These conditions, three in number, are now discussed in reference to electromagnetic tubes.

(1) The flux must remain constant with the time. This is satisfied for electromagnetic tubes as regards the proper flux for we have by (26d), since here

$$\frac{\partial u_y}{\partial y} = \frac{1}{y_1} \frac{\partial y_1}{\partial t}, \quad \frac{\partial u_z}{\partial z} = \frac{1}{z_1} \frac{\partial z_1}{\partial t},$$

$$\frac{1}{R y_1 z_1} \frac{\partial}{\partial t} (R y_1 z_1) = 0. \quad (28^*)$$

It must be observed, however, that the condition is not satisfied for the flux of  $R$  in the space-time system of a fixed observer. From (19c, d) and (20) we find in fact

$$\frac{1}{R y_1 z_1} \frac{\delta}{\delta t} (R y_1 z_1) = - \frac{u}{1 - u^2} \frac{\delta u}{\delta t}. \quad (29)$$

Nevertheless, a vector may be constructed the flux of which does remain constant during the motion to a fixed observer, for (29) can be re-written in the form

$$\frac{(1 - u^2)^{\frac{1}{2}}}{R y_1 z_1} \frac{\delta}{\delta t} \left\{ \frac{R}{(1 - u^2)^{\frac{1}{2}}} y_1 z_1 \right\} = 0, \quad (30)$$

which shows that the flux of the vector  $\frac{R}{(1 - u^2)^{\frac{1}{2}}}$  over the cross section of the tube does not change with the time. Because of the constancy of its flux this vector would be appreciated more directly than  $R$  itself by a fixed observer.

(2 and 3) The nature of the further conditions will be evident from fig. 4

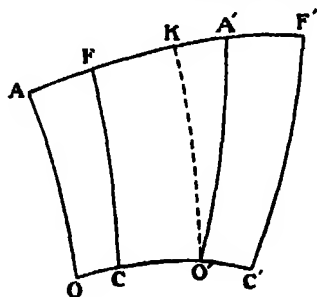


FIG. 4.

which represents the  $xz$  face of a short length of a tube  $OF$  and the same tube  $O'F'$  after the lapse of a short time  $\delta t$ . Drawing  $O'K$  parallel to  $OA$ , we have

$$AK = OO' = u\delta t, AA' = \left(u + x_1 \frac{\partial u}{\partial x}\right)\delta t, \quad \angle KO'A' = \frac{\partial \theta_{xz}}{\partial t} \delta t,$$

whence

$$\frac{\partial \theta_{xz}}{\partial t} = \frac{\partial u}{\partial x}. \quad (31a)$$

Similarly for the rate of bending in the  $xy$  plane we get

$$\frac{\partial \theta_{xy}}{\partial t} = \frac{\partial u_y}{\partial x} = u \frac{\partial \theta_{xy}}{\partial x}. \quad (31b)$$

It is only when these equations are satisfied that the points of each  $R$  line which bounds a tube will move to corresponding points of a displaced line, *i.e.*, that the tube will move without breaking up and losing its identity. Translated into Cartesian notation the three conditions (29) become identical with the three components (1) in the direction of  $R$ , (2 and 3) perpendicular to it, of the vector equation

$$\frac{\partial \mathbf{R}}{\partial t} = \text{curl} [\mathbf{uR}]. \quad (32)$$

Reference to equations (19) shows that the conditions (31) are not satisfied except in special cases. If the derivatives of  $\alpha$  are everywhere zero, a condition which includes the important case of all fields in which the electric and magnetic forces are perpendicular to each other, the conditions (31) are satisfied by (19  $f, g, h$ ) and the electromagnetic tubes will keep their identity as they move. In this case  $\mathbf{R} = \mathbf{e} (1 - u^2)^{1/2}$  and the electromagnetic tube becomes identical with a moving Faraday tube, having for a fixed observer a constant flux of  $\mathbf{e}$  (*cf.* (30)). The whole of the equations (19), and the results deduced from them, in this case ( $\alpha = 0$ ) become directly applicable as a theory of moving ordinary Faraday tubes. However, when  $\mathbf{e}$  and  $\mathbf{h}$  are not perpendicular,  $\alpha$  and its derivatives are not zero; the equations (31) are then not satisfied and we must infer that a theory of moving permanent tubes, whether simple Faraday tubes, or the more general electromagnetic tubes, is not possible in the general field.

*Rotations of field elements.*—Nevertheless, a theory of moving field elements, short lengths of tubes of  $R$  such as have been described, is not only possible but may be readily developed from the equations. The second half (*e...h*) of equations (19) contains a description of the way in which the electromagnetic tubes (including the Faraday tubes to which they reduce when  $\alpha = 0$ ) break up when they do not possess permanence. The physical ideas involved can

be seen best by considering the simpler proper equations (26) instead of the more general ones (19). The latter represent the same things but the expressions for relative rotations of moving elements are more complicated when stated in the space-time system of a fixed observer.

(26f) may be written

$$\Omega_v = \frac{\partial \theta_{xz}}{\partial t} = -\frac{\partial u}{\partial x} + \frac{\partial \alpha}{\partial y} = -\frac{\partial u}{\partial x} + \omega_v. \quad (*)$$

Here  $\partial \theta_{xz}/\partial t$  denotes the proper angular velocity  $\Omega_v$  with which the  $x$  or tensional axis of an element is rotating in the plane  $xz$ . According to the equation it is composed of two parts. The first,  $-\partial u/\partial x$ , is produced by the motion of the tube of which the element forms a part: if this existed alone the tube would maintain continuity of existence (cf. 31a). But there is a second part,  $\partial \alpha/\partial y = \omega_v$ , of the total angular velocity  $\Omega_v$ , which makes the stress axis rotate faster (or slower, according to sign) than it would do were the motion of the whole tube the only cause of rotation.

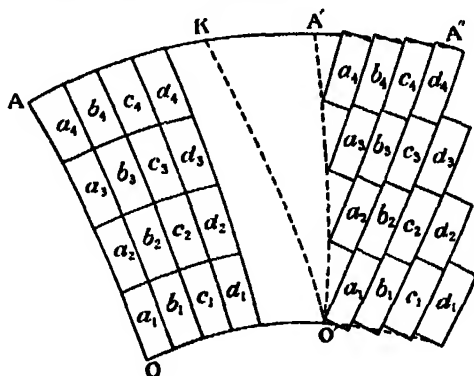


FIG. 5.

The effect of both terms is shown in fig. 5 which represents in the  $xz$  plane several contiguous elements  $a_1, a_2, b_1$ , etc., all having the same proper flux and the positions of each a short time later. In the initial position R-tubes such as  $a_1 \dots a_4, b_1 \dots b_4$  of constant proper flux can be formed from adjacent elements, and the motion is such that at a time  $\delta t$  later the line  $OA$  of the tube  $a_1 \dots a_4$  has been displaced to  $O'A'$ . The angle  $KO'A'$  is thus  $\frac{\partial u}{\partial x} \delta t$ . The actual rotation of the axes of the elements  $\frac{\delta \theta_{xz}}{\delta t} \delta t$  is, however, not  $KO'A'$  but  $KO'A''$ , where  $A'O'A'' = -\frac{\partial \alpha}{\partial y} \delta t$ , and the only tubes of constant proper flux which

can be formed now lie along the line  $O'A''$ . Elements constructed in the new field must lie along this line, and the only way in which we can get a *physical* picture of this change, i.e., one in which there is continuity in time of something objective in the field, is by viewing the elements themselves as rotating into the new positions along  $O'A''$ . We may then say the old tube  $a_1 \dots a_4$  is broken up and the elements align themselves along their tensional axes into a new tube  $a_1 b_2 c_3 d_4$  which is again immediately broken up by the motions. Thus while the instantaneous tubes have no continuity of existence, being continually formed from different elements, the elements themselves, each characterised by its proper flux of  $R$  constant with the time, may be supposed to keep their identities permanently in the field. Each element is in a state of independent rotation relatively to the tube of which it forms instantaneously a part.  $\partial\alpha/\partial y$  is its proper angular velocity about the  $y$  axis relative to the tube and similarly by (26g)  $\partial\alpha/\partial z = \omega_z$  is that about the  $z$  axis.

There is also in general a rotation of each element about  $Ox$ , the axis of its instantaneous tube, for by (26e) we have

$$2\Omega_x = \frac{\partial u_z}{\partial y} - \frac{\partial u_y}{\partial z} = -\frac{\partial \alpha}{\partial x}. \quad (*)$$

This formula is different from the two previous ones, since in orthogonal fields ( $\alpha = 0$ )  $\Omega_x$  is zero, and a tube has no rotation about its own axis due to its velocity  $u$ . Accordingly in the general case  $-\frac{\partial \alpha}{\partial x}$  measures twice the absolute proper angular velocity of an element about the tube axis, a velocity relative to the tube not coming here into consideration.

The last equation of (26) completes the scheme for  $\alpha$  by giving its proper time rate of increase as being equal to  $\frac{\partial \theta_{xz}}{\partial y} + \frac{\partial \theta_{xy}}{\partial z}$ , which is twice the space rate of twist of a tube or element about its  $x$  axis.

The scalar product of  $e$  and  $h$  in the electromagnetic field has not hitherto been recognised to have any special mechanical significance, but these considerations show that there is a certain mechanical interpretation for it.  $\alpha$  is a measure of  $(eh)$ , and the gradient of  $\alpha$  at each point determines a certain intrinsic angular velocity of rotation of the stress axes which in non-orthogonal fields is present superposed on the rotation produced by the motion of the tubes.

The proper equations developed above are identical with those which have

be deduced in a previous paper† dealing with the properties of four dimensional electromagnetic tubes, except for the fact that there the equations were expressed in terms of imaginary time. The results of this paper are thus the interpretation in space and time of the properties of electromagnetic tubes which were there derived in four dimensional form. As time elapses, *i.e.*, as the observer's hyperplane moves through the four dimensional field in the direction of his time axis, the section which it makes of the four dimensional entity is such that it can be divided into moving elements  $x_1y_1z_1$ , which have the properties described above.

*An element of action in the field.*—The conception of the field elements in states of individual rotation, whereby old tubes or R are broken up and new ones continually formed, may be used to determine a characteristic time  $t_1$  which can be associated with each element. This is most naturally taken to be the time between the corresponding points of two successive breaks, *e.g.*, the time elapsing between the two states shown in fig. 5.

The action of an element reckoned over this characteristic time will then provide a naturally determined infinitesimal element of action in the four dimensional field, the magnitude of which we proceed to determine. In the special axes on which the proper equations (26) are expressed, the  $y$  and  $z$  axes are not fixed, other than being confined to lie in the given plane  $yz$ . We can consequently choose them so as to make the rotation  $\omega$  which tends to break up the tubes be wholly in the plane  $xz$ . With this choice  $\omega_z = \partial\alpha/\partial z = 0$ , and  $\partial\alpha/\partial y$  is the whole angular velocity  $\omega$  of the element relative to the tube of which it forms a part.

If the field elements are drawn as in fig. 5, even when  $x_1y_1z_1$  are infinitesimal, the consideration of the intermediate stages between corresponding points of successive breaks presents obvious difficulties, since the only successive tubes which can be formed are separated by finite angles. For the same reason, moreover, elements of this shape cannot represent *on the microscopic scale* the changes in the field given by Maxwell's laws. If Maxwell's laws are to apply microscopically, the successive R-tubes must be capable of being drawn at infinitesimal angles with their predecessors. To accomplish this we must construct the elements of such shapes that  $z_1$  is infinitesimal compared with  $x_1$ . When this is the case we can determine  $t_1$  by writing

$$\omega t_1 = \frac{z_1}{x_1}. \quad (*)$$

† 'Phil. Mag.', vol. 44, p. 705 (1922).

From this we get the following relation between the  $yz$  and  $xt$  faces of the space time element  $x_1y_1z_1t_1$  :

$$\frac{y_1z_1}{x_1t_1} = y_1\omega = y_1 \frac{\partial \alpha}{\partial y} = \Delta_1 \alpha, \quad (33^*)$$

where  $\Delta_1 \alpha$  is the change in  $\alpha$  which occurs in passing from one element to a corresponding part of the next in the  $y$  direction, this being now defined as the line in the  $yz$  plane along which  $\alpha$  has the maximum gradient. We may also suppose that an element is characterised by the magnitude of its proper flux, and write

$$Ry_1z_1 = \Delta F. \quad (34^*)$$

In the ordinary theory, as there is nothing supposed to be moving, there is no definite indication of what ought to be taken as the action density of an electromagnetic field ; it is usually taken, somewhat arbitrarily, as

$$\frac{1}{2} (e^2 - h^2) = \frac{1}{2} R^2 \cos 2\alpha.$$

We shall here, however, take it as  $\frac{1}{2} R^2$ , since this may be proved to represent the density of the Lagrangian function of a field element in motion. In the case under consideration where the element is viewed at rest, this gives for the action  $A$  of the element its proper energy  $\frac{1}{2} R^2 x_1 y_1 z_1$  considered for the proper interval  $t_1$  which elapses between its alignment with its neighbours into two successive tubes. We then get for it the expression

$$A = \frac{1}{2} R^2 x_1 y_1 z_1 t_1 = \frac{1}{2} \frac{(\Delta F)^2}{\Delta_1 \alpha}. \quad (35)$$

The magnitude of this infinitesimal element of action is fixed when  $\Delta F$  and  $\Delta_1 \alpha$  are assumed given ; it is invariant to the Lorentz transformation with the velocity in any direction. It should be observed, however, that the element  $x_1 y_1 z_1 t_1$  does not stand for a uniquely defined region of space-time. While  $y_1$  and  $z_1$  are fixed in magnitude and direction by  $\Delta_1 \alpha$  and  $\Delta F$ , this is not the case with  $x_1$  and  $t_1$  individually. By (33) only the element of surface  $x_1 t_1$  and the plane in which it lies are fixed. This point is of importance in the next section.

*Differences between field elements and ordinary matter. "Longitudinal" Transformation.*—The properties of the field elements which have been found above are to a large extent those by which we distinguish objective existence. A field element, unlike the tube from which it is constructed, possesses a permanent identity, that is to say, if we construct at any point an element in a known electromagnetic field, we know its velocity and direction of motion and also its angular velocity at each instant, so that we can, theoretically, trace its

position, size, and shape as an individual entity characterised by a constant flux throughout the whole history of the field. Moreover the local values of  $\epsilon$  and  $h$  are fixed by the dimensions and motion of the element, and the alterations in these can be pictured as caused by the action according to the laws of mechanics of the mutual stresses of adjacent elements on each other. This brings us near to the possibility of constructing an atomic theory of the electromagnetic field, but one must guard against attributing to an element more of the properties of ordinary matter than it possesses. There is an important respect in which its properties differ from those of ordinary matter, in that it has been regarded as capable of moving only in a direction at right angles to its length. An element of ordinary matter must necessarily be considered capable of moving in *any* direction, since its motion in any direction can always be produced by giving a velocity in the opposite direction to the observer. On the other hand, in a theory of moving lines, such as that to which in the first place the transformed electromagnetic equations led, no conception other than that of perpendicular motion is feasible, for unless we can identify the points on a line, motion *along* its length has no meaning. The equations, however, lead finally to the consideration of field elements which do, so to speak, identify the points on a line, and it is necessary to consider whether the motion of a field element *along* an electromagnetic tube is a possible conception and if so what it means.

The question can be examined by transforming the equations (12) or (26) to a co-ordinate system having an arbitrary velocity  $v$  in the  $x$  direction. The equations of transformation are readily obtained in the same way as equation (14) for transformation with velocity in the  $z$  direction. They are very complicated except when  $u = 0$ , in which case they reduce to the following simple forms

$$\begin{aligned} d\theta_{xx} &= \frac{d\theta_{xx}' - v du_z'}{(1 - v^2)^{\frac{1}{2}}}, & d\theta_{xy} &= \frac{d\theta_{xy}' - v du_y'}{(1 - v^2)^{\frac{1}{2}}}, \\ du_x &= \frac{du_x' - v d\theta_{xx}'}{(1 - v^2)^{\frac{1}{2}}}, & du_y &= \frac{du_y' - v d\theta_{xy}'}{(1 - v^2)^{\frac{1}{2}}}, \\ \frac{\partial}{\partial x} &= \frac{1}{(1 - v^2)^{\frac{1}{2}}} \left( \frac{\partial}{\partial x'} - v \frac{\partial}{\partial t'} \right), & \\ \frac{\partial}{\partial t} &= \frac{1}{(1 - v^2)^{\frac{1}{2}}} \left( \frac{\partial}{\partial t'} - v \frac{\partial}{\partial x'} \right). \end{aligned} \quad (36)$$

These transformations must only be applied to the proper equations (26). The undashed quantities are the field variables of (26), the dashed ones the corresponding variables for an observer  $A'$  moving with a velocity  $v$  along  $x$

relative to  $A^\circ$ , the observer of the undashed system. Now if we express (26) in terms of the dashed variables by substituting in it the values (36), the result is to leave it entirely unchanged in form. Consequently, the possibility of constructing a field element  $x_1'y_1'z_1'$  which may be viewed either as being at rest or moving only in the direction perpendicular to its length is a matter entirely independent of any velocity along the tube which may be assigned to  $A'$ .

$A'$  may of course consider the old element  $x_1y_1z_1$ , which to him will appear in motion along the tube, and express the properties of the field in terms of this. This would necessitate the postulation of a flux of energy and momentum along the tube, carried by the moving element. It is well known that on the Poynting flux of energy in the field we can superpose a flux of arbitrary magnitude in a closed circuit, accompanied by a corresponding momentum, without destroying the validity of the electromagnetic relations. The energy and momentum carried by the longitudinally moving element would form a flux of this character. There is no logical inconsistency in this, but there is also no necessity for it. A new element,  $x_1'y_1'z_1'$  constructed so as to have the simpler property of being at rest or in motion only transversely, and in agreement with the ordinary expressions for the flux of energy and momentum, is the one on which  $A'$  would naturally focus his attention.

It is to be observed that the new element  $x_1'y_1'z_1'$  with its corresponding time  $t_1'$  does not map out, as a portion of matter would, identically the same region of space-time as the old element  $x_1y_1z_1$  with its  $t_1$ . The space-time elements  $x_1y_1z_1t_1$  and  $x_1'y_1'z_1't_1'$  nevertheless differ from each other only in that the equal rectangular faces  $x_1t_1$  and  $x_1't_1'$  are constructed with their sides  $x_1$  and  $x_1'$  drawn in different directions in the same fixed  $xt$  plane. This arbitrariness of the  $xt$  face in the construction of an element of action is one to which reference has already been made. It is precisely of the same type as a similar arbitrariness in the  $yz$  face, but in consequence of the hyperbolic geometry of the  $xt$  plane it shows itself in this physically different way.

An interesting result of this analysis is that properties of field elements have been deduced which from a physical point of view it is difficult to reconcile with the idea of elements of infinitesimal size. Can we imagine really infinitesimal physical elements, in states of independent (although co-ordinated) rotation with respect to each other, and separated from each other by surfaces of slip as indicated crudely in fig. 5, unless they are finite in size? It is true that similar cases present themselves in hydrodynamics, where infinitesimal elements of matter in rotation are assumed in dealing with the vortical motion of liquids, but here this neglect of the real molecular constitution of the medium is only



made as a mathematical convenience. It must be admitted, however, that from a purely mathematical point of view the difficulty raised need not exist. A field element is essentially a constructed quantity, mapped out along the natural lines of the electromagnetic field in the same way as a Faraday tube element (of which it is the generalisation) is mapped out in an electrostatic field. In consequence of the rotation of the stress axes, constructed elements in the field successive in time lie at small angles with respect to their predecessors. Mathematically there is no necessity to assert that there is any continuity between them, i.e., that they are their predecessors turned round through a small angle. There is, however, some justification for the more physical point of view which would regard an element itself as being in rotation, because it possesses in the constancy of its proper flux the chief, if not the only, property by which an entity in the field can be distinguished.

Without attempting here to discuss further the question of the actual finiteness or otherwise of an element, it is nevertheless interesting to observe that the assumption that in an electromagnetic field finite and discrete field elements actually do exist would not be inconsistent in any way with the truth of Maxwell's equations as *macroscopic* equations of the field. A collocation of finite elements, endowed with the property of permanence, and subject to the stress and laws of motion which have been deduced for them, could by a reversal of the argument be shown to give rise exactly to Maxwell's equations for the average field over regions containing a sufficient number of elements, although inside the elements only a limited form of the general equations would be valid. It is further a point of interest to note that, since field elements are the space sections of four-dimensional elements of action, such a theory would formulate the general electromagnetic field in space-time as being constituted of finite elements of action.

---

## *Stark Patterns Observed in Helium.*

By J. STUART FOSTER, B.Sc., Ph.D., Assistant Professor of Physics, McGill University.

(Communicated by A. S. Eve, F.R.S.—Received November 1, 1926.)

[PLATES 6-8.]

This paper\* is mainly a report of further observations on the Stark-effect in helium made with a view to establishing various definite Stark patterns for the series lines. It thus appears as an extension to an earlier paper† in which it was pointed out that a plan for Stark patterns is contained implicitly in the Bohr perturbation theory of the Stark-effect as developed by Kramers‡ to predict connections between the hydrogen fine structure and the components observed in high fields. This plan, which on the perturbation theory might be expected to make its appearance in helium,§ receives somewhat detailed support from the present data, and will be outlined in later paragraphs. It should be stated now, however, that while the detailed analyses here given may be regarded as an extension to the observations by Stark|| and Nyquist,¶ they offer definite reasons for a rather extensive revision of the complex analyses reported by Takamine and Kokubu.\*\*

Soon after his discovery of this effect Stark†† suggested that it might be found to be of the same nature for the various members of a single spectral series. He noted, in particular, that on the early plates certain principal and sharp series lines of helium were merely displaced without being split by the applied electric field. In the following paper Stark and Kirschbaum‡‡ gave the results of a more complete examination of the Stark-effect for the series lines of orthohelium, parhelium, lithium, and the doublets of calcium. With the

\* A brief report of part of the present research was given in 'Nature,' vol. 116, p. 135 (1925).

† Foster, 'Phys. Rev.,' vol. 23, p. 667 (1924).

‡ 'Z. f. Physik,' vol. 3, p. 199 (1920).

§ For a general discussion of the Stark-effect in helium see N. Bohr, 'The Quantum Theory of Line Spectra,' Part III, p. 108 (1922).

|| 'Elektrische Spektralanalyse chemischer Atome,' Leipzig, 1914.

¶ 'Phys. Rev.,' vol. 10, p. 226 (1917).

\*\* 'Mem. Coll. Sci., Kyoto,' vol. 3, p. 275 (1919).

†† 'Ann. d. Physik,' vol. 43, p. 965 (1914).

‡‡ 'Ann. d. Physik,' vol. 43, p. 1017 (1914).

single exception of the parhelium line  $\lambda$  3614, which appeared to be double, they found all principal and sharp series lines simply displaced. The two components of each calcium doublet were shifted in the same direction, and by nearly the same amounts.

The above results for helium in the visible region were confirmed by Nyquist, who used very high dispersion and in some cases higher fields. As regards the analysis of the line  $\lambda$  3614, it is highly probable that the additional "component" was in reality the new combination line 2P-5G, Plate 7 (H). Evidence for such a conclusion was supplied by the writer in the above-mentioned paper. Simple displacements of principal and sharp series lines were also observed by Takamine\* during his examination of the Stark-effect in the spectra of many metals.

It is thus the observed general rule that in electric fields all single lines of the above mentioned series have but one parallel component and one perpendicular component; commonly the former has the greater displacement. So far as the writer is aware, there is no conclusive evidence of an exception to this rule.

Stark† and his pupils‡ have presented an attractive view of the effects in the diffuse and "diffuse principal" series of both parhelium and orthohelium, according to which the number of Stark components increases by unity as we pass from one member to the next in each series. This view does not agree, however, with the earlier observations by Brunetti§ and Nyquist, both of whom adopted the Lo Surdo method for the examination of Stark-effects. The former found the components in the diffuse series more numerous than those accepted by Stark; the latter first showed quite clearly, with published photographs, that new and entirely separate lines were included in the groups which previously had been regarded as components of the diffuse series alone. Moreover, as suggested by Bohr|| and the writer,¶ the "diffuse principal" series of Stark must be regarded as series of line groups of the type  $2S-mQ$  ( $2s-mq$  in orthohelium). Evidently we must abandon Stark's view, and look a little more closely into these groups to determine the nature of the splitting of the various lines which have a single frequency in very low or zero field.

By means of a suitably modified Lo Surdo source, the Stark analysis of the

\* 'Astrophys. Journ.,' vol. 50, p. 23 (1919).

† 'Ann. d. Physik,' vol. 56, p. 577 (1918).

‡ Liebert, 'Ann. d. Physik,' vol. 56, p. 589 (1918).

§ 'Accad. Lincei,' vol. 24, pp. 719-723 (1915).

|| *Loc. cit.*

¶ *Loc. cit.* The paper contains an example of a method by which a combination line may sometimes be identified even in cases where it appears only in high fields.

helium line groups has been somewhat extended in the present research. The new data are in harmony with a definite scheme for Stark patterns, which will now be described.

In the definition of the states of the hydrogen atom in low fields Kramers employs, in addition to the total and azimuthal quantum numbers,  $n$ ,  $n_1$ , a third number  $n_2$  which determines the component of angular momentum about an axis parallel to the field. The orbit rotates uniformly about this axis. With the consequent restrictions (1)  $n \geq n_1 \geq n_2 \geq 1$  and (2)  $\Delta n_2 = 0, \pm 1$  (corresponding to parallel and perpendicular components, respectively) the character of the splitting of the fine structure lines is determined. Kramers showed that with increasing field the energy remains a single-valued function of the quantum numbers, so that the components remain sharp and become identified with the Stark-Epstein\* components through the relation

$$(n_1, n_2, n_3) \text{ Epstein} \equiv [(n_1 - n_2), (n - n_1), n_3] \text{ Kramers.}$$

We note that the Stark patterns for the fine structure lines are dependent upon the azimuthal quantum in initial and final orbits, that is, are constant within a fine structure "series." Owing to the restriction  $\Delta n_2 = 0, \pm 1$ , only four patterns are expected in the Balmer groups†; viz.,

$$\begin{array}{l} \frac{\text{par. compts.}}{\text{perp. compts.}}, \frac{2}{3} \text{ in the series } 2_k - n_k, k = 3, 4, 5 \dots \\ \frac{2}{2} \text{ in the series } 2_2 - n_2 \text{ only.} \\ \frac{1}{1} \quad \text{,,} \quad \text{,,} \quad 2_2 - n_1 \text{ and } 2_1 - n_k, k = 2, 3, 4 \dots \\ \frac{1}{0} \quad \text{,,} \quad \text{,,} \quad 2_1 - n_1 \text{ only.} \end{array}$$

As examples of all four patterns have been found in the corresponding series of both orthohelium and parhelium during the present investigation, it seems probable that this plan may serve as a more general key to the Stark-effect than was at first anticipated. Fig. 1 has been prepared, therefore, to indicate more clearly the detailed connections in the first three members of the Balmer series. The upper figures represent components produced by light in which the electric vector is parallel to the applied electric field; the lower figures represent perpendicular components. The theoretical fine structure triplets are shown at zero field. Upon application of a very weak field, many additional fine structure lines are expected to appear. With a scale chosen to restrict

\* P. Epstein, 'Ann. d. Physik,' vol. 50, p. 489 (1916).

† The spin on the electron is neglected.

the diagram to a single page, not all of these can be represented as separate lines.

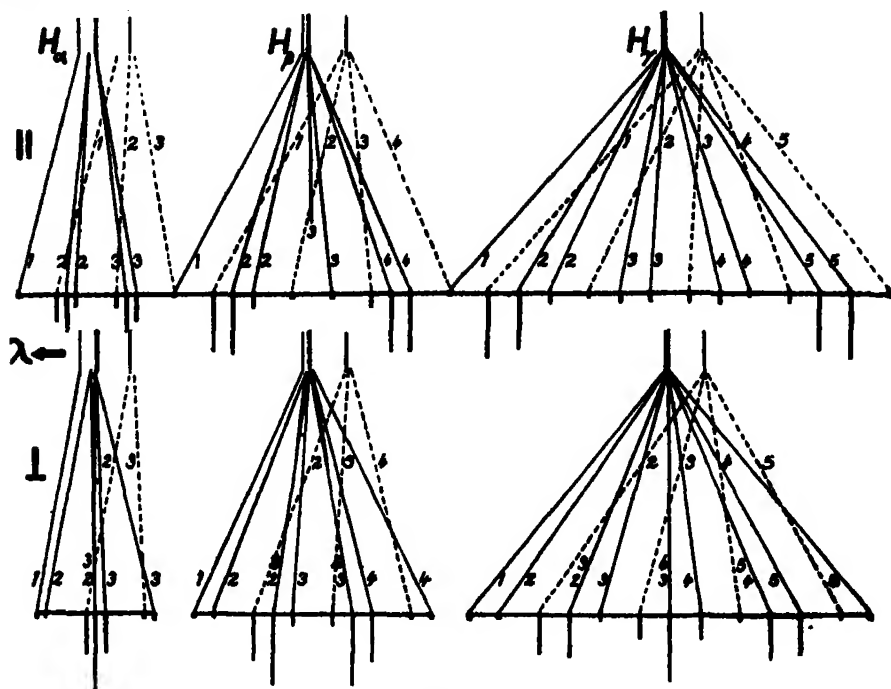


FIG. 1.

The Stark components appear in two groups corresponding to the two fine structure groups in which they originate. The dotted lines represent those contributed by fine structure lines emitted when the electrons pass to the  $2_1$  orbit. The full lines indicate the more numerous components connected with the fine structure lines produced when the electrons fall into the  $2_2$  orbit. Again to save space, the Stark components are assumed to have a perfectly symmetrical Stark-Epstein arrangement at a field of about 1400 v./cm. Straight lines are used to show the connections with the fine structure. The actual variations of the displacements with increasing fields has not been calculated for all field strengths. According to Kramers the relation is quadratic in very low fields.

The Stark components are labelled with the initial azimuthal quantum number associated with the fine structure line in which they originate. This emphasises connections not everywhere evident in the diagram, and enables one to recognise the above-mentioned patterns, which are contributed by the various series within the fine structure.

It will be noticed that in many cases two perpendicular components from different fine structure lines take nearly identical positions at moderate fields, and thus form a single component in the Stark-Epstein group pattern. To make clear the theoretical connections, these are labelled with two appropriate numbers. Such connections are, of course, essential to the theoretical recognition of the pattern  $\frac{2}{3}$ .

The intensity of each component in high fields, as calculated by Schrödinger\* on a quantum mechanics basis, is represented in the figure by the length of the vertical line immediately under it. Some of these intensities have already been checked quantitatively by Chalk and the writer.† It is to be emphasised, however, that the central  $p$ -components of  $H_\alpha$  and  $H_\beta$ , which experimentally as well as theoretically appear to vanish in high fields, are nevertheless essential to the complete picture of the Stark-effect in hydrogen.

Even in hydrogen, experimental gaps still remain in the theoretical patterns just mentioned. Several components have not been observed ( $H_\alpha$ ,  $p$ ,  $\Delta = \pm 8$ ;  $H_\beta$ ,  $p$ ,  $\Delta = \pm 14$ ) or are doubtful ( $H_\gamma$ ,  $p$ ,  $\Delta = \pm 22$ ;  $H_\delta$ ,  $p$ ,  $\Delta = \pm 32$ , and  $s$ ,  $\Delta = \pm 30$ ). We are here considering the combined researches of Stark and many others. In any single investigation the gaps are more serious. This fact is mentioned as a warning that complete analyses can scarcely be hoped for in other elements, where the displacements and separations are less.

### *Experimental Arrangements.*

The main features of the Lo Surdo source were mentioned very briefly in an earlier paper. The portion which is of most interest is that near the cathode (fig. 2). The pyrex glass tube has an internal diameter of 1.3 cm., and contains, besides the electrode E and means for adjusting the same, a block of lavite A. This material is easily worked into the desired shape and is then hardened by heat treatment before being placed in position. The seal between the glass and the lavite is made as good as possible without actually obtaining adhesion through excessive heating. B is a hole 2.5 mm. in diameter; its centre is 1.5 mm. from the axis of the main tube. As is well known, the light is rather intense within the Crookes' dark space of

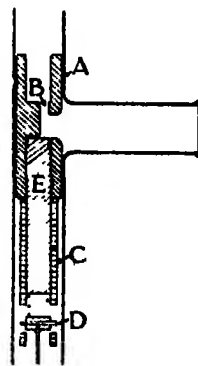


FIG. 2.

\* 'Ann. d. Physik,' vol. 80, p. 437 (1926).

† Foster and Chalk, 'Nature,' vol. 118, p. 592 (1926).

Lo Surdo tubes. A slit 0.5 mm. wide is cut through the lavite wall to allow this light to pass through the side tube and out to the spectrograph. For the study of central components it is necessary to use a still narrower slit, and thus prevent any glow in the side tube. Normally, however, the glow is very useful, as it produces an excellent comparison line at zero field. The width of the slit is never greater than 0.75 mm. It passes through 3 mm. of lavite, and has a vertical height of 5 mm. At the gas pressures employed, this includes a little more than the so-called dark space. The cathode itself is an aluminium rod 6 mm. in diameter and 4 cm. long. It is clamped in an adjustable sleeve C, which rests against the lavite. By means of this arrangement, the cathode surface is drawn back about 0.3 mm. from the lavite immediately above it. The cylindrical surface of the rod is reduced slightly in diameter at the top. An annular space about 0.3 mm. wide is thus formed between the cathode and the surrounding lavite wall. The electrode may be revolved about its vertical axis by means of a ground glass joint, to one portion of which is attached a flexible steel wire. At the other end of the wire is a brass plug, which fits loosely in the sleeve already mentioned. Between this plug and the cathode a coiled spring is compressed. The various parts are held together by a pin D, which may move in limiting slots through the sleeve. The spring holds the cathode firmly in position. The anode, placed 12 cm. from the cathode, is a heavy aluminium disc 4 cm. in diameter. The surfaces of both electrodes are initially clean and smooth.

The tube contains a mixture of pure helium and hydrogen gases. The discharge is produced by applying 5 to 10 k.v. from a source of direct current to be described in a later paragraph. Under these conditions, high fields are developed in the Crookes' dark space. When the cathode surface is placed very close to the lavite immediately above it, the field reaches a maximum at the cathode. Upon drawing the electrode back to the position indicated in the diagram, it is found that the maximum field is developed a fraction of a millimeter above the cathode. The latter distribution may also be obtained by enlarging slightly the hole in the lavite near the cathode surface with the cone-shaped end of a somewhat larger drill. In these cases, the effective removal of the surrounding lavite wall, with consequent decrease in density of charges, is probably the principal factor determining the distribution of the field. We shall not discuss this very complex phenomenon further; but simply state that the distribution can be controlled and reproduced. Best Stark analyses are obtained by arranging to have a maximum field slightly above the cathode as first observed by Nyquist.

This source gives a strong steady light, and has a relatively long life. The design is such as to effectively insulate the cathode from the sputtered metal which covers the wall of the small hole through the lavite.

The bombardment of the positive ions produces a small conical hole in the exposed cathode surface. This has a diameter of 0.75 mm., and with a normal current (8–10 mil. amp.) reaches a depth of 1 mm. in about three hours. The photographs indicate that during this time the equipotential surfaces near the cathode are slightly modified as well as shifted. The disturbance to the original potential distribution is less in the smaller tubes.

The cathode was rotated continuously in preliminary experiments; but this procedure was later abandoned. A cathode which fits well enough to prevent the discharge from flashing back of the cathode surface (with accompanying drop in applied voltage) cannot be turned with certainty by a small electromagnet. It is found more practical to turn the electrode by means of a ground glass joint when the need arises, *i.e.*, when the pitting is excessive or the discharge unstable. The position of the cathode is read on a scale attached to one member of the glass joint. In the examination of weak lines the cathode is turned to a new position after about three hours, and the exposure continued. Provided both pits are of normal character, this motion does no harm to the analysis. During the first ten hours the source improves with age.

When necessary the cathode is refinished, and the lavite surface cleaned with suitable tools. Each such treatment enlarges the diameter of the effective discharge tube, and so leads to the establishment of weaker fields.

The high potential apparatus is designed to supply 100 mil. amps. at 10,000 volts. It is a compact portable unit assembled from parts supplied by the General Electric Co. Sixty-cycle alternating current passes through a controlling rheostat and the primary of the high potential transformer. The centre of the secondary coil is used as a neutral point, and the half-waves are rectified by two kenotrons. The pulses are reduced by two 2 mf. condensers connected in series, and placed in parallel with the tube. Still further reduction is effected, and the discharge made more steady, by an inductance of 400 henrys and a water resistance in series with the tube. The applied voltage is read on an electrostatic voltmeter, and is kept constant by small adjustments of the rheostat.

The vacuum system needs no detailed description. A large capacity assists in maintaining constant gas pressure during exposures. Various mixtures of hydrogen and helium are kept sufficiently pure by constant communication with a charcoal bulb immersed in liquid air. The total pressure was 2 mm. during most of the experiments.



The light from the tube first passes through a Wollaston prism and is then focussed on the slit, with suitable magnification, by an F. 6.3 Tessar lens. While the total spreading of the components is determined by the maximum field and the dispersion, the slope of the lines on the plate depends upon the magnification, which in each case is made large enough to permit good resolution.

A Hilger E 1 quartz spectrograph has proved satisfactory for the examination of the Stark-effect in the series  $2S-mS$  and  $2s-ms$  of helium. In the case of the latter series, the Tessar lens was replaced by a quartz-fluorite achromat supplied by Hilger. This investigation has been carried out at McGill University, particular attention being paid to polarisations. The remaining photographs were taken in a glass spectrograph the dispersion of which varies from 1.5 to 8 Å/mm. They were obtained by the writer while National Research Fellow at Yale University, and have been withheld from publication until the opportunity arose for the completion of the group of Stark patterns reported below.

### *Observed Stark Patterns.*

In the following analyses of Stark effects for certain typical series lines of helium each complex pattern which is in harmony with the present scheme contains one or more components first observed by the writer.

*The Pattern  $\frac{2}{3}$ .*—This is a most interesting pattern; since its appearance in hydrogen necessitates the overlapping of certain  $s$ -components. Great difficulties must be overcome to obtain direct experimental evidence of its existence there, and this fact lends added interest to its actual appearance in helium.

Measurements in fields up to about 50 kv./cm. have been made for the parhelium diffuse series line  $2P-4D$ ,  $\lambda$  4922, Plate 7 (J); the orthohelium combination line  $2p_1-4f$ ,  $\lambda$  4470, Plate 6 (B); and the  $s$ -components of  $2p_1-5f$ ,  $\lambda$  4025, Plate 6 (C). These are given in Table I and plotted in figs. 3 and 4.

In the case of  $\lambda$  4922, field strengths are accurately known from the displacements in  $H_\beta$  appearing on the same plate. Most of the remaining new measurements are for lines unaccompanied by Balmer lines. The field strengths have been found indirectly, therefore, from simultaneous photographs of H and He lines which appear on other plates obtained with less dispersion and more intense light. As a result, the measurements of the relative displacements of components is in general more accurate than that of the field strengths.

Table I.

 (a)  $2P-4D$  and  $2P-4F$  in electric fields.

p-components.			s-components.		
Field in kv./cm.	$\Delta\nu$ in cm. <sup>-1</sup> .		Field in kv./cm.	$\Delta\nu$ in cm. <sup>-1</sup> .	
	2P-4D.	2P-4F.		2P-4D.	2-4F.
6.6	-1.0	+7.0	2.5	--	+6.0
16.8	3.5	8.5	7.6	--	7.0
22.8	7.0	10.8	16.8	-2.1 3.8	8.0
34.5	11.5	12.5	27.2	9.0, 8.2, 4.8	10.7
44.5	16.8, 15.5	14.4	35.5	12.8, 11.5, 6.6	13.0
			44.8	17.5, 15.4, 9.2	15.0

 (b)  $2p_1-4f$  and  $2p_1-4d$  in electric fields.

	$2p_1-4f$ .	$2p_1-4d$ .
Field in kv./cm.	$\Delta\nu$ in cm. <sup>-1</sup> ; $\frac{p\text{-comp.}}{s\text{-comp.}}$	$\Delta\nu$ in cm. <sup>-1</sup> ; $\frac{p\text{-comp.}}{s\text{-comp.}}$
18.5	$\frac{+11.6}{10.8, 12.4}$	$\frac{-3.6}{-3.2}$
33.5	$\frac{16.8}{14.4, 17.2, 18.0}$	$\frac{9.2, 7.8}{9.2, 7.2}$
50.0	$\frac{22.9, 24.3}{18.0, 22.8, 24.4}$	$\frac{13.3, 14.7}{11.6, 14.0}$

 (c)  $2p_1, 2-5f$ ; s-components only.

Field in kv./cm.	$\Delta\nu$ in cm. <sup>-1</sup> measured from d line. $2p_1 - 5f$ only.
34	2.28, 4.25
44	2.10, 5.38, 6.10

 Doublet separation : 1.00 cm.<sup>-1</sup>.

In order to show the necessary detail, the photographs are enlarged from the original plates. The magnification may be determined from the contact prints, which are marked with the corresponding small letter. Since it is

desired to reproduce the relative intensities of components as faithfully as possible, retouching has been avoided during the preparation of the enlargements.

(In Plate 6 the engraver has slightly enhanced 2S-4P and 2S-5F in low fields.)

The present photograph of the  $\lambda$  4471 group shows rather marked differences

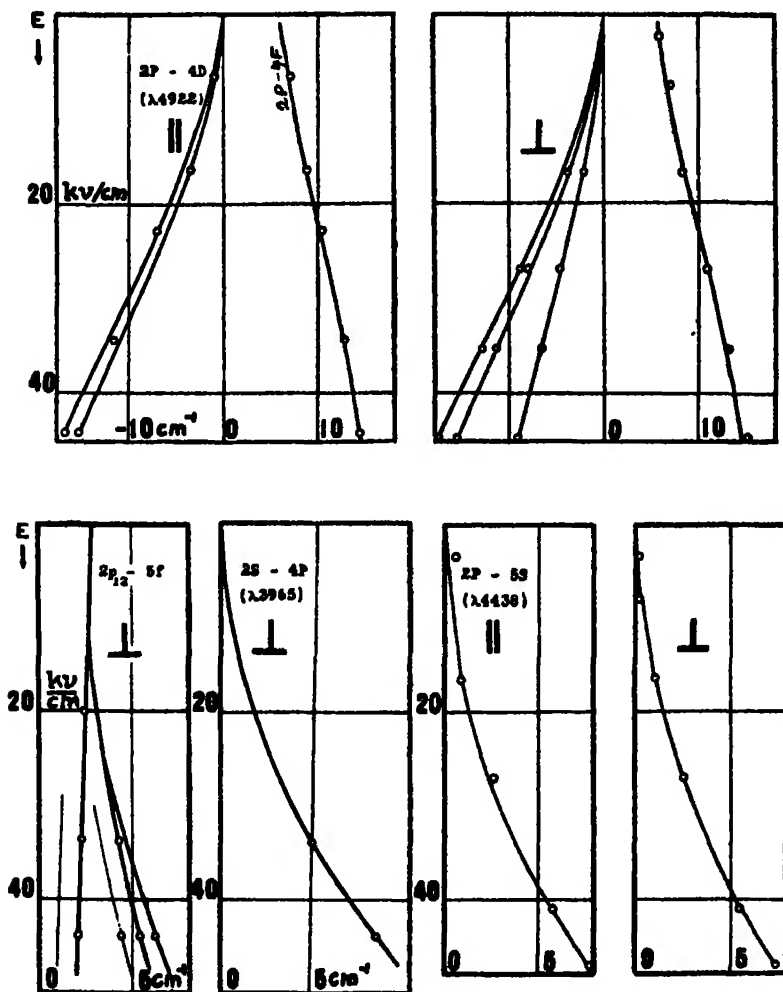


FIG. 3.

between the  $p$  and  $s$ -components as compared with the earlier analyses reported by Nyquist and by Takamine and Kokubu. The analysis is assumed to apply to the stronger component (itself a doublet on the Heisenberg\* theory); since the spectrograph could not resolve the normal components of the diffuse series

\* 'Z. f. Physik,' vol. 38, p. 411 (1926).

line at zero field. In the latter respect the analysis of the following group in the series, viz.,  $\lambda$  4026, has been more successful. Here the diffuse "doublet"

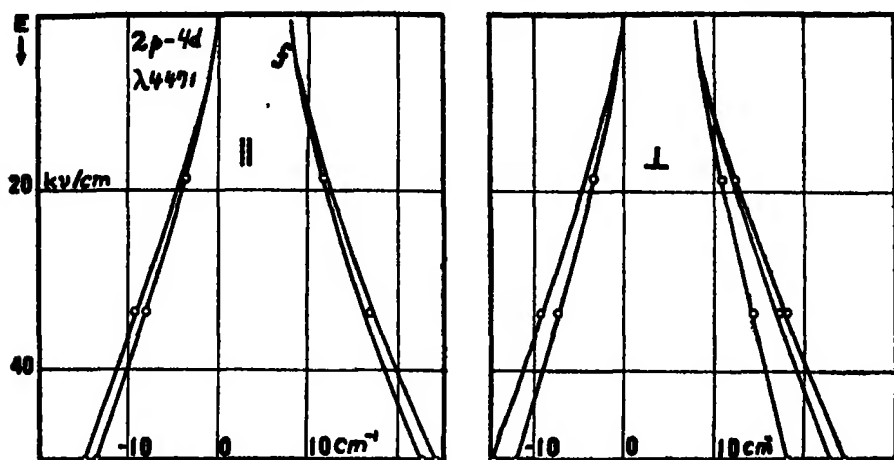


FIG. 4.

is clearly resolved; but the large magnification used at the slit allowed the examination of only the  $s$ -components. There are three such components arranged like the  $s$ -components of  $2p-4f$  as regards both relative positions and intensities. Moreover, two of the components have weak companions running parallel to them. The separations are just equal to that of the diffuse "doublet," while the relative intensity shows a noticeable variation. Apparently the two commonly observed fine structure components trace out almost identical patterns, the one being slightly displaced from the other. This constant displacement observed over a range of high fields makes it seem almost certain that the stronger component (Heisenberg doublet) remains unresolved in this analysis.

By reference to fig. 1 it is seen that the hydrogen  $p$ -components of this pattern have small separations, whereas one  $s$ -component is rather well spaced from the remaining close pair. The  $p$ -components are usually of nearly equal intensity. One  $s$ -component is strong in each pattern, and one at least is relatively weak. All these characteristics are found in the helium patterns of this type which have been photographed.

*The pattern  $\frac{2}{2}$ .*—This pattern has been found during the present series of experiments, for all members of the parhelium combination series  $2P-mP$  which appear on the plates. Some uncertainty arises in the case of  $2P-7P$  however, since the connections of the  $s$ -components are not clear. As already

noted, this is the only parhelium series which might be expected to have this pattern.

The chief experimental difficulty lies in the fact that one  $s$ -component of each line is relatively very weak. The examples, 2P-4P, Plate 6 (E), and 2P-5P, Plate 7 (K) (wide slit) are typical. The measurements made on these lines and on other members of the series 2P- $m$ P are given in Table II, and plotted in fig. 5.

Table II.—Series 2P- $m$ P.

(a)  $m = 4$ ;  $\nu_{\text{calc.}} = 20357.96$ . (In  $\lambda$  4922 group.)

$p$ -components.		$s$ -components.	
Field in kv./cm.	$\Delta\nu$ in cm. <sup>-1</sup> .	Field in kv./cm.	$\Delta\nu$ in cm. <sup>-1</sup> .
14.4	0.3	14.9	0.8
22.8	2.0, 2.6	26.9	2.5
34.4	4.0, 6.2	35.4	4.5, 6.2
44.2	6.5, 9.5	44.7	7.1, 9.8

(b)  $m = 5^*$ ;  $\nu_{\text{calc.}} = 22807.72$ . (In  $\lambda$  4388 group.)

7.9	1.2		
10.6	2.3		
14.2	3.9, 5.3		
18.4	6.4, 9.0		
23.3	9.9, 13.2		
28.9	14.4, 18.7		
34.7	19.3, 24.7		
38.0	22.5, 28.3	40	25.1, 31.3

·65.

Field in kv./cm.	$\Delta\nu$ in cm. <sup>-1</sup> ; $\frac{p\text{-comp.}}{s\text{-comp.}}$	$\Delta\nu$ in cm. <sup>-1</sup> ; $\frac{p\text{-comp.}}{s\text{-comp.}}$
3.2	$\frac{1.0}{(-)}$	$\frac{4.0}{(-)}$
7.0	$\frac{6.5}{4.0}$	$\frac{13.0}{10.0}$
15.2	$\frac{17.0}{15.0}$	$\frac{31.0}{29.0}$
26.8	$\frac{33.0, 39.0}{32.0, 36.0}$	$\frac{54.5}{55.0, 41.0}$
34.8	$\frac{44.0, 54.0}{44.0, 50.0}$	$\frac{72.5, 63.5}{67.7, 52.7}$

\* Data taken from an earlier paper, *loc. cit.*

Quite recently I have found a similar analysis for  $2p-5p$  on plates where the maximum field is 130 kv./cm. As the separations are still very small, however,

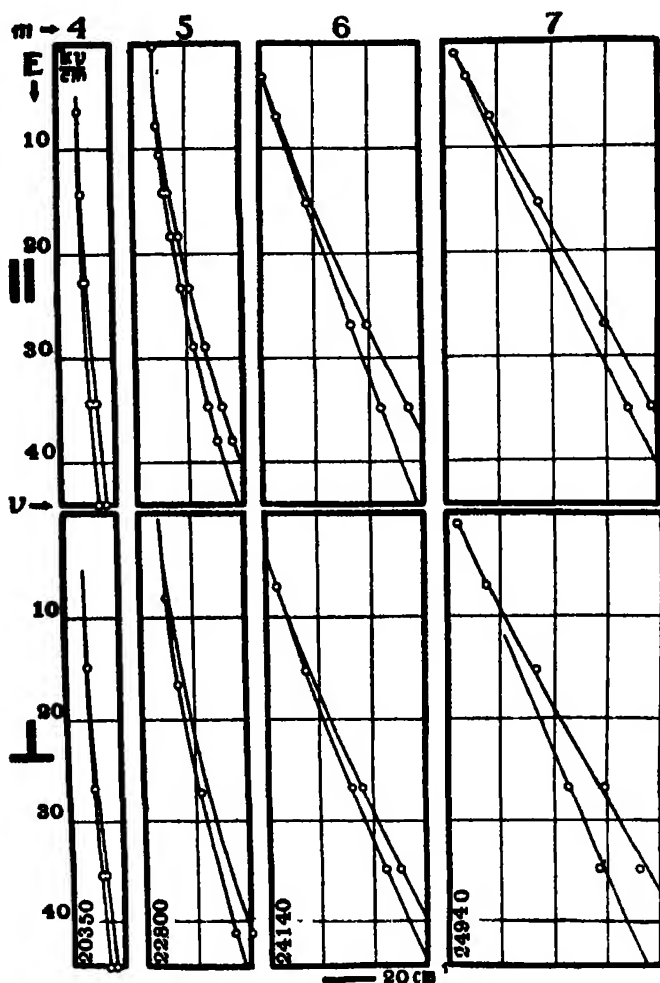


FIG. 5.

and the check from other lines not wholly satisfactory, this is not reported as a final analysis.

*The Pattern  $\frac{1}{1}$ .*—Particular interest is attached to this simple pattern, which Stark, Nyquist, Takamine, and others have observed for the members of principal and sharp series of many elements. Owing to the isolation of the lines and the simplicity of the pattern, any variations therefrom should be most easily

detected. Takamine and Kokubu\* have, in fact, reported a splitting of the helium lines  $\lambda\lambda$  4438, 4121, and 3965, in a fine analysis. This has the appearance of direct experimental proof that Stark patterns, in helium at least, do not remain constant within a single spectral series. As these few lines thus assume a prominent position in the Stark-effect, they have been re-examined by the writer.

The spectrograph† has a dispersion of 1.6 Å/mm. at  $\lambda$  3965; hence a magnification of 3 was used at the slit during the examination of this line and the  $\lambda$  4026 group. This magnification permitted the analysis of light of but one polarisation. On several plates the  $s$ -component of  $\lambda$  3965, Plate 6 (G), is unusually sharp, and simply displaced. The new components found for  $2p_{1,2}-5f$  on these plates indicate that the analysis is probably complete. A similar and equally satisfactory analysis of  $\lambda$  4438 is shown in fig. 3. The line  $\lambda$  4121 also has single components. Observations on the lines 4438 and 3965 are recorded in the following table, and plotted in fig. 3. The displacements of 4438 are negative, not positive as represented in the figure.

Table III.

(a)  $2S-4P$  in electric field;  $s$ -component only.

Field in kv./cm.	$\Delta\nu$ in cm. <sup>-1</sup> .
34	5.0
44	8.3

(b)  $2P-5S$ .

Field in kv./cm.	$\Delta\nu$ in cm. <sup>-1</sup> . $p$ -component.	$\Delta\nu$ in cm. <sup>-1</sup> . $s$ -component.
3.5	- 0.5	- 0.2
8.1	—	0.2
10.0	0.82	1.07
27.3	2.00	2.60
41.1	5.75	5.28
47.4	7.65	7.45

These results definitely disagree with those published by Takamine and Kokubu. In fact, the disagreement is not limited to the few lines just mentioned,

\* *Loc. cit.*

† Foster, 'Journ. Op. Soc. Am. and R.S.L.' vol. 8, p. 373 (1924).

but extends to include the line groups  $\lambda\lambda$  4922, 4472, 4388, 4026, i.e., the greater part of that section of the Stark-effect in helium which was examined by these authors. According to them, the patterns  $\frac{2}{3}$  and  $\frac{2}{2}$  do not exist. More complex analyses are found for many of the lines. In a comparative study of these conflicting analyses, we have to deal with the fact that within a single line group (e.g.,  $\lambda$  4026) Takamine and Kokubu find for one line ( $2p-5d$ ) more components than the writer, for another ( $2p-5f$ ) less. The explanation is very simple, and lies in the instability which may arise in Lo Surdo tubes containing high fields and high current density. Abrupt changes in the field distribution sometimes produce spurious components, as represented in Plate 7 (M). Here the analysis of the He  $\lambda$  4388 group is in good agreement with Takamine and Kokubu; yet from H, it is seen to be wrong. Evidently during part of the exposure (2 hrs.) the well-known pair of strong  $p$ -components on either side of the normal H, have remained in a certain position, and later shifted (following rather abrupt change of current from 8 ma. to 2 ma., the voltage being kept constant for an additional exposure of six hours) in such a way, let us assume, that the inside component took approximately the position formerly occupied by the outside one, while the latter moved out to form a spurious component. This explains the relative intensities in this photograph as well as in the drawings by Takamine and Kokubu. It also explains the appearance of analyses which are often too complex where strong components exist, while for the same reason weak components are lost. Finally, in accord with this interpretation of their plates, the spurious  $p$ - and  $s$ -components of the sharp and principal series lines (as represented in their drawings) have the same relative displacements and intensities.

*The Pattern  $\frac{1}{0}$ .*—This simplest of all patterns might be expected in the combination series  $2S-mS$  and  $2s-ms$  only. Stark has already reported the orthohelium lines with single displacements; the present experiments were undertaken simply to determine the polarisation, not previously mentioned, and to see if any perpendicular components could be found.

The orthohelium lines  $2s-ms$ ;  $m = 5, 6, 7$ , together with the accompanying  $2s-mq$  groups have been examined by Mr. H. B. Hachey and the writer, and will be reported in detail later. The line  $2s-6s$ ,  $\lambda$  2850, is shown in Plate 6 (D). The light was so directed through the spectrograph that the  $s$ -components of unpolarised lines were much the stronger, yet no such component of this line appeared. The other members of the series presented a similar appearance.



In these experiments a field of about 5-10 kv./cm. was needed to give the 2s-ms combination lines appreciable intensity.

Liebert has reported 2S-6S with a single displacement, polarisation not being given. 2S-5S is now found with the pattern  $\frac{1}{0}$ , Plate 6 (F). The displacement toward the red is 20.1 cm.<sup>-1</sup> in a field of 87 kv./cm. This value for the field is found by extrapolation from earlier measurements of the D line, according to which the displacement is proportional to the field except in very low fields.

As a supplement to the earlier paper, measurements of the s-components of the group 2P-5Q,  $\lambda$  4388, are given in Table IV, and plotted in fig. 6. The

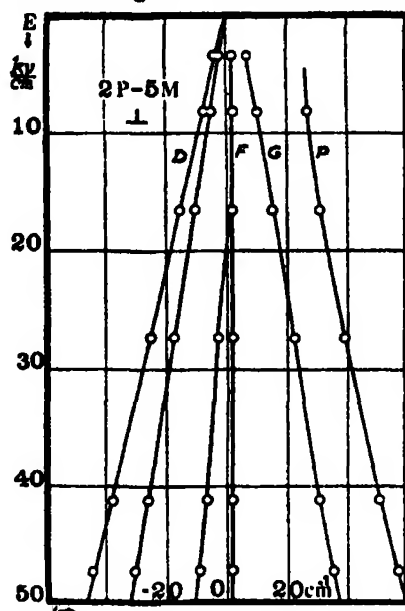


FIG. 6.

Table IV.— $\lambda$  4388 Group in Electric Field ; s-components only.

Field in kv./cm.	$\Delta\nu$ in cm. <sup>-1</sup> measured from D line in zero field.			
	2P-5P.	2P-5G.	2P-5F.	2P-5D.
3.5	—	6.75	1.0	— 2.50, — 4.00
8.1	26.6	10.0	1.95	— 5.30, — 7.85
16.6	30.6	14.8	1.8	— 10.6, — 15.6
27.3	38.8	22.0	1.8, — 3.00	— 17.6, — 25.0
41.1	50.9	30.6	1.9, — 6.55	— 26.0, — 37.6
47.4	57.6	35.6	1.8, — 8.85	— 30.5, — 44.5

displacements are conveniently measured from the normal position of the diffuse series line.

*Comparative Review of the Stark-effect in Hydrogen and Helium.*

Since the observed Stark patterns of neutral helium have been found to be of exactly the same character as those in the theoretical relativistic Stark-effect predicted for hydrogen, it is reasonable to assume that the hydrogen picture is essentially correct, and need receive only slight unobservable modifications due to the spinning electron. On this view, it is found, in accord with general theoretical expectations, that all the outstanding characteristics of the Stark-effect are the same for the two elements. First, as regards individual lines : - -

- (i) Asymmetric displacements. The only symmetric Stark-effect in hydrogen is for the first member of the Lyman series, and its symmetry is limited to the first order effect. (In hydrogen, as well as in helium, the line groups presenting a symmetrical appearance as a whole are in reality composed of highly asymmetric individual patterns.)
- (ii) Appearance of " new " combination lines in electric field.
- (iii) Change in relative intensity of components with increasing field.  
This phenomenon exists in hydrogen as well as in helium, where it is well known.
- (iv) Vanishing  $p$ -components.
- (v) Displacements showing non-linear relation with the field in low fields.
- (vi) Second order shift toward red in very high fields.\*
- (vii) Constant patterns within a single spectral series.
- (viii) Change in direction of displacements within a series. Examples of this phenomenon are found in  $2P-mF$  and  $2p_1-mf$ .

Since all these characteristics have been directly observed in helium, it is evident that, experimentally, the Stark-effect is in reality much better known in helium than in hydrogen.

*Group Similarity.*—The individual lines are grouped to form symmetric patterns, which are somewhat similar in the spectra being compared. There are, of course, no single groups in helium comparable to complete Balmer lines. The helium groups due to transitions to the  $2S$  (and  $2s$ ) orbit correspond to the dotted components in fig. 1, and are far removed toward the ultra-violet region.

\* Takamine, 'Mem. Coll. Sci., Kyoto,' vol. 3, p. 271 (1919); also Foster, 'Astrophys. Journ.,' vol. 63, p. 191 (1926).

Within each of these groups the relative intensities\* are quite similar to the asymmetric gradation in the hydrogen dotted groups, Plate 7, (H); 6, (F); fig. 7.

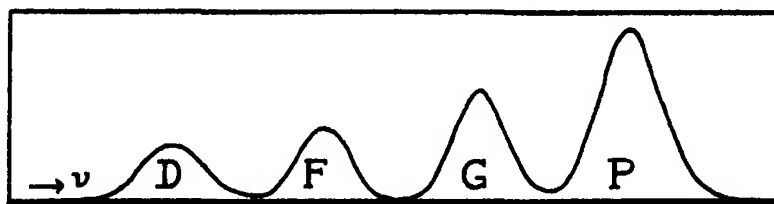


FIG. 7.—Densities of  $p$ -components of  $2S-5Q$  at 35 kv/cm.

Because of the different types of lines involved, more interesting complex group patterns are possible for the other set of helium lines ( $2P-mQ$ ) and ( $2p-mq$ ), which appear mainly in the visible region. These we may compare with the Stark-effect for hydrogen, keeping in mind that gaps must occur corresponding to the absence of the violet lines just mentioned. Moreover, the series lines are not arranged in the same order in the three systems owing to the inversion of the parhelium  $mP$  terms. This, together with the large separations, within the groups, of the sharp and orthohelium  $p-p$  combination lines, leads to certain modifications in the displacements and intensities within the individual patterns. Part of these modifications are understood on present theory.

As early as 1913 Bohr† showed that a weak external electric field can have but small influence on a series line in cases where the initial orbit is greatly perturbed by the inner electrons. The rapid rotation of the orbit then leads to a small time mean value of the perturbing potential due to the applied field. Thus terms far removed from hydrogen terms are little affected, as may be seen best in data recently collected by Stark.‡ This explains, at least in part, the fact that the magnitude of the Stark-effect for any line within a group is largely governed by its position relative to its neighbours. Especially in the groups of lines due to transitions from levels of low principal quantum number, this is rather marked.

The spacing of the helium components of a single line necessarily shows a deviation from that of the hydrogen components, owing to the relatively small effect of experimentally high fields on the  $2P$  and  $2S$  levels ( $2p$  and  $2s$

\* The writer wishes to thank Dr. Stetson of Harvard University for the use of a suitable photometer, and Drs. J. B. Green and F. Kurrelmeyer for assistance in observing photographic densities.

† 'Phil. Mag.,' vol. 27, p. 506 (1913).

‡ 'Ann. d. Physik,' vol. 78, p. 425 (1926).

also). Further, many helium components vanish when they show, in any field, a displacement noticeably less than that expected from the behaviour in lower fields. This phenomenon has been observed for  $p$ -components in the  $2P-mQ$  (and  $2p-mq$ ) groups only. It leaves permanent gaps in the group patterns of the  $p$ -components, and makes it impossible ever to observe complete individual patterns for all of these lines. Many of them are weak, and they all vanish in fields less than that needed for their resolution.

Examples of the great similarity which develops between the Stark-effects for hydrogen and helium when  $n$  becomes larger are shown in Plate 8 (A, N), where the arrow indicates a newly observed component of  $2P-6G$ . This similarity is, of course, almost entirely due to the hydrogen-like character of the initial orbits. The patterns can never become identical, even for large  $n$  and large fields, because of the relatively small effects on the final orbit. The great similarity as regards relative intensities of  $s$ -components is not surprising if one observes that Kramers' estimates of intensities of Stark components in hydrogen may be made to agree very much better with experiment by total neglect of amplitudes in the final orbits.

A detailed explanation of the principal experimental facts contained in this paper will be published shortly. It is based on quantum mechanics, and agrees satisfactorily with the observations at all field strengths.

### *Summary.*

1. A modified Lo Surdo discharge tube is described.
2. Four Stark patterns, each constant within its appropriate spectral series, and in harmony with a scheme based on the theory of the relativistic Stark-effect, have been found in parhelium and in orthohelium.
3. The general characteristics of the Stark-effect in hydrogen and in helium are reviewed, and found to vary mainly in the range of field strength at which the more interesting features appear. The experimental facts are more completely known in helium.
4. Reasons are given for an extensive revision of the Stark-effect in helium, as reported by Takamine and Kokubu.

## DESCRIPTION OF PLATES 6-8.

PLATE 6.—(B) is from the glass spectrograph; six prisms; exposure 30 minutes. The line  $\lambda$  4471 is particularly difficult to analyse. The spectrograph having slightly less resolving power than is needed to separate the components of the "doublet," each strong Stark component is for this reason diffuse on the red side. The diffuse character is possibly further enhanced by the unresolved third  $s$ -component. While two  $p$ -components are clearly seen on many plates, it has been observed that their separation increases very little in the higher fields employed in these experiments. It is nearly the same at 50 kv./cm. and 75 kv./cm., ( $b_1$ ) and ( $b_2$ ).

(C) taken with six prisms; exposure 40 min.; shows unusual detail in the central section of the  $\lambda$  4026 group.

(D) is from the El quartz spectrograph, exposure 2 hours. Two of the  $2s - mQ$  groups may be seen in ( $d$ ).

(E) The outside  $s$ -component appears to be newly observed; since its low relative intensity is quite different from any earlier reported.

(F) This photograph, from the quartz spectrograph, exposure 2 hours, shows the marked symmetry of the  $2S - mQ$  groups which develops in high fields (compare Plate 7 (H)), Here the G line is the strongest member of the group in the maximum field of 87 kv./cm. whereas the corresponding line in the  $2P - 5Q$  group (see ( $k$ )) vanishes at 28 kv./cm. ('Phys. Rev.' 23, 667, 1924). Throughout the group, the  $p$ -components are displaced more than the  $s$ -components.

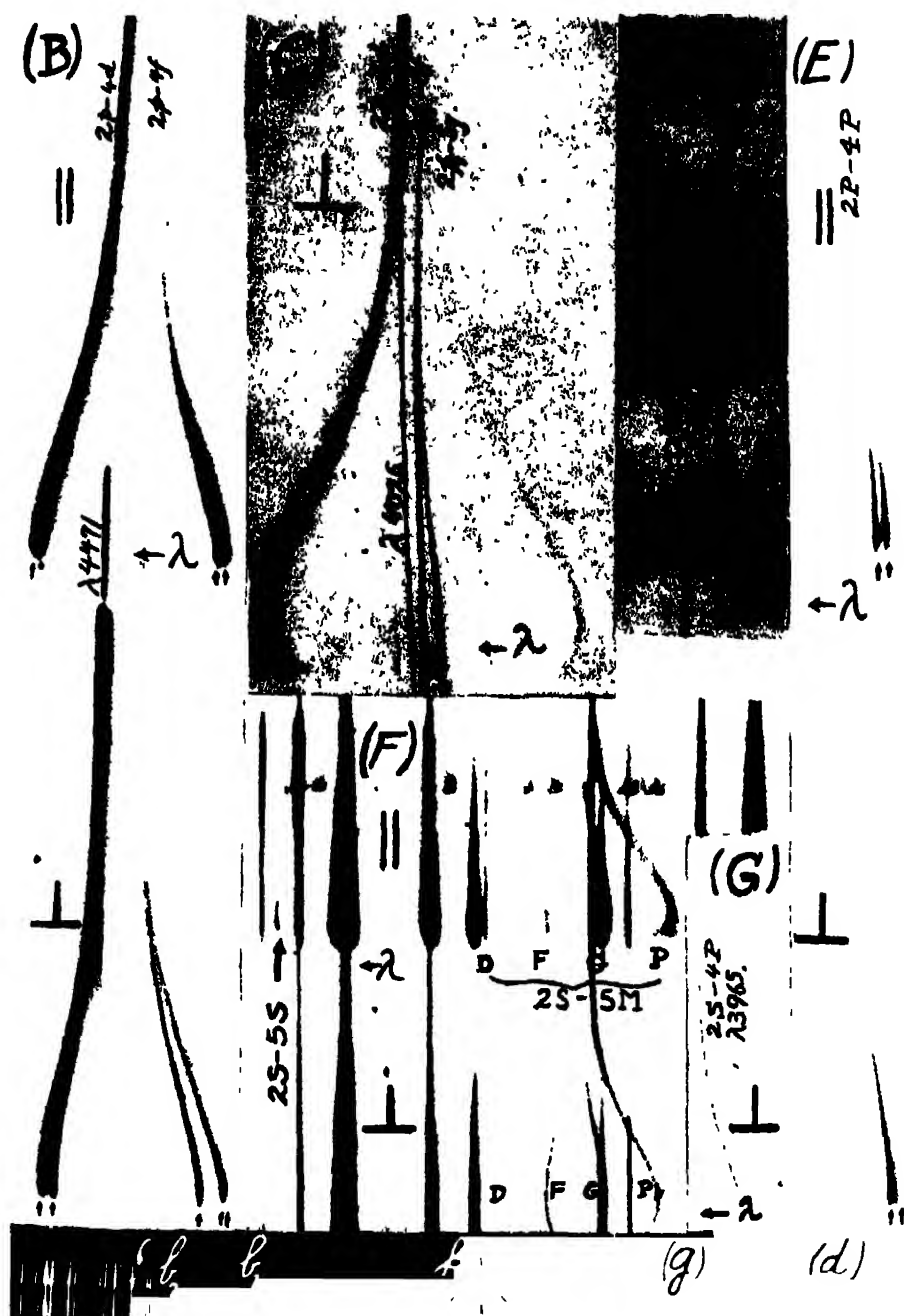
PLATE 7.—(I) is from a plate taken with six prisms, exposure 1 hour. The spur on the D line is probably due to a faint ordinary discharge in the side tube. The strong component of the D line is double. As the helium lines are much sharper than the hydrogen lines, the latter do not act as a check on the present very small separation. Since the double line is the strongest component with a large displacement, it may have become double through an unsteady discharge. Such an action could not be detected in this particular photograph. The D line is seen to be split at about 3 kv./cm., whereas the F line remains sharp up to 18 kv./cm. at which field a weak component breaks away rather abruptly.

(J) This analysis was obtained with six prisms, exposure 1 hour. The two  $p$ -components of the diffuse line are difficult to separate, as was the case with  $\lambda$  4471.

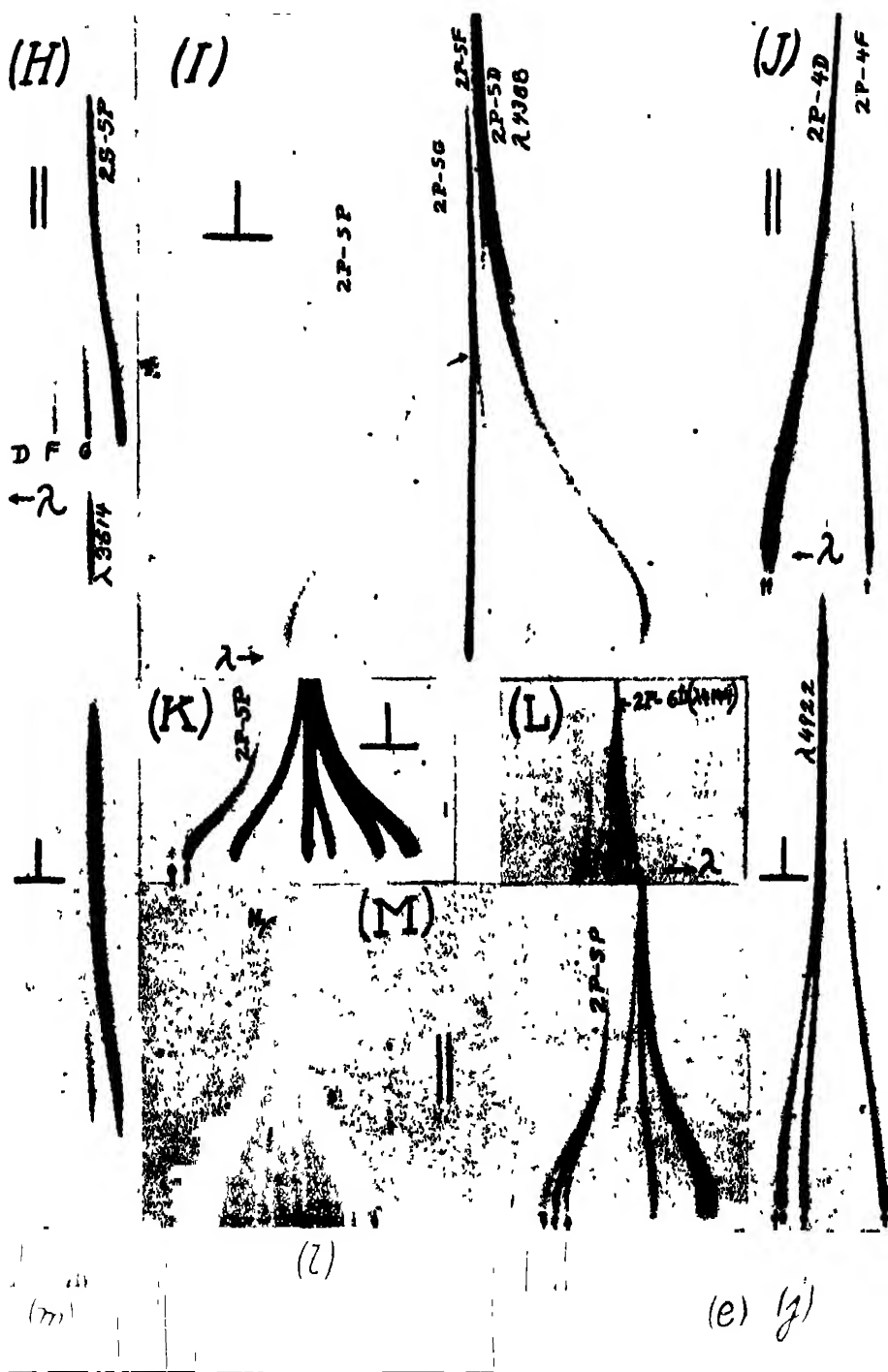
(L) Exposure 8 hours. This photograph shows a new combination line,  $2P - 6F$ , reported in the earlier paper.

PLATE 8.—The photograph (A) of  $H_2$  and the parhelium group  $\lambda$  4144, was taken in the glass spectrograph with three prisms, exposure 50 minutes. The maximum field is 38 kv./cm. The corresponding orthohelium group  $\lambda$  3820 is seen in much higher fields at (N). The latter print is from a plate exposed for one hour in the quartz spectrograph.

---



Examples of Four Stark Patterns.









# *On the Mutual Potential Energy of a Plane Network of Doublets.*

By J. TOPPING, M.Sc., Ph.D., Beit Scientific Research Fellow.

(Communicated by Prof. S. Chapman, F.R.S.—Received November 25, 1926.)

## *Introduction.*

§ 1. The object of this note is the determination of the mutual potential energy of a distribution of small electric or magnetic doublets lying in a plane with their axes perpendicular to the plane; reckoning the potential energy from a state of infinite dispersion of the doublets. The doublets are supposed to have a definite electric or magnetic moment, the same for all, whose value is determined by their constitution and does not depend on their mutual action. The problem bears on the energy of a layer of polarised molecules on the surface of a fluid, and the question as to the value of the energy, for a given number of molecules of given moment per unit area, was put by Dr. E. K. Rideal to Prof. S. Chapman, at whose suggestion the writer undertook this investigation.

In actual surface layers the mode of packing of the molecules is not always known, and therefore two special cases are considered, in order to determine how the mode of packing influences the energy, the number of doublets per unit area being given. It is supposed that the doublets form either a simple square network, or an equi-triangular network; and it appears that the mutual potential energy differs only by about 2 per cent. in the two cases. It is therefore possible to give (§ 4) a fairly definite estimate of the energy, which is likely to be approximately true for any probable mode of packing of the molecules.

§ 2. The mutual potential energy of two doublets of moments  $\mu$  and  $\mu'$  respectively is given by :

$$W = \frac{\mu\mu'}{r^3}(\cos \epsilon - 3 \cos \theta \cos \theta'), \quad (1)$$

where  $\epsilon$  is the angle between the axes of the doublets and  $\theta, \theta'$  the angles between the line joining the doublets and the axes of the doublets respectively.

If the two doublets are parallel, and perpendicular to the line joining them.  $\epsilon = 0$  and  $\theta = \theta' = 90^\circ$ , so that

$$W = \frac{\mu\mu'}{r^3}. \quad (2)$$

Hence the mutual potential energy per doublet of a series of co-planar doublets of equal moments  $\mu$ , with their axes all perpendicular to the plane, is given by :

$$W = \frac{1}{2} \sum \mu^2/r^3 \quad (3)$$

where  $r$  is the distance of any doublet from the particular one considered, and the summation extends over all the doublets of the plane.

We shall consider two special cases: viz., when the doublets are situated at the net-points of (1) a square network, and (2) an equi-triangular network.

*Case I.*—Taking the side of the elementary squares of the lattice to be  $a$ , we can express the distance  $r$  of any doublet from the given doublet (taken as the origin) in the form:—

$$r^2 = (l^2 + m^2) a^2 \quad (4)$$

where  $l$  and  $m$  are two integral parameters, measured in perpendicular directions along adjacent sides of the squares. All the net-points of an infinite network will be included by both  $l$  and  $m$  assuming integral values from  $-\infty$  to  $+\infty$ .

Thus, the mutual potential energy per doublet of an infinite series of doublets, each of moment  $\mu$  arranged at the net-points of a square network of side  $a$ , with their axes all perpendicular to the plane, is given by:

$$W = \frac{1}{2} \cdot \frac{\mu^2}{a^3} \sum' \sum \frac{1}{(l^2 + m^2)^{3/2}}, \quad (5)$$

the dash in the summation sign indicating that  $l$  and  $m$  do not assume simultaneous zero values.

*Case II.*—If  $a$  be the length of side of the elementary triangles of the network, the distance  $r$  of any doublet from any given doublet (taken as origin), can be written:

$$r^2 = a^2 (l^2 - lm + m^2) \quad (6)$$

where  $l$  and  $m$  are integral parameters, measured in directions along two sides of the triangles inclined at  $120^\circ$  to each other.

Thus the mutual potential energy per doublet of such an infinite equi-triangular network of doublets, each of moment  $\mu$  and with their axes perpendicular to the plane, is given by:

$$W = \frac{1}{2} \cdot \frac{\mu^2}{a^3} \sum' \sum \frac{1}{(l^2 - lm + m^2)^{3/2}}, \quad (7)$$

where  $l$  and  $m$  take all negative, zero, and positive integral values excepting simultaneous zero values.

§ 3. The double summations on the right-hand sides of equations (5) and (7) are Zeta-functions of the second order, and they can be evaluated by means of some formulæ which have been recently given by Lennard-Jones and Ingham.\*

\* 'Roy. Soc. Proc.,' A, vol. 107, p. 636 (1925).

In the notation of their paper the generalised Zeta-functions of Epstein are defined as follows. Let

$$q(u) = q(u_1, \dots, u_k) = \sum_{\lambda, \mu=1}^k d_{\lambda\mu} u_\lambda u_\mu \quad (d_{\lambda\mu} = d_{\mu\lambda}),$$

be a positive definite quadratic form in the  $k$  variables  $u_1, \dots, u_k$ , with the determinant

$$\begin{vmatrix} d_{11} & \dots & d_{1k} \\ \dots & \dots & \dots \\ d_{k1} & \dots & d_{kk} \end{vmatrix} = D \quad (>0),$$

and let  $g_1, \dots, g_k$  and  $h_1, \dots, h_k$  be two series each of  $k$  real numbers. Then the generalised Zeta-functions associated with the form  $q$  and with the "characteristics"  $(g)$  and  $(h)$  is defined by:

$$Z \begin{vmatrix} g_1 & \dots & g_k \\ h_1 & \dots & h_k \end{vmatrix} (s)_q = \sum_{q>0} e^{2\pi i(h_1 l_1 + \dots + h_k l_k)} \{q(l_1 + g_1, \dots, l_k + g_k)\}^{-s}, \quad (8)$$

the summation extending to all integral values of  $l_1, \dots, l_k$ , for which  $q(l_1 + g_1, \dots, l_k + g_k) > 0$ , and so to all integer values except, in case  $g_1, \dots, g_k$  are integral, the combination  $-g_1, \dots, -g_k$  which makes,  $q = 0$ .

Equation (8) may be written in the more compact form:

$$Z \begin{vmatrix} g \\ h \end{vmatrix} (s)_q = \sum_{q>0} e^{2\pi i(hl)} [q(l + g)]^{-s}. \quad (8')$$

From this definition it follows that:

$$\sum_{-\infty}^{\infty} \sum_{-\infty}^{\infty} \frac{1}{(l^2 + m^2)^{3/2}} = {}^2Z \begin{vmatrix} 0 \\ 0 \end{vmatrix} (3)_{q_1} \equiv \sum_{n=1}^{\infty} \frac{a_n}{n^{3/2}}, \quad (9)$$

where  $q_1 = u_1^2 + u_2^2$  and  $a_n$  is the number of representations of  $n$  as the sum of two squares.

From lemma 1 of Lennard-Jones and Ingham's paper, taking  $x = 25 (>0)$  and  $\kappa = 5$  (an integer  $\geq 0$ ), we have on effecting some simple reductions:

$$\begin{aligned} {}^2Z \begin{vmatrix} 0 \\ 0 \end{vmatrix} (3)_{q_1} &= \sum_{n=1}^{20} \frac{a_n}{n^{3/2}} + \frac{\pi}{6!} \cdot \frac{3 \cdot 5 \cdot 7 \cdot 9 \cdot 11 \cdot 13}{2^5 \cdot 5} - \frac{1}{5!} \cdot \frac{5 \cdot 7 \cdot 9 \cdot 11 \cdot 13}{2^5 \cdot 125} \\ &\quad - \sum_{v=0}^5 \frac{3 \cdot 5 \dots (2v+1)}{2^v \cdot v!} \cdot \frac{Q_v(25)}{25^{v+5/2}} + R_1 \end{aligned} \quad (10)$$

where

$$Q_v(25) = \sum_{n=1}^{20} (25 - n)^v \cdot a_n,$$

and

$$|R_1| < \frac{3 \cdot 5 \dots 13}{2^6 \cdot \pi^7} \cdot \frac{G_{51}(25\pi^2)}{5^{51}} \cdot {}^2Z \begin{vmatrix} 0 \\ 0 \end{vmatrix} (15/2)_{q_1}$$

by lemma 4, in which the function  $G$  is such that

$$G_{\mu}(X) < 1 + \frac{3(\mu+1)(\mu+6)}{16X} \left(1 + \frac{11}{X} + \frac{54}{X^2}\right), \quad (11)$$

if  $0 \leq \mu \leq 6$ ,  $X > 0$  by lemma 5.

It is therefore necessary to evaluate  $Q_{\nu}$  (25), and this can be done without much difficulty, the values being as follows :

$\nu$	0	1	2	3	4	5
$Q_{\nu}$ (25)	68	948	15 748	291 252	5 745 124	118 062 228

which are useful in the evaluation of the summation given by equation (9) for other values of  $s$  ( $s = 3$  in this case).

Also from equation (11) it can be shown that  $G_{5\frac{1}{2}}(25\pi^2) < 1.07$  and since

${}^2Z \begin{vmatrix} 0 \\ 0 \end{vmatrix} (15/2)_n < 6$  certainly, it follows that

$$|R_1| < 0.000\ 006.$$

Thus evaluating the expression on the right-hand side of equation (10) it is found that :

$${}^2Z \begin{vmatrix} 0 \\ 0 \end{vmatrix} (3)_n = 9.033\ 623 + R_1 \quad \text{where} \quad |R_1| < 0.000\ 006 \\ = 9.033\ 6_{17}^{29}, \quad (12)$$

where the double set of figures indicates the limits of error.

Again from the definitions of the generalised Zeta-function it follows that :

$$\sum_{-\infty}^{\infty} \sum \frac{1}{(l^2 - lm + m^2)^{3/2}} \equiv \sum_{n=1}^{\infty} \frac{b_n}{n^{3/2}} = {}^2Z \begin{vmatrix} 0 \\ 0 \end{vmatrix} (3)_n, \quad (13)$$

where  $q_2 = u_1^2 - u_1u_2 + u_2^2$ , and  $b_n$  is the number of representations of  $n$  in the form  $(l^2 - lm + m^2)$  with  $l$  and  $m$  integral.

In this case  $D = \frac{2}{3}$  ( $> 0$ ) and we have :

$${}^2Z \begin{vmatrix} 0 \\ 0 \end{vmatrix} (3)_n = \sum_{n=1}^{21} \frac{b_n}{n^{3/2}} + \frac{\pi}{6! \left(\frac{2}{3}\right)^{\frac{1}{2}}} \cdot \frac{3.5.7.9.11.13}{2^5.5} - \frac{1}{5!} \cdot \frac{5.7.9.11.13}{2^5.125} \\ - \sum_{\nu=0}^5 \frac{3.5 \dots (2\nu+1)}{2^{\nu} \cdot \nu!} \cdot \frac{Q'_{\nu}(25)}{25^{\nu+3/2}} + R_2, \quad (14)$$

where  $Q'_{\nu}(25) = \sum_{n=1}^{21} (25-n) b_n$ ,

and

$$|R_2| < \frac{3.5.7 \dots 13}{2^5 \cdot \pi^7 \left(\frac{2}{3}\right)^{\frac{1}{2}}} \cdot \frac{G_{5\frac{1}{2}}(25\pi^2)}{5^{2\frac{1}{2}}} \cdot {}^2Z \begin{vmatrix} 0 \\ 0 \end{vmatrix} (15/2)_{\frac{1}{2}},$$

$\bar{q}_2$  being the form reciprocal to  $q_2$  so that

$$\bar{q}_2 = 4/3 (u_1^2 - u_1u_2 + u_2^2).$$

The values of  $Q'_v$  (25) have to be found and they are as follows :—

$v$	0	1	2	3	4	5
$Q'_v$ (25)	84	1 110	18 282	338 610	6 694 194	137 842 050

In fixing an upper limit to  $|R_2|$  we need some estimate of  ${}^2Z \begin{vmatrix} 0 \\ 0 \end{vmatrix} (15/2)_{q_1}$ , which equals  $(3/4)^{3/2} \cdot {}^2Z \begin{vmatrix} 0 \\ 0 \end{vmatrix} (15/2)_{q_1}$ . By comparison with the value of  ${}^2Z \begin{vmatrix} 0 \\ 0 \end{vmatrix} (3)_{q_1}$  we can safely say that  ${}^2Z \begin{vmatrix} 0 \\ 0 \end{vmatrix} (15/2)_{q_1} < 9$ , whence it follows that :

$$|R_2| > 0.000\ 007.$$

Hence by equation (14) we have :

$$\begin{aligned} {}^2Z \begin{vmatrix} 0 \\ 0 \end{vmatrix} (3)_{q_1} &= 11.034\ 177 + R_2 \\ &= 11.034\ 1\frac{84}{70}, \end{aligned} \quad (15)$$

the double set of figures indicating the limits of error.

It might be noted that the double summation represented in equation (13), may also be evaluated as follows :

The equi-triangular network can be divided into six exactly similar networks. The net-points of one such sector are represented by  $l$  varying from 1 to  $\infty$ , and  $m$  from 0 to  $(l-1)$ , (the origin (0, 0) excluded). It follows therefore that :

$$\begin{aligned} \sum_{-\infty}^{\infty} \sum_{-\infty}^{\infty} \frac{1}{(l^2 - lm + m^2)^{3/2}} &= 6 \sum_{l=1}^{\infty} \sum_{m=0}^{l-1} \frac{1}{(l^2 - lm + m^2)^{3/2}} \\ &= 6 \left[ \frac{1}{1^{3/2}} + \frac{1}{4^{3/2}} + \frac{1}{3^{3/2}} + \sum_{l=3}^{\infty} \sum_{m=0}^{l-1} \frac{1}{(l^2 - lm + m^2)^{3/2}} \right]. \end{aligned} \quad (16)$$

The summation included in the right-hand side expression can be evaluated by an algebraic method, and its value has recently been given,\* viz. :

$$\sum_{l=3}^{\infty} \sum_{m=0}^{l-1} \frac{1}{(l^2 - lm + m^2)^{3/2}} = 0.5215\ 793. \quad (17)$$

Hence we have :

$$\sum_{-\infty}^{\infty} \sum_{-\infty}^{\infty} \frac{1}{(l^2 - lm + m^2)^{3/2}} = 6 [1.839\ 0294] = 11.034\ 1764. \quad (18)$$

This result is in excellent agreement with that found from the Zeta-function formulæ given in equation (15).

\* Chapman, Topping and Morrall, 'Roy. Soc. Proc.,' A, vol. 111, p. 41 (1926).

## 72 *Mutual Potential Energy of Plane Network of Doublets.*

§ 4. Returning to equation (5), the mutual potential energy per doublet of the infinite square network of doublets is therefore given by :

$$W = \frac{1}{2} \cdot \frac{\mu^2}{a^3} \cdot 9.033 \ 6.$$

The number  $n$  of doublets per unit area is  $1/a^2$ , so that the mutual potential energy per unit area in the presence of an infinite square network of doublets is

$$W = \frac{1}{2} \cdot \frac{\mu^2}{a^3} \cdot 9.033 \ 6 = \frac{1}{2} n^{5/2} \mu^2 \cdot 9.033 \ 6. \quad (19)$$

This is given in ergs per square cm. if  $n$  be the number of doublets per square cm. and  $\mu$  be expressed in C.G.S. units. It can easily be transferred into heat units (calories) on dividing by the mechanical equivalents of heat  $J$ .

Similarly from equation (7), the mutual potential energy per doublet of an infinite equi-triangular network of doublets is :

$$W = \frac{1}{2} \cdot \frac{\mu^2}{a^3} \cdot 11.0342,$$

and since there is one doublet to each rhombus of area  $\frac{1}{2}a^2\sqrt{3}$ , so that  $n = 2\sqrt{3}/3a^2$ , the mutual potential energy per unit area of an infinite equi-triangular network of doublets is :

$$W = \frac{1}{2} \cdot \frac{2\sqrt{3}}{3} \cdot \frac{\mu^2}{a^3} \cdot 11.0342 = \frac{1}{2} n^{5/2} \mu^2 \cdot 8.892 \ 7 \quad (20)$$

the units being as given above.

It appears therefore from equations (19) and (20) that the mutual potential energy per unit area is practically the same for a square network of doublets as for an equi-triangular network, provided there be the same number of doublets per unit area in each case.

Thus for chemical purposes, as in the case of surface films, owing to the limits of accuracy of the experimental results, it will be immaterial whether the network be considered square or equi-triangular. The mutual potential energy per unit area of the surface may therefore be written in the form :—

$$W = \frac{1}{2} n^{5/2} \mu^2 \cdot \kappa, \quad (21)$$

where  $\kappa$  is approximately equal to 9, and  $n$  is the number of doublets per unit area.

---

*On the Sparking Potentials of Discharge Tubes containing carefully Purified Electrodes.*

By JAMES TAYLOR, M.Sc., Ph.D., A.Inst.P., Fellow of the International Education Board, Physics Laboratory of the University of Utrecht.

(Communicated by O. W. Richardson, F.R.S.—Received December 2, 1926.)

*Introduction.*

The present paper describes the results obtained in a continuation of some earlier work carried out on the electrode surface phenomena of discharge tubes in their relation to the sparking potential function.\*

The discharge tubes used previously contained a filling-gas of neon-helium mixture, and the electrodes were of nickel or iron. It was found that there was an increase of the sparking potential with "flashing" or discharge. This increase was termed "polarisation." In certain cases relatively large polarisations were observed. Polarisation could be reduced or eliminated in many cases by passing a discharge in the reverse direction through a polarised tube, or by resting it for a few hours.

Experiments showed that the polarisations were reduced to small values by the introduction of sodium on to the electrodes, and that the actual values of the sparking potentials were concurrently considerably lowered.

A theory of the sparking potential was given. It was assumed that electrons were given off from the kathode by the photo-electric effect of the radiation accompanying the neutralisation of the positive ions at the kathode surface. According to this hypothesis, the sparking potential should be a function of the photo-electric emissivity of the kathode surface.

Assuming the above hypothesis a theory of the electrode surface phenomena was given in which it was assumed that the passage of a discharge modified layers of gas occluded or absorbed on the electrode surfaces. Results indicated that the modifications were of two kinds—one of a permanent nature which changed the photo-electric emissive power of the kathode, and was consequently accompanied by a change in the sparking potentials, the other of a temporary nature due to the charging up of the surface layers and the consequent formation of electrical double layers. The layers were supposed to inhibit electronic emission from the kathode and bring about the polarisation effects.

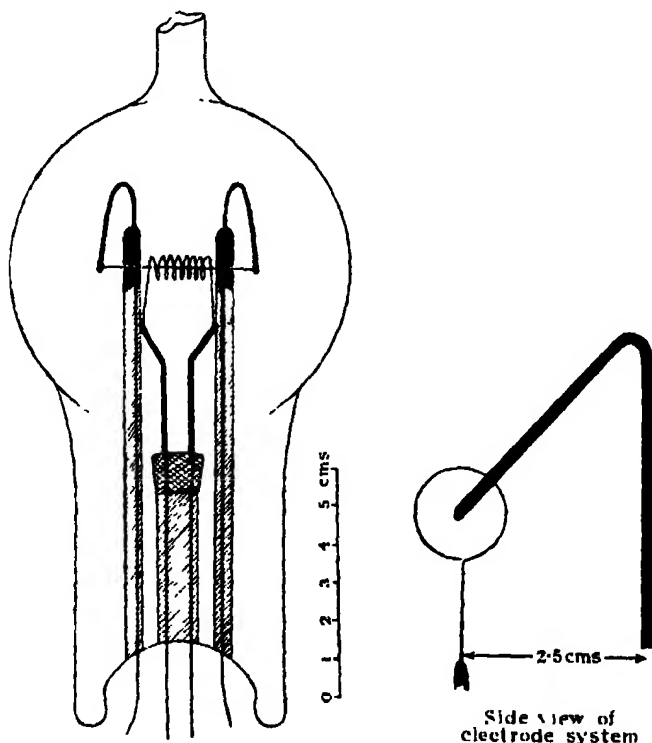
\* J. Taylor, "On the Sparking Potentials of Glow Discharge Tubes," 'Phil. Mag.', vol. 3 (1927).



The work to be described in the present paper deals with the first type of electrode surface phenomena in which the changes of the sparking potential function are due, not to a transient charging up of the surface layer, but to permanent surface modifications.

*Description of Apparatus.*

For the purpose of investigating the sparking potential function for pure metal electrodes—or rather for electrodes of which the surfaces were as pure as possible—a discharge tube of special form was constructed. It comprised an electrode in the form of a tungsten wire, surrounded by a coaxial tungsten wire spiral, the whole system being therefore of the same form as the filament-grid system of a thermionic valve. The geometrical disposition of the supports, etc., was such that discharge always took place between the inner wire and the surrounding spiral. A diagram of the tube is given in the figure. It was “baked



out” for many hours at high vacuum at a temperature of over  $300^{\circ}\text{C}$ . The tungsten wire electrodes were thoroughly cleaned and “degassed” by heating them strongly electrically for six hours in high vacuum. When the electrodes

had been brought to this condition which at least approximated to a clean, "gas free" state, carefully purified dried argon gas was introduced into the tube to the required pressure.

The filling-gas was continuously purified by utilisation of a quartz furnace containing heated calcium. In order to test the quality of the gas, a discharge tube with plane-parallel electrodes was included in the apparatus. Any change in gas quality was denoted by a change in the sparking potential of this test-tube. Tests were made from time to time during the work, but the sparking potential was found to be constant, consequently in the later experiments this test was dispensed with, because of the excessive gas-capacity of the test-tube.

The experimental arrangements for the determination of the sparking potentials were similar to those used in previous work.\* A source of constant and adjustable potential was connected in series with a resistance of 450,000 ohms to the discharge tube which was shunted by an electrostatic voltmeter. The potential was gradually raised until discharge occurred. The discharge was of a feeble nature (usually of the "corona" type,\* and of a few microamps. in magnitude), and was confined to the space between the wire and the coaxial spiral.

#### *Experimental Results for Tungsten Electrodes formed in High Vacuum.*

Experiments were carried out on two tubes of similar form and similar results were obtained in the two cases. Using S as kathode, it was found that the first discharge took place at a definite potential and the succeeding ones at progressively decreasing potentials. The value of the sparking potential decreased gradually under the action of the discharge to a minimum value after which it increased again. Table I is illustrative of the results obtained with one tube. In the results given the first discharge took place with S as kathode, so that the value (2) given for W as kathode does not represent the actual value for a vacuum-formed surface on W. In the example given the values for the sparking potentials with both S and W as kathodes finally attained values approximating to the initial ones. This, however, was by no means always the case. There appeared to be great differences in behaviour according to conditions, and the previous treatment of the wires.† In all cases, however, it was found that the sparking potentials for both S and W as kathode

\* Taylor, *loc. cit.*

† Compare with experiments on the photoelectric emission of metals as influenced by temperature, e.g., Welo, 'Phil. Mag.' vol. 2, p. 463 (1926).

were higher initially with the "clean tungsten" electrodes (the initial sparking potential was constant and definite) and decreased with discharge to a minimum value which varied according to conditions.

Table I.

S denotes tungsten spiral, W coaxial wire. The numbers at the side of the sparking potential values give the number of the discharge in the time order in which they occurred. Tungsten electrodes "formed" in *vacuum*. Pressure of argon 3.94 mm. Diameter of tungsten wire 0.3 mm.; diameter of spiral, 6 mm.; length, 16 mm.; number of turns, 10.

Sparking potentials	S kathode.	(1) 273	(3) 249	(5) 249	(7) 250	(9) 251	
	W kathode.	(2) 245	(4) 235	(6) 237			(10) 237
	W kathode.	(11) 239	(12) 239	(13) 241	(14) 242	(15) 244	
	W kathode.	(16) 245	(17) 246	(18) 247	(19) 247.5		
		Remained fairly steady at this value.					
	S kathode.	(20) 251	(21) 254	(22) 257	(23) 261	(24) 262.5	
	S kathode.	(25) 263	remained fairly steady at this value.				

After this point, in almost all, though not quite all, cases, a considerable but slow increase in the sparking potential values occurred. In some few cases the final values were even higher than those characteristic of the "clean tungsten."

The changes were definitely due to the passage of the discharge and were not in any way attributable to the change in the gas condition.\* This was proved by experiments which showed that the gas quality remained constant, and further from the fact that the sparking potential values did not change when the discharge tube was rested for time periods long in comparison with the duration of the experiments determining the sparking potentials. The lack of change of the values with time and the fact that they were not altered appreciably by passing discharges in the reverse direction through the tube, showed that the changes were not due to temporary electrical double layers, but to permanent alterations in the nature of the electrode surface.

#### *Experimental Results for Tungsten Electrodes formed in Pure Argon.*

A series of experiments were undertaken in which the tungsten electrodes previously "formed" in high vacuum were reheated for various periods of time in argon gas which was continuously purified.

\* It was also definitely proved that the changes were in no way connected with lack of initial ionisation to produce the discharge.

The proceeding was as follows :—S or W was heated electrically to the desired temperature for the required time and the tube was then rested for about 10 minutes before taking readings. Any impurities given off by the heating were absorbed by the calcium and by a liquid air trap which was continuously used throughout all the experiments. Actually, the quantity of impurity given off was exceedingly small for the tube had been “baked out” previously, and S and W heated for many hours at the highest temperature consistent with safety. In any case, no time changes apart from the actual change due to the discharge were observed.

The results obtained were almost the same as those for the vacuum-formed electrodes, except that the initial sparking potentials were usually lower than for those. Nevertheless, in many instances, the values approached those for the vacuum-formed surfaces. Tables II and III give some of the results obtained.

Table II.—Pressure of Argon, 3·94 mm.

Sparking Potential of first discharge. S Kathode.	Treatment of Tube.
Volts.	
273	S and W heated strongly <i>in vacuum</i> .
268	S heated strongly for 10 minutes in the gas.
263	Ditto. Ditto.
264	S heated dull red for 0·5 minutes in the gas.
261	S heated strongly for a few minutes in the gas.
264	S and W heated strongly a few minutes in the gas.
267	S heated very strongly a few minutes in the gas.

Table III.—Pressure of argon, 3·94 mm.

Sparking potential of first discharge. W Kathode.	Treatment of tube. (All heatings took place in the gas.)
Volts.	
249	W heated strongly for 10 minutes.
241	Do.
239	Do.
251	W heated strongly a few minutes.
245	S and W heated a few minutes together.
255	W heated very strongly for a few minutes.
251	W heated a few minutes.

The result of heating appears to be as follows:—If S was heated, then its final condition was very similar to that which it would have attained in vacuum, but the condition of W was unaffected except for an indirect effect due to the heating it underwent by conduction and radiation. If, however, S was heated very strongly, tungsten from its surface evaporated on to W and formed a new surface there. Whatever the nature of the surface layers that were formed under the action of the discharge they were modified or done away with when the wires were heated in the pure argon gas. The sparking potentials were not quite the same as those attained by heating in vacuum, so that it must be assumed that the heating did not drive off so much of the surface layers in the gas as in vacuum, or alternatively, that the change in the surface structure was not so great as that obtained by heating in vacuum.

Another important point which will be considered later, is that the actual relative values of the sparking potential for S and W as cathodes depended largely upon the condition of the electrodes and not merely upon the geometrical distribution of the electric field between the wire and the coaxial spiral, a result which follows the assumption, until recently held, that the sparking potential was independent of the nature of the cathode surface.\* By comparing the results in Table III for W as cathode, with those in Table II for S as cathode, it is seen that normally, when the electrodes were most probably in the same condition, the sparking potential was lower for W as cathode than for S as cathode. This is in accordance with the usually accepted results.\* In cases where S and W had undergone different treatment, and were, therefore, presumably of different surface conditions, the sparking potential for W as cathode could be less than, equal to, or greater than, that for S as cathode, according to circumstances. Table IV gives some illustrative results.

Table IV.—Pressure of Argon, 3·9 mm.

Sparking Potentials of first discharges.		Treatment of tube.  (All heatings took place in the gas.)
S Kathode.	W Kathode.	
Volts.	Volts.	
275	251	W heated strongly a few minutes.
244·5	245	S and W heated for a few minutes.
264	247	S and W heated strongly for 10 minutes.
247	255	W heated very strongly for a few minutes.
267	255	S heated strongly a few minutes.
251	251	W heated for a few minutes.

\* Townsend, "Electricity in Jars."

The condition of the anode was found to exert little, if any, action on the values of the sparking potential. We may conclude, therefore, that the value of the sparking potential depends upon the surface condition of the kathode.

*Experiments with "Untreated" Electrodes.*

A tube of similar form to that described above was used, and it was filled with gas, etc., in exactly the same manner, the sole difference being that the electrodes were not "cleaned" by electrical heating. Table V gives the results obtained. The initial values of the sparking potentials were small and increased both for S and W as kathode as the process of "degassing" or driving off the surface layers of gas was carried out.

Table V.—Tungsten Tube with Argon as filling Gas, Pressure = 2.86 mm.

Sparking potentials		Treatment of tube (All heatings in gas)
W Kathode.	S Kathode.	
Volts. 197-200 193-195 217 225	Volts. 245 243-245 255 271	Untreated. W heated dull red 3 minutes W heated dull red 20 minutes. W heated dull red 10 minutes.

*Experiments on Nickel Surfaces.*

Some experiments were carried out in which nickel was evaporated upon the tungsten electrodes in an atmosphere of argon. The results appear to be quite different from those obtained with tungsten electrodes. The first discharges occurred at a less potential than the succeeding ones, and the sparking potential rose to a maximum and approximately constant value. With S as kathode the sparking potential for the initial discharge was 217 volts and rose to 244 volts with discharge. A similar increase took place with W as kathode.

*Experiments with "Sodiated" Electrodes.*

Sodium was introduced electrolytically through a side tube provided for the purpose,\* and was evaporated on to the tungsten electrodes. After the tube had been rested for a few hours, the sparking potentials were redetermined.

\* For method see Taylor, *loc. cit.* Cf. Warburg, 'Ann. d. Physik,' vol. 40, p. 1 (1890); Burt, 'Phil. Mag.,' vol. 49, p. 1168 (1925); and 'Journ. Opt. Soc.,' vol. 11, p. 87 (1925). See also Taylor, 'J. Sci. Inst.,' vol. 4, p. 78 (1927).

Previous to introduction of the sodium the values were 265 volts with S as kathode, and 251 volts with W as kathode. These values were those determined after S and W had been heated to yellow white heat for ten minutes and then rested. When the electrodes were sodiumated the values were 122 volts with S kathode and 106 with W kathode. The falls of the sparking potential values were consequently great. The electrodes were then treated in a manner described in Table VI, in order to drive off some sodium from one or the other electrode. After each heating the tube was rested several minutes and the sparking potentials were then redetermined.

Table VI.—Pressure of Argon = 3.9 mm.

Sparking potentials.		Treatment of tube.
S Kathode.	W Kathode.	
Volts.	Volts.	
122	106	Both electrodes "sodiumated."
136	214	W heated at dull red heat for 1.5 minutes.
142	98	S heated for an instant to dull red.
152	95	S heated dull red for a second or two.
157	93	Do.
183	101	S heated dull red for 10 seconds.
230	108	Do.
254	110	Do.
254	111	Do.
253	112	S heated dull red for 20 seconds.

From the table (second line) it is seen that when W was heated to a dull-red for 1.5 minutes the sparking potential had risen by 108 volts (W kathode). The value attained was not that characteristic of the original tungsten electrode, so that it is evident that the heating had not entirely reproduced a tungsten surface. At the same time S had evidently become heated to a slight extent by conduction and radiation, and some of the sodium had evaporated. This brought about an increase of 14 volts in the sparking potential with S as kathode. In the next operation S was heated for an extremely short time. It was found that the sparking potential (S kathode) had risen a further 6 volts, whilst the value for W had fallen from 214 volts to the value 98, showing that sodium had evaporated from S on to W. The table shows the continuation of similar treatments. It is seen that when S was heated for 10 secs. or more, that W also became heated by conduction, etc., and lost some of its sodium, so that the sparking potential increased in value. In

some previous work\* with parallel-electrode discharge tubes in which the electric field was uniform over considerable areas, results on sodiumated electrodes indicated that the "sparking potential is a function of the composition of the kathode over a considerable area." The results given in Table VI further support this conclusion. The effect of introducing sodium upon the kathode is to diminish progressively the sparking potential as the amount of sodium is increased, until a constant value is attained when the electrode is completely sodiumated. The heating reduces the quantity of sodium per unit area. We may assume that a film of a few atoms in thickness will act in all ways as a sodium electrode. With an insufficient quantity to produce such a film there will be "bare patches" and the electrodes will be "mixed" ones.

### *General Results.*

The above described results are in accordance with those of the previous work.

The sparking potential is a function of the nature and condition of the kathode surface, and varies continuously with changes of the latter, depending upon the mean composition of the "working" part of the kathode surface. In other words, the sparking potential is a gross effect of ions, a result in accordance with the theory of the sparking potential described in the introduction to this paper.

### *Simple Theory for Parallel-Plate Electrodes.*

The actual mechanism of the initiation of the self-sustained electric discharge is still obscure. The usually accepted hypothesis is that of Townsend.† Another theory has been advanced more recently by Holst and Oosterhuis.‡

The experimental results obtained on the development of the currents before the self-sustained electric discharge sets in, is fairly conclusive "in showing that ionisation is principally due to the direct effect of collisions of electrons with molecules of the gas."§

Adopting Townsend's method of regarding the production of currents by the above process, for the simple case of a uniform field between plane-parallel electrodes, we arrive at the well-known expression for the number of positive

\* Taylor, *loc. cit.*

† Townsend, "Electricity in Gases," 'Hand. d. Rad.,' vol. 1, p. 283 (1920).

‡ Holst and Oosterhuis, 'Phil. Mag.,' vol. 46, p. 1117 (1923).

§ Townsend, 'Phil. Mag.,' vol. 45, p. 44 (1923).



ions arriving at the kathode, if  $N_0$  be the number of electrons produced at the kathode by the action of external "ionising agents,"

$$N = N_0 (\epsilon^{\alpha x} - 1) \quad (1)$$

where " $\alpha$  is the average number of molecules of the gas ionised by an electron in moving through a centimetre in the direction of the electric force," and  $x$  is the distance between the electrodes;  $\alpha$  is a function of the pressure of the gas, and the magnitude of the electric field. The neutralisation of these positive ions at the kathode surface will be accompanied by the emission of radiation,\* of which some falls upon the electrode surface and produces the emission of photo-electrons. Let the ratio of the number of electrons given off the kathode by the photoelectric effect to the number of positive ions neutralised there be  $\gamma$ . Then we obviously have the following condition for the production of a self-sustained discharge,

$$\gamma N_0 (\epsilon^{\alpha x} - 1) \geq N_0, \quad (2)$$

and consequently the sparking distance  $x_1$ , for an electric field of  $X$  volts per centimetre (which corresponds to the value  $\alpha$  for the number of electrons produced per centimetre by one electron), is given by

$$\gamma (\epsilon^{\alpha x_1} - 1) = 1. \quad (3)$$

and the sparking potential  $v_c$  is given by

$$v_c = X x_1 = \frac{X}{\alpha} \log \frac{1 + \gamma}{\gamma}. \quad (4)$$

Equation (3) is precisely the same as the equation given by Townsend, except that  $\gamma$  has a different significance.† It is readily seen how this hypothesis can be fitted into the relation obtained by Holst and Oosterhuis.‡

The variation of the function  $\gamma$ , which is a measure of the photoelectric emissivity of the cathodic surface for the radiation accompanying the neutralization of the positive ions of the gas, would entail a whole manifold of possible variations of the sparking potential function  $v_c$ .  $\gamma$  would be variable according to the condition and mean composition of the "working" part of the kathode surface, and would be subject to variations with the gas-to-metal potential changes, and the transient electric double layers set up by electrical charges on the kathode surface.

We may reasonably attribute the effects of the change of the sparking potential in the case of the tungsten electrodes to changes in the surface layers

\* Thomson, 'Phil. Mag.' (May, 1925); *ibid.*, vol. 2, p. 9, p. 674 (1926).

† Townsend, *loc. cit.*

‡ Holst and Oosterhuis, *loc. cit.*

of gas on the kathode. This was the position maintained in previous work on the electrode surface effects. It is, of course, also conceivable that many of the above described effects were due to changes in the surface structure of the metal of the kathode; in any case, such changes would be accompanied by a corresponding change in the function  $\gamma$ .

The results, indeed, are very analogous to some of those obtained for the variation of the photoelectric emissivity of metals.\* It is hoped to continue experiments in which both  $\gamma$  and  $v_c$  will be measured simultaneously.

### Summary.

A description is given of experiments on the sparking potentials of a discharge tube containing a filling gas of argon and comprising a tungsten wire electrode surrounded by a coaxial tungsten wire spiral electrode, both of which could be purified by heating electrically *in vacuo* or in argon.

Experiments with "sodiumated" electrodes are also described.

The conclusions are :-

The sparking potential is a function of the nature and condition of the kathode surface and varies continuously with changes of the latter, depending upon the mean composition of the "working" part. It is higher for the first discharge between "vacuum-formed" tungsten electrodes, falls to a minimum value with continued discharge, and then increases again to a definite value.

The results are interpreted as being due to the change of the photoelectric emissivity of the kathode, due to changes in surface gas layers.

A theory of the sparking potential is given in which it is assumed that the extra ionisation required to initiate the self-sustained electric discharge is brought about by the emission of electrons from the kathode surface due to the photoelectric action of the radiation accompanying the neutralisation of the positive ions at the kathode surface.

For parallel-plate electrodes the hypothesis yields an exactly similar relation to that given previously by Townsend,†

$$\gamma (\epsilon^{\alpha x_1} - 1) = 1,$$

$\gamma$ , however, has a different significance; it represents the ratio of the number of electrons given off by the kathode by the photoelectric effect, to the number of positive ions neutralised there. " $\alpha$  is the average number of molecules of the gas ionised by an electron in moving through a cm. in the direction of the electric force" ( $X$  volts per cm.), and  $x_1$  is the sparking distance.

$\gamma$  varies with the condition of the kathode surface.

\* See (†) footnote, p. 75.

† Townsend, *loc. cit.*

I have great pleasure in acknowledging my indebtedness to the International Education Board for the Fellowship which enabled the work to be carried out, to Prof. Ornstein for his continuous help and interest in the research, to Mr. Willemse, and to Mr. Kuipers for his care in constructing all the glasswork used in the experiments.

---

*Quasi-unimolecular Reactions. The Decomposition of Diethyl Ether in the Gaseous State.*

By C. N. HINSHELWOOD, Fellow of Trinity College, Oxford.

(Communicated by H. Hartley, F.R.S.—Received December 8, 1926.)

*Introduction.*

During the last few years we have made in Oxford an investigation of a number of gaseous reactions with the chief object of applying the principles of the kinetic theory and discovering the mechanism of "activation." In order to make clear the bearing of the fresh experiments described in this paper it will be convenient first to give a brief summary of the general development of the enquiry.

1. At first the only homogeneous reactions which could be discovered were bimolecular reactions. The rate of these could be expressed by the equation— $\text{number of molecules reacting} = \text{number entering into collision} \times e^{-E/RT}$ —which had been applied by W. C. M. Lewis to the decomposition of hydrogen iodide.  $E$  is the "energy of activation." The conditions under which this equation is rigidly applicable are—(a) the two molecules participating in the reaction require independent activation to the extents  $E_1$  and  $E_2$  respectively, where  $E_1 + E_2 = E$ , though the separate values need not be known; (b) the energy of activation in each molecule is confined to two degrees of freedom, and (c) nearly all the collisions where (a) is satisfied are fruitful. Assumption (a) is very general and a highly probable one; assumption (b) is approximate only, but the equation remains very nearly true for any small number, one, two or three degrees of freedom. Since it is found to agree with experiment we may conclude that in most bimolecular reactions activation of the two colliding molecules in some simple manner in a few degrees of freedom is a necessary and sufficient condition for chemical change.

2. The decomposition of acetone\* at about 500° C. now proved to be a unimolecular reaction, and the number of molecules reacting in unit time appeared to be about  $10^5$  times greater than the number which could be activated by collision in a manner at all similar to that characteristic of a bimolecular reaction. Analogous results had been found by Daniels and Johnston for nitrogen pentoxide.† It thus seemed that there must be some fundamental difference between the mechanisms of bimolecular and unimolecular reactions. This was brought out more sharply by the observation that the decomposition of acetaldehyde—a bimolecular reaction—although chemically similar to that of acetone, fell into line completely with other bimolecular reactions.

3. It was natural to turn at first to some form of radiation theory for unimolecular reactions, since, in spite of all its difficulties, this theory is not completely excluded from the realm of possibility. It must be emphasised that the difficulty does not lie in explaining how a unimolecular reaction can be determined by collisions—the theory of Lindemann provides for this—but in the apparent insufficiency of collisions. In the course of a discussion Prof. Lindemann suggested to me that the best plan would be to extend the idea of energy of activation to include not merely energy of some specific kind but energy of all kinds in every possible distribution in a large number of degrees of freedom, the only condition being that the total should exceed  $E$ . Plenty of collisions might be available to produce this kind of activated molecule. Some of the consequences of this suggestion were worked out in a recent paper‡ and may be summarised as follows.

The chance that a molecule contains in  $n$  degrees of freedom energy greater than  $E$  is no longer  $e^{-E/RT}$  but

$$e^{-E/RT} (E/RT)^{n-1}$$

A correction  $(\frac{1}{2}n - 1) RT$  has, however, to be added to the value of  $E$  which is derived in the usual way from the Arrhenius equation.

In a unimolecular reaction it is only necessary that one of the molecules in a collision should be activated. We might assume that under favourable conditions all the energy of two molecules in collision could pass into one, but this is very unlikely. To calculate the number of collisions from which a molecule emerges with energy greater than  $E$  it is best to proceed as follows.

\* 'Roy. Soc. Proc.,' A, vol. 111, p. 245 (1926). 'J. Amer. Chem. Soc.,' vol. 43, p. 53 (1921). Cf. Tolman, *ibid.*, vol. 47, p. 1524 (1925).

† 'Roy. Soc. Proc.,' A, vol. 113, p. 230 (1926).

Suppose statistical equilibrium to be established in the gas, and let the chemical change be ignored. Then—number of molecules ( $N_1$ ) of which the energy rises above the limit  $E$  in unit time = number ( $N_2$ ) the energy of which falls below  $E$ . Since  $E$  is a very large amount, possessed by exceptional molecules only, the vast majority of activated molecules which suffer collisions will have their energy reduced below  $E$ . Thus  $N_2$  is very nearly equal to number of collisions  $\times$  fraction of molecules with energy greater than  $E$ , i.e., to

$$\frac{Z \cdot e^{-E/RT} (E/RT)^{\frac{1}{2}n-1}}{\frac{1}{2}n-1}.$$

Hence from the condition for statistical equilibrium  $N_1$  is also nearly equal to this. This argument was tacitly assumed in the former paper.

If  $n$  is large this expression is much greater than the simple exponential and the discrepancies of the order  $10^5$  which were mentioned above can be wiped out by assuming a sufficient number of degrees of freedom in the molecule.

Turning now to the experimental evidence, it is in fact observed that whereas bimolecular reactions which only require the simple exponential expression are usually transformations of comparatively simple molecules such as HI,  $\text{Cl}_2\text{O}$  and  $\text{N}_2\text{O}$ , unimolecular reactions seem to be characteristic of more complex molecules. The next step in the experimental investigation is therefore to test more thoroughly the definite hypothesis that unimolecular reactions are mainly confined to molecules with large numbers of internal degrees of freedom.

For these molecules, with the usual sort of values of  $E$  and the extended idea of energy of activation, there will be enough collisions for Lindemann's mechanism\* to work. We must now consider this mechanism. Unlike the simple molecules such as HI, which probably react at once if at all, the more complex molecules have an appreciable time of relaxation, and having gained the total energy  $E$  in  $n$  degrees of freedom will not, on the average, react until after a small finite time, before the lapse of which they may lose their energy again in another collision. Thus at high pressures the rate of activation and de-activation may be great compared with the rate of chemical change. Under these circumstances the removal of molecules by chemical transformation does not seriously affect the Maxwell distribution. The number of molecules reacting in unit time is then a small constant fraction of the number of activated molecules, which in turn is a small constant fraction of the total number. Hence the reaction satisfies the unimolecular law.

But it can only satisfy the law exactly at pressures above a certain limit :

\* 'Trans. Faraday Soc.,' vol. 17, p. 598 (1922).

at some pressure sufficiently low the law must begin to fail and give place to one approximating more closely to a bimolecular law the lower the pressure. Attempts to detect this phenomenon in the decomposition of nitrogen pentoxide\* have given negative results so far, but the unimolecular velocity constant of the decomposition of propionic aldehyde† appears to fall sharply at pressures below about 80 mms. If it is assumed that at this point there are just enough collisions to activate the molecules it can be calculated that 12 to 14 degrees of freedom in the molecule are necessary. This is a very plausible result, but standing alone can hardly be considered conclusive. There is always the possibility of some undiscovered complication, and although the existence of any factor which would make the results of the experiments with propionic aldehyde unreliable was shown to be exceedingly unlikely, it is none the less desirable to examine as many examples as possible. If a whole series of substances appear to react by the Lindemann mechanism it is very improbable that all the results can be due to a deceiving coincidence.

To study the behaviour of molecules with large numbers of degrees of freedom we have to rely chiefly on organic compounds in the gaseous state. The present paper deals with the decomposition of diethyl ether. The decomposition of dimethyl ether is also being investigated and an account of the experiments will be published later.

The diethyl ether reaction proves to be simple kinetically. It is unimolecular over a wide range of pressures, but falls off in its specific rate at lower pressures. This falling off does not occur, however, in presence of an excess of hydrogen, which appears to be able to keep the number of activating collisions above the critical limit. The chemical result of the decomposition is not quite a simple one, though reasons are given in one of the following sections for believing that this fact does not affect the simplicity of the reaction kinetics. It was satisfactory, however, to find that the decomposition of dimethyl ether proceeds in accordance with the simple equation  $\text{CH}_3\text{OCH}_3 = \text{CH}_4 + \text{CO} + \text{H}_2$ , where there is less room for complications which might produce an illusory effect of simplicity. None the less the reaction of the dimethyl ether is exactly analogous kinetically to that of the diethyl ether. This fact is mentioned in anticipation because it strengthens very much the conclusions of this paper about the nature of the diethyl ether reaction.

\* Hunt and Daniels, 'J. Amer. Chem. Soc.,' vol. 47, p. 1602 (1925); Hirst and Rideal, 'Roy. Soc. Proc.,' A, vol. 109, p. 526 (1925).

† Hinshelwood and Thompson, 'Roy. Soc. Proc.,' A, vol. 113, p. 221 (1926).

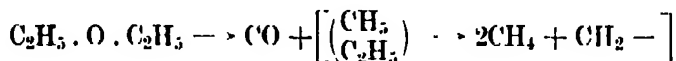
The following table shows the influence of the complexity of the molecule upon the type of reaction mechanism by which it decomposes thermally :—

Bimolecular.	Unimolecular.	
HI	N <sub>2</sub> O <sub>5</sub>	constant has normal value at 0.01 mm.
N <sub>2</sub> O	(SO <sub>2</sub> Cl <sub>2</sub> )	data incomplete.
Cl <sub>2</sub> O	CH <sub>3</sub> COCH <sub>3</sub>	no observations on falling of constant.
O <sub>3</sub>	C <sub>2</sub> H <sub>5</sub> CHO	constant falls off below 80 mm.
CH <sub>3</sub> CHO	C <sub>2</sub> H <sub>5</sub> .O.C <sub>2</sub> H <sub>5</sub>	" " " 150 "
	CH <sub>3</sub> .O.CH <sub>3</sub>	" " " 350 "

We have also made experiments with methyl acetate and with methyl alcohol, but the reactions of each were too much influenced by the surface of the silica vessel to allow the isolation and measurement of the true gas reaction.

*The nature of the products of decomposition of diethyl ether.*

The decomposition of ether in the gas phase does not yield ethylene and water according to the equation  $C_2H_5 \cdot O \cdot C_2H_5 = 2C_2H_4 + H_2O$ , but consists in the separation of carbon monoxide from the molecule. The hydrocarbon residue, of the empirical composition  $C_3H_{10}$ , is relatively somewhat richer in carbon than methane, the most stable hydrocarbon, and re-arranges itself to give mainly methane, a little ethylene, and a certain amount of a higher hydrocarbon which is probably ethane. The process of decomposition seems to take place more or less thus —



with a rapid combination of the  $CH_2-$  residues to give ethylene.

The net result is thus  $CO + 2CH_4 + \frac{1}{2}C_2H_4$ . According to this equation there would be about twice as much methane as carbon monoxide and about four times as much methane as ethylene. Actually the amount of ethylene is slightly less, and there is a little ethane. The following are the analyses of the products of complete decomposition at temperatures towards the extremes of the range over which the velocity measurements were made

	587°	477°
	Per cent.	Per cent.
CO	28.7	27.9
CH <sub>4</sub>	55.3	54.4
C <sub>2</sub> H <sub>4</sub>	7.8	8.9
C <sub>2</sub> H <sub>6</sub>	8.2	8.8
CO <sub>2</sub>	0.0	0.0

It is to be noted that the character of the decomposition does not alter over this range of temperature.

It has long been recognised that a rather complex set of products may be formed from one molecule in a single act of decomposition. There may be a rapid re-arrangement of the residual fragments after a part of the molecule has been split off, and it is not necessary to suppose a complicated series of consecutive reactions. Bone observed,\* for example, that acetaldehyde, which decomposes at 500° C. into carbon monoxide and methane, could at higher temperatures yield free carbon and hydrogen. These were not formed by the subsequent decomposition of methane first produced, since at the temperatures in question methane was still quite stable. Sabatier also supposes the rapid re-arrangement of the residual fragments from a simple decomposition to be responsible for the large variety of products which are formed in certain pyrogenic reactions.

In making the measurements of reaction velocity the method employed was exactly similar to that described in previous papers, and depended upon observing the rate of increase of the total pressure as the decomposition proceeded. This can be regarded as a measure of the rate of reaction of the ether itself as long as any subsequent re-arrangements are rapid compared with the primary breaking up of the ether molecules. Apart from the general probability of the assumption that this condition is fulfilled, the following direct observations are evidence that it is. First, the reaction obeys a unimolecular law in a way which would be unlikely if the rate of pressure increase were determined by a series of consecutive changes of comparable rates. Secondly, the approach to the "end-point" of the reaction is quite definite as may be seen by reference to the figures in the next section.

There is, however, another possible source of disturbance to which careful attention must be given. If hydrocarbon residues such as  $\text{CH}_2$  — exist momentarily in the free state, then their fate may be influenced by pressure and by temperature in a way which makes the rate of pressure increase at one temperature or pressure bear a relation to the actual rate of ether decomposition different from that which it bears at another temperature or pressure. However, the table already given shows the products to be the same at different

\* 'J. Chem. Soc.,' vol. 87, p. 910 (1905). In this paper Bone and Smith describe the thermal decomposition of acetaldehyde and of formaldehyde—though not from the kinetic standpoint. Reference to this very important work should have been made in the introduction to the paper by Hinshelwood and Hutchison on the kinetics of the former reaction.



temperatures. The total pressure increase is also constant, as the following figures show.

Temp. (°C.)	Initial Pressure.	Total increase of Pressure	Ratio.
525	190	384	1.93
555	194	357	1.84
588	218	407	1.86

In all calculations the increase will be taken as 188 per cent. of the initial pressure.

If pressure influenced the course of the re-arrangement, more condensed products would probably be formed at higher pressures. The total pressure increase, if it varied at all, would therefore be expected to be smaller for high than for low initial pressures of the ether. At 32 mm. the total increase was about 2.1 instead of 1.9 times the initial pressure. This is not a very accurate result but such deviation as there is agrees with expectation. When, therefore, the initial rate of reaction is measured by the actual rate of pressure increase the values obtained for the lower pressures will be slightly too high relatively to those for the higher pressures. Such small error as this introduces makes the unimolecular velocity constants appear to rise at lower pressures. Since the real fact is that they fall markedly, in the manner predicted by Lindemann's theory, it does not appear that this error can be appreciable.

The decomposition of dimethyl ether,  $\text{CH}_3 \cdot \text{O} \cdot \text{CH}_3 = \text{CH}_4 + \text{CO} + \text{H}_2$ , in which no unstable residues need be supposed to play a part, is kinetically similar in every respect to that of diethyl ether. This gives further reason for believing that the diethyl ether results are not in any way illusory.

As far as can be seen, therefore, there is no reason to suppose that what is measured is anything but the actual rate of decomposition of ether.

### *The Kinetics of the Reaction.*

The reaction taking place in a silica bulb is predominantly homogeneous. Half-filling the bulb with powdered silica, which had increased the rate of decomposition of methyl formate sixteen times, caused little acceleration of the reaction.

Average value of  $k$ .

	594° C.	554°	525°	476°	434°
Bulb empty	0.0115	0.00247	0.00071	0.000088	0.0000090
Bulb and powdered silica	0.0097	0.00249	(0.00122)	0.000096	0.000025

The bracketed value is probably too high as it includes the first two experiments of the series, which showed an abnormal behaviour probably attributable to adsorbed air not completely pumped off from the finely powdered silica. There is therefore very little surface reaction in the empty bulb, except at the lowest temperatures, where it may amount to about 10 per cent. of the total.

In these experiments a wide necked bulb had to be used in order that the powdered silica might be introduced easily. This leads to a certain inaccuracy. In all the other experiments, therefore, bulbs with capillary connections were used. Two samples of ether, one specially purified in the laboratory, the other obtained from Kahlbaum, were used. The former was kept over sodium in a bulb sealed to the apparatus throughout the course of the experiments. Two different capillary-necked bulbs were used. The various results were concordant as the following examples show.

Temperature 525° C. The times are those required for the initial pressure to increase by 50 per cent., that is, for 26.6 per cent. of the reaction to take place. The initial pressure was about 200 mm. in all the experiments.

Bulb.	Ether Sample.	Time.
		5' 53"
		5' 36"
		5' 47"

When the initial pressure of the ether is fairly high the reaction is kinetically unimolecular. One of the simplest criteria of a unimolecular reaction is that the time required for three-quarters of the change is exactly double that required for one half.

Temperature C.	Initial Pressure of Ether.	" Half- life."	" Three- quarter life."	Ratio.
525°	199	14' 10"	29' 10"	2.06
555°	194	4' 20"	9' 3"	2.09
588°	218	59"	127"	2.15

The complete course of these experiments is shown in the table below.

$a$  is the total increase in pressure at the end of the reaction.

$x$  is the increase at time  $t$ ;  $k_{10} = \frac{1}{t} \log_{10} \frac{a}{a-x}$ .

525° C.			555° C.		
$a = 384.$			$a = 357.$		
$t$ (seconds).	$x$ (mm.).	$k_{10}$	$t$	$x$	$k_{10}$
158	43	0.000326	67	53	0.00104
273	73	0.000335	106	83	0.00118
390	103	0.000350	176	133	0.00115
616	153	0.000358	270	183	0.00116
951	210	0.000362	340	213	0.00116
1,210	243	0.000360	523	263	0.00111
1,666	283	0.000348	900	313	0.00101
2,390	318	0.000320	1,680	343	
$\infty$	384		2,350	353	
			3,380	357	

588° C.			$a = 407.$		
$t$	$x$	$k_{10}$			
22	80	0.00432			
30	110	0.00456			
40.5	150	0.00493			
54	190	0.00505			
82	250	0.00505			
103	280	0.00491			
147	320	0.00456			
245	360	0.00383			
600	395				
1,920	407				
2,700	407				

} The sharp end point is to be noted.

At lower pressures the rate of reaction falls much below that required by the unimolecular law; this is shown to some extent by the falling in the values of  $k$  during the later stages, but is made more evident by plotting against the initial pressure of the ether the time required for a given fraction of the total reaction to complete itself. In fig. 1 the time required for 26.6 per cent. is plotted. In a truly unimolecular reaction the graph would be a straight line parallel to the pressure axis. Above 200 mm. this is nearly realised; the increase in the time at lower initial pressures corresponds to a fall in the velocity constant.

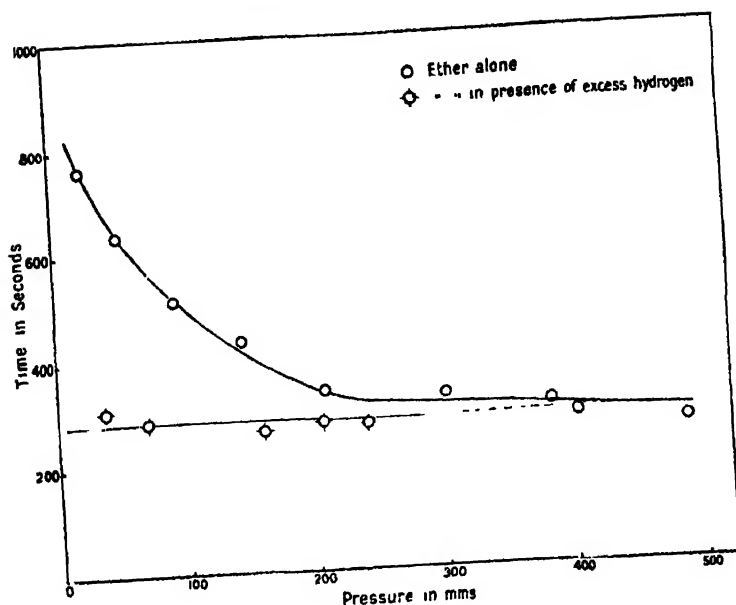


FIG. 1.

The curve is plotted from the values tabulated below, which were obtained in a random order. Bulb 1 was used.  
Temperature 525° C.

Initial pressure of ether (millimetres).	Time required for 26.6 per cent. change, i.e., for pressure to increase by 50 per cent.
487	4' 22"
403	4' 40"
382	5' 6"
302	5' 28"
210	5' 33"
145	7' 14"
93	8' 32"
51	10' 38"
25	12' 45"

In seeking an explanation of this curve the following possibilities have to be considered: (a) the falling in the value of the velocity constant is due to the effect predicted by Lindemann's theory—(b) a unimolecular and a bimolecular reaction take place simultaneously—(c) a surface reaction comes in to a relatively much greater extent at low pressures. Neither (b) nor (c) is admissible.

(b) would require the composite reaction to become more and more nearly bimolecular as the pressure increased, since the rate of a bimolecular reaction increases with pressure more rapidly than that of a unimolecular reaction. The actual transition is, however, in the opposite direction; (c) must be ruled out because the superposition of a surface reaction on a unimolecular gas reaction could only cause the constant to be increased relatively at lower pressures; (a), therefore, seems to be the probable explanation.

*The effect of other gases on the rate of reaction.*

Helium has no appreciable influence on the rate of reaction. The following results were obtained at 525° C., using bulb II.  $\tau$  is the time required for 26.6 per cent. of the reaction to take place.

Initial pressure of ether (mm.).	Pressure of helium.	$\tau$ (observed).	$\tau$ (absence of helium).
195	0	5' 52"	5' 45"
293	0	5' 42"	5' 15"
108	200	7' 44"	8' 5"
135	300	7' 35"	7' 12"

Nitrogen has little influence.

Initial pressure of ether.	Pressure of nitrogen	$\tau$ (observed)	$\tau$ (absence of nitrogen).
190	292	6' 41"	5' 53"
109	287	7' 45"	8' 3"
71	288	8' 50"	9' 36"

The products of reaction in excess have a slight but definite retarding influence at all pressures of ether.

Initial pressure of ether.	Pressure of reaction products present initially.	$\tau$ observed.	$\tau$ (no products added).
209	0	5' 50"	5' 35"
237	290	6' 51"	5' 26"
94	290	10' 24"	8' 40"
60	290	14' 10"	10' 10"

None of these effects are very marked. The influence of hydrogen on the reaction is, however, very remarkable. A sufficient excess completely prevents

the falling off in the rate of reaction at low partial pressures of ether. This can be seen clearly from the lower curve in fig. 1.

Temperature 525° C.

Initial pressure of ether (mm.).	Pressure of hydrogen (mm.).	$\tau$ .
240	292	4' 31"
200	293	4' 40"
164	287	4' 21"
60	292	4' 47"
30	295	5' 10"

An independent chemical interaction of the hydrogen and the ether seems improbable, since under no circumstances can the hydrogen increase the total rate above the limiting rate characteristic of high partial pressures of ether.

It seems as if collisions with hydrogen molecules can keep up the supply of activated ether molecules almost as effectively as collisions with other ether molecules. Why the effect of hydrogen should be so specific is not evident.

*Temperature Coefficient, Heat of Activation.*

The following table contains all the important data :—

T (abs.)	$\tau$ (seconds)	$k_{\text{observed}}$	$k_{\text{calculated}}$
861°	30	0.0103	0.0099
828.5°	118	0.00262	0.00291
798°	347	0.000892	0.000851
747°	3,634	0.0000852	0.0000861
699°	42,050	0.0000074	0.00000736

$\tau$  is the time in seconds required for the initial pressure to increase by 50 per cent. Each value is the average result of at least two determinations at pressures in the steady region.  $k_{\text{observed}}$  is found from  $\tau$  by the relation  $k = \frac{1}{\tau} \log \frac{188}{188 - 50}$ , the total pressure increase being 188 per cent.  $k_{\text{calculated}}$  is obtained from the formula

$$\ln k = 26.47 - \frac{53,000}{RT}.$$

The heat of activation, 53,000 calories, is not very different from that of propionic aldehyde 55,000 calories. The absolute rates of the two decom-

positions are nearly the same. At  $800^\circ$  abs.  $k$  for propionic aldehyde is  $2.1 \times 10^{-3}$  while  $k$  for diethyl ether is  $0.92 \times 10^{-3}$ .

In the diethyl ether decomposition the value of  $k$  begins to fall at about  $1/5$  atmosphere.

At  $800^\circ$  abs. and this pressure the number of molecules,  $N$ , which react per second in 1 c.c. is  $1.7 \times 10^{15}$ . The total number of collisions,  $Z$ , is  $\sqrt{2}\pi\sigma^2\bar{u}n^2$ , where  $\sigma$ , the molecular diameter, is taken as  $5 \times 10^{-8}$  cm.,  $\bar{u}$ , the root mean square velocity, is  $5.19 \times 10^4$  cm. per sec.,  $n$ , the number of molecules per c.c. is  $9.23 \times 10^{18}$  at  $800^\circ$  and 760 mm.

At  $1/5$  atmosphere  $Z = 2.0 \times 10^{27}$ .

If  $E = 53,000$  calories,  $Ze^{-E/RT} = 6.0 \times 10^{12}$ .  $N$ , the number reacting, is  $1.7 \times 10^{15}$  or 280 times greater than  $Ze^{-E/RT}$ .

Introducing the expression for  $n$  degrees of freedom, and assuming that at  $1/5$  atmosphere there are just enough collisions to account for the number of molecules which react

$$N = \frac{Z \cdot e^{-\frac{53,000 + (\frac{1}{2}n-1)RT}{RT}} \left( \frac{53,000 + (\frac{1}{2}n-1)}{RT} \right)^{n-1}}{1}$$

$$\frac{N}{Z \cdot e^{-53,000/(1.98 \times 800)}} = \frac{e^{-(\frac{1}{2}n-1)\{33.46 + (\frac{1}{2}n-1)\}} (\frac{1}{2}n-1)^{n-1}}{1}$$

If  $n = 6$ , the right hand side is 85, while if  $n = 8$ , the right hand side is 402. The experimental value of the left hand side is 280, whence we may conclude that the participation of about 8 degrees of freedom will allow activation by Lindemann's mechanism.

#### *General conclusions.*

Whatever views may be held about the interpretation of the results described in this paper, the experimental fact is certain that three reactions—namely, the decomposition of propionic aldehyde, of diethyl ether and of dimethyl ether—appear to be unimolecular at high pressures and assume a bimolecular character at lower pressures.

It will probably be conceded that this proves collisions to be responsible for the activation of the molecules, and since the reactions are not in a strict sense transformations of isolated molecules they might be called quasi-unimolecular at the higher pressures.

These quasi-unimolecular reactions can be explained most simply by assuming that Lindemann's mechanism is operative, an assumption which is supported

by the observations on the influence of hydrogen, but can hardly be regarded as proved.

It is premature to say whether all reactions which obey the unimolecular law are of this kind. The decomposition of acetone is probably quasi-unimolecular, but the decomposition of nitrogen pentoxide still betrays no evidence of dependence on collisions at very low pressures. This can probably be accounted for by assuming that enough degrees of freedom are involved; but also it is true to say that nowhere must more care be exercised than in making inductions about the mechanism of chemical reactions. At the moment it is better to make reactions which are shown to be quasi-unimolecular into a separate class, in which the nitrogen pentoxide decomposition may or may not turn out to be included.

All the effects of foreign gases on the decomposition of diethyl ether can be explained in terms of the suggested mechanism, which allows for the most specific influences, without, however, providing the means by which these may be predicted.

#### *Summary.*

The decomposition of gaseous diethyl ether is a reaction which follows the unimolecular law at high pressures, but becomes more nearly bimolecular at lower pressures. The velocity is represented by the equation

$$\ln k = 26.47 - \frac{53,000}{RT}.$$

A sufficient amount of hydrogen completely stops the falling-off in the unimolecular velocity constant at low pressures; helium and nitrogen have little or no influence, while the reaction products in considerable excess have a slight retarding influence.

There are enough collisions to activate the molecules if the energy of activation is assumed to be distributed among about eight degrees of freedom.

These and other "quasi-unimolecular" reactions are most simply explained on Lindemann's theory; further evidence is needed however to confirm this interpretation.

A table is given showing the relation between the complexity of a molecule and the type of mechanism by which it decomposes. Simple molecules usually decompose bimolecularly; more complex ones in a quasi-unimolecular way, as might be expected on theoretical grounds.



*The Nature and Artificial Production of the (so-called) Voiced  
and Unvoiced Consonants.*

By SIR RICHARD A. S. PAGET, Bart.

(Communicated by Sir William Bragg, F.R.S.—Received December 21, 1926.)

In a previous paper\* experiments were described in which the various English consonant sounds were defined in terms of the combinations and changes of resonance observed by ear when these sounds were articulated, without phonation. It was also shown how these sounds could be imitated by models which produced similar combinations and changes of resonance, without imitating the shapes of the natural vocal cavities.

These observations indicated that, in certain cases, no difference of resonance was observable between the (so-called) voiced and unvoiced forms of a given consonant type, *e.g.*, between *p* and *b*, *θ* and *ð*, *s* and *z*, *f* (*sh*) and *ʒ* (*zh*), and *t* and *d* respectively.

It was clear that the usual phonetic distinction, that *p*, *t*, *k*, *θ*, *s*, and *f* are unvoiced, while *b*, *d*, *g*, *ð*, *z*, and *ʒ* are voiced, was not fundamental, since both series could be recognisably articulated in a whisper, *i.e.*, without phonation or voicing.

In some cases—such as *p* and *b*, and *t* and *d*—the difference between the two types of whispered sounds appeared to be mainly one of air pressure—the greater pressure producing the so-called “unvoiced” sounds *p* and *t*. In other cases, such as *θ* and *ð*, the relative loudness of the various component resonances appeared to be different for the two types of sound.

In the cases of *θ*, *ð*, and *s*, *z*, the air pressure appeared to be greater in the case of the “voiced” sounds *ð* and *z*.

In the other cases it was found that the difference (in models) could be produced by a combination of differential air pressure and type of closure; the latter difference producing a variation in the rate of change of one or more of the resonances.

It was observed that with a vowel sounding model giving the vowel *i* as in it,† an unphonated *b* sound, breathed by the mouth into the reed of the model, became a voiced *p*, while a similar unphonated *d* sound was converted into a

\* ‘Roy. Soc. Proc.’ A, vol. 106, pp. 150–174 (1924).

† Compare (cat) model, ‘Roy. Soc. Proc.’ A, vol. 102, p. 759, fig. 14 (1923).

voiced *t*. These observations were not followed up at the time of the original experiment.

The experiment evidently indicated (1) that the resonances of the model were in some way characteristic of the *t/d* type of consonant; and (2) that the distinction between *t* and *d* was (in some way) formed in the operator's own mouth, and was transmitted through the reed and resonators of the model so as to produce the corresponding (so-called) voiced or unvoiced sound in the model. In other words, the distinction between "voiced and unvoiced" consonants appeared to be one of resonance in the mouth, with or without a difference of air pressure.

Experiments were made to test the position in the mouth in which the essential change was produced.

To investigate the distinction between *p* and *b*, a perforated mouth stopper was formed in plasticene and held between the lips, so that the orifice could be closed and released by the thumb or finger so as to eliminate the possibility of differential action of the lips. It was found that *p* or *b* could be whispered at will, with identical actions of closure and release of the mouth orifice and independently of differences of air pressure.

It was also found that a *p* or *b*, or alternatively an *f* or *v*, could be made between the lips and the exterior of a solid mouth stopper.

To investigate the action inside the mouth, while whispering *p/b* or *f/v*, a mouth stopper was made of cork with a glass window inserted, as shown in fig. 1, and an electric torch bulb was fitted to the inside of the window frame so as to illuminate the interior of the mouth while the consonants *p/b* or *f/v* were articulated between the lips and the outer margin of the windowed stopper.

There was no visible change in the position of the tongue or soft palate in changing from *f* to *v*, or from *p* to *b*; it was clear, therefore, that the essential difference was produced in the pharyngeal or laryngeal regions.

An attempt was made to observe these regions during articulation by means of a laryngeal mirror with small attached electric light, the mirror handle being passed through the cork frame of the windowed mouth stopper, but the observation proved too difficult.

A model was made in plasticene, as in fig. 2, in which the soft palate and palatal arch were approximately copied full size; the pharyngeal portions were replaced by a 1-inch internal diameter rubber tube connected to the

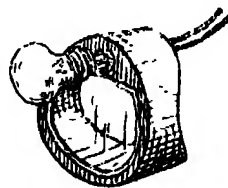


FIG. 1. — Mouth Stopper and Electric Torch Lamp.

air-supply pipe (from a foot bellows) by means of a perforated cork and short length of tube.

Fixed vocal chords, in plasticene, were formed at the base of the rubber tube, with a lenticular aperture of about 15 mm.  $\times$  between 0.75 and 0.5 mm., as shown in section in fig. 3; the tube is shown expanded laterally (due to external constriction) at a point about 2 cm. above the vocal chords.

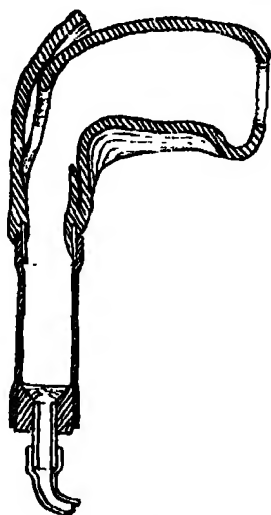


FIG. 2.



FIG. 3.

FIG. 2.— Plasticene Model with Rubber Tube Pharynx and Fixed Plasticene Vocal Chords.

FIG. 3. Fixed Vocal Chords. Pharyngeal Constriction and Connection to Air Supply.

When air was blown through the model under these conditions, and the mouth of the model was closed and released by hand, the whispered consonant was *p* or *f*, according as the closure of the mouth of the model was complete or partial.

The aperture of the plasticene vocal chords was progressively enlarged, and the whispered consonant—produced by closure and release of the mouth of the model—observed.

The result was as follows :—

Dimensions of lenticular aperture.	Consonant produced.
15 mm. $\times$ 2 mm. ....	<i>p</i> or <i>f</i> .
15 mm. $\times$ 3.5 mm. ....	<i>p</i> at high pressure, <i>b</i> at low pressure.
15 mm. $\times$ 5 mm. ....	<i>b</i> at all pressures.

The experiment was tried of constricting the pharyngeal (rubber) tube to different degrees of closure and in different positions relative to that of the plasticene vocal chords.

With a vocal chord aperture of 15 mm.  $\times$  5 mm., constriction to a slit of 2 to 3 mm. at 3.5 cm. above the vocal chords further improved the unphonated *b*. Such a constriction was conveniently produced by bending the rubber tube sharply at an angle of between 45° and 90°.

With the vocal-chord aperture reduced to between 0.75 and 0.5 mm., so as to give a *p* or *f* constriction of the pharyngeal tube at a point about 1 cm. above the vocal chords to a slit of 4 to 5 mm. produced no change in the *p* or *f* sound.

Further constriction of the pharynx tube to a 2 to 3-mm. slit changed the *p* or *f* to a clear *b* or *v* respectively.

There was a marked increase of resonance in the model under the conditions which produced the *b* or *v* sounds.

Constriction of the pharynx tube to a slit of 1 to 2 mm. aperture at any position from 1 cm. to 5 cm. above the vocal chords could be made to produce the same effect —i.e., to convert a *p* or *f* into *b* or *v* —by adjusting the degree of constriction in each case.

A further constriction of the pharynx tube, so as nearly to close the slit, converted the *b* or *v* back to *p* or *f*.

The same effect was produced by a close constriction at 6 cm. above the vocal chords, but the best effect was produced by constriction at about 1 cm. above the vocal chord level.

It was found that, in the case of the writer's own voice, an unphonated *b*, *d*, *g*, *v*, *z*, *ʒ*, or *ʒ* could be forcibly converted into its "unvoiced" equivalent *p*, *t*, *k*, *f*, *s*, *ʃ* and *θ*, viz., by external pressure on the front of the throat at about 3 cm. above the centre of the larynx, while whispering any one of the "voiced" series.

### *Conclusions.*

It appears that the unphonated *b*, *d*, *v*, etc., or *p*, *t*, *f*, etc., series of consonants can be produced in two alternative ways.

Large aperture at the vocal chords with the small aperture above them produces the *p*, *t*, *f* series; large aperture at the vocal chords and large aperture above them, produces the *b*, *d*, *v* series.

Small aperture at the vocal chords and large aperture above them, produces

## 102 *Artificial Production of Voiced and Unvoiced Consonants.*

the *p, t, f* series; small aperture at the vocal chords (as in the case of actual phonation) and small aperture above them, produces the *b, d, v* series.

In other words, both apertures large, or both apertures small, produce the *b, d, v* series, whereas one large and one small aperture produce the *p, t, f* sounds.

The constriction in the model above the position of the vocal chords seems to correspond with a possible action of the false vocal chords, but conclusive observations on the point have not yet been made.

The results, which were obtained during August and September, 1926, have been recently confirmed by a further series of experiments carried out jointly by Dr. R. S. Clay, of the Northern Polytechnic, and the present writer, using a 1-inch diameter rubber tube 15 cm. long (in the clear) as the resonator and an adjustable tube clip for producing the upper constriction.

The lower constriction (corresponding to that of the vocal chords) was produced, as before, by a slit in a plug of plasticine, and the unphonated sounds were produced by air from a compression plant passed through the model.

By closure (complete or partial) and release of the tube in various positions, it was found possible, for example, to produce *p, f, s* and *k*, or *b, v, z* and *g*, by adjusting the clip so as to give a slit aperture of 16 mm. for the *p-k* series, or 6 mm. for the *b-g* series.

The resonance changes produced by the variations of aperture described have not yet been investigated.

---

## *Anodic Overvoltage Measurements with the Cathode Ray Oscillograph.*

By EDGAR NEWBERRY, D.Sc., F.I.C., University of Cape Town.

(Communicated by Sir Ernest Rutherford, Pres.R.S.—Received December 8, 1926.)

[PLATES 9 AND 10.]

Anodic phenomena are more complex and more interesting in many ways than cathodic, inasmuch as we encounter not only overvoltage and transfer resistance but also solution of the electrode, passivity and valve action. Since the underlying principles of passivity and of valve action are still controversial matters, the following work was undertaken with the hope that fresh light would be thrown on these phenomena.

*Experimental.*—The apparatus used was identical with that previously described\* except that the experimental electrode C, being now the anode, was connected to the grid of the thermionic valve and the standard mercurous sulphate electrode to the filament.

In all cases the electrolyte was a normal solution of sulphuric acid.

The electrodes chosen were of three types :—

- (a) Unattackable electrodes—platinum, gold, lead.
- (b) Electrodes showing passivity—nickel, iron, chromium.
- (c) Electrodes showing valve action—antimony, tantalum, bismuth.

All the electrodes were cleaned with No. 000 emery paper before use, and all had an exposed surface of 1 sq. cm.

Some of the curves obtained are shown in figs. 1–31, on Plates 9 and 10.

Assuming that the E.M.F. of the oxy-hydrogen cell is 1.23 volts, the potential difference between an oxygen electrode and the mercurous sulphate electrode used would be 0.53 volt. In the given solution, however, hydroxyl ions are far more plentiful than oxygen ions, and, in fact, it is doubtful if the latter exist at all. It is therefore more reasonable for comparison with other overvoltages to assume the hypothetical hydroxyl electrode as standard, and the potential difference between this and the mercurous sulphate electrode then becomes 0.83 volt. Overvoltages in the following table are calculated on this basis. For comparison with anodic values by other workers they must be increased by 0.3 volt.

\* 'Roy. Soc. Proc.,' A, vol. 107, p. 486 (1925), and vol. 111, p. 182 (1926).

Fig.	Electrode.	Current density.	Applied voltage.	Over-voltage.	Transfer resistance.	Remarks.
		ma.	volt.	volt.	ohms.	
1	Platinum	10	—	0.4	5	—
2	"	100	—	0.4	2.5	—
3	Gold	10	—	0.5	7.5	—
4	"	100	—	0.5	3	—
5	Lead	0.1	1	—	—	—
6	"	0.1	2	—	—	—
7	"	10	—	0.65	—	—
8	"	100	—	0.7	2.5	—
9	Nickel	1	—	-1.2	—	—
10	"	10	—	-1.1	—	—
11	"	100	—	0.2	3	—
12	"	1000	—	0.2	0.75	—
13	Iron	200	—	—	—	Partly active
14	"	300	—	—	—	"
15	"	100	—	0.4	1.5	Passive
16	"	1000	—	0.4	0.75	"
17	Chromium	10	—	-0.2	8	—
18	"	100	—	-0.2	3	—
19	Antimony	0.1	1	—	—	—
20	"	0.1	2	—	—	—
21	"	0.1	3	—	—	—
22	"	0.1	4	—	—	—
23	Tantalum	0.01	1	—	—	—
24	"	0.01	2	—	—	—
25	"	0.01	2.5	—	—	—
26	"	0.01	3.5	—	—	—
27	"	0.01	2.5	—	—	After 10 volts applied
28	Bismuth	20-15	1.5	—	—	—
29	"	16-15	2.5	—	—	—
30	"	15	3.5	—	—	—
31	"	10	6	—	—	—

The measurements from which the above data have been calculated were taken on the original negatives and not from the prints. More accurate values are obtained in this way.

*Discussion of the unattackable and passive electrodes.*—It will be at once evident from an examination of the photographs, figs. 1-18, that anodic and cathodic behaviour of electrodes show so many points of resemblance, when the electrodes are not attacked, that similar forces must be at work in both cases, and any theory which is applied to the one must also be applicable to the other. This holds good also for passive electrodes but only when they are in the passive condition. Comparison of figs. 1-4 with figs. 11, 12, 15, and 16 shows no essential differences in the general characteristics of the curves for attackable electrodes and passive electrodes. This also applies to the case of lead when a moderate current is flowing, but at very low current densities a remarkable

change in the character of the curves is evident—figs. 5, 6, and 6A. Lead is usually classed as an unattackable anode in dilute sulphuric acid, in spite of the known fact that it acquires a coating of dioxide, but these curves appear to indicate that a far more suitable place would be among the passive metals. Fig. 5 is obtained when a constant potential difference of 1 volt is applied between a lead anode and a platinum cathode. A very small current (0.1 milliamperes) flows under these conditions and the single potential of the lead remains very low. When the applied potential was raised to 2 volts, the current at first rose slightly, but then rapidly fell to the previous value of 0.1 milliamperes. The single potential of the lead after cutting off the current remained low as before. This is shown in fig. 6 where the lowest curve was obtained by switching off the main battery after the upper part of the photograph had been taken. It may be noted that, in these two cases, transfer resistance appears to be absent since the upper and lower parts of the curves are continuous although the photographs do not show this well.

After taking fig. 6, it was observed that the curve suddenly began to change its position and shape, the lower part rising in exactly the same way as is observed with nickel or iron when passivation occurs. To illustrate this two further photographs were taken and both printed together on one paper—fig. 6A. For these the applied potential was kept constant at 2 volts throughout. At first the curve to the left of the figure was obtained, and is a reproduction (on a slightly reduced scale) of fig. 6. Then the current was allowed to flow for 5 minutes without altering any part of the apparatus and a second photograph taken. During this time the current rose to three times its former value though the applied potential was unchanged. The curve obtained is the upper one to the right of the figure. Finally the main current was cut off as in fig. 6 and the lower right-hand line was obtained. Comparing this with the corresponding portion of fig. 6 it will be seen that the single potential of the anode has risen by about 1.2 volts, which is much the same as the change of potential which occurs when nickel becomes passive. The increase in the current is evidently due to the change of a non-conducting film of  $\text{PbSO}_4$  into a conducting film of  $\text{PbO}_2$ .

It appears quite certain therefore that a lead anode in dilute sulphuric acid must be classed as a passive metal, and further that it owes its passive properties to the presence of an insoluble, electrically conducting coating of higher oxide.

This affords strong evidence in support of the so-called "oxide" theory of passivity, but it must be realised that other anodic overvoltage compounds



such as higher chlorides, iodides, etc., may possess similar properties and also show the phenomena of passivity. Further, in some cases the higher oxide, chloride, etc., may form a solid solution in the electrode surface, though this is probably not the case with lead in dilute sulphuric acid.

The fact that lead gives a visible coating of appreciable thickness is merely due to the porosity of the coating, and this appears to be an inherent property of lead and of its compounds. It is well known that lead plating on iron will not protect the iron from rust, etc., unless the coating is extremely thick compared with other electroplated metals. Similarly lead chloride will not protect a lead anode from further attack by chloride ions. If the anodic overvoltage compound is non-porous a coating of molecular thickness may be sufficient to show passivity phenomena, and such a coating would be invisible if its colour is similar to that of the underlying metal, or if it forms a solid solution in the metal surface. It may here be noted that the lead electrode, after the treatment described under 6A, was covered with a brilliant red coating closely resembling polished metallic copper.

Figs. 9 and 10 show the behaviour of nickel in the active state; figs. 11 and 12 in the passive state. The sudden rise of single potential together with the simultaneous appearance of transfer resistance when oxygen gas is liberated are well shown by these curves.

The curves for iron in the active state are similar to those for nickel, and it was considered unnecessary to reproduce them. Figs. 15 and 16 showing iron in the active state may be compared with figs. 11 and 12—the corresponding curves for nickel.

Figs. 13 and 14 were obtained by allowing the iron electrode to remain in the acid in the active state for some time until it was deeply etched, under which conditions it is much more difficult to render passive. When the current was increased to 200 milliamperes which would have been sufficient to induce passivity with the original electrode, the curve separated into three portions of which the two upper parts are really continuous although the photographs hardly show this. As the current was increased, the top portion became longer and brighter but maintained the same position vertically. At the same time the middle portion rose and finally coalesced with the top portion. Then, and not till then, the lowest portion suddenly rose to the position shown in figs. 15 and 16. The presence of the middle portion during partial passivity shows the existence of a "charging period" during which the passivity compound is being formed, and this compound is evidently destroyed very rapidly by local action on the electrode when the charging current is interrupted. The case of chromium,

figs. 17 and 18, is peculiar. Chromium is usually looked upon as a passive metal and it certainly has pre-eminently the power of inducing easy passivation in iron, a high-chromium steel electrode being rendered passive in 2 seconds by a current of 1 milliampere per square centimetre. Chromium metal, however, in dilute sulphuric acid or in dilute sodium hydroxide, solution fails to show some of the most characteristic features of true passivity.

(1) No sudden rise of single potential is observed in acid or alkali electrolyte. This may be due to passivity being induced by mere immersion.

(2) The observed anodic overvoltage is a negative quantity referred to a hydroxyl electrode, whereas that for the typically passive metals is strongly positive. Even highly attackable metals like aluminium or magnesium show positive overvoltages of 0.6 volt or more when passivated in alkali.

(3) Very little oxygen is liberated and the metal dissolves as chromate almost in accordance with Faraday's laws.

(4) The behaviour of chromium in hydrochloric acid is similar to that described above. At high current densities the anodic overvoltage with respect to chlorine is the same as that found with respect to hydroxyl in the present work, — 0.2 volt.

It appears, therefore, that although chromium may be regarded as a metal which is easily passivated with respect to the formation of  $\text{Cr}^{+++}$  ions, it cannot be passivated with respect to the formation of  $\text{Cr}^{VI}$  ions.

*The valve metals.*—It will be at once evident from an inspection of figs. 19-31 that we are here dealing with quite a different type of phenomena. Overvoltage and transfer resistance are absent and the curves are no longer discontinuous. The current passing is so small even with high applied potentials, and so rapidly falls when the applied potential is kept constant, that it is impossible to obtain curves for definite current densities. In these experiments, therefore, the applied potential was fixed, and only the average current observed. The appearance of the curves at once suggests the charging of a condenser through a low resistance and its discharge through a very high resistance. The condenser in this case is made up of the electrode as one plate and the electrolyte as the other, the dielectric being formed by a film of metallic oxide of high insulating power. The nature of this film determines the nature of the curves obtained. In the case of antimony the film is invisible but appears to dissolve very slowly in the acid, since a small current, 0.1 milliampere, persists at all voltages. With a tantalum anode the current was too small to detect with the milliammeter until 12 volts were applied, when a current of 0.02 ma. was observed. The film of oxide produced is therefore very thin, extremely

insoluble, and an excellent insulator, but at the same time this electrode shows a peculiar property not shared by antimony or bismuth. When the electrode is freshly cleaned and the experiments conducted fairly rapidly, the curves obtained are similar to those obtained with antimony. When, however, the electrode is used for some time with a high anodic voltage or still more so when the electrode has been exposed to the air for some time, it acquires a single potential of about 2 volts referred to the mercurous sulphate electrode. If this potential is disturbed by passing a current or by short-circuiting anode and cathode, and the disturbing force then removed, the single potential of the tantalum persistently but slowly returns to this value, usually taking from 1 to 3 seconds to do so. At the same time the electrode acquires a peculiar tendency to resist rapid changes of potential so that if a potential difference, of, say, 1 volt, be applied while the commutator is rotating at the usual speed, the rate of the return to 2 volts is so slow that the curve obtained is practically a straight line, and a series of such lines may be obtained by varying the applied voltage between 0.1 and 3 volts (see fig. 27). This behaviour, which is probably connected with the excellent rectifying power of tantalum for alternating currents, is difficult to explain, and the following suggestions are, therefore, made somewhat tentatively.

The tendency to acquire a definite potential of 2 volts referred to a mercurous sulphate electrode may be due either to the formation of minute quantities of an overvoltage oxide or to the very slow ionisation of the normal oxide. It cannot be due to ionisation of the metal itself as that would give a potential opposite in sign and differing by about 3 volts from that observed. A difficulty arises if the ionisation of the normal oxide be taken to account for the observed behaviour inasmuch as all the known ionising oxides are good electrical conductors (*e.g.*,  $\text{PbO}_2$ ,  $\text{MnO}_2$ , etc.), and this oxide is an excellent insulator. Possibly, therefore, a very small quantity of an ionising, electrically conducting, over-voltage oxide is formed and disseminated through the mass of non-conducting normal oxide. This would form a large number of very small condensers which could only discharge slowly through the insulating medium round them although that medium is intensely thin, and would thus account for the observed tendency to resist sudden changes of potential. A further suggestion is made later.

In the case of bismuth, the oxide coating is clearly visible and of appreciable thickness, and at the same time the current passing, though variable, is much greater than with antimony or tantalum. This is due, not to the lack of insulating power of the oxide itself but to the porosity of the film formed, being in fact parallel with the case of lead. The condenser formed is therefore a very

leaky one, and until the coating has attained a thickness of about 0.1 mm. its discharge is so rapid that the curves obtained, figs. 28-30, look like overvoltage curves. Careful examination of the oscillograph screen, however, shows that the curves are really continuous. The upper extremities of the lower portions of these curves are very hazy and attenuated, in marked contrast to the sharply defined ends of a true overvoltage curve. Unfortunately the photographs do not show this well, but fig. 31, taken when the coating had thickened considerably, shows it better than the other three.

In alkali electrolyte, bismuth behaves like antimony in acid. Bismuth and nickel in alkali, antimony and lead in acid or tantalum, and lead in acid may, therefore, be used as electrolytic rectifying cells for alternating current, but rectifying action may depend also upon the oxide film acting as a membrane permeable to hydrogen ions but not to hydroxyl.

It is possible with the data available from the curves, to calculate roughly the capacity of the condenser and also the thickness of the film of oxide forming the dielectric.

Thus in fig. 21 the potential of the antimony condenser falls from 2 volts to 1 volt during one-quarter revolution of the commutator, and the resistance between the filament and grid of the valve across which the condenser is discharging is of the order of one megohm.

The capacity of a condenser discharging from  $V_1$ -V through a resistance R in time  $t$  is given by

$$C = \frac{t}{R \log_e \frac{V_1}{V}}$$

In this case, therefore,  $C = \frac{3}{10} \times 10^{-6} / 0.7 = 10^{-7}$  farads approx.

$$\text{or} = 10^5 \text{ cms.}$$

This capacity, 0.1 micro-farad, is surprisingly large for a plate only 1 sq. cm. in area, and is due to the thinness of the oxide film.

Since most of the solid dielectrics known have a specific inductive capacity between 3 and 10, we shall probably be not far wrong in assuming that of the antimony oxide film to be about 5.

$$\text{Then} \quad C = \frac{KA}{4\pi d} \quad \text{or} \quad 10^5 = \frac{5 \times 1}{4\pi d}$$

$$\text{Whence} \quad d = 4 \times 10^{-5} \text{ mm. approx.}$$

Since molecular thickness is of the order of  $10^{-7}$  mm., it is quite conceivable that, in certain cases, condensers may be formed having a capacity of the order

of 10 microfarads per square centimetre. This suggests another possible explanation of the peculiar behaviour of tantalum. If the oxide film in this case is of molecular thickness, the time taken to discharge from 2 volts to 1 volt through a megohm resistance would be of the order of 30 seconds. The change of potential during 0.1 second under these circumstances would not appreciably affect the position of the oscillograph spot, and a nearly straight line would be obtained. This, however, does not account for the tendency shown by this electrode to acquire the definite potential of 2 volts already referred to, and it still appears necessary to assume the formation of traces of a true overvoltage oxide.

#### *Summary.*

The behaviour of a series of metallic anodes in dilute sulphuric acid has been investigated with the aid of the cathode ray oscillograph.

Unattackable electrodes and passive electrodes (when in the passive state) show the phenomena of overvoltage and transfer resistance similar in all respects to those observed during cathodic treatment.

Lead must be definitely placed among the passive electrodes along with nickel and iron, and the lead dioxide looked upon as an overvoltage compound.

Chromium is readily rendered passive with respect to the formation of tri-valent ions, but is still active with respect to the formation of hexavalent ions.

The cause of passivity is the formation of an insoluble, electrically conducting coating of an overvoltage compound which may or may not form a solid solution in the electrode surface.

The reason why the coating is of measureable thickness in the case of lead, but invisible with iron or nickel, is that the lead dioxide is slightly porous and permits deeper action on the electrode surface.

Valve action is due to the formation of an insoluble, electrically insulating coating of oxide or other compound forming the dielectric of a condenser of which the plates are electrode and electrolyte. The capacity of such condensers may be of the order of a micro-farad per square centimetre. The thickness of the coating in the case of antimony is calculated to be of the order of  $4 \times 10^{-5}$  mm., and in the case of tantalum it is probably of the order of  $10^{-6}$  mm.

It is suggested that the action of an electrolytic rectifier may be due partly to the condenser action outlined above, and partly to the oxide film acting as a semi-permeable membrane, permeable only to hydrogen ions.

[REDACTED]

1

2

3

4

5

6

7

8

9

10

11

12

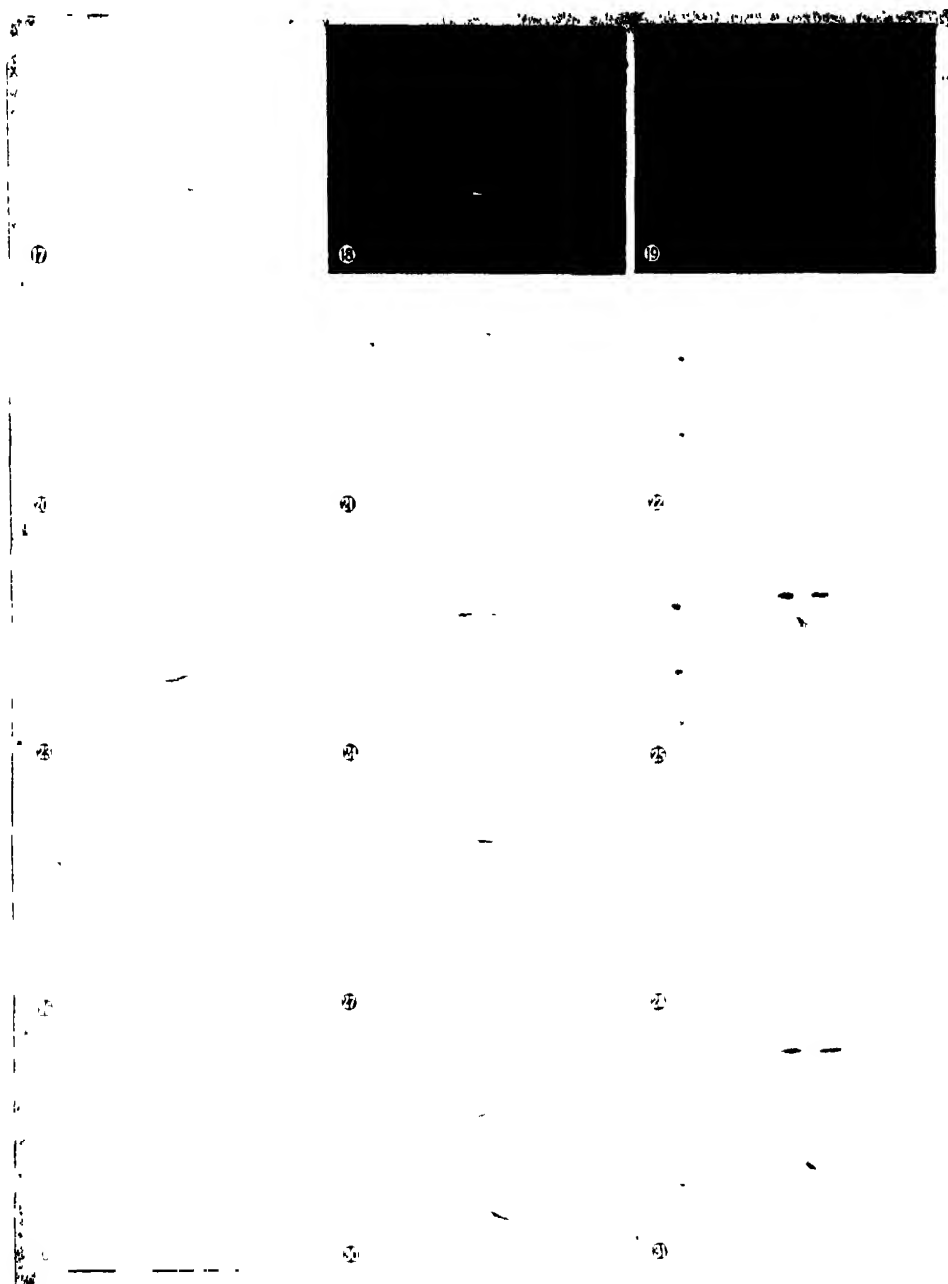
13

14

15

16

17



*The Energy of the Struck String.—Part I.*

By W. H. GEORGE, M.Sc., Ph.D., F.Inst.P., Moseley Student, and H. E. BECKETT, B.Sc., Research Student, University College, Nottingham.

(Communicated by Sir William Bragg, F.R.S.—Received December 24, 1926.)

[PLATES 11 AND 12.]

The paper deals with an investigation of the energy of the struck string studied by observation of the energy lost by the hammer during the impact. A systematic investigation was made of the influence of the position of the impact along the string and of the relative mass of hammer and string. For each value of the mass of the hammer a sharply defined position of impact was found at which maximum energy loss by the hammer occurs and the necessary conditions were studied in detail.

In the summary of results given at the end of the paper references are given to the figures in the text in which the results are shown graphically.

# 1. OBJECT OF THE EXPERIMENTS.

The subject seems of interest from two rather different points of view.

(1) The more obvious application of the work is to the acoustics of the pianoforte. This instrument is unique among important musical instruments, in that almost the whole of the desired amount of energy has to be given to the system in some small fraction (*e.g.*,  $1/500$ ) of a second before any sound is heard. In contrast with this, in the important families of the bowed-string instruments (violin, viola, 'cello, etc.) and in the wind instruments (organ, flute, oboe, clarinet, horn, trumpet, etc.) energy is given to the system almost continuously so long as sound is desired. One of the most fundamental problems of pianoforte acoustics would therefore appear to be that of determining the conditions under which the energy communicated to the system during the impact shall be a maximum consistent with certain qualitatively fixed conditions. Although the design of the pianoforte has been evolved entirely by empirical methods, it was from the first realised that its sounds were too weak and of too short duration, and it is of interest to note in the evolution of the instrument the gradual increase in the mass and tension of the strings, and the use of more than one string tuned to a given frequency as means to increase the initial energy of the system.



In the literature of the subject we have been unable to find any references to theoretical or experimental work on the energy of the struck string.

(2) The second point of view from which the work would appear to be of interest lies in its connection with the more general problem of absolute quantitative energy measurements in acoustics. The essential difficulty of these measurements lies in the minuteness of the absolute value of the energy of a single vibration of any sound of normal intensity. However, it may well be, as for example in the present work, that the complete time-integral of the energy can be measured. It would be of interest to investigate along similar lines the possibility of the use of a struck tuning fork as a standard source of sound and the method would be suitable for investigating the acoustics of bells and other percussion instruments.

## II. THEORY.

In the experimental work a small metal cylinder, suspended by threads so as to form a pendulum, could be made to impinge upon a horizontally stretched wire. The speed and hence the energy of the hammer before and after impact could be calculated from readings, upon a scale, of the position of the shadow of the hammer formed by a point source of light.

If the hammer, taken as a *particle* of mass  $m$ , impinges upon the string with speed  $v_0$  and rebounds with speed  $v$ , then, in the ideal case, the energy given to the string is equal to the energy lost by the hammer [ $\frac{1}{2}m(v_0^2 - v^2)$ ]. This quantity cannot in general be calculated, but the calculation can be made for a number of special cases by the aid of the Kaufmann\* theory. Although more general equations can be written, they can be solved only by very tedious approximate graphical or numerical methods. As the more general equations,† giving the duration of the impact and the speed of the hammer, which would have to be used to calculate the energy of the string cannot be solved analytically, and have not yet been tested experimentally over the range of the present work, their use here would hardly justify the labour involved. It is evident from an examination of figs. 1 to 8 which show the form of the relation between the position of the impact and the fraction of the initial energy lost by the hammer during the impact, each for a special value of the relative mass of hammer and string, that the analytical expression of the results will be very complicated.

\* 'Wied. Ann.,' vol. 54, pp. 675-712 (1895).

† Raman and Banerji, 'Roy. Soc. Proc.,' A, vol. 97, pp. 99-110 (1920); Das, 'Proc. Ind. Assoc.,' vol. 7, pp. 13-20 (1921), and vol. 9, pp. 297-322 (1926).

The following analysis refers to the part of the string between the bridge and the point at which the energy lost by the hammer during the impact is a maximum.

*Notation.* We shall assume that the string is infinitely thin, is perfectly flexible, is stretched between fixed supports, and that the motion is confined to the horizontal plane so that the influence of gravity may be neglected.

- $l$  = length of string between bridges.
- $a$  = distance of struck point from nearer bridge.
- $b$  = distance of struck point from farther bridge.
- $x$  = variable distance measured from a bridge along the equilibrium position of the string.
- $y$  = variable displacement of string perpendicular to the  $x$ -axis, parallel to and reckoned positive in the direction of the approaching hammer.
- $r$  = distance between string and axis of rotation of hammer.
- $v_0$  = initial velocity of hammer.
- $v$  = velocity of hammer at instant of separation of hammer and string.
- $c$  = speed of propagation of transverse waves on the string.
- $\mu$  = linear density of string.
- $m$  = effective mass of hammer -- mass of a particle distant  $r$  from axis of rotation and equimomental with the hammer.
- $m_0$  =  $m + \mu a/3$ .
- $m'$  = actual mass of hammer.
- $M$  = mass of string between bridges =  $\mu l$ .
- $s$  = number of partial tone.
- $0_s$  = period of  $s$ th partial.
- $n_s$  = frequency of  $s$ th partial.
- $\tau$  = duration of impact.
- $t$  = variable time reckoned from the beginning of the impact or as stated in the text.
- $A_s$  or  $B_s$  = amplitude of the  $s$ th partial.
- $E$  = Young's Modulus for the material of the string.
- $\omega k^2$  = moment of inertia of cross-section of string.
- $d_0$  = diameter of wire.

*Energy of the Hammer.*

*Impact at Mid-Point of String.*—We must assume that the duration ( $\tau$ ) of the impact is less than one period ( $\theta$ ) of the fundamental tone of the string. Then Kaufmann has shown that

$$\left(0 < \frac{t}{\theta} < \frac{1}{2}\right) \quad y = v_0 \theta \frac{m}{4M} \left(1 - e^{-\frac{4M}{m} \frac{t}{\theta}}\right), \quad (1)$$

$$\left(\frac{1}{2} < \frac{t}{\theta} < 1\right) \quad y = v_0 \theta \left\{ e^{-\frac{4M}{m} \frac{t}{\theta}} \left[ 2e^{\frac{2M}{m} \left(\frac{t}{\theta} - \frac{1}{2}\right)} - \frac{m}{4M} \right] - \frac{m}{4M} \right\}, \quad (2)$$

and

$$\frac{\tau}{\theta} = \frac{1}{2} + \frac{1}{4} \frac{m}{M} \left(1 + \frac{1}{2} e^{-\frac{2M}{m}}\right). \quad (3)$$

If we assume the hammer to be unyielding then  $\tau$  cannot be less than  $\theta/2$ . In our experiments the smallest value of  $\tau/\theta$  when  $a/l = 1/2$  was found to be 0.58 (when  $m/M = 0.137$ ), we are not, therefore, concerned with velocities derivable from equation (1). From (2) we have

$$\left(\frac{1}{2} < \frac{t}{\theta} < 1\right) \quad \frac{dy}{dt} = v_0 e^{-\frac{4M}{m} \frac{t}{\theta}} \left\{ -\frac{4M}{m} \left[ 2e^{\frac{2M}{m} \left(\frac{t}{\theta} - \frac{1}{2}\right)} - \frac{m}{4M} \right] \right\}, \quad (4)$$

whence using (3) we have

$$\left(\frac{1}{2} < \frac{t}{\theta} < 1\right) \quad \frac{1}{2} m (v_0^2 - v^2) = \frac{1}{2} m v_0^2 \left\{ 1 - 4e^{-2\left(1 + \frac{1}{2} e^{-\frac{2M}{m}}\right)} \right\}. \quad (5)$$

*Impact near a Bridge.*—In this case Kaufmann did not solve the equations rigorously, but introduced an approximation by supposing that the shorter portion of the string remains straight during the impact, that is the influence of its vibrations is neglected. The influence of its inertia is included in the factor  $m_0 = m + \mu a/3$ . The solutions obtained were:—

$$\left(0 < \frac{t}{\theta} < \frac{b}{l}\right) \quad y = \frac{v_0 \theta}{\sqrt{\frac{M}{m_0} \left(4 \frac{l}{a} - \frac{M}{m_0}\right)}} e^{-\frac{M}{m_0} \frac{t}{\theta}} \cdot \sin \left\{ \frac{t}{\theta} \sqrt{\frac{M}{m_0} \left(4 \frac{l}{a} - \frac{M}{m_0}\right)} \right\}, \quad (6)$$

and

$$\left(\frac{b}{l} \leq \frac{t}{\theta}\right) \quad \frac{\tau}{\theta} = \frac{1}{\sqrt{\frac{M}{m_0} \left(4 \frac{l}{a} - \frac{M}{m_0}\right)}} \tan^{-1} \left\{ \frac{\sqrt{\frac{M}{m_0} \left(4 \frac{l}{a} - \frac{M}{m_0}\right)}}{-2 \frac{l}{a} + \frac{M}{m_0}} \right\}. \quad (7)$$

From (6) we have

$$\left(0 < \frac{t}{\theta} < \frac{b}{l}\right) \frac{dy}{dt} = \frac{v_0 e^{-\frac{M}{m_0} \cdot \frac{t}{\theta}}}{\sqrt{\frac{M}{m_0} \left(4 \frac{l}{a} - \frac{M}{m_0}\right)}} \cdot \left\{ \sqrt{\frac{M}{m_0} \left(4 \frac{l}{a} - \frac{M}{m_0}\right)} \cos \left[ \frac{t}{\theta} \sqrt{\frac{M}{m_0} \left(4 \frac{l}{a} - \frac{M}{m_0}\right)} \right] - \frac{M}{m_0} \sin \left[ \frac{t}{\theta} \sqrt{\frac{M}{m_0} \left(4 \frac{l}{a} - \frac{M}{m_0}\right)} \right] \right\}, \quad (8)$$

whence using (7) we have : -

$$\frac{1}{2} m (v_0^2 - v^2) = \frac{1}{2} m v_0^2 \left\{ 1 - e^{-\frac{2M}{m_0} \frac{t}{\theta}} \frac{1}{\sqrt{\frac{M}{m_0} \left(4 \frac{l}{a} - \frac{M}{m_0}\right)}} \tanh^{-1} \left[ \frac{\sqrt{\frac{M}{m_0} \left(4 \frac{l}{a} - \frac{M}{m_0}\right)}}{-2 \frac{t}{\theta} + \frac{M}{m_0}} \right] \right\}. \quad (9)$$

### Energy of the Vibrating String.

In the ideal case the energy of the vibrating string in terms of the amplitudes of the partials can readily be determined by simple physical considerations. As the ideal conditions are never completely realised in experimental work it is important to note them. They are that the string is (i) infinitely thin ; (ii) perfectly flexible ; (iii) stretched between fixed supports ; (iv) vibrating in a horizontal plane ; (v) not giving up energy to the surrounding space, and that the vibrations are of such small amplitude that (vi) the square of the inclination of any part of the string to its initial direction may be neglected ; and (vii) the tension remains constant throughout the motion. The third of these conditions is the most difficult to realise as is shown by the very considerable intensity of the sounds heard when a string is vibrating. The energy radiated by the string itself is exceedingly small.

In the present work the ratio (i) of diameter to length of string is 1/3430. To avoid the difficulty which arises through the change in the plane of vibration of the string, observations of the amplitude of vibration were made upon the *initial* vibrations. The optical system used for obtaining the photographic records was accurately focussed for motion in a horizontal plane so that with the large magnification used any departure from this plane by the vibration string causes the effects of bad focussing in the resulting photograph. The ratio of the *largest* amplitude to the appropriate length of the string was 1/1024.

The shape of the string is given by :—

$$y = \sum_{n=1}^{\infty} \sin \frac{\pi n x}{l} \left( A_n \cos \frac{\pi n c t}{l} + B_n \sin \frac{\pi n c t}{l} \right), \quad (10)$$

and the velocity of any point at any time by :—

$$\frac{dy}{dt} = \sum_{s=1}^{\infty} \frac{s\pi c}{l} \sin \frac{s\pi x}{l} \left[ B_s \cos \frac{s\pi ct}{l} - A_s \sin \frac{s\pi ct}{l} \right]. \quad (11)$$

If we consider the string to be sounding only the  $s$ th partial then at times given by an integral multiple of 0,  $y$  is zero for all values of  $x$ , and the energy of the string's vibration is wholly kinetic. Equation (11) then reduces to

$$\frac{dy}{dt} = \pm \frac{s\pi c}{l} B_s \sin \frac{s\pi x}{l}, \quad (11a)$$

and the kinetic energy due to the sounding of the  $s$ th partial is given by :—

$$\frac{1}{2} \mu \int_0^l \left( \frac{dy}{dt} \right)^2 dx = \frac{1}{2} \mu \frac{s^2 \pi^2 c^2}{l^2} B_s^2 \int_0^l \sin^2 \frac{s\pi x}{l} dx = \frac{1}{4} \mu \frac{s^2 \pi^2 c^2}{l} B_s^2 = \pi^2 n_s^2 M B_s^2.$$

Hence the total energy of motion of the vibrating string is given by :—

$$\pi^2 n_1^2 M \sum_{s=1}^{\infty} s^2 B_s^2. \quad (12)$$

This expression agrees with that derived by a different method by Rayleigh.\*

*Effect of Stiffness of String.*—We may determine the increase in the potential energy of the deformations of the string due to its stiffness by assuming that the shape of the deformations is still that given by equation (10) from which we have

$$\frac{d^2 y}{dx^2} = - \sum_{s=1}^{\infty} \frac{s^2 \pi^2}{l^2} \sin \frac{s\pi x}{l} \left( A_s \cos \frac{s\pi ct}{l} + B_s \sin \frac{s\pi ct}{l} \right).$$

Since the curvature at any point of the string is small the potential energy of the deformation is then given by :—

$$\begin{aligned} \frac{1}{2} E \omega k^2 \sum_{s=1}^{\infty} \frac{s^4 \pi^4}{l^4} \left( A_s \cos \frac{s\pi ct}{l} + B_s \sin \frac{s\pi ct}{l} \right)^2 \int_0^l \sin^2 \frac{s\pi x}{l} dx \\ = \frac{1}{128} \pi E d^4 \sum_{s=1}^{\infty} \frac{s^4 \pi^4}{l^4} \left( A_s \cos \frac{s\pi ct}{l} + B_s \sin \frac{s\pi ct}{l} \right)^2 \cdot \frac{l}{2}. \end{aligned} \quad (13)$$

Since when  $t = 0$ ,  $y = 0$  for all values of  $x$ , we have  $A_s = 0$ . The potential energy of deformation due to a single partial is a maximum when  $t = 0_s/4$  and the value is then given by :—

$$\text{P.E.}_{\max} = \frac{1}{256} \frac{\pi^5 E d^4}{l^3} \cdot s^4 B_s^2. \quad (13a)$$

Throughout the present work this is equivalent to  $2.467 s^4 B_s^2$  ( $E = 9 \times 10^{11}$ ;  $d = 0.0926$  cm.;  $l = 317.6$  cm.)

\* 'Sound,' vol. 1, p. 186.

*Special Cases.*—When  $s = 1$  the maximum value of  $B_s$  was 0.3 cm., giving  $P.E._{max} = 0.222$  ergs. The corresponding vibrational energy was 45,820 ergs.

When  $s = 3$  the maximum value of  $B_s$  was 0.0358 cm., giving

$$P.E._{max.} = 0.256 \text{ ergs (vibrational energy} = 5492 \text{ ergs).}$$

When  $s = 7$  the maximum value of  $B_s$  was 0.008 cm., giving

$$P.E._{max} = 0.409 \text{ (vibrational energy} = 1614 \text{ ergs).}$$

Hence we may conclude that under the conditions of the present work the influence of the stiffness of the string may be neglected.

### III. EXPERIMENTS.

A portion of the apparatus is shown in Plate 11.

*The String*, consisting of steel piano wire of diameter 0.0926 cm., was stretched horizontally across bridges (B) supported about 3 metres apart on massive iron brackets which were firmly clamped to roof posts of the laboratory. Tuning was effected by altering the tension of the wire by screw devices attached to the brackets.

*The Hammer* (H) which in conception was a simple pendulum consisted of a metal (brass or steel) cylinder suspended from two points (S) by four threads. In the equilibrium position the axis of the cylinder was horizontal and perpendicular to the string, and the wedge shaped end of the cylinder just touched the string. The width of the contact as shown by measuring the width of the bright speck left when the hammer had impinged on the smoked string was less than 0.2 mm., or about  $1/16000$  of the string's length. The impact may, therefore, be said to occur at a *point*.

*Optical Arrangements.*—The two points of suspension of the hammer threads were on a framework which could be moved upon joists (J) parallel to the string. The same framework carried a "Pointolite" lamp (P) so fixed that the point source lay in the axis of rotation of the hammer. This source cast upon a horizontal scale (outside the field shown), situated about 1 metre below the string, a shadow of a fine wire pointer passing through the centre of gravity of the hammer. The whole apparatus is so designed that the position of any important part of it is adjustable in three mutually perpendicular directions.

*The Hammer-Velocity* ( $v_0$ ) at the beginning of the impact is adjustable by varying the original inclination ( $\phi_0$ ) with the vertical, of the radius vector. In order that the initial energy of the hammer can be calculated from observations of  $\phi_0$  it is necessary to ensure that the hammer falls *freely* from *rest*. This

was secured by using an electro-magnetically operated mechanical release (M) in which the part in contact with a wire loop attached to the back of the hammer moved initially with high speed along the path of the hammer and in the same direction. Since the path of the hammer is a circular arc of radius about 55 cm., whilst its shadow moves along a plane scale perpendicular to the equilibrium vertical radius vector ( $h$ ), small differences in the position ( $d$ ) of the hammer when at rest at the end of its rebound from the string are easily read ( $\Delta d = h \sec^2 \phi \Delta \phi$ ).

If  $\phi_0$  be the initial inclination with the vertical of the line joining the centre of gravity of the hammer with the axis of its path, then the speed  $v_0$  of the centre of gravity of the hammer immediately before the impact is given by:—

$$v_0 = \left\{ \frac{2m'r^2g}{I} [1 - \cos \phi_0] \right\}^{\frac{1}{2}},$$

where  $m'$  is the actual mass of the hammer and  $I = m' \left[ \frac{d_0^2}{16} + \frac{l_0^2}{12} + r^2 \right]$ . If the

hammer were taken as a particle we should have  $I = mr^2$ . In order to show how nearly the hammer system approximates to a simple pendulum the values of  $m$  and  $m'$  for three of the hammers are shown in Table I.

Table I.—Approximation of Hammer System to a Simple Pendulum.

$m/M$	Diameter of hammer $d_0$ .	Effective length of hammer $l_0$ .	$r$	Actual mass of hammer $m'$ .	$m$ .	Per cent. difference.
0.5	cm. 0.53	cm. 5.0	cm. 55.5	gm. 8.49	gm. 8.496	0.07
1.0	0.65	6.4	55.9	16.99	17.01	0.12
4.77	1.26	7.7	55.8	81.04	81.17	0.16

#### *Distribution of the Energy of the Hammer.*

In the design of the hammer system the chief aim was simplicity in order that the greater part of the energy of the hammer should be represented by the kinetic and potential energy of its mass as a whole, these quantities being easily measureable. The compound pendulum used in previous work was rejected because of the uncertainty of the energy losses due to flexure of the shaft and friction of the axle in its bearings. The system actually used has been shown to approximate very closely to a simple pendulum. That part of its energy

due to the initial displacement from the vertical becomes distributed as follows :—

- (i) In the rebound.
- (ii) In vibrations set up in the string system.
- (iii) In vibrations set up in the hammer system.
- (iv) In permanent deformations of hammer and string due to their imperfectly elastic properties ; and
- (v) In friction losses.

The study of (i) forms the main part of the present work. Some work has, however, been done on (ii). For 32 special cases the necessary experimental observations were made to determine the amplitude of the vibration of the first seven partials of the string, and the results will be given in a later part of the work.

Since the hammer never quits the string before the original wave set up by the impact has again reached it after reflection at the nearer bridge, it follows that the energy given up to the string will depend also on the nature of the bridges and supports. Except for the very lightest hammer ( $m/M = 0.137$ ) waves are reflected several times before the impact is ended. The energy of the vibration of the bridges and supports is not dealt with in the present instalment of the work throughout which the same string, bridges and supports were used.

(iii) The vibration of the hammer system consists of two parts :—the vibration of the hammer as a whole, and the longitudinal elastic vibration of the metal rod. The mass of the four threads by which the hammer was supported was of the order 0.1 gm., whilst the mass of the hammers varied from 2.32 to 81.04 gm. Hence the energy lost by the vibration of the threads may be neglected. The supports to which they were attached were sufficiently massive and firm to be unaffected by the motion. Considering now the vibration of the metal rod as a whole, it may be noted that the vertical motion is unaffected by the impact. There is, therefore, no tendency to set up vibration in a vertical plane about an axis parallel to the string. The absence of vibration in a horizontal plane about a vertical axis was found by observation of the shadow of the hammer.

The energy of the longitudinal elastic vibrations of the metal rod, which are evident in the high pitched metallic ringing sound heard as the hammer rebounds from the string whose vibrations have been quickly damped immediately after the impact, will be discussed in a later instalment of the work.

(iv) With the actual experimental conditions of this work permanent deforma-



tion of the hammer faces or the string could not be detected. Any influence due to lack of uniformity in the elastic properties of the string would not be detected as the identical string was used throughout.

(v) Friction losses between the hammer face and the string may be neglected as there would be little if any tendency for relative motion between the hammer and the struck point of the string on account of the large radius (55 cm.) of the arc along which the hammer moves, and the small amplitude (say, 0.2 cm.) of the motion at the struck point.

The loss due to air friction on the hammer could be determined experimentally by raising the framework (P in Plate 11) so that the hammer passed over the string instead of striking it. The logarithmic decrement was thus determined for the hammer  $m/M = 0.5$  and was found to be 0.0084. Observations showed that for any hammer the displacement after three half swings from rest was almost equal to the original displacement. The loss due to air friction may, therefore, be neglected.

Another slight loss of energy is that due to the air pulse set up by the sudden retardation of the hammer during the impact. In a typical case (see Plate 12, fig. 8) the hammer originally moving with a speed of 65 cm./sec. is brought to rest in a space of about 0.3 cm. and in a time of about 0.0075 second. This pulse together with the vibrations of the metal cylinder causes the noise of the impact.

#### IV. RESULTS.

On account of the large number of variables which are known, or which might reasonably be expected, to influence the phenomena of the struck string a preliminary survey was made to determine which factors had the greatest influence on the energy changes during the impact, and it was found that the relative striking place and mass of the hammer were the two most important variables. These two were studied in considerable detail, but before giving the results of this, the larger part of the work, some consideration will be given to the influence of other variables.

##### *Influence of Single Variables.*

*Tension of String.*—Throughout the whole of the present work the string was stretched under high tension (125.4 lbs. wt. as compared with 170 lbs. wt. used in pianofortes) and the influence of change of tension was not studied experimentally. It may, however, be shown theoretically that when high tensions are used *the fraction of its initial energy lost by the hammer is independent of the*

*tension.* By substituting for  $l$  in equations (4) and (8) the values of  $\tau$  given by equations (3) and (7) respectively we have

$$\frac{v/v_0}{(a/l = 1)} = 2e^{-\left(1 + 4e^{-\frac{2M}{m}}\right)}$$

and

$$\frac{v/v_0}{(a/l = 1)} = e^{-\frac{M}{m_0} \frac{1}{\sqrt{\frac{M}{m_0} \left(1 + \frac{l}{a} - \frac{M}{m_0}\right)}} \tan^{-1} \left\{ \frac{\sqrt{\frac{M}{m_0} \left(1 + \frac{l}{a} - \frac{M}{m_0}\right)}}{1 + \frac{l}{a} + \frac{M}{m_0}} \right\}}$$

and the right-hand sides of these expressions are quite independent of the tension. It is important to note this for it follows that small changes in the velocity of rebound of the hammer would not be produced by the change of tension of the wire caused by unavoidable changes in the temperature of the laboratory and other factors.

*Stiffness of the String.*—It has already been shown theoretically that under the conditions of the present work this factor has not an important influence on the energy changes.

*Initial Velocity ( $v_0$ ) of the Hammer.*—The influence of this factor has been studied in considerable detail, and an account of the results will be given in Part II of the work. It may be stated here that the initial velocity of the hammer is not an important variable, and its value in the work here discussed was kept constant at about 65 cm. per second, the exact value in any case is given in the tables.

*Relative Position ( $a/l$ ) of Impact and Mass ( $m/M$ ) of Hammer.*—The influence of these two factors is set out in Table II. The first column gives the distance ( $a$ ) in cm. of the impact from the nearer bridge. The other columns giving the actual observed scale readings of the position of the hammer after its rebound from the string show for each value of  $a$  in column V the mean of 10 readings of  $d$  and in columns II to IV and VI to X the mean of five readings. In no case was the difference between the greatest and smallest reading of  $d$ , for any given value of  $a$  and  $m$ , greater than 1 mm.

The general nature of the results is best seen in figs. 1 to 8 in each of which the fraction of its initial energy lost by the hammer during the impact is plotted against the distance ( $a$ ) of the impact from the nearer bridge. Assuming the string system to be symmetrical about the central plane the complete figures are all symmetrical about the mid-point ordinate of ( $a$ ). The individual points used in plotting the curves are too close together to be indicated, and no attempt has been made to draw smooth curves through series of points. The curves

Table II.  $-l = 317.6$  cms.;  $\theta = 0.01875$  sec.;  $\mu = 0.0535$  grs./cm.; $d_0 = 45.0$  cms.

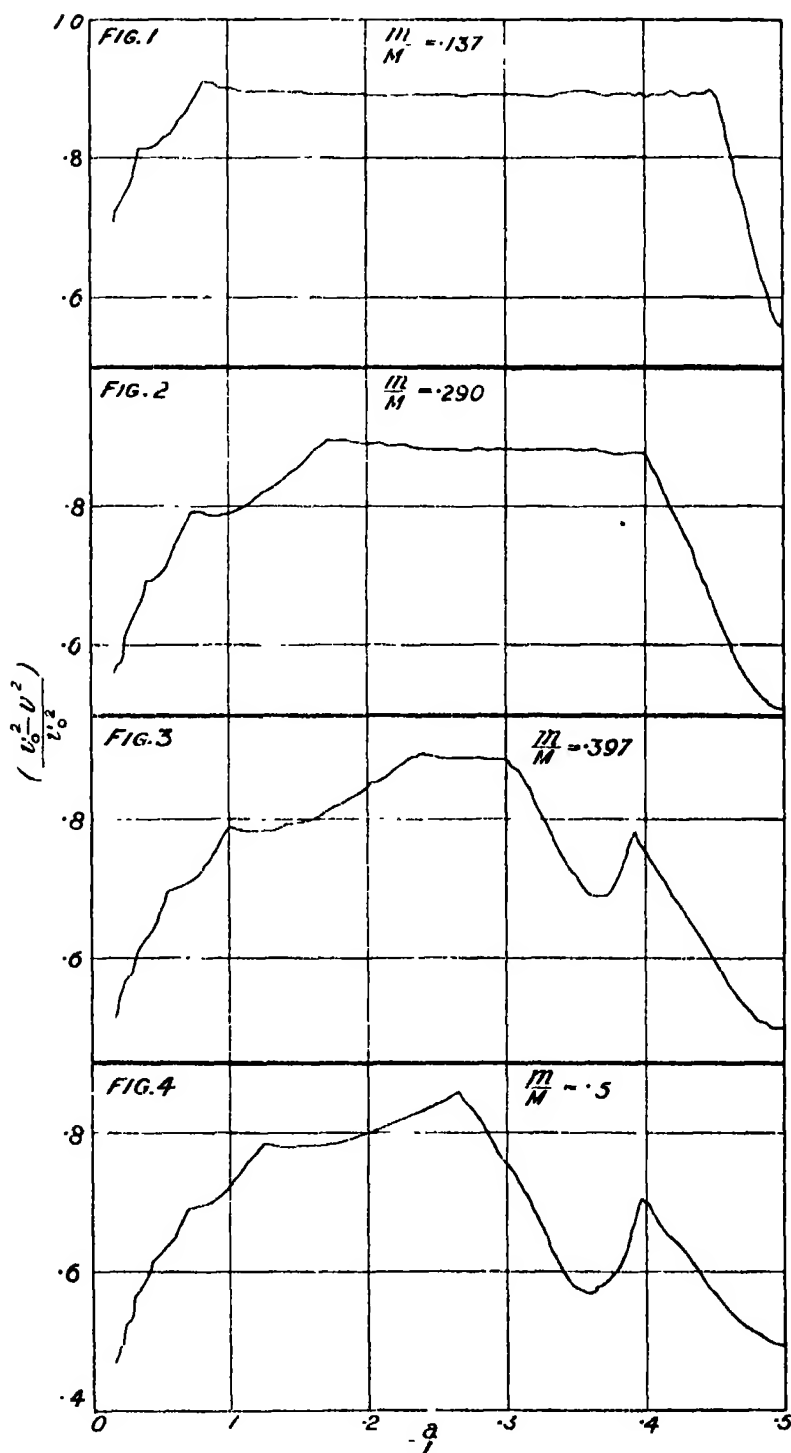
$m$ M $r_0$ cm. sec. $r$ cm. $h$ cm.	0.137 61.89 55.2 156.6	0.200 64.89 55.2 156.6	0.397 64.85 55.1 156.6	0.5 64.83 55.5 157.3	0.5 64.89 55.6 157.3	1.0 65.00 55.9 157.3	1.686 65.00 55.8 157.3	3.0 65.06 55.9 157.3	4.769 65.00 55.8 157.3
$a$ cm.	mean $d$ cm.								
5.2	--	--	--	32.51	--	35.60	--	--	--
5.3	--	--	--	--	--	--	--	38.90	--
5.5	23.92	--	--	--	32.40	--	37.40	--	--
5.6	--	29.1	--	--	--	--	--	--	--
5.7	--	--	31.0	--	--	--	--	--	--
5.8	--	--	--	--	--	--	--	--	39.90
6.0	23.00 <sup>c</sup>	28.9	30.5	31.91	31.90	35.28	--	38.80	--
7	22.80	28.4	30.0	31.51	31.48	34.60	36.72	38.46	39.50
8	22.10	27.4	29.0 <sup>x</sup>	30.43	30.50	34.00	36.40	37.98	39.38
9	21.48	26.9 <sup>d</sup>	28.9	30.33	30.40	33.50	35.92	37.70	39.10
10	20.56	26.5	28.2	29.17 <sup>b</sup>	29.30	33.36	35.60	37.50	38.98
11	19.00 <sup>h</sup>	25.9	27.4	28.96	29.10	32.50	35.08	37.00	38.70
12	19.00 <sup>h</sup>	25.0	27.0	--	28.70	32.50	34.98	36.82	38.48
12.7	--	--	--	28.35	--	--	--	--	--
13	19.10	24.0 <sup>c</sup>	26.9 <sup>d</sup>	--	28.30	32.00	34.50	36.78	38.10
14	19.00	24.0 <sup>c</sup>	26.5	27.46 <sup>b</sup>	27.40	31.60	34.40	36.50	38.00
15	18.90	24.0 <sup>c</sup>	26.0	--	27.20	31.00	33.98	36.40	37.90
15.9	--	--	--	26.94	--	--	--	--	--
16	18.60	--	25.5	--	27.00	31.00	33.78	36.00	37.50
17	18.10	23.5	24.8	--	26.92	30.80	33.50	35.94	37.50
17.8	18.10	--	--	26.61	--	--	--	--	--
18	18.10	23.0	24.2 <sup>c</sup>	--	26.70	30.50	33.30	35.50	37.40
18.9	--	--	--	26.41	--	--	--	--	--
19	17.50	22.5	24.2 <sup>c</sup>	--	26.14	30.00	32.88	35.44	37.10
20	17.00	22.0	24.1	25.54	25.70	29.50 <sup>x</sup>	32.62	35.10	37.00
21	16.60	21.5	--	--	25.10	29.50 <sup>x</sup>	32.50	35.00	36.90
21.2	--	--	--	25.00	--	--	--	--	--
22	16.08	20.7	23.9	--	24.52	29.48	32.48	34.80	36.60
23	15.40	20.0 <sup>h</sup>	--	--	24.50	29.34	32.10	34.60	37.00
24	14.90	20.0 <sup>h</sup>	23.4	24.30 <sup>c</sup>	24.50	--	31.90	34.40	37.50
25	14.00	--	--	--	24.50	28.62	31.50	34.30	38.02
26	13.20 <sup>a</sup>	20.1	22.8	--	24.44	28.50	31.50	34.02	38.62
26.5	--	--	--	24.33	--	--	--	--	--
27	13.10	--	--	--	24.30	28.10	31.30	34.00	39.26
28	13.20	20.3	22.1	24.10	24.10	27.60 <sup>b</sup>	31.10	33.88	39.54
29	13.36	--	--	--	23.98	27.46	31.00	33.88	40.10
30	13.50	20.2	21.0	23.52	23.80	--	30.98	33.80	40.60
31	13.50	--	--	--	23.50	27.48	30.60	33.50	41.00
31.8	--	--	--	23.22	--	--	--	--	--
32	13.58	20.0	20.0 <sup>h</sup>	--	23.30	--	30.40	33.48	41.12
33	13.60	--	--	--	22.90	27.20	29.98	33.80	41.48
33.5	--	--	--	22.56	--	--	--	--	--
34	13.88	19.8	20.3	--	22.60	--	29.90	34.48	41.90
35	13.90	--	--	--	22.20	27.00	29.90	35.00	42.00
35.3	--	--	--	21.95	--	--	--	--	--
36	13.96	19.5	20.4	21.63	21.72	--	29.80	35.60	42.38
37	13.90	--	--	--	21.40	26.80	29.60	36.10	42.30
38	13.96	19.0	20.4	21.01	21.00	26.50	29.60	37.00	42.44
39	13.96	--	--	--	20.50	26.24	29.60	37.44	42.50
39.7	--	--	--	20.43 <sup>h</sup>	--	--	--	37.98	--
40	14.00	18.7	20.3	--	20.46	26.00	--	37.98	42.60
41	14.00	--	--	20.46	20.48	25.80	29.38	38.00	42.90
42	14.02	18.4	20.3	--	20.50	25.40	29.10	38.50	42.84

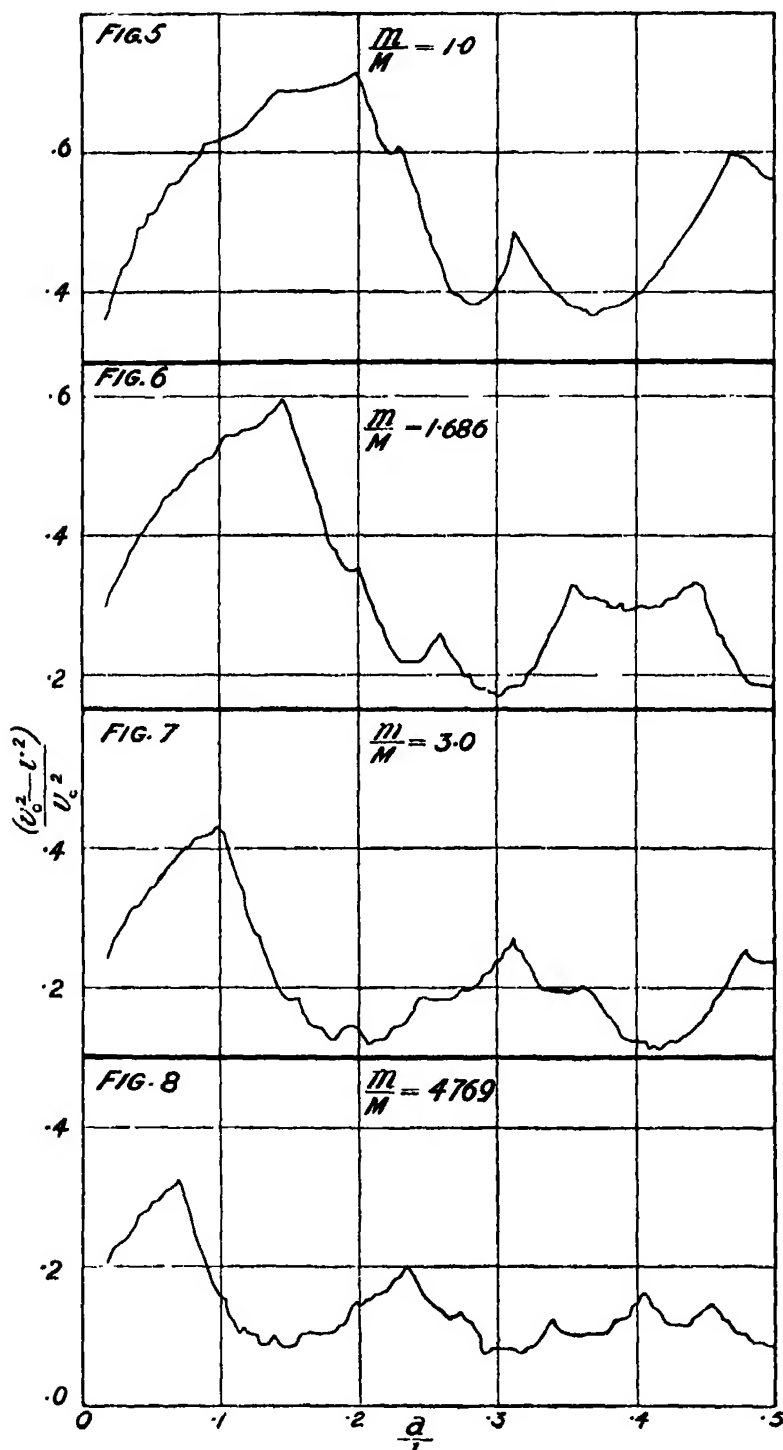
Table II—(continued).

$a$ cm	mean $d$ cm.								
43	14.08	—	—	20.56	20.52	25.02	28.96	39.00	42.80
44	14.10	17.7	20.0	—	20.58	24.80	28.76	39.50	42.60
45	14.12	—	—	—	20.60	24.60 <sup>c</sup>	28.52	39.96	42.80
45.1	—	—	—	20.60	—	—	—	—	—
46	14.10	17.0	19.9	—	20.60	24.60 <sup>c</sup>	28.20	40.12	42.92
47	14.10	—	—	—	20.56	—	28.40	40.42	42.92
48	14.10	16.5	19.8	20.54	20.50	24.60 <sup>c</sup>	28.86	40.50	42.90
49	14.20	—	—	—	20.50	24.60 <sup>c</sup>	29.52	40.50	42.90
50	14.20	15.8	19.6	20.54	20.50	24.56	30.10	40.50	42.60
51	14.20	—	—	—	20.50	—	30.70	40.90	42.60
52	14.20	15.0	19.3	—	20.50	24.54	31.40	41.04	42.48
52.9	—	—	—	20.47	—	—	—	—	—
53	14.20	—	—	—	20.40	—	31.94	41.42	42.50
54	14.20	14.2	19.0	—	20.36	21.48	32.50	41.50	42.50
55	14.30	—	—	—	20.40	—	33.08	41.50	42.50
56	14.30	14.0 <sup>A</sup>	18.7	20.41	20.30	24.40	33.90	41.00	42.50
57	14.30	—	—	—	20.12	—	34.48	41.80	42.40
58	14.30	14.0	18.4	—	20.10	24.20	34.96	41.90	42.34
59	—	—	—	—	20.08	—	35.02	41.80	42.12
60	14.30	14.1	18.1	20.01	20.00	23.98	35.50	41.58	42.00
61	—	—	—	—	19.94	23.90	35.80	41.48	41.90
62	14.30	14.2	17.6	—	19.86	23.72	35.90	41.48	41.52
63	—	—	—	—	19.80	23.60	35.80	41.50	41.30
63.5	—	—	—	19.60	—	—	—	—	—
64	14.40	14.3	17.0	—	19.62	24.10	35.76	41.62	41.40
65	—	—	—	—	19.50	24.70	36.40	41.82	41.28
66	14.40	14.4	16.6	—	19.42	25.50	36.98	41.90	41.22
67	—	—	—	—	19.40	26.08	37.48	41.98	41.06
68	14.40	14.5	16.2	19.02	19.30	27.00	37.92	41.90	41.00
69	—	—	—	—	19.10	27.50	38.12	41.90	40.98
70	14.40	14.5	15.6	—	18.98	27.80	38.50	41.90	40.90
71	—	—	—	—	18.90	28.00	39.00	41.62	40.70
72	14.40	14.6	15.0	18.54	18.70	27.92	39.10	41.52	40.48
73	—	—	—	—	18.56	27.70	39.42	41.50	40.40
74	14.30	14.7	14.5	—	18.46	28.22	39.48	41.40	40.00
75	—	—	—	—	18.40	28.90	39.50	41.08	39.94
76	14.30	14.8	14.3 <sup>A</sup>	18.04	18.02	29.50	39.50	41.00	40.21
77	—	—	—	—	17.96	30.02	39.50	40.52	40.60
78	14.30	14.8	14.3 <sup>A</sup>	—	17.80	30.64	39.48	40.40	40.90
79	—	—	—	—	17.52	31.48	39.32	40.48	41.10
79.4	—	—	—	17.48	—	—	—	—	—
80	14.30	14.9	14.4	—	17.42	32.00	39.00	40.48	41.40
81	—	—	—	17.06	17.30	32.56	38.82	40.50	41.48
82	14.40	14.9	14.5	16.92	17.10	33.04	38.40	40.50	41.58
83	—	—	—	16.67	16.96	33.50	38.66	40.48	41.70
84	14.50	15.0	14.5	—	16.60	33.98	38.98	40.48	41.90
85	—	—	—	16.44	16.42	34.38	39.30	40.44	41.80
86	14.50	15.0	14.5	17.06	17.20	34.50	39.50	40.34	41.86
87	—	—	—	17.60	17.98	34.54	39.70	40.10	41.64
88	14.40	15.0	14.5	17.77	18.00	34.80	39.98	40.10	41.32
89	—	—	—	—	18.20	34.90	40.00	40.02	42.04
90	14.36	15.0	14.5	18.83	19.00	34.90	40.40	39.98	42.30
91	—	—	—	—	19.60	34.90	40.50	39.90	42.48
92	14.30	15.1	14.5	20.08	20.40	34.70	40.52	39.60	42.80
93	—	—	—	—	20.90	—	40.52	39.48	42.80
94	14.20	15.0	14.6	20.99	21.30	34.50	40.70	39.42	42.96
95	—	—	—	—	21.70	—	40.70	39.02	43.00
96	14.20	15.0	14.7	—	22.00	33.90	40.80	38.98	43.06
97	—	—	15.4	22.23	22.50	—	40.60	38.60	43.06
98	14.30	15.0	15.5	22.60	23.00	32.90	40.52	38.50	43.08
99	—	—	16.1	—	23.50	33.30	40.50	38.10	43.10

Table II—(continued).

a cm.	mean d cm.								
100	14.40	15.0	17.0	23.69	24.10	33.50	40.48	38.40	43.20
101	—	—	17.4	—	24.52	33.90	40.40	38.62	43.20
102	14.40	15.0	18.3	24.89	25.10	34.10	40.00	38.90	43.00
103	—	—	19.0	—	25.70	34.50	39.90	39.20	43.00
104	14.46	15.0	19.5	25.77	26.20	34.90	39.80	39.50	42.90
105	—	—	19.8	—	26.80	35.06	39.42	39.90	42.68
106	14.40	14.9	20.9	26.53	27.10	35.40	39.00	40.00	42.48
107	—	—	21.4	—	27.60	35.60	38.58	40.00	42.10
108	14.20	15.0	21.8	27.58	28.00	35.80	38.30	40.01	42.00
109	—	—	22.4	—	28.50	35.96	38.00	40.10	42.20
110	14.00	15.0	23.0	28.52	28.90	36.10	37.62	40.10	42.40
111	—	—	23.1	—	29.10	36.40	37.30	40.20	42.48
112	14.00	15.1	23.4	28.90	29.40	—	36.52	40.20	42.50
113	—	—	24.0	—	29.50	36.50	36.52	40.20	42.50
114	13.98	15.1	24.4	29.01	29.50	36.52	36.70	40.00	42.52
115	—	—	24.5	—	29.50	36.66	36.94	39.88	42.50
116	14.10	15.1	24.5	28.74	29.46	36.66	37.00	40.00	42.50
117	14.20	—	24.5	—	29.30	36.90	37.00	40.14	42.50
118	14.48	15.2	24.5	28.45	29.00	36.80	37.00	40.48	42.50
119	14.48	—	24.4	—	28.90	36.70	37.06	40.60	42.50
120	14.40	15.2	24.0	28.00	28.40	36.60	37.20	40.90	42.38
121	14.20	—	23.4	—	28.10	36.60	37.40	41.02	42.30
122	14.38	15.2	22.5	26.98	27.50	36.50	37.40	41.20	42.06
123	14.40	—	22.0	—	27.00	36.00	37.40	41.50	42.00
124	14.40	15.2	20.9	25.77	26.40	36.48	37.30	41.82	41.90
125	13.82	—	20.5	—	25.40	36.30	37.50	41.90	41.80
126	14.00	15.2	21.1	23.92	24.48	36.20	37.50	41.98	41.50
127	14.40	15.4	21.8	24.25	24.68	36.00	37.48	42.02	41.40
128	13.82	16.0	22.1	24.49	25.00	35.96	37.40	42.04	41.02
129	14.20	16.6	22.6	—	25.20	35.84	37.40	42.02	41.00
130	14.20	17.5	23.0	25.26	25.58	35.56	37.41	42.20	41.30
131	14.40	18.3	23.5	—	25.90	35.40	37.40	42.10	41.50
132	14.10	18.9	23.9	25.86	26.40	35.04	37.40	42.20	41.60
133	13.90	19.8	24.3	—	26.50	34.98	37.40	42.26	41.90
134	14.30	20.2	24.6	—	26.90	34.54	37.08	42.10	42.00
135	14.40	20.8	25.0	26.59	27.10	34.30	37.00	42.02	42.00
136	14.50	21.5	25.4	26.86	27.32	34.04	37.00	42.00	42.00
137	14.50	22.2	25.9	—	27.76	33.84	36.82	41.98	42.02
138	14.30	22.9	26.3	27.55	28.00	33.50	36.68	41.84	42.00
139	14.20	23.4	26.5	27.85	28.22	33.30	36.60	41.74	42.00
140	14.40	24.0	26.9	28.07	28.48	33.00	36.50	41.68	41.90
141	14.40	24.5	27.4	—	28.80	32.70	36.48	41.48	41.80
142	13.90	25.1	27.8	28.78	29.10	32.40	36.54	41.30	41.70
143	14.00	25.8	28.1	—	29.40	32.00	37.00	41.00	41.58
144	14.90	26.4	28.5	29.33	29.66	31.66	37.50	40.88	41.40
145	16.50	26.9	28.9	—	30.00	31.40	37.92	40.50	41.50
146	18.40	27.4	29.1	29.85	30.20	31.00	38.50	40.30	41.60
147	19.40	27.8	29.4	—	30.40	30.50	38.60	40.00	41.90
148	21.00	28.4	29.9	30.41	30.50	29.98	39.00	39.78	42.00
149	21.94	28.9	30.0	—	30.88	29.80	39.20	39.46	42.20
150	22.90	29.2	30.3	30.58	30.90	—	39.50	39.00	42.40
151	24.00	29.6	30.5	—	31.00	30.00	39.88	38.70	42.50
152	25.40	29.9	30.9	30.88	31.08	30.00	40.02	38.60	42.50
153	26.40	30.3	31.0	—	31.26	—	40.28	38.78	42.70
154	27.20	30.5	31.0	31.13	31.40	30.36	40.48	38.92	42.80
155	27.70	30.6	31.2	—	31.40	30.50	40.50	39.00	42.80
156	28.60	30.9	31.3	31.38	31.50	—	40.48	39.00	42.80
157	29.00	31.0	31.3	—	31.50	30.90	40.48	39.00	42.90
158	29.30	—	—	—	—	—	—	—	—
158.8	29.30	31.0	31.4	31.53	31.50	31.00	40.48	39.00	42.90





follow the values directly calculated from the observed readings of the rebound of the hammer, and *no* corrections have been applied. Emphasis is not laid upon the small variations, of the order  $1/40$  of the large squares indicated on the figures, as these are possibly within the limits of experimental error. The effect upon the value of  $1 - (v^2/v_0^2)$  of an error of 1 mm. in the scale reading ( $d$ ) of the rebound of the hammer is shown in Table III for several values of  $d$ , when  $d_0 = 45$ .

Table III.

$d$ .	Per cent. error in $d$ .	Value of $1 - (v^2/v_0^2)$ ( $d_0 = 45$ ).	Per cent. error in $1 - (v^2/v_0^2)$ ( $d_0 = 45$ ).
13.1	0.76	0.910	0.15
21.6	0.46	0.761	0.29
31.6	0.32	0.492	0.65
38.5	0.26	0.256	1.51
41.0	0.24	0.161	2.55
42.2	0.24	0.114	3.68
42.8	0.23	0.091	4.70
43.2	0.23	0.078	5.48

A comparison of this table with figs. 1 to 8 will show that all the main fluctuations of the curves are outside the limits of experimental errors. The greatest percentage error of 5.5 is represented by  $1/50$  of the large squares. Before these results are discussed it is important to note that *wherever an attempt at repetition was made the results here given were always obtained*. The results shown in Table II, Column VI, were obtained quite independently after an interval of three months and should be compared with those shown in Column V.

It will be seen that for very light hammers,  $m/M = 0.4$  or less (figs. 1 to 3), the energy lost by the hammer increases rapidly as the impact occurs further and further from the bridge until a maximum point is reached. After this the energy lost remains constant until the mid-point of the string is approached, when the energy lost rapidly decreases. The length of string over which the energy changes are constant is shorter the heavier the hammer, until for a hammer of mass one-half that of the whole string the feature is lost altogether and we have a sharply defined maximum. With further increase of the mass of the hammer this maximum moves nearer and nearer to the bridge and at the same time diminishes, that is the *fractional* loss of energy by the hammer diminishes. Subsidiary maxima between the mid-point of the string and the

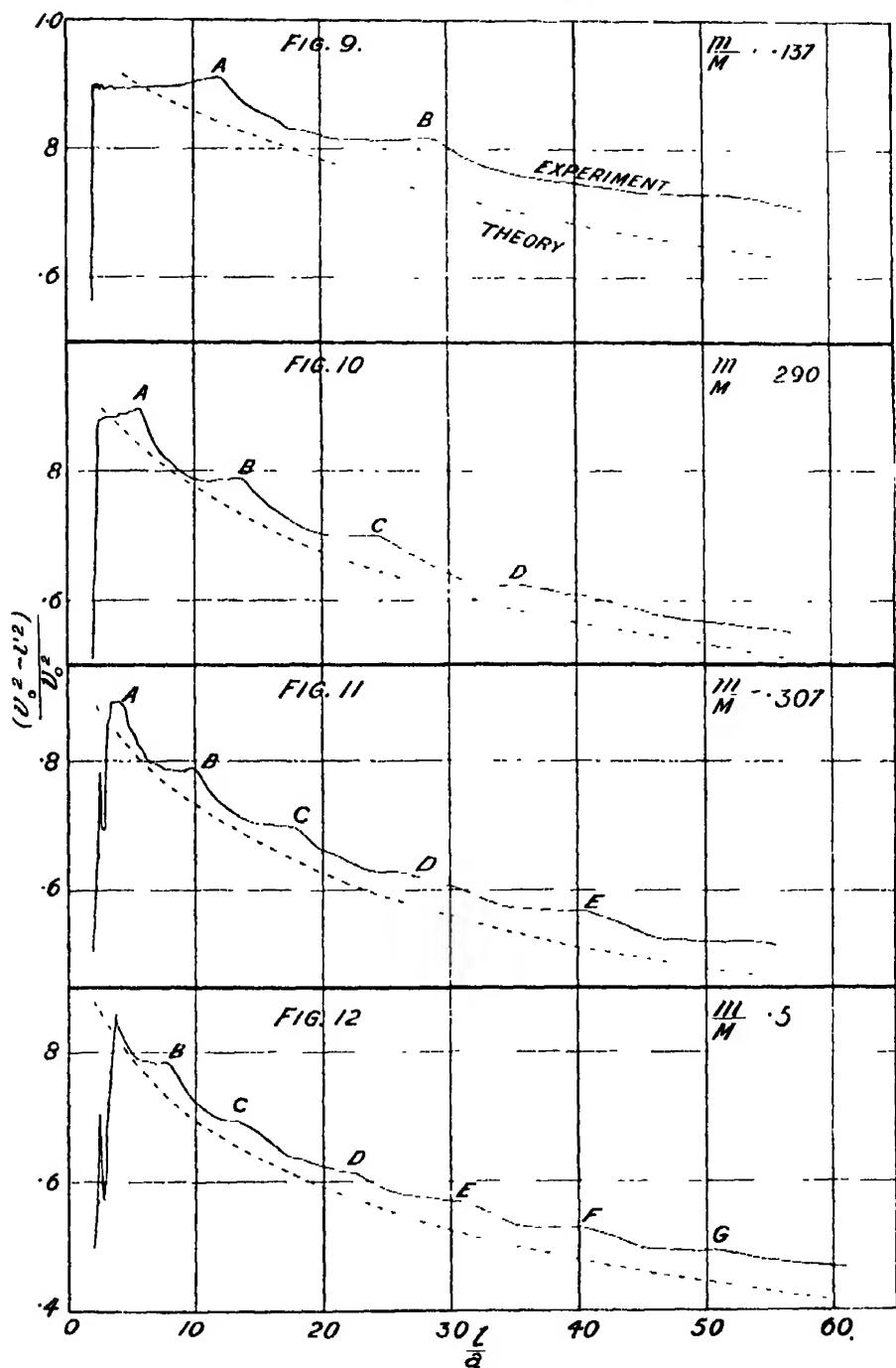


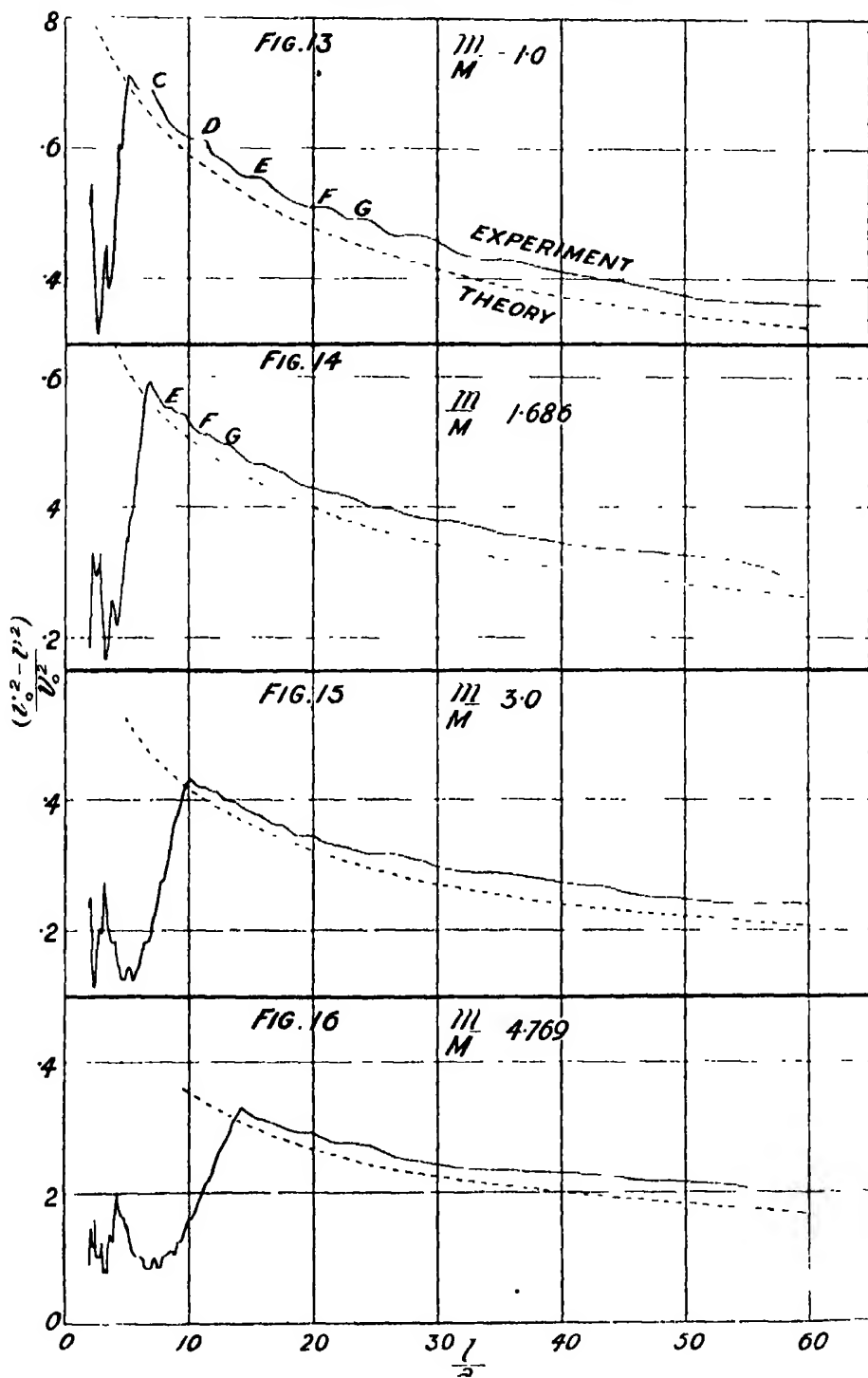
point of maximum energy loss by the hammer become more and more important as the mass of the hammer is increased.

*Wave Propagation along the String.* It is natural to suppose that this factor has an important influence on the phenomena of the struck string. Under the conditions of this work the speed of propagation of transverse disturbances is constant, the waves travelling the length of the string twice in one period of the fundamental tone. This is, of course, quite independent of the mass of the hammer. The duration of the impact is, however, strongly influenced by the mass of the hammer. On the whole, when other conditions are the same, the duration of the impact is greater the greater the mass of the hammer. Hence we may suppose that the complex subsidiary maxima especially shown in figs. 5 to 8 are due to the fact that the heavier hammers remain in contact with the string for a longer period of time and waves reflected from *both* bridges become increasingly important. Proceeding on these lines it seems natural to consider each of the curves of figs. 1 to 8 in two parts, i.e., the portion between the nearer bridge and the point of maximum energy transference and the remaining portion between this point and the mid-point of the string. The physical justification for this division is given later in fig. 18. Considering now the first portion of the curves reference should be made to figs. 9 to 16 in which the fraction of the hammer's initial energy lost during the impact is, in each figure, plotted against the position ( $l/a$ ) of the impact. The broken curves show the theoretical values obtained by *neglecting* the vibrations of the shorter piece of string (see equation (9)). It is hoped in a later instalment of the work to give the more exact treatment which involves data on the duration of the impact. It will be seen that the increase in the energy loss of the hammer as the impact occurs further and further from the bridge, follows, in the main, an exponential law. It is probable that the small fluctuations superimposed on this exponential curve are due to the vibrations of the shorter piece of the string, and it is natural to suppose that at such points as those marked in figs. 9 to 14 with the same letters A, B, etc., the later experimental work will show that at these positions in spite of the change in mass of the hammer the records of the impact will be of the same type.

A note may here be made on the second and more complex part of the curves shown in the right-hand sides of figs. 1 to 8. The necessary data on the duration of the impacts and on the pressure changes are not yet available, but some qualitative information is given in a paper by Prof. Raman and B. Banerji.\* A graph is there reproduced showing the change with the position of the striking

\* 'Roy. Soc. Proc.,' A, vol. 97. p. 108 (1920).





point in the value of the duration of the impact as measured by the ballistic galvanometer method for the value  $m/M = 1.68$ . No scale is indicated, no list of experimental values is given, and the theoretical and experimental curves are shown in different figures so that it is not possible to make numerical comparisons. However, if the right-hand portion of fig. 6 of the present paper be inverted and placed so that the mid-point ordinate of the curve lies on that of the Raman-Banerji curve it will be seen that this ordinate is a line of approximate symmetry. This would indicate that there is a tendency for the energy lost by the hammer during the impact to be less the greater the duration of the impact. This would not be inconsistent with the physical mechanism of the impact, for the longer the hammer remains in contact with the string, the more chance there is of its regaining some of its lost energy from the impulse travelling in both directions along the string.

#### V. SOME PROPERTIES OF THE POINT OF MAXIMUM ENERGY TRANSFERENCE.

We discuss now the maximum point on each of figs. 1 to 8 at which points the energy lost by the hammer is a maximum.

*Influence of Mass of Hammer on Position of Maximum.* -In the full curve of fig. 17 the relative position ( $a/l$ ) of the impact when the energy lost by the hammer is a maximum, is plotted against the relative mass ( $m/M$ ) of the hammer. In the broad straight line the position is plotted in terms of ( $l/a$ ). The branched

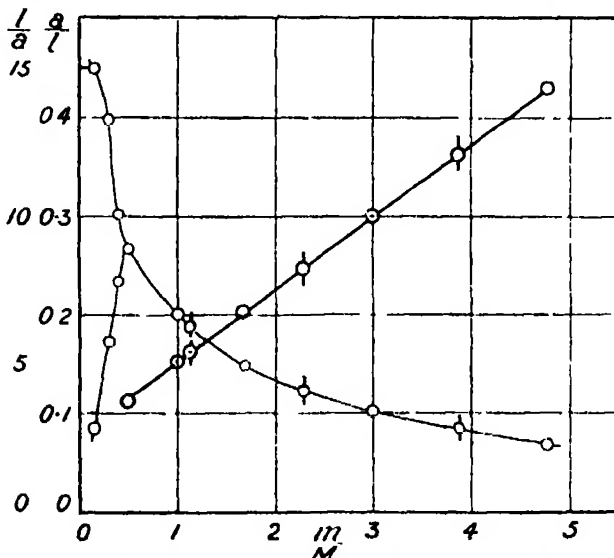


FIG. 17.—Influence of mass ( $m$ ) of hammer upon position of impact for maximum energy transference from hammer to string.

portion of the full curve shows the limits of the two ends of the flat part of the energy curves (figs. 1 to 3).

In order to test the linear relation between the relative position ( $l/a$ ) of the impact for maximum energy change and the relative mass ( $m/M$ ) of the hammer, observations were made for two other values of  $m/M$  (2.28 and 3.86) in the regions where the maximum points were expected to occur. The observations are shown in Table IV, and the points on the graph are shown by the special mark of a vertical line through them. The value for  $m/M = 1.12$  was obtained from a complete survey with this hammer, the results of which are not given in this paper.

Table IV.—Verification of Linear Relation shown in fig. 17.

$$l = 317.6 \text{ cm.}; h = 150.6 \text{ cm.}$$

$m = 38.77 \text{ gm.}; m/M = 2.282; r = 55.1$   
 cm.;  $v_0 = 64.85 \text{ cm./sec.}$ ; initial energy  
 $= (1/2) mv_0^2 = 81530 \text{ ergs.}$

$m = 65.65 \text{ gm.}; m/M = 3.864; r = 55.2$   
 cm.;  $v_0 = 64.89 \text{ cm./sec.}$ ; initial energy  
 $= 138220 \text{ ergs.}$

$a \text{ cm.}$	Mean $d \text{ cm.}$	$\frac{v_0^2 - v^2}{v_0^2}$	$a \text{ cm.}$	Mean $d \text{ cm.}$	$\frac{v_0^2 - v^2}{v_0^2}$
32	32.00	0.478	21	36.20	0.339
33	31.82	0.486	22	36.00	0.347
34	31.50	0.493	23	35.80	0.352
35	31.50	0.493	24*	35.50	0.362*
36	31.50	0.493	25	35.50	0.362*
37	31.50	0.493	26	35.50	0.362*
38*	31.40	0.498*	27	35.60	0.357
39	31.44	0.496	28	36.00	0.347
40	32.00	0.478	29	36.62	0.324
41	32.50	0.463	30	37.30	0.300
42	33.18	0.442			

*Duration of Impact.*—There are considerable difficulties in the measurement of this quantity and for accurate work it is desirable to use both the photographic and the oscillograph methods,\* each of which gives at the same time information on the pressure changes occurring during the impact.

As the oscillograph used in previous work was not available, the duration of the impact at the maximum points was determined by the photographic method, and the results are shown in Plate 12, figs. 1 to 8, and in fig. 18. In Plate 12, figs. 1 to 8, are reproduced photographic displacement-time records of the

\* George, 'Roy. Soc. Proc.,' A, vol. 108, pp. 284–295 (1925), and 'Phil. Mag.,' vol. 84, pp. 34–43 (1924).

impact In each figure the time axis is horizontal and positive from right to left. The upper line records the motion of the observed *point* of the string and in each case begins with a straight line showing the point to be at rest. Beneath this straight line is the edge of a dark patch inclined to the straight line, showing the motion of the hammer. This shows in each figure that the hammer approaches with uniform velocity, and rebounds with a smaller uniform velocity. (see especially fig. 1) corresponding to the energy lost during the impact. In fig. 8 it is difficult to see any difference in the slope of the two edges of the dark patch since the fractional loss of energy here is so small. At the point where the dark patch and the straight line meet contact begins. It will be seen that at first there is no change in the slope of the straight edge, indicating that at the beginning of the impact the observed point of the string starts to move with the velocity of impact of the hammer. When the maximum displacement is reached the hammer has lost all its kinetic energy since it is momentarily at rest. Although the struck point of the string is also at rest other parts of the string are in motion, and at this instant the energy of the string is partly kinetic and partly potential, whilst the energy of the hammer is wholly potential. The rebound then commences and differences in the motion of the hammer and the struck point of the string are evident.

In order to measure the duration of the impact the point on the photographic record at which separation of hammer and string is shown must be determined. An examination of the records will show the difficulty of this determination. In fig. 4 the hammer and string appear to separate and then make contact again twice before the impact is ended, whilst in fig. 1 there is only one separation. It is clearly desirable to obtain in each case information concerning the pressure changes during the impact, and to define clearly what is meant by "duration of impact." It is hoped to discuss this in later instalments of the work. Examination of many records of the type shown in Plate 12 suggests that in many cases the impact consists of a direct contact and separation followed by one or more contacts and separations, and the oscillograph method has shown that these subsequent contacts are sufficient to make electrical contact between hammer and string. It has not yet been determined whether the subsequent contacts affect the motion of the string.

To revert now to the records shown in Plate 12: measurements were made of the times, reckoned from the beginning of the impact, at which separations occurred. For example, from fig. 6 two values were obtained. The results, expressed as fractions of the fundamental free period of the string, are plotted in fig. 18 against the relative mass of the hammer. The highest values lie on

a horizontal straight line for which  $\tau/\theta = 1$ , and are clearly due to the original wave which has traversed the whole length of the string twice. Taking the next

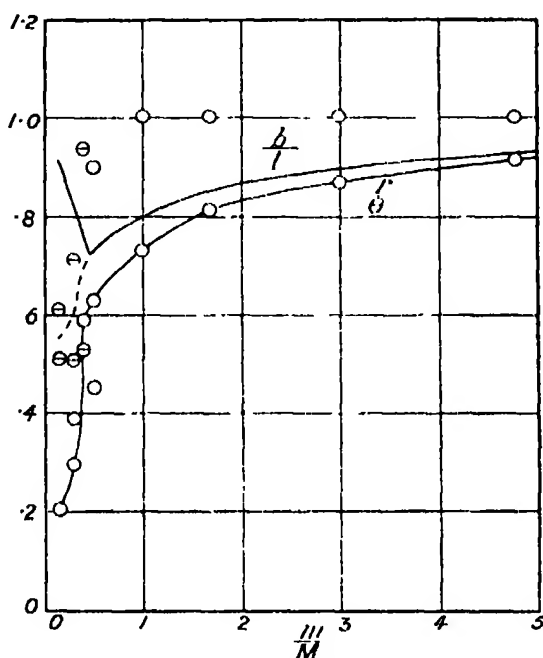


FIG. 18.—Relation of wave propagation along the string to the conditions giving maximum energy transference from hammer to string.

set of values of  $\tau/\theta$  and plotting for comparison the corresponding values of the ratio of the longer portion of the string ( $b$ ) to the whole length ( $l$ ), it will be seen that  $\tau/\theta$  is nearly equal to, but is always less than,  $b/l$ . Hence we may conclude that *when the energy lost by the hammer is greatest the conditions are such that the hammer rebounds just before the wave reflected from the farther bridge has again reached the place of impact.*

**Maximum Energy Changes.**—An examination of the upper full curve of fig. 19, in which the fraction of the hammer's initial energy lost during the impact is plotted against the relative mass ( $m/M$ ) of the hammer, will show that as the mass of the hammer increases the maximum fraction of its energy lost decreases continuously. The points marked with a vertical line show, as before, values obtained by a restricted survey near the positions predicted from the previous work. The dotted curve shows the theoretical values given by equation (9). That the theoretical values are always less than the experimental is to be expected as no corrections are here made to allow for the violation of the conditions set out at the beginning of the theoretical part. It will be noted

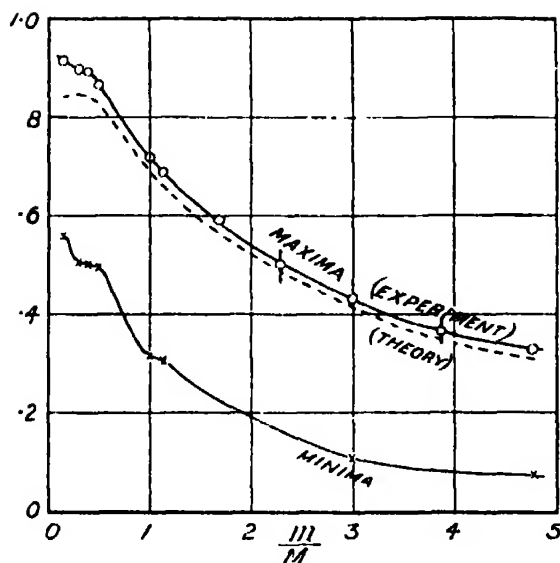


FIG. 19. Influence of mass ( $m$ ) of hammer upon the maximum fraction of its initial energy transferable to the string.

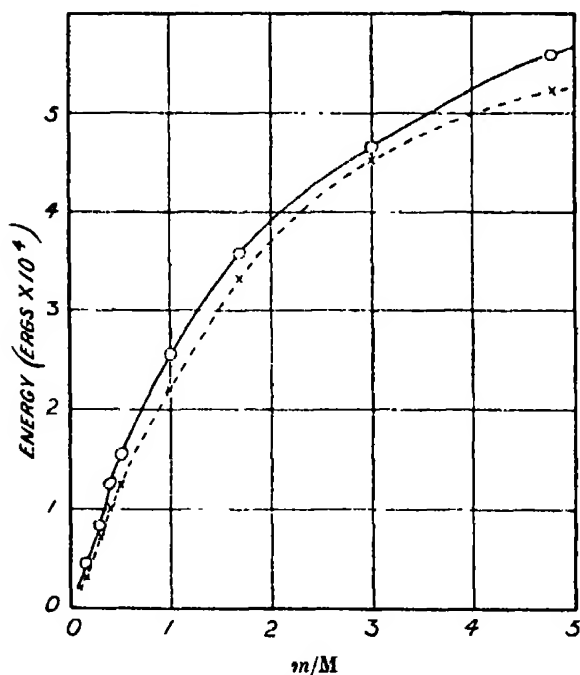


FIG. 20.— Influence of mass ( $m$ ) of hammer upon the maximum energy transferable to the string when the initial velocity of the hammer is constant (*cf.* fig. 19).



that the theory agrees with experiment over the range of values of  $m/M = 0.5 - 5.0$ . The lower full curve shows the minimum values and is given for comparison.

When the initial value of the velocity of the hammer is kept constant the absolute value of the maximum energy lost by the hammer *increases continuously* with increase in the mass of the hammer. This is shown in the full curve of fig. 20 in which the absolute value in ergs of the energy lost by the hammer is plotted against the relative mass ( $m/M$ ) of the hammer. For comparison the broken curve is given showing the absolute value in ergs of the sum of the energies of the first seven partials of the vibrating string (see equation (12)) as determined experimentally. Details will be given in a later part.

## VI. SUMMARY OF RESULTS.

For the impact of a metal hammer at a point of a struck string : -

(1) The energy lost by the hammer is a discontinuous function of the position of the impact (figs. 1 to 8).

(2) As the position of the impact moves away from a bridge the energy lost by the hammer increases exponentially until a point of maximum energy loss is reached (figs. 9 to 16).

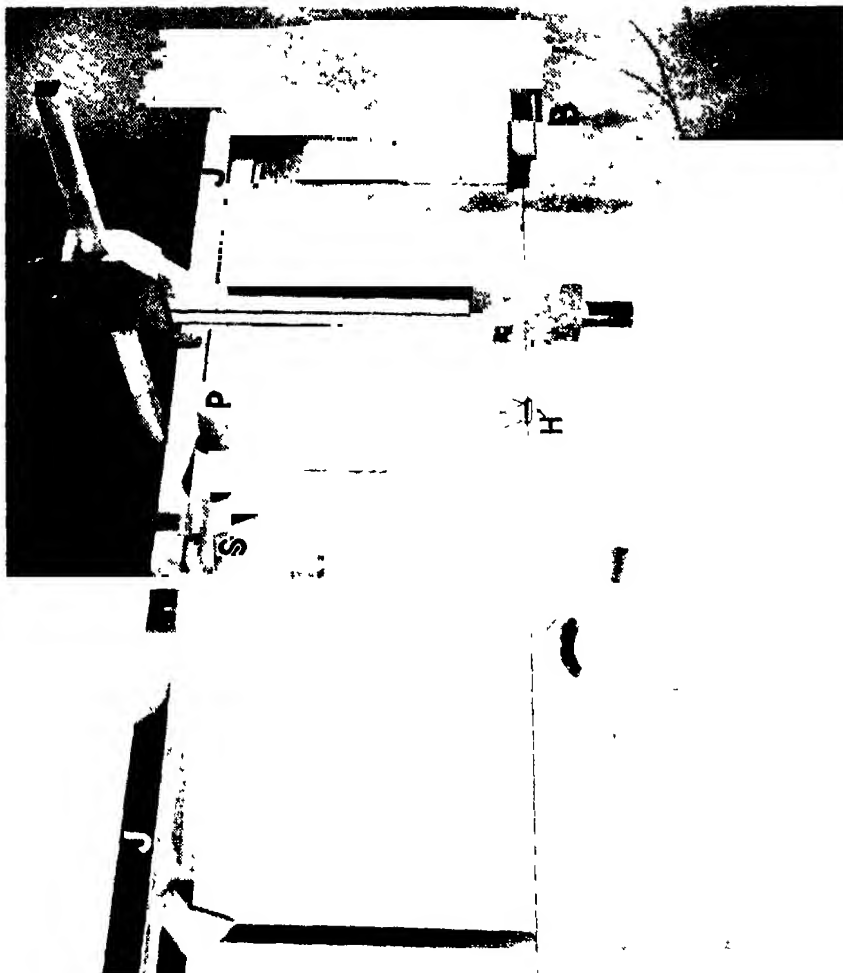
(3) The position of the point of maximum energy loss is a continuous function of the mass of the hammer and is nearer the bridge the heavier the hammer. A linear relation holds between the relative mass ( $m/M$ ) of hammer ( $m$ ) and string ( $M$ ) and the relative position ( $l/a$ ) of the impact, for the range of values  $m/M = 0.5 - 5.0$  (fig. 17).

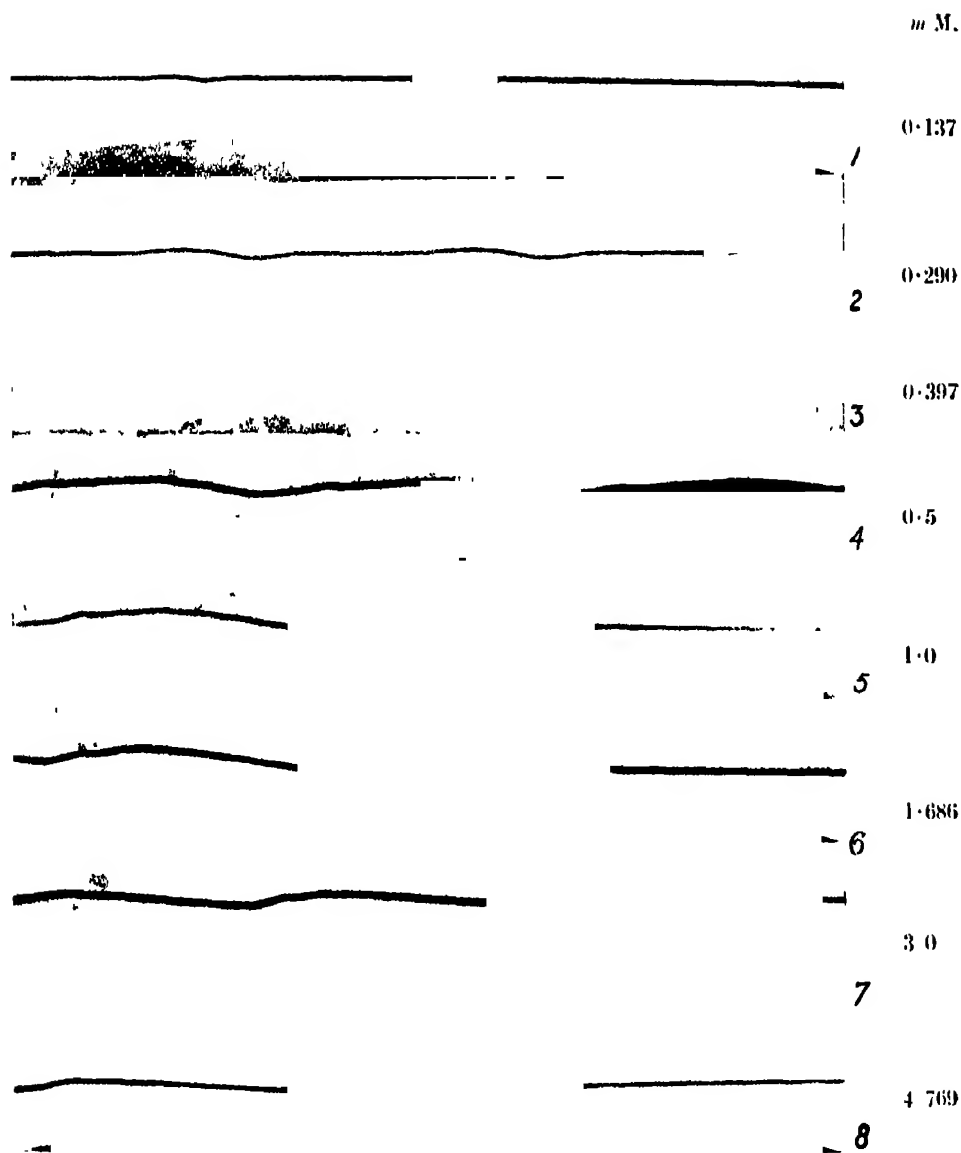
(4) Measurement of the duration of the impact shows that for maximum energy loss by the hammer, the conditions are such that the hammer rebounds just before the wave reflected from the farther bridge reaches the point of impact (fig. 18).

(5) The maximum fraction of the hammer's initial energy lost during the impact *decreases* continuously with increase in the mass of the hammer (fig. 19), but the absolute value of the energy lost *increases* continuously with increase in the mass of the hammer (fig. 20).

(6) For very light hammers,  $m/M$  of the order 0.3, the energy lost by the hammer remains almost constant at its maximum value as the position of the impact is moved for a considerable distance along the string (figs. 1 and 2).

Since the phenomena of the struck string are influenced by the *relative* position of the impact and not by its absolute value, Table II serves to





Photographic displacement-time curves of impact when maximum transference of energy from hammer to string takes place. For explanation see text, p. 133.

indicate at what positions of impact, for each of the eight values of the relative mass of the hammer, future investigations of other phenomena might suitably be made.

*Acknowledgments.*

We wish to thank the Royal Society and the Department of Scientific and Industrial Research for financial aid, and Prof. P. E. Shaw for his kindness in continuing to provide for the work the facilities originally provided by the late Prof. W. H. Barton, F.R.S.

---

*On Detonation of Gaseous Mixtures of Acetylene and of Pentane.*

By A. EGERTON, F.R.S., and S. F. GATES, B.Sc., M.A.

(Received December 2, 1926)

[PLATES 13-16.]

If a combustible gas at atmospheric pressure is ignited near one end of a tube and the rate of supply of heat by combustion is greater than the loss by radiation and conduction, the progress of the flame will be rapidly accelerated. Of a sudden, detonation may occur. A detonation wave travels forward at a nearly uniform rate, combustion proceeding simultaneously and a "retonation" wave travels back through the burnt gases from the "position of detonation." The discovery of the detonation wave by Berthelot and the researches of Mallard and Le Chatelier and of Dixon thereon are matters of history.

The purpose of the work described in this communication was to find the position at which a burning mixture of gases would develop a detonation wave under certain fixed conditions. The influence on such position of a change of strength of the combustible gas mixture and then of the nature of the diluent gas was studied. The effect of the addition of small quantities of certain "antiknock" compounds has also been investigated.

It is obvious that with so many combustible vapours and so many diluent gases and variable conditions of initial temperature and pressure, it was necessary to confine the investigation to certain substances and certain mixtures. The work was limited to the study of detonation in mixtures of acetylene and of pentane vapour in presence of the amount of oxygen required for complete

combustion and diluted with varying amounts of nitrogen, oxygen, argon, carbon dioxide and excess of fuel.

Investigations have shown\* that a change of rate of combustion is produced by a change in the diameter of the tube in which the combustion is carried out. The wider the tube up to a certain limit, the later will detonation set in. Tubes of the same diameter and material have therefore been used throughout this work.

*II. Experimental Methods.*—It is unnecessary to give a detailed description of the apparatus employed. Tubes 150 cm. by 0.9 cm. internal diameter, flanged at both ends, were closed by movable brass plates ground flat to the flange on the tubes. Strings attached to the plates were arranged to remove either or both ends, and at the moment of removal to make the contact for the igniting spark. A condensed discharge between rounded platinum points, sealed in 9 cm. from one end of the tube, was employed to effect ignition. One of the plates carried a small brass tube and tap through which the explosion tube was exhausted and filled.

The charge was made by means of two burettes containing mercury, one of which acted as a reservoir, the other being used for measuring out the volume of gas. In the case of pentane the liquid was let into the burette from a weight pipette with a grinding fitting on to the top of the burette, air was then added to the vaporised pentane. Mixing was effected by a small heating coil outside the lower end of the burette. This small coil gently warmed a small part of the glass and set up convection currents. The tube was evacuated by an oil pump, the charge let in from the burette or storage vessel and adjusted accurately to atmospheric pressure by means of a small manometer and left to stand in the tube for some minutes before firing. (For details of apparatus see fig. 1.) The gases employed were from ordinary compressed gas cylinders, and the pentane was supplied by Shell-Mex, Ltd.

The photographs were taken by means of a rotating wheel camera. The duralmin wheel of 1 metre circumference was mounted on ball bearings; it was accurately balanced and could be spun 10,000 revs. per minute or a peripheral speed of 170 metres per second. The speed employed in the present experiments was usually only about 10 metres per second. A tachometer with several ranges was mounted on the axis of the wheel and was sufficient to indicate the speed of rotation. The lens employed was a Taylor, Taylor, Hobson F2 cinema lens. The distance of lens to tube was 2 metres. Lumière

\* *Vide Lafitte, 'C.R.,' vol. 176, p. 392 (1923).*

negative paper was affixed to the 4 inch rim of the wheel, and was found more convenient than the film which was used in the earlier experiments. Identifica-

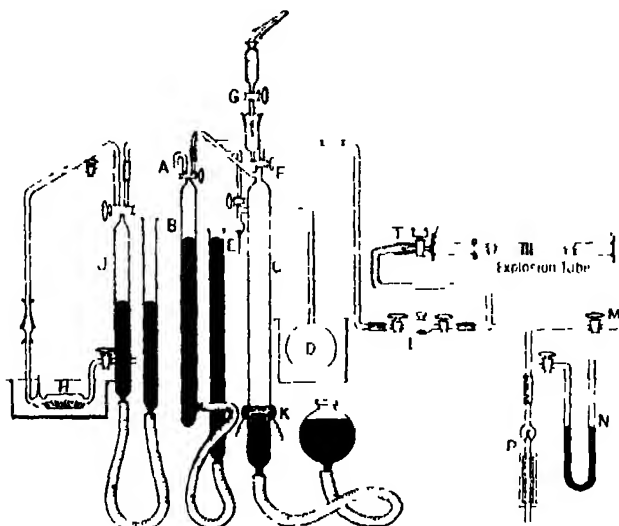


FIG. 1.—Charging Apparatus.

- |                                       |                                        |
|---------------------------------------|----------------------------------------|
| A.—Intake to burette.                 | J. Burette to mix air with anti-knock. |
| B. Measuring burette.                 | K. Mixing heating coil.                |
| C. Mixing burette.                    | L. Intake for anti-knock (low v.p.).   |
| D. Storage for mixed gas.             | M. Tap to vacuum.                      |
| E. Trap.                              | N. Water gauge.                        |
| F. Tap for charging tube.             | P. Manometer.                          |
| G. Intake for liquid combustible.     | T. Sleeve joint to tube.               |
| H. Intake for anti-knock (high v.p.). |                                        |

tion marks were necessary which appear as white vertical lines on the photographs.

III. *Conditions for Constancy of Position of Detonation.*—The conditions for constancy of position of detonation were found to be accurate and thorough mixture of the components of the gas mixture, uniformity in the bore of the tube and as little movement in the gas as possible. The degree of humidity of the gas, the method of ignition, and the presence of ions in the gas (produced from  $\beta$ -rays from radium) did not appear to affect the position to any definite extent. In weak mixtures it was much more difficult to obtain concordant results than in the stronger mixtures. The later the detonation the more effects of movement in the gas and lack of homogeneity disturb normal combustion. As is well known there is a difference in the behaviour on combustion in an open tube and in a closed tube. In a closed tube the burnt gases expand

and compress the unburnt mixture, the pressure rises approximately as the mass of mixture burnt; in an open tube with very rapid combustion, the conditions are not very different from those in a closed tube provided ignition occurs near a closed end. If, on the other hand, the tube is open at both ends and the gas is free to expand, the behaviour is very different.

A jerky type of combustion, such as described by Le Chatelier,\* is obtained in tubes open at both ends if the distance of spark to near end is less than a certain distance (see Photo. 9, Plate 15). Under such circumstances detonation may occur almost any time, no regularity in the position being obtainable. If the near end of the tube is closed by a movable plate the effect is entirely done away with and the combustion becomes regular. The photographs 1 to 5 (Plate 13) illustrate this difference between explosion in an open tube and in a closed tube. The last photograph (No. 5) shows the rarefaction caused by the release of pressure when the combustion front reaches the end of the tube, travelling back at about 1,400 metres per second through the hot burnt gases. In this case it has too far to go and does not catch up the forward combustion front or interfere with combustion as it does in the cases shown in photographs 1 and 3, where the distance from spark to end is only 9 cms. In order to avoid such disturbances the measurements here described have been carried out with the end plate near the spark left on. (The end plate does not move away appreciably from the end of the tube during the explosion period.)

In many cases the tubes are shattered at and beyond the detonation point. The only difference in the records then being that "the after burn" only shows for a period of about  $5 \times 10^{-4}$  seconds instead of about 2 or 3 times as long. Chance of shattering was found to be diminished by surrounding the tube with a water jacket, but increased by successive detonations in the same tube.

Photo. 8, Plate 14, shows detonations in identical positions, one record was taken, however, with the wheel rotating about 8 times as fast as the other: elongation of the record in a vertical direction results. Chance superposed the start of the two explosions as recorded on the film. Detonation occurred slightly earlier at the end nearer the spark than towards the far end due presumably to the increase in pressure occasioned by the near end plate. A detonation wave was reflected from the end plate and cut across the slower moving detonation waves which travelled inwards from the two detonation points. For a given mixture the shape of the combustion track and therefore the increase in the rate of combustion should be the same. Two photographs (see Photo. 6, Plate 13) with the same mixture (1 pentane, 8 oxygen, 6 nitrogen)

\* 'Ann. d. Mines,' vol. 4, p. 350 (1883).

have by chance (1 in 1,000) closely superposed themselves and illustrate this point well. It has already been pointed out that combustion in weak mixtures is readily disturbed by movement in the gas, lack of homogeneity and slight change of composition so that results were not always so satisfactory as afforded by this illustration of the reproducibility possible. Weak mixtures often exhibited "pseudo-detonation" points (see Photo. 13, Plate 16), the combustion accelerated rapidly and developed a weak retonation wave of about the usual velocity. A true detonation wave was not developed but combustion proceeded with fairly uniform velocity; the real detonation point was reached at a later stage. Sometimes early detonation occurred where a pseudo-detonation tended to arise. It is possible that particles of dust or irregularities in the tube have something to do with the tendency to change over to the detonation type of combustion.\* In support of this view one photograph showed a number of retonation waves generated at the back of the accelerating combustion front at fairly regular intervals.

A compression wave travelling at about the speed of the retonation waves, *i.e.*, of sound waves in the hot gases, is nearly always set up at every irregularity or constriction in the tube, and the removal of energy in this way affects momentarily the progress of the combustion. Dixon† showed that detonation will not be transmitted if energy is absorbed from the wave at a flexible joint. Lafitte‡ has shown that in passing from a narrow into a wide tube, the detonation wave is extinguished, but may be set up again at a later stage in the wider tube.§ Photographs of explosions in tubes of transparent rubber illustrate this point well. (See Photo. 7, Plate 13, in which two detonations occur in a length of about 30 cms.) Compression waves may develop into detonation waves in the forward direction, if sufficiently intense. Sound waves from the spark reflected from the back of the combustion zone do not appear to influence to any great extent the progress of the combustion or the normal detonation point. Most of the photographs show that a sound wave produced on ignition travels to the near end plate and is there reflected passing back through the burning gases at a rate depending on their temperature. This wave is reflected and thrown back from the combustion front, which it leaves hardly disturbed. On reaching the end plate it is again reflected back; generally this wave is deflected by the gases flowing

\* Lafitte, 'C.R.', vol. 176, p. 1392 (1923).

† 'Phil. Trans.' A, vol. 200, p. 335 (1903).

‡ 'C.R.', vol. 179, p. 1394 (1924).

§ See also Chapman and Wheeler, 'J. Chem. Soc.' vol. 128, p. 2139 (1926).



backward from the region of detonation point and never again reaches the advancing combustion. The refraction of the sound waves in passing the region of the detonation waves or reflection waves is clearly visible in the photographs; this is partly due to the change of temperature and partly to local movements in the gas. There is no definite indication from the records other than a weak reflection, that the sound waves propagated from the spark in the forward direction in the unburnt gas influence the course of the combustion. The combustion front overtakes such a wave and in fact itself becomes an accelerating compression wave, before the detonation point is reached.

The above remarks on the conditions affecting the position of detonation indicate that close concordance in position is not always to be expected, particularly with weak mixtures.

IV. *Results.*—Table I summarises the results obtained for different mixtures. Sufficient oxygen is added in each case to burn the fuel completely except when excess of the latter is intentionally added. Oxygen accelerates combustion, and detonation occurs earlier than with a similar quantity of nitrogen. In argon detonation occurs considerably earlier than in a corresponding mixture with nitrogen, but not quite so early as in oxygen except for weak mixtures. (See Photos. 11 and 12, Plate 16.) Excess of combustible has a great delaying effect in *large* excess. But early detonation occurs with mixtures containing up to double the amount required for complete combustion with the oxygen present. Carbon dioxide has a greater delaying effect than nitrogen. In a mixture  $1C_2H_2 \cdot 2.5 O_2$  and  $3X$  the position of detonation obtained in mixtures with the following diluents  $X$  are:  $-O_2$ , 30 cms.;  $A$ , 35 cms.;  $N_2$ , 48 cms.;  $C_2H_2$ , 53 cms.;  $CO_2$ , 95 cms.; or in a mixture  $1C_2H_2 \cdot 8O_2 \cdot 2X$  the following:— $O_2$ , 12 cms.;  $A$ , 34 cms.;  $N_2$ , 50 cms.;  $C_2H_2$ , 80 cms.;  $CO_2$ , 62 cms. The rate of rise of temperature in a combustible mixture will depend on the thermal conductivity, the specific heat per unit volume and the reaction velocity. On account of the smaller specific heat of the argon one would expect earlier detonation than in the nitrogen and earlier in nitrogen than in carbon dioxide. The earlier detonation in mixtures with excess of oxygen must be ascribed to the effect of excess of the latter on the reaction velocity. In the case of acetylene, heat is available from its decomposition, the delaying effect is less than might be expected from its specific heat alone. The dissociation of  $CO_2$  may also be an influence favouring delay. Le Chatelier\* determined the change of position of

\* 'C.R.,' vol. 130, p. 1756 (1900).



detonation in mixtures of acetylene with varying quantities of oxygen. He obtained for a mixture  $C_2H_2 + 0.5 O_2$ , 1 metre,  $+ 1 O_2$ , 5 cms.,  $+ 6 O_2$ , 15 cms.

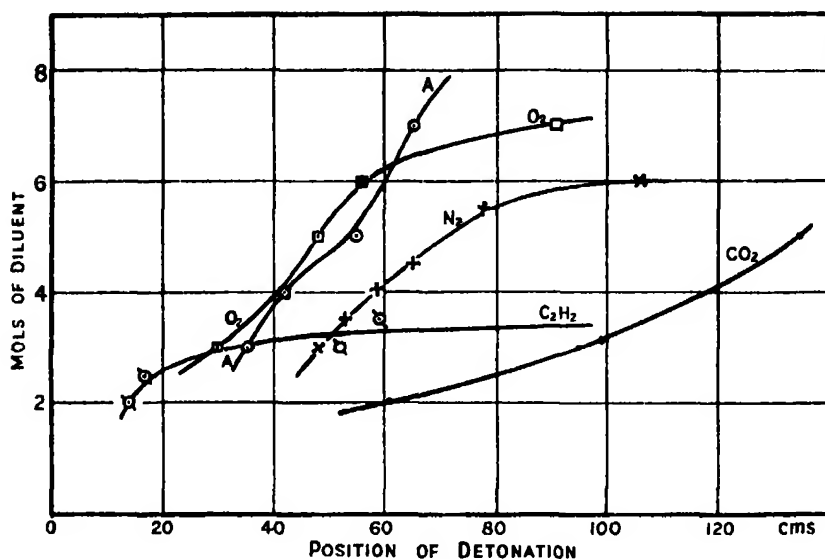


FIG. 2. Effect on Position of Detonation in various Gases in mixture with  $C_2H_2 + 2.5 O_2$ .

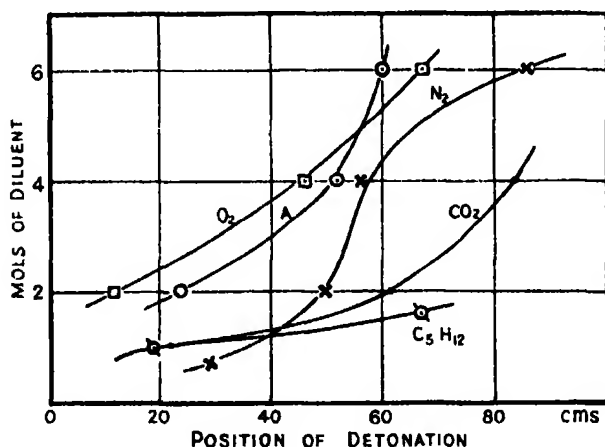


FIG. 3.—Effect on Position of Detonation in various Gases in mixture with  $C_5H_{12} + 8 O_2$ .

$+ 10 O_2$ , 80 cms. These results are in tolerable agreement with the present measurements. Dixon has pointed out\* that mixtures of acetylene of com-

\* 'J.S. Aut. Eng.,' vol. 9, p. 237 (1921).

position to give CO on combustion, burn faster and detonate sooner than those burning to CO<sub>2</sub>. As data are not available for heat conductivity in gases at high temperatures, it is hardly possible to make more than qualitative observations on these results, but by accurate observations of the velocities of the detonation waves, it may be possible to arrive at a more precise knowledge of the influence of various diluents on the progress of combustion.

These measurements were not carried out with a view to determine the velocity of the detonation waves but only the position of detonation. Records, however, were measured (see Table II), but are not reliable to less than 50

Table II.—Velocity of Detonation.

Mixture	Mean Veloc m. sec.	Mixture.	Mean Veloc m. sec.
C <sub>2</sub> H <sub>2</sub> + 2 5O <sub>2</sub> + 3 to 5N <sub>2</sub>	2,070	C <sub>2</sub> H <sub>2</sub> + 8O <sub>2</sub> + 3 to 6N <sub>2</sub>	2,200
C <sub>2</sub> H <sub>2</sub> + 2 5O <sub>2</sub> + 3 to 6O <sub>2</sub>	1,930	C <sub>2</sub> H <sub>2</sub> + 8O <sub>2</sub> + 2 to 6O <sub>2</sub>	2,100
C <sub>2</sub> H <sub>2</sub> + 2 5O <sub>2</sub> + 3 to 5A	2,020	C <sub>2</sub> H <sub>2</sub> + 8O <sub>2</sub> + 2 to 6A	2,110
C <sub>2</sub> H <sub>2</sub> + 2 5O <sub>2</sub> + 2 to 3CO <sub>2</sub>	2,030	C <sub>2</sub> H <sub>2</sub> + 8O <sub>2</sub> + 1 to 4CO <sub>2</sub>	2,170
C <sub>2</sub> H <sub>2</sub> + 2 5O <sub>2</sub> + 2C <sub>2</sub> H <sub>2</sub>	2,400	C <sub>2</sub> H <sub>2</sub> + 8O <sub>2</sub> + 1C <sub>2</sub> H <sub>2</sub>	2,550
C <sub>2</sub> H <sub>2</sub> + 2 5O <sub>2</sub> + 3C <sub>2</sub> H <sub>2</sub>	2,330	C <sub>2</sub> H <sub>2</sub> + 8O <sub>2</sub> + 1.67C <sub>2</sub> H <sub>2</sub>	2,475

metres per second. Dilution decreases the velocity. More accurate and extensive measurements are being made. The noteworthy results are that the velocity appeared to be less in argon and in oxygen than in nitrogen, and greater in mixtures rich in combustible. Dixon's observations (*loc. cit.*) appear to be in agreement with this conclusion. (See next page.)

The following are results of measurements on Photo. 8 :

Speed of Detonation Wave .. .. .	2,100 metres sec.
(Early part of do.) .. .. .	2,400 ..
Reflected Detonation Wave .. .. .	1,900 ..
Retonation Wave (at near end) .. .. .	1,700 ..
„ „ (from centre point) .. .. .	1,700 ..
Speed prior to Detonation about .. .. .	1,100 ..

Most of the photographs show that during the early part of the detonation the speed is considerably faster, but after about 20 cms. settles down to uniform rate.

*V. General Observations.* Nernst\* describes the processes which follow upon the ignition of a combustible gas mixture in a tube thus: "first we have the condition of slow combustion, heat is conveyed by conduction to the adjacent layers, and there follows a velocity of propagation of a few metres per second. But since the combustion is accompanied by a high increase of pressure, the adjacent still unburnt layers are simultaneously compressed whereby the reaction velocity increases and ignition proceeds faster. This involves still greater compression of the next layer, and so, if the mixture be capable of sufficiently rapid combustion, the velocity of propagation of the ignition must continually increase. As soon as the compression in the still unburnt layers becomes so great that spontaneous ignition results the now much more pronounced compression waves excited with simultaneous combustion must be propagated with very great velocity, *i.e.*, we have the spontaneous development of a detonation wave." The wave travels with a velocity one and a half to twice the velocity of sound in the mixture at the temperature to which the gases are raised by the explosion. On the work of Riemann and Hugoniot, Jouguet† obtained formulæ for the calculation of the velocity of the detonation wave. The following figures were obtained for mixtures similar to those used in this work.

Mixture.	Caled.	T° C.	Obsd.	Observer.
$C_2H_2 + 2.5O_2 + 1.5 C_2H_2$	3,091 m /sec.	5,570°	2,961 m /sec.	Dixon.
$C_2H_2 + 2.5O_2 + 0.5O_2$	2,120 "	4,890°	2,220 "	Le Chatelier.
$C_2H_2 + 2.5O_2 + 7.5O_2$	1,858 "	3,560°	1,850 "	Dixon.

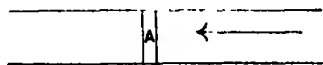
Dissociation was not taken into account, nor incompleteness of reaction, but agreement is good. In the case of hydrogen and oxygen mixtures, agreement was not so satisfactory. The theory requires that the reaction velocity should change rapidly in and behind the wave front. The combustion must occur in the wave front and not behind it. While theory provides means of explaining and calculating the velocity of propagation of a detonation wave, the conditions which govern its establishment are not so clear.

Instead of imagining a hot zone of combustion travelling along a tube, let the gas be considered streaming back through a stationary zone in which reaction occurs. Suppose the gas, already compressed and heated to just

\* 'Physikalisch-chemische Betrachtungen über den Verbrennungsprozess in den Gasmotoren.

† 'Jour. de Math.,' vol. 2, p. 5 (1906).

below ignition temperature but still losing just too much heat to ignite, to be streaming through the tube. If at some point the loss of heat becomes slightly less, then that region will be the hottest and will become the region A where inflammation sets in. The gas can be passed through quicker and quicker as the reaction rate increases and more heat becomes available to raise the temperature of the gas. Finally the reaction rate becomes so great that the heat available is sufficient for the gas to pass through at the average rate of translation of the molecules, and where this occurs a quasi-stationary detonation wave of uniform velocity would be formed. (The wave would have the velocity of sound in the gases heated to the temperature of the reaction zone referred to their initial state, not to their state after combustion.) In order to make this mechanism reasonable it would seem necessary that, as the temperature rises, more and more of the molecules arrive in the zone in an "activated" state ready to combine immediately in the time available to pass the zone. Le Chatelier (*loc. cit.*) attributed to the zone a thickness of less than  $10^{-5}$  sec. (about 1 cm.); Becker\* gives a finite but much smaller width to the boundary of action. Above a certain temperature all the molecules may become available for combination and at this stage detonation sets in. This view demands more than adiabatic compression to the ignition point, the necessary activation by radiation, ionisation or encounter must occur before or on entering the combustion zone. Ignition by adiabatic compression alone does not lead to immediate detonation.



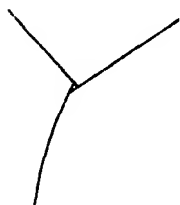
There are certain peculiarities of the detonation point which exhibit a difference between the conditions necessary for initiation of a detonation wave and those necessary for its propagation when once initiated.

In the first place the detonation position is generally marked by a specially dark spot on the resulting photograph. (On a film this spot usually seems to be discontinuous from the rest of the image of the detonation wave, but on paper this is not so and that effect must be due to halation.) By taking photographs on the wheel rapidly rotating (3 to 6 thousand revs. per minute), the point where detonation sets in seems to be slightly forward of the visible combustion front, and the first few millimetres of the path of the detonation wave is much brighter than the rest. Apparently the wave is passing through unburnt gas for the first few millimetres (see Photo. 10, Plate 15). Le Chatelier† held the view that detonation occurred slightly forward of the combustion front.

\* 'Z. f. Physik,' vol. 8, p. 321 (1921).

† 'C.R.' vol. 130, p. 1756 (1900).

The combustion curve and the detonation wave are not continuous at the detonation point. Dixon's photographs showed the effect pronouncedly, but he demonstrated that the discontinuity was due to halation. Our photographs on films exhibit the discontinuity to a much greater extent than on paper, and there is no doubt that Dixon's view (*loc. cit.*, p. 347) was in the main correct so far as photographs on films were concerned. There appears, however, that there is a slight real discontinuity, which cannot be explained by light scattering or halation (it is found on faint as well as strong records on the negative paper), and the detonation point can always be resolved at high speed into a mark in the line of the detonation wave. There are therefore grounds for Le Chatelier's contention, though the distance is only a small fraction of that mentioned in his communication (0.05 metre). Careful examination of the high speed records appear to show a structure thus:—



The detonation and detonation wave definitely starts ahead of the line of the combustion, but there is a tendency for the latter to change to the speed of the detonation wave prior to actual detonation.

Secondly, many photographs show that detonation does not necessarily occur during rapid acceleration of combustion, but often during a state of fairly uniform but rapid burning (see Photo. 6, Plate 13). Further, most of the photographs show that rapid expansion and projection of gas away from the point of detonation occurs. The density of the gas after detonation is less in the neighbourhood of the point as shown by the rate of passage of the reflected waves through this region. Complete and instantaneous reaction and sudden cooling by expansion account for the absence of luminosity in this neighbourhood. The detonation wave, on the other hand, does not cause instantaneous combustion, and luminosity continues for about 1/500th second after the detonation wave has passed—perhaps partly connected with reassociation on cooling. Lastly, it is noted that the rate of passage of the detonation wave is abnormally rapid in the neighbourhood of the detonation point.

These characteristics indicate that detonation appears to be initiated as a spontaneous explosion of a region of gas, and that once initiated the condition for combustion of the detonating type is more readily attained. It is as if a certain region of gas became activated so as all to combine momentarily, and that when once this has occurred such activation is more rapidly engendered than by the ordinary type of combustion, the temperature in the wave being higher.

These views are only put forward tentatively as a result of the records obtained, and further study is desirable. Some of the records show a very short predetonation period, the time of combustion from spark to detonation point is of the order of  $10^{-4}$  second. In Photo. 14, Plate 16, detonation occurs at the end plate, and the reflection wave closely follows the forward detonation wave. The retonation wave from the forward detonation wave is faint because it travels through a region where nearly complete combustion has been occasioned. In some cases, when excess of pentane and acetylene are present, plumes of nearly stationary incandescence are recorded. In all probability they consist of glowing particles of carbon. (See Photo. 15, Plate 16, for excess of acetylene and Photo. 16 for excess of pentane.)

VI. Action of "Antiknocks" on Position of Detonation.—Experiments have been made to ascertain whether antiknocks like lead ethyl or diethyl selenide would render the position of detonation later when mixtures of acetylene or of pentane with oxygen and nitrogen, etc., were exploded.

The diethylselenide was introduced from the small burette and added to the mixture in the desired quantities. The lead ethyl was introduced by passing the mixed gases on the way to the explosion tube through a small tube containing the liquid which could be weighed before and after. The weighings showed that between one volume of lead ethyl in 750 down to one volume in 1,500 of the mixture was present in the tube. There was invariably a smell of lead ethyl in the tube even after explosion. The results are given in the following table:—

Table III.

Mixture.	With Pb(Et) <sub>2</sub> .	Without.
$1C_2H_2 : 2.5O_2 : 3N_2$	40 cms.	{ 48 cms.
$1C_2H_2 : 2.5O_2 : 6N_2$	{ 77 "	48 "
	77 "	110 "
	77 "	116 "
$1C_2H_{12} : 8O_2 : 2N_2$	{ 47 "	66 "
	50 "	64 "
	62 "	62 "
$1C_2H_{12} : 8O_2 : 2CO_2$	{ 61 "	62 "

There is no evidence that the presence of lead ethyl causes any delay of detonation under these conditions, but rather the reverse. The measurements without lead ethyl were made in most cases with a batch of gas made at the same time as that for the lead ethyl experiments, so that the results



obtained are closely comparative. There was no difference in the type of record obtained.

Other experiments were made with mixtures containing excess oxygen, the results being in agreement with the above conclusion.

Similar results were obtained for the effect of diethylselenide (1/200 part by volume) on an acetylene mixture(  $1\text{C}_2\text{H}_2 \cdot 2.5\text{O}_2 \cdot 4.0\text{N}_2$ ). These records showed a slightly earlier detonation in the presence of diethylselenide. For the strong mixtures the preliminary burn before detonation was slightly more rapid with than without lead ethyl and the light was bluer, but in other cases the time of burn appeared to be exactly the same. From measurements of the velocity there was no evidence of any slowing down of the detonation wave by the lead ethyl.

Experiments have been described by Midgley\* and later by Church, Mack and Boord† in which mixtures of acetylene and air were exploded in an open tube, 1 m.  $\times$  3 cms. diameter in the presence of diethylselenide and other antiknocks. From the violence of the explosion their effectiveness in suppressing detonation was gauged by ear. The gases were probably allowed to bubble through the antiknocks, and, flowing continuously, were allowed to mix on entering the tube. A very little change in mixture would affect the point of detonation.

#### *Summary.*

(1) The conditions for detonation to occur in the same place in a tube of certain dimensions have been investigated for acetylene and for pentane mixtures of definite composition.

(2) The effect of change of composition and of nature of diluent gas on such position has been determined.

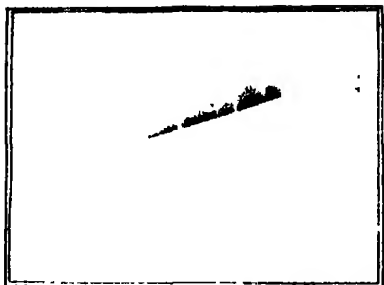
(3) Detonation appears to take place slightly ahead of the combustion front.

(4) The "antiknock" compounds, lead tetraethyl and diethylselenide, were not found to affect the position of detonation at ordinary initial pressures and temperatures.

It is to the Asiatic Petroleum Company that we are indebted for the funds necessary to carry out this work, and to Messrs. Kewley and Marshall, of their technical staff, for their interest in it. We have also to thank Mr. R. J. Schaffer, B.A., B.Sc., and Mr. C. Moore for assistance at various stages.

\* 'J. Ind. Eng. Chem.,' vol. 14, p. 894 (1922).

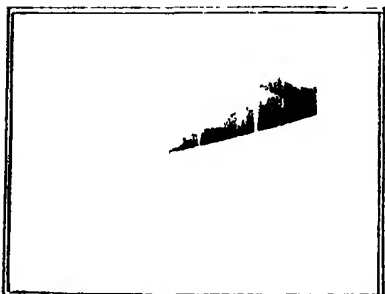
† 'J. Ind. Eng. Chem.,' vol. 18, p. 304 (1926).



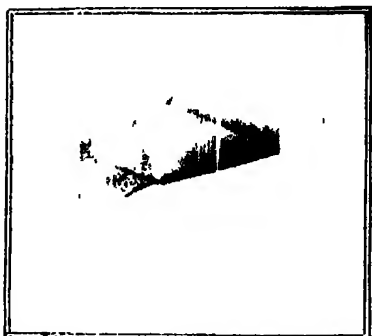
1



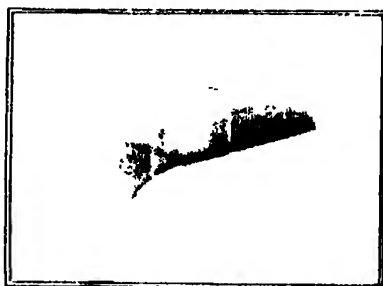
2



3



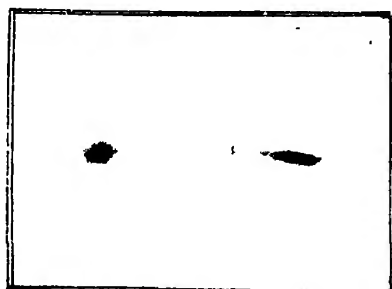
4



5

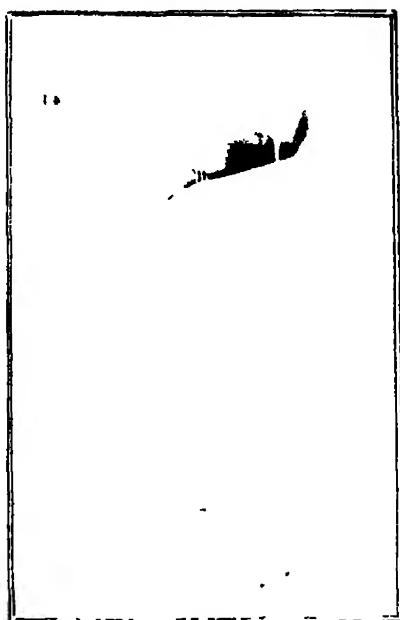


6

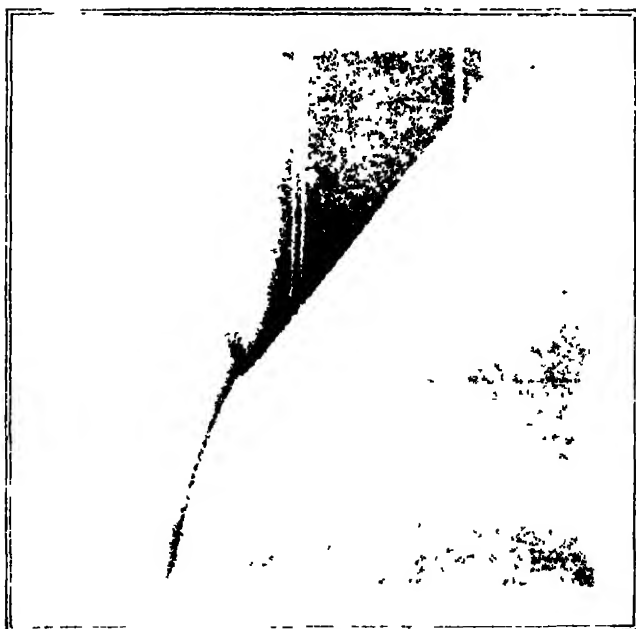


7

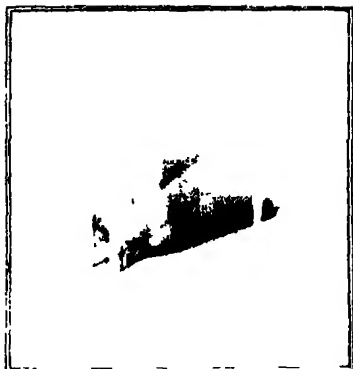




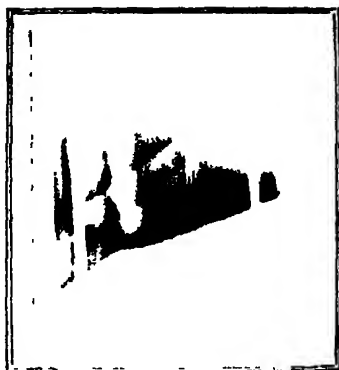
9



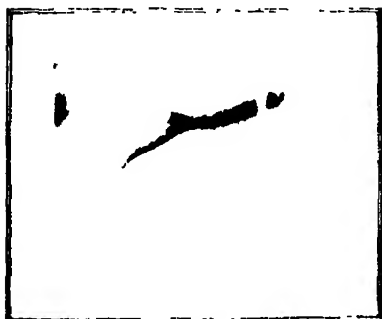
10



11



12



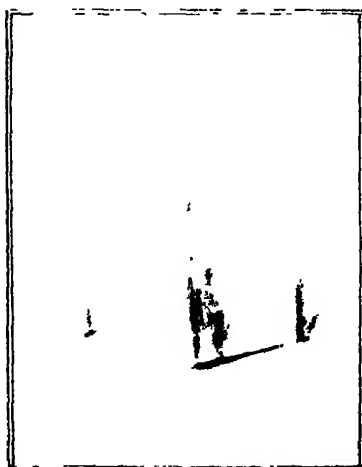
13



14



15



16

EXPLANATION OF PLATES.

PLATE 13.

- PHOTO. 1.—Both ends removed before ignition. Mixture  $C_2H_2 + 2.5 O_2 + 3.6 N_2$ . Detonation at 31 cms.
- PHOTO. 2.—Near end plate not removed before ignition. Same mixture. Detonation at 50 cms.
- PHOTO. 3.—Far end plate not removed before ignition. Same mixture. Detonation at 37 cms. Reflection wave.
- PHOTO. 4.—Neither end removed before ignition. Same mixture. Detonation at 49 cms. Reflection wave.
- PHOTO. 5.—Spark 37 cms. instead of 9 cms. from the end. Both ends removed. Detonation at 49 cms.
- PHOTO. 6.—Superposition of two explosion records. Mixture  $1C_2H_{12} + 8O_2 + 6N_2$ . Detonation at 87 cms.
- PHOTO. 7.—Explosion in transparent rubber (panchromatic plate). Mixture  $C_2H_2 + 2.5O_2 + 4.5N_2$ .

PLATE 14.

- PHOTO. 8.—Two explosion records at 650 revs. and 5,400 revs. respectively. Mixture  $C_2H_2 + 2.5O_2 + 3.6N_2$ .

PLATE 15.

- PHOTO. 9.—Jerky type of explosion in open tube. Mixture  $C_2H_2 + 2.5 O_2 + 3.6 N_2$ . Detonation at 87 cms.
- PHOTO. 10.—Enlargement of detonation point. 3,100 revs. Mixture  $C_2H_2 + 2.5 O_2 + 3.6 N_2$ .

PLATE 16.

- PHOTO. 11.—Mixture  $1C_2H_2 + 2.5O_2 + 4O_2$ . Detonation at 41 cms.
- PHOTO. 12.—Mixture  $1C_2H_2 + 2.5O_2 + 4A$ . Detonation at 40 cms.
- PHOTO. 13.—Mixture  $1C_2H_{12} + 8O_2 + 4N_2$ . Exhibiting pseudo-detonation at 47 cms. and detonation at 91 cms.
- PHOTO. 14.—Mixture  $1C_2H_2 + 2.5O_2 + 1CO_2$ . Detonation at 25 cms.
- PHOTO. 15.—Mixture  $1C_2H_2 + 2.5O_2 + 3.5C_2H_2$ . Detonation at 59 cms.
- PHOTO. 16.—Mixture  $1C_2H_{12} + 8O_2 + 1.7C_2H_{12}$ . Detonation at 67 cms.
-

*On Detonation in Gaseous Mixtures at High Initial Pressures and Temperatures.*

By A. EGERTON, F.R.S., and S. F. GATES, B.Sc., M.A.(Oxon).

(Received December 2, 1926)

[PLATES 17, 18.]

1. *Detonation in Acetylene and Pentane Mixtures.*— Observations on detonation in acetylene and pentane mixtures at ordinary pressures with the object of finding the position of detonation in a tube under set conditions, were described in the previous paper. The present paper extends this work, but at higher initial pressures and temperatures.

Apart from the study of detonations in engines, and experiments in explosion bombs where the pressure rise is observed, very little appears to have been done to extend the work of Le Chatelier and of Dixon on rate of propagation of combustion to regions of high pressure. The highest pressure at which explosions were photographed by Le Chatelier and by Dixon were about one and a half to two atmospheres. Woodbury, Canby and Lewis\* using a bomb of 12 inches length succeeded in photographing explosions in acetylene air mixtures at pressures up to 4 atmospheres. They also investigated the effect of initial temperature (up to 125° C.). The results are referred to by Brown, Leslie and Hunn† who find that for any initial density or pressure there should be a certain maximum value of the initial temperature to provide a maximum rate of rise of pressure on exploding a given gaseous mixture; decrease in density of charge on rise of temperature overcomes the effects of increase in reaction velocity.‡

In the present work a steel explosion tube is used provided with a number of windows so that the progress of combustion can be followed by photographing the flame through the windows in the same way as described in the previous paper. The conditions under which explosion is effected in these experiments are nearer those which hold in an internal combustion engine. The region of the usual compression which is employed in an engine is covered by the

\* 'J.S. Aut. Eng.,' vol. 8, p. 209 (1921).

† 'J. Ind. Eng. Chem.,' vol. 17, p. 397 (1925).

‡ Dumanois and Lafitte, 'C.R.,' vol. 183, p. 284 (1926), have investigated the effect of pressure on detonation of electrolytic gas, giving results in agreement with recent observations of the present authors.

measurements. It is not possible, however, to maintain the explosive mixture at the temperature (about  $400^{\circ}\text{C.}$ ) reached by the charge in an engine prior to ignition, without the occurrence of self-ignition. Further there are other conditions which apply in an engine such as turbulence, large differences in temperature of cylinder walls and valves which cannot be imitated by the method here employed. Nevertheless the present results are not without some interest from the point of view of engine behaviour. The measurements are limited to mixtures of acetylene or of pentane with nitrogen or oxygen.

II. *Experimental Arrangements.*—A steel tube 5 feet long by  $1\frac{1}{8}$  inches external diameter and  $\frac{5}{8}$  inch internal diameter was capped at each end by stout hexagon nuts rendered tight by copper washers. Along one side of the tube 13 holes were bored at 10 cms. intervals to accommodate glass windows measuring 1 cm. diameter by 0.5 cm. thick. The windows seated down on to very thin rubber washers for ordinary temperatures, or special asbestos composition washers for the higher temperatures. Between the windows and the steel screw head which held them in position was placed another washer of softened copper. One of the hexagon nuts carried the stem of a high-pressure valve. This could be attached to the mixing bomb direct or to the tubes leading to the Bourdon gauge, vacuum pump and mixing bomb. The mixing bomb measured 2 feet by  $2\frac{1}{4}$  inches internal diameter. It contained a loose fitting ball to assist mixing by rocking the cylinder about a horizontal position. The gases for the mixture were introduced from cylinders into the bomb, the quantity being measured by means of the pressures registered on the Bourdon gauge. In the case of mixtures made from volatile liquids a weighed quantity of liquid, sealed in a glass vessel, was placed in the bomb and held in position under a piece of wire gauze. The valve of the mixing bomb having been closed and the rest of the gases added, the bomb was removed and the ball rolled to the top and allowed to fall quickly on the glass vessel. The small vessel was smashed and the mixing of the vapour allowed to proceed. In some cases it was necessary to heat the bomb in order to assist vaporisation of the liquid. A heating jacket was constructed to slide over the bomb with thermocouples arranged to measure the temperature. Electrical heating jackets could also be slid over the explosion tube, a space being left for the windows. The whole tube could be heated to about  $400^{\circ}\text{C.}$  Temperature was measured by 3 thermocouples screwed into the body of the tube. The windows are so arranged that there is as little interference with the smoothness of the bore of the tube as possible.

Analyses of the mixtures were not carried out, as it was found possible to repeat the results by the above method of making the mixtures.



The steel explosion tube was mounted between two vertical stanchions at 2 metres distance from the camera. Ignition could be effected from the centre or 16 cms. from the near end. A K.L.G. sparking plug was connected to a 1 inch spark coil. Photo. 4, Plate 17, shows the kind of symmetrical record obtained if ignition is started in the centre of the tube. The detonation point, retonation wave, detonation wave and reflection waves are clearly seen. The exact position of the detonation point, though it may fall between the windows, can be obtained by producing the retonation wave to meet the detonation wave. In this case it occurs just about the second window from the spark. Detonation produces particles of metallic iron, probably by shattering the surface of the metal. This is deposited as a film on the windows which have to be cleaned after several explosions. At high pressures the windows are sometimes cracked by the detonation and the inner surfaces are frequently damaged.

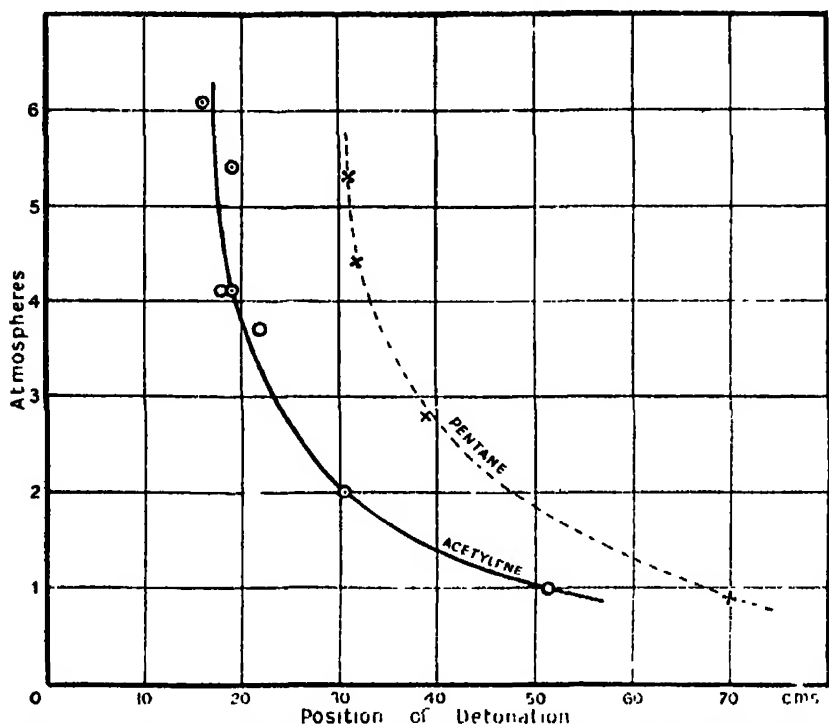
III. *Results*.—The results are collected in Table I and are also shown on the graph. Increase in the initial pressure increases the tendency to detonate very considerably, but the limit is reached at about 3 atmospheres; further increase in initial pressure has very little effect. This rather remarkable result agrees with the observations of Woodbury, Canby and Lewis.\* They state that for acetylene-air mixtures under pressure of 1 to 4 atmospheres, the rate of propagation of combustion increases with increase of pressure up to a certain

Table I.

Mixture	Initial Pressure in atmos. (absolute).	Position of Detonation. cms. from Spark.	Mixture.	Initial Pressure in atmos. (absolute).	Position of Detonation cms. from Spark.
$C_2H_2 + 2.5O_2 + 4N_2$	1	50	$C_2H_{12} + 8O_2 + 6N_2$	1	70
	1	52		1	(58)
	1	52		2.7	37
	2	31		2.7	(31)
	2	30		4.4	32
	3.7	22		4.4	32
	4.1	18		4.4	32
	4.1	19		5.3	32
	5.4	(19)		5.3	31
	6.1	(16)			
			$C_2H_{12} + 8O_2 + 12N_2$	5.4	60
			$C_2H_{12} + 8O_2 + 15N_2$	2	100
				5.4	72
				9.3	74
			$C_2H_{12} + 8O_2 + 32N_2$	8.0	no detonation
				9.6	

\* 'J. Soc. Aut. Eng.,' vol. 8, p. 209 (1921).

critical pressure (2 to 3 atmospheres), beyond which no increase was obtained. It is noteworthy that a mixture (1 pentane,  $80\text{O}_2$ ,  $32\text{N}_2$ ) which is about the



Change of Position of Detonation Point with Pressure —  $\text{C}_2\text{H}_2 \cdot 2.5\text{O}_2 \cdot 4\text{N}_2 \dots$   
 $\text{C}_5\text{H}_{12} \cdot 80\text{O}_2 \cdot 6\text{N}_2$ .

composition of a mixture of pentane and air, which might be employed in an internal combustion engine, does not detonate in the steel tube (150 cms. long) even at 9 atmospheres initial pressure. Photos. 1, 2 and 3 (Plate 17) show the effect of increasing the pressure of a mixture  $1\text{C}_5\text{H}_{12} + 2.5\text{O}_2 + 4\text{N}_2$  from 15 to 30 and then to 60 lbs. Detonation occurred at 52, 31, and 18 cms. respectively. The position of detonation at ordinary pressure was a little earlier than that determined in the glass tubes. Photo. 5 (Plate 17) shows a detonation in a mixture ( $1\text{C}_5\text{H}_{12} + 80\text{O}_2 + 15\text{N}_2$ ) at 136 lbs. pressure; such a mixture does not detonate in a tube 150 cms. long at atmospheric pressure.

IV. *Effect of Temperature.*—Using a mixture  $1\text{C}_2\text{H}_2 + 2.5\text{O}_2 + 5\text{A}$ , no change of position of detonation for two initial temperatures  $17^\circ\text{C}$ . and  $40^\circ\text{C}$ . had been found during the experiments, using glass tubes at ordinary pressures. The glass tube was jacketed with a water jacket at the required temperature. Detonation in each case occurred at 55 cms. (see Photos. 6 and 7, Plate 18).

In the steel apparatus experiments were carried out at 230° C. on a mixture 1 pentane, 8O<sub>2</sub> + 15N<sub>2</sub>. At 138 lbs. pressure, ignition occurred before the spark was passed, at 79 lbs. the charge was not ignited in the hot explosion tube, and on passing the spark a record was obtained. Detonation occurred as late as 85 cms. At 30 lbs. detonation occurred at 110 cms., both these are slightly later than the results for normal temperatures at the same pressures. Correcting, however, to 15° C., the mixtures at above pressures become of equal density to mixtures at 45 lbs. and 17.5 lbs. respectively. Between 230° C. and 240° C., the reaction rate for such a mixture increases in such a way that at 230° C. the oxidation of the pentane is hardly appreciable, but at 240° C. it is rapid enough to cause self-ignition of the mixtures. This is similar to Fenning's results with hexane mixtures.\* At 240° C., and at 122 lbs. pressure the record showed that self-ignition occurred at the far end of the tube, and a slow moving explosion travels back towards the inlet valve. Ignition probably would occur first near the dead end of the tube owing to compression, but the explosion cannot travel fast enough against the inflowing stream of gas, and did not pass through the valve into the mixing vessel. These effects illustrate pre-ignition and prevention of detonation by the motion of the combustible gas.

From the photograph at 230° C. (see Photo. 8, Plate 18) the flame appears to travel slower than at normal temperature, and the change of rate of combustion was more abrupt before combustion set in. According to the experiments of Woodbury, Canby and Lewis rise of the initial temperature in 10 per cent. acetylene mixture from 25° C. to 80° C. decreased the rate of combustion at constant pressure, though with rich mixtures there was a slight increase up to 75° C. followed by a decrease up to 125° C. Dixon had already observed that initial temperatures do not appear to add to the flame temperature. It is possible that slight partial combustion occurs before the passage of the spark, but Fenning's experiments (*loc. cit.*), and agreement of position with a repeat experiment in our case, make this improbable.

Measurements of velocity of the detonation wave from the slope of the start of the bands of light from the windows indicated that the velocity decreased with dilution of the mixture. Rise of initial pressure or temperature did not alter the velocity to any great extent: further measurements are being made to determine the precise extent of the slight increase in velocity with rise of pressure. The charge density corrected for temperature was 46 lbs. in the experiment at 230° C., and a higher combustion temperature than for the same pressure at 20° C. might have been expected, nevertheless the detonation wave

\* 'Rep. Aero. Res. Comm.,' No. 979, p. 20 (1925).

appeared to be travelling at much the same rate. Further careful measurements are necessary ; the rate should depend on the maximum flame temperature, though not on the pressure, unless the number of molecules change on reaction, then a slight increase or decrease in velocity might occur. Increase of specific heat with rise of initial temperature would tend to reduce the velocity.

V. *Influence of "Antiknocks" on detonation at High Pressure.*—The following results leave no doubt that for the conditions under which gaseous mixtures are exploded in the steel tube, the presence of lead ethyl does not delay detonation or appreciably modify the course of combustion. (See Photos. 8, 9, 10, 11, Plate 18, and Table II (A) and (B).)

Table IIA. Pentane 1 : 8O<sub>2</sub> : 6N<sub>2</sub>. Temp. 15° C.

Pressure (atmos.).	Without PbEt <sub>4</sub> .	With PbEt <sub>4</sub> .	Without PbEt <sub>4</sub> (check).
	cms.	cms.	cms.
5.3	32	30	31
4.4	32	32	32
2.7	37	32	31
1.0	70	60	58

Table IIB.—Pentane 1 : 8O<sub>2</sub> : 15N<sub>2</sub>. Temp. 230 to 240° C.

Pressure (atmos.).	Without PbEt <sub>4</sub> .	With PbEt <sub>4</sub> .
	cms.	cms.
5.8	85	88
2.2	111	109

The concentration of the first mixture was 1 per cent. of Pb (C<sub>2</sub>H<sub>5</sub>)<sub>4</sub> in the pentane or a vapour concentration of 1 in 6300 molecules of vapour mixture. The concentration in the second was 10 per cent. Pb (C<sub>2</sub>H<sub>5</sub>)<sub>4</sub> in the pentane or 1 in 1,000 molecules of the mixture. There might be an effect at higher temperatures, but difficulties with pre-ignition of the mixture prevent such experiments being made in the way here described.\*

\* Experiments have also been made upon the effect of nickel carbonyl on similar mixtures at 200° C. and 100° C. up to 130 lbs. initial pressure. There was no measurable effect on the position of detonation. It was doubtful, however, how much Ni(CO)<sub>4</sub> was present in the gas at the moment of ignition as it undergoes rapid oxidation. In the lead ethyl experiments chemical tests proved beyond doubt that lead ethyl was present in the explosion tube at the moment of ignition.

Experiments in other directions have led to the view that lead ethyl has little effect on combustion till a temperature of nearly  $400^{\circ}$  C. is reached. The seat of its effect on detonation in an engine therefore appears to be prior to ignition.

VI. *General Observations on Detonation in Gases.*—Woodbury, Canby and Lewis (*loc. cit.*) did not obtain detonation of any mixtures of air and acetylene (from 5 to 20 per cent. acetylene) in their 12 inch bomb, but mixtures enriched with oxygen (*e.g.*,  $1\text{C}_2\text{H}_2 + 1.5\text{O}_2 + 2.5\text{N}_2$ ), so as to burn to CO, could be made to detonate before the explosion reached the walls. This, and the observations on the effect of pressure and temperature are in general agreement with the present results. They quote, however, experiments which indicate that auto-ignition occurs considerably ahead of the combustion front. None of the present records show any trace of this. They state that auto-ignition was observed in a mixture ( $1\text{C}_2\text{H}_2 + 2.7\text{O}_2 + 2.9\text{N}_2$ ), but similar and richer mixtures have been ignited in the long steel tube at pressures up to 10 atmospheres, and no such effect has been observed to occur. It seems possible that the records obtained might be explained by the setting up of jerky explosions (described on p. 140), occasioned perhaps by leakage of gas from the bomb.

Fenning has carefully investigated detonation in petrol-air, hexane-air and benzene-air mixtures in a bomb 20 cms. long  $\times$  17.5 cms. diameter. It was found that only rich mixtures could develop detonation under such conditions, and that rise of temperature increased the tendency to detonate. In the work here described complete combustion mixtures of pentane, as dilute as those employed by Fenning for hexane or petrol, do not detonate even after a run of 150 cms., much less in 20 cms. Experiments with dilute mixtures rich in combustible have not yet been carried out in the explosion tube. In a short bomb rise of pressure at the combustion front would be more rapid and consequently detonation might occur more readily.

There appear to be several views of the phenomenon known as "knocking" in internal combustion engines:—

- (1) Combustion changes to detonation, a detonation wave being set up.
- (2) Combustion changes to detonation locally, but the wave is not transmitted throughout the charge.
- (3) Self-ignition of portions of the charge occurs.

Depending on circumstances, any of these views may represent what happens. It is probable that when violent knocking takes place, detonation is set up

and the detonation wave passes through the unburnt gases. Reflection waves would travel back and forth through the burnt gases getting slower and slower as they cooled. On the other hand, since conditions in an engine are such that (a) the mixture is near the limiting mixture strength in which a detonation wave can transmit itself, (b) the detonation may occur when the bulk of the charge is burnt, (c) the piston has commenced to move out, and (d) the charge is in a state of turbulence, mild detonation may indicate that a local change to the detonating type of combustion occurs, but that a detonation wave is not propagated ; many of the photographs indicate this possibility.

Wendlandt\* has determined the composition of the *limit* mixtures (at ordinary pressures) for hydrogen-air and carbon monoxide-oxygen mixtures, which will transmit a detonation wave. A very slight change of composition makes a great difference to the propagation of the wave, and probably a slight difference of pressure would make similar differences. It is thus quite possible that local detonation might occur without transmission of a wave throughout the unburnt gas.

The conditions which give rise to detonation are, no doubt, high local pressure and high local temperature. Sound waves from the spark, self-ignition centres and obstructions may occasion high local pressures ; hot valves, hot intake or exhaust gases, carbon deposit or any influence reducing heat loss might produce high temperatures. Adiabatic compression during the compression stroke and the additional temperature from the hot exhaust gases generally provide a high enough temperature at the end of the compression stroke to ignite the charge were more time available before passage of the spark. It is possible, therefore, that part of the charge might ignite of itself after the spark had passed, particularly as the pressure would be rising rapidly. Such an action ought however to assist, rather than otherwise, normal combustion, just as multiple ignition centres are well known to do. Compression waves set up by the ignited charge may cause auto-ignition of another part of the charge, giving rise to stronger compression waves which occasion knocking. The present work does not provide any evidence for such a view, but it is intended to carry out further experiments on the point.

## VII. Summary.

(1) Detonation in acetylene and in pentane mixtures at high initial temperatures (230° C.) and pressures (10 atmospheres) has been investigated photographically, using a steel tube fitted with glass windows.

\* 'Z. Phys. Chem.,' vol. 116, p. 227 (1925), and vol. 110, p. 637 (1924).

(2) Increase of initial pressure engenders earlier detonation up to a certain limit, when further increase makes very little difference.

(3) The effect of increase of initial temperature was also investigated. At a given initial pressure, rise of initial temperature appeared to render detonation slightly later.

(4) Lead tetraethyl was not found to affect the position of detonation of the mixtures investigated at high pressure either at normal initial temperature or at 230° C.

This work has been carried out with funds provided by the Asiatic Petroleum Company. We are indebted to the Company and their technical staff for their interest in it.

#### KEY TO PHOTOGRAPHS.

##### PLATE 17.

PHOTO. 1.—Effect of pressure on position of detonation. Mixture  $1C_2H_2 + 2.5O_2 + 4N_2$ , 15 lbs. pressure. Detonates at 52 cms.

PHOTO. 2.—Effect of pressure on position of detonation. Mixture  $1C_2H_2 + 2.5O_2 + 4N_2$ , 30 lbs. pressure. Detonates at 31 cms.

PHOTO. 3.—Effect of pressure on position of detonation. Mixture  $1C_2H_2 + 2.5O_2 + 4N_2$ , 60 lbs. pressure. Detonates at 18 cms.

PHOTO. 4.—Mixture  $1C_2H_2 + 2.5O_2 + 4N_2$ , ignited at centre of tube (55 lbs. pressure). Detonates at 22 cms.

PHOTO. 5.—Mixture  $1C_2H_{12} + 8O_2 + 15N_2$ , 136 lbs. pressure. Detonates at 74 cms.

##### PLATE 18.

PHOTO. 6.—Effect of temperature on position of detonation. Mixture  $C_2H_2 + 2.5O_2 + 5A$ , 17° C. 15 lbs. pressure. Detonates at 55 cms.

PHOTO. 7.—Ditto at 40° C. Detonation at same position.

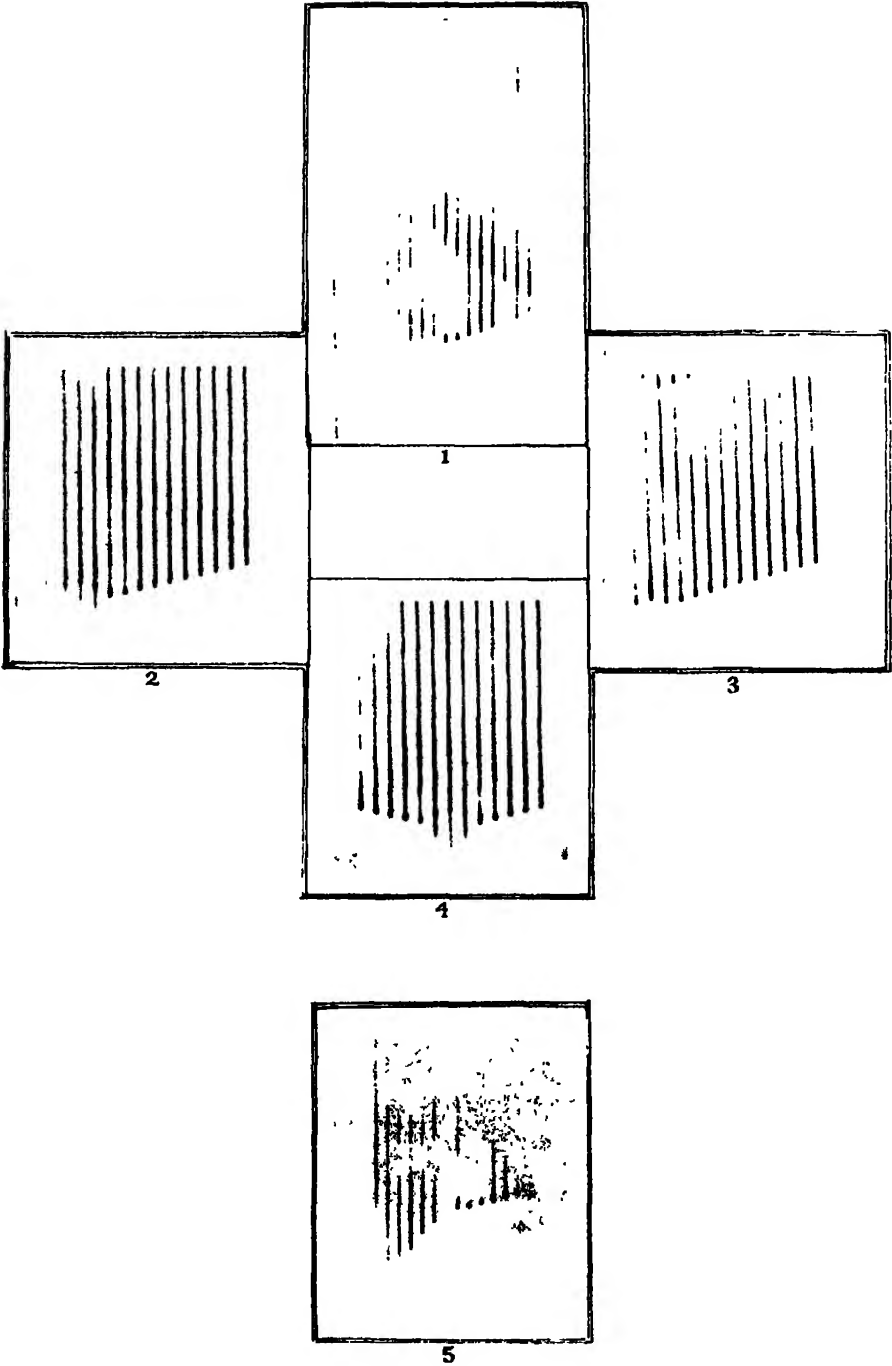
PHOTO. 8.—Effect of lead ethyl and temperature.  $C_2H_{12} + 8O_2 + 15N_2$ , 79 lbs. 230° C. Detonates at 85 cms.

PHOTO. 9.—Effect of temperature alone.  $C_2H_{12} + 8O_2 + 15N_2$ , 79 lbs. 230° C. Detonates at 88 cms.

PHOTO. 10.—Mixture  $C_2H_{12} + 8O_2 + 6N_2$ , 79 lbs. Normal temperature. Detonates at 32 cms.

PHOTO. 11.—Effect of lead ethyl. Mixture  $C_2H_{12} + 8O_2 + 6N_2$ , 79 lbs. Normal temperature. Detonates at 30 cms.

---



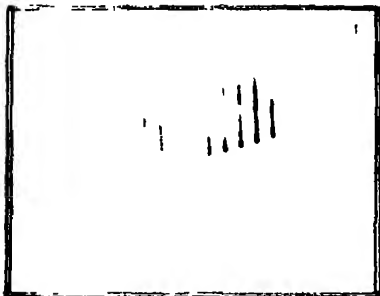




6



7



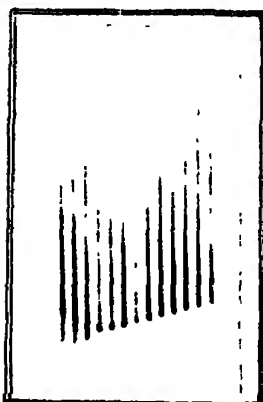
8



9



10



11

*Some Physical Properties of Icebergs and a Method for their Destruction.*

By HOWARD T. BARNES, D.Sc., F.R.S., Professor of Physics and former Director, McGill University, Montreal.

(Received November 4, 1926.)

[PLATES 19-22.]

The icebergs which infest the North Atlantic have their origin in the glaciers of Greenland. The ice composing them is formed by compression of snow and frost, and in consequence possesses structural characteristics very different from those of ordinary ice, which we may call thermal ice.

Glacial ice has been studied a great deal, and the literature on the subject is voluminous.

From all of this material it may be learned that the structure of glacier ice and icebergs is granular in nature. The nuclei of these grains are obviously the snow crystals which have in the course of ages grown to considerable size. With the depression of the snow under the accumulations of fresh deposits, a great deal of air is entangled and pressed into the mass. During the movement of the ice downwards and outwards, cracks and crevices result in ways well understood. These become filled with melted glacier ice water of great purity and refreeze free of air. The natural colour of pure ice is a deep blue by the scattering of the light from the large ice molecules, and in these refrozen cracks are found the remarkable deep blue bands which are characteristic of iceberg masses.

Solid pressure ice, which contains air, is a deep green, but rapidly weathers on the exposed surface under a bright sun to pure white.

The appearance of the surface is caused by innumerable air bubbles which have been released in the ice by the sun's rays, and have assumed measurable proportions. It is not the purpose here to go into the theory of glacial movement, or discuss the purely geological or climatological aspect of glaciers, as this is very little connected with the object of the present investigation, which has been carried out in an attempt to gain sufficient knowledge of icebergs to find some way to hasten their disruption.

It is only by a careful physical study of icebergs that suggestion can be gathered towards this end.

The author has had this matter under study for a great many years, his first

iceberg pictures having been obtained in 1893, but it was not until 1910, after many years devoted to ice research on the St. Lawrence River, that he was able to give special attention to the problem.

The first iceberg expedition sent out by the writer was in the summer of 1910 when, through the help of the Canadian Government, passage was given on one of the Government boats from Quebec to Hudson Bay and return. During this voyage microthermometer observations were made of sea temperatures in the proximity of icebergs, and it was found that an iceberg is surrounded by a zone of water in general higher in temperature than the currents in which it was being carried.

Other expeditions were organised and carried out around the Strait of Belle Isle, the Coast of Labrador, and several across the Atlantic through the kindness of the steamship lines (C.P.R., Royal and Allan lines). The final result of this work has already been published.\*

In 1924 the author went out on one of the ice patrol trips of the U.S. Coast-guard ships (U.S.C.G. "Modoc") to study their methods of ice patrol. Fortunately this time was spent floating alongside a single berg 60 miles off the Newfoundland Coast. Much valuable information was obtained as to the way in which an iceberg breaks up under natural conditions. Two weeks were consumed in this study, and the interesting fact was noticed by the writer that the greatest calving and most numerous cracking took place in the early morning at and immediately after sunrise.

Observation showed that during the night the berg stopped running with water over its surface and froze again.

With the advent of sunlight, and before the surface-melting started, the heat of the returning day apparently penetrated the ice and, it was thought, caused an unequal expansion, resulting in the cracking.

All day the berg ran with water and washed away this heat, maintaining a surface temperature of 0° C.

During the night and towards morning the largest growlers fell off and floated away. This suggested to the writer that strains could be set up at will in the great ice mass by the local application of heat at a high enough temperature to cast powerful rays into the ice.

\* "43rd Annual Report, Department of Marine and Fisheries of Canada," 1909-10, 'Royal Institution Report,' May, 1912. The voyage of the "Sootia" in 1913 and U.S.S. "Seneca" in the same year failed to pick out the iceberg effect owing to the lack of a suitable microthermometer. An ordinary recorder is not sensitive enough to detect the warm layers.

The actual experiment of applying heat in an iceberg was not tried, however, until two years later, but the idea then obtained was productive of helpful methods for general ice control on a very large scale.\*

### *Physical Properties.*

Several were considered of interest, but all of them could not be studied during the recent expedition to Notre Dame Bay, Newfoundland, made by the writer during the past summer.

Information was gathered on the purity of the iceberg ice, and the amount and quality of the air compressed in the berg. By inference the density of the co-volume of ice and air which composes the bulk of the iceberg was obtained. The other physical properties, such as hardness and elastic constants, must be reserved for a later series of tests.

The chemical work of this expedition was done entirely by my son, Mr. W. H. Barnes, Demonstrator of Chemistry in McGill University.

Comfortable quarters were given the writer in the Notre Dame Bay Memorial Hospital situated at Twillingate, which was the headquarters during the stay in Newfoundland. The director, Dr. Charles E. Parsons, was most kind in giving us a room for a laboratory. The photographic rooms connected with the X-ray department of the hospital gave us an opportunity for developing the colour plates which were made to show the wonderful deep blue and green of the ice masses. The Agfa colour process plates were found very satisfactory.

### *Results of the Chemical Tests.*

*Total Solids.*—About one litre of water was evaporated to dryness in a weighed platinum dish, and the dish and residue was re-weighed. The following results were obtained :—

Nature of Water	Volume Evaporated.	Residue.	Total Solids. Parts per (100000)
Melted iceberg ice	1079 c.c.	0.0045 gms.	0.41
Distilled water	1044 c.c.	0.0055 gms.	0.52

The residue, which in each case was black and insoluble in water, was probably made up of dust particles from the air accumulated during the evaporations.

\* "Engineering Features in Breaking the Allegheny Ice Gorge," 'The Journal of the Engineering Institute of Canada,' vol. 9, p. 453 (1926).

*Relative Volume of Air in Iceberg Ice.*—A large test tube having a thin paper strip down one side was partially filled with toluene and placed in an ice-salt freezing mixture. When the temperature of the toluene had become constant its level in the tube was marked on the paper strip. A piece of iceberg ice was then quickly dried with filter paper and placed in the toluene, the new level of the toluene being marked on the paper strip as before. The piece of ice was then rapidly transferred by means of a long forceps to a bath of melted ice-water at room temperature, where it was allowed to melt under an inverted funnel.

The air on escaping passed into an eudiometer tube, where it collected by displacing the melted ice water with which the tube was filled. Care was taken that no bubbles adhered to the stem of the funnel or the walls of the eudiometer tube. The volume of air collected was read at atmospheric pressure from the graduations on the eudiometer tube.

The volume of the ice was obtained by replacing the toluene in the large test tube by water run in from a burette, the volume between the two marks on the paper strip being carefully noted.

The following results were obtained with two samples of ice:—

Temperature of Toluene.	Volume of Air (reduced to temperature of Toluene).	Volume of Ice and Air.	Per cent. Volume of Air.
— 0.8° C	0.28 c.c.	1.85 c.c.	15.1
— 2.1° C.	0.55 c.c.	7.4 c.c.	7.4

The calculations involved in the above results assume that the air in the iceberg ice is at atmospheric pressure. Observation of the behaviour of the ice on melting and the sizes of the bubbles in the ice, and after being released from the ice, support this assumption.

*Analysis of Air Enclosed in Iceberg Ice.*—Ground-glass stoppered bottles of about 500 c.c. capacity were filled with melted ice-water and inverted in a bath of melted iceberg ice. The iceberg ice was allowed to melt under a funnel, the stem of which passed through a rubber cork into the neck of the bottle to be filled. Two of the bottles were completely filled with the air, whereas three others were sealed up with water. The ground-glass stoppers were wired to the bottles and sealing was completed with paraffin.

At a later date the bottles were opened under water which had previously been aerated for 10 hours. A long bent glass tube filled with water was inserted

through the neck of the bottle into the gas, the other end being connected to a gas burette. A sample of the air was taken and analysed for carbon dioxide and oxygen in the usual manner, using the Hempel apparatus, potassium hydroxide and alkaline pyrogallate being employed for absorption of carbon dioxide and oxygen respectively.

The following are the results obtained, together with particulars of each sample :—

*Sample 1.*—Air from growler shortly after it broke away from berg, collected over seawater at 46·5° F. Sealed up with seawater in bottle.

Analysis :—

CO <sub>2</sub> .....	0·0 per cent.
O <sub>2</sub> .....	20·0 „

*Sample 2.*—Air from growler collected over melted iceberg ice without regard to temperature of bath. Sealed up with water through which bubbles passed.

Analysis :—

	CO <sub>2</sub>	O <sub>2</sub>
1 .....	0·2 per cent.	17·7 per cent.
2 .....	0·0 „	17·9 „
Mean .....	0·1 „	17·8 „

*Sample 3.*—Air from growler collected over melted iceberg ice. Temperature of bath, 40–45° C. Bottle completely filled with air.

Analysis :—

Mean of six analyses agreeing with one another to 0·6 per cent. oxygen.

CO <sub>2</sub> .....	—0·1 per cent.
O <sub>2</sub> .....	19·0 „

*Sample 4.*—Air from 2 feet below surface of berg collected over melted iceberg ice. Temperature of bath, 45–50° C. Only a very small sample (23 c.c.) of air was collected. Bottle sealed up containing water from the bath.

Analysis :—

CO <sub>2</sub> .....	0·4 per cent.
O <sub>2</sub> .....	13·8 „

*Sample 5.*—Air from growler collected over melted iceberg ice at temperature of 40–45° C. Bottle filled completely with air.

Analysis :—

Mean of six analyses agreeing with one another to 0·6 per cent. oxygen.

CO <sub>2</sub> .....	—0·1 per cent.
O <sub>2</sub> .....	18·8 „

*Discussion.*

With regard to the determination of total solids, it will be seen that melted iceberg ice is at least as pure as distilled water. At some future date it is planned to make conductivity measurements on this water.

The two determinations of the relative amount of air contained in iceberg ice are only approximate because of the difficulty in reading such small volumes of gas in the eudiometer tube, which was only graduated to tenths of a cubic-centimetre. The next determinations will be made with a specially constructed tube of small bore, with which readings can be taken to a further number of decimal places. The values already found, however, are probably a minimum because the ice on melting undoubtedly dissolved a small fraction of the air liberated. There was probably very little loss of air from the bubbles passing through the water in the eudiometer tube, because it was obtained by melting iceberg ice and allowing it to stand in an open pail for some length of time before use as a bath.

It is also planned to make tests at some future time on the relative amount of air at different depths through the bergs.

The air analyses indicate that the air contained in the iceberg ice has probably the same composition as the atmosphere at the present day.

The peculiar values for carbon dioxide obtained are due to experimental error. The carbon dioxide found was zero after the first few analyses due probably to the fact that the air sample was allowed to remain in the gas burette for 15 to 20 minutes before passing into KOH. This enabled it to come to the temperature of the room before the first volume was read. A very slight change in temperature would have a marked effect on the volume of the gas, since in most cases from 50 to 100 c.c. were used for each analysis.

That the composition of the air is probably the same as that of the atmosphere of the present day is shown by the following rough calculation.

Taking the results of Sample 3, namely, 19.0 per cent. oxygen and neglecting the value for carbon dioxide recorded and assuming that the relative volume of air is, say, 10 per cent., then the relative amounts of oxygen and nitrogen in the original air are given by  $(0.19 \times 100) + (0.0045 \times 1000)$ , for oxygen at 40–45° C. from air is equal to  $\frac{1}{5} \times 0.0225$  vol. of O<sub>2</sub> per vol. of water and  $(0.81 \times 100) + (0.0092 \times 1000)$  for nitrogen, since the solubility of the nitrogen at 40–45° C. from air is equal to  $\frac{4}{5} \times 0.0116$  vol. of N<sub>2</sub> per vol. of water.

The amount of oxygen in the original air is then equal to

$$\frac{(0.19 \times 100) + (0.0045 \times 1000)}{[(0.81 \times 100) + (0.0092 \times 1000)] + [(0.19 \times 100) + (0.0045 \times 1000)]}$$

$$= \frac{23.5}{113.7} = 20.7 \text{ per cent.}$$

assuming saturation of the iceberg ice with oxygen and nitrogen as it melts.

The slightly larger value of 20.0 per cent. oxygen obtained for sample 1 is probably due to the lesser solubility of air in sea water. The lower value obtained for sample 2 can be accounted for by the fact that no attention was paid to the temperature of the bath, and consequently it was usually at a much lower value than for samples 3 and 5.

Samples 3 and 5, although from growlers from different bergs, were collected in exactly the same manner with the temperature of the bath maintained between 40 and 45° C.

The results obtained for the two samples agree closely with one another.

The peculiarly low result obtained for sample 4 may be due to experimental error because the sample obtained was only 23 c.c. Unfortunately, no check could be made on this sample. The result, however, remains interesting, although not necessarily of special significance. It is hoped that at the next opportunity of obtaining iceberg ice a chamber capable of being evacuated will be available. The ice will be broken up by a magnetic crusher in vacuum and the air collected and analysed very carefully over mercury. It is also planned to collect samples of the air from different depths in the berg in this way.

#### *Effect of Applying High Temperature Heat to Icebergs.*

The experiments with thermit were conducted on three bergs. The biggest one we could find was treated first with a hundred pound charge let into the ice about three feet. The result of firing was the emission of flame and fire to a height of 125 feet or more with a great explosion of the ice and the throwing off of great masses of the ice from the sides and ends of the main plateau treated. This iceberg was, we estimated from our survey, 500 feet long by as many wide, and its mountainous cliffs rose on one side to a height of between 75 to 100 feet with a second plateau 60 feet up. These measurements were made all from the water line and no estimate was made of the mass under the water. The whole berg was stable and oscillating very slowly from the swell with a period of from 4 to 5 minutes. As anticipated, the effect of the intense heat in direct contact with the hard ice was to send a temperature wave into the mass which produced a great deal of cracking and visible disruption, apart from the explosive shock (figs. 3 and 4) of the dissociated ice itself. This cracking went on all the evening after we returned to the village and could be distinctly heard out at sea 5 miles away. Toward the early morning a very loud report resulted which woke many of the people of Twillingate, and when we visited the berg the next day we found the great bulk of the interior had come away. The day following witnessed the



full effect of the cracking when the whole plateau on which the charge had been fired split, and came away almost across the thermit hole.

The disintegrating effect of the heat treatment can be seen by comparing photographs 1 and 2 which were taken before and after the charge of thermit was set off. The whole berg could have been broken up had we placed more heat-charges in at different points. As it was about a third of the ice was broken off and the whole berg turned through 45 degrees through the lightening of the side treated.

On the last day two charges of the high explosive, bermite, were set off on the berg illustrated in photograph 2, which pulverised the ice surface a great deal. The second berg treated was a small one aground in Jenkin's Cove, in the harbour. Fig. 5 shows firing the charge on this mass. 500 pounds placed about 4 feet in the ice was fired at sundown in order to allow the people of Twillingate an opportunity to see the spectacle of the burning and disrupting ice. The whole thing was a most wonderful sight when the mighty charge fired and roared, lighting up the iceberg and surrounding hills like Vesuvius in eruption. Flames and molten thermit and ice were shot upwards 100 feet or more by the explosion which followed. Much of this berg was disrupted but the full effect of the big charge was lost into the air. As before the real change in the berg did not take place until the next day, when most of the off-side nearly through the thermit hole came away (fig. 6). For two days after this berg continued to break away and rolled from one side to the other shifting its position as it was lightened by breaking masses.

The third berg treated was a small one of the mushroom type (fig. 7), outside the harbour, but aground off the shore of the North Island. The berg was roughly 100 feet in diameter and almost round with a central cup-shaped dome. On the summit of this were planted two charges of thermit, the first of 60 pounds and a second of 100 pounds. Explosions came in both cases, but no visible sign of disrupting ice. On returning the next morning this berg could not be found for it had fallen away along the thermit hole, becoming honeycombed with cracks. A floating fragment was identified by marks of the molten thermit and the hole blown out by the reaction which was now on the water-line half hidden under the surface, see fig. 8. Three other bergs close by were still in place. There is no doubt of the disrupting action of the high temperature of the thermit, and another time means shall be found to sink the charge down 50 or 100 ft. into the ice, which can easily be done by means of a rock drill in a very few minutes. Indeed, the bergs can be drilled from a boat without going on them where this is impracticable.



FIG. 1.—Large iceberg before treating with thermit.



FIG. 2.—The same iceberg two days later after thermit treatment test of a high explosive without much result.

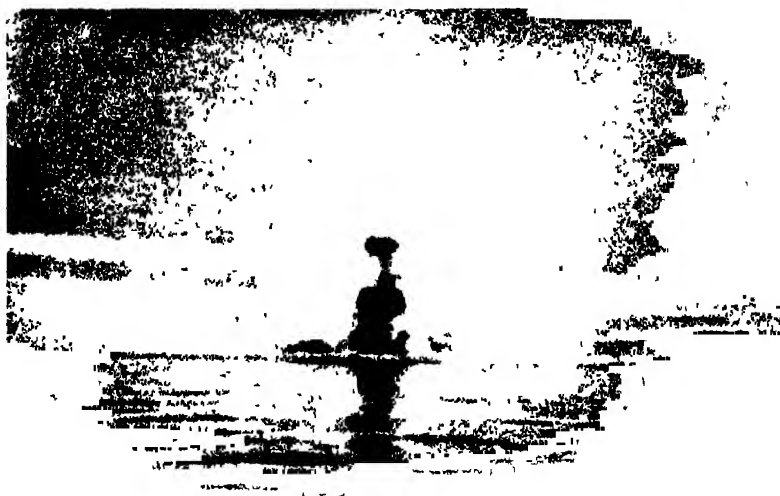


FIG. 3.—Explosion of the ice from the reaction of 100 lb. of thermut.



FIG. 4.—Fragments of ice scattered over the sea from the force of the exploding ice.



FIG. 5 —A small iceberg exploded from the reaction of 500 lb. of thermit.

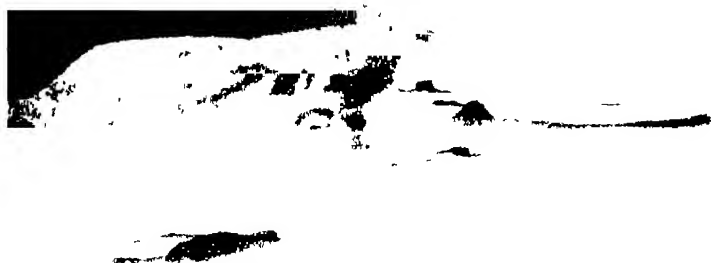


FIG. 6.—The same iceberg taken the next morning rapidly breaking up from the honey combing and cracks of the intense heat reaction.

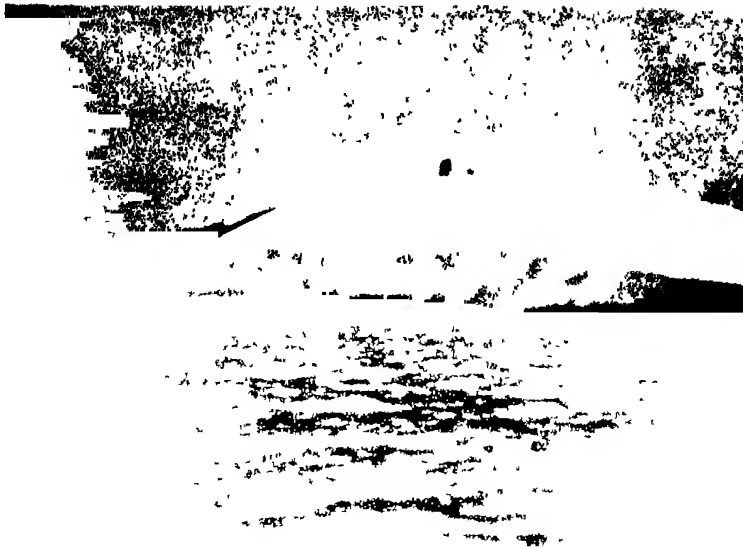


FIG. 7.—Last iceberg to be treated. Lighting the fuse for setting off a 100 lb. charge.

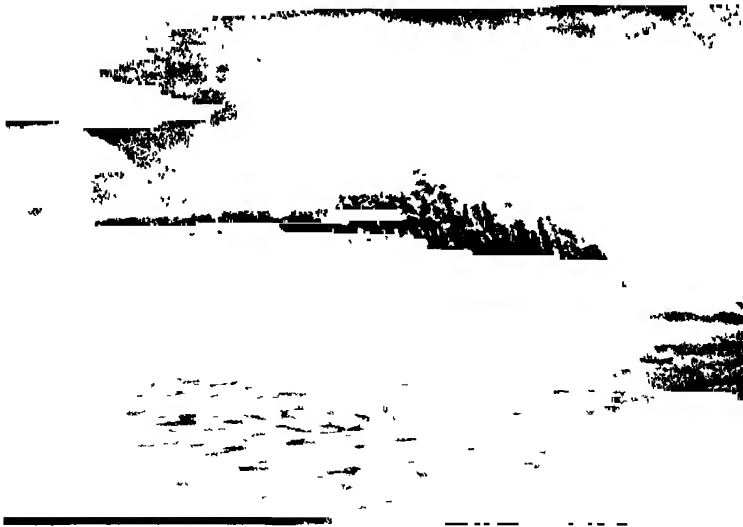


FIG. 8.—Fragment of the above iceberg recognised by the marks of the thermit slag, and the hole blown out of the ice by the heat reaction. This piece was the only remains of the berg found the next morning, and was rapidly going to pieces. It was not safe to go on again. Three other bergs in the immediate vicinity remained in place. The thermit hole is nearly submerged.

*Studies upon Catalytic Combustion.—Part V. The Union of Carbonic Oxide and other Gases with Oxygen in Contact with a Fireclay Surface at 500° C.*

By WILLIAM A. BONE, D.Sc., F.R.S., and A. FORSHAW, M.Sc.

(Received December 24, 1926.)

*Introduction.*

In a former communication to the Society, Bone and Wheeler dealt very fully with the action of a porous porcelain surface in promoting the slow combination of hydrogen and oxygen at 430° C.\* It was shown (*inter alia*) (i) that previous exposure of the surface to hydrogen at such temperature stimulates its catalysing power towards normal electrolytic gas in a very remarkable degree, and (ii) that when excess of one or other of the reacting gases is present, the rate of combination is always proportional to the partial pressure of the hydrogen.

In Sections *A* and *B* of the present communication, similar experiments will be described upon the behaviour of a fireclay surface at 500° C. towards mixtures of carbonic oxide and oxygen, showing (i) that previous exposure of carbonic oxide has much the same stimulating effect upon its catalysing power as was previously observed by Bone and Wheeler in regard to a porcelain surface and hydrogen, and (ii) that in most other respects the surface catalysed the combination of CO-oxygen mixtures in much the same way as does one of porcelain that of hydrogen and oxygen mixtures, except that in the former case the catalysing power is feebler than in the latter. In Sections *C* and *D* will be described comparative experiments upon the relative speeds of the catalytic combustion of carbonic oxide, hydrogen and methane, respectively, in contact with a fireclay surface at 500° C.

It should be understood that in all experiments the Bone and Wheeler circulation apparatus was employed, a series of bulbs containing a solution of barium hydroxide being inserted to ensure the continuous and rapid removal from the system of the carbon dioxide produced. The general arrangement of the apparatus was in all essential respects that shown in the diagram published in Part I hereof (*q.v.*)†; its total capacity would be about 1,500 c.c., and the

\* 'Phil. Trans.,' A, vol. 206, p. 13 (1906).

† 'Proceedings,' A, vol. 109, p. 465 (1925).

gaseous mixtures were circulated through the system at a rate such that each circuit was completed in about an hour. The experiments will be described in their chronological sequence, adopting the same symbols as before, so that the reader may better understand how the "surface activity" varied with such factors as previous history, pressure, and the actual composition of the reacting mixtures concerned. For we would again emphasise how important it is for the correct interpretation of such experiments always to have the fullest information as to the conditions throughout. It may be assumed that in all the cases the reacting mixtures were saturated with water vapour at the room temperature, which will be indicated by  $\theta$  in the text.

### *Experimental.*

The catalysing surface employed was prepared by crushing a high-grade firebrick, removing the finer particles by sieving, and then using those which would be retained on a mesh of 5 and pass through one of 3 per linear inch. The material was strongly ignited at  $900^{\circ}\text{C}$ . in air before being packed into the reaction tube of the circulation apparatus.

The gases used were quite pure, save for the presence of less than 1 per cent. of adventitious nitrogen, which may be regarded as negligible. All the pressure values recorded in the paper refer to the dry "nitrogen-free" gas.

It should also be understood that, throughout any given series of experiments, the furnace used for heating the reaction tube was never turned out, but kept going continuously at the experimental temperature for the whole duration of the series.

### *A.*

This series of experiments was carried out at Manchester University by one of us (W. A. B.) in conjunction with G. W. Andrew in the summer of 1906, just before the apparatus was dismantled for removal to Leeds University where it was reinstalled two years later for the remainder of the research.

At the outset of the series, the "activity" of the surface was very low, a value of  $k = 0.015$  (approx.) being obtained when a "moist" normal mixture  $2\text{CO} + \text{O}_2$  was circulated over it, the rate of combination throughout being proportional to the pressure of the reacting mixture as follows:—

*Experiment I (14/6/1906) with a 2CO + O<sub>2</sub> Mixture.*

$$T = 490^{\circ} \text{C.} \quad \theta = 25.5^{\circ}.$$

$t$ Hours.	$P_{2\text{CO} + \text{O}_2}$ mm.	$k_1 = \frac{1}{t} \log \frac{P_0}{P_t}$
0	408	—
2	380	0.0154
4	355	0.0151
6	331	0.0151
10	287	0.0153

At the conclusion of the experiment a sample of the residual gas was removed from the apparatus for analysis, when it was found to contain 65.0 per cent. of carbonic oxide. The ratio C/A obtained in the explosion analysis was, however, 0.523, showing that a little hydrogen had been generated by the interaction  $\text{CO} + \text{H}_2 \rightleftharpoons \text{CO}_2 + \text{H}_2$  during the experiment.

*Experiments II to IV with Mixtures containing Excess of Carbonic Oxide.*

In three successive experiments a mixture originally containing a large excess of carbonic oxide, namely,  $4\text{CO} + \text{O}_2$ , was circulated over the surface at  $490^{\circ}$ , and after each experiment the residual gas, after all the oxygen had disappeared, was kept circulating over it at the same temperature for many hours. In these circumstances, not only was the activity of the surface, as indicated by the  $k_{\text{O}_2}$  values, greatly enhanced, but the rate of combination was much more proportional to the partial pressure of the carbonic oxide than to that of the oxygen, as the following observations (Experiment IV  $T = 490^{\circ}$ ,  $\theta = 26^{\circ}$ ) show :-

$t$ Hours.	$P_{\text{CO}}$ mm.	$P_{\text{O}_2}$ mm.	$k_{\text{CO}}$	$k_{\text{O}_2}$
0	299	76	—	—
2	246	49	0.0427	0.0953
4	207	29	0.0400	0.1046
$6\frac{1}{2}$	167	9	0.0390	0.1425

A sample of the gas removed from the apparatus at the end of  $6\frac{1}{2}$  hours, whilst there was still a small proportion of oxygen in it, gave on subsequent explosion analysis a C/A ratio = 0.510, showing that only a small amount of



hydrogen had been generated by interaction between steam and carbonic oxide up to that point. When, however, the circulation of the residual gas, whose oxygen-content soon vanished, was continued over the surface, hydrogen rapidly accumulated in it, as the following figures indicate :—

Percentage Composition of the  $N_2$ -free Residual Gas in the Apparatus after—

			18 hours.	42 hours.
CO	..	..	86.7	72.4
H <sub>2</sub>	..	..	13.3	27.6

Such indeed was typical of our usual experience during the investigation ; for so long as free oxygen was present in the reacting mixture little or no free hydrogen accumulated in it, but afterwards it would do so.

It will be seen from experiments to be described in Section C hereof, that the rate of oxidation of hydrogen at the experimental temperature over the surface was very much greater than that of moist carbonic oxide.

*Experiment V (29/6/1906) with a  $2CO + O_2$  Mixture showing the Stimulating Effect of the Residual Gas from IV.*

$$T = 490^\circ. \quad 0 = 22.6.$$

The residual gas from Experiment IV having been circulated over the surface at  $490^\circ$  for 48 hours and then withdrawn from the apparatus, the catalysing power of the surface towards the "normal"  $2CO + O_2$  mixture was found to be many times greater than in Experiment I, as the following results show :—

$t$	$P_{2CO+O_2}$	$k_1$
Hours	mm.	
0	400	—
2	237	0.1137
4	150	0.1065

*Experiment VI (2/7/1906) with a Mixture containing Excess of Oxygen.*

$$T = 490^\circ. \quad 0 = 23^\circ.$$

The surface having thus been brought into a highly active condition, a mixture initially containing equal volumes of the reacting gases (i.e.,  $CO + O_2$ ) was circulated over it at  $490^\circ$ , with the result that the rate of combination,

which still remained very super-normal, was found to be nearly proportional to the partial pressure of the CO, as follows :—

$t$ Hours.	$P_{CO}$ mm.	$P_{O_2}$ mm.	$k_{1CO}$	$k_{1O_2}$
0	201	200	—	—
1	157	178	0.1073	0.0506
2	126	162	0.1014	0.0457
4	85	142	0.0934	0.0372
10	19	109	0.1024	0.0263

*Experiments VII to IX with a  $2CO + O_2$  Mixture showing the Depressing Effect of Oxygen-treatment.*

Finally, after a prolonged treatment of the surface with oxygen at  $490^\circ$ , during which its catalysing power continuously decreased, a stable condition of very low activity was reached (Experiment IX) which left the surface in much the same condition as it had been at the commencement of the series (compare Experiment I), as follows :—

*Experiment IX (16/7/1906).*

$$T = 490^\circ. \quad \theta = 23^\circ.$$

$t$ Hours.	$P_{2CO+O_2}$ mm.	$k_1$
0	400	—
5	334	0.0157
24	165	0.0160
42	80	0.0167

*B.*

Two years later, after the apparatus had been re-installed at the University of Leeds, another series of experiments was carried out by A. Forshaw with a similar surface at a temperature which did not vary more than 2 or  $3^\circ$  on either side of  $500^\circ$  C. during the whole period covered by them.

At the outset of the experiments the catalysing power of the surface was feeble ( $k_1 = 0.0247$ ), but it gradually increased as successive "normal"  $2CO + O_2$  mixtures were circulated over it, until eventually it reached a fairly steady state with  $k_1 = 0.030$ , which was considered to represent the "normal" condition for the series. It will suffice to give the details of one typical group

of successive experiments (Nos. XX to XXVII) of the series, in order to show how the results previously obtained in Manchester were generally confirmed.

*Experiment XX (30/6/1908) with a  $2\text{CO} + \text{O}_2$  Mixture showing the "normal" Catalysing Power of the Surface.*

$$T = 501 \text{ to } 503^\circ. \quad \theta = 22.5^\circ.$$

$t$	$P_{2\text{CO} + \text{O}_2}$	$k_1$
Hours.	mm.	
0	448.4	—
1	418.9	0.0296
4	345.0	0.0285
$19\frac{1}{4}$	116.8	0.0303

The apparatus was now rapidly evacuated, and a mixture  $4\text{CO} + \text{O}_2$  introduced.

*Experiment XXI (1/7/1908) with Mixture containing Excess CO.*

$$T = 498 \text{ to } 504^\circ. \quad \theta = 22 \text{ to } 24^\circ.$$

$t$	$P_{\text{CO}}$	$P_{\text{O}_2}$	$k_{1\text{CO}}$	$k_{1\text{O}_2}$
Hours.	mm.	mm.		
0	362.9	94.5	—	—
2	326.2	76.2	0.0231	0.0467
4	292.8	59.5	0.0233	0.0502
$6\frac{1}{2}$	255.7	40.9	0.0234	0.0559
$10\frac{1}{4}$	202.0	14.0	0.0236	0.0771

It is clear that the catalysing power of the surface, which is best indicated by the  $k_{\text{O}_2}$  values, steadily increased during the experiment, the rate of reaction being strictly proportional to the partial pressure of the carbonic oxide throughout. Analysis again showed that there had been no appreciable liberation of hydrogen by the interaction of carbonic oxide and steam during the first  $10\frac{1}{4}$  hours, i.e., whilst any free oxygen remained in the system. On continuing the circulation of the residual gas, after all the oxygen had disappeared, however, hydrogen slowly appeared, as the following figures show:—

$t$	20 $\frac{1}{4}$	45	93 Hours.
Percentage composition of Gas in Apparatus	$\left\{ \begin{array}{l} \text{CO} = 88.4 \\ \text{H}_2 = 10.4 \\ \text{N}_2 = 1.2 \end{array} \right.$		
	69.0	29.5	47.0
	1.5	1.2	1.2

The residual gas having been continuously circulated for upwards of 80 hours over the surface and then withdrawn, the catalysing power of the surface towards a normal  $2\text{CO} + \text{O}_2$  mixture (Experiment XXII) was found to have been greatly enhanced, as follows :—

*Experiment XXII (5/7/1908) with a  $2\text{CO} + \text{O}_2$  Mixture.*

$$T = 500^\circ, \quad \theta = 22^\circ.$$

$t$ Hours.	$P_{2\text{CO} + \text{O}_2}$ mm.	$k_1$
0	150.8	—
2	294.5	0.0925
4	210.8	0.0826
8	114.5	0.0744

On continuing to circulate a  $2\text{CO} + \text{O}_2$  mixture over the surface at  $500^\circ$  during the next 48 hours, the catalysing power gradually diminished until  $k_1$  had fallen to 0.048 (in Experiments XXIII and XXIV) the details of which need not be reproduced). Whereupon, the apparatus was evacuated and an approximately equimolecular  $\text{CO} + \text{O}_2$  mixture was introduced after which the following observations (Experiment XXV) were made :—

*Experiment XXV (7/7/1908) with a Mixture containing Excess of  $\text{O}_2$ .*

$$T = 500^\circ, \quad \theta = 20^\circ.$$

$t$ Hours.	$P_{\text{CO}}$ mm.	$P_{\text{O}_2}$ mm.	$k_{1\text{CO}}$	$k_{1\text{O}_2}$
0	171.2	198.9	—	—
2	131.9	179.3	0.0566	0.0225
4	101.6	164.1	0.0567	0.0209
7	68.9	147.7	0.0565	0.0185
12	35.4	131.0	0.0570	0.0151
25½	4.6	115.6	0.0616	0.0092

Attention is again directed to the remarkable constancy of the  $k_{\text{O}_2}$  values throughout (cf. also Experiment XXI). Finally, after the residual oxygen had been circulated in the apparatus for 48 hours longer, and then pumped out, the catalysing power of the surface towards the theoretical  $2\text{CO} + \text{O}_2$  mixtures was redetermined (Experiment XXVI) as follows :—

*Experiment XXVI (9/7/1908) with a  $2\text{CO} + \text{O}_2$  Mixture after 48 hours  $\text{O}_2$  treatment.*

$$T = 501 \text{ to } 503^\circ. \quad \theta = 20^\circ.$$

$t$ Hours.	$P_{2\text{CO} + \text{O}_2}$ mm.	$k_1$
0	432.6	—
2	354.1	0.0435
4	295.8	0.0413
5	272.9	0.0400

After the conclusion of this experiment the furnace was turned out, and the apparatus evacuated; it was then allowed to remain vacuum at the room temperature for a period of six weeks, after which the furnace was re-lighted and the temperature of the reaction tube raised to  $500^\circ \text{C}$ . again. Unfortunately, however, the tube cracked during the process, admitting air to the surface; but it was quickly mended and the apparatus re-exhausted. On subsequently re-determining the catalysing power of the surface towards a theoretical  $2\text{CO} + \text{O}_2$  mixture (Experiment XXVII) it was found to have fallen nearly to the same "normal" value as had been observed at the commencement of the series (*cf.* Experiment XXI), as follows:—

*Experiment XXVII (26/8/1908) with a  $2\text{CO} + \text{O}_2$  Mixture.*

$$T = 500 \text{ to } 504^\circ. \quad \theta = 20^\circ.$$

$t$ Hours	$P_{2\text{CO} + \text{O}_2}$ mm.	$k_1$
0	218.8	—
2	185.8	0.0355
6	137.6	0.0336

*C.—Comparison of the relative Catalysing Powers of the Surface at  $500^\circ$  towards (a)  $2\text{H}_2 + \text{O}_2$  and (b)  $2\text{CO} + \text{O}_2$  Mixtures respectively.*

As it seemed of interest to compare the relative catalysing power of the surface towards theoretical  $2\text{H}_2 + \text{O}_2$  and  $2\text{CO} + \text{O}_2$  mixtures, respectively, at  $500^\circ$  under like conditions, another series of experiments, extending altogether over about a month was undertaken. The reaction tube containing the surface was maintained within  $5^\circ$  on either side of  $500^\circ \text{C}$ . throughout the whole series. Theoretical mixtures of (a)  $2\text{H}_2 + \text{O}_2$  or (b)  $2\text{CO}_2 + \text{O}_2$ , each

saturated with water vapour at the room temperature (16 to 20° C.), were alternately circulated over the surface, and the reaction constant determined in each case. In this way a series of comparative results was obtained, which proved unmistakably that the rate of catalytic combustion of hydrogen far exceeded that of carbonic oxide over the surface, as the following summarised results show :—

Mean $k_1$ Values in Experiments with					
		$2\text{H}_2 + \text{O}_2$	0		
			°		
				$2\text{CO} + \text{O}_2$	0
					°
XXIX ..	..	0.1194	20.0	XXVIII ..	0.0354 20.5
XXX ..	..	0.1130	18.5	XXXI ..	0.0500 —
XXXIII ..	..	0.1071	18.0	XXXII ..	0.0444 18.0
XXXIV ..	..	0.1005	17.0	XXXVII ..	0.0461 16.0
XXXV ..	..	0.1093	17.0	XXXIX ..	0.0358 —
XXXVI ..	..	0.1099	16.0		
				Mean =	0.0423
Mean	-	0.1100			

It should be noted that whereas the  $k_1$  values for  $2\text{H}_2 + \text{O}_2$  varied but little from the general mean, those for  $2\text{CO} + \text{O}_2$  showed somewhat greater divergence. Possibly this circumstance may be due to the last-named mixtures being more sensitive than the former to variations in the hygroscopic conditions, because the  $k_1$  values for the  $2\text{CO}_2 + \text{O}_2$  mixtures varied fairly regularly with the saturation temperature  $\theta$ . On an average, the moist  $2\text{H}_2 + \text{O}_2$  mixtures combined about 2.5 times as quickly as did the moist  $2\text{CO}_2 + \text{O}_2$  mixtures over the surface.

This conclusion was subsequently confirmed by two experiments (XLVIII and XLIX) in each of which a mixture of hydrogen, carbonic oxide and oxygen in approximately equimolecular proportions was circulated over the surface at 500°, and the partial pressure of each of its three constituents determined at stated intervals as shown by the hereunder figures, which leave no room for doubt concerning the faster burning of the hydrogen.

*Experiments XLVIII and XLIX with a  $H_2 + CO + O_2$  Mixture.*

T = 500°.

						Partial Pressures of		
Time						$H_2$	CO	$O_2$
Hours.						mm.	mm.	mm.
XLVIII	{	0	..	..	..	147	143	150
		3½	..	..	..	33	118	(80)
		6½	..	..	..	8	53	34
XLIX	{	0	..	..	..	151	143	159
		1	..	..	..	92	128	118
		3	..	..	..	47	95	82
		5½	..	..	..	19	65	52

It may be mentioned that in the second experiment there seemed to be some indication of a slight absorption of oxygen by the surface.

*D. Comparison of the Rates of Catalytic Combustion of Methane and Hydrogen respectively over the surface at 500° C.*

In this final series of experiments, which were carried out for us by Dr. Harold Hartley at the University of Leeds in November, 1909, the relative rates of the catalytic combustion of hydrogen and methane over the same fireclay surface at 500° were compared.

It has long been known that in flames and explosions the affinity of methane far exceeds that of hydrogen for oxygen. Thus in 1915 one of us (W. A. B.) found that when a mixture of methane, hydrogen and oxygen corresponding to  $CH_4 + 2H_2 + O_2$  is exploded in bombs at initial pressures between 18 and 48 atmospheres, the resulting oxygen distribution between the two combustible gases showed the affinity of methane to be at least twenty or thirty times greater than that of hydrogen for oxygen in such circumstances.\*

We have found, however, that in their catalytic combustion over a fireclay surface at 500°, the foregoing order of things is completely reversed, the hydrogen now burning at a very much faster rate than the hydrocarbon, as the following experimental results show :—

\* W. A. Bone, 'Phil. Trans.', vol. 215, p. 298 (1915).

*Experiments I. to LII with a  $\text{CH}_4 + 2\text{H}_2 + \text{O}_2$  Mixture.*

T 500°.

					Partial Pressures of			0
<i>t</i>					$\text{CH}_4$	$\text{H}_2$	$\text{O}_2$	
Hours.					mm.	mm.	mm.	"
I.	..	..	{	0 .. ..	106.4	192.0	99.4	20
				4 .. .	94.7	16.8	13.0	
				Difference	11.7	145.2	86.4	
II	..	..	{	0 . ..	107.2	191.1	103.5	20
				7½ .. .	95.2	28.8	2.9	
				Difference	12.0	162.3	100.6	
LII	..	..	{	0 .. ..	101.3	203.0	97.5	21
				7 .. ..	96.5	27.2	0.8	
				Difference	4.8	175.8	96.7	

It should be understood that, as the baryta absorption bulbs were kept in the circuit during the experiments, any carbon dioxide resulting from the methane-oxidation would be quickly removed from the system. No carbon was ever deposited on the surface, but as an experiment proceeded a small amount (up to about 2 per cent.) of carbonic oxide accumulated in the reacting gases.

*Summary.*

The principal conclusions established by the research in regard to the action of a fireclay surface in catalysing the combustion of carbonic oxide at 500° may be summarised as follows :—

(1) That the surface catalyses the combination of (moist) carbonic oxide and oxygen much in the same way as it does that of hydrogen and oxygen at the same temperature though in a less degree.

(2) That, with a moist mixture of the carbonic oxide and oxygen in their combining proportions, the rate of combination is always directly proportional



to the pressure of the dry mixture, provided that the surface is in a "normal" condition, and the reaction-product quickly removed from the system.

(3) That the catalysing power of the surface can be greatly stimulated by previous exposure at the reaction temperature to the combustible gas. The stimulus so imparted is not, however, permanent, but gradually dies away after the exciting cause is removed. It may also be removed by exposing the surface to oxygen at the reaction temperature. Indeed an oxygen-treated surface becomes either "normally" active, or only slightly more so, according to conditions.

(4) That when the carbonic oxide and oxygen are present in other than their combining proportions, their rate of combination is proportional to the partial pressure of the carbonic oxide, which thus becomes the controlling factor in the process.

(5) That of hydrogen, carbonic oxide and methane, the first named is the most, and the last-named the least, amenable to the catalytic combustion.

Further discussion as to the interpretation of the experiments is deferred until a future paper which one of us proposes to publish in conjunction with Dr. Harold Hartley, who, in addition to carrying out a long experimental research on the action of silver in catalysing the combustion of carbonic oxide, the results of which have yet to be reported, has given much attention to the theoretical aspects of the subject. Meanwhile, we desire to express our indebtedness to the Government Grant Committee of the Society for grants out of which part of the expenses of the investigation were defrayed.

---

*The Theoretical Prediction of the Physical Properties of Many-Electron Atoms and Ions. Mole Refraction,\* Diamagnetic Susceptibility, and Extension in Space.*

By LINUS PAULING, Fellow of the John Simon Guggenheim Memorial Foundation.

(Communicated by A. Sommerfeld, For. Mem R.S. -Received January 1, 1927.)

I. --Introduction.

It is customary to express the empirical data concerning term values in the X-ray region by introducing an effective nuclear charge  $Z_{\text{eff}}e$  in the place of the true nuclear charge  $Ze$  in an equation theoretically applicable only to a hydrogen-like atom. Often a screening constant  $S$  is used, defined by the equation

$$Z_{\text{eff}} = Z - S;$$

and this screening constant is qualitatively explained as due to the action of electrons which are nearer the nucleus than the electron under consideration, and which in effect partially neutralise the nuclear field. Thus the relativistic or magnetic doublet separation may be represented by the equation

$$\Delta\nu = \frac{R\alpha^2}{n^3k(k-1)} (Z - s_0)^4 + \dots$$

This equation, including succeeding terms, was obtained originally by Sommerfeld from relativistic considerations with the old quantum theory; the first term, except for the screening constant  $s_0$ , has now been derived by Heisenberg and Jordan† with the use of the quantum mechanics and the idea of the spinning electron. The value of the screening constant is known for a number of doublets, and it is found empirically not to vary with  $Z$ .

It has been found possible to evaluate  $s_0$  theoretically by means of the following treatment: (1) Each electron shell within the atom is idealised as a uniform surface charge of electricity of amount  $-ze$  on a sphere whose radius is equal to the average value of the electron-nucleus distance of the electrons in the shell. (2) The motion of the electron under consideration is then determined by the use of the old quantum theory, the azimuthal quantum number being chosen so as to produce the closest approximation to the quantum

\* The phrase "mole refraction" will be used in this paper in place of "coefficient of refraction" or "molal coefficient of refraction," in conformity with the use of the German word *Molrefraktion*.

† 'Z. f. Physik,' vol. 37, p. 263 (1926).

mechanics. (3) Since  $s_0$  does not depend on  $Z$ , it is evaluated for large values of  $Z$ , by expanding in powers of  $z_i/Z$  and neglecting powers higher than the first, and then comparing the expansion with that of the expression containing  $Z - s_0$  in powers of  $s_0/Z$ . The values of  $s_0$  obtained in this way\* are in satisfactory agreement with the empirical ones, the agreement being excellent in the case of orbits of large excentricity, for which the idealisation of the electron shells would be expected to introduce only a small error.

The important problem of the theoretical evaluation of the properties of many-electron atoms and ions has so far received little attention, compared with that devoted to spectral term values. The wave mechanics of Schrödinger provides an atomic model which suggests that the method of treatment given  $s_0$  can be used in deriving theoretical values of screening constants to be used in the equations representing the mole refraction or polarisability, diamagnetic susceptibility, extension in space, and other properties of atoms and monatomic ions. This procedure is followed in this paper, the assumption being made that the nuclear charge is large in comparison with the charge of an electron shell. This requirement is not well fulfilled by actual atoms and ions. However, from a comparison with the accurately known experimental values of the mole refraction of the rare gases and of some ions in aqueous solution it is found that the calculated values of the mole refraction screening constant are not greatly in error. The indicated corrections are made; so that, with the aid of this one empirical change, theoretical values are obtained for the mole refraction and the diamagnetic susceptibility of a large number of atoms and ions. A third screening constant is also evaluated, which permits the calculation of the electron distribution in atoms and ions and the estimation of inter-atomic distances. In this connection it is shown that the investigation of the diffraction of X-rays by crystals provides a method for the direct experimental verification of the form of Schrödinger's eigenfunctions.

## II.—*The Wave Mechanics of the Hydrogen Atom and the Idealisation of an Electron Shell.*

In the wave mechanics of Schrödinger† a conservative Newtonian dynamical system is represented by a wave function or amplitude function  $\psi$ , obtained from the partial differential equation

$$\text{div. grad. } \psi + \frac{8\pi^2}{h^2} (W - V(q_i)) \psi = 0,$$

\* Pauling, 'Z. f. Physik,' vol. 40, p. 344 (1926).

† Schrödinger, 'Ann. d. Physik,' vol. 79, p. 361 (1926); vol. 79, p. 489; vol. 80, p. 437; vol. 81, p. 109; cited hereafter as I, II, III, IV.

with the conditions that  $\psi$  be everywhere continuous, single-valued, and bounded.  $W$  and  $V(q_r)$  are the energy constant and the potential energy; and the indicated operations are with respect to co-ordinates whose line element is given by

$$ds^2 = 2T(q_r, \dot{q}_r) dt^2,$$

in which  $T$  is the kinetic energy expressed as a function of the velocities. Only certain functions (called eigenfunctions) satisfy these requirements in any given case; correspondingly there are certain characteristic values of the energy constant  $W$ . For the hydrogen-like atom with fixed nucleus the potential energy is  $-e^2Z/r$ ; on writing for the eigenfunctions

$$\Psi_{nlm} = X_{nl}(r) Y_{lm}(\vartheta) Z_m(\phi), \quad (1)$$

the wave equation can be resolved into three total differential equations, with the solutions\*

$$\begin{aligned} X_{nl}(r) &= \left\{ \left( \frac{2Z}{na_0} \right)^3 \frac{(n-l-1)!}{2n[(n+l)!]^3} \right\}^{\frac{1}{2}} e^{-\xi/2} \xi^l L_{n+l}^{(2l+1)}(\xi) \\ &\quad \text{with } \xi = \frac{2Z}{a_0 \cdot n} \cdot r \\ Y_{lm}(\vartheta) &= \left\{ (l+\frac{1}{2}) \frac{(l-m)!}{(l+m)!} \right\}^{\frac{1}{2}} P_l^m(\cos \vartheta) \\ Z_m(\phi) &= \frac{1}{\sqrt{2\pi}} e^{im\phi} \end{aligned} \quad (2)$$

$L_{n+l}^{(2l+1)}(\xi)$  represents the  $(2l+1)$ th derivative of the  $(n+l)$ th Laguerre polynomial; and  $P_l^m(\cos \vartheta)$  is Ferrer's associated Legendre function of the first kind, of degree  $l$  and order  $m$ .  $Y_{lm} Z_m$  thus constitutes a surface harmonic. The  $\Psi$ 's are in this form orthogonal and normalised with respect to unity, so that they fulfil the conditions

$$\int \Psi_{nlm} \Psi_{n'l'm'} dV = \begin{cases} 1 & \text{for } n = n', l = l', m = m' \\ 0 & \text{otherwise.} \end{cases}$$

The parameter  $n$  can assume the values 1, 2, 3, ..., and is to be identified with the principal quantum number characterising the energy of the atom;  $l$  can assume the values 0, 1, 2, ...  $n-1$ , and is to be identified with  $k-1$ ,  $k$  being the azimuthal quantum number of the old quantum theory; while  $m$ , the magnetic quantum number, can assume the values 0,  $\pm 1$ ,  $\pm 2$ , ...  $\pm l$ .

Schrödinger (IV) has interpreted  $\Psi \bar{\Psi}$  ( $\bar{\Psi}$  being the conjugate complex of  $\Psi$ ) as giving the weight or probability to be assigned to the corresponding micro-

\* See Schrödinger I; Waller, 'Z. f. Physik,' vol. 38, p. 635 (1926).

scopic state of the system; in the hydrogen-like atom  $\Psi \bar{\Psi}$  would then give the *electron density* as a function of  $r$ ,  $\vartheta$ , and  $\phi$ , the electron being considered as distributed through space in accordance with this expression (following Schrödinger), or as achieving this distribution through a time average of its instantaneous positions. Unsöld\* has shown that this conception provides a simple explanation of Schrödinger's perturbation theory, to the effect that it gives the interaction of the perturbing field and this distribution of electricity. Thus it can easily be shown that the first-order Stark effect energy given by the wave mechanics (Schrödinger, III) is just the field energy of the electric dipole corresponding to such an electron density (the wave equation being separated in parabolic co-ordinates in this case). Accepting these views, the fractional number of electrons in a spherical shell of unit thickness at the distance  $r$  from the nucleus is

$$D = 4\pi r^2 \Psi \bar{\Psi} = r^2 X_n^2(r). \quad (3)$$

An atom in the S state, with  $l = m = 0$ , has  $Y_{00}^2(\vartheta) Z_0^2(\phi) = 1/4\pi$ , so that  $\Psi_{n00}$  is spherically symmetrical. Unsöld has further shown that the sum of the quantities  $\Psi \bar{\Psi}$  for the electrons of a completed sub-group ( $n$  and  $l$  constant,  $m = -l, -l+1, \dots, 0, \dots, +l$ ) is not dependent on  $\vartheta$  and  $\phi$ . Accordingly the electron distribution in an atom in the S state or containing only completed sub-groups† is spherically symmetrical, and a function of  $r$  alone.

The dependence on  $r$  of several eigenfunctions is shown by the following equations, and by fig. 1, in which  $-X_n(r) \cdot Z^{-3/2} \cdot 10^{-12}$  is plotted as a function of  $\xi$ .

$$X_{10}(r) = -2 \left( \frac{Z}{a_0} \right)^{3/2} \cdot e^{-\xi/2},$$

$$X_{20}(r) = \frac{2}{2^{5/2}} \left( \frac{Z}{a_0} \right)^{3/2} \cdot e^{-\xi/2} (\xi - 2),$$

$$X_{30}(r) = -\frac{2}{3^{5/2} 2!} \left( \frac{Z}{a_0} \right)^{3/2} \cdot e^{-\xi/2} (\xi^2 - 6\xi + 6),$$

$$X_{40}(r) = \frac{2}{4^{5/2} 3!} \left( \frac{Z}{a_0} \right)^{3/2} \cdot e^{-\xi/2} (\xi^3 - 12\xi^2 + 36\xi - 24),$$

$$X_{50}(r) = -\frac{2}{5^{5/2} 4!} \left( \frac{Z}{a_0} \right)^{3/2} \cdot e^{-\xi/2} (\xi^4 - 20\xi^3 + 120\xi^2 - 240\xi + 120),$$

\* 'Dissertation,' Munich, 1927.

† The sub-groups for which this theorem is derived are not the Stoner sub-groups. However, it is highly probable that the inclusion of the spinning electron in the theory will lead to the result that the theorem is actually true for the Stoner sub-groups.

$$X_{21}(r) = -\frac{2}{2^2\sqrt{3!}}\left(\frac{Z}{a_0}\right)^{3/2}e^{-\xi/2}\cdot\xi,$$

$$X_{31}(r) = \frac{2}{3^2\sqrt{4!}}\left(\frac{Z}{a_0}\right)^{3/2}e^{-\xi/2}\cdot\xi(\xi-4),$$

$$X_{41}(r) = -\frac{2}{4^2\sqrt{5!}\cdot 2!}\left(\frac{Z}{a_0}\right)^{3/2}e^{-\xi/2}\cdot\xi(\xi^2-10\xi+20),$$

$$X_{61}(r) = \frac{2}{5^2\sqrt{6!}\cdot 3!}\left(\frac{Z}{a_0}\right)^{3/2}e^{-\xi/2}\cdot\xi(\xi^3-18\xi^2+90\xi-120).$$

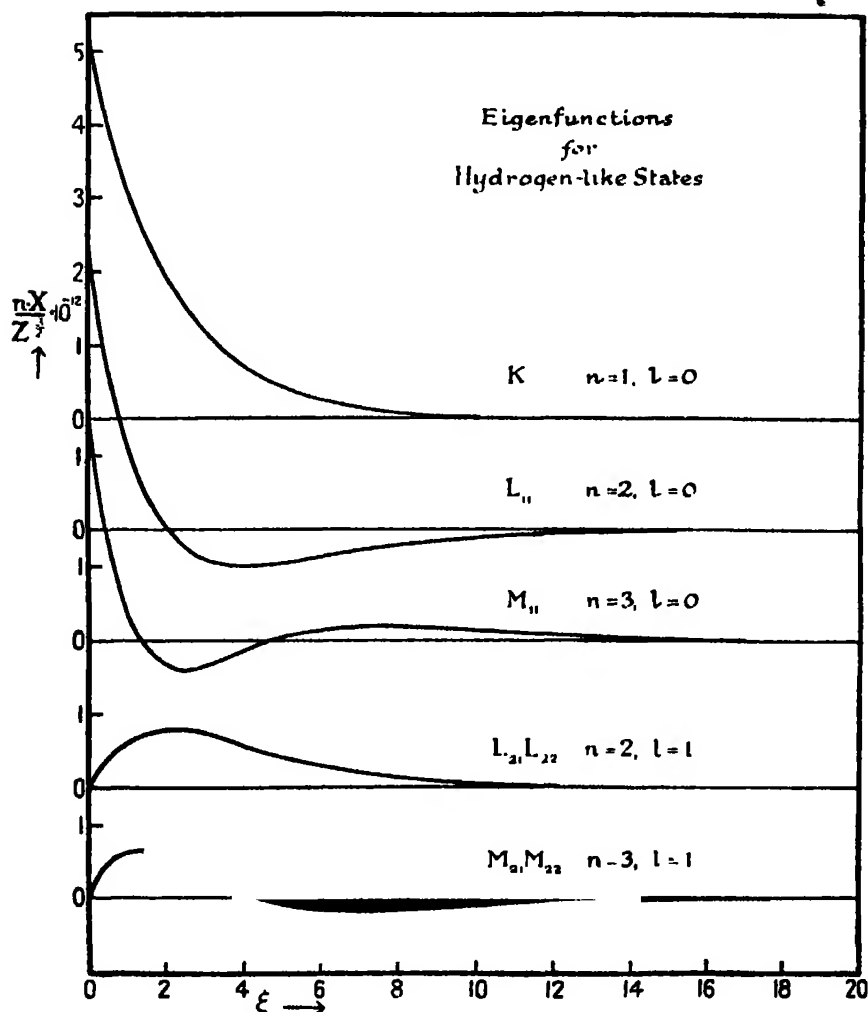


FIG. 1.—Eigenfunctions for hydrogen-like states; as ordinates are shown values of  $-nX_{nl}(\xi) \cdot Z^{-3/2} \cdot 10^{-12}$  with values of  $\xi$  as abscissae.

It will be observed that the function differs appreciably from zero only within a radius of the order of magnitude of the major axis of the corresponding ellipses of the old quantum theory; namely,  $r = 2a_0 n^2/Z$ , or  $\xi = 4n$ , as was remarked by Schrödinger (I). In fig. 2 are given values of  $D$  as a function of

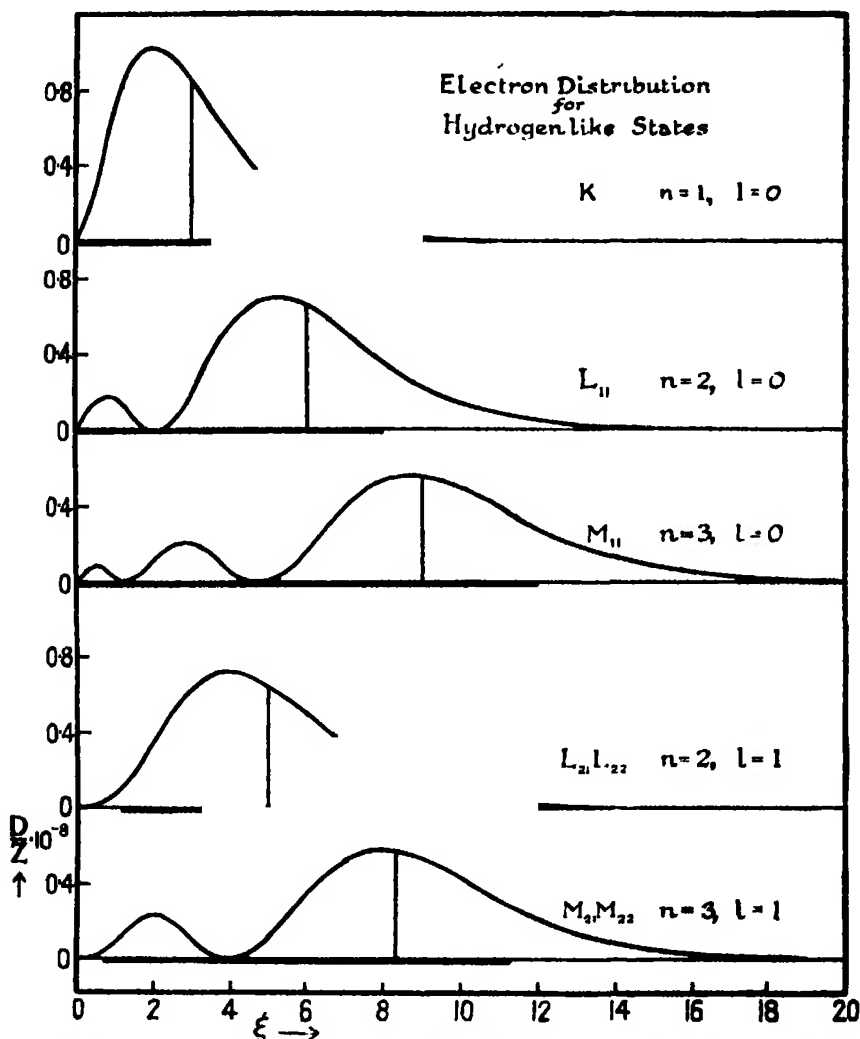


FIG. 2.—Electron distribution for hydrogen-like states; the ordinates are values of  $D \cdot Z^{-1} \cdot 10^{-3}$ , in which  $D = 4\pi r^2 \rho$ , with  $\rho$  the electron density. The vertical lines correspond to  $\bar{r}$ , the average value of  $r$ .

$\xi$ , showing the distribution of the electron with respect to  $r$ . The limits indicated on the  $\xi$ -axis correspond to the electron-nucleus distances at aphelion

and perihelion given by the old quantum theory with  $k^2$  placed equal to  $l(l+1)$ .

The idealisation of an electron shell as a uniform distribution of electricity on the surface of a sphere was innovated by Schrödinger,\* who calculated the term-values of penetrating orbits by this method, with the old quantum theory. It was pointed out by Heisenberg† and Unsöld‡ that the same idealisation is permitted by the wave mechanics, the potential of the  $e\Psi^*\Psi$  distribution of electricity approximating  $-e^2/r$  for large values of  $r$ , and being equal to  $-e^2Z/a_0n^2$  for  $r=0$ . The spherical symmetry shown by Unsöld to hold for completed sub-groups is, of course, retained in this idealisation. As the best value for the radius  $\rho_0$  of the equivalent shell we shall choose the average value of  $r$ ,

$$\bar{r} = \int r \Psi^* \Psi dV.$$

The method of evaluating this integral has been given by Waller,§ whose equations lead to the result

$$r = \frac{a_0 n^2}{Z} \left[ 1 + \frac{1}{2} \left\{ 1 - \frac{l(l+1)}{n^2} \right\} \right]. \quad (4)$$

(The old quantum theory expression for the time average of  $r$  contained  $k^2$  in place of  $l(l+1)$ .)

Following Heisenberg and Unsöld, let us consider the potential for the state  $n=1$ . It is, at the radius  $R$ ,

$$\begin{aligned} \Phi_{10} &= -e \left\{ \int_0^R \frac{1}{R} \cdot X_{10}^2(r) r^2 dr + \int_R^\infty \frac{1}{r} X_{10}^2(r) r^2 dr \right\} \\ &= -e \left\{ \frac{1}{R} - e^{-(2Z/a_0)R} \left( \frac{Z}{a_0} + \frac{1}{R} \right) \right\}. \end{aligned}$$

The potential of the electron distributed over the surface of a sphere of radius  $\rho_0$  is

$$\begin{aligned} \Phi &= -\frac{e}{R} \quad \text{for } R > \rho_0 \\ &= -\frac{e}{\rho_0} \quad \text{for } R < \rho_0. \end{aligned}$$

$\Phi$  will provide the most satisfactory approximation to  $\Phi_{10}$  when the difference  $\Phi - \Phi_{10}$ , properly weighted and integrated throughout space, is zero.

\* 'Z. f. Physik,' vol. 4, p. 347 (1921).

† 'Z. f. Physik,' vol. 39, p. 499 (1926).

‡ 'Dissertation,' Munich, 1927.

§ Waller, 'Z. f. Physik,' vol. 38, p. 635 (1926).



Reference to fig. 2 shows that for small values of  $r$ , for which  $\Phi$  and  $\Phi_{10}$  differ appreciably, the dependence of  $D$  on  $r$  is roughly linear for all states, which we may consider to represent other electrons which interact with the electron in the state  $n = 1$ . Hence the weight may be taken as linear in  $r$ , and we obtain

$$\int_0^{\bar{r}} (\Phi - \Phi_{10}) r dr = \text{const.} \left( 3 - \frac{2Z}{a_0} \rho_0 \right),$$

which vanishes for

$$\rho_0 = \frac{3}{2} \frac{a_0}{Z};$$

that is, for exactly the value  $\bar{r}$  as given by equation (4). It is probable that the explicit consideration of further cases would lead to similar conclusions. The  $\xi$  values corresponding to  $r = \bar{r}$  are shown in fig. 2.

In the following discussion we shall use  $m_i$  to denote the principal quantum number of the  $i$ th shell, i.e., instead of  $n$ . We shall introduce for convenience the numerical factor  $\gamma_i$ , such that

$$\bar{r} = \gamma_i \frac{a_0 m_i^2}{Z}. \quad (5)$$

From equations (4) and (5) we accordingly obtain for an electron with the quantum numbers  $m_i$  and  $l_i$  the expression

$$\gamma_i = 1 + \frac{1}{2} \left\{ 1 - \frac{l_i(l_i + 1)}{m_i^2} \right\}. \quad (6)$$

It has been found that no significant error is introduced by combining the subgroups of an entire shell, using an average value of  $\gamma$  for the entire K, L, M, ... shell. With the Stoner distribution of electrons among the levels, this average value is

$$\gamma(m_i) = 1 + \frac{1}{2m_i} + \frac{(m_i - 1)^2}{4m_i^2} \quad (7A)$$

for completed shells,

$$\gamma(m_i) = \frac{3}{2} - \frac{3}{4m_i} \quad (7B)$$

for eight-shells (octets), and

$$\gamma(m_i) = \frac{5}{2} - \frac{2}{m_i^2} \quad (7C)$$

for eighteen-shells.

It might be thought that these values of  $\gamma$  are not correct because of the fact that the electron shells actually do not consist of hydrogen-like electrons, but rather themselves of "penetrating" electrons. However, as  $Z$  increases the "penetrating orbits" become more and more hydrogen-like; and these

values of  $\gamma$  can accordingly be used in our later treatment, which postulates that  $Z$  is large, the error introduced being quadratic in  $z/Z$ , and so negligible.

### III.—The Quantisation of Penetrating Orbits.

Let us now consider an electron orbit  $n_k$  (in which  $k = k_1$ , in the X-ray nomenclature of Sommerfeld), which penetrates a number of electron shells. We shall determine the orbit with the methods of classical mechanics, quantising with the rules of the old quantum theory; values of the azimuthal quantum number  $k$  will later be chosen in such a way as to cause our formulas to approximate as closely as possible to the quantum mechanics. In accordance with the previous discussion, the  $i$ th electron shell is idealised as a homogeneous surface charge of amount  $-z_i e$  on a sphere of radius  $\rho_i = \bar{r}_i$ . We shall let  $Z_i e$  be the effective nuclear charge in the  $i$ th region, which is the region between the radii  $\rho_{i-1}$  and  $\rho_i$ ; accordingly  $Z_{i+1} = Z_i - z_i$ , and  $Z_1 = Z - z$ , in which  $Z$  is the atomic number of the atom and  $z$  the number of electrons entirely within the orbit under consideration. With the use of Newtonian dynamics, *i.e.*, neglecting the relativistic effect and the perturbations due to the spinning electron, the motion of the electron is described by the Hamiltonian equation

$$\frac{1}{2m} \left( p_r^2 + \frac{p_\phi^2}{r^2} \right) + V(r) = W, \quad (8)$$

in which  $W$  is the energy constant and

$$V(r) = V_i(r) = -\frac{Z_i e^2}{r} - \frac{z_i e^2}{\rho_i} - \frac{z_{i+1} e^2}{\rho_{i+1}} - \dots \quad (9)$$

in the  $i$ th region. Since  $\phi$  is cyclic, the quantum rules require

$$p_\phi = \frac{k\hbar}{2\pi}.$$

Let us now define for the  $i$ th region a radial quantum number  $n_i'$ , which we shall call the *segmentary* radial quantum number, by means of the equation

$$n_i' \hbar = \oint \sqrt{2m \{W - V_i(r)\} - \frac{k^2 \hbar^2}{4\pi^2} \cdot \frac{1}{r^2}} dr. \quad (10)$$

$n_i'$  is thus the radial quantum number which would characterise the orbit if the  $i$ th region were large enough to include the entire orbit. The true radial quantum number, on the other hand, is given by the equation

$$n' \hbar = \sum_{i=1}^j \int_{i\text{th region}} \sqrt{2m \{W - V(r)\} - \frac{k^2 \hbar^2}{4\pi^2} \cdot \frac{1}{r^2}} dr. \quad (11)$$

From equations (8), (9) and (10) it is evident that the path of the electron in the  $i$ th region is a segment of the Kepler ellipse defined by the segmentary radial and the azimuthal quantum numbers  $n_i'$  and  $k$ , so that it can be described by the known equations

$$r = \frac{a_0 k^2}{Z_i} \cdot \frac{1}{(1 - \epsilon_i \cos \phi)} = \frac{a_0 n_i^2}{Z_i} (1 + \epsilon_i \cos u)$$

$$t = \frac{n_i^3}{4\pi R Z_i^2} (u + \epsilon_i \sin u).$$

In these equations  $\phi$  and  $u$  are the segmentary true anomaly and excentric anomaly, respectively, measured from aphelion; while  $n_i$  and  $\epsilon_i$  are the segmentary principal quantum number and excentricity, given by the equations

$$n_i = n_i' + k, \quad \epsilon_i = \sqrt{1 - \frac{k^2}{n_i^2}}.$$

To evaluate the segmentary quantum numbers we observe from a comparison of equations (9) and (10) with the corresponding ones for a hydrogen-like orbit that

$$W = -\frac{e^2}{2a_0} \cdot \frac{Z_i^2}{n_i^2} + \frac{z_i e^2}{\rho_i} + \frac{z_{i+1} e^2}{\rho_{i+1}} + \dots = -\frac{e^2}{2a_0} \cdot \frac{Z_{i+1}^2}{n_{i+1}^2} + \frac{z_{i+1} e^2}{\rho_{i+1}} + \dots = \text{const.} \quad (12)$$

From this there is obtained, neglecting powers of  $z_i/Z$  higher than the first, the expression

$$n_{i+1} = n_i \left( 1 + \frac{z_i}{Z} \cdot \beta \right), \quad \text{with} \quad \beta = \frac{n^2}{\gamma_i m_i^2} - 1. \quad (13)$$

On carrying out the integrations in equation (11), it becomes

$$n' = n_1 \{F(\pi) - F(u_1)\} + n_2 \{F(u_2') - F(u_2)\} + \dots + n_j \{F(u_j') - F(0)\}, \quad (14)$$

in which

$$F(u_i) = \frac{1}{\pi} \left[ u_i - \epsilon_i \sin u_i - \sqrt{1 - \epsilon_i^2} \arcsin \left( \frac{\sqrt{1 - \epsilon_i^2} \sin u_i}{1 + \epsilon_i \cos u_i} \right) - \pi (1 - \sqrt{1 - \epsilon_i^2}) \right], \quad (15)$$

the initial and final values  $u_i$  and  $u_i'$  of the excentric anomaly in the  $i$ th region being given by the equations

$$1 + \epsilon_i \cos u_i = \frac{\rho_i Z_i}{a_0 n_i^2}, \quad 1 + \epsilon_{i+1} \cos u_{i+1}' = \frac{\rho_i Z_{i+1}}{a_0 n_{i+1}^2}. \quad (16)$$

From this, with the use of equation (13), and again neglecting powers of  $z_i/Z$

higher than the first, there is derived the following relation between  $n_1$  and the true quantum number  $n$  :

$$n_1 = n \left[ 1 - \sum_{i=1}^{\prime} \frac{1}{\pi} \cdot \frac{z_i}{Z} \{ \beta_i u_i + (1 + \beta_i) \varepsilon \sin u_i \} \right]. \quad (17)$$

The equation connecting  $\varepsilon_i$  and  $\varepsilon$  is easily obtained from the definition of  $\varepsilon_i$  with the use of equations (13) and (17).

In order to approximate as closely as possible to the quantum mechanics we shall use throughout for  $k^2$  the quantity  $l(l+1)$ ; for often in the quantum mechanics  $l(l+1)$  occupies the place formerly given to  $k^2$ , as we have seen in the case of  $\tilde{r}$ .

The use of these expressions describing the penetrating orbit in predicting the physical properties of many-electron atoms will be exemplified in the following sections.

#### IV.—The Theoretical Determination of the Mole Refraction.

A simple consideration involving a slow mechanical transformation\* shows that if the energy quantity corresponding to the second-order Stark effect of a system is

$$\Delta E = -\frac{1}{2} \alpha F^2, \quad (18)$$

then the electric moment induced in the system is

$$\bar{\mu} = \alpha F. \quad (19)$$

The polarisation in unit volume can be expressed in terms of the index of refraction  $n$  as

$$P = \frac{N}{V} \bar{\mu} = \frac{N}{V} \alpha F = \frac{3}{4\pi} \frac{n^2 - 1}{n^2 + 2} \cdot F \quad (20)$$

in which  $N$  is Avogadro's number and  $V$  the volume occupied by one mole of the molecules under consideration,  $\alpha$  referring to one molecule. The mole refraction  $R$  is defined by the equation

$$R = V \cdot \frac{n^2 - 1}{n^2 + 2} = \frac{4\pi N}{3} \cdot \alpha. \quad (21)$$

Wentzel,† Waller‡ and Epstein§ have derived a formula for the second-order

\* Jones, 'Roy. Soc. Proc.' A, vol. 105, p. 650 (1924). The first attempt to calculate the mole refraction from the quadratic Stark effect formula was made by Lennard-Jones (Jones), with the old quantum theory.

† 'Z. f. Physik,' vol. 38, p. 518 (1926).

‡ 'Z. f. Physik,' vol. 38, p. 635 (1926).

§ Epstein, 'Nature,' vol. 118, p. 444 (1926), 'Phys. Rev.,' vol. 28, p. 695 (1926).

Stark effect of a hydrogen-like atom, using the Schrödinger wave mechanics. Their equation, obtained independently and by different methods, is

$$\Delta E = - \frac{\hbar^6}{16 (2\pi)^6 m^3 e^6 Z^4} n^4 (17n^2 - 3m^2 - 9n_3^2 + 19) \cdot F^2, \quad (22)$$

which gives

$$R = \frac{N \cdot \hbar^6}{12 (2\pi)^6 m^3 e^6 Z^4} n^4 (17n^2 - 3m^2 - 9n_3^2 + 19), \quad (23A)$$

or, introducing for the physical constants their accepted values,

$$R = \frac{0.0470}{Z^4} n^4 (17n^2 - 3m^2 - 9n_3^2 + 19). \quad (23B)$$

Here  $n$  is the principal quantum number, and  $m$  and  $n_3$  are given by the equations

$$m = n_2 - n_1, \quad n_3 = n - 1 - n_1 - n_2.$$

The quantum numbers  $n_1$  and  $n_2$  have the integral values

$$0 \leq n_1 \leq n - 1, \quad 0 \leq n_2 \leq n - 1.$$

These conditions suffice to determine the possible values of  $m$  and  $n_3$ . As was shown by Pauli,\* they are compatible with the experimental evidence, and explain many previously difficultly explicable facts involving the exclusion of certain quantum states.†

The electrons within the atom are actually not quantised in parabolic co-ordinates, but instead, on account of the central field of the atom core, in polar co-ordinates. It would, then, not be logical to attempt to select favoured values of  $m$  and  $n_3$ . Instead, we shall calculate the quantity

$$n^4 (17n^2 - 3m^2 - 9n_3^2 + 19)$$

for each set of values of the quantum numbers, and then average the result. This procedure is justified to a considerable extent by the fact that the polarisation does not depend largely on the subsidiary quantum numbers, but is a function mainly of the principal quantum number, which is not changed by quantisation in a central field. On averaging over all values of  $m^2$  and  $n_3^2$ ,

\* 'Z. f. Physik,' vol. 36, p. 336 (1926).

† Equation 22 differs from that derived by Epstein with the old quantum theory only in the inclusion of the number 19, and in the values given to  $n_3$  (previously  $n_3 = n - n_1 - n_2$ ). Wentzel and Waller have shown that the new equation is in somewhat better agreement with the best experimental data than the old one.

assigning equal weight to each set of values of  $n_1$  and  $n_2$ , there is obtained the result  $\overline{m^2} = \overline{n_3^2} = \frac{1}{8}(n^2 - 1)$ , which on substitution in equation (23) gives

$$R = 0.0470 \cdot n^4 (15n^2 + 21) \cdot \sum_k \frac{1}{(Z - S_{R_k})^4}, \quad (24)$$

in which the summation is to be taken over all electrons in the  $n$ th shell.\*  $S_R$  is called the mole refraction screening constant.

We shall now predict values of  $S_R$  for ions for which  $z_i/Z$  is small, i.e., for  $Z$  large. If this screening constant is constant, and does not depend on  $Z$ , these values hold for all atoms and ions with the structures considered. The nature of the agreement between the theoretical and the experimental values of  $R$  or of  $S_R$  will show to what extent this is true.

From equation (24) it is seen that, except for a small additive term in  $n^4 Z^{-4}$ , the mole refraction of a hydrogen-like electron is proportional to  $n^6 Z^{-4}$ . Now most of the polarisation occurs in the outermost part of the orbit, for here the externally applied field has its greatest value relative to the nuclear field. Accordingly we shall assume that the polarisation produced in a penetrating orbit is equal to that produced in a hydrogen-like orbit having the same parameters as those effective in the outermost ( $j$ th) region. This assumption is reasonable in view of the fact that in every case nearly the entire outer half of the orbit lies in this region. We accordingly write

$$R = \text{const. } n_j^6 Z_j^{-4} = \text{const. } n^6 (Z - S_R)^{-4}, \quad (25)$$

and from this determine  $S_R$ .

For generality let us consider a property proportional to  $n^r Z^{-t}$ , so that we have

$$\text{const. } n_j^r Z_j^{-t} = \text{const. } n^r (Z - S)^{-t}.$$

On expanding the left hand expression in powers of  $z_i/Z$ , using equations (13) and (17), and comparing the first term of the expansion with the corresponding term in the expansion of the right-hand expression in powers of  $S/Z$ , it is found that

$$S = z + \sum_i z_i - \sum_i^r \sum_i^t z_i D_i, \quad (26A)$$

in which  $D_i$ , which we shall call the unit screening defect for an electron in the  $i$ th shell, is given by the equation

$$D_i = \frac{1}{\pi} \{ \beta_i u_i + (1 + \beta_i) \varepsilon \sin u_i \} - \beta, \quad (26B)$$

with 
$$1 + \varepsilon \cos u_i = \frac{\gamma_i m_i^2}{n^2}. \quad (27)$$

\* This equation is, of course, rigorously true for H, He<sup>+</sup>, etc., for which  $S_R$  is zero.

Internal shells are thus seen to screen completely, and the screening effects of penetrated shells are additive. Moreover, it is seen that for properties proportional to different powers of  $n$  and  $Z$  the total screening defect varies directly with  $r/\ell$ .

For the mole refraction screening constant we accordingly have

$$S_{R\infty} = z + \sum_i z_i - \frac{1}{2} \sum_i z_i D_i. \quad (28)$$

Table I.—The Mole Refraction Screening Constant.

	$Z_0$		$S_{R\infty}$	$S_{R_0}$	$S_{R_0} - S_{R\infty}$	$\Delta S_R$
He	2	K	0.391	0.397		0
Ne	10	$L_{II}$	4.45	4.31	-0.14	0
		$L_{II} L_{III}$	5.64	5.50		
Ar	18	$M_{II}$	9.70	11.11	1.41	0.05
		$M_{II} M_{III}$	10.99	12.40		
Kr	36	$N_{II}$	21.28	26.69	5.41	0.19
		$N_{II} N_{III}$	22.92	28.33		
Xe	54	$O_{II}$	34.29	42.26	7.97	0.29
		$O_{II} O_{III}$	36.63	44.60		
[Cu <sup>+</sup> ] <sub>0</sub>	28	$M_{II}$	14.4	14.9	0.5	0.02
		$M_{II} M_{III}$	16.1	16.6		
		$M_{II} M_{III}$	19.5	20.0		
[Ag <sup>+</sup> ] <sub>0</sub>	46	$N_{II}$	25.7	32.15	6.5	0.23
		$N_{II} N_{III}$	27.5	33.85		
		$N_{II} N_{III}$	31.1	37.55		
[Au <sup>+</sup> ] <sub>0</sub>	78	$O_{II}$	46.0	59.9	13.9	0.50
		$O_{II} O_{III}$	48.1	62.0		
		$O_{II} O_{III}$	52.4	66.3		

In column 4 of Table I are given the values of  $S_{R\infty}$  obtained by the application of this equation to the structures included. (We have written  $S_{R\infty}$  because the values are derived for very large values of  $Z$ .) The symbols [Cu<sup>+</sup>]<sub>0</sub>, [Ag<sup>+</sup>]<sub>0</sub>, and [Au<sup>+</sup>]<sub>0</sub> denote atoms with the corresponding structures and the atomic numbers 28, 46, and 78. In column 5 are given values of  $S_R$  obtained from the experimental values of  $R$  (for light of infinite wave-length) shown in Table II by the following procedure. It is assumed that the differences in  $S_R$  for different sub-levels within a shell are those given by the theory; the solution of equation (24), with  $R$  given its experimental values, then gives the "experimental" values,  $S_{R_0}$ .

Table II.—Experimental Values of the Mole Refraction.\*

—	R.	—	R.
He	0.513	Zn <sup>++</sup>	0.72
Ne	0.995	Cd <sup>++</sup>	2.74
Ar	4.132	Hg <sup>++</sup>	3.14
Kr	6.25	Ag <sup>+</sup>	4.33
Xe	10.16		

\* The experimental values for the rare gases are those of C. and M. Cuthbertson ('Roy. Soc. Proc.,' A, vol. 84, p. 13 (1911)) extrapolated to infinite wave-length by Born and Heisenberg ('Z. f. Physik,' vol. 23, p. 388 (1924)). The silver ion value is obtained from the solution value given by Heydweiller ('Phys. Z.,' vol. 26, p. 526 (1925)) by taking 2.17 for the potassium ion. The cadmium ion value was calculated from this by the methods in the text, and the zinc and mercury ion values obtained from Heydweiller's by correcting by the difference between his cadmium value and ours; this procedure being adopted to correct for the effect of hydration of these highly charged ions.

The agreement between the theoretical and the experimental values of  $S_R$  is most encouraging. It is seen that for elements with only a few electrons the agreement is complete, and that it becomes less satisfactory as the electron number of the structure increases, the difference  $S_{R_0} - S_{R_\infty}$  showing a uniform increase. We can hence draw the conclusions that for light atoms all of the assumptions involved in the derivation of equations (24) and (28) are justified, that for these atoms the theoretical treatment of the electron orbits proposed in this paper is in general acceptable, and that it is permissible, in addition, to suppose the screening constants to be constant, and not to vary with  $Z$ . For heavier atoms the theoretical derivation of screening constants (valid for  $Z$  large) is only approximate, and the assumption that the screening constants are independent of  $Z$  is only approximately true, for they approach the theoretical values as  $Z$  becomes large. Evidence tending to show the fundamental correctness of our theoretical procedure, other than the good agreement of theory and experiment for light atoms, is provided by the regularity in the increase of  $S_{R_0} - S_{R_\infty}$  as the electron number of the structure increases, and by the similarity in the values of  $S_{R_0} - S_{R_\infty}$  for corresponding eight-shell and eighteen-shell structures.

It is of interest to note that on introducing the theoretical value of  $S_{R_\infty}$  for helium in equation (24), the result  $R = 0.506$  is obtained. The experimental data of C. and M. Cuthbertson were extrapolated to 0.513 for light of infinite wave-length by Born and Heisenberg, and to 0.518 by Heydweiller; so that our *entirely theoretically derived* value agrees with experiment within the limit of error of the extrapolation.

By introducing in equation (24) the values of  $S_{R_0}$  given in Table I we obtain



tentative predicted values for the mole refraction of univalent ions with the structures considered (Table III). These values apply only to free ions

Table III.—Mole Refraction of Univalent Ions.

Ion.	R predicted.	R solution.	R crystal.
Na <sup>+</sup>	0.457	0.11	0.04 to -0.55
K <sup>+</sup>	2.17	(2.17)	(2.17)
Rb <sup>+</sup>	3.88	3.56	3.77 to 4.10
Cs <sup>+</sup>	6.82	6.17	6.23 to 6.42
F <sup>-</sup>	2.65	2.71	2.96
Cl <sup>-</sup>	8.92	8.76	8.04 to 8.48
Br <sup>-</sup>	10.75	12.14	11.06 to 11.80
I <sup>-</sup>	15.71	18.07	16.24 to 17.02

in the gaseous state. It is difficult to say *a priori* whether measurements made on alkali halide crystals or those made on dilute aqueous solutions of the alkali halides would give mole refraction values in the better agreement with those holding for the gaseous ions. Previous investigators, in attempting to derive values of the polarisabilities of gaseous ions from experimental data for salts, have decided differently; Born and Heisenberg\* chose to use crystals, while Fajans and Joos† and Heydweiller‡ used dilute aqueous solutions. One fact showing that the perturbing effects in crystals are large is the large deviation from additivity exhibited by their mole refraction, amounting to as much as 1.5 units for the alkali halides.§ Our predicted values for gaseous ions show that ions in solution are indeed more similar to gaseous ions than are ions in crystals, as far as the mole refraction is concerned. In column 3 of Table III are given experimental values of R for ions in dilute solution, obtained from Heydweiller's tables by assuming the value 2.17 for potassium ion to be correct; and in column 4 values of R for the ions in the alkali halide crystals, calculated from the data given by Born and Heisenberg by again assuming the same value for potassium ion. Only the sodium, fluoride, and chloride ions can be compared

\* Born and Heisenberg, 'Z. f. Physik,' vol. 23, p. 388 (1924); for criticism of their derivation of polarisabilities from spectral term values see Hartree, 'Proc. Camb. Phil. Soc.,' vol. 22, p. 409 (1924); 'Roy. Soc. Proc.,' A, vol. 106, p. 552 (1924); and Schrödinger 'Ann. d. Physik,' (4), vol. 77, p. 43 (1925).

† Fajans and Joos, 'Z. f. Physik,' vol. 23, p. 1 (1924). These authors also discussed the data for crystals, and showed that the mole refraction values for ions in solution are usually only slightly different from those for gaseous ions.

‡ Heydweiller, 'Phys. Z.,' vol. 26, p. 526 (1925); for a discussion of the experimental and previous theoretical work on mole refraction see the two preceding papers.

§ Fajans and Joos; also Spangenberg, 'Z. f. Krist.,' vol. 53, p. 499 (1923).

with the theoretical results, for only in these cases have we shown  $S_R$  to be practically independent of  $Z$ . In each of these three cases the solution results agree better with the theoretical values than do the crystal results, so that the conclusion can be safely drawn that in general ions in solution resemble gaseous ions more closely than do ions in crystals. The agreement between the solution values and the theoretical ones is good for the fluoride and chloride ions; the solution value for the sodium ion is low, without doubt on account of the action of this very small ion on the surrounding water molecules, which has previously been estimated by Fajans and Joos to cause a decrease of about 0.3 in  $R$ .

We are now led to introduce a second empirical correction into our calculations. The theoretical values for the rubidium, caesium, bromide, and iodide ions in Table III resulted from the assumption that  $S_R$  is independent of  $Z$ , which is known not to be true for these structures, on account of the difference between  $S_{R_0}$  and  $S_{R_\infty}$ . The solution values of  $R$ , which we may assume to hold also for gaseous ions in these cases, also show that the screening constant for the negative ions should be larger and for the positive ions smaller than that used; that is, as  $Z$  increases  $S_R$  decreases, presumably approaching our theoretical values for  $Z$  large. We shall assume that  $S_R$  is a linear function of  $Z$  in this region, and evaluate the parameters of the function with the use of the solution values for the bromide and iodide ions. If we write

$$S_R = S_{R_0} - (Z - Z_0) \Delta S_R, \quad (29)$$

within a range of values of  $Z$  not too far removed from  $Z_0$  (the electron number of the structure), then  $\Delta S_R$  is found to be 0.19 and 0.29 for the krypton and xenon structures respectively. These values are approximately proportional to  $S_{R_0} - S_{R_\infty}$ ; hence we may safely accept 0.23 and 0.50 for the silver and aurous ion structures, respectively; and for consistency the corresponding values 0.05 and 0.02 will be used for the argon and cuprous ion structures also.

In Table IV are given values\* of the mole refraction of gaseous ions calculated from equations (24) and (29) with the use of the values found above for  $S_{R_0}$  and  $\Delta S_R$ . Values for hydrogen-like atoms and ions are also included; these are, of course, accurate, since no screening constant is needed. Table IV is

\* Throughout we have considered only the portion of the mole refraction produced in the outermost shell. In the case of xenon one finds by our methods that as much as 4 per cent. of the total mole refraction is due to the N shell; accordingly our values of  $S_R$  for the O electrons would be decreased by about 0.1 on making this correction. The values of  $R$  for ions would in most cases not be changed materially by the explicit consideration of the polarisation of inner shells, and so the less complicated treatment of this paper has been adopted.

Table IV.—The Mole Refraction and Diamagnetic Susceptibility of Atoms and Ions.

H		He <sup>+</sup>		Li <sup>++</sup>																																																																																																																																																																																																																																																																																																																																																																																																																																																																																																																																																																																																																																																																																																																																																																																																																																																																																																																																																																																																																																																																																																																																																																																																											
---	--	-----------------	--	------------------	--	--	--	--	--	--	--	--	--	--	--	--	--	--	--	--	--	--	--	--	--	--	--	--	--	--	--	--	--	--	--	--	--	--	--	--	--	--	--	--	--	--	--	--	--	--	--	--	--	--	--	--	--	--	--	--	--	--	--	--	--	--	--	--	--	--	--	--	--	--	--	--	--	--	--	--	--	--	--	--	--	--	--	--	--	--	--	--	--	--	--	--	--	--	--	--	--	--	--	--	--	--	--	--	--	--	--	--	--	--	--	--	--	--	--	--	--	--	--	--	--	--	--	--	--	--	--	--	--	--	--	--	--	--	--	--	--	--	--	--	--	--	--	--	--	--	--	--	--	--	--	--	--	--	--	--	--	--	--	--	--	--	--	--	--	--	--	--	--	--	--	--	--	--	--	--	--	--	--	--	--	--	--	--	--	--	--	--	--	--	--	--	--	--	--	--	--	--	--	--	--	--	--	--	--	--	--	--	--	--	--	--	--	--	--	--	--	--	--	--	--	--	--	--	--	--	--	--	--	--	--	--	--	--	--	--	--	--	--	--	--	--	--	--	--	--	--	--	--	--	--	--	--	--	--	--	--	--	--	--	--	--	--	--	--	--	--	--	--	--	--	--	--	--	--	--	--	--	--	--	--	--	--	--	--	--	--	--	--	--	--	--	--	--	--	--	--	--	--	--	--	--	--	--	--	--	--	--	--	--	--	--	--	--	--	--	--	--	--	--	--	--	--	--	--	--	--	--	--	--	--	--	--	--	--	--	--	--	--	--	--	--	--	--	--	--	--	--	--	--	--	--	--	--	--	--	--	--	--	--	--	--	--	--	--	--	--	--	--	--	--	--	--	--	--	--	--	--	--	--	--	--	--	--	--	--	--	--	--	--	--	--	--	--	--	--	--	--	--	--	--	--	--	--	--	--	--	--	--	--	--	--	--	--	--	--	--	--	--	--	--	--	--	--	--	--	--	--	--	--	--	--	--	--	--	--	--	--	--	--	--	--	--	--	--	--	--	--	--	--	--	--	--	--	--	--	--	--	--	--	--	--	--	--	--	--	--	--	--	--	--	--	--	--	--	--	--	--	--	--	--	--	--	--	--	--	--	--	--	--	--	--	--	--	--	--	--	--	--	--	--	--	--	--	--	--	--	--	--	--	--	--	--	--	--	--	--	--	--	--	--	--	--	--	--	--	--	--	--	--	--	--	--	--	--	--	--	--	--	--	--	--	--	--	--	--	--	--	--	--	--	--	--	--	--	--	--	--	--	--	--	--	--	--	--	--	--	--	--	--	--	--	--	--	--	--	--	--	--	--	--	--	--	--	--	--	--	--	--	--	--	--	--	--	--	--	--	--	--	--	--	--	--	--	--	--	--	--	--	--	--	--	--	--	--	--	--	--	--	--	--	--	--	--	--	--	--	--	--	--	--	--	--	--	--	--	--	--	--	--	--	--	--	--	--	--	--	--	--	--	--	--	--	--	--	--	--	--	--	--	--	--	--	--	--	--	--	--	--	--	--	--	--	--	--	--	--	--	--	--	--	--	--	--	--	--	--	--	--	--	--	--	--	--	--	--	--	--	--	--	--	--	--	--	--	--	--	--	--	--	--	--	--	--	--	--	--	--	--	--	--	--	--	--	--	--	--	--	--	--	--	--	--	--	--	--	--	--	--	--	--	--	--	--	--	--	--	--	--	--	--	--	--	--	--	--	--	--	--	--	--	--	--	--	--	--	--	--	--	--	--	--	--	--	--	--	--	--	--	--	--	--	--	--	--	--	--	--	--	--	--	--	--	--	--	--	--	--	--	--	--	--	--	--	--	--	--	--	--	--	--	--	--	--	--	--	--	--	--	--	--	--	--	--	--	--	--	--	--	--	--	--	--	--	--	--	--	--	--	--	--	--	--	--	--	--	--	--	--	--	--	--	--	--	--	--	--	--	--	--	--	--	--	--	--	--	--	--	--	--	--	--	--	--	--	--	--	--	--	--	--	--	--	--	--	--	--	--	--	--	--	--	--	--	--	--	--	--	--	--	--	--	--	--	--	--	--	--	--	--	--	--	--	--	--	--	--	--	--	--	--	--	--	--	--	--	--	--	--	--	--	--	--	--	--	--	--	--	--	--	--	--	--	--	--	--	--	--	--	--	--	--	--	--	--	--	--	--	--	--	--	--	--	--	--	--	--	--	--	--	--	--	--	--	--	--	--	--	--	--	--	--	--	--	--	--	--	--	--	--	--	--	--	--	--	--	--	--	--	--	--	--	--	--	--	--	--	--	--	--	--	--	--	--	--	--	--	--	--	--	--	--	--	--	--	--	--	--	--	--	--	--	--	--	--	--	--	--	--	--	--	--	--	--	--	--	--	--	--	--	--	--	--	--	--	--	--	--	--	--	--	--	--	--	--	--	--	--	--	--	--	--	--	--	--	--	--	--	--	--	--	--	--	--	--	--	--	--	--	--	--	--	--	--	--	--	--	--	--	--	--	--	--	--	--	--	--	--	--	--	--	--	--	--	--	--	--	--	--	--	--	--	--	--	--	--	--	--	--	--	--	--	--	--	--	--	--	--	--	--	--	--	--	--	--	--	--	--	--	--	--	--	--	--	--	--	--	--	--	--	--	--	--

made complete because it is often desirable to have even approximate values of  $R$  for ions, even for those which are not capable of existence in solution. Thus, for example, they may be compared with core polarisabilities deduced from the energy levels of non-penetrating alkali-like electron states in order to test the spectral theory used in the deduction. Moreover, the deviation of the observed mole refraction from the calculated value for a crystal or complex ion can be considered as a measure of the deformation experienced by the individual ions composing the crystal or ion, as was especially emphasised by Fajans and Joos. For example, they give for  $\text{PO}_4^{3-}$ ,  $\text{SO}_4^{2-}$ , and  $\text{ClO}_4^-$  the values 16.3, 14.6, and 13.3 respectively; from Table IV we obtain 39.5 in each case, assuming the complex ion to consist of undeformed monatomic ions. They give also for  $\text{CO}_3^{2-}$  12.3 and for  $\text{NO}_3^-$  11.0; our values are 29.6 in each case.\* The reasonable conclusion can hence be drawn that in each series the deforming influence of the central ion increases with its electrical charge.†

No extensive comparison with experiment to test the values in Table IV will be made. The close agreement between the purely theoretical and the experimental results in the case of helium and neon allows one to place confidence in the  $R$  values for ions with these structures; and the same remark applies with less force in the case of the argon structure, where only a small empirical correction was introduced. It is interesting to note that the theoretical values 3.57 and 6.15 for the rubidium and the caesium ion agree very well with the experimental ones, 3.56 and 6.17 (Table III), which were not used at all in the evaluation of the empirical corrections for these structures. Finally, we may mention that our values agree in general with those of Fajans and Wulff,‡ obtained by them from the experimental  $R$  values for salt solutions by the application of only the simplest theoretical considerations.

\* The experimental values are for the sodium D-lines, but are only slightly changed on extrapolation to infinite wave-length.

† For other uses of the ionic polarisability reference may be made to its rôle in the theoretical discussion of the structures of molecules (Heisenberg, 'Z. f. Physik,' vol. 26, p. 196 (1924); Kornfeld, *ibid.*, vol. 26, p. 205 (1924); Hund, *ibid.*, vol. 31, p. 81 (1925); vol. 32, p. 1 (1925); and in simple thermodynamic quantities such as the heat of vaporisation of crystals (Born and Heisenberg), and the heat of ionisation (into  $\text{H}^+$  and  $\text{X}^-$ ) of the hydrogen halides (Kemble, 'Journ. Opt. Soc. Am.,' vol. 12, p. 1 (1926)).

‡ Fajans and Wulff, not yet published. Their ionic refraction values for light of infinite wave-length are found by the methods applied by Fajans and Joos to the refraction for the sodium D-lines.

V.—*Diamagnetic Susceptibility.*

According to the classical theory, the effect of a magnetic field on a system composed of electrons in motion about a fixed nucleus is equivalent to the first order of approximation to the imposition on the system of a uniform rotation about the field direction (the Larmor precession) with the angular velocity  $2\pi\omega_H = He/2mc$ . This rotation of electrons produces a magnetic moment opposed to the field, such that the molal diamagnetic susceptibility is

$$\chi = - \frac{Ne^2}{4mc^2} \cdot \sum_{\kappa} \overline{r_{\kappa}^2 \sin^2 \vartheta_{\kappa}},$$

in which  $r_{\kappa} \sin \vartheta_{\kappa}$  is the projection normal to the field direction of the distance  $r_{\kappa}$  of the  $\kappa$ th electron from the nucleus;  $\overline{r_{\kappa}^2 \sin^2 \vartheta_{\kappa}}$  denotes the time average of  $r_{\kappa}^2 \sin^2 \vartheta_{\kappa}$ . For S states and for completed groups and sub-groups the new quantum mechanics gives  $\overline{r_{\kappa}^2 \sin^2 \vartheta_{\kappa}} = \frac{2}{3} \overline{r_{\kappa}^2}$ , so that we obtain

$$\chi = - \frac{Ne^2}{6mc^2} \cdot \sum_{\kappa} \overline{r_{\kappa}^2}. \quad (30)$$

Adhering to our general method of treatment, we shall now evaluate a screening constant  $S_M$  valid in the case of  $Z$  large. Taking the time average of  $r^2$  in the various regions traversed, we write

$$\overline{r^2} = \frac{\sum_{i=1}^j \int_{\text{ith region}} r^2 dt}{\sum_{i=1}^j \int_{\text{ith region}} dt},$$

which gives, on evaluating the integrals,

$$\overline{r^2} = a_0^2 \frac{\sum_{i=1}^j n_i^7 Z_i^{-4} \{U(u_i') - U(u_i)\}}{\sum_{i=1}^j n_i^3 Z_i^{-2} \{(u_i' + \epsilon_i \sin u_i') - (u_i + \epsilon_i \sin u_i)\}},$$

in which

$$U(u_i) = u_i (1 + \frac{2}{3} \epsilon_i^2) + 3 \epsilon_i \sin u_i + \frac{2}{3} \epsilon_i^2 \sin u_i \cos u_i + \epsilon_i^3 \sin u_i - \frac{1}{3} \epsilon_i^3 \sin^3 u_i,$$

and  $u_i$  and  $u_i'$  are given by equation (16). On expanding this in powers of  $z_i/Z$ , with the use of equations (13) and (17) and neglecting terms other than linear, and comparing the expansion with that of

$$\overline{r^2} = a_0^2 \frac{n^4}{(Z - S_M)^2} (1 + \frac{2}{3} \epsilon^2), \quad (31)$$

in powers of  $S_{M_\infty}/Z$ , there is obtained for  $S_{M_\infty}$  the value

$$S_{M_\infty} = z + \sum_i S_{M_i} = z + \sum_i z_i - \sum_i D_{M_i} \quad (32A)$$

$$\text{with } S_{M_i} = \frac{z_i}{\pi} \left\{ u_i + \frac{\epsilon \sin u_i \left( \frac{3}{2} - \frac{1}{2} \epsilon^2 - \epsilon \cos u_i + \frac{1}{12} \epsilon^2 \sin^2 u_i \right)}{\left( 1 + \frac{3}{2} \epsilon^2 \right) \left( 1 + \epsilon \cos u_i \right)} \right\} \quad (32B)$$

with  $u_i$  as given in equation (27).

In column 4 of Table V are given values of  $S_{M_\infty}$  calculated by means of equation (32). The mole refraction results show that we may expect the

Table V.—The Diamagnetism Screening Constant.

	$Z_0$		$S_{M_\infty}$	$S_{M_0}$	$\Delta S_M$
He	2	K	0.228	0.228	0
Ne	10	$L_{11}$	3.26	3.26	0
		$L_{21} L_{22}$	4.11	4.11	
Ar	18	$M_{11}$	7.57	9.40	0.07
		$M_{21} M_{22}$	8.68	10.63	
Kr	36	$N_{11}$	17.19	24.21	0.25
		$N_{21} N_{22}$	18.94	26.13	
Xe	54	$O_{11}$	27.34	38.28	0.39
		$O_{21} O_{22}$	29.38	40.87	
[Cu <sup>+</sup> ] <sub>0</sub>	28	$M_{11}$	10.8	11.45	0.03
		$M_{21} M_{22}$	12.2	12.9	
		$M_{31} M_{32}$	14.4	15.25	
[Ag <sup>+</sup> ] <sub>0</sub>	46	$N_{11}$	20.0	28.35	0.31
		$N_{21} N_{22}$	21.8	30.35	
		$N_{31} N_{32}$	25.0	34.3	
[Au <sup>+</sup> ] <sub>0</sub>	78	$O_{11}$	36.7	54.8	0.65
		$O_{21} O_{22}$	39.1	57.35	
		$O_{31} O_{32}$	43.3	62.35	

theoretical values to be correct in the case of the helium and neon structures, and to show an increasing error with increasing electron number for the other structures. The form of equation (26), which gives the screening constant for a property proportional to  $n^2 Z^{-1}$ , immediately suggests a method for correction by means of the empirical changes introduced in the mole refraction screening constant  $S_R$ ; namely, with the assumption that the various screening constants (for various physical properties) of an atom or ion deviate from their values calculated for  $Z$  large in such a way as to keep constant the ratios of the corresponding screening defects of the penetrated shells. Thus we would assume that  $D_M/D_R$  for argon, krypton, etc., has the values holding for  $Z$  large;

and from this ratio and the empirical  $D_R$  values  $D_M$  and hence  $S_M$ , and  $\Delta S_M$  can be found. The results are given in Table V, which accordingly contains theoretical values of the diamagnetism screening constant, corrected for all structures but helium and neon by the empirical mole refraction data. For each ion  $S_M$  is obtained by an equation of the form of equation (29).

The quantum mechanics treatment of diamagnetism has not been published.\* It seems probable, however, that Larmor's theorem will be retained essentially, in view of the marked similarity between the results of the quantum mechanics and those of the classical theory in related problems, such as the polarisation due to permanent electric dipoles and the paramagnetic susceptibility.† Thus we are led to use equation (30), introducing for  $\bar{r}_{nlm}^2$  the quantum mechanics value

$$\bar{r}_{nlm}^2 = \int r^2 \Psi_{nlm} \bar{\Psi}_{nlm} dV = a_0^2 \cdot \frac{n^4}{(Z - S_M)^2} \left[ 1 + \frac{1}{2} \left\{ 1 - \frac{l(l+1) - \frac{1}{2}}{n^2} \right\} \right], \quad (33)$$

differing from the value of the old quantum theory in the number  $\frac{1}{2}$ , and in having  $l(l+1)$  instead of  $k^2$ . Substituting this in equation (30), and introducing the numerical values of the physical constants, there results

$$\chi = -2.010 \cdot 10^{-6} \cdot \sum_{\kappa} \frac{n_{\kappa}^4}{(Z - S_{M_{\kappa}})^2} \left[ 1 - \frac{\{3l_{\kappa}(l_{\kappa} + 1) - 1\}}{5n_{\kappa}^2} \right], \quad (34)$$

in which the summation over  $\kappa$  denotes over all the electrons in the atom.

The molal diamagnetic susceptibilities of rare gas atoms and a number of monatomic ions obtained by the use of equation (34) are given in Table IV. The values for the hydrogen-like atoms and ions are accurate, since here the screening constant is zero. It was found necessary to take into consideration in all cases except the neon (and helium) structure not only the outermost electron shell but also the next inner shell, whose contribution is for argon 5 per cent., for krypton 12 per cent., and for xenon 20 per cent. of the total.

The available experimental data, because of their paucity and their inaccuracy, do not permit the extensive testing of these figures. The directly determined susceptibilities for helium, neon, and argon are in gratifying agreement with the theoretical ones (Table VI). From the mole refraction results we may expect ions in solution to have values of  $\chi$  near those for gaseous ions. Koenigsberger‡ has made determinations of  $\chi$  for seven alkali halides in aqueous solution, in

\* Schrödinger (IV) has tentatively advanced a form of the wave equation in which magnetic fields are considered.

† Mensing and Pauli, 'Phys. Z.', vol. 27, p. 509 (1926); Van Vleck, 'Nature,' vol. 118, p. 226 (1926).

‡ Koenigsberger, quoted in Landolt-Börnstein.

Table VI.—Diamagnetic Susceptibilities of the Rare Gases.

	$-\chi \cdot 10^6$ Calculated.	Observed.*	From salt solutions.
He	1.54	1.88	1.8
Ne	5.7	6.7	9
Ar	21.5	18.1, 20.3	18
Kr	42		37
Xe	66		59

\* The three numbers in the first column are from Hector, 'Phys. Rev.', vol. 24, p. 418 (1924); the second value for argon is from Lehrer, 'Ann. d. Physik, vol. 81, p. 229 (1926).

each case obtaining a specific susceptibility of  $-0.45 \cdot 10^{-6}$  units per gram. Assuming this rule to hold in general, one obtains the rare gas susceptibilities given in the last column of Table VI, in satisfactory agreement with those calculated. He also gives for the halides of calcium, barium, and strontium specific susceptibilities somewhat lower, about  $-0.41 \cdot 10^{-6}$ , corresponding satisfactorily with the decrease observed in Table IV on going from a univalent to the adjoining divalent cation.

The experimental specific susceptibilities of solid salts obtained by different investigators (quoted in Landolt-Börnstein) show wide variations, but in general agree roughly with those from solutions. Thus for sodium chloride five investigators report five values, varying from  $-0.38$  to  $-0.58 \cdot 10^{-6}$ . Of these the most trustworthy seems to be that of Ishiwara,  $-0.498 \cdot 10^{-6}$ . This corresponds to  $\chi = -29.2 \cdot 10^{-6}$ , in satisfactory agreement with our value  $-33 \cdot 10^{-6}$ . Pascal has also made extensive experimental investigations, from which he deduced a set of atomic susceptibilities,\* choosing them in such a way as to give agreement with those for the elementary substances in a number of cases. These values are of little use to us because of lack of information regarding the nature of the compounds studied.† Pascal‡ has later reported the susceptibilities of several salts of each of the alkali and alkali earth metals, from which ionic susceptibilities can be derived after the choice of one as a starting point. We shall take for  $-\chi \cdot 10^6$  for sodium ion 5.2 and for potassium ion 14.5 (compatible values), which are 4 smaller than those chosen by Pascal; in this way the "experimental" values in Table VII are obtained. For helium-, neon- and argon-like ions, as well as for the cuprous ion, the agreement with our

\* 'C. R.', vol. 158, p. 1895 (1914).

† Despite the improbability that these atomic susceptibilities correspond at all with true ionic susceptibilities, they have been made the basis of a theoretical discussion by Cabrera, 'Journ. de physique et le radium,' VI, vol. 6, p. 241 (1925).

‡ 'C. R.', vol. 158, p. 37 (1914); vol. 159, p. 429 (1914); vol. 173, p. 144 (1921).



Table VII.—Ionic Susceptibilities, from Pascal.

—	$-\chi \cdot 10^6$ Experiment.	Theory.	—	$-\chi \cdot 10^6$ Experiment.	Theory.
Li <sup>+</sup>	0.2	0.6	F <sup>-</sup>	10.3	8.1
Na <sup>+</sup>	5.2	4.2	Cl <sup>-</sup>	24.1	29
K <sup>+</sup>	14.5	16.7	Br <sup>-</sup>	34.6	54
Rb <sup>+</sup>	23.2	35	I <sup>-</sup>	48.6	80
Cs <sup>+</sup>	37.0	55			
Be <sup>++</sup>	0.2	0.3	CO <sub>3</sub> <sup>=</sup>	30.2	38
Mg <sup>++</sup>	3.3	3.2	NO <sub>3</sub> <sup>-</sup>	18.2	38
Ca <sup>++</sup>	7.8	13.3	PO <sub>4</sub> <sup>=</sup>	47.1	52
Sr <sup>++</sup>	16.5	28	SO <sub>4</sub> <sup>=</sup>	41.6	51
Ba <sup>++</sup>	29.8	46	OH <sup>-</sup>	11.5	12.6
Cu <sup>+</sup>	ca. 14	13			
Ag <sup>+</sup>	27	44			

predicted values is satisfactory ; but for the more complicated ions the experimental values are low. It is impossible to give with certainty the explanation of this difference. The experimental values from solutions indicate that our predicted values are at least approximately correct for isolated ions, so that probably the differences are real, and are to be attributed to the mutual action of the ions in crystals. In regard to this effect of mutual action it is significant that the crystals show deviations from additivity (as in the case of the mole refraction), amounting, however, to only a few per cent.

We can draw conclusions regarding deformation of ions from observations of the diamagnetic susceptibility just as from those of the mole refraction. Thus in the series CO<sub>3</sub><sup>=</sup>, NO<sub>3</sub><sup>-</sup> and PO<sub>4</sub><sup>=</sup>, SO<sub>4</sub><sup>=</sup> the experimental values of  $\chi$  show successively greater deviations from the theoretical ones (assuming undeformed O<sup>-</sup> ions) with increasing electrical charge of the central ion.\*

We may accordingly conclude that our theoretical values of the diamagnetic susceptibility of atoms and ions are not incompatible with the experimental data.

#### VI.—*The Electron Distribution in Atoms and Ions. Atomic Sizes.*

According to the discussion in Section II, the quantity  $\Psi^*\bar{\Psi}$  represents the electron density about the nucleus in a hydrogen-like atom. The electron

\* Larmor's Theorem is, of course, valid only for systems of electrons and one nucleus, so that complexes of atoms presumably do not permit the usual treatment. It seems probable, however, that the introduction of a hydrogen nucleus into an ion would cause a diminution in the susceptibility (in absolute value). The value of  $-\chi \cdot 10^6$  for water, 13.0, suggests that 12.6 for O<sup>-</sup> is low, in agreement with the fact that the value 5.7 for neon is smaller than Hector's 6.7.

density corresponding to a "penetrating orbit" could be found by the solution of the boundary problem resulting on giving the potential energy  $V$  in the wave equation the value shown in equation (4). An approximation to this result is obtained by the introduction of a screening constant  $S_s$ , which we shall call the size screening constant, the shape of the distribution curve being considered to remain unaltered.

To evaluate this screening constant, we observe that in the penetrating orbits of the old quantum theory the electron remains for most of its period in the outer half of its orbit, *i.e.*, in the outermost or  $j$ th region. Hence we may consider that the entire orbit corresponds to one characterised by the segmentary quantum number  $n_j$  of the outermost region. It is desirable to evaluate  $S_s$  in such a way as to give the correct value to  $\bar{r}$ , the average distance of the electron from the nucleus. This distance is given by equation (4). Omitting for simplicity the factor  $1 + \frac{1}{2} \left\{ 1 - \frac{l(l+1)}{n^2} \right\}$ , which is of little significance in the result obtained, we then write

$$a_0 \cdot \frac{n_j^2}{Z_j} = a_0 \cdot \frac{n^2}{(Z - S_{s_w})}.$$

The value of the size screening constant  $S_{s_w}$  is accordingly given by equation (26),  $r/t$  being replaced by 2.

As before, we may expect the values of  $S_{s_w}$  calculated for  $Z$  large to be valid for actual ions with the helium and neon structures. For the other structures we introduce the empirical corrections based upon those used for the mole refraction screening constant, with the aid of the principle of the constancy of the ratios of corresponding screening defects, already used for the diamagnetism screening constant. In this way the values of  $S_{s_w}$  and  $\Delta S_s$  given in Table VIII are obtained. An equation similar to equation (29) is to be used to find individual values of  $S_s$ .

The most instructive method of representing the electron distribution is by a graph showing it as a function of the distance  $r$  from the nucleus; that is, by the use of  $D = 4\pi r^2 \rho$ , where  $\rho$  is the electron density. Such a graph is shown in fig. 3, in which is represented the total value of  $D$  for the sodium ion and the chloride ion, the  $D$  values being calculated as in Section II, but with the use of the appropriate effective atomic numbers  $Z - S_s$ . The vertical line for each shell is drawn at the average position  $\bar{r}$  of the electrons in that shell, and its height gives the contribution of these electrons to  $D$  at this point. The distribution curves of the individual shells are those of fig. 2, with the scale

Table VIII.—The Size Screening Constant.

	$Z_0$		$S_{K_0}$	$\Delta S_s$
He	2	K	0.188	0
Ne	10	$L_{11}$	2.84	0
		$L_{21} L_{22}$	4.52	
Ar	18	$M_{11}$	9.15	0.07
		$M_{21} M_{22}$	10.87	
Kr	36	$N_{11}$	23.91	0.25
		$N_{21} N_{22}$	26.83	
Xe	54	$O_{11}$	38.68	0.49
		$O_{21} O_{22}$	41.80	
[Cu <sup>+</sup> ] <sub>0</sub>	28	$M_{11}$	10.9	0.03
		$M_{21} M_{22}$	13.15	
		$M_{31} M_{32}$	17.7	
[Ag <sup>+</sup> ] <sub>0</sub>	46	$N_{11}$	27.9	0.31
		$N_{21} N_{22}$	30.3	
		$N_{31} N_{32}$	35.1	
[Au <sup>+</sup> ] <sub>0</sub>	78	$O_{11}$	54.2	0.67
		$O_{21} O_{22}$	57.0	
		$O_{31} O_{32}$	62.7	

varied as indicated by the positions and heights of the corresponding vertical lines.\*

We are thus led to the following picture of atoms and ions containing only completed sub-groups of electrons; the chloride ion, for example. The electron distribution about the nucleus is spherically symmetrical. The two K electrons in the chloride ion form a ball about the nucleus extending to the radius of about 0.1 Å, the electron density  $\rho$  decreasing monotonically as  $r$  increases. (This meaning will be implied by the word "ball." See fig. 1, in which the ordinates are proportional to  $\pm\sqrt{\rho}$ , to find the electron density.) The two  $L_{11}$  electrons provide a small ball extending to 0.07 Å, and then a thick shell, of maximum density at a distance of about 0.15 Å. The six  $L_{21}$   $L_{22}$  electrons form one shell only, its density increasing from zero at  $r = 0$  to a maximum at  $r = 0.1$  Å, and then decreasing. A small portion (1 per cent.) of the two  $M_{11}$  electrons forms a ball about the nucleus, extending to 0.13 Å; from this distance to 0.48 Å extends a shell containing about 10 per cent. of

\* In fig. 3  $L_1$  represents  $L_{11}$ ,  $L_2$  represents  $L_{21}$   $L_{22}$ , &c. Through a mistake the  $L_1$  and  $L_2$  vertical lines for the chloride ion are drawn to the wrong heights; the  $L_2$  line should have the height shown for the  $L_1$  line, and *vice versa*.

the two electrons, of maximum density at about  $0.2 \text{ \AA}$ , and the remainder forms still another shell of maximum density at  $0.8 \text{ \AA}$ . The six  $M_{21} M_{22}$  electrons

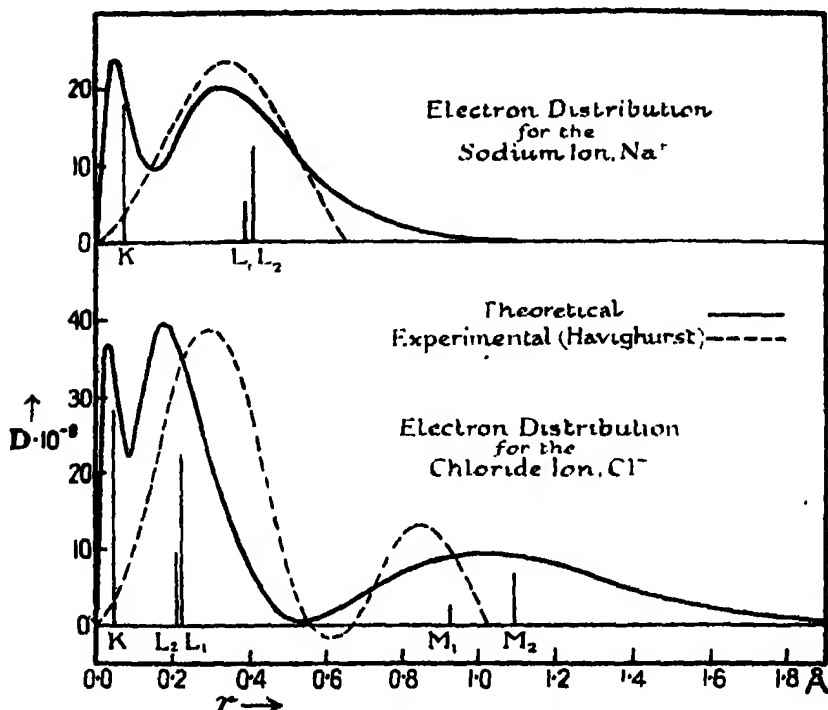


FIG. 3.—The theoretical and the experimental electron distribution (as a function of the distance from the nucleus) for the sodium and the chloride ion.

form two shells, one, containing about 10 per cent. of the electrons, having its maximum density at  $0.13 \text{ \AA}$ , and the other with maximum density at  $0.9 \text{ \AA}$ .\*

We may accordingly say that an atom is composed of a nucleus embedded in a ball of electricity (the two K electrons with small contributions from other shells), which in turn is surrounded by more or less distinctly demarcated thick concentric shells, containing essentially the L, M, N, etc., electrons.†

Of particular interest is the result that for a radius of around  $0.55 \text{ \AA}$  the electron density in the chloride ion falls nearly to zero; for this conclusion has

\* The details of this description would be changed slightly, but not essentially, by the introduction of the spinning electron into the theory.

† The experiments of Davison and Kunsman, 'Phys. Rev.', vol. 22, p. 242 (1923), on the distribution in angle of electrons scattered by metals provide some experimental verification of this layer structure of atoms; for the investigators remark that their results are explicable by the atomic model involving the surface layer idealisation of electron shells.

been previously drawn from the experimental intensities of reflection of X-rays from sodium chloride crystals. It was remarked by Duane\* that if the distribution of diffracting power (the electron density) within a crystal be represented by a triple Fourier series, then the intensity of reflection of X-rays from the plane ( $hkl$ ) of the crystal† is proportional to the square of the coefficient of the corresponding term in the series; which for a crystal such as sodium chloride has the form,

$$\rho(x, y, z) \sim \sum_h \sum_k \sum_l A_{hkl} \cos 2\pi h \frac{x}{a} \cos 2\pi k \frac{y}{a} \cos 2\pi l \frac{z}{a}. \quad (35)$$

The quantity  $A_{hkl}^2$  can be obtained from the measured intensities of reflection of X-rays by making various corrections (for dependence on angle of reflection, extinction of the beam of X-rays, etc.). With the aid of a reasonable assumption regarding the sign of  $A_{hkl}$ , Havighurst‡ has in this way obtained the Fourier series representation of the distribution of refracting power in sodium chloride, using planes as complex as (10.0.0). From this he calculated the electron distribution  $D$  as a function of  $r$  for the sodium and the chloride ion, obtaining the curves§ shown in fig. 3. On comparing the curve for sodium ion with the theoretical curve it is seen that except for the maximum made by the K electrons there is satisfactory agreement. The experimental chloride ion curve also does not show the maximum due to K electrons, and, moreover, the ratio of the area of the M to that of the L hump is smaller than the theoretical one. It is gratifying, however, to observe the experimental verification of the existence of the M shell, and of the minimum in the electron density in the region at 0.6 Å from the nucleus. In explanation of the small size of the M hump found by Havighurst we observe that the densities  $\rho$  in this region as given by equation (35) are very small, not much larger than the random fluctuations shown by the series, so that this portion of the curve may be in considerable error. The non-appearance of the K maxima may be attributed to several co-operating causes. In order for the Fourier series to be sensitive enough to show such sharp maxima, accurate values of the coefficients  $A_{hkl}$  for a large number of planes with indices of the order of 15 would be required. Furthermore, it is probable that

\* 'Proc. Nat. Acad. Amer.,' vol. 11, p. 489 (1925).

† ( $hkl$ ) represents here the Miller indices multiplied by the order of reflection.

‡ 'Proc. Nat. Acad. Amer.,' vol. 11, p. 502 (1925). Havighurst used the intensity measurements of W. L. Bragg, James, and Bosanquet, 'Phil. Mag.,' vol. 41, p. 309 (1921); vol. 42, p. 1 (1921).

§ A somewhat similar but not identical electron distribution for these ions has been derived by A. H. Compton, 'Phys. Rev.,' vol. 27, p. 510 (1926), from the same experimental data.

thermal motion of the ions in the crystal at ordinary temperatures would smooth the curve somewhat, and displace it towards larger values of  $r$ . It is also possible that for the tightly bound K electrons the reflecting power and the electron density are no longer proportional. The careful determination of many coefficients  $A_{kk}$  for sodium chloride and other crystals will no doubt provide much valuable information regarding the electron distribution in atoms, permitting a decision to be reached concerning the validity of Schrödinger's interpretation of his eigenfunctions, and incidentally testing the procedure of this paper for evaluating the screening constants.

The theoretically obtained electron densities of ions may be used for the calculation of the so-called F curves, which give the effective reflecting power of the ion as a function of the angle of reflection and the wave-length of X-rays, and which are of use in the determination of crystal structures. It may be mentioned that the high maximum value of the electron density at the nucleus given by our calculations provides considerable justification for the method\* of determining crystal structures with the aid of the relative intensities of Laue spots produced by crystal planes with complicated indices.

#### VII.—Interatomic Distances.

Schrödinger's ideas lead to a simple explanation of the forces between atoms, in particular of the previously difficultly understandable repulsive force.† As an illustration we shall calculate the internuclear distances for the hydrogen halides.

For simplicity we shall assume the fluoride ion to consist of the nucleus, two K electrons very close to it, and eight  $L_{21}$   $L_{22}$  electrons; for as can be seen from the representation of the sodium ion in fig. 3 the  $L_{11}$  electrons show nearly the same distribution along  $r$  as the  $L_{21}$   $L_{22}$  electrons. The potential energy of a hydrogen nucleus at the distance  $R$  from the fluorine nucleus is then

$$\Phi = \frac{7e^2}{R} - 8e^2 \left\{ \int_0^R X_{21}^2(r) \frac{r^2}{R} dr + \int_R^\infty X_{21}^2(r) \frac{r^2}{r} dr \right\}, \quad (36)$$

assuming that the fluoride ion is not deformed by the hydrogen ion. The first term in  $\Phi$  is due to the nucleus and the K electrons, with a charge of  $7e$ , and the second term to the eight L electrons. For equilibrium we have the condition

$$\left( \frac{d\Phi}{dR} \right)_{R=R_0} = -\frac{7e^2}{R_0^2} + \frac{8e^2}{R_0^2} \int_0^{R_0} X_{21}^2(r) r^2 dr = 0, \quad (37)$$

\* Used principally in the United States, by Wyckoff, Dickinson, etc.

† This was remarked by Unsöld, 'Dissertation,' Munich, 1927.

with the simple interpretation that the number of electrons within the radius  $R_0$  is  $Z$ , so that the repulsive force of the nucleus on the hydrogen ion just balances the attractive force of an equivalent number of electrons.

The solution of this equation is  $R_0 = 0.91 \text{ \AA}$ , in deceptively good agreement with the band spectra value given in Table IX. For there are two important

Table IX.—Internuclear Distances in the Hydrogen Halides.

	Theoretical.	Experimental.*
	$\text{\AA}$	$\text{\AA}$
HF	0.91	0.92
HCl	1.55	1.265, 1.28
HBr	2.12	1.407

\* The experimental figures, with one exception, were obtained from oscillation-rotation spectra with the use of integral rotational quantum numbers by Kratzer, 'Z. f. Physik,' vol. 3, p. 289 (1920). The second figure for hydrogen chloride was calculated by Colby, 'Astrophys. Journ.,' vol. 58, p. 303 (1923), from the same data, with the use of half quantum numbers, and by Czerny, 'Z. f. Physik,' vol. 34, p. 227 (1925), from pure rotation spectra with half quantum numbers.

considerations which must be introduced in the more detailed treatment of interatomic forces, and which in this case apparently effectively neutralise each other. Our evaluation of the electron distribution provides only an approximation to that corresponding to a "penetrating orbit," so that the average electron-nucleus distance  $\bar{r}$  is correctly given, but for large values of  $r$  the electron density is given a smaller value than the actual one. This effect, if taken into consideration, would increase the repulsive force at large values of  $R$ , and would tend to give a larger value of  $R_0$ . But the deforming action of the hydrogen ion on the fluoride ion must also be taken into account. This can be thought of as the polarisation of the fluoride ion in the field of the positive ion, resulting in an attractive force between the two ions of amount  $2\alpha e^3/R_0^5$ , if the polarisability  $\alpha$  be assumed constant. The potential of this term, introduced in equation (37), would tend to decrease the value of  $R_0$ . The higher order effects, induced quadrupole, etc., moments, also in reality are of importance.

The values of  $R_0$  similarly calculated for hydrogen chloride and hydrogen bromide, with the substitution of  $X_{31}(r)$  and  $X_{41}(r)$  for  $X_{21}(r)$  in equation (37), are somewhat larger than the experimental ones. This indicates that the deforming effect of the hydrogen ion on the halide ions is of greater relative importance for these ions than for the fluoride ion.

A similar procedure can be used in predicting interatomic distances in ionic crystals, by evaluating the potential energy of a three-dimensional array of

undeformed ions, and determining the condition that this be a minimum. Such a procedure leads to interatomic distances of the order of magnitude of the actual ones; because of the approximate nature of our determination of the electron distribution it is not worth while to carry out accurately the lengthy calculations involved.

#### VIII.—*Conclusion.*

The general method followed in this paper is capable of refinements which should make possible the accurate prediction of the properties of any atom or ion. The most obvious one is the use of the wave mechanics in determining the state of an electron under the influence of a positive nucleus and several idealised electron shells. Explicit expressions for the properties of an electron in such a state may then be derived, eliminating the necessity of the more or less inaccurate adaptation of the equations obtained for hydrogen-like atoms. Further progress may also be made in approximating an electron shell more closely than is possible with a spherical surface charge. All of these refinements will greatly complicate the treatment, however; and while without doubt they will sooner or later be introduced, the relatively simple, if less exact, procedure which we have used suffices to show the general applicability of the method, and to provide approximate values of the physical properties of ions which may not exist under conditions permitting experimental investigation. The usefulness of these values in the consideration of the structure of molecules and of crystals will be illustrated elsewhere.

I wish to express my sincere thanks to Prof. A. Sommerfeld, from whose Seminar much of the inspiration for this research was obtained. I am also indebted to the John Simon Guggenheim Memorial Foundation and to the California Institute of Technology for providing the opportunity for its prosecution.

[*Added February 10, 1927.*—J. H. Van Vleck in 'Proc. Nat. Acad. America,' vol. 12, p. 662 (December, 1926), has discussed the mole refraction and the diamagnetic susceptibility of hydrogen-like atoms with the use of the wave mechanics, obtaining results identical with our equations (24) and (34). He also considered the effect of the relativity corrections (which is equivalent to the effect of a central field) and concluded that equation (24), derived by the use of parabolic instead of spherical co-ordinates, is not invalidated.]



*The Effective Cross Section of the Oriented Hydrogen Atom.*

By RONALD G. J. FRASER, Ph.D., Exhibition of 1851 Senior Student.

(Communicated by H. M. Macdonald, F.R.S.—Received December 15, 1926.)

*Introduction.*

1. Evidence has recently been accumulating that atoms may show an isotropy far greater than would be anticipated on the basis of the atom model developed by Bohr and Sommerfeld; a suggestion which is thrown into strong relief by the examination of matter under conditions of space quantisation in a magnetic field. Evidently, the possibility of orienting at will the momentum axes of certain atoms in a prescribed direction in space offers an ideal means of investigating atomic symmetry.

One must be careful, however, in drawing deductions from observations of this kind. Sommerfeld\* has clearly shown that those atoms which possess a closed electron group in the sense of the Stoner classification of electron levels cannot orient when in the normal state. The experiments of Stern and Gerlach† on zinc, cadmium, mercury, tin and lead are in excellent agreement with this idea. In this regard, the observations of, for example, Dymond‡ on the excitation of helium by electron impacts, Rusch§ on the cross section of argon, and of Weatherby and Wolf|| on the dielectric constant of helium cannot be interpreted as indicating marked atomic isotropy; because the inert gases possess a closed group.

The same may be said of observations on the double refraction, dielectric constant, etc., of diamagnetic molecules; for the theory of molecular orientation, so far as it has been developed, demands so large a number of prescribed directions at ordinary temperatures that unless observations are made at very low temperature no certain deductions can be drawn from them. Further search for orientation effects in diamagnetic gases has led so far to quite contradictory results.¶

\* 'Physikal. Z.,' vol. 26, p. 70 (1925).

† See Sommerfeld, "Atombau und Spektrallinien." 4th German Ed., p. 632; Gerlach, 'Ann. Physik,' vol. 76, p. 163 (1925).

‡ 'Roy. Soc. Proc.,' A, vol. 107, p. 291 (1925).

§ 'Ann. Physik,' vol. 80, p. 707 (1926).

|| 'Phys. Rev.,' vol. 27, p. 709 (1926).

¶ Glaser, 'Ann. Physik,' vol. 75, p. 459 (1924); *ibid.*, vol. 78, p. 641 (1925); Lehrer, 'Ann. Physik,' vol. 81, p. 229 (1926); Hammar, 'Proc. Nat. Acad. Sci.' vol. 12, pp. 594, 597 (1926).

2. It is clear that observation of the normal hydrogen atom under conditions of space quantisation forms the most suitable point of departure in an investigation of different atoms for isotropy or anisotropy. For, according to orbit theory: first, the hydrogen atom in the normal state should possess a magnetic moment of one Bohr magneton, and should orient with its momentum axis parallel and anti-parallel to the field\* ; that is without regard to sign, in a single prescribed direction ; second, the single plane orbit of the hydrogen atom forms a highly anisotropic system.

### *The Method.*

1. By proper choice of the discharge tube conditions, a beam of fast hydrogen canal rays may be made to consist very largely of atoms, charged and neutral. At a sufficiently great distance behind the cathode, there exists a dynamic equilibrium between the charged and neutral atoms, the mechanism of which depends *entirely* on collisions between the particles of the beam and the molecules of the resting gas.† If, now, the neutral atoms are oriented parallel and anti-parallel to a field direction coinciding with the direction of their motion, then it follows, if one accepts the Bohr-Sommerfeld atom model, that the *effective collision area* presented by them to the molecules of the resting gas is increased in the ratio of  $\pi^2 : 4$ . The charged atoms, being single protons, are uninfluenced by the field. As a result, the mean free path of the neutral atoms ( $L_2$ ) is decreased, that of the protons ( $L_1$ ) is unaffected by the presence of the field. In other words, the fact of orientation appears to demand a new set of equilibrium conditions, for which there is present less than the normal proportion of neutral atoms.

2. The number of neutral atoms is very simply determined by methods which have been developed by Wien and by Rüchardt.‡ All the positive particles are removed from the beam at a certain point by a sufficiently strong transverse electric field. The neutral atoms remaining fall on a thermopile connected with a galvanometer, producing a deflection proportional to their number. If  $d'_2$ ,  $d_2$  denote the galvanometer deflections with and without magnetic field,

\* [Added January 20, 1927.—The determination of the atomic magnetic moment of hydrogen as 1 Bohr magneton was recently announced by E. Wrede ('Verh. d. Deutsch. Physikal. Ges.,' III, vol. 7, p. 37 (1926)), and appears in 'Z. f. Physik,' 1927, under "Untersuchungen zur Molekularstrahlmethode aus dem Institut für physikalische Chemie der Hamburgischen Universität," No. 6.]

† Baerwald, 'Ann. Physik,' vol. 65, p. 167 (1921); *ibid.*, vol. 70, p. 255 (1923).

‡ Wien, 'Ann. Physik,' vol. 39, p. 528 (1912); Rüchardt, *ibid.*, vol. 71, p. 377 (1923).

then the ratio  $d_2/d'_2 = n_2/n'_2$ , where  $n'_2, n_2$  are the numbers of neutral atoms with and without field.

If, then,  $d_2/d'_2 > 1$ , one must conclude that the number of neutral particles has been decreased by the presence of the field, in accordance with the argument above.

3. When the condenser is earthed the total beam falls on the thermopile; if the corresponding galvanometer deflections with and without field be  $d'_1, d_1$ , then

$$d_1 = k(n_1 + n_2), \quad d'_1 = k(n'_1 + n'_2),$$

where  $n'_1, n_1$  are the numbers of protons with and without the field, and  $k$  is a constant. Evidently,  $d_1 = d'_1$ . If  $L_1, L_2$  are the mean free paths of protons and atoms without field,  $L'_1, L'_2$  the same quantities with field, it follows from the theory of the charge exchange given by Wien that

$$\frac{d_1 - d_2}{d_2} = \frac{L_1}{L_2} = w, \quad \frac{d'_1 - d'_2}{d'_2} = \frac{L'_1}{L'_2} = w'.$$

We are assuming that  $L_1 = L'_1$ , hence

$$\frac{w}{w'} = \frac{L'_2}{L_2}.$$

Now, in general,

$$\frac{1}{L_2} = Nr_2^2\pi,$$

where  $N$  is the number of gas molecules per cubic centimetre at the temperature and pressure of the experiment, and  $r_2$  is the collision radius of the neutral atom. Then if  $r'_2$  denote the collision radius of the oriented atom

$$\frac{1}{L'_2} = Nr'^2_2\pi$$

and

$$\frac{r_2^2}{r'^2_2} = \frac{L'_2}{L_2} = \frac{w}{w'}.$$

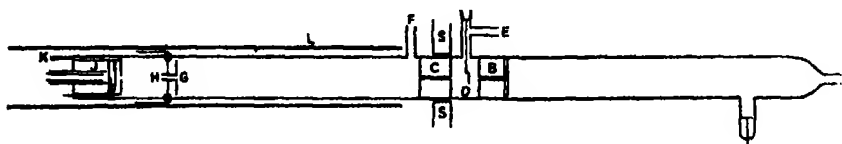
Since  $w$  can be determined correct to within 2 per cent., it is clear that a difference of 2 or 3 per cent. in the target area of the hydrogen atom following orientation would be detected by the present method.

#### *The Apparatus.*

A sketch of the apparatus is seen in the figure. AB is the discharge tube, cylindrical in form as giving a relatively small proportion of molecules.\* BC is the double cathode, of brass and Swedish iron respectively, which, with the

\* Döpel, 'Ann. Physik,' vol. 76, p. 1 (1925).

whole observation tube, is earthed. C forms part of the magnetic shield S, built up to 2 cm. thickness of stalloy stampings 1 foot square. B and C have



each a circular canal of 1.8 mm. in diameter. They are soldered into the observation tube. At E works a rotary Gaede pump. Hydrogen, prepared from carbonate-free sodium hydroxide, freed from traces of oxygen by combustion at a glowing spiral, and dried for 12 hours over phosphorus pentoxide, is drawn in at A through a capillary, and out at E. At F works a small Gaede steel diffusion pump. A separate supply of gas, either hydrogen or argon, is led into the observation tube at K. The arrangement is designed to allow the maintenance of a considerable difference of pressure between the discharge and observation tubes. The observation pressure is determined by a McLeod gauge (McLeod II); the discharge pressure by a separate gauge (McLeod I). Mercury vapour was carefully held back from discharge and observation tubes by liquid air or solid carbon dioxide.

At a distance of 30.5 cm. behind C is G, a brass diaphragm with aperture 5 mm. diameter, immediately in front of the brass condenser H, with plates 2 cm. by 1 cm., and a gap of 6 mm. It is insulated from the observation tube by vulcanite. A P.D. of 540 volts between the plates is sufficient to remove all the protons from the beam. The distance between C and H is large enough to ensure that equilibrium is attained at H.\* I is the thermopile, furnished with a diaphragm of 4 mm. aperture. It is a 6-element copper-bismuth pile, resistance about 6 ohms, specially constructed for this work. It attains within 1 per cent. of its equilibrium deflection in 25 seconds, in a pressure range of  $10^{-2}$  to  $10^{-3}$  mm. The zero is stable to within  $\pm 10$  scale divisions daily variation. It is mounted on a water jacket, J, fed from a thermo-syphon reservoir. The wires to the galvanometer are led out together, in order to avoid any "search coil" effect on throwing on the field. The galvanometer is a Cambridge high sensitivity instrument; total internal resistance 13.1 ohms, resistance of coil 10 ohms; having a half period of 7.5 seconds, and a sensitivity of some  $3 \times 10^{-9}$  amp. per scale division at 1 metre. It is mounted on a concrete pier, and screened from external magnetic action by a cylindrical shield of stalloy. The

\* Rüchardt, *loc. cit.*

arrangement is very sensitive ; with a discharge output of 1 watt, the deflection is of the order 400 mm. D is a shutter to cut off the canal rays from the pile when the latter is not in use.

The observation tube is surrounded for its whole length by a solenoid L, of six layers No. 16 S.W.G., capable of giving a field of some 450 gauss with a current of 12 amps. The strength of the field is measured both by the amps. turns ; and by means of a search coil, carried on the observation tube itself, and a Grassot fluxmeter. The full carrying capacity could not of course be used, due to the temperature effect on the thermopile ; with a current of some 2 amps., however, no temperature creep of the thermopile could be detected within a period of 20 to 30 minutes.

The potential across the discharge tube was measured by a spark gap between aluminium balls 5 cm. diameter, connected in parallel with the tube ; the current by a milliammeter.

#### *Experimental Procedure.*

*Pressure Conditions.*—It is essential that the pressure conditions both in the discharge tube and in the observation tube, should be carefully chosen.

1. *Discharge Tube.*—In order to obtain a high proportion of atoms in the beam, the discharge pressure must be fairly high ( $2 \times 10^{-2}$  to  $5 \times 10^{-2}$  mm. in the present experiments) ; and the potential rather large\* (here 10 to 20 kilovolts). Under such conditions, even with the use of earth valves, static "flashing" is very troublesome. When a thermopile is used, extremely steady discharge conditions are essential. Several arrangements for producing the discharge were tried, and excellent results were finally got by using a small coil (6-inch spark gap), and a heavy mercury break. Moreover, the current must be small. In all the experiments it was about 1/10 milliamp. The discharge tube current was controlled by a sliding resistance in the primary circuit of the coil. A point and cup rectifier was used. With these arrangements, the discharge conditions could be held constant for several hours in a good run.

2. *Observation Tube.*—The first essential here is a pressure sufficiently high to ensure the establishment of the equilibrium charge exchange in the beam. On the other hand, the pressure must be low enough to ensure that the time for the neutrals to traverse the mean free path ( $L_2$ ) is long enough for space quantisation to be assured. The time required for the establishing of space quantisation is not as yet very certainly known. Recent theoretical and experimental considerations seem to show, however, that the time of quantisation in a magnetic field is of the same order as the period of the Larmor

\* Döpel, *loc. cit.*

precession. Next, the chance of the neutral atoms making ionising collisions should be very much higher for the normal state than for other, excited, states ; otherwise the simple considerations upon which the experiments are based cannot apply. This is assured if, in comparison with  $L_2$ , (1) the mean free path ( $l$ ) of the natural time of excitation is small ; (2) the mean free path ( $l_1$ ) of an atom in an excited (including a metastable) state, until its return to the normal state due to a collision of the second kind, is small ; (3) the mean free path ( $l_2$ ) of a normal atom, until excited to the emission of a given spectral line, is large.

With these considerations in view, the selected pressure range in the observation tube was  $3 \times 10^{-3}$  to  $4.5 \times 10^{-3}$  mm. Rüchardt has shown that the mean free path ( $L_2$ ) of the neutral atoms does not depend very markedly on the discharge potential  $V$  ; nevertheless, there is a tendency for  $L_2$  to assume smaller values with lower voltages. For the least favourable of our experimental conditions, namely,  $V = 10$  kilovolts and observation tube pressure,  $p = 4.5 \times 10^{-3}$  mm., he finds  $L_2$ , for hydrogen in hydrogen, to be about 30 cm. A simple calculation then shows that the time between two charge exchanges is  $2.2 \times 10^{-7}$  seconds. The strength of the field used throughout the experiments was uniformly 75 gauss ; the corresponding Larmor period is  $0.93 \times 10^{-8}$  seconds. Thus some twenty complete Larmor periods can be described between two charge exchanges ; and "sharp" quantisation is assured. Further, assuming a time of excitation of the order  $10^{-8}$  seconds,  $l \sim 1$  cm. ; the observations of Wien\* give, for hydrogen in hydrogen,  $l_1 = 3.4$  cm. for the  $4_2$  state, when  $p = 4.5 \times 10^{-3}$  mm. and  $V = 5$  kilovolt ; while Dasannacharya† finds, for the same pressure,  $l_2 (H_\beta) = 0.54 \times 10^4$  cm. and  $l_2 (H_\gamma) = 2.4 \times 10^4$  cm. Thus the existing data, so far as they go, justify the conclusion that the conditions (1), (2) and (3) above are fulfilled ; confirmatory evidence is furnished by measurements of the cross section of the neutral atoms by the mean free path method, which give values not very different from that of the innermost Bohr orbit.‡

*Stray Magnetic Effects.*—A small inductive effect on the galvanometer was still detectable when the solenoid field was thrown on, even after the adoption of shielding and non-inductively wired leads. This was completely eliminated by building up the field, gradually but quite rapidly, by means of a sliding

\* Wien, 'Ann. Physik,' vol. 70, p. 1 (1923).

† Dasannacharya, 'Ann. Physik,' vol. 77, p. 597 (1925).

‡ Rüchardt, *loc. cit.*

resistance in the solenoid circuit. The further precaution was taken of periodically reversing the direction of the magnetising current during a run.

*Readings.*—The method of taking observations is as follows. Let  $d'$ ,  $d$  denote in general galvanometer deflections with and without field.  $d$  is first observed; 15 seconds later, the field is built up; after a lapse of 30 seconds,  $d'$  is observed; 15 seconds later, the field is rapidly reduced to zero by building up the resistance in the solenoid circuit, and opening the switch; after a further 30 seconds,  $d$  is again observed, and so on. At the end of a run, the zero is checked. The number of readings taken in a single run varied from 40 to 110. By adopting this method of timed readings, the effect of slight variations in the discharge conditions is practically entirely eliminated.

### Experimental Results.

1. *Resting Gas, Hydrogen.*—The discharge tube pressures were varied between  $2 \times 10^{-2}$  and  $6 \times 10^{-2}$  mm.; the observation tube pressures between  $3 \times 10^{-3}$  and  $4 \times 10^{-3}$  mm. The ratio  $d_2/d'_2$  was determined for each set of pressure conditions, the observations being in each case many times repeated. Table I shows typical data. In no case is any magnetic effect detectable.

Table I.

Milliamps.	V. kilovolt.	McLeod I. mm. $\times 10^{-2}$ .	McLeod II. mm. $\times 10^{-2}$ .	Flux gauss.	No. of readings.	$d_2$ .	$d'_2$ .	$d_2/d'_2$ .
0.1	20	2.0	4.0	75	60	405.7	405.6	1.000 <sub>2</sub>
0.1	20	3.5	3.0	75	78	313.2	312.5	1.002
0.1	15	6.0	4.0	75	80	371.4	371.7	0.999
0.1	10	5.5	4.0	75	44	297.8	297.7	1.000 <sub>3</sub>
0.1	12	5.0	3.0	75	110	320.1	318.7	1.004

The quantities  $w$ ,  $w'$  were frequently determined at the same time as  $d_2$ ,  $d'_2$ . The following values are typical:  $w = 0.169$ ;  $w' = 0.171$ ; whence  $r_2/r'_2 = \sqrt{w/w'} = 0.994$ .

2. *Resting Gas, Argon.*—It was considered just possible that for hydrogen the molecules of the resting gas might orient in the field, in such a manner as to annul the effect of an increase in the target area of the moving neutral hydrogen atoms. The experiments were therefore repeated, the resting gas being now argon, which, as an inert gas possessing a closed electron group, may be assumed incapable of orientation. The argon was carefully purified by circulation for many hours in a quartz tube over glowing calcium, before admission to the apparatus.

The following shows the individual readings in a typical determination of  $d_2$  and  $d'_2$ ; an idea may thus be gained of the conditions of stability attained. Here, again, in no case could any magnetic effect be observed.

August 12, 1926. Resting gas, Argon; milliamps, 0.05; potential, 15 kilovolts. McLeod I,  $5 \times 10^{-2}$  mm.; McLeod II,  $4.5 \times 10^{-2}$  mm.; flux, 75 gauss.

*Galvanometer Deflections.*—(mm.) (Figures in ordinary type indicate observations taken *without* field; those in italics observations *with* field.)

432,	433,	432,	431,	433,	434,	436,	437,	439,	439,	436,	429
430,	430,	430,	431,	433,	440,	443,	439,	436,	436,	436,	435
435,	436,	438,	440,	433,	429,	431,	433,	434,	431,	428,	433
434,	436,	434,	434,	436,	436,	439,	441,	438,	436,	441,	441
443,	444,	443,	440,	442,	443,	441,	438,	437,	436,	436,	439
441,	441,	443,	441								

Total number of readings, 64;  $d_2$  (av.), 436.34 mm.;  $d'_2$  (av.), 436.31 mm.

### *Conclusions.*

The results, particularly with argon as resting gas, where the possibility of molecular orientation is excluded, are conclusive:  $d_2/d'_2 = 1$  to within the experimental error. This means that the effective collision area presented to the molecules of the resting gas by the neutral hydrogen atoms in a beam of canal rays is unaltered by space quantisation. The hydrogen atom is shown to be isotropic.

### *Discussion.*

1. The result of the present experiments receives notable spectroscopic confirmation. Unsöld\* has recently shown from an analysis of the helium arc spectrum, that the helium atomic core is not an electric quadrupole, as would follow from the assumption of a plane orbit for the inner electron. This argues an advanced symmetry for the helium atomic core, and hence immediately for the normal hydrogen atom.

A similar high degree of isotropy is evinced by the normal sodium atom. The magnetic behaviour of sodium is known.† Only two orientations, parallel and anti-parallel to the field, are possible for the normal sodium atom. Nevertheless Schütz‡ has established the fact that sodium vapour shows no trace of double refraction independent of field strength and wave-length.

2. These facts receive a remarkably satisfying interpretation on the basis

\* 'Z. f. Physik.' vol. 36, p. 92 (1926).

† Taylor, 'Phys. Rev.', vol. 28, p. 576 (1926).

‡ 'Z. f. Physik.' vol. 38, p. 859 (1926).



of the Schrödinger mechanics. In his first paper, Schrödinger\* shows that, adopting polar co-ordinates,  $r$ ,  $\theta$ ,  $\phi$ , the eigenfunction,† for any state of the hydrogen atom may be expressed as the product of two functions; one containing  $r$  alone, the other a spherical harmonic in  $\theta$  and  $\phi$ . This result may be thrown into the form

$$\psi = X_{n,l}(r) P_l^m(\cos \theta) \frac{\cos}{\sin} m\phi, \quad (1)$$

where the usual spectroscopic conventions (not used by Schrödinger) are adopted; namely,  $n$  = principal quantum number;  $l$  = (azimuthal quantum number) — 1;  $m$  = magnetic quantum number.

The normal state of the hydrogen atom is a  $1s$  state; for which  $n = 1$ ,  $l = 0$ ,  $m = 0$ ; and the corresponding eigenfunction becomes

$$\psi = X_{1,0}(r) P_0^0(\cos \theta) \cos(0 \cdot \phi) \sim X(r). \quad (2)$$

That is  $\psi$  depends on  $r$  alone.

Next, we observe that, in his fourth paper, Schrödinger‡ has sustained the hypothesis that  $e.\psi^2$  expresses the mean space charge,  $\rho$ , of the distributed electron;  $e$  being the classical point charge. It follows at once from (2) that for the normal hydrogen atom

$$\rho = \rho(r). \quad (3)$$

That is, the electric field of the normal hydrogen atom possesses spherical symmetry. The hydrogen atom must, therefore, under all circumstances show perfect isotropy in collisions with other atoms.

It is evident that the above treatment leads to zero magnetic moment for the  $1s$  state ( $m = 0$ ). The reason is that no account has been taken of the angular momentum of the spinning electron,§ the eigenfunctions for a system with spinning electron having not so far been developed. That which orients in such case is apparently the *electron* momentum vector,  $\frac{1}{2} \cdot \hbar/2\pi$ . It seems clear that the corresponding magnetic moment equals *one* Bohr magneton,|| in agreement with the experimental results for atoms with a doublet  $s$  ground

\* 'Ann. Physik,' vol. 79, p. 361 (1926).

† We follow Dirac, 'Roy. Soc. Proc.' A, vol. 112, p. 664 (1926), in taking over the German term "Eigenfunktion."

‡ 'Ann. Physik,' vol. 81, p. 109 (1926).

§ Goudsmit and Uhlenbeck, 'Nature,' vol. 117, p. 264 (1926).

|| Thomas, 'Nature,' vol. 117, p. 514 (1926); Frenkel, 'Z. f. Physik,' vol. 37, p. 243 (1926); Heisenberg and Jordan, *ibid.*, vol. 37, p. 263 (1926).

term (copper, silver, gold ; sodium, potassium). The assumption of a spinning electron does not, of course, invalidate equations (2) and (3).

Finally, since the ground term of sodium is, as for hydrogen, an *s*-term, the sodium atom must be optically isotropic, as Schütz has found.

*Summary.*

Search for a change in the collision area of the hydrogen atom following space quantisation yields a negative result. The hydrogen atom in the normal (*1s*) state is thus shown to be isotropic. Spherical symmetry for an *s*-state follows as a necessary consequence of the Schrödinger atom theory ; hence the present result and also the absence of double refraction in space quantised sodium vapour (Schütz) are satisfactorily explained.

My thanks are due, in the first place, to Prof. G. P. Thomson, for his constant interest in the work, to which he contributed very many helpful suggestions. I am indebted to Mr. C. G. Fraser, instrument maker in the Natural Philosophy Department of the University of Aberdeen, to whom the design and construction of the thermopile used are due, for invaluable technical assistance ; and to Mr. James McKay.

For the information that the Schrödinger mechanics might be used to interpret the negative result of the present experiments I am indebted to Prof. Sommerfeld, to whom my grateful thanks are due for valuable discussion and advice.

---

*An X-Ray Investigation of Optically Anomalous Crystals of Racemic Potassium Chlorosulphoacetate.*

By W. G. BURGERS (Ramsay Memorial Fellow).

(Communicated by Sir William Bragg, F.R.S.—Received December 9, 1926.)

[PLATE 23.]

A crystallographic description of racemic potassium chlorosulphoacetate,  $\left\{ \begin{array}{l} \text{CHCl} \cdot \text{SO}_3\text{K} \\ | \\ \text{COOK} \end{array} \right. + 1\frac{1}{2} \text{HO}$ , has been given by Rathke\* and Doelter,† who came

to different conclusions with regard to the crystal symmetry. Rathke described the crystals as tetragonal, Doelter as orthorhombic. Recently, in a detailed investigation of crystals of this substance by F. M. Jaeger,‡ it was shown that the crystals are apparently orthorhombic-bipyramidal and markedly pseudo-tetragonal. The axial ratio is :—

$$a : b : c = 0.9973 : 1 : 2.7650.$$

The beautiful crystals which were used in the last-mentioned investigation showed remarkable optical anomalies. For particulars concerning them reference should be made to the original paper. To avoid misunderstanding only the general appearance of these anomalies may be described here :—

In parallel polarised light the crystals, which have often the shape of square plates parallel to {001}, the *a* and *b* axes forming their diagonals, show diagonal extinction on {001}. They are more or less divided into four triangular quadrants, separated by boundary lines parallel to the *a* and *b* axes, the resulting appearance being a zonal structure parallel to the boundaries of the square plates.

In convergent polarised light the interference image is only centrosymmetrical, showing a strong crossed dispersion of monoclinic character.

From these anomalies, and also from the facts that, *e.g.*, the planes (001) and (00 $\bar{1}$ ) were never exactly parallel and showed microscopical striations, Jaeger concluded that the apparently orthorhombic crystals are built up of perpendicularly crossed monoclinic lamellæ.

The crystals which were used in the present investigation were either the

\* 'Lieb. Ann. Chemie,' vol. 161, p. 166 (1872).

† 'Monatshefte,' vol. 7, p. 159.

‡ 'Proc. Roy. Acad. Amsterdam,' vol. 28, p. 423 (1925)

same as those above mentioned, or they had been grown under similar circumstances, i.e., from aqueous solutions which contained also KBr or KCl.\* The investigation was undertaken for the purpose of throwing some light on the composition of these crystals by means of X-rays.

A number of oscillation photographs about different crystallographic directions were taken with a Shearer gas-tube of copper anticathode. The greater part of the spots on the oscillation photographs were doubled. The doubling was not caused by any twin structure, but simply due to the high absorbing power of the crystals for copper rays; this could be definitely established by the character of their appearance and the dimensions of the crystal which was smaller than the beam.

With regard to X-rays the crystals behaved as true orthorhombic pseudotetragonal crystals. From the photographs the following preliminary values were calculated for the axes:—

$$a = 8.7 \text{ \AA}, \quad b = 8.6 \text{ \AA}, \quad c = 23.9 \text{ \AA}.$$

Accurate values were determined with the aid of a Bragg ionisation spectrometer. The crystals gave good reflections. Only a small number of planes were investigated in this way (Table I).

Table I.

Plane.	Spacing.		Relative intensities from successive orders.
	calc.	obs.	
001	23.76	11.88	II. v.w.; IV, VI mod. w.; VIII str., X, XII abs.; XIV, XVI w.
100	8.58	4.28	II w.; IV, VI mod.
010	8.60	4.28	II, IV mod. str.; VI w.
101	8.07	8.08	I abs.; II mod. str.; III str.; IV mod. str.
102	6.96	3.48	II mod. str.; IV w.
201	4.22	2.11	II mod.; IV w.
103	5.83	5.83	I w.; II, III mod. str.; IV w
301	2.84	2.84	I mod. str.; II abs.
105	4.16	4.17	I vw.; II w.; III mod.
025	3.19	3.19	I mod.

\* The crystals were kindly given to me by Prof. Backer and Prof. Jaeger of Groningen, to whom my best thanks are due. According to Prof. Backer, by whom the crystals had been grown, it seemed difficult to obtain measurable crystals from aqueous solutions which contained the pure sulphoacetate only. However the presence of KCl or KBr in such a solution was favourable to the growth of good crystals on slow evaporation of the solvent.

Especially the  $c$ -spacing could be carefully measured because several orders were observed; its value is 11.88 Å. Using this value and the axial ratio given by Jaeger, one finds:—

$$a = 8.58 \text{ Å}, \quad b = 8.60 \text{ Å}, \quad c = 23.76 \text{ Å}.$$

The calculated spacings in Table I refer to these axes. They determine a unit-cell which contains eight groups  $\left\{ \begin{array}{l} \text{CHCl} \cdot \text{SO}_3\text{K} \\ | \\ \text{COOK} \end{array} \right. + 1\frac{1}{2}\text{H}_2\text{O}$  (the figures quoted give 8.00).\*

The indices of the spots on the photographs were found by means of Bernal's method of analysis.† Table II gives the planes from which reflections were observed.

Table II.—Planes observed on Oscillation Photographs.

Axial Planes.	Planes $\{h k 0\}$ .	Planes $\{0 k l\}$ .	Planes $\{h 0 l\}$ .	Planes $\{h k l\}$ .				
200	210	021	103	301	111	211	134	231
400	220	022	105	303	112	212	135	232
020	230	023	107	305	113	214	136	233
040	410	025	109	307	114	216	137	234
002	240	026	202	309	116	217	138	235
004	420 ?	027	204	402	117	221	139	237
006	430	029	206	404	118	223	312	412
008		041		406	119	225	313	413
				408	121	226	314	416
					122	227	315	241
					126	228	316	243
					127	131	317	246
					128	133	318	421
							321	422
							322	423
							323	432
							324	
							325	
							326	

This table and Table I show that the following sets of planes are halved:—

- (a)  $\{h k 0\}$  if  $h$  is odd,
- (b)  $\{0 k l\}$  if  $k$  is odd,
- (c)  $\{h 0 l\}$  if  $(h + l)$  is odd.

\* The specific gravity of a small beautiful crystal was determined by the suspension method in a mixture of tetrabromoethane ( $\rho_{40}^{20} = 2.967$ ) and alcohol ( $\rho_{40}^{20} = 0.789$ ). Its value was  $\rho_{40}^{16} = 2.09$ .

† 'Proc. Roy. Soc.,' A, vol. 113, p. 117 (1926).

The given halvings correspond to the space-group  $Q_1^4$ , the underlying lattice being the simple orthorhombic lattice  $\Gamma_0$ .\* This is a strong argument in favour of the assumption that the crystals are truly orthorhombic.

A possibility which ought to be considered is that the unit-cell might not be truly orthorhombic, but pseudo-tetragonal monoclinic. However, this seems impossible for the following reason. It follows from the optical anomalies that our  $c$ -axis would be the  $b$ -axis of this monoclinic cell. Therefore, if we consider the unit-cell as monoclinic, the indices of the sets of halvings become :

- (a)  $\{h0l\}$  if  $h$  is odd,
- (b)  $\{0kl\}$  if  $l$  is odd,
- (c)  $\{hko\}$  if  $(h+k)$  is odd.

In order to see how far we can account for these halvings in the monoclinic system, we need only consider space-groups which are based on the simple monoclinic lattice  $\Gamma_m$ . In fact, the presence of first order reflections of forms such as  $\{111\}$  and  $\{112\}$ † excludes the possibility of  $\Gamma_m'$ , because the required halvings would not be affected by the simultaneous presence of pseudo-tetragonal unit-cells which are rotated with regard to each other through  $90^\circ$  about the  $b$ -axis. In the space-groups based on  $\Gamma_m$ , the planes which may be halved are  $\{010\}$ , and planes of the orthodiagonal zone  $\{h0l\}$ . As a consequence of this it seems impossible to account for the sets of halvings (b) and (c) by a perpendicular crossing of monoclinic lamellæ.

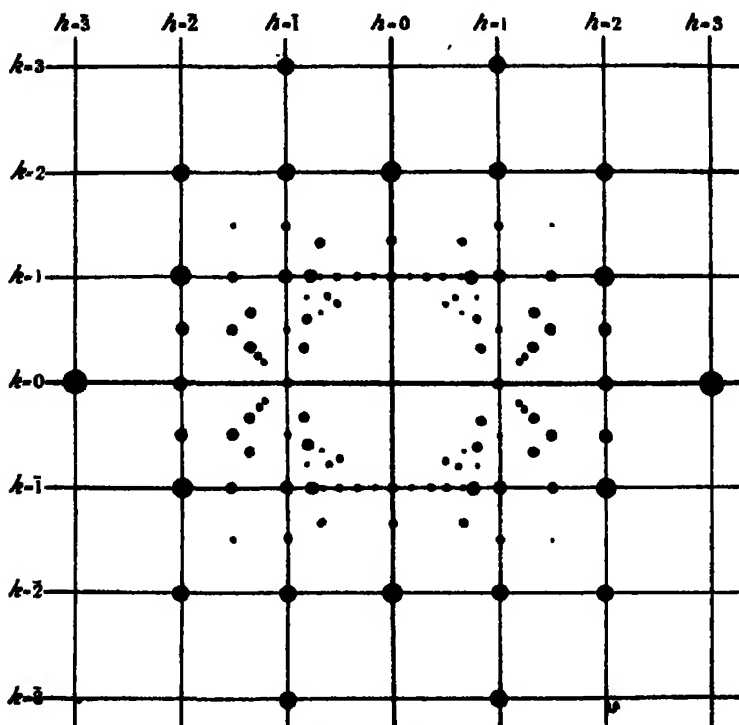
Therefore it seems necessary to assume that the successive zones of the crystals, which show themselves clearly in polarised light, are orthorhombic themselves and produced by a crystal growth which has taken place in steps. This is also confirmed by Laue-photographs. A number of such photographs were taken with copper and molybdenum rays, perpendicular to the basal plane. For some of them the whole of a crystal was used, for others only a part. These parts had been cut so that sometimes only zones of one direction, sometimes of two directions were present. All photographs showed two planes of symmetry perpendicular to each other, as is expected for orthorhombic crystals. Two of the photographs (Plate 23) and a gnomonic projection are given. They show clearly a pseudo-tetragonal character.

The zonal structure of the crystals gives a possible explanation of the fact that several of the Laue-photographs showed a considerable number of multiple spots, some of which consisted of an intense sharp part, and a weaker part,

\* Artbury and Yardley, 'Phil. Trans.,' A, vol. 224, p. 235 (1924).

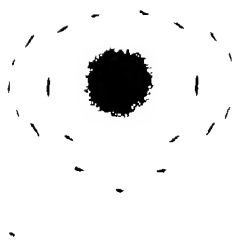
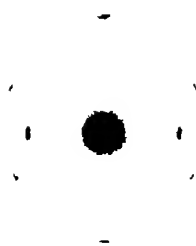
† With regard to the monoclinic cell the indices of  $\{111\}$  and  $\{112\}$  become  $\{111\}$  and  $\{121\}$ .

but generally these spots were broad or consisted of parts which had more or less the same intensity. Moreover, although the general appearance of the



Gnomonic Projection of Laue Photograph perpendicular to  $\{001\}$ , Copper Anticathode.

photographs was alike, this was never exactly the case, in so far as a certain spot never looked the same on two photographs of different crystal parts. Only the intense sharp reflections were always found as part of the same spots. A slight difference in orientation of successively crystallised layers, which shows itself in the deviations from parallelism between opposite faces (observed by Jaeger), must be the cause of this "multiplying" effect. This effect will be accentuated by the divergence of the X-ray beam. It was, for example, much more pronounced on the photographs, taken with Cu-rays, than on those taken with Mo-rays. For the former a copper anticathode was used of such a shape that a beam of rays was produced which was practically equally divergent in all directions, whereas the divergence of the rays from an almost flat molybdenum anticathode was considerably different in two directions which were perpendicular to each other. As a consequence of this, a photograph taken



Laue photographs of Racemic Potassium Chlorosulphoacetate, perpendicular to {001}, taken with copper anticathode (upper figure) and molybdenum anticathode (lower figure).





with Mo-rays showed the effect to a marked degree in one direction only. Calculation showed that the "intense sharp" reflections, mentioned above, were due to characteristic rays. Laue-photographs in directions which were not exactly perpendicular to {001} showed such reflections as part of quite different spots.

It is probable that the optical anomalies of the investigated crystals can be explained, after the manner of Brauns,\* and others, by the presence of internal strains. These latter may be caused for example by outer influences, or by the inclusion of isomorphous or other foreign substances. With regard to this, it should be pointed out that the crystals were grown from solutions containing KCl or KBr. It turned out that the crystals investigated contained small quantities of KCl. Indeed, included in one of the larger crystals, a small crystal of KCl was visible to the naked eye. It was identified both chemically and by measurement of the spacings of its cube-faces, which had the value 3.14. But even small transparent crystals gave a very faint but definite turbidity after addition of  $\text{HNO}_3$  and  $\text{AgNO}_3$ . It is therefore suggested that the presence of alkali halides in the mother liquor was directly (by giving rise to inclusions) or indirectly† the cause of a more or less strained lamellar growth.

The fact that the Laue-photographs of all sections possess orthorhombic symmetry, although the crystals show a monoclinic character in convergent polarised light, is in accordance with a recent investigation of F. Rinne.‡ This author showed that the atomic displacements which are a consequence of stresses in a crystal, and which are quite large enough to bring about a change in its optical character, are so small that they do not show themselves in Laue-photographs.

If the crystals are really orthorhombic, the substance is a true racemate, in the sense that right- and left-handed molecules are present in the same unit-cell. The latter contains eight salt molecules. For the sake of com-

\* R. Brauns, 'Die Optischen Anomalien' (1891). See also F. M. Jaeger, 'Lectures on the Principle of Symmetry.'

† It ought to be stated that an analysis of some of the crystals by Prof. Backer gave the following figures :

$$\text{C}_2\text{H}_3\text{O}_2\text{ClSk}_2 + 1\frac{1}{2}\text{H}_2\text{O} \begin{cases} \text{found : H}_2\text{O } 9.50 \text{ per cent. ; K } 28.21 \text{ per cent.} \\ \text{calc. : H}_2\text{O } 9.73 \text{ per cent. ; K } 28.16 \text{ per cent.} \end{cases}$$

This shows that the quantity of inclusion may be sometimes very small indeed, and the question arises if in those cases also the inclusion can be considered as the cause of the strains.

‡ 'Centr. bl. f. Min.' (1925), A, p. 225 ; also 'Z. f. Krist.', vol. 63, p. 236 (1926).

pletteness, the co-ordinates of the eight corresponding equivalent points are given :—

$$\begin{array}{ccccccc}
 x & y & z & \frac{1}{2} - x & \frac{1}{2} - y & \bar{z} & \\
 x & \frac{1}{2} + y & \frac{1}{2} - z & \frac{1}{2} + x & \bar{y} & \frac{1}{2} + z & \\
 \bar{x} & \frac{1}{2} - y & \frac{1}{2} + z & \frac{1}{2} + x & y & \frac{1}{2} - z & \\
 x & \bar{y} & \bar{z} & \frac{1}{2} - x & \frac{1}{2} + y & z & *
 \end{array}$$

There are twelve water molecules. Eight of them are probably connected with the sulpho-groups of the eight salt molecules. It is well known that the sulpho-carboxylic acids generally contain one molecule of water of crystallisation. The four remaining water molecules must occupy special positions, either at centres of symmetry or on dyad axes.

It is possible that a right- and a left-handed salt molecule have combined to form a racemic double molecule, but no particular argument, either for or against this supposition, was found.

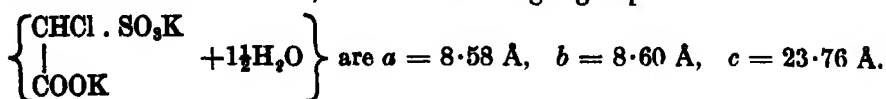
[*Note added January, 1927.*—Since this work was concluded crystals of racemic potassium chlorosulphoacetate have been grown by Prof. Backer from a pure aqueous solution by inoculating with a crystal of the salt prepared by the previous method. The crystals obtained in this way show the same zonal appearance in parallel polarised light. This shows that the presence of KCl or KBr in the solutions from which the crystals investigated were grown is not essential for the occurrence of a strained lamellar growth.]

### *Summary.*

In an investigation of crystals of racemic potassium chlorosulphoacetate  $\left\{ \begin{array}{l} \text{CHCl} \cdot \text{SO}_3\text{K} \\ \text{COOK} \end{array} + 1\frac{1}{2}\text{H}_2\text{O} \right\}$  by F. M. Jaeger, it was shown that these crystals exhibit an anomalous optical behaviour, and that variations occur in the angles between some of their faces. These facts led to the conclusion that the apparently orthorhombic crystals were in reality built up of perpendicularly crossed monoclinic lamellæ. The present investigation of the crystals by X-rays shows that the crystals are truly orthorhombic, and that the irregularities of their habit must be caused by a slight difference in orientation of successively crystallised layers. It is suggested that the optical anomalies are due to strains in the crystals.

\* Deduced from Astbury and Yardley's diagrams and from Wyckoff's tables.

The space-group of the crystals is  $Q_h^{14}$ , the underlying lattice  $\Gamma_0$ . The dimensions of the unit cell, which contains eight groups



This investigation was carried out by aid of a grant from the Ramsay Memorial Fund. My sincere thanks are due to Sir William Bragg for his kindness and encouragement, and to the Managers of the Royal Institution of Great Britain for continuing to place at my disposal the facilities of the Davy Faraday Research Laboratory.

*The Electric Fields of South African Thunderstorms.*

By B. F. J. SCHONLAND, M.A., Ph.D., Senior Lecturer in Physics, University of Cape Town, and J. CRAIB, M.A.

(Communicated by C. T. R. Wilson, F.R.S.—Received January 3, 1927.)

[PLATES 24, 25.]

§ 1. *Introduction.*

The quantitative study of the electrical changes taking place in thunderstorms was initiated and has been developed by Prof. C. T. R. Wilson in two important papers.\* Measurements of the electric fields due to charged clouds and of the field changes associated with lightning discharges have led him to put forward certain views according to which the thunderstorm is an important factor in the production and maintenance of several electro-meteorological phenomena with which it has not previously been considered connected. Chief amongst these is the negative charge on the surface of the earth, for the replenishment of which the views of Wilson require a certain preponderance of thunderclouds of positive polarity, *i.e.*, positively charged above and negatively charged below, over clouds of negative polarity, the ionisation currents between the bases of the clouds of the former type and the ground serving to maintain the earth's charge at a steady value in spite of the reverse current flowing in regions of fine weather.

\* Wilson, 'Roy. Soc. Proc.,' A, vol. 92, p. 555 (1910), referred to as W1; Wilson, 'Phil. Trans.,' A, vol. 221, p. 73 (1921), referred to as W2.

It is necessary, in order to test this theory, that observations be made in different parts of the world to examine whether the required preponderance of clouds of positive polarity exist. For this purpose South Africa, which contributes largely to the world's supply of thunderstorms, is very suitable.

The measurements described in this paper are mainly concerned with the question of cloud polarity, and seem to show an overwhelming preponderance of clouds of positive polarity, amongst those examined. Opportunity has also been taken to discuss other matters connected with the electrical effects of thunderstorms.

### § 2. *Site and Apparatus.*

Thunderstorms being rare at Cape Town, the necessary apparatus was installed in January, 1926, on the farm Gardiol, two miles south-east of the town of Somerset East, Cape Province, situated in what is called the East Central Karroo. The altitude of the station is 2460 feet above sea-level.

The site was chosen to give a good view of the surrounding country, especially in the westerly direction, from which most of the storms come. The nearest trees and the only near house are more than 100 yards away. The grass in the neighbourhood of the station is naturally very short and dry.

The storms examined were for the most part violent thunderstorms travelling across the country from west to east. A few were purely local, caused by convection currents due to surface heating. The total number of storms between January and June, 1926, was considerably below the average, and drought conditions prevailed.

The apparatus was installed in a wooden hut 9 feet by 8 feet in area, having a sloping gavanised iron roof of maximum height 9 feet. The whole installation was copied almost directly from that described by Wilson.

For the measurement of the electric fields of distant storms a copper ball 30·6 cm. in diameter was used, mounted and insulated exactly as described by Wilson.\* This ball could be raised to a height of 5·00 metres above the ground. For nearer storms a copy of the exposed testplate† was constructed from a wooden circular sieve 54·6 cm. in diameter and 14 cm. in depth. This was filled with earth to the level of the surrounding ground and mounted on sulphur-ebonite insulators inside a concentric pit 59·5 cm. in diameter and 60 cm. deep. The insulators were suitably shielded against dust and dripping water. The device for swinging a cover over the testplate, the insulation and shielding of the lead-in wires, and the earthing arrangements were similar to those of Wilson.

\* W.2, p. 75.

† W.1, p. 561.

The base of the vertical pipe carrying the ball was 550 cm. to the south of the nearest end of the hut, while the centre of the testplate was 600 cm. to the west. An outside view of the station is shown in fig. 1, Plate 24, a cross being placed immediately above the testplate. On the right is the metal-lined box to hold the ball when it is lowered.

The arrangements inside the hut for measuring the quantities of electricity which passed between the exposed conductors and the earth—the capillary electrometer, microscope objective, slit and moving photographic plate—did not differ essentially from the descriptions given by Wilson.\* The rate of motion of the plate was regulated by means of a needle valve controlling the flow of oil into a cylinder. Some difficulty was experienced with this device owing to alteration in the viscosity of the oil with temperature, for the temperature in the hut often exceeded 105° F. A convenient arrangement was introduced whereby two photographic records could be taken on one plate. The usual wooden plateholder was slipped into a larger box sliding across the slit in guides. When moved to one side of this box one half of the plate was exposed, after which it could be quickly shifted to the other side and a second photograph taken on the other half. Fig. 2, Plate 24, is a general view of the recording apparatus.

The sensitiveness of the electrometer was checked by means of a standard condenser charged to a known potential difference and was such that a displacement of 1 mm. on the photographs corresponded to the passage of  $1.03 \times 10^{-8}$  coulombs, or 30.8 e.s.u., through the capillary electrometer. From the data given it may easily be shown that this displacement corresponds to a change in the vertical electric field of 127 volts per metre when the ball was used and of 4950 volts per metre in the case of the testplate. These figures include corrections of 6 per cent. and 9 per cent. for the effect of the charge induced on the hut and on the earth-connected testplate cover and supporting arm. The effective area of the testplate was 2560 sq. cm.

### § 3. *The Electric Field of a Bipolar Thundercloud.*

In discussing the observations it will be convenient to adopt, as a working hypothesis, the view that a thundercloud is essentially bipolar, electric charges of opposite sign being liberated at different heights in the cloud. Thus we may speak of the upper and lower charges without specifying at the moment their exact positions or their relative magnitudes. All the evidence which will

\* W2, p. 76.

be put forward is in agreement with this view of the nature of the electrification of the cloud.

At distances which are large compared with the dimensions of the charged portions of the cloud, we may treat these as point charges.

In fig. 3 let A represent the upper charge,  $Q_2$ , at a height  $H_2$  above the earth,

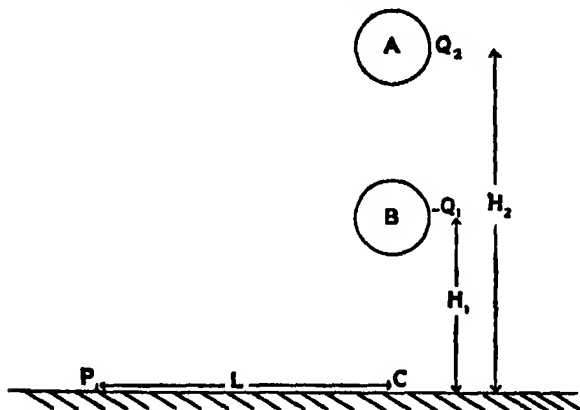


FIG. 3.

and B the lower charge,  $-Q_1$ , of opposite sign, at a height  $H_1$ . Let P be the point at which the vertical electric field is measured. According to the usual convention, this field is called positive if its direction is downwards and negative if it is upwards. It will be convenient to use the term "steady field" to denote the field at P when neither pole of the cloud is discharging or recovering from a discharge.

The steady vertical field at P due to the cloud will be given by the expression

$$F = \frac{2Q_2H_2}{(H_2^2 + L^2)^{3/2}} - \frac{2Q_1H_1}{(H_1^2 + L^2)^{3/2}}. \quad (1)$$

In general this expression shows that for distances L less than a certain critical value the second term and, consequently, the effect of the lower charge B predominates, while for distances greater than this critical value the first term is the greater and the sign of the field at P is set by that of the upper charge A. Thus with increasing distance L between the cloud and the station the field will first be of the same sign as the charge upon the lower part, then become zero, and then reverse so as to be of the same sign as the upper charge. This reversal of the sign of the field with distance will only occur provided that the lower charge  $Q_1$  is not less than  $H_1^3/H_2^3$  times, nor greater than  $H_2/H_1$  times, the upper charge  $Q_2$ .

\* W2, p. 96.



FIG. 1.



FIG. 2.





FIG. 4.



FIG. 5.



FIG. 6.

A reversal of the steady field as a thundercloud approached or receded from the station has been observed in several cases and these will be described in the next section. It would have perhaps been observed more often were it not for practical difficulties in the way of measuring the field due to a single thundercloud. These arise from the fact that the observed field is often the resultant of the effects of several clouds, and, unless local clouds and other distant storms are absent or negligible, a definite observation of the steady field due to a single distant storm is not possible.

Information as to the electrical nature of the cloud may, however, be obtained in another way, by examining the sign and magnitude of the changes of field caused by lightning discharges. Let us consider fig. 3 to represent an isolated cloud in which the flashes of lightning pass nearly vertically between the poles and the ground or between the two poles of the cloud. We may represent the two former types of discharge by the symbols AC and BC, and the latter by AB. Then equation (1) shows that the sudden changes of field resulting from these three types of discharge are given by the following expressions :

Discharge AC

$$\Delta F = - \frac{2Q_2 H_2}{(H_2^2 + L^2)^{3/2}},$$

discharge BC

$$\Delta F = + \frac{2Q_1 H_1}{(H_1^2 + L^2)^{3/2}},$$

discharge AB

$$\Delta F = -2Q_2 \left[ \frac{H_2}{(H_2^2 + L^2)^{3/2}} - \frac{H_1}{(H_1^2 + L^2)^{3/2}} \right] \text{ if } Q_1 > Q_2,$$

or

$$\Delta F = -2Q_1 \left[ \frac{H_2}{(H_2^2 + L^2)^{3/2}} - \frac{H_1}{(H_1^2 + L^2)^{3/2}} \right] \text{ if } Q_1 < Q_2.$$

For the two single-pole discharges the sign of  $\Delta F$ , the field change, is independent of the distance, but for the pole to pole discharge it evidently reverses as the distance  $L$  increases.

Consider a cloud of positive polarity, one in which the upper pole is positive and the lower negative. The effects to be expected from such a cloud are shown in the tables below.

Table I.—Distant Positive Cloud.

Discharge.	Sign of sudden field change.
AB	Negative
BC	Positive
AC	Negative

Table II.—Near Positive Cloud.

Discharge.	Sign of sudden field change.
AB	Positive
BC	Positive
AC	Negative

For a cloud of polarity opposite to this, negative above and positive below, the sign of each of these field changes would be reversed. It is necessary to add some remarks to the above simplified discussion of the effects of discharges.

(a) The critical distance at which the change of field due to a discharge AB reverses its sign on passing through zero is not identical with the distance at which the same thing happens to the steady field of the cloud. The latter is given by

$$H_2(H_1^2 + L^2)^{3/2} = \frac{Q_1}{Q_2} \times H_1(H_2^2 + L^2)^{3/2}, \quad (2)$$

and the former by

$$H_2(H_1^2 + L^2)^{3/2} = H_1(H_2^2 + L^2)^{3/2}. \quad (3)$$

The two values of  $L$  are only equal when  $Q_1 = Q_2$ . The relative magnitudes of  $Q_1$  and  $Q_2$  depend upon a number of factors, and there is no reason to suppose that they are equal. They may even be so different that no value of  $L$  will satisfy (2), in which case the steady field will not reverse its sign.

(b) It is possible that discharges may occur between the upper pole A and the conducting upper atmosphere. Such discharges have been observed by us at night as an intermittent glow upwards from the top of a distant cloud. The effect of such a discharge on the field would be the same as that given in the tables under AC.

(c) A discharge from pole to pole involves the disappearance of equal and opposite quantities of electricity, and may be followed by a second flash from the pole which originally had the greater charge. This second discharge may pass to earth or to the upper atmosphere, as suggested in (b) above. It is

possible that the two flashes may occur almost simultaneously, the discharge from pole to pole extending downwards or upwards from the cloud. At great distances the resultant effect would be of the same sign as that produced by a discharge AB, while at small distances it would be of the same sign as a discharge BC, provided that the relative magnitudes of the charges lie between the limits mentioned at the beginning of this section.

Fortunately, a considerable simplification of the results to be expected from observations of field changes can be made in the case of the measurements to be described. For in South Africa, as in India,\* it is a matter of common observation that the great majority of lightning discharges pass between the upper and lower parts of the cloud and do not strike to the ground. Discharges from the bottom of the cloud to the ground are much less frequent and from the upper pole to the ground comparatively rare.

We should therefore expect for distant storms of positive polarity a preponderance of negative changes of field (Table I, discharge AB) and for near storms a preponderance of positive changes (Table II, discharge AB). The signs of these changes will be reversed for storms of negative polarity.

#### § 4. *Observations of Fields and Sudden Field Changes.*

The measurements have been separated into two sets corresponding to what are called near and distant storms. A storm at a distance of more than 8 kilometres from the station is placed in the latter category, while storms occurring within a distance of 6 kilometres are considered as near. The information obtained from visual and photographic observation of 18 distant storms is summarised in Table III. The first column contains the serial number under which the storm was recorded, the second its approximate distance in kilometres. The third column contains the sign and magnitude of the steady field due to the undischarged cloud together with the normal fine-weather field. [This fine-weather field was never found to exceed 60 volts per metre at any time of the day or night, and its usual value was between 30 and 50 volts per metre. More accurate determinations of what seems a remarkably low value will shortly be made.]

When this steady field was not definitely ascertained, owing to the interfering effects of other clouds or to other reasons, the column is left blank. The number of sudden positive and negative changes of field observed visually and photographically are next entered in separate columns, and finally the results of the two methods of observation are shown combined.

\* Simpson, 'Phil. Trans.' A, vol. 209, p. 412 (1909).

Table III.

Storm.	Distance.	Steady field.	Sudden field changes.						Remarks.
			Visual.		Photographic.		Combined.		
			Pos.	Neg.	Pos.	Neg.	Pos.	Neg.	
1	km. 24	v m. +250	3	29	—	—	3	29	Approaching. Receding.
2	8-31	—	—	—	8	3	8	3	
3	11-7	—	8	21	1	8	9	29	
4	6-16	—	—	—	0	5	0	5	
5	35	—	12	35	—	—	12	35	
6	10*	—	26	95	—	—	26	95	
6	15*	+ 30	—	—	4	8	4	8	
7	23	—	—	—	0	13	0	13	
8	15*	—	—	—	2	25	2	25	Approaching. Receding. Flashes in clouds. (upwards). Two storms in action. Flashes in clouds.
9	20*	—	12	118	—	—	12	118	
10	14*	+100	1	14	4	28	5	42	
11	30-10	—	4	39	—	—	4	39	
11	14-25	—	3	40	—	—	3	40	
12	10	+100	0	27	—	—	0	27	
13	24	—	—	—	9	14	9	14	
14	8	+ 40	23	13	—	—	23	13	
15	10*	—	4	50	—	—	4	50	Flashes in clouds.
16	30*	+ 40	1	10	0	4	1	14	
17	20	+260	—	—	1	39	1	30	
18	14-17	+800	—	—	6	28	6	28	
		Total	97	491	35	175	132	666	

\* Indicates that the distance is a rough estimate.

The results in the above table may be summarised as follows :—

- Out of 18 distant storms, ranging in distance from 8 to 35 km., the steady field could be definitely ascertained in the case of 8 storms. For 4 of these it was positive and easily separable from the normal fine weather field, while for the remaining 4 it was too small to be separated from it.
- Out of 798 sudden changes of field, 666 were negative changes and 132 positive changes, a ratio of 5.0 to 1.
- This preponderance of negative changes is shown by 16 out of the 18 storms. The remaining 2 storms showed a preponderance of positive over negative changes in the ratio of 8/3 and 23/13 respectively.

Storm 2 is discussed in greater detail in § 5.

The next table contains similar data for five near storms.

Table IV.

Storm.	Distance.	Steady field.	Sudden field changes.						Remarks.
			Visual.		Photographic.		Combined.		
			Pos.	Neg.	Pos.	Neg.	Pos.	Neg.	
6	km.	v.m.							Flashes in clouds.
7	4.3	— 5000	2	6	3	0	5	6	
7	4.5	— 10500	—	—	7	2	7	2	
7	5.6	— 2500	—	—	5	0	5	0	
8	3.1	— 11200	—	—	2	0	2	0	
12	5.2	2000	19	0	—	—	19	0	
10	3.1	— 10000	0	1	1	0	1	1	
		Total	21	7	18	2	39	9	

It will be seen that in the case of these five near storms—

- (d) The steady fields were all definitely and strongly negative.
- (e) The sudden changes of field were predominately positive in sign, the ratio of positive to negative discharges being 39 to 9 or 4.3 to 1.

Comparing the results in the two tables, it is evident that the predominant sign of the sudden changes of field undergoes a striking reversal as the distance is increased. Thus, while the ratio of positive to negative changes for the five near storms in Table IV is 39/9, the same ratio for the *same* five storms when more than 10 km. distant is 27/210. Such a reversal cannot occur if the majority of the discharges take place from a single pole to the ground or the upper atmosphere, so that the results in these tables are in accord with the observation that the discharges are mainly between the poles of the cloud.

It appears also that the steady field of a thundercloud may undergo a reversal of sign as the distance is increased. That this is probable is indicated by (a) and (d) and quite well shown by storms 10 and 12, which gave positive fields when distant from, and negative ones when near to the station.

A comparison of the actual signs of the fields and field changes with the discussion given in § 3 leads to the conclusion that the observed effects were due to bipolar clouds, most of which, if not all, were of positive polarity. Further support for this conclusion is given by the details of certain storms discussed in the next section.

### § 5. *Discussion of Storms.*

Some attempt will be made in this section to correlate the field observations with the appearance of the lightning discharges to an outside observer.

(a) *Storm No. 12.*—This storm first came under observation when at a distance of 9·6 km. from the station, giving a small positive field which underwent 27 sudden negative changes. During this time it was approaching the station, and after reaching a distance of about 5 km. the field became strongly negative and 19 sudden large positive changes of field were observed from discharges at distances ranging from 5 to 2 km., all of the order of + 2000 volts per metre. During this time no sudden negative field changes occurred.

Outside observations showed that the lightning did not strike down, but was entirely between two portions of the cloud vertically above each other.

(b) *Storm No. 9.*—This took place at night at a distance of about 20 km. One observer noted the sign of the sudden changes of field while another made visual observations of the nature of the flashes of lightning. One hundred and seventeen negative and 12 positive changes of field were observed. The outside observer identified the positive changes with discharges between the base of the cloud and the ground and the negative changes with discharges in the cloud. The former were clearly visible as short distinct flashes, while the latter produced a general lighting up of the cloud.

(c) *Storms at the Reversal Point.*—On two occasions storms were observed to be taking place at a distance of from 6 to 8 km., but an examination of the field changes showed that the flashes of lightning produced no appreciable effect on the field. These storms occurred before the nature of the phenomenon was fully realised, and attention was unfortunately directed to testing whether the apparatus was in order and to other storms. In one case the flashes were observed to be taking place within the cloud, and there can be little doubt that both these storms were at the critical distance at which the effect of a discharge between the poles becomes zero and beyond which it reverses sign.

(d) *Rarity of Strong Positive Fields.*—Strong positive fields, in contrast to strong negative fields, were rarely observed and were always due to the *dissecta membra* of a worked-out storm. On one occasion such a cloud with a pronounced mammatiform appearance on its lower surface produced a field of between + 2000 and + 1000 volts per metre for about half an hour. It passed directly over the station and produced neither rain nor lightning. The only other occasions were during the observation of storm 2 described in (e) below, when a local cloud produced fields of + 3000 and + 1400 volts per metre for two periods of about 5 minutes each, without discharging.

(e) *Storm No. 2.* This storm is of some interest in view of its exceptional position in Table III, for it was one of the two distant storms which gave more positive (8) than negative (3) changes of field. The meteorological conditions were of a character quite different to those of any other storm investigated, for instead of the afternoon the storm took place in the early morning, at 6 a.m. The sky was covered with dark rain clouds as far as the eye could see, but the storm itself was of a mild character, only 11 discharges being observed in the course of an hour, after which the active centre moved away to the south-east. The potential gradient at the station was mainly due to local clouds which produced fields ranging from  $-1000$  to  $-5000$  volts per metre for about an hour, with the two short positive intervals mentioned in (d) above, but never discharged.

The flashes were all distant, ranging from 8.6 to 31 km. and 8 positive and 3 negative changes of field were photographically recorded. Outside observation showed that all the positive changes and one negative change were due to discharges between the base of the cloud and the ground. The remaining two negative changes were not observed as flashes at all, and it seems probable that they occurred between the poles of the cloud.

The predominance of positive over negative changes of field can therefore be ascribed in this case to the exceptional number of discharges between the base of the cloud and the ground, the cloud being of positive polarity.

This storm is instructive in making a comparison between the results obtained in the present series of storms and those examined by Wilson in England. Wilson\* found a predominance of positive over negative sudden changes of field, the numbers being 528 and 336 respectively. The descriptions of the storms indicate that a large proportion, possibly the majority, of the flashes passed between the base of the cloud and the ground. Such discharges, whatever the distance of the storm, would always produce a field change of opposite sign to the charge on the lower pole. If they were of frequent occurrence, as in storm 2 above and as is indicated by Wilson's description, their effect would be to hide the evidence for reversal of sign afforded by discharges within the cloud. In this connection it has been pointed out by Appleton, Watt, and Herd† that Wilson's observations for distances less than 5 km. show a preponderance of positive over negative changes of field in the ratio of 4 to 1, while at greater distances (5 to 30 km.) the ratio is only 1.5 to 1. This is what would be expected if the thunderclouds were, as in the present instance, largely positive in polarity,

\* W2, p. 85.

† 'Roy. Soc. Proc.' A, vol. 111, p. 654 (1926).



but discharges from the lower pole to the ground were of more frequent occurrence.

Appleton, Warr, and Herd have examined thunderclouds at distances ranging from 20 to more than 500 km. and found a strong predominance of negative changes of field associated with these distant discharges. They have also recorded an interesting case of reversal of the sign of the field changes at a distance of about 8 km., and some observations which closely resemble those described in (b) above, correlating the sign of the field changes with the appearance of the flashes.

### § 6. *Some Typical Records.*

(a) *Storm -May 1, 1926 (fig. 4).*—This is a typical record of a distant storm obtained by means of the ball when it was at a distance of from 13 to 17 km. The slightly skew appearance of the record is due to a wrong setting of the slit.

The record runs from 16 h. 51 m. 10 s. to 17 h. 1 m. 7 s. The ball was lowered for a few seconds at 16 h. 57 m. 30 s., and the record shows a potential gradient of + 800 volts per metre at this moment. Five sudden positive changes of field and 28 negative changes are shown. The three large negative changes altered the field by 384, 576, and 512 volts per metre, and occurred at distances, determined by stop watch outside the hut, of 17.2, 13.5 and 15.5 km. The electric moments of the flashes were thus 1.95, 1.52, and 1.92 volts per metre  $\times$  km.<sup>3</sup>  $\times 10^6$ . The outside observer reported all the flashes as taking place within the cloud.

(b) *Storm 8—February 24, 1926 (figs. 5 and 6).*—Fig. 5 shows the record obtained on the ball when the storm was approaching the station from a distance of about 15 km. A strong wind made thunder observations impossible. The record ran from 17 h. 10 m. 10 s. to 17 h. 23 m. 40 s. The potential gradient immediately before the record was — 520 volts per metre, and at 17 h. 12 m. 12 s., when the ball was lowered, it had fallen to — 256 volts per metre. A local cloud was producing rain throughout the record. Twenty-seven negative and five positive sudden changes of field are shown, the largest being — 130 volts per metre. The increasing negative field drove the mercury meniscus out of the field of view before the completion of the record.

At the close of the above record the storm was found to have approached so near that the testplate had to be employed. The record thus obtained is shown in fig. 6. It ran from 17 h. 30 m. 0 s. to 17 h. 40 m. 30 s. At 17 h. 30 m. 36 s., when the cover was swung over the testplate for a few seconds,

the field was — 11,200 volts per metre. Two positive discharges causing changes of + 12,300 and + 10,000 volts per metre are shown, the latter at a distance of 3.10 km., as determined from the thunder mark immediately following it. It was noted that heavy rain occurred at 17 h. 24 m. 15 s., which accounts for the rapid upward movement of the meniscus at 17 h. 33 m. 30 s. if the rain was positively charged. The cover was replaced before the end of the record, and the failure of the meniscus to return to the field of view showed that the system received a positive charge from the rain.

§ 7. *Electric Moments of the Discharges.\**

For a distant discharge the product  $\Delta F \times L^3$  of the sudden change of field and the cube of the distance gives the electric moment  $2QH$  or  $2Q(H_2 - H_1)$  according as the discharge passes to the ground or from pole to pole. This is only true when the discharge is sufficiently far off for  $H^2$  to be negligible in comparison with  $L^2$ . For less distant cases it gives too small a value.

The table below contains the mean values of  $\Delta F \times L^3$  for positive and negative discharges at distances (1) below 10 km. and (2) between 10 and 30 km. The number of observations used in getting the means is in each case shown in brackets.  $\Delta F \times L^3$  is given in volts per metre  $\times$  km.<sup>3</sup>  $\times 10^5$ .

Table V.

	0-10 km.		10-30 km.	
	Positive.	Negative.	Positive.	Negative.
$\Delta F \times L^3$	3.1 (7)	3.9 (2)	7.6 (10)	8.6 (63)

The mean value is not appreciably different for positive and negative discharges. It should be pointed out that the table is not representative of the 18 storms examined, for some yielded but little information on this point, while others furnished a large number of discharges at known distances.

For discharges between 10 and 30 km. the mean value of  $\Delta F \times L^3$  for both positive and negative changes of field is 8.45 volts per metre  $\times$  km.<sup>3</sup>  $\times 10^5$ , or 94 coulomb-kilometres. This is rather less than the corresponding figure of 148 coulomb-kilometres found by Wilson,\* but the agreement as regards order of magnitude is quite satisfactory. The actual values obtained ranged from

\* Compare W2, p. 90, between 10 and 30 km.

6.2 to 0.10 times the above mean, the former being almost certainly a very long discharge from the top of a cloud.

### § 8. *Discussion of Results.*

No further discussion of the information yielded by the photographic records will be attempted here. The main purpose of the present paper is to present what appears to be very clear evidence of the bipolar nature of thunderclouds, and of the strong predominance amongst such clouds of a type in which the upper pole is positive and the lower pole negative.

The observations given in sections 4 and 5 seem to make it doubtful whether more than one, if any, of the 18 thunderstorms examined were of negative polarity. Such a predominance of the positive type suggests that Simpson's\* theory of the production of the charge by the breaking up of large water-drops in an ascending air-current, which would produce a cloud of negative polarity must either be rejected or radically altered.

The conclusion that thunderclouds of positive polarity were mainly, if not always, observed is of importance in connection with Wilson's theory of the maintenance of the negative charge on the surface of the earth.† The ionisation currents above and below clouds of this type would feed positive electricity to the upper atmosphere and negative electricity to the earth. The thunderstorm, to use Wilson's simile,‡ would thus act as an electric generator connected between upper atmosphere and earth, the return circuit being provided by the feebly conducting air in the regions of fine weather.

The frequent references to Prof. Wilson's papers indicate to what extent we are indebted to them, both for the design of the apparatus and for the interpretation of the observations. We have also to thank him for kind advice in connection with certain experimental difficulties. Our grateful thanks are also due to Mr. J. Linton for constructing the apparatus required and assisting in its assembly and in the observations, to Prof. A. Ogg for providing many facilities for the work, and to the South African Research Grant Board for a grant in aid.

### § 9. *Summary.*

(1) A description is given of the installation and equipment of a station for measurements in electrical meteorology, which has been established at Somerset East, Cape Province, South Africa.

\* Simpson, *loc. cit.*

† W2, p. 113.

‡ W2, p. 109.

(2) Observations have been made of the electric fields and field changes associated with 18 distant and 5 near thunderstorms. The sudden changes of field due to distant lightning discharges ( $> 8$  km.) were predominantly negative in sign, those due to near discharges ( $< 6$  km.) predominantly positive. The relative frequencies of positive and negative changes were 1 : 5 in the former case and 4·3 : 1 in the latter. The steady electric fields below the 5 near storms were all strongly negative.

(3) It is shown that these results indicate that the thunderclouds were bi-polar in nature and that the polarity was generally, if not always, positive, the upper pole being positive and the lower pole negative. It is doubtful if any active storms of opposite polarity were observed at all.

(4) The electric moments of the charges removed by 82 lightning discharges have been measured. The mean value is 94 coulomb-kilometres.

---

### *The Quantum Theory of the Emission and Absorption of Radiation.*

By P. A. M. DIRAC, St. John's College, Cambridge, and Institute for Theoretical Physics, Copenhagen.

(Communicated by N. Bohr, For Mem. R S.—Received February 2, 1927.)

#### *§ 1. Introduction and Summary.*

The new quantum theory, based on the assumption that the dynamical variables do not obey the commutative law of multiplication, has by now been developed sufficiently to form a fairly complete theory of dynamics. One can treat mathematically the problem of any dynamical system composed of a number of particles with instantaneous forces acting between them, provided it is describable by a Hamiltonian function, and one can interpret the mathematics physically by a quite definite general method. On the other hand, hardly anything has been done up to the present on quantum electrodynamics. The questions of the correct treatment of a system in which the forces are propagated with the velocity of light instead of instantaneously, of the production of an electromagnetic field by a moving electron, and of the reaction of this field on the electron have not yet been touched. In addition, there is a serious difficulty in making the theory satisfy all the requirements of the restricted

principle of relativity, since a Hamiltonian function can no longer be used. This relativity question is, of course, connected with the previous ones, and it will be impossible to answer any one question completely without at the same time answering them all. However, it appears to be possible to build up a fairly satisfactory theory of the emission of radiation and of the reaction of the radiation field on the emitting system on the basis of a kinematics and dynamics which are not strictly relativistic. This is the main object of the present paper. The theory is non-relativistic only on account of the time being counted throughout as a c-number, instead of being treated symmetrically with the space co-ordinates. The relativity variation of mass with velocity is taken into account without difficulty.

The underlying ideas of the theory are very simple. Consider an atom interacting with a field of radiation, which we may suppose for definiteness to be confined in an enclosure so as to have only a discrete set of degrees of freedom. Resolving the radiation into its Fourier components, we can consider the energy and phase of each of the components to be dynamical variables describing the radiation field. Thus if  $E_r$  is the energy of a component labelled  $r$  and  $\theta_r$  is the corresponding phase (defined as the time since the wave was in a standard phase), we can suppose each  $E_r$  and  $\theta_r$  to form a pair of canonically conjugate variables. In the absence of any interaction between the field and the atom, the whole system of field plus atom will be describable by the Hamiltonian

$$H = \sum_r E_r + H_0 \quad (1)$$

equal to the total energy,  $H_0$  being the Hamiltonian for the atom alone, since the variables  $E_r, \theta_r$  obviously satisfy their canonical equations of motion

$$\dot{E}_r = -\frac{\partial H}{\partial \theta_r} = 0, \quad \dot{\theta}_r = \frac{\partial H}{\partial E_r} = 1.$$

When there is interaction between the field and the atom, it could be taken into account on the classical theory by the addition of an interaction term to the Hamiltonian (1), which would be a function of the variables of the atom and of the variables  $E_r, \theta_r$  that describe the field. This interaction term would give the effect of the radiation on the atom, and also the reaction of the atom on the radiation field.

In order that an analogous method may be used on the quantum theory, it is necessary to assume that the variables  $E_r, \theta_r$  are q-numbers satisfying the standard quantum conditions  $\theta_r E_r - E_r \theta_r = i\hbar$ , etc., where  $\hbar$  is  $(2\pi)^{-1}$  times the usual Planck's constant, like the other dynamical variables of the problem. This assumption immediately gives light-quantum properties to

the radiation.\* For if  $\nu_r$  is the frequency of the component  $r$ ,  $2\pi\nu_r\theta_r$  is an angle variable, so that its canonical conjugate  $E_r/2\pi\nu_r$  can only assume a discrete set of values differing by multiples of  $h$ , which means that  $E_r$  can change only by integral multiples of the quantum  $(2\pi h)\nu_r$ . If we now add an interaction term (taken over from the classical theory) to the Hamiltonian (1), the problem can be solved according to the rules of quantum mechanics, and we would expect to obtain the correct results for the action of the radiation and the atom on one another. It will be shown that we actually get the correct laws for the emission and absorption of radiation, and the correct values for Einstein's A's and B's. In the author's previous theory,† where the energies and phases of the components of radiation were c-numbers, only the B's could be obtained, and the reaction of the atom on the radiation could not be taken into account.

It will also be shown that the Hamiltonian which describes the interaction of the atom and the electromagnetic waves can be made identical with the Hamiltonian for the problem of the interaction of the atom with an assembly of particles moving with the velocity of light and satisfying the Einstein-Bose statistics, by a suitable choice of the interaction energy for the particles. The number of particles having any specified direction of motion and energy, which can be used as a dynamical variable in the Hamiltonian for the particles, is equal to the number of quanta of energy in the corresponding wave in the Hamiltonian for the waves. There is thus a complete harmony between the wave and light-quantum descriptions of the interaction. We shall actually build up the theory from the light-quantum point of view, and show that the Hamiltonian transforms naturally into a form which resembles that for the waves.

The mathematical development of the theory has been made possible by the author's general transformation theory of the quantum matrices.‡ Owing to the fact that we count the time as a c-number, we are allowed to use the notion of the value of any dynamical variable at any instant of time. This value is

\* Similar assumptions have been used by Born and Jordan [*Z. f. Physik*, vol. 34, p. 886 (1925)] for the purpose of taking over the classical formula for the emission of radiation by a dipole into the quantum theory, and by Born, Heisenberg and Jordan [*Z. f. Physik*, vol. 35, p. 606 (1925)] for calculating the energy fluctuations in a field of black-body radiation.

† *Roy. Soc. Proc.*, A, vol. 112, p. 661, § 5 (1926). This is quoted later by, *loc. cit.*, I.

‡ *Roy. Soc. Proc.*, A, vol. 113, p. 621 (1927). This is quoted later by *loc. cit.*, II. An essentially equivalent theory has been obtained independently by Jordan [*Z. f. Physik*, vol. 40, p. 809 (1927)]. See also, F. London, *Z. f. Physik*, vol. 40, p. 193 (1926).

a q-number, capable of being represented by a generalised "matrix" according to many different matrix schemes, some of which may have continuous ranges of rows and columns, and may require the matrix elements to involve certain kinds of infinities (of the type given by the  $\delta$  functions\*). A matrix scheme can be found in which any desired set of constants of integration of the dynamical system that commute are represented by diagonal matrices, or in which a set of variables that commute are represented by matrices that are diagonal at a specified time.† The values of the diagonal elements of a diagonal matrix representing any q-number are the characteristic values of that q-number. A Cartesian co-ordinate or momentum will in general have all characteristic values from  $-\infty$  to  $+\infty$ , while an action variable has only a discrete set of characteristic values. (We shall make it a rule to use unprimed letters to denote the dynamical variables or q-numbers, and the same letters primed or multiply primed to denote their characteristic values. Transformation functions or eigenfunctions are functions of the characteristic values and not of the q-numbers themselves, so they should always be written in terms of primed variables.)

If  $f(\xi, \eta)$  is any function of the canonical variables  $\xi_k, \eta_k$ , the matrix representing  $f$  at any time  $t$  in the matrix scheme in which the  $\xi_k$  at time  $t$  are diagonal matrices may be written down without any trouble, since the matrices representing the  $\xi_k$  and  $\eta_k$  themselves at time  $t$  are known, namely,

$$\left. \begin{aligned} \xi_k(\xi'\xi'') &= \xi_k' \delta(\xi'\xi''), \\ \eta_k(\xi'\xi'') &= -i\hbar \delta(\xi_1' - \xi_1'') \dots \delta(\xi_{k-1}' - \xi_{k-1}'') \delta'(\xi_k' - \xi_k'') \delta(\xi_{k+1}' - \xi_{k+1}'') \dots \end{aligned} \right\}. \quad (2)$$

Thus if the Hamiltonian  $H$  is given as a function of the  $\xi_k$  and  $\eta_k$ , we can at once write down the matrix  $H(\xi'\xi'')$ . We can then obtain the transformation function,  $(\xi'/\alpha')$  say, which transforms to a matrix scheme  $(\alpha)$  in which the Hamiltonian is a diagonal matrix, as  $(\xi'/\alpha')$  must satisfy the integral equation

$$\int H(\xi'\xi'') d\xi'' (\xi'/\alpha') = W(\alpha') \cdot (\xi'/\alpha'), \quad (3)$$

of which the characteristic values  $W(\alpha')$  are the energy levels. This equation is just Schrödinger's wave equation for the eigenfunctions  $(\xi'/\alpha')$ , which becomes an ordinary differential equation when  $H$  is a simple algebraic function of the

\* *Loc. cit.* II, § 2.

† One can have a matrix scheme in which a set of variables that commute are at all times represented by diagonal matrices if one will sacrifice the condition that the matrices must satisfy the equations of motion. The transformation function from such a scheme to one in which the equations of motion are satisfied will involve the time explicitly. See p. 628 in *loc. cit.*, II.

$\xi_k$  and  $\eta_k$  on account of the special equations (2) for the matrices representing  $\xi_k$  and  $\eta_k$ . Equation (3) may be written in the more general form

$$\int H(\xi'\xi'') d\xi'' (\xi'/\alpha') = i\hbar \partial (\xi'/\alpha') / \partial t, \quad (3')$$

in which it can be applied to systems for which the Hamiltonian involves the time explicitly.

One may have a dynamical system specified by a Hamiltonian  $H$  which cannot be expressed as an algebraic function of any set of canonical variables, but which can all the same be represented by a matrix  $H(\xi'\xi'')$ . Such a problem can still be solved by the present method, since one can still use equation (3) to obtain the energy levels and eigenfunctions. We shall find that the Hamiltonian which describes the interaction of a light-quantum and an atomic system is of this more general type, so that the interaction can be treated mathematically, although one cannot talk about an interaction potential energy in the usual sense.

It should be observed that there is a difference between a light-wave and the de Broglie or Schrödinger wave associated with the light-quanta. Firstly, the light-wave is always real, while the de Broglie wave associated with a light-quantum moving in a definite direction must be taken to involve an imaginary exponential. A more important difference is that their intensities are to be interpreted in different ways. The number of light-quanta per unit volume associated with a monochromatic light-wave equals the energy per unit volume of the wave divided by the energy  $(2\pi\hbar)\nu$  of a single light-quantum. On the other hand a monochromatic de Broglie wave of amplitude  $a$  (multiplied into the imaginary exponential factor) must be interpreted as representing  $a^2$  light-quanta per unit volume for all frequencies. This is a special case of the general rule for interpreting the matrix analysis,\* according to which, if  $(\xi'/\alpha')$  or  $\psi_{\alpha'}(\xi_k')$  is the eigenfunction in the variables  $\xi_k$  of the state  $\alpha'$  of an atomic system (or simple particle),  $|\psi_{\alpha'}(\xi_k')|^2$  is the probability of each  $\xi_k$  having the value  $\xi_k'$ , [or  $|\psi_{\alpha'}(\xi_k')|^2 d\xi_1' d\xi_2' \dots$  is the probability of each  $\xi_k$  lying between the values  $\xi_k'$  and  $\xi_k' + d\xi_k'$ , when the  $\xi_k$  have continuous ranges of characteristic values] on the assumption that all phases of the system are equally probable. The wave whose intensity is to be interpreted in the first of these two ways appears in the theory only when one is dealing with an assembly of the associated particles satisfying the Einstein-Bose statistics. There is thus no such wave associated with electrons.

\* *Loc. cit.*, II, §§ 6, 7.



## § 2. *The Perturbation of an Assembly of Independent Systems.*

We shall now consider the transitions produced in an atomic system by an arbitrary perturbation. The method we shall adopt will be that previously given by the author,† which leads in a simple way to equations which determine the probability of the system being in any stationary state of the unperturbed system at any time.‡ This, of course, gives immediately the probable number of systems in that state at that time for an assembly of the systems that are independent of one another and are all perturbed in the same way. The object of the present section is to show that the equations for the rates of change of these probable numbers can be put in the Hamiltonian form in a simple manner, which will enable further developments in the theory to be made.

Let  $H_0$  be the Hamiltonian for the unperturbed system and  $V$  the perturbing energy, which can be an arbitrary function of the dynamical variables and may or may not involve the time explicitly, so that the Hamiltonian for the perturbed system is  $H = H_0 + V$ . The eigenfunctions for the perturbed system must satisfy the wave equation

$$i\hbar \partial\psi/\partial t = (H_0 + V) \psi,$$

where  $(H_0 + V)$  is an operator. If  $\psi = \sum_r a_r \psi_r$  is the solution of this equation that satisfies the proper initial conditions, where the  $\psi_r$ 's are the eigenfunctions for the unperturbed system, each associated with one stationary state labelled by the suffix  $r$ , and the  $a_r$ 's are functions of the time only, then  $|a_r|^2$  is the probability of the system being in the state  $r$  at any time. The  $a_r$ 's must be normalised initially, and will then always remain normalised. The theory will apply directly to an assembly of  $N$  similar independent systems if we multiply each of these  $a_r$ 's by  $N^{1/2}$  so as to make  $\sum_r |a_r|^2 = N$ . We shall now have that  $|a_r|^2$  is the probable number of systems in the state  $r$ .

The equation that determines the rate of change of the  $a_r$ 's is§

$$i\hbar \dot{a}_r = \sum_s V_{rs} a_s, \quad (4)$$

where the  $V_{rs}$ 's are the elements of the matrix representing  $V$ . The conjugate imaginary equation is

$$-i\hbar \dot{a}_r^* = \sum_s V_{rs}^* a_s^* = \sum_s a_s^* V_{sr}. \quad (4')$$

† *Loc. cit.* I.

‡ The theory has recently been extended by Born [*Z. f. Physik*, vol. 40, p. 167 (1926)] so as to take into account the adiabatic changes in the stationary states that may be produced by the perturbation as well as the transitions. This extension is not used in the present paper.

§ *Loc. cit.*, I, equation (25).

If we regard  $a_r$  and  $i\hbar a_r^*$  as canonical conjugates, equations (4) and (4') take the Hamiltonian form with the Hamiltonian function  $F_1 = \sum_r a_r^* V_r a_r$ , namely,

$$\frac{da_r}{dt} = \frac{1}{i\hbar} \frac{\partial F_1}{\partial a_r^*}, \quad i\hbar \frac{da_r^*}{dt} = - \frac{\partial F_1}{\partial a_r}.$$

We can transform to the canonical variables  $N_r$ ,  $\phi_r$  by the contact transformation

$$a_r = N_r^{1/2} e^{-i\phi_r/\hbar}, \quad a_r^* = N_r^{1/2} e^{i\phi_r/\hbar}.$$

This transformation makes the new variables  $N_r$  and  $\phi_r$  real,  $N_r$  being equal to  $a_r a_r^* = |a_r|^2$ , the probable number of systems in the state  $r$ , and  $\phi_r/\hbar$  being the phase of the eigenfunction that represents them. The Hamiltonian  $F_1$  now becomes

$$F_1 = \sum_{rs} V_{rs} N_r^{1/2} N_s^{1/2} e^{i(\phi_r - \phi_s)/\hbar},$$

and the equations that determine the rate at which transitions occur have the canonical form

$$\dot{N}_r = - \frac{\partial F_1}{\partial \phi_r}, \quad \dot{\phi}_r = \frac{\partial F_1}{\partial N_r}.$$

A more convenient way of putting the transition equations in the Hamiltonian form may be obtained with the help of the quantities

$$b_r = a_r e^{-iW_r t/\hbar}, \quad b_r^* = a_r^* e^{iW_r t/\hbar},$$

$W_r$  being the energy of the state  $r$ . We have  $|b_r|^2$  equal to  $|a_r|^2$ , the probable number of systems in the state  $r$ . For  $b_r$  we find

$$\begin{aligned} i\hbar \dot{b}_r &= W_r b_r + i\hbar \dot{a}_r e^{-iW_r t/\hbar} \\ &= W_r b_r + \sum_s V_{rs} b_s e^{i(W_r - W_s)t/\hbar} \end{aligned}$$

with the help of (4). If we put  $V_{rs} = v_{rs} e^{i(W_r - W_s)t/\hbar}$ , so that  $v_{rs}$  is a constant when  $V$  does not involve the time explicitly, this reduces to

$$\begin{aligned} i\hbar \dot{b}_r &= W_r b_r + \sum_s v_{rs} b_s \\ &= \sum_s H_{rs} b_s, \end{aligned} \tag{5}$$

where  $H_{rs} = W_r \delta_{rs} + v_{rs}$ , which is a matrix element of the total Hamiltonian  $H = H_0 + V$  with the time factor  $e^{i(W_r - W_s)t/\hbar}$  removed, so that  $H_{rs}$  is a constant when  $H$  does not involve the time explicitly. Equation (5) is of the same form as equation (4), and may be put in the Hamiltonian form in the same way.

It should be noticed that equation (5) is obtained directly if one writes down the Schrödinger equation in a set of variables that specify the stationary states of the unperturbed system. If these variables are  $\xi_\lambda$ , and if  $H(\xi, \xi')$  denotes

a matrix element of the total Hamiltonian  $H$  in the  $(\xi)$  scheme, this Schrödinger equation would be

$$i\hbar \partial \psi(\xi') / \partial t = \sum_{\xi''} H(\xi' \xi'') \psi(\xi''), \quad (6)$$

like equation (3'). This differs from the previous equation (5) only in the notation, a single suffix  $r$  being there used to denote a stationary state instead of a set of numerical values  $\xi_k$  for the variables  $\xi_k$ , and  $b_r$  being used instead of  $\psi(\xi')$ . Equation (6), and therefore also equation (5), can still be used when the Hamiltonian is of the more general type which cannot be expressed as an algebraic function of a set of canonical variables, but can still be represented by a matrix  $H(\xi' \xi'')$  or  $H_{r's}$ .

We now take  $b_r$  and  $i\hbar b_r^*$  to be canonically conjugate variables instead of  $a_r$  and  $i\hbar a_r^*$ . The equation (5) and its conjugate imaginary equation will now take the Hamiltonian form with the Hamiltonian function

$$F = \sum_{r,s} b_r^* H_{rs} b_s. \quad (7)$$

Proceeding as before, we make the contact transformation

$$b_r = N_r^{\frac{1}{2}} e^{-i\theta_r/\hbar}, \quad b_r^* = N_r^{\frac{1}{2}} e^{i\theta_r/\hbar}, \quad (8)$$

to the new canonical variables  $N_r, \theta_r$ , where  $N_r$  is, as before, the probable number of systems in the state  $r$ , and  $\theta_r$  is a new phase. The Hamiltonian  $F$  will now become

$$F = \sum_{r,s} H_{rs} N_r^{\frac{1}{2}} N_s^{\frac{1}{2}} e^{i(\theta_r - \theta_s)/\hbar},$$

and the equations for the rates of change of  $N_r$  and  $\theta_r$  will take the canonical form

$$\dot{N}_r = -\frac{\partial F}{\partial \theta_r}, \quad \dot{\theta}_r = \frac{\partial F}{\partial N_r}.$$

The Hamiltonian may be written

$$F = \sum_r W_r N_r + \sum_{r,s} v_{rs} N_r^{\frac{1}{2}} N_s^{\frac{1}{2}} e^{i(\theta_r - \theta_s)/\hbar}. \quad (9)$$

The first term  $\sum_r W_r N_r$  is the total proper energy of the assembly, and the second may be regarded as the additional energy due to the perturbation. If the perturbation is zero, the phases  $\theta_r$  would increase linearly with the time, while the previous phases  $\phi_r$  would in this case be constants.

### §3. *The Perturbation of an Assembly satisfying the Einstein-Bose Statistics.*

According to the preceding section we can describe the effect of a perturbation on an assembly of independent systems by means of canonical variables and Hamiltonian equations of motion. The development of the theory which

naturally suggests itself is to make these canonical variables q-numbers satisfying the usual quantum conditions instead of c-numbers, so that their Hamiltonian equations of motion become true quantum equations. The Hamiltonian function will now provide a Schrödinger wave equation, which must be solved and interpreted in the usual manner. The interpretation will give not merely the probable number of systems in any state, but the probability of any given distribution of the systems among the various states, this probability being, in fact, equal to the square of the modulus of the normalised solution of the wave equation that satisfies the appropriate initial conditions. We could, of course, calculate directly from elementary considerations the probability of any given distribution when the systems are independent, as we know the probability of each system being in any particular state. We shall find that the probability calculated directly in this way does not agree with that obtained from the wave equation except in the special case when there is only one system in the assembly. In the general case it will be shown that the wave equation leads to the correct value for the probability of any given distribution when the systems obey the Einstein-Bose statistics instead of being independent.

We assume the variables  $b_r, \hbar b_r^*$  of § 2 to be canonical q-numbers satisfying the quantum conditions

$$b_r \cdot \hbar b_r^* - \hbar b_r^* \cdot b_r = \hbar$$

or

$$b_r b_r^* - b_r^* b_r = 1,$$

and

$$b_s b_s - b_s b_r = 0, \quad b_r^* b_s^* - b_s^* b_r^* = 0,$$

$$b_s b_r^* - b_r^* b_s = 0 \quad (s \neq r).$$

The transformation equations (8) must now be written in the quantum form

$$\left. \begin{aligned} b_r &= (N_r + 1)^{\frac{1}{2}} e^{-i\theta_r/\hbar} = e^{-i\theta_r/\hbar} N_r^{\frac{1}{2}} \\ b_r^* &= N_r^{\frac{1}{2}} e^{i\theta_r/\hbar} = e^{i\theta_r/\hbar} (N_r + 1)^{\frac{1}{2}} \end{aligned} \right\} \quad (10)$$

in order that the  $N_r, \theta_r$  may also be canonical variables. These equations show that the  $N_r$  can have only integral characteristic values not less than zero,† which provides us with a justification for the assumption that the variables are q-numbers in the way we have chosen. The numbers of systems in the different states are now ordinary quantum numbers.

† See § 8 of the author's paper 'Roy. Soc. Proc.,' A, vol. 111, p. 281 (1926). What are there called the c-number values that a q-number can take are here given the more precise name of the characteristic values of that q-number.

The Hamiltonian (7) now becomes

$$\begin{aligned} F &= \sum_r b_r^* H_r b_r = \sum_{rs} N_r^{\frac{1}{2}} e^{i\theta_r/\hbar} H_{rs} (N_s + 1)^{\frac{1}{2}} e^{-i\theta_s/\hbar} \\ &= \sum_{rs} H_{rs} N_r^{\frac{1}{2}} (N_s + 1 - \delta_{rs})^{\frac{1}{2}} e^{i(\theta_r - \theta_s)/\hbar} \end{aligned} \quad (11)$$

in which the  $H_{rs}$  are still c-numbers. We may write this  $F$  in the form corresponding to (9)

$$F = \sum_r W_r N_r + \sum_{rs} v_{rs} N_r^{\frac{1}{2}} (N_s + 1 - \delta_{rs})^{\frac{1}{2}} e^{i(\theta_r - \theta_s)/\hbar} \quad (11')$$

in which it is again composed of a proper energy term  $\sum_r W_r N_r$  and an interaction energy term.

The wave equation written in terms of the variables  $N_r$  is†

$$i\hbar \frac{\partial}{\partial t} \psi(N_1', N_2', N_3' \dots) = F \psi(N_1', N_2', N_3' \dots), \quad (12)$$

where  $F$  is an operator, each  $\theta_r$  occurring in  $F$  being interpreted to mean  $i\hbar \partial/\partial N_r'$ . If we apply the operator  $e^{\pm i\theta_r/\hbar}$  to any function  $f(N_1', N_2', \dots N_r', \dots)$  of the variables  $N_1', N_2', \dots$  the result is

$$\begin{aligned} e^{\pm i\theta_r/\hbar} f(N_1', N_2', \dots N_r', \dots) &= e^{\mp \partial/\partial N_r'} f(N_1', N_2', \dots N_r' \dots) \\ &= f(N_1', N_2', \dots N_r' \mp 1, \dots). \end{aligned}$$

If we use this rule in equation (12) and use the expression (11) for  $F$  we obtain‡

$$\begin{aligned} i\hbar \frac{\partial}{\partial t} \psi(N_1', N_2', N_3' \dots) \\ - \sum_{rs} H_{rs} N_r^{\frac{1}{2}} (N_s' + 1 - \delta_{rs})^{\frac{1}{2}} \psi(N_1', N_2' \dots N_r' - 1, \dots N_s' + 1, \dots). \end{aligned} \quad (13)$$

We see from the right-hand side of this equation that in the matrix representing  $F$ , the term in  $F$  involving  $e^{i(\theta_r - \theta_s)/\hbar}$  will contribute only to those matrix elements that refer to transitions in which  $N_r$  decreases by unity and  $N_s$  increases by unity, i.e., to matrix elements of the type  $F(N_1', N_2' \dots N_r' \dots N_s'; N_1', N_2' \dots N_r' - 1 \dots N_s' + 1 \dots)$ . If we find a solution  $\psi(N_1', N_2' \dots)$  of equation (13) that is normalised [i.e., one for which  $\sum_{N_1', N_2', \dots} |\psi(N_1', N_2' \dots)|^2 = 1$ ] and that satisfies the proper initial conditions, then  $|\psi(N_1', N_2' \dots)|^2$  will be the probability of that distribution in which  $N_1'$  systems are in state 1,  $N_2'$  in state 2, ... at any time.

Consider first the case when there is only one system in the assembly. The probability of its being in the state  $q$  is determined by the eigenfunction

† We are supposing for definiteness that the label  $r$  of the stationary states takes the values 1, 2, 3, ....

‡ When  $s = r$ ,  $\psi(N_1', N_2' \dots N_r' - 1 \dots N_s' + 1)$  is to be taken to mean  $\psi(N_1' N_2' \dots N_r' \dots)$ .

$\psi(N_1', N_2', \dots)$  in which all the  $N$ 's are put equal to zero except  $N_q'$ , which is put equal to unity. This eigenfunction we shall denote by  $\psi\{q\}$ . When it is substituted in the left-hand side of (13), all the terms in the summation on the right-hand side vanish except those for which  $r = q$ , and we are left with

$$i\hbar \frac{\partial}{\partial t} \psi\{q\} = \Sigma_r H_{qr} \psi\{r\},$$

which is the same equation as (5) with  $\psi\{q\}$  playing the part of  $b_q$ . This establishes the fact that the present theory is equivalent to that of the preceding section when there is only one system in the assembly.

Now take the general case of an arbitrary number of systems in the assembly, and assume that they obey the Einstein-Bose statistical mechanics. This requires that, in the ordinary treatment of the problem, only those eigenfunctions that are symmetrical between all the systems must be taken into account, these eigenfunctions being by themselves sufficient to give a complete quantum solution of the problem.<sup>†</sup> We shall now obtain the equation for the rate of change of one of these symmetrical eigenfunctions, and show that it is identical with equation (13).

If we label each system with a number  $n$ , then the Hamiltonian for the assembly will be  $H_A = \Sigma_n H(n)$ , where  $H(n)$  is the  $H$  of §2 (equal to  $H_0 + V$ ) expressed in terms of the variables of the  $n$ th system. A stationary state of the assembly is defined by the numbers  $r_1, r_2 \dots r_n \dots$  which are the labels of the stationary states in which the separate systems lie. The Schrödinger equation for the assembly in a set of variables that specify the stationary states will be of the form (6) [with  $H_A$  instead of  $H$ ], and we can write it in the notation of equation (5) thus:

$$i\hbar b(r_1 r_2 \dots) = \Sigma_{s_1, s_2, \dots} H_A(r_1 r_2 \dots; s_1 s_2 \dots) b(s_1 s_2 \dots), \quad (14)$$

where  $H_A(r_1 r_2 \dots; s_1 s_2 \dots)$  is the general matrix element of  $H_A$  [with the time factor removed]. This matrix element vanishes when more than one  $s_n$  differs from the corresponding  $r_n$ ; equals  $H_{r_n r_n}$  when  $s_n$  differs from  $r_n$  and every other  $s_n$  equals  $r_n$ ; and equals  $\Sigma_n H_{r_n r_n}$  when every  $s_n$  equals  $r_n$ . Substituting these values in (14), we obtain

$$i\hbar \dot{b}(r_1 r_2 \dots) = \Sigma_n \Sigma_{s_n \neq r_n} H_{r_n s_n} b(r_1 r_2 \dots r_n s_n r_{n+1} \dots) + \Sigma_n H_{r_n r_n} b(r_1 r_2 \dots). \quad (15)$$

We must now restrict  $b(r_1 r_2 \dots)$  to be a symmetrical function of the variables  $r_1, r_2 \dots$  in order to obtain the Einstein-Bose statistics. This is permissible since if  $b(r_1 r_2 \dots)$  is symmetrical at any time, then equation (15) shows that

<sup>†</sup> *Loc. cit.*, I, § 3.

$\dot{b}(r_1 r_2 \dots)$  is also symmetrical at that time, so that  $b(r_1 r_2 \dots)$  will remain symmetrical.

Let  $N_r$  denote the number of systems in the state  $r$ . Then a stationary state of the assembly describable by a symmetrical eigenfunction may be specified by the numbers  $N_1, N_2 \dots N_r \dots$  just as well as by the numbers  $r_1, r_2 \dots r_n \dots$ , and we shall be able to transform equation (15) to the variables  $N_1, N_2 \dots$ . We cannot actually take the new eigenfunction  $b(N_1, N_2 \dots)$  equal to the previous one  $b(r_1 r_2 \dots)$ , but must take one to be a numerical multiple of the other in order that each may be correctly normalised with respect to its respective variables. We must have, in fact,

$$\sum_{r_1, r_2 \dots} |b(r_1 r_2 \dots)|^2 = 1 = \sum_{N_1, N_2 \dots} |b(N_1, N_2 \dots)|^2,$$

and hence we must take  $|b(N_1, N_2 \dots)|^2$  equal to the sum of  $|b(r_1 r_2 \dots)|^2$  for all values of the numbers  $r_1, r_2 \dots$  such that there are  $N_1$  of them equal to 1,  $N_2$  equal to 2, etc. There are  $N!/N_1! N_2! \dots$  terms in this sum, where  $N = \sum_r N_r$  is the total number of systems, and they are all equal, since  $b(r_1 r_2 \dots)$  is a symmetrical function of its variables  $r_1, r_2 \dots$ . Hence we must have

$$b(N_1, N_2 \dots) = (N!/N_1! N_2! \dots)^{\frac{1}{2}} b(r_1 r_2 \dots).$$

If we make this substitution in equation (15), the left-hand side will become  $i\hbar (N_1! N_2! \dots / N!)^{\frac{1}{2}} \dot{b}(N_1, N_2 \dots)$ . The term  $H_{r_m s_m} b(r_1 r_2 \dots r_{m-1} s_m r_{m+1} \dots)$  in the first summation on the right-hand side will become

$$[N_1! N_2! \dots (N_r - 1)! \dots (N_s + 1)! \dots / N!]^{\frac{1}{2}} H_{r,s} b(N_1, N_2 \dots N_r - 1 \dots N_s + 1 \dots), \quad (16)$$

where we have written  $r$  for  $r_m$  and  $s$  for  $s_m$ . This term must be summed for all values of  $s$  except  $r$ , and must then be summed for  $r$  taking each of the values  $r_1, r_2 \dots$ . Thus each term (16) gets repeated by the summation process until it occurs a total of  $N_r$  times, so that it contributes

$$\begin{aligned} N_r [N_1! N_2! \dots (N_r - 1)! \dots (N_s + 1)! \dots / N!]^{\frac{1}{2}} H_{r,s} b(N_1, N_2 \dots N_r - 1 \dots N_s + 1 \dots) \\ = N_r^{\frac{1}{2}} (N_s + 1)^{\frac{1}{2}} (N_1! N_2! \dots / N!)^{\frac{1}{2}} H_{r,s} b(N_1, N_2 \dots N_r - 1 \dots N_s + 1 \dots) \end{aligned}$$

to the right-hand side of (15). Finally, the term  $\sum_n H_{r,n} b(r_1, r_2 \dots)$  becomes

$$\sum_r N_r H_{r,r} b(r_1 r_2 \dots) = \sum_r N_r H_{r,r} (N_1! N_2! \dots / N!)^{\frac{1}{2}} b(N_1, N_2 \dots).$$

Hence equation (15) becomes, with the removal of the factor  $(N_1! N_2! \dots / N!)^{\frac{1}{2}}$ ,

$$\begin{aligned} i\hbar \dot{b}(N_1, N_2 \dots) = \sum_r \sum_{s \neq r} N_r^{\frac{1}{2}} (N_s + 1)^{\frac{1}{2}} H_{r,s} b(N_1, N_2 \dots N_r - 1 \dots N_s + 1 \dots) \\ + \sum_r N_r H_{r,r} b(N_1, N_2 \dots), \quad (17) \end{aligned}$$

which is identical with (13) [except for the fact that in (17) the primes have been omitted from the  $N$ 's, which is permissible when we do not require to refer to the  $N$ 's as  $q$ -numbers]. We have thus established that the Hamiltonian (11) describes the effect of a perturbation on an assembly satisfying the Einstein-Bose statistics.

#### § 4. *The Reaction of the Assembly on the Perturbing System.*

Up to the present we have considered only perturbations that can be represented by a perturbing energy  $V$  added to the Hamiltonian of the perturbed system,  $V$  being a function only of the dynamical variables of that system and perhaps of the time. The theory may readily be extended to the case when the perturbation consists of interaction with a perturbing dynamical system, the reaction of the perturbed system on the perturbing system being taken into account. (The distinction between the perturbing system and the perturbed system is, of course, not real, but it will be kept up for convenience.)

We now consider a perturbing system, described, say, by the canonical variables  $J_k, \omega_k$ , the  $J$ 's being its first integrals when it is alone, interacting with an assembly of perturbed systems with no mutual interaction, that satisfy the Einstein-Bose statistics. The total Hamiltonian will be of the form

$$H_T = H_p(J) + \sum_n H(n),$$

where  $H_p$  is the Hamiltonian of the perturbing system (a function of the  $J$ 's only) and  $H(n)$  is equal to the proper energy  $H_0(n)$  plus the perturbation energy  $V(n)$  of the  $n$ th system of the assembly.  $H(n)$  is a function only of the variables of the  $n$ th system of the assembly and of the  $J$ 's and  $\omega$ 's, and does not involve the time explicitly.

The Schrödinger equation corresponding to equation (14) is now

$$i\hbar \dot{b}(J', r_1 r_2 \dots) = \sum_{J'', s_1 s_2 \dots} H_T(J', r_1 r_2 \dots; J'', s_1 s_2 \dots) b(J'', s_1 s_2 \dots),$$

in which the eigenfunction  $b$  involves the additional variables  $J_k'$ . The matrix element  $H_T(J', r_1 r_2 \dots; J'', s_1 s_2 \dots)$  is now always a constant. As before, it vanishes when more than one  $s_n$  differs from the corresponding  $r_n$ . When  $s_m$  differs from  $r_m$  and every other  $s_n$  equals  $r_n$ , it reduces to  $H(J'r_m; J''s_m)$ , which is the  $(J'r_m; J''s_m)$  matrix element (with the time factor removed) of  $H = H_0 + V$ , the proper energy plus the perturbation energy of a single system of the assembly; while when every  $s_n$  equals  $r_n$ , it has the value  $H_p(J') \delta_{J, J'} + \sum_n H(J'r_n; J'r_n)$ . If, as before, we restrict the eigenfunctions



to be symmetrical in the variables  $r_1, r_2 \dots$ , we can again transform to the variables  $N_1, N_2 \dots$ , which will lead, as before, to the result

$$i\hbar \dot{b}(J', N_1', N_2' \dots) = H_P(J') b(J', N_1', N_2' \dots)$$

$$+ \sum_{r,s} \sum_{r,s} N_r^{-1} (N_s' + 1 - \delta_{rs})^{\frac{1}{2}} H(J'r; J''s) b(J'', N_1', N_2' \dots N_r' \dots 1 \dots N_s' + 1 \dots) \quad (18)$$

This is the Schrödinger equation corresponding to the Hamiltonian function

$$F = H_P(J) + \sum_{r,s} H_{rs} N_r^{\frac{1}{2}} (N_s + 1 - \delta_{rs})^{\frac{1}{2}} e^{i(\theta_r - \theta_s)/\hbar}, \quad (19)$$

in which  $H_{rs}$  is now a function of the  $J$ 's and  $w$ 's, being such that when represented by a matrix in the  $(J)$  scheme its  $(J' J'')$  element is  $H(J'r; J''s)$ . (It should be noticed that  $H_{rs}$  still commutes with the  $N$ 's and  $\theta$ 's.)

Thus the interaction of a perturbing system and an assembly satisfying the Einstein-Bose statistics can be described by a Hamiltonian of the form (19). We can put it in the form corresponding to (11') by observing that the matrix element  $H(J'r; J''s)$  is composed of the sum of two parts, a part that comes from the proper energy  $H_0$ , which equals  $W_r$  when  $J_s'' = J_s'$  and  $s = r$  and vanishes otherwise, and a part that comes from the interaction energy  $V$ , which may be denoted by  $v(J'r; J''s)$ . Thus we shall have

$$H_{rs} = W_r \delta_{rs} + v_{rs},$$

where  $v_{rs}$  is that function of the  $J$ 's and  $w$ 's which is represented by the matrix whose  $(J' J'')$  element is  $v(J'r; J''s)$ , and so (19) becomes

$$F = H_P(J) + \sum_r W_r N_r + \sum_{r,s} v_{rs} N_r^{\frac{1}{2}} (N_s + 1 - \delta_{rs})^{\frac{1}{2}} e^{i(\theta_r - \theta_s)/\hbar}. \quad (20)$$

The Hamiltonian is thus the sum of the proper energy of the perturbing system  $H_P(J)$ , the proper energy of the perturbed systems  $\sum_r W_r N_r$ , and the perturbation energy  $\sum_{r,s} v_{rs} N_r^{\frac{1}{2}} (N_s + 1 - \delta_{rs})^{\frac{1}{2}} e^{i(\theta_r - \theta_s)/\hbar}$ .

### §5. *Theory of Transitions in a System from One State to Others of the Same Energy.*

Before applying the results of the preceding sections to light-quanta, we shall consider the solution of the problem presented by a Hamiltonian of the type (19). The essential feature of the problem is that it refers to a dynamical system which can, under the influence of a perturbation energy which does not involve the time explicitly, make transitions from one state to others of the same energy. The problem of collisions between an atomic system and an electron, which has been treated by Born,\* is a special case of this type. Born's method is to find a *periodic* solution of the wave equation which consists, in so far as it involves the co-ordinates of the colliding electron, of plane waves,

\* Born, 'Z. f. Physik,' vol. 38, p. 803 (1926).

representing the incident electron, approaching the atomic system, which are scattered or diffracted in all directions. The square of the amplitude of the waves scattered in any direction with any frequency is then assumed by Born to be the probability of the electron being scattered in that direction with the corresponding energy.

This method does not appear to be capable of extension in any simple manner to the general problem of systems that make transitions from one state to others of the same energy. Also there is at present no very direct and certain way of interpreting a periodic solution of a wave equation to apply to a non-periodic physical phenomenon such as a collision. (The more definite method that will now be given shows that Born's assumption is not quite right, it being necessary to multiply the square of the amplitude by a certain factor.)

An alternative method of solving a collision problem is to find a *non-periodic* solution of the wave equation which consists initially simply of plane waves moving over the whole of space in the necessary direction with the necessary frequency to represent the incident electron. In course of time waves moving in other directions must appear in order that the wave equation may remain satisfied. The probability of the electron being scattered in any direction with any energy will then be determined by the rate of growth of the corresponding harmonic component of these waves. The way the mathematics is to be interpreted is by this method quite definite, being the same as that of the beginning of §2.

We shall apply this method to the general problem of a system which makes transitions from one state to others of the same energy under the action of a perturbation. Let  $H_0$  be the Hamiltonian of the unperturbed system and  $V$  the perturbing energy, which must not involve the time explicitly. If we take the case of a continuous range of stationary states, specified by the first integrals,  $\alpha_k$  say, of the unperturbed motion, then, following the method of §2, we obtain

$$i\hbar a(\alpha') = \int V(\alpha'\alpha'') d\alpha'' \cdot a(\alpha''). \quad (21)$$

corresponding to equation (4). The probability of the system being in a state for which each  $\alpha_k$  lies between  $\alpha_k'$  and  $\alpha_k' + d\alpha_k'$  at any time is  $|a(\alpha')|^2 d\alpha_1' \cdot d\alpha_2' \dots$  when  $a(\alpha')$  is properly normalised and satisfies the proper initial conditions. If initially the system is in the state  $\alpha^0$ , we must take the initial value of  $a(\alpha')$  to be of the form  $a^0 \cdot \delta(\alpha' - \alpha^0)$ . We shall keep  $a^0$  arbitrary, as it would be inconvenient to normalise  $a(\alpha')$  in the present case. For a first approximation

we may substitute for  $a(\alpha')$  in the right-hand side of (21) its initial value. This gives

$$i\hbar \dot{a}(\alpha') = a^0 V(\alpha' \alpha^0) = \alpha^0 v(\alpha' \alpha^0) e^{i[W(\alpha') - W(\alpha^0)]t/\hbar},$$

where  $v(\alpha' \alpha^0)$  is a constant and  $W(\alpha')$  is the energy of the state  $\alpha'$ . Hence

$$i\hbar a(\alpha') = a^0 \delta(\alpha' - \alpha^0) + a^0 v(\alpha' \alpha^0) \frac{e^{i[W(\alpha') - W(\alpha^0)]t/\hbar} - 1}{i[W(\alpha') - W(\alpha^0)]/\hbar}. \quad (22)$$

For values of the  $\alpha_k'$  such that  $W(\alpha')$  differs appreciably from  $W(\alpha^0)$ ,  $a(\alpha')$  is a periodic function of the time whose amplitude is small when the perturbing energy  $V$  is small, so that the eigenfunctions corresponding to these stationary states are not excited to any appreciable extent. On the other hand, for values of the  $\alpha_k'$  such that  $W(\alpha') = W(\alpha^0)$  and  $\alpha_k' \neq \alpha_k^0$  for some  $k$ ,  $a(\alpha')$  increases uniformly with respect to the time, so that the probability of the system being in the state  $\alpha'$  at any time increases proportionally with the square of the time. Physically, the probability of the system being in a state with exactly the same proper energy as the initial proper energy  $W(\alpha^0)$  is of no importance, being infinitesimal. We are interested only in the integral of the probability through a small range of proper energy values about the initial proper energy, which, as we shall find, increases linearly with the time, in agreement with the ordinary probability laws.

We transform from the variables  $\alpha_1, \alpha_2 \dots \alpha_u$  to a set of variables that are arbitrary independent functions of the  $\alpha$ 's such that one of them is the proper energy  $W$ , say, the variables  $W, \gamma_1, \gamma_2, \dots \gamma_{u-1}$ . The probability at any time of the system lying in a stationary state for which each  $\gamma_k$  lies between  $\gamma_k'$  and  $\gamma_k' + d\gamma_k'$  is now (apart from the normalising factor) equal to

$$d\gamma_1' \cdot d\gamma_2' \dots d\gamma_{u-1}' \int |a(\alpha')|^2 \frac{\partial(\alpha_1', \alpha_2' \dots \alpha_u')}{\partial(W', \gamma_1' \dots \gamma_{u-1}')} dW'. \quad (23)$$

For a time that is large compared with the periods of the system we shall find that practically the whole of the integral in (23) is contributed by values of  $W'$  very close to  $W^0 = W(\alpha^0)$ . Put

$$a(\alpha') = a(W', \gamma') \quad \text{and} \quad \partial(\alpha_1', \alpha_2' \dots \alpha_u') / \partial(W', \gamma_1' \dots \gamma_{u-1}') = J(W', \gamma').$$

Then for the integral in (23) we find, with the help of (22) (provided  $\gamma_k' \neq \gamma_k^0$  for some  $k$ )

$$\begin{aligned} & \int |a(W', \gamma')|^2 J(W', \gamma') dW' \\ &= |a^0|^2 \int |v(W', \gamma'; W^0, \gamma^0)|^2 J(W', \gamma') \frac{[e^{i(W' - W^0)t/\hbar} - 1][e^{-i(W' - W^0)t/\hbar} - 1]}{(W' - W^0)^2} dW' \\ &= 2|a^0|^2 \int |v(W', \gamma'; W^0, \gamma^0)|^2 J(W', \gamma') [1 - \cos(W' - W^0)t/\hbar] / (W' - W^0)^2 dW' \\ &= 2|a^0|^2 t/\hbar \cdot \int |v(W^0 + \hbar x/t, \gamma'; W^0, \gamma^0)|^2 J(W^0 + \hbar x/t, \gamma') (1 - \cos x) / x^2 dx, \end{aligned}$$

if one makes the substitution  $(W' - W^0)t/\hbar = x$ . For large values of  $t$  this reduces to

$$2|a^0|^2 t/\hbar \cdot |v(W^0, \gamma'; W^0, \gamma^0)|^2 J(W^0, \gamma') \int_{-\infty}^{\infty} (1 - \cos x)/x^2 \cdot dx \\ = 2\pi |a^0|^2 t/\hbar \cdot |v(W^0, \gamma'; W^0, \gamma^0)|^2 J(W^0, \gamma').$$

The probability per unit time of a transition to a state for which each  $\gamma_k$  lies between  $\gamma_k'$  and  $\gamma_k' + d\gamma_k'$  is thus (apart from the normalising factor)

$$2\pi |a^0|^2/\hbar \cdot |v(W^0, \gamma'; W^0, \gamma^0)|^2 J(W^0, \gamma') d\gamma_1' \cdot d\gamma_2' \dots d\gamma_u' \dots, \quad (24)$$

which is proportional to the square of the matrix element associated with that transition of the perturbing energy.

To apply this result to a simple collision problem, we take the  $\alpha$ 's to be the components of momentum  $p_x, p_y, p_z$  of the colliding electron and the  $\gamma$ 's to be  $\theta$  and  $\phi$ , the angles which determine its direction of motion. If, taking the relativity change of mass with velocity into account, we let  $P$  denote the resultant momentum, equal to  $(p_x^2 + p_y^2 + p_z^2)^{1/2}$ , and  $E$  the energy, equal to  $(m^2c^4 + P^2c^2)^{1/2}$ , of the electron,  $m$  being its rest-mass, we find for the Jacobian

$$J = \frac{\partial(p_x, p_y, p_z)}{\partial(E, \theta, \phi)} = \frac{EP}{c^2} \sin \theta.$$

Thus the  $J(W^0, \gamma')$  of the expression (24) has the value

$$J(W^0, \gamma') = E'P' \sin \theta'/c^2, \quad (25)$$

where  $E'$  and  $P'$  refer to that value for the energy of the scattered electron which makes the total energy equal the initial energy  $W^0$  (i.e., to that value required by the conservation of energy).

We must now interpret the initial value of  $a(\alpha')$ , namely,  $a^0 \delta(\alpha' - \alpha^0)$ , which we did not normalise. According to §2 the wave function in terms of the variables  $\alpha_k$  is  $b(\alpha') = a(\alpha') e^{-iW^0 t/\hbar}$ , so that its initial value is

$$a^0 \delta(\alpha' - \alpha^0) e^{-iW^0 t/\hbar} = a^0 \delta(p_x' - p_x^0) \delta(p_y' - p_y^0) \delta(p_z' - p_z^0) e^{-iW^0 t/\hbar}.$$

If we use the transformation function\*

$$(x'/p') = (2\pi\hbar)^{-3/2} e^{i\sum_{k=1}^3 p_k^0 x'_k/\hbar},$$

and the transformation rule

$$\psi(x') = \int (x'/p') \psi(p') dp_x' dp_y' dp_z',$$

we obtain for the initial wave function in the co-ordinates  $x, y, z$  the value

$$a^0 (2\pi\hbar)^{-3/2} e^{i\sum_{k=1}^3 p_k^0 x_k/\hbar} e^{-iW^0 t/\hbar}.$$

\* The symbol  $x$  is used for brevity to denote  $x, y, z$ .

This corresponds to an initial distribution of  $|\alpha^0|^2 (2\pi\hbar)^{-3}$  electrons per unit volume. Since their velocity is  $P^0 c^2/E^0$ , the number per unit time striking a unit surface at right-angles to their direction of motion is  $|\alpha^0|^2 P^0 c^2/(2\pi\hbar)^3 E^0$ . Dividing this into the expression (24) we obtain, with the help of (25),

$$4\pi^2 (2\pi\hbar)^2 \frac{E'E^0}{c^4} |v(p'; p^0)|^2 \frac{P'}{P^0} \sin \theta' d\theta' d\phi'. \quad (26)$$

This is the effective area that must be hit by an electron in order that it shall be scattered in the solid angle  $\sin \theta' d\theta' d\phi'$  with the energy  $E'$ . This result differs by the factor  $(2\pi\hbar)^2/2mE'$  .  $P'/P^0$  from Born's.\* The necessity for the factor  $P'/P^0$  in (26) could have been predicted from the principle of detailed balancing, as the factor  $|v(p'; p^0)|^2$  is symmetrical between the direct and reverse processes.†

#### § 6. Application to Light-Quanta.

We shall now apply the theory of § 4 to the case when the systems of the assembly are light-quanta, the theory being applicable to this case since light-quanta obey the Einstein-Bose statistics and have no mutual interaction. A light-quantum is in a stationary state when it is moving with constant momentum in a straight line. Thus a stationary state  $r$  is fixed by the three components of momentum of the light-quantum and a variable that specifies its state of polarisation. We shall work on the assumption that there are a finite number of these stationary states, lying very close to one another, as it would be inconvenient to use continuous ranges. The interaction of the light-quanta with an atomic system will be described by a Hamiltonian of the form (20), in which  $H_P(J)$  is the Hamiltonian for the atomic system alone, and the coefficients  $v_{rn}$  are for the present unknown. We shall show that this form for the Hamiltonian, with the  $v_{rn}$  arbitrary, leads to Einstein's laws for the emission and absorption of radiation.

The light-quantum has the peculiarity that it apparently ceases to exist when it is in one of its stationary states, namely, the zero state, in which its momentum, and therefore also its energy, are zero. When a light-quantum is absorbed it can be considered to jump into this zero state, and when one is emitted it can be considered to jump from the zero state to one in which it is

\* In a more recent paper ('Nachr. Gesell. d. Wiss.' Gottingen, p. 146 (1926)) Born has obtained a result in agreement with that of the present paper for non-relativity mechanics, by using an interpretation of the analysis based on the conservation theorems. I am indebted to Prof. N. Bohr for seeing an advance copy of this work.

† See Klein and Rosseland, 'Z. f. Physik,' vol. 4, p. 46, equation (4) (1921).

physically in evidence, so that it appears to have been created. Since there is no limit to the number of light-quanta that may be created in this way, we must suppose that there are an infinite number of light-quanta in the zero state, so that the  $N_0$  of the Hamiltonian (20) is infinite. We must now have  $\dot{0}_0$ , the variable canonically conjugate to  $N_0$ , a constant, since

$$\dot{0}_0 = \partial F / \partial N_0 = W_0 + \text{terms involving } N_0^{-1} \text{ or } (N_0 + 1)^{-1}$$

and  $W_0$  is zero. In order that the Hamiltonian (20) may remain finite it is necessary for the coefficients  $v_{r0}$ ,  $v_{0r}$  to be infinitely small. We shall suppose that they are infinitely small in such a way as to make  $v_{r0}N_0^{\frac{1}{2}}$  and  $v_{0r}N_0^{\frac{1}{2}}$  finite, in order that the transition probability coefficients may be finite. Thus we put

$$v_{r0}(N_0 + 1)^{\frac{1}{2}} e^{-i\theta_0/h} = v_r, \quad v_{0r}N_0^{\frac{1}{2}} e^{i\theta_0/h} = v_r^*,$$

where  $v_r$  and  $v_r^*$  are finite and conjugate imaginaries. We may consider the  $v_r$  and  $v_r^*$  to be functions only of the  $J$ 's and  $w$ 's of the atomic system, since their factors  $(N_0 + 1)^{\frac{1}{2}} e^{-i\theta_0/h}$  and  $N_0^{\frac{1}{2}} e^{i\theta_0/h}$  are practically constants, the rate of change of  $N_0$  being very small compared with  $N_0$ . The Hamiltonian (20) now becomes

$$F = H_P(J) + \sum_r W_r N_r + \sum_{r \neq 0} [v_r N_r^{\frac{1}{2}} e^{i\theta_r/h} + v_r^* (N_r + 1)^{\frac{1}{2}} e^{-i\theta_r/h}] \\ + \sum_{r \neq 0} \sum_{s \neq 0} v_{rs} N_r^{\frac{1}{2}} (N_s + 1 - \delta_{rs})^{\frac{1}{2}} e^{i(\theta_r - \theta_s)/h}. \quad (27)$$

The probability of a transition in which a light-quantum in the state  $r$  is absorbed is proportional to the square of the modulus of that matrix element of the Hamiltonian which refers to this transition. This matrix element must come from the term  $v_r N_r^{\frac{1}{2}} e^{i\theta_r/h}$  in the Hamiltonian, and must therefore be proportional to  $N_r^{\frac{1}{2}}$  where  $N_r'$  is the number of light-quanta in state  $r$  before the process. The probability of the absorption process is thus proportional to  $N_r'$ . In the same way the probability of a light-quantum in state  $r$  being emitted is proportional to  $(N_r' + 1)$ , and the probability of a light-quantum in state  $r$  being scattered into state  $s$  is proportional to  $N_r' (N_s' + 1)$ . Radiative processes of the more general type considered by Einstein and Ehrenfest,† in which more than one light-quantum take part simultaneously, are not allowed on the present theory.

To establish a connection between the number of light-quanta per stationary state and the intensity of the radiation, we consider an enclosure of finite volume,  $A$  say, containing the radiation. The number of stationary states for light-quanta of a given type of polarisation whose frequency lies in the

† 'Z. f. Physik,' vol. 19, p. 301 (1923).

range  $\nu_r$  to  $\nu_r + d\nu_r$  and whose direction of motion lies in the solid angle  $d\omega_r$  about the direction of motion for state  $r$  will now be  $A\nu_r^2 d\nu_r d\omega_r / c^3$ . The energy of the light-quanta in these stationary states is thus  $N_r' \cdot 2\pi\hbar\nu_r \cdot A\nu_r^2 d\nu_r d\omega_r / c^3$ . This must equal  $Ac^{-1}I_r d\nu_r d\omega_r$ , where  $I_r$  is the intensity per unit frequency range of the radiation about the state  $r$ . Hence

$$I_r = N_r' (2\pi\hbar)\nu_r^3/c^2, \quad (28)$$

so that  $N_r'$  is proportional to  $I_r$  and  $(N_r' + 1)$  is proportional to  $I_r + (2\pi\hbar)\nu_r^3/c^2$ . We thus obtain that the probability of an absorption process is proportional to  $I_r$ , the incident intensity per unit frequency range, and that of an emission process is proportional to  $I_r + (2\pi\hbar)\nu_r^3/c^2$ , which are just Einstein's laws.\* In the same way the probability of a process in which a light-quantum is scattered from a state  $r$  to a state  $s$  is proportional to  $I_r[I_s + (2\pi\hbar)\nu_r^3/c^2]$ , which is Pauli's law for the scattering of radiation by an electron.†

### §7. *The Probability Coefficients for Emission and Absorption.*

We shall now consider the interaction of an atom and radiation from the wave point of view. We resolve the radiation into its Fourier components, and suppose that their number is very large but finite. Let each component be labelled by a suffix  $r$ , and suppose there are  $\sigma_r$  components associated with the radiation of a definite type of polarisation per unit solid angle per unit frequency range about the component  $r$ . Each component  $r$  can be described by a vector potential  $\kappa_r$  chosen so as to make the scalar potential zero. The perturbation term to be added to the Hamiltonian will now be, according to the classical theory with neglect of relativity mechanics,  $c^{-1}\sum_r \kappa_r \cdot \dot{X}_r$ , where  $X_r$  is the component of the total polarisation of the atom in the direction of  $\kappa_r$ , which is the direction of the electric vector of the component  $r$ .

We can, as explained in §1, suppose the field to be described by the canonical variables  $N_r, \theta_r$ , of which  $N_r$  is the number of quanta of energy of the component  $r$ , and  $\theta_r$  is its canonically conjugate phase, equal to  $2\pi\hbar\nu_r$  times the  $\theta_r$  of §1. We shall now have  $\kappa_r = a_r \cos \theta_r / \hbar$ , where  $a_r$  is the amplitude of  $\kappa_r$ , which can be connected with  $N_r$  as follows:—The flow of energy per unit area per unit time for the component  $r$  is  $\frac{1}{2}\pi c^{-1}a_r^2\nu_r^2$ . Hence the intensity

\* The ratio of stimulated to spontaneous emission in the present theory is just twice its value in Einstein's. This is because in the present theory either polarised component of the incident radiation can stimulate only radiation polarised in the same way, while in Einstein's the two polarised components are treated together. This remark applies also to the scattering process.

† Pauli, 'Z. f. Physik,' vol. 18, p. 272 (1923).

per unit frequency range of the radiation in the neighbourhood of the component  $r$  is  $I_r = \frac{1}{2}\pi c^{-1} a_r^2 \nu_r^2 \sigma_r$ . Comparing this with equation (28), we obtain  $a_r = 2(h\nu_r/c\sigma_r)^{\frac{1}{2}} N_r^{\frac{1}{2}}$ , and hence

$$\kappa_r = 2(h\nu_r/c\sigma_r)^{\frac{1}{2}} N_r^{\frac{1}{2}} \cos \theta_r/h.$$

The Hamiltonian for the whole system of atom plus radiation would now be, according to the classical theory,

$$F = H_P(J) + \sum_r (2\pi h \nu_r) N_r + \frac{1}{2} 2c^{-1} \sum_r (h\nu_r/c\sigma_r)^{\frac{1}{2}} X_r N_r^{\frac{1}{2}} \cos \theta_r/h, \quad (29)$$

where  $H_P(J)$  is the Hamiltonian for the atom alone. On the quantum theory we must make the variables  $N_r$  and  $\theta_r$  canonical q-numbers like the variables  $J_k, w_k$  that describe the atom. We must now replace the  $N_r^{\frac{1}{2}} \cos \theta_r/h$  in (29) by the real q-number

$$\frac{1}{2} \{N_r^{\frac{1}{2}} e^{i\theta_r/h} + e^{-i\theta_r/h} N_r^{\frac{1}{2}}\} = \frac{1}{2} \{N_r^{\frac{1}{2}} e^{i\theta_r/h} + (N_r + 1)^{\frac{1}{2}} e^{-i\theta_r/h}\}$$

so that the Hamiltonian (29) becomes

$$F = H_P(J) + \sum_r (2\pi h \nu_r) N_r + h^{\frac{1}{2}} c^{-\frac{1}{2}} \sum_r (\nu_r/\sigma_r)^{\frac{1}{2}} X_r \{N_r^{\frac{1}{2}} e^{i\theta_r/h} + (N_r + 1)^{\frac{1}{2}} e^{-i\theta_r/h}\}. \quad (30)$$

This is of the form (27), with

$$v_r = v_r^* = h^{\frac{1}{2}} c^{-\frac{1}{2}} (\nu_r/\sigma_r)^{\frac{1}{2}} \dot{X}_r \quad (31)$$

and

$$v_{rs} = 0 \quad (r, s \neq 0).$$

The wave point of view is thus consistent with the light-quantum point of view and gives values for the unknown interaction coefficient  $v_{rs}$  in the light-quantum theory. These values are not such as would enable one to express the interaction energy as an algebraic function of canonical variables. Since the wave theory gives  $v_{rs} = 0$  for  $r, s \neq 0$ , it would seem to show that there are no direct scattering processes, but this may be due to an incompleteness in the present wave theory.

We shall now show that the Hamiltonian (30) leads to the correct expressions for Einstein's A's and B's. We must first modify slightly the analysis of §5 so as to apply to the case when the system has a large number of discrete stationary states instead of a continuous range. Instead of equation (21) we shall now have

$$i\hbar \dot{a}(\alpha') = \sum_{\alpha''} V(\alpha'\alpha'') a(\alpha'').$$

If the system is initially in the state  $\alpha^0$ , we must take the initial value of  $a(\alpha')$  to be  $\delta_{\alpha'\alpha^0}$ , which is now correctly normalised. This gives for a first approximation

$$i\hbar \dot{a}(\alpha') = V(\alpha'\alpha^0) = v(\alpha'\alpha^0) e^{i[W(\alpha') - W(\alpha^0)]t/\hbar},$$

which leads to

$$i\hbar a(\alpha') = \delta_{\alpha'\alpha^0} + v(\alpha'\alpha^0) \frac{e^{i[W(\alpha') - W(\alpha^0)]t/\hbar} - 1}{i[W(\alpha') - W(\alpha^0)]/\hbar},$$



corresponding to (22). If, as before, we transform to the variables  $W, \gamma_1, \gamma_2 \dots \gamma_{u-1}$ , we obtain (when  $\gamma' \neq \gamma^0$ )

$$a(W'\gamma') = v(W', \gamma'; W^0, \gamma^0) [1 - e^{i(W' - W^0)/\hbar}] / (W' - W^0).$$

The probability of the system being in a state for which each  $\gamma_k$  equals  $\gamma'_k$  is  $\sum_{W'} |a(W'\gamma')|^2$ . If the stationary states lie close together and if the time  $t$  is not too great, we can replace this sum by the integral  $(\Delta W)^{-1} \int |a(W'\gamma')|^2 dW'$ ,

where  $\Delta W$  is the separation between the energy levels. Evaluating this integral as before, we obtain for the probability per unit time of a transition to a state for which each  $\gamma_k = \gamma'_k$

$$2\pi/\hbar \Delta W \cdot |v(W^0, \gamma'; W^0, \gamma^0)|^2. \quad (32)$$

In applying this result we can take the  $\gamma$ 's to be any set of variables that are independent of the total proper energy  $W$  and that together with  $W$  define a stationary state.

We now return to the problem defined by the Hamiltonian (30) and consider an absorption process in which the atom jumps from the state  $J^0$  to the state  $J'$  with the absorption of a light-quantum from state  $r$ . We take the variables  $\gamma'$  to be the variables  $J'$  of the atom together with variables that define the direction of motion and state of polarisation of the absorbed quantum, but not its energy. The matrix element  $v(W^0, \gamma'; W^0, \gamma^0)$  is now

$$\hbar^{1/2} c^{-1/2} (v_r/\sigma_r)^{1/2} \dot{X}_r(J^0 J') N_r^0,$$

where  $X_r(J^0 J')$  is the ordinary  $(J^0 J')$  matrix element of  $X_r$ . Hence from (32) the probability per unit time of the absorption process is

$$\frac{2\pi}{\hbar \Delta W} \cdot \frac{\hbar v_r}{c^3 \sigma_r} |X_r(J^0 J')|^2 N_r^0.$$

To obtain the probability for the process when the light-quantum comes from any direction in a solid angle  $d\omega$ , we must multiply this expression by the number of possible directions for the light-quantum in the solid angle  $d\omega$ , which is  $d\omega \sigma_r \Delta W / 2\pi\hbar$ . This gives

$$d\omega \frac{v_r}{\hbar c^3} |\dot{X}_r(J^0 J')|^2 N_r^0 = d\omega \frac{1}{2\pi\hbar^2 c v_r^2} |\dot{X}_r(J^0 J')|^2 I_r,$$

with the help of (28). Hence the probability coefficient for the absorption process is  $1/2\pi\hbar^2 c v_r^2 \cdot |X_r(J^0 J')|^2$ , in agreement with the usual value for Einstein's absorption coefficient in the matrix mechanics. The agreement for the emission coefficients may be verified in the same manner.

The present theory, since it gives a proper account of spontaneous emission, must presumably give the effect of radiation reaction on the emitting system, and enable one to calculate the natural breadths of spectral lines, if one can overcome the mathematical difficulties involved in the general solution of the wave problem corresponding to the Hamiltonian (30). Also the theory enables one to understand how it comes about that there is no violation of the law of the conservation of energy when, say, a photo-electron is emitted from an atom under the action of extremely weak incident radiation. The energy of interaction of the atom and the radiation is a q-number that does not commute with the first integrals of the motion of the atom alone or with the intensity of the radiation. Thus one cannot specify this energy by a c-number at the same time that one specifies the stationary state of the atom and the intensity of the radiation by c-numbers. In particular, one cannot say that the interaction energy tends to zero as the intensity of the incident radiation tends to zero. There is thus always an unspecifiable amount of interaction energy which can supply the energy for the photo-electron.

I would like to express my thanks to Prof. Niels Bohr for his interest in this work and for much friendly discussion about it.

### *Summary.*

The problem is treated of an assembly of similar systems satisfying the Einstein-Bose statistical mechanics, which interact with another different system, a Hamiltonian function being obtained to describe the motion. The theory is applied to the interaction of an assembly of light-quanta with an ordinary atom, and it is shown that it gives Einstein's laws for the emission and absorption of radiation.

The interaction of an atom with electromagnetic waves is then considered, and it is shown that if one takes the energies and phases of the waves to be q-numbers satisfying the proper quantum conditions instead of c-numbers, the Hamiltonian function takes the same form as in the light-quantum treatment. The theory leads to the correct expressions for Einstein's A's and B's.

---

## *The Photographic Action of $\beta$ -Rays.*

By C. D. ELLIS, Ph.D., Fellow of Trinity College, and Lecturer in the University  
of Cambridge, and W. A. WOOSTER, B.A., Charles Abercombe Smith  
Student of Peterhouse, Cambridge.

(Communicated by Sir Ernest Rutherford, P.R.S.—Received January 19, 1927.)

### *Introduction.*

The study of  $\beta$ -ray spectra has now advanced to that stage at which, for the majority of radioactive substances, the velocities of the homogeneous electrons forming the "lines" have been measured with a fair accuracy. The relative intensities of the "lines" have in the past been obtained by visual estimation of the photographic blackening of the plates on which they have been recorded, and it has become important to obtain more precise information on this subject. The most direct method of determining the relative intensities would be to count the number of, or measure the total charge carried by, the particles forming the lines. This is not practicable, to any high degree of accuracy, because of the small effects which are obtainable, and it is obvious that the photographic plate, in giving quite intense and sharp lines, in addition to a permanent record, presents many advantages. The use of this method, however, necessitates the calibration of the plate both for the variation of the blackening with exposure and also with velocity of the rays. The corresponding calibrations for ordinary light have now become a matter of routine, but since there has, as yet, been little systematic work on the behaviour of the photographic plate to  $\beta$ -rays, we have thought it best to record in this paper such experiments as we have found necessary before undertaking the main intensity problem. It is the dependence of blackening on exposure which is mainly treated in this paper, although we have in addition obtained some interesting results on the effect of  $\beta$ -particles of different velocities.

In an investigation on the relationship between blackening and exposure, *i.e.*, the characteristic curve of a type of plate, it is first necessary to find the dependence of the blackening\*  $D$  on the time of exposure  $t$ , when the product of intensity  $I$  and time of exposure  $t$  is kept constant. If  $D$  is independent of  $t$ , when  $I \cdot t$  is constant, then the Reciprocity Law of Bunsen and Roscoe is said to be valid for the plate. This law, although it has to be slightly modified

\* Blackening or density is defined thus,  $D = \log I_0/I$ , where  $I_0/I$  is the ratio of the incident to transmitted light passing through the darkened patch.

for luminous radiation, has been shown to be true in the case of X-rays and also for heterogeneous  $\beta$ -rays.\* In all previous work on the photographic action of  $\beta$ -rays† the particles were of heterogeneous velocities, but in view of the ultimate object of this investigation it was thought unsatisfactory to employ heterogeneous particles, and although the procedure was thereby made rather more laborious, beams of practically homogeneous particles, taken from the continuous  $\beta$ -ray spectrum, were used. It is in general important, when dealing with an unknown type of plate, after investigating the validity of the Reciprocity Law, to determine the variation of the characteristic curve with time of development, and thereby find the optimum value. Our general experience in photographing  $\beta$ -ray spectra had led us to employ a particular type of plate and method of development, and the main value of our experiments on the variation of the characteristic curve with time of development was that it indicated the error introduced into the value of the density for a given uncertainty in the time of development.

Having settled these preliminary points, it was possible to attack the main problem of the variation of photographic action with velocity. It might have been expected that the characteristic curves of density plotted against total exposure, for equal numbers of  $\beta$ -particles of different velocities, would have differed not only in magnitude but in form; however, we were able to show that, fortunately, matters were somewhat simpler. The form of the curve was always the same, and we may say that, when the specific photographic action of different velocities is taken into account, the response of the photographic plate is the same to  $\beta$ -rays of all velocities.

In so far as the Reciprocity Law is concerned our present results agree with previous work, namely, that it holds also in the case of homogeneous particles, but it would appear that the characteristic curve of the Ilford X-ray plate used by us, is linear over a much shorter range of density than the Agfa film cited in Bothe's experiments.

### *Method.*

The usual  $\beta$ -ray spectrograph, modified in certain particulars, was employed. Normally the photographic plate is pressed against the long slot CD, through which the rays pass after completing their semicircular tracks. In the present experiment, the slot CD was filled up except for a small rectangular opening AB ( $0.5 \times 1.0$  cm.) having its long side perpendicular to CD. The photographic

\* Bothe, 'Z. f. Physik,' vol. 8, p. 243 (1922).

† See also Salbach, 'Z. f. Physik,' vol. 11, p. 107 (1922).

plate was not pressed against CD but supported on a tray *ef*, which could be moved along under the slot by a thread operated from outside by a vacuum-tight winch.

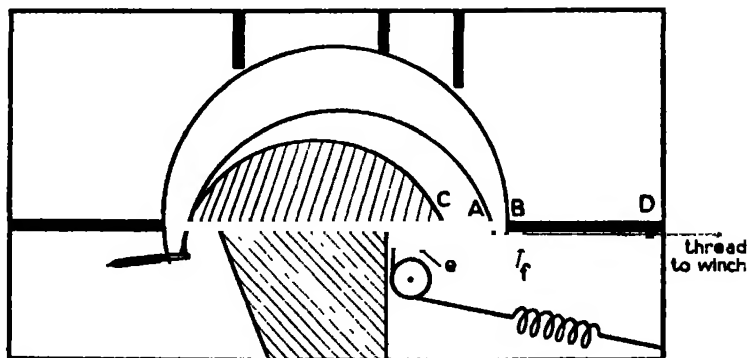


FIG. 1.

The magnetic field being applied in the appropriate direction, the plate was moved along to its first position. After the first exposure the tray was moved to an adjoining position and a different exposure made. This was repeated again, giving three exposures on each plate. The same process was carried out several times for the same value of the magnetic field. The latter was then changed and exposures made to rays of another velocity. A thick emanation tube was used as source, and in order to avoid the presence of  $\beta$ -ray lines on the patches, it was placed longitudinally instead of laterally in the apparatus. The mean value of  $\rho$ , the radius of the  $\beta$ -ray tracks, was 6.5 cm.

The plates were developed in the usual way, 1:20 rodinal being used as developer and the time of development in general five minutes. Development was carried out in dishes immersed in a thermostat at 18° C., and as many plates as possible were developed at the same time. A single (5 × 4) Ilford X-ray plate was cut into five portions, four of which were exposed to the  $\beta$ -rays; the fifth was not exposed but developed in the same dish as the others.

The density of the blackened patches of the plates were determined by means of a Dobson photo-electric microphotometer in the following manner. The light passing through the portion of the plate under investigation was balanced against the standard wedge of the instrument and all densities were determined in terms of this wedge. The difference in wedge readings corresponding to an absolute density difference of unity is equal to  $30.0 \pm 0.6$  mm.; but it should be noted, that the differences in density, as recorded by the microphotometer, are not necessarily equal to those which would be obtained by other

instruments often employed in photographic work, which determine the "contact density" of the darkened patch. Whereas the Dobson microphotometer utilises a narrow cone of the light emerging from the plate, the latter type of instrument absorbs the whole of the transmitted radiation. For purposes of reference, densities in the following curves are expressed in millimetres of the photometer wedge as well as in absolute measure.

Three densities were measured for each patch, namely those of—

- (1) the unexposed plate, constituting a blank ;
- (2) the background on either side of the patch ;
- (3) the patch itself.

The difference (3) — (1) gives the increase in density due to  $\beta$ -rays and general  $\beta$ - and  $\gamma$ -ray fog, whilst the difference (2) — (1) gives the density due to general  $\beta$ - and  $\gamma$ -ray fog alone, outside the patch. Whilst the density of this fog inside the patch is not in general the same as that outside, due to the fewer number of unaffected grains present at any given time, the values of (3) — (1) and (2) — (1) were small enough to justify this assumption being made. Correction was made for the increase of (3) — (1) due to this fog by increasing the numerical value of the exposure by an amount equal to that required to give a density (2) — (1).

#### *Experimental Results.*

(a) *Test of Reciprocity Law.*—In order to test the validity of the Reciprocity Law under the present experimental conditions a density-exposure, *i.e.*,  $D/I \cdot t$  curve ( $I$  representing the intensity of the radiation was taken equal to the number of millicuries of radioactive material, and  $t$  was simply the number of hours exposure), was drawn for each plate, successive plates being exposed to sources of different intensity and the time of exposure being suitably chosen. Where the curves overlapped, the values of  $D$  for a given  $I \cdot t$  were read off. If the Reciprocity Law holds, the values of  $D$  for the same  $I \cdot t$  should be independent of the value of  $t$ . In the accompanying figure  $D$  is plotted against  $t$ .

It will be seen that corresponding points are distributed about a mean horizontal straight line, the difference between the observed and the mean value being always within the experimental error. In the curves C and H the points lie quite close to the horizontal straight line, and in the cases of the other three there is no systematic divergence therefrom. When the Reciprocity Law fails, as in the case of luminous radiation, it is customary to apply the Schwartzchild relation

$$D = f(I \cdot t^p)$$

where  $p$  is a constant.

The curves A, B in fig. 2 give the variation of  $D$  for constant  $I \cdot t$  when values  $p = 1.2$  and  $0.8$  are taken. It is clear that the value of  $p$ , even if the experi-

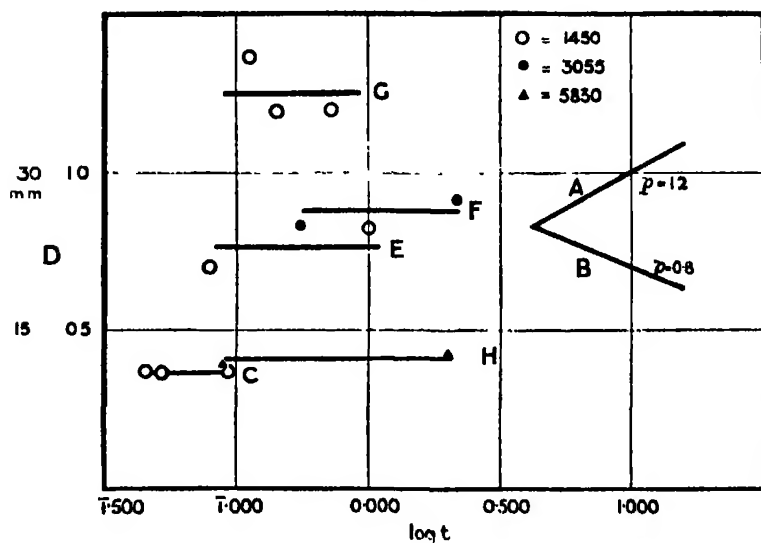


FIG. 2.

mental points of curves E, F, G were taken as accurate, would be nearer to unity than either 1.2 or 0.8. Thus we may conclude, taking also into account the fact that the Reciprocity Law has been shown to hold both for X-rays\* and heterogeneous  $\beta$ -rays,† that the law also applies to homogeneous particles.

(b) *Variation of Density with Time of Development.* The effect of variation in the time of development  $Z$  on the characteristic  $D/I \cdot t$  curve is a large problem more associated with the study of the photographic plate than with measurements on the intensity of  $\beta$ -ray lines by a photographic method. Our general experience has shown that, with the relatively powerful sources of radium B and C at our disposal, that development for five minutes gives the most satisfactory photographs. There was no need, therefore, to seek for an optimum value of  $Z$ , as would normally be done with an unknown type of plate, but rather we used the results, indicated in fig. 3, to determine the error introduced in the density by a variation in the time of development about the mean value of five minutes.

The curves of fig. 3 were obtained by using  $\beta$ -rays of mean velocity  $H_p = 3055$ ; the points lie evenly about the smooth curves plotted according to a

\* Glocker u. Traub, 'Phys. Z.', vol. 22, p. 345 (1921); also Bouwers, 'Z. f. Physik, vol. 14, p. 374 (1923).

† Salsbach and Bothe, *loc. cit.*

theoretical formula which is stated in the next paragraph, and from them it was deduced that a change of 7 seconds in the time of development, which we con-

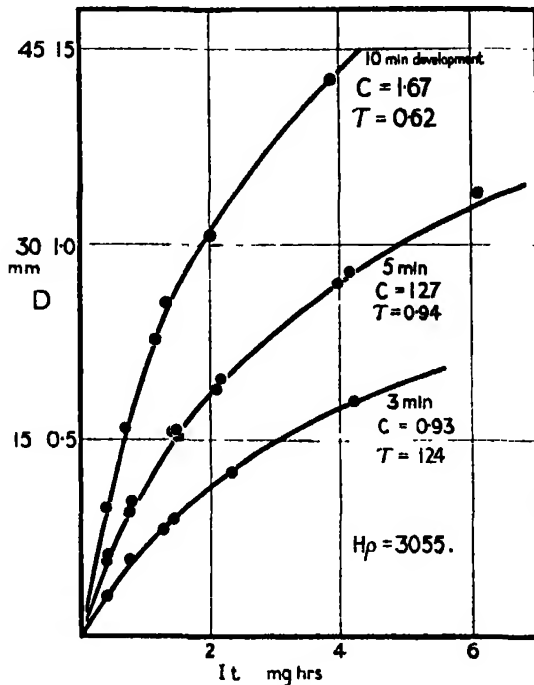


FIG. 3.

sider is probably the maximum error, gave rise to a variation of 3 per cent. in the value of the density.

It is of some interest to note that these curves appear to show that 10 minutes is the most advantageous value of  $Z$ , since a given density can be obtained with greater contrast for a smaller exposure. However these curves are, from the nature of the way in which they are plotted, independent of the amount of chemical fog, and whilst this is quite small between  $Z = 3$ –5 minutes it increases considerably between  $Z = 5$ –10 minutes. It is the appearance of an appreciable amount of chemical fog beyond  $Z = 5$  minutes which makes this the most advantageous value.

The problem of obtaining the  $\beta$ -ray "lines" of weak sources or the faint "lines" of strong sources is outside the scope of this work, but it is generally known that long development by special methods, which avoid the appearance of chemical fog, are advantageous, as is suggested by the above curves.

In the next paragraph we shall show that the characteristic curve obtained



with a time of development of five minutes is independent, as regards its shape, of the velocity of the particles, and is given by a simple formula suggested by theoretical considerations. This formula is

$$D = C \log (I \cdot t / \tau + 1), \quad (1)$$

where  $C$  and  $\tau$  are constants. The same would appear to be true for other times of development as is to be expected, since by varying the ordinates appropriately the three curves can be made to coincide. It would thus appear that only the constant  $C$  is affected by varying the time of development.

*Variation of Density with Exposure, for different velocities of  $\beta$ -particle.*

The variation of density with exposure  $I \cdot t$  for various velocities of  $\beta$ -particle and constant time of development (5 minutes) is shown in the diagram below.

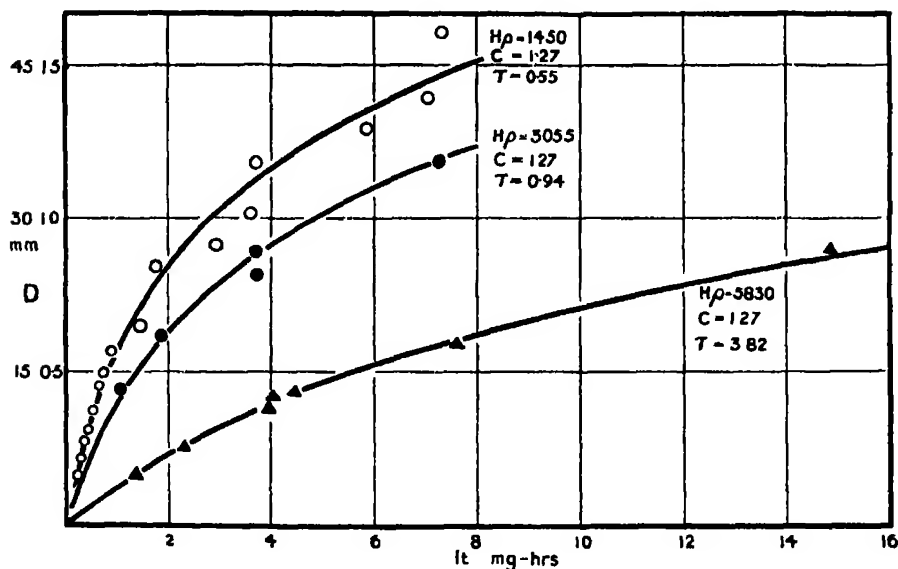


FIG. 4.

The smooth curves are based on the theoretical formula (1) and the points indicated are all actual experimental values. The divergences from the smooth curves are within the experimental error, and it is clear that the formula forms at least a good basis for interpolation.

The abscissæ of the curves given above though proportional to, are not in the ratio of the number of particles of the three velocities incident upon the plate, since the relative numbers emerging from the emanation tube were unknown. We can therefore obtain no evidence from these curves as to the

relative photographic action of particles of different velocities, but we may obtain some very useful information by proceeding in the following manner. Consider very small numbers  $n_1, n_2, n_3$ , of particles of the three velocities incident in different places upon an otherwise blank plate. We may choose a ratio  $n_1 : n_2 : n_3$  such that they produce equal blackenings. Suppose now that the streams of particles continue to be incident upon the plates in the same ratio, then we want to know whether the blackening produced in each case also continues to be the same. To return to the above curves, we may alter their abscissæ so that in each case the blackening for a given very small exposure  $I \cdot t$  is the same. This is, of course, equivalent to making the tangents at the origin the same in each case. When this is done the curves coincide and all the experimental points lie evenly about the one smooth curve as shown in the next figure.

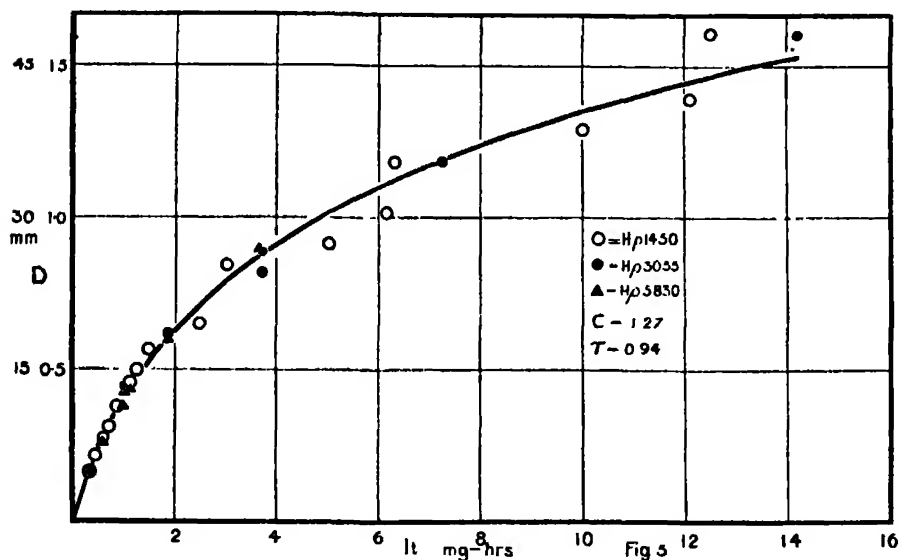


FIG. 5.

This is an extremely interesting result which greatly simplifies the comparison of lines due to  $\beta$ -rays of different velocities.

We have not attempted any detailed theoretical explanation of our results, but it might be noted that the natural interpretation of fig. 5 is that a  $\beta$ -particle has a certain probability of rendering developable a grain through which it passes, and this probability is analogous to ionising power and varies with the velocity. Except for this feature, introducing a simple multiplying factor, all  $\beta$ -particles within the range investigated behave identically towards a photo-

graphic plate. The form of the curve in fig. 5 is determined entirely by the photographic plate, in fact by the size and arrangement of the grains, but it is not affected by the agency, external to the plate, which renders the grain developable. The problem of comparing the intensities of two  $\beta$ -ray beams by their photographic action can now be seen to fall into two parts. The first is the determination of the curve of the plate valid for all velocities, as we have done above, the second the determination of the specific photographic action of different velocities. Unfortunately, this latter point is uncertain and methods of estimating it are discussed in the following paper.

### *Discussion.*

Our experimental results can be summarised by stating that independently of the time of development or the velocity of the  $\beta$ -particles, the density  $D$  is connected with the total exposure  $I \cdot t$  by the equation

$$D = C \log (I \cdot t / \tau + 1)$$

where  $C$  and  $\tau$  are constants. The effect of varying either the time of development, or the velocity of the particles is only to change these constants, but it appears that there is still a further simplification in that the constant  $C$  is determined only by the time of development, and the constant  $\tau$  by the velocity of the particles. The manner in which  $C$  varies with the time of development is not relevant to the present paper. So far although we have frequently quoted the above equation, we have made no reference to the assumptions on which it was deduced by Busé\* and Silberstein. The first point which strikes one is that Silberstein† only obtains this formula for a plate having a single layer of sensitive grains, whereas Ilford X-ray plates are specially arranged to have several layers, that is a thick coating, to increase the absorption. Again, although the only physical assumption that is made is that the amount of blackened silver halide is the result of the probability distribution of effective hits by the  $\beta$ -particles on the sensitive grains, the calculation of this amount of silver halide would in this case be complicated by the many layers of grains and by the fact that the grains are not all of the same size. We are greatly indebted to Ilford Ltd., and especially to Mr. B. V. Storr, of Ilford Ltd., for providing us with data about the distribution of grain size in these X-ray plates, but finally, following their advice, we thought it unjustifiable to assume any simple law for this distribution. The result is that we do not attempt any deduction of Silberstein's equation such as might be thought to be applicable

\* Busé, 'Physica,' March, 1922, Nr. 3.

† L. Silberstein, 'Phil. Mag.,' vol. 45, p. 1062 (1923).

to our present case. However, it appears to us that the simple logarithmic connection is essentially a property of single layered plates, but that to penetrating radiations like  $\beta$ -rays or X-rays even a many-layered plate will behave in the same way. This suggests that with  $\beta$ -particles of velocity below  $H_p = 800$ , when most of them will be stopped completely in the film, the form of the characteristic curve might alter.

It is a matter of great interest that Silberstein showed this same formula to hold for blackening by X-rays, and the results of a very thorough investigation by Bouwers\* renders a still closer comparison possible. It is to be expected that X-rays would give the same blackening law as  $\beta$ -rays since the photographic action of X-rays, like the ionisation, is to be ascribed to the high-speed photo-electrons which are liberated. Since the velocity of these electrons increases as the wave-length diminishes, we might expect the same changes to be produced by faster particles or shorter wave-length X-rays. This is exactly what is observed. Bouwers found that while  $\tau$  was independent of the time of development, it increased with decreasing wave-length just as we found it to increase with increasing velocity of the  $\beta$ -rays. Further the variation of  $U$  with time of development was in the same sense and of the same order.

Finally, reference must be made to the divergence of these results from those of Bothe,† who also investigated the blackening effect of  $\beta$ -particles. He found a characteristic curve linear up to  $D = 1$ , whereas it can be seen that it is not possible to draw a straight line through the initial points of our curves above a density of 0.35–0.40 for 5 minutes' development. The cause of this difference is probably not to be found in the fact that he used the heterogeneous particles of radium E, since the maximum intensity of this spectrum occurs at a value of  $H_p = 2,900$  approximately, and it has been shown in the above that within the range  $H_p = 1,450$ – $5,830$ , particles of different velocities have the same form of blackening curve. Since the experimental procedure was the same in both cases, it would appear that the Agfa film has a characteristic curve with a much longer initial linear part than is the case for Ilford X-ray plates.

#### Summary.

The blackening of Ilford X-ray plates by  $\beta$ -rays has been investigated under varying conditions, and it has been found that —

1. The Reciprocity Law holds.

\* Bouwers, *loc. cit.*

† *Loc. cit.*

2. The form of the characteristic curve is independent of the velocity of the particle.
3. The characteristic curve, as in the case of X-rays, follows the equation  $D = C \log (It/\tau + 1)$  giving an initial part which may be considered linear up to a density of 0.3.

We wish to thank Dr. H. W. B. Skinner for much assistance in the manipulation of the photometer, Mr. B. V. Storr, of Ilford Ltd., for many valuable suggestions in the handling of the plates, and Mr. G. R. Crowe for the preparation of the radioactive sources.

### *The Relative Intensities of the Groups in the Magnetic $\beta$ -Ray Spectra of Radium B and Radium C.*

By C. D. ELLIS, Ph.D., Fellow of Trinity College and Lecturer in the University of Cambridge, and W. A. WOOSTER, B.A., Charles Abercrombie Smith Student of Peterhouse, Cambridge.

(Communicated by Sir Ernest Rutherford, P.R.S.—Received January 19, 1927.)

#### *Introduction.*

It is well known that the study of the energy of the groups of homogeneous  $\beta$ -particles emitted by radio-active bodies has led to many important results, of these the chief is that these groups are due to the conversion of the characteristic  $\gamma$ -rays emitted by the body during the disintegration. From the measurement of the energy of these groups, it has been possible to deduce the energy or frequency of the  $\gamma$ -rays, and there appears to be evidence indicating that the  $\gamma$ -rays are associated with a nuclear level system in the manner familiar from X-ray and optical spectra. This opens up a promising field of work, since a knowledge of these level systems, and the way they varied from body to body would be an important addition to our all too scanty knowledge of the nucleus. Unfortunately, it must be admitted that the existing measurements of the  $\beta$ -ray groups are not of sufficient accuracy to provide a unique determination of the level system, they indicate strongly that the level systems exist, but it is difficult to deduce the actual arrangement with any certainty. An increase in the accuracy of the  $\beta$ -ray measurement would undoubtedly lead to interesting

conclusions, but no simple way has as yet been proposed by which this can be achieved. Instead of attempting this method we have attacked the  $\beta$ - and  $\gamma$ -ray problem from another side.

Previous investigations have been concerned chiefly with the energy of the individual electrons comprising the  $\beta$ -ray groups and of the  $\gamma$ -rays which can be deduced from them, but it is clear that any theory of their rôle in the disintegration must also take into consideration their intensities. This seems to be a more promising method of advance than that of trying to increase the accuracy of measurements already carried to a fraction of a per cent., since even approximate values of the intensities would be valuable. There are three main lines along which intensity measurements can usefully be made, one of which is the subject of the present paper. Considered by itself, each is interesting, but since it appears likely that the most valuable results will be obtained by comparing all three, it is permissible to refer briefly to them here.

During the disintegration there are believed to occur in the nucleus certain quantum transitions, which sometimes result in the ejection of an electron from the electronic structure to form one of the  $\beta$ -ray lines, but more often give rise to a  $\gamma$ -ray escaping from the atom. Opinions differ whether the  $\gamma$ -ray may always be considered to be emitted from the nucleus, and sometimes internally absorbed before it leaves the atom, or whether it is better to keep to the more general standpoint above. However, in either case we can speak of the probability  $p$  of a certain nuclear transition occurring at any one disintegration, and we can denote by  $\alpha$  the fraction of these transitions resulting in  $\beta$ -ray groups. The more detailed view would describe  $\alpha$  as the internal conversion coefficient of the  $\gamma$ -rays. The amount of  $\gamma$ -ray energy issuing from the atom will be  $\Sigma h\nu_1 p_1 (1 - \alpha)$  and the corresponding number of secondary electrons will be  $\Sigma p_1 \alpha_1$ . Actually, it is necessary to consider that electrons may come from any of the K,  $L_I$ ,  $L_{II}$ , ..., etc., levels, and one coefficient  $\alpha$  is not sufficient. Using an obvious notation it will be seen that the present measurements of the relative intensities of the  $\beta$ -ray lines consist in a determination of the relative values of the quantities  $p_{1K}\alpha_1$ ,  $p_{1L}\alpha_1 \dots p_{2K}\alpha_2$ .

It is to be expected that the most interesting results would be obtained if the two factors  $p$  and  $\alpha$  could be separated and determined in absolute measure, and this introduces the need for the other intensity measurements already referred to. A comparison of the number of secondary electrons ejected from the radioactive atoms with the number of quanta of the corresponding  $\gamma$ -rays actually emitted, would give  $\alpha/(1-\alpha)$ . Many estimates of these quantities have already been made, but since we hope soon to publish some measurements

by a new method, it is sufficient here to note that the quantities  $\alpha$  can be determined independently of the  $p$ 's. All that then remains in order to be able to give a complete account of the disintegration in terms of the  $p$ 's and  $\alpha$ 's is to fix the absolute values of the intensities of the  $\beta$ -ray groups. This may be done by a variety of methods, by a direct measurement of the stronger groups as carried out by Gurney,\* or indirectly from the total  $\gamma$ -ray energy emitted as indicated by the present writers on another occasion.†

The object of this introduction is to show that although the present measurement presents many points of interest considered by itself, its chief importance lies in the fact that it is an essential step towards combining several different intensity measurements which will then yield values for the probabilities of the occurrence of the various fundamental stages in the  $\beta$ -ray disintegration.

*Methods of Measuring the Relative Intensities of the  $\beta$ -ray Lines.*

There are several ways of recording  $\beta$ -ray spectra, any of which might at first sight appear suitable for determining the relative intensities of the groups, but a closer consideration shows that the photographic method, in spite of one serious disadvantage, is alone suitable.

In every case a magnetic field must be used to separate out the groups of different velocity, but there are four main ways of recording them. In the first place with any one setting of the magnetic field  $\beta$ -particles within a narrow range of velocities can be allowed to enter an ionisation chamber or electrical counter, and, by varying the magnetic field, the entire spectrum can be recorded. In both cases, the slit of the ionisation chamber or counter must be covered with thin mica which involves difficult corrections for reflection, and, further, in the case of the ionisation chamber the ionising effect for a fixed number of particles varies with the velocity and to a lesser extent there is probably a similar effect with a counter. These difficulties would be avoided if the  $\beta$ -particles were received in an open Faraday cylinder and their number determined directly by measurement of the charge. This method has been used by Gurney, and he has made some important measurements which will be referred to later; but it shares with the other two methods the fundamental disadvantage that only the stronger lines of the spectrum are detectable.

It must be remembered that the  $\beta$ -ray groups only form a small portion of the total electronic emission, the main part of which is due to the disintegration electrons. These are spread out over a wide range of velocities and form a

\* *Vide infra.*

† 'Phil. Mag.', vol. 50, p. 521 (1925).

continuous background on which the groups are superimposed. In most cases the groups represent only a small increase of a few per cent. over this background, and a direct determination by subtracting two ionisation currents is impracticable, in fact with measurements of the ordinary type most of the lines escape detection. The photographic method of recording the  $\beta$ -ray spectra, on the other hand, seems specially adapted for investigating the lines since, in general, if a line can be seen on the plate its density can be measured by a photometer. It should be noted that with this method the difficulty of the continuous spectrum still exists, for the usual statement that the photographic plate shows up the lines at the expense of the background is, of course, untrue. The density of a photographic plate does not increase linearly with the exposure, in general the sensitivity of the plate falls off at higher densities, which is a distinct disadvantage as compared with the linear relations of the electrical methods; but still it reproduces the relative intensities, and on the photographic plate the lines will represent on the whole a smaller percentage increase of the density than on an ionisation curve. The reason why they can be detected in the latter case and not in the former, depends entirely on the fact that while it is very difficult to balance out 95 per cent. of an ionisation current with its probability fluctuations, it is very simple with modern photometers to balance out 95 per cent. of the opacity of a plate and still have a sufficiently sensitive optical balance to be able to concentrate on the remaining 5 per cent.

While the photographic plate seems for these reasons to offer the only method of measuring the intensities, it suffers from the disadvantage that the photographic effect of the  $\beta$ -particles varies with the velocity. At the moment the correction for this has to be estimated, but we have presented our results in such a way that should subsequent experiment show our method of correction to be in error, it will be quite easy to apply any other.

The method of taking the photographs needs no remarks since we used the standard focussing method with a very thin walled glass tube filled with radium emanation as source, or in the case of the slower groups a bare activated wire.

#### *Experimental Procedure.*

The density of the photographic blackening of the line was measured by means of a micro-photometer. In the form of instrument used in this work one beam of light was passed through a uniform wedge, and the "thickness" of the wedge was varied until the intensity of the beam of light passing through it became equal to that of the light passing through a strip of the line 1/50th mm. wide. In this way the density of the line at any point could be expressed in terms of



the length of the standard wedge. In the case of the lines produced by wire sources it was sufficient to determine the density at the peak of the line, but when an  $\alpha$ -ray tube was used as source the intensity was found at a large number of points along the line. In the preceding paper the present authors have shown that the photographic density is related to the number of particles hitting the plate according to the following equation

$$D = C \log (E/\tau + 1)$$

where  $D$  = density.

$E$  = number of particles hitting the plate.

$C$  and  $\tau$  are constants.

Values for  $C$  and  $\tau$  appropriate to our conditions were determined in the previous experiments referred to, and the measured densities were converted into their equivalent values of  $E$  by means of this equation. Curves were then plotted for each line showing the variation of  $E$  along the plate—such curves are here termed intensity-distribution curves. When due allowance has been made for the continuous background, the number of particles falling into the line is proportional to the area under the intensity-distribution curve. It was somewhat difficult in the present work to determine this area accurately, as the intensities of most of the lines were small. Though the density at the peak of the faint lines was measurable with fair accuracy, the total area under the curve was uncertain because the tail of the line merged slowly into the continuous background. For determining the intensities of the weaker lines the following method was, therefore, adopted. A curve was drawn from the results for the stronger lines, showing the variation with  $H\rho$  of the particles of the ratio of the total area of the line to the density at the peak. From this curve the appropriate ratio was read off for each of the weaker lines, and this when multiplied by the measured density at the peak gave a value of the area, which is probably more accurate than that obtained by measuring the area directly. Corrections were applied to these values to reduce them all to a standard radius of curvature (6 cm.) of the particles.

In the case of the lines obtained with wire sources, the calculation given by one of us provided values for the ratio of area to peak density, and hence it was only necessary to measure the latter in each case.\*

No mention has as yet been made of the variation of the photographic action of the  $\beta$ -rays with velocity. It has been tacitly assumed in applying the equation (1), that all particles have the same specific action. This is certainly

\* It is hoped shortly to publish full details of these and allied calculations which have been carried out by one of us (W. A. W.).

not true, but unfortunately there is no direct experimental evidence as to the appropriate correction. We have assumed that the activity of the  $\beta$ -rays is proportional to the energy lost in the film during their transit through it, i.e., proportional to  $\beta^2$ . This assumption seems reasonable, and is supported by the fact that W. Wilson's\* results on the ionisation of gases indicate the same variation with velocity. The final results include this correction but should it be necessary to apply subsequently some other correction for velocity this may readily be done since our uncorrected values can be obtained from the table by dividing by  $\beta^2$ .

Before giving the experimental results we would emphasise that it was a special point of these measurements to determine the intensities of the radium B lines on the same scale as those of radium C, or in other words on the basis of equal numbers of disintegrating atoms of the two bodies. There was no difficulty in doing this since the amounts of radium B and radium C present on a source are easily determinable.

### Experimental Results.

The lines whose intensities we have been able to measure in the manner described in the last paragraph are marked by a star in Table I. The intensities

Table I.—Intensity of the  $\beta$ -Ray Groups emitted by Radium B and Radium C for equal number of disintegrating atoms.

(For origin of groups see 'Roy. Soc. Proc.,' A, vol. 105, p. 174 (1924), and 'Camb. Phil. Soc. Proc.,' vol. 22, p. 374 (1924).)

#### RADIUM B.

H $\rho$ .	Intensity in arbitrary units.	Values of pa.	H $\rho$ .	Intensity in arbitrary units.	Values of pa.
660.9†	17	0.0083	1410*	57	0.0314
667.0†	5	0.0027	1496*	7	0.0038
687.0†	1	0.0005	1576*	3.5	0.0019
768.8†	11	0.0060	1677*	79	0.0435
793.1†	8	0.0044	1774*	12	0.0066
799.1†	4	0.0022	1850*	1.5	0.0008
833.0	2	0.0011	1938*	100	0.0.50
838.0	5	0.0027	2015*	15	0.0082
855.4	2	0.0011	2064*	5	0.0027
860.9	5	0.0027	2110	1.5	0.0008
877.8	1.5	0.0008	2256*	22	0.0121
896.0	1.5	0.0008	2307*	8.0	0.0044
926.2	3	0.0016	2321	1.5	0.0008
949.2	3	0.0016	2433	1.5	0.0008
1155	2	0.0011	2480	1.5	0.0008
1209	1	0.0005			

† Values less certain for these lines.

\* Wilson 'Roy. Soc. Proc.,' A, vol. 85, p. 240 (1911).

Table I--(continued).

## RADIUM C.

$H\beta$	Intensity in arbitrary units.	Values of $p\alpha$ .	$H\beta$ .	Intensity in arbitrary units.	Values * of $p\alpha$ .
1379	0.05	0.00002	5428	0.15	0.00008
1438	0.05	0.00002	5552	0.2	0.00011
1557	0.4	0.00022	5708	0.15	0.00008
1586	0.1	0.00005	5904*	4.06	0.00223
1834	0.1	0.00005	5948	0.2	0.00011
1912	0.1	0.00005	6030	0.2	0.00011
2085	0.5	0.00027	6161*	0.99	0.00054
2156	0.1	0.00005	6212*	0.37	0.00020
2256	0.3	0.00015	6350	0.09	0.00005
2390	0.1	0.00005	6523	0.07	0.00004
2550	0.1	0.00005	6656	0.07	0.00004
2720	0.2	0.00011	6800	0.07	0.00004
2840	0.1	0.00005	6932	0.15	0.00008
2890	0.1	0.00005	6998	0.15	0.00008
2980*	7.2	0.00398	7109*	0.85	0.00046
3145	0.5	0.00027	7240	0.07	0.00004
3203	0.5	0.00027	7380	0.20	0.00011
3271*	1.7	0.00094	7530	0.05	0.00003
3307	0.5	0.00027	7690	0.05	0.00003
3326	0.5	0.00027	7974	0.05	0.00003
3584	0.5	0.00027	8090	0.05	0.00003
3824	0.5	0.00027	8313	0.05	0.00003
4196*	0.86	0.00047	8617	0.20	0.00011
4404	0.5	0.00027	8885	0.05	0.00003
4866*	1.94	0.00107	9165	0.05	0.00003
4991	0.3	0.00015	9425	0.05	0.00003
5136	0.3	0.00015	9655	0.05	0.00003
5178	0.3	0.00015	10020	0.05	0.00003
5281*	0.81	0.00044			

Intensities of lines marked with \* were measured directly, and those of the remainder interpolated from visual estimates.

of the numerous weaker lines were estimated by a method which is discussed later and for the moment the figures in the third column headed  $p\alpha$  will not be referred to.

We could not expect our measurements to be more accurate than about 5 per cent. even in the case of the strongest lines, while the weaker lines would be even less accurate. However, within these limits there is fair agreement with the results of Gurney.\* Using an electrical method he measured directly the number of electrons in the four strong lines of radium B, and his results are compared with the values from Table I in Table II. As it is only a question of relative intensity, the intensity of the strongest line  $H\beta$  1938 is put equal to 100 in each case.

\* 'Roy. Soc. Proc.,' A, vol. 109, p. 540 (1925).

Table II.

H $\rho$ of line :	1410	1677	1938	2256
Gurney ....	46	74	100	23
Ellis and Wooster	57	79	100	23

Two of the three comparisons are in sufficient agreement but for H $\rho$  1410 the divergence is 20 per cent. This is not so serious as it might seem since Gurney's measurements were bound to be uncertain for this line. As he explains in his paper, the intensity of a line can be deduced from his curves by taking the height of the peak above the continuous spectrum, and to carry this out the curve of the continuous spectrum has to be extrapolated through the region of the line. While this can be done with fair accuracy where the run of the curve is flat or only slightly inclined, as is the case for the three higher lines, the process becomes uncertain for H $\rho$  1410 where the curve ascends sharply.

We have already mentioned that it was not possible to measure directly the intensities of the weakest lines, but it is not difficult to form an estimate by comparing the present measurements with the visual estimates made by previous observers.\* It is found that on the whole the visual estimates were surprisingly correct except in the case of lines differing considerably in intensity, when the weaker line is usually overestimated. Again, as was pointed out in the papers cited, it is difficult to give relative intensities valid over a wide range, and here again we find that there has been a steady tendency to overestimate the lines of higher H $\rho$ . In general, however, the visual estimates may be used with fair accuracy as giving the intensities of the faint lines relative to those actually measured, provided the extrapolation is between lines not differing by more than a factor of three in intensity or by 1.5 in H $\rho$ . In this way we have found the values in Table I which are not marked with a star.

A more difficult problem is presented by the group of lines between H $\rho$  663 and H $\rho$  1300. The faint lines around H $\rho$  800-950 can only be estimated by the above method, but the lower group are sufficiently intense to be measured photometrically. Unfortunately, this has little value, since this is just the region where the velocity correction if applied would produce large differences, and where further it is very uncertain. These  $\beta$ -particles have not sufficient energy to penetrate completely the photographic film with small loss of energy,

\* Ellis and Skinner, Roy. Soc. Proc., A, vol. 105, p. 174 (1924); Ellis, 'Proc. Camb. Phil. Soc.,' vol. 22, p. 374 (1924).

but will be very largely absorbed. For  $\beta$ -particles of still lower velocity, none of which penetrated the film completely, it would be possible to find another basis for comparing the photographic action by means of the total energy, but with the groups about  $H\beta$  663 it is difficult to know what correction to apply. We therefore decided it was necessary to treat these lines by a different method, and in the meanwhile to complete the table we give figures taken from Gurney's paper. Taking his measurements of the intensity of  $H\beta$  663, 668, etc., relative to that of  $H\beta$  1938 we obtained directly the figures shown in the table, and the intensities of the remaining lines in this region were interpolated from these using the visual estimates. In the table these intensities are marked to show they may be less accurate than the remainder.

### *Discussion of Results.*

A point of great interest is to compare the intensities of the lines due to the conversion of the same frequency  $\gamma$ -ray in different levels, such as the K and  $L_1$ . This is shown in Table III where in order to show the accuracy attainable the ratio for each pair of lines is tabulated for each plate on which they both occurred. The reason why there is only a single entry against  $H\beta$  1496 and  $H\beta$  1938 is that satisfactory photographs of both K and L lines were not obtained on the same plate, so in these cases the mean values from Table I are used.

Table III.—Ratio of the Intensities of  $\beta$ -Ray Groups due to the Conversion of the same frequency  $\gamma$ -Ray in the K and  $L_1$  levels.

H $\beta$ of groups compared.		Energy of $\gamma$ -ray in volts.	Ratio $L_1/K$ .
K.	$L_1$ .		
1410	1744	$2.43 \times 10^5$	0.24 0.17
1496	1850	2.60	0.21
1677	2015	2.97	0.16 0.20
1938	2256	3.54	0.22
2980	3271	6.12	0.21 0.26 0.21 0.27
5904	6161	14.3	0.22 0.24

It is possible to treat six  $\gamma$ -rays in this way, and taking into account the difficulty of the measurements it appears that the  $L_I/K$  ratio is sensibly constant. This is a very striking result, since the range of energy of the  $\gamma$ -rays is from  $2.4 \times 10^5$  volts to  $14.3 \times 10^5$  volts, a sixfold increase. As we have already mentioned, the  $\beta$ -ray groups can be considered as being due to internal absorption of the  $\gamma$ -rays, and on this view the constancy of the  $L_I/K$  ratio would mean a constant ratio for the probability of internal absorption in the  $L_I$  and  $K$  levels, independent of the frequency. This is precisely what is found, to a first approximation, for ordinary external absorption in the X-ray region, and what is still more significant, according to the latest measurements of Allen,\* the ratio at the  $K$  jump for atomic numbers near to 83 is 0.2, while the mean of the above values is 0.22.

These measurements would indicate, in this respect, a close parallel between ordinary external absorption and what has been termed internal absorption, and if this should subsequently be found to be the case for all  $\gamma$ -rays, the phenomenon has an important bearing on the much discussed question of the physical reality of internal absorption. Smekal† has recently given a clear statement of the difficulties raised by the phenomenon, and he pointed out that what had been observed was only a numerical connection between the energies of the  $\gamma$ -rays and the energies of the groups in the  $\beta$ -ray spectra. This connection could be explained by postulating emission of the  $\gamma$ -rays from the nucleus and subsequent reabsorption, but he was of the opinion that nothing was gained unless some connection could be established between this internal absorption and ordinary absorption. No obvious connection had previously been discovered and for this reason Smekal questioned the utility of this conception, but the results obtained in the present investigation certainly support the original idea. The internal absorption appears to have one characteristic in common with external absorption, namely, the constancy of the  $L/K$  absorption ratio over a wide range of frequencies, and further the numerical values for this ratio in the two cases are in agreement. There is too little evidence to speak with certainty on this point, but it is our opinion that in the case of  $\gamma$ -rays it is both useful and probably correct to consider the  $\beta$ -ray groups as due to a true internal absorption, and that this absorption is similar to ordinary external absorption when the special conditions under which it occurs are taken into account.

The most striking characteristic of the ordinary absorption is the rapid varia-

\* 'Phys. Rev.' p. 920 (Nov., 1926).

† 'Ann. d. Physik,' vol. 8, p. 374 (1926).

tion with the wave-length. There is no direct evidence on this point for the  $\gamma$ -ray region, but Ahmad's\* results suggest that the same laws hold for these high frequencies as for ordinary X-rays. We should, therefore, expect the photoelectric absorption, with which we are comparing the internal absorption, to vary approximately as  $\lambda^3$ . It is scarcely within the province of the present investigation to consider the actual values of the internal absorption coefficient, but it may be pointed out that again, in the question of variation with wave-length, our results indicate that there is a general similarity between the two types of absorption. This is best brought out by considering a special case. From the third column of Table I, whose derivation will be explained in the next paragraph, it can be deduced that the prominent  $\gamma$ -rays of radium C, of energies between  $10^6$  and  $2 \times 10^6$  volts, lead to the emission of 5 K electrons from every 1000 disintegrating atoms, whereas the three strong  $\gamma$ -rays of radium B of energies about  $0.3 \times 10^6$  volts give about 130 K electrons from the same number of disintegrations. There are several lines of evidence which indicate that the total number of  $\gamma$ -rays emitted in these two cases is of the same order of magnitude, so that a change of energy of the  $\gamma$ -ray from  $0.3$  to  $1 - 2 \times 10^6$  volts changes the internal conversion coefficient by a factor of the order of magnitude of  $5/130$ . Although rough calculations of this type, in which  $\gamma$ -rays of different frequencies are grouped together, cannot be used to find the rate of variation of the internal absorption coefficient with frequency, they do show that like the external absorption it must decrease rapidly with increasing frequency.

We have taken up a cautious attitude on the question of the reality of the internal absorption, because as yet the evidence for a final decision is incomplete, but we consider that such evidence as there is points strongly to the existence of a true internal absorption.

An essential feature of Gurney's work was that he was able to find directly the number of electrons in the stronger groups from a given amount of radioactive substance. Using the previous notation of  $p$  being the probability of a certain  $\gamma$ -ray being emitted at any one disintegration, and  $\alpha$  the probability of its conversion inside the parent atom, then Gurney determined the quantities  $p\alpha$  for five of the stronger lines. It appears that on our arbitrary scale a line of intensity 100 corresponds to a value of  $p\alpha$  of  $0.055$ , that is 55 electrons would go to form such a line from every 1000 atoms that disintegrate. The  $p\alpha$  values for all the lines are given in columns 3 and 6 of Table I, and were obtained by simple multiplication of the intensities in columns 2 and 4 by this factor  $0.055$ .

\* 'Roy. Soc. Proc.,' A, vol. 105, p. 507 (1924).

By adding together all the figures in columns 3 and 6 of Table I it appears that radium B emits 213 secondary electrons for every 1000 atoms that disintegrate, and radium C 16. Taking into account the disintegration electrons of which there is one per atom, radium B emits 1.21 electrons per disintegrating atom, and radium C 1.016 or together 2.23. It is a matter of great interest to compare this figure with the direct determination made by Gurney. His final value depended on whether the number " $n$ " of atoms disintegrating per second in 1 millicurie was taken as 3.4 or  $3.72 \times 10^7$ , the first being the value found by Geiger and Werner,\* and the second that of Hess and Lawson.† According as to which figure was taken Gurney found respectively 2.48 or 2.27 electrons to come from each pair of disintegrating radium B and radium C atoms. At first sight the value 2.23 found in the present work appears to be in excellent agreement with the second value, but to appreciate the accuracy with which agreement might be expected it is necessary to enter into a little more detail.

Using the values of Table I we have deduced that from 1000 atoms each of radium B and radium C 230 secondary electrons are emitted, but since this figure is based on Gurney's measurement of the number of electrons in the strong radium B line  $H\beta$  1938, which in its turn depends on the number of atoms disintegrating per second in a millicurie, it can be seen that our experimental figure of 230 secondary electrons is uncertain to 10 per cent. from this cause alone. Adding another 5 per cent. for our own experimental error we arrive at a total uncertainty of 15 per cent. We can, therefore, say that our experimental figure of 230 electrons from every 1000 disintegrating atoms should be correct to 15 per cent. after allowing for the divergence between the existing determinations of " $n$ ." This will be found repeated as the first entry of Table IV below. We will now deduce directly from Gurney's measurements another estimate for the number of secondary electrons. According to the value chosen for " $n$ " (number of atoms disintegrating per second) he found that 1000 atoms each of radium B and radium C gave either 2480 or 2270 electrons. Since each atom gives one disintegration electron 2000 of these electrons are nuclear, leaving respectively either 480 or 270 as the number of secondary electrons. These two estimates form the second and third entry in Table IV, and since the value of the total emission is probably accurate to 3 per cent., the values for the secondary emission determined by subtraction will be accurate to 16 per cent. and 25 per cent. respectively.

\* 'Z. f. Physik,' vol. 21, p. 107 (1924).

† 'Phil. Mag.,' vol. 48, p. 200 (1924).



Table IV.—Total number of photoelectrons from 1000 disintegrating atoms each of radium B and radium C.

230	Using Gurney's value for number of electrons in line $H\beta$ 1938 and also measurements of present paper. Probable error 15 per cent., which includes uncertainty in " $n$ ."
480	Using Gurney's value for total number of electrons emitted by RaB and RaC and calculating with " $n$ " = $3.4 \times 10^7$ . Probable error 16 per cent.
270	The same, but using " $n$ " = $3.72 \times 10^7$ . Probable error 25 per cent.

It would thus appear that either Gurney included in his measurements, in spite of all his precautions, some electrons which did not come directly from the radioactive material, or the value of " $n$ " is nearer  $3.7 \times 10^7$  than  $3.4 \times 10^7$ .

In the course of this paper we have discussed several interesting points which arise naturally from the measurements of the intensities of the groups, but we would emphasise again that this does not exhaust the information which can be obtained. It is to be hoped that a suitable comparison of these values with the other intensity measurements referred to, will lead to an estimate of magnitudes of a more fundamental nature, the absolute probabilities of the nuclear quantum transitions.

#### *Summary.*

1. The relative intensities of the  $\beta$ -ray groups of the radium B and radium C magnetic spectrum have been measured for equal number of disintegrating atoms.

2. The ratio of the intensities of the groups arising by internal absorption of a  $\gamma$ -ray in the L and K levels is independent of the frequency of the  $\gamma$ -ray, and approximately equal to that applying in the case of the external absorption of X-rays.

In conclusion we would like to express our thanks to Prof. Sir Ernest Rutherford for his interest and help in these experiments and for providing us with the radioactive material, and also to Mr. G. R. Crowe for the preparation of the sources.

*Experiments to Test the Possibility of Transmutation by  
Electronic Bombardment.*

By M. W. GARRETT, D.Phil., Exeter College, Oxford.

(Communicated by F. A. Lindemann, F.R.S.—Received December 15, 1926.)

*Experiments upon Tin.*

In an earlier paper\* experiments were described which were carried out in order to test the production of gold from mercury, as reported by Miethe and Stammreich, and by Nagaoka. These experiments led to conclusively negative results, but it was considered desirable to repeat also the work of Smits and Karssen† upon the conversion of lead into thallium and mercury. To this end it was decided to adapt the quartz tube apparatus with sealed in tungsten leads, already used in the case of mercury, and described and illustrated in the previous paper (interrupted arc method).

While waiting for a specially pure preparation of lead, tin suggested itself as a suitable metal for further experimentation. Besides its low melting point, there is the further advantage that indium, the most probable product of any transmutation of tin, can be spectroscopically detected in exceedingly minute traces, whilst its occurrence is so limited that the danger of accidental contamination from the ordinary materials of the laboratory is much smaller than is the case with most elements. In this respect, a positive result with indium would be more convincing than the production of mercury reported by Smits.

The quartz tubes employed were similar to those already used in the case of mercury, but a burner was added to the apparatus for heating the metal to its melting point. The tubes were run from the 100 volt mains, with a large inductance in series. With a short circuit current of 40–50 amperes, and a mean heating current of 18–22 amperes, they remained red hot without the aid of the burner, which was extinguished as soon as the arc had started. These currents were supported without overheating by the 0.5 mm. tungsten-lead seals, which remained at a temperature below the melting point of tin in spite of heat conduction from above. The flickering light from the arc was focussed upon the slit of a small Hilger quartz spectrograph and the spectrum photographed.

The tin was freed from oxide by being melted once or twice *in vacuo* and

\* 'Roy. Soc. Proc.,' A, vol. 112, p. 391 (1926).

† Smits and Karssen, 'Nature,' vol. 117, p. 13 (1926).

forced through a fine constriction, after which it was sealed up in the quartz tube under a pressure of a centimetre or two of hydrogen. But it was found necessary to leave a minute trace of oxide contaminating the tin. Otherwise the bright metal adhered so firmly to the quartz walls as to crack the tubes on cooling.

Considerable difficulty was experienced in obtaining tin free from all traces of indium. The spark or arc spectrum of ordinary commercial tin showed a very strong line at 4511, and this line could be detected under favourable circumstances in all the samples of "pure" tin which were at first available. An attempt was made to remove the indium from the tin by distillation *in vacuo* for 40 hours, in a quartz tube, at a temperature of about 800°. The indium lines were weakened by this treatment to such an extent that they could no longer be detected with certainty in the open arc spectrum, but the four most prominent ones came up clearly in the spectrum of the arc in the sealed quartz tube. This constitutes a more delicate test than the ordinary open arc method.

A sample of Kahlbaum's purest tin was ultimately obtained, and this failed to show any trace of the blue indium line, either in the carbon arc in air or in the quartz tube. A careful examination of the photographs of the quartz arc showed faint traces of 4102 (indium) and of 4058 (lead). All the other lines measured, with the exception of H $\alpha$  and the mercury spectrum (see below), were due to tin. It is interesting to note that in this case 4102 proved to be the most persistent indium line, in place of 4511 (de Gramont) or one of the ultra-violet lines (Hartley and Adeney). When all four lines were present, their intensity followed the order of decreasing wave length, 4511 being the strongest.

Decisive results were obtained from the first tube which was filled with Kahlbaum's tin. This tube was run at an average current of 18 amperes, and maximum instantaneous current of 45 amperes, for 50 hours before it was punctured by an intense local arc. Photographs of its spectrum were obtained at short intervals, from a few minutes after starting to one hour before its collapse, and since these photographs showed uniformly the same faint indication of the line 4102 without any trace of the other indium lines, or of cadmium, the attempt to transmute tin was abandoned.

A sample was now obtained of Kahlbaum's purest lead, which, upon spectroscopic examination in an open carbon arc, failed to show any indication of the mercury or thallium lines. It was found, however, on attempting to run lead in the quartz tubes in the same way as the tin, that the tubes invariably cracked, either upon cooling or reheating, and it was evident that a new technique would have to be evolved before successful runs could be made. At

just this time a paper appeared by Smits,\* in which he reported considerable difficulty in duplicating his earlier results, and concluded that the conditions favourable to transmutation were so obscure and so difficult to reproduce that "even an extended series of negative results would not necessarily be convincing." For this reason the experiments upon lead were discontinued as unprofitable; for any negative results which might have been forthcoming would be no more convincing than those already obtained by Smits, whereas a positive result was considered unlikely.

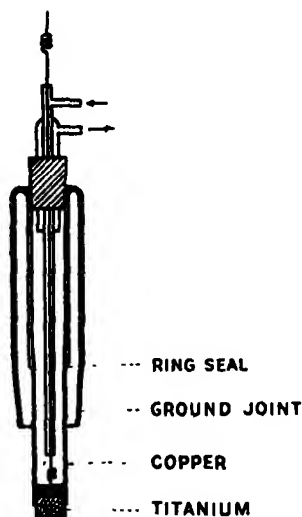
The test for mercury under the conditions of Smits's experiment is so extraordinarily sensitive that the utmost rigour of proof, in a considerable series of consistent experiments, is required before the possibility of accidental contamination from so common a substance is altogether eliminated. The difficulty of excluding mercury was brought out in the experiments upon tin, where, in spite of careful handling, the mercury lines appeared quite distinctly in several of the tubes, though the almost complete absence of this element from the original tin was shown by the fact that several tubes showed merely a very faint trace of 2537, without any of the other mercury lines. The most interesting case was that of the tube already described at length, in which the strongest mercury lines were all present from the beginning, but in which they increased unmistakably in intensity, by comparison with the tin lines, during the course of the run. Since the tube was sealed throughout this time, such an effect is difficult of explanation, but it may possibly have a bearing upon the earlier results of Smits.

#### *Experiments upon Titanium.*

These experiments differed from those previously described in that high speed electrons capable of penetrating the innermost electronic orbits of the titanium atom were employed, the bombardment being carried out *in vacuo*. Titanium was chosen because of its non-volatility and low atomic number ( $K\alpha$  voltage under 5000), and the fact that it might be expected to yield scandium, also a non-volatile element, and one which, though spectroscopically detectable in very minute traces, is of very limited occurrence. Furthermore, though scandium is one of the rarest of all the elements upon this planet, its lines are more prominent in stellar spectra than are those of titanium, which suggests a possibility that the two elements may be mutually convertible under certain conditions which may occur in the hot stars.

\* Smits, 'Z. anorg. Ch.,' vol. 155, p. 269 (1926). See also 'Nature,' vol. 117, p. 613 (1926).

A 20 cm. glass bulb was employed, provided with a Coolidge cathode, and a water-cooled anticathode which is sketched in the accompanying figure.



With an input of 300 watts, only a small dull, red spot was observable at the focus, and since only about half this power was actually employed during the course of the experiment, the anticathode was not heated to a temperature at which any scandium formed might be expected to volatilise off. Several runs were made, the longest being of 30 hours, with an average current of 12 milliamperes at 12,000 volts. The arc and spark spectra were photographed with a small concave grating spectrograph, but no trace of scandium could be detected.

#### *Summary.*

An attempt to transmute tin into indium, in a quartz apparatus similar to that used in the case of mercury (described in a previous paper), and to the apparatus in which Smits reported evidence of the formation of thallium and mercury from lead, proved a failure, in spite of the employment of high current densities and the extraordinary sensitiveness of the spectroscopic method. Indium was detected in all the samples of "pure" tin examined, though in barely detectable traces in the purest tin of C. A. F. Kahlbaum. The 4102 line was found to be the most persistent in the spectrum of this element (de Gramont lists, 4511).

Attempts were made to prepare scandium from titanium, using electrons of sufficient speed to be certain of penetrating the K ring of this element. Titanium was bombarded with 12,000 volt electrons from a hot filament in an evacuated bulb, but no evidence of any transmutation was obtained.

Grateful acknowledgment is due to Prof. F. A. Lindemann for numerous helpful suggestions, and to the International Education Board for a generous financial grant.

### *Bands in the Secondary Spectrum of Hydrogen.*

By H. STANLEY ALLEN, M.A., D.Sc., Professor of Natural Philosophy in the University of St. Andrews, and IAN SANDEMAN, Ph.D., late Carnegie Research Scholar in the University of St. Andrews.

(Communicated by O. W. Richardson, F.R.S.—Received December 17, 1926.)

Fulcher's discovery of bands in the secondary spectrum of hydrogen at low pressures proved the starting point of a number of investigations, including those, based on the valuable tables of Merton and Barratt, which have been carried out in the University of St. Andrews.\* The application of the quantum theory to these bands has been discussed by one of us (H. S. A.), by Curtis, and in particular by Richardson who, partly in association with Tanaka, has added greatly to the number of known regularities and done much to bring them into line with the theory of band spectra. Nevertheless, apart from the Fulcher system, of which Richardson has recently given a very complete account,† there remains a very large number of lines which have not yet been classified.

One of the present writers (I. S.) has been engaged in a study of the secondary spectrum at higher pressures, and among the regularities which have been selected by this method is a band with head at  $4582\cdot58$  A.U. and shading towards the violet, which has been described in a recent communication.‡ This band yielded an initial moment of inertia agreeing closely with a value deduced from a static model of triatomic hydrogen,  $H_3$ .§ This band has since been found to be one of a large number of similar bands which it will be the purpose of this paper to describe. We shall refer to it for convenience as "Band II<sub>A</sub>, a."

A very remarkable feature of the blue and violet regions of the spectrum is the number of times series occur parallel to the Q series of Band II<sub>A</sub>, a. These

\* (1) Allen, 'Proc. Roy. Soc., Edin.,' vol. 43, p. 180 (1923); (2) Allen, 'Roy. Soc. Proc., A, vol. 106, p. 69 (1924); (3) Sandeman, 'Roy. Soc. Proc.,' A, vol. 108, p. 607 (1925); (4) Sandeman, 'Roy. Soc. Proc.,' A, vol. 110, p. 326 (1926).

† See, *inter alia*, 'Roy. Soc. Proc.,' A, vol. 111, p. 714 (1926), and a letter in 'Nature,' of July 24, 1926.

‡ Sandeman, *loc. cit.* (3).

§ Allen, *loc. cit.* (1). It is not claimed that such a model represents all the properties of the molecule, but it is reasonable to suppose that it gives at least the right order of magnitude for the moment of inertia.

series involve a considerable number of the faint lines recorded by Tanaka,\* and generally occur in groups, the individual series of each group being separated by about 92 wave-numbers. We shall designate all the regularities of this type by the roman numeral "II" to discriminate them from all other known types of bands, and, further, use the capital letters, A, B, C, ..., as suffixes to distinguish the systems to which the various groups belong.

In Table I we give a well-marked group which occurs just on the short-wave side of the primary line  $H_\beta$ . The individual series forming the group have been allotted the small letters,  $a, b, c, \dots$ , starting from the most intense series which occurs in this case on the right-hand edge of the group, while the system to which the group belongs has been allotted the suffix "B." Thus we can refer to the band to which the  $a$  column of Table I belongs as "Band II<sub>B</sub>,  $a$ ." This nomenclature has been chosen as providing a convenient way of referring to the various series independently of any assumption as to the structure of the group.†

Table I shows the wave-numbers of the lines with intensities in brackets underneath. The first figure given is the intensity recorded by Merton and Barratt or by Tanaka, an "M" or "T" being prefixed to indicate which observations are referred to. The other two figures refer to observations of the arc spectrum at atmospheric pressure and at 45 cm. of mercury made in this Laboratory, to which reference has been made in previous papers.‡ The letter "H" or "L" indicates that the line is recorded by Merton and Barratt as enhanced at high or low pressure. "Z" indicates lines showing normal Zeeman effect, "NZ" lines not showing Zeeman effect, and "ZA" lines given by Dufour§ as showing abnormal Zeeman effect.

Both horizontal and vertical differences are given in italics. The horizontal differences are everywhere nearly 92 wave-numbers, but appear to increase slightly in passing from the left-hand to the right-hand edge of the table. The

\* Tanaka, 'Roy. Soc. Proc.' A, vol. 108, p. 592 (1925).

† This notation is consistent with that employed in a recent Paper for Band System IV<sub>A</sub> (Sandeman, *loc. cit.* (4)). It is probable that the bands to which the series belong correspond to various transitions,  $n \rightarrow n'$ , of the vibration quantum number, so that the letters,  $a, b, c, \dots$ , can be assumed to stand for bracket expressions  $(n, n')$ . Further, we have provisionally supposed the different groups to belong to different systems. When the structure of these regularities becomes better known, the suffix allotted to the strongest group may be extended to the whole of the related system, and the electron quantum numbers inserted in the expressions for the bands, as has been done in the case of Band System IV<sub>A</sub>.

‡ Sandeman, *loc. cit.*

§ Dufour, 'Journ. de Phys.' Ser. 4, vol. 8, p. 237 (1909).

Table I.—Band Group II<sub>B</sub>.

## Q Series.

	e.	d.	c.	b.	a.
Q(1)	..	(20795.77) <sup>§</sup> (M2H, 6, 4)	92.53	(20888.30) <sup>§</sup> (M2H, 7, 5)	93.23
		5.15	5.20	5.69	6.71
Q(2)	..	20708.6 (Tr, 0, -)	92.3	20800.92 (Tr, -, -)	93.25
		25.6		20893.50 <sup>  </sup> (M1H, -, -)	21078.98* (M3L, 4, 2)
		20734.24 (Tr, -, -)		24.42	23.84
Q(3)	...	42.78	92.15	20826.39* (Tr, 0, -)	21102.79 <sup>†</sup> (Tr, p, -)
		20777.02* (M0, 4, 3)		23.94	43.41
Q(4)	..	60.22	91.85	42.80	21146.20 <sup>‡</sup> (M0H, -, -)
		20837.24) <sup>§</sup> (M4, **, **)		20960.72* (M0, p, -)	61.63
Q(5)	...			62.17	21207.83 (M3, 1, -)
				21022.89 (M0L, -, -)	79.56
Q(6)	..			79.90	21287.39 (Missing)
				21102.79 <sup>†</sup> (Tr, p, -)	99.18
Q(7)	.				21380.57 (M2, p, p)

\* Members of Richardson's Blue Fulcher System.

† An overlap. Since Q(6) is missing in columns a and b, this line is probably to be allotted to II<sub>B</sub>, a, Q(3).

‡ Also 41 Q(6).

§ These lines probably do not belong to the present system, but have been included, because they may overshadow fainter members. 20888.30 is also 53 P(1) and 41 Q(5), and 20795.77 is also 110 Q(5).

|| Also 110 Q(4).

¶ The line 20867.46 (M1H, 1, 0) comes near this value.

\*\* Not resolved from 20840.45 (M3). The arc intensities of the combined line are: At. Press. 6, 45 cm. 4.



vertical differences are very nearly the same as those of the Q Series of Band II<sub>A</sub>, *a*,\* which are 6·83, 25·15, 43·39, 61·12, 79·52, and 99·11.

If we except the three doubtful members which have been placed in brackets and the lines 21009·64 and 20777·02 which are overlaps with the Blue Fulcher System, the various series of Table I are similar in intensity sequence.

It must be admitted that Table I shows a number of coincidences with the lines of Richardson's Blue Fulcher System. It is, however, noteworthy that the lines 21078·95 and 20985·70, which appear as Q(2)'s of the *a* and *b* columns, are somewhat intense for their positions in Richardson's† series, so that they may well be genuine overlaps. The numerical coherence of Table I is sufficiently striking to warrant a conviction that the series are actually related to II<sub>A</sub>, *a*, Q, a conviction which is strengthened when we find the same configuration of lines cropping up in other parts of the spectrum.

The intensity sequence shown by the first four members of the *a* column of Table I suggests that this series is of the alternating-intensity type, since Q(2) and Q(4) are stronger than Q(1) and Q(3). There is, however, a curious rise in intensity at Q(5) both in the arc and in the Geissler-tube observations. A rise in intensity at Q(5) is also apparent in the *b* column. In a series like this, where Q(2) is moderately strong, Q(3) and Q(4) weak, and Q(5) again moderately strong, we seem to have indications of the enhancement of every third line instead of every second, a state of things which we may call "threefold intensity alternation." This peculiarity appears again in other groups, and calls for theoretical explanation. If we could assume the operation of a principle of threefold intensity alternation simultaneously with one of twofold alternation, the intensity sequence of the *a* series of Table I would, in fact, cease to be peculiar. We shall later return to this question.

The group shows signs of extrapolating horizontally in the direction of longer wave-lengths, and, at least as far as the more intense lines Q(2) and Q(5) are concerned, also in the direction of shorter wave-lengths. We have not, however, included these lines in Table I, since it is doubtful whether they are really members of the system.

In Table II we give another group (II<sub>C</sub>) which bears a striking similarity to

\* Sandeman, *loc. cit.* (3). The numeration adopted in the present paper differs from that previously given for Band II<sub>A</sub>, *a*. The values of *m* have each been decreased by 1, so that the line of lowest quantum number is now taken as Q(1) instead of Q(2). While the experimental evidence is insufficient to enable us to regard either numeration as preferable, the one here adopted seems better suited for a preliminary study of these bands, since it yields values of the E and *e* constants of reasonable magnitude.

† Richardson, *loc. cit.*

Table II.—Band Group IIc.

Q Series.

	a.	b.	c.	d.	e.
Q(1)	24005.68 (Tp)	5.71			
Q(2)	24011.39 (M2H)	91.44	92.44	23735.49 (Tv)	
Q(3)	24035.69† (M1L)	91.05	92.07	23760.42 (Tq)	23668.19 (M2)
Q(4)	44.91	43.24	43.61	43.71	43.49
Q(5)	24080.60 (Mu)	92.72	91.70	23804.13 (M2)	23711.68 (Tp)
Q(6)	62.56	62.89	62.46	62.29	62.29
Q(7)	24143.16 (Tv)	92.39	92.13	23858.64 (Trd)	23773.97 (M5)
	80.81	80.74			
	24223.97 (Missing)	92.46	24131.51 (Tv)		
	99.06				
	24323.03 (Mo)				

\* The same line as 20 Q(2).

† The same line as 20 Q(5).

‡ The wave-number of this line is a little too low. Richardson informs us that he claims the line as his  $\beta_1$  Q(1), but that Tanaka has recorded it as of strength 3 on one plate. This would make it too strong for either band, and tend to support a real coincidence.

Group II<sub>B</sub>. This group occurs on the short-wave side of the primary line H<sub>γ</sub>. Table II shows only the intensities recorded by Merton and Barratt or by Tanaka. The continuous spectrum is so strong in the arc in this region, that measurement of the fainter lines was difficult. Besides the lines given, 23577·1 (T) and 23619·05 (T0) may be Q(3) and Q(4) respectively of column *f*.

The horizontal differences are again everywhere about 92 wave-numbers, but do not appear to increase towards the short-wave side of the group as in Table I. There is, however, considerable similarity between the two tables. The best marked series again occurs on the right-hand edge of the group; columns *a* and *b* are again more intense than the others; and the Q(1)'s are again faint or missing. It is also interesting that Q(5) of the *d* column is missing in both tables, while Q(2) of the *e* column is missing in Table II and very faint in Table I. Again in both tables *a*, Q(7), is present, while *a*, Q(6), is not.

There are three lines, 23773·97, 23668·19, and 23804·13, which appear to be rather intense, but, apart from these and the two lines noted as overlaps, the intensity distribution of the series in Table II is reasonable. The vertical differences are nearly the same in the two groups.

Interspersed with the Q series of Group II<sub>C</sub> are other lines which show horizontal differences of the same order, and presumably belong to related series. We have not succeeded in finding any convincing arrangement of these. Nor have we been able definitely to identify P and R series in the case of the previous group. A difficulty which presents itself in searching for R series parallel to the R series of Band II<sub>A</sub>, *a*, is that the distance between R(1) and R(3) is nearly the same as the horizontal interval separating the series: in fact, in Band II<sub>A</sub>, *a*,  $R(3) - R(1) = 93\cdot63 \text{ cm.}^{-1}$ , so that it is hard to say whether a given line should be identified as R(1) or as R(3) of the band immediately on the long-wave side.

As we shall show later, groups of the type considered exist in which both P and R series can be identified, and others in which apparently only R series are present.\* We shall leave the question of the identification of P and R series for Groups II<sub>B</sub> and II<sub>C</sub> until further experimental evidence is available.

In Table III is given a remarkable group of lines occurring on the short-wave side of the primary line H<sub>β</sub> in a region where lines are comparatively scarce. This group differs from the last in having its best marked series on the long-wave side of the group, and in showing the horizontal differences between the columns to increase regularly in passing up the group. The Q(1)'s are, in fact,

\* In the present paper we shall deal in detail only with groups showing both P and R series.

Table III.—Band Group II<sub>D</sub>.

## Q Series.

	a.	b.	c.	d.	e.
Q(1)	24632.85 (M0)	90.80	24723.65 (M1)	93.44	24817.09 (M2)
	5.95	6.06	5.74	5.68	5.68
Q(2)	24638.80 (M0)	90.91	24729.71 (Missing)	93.12	24822.83 (M0)
	23.82	24.60	24.85	24.06	24.07
Q(3)	24669.62 (Tp)	91.69	24754.31 (M0)	93.37	24847.68* (Tr)
	43.32	42.79	42.43	43.55	
Q(4)	24705.94 (Tr)	91.16	24797.10 (M0)	93.01	24890.11 (Tp)
	61.37	61.52			61.60
Q(5)	24767.31 (Tg)	91.31	24858.62 (T0d)	96.69	24987.00† (Missing)
	80.37	80.09			25048.00 (M0)
Q(6)	24847.68* (Tr)	91.03	24938.71 (Tp)		80.50
	99.62				25129.10 (M0)
Q(7)	24947.30 (Tgd)				
	116.56				
Q(8)	25065.86 (Tr)				

\* An overlap. A similar overlap between a Q(3) line and a Q(6) line occurs in other instances, e.g., Tables I, V, and VII.

† Merton and Barratt record a line 24967.63 (0).

spaced out according to a quadratic law. The  $a$  series is one of considerable length and is of the alternating-intensity type. There are, moreover, indications of intensity-alternation horizontally as well as vertically, since the  $b$  and  $d$  columns are more intense than the  $a$ ,  $c$ , and  $e$  columns.

Table III shows one or two missing lines besides a few intensity peculiarities, and since little is known about structure in this region, not much can be said about the latter. Nevertheless, the horizontal differences are exceedingly regular, and the vertical differences closely resemble those of the other groups and yield a nearly constant second difference. Besides the lines given, 24545·18 (M1) may be Q(1) of the column immediately on the long-wave side of the  $a$  column, which we may call the “ $z$ ” column. It may be mentioned that there are two lines, 24645·41 (M0) and 24676·85 (M0), which appear to continue the  $a$  series of Table III in the direction of lower quantum numbers, i.e., on the numeration adopted these lines would be Q(0) and Q(−1). These have not been included in Table III, since we have no definite analogy for the existence of such members in the other groups.\*

Group II<sub>n</sub> shows indications of possessing R series parallel to that of Band II<sub>A</sub>,  $a$ . Moreover, a little farther up the spectrum there is a similar parallel group which seems to bear a particularly intimate relation to it. We shall defer consideration of these related regularities to a later paper.

It is worthy of mention that the original Q series, II<sub>A</sub>,  $a$ , Q, itself shows indications of fitting into a scheme similar to that of Tables I and II. Table IV shows a scheme incorporating this series (column  $a$ ). The horizontal differences here seem to be in the neighbourhood of 93 instead of 92. Table IV shows a considerable number of missing lines besides overlaps with lines of other systems. However, since we have indications of a threefold intensity alternation in column  $a$ , such as was found to hold in Table I, and as this peculiarity repeats itself in columns  $b$ ,  $c$ , and  $d$ , the scheme seems not unlikely.

*A Band System in the Infra-red showing P, Q, and R Combinations similar to Band II<sub>A</sub>,  $a$ .*—Recent measurements of the infra-red secondary spectrum of hydrogen by T. E. Allibone† have made possible a more thorough study of the spectral region beyond H<sub>2</sub>, and have shown the existence of another group of lines bearing a close resemblance to those given in the preceding tables. This

\* Some of the groups show doubtful extrapolations in the direction of lower quantum numbers. These are, in most cases, such a bad fit that it seems likely that such lines are members of some other related series coming accidentally near the positions which the extrapolations of the Q series should occupy.

† Allibone, ‘Roy. Soc. Proc.’ A, vol. 112, p. 196 (1926).

Table IV.—Band Group II<sub>A</sub>.

## Q Series.

	a.	b.	c.	d.
Q(1)	21830·67 <sub>  </sub> (M1NZ, q, p)	¶ <sub>  </sub>		
	6·83			
Q(2)	21837·50 (M3NZ, 4, 4)	93·13	21930·93*§ 93·46 (M2ZA, 6, 6)	22024·39 93·58 (M2HZ, —, —) 22117·97 (M0ZA, 2, 1)
	25·15		24·18	
Q(3)	21862·65 (M4H, 10, 8)		22048·57* (M3, —, —)	
	43·39		43·31	
Q(4)	21906·04 (M1HNZ, 5, 5)		22091·88 (T***, —, —)	
	61·12		61·08	
Q(5)	21967·16† (M3HNZ, 8, 7) 79·52	92·11	22059·27 93·69 (M0ZA, 3, 1) 80·64	22152·96* 94·33 (M1, —, —) 22217·29* (M2L, —, —)
Q(6)	22046·68 (M3NZ, 6, 4)	93·23	22139·91*† (M1H, —, —)	
	99·11	99·36		
Q(7)	22145·79* (M1HNZ, 6, 5)	93·48	22239·27 94·52 (Tpd, 0d, p)	22333·79 (Tq, —, —)
	117·45			
Q(8)	22263·24* (M5LZ, 1, 1)			

\* Members of Richardson's Blue Fulcher System.

† The same line as 101 R(4).

‡ The same line as 60 R(6).

§ Recorded by Merton and Barratt as an unresolved doublet. This line also appears as 101 R(3) and 26 P(5).

|| The intensity of this line was given before as (M1, 0, —). Later measurements would indicate the above as a better ratio of the intensities at atmospheric pressure and at 45 cm.

¶ 21922·75 (M0L, 1, p) may be b, Q(1).

\*\* Tanaka describes this line as of "quite variable" intensity, perhaps meaning that some parts of the line looked more intense than others.

group, Band Group II<sub>F</sub>, is given in Table V in which the letter "A" before the intensities indicates that the observations are Allibone's. Three parallel Q series can be identified showing horizontal and vertical differences of the same magnitude as before and possessing an intensity distribution not unlike that of the other groups. The rise of intensity at Q(5) is specially well marked in all three series. Moreover, an R and a P series can also be identified closely parallel to the R and P series of Band II<sub>A</sub>, *a*, and fitting into a P, Q, and R

Table V.—Band Group II<sub>F</sub>.  
Q Series.

Q(1)	a.	b.	c.
Q(2)	13470.42 (A4) 25.13	94.29 13504.71 (A1) 23.95	93.24 13657.95 (A3) 23.44
Q(3)	13495.55 (A1) 43.37	93.11 13588.66 (A1) 43.43	92.73 13681.39* (A6) 43.35
Q(4)	13538.92 (A4) 61.81	93.17 13632.09 (A3) 62.23	92.65 13724.74 (A1) 62.43
Q(5)	13600.73 (A12) 80.66	93.59 13694.32 (A4) 80.73	92.85 13787.17 (A6)
Q(6)	13681.39* (A6) 99.93	93.66 13775.05 (Missing) 99.22	
Q(7)	13781.32† (A10)	92.95 13874.27 (A1)	

\* An overlap. (Cf. Tables I and III.)

† This is probably a strong line of another system overshadowing a weaker member.

Table VI.—Band Group II<sub>F</sub>.  
An R and a P series in conjunction with II<sub>F</sub>, a, Q.

R(1)	II <sub>F</sub> , a, R(m).	P(2)	II <sub>F</sub> , a, P(m).
R(2)	13512.95 (A1) 55.25	P(3)	13453.02 (A2) 13.80
R(3)	13568.20 (A1) 73.79	P(4)	13466.82 (A*) 31.67
R(4)	13641.99 (A8) 91.35	P(5)	13498.49 (A1) 50.29
R(5)	13733.34† (Calculated)	P(6)	13548.78‡ (A1)

\* The intensity of this line differed widely on Allibone's two plates, being recorded as 1 on Plate A and 5 on Plate B.

† The line 13732.28 (A5) comes near this value. This line seems, however, more likely to be II<sub>F</sub>, b, R(4), since it gives 13593.98 (A4) as II<sub>F</sub>, b, P(5) in agreement with the Combination Principle.‡ Richardson informs us that this line coincides with his  $\alpha_5$  Q(2).

combination along with the Q series of column *a*. These series are given in Table VI. The first differences of the R series closely resemble the corresponding first differences of the series II<sub>A</sub>, *a*, R, which are 56·52,\* 73·52,\* and 91·29, while the first differences of the P series are not unlike the corresponding first differences calculated for the incomplete P series of Band II<sub>A</sub>, *a*, which are 12·10, 30·58, and 49·35.

The Simple Combination Principle applied to Band II<sub>F</sub>, *a*, gives:—

		Difference.
Q(2) + Q(3) = 26965·97,	R(2) + P(3) = 26965·97,	<sub>2</sub> Δ <sub>3</sub> = 0·00,
Q(3) + Q(4) = 27034·47,	R(3) + P(4) = 27035·02,	<sub>3</sub> Δ <sub>4</sub> = +0·55,
Q(4) + Q(5) = 27139·65,	R(4) + P(5) = 27140·48,	<sub>4</sub> Δ <sub>5</sub> = +0·83.

A curious feature of the band is the apparent capriciousness in the intensity of the line P(4) observed by Allibone, suggesting that some of the other observed intensity-peculiarities may be traceable to some such "capriciousness" rather than to overlaps with lines of other systems. The possibility presents itself that the lines of the system may be peculiarly sensitive to changes in the conditions of excitation. There is, for example, in the arc† some condition which causes enormous enhancement of the lines of Band II<sub>A</sub>, *a*—see Table IV. We shall later return to this point in considering the question of the identity of the emitter.

Besides the lines given in Tables V and VI there are other lines which may be members of the R and P series belonging to the other bands of the group, but, as these series are uncertain owing to their fragmentary character, we shall leave them until further experimental evidence is available.

A circumstance which provides strong evidence for the validity of Group II<sub>F</sub> is that an almost parallel configuration of lines occurs a little farther up the spectrum (Group II<sub>G</sub>). This second group occurs astride the primary line H<sub>ε</sub> in the region between the observations of Merton and Barratt and those of Allibone, and some of its members come out in the arc,† which are not recorded by other observers. Although no high accuracy is claimed for these determinations, these lines fit into the general scheme, and the R and P series of the *a* band are in moderate agreement with the Combination Principle. The details of this group are given in Tables VII and VIII.

\* These values are based on an approximate determination of an arc line. The first is probably too large, and the second too small. See Sandeman, *loc. cit.* (3).

† The arc observations referred to throughout the present paper are those made at St. Andrews, see Sandeman, *loc. cit.*



The Simple Combination Principle applied to Band II<sub>G</sub>,  $\alpha$ , gives :—

				Difference.
Q(2) + Q(3) = 30173·04,	R(2) + P(3) = 30172·65,	${}_2\Delta_3 = -0\cdot39,$		
Q(3) + Q(4) = 30242·59,	R(3) + P(4) = 30242·52,	${}_2\Delta_4 = -0\cdot07,$		
Q(4) + Q(5) = 30347·49,	R(4) + P(5) = 30348·34,	${}_4\Delta_5 = +0\cdot85,$		
Q(5) + Q(6) = 30489·76,	R(5) + P(6) = 30490·66,	${}_5\Delta_6 = +0\cdot90.$		

Table VII.—Band Group II<sub>G</sub>.

Q Series.

	$\alpha$ .		$b$ .		$c$ .
Q(1)	..		15162·68§ (-, 1, 1)	91·87	15254·55   (P1, 0, 2)
			6·09		6·26
Q(2)		15073·25† (-, 4, 2)	95·52	15168·77   (P1, 0, 0)	92·04
		26·54		23·16	24·26
Q(3) ....	...	15099·79 (A0, -, -)	92·14	15191·93¶ (-, 3, 1d)	93·14
		43·01			43·21
Q(4) ....	...	15142·80 (A3, -, p)			15328·28** (Missing)
		61·89			62·08
Q(5) ....	....	15204·69‡ (-, -, 2)			15390·36 (M0, 0, 1)
		80·38			
Q(6) ....	..	15285·07* (M2, 2, 1)			
		100·32			
Q(7) .	.	15385·39 (M0, 1, 0)			

\* An overlap. Cf. Table V. The line 15285·07 is also a member of Richardson's Red Fulcher System. The strength of this line in the arc at higher pressures is sufficient to indicate a real coincidence.

† Arc line, W.L. 6632·44 (Cf. Piazzzi Smith 6632·7 R.A. (6) ) not completely resolved from 6633·86 (A3, 1, 2). The wave-number seems rather low.

‡ Arc line, W.L. 6575·11.

§ Arc line, W.L. 6593·32.

|| Porlezza's measurements reduced to I.A., 'Atti. Acad. Lincei,' vol. 20 (2), p. 176 (1911). The wave-lengths are 6590·90 and 6553·83 R.A.

¶ Arc line, W.L. 6580·63. The intensity at atmospheric pressure seems rather high, and the wave-number is too low, so that there is probably an interference here with a line of some other system.

\*\* The line 15327·31 (M0, 3, 2), a member of Richardson's Red Fulcher System, comes near this value.

Table VIII.—Band Group II<sub>G</sub>.An R and a P series in conjunction with II<sub>G</sub>,  $\alpha$ , Q.

R(1)	II <sub>G</sub> , $\alpha$ , R( $m$ ). †	P(2)	II <sub>G</sub> , $\alpha$ , P( $m$ ).
R(2)	15115.79‡ (-, 3, 2)  56.71	P(3)	15056.86* (-, 0, 1)  13.16
R(3)	15172.50§ (A3, 2, 1)  73.84	P(4)	15070.02 (A3, 1, 2)  31.98
R(4)	15240.34   (-, 2, -)  92.30	P(5)	15102.00 (A2, 4, 4)  50.02
R(5)	15338.64 (M4H, 4, 3)	P(6)	15152.02 (A4, -, -)

\* Arc line, W.L. 6639.66.

† The line 15078.11 (A4, 5, 3) may be R(1), but seems rather too intense.

‡ Arc line, W.L. 6613.78.

§ The same line as IV<sub>A</sub>, 6 P(5).|| Arc line, W.L. 6557.14. This line was difficult to measure owing to its proximity to H <sub>$\alpha$</sub> .

It is noteworthy that, although the Q(2)'s of Table VII are somewhat irregular, the difference Q(3) — Q(2) varies from column to column in much the same way as it does for Table V.

The fact that the  $\alpha$  bands of the two groups are very nearly parallel is best shown by means of the scheme of term differences for the two bands (Table IX). Both initial- and final-term differences seem very slightly greater for Band II<sub>G</sub>,  $\alpha$ , than for Band II<sub>F</sub>,  $\alpha$ . In Table IX the initial-term difference,  $F(m+1) - F(m)$ , has, for each value of  $m$ , been taken as the mean of the two quantities  $R(m) - Q(m)$  and  $Q(m+1) - P(m+1)$ , and similarly the final-term difference,  $f(m+1) - f(m)$ , as the mean of the two quantities  $R(m) - Q(m+1)$  and  $Q(m) - P(m+1)$ . Although the accuracy of the observational data, at least in the case of the second band, is insufficient to warrant the attaching of much importance to the small quantities  $\Delta^2\{F(m+1) - F(m)\}$  and  $\Delta^2\{f(m+1) - f(m)\}$ , yet the fact that the Simple Combination Principle holds with moderate closeness enables us with confidence to use the scheme of term differences to draw a number of conclusions regarding the structure of the bands.

The first question to be decided is what formula to employ to represent the terms. The fact that the quantities  $\Delta^2\{F(m+1) - F(m)\}$  and  $\Delta^2\{f(m+1) - f(m)\}$  in Table IX contain so many + signs makes it appear very unlikely that

the formula of Kramers and Pauli\* will be found to give a reasonable representation of the bands, and, indeed, this formula has already been found to be unsatisfactory in the case of Band II<sub>A</sub>,  $\alpha$ . In default of a better term representation, we have used the general quadratic expressions :-

$$F(m) = B(m + E)^2,$$

$$f(m) = b(m + e)^2.$$

Table IX.—Bands II<sub>F</sub>,  $\alpha$ , and II<sub>G</sub>,  $\alpha$ . Term differences.

Initial Term Differences.

Band.	$m$ .	$F(m+1) - F(m)$ .	$\Delta \{F(m+1) - F(m)\}$ .	$\Delta^2 \{F(m+1) - F(m)\}$ .
II <sub>F</sub> , $\alpha$	1			
	2	42.53	29.845	+0.435
	3	72.375	30.28	-0.325
	4	102.655	29.955	
	5	132.61		
II <sub>G</sub> , $\alpha$	1			
	2	42.735	30.01	+0.36
	3	72.745	30.37	+0.015
	4	103.115	30.385	
	5	133.50		

Final Term Differences.

Band.	$m$ .	$f(m+1) - f(m)$ .	$\Delta \{f(m+1) - f(m)\}$ .	$\Delta^2 \{f(m+1) - f(m)\}$ .
II <sub>F</sub> , $\alpha$	1			
	2	17.40	11.605	+0.235
	3	29.005	11.84	-0.735
	4	40.845	11.105	
	5	51.95		
II <sub>G</sub> , $\alpha$	1			
	2	16.195	13.54	-2.05
	3	29.735	11.49	+0.405
	4	41.225	11.895	
	5	53.12		

Here  $B$ , in agreement with mathematical theories of band spectra, may be taken to represent the expression  $h/8\pi^2 I_1$ ,  $I_1$  being the initial moment of inertia of the molecule, and  $E$  is a constant for a given band,  $m + E$  representing the

\*  $F(m) = B(\sqrt{m^2 - \sigma^2} \mp \rho)^2$ . See Kramers and Pauli, 'Zeits. für Physik,' vol. 13, p. 351 (1923). For a discussion of the applicability of this formula to Band II<sub>A</sub>,  $\alpha$ , see Sandeman, *loc. cit.* (3).

"effective" initial quantum number, and similarly for the quantities  $b$  and  $e$  which appear in the expression for the final term,  $f(m)$ . Further, taking the P, Q, and R lines to correspond to transitions of the rotation quantum number as follows :—

$$P(m), \quad m - 1 \rightarrow m,$$

$$Q(m), \quad m \rightarrow m,$$

$$R(m), \quad m + 1 \rightarrow m,$$

the assumption adopted by Kratzer\* and again by Kramers and Pauli and followed in his experimental work by Richardson, we obtain the expressions for the band lines as :—

$$P(m) = \nu_0 + F(m - 1) - f(m),$$

$$Q(m) = \nu_0 + F(m) - f(m),$$

$$R(m) = \nu_0 + F(m + 1) - f(m).$$

From these expressions the constants  $B$ ,  $I_1$ ,  $E$ ,  $b$ ,  $I_2$ ,  $e$ , and the null line,  $\nu_0$ , can be deduced by the methods described in a previous paper.† The constants deduced for Bands II<sub>F</sub>,  $a$ , and II<sub>G</sub>,  $a$ , are shown in Table X. In Table X owing to the uncertainty attaching to the line II<sub>G</sub>,  $a$ , Q(2) we have used only the data corresponding to  $m = 3, 4, 5$ , and  $6$ . This procedure, although admittedly approximate, was the only one that seemed to promise a fair comparison between the bands. Further, since we cannot hope to obtain very accurate values of the null lines,  $\nu_0$ , from the present data, these have been calculated from the Q series only, and in fact from the lines Q(3), Q(4), Q(5), and Q(6). Table X also gives the constants for Band II<sub>A</sub>,  $a$ , deduced from the corresponding data for comparison.

Table X.—Band Constants.

Band.	B cm. <sup>-1</sup>	I <sub>1</sub> gm. (cm.) <sup>2</sup>	E	b cm. <sup>-1</sup>	I <sub>2</sub> gm. (cm.) <sup>2</sup>	e	ν <sub>0</sub> cm. <sup>-1</sup>
II <sub>F</sub> , $a$	15.059	$18.35 \times 10^{-41}$	-1.095	5.736	$48.18 \times 10^{-41}$	-0.961	13164.75
II <sub>G</sub> , $a$	15.189	$18.19 \times 10^{-41}$	-1.105	5.846	$47.28 \times 10^{-41}$	-0.963	15069.53
II <sub>A</sub> , $a$	15.178	$18.21 \times 10^{-41}$	-0.919	6.145	$44.98 \times 10^{-41}$	-0.648	21830.95

Table X shows that the initial moment of inertia is very nearly the same for the three bands, while the final moments of inertia are all different. The E

\* Kratzer, 'Ann. der Physik,' vol. 672, p. 127 (1922).

† Sandeman, *loc. cit.* (4).

and  $e$  constants of Band II<sub>A</sub>,  $\alpha$ , are markedly smaller numerically than those of the other bands, showing that the molecular configuration is somewhat different for this band. Another curious conclusion arises from a consideration of Table X. Although at a first glance we might be inclined to suppose that the small changes in the term differences in passing from Band II<sub>F</sub>,  $\alpha$ , to Band II<sub>G</sub>,  $\alpha$ , are to be attributed to the same cause, yet Table X indicates that, while the small change in the initial-term differences is to be traced to a change in the initial moment of inertia as well as to a change in the  $E$  constant, the small change in the final-term differences is entirely attributable to a change in the final moment of inertia, since the  $e$  constant is noticeably the same for both bands.

Although the data at present available make it impossible as yet to unravel these peculiarities, Tables IX and X indicate clearly that there is some intimate relationship between Band Groups II<sub>F</sub> and II<sub>G</sub>. On the basis of current band theory, three possibilities seem to be present, which we may call (1), (2), and (3) :-

(1) It is possible that, while the corresponding columns of the two groups have the same vibrational quantum numbers, the groups have the final electronic state in common and correspond to different initial electronic states. On the basis of this supposition we should expect the groups to be given by some formula analogous to that of Rydberg. In justice to this view it may be pointed out that a decrease in the final moment of inertia has also been found to take place with rise of electron quantum number in the case of Band System IV<sub>A</sub>.\* Nevertheless, it is hard to see why the initial moment of inertia should also decrease, as it appears to do, with rise of electron quantum number.

(2) It is possible that the groups have both electronic states in common, and correspond to different "groups" of a Deslandres system. For example, it is possible that the  $a$ ,  $b$ , and  $c$  bands of II<sub>F</sub> correspond to vibrational transitions such as  $0 \rightarrow 0$ ,  $1 \rightarrow 1$ ,  $2 \rightarrow 2$ , and those of II<sub>G</sub> to transitions such as  $1 \rightarrow 0$ ,  $2 \rightarrow 1$ ,  $3 \rightarrow 2$ . An objection to this view is that, by making all likely assumptions, it should be possible to forecast the remaining groups of the Deslandres system. Although the writers have tried a number of likely assumptions, their efforts to find the other Deslandres groups have so far proved abortive. It may be said, however, that much of the system of Type-II regularities is so faint that this possibility may conceivably be found to be a solution of the problem, once it has been found possible to devise experimental conditions which would favour the lines of the system.

\* Sandeman, *loc. cit.* (4).

(3) A third possibility which is worthy of mention is that the groups, while having their electronic states in common, may each represent a one-dimensional system of bands with a common vibrational state. On this assumption, for example, the *a*, *b*, and *c* bands of  $\text{II}_F$  may correspond to vibrational transitions  $0 \rightarrow 2$ ,  $0 \rightarrow 1$ ,  $0 \rightarrow 0$ , and those of  $\text{II}_G$  to transitions  $1 \rightarrow 2$ ,  $1 \rightarrow 1$ ,  $1 \rightarrow 0$ . This possibility seems less likely, since it would lead to a Deslandres formula in which the coefficients of the linear terms in the vibrational quantum numbers would be of very different orders of magnitude. One would, in fact, be of the order  $92 \text{ cm.}^{-1}$ , and the other of the order  $1605 \text{ cm.}^{-1}$  (the interval separating the groups).

Another objection to Possibility (3) is that neither the initial nor the final state seems to be the same for the two *a* bands, although these bands occupy the same positions in the two groups. Indeed, the variation in the band constants in passing from Band  $\text{II}_F$ , *a*, to Band  $\text{II}_G$ , *a*, is so peculiar, that it is difficult to admit any explanation purely in terms of vibration quantum numbers. It must also be remembered that we are dealing with bands the presumable emitter of which is  $\text{H}_3$ , and have no adequate theory to guide us in the study of triatomic spectra.

Other regularities of the same type as the above have been detected, and serve to throw some light on the questions just considered. A consideration of these is reserved for a subsequent paper. We shall conclude the present paper with some remarks as to the identity of the emitter.

*The Emitter.*—One of the difficulties raised by the bands which have just been described is the very large difference between the initial and final moments of inertia which are of the order  $18 \times 10^{-41} \text{ gm. (cm.)}^2$  and  $45 \times 10^{-41} \text{ gm. (cm.)}^2$  respectively. As has been mentioned earlier in the present paper, the initial moment of inertia comes near the value  $19.33 \times 10^{-41} \text{ gm. (cm.)}^2$  deduced from a static model of triatomic hydrogen,  $\text{H}_3$ .\* This static model is one in which the three protons and three electrons are imagined to be situated at alternate corners of a regular hexagon, and as a tentative explanation of the facts the writers have supposed that all the bands of Type II correspond to a transition of the molecule from some such simple hexagonal configuration to an unsymmetrical configuration with one of the protons relatively distant from the other two, which would possess a much larger moment of inertia.

In addition to the evidence provided by the moments of inertia, there are three considerations which support the allocation of the Type-II bands to triatomic hydrogen :—

\* Allen, *loc. cit.* (1).

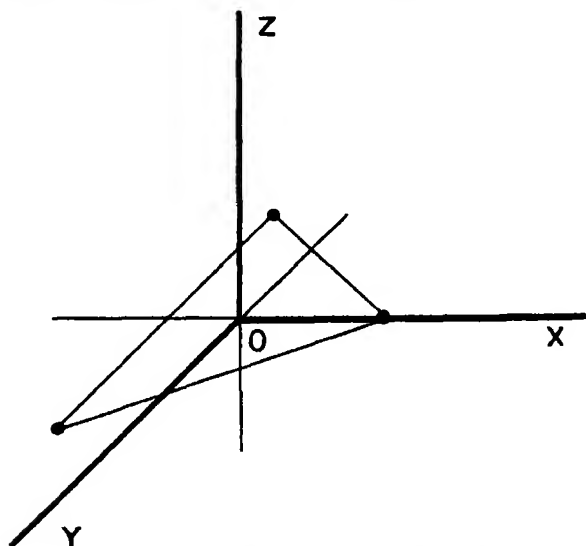
(1) The faintness of the system. We should not expect  $H_3$  to be very abundant in the Geissler-tube discharge compared with  $H_2$ .

(2) The enhancement of some of the lines in the arc at higher pressures. It is not surprising to find some of the bands due to  $H_3$  to come out strongly in the arc, *e.g.*, Band  $II_A, a$ —since the striking of an arc in hydrogen has long been known to chemists as a method of preparing “active hydrogen.”

Related to this may be the variable intensity shown by some of the lines. (See the foot-note on the line  $II_P, a, P(4)$ .) Again, the lines  $II_A, a, R(5)$  and  $II_D, a, Q(1)$  are recorded by Merton and Barratt as measured on one plate only, while Allibone's tables record a similar observation for  $II_P, a, Q(3)$ .) Such variable intensity is what we should expect from the unstable character of  $H_3$ , since the amount of  $H_3$  present during an exposure is likely to be very sensitive to small changes in the conditions of excitation.

(3) The peculiar intensity distribution of the series. We might expect to find diatomic spectra show twofold intensity alternation in the series, but hardly threefold intensity alternation such as appears in the recrudescence of intensity at  $Q(5)$  in some of the groups, since we have no analogy for this in the known diatomic bands.

In a recent letter to ‘Nature,’ J. C. Slater\* has given an explanation, based on a suggestion made by Ehrenfest and Tolman, of how twofold and threefold intensity alternation in band series may come about. A brief idea of this theory may be given diagrammatically as follows :—



\* Slater, ‘Nature,’ vol. 117, p. 555 (1926).

Suppose we regard the three atoms of a triatomic molecule as being at the corners of an equilateral triangle in the XY plane of the diagram, O being the centre of gravity of the triangle and the X axis coinciding with a median. During a complete rotation about an axis such as OY there is only one position corresponding to that of the figure. During a complete rotation about an axis such as OX, however, there are two positions, viz., the second position occurs when the two atoms not on the axis of rotation have changed places. And during a complete rotation about an axis such as OZ there are three similar positions. Taking  $\phi$  as the azimuthal co-ordinate about the last axis, it is uncertain whether the integral

$$\int p_{\phi} d\phi$$

has to be taken from 0 to  $2\pi$ , or from 0 to  $2\pi/3$ . On the latter assumption we should have

$$\int_0^{2\pi/3} p_{\phi} d\phi = mh,$$

giving

$$p_{\phi} = 3m \cdot \frac{h}{2\pi}$$

Thus every third line would be intensified.

Although such an explanation is somewhat conjectural, it is interesting to note that the symmetrical hexagonal configuration which we have assumed for the initial state in the Type-II bands would admit of just such a possibility as this, so that it is not surprising to find the lines Q(2) and Q(5) simultaneously intense.\* Moreover, if the threefold intensity alternation is traceable to the initial term,† we should expect to find R(4) simultaneously intense with Q(5). This is certainly the case for Band II<sub>F</sub>,  $\alpha$ , in which Q(5) and R(4) are noticeably intense lines. P(6) should also be simultaneously intense, although we should not expect it to be as intense as R(4). The line II<sub>F</sub>,  $\alpha$ , P(6) is scarcely a satisfactory member of the system, since it is claimed as Richardson's  $\alpha_5$  Q(2), yet it is noteworthy that there is not a single R(4), Q(5) or P(6) line which is certainly absent. Again, R(4) is noticeably stronger than R(3) in Band II<sub>A</sub>,  $\alpha$ , which shows strength in Q(5).

\* The theory suggests that Q(3) and Q(6) would have been a better numeration for these lines.

† A difficulty arises in reconciling the foregoing explanation with the writers' assumption that the bands are due to a transition from a symmetrical to an unsymmetrical molecular configuration, particularly when the Selection Principle is taken into account. Our present object is to examine various possibilities, which can be judged in their proper perspective, as the structure of these regularities becomes better known.



Whether we accept the foregoing explanation or not, it seems probable that the peculiar intensity sequence of the bands is attributable to the triatomic molecule.

*Summary.*

In a recent communication [Sandeman, 'Roy. Soc. Proc.,' A, vol. 108, p. 607, (1925)] on the secondary spectrum of hydrogen at higher pressures a band has been described, comprising a P, Q and R combination, and attributed to triatomic hydrogen. This has since been found to be one of a very considerable system of bands. These bands occur in groups, the bands of a group being spaced out at intervals of very nearly 92 wave-numbers, the spacing being in some cases approximately constant and in others conforming to a quadratic law. The bands are found both in the range of wave-lengths measured by Merton and Barratt and by Tanaka, and also in the infra-red region recently investigated by Allibone. Two groups occurring in the latter region have been considered in detail.

Experiment has shown that in some cases the lines of the groups are enhanced in the spectrum of the arc in hydrogen at higher pressures. The bands must originate in molecules with large moments of inertia, and other reasons are also advanced for believing that they are due to active or triatomic hydrogen. A complete analysis of their structure would prove an important step towards an understanding of triatomic spectra.

We wish to thank the Department of Scientific and Industrial Research for a grant towards instrumental equipment, and Prof. O. W. Richardson for helpful information and advice.

[*Note added December 13, 1926.*—In a communication which has just appeared ('Roy. Soc. Proc.,' A, vol. 113, p. 420 (1926)) Deodhar gives a list of faint hydrogen lines between 6601·99 and 3357·52 I.A. among which are the following lines which serve to fill gaps and extend the series of the above system :—

Table I, II<sub>B</sub>, b, Q(6), 21194·30 (*r*).

II<sub>B</sub>, c, Q(7), 21201·58 (*g*)

II<sub>B</sub>, d, Q(4), 20869·07 (*qd*)

Table II, II<sub>C</sub>, a, Q(6), 24223·28 (*rd*)

Table III, II<sub>D</sub>, e, Q(2), 25018·64 (*r*)

Table IV, II<sub>A</sub>, b, Q(3), 21956·50 (*r*) (Wave-number rather high.)

II<sub>A</sub>, b, Q(4), 21998·42 (*r*)

II<sub>A</sub>, c, Q(6), 22232·34 (*Od*)

Table VII, II<sub>G</sub>, a, Q(8), 15503·84 (*rd*<sup>2</sup>).

Deodhar also confirms the lines  $\text{II}_G$ ,  $b$ ,  $Q$  (1) and  $\text{II}_G$ ,  $c$ ,  $Q$  (1), his wave numbers being  $15162\cdot24$  ( $rd^2$ ) and  $15253\cdot88$  ( $rd$ ).

The missing line  $P$  (5) of the original band  $\text{II}_A$ ,  $a$ , the value of which was predicted from the Combination Principle as  $21858\cdot35$ , is present on his list as  $21857\cdot96$  ( $q$ ).  $P$  (6) is not given by Deodhar, but its predicted value occurs very near the comparatively strong line  $21906\cdot04$  ( $\text{M1H}$ , 5, 5).]

### *The Straggling of $\alpha$ Particles from Radium C.*

By G. H. BRIGGS, Ph.D., Lecturer in Physics in the University of Sydney.

(Communicated by Sir Ernest Rutherford, Pres.R.S.—Received January 19, 1927.)

[PLATE 26.]

#### § 1. *Introduction.*

It is well known that a pencil of homogeneous  $\alpha$  particles in passing through matter decrease in energy and become increasingly heterogeneous with the amount of matter traversed. It can be shown that this straggling of the  $\alpha$  particles, so named by Darwin,\* is a necessary consequence of any theory of absorption of  $\alpha$  particles in which the loss of energy depends on the transfer of energy to the electrons or nuclei of the atoms which it encounters. The well-known fact that the ranges of individual  $\alpha$  particles, whether measured by the scintillation, photographic, or Wilson cloud method, are subject to fluctuations, is an illustration of this phenomenon. This straggling is most clearly shown by observing the broadening in a magnetic field of a narrow pencil of homogeneous  $\alpha$  rays after their passage through a definite thickness of absorbing matter. No quantitative measurements have hitherto been made by this method, but this broadening was clearly shown by Rutherford† in experiments on the capture and loss of electrons by  $\alpha$  particles. It is also seen in the photographs obtained by Henderson‡ in experiments on the same subject.

The first experiments on the straggling of  $\alpha$  particles were made in 1910 by Geiger,§ who measured the variation in range of  $\alpha$  particles by the scintillation

\* 'Phil. Mag.,' vol. 23, p. 901 (1912).

† 'Phil. Mag.,' vol. 47, p. 277 (1924).

‡ 'Roy. Soc. Proc.,' A, vol. 109, p. 157 (1925).

§ 'Roy. Soc. Proc.,' A, vol. 83, p. 505 (1910).

method. This method was also used by other observers,\* but the values obtained were all several times too great, as was shown by the experiments of Makower,† who detected the  $\alpha$  particles by their photographic action and pointed out that the failure of the scintillation method is probably to be ascribed to the difficulty of counting extremely feeble and comparatively bright scintillations simultaneously. Recently the straggling of particles has been measured by the Wilson cloud method by I. Curie,‡ Meitner and Freitag§ and I. Curie and Mercier.|| The results of these experiments will be discussed in § 10.

The only aspect of the straggling of  $\alpha$  particles which has hitherto been investigated quantitatively is the straggling of the ranges at the end of the path. At any point in the range of a beam of  $\alpha$  particles, however, straggling must produce variations in the energies and velocities of particles which have traversed the same distance. At the same time there will be variations in the distances traversed by particles which have all lost the same amount of energy. At the end of the range the latter becomes the total straggling of the ranges.

In the experiments to be described below the distribution of the velocities has been measured by the magnetic deflection method for  $\alpha$  particles from radium C after passing through mica for a range of emergent velocities from  $0.98 V_0$  to  $0.22 V_0$ . From these data and the velocity curve which has also been measured over the same range of velocities, as will be described in a later paper and which will be referred to here as Part II, the straggling of the energies and ranges at any point in this region may be calculated. Thus, it has been possible to study the phenomenon of straggling over nearly the whole of the range of the  $\alpha$  particles and to determine the contribution to the total straggling of various parts of the range.

## § 2. *Description of Apparatus.*

The apparatus used for experiments with mica of stopping power less than 3.5 cm. of air is shown diagrammatically in fig. 1. A is the source of  $\alpha$  rays, a platinum wire 0.10 or 0.125 mm. diameter on which radium active deposit was collected by exposure to radium emanation in an electric field. The wire was stretched taut by a spring holding it normal to the plane of the diagram. A length of about 8 mm. of wire was effective in producing useful rays. B is

\* Taylor, 'Phil. Mag.,' vol. 26, p. 377 (1913); Friedmann, 'Wien. Ber.,' vol. 122, p. 1269 (1913).

† 'Phil. Mag.,' vol. 32, p. 222 (1916).

‡ 'Ann. de Physique,' vol. 3, p. 299 (1925).

§ 'Z. f. Physik,' vol. 37, p. 481 (1926).

|| 'J. Phys.,' vol. 7, p. 289 (1926).

a sheet of mica almost touching the wire. Mica was chosen as the absorbing material because it is practically the only substance which can readily be

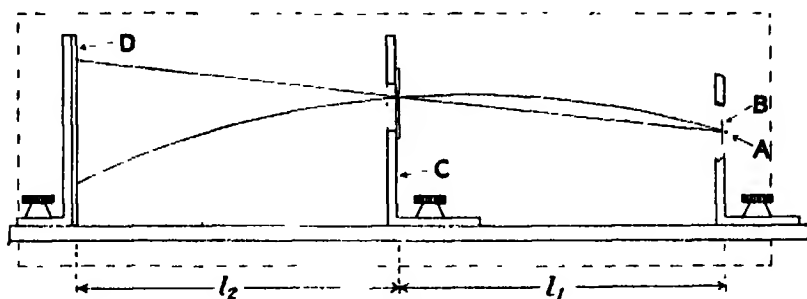


FIG. 1.

obtained in sufficiently thin uniform sheets. Four slits spaced at distances of about 2 mm. were mounted on C; only one slit is shown in the diagram. The slits were made of copper, the edges were accurately ground and polished, and the angle between the two faces forming an edge was about  $130^\circ$ . The widths of the slits were 0.48, 0.88, 0.51 and 0.80 mm. wide. D is a photographic plate, 6 by 1.8 cm. The distance from A to D was 21 cm. and C was placed midway between the source and the plate. The supports carrying A, B and C were fastened to a brass base and the whole could be slid into a brass box between the poles (shown by dotted lines) of a large electro-magnet. This electro-magnet had been designed for use in the Cavendish Laboratory in experiments with large deflections of  $\alpha$  particles. The rectangular ends of the pole pieces are 24 by 8.5 cm. and for a gap of 2.7 cm., and a field of 10,000 gauss, the variation is only a few gauss over the greater part of the area. The pressure in the brass box could be reduced rapidly to less than  $10^{-4}$  mm. of mercury by a diffusion pump. Mercury vapour was kept out by liquid-air traps. A shutter worked by a windlass could be lowered over the slits to prevent  $\alpha$  particles from reaching the plate before the pressure was sufficiently reduced. With a field of 10,000 gauss the deflection with a bare source was about 23 mm. Fluctuations in the current through the electro-magnet were detected by a potentiometer, and it was found quite possible to keep the current constant to within 1 in 20,000.

The exposure for the deflected lines was made first and was generally begun 15 to 20 minutes after the source was removed from the activating apparatus. If the mica was less than 2 cm. equivalent air stopping power, an exposure of 15 to 20 minutes was sufficient with a source of  $\gamma$ -ray activity equivalent to 15

milligrams, and the undeflected lines would then require an exposure of 30 to 90 minutes, depending on the broadening to be expected.

To find the mean reduction in velocity produced by the particular piece of mica employed, it was generally arranged that the mica did not completely cover the source, so that simultaneously with the deflected lines from the four slits a set of lines, due to particles having the initial velocity of  $\alpha$  particles from radium C, were produced. The residual field of the electro-magnet was so small that these faster particles did not produce any alteration in the width of the undeflected bands. A gap of two- or three-tenths of a millimetre was sufficient to give satisfactory lines of this kind. Except for a small correction due to the fact that the deflection is not exactly a linear function of  $1/r$  ( $r$  being the radius of curvature of the path), the value of  $V/V_0$  is given by the ratio of the deflection of this no-mica line to that of the main deflected line.

### § 3. Calibration of the Photographic Plates.

Ilford process plates were found to be the most satisfactory among several kinds tried. They were calibrated by making a series of exposures in overlapping steps under conditions very similar to those in the straggling experiments. The plates were exposed in pairs, one on either side of a wire activated with radium C, and care was taken to see that the obliquity effect noted by Bothe\* did not produce serious errors. When the plates were measured with a microphotometer it was found that the relation between the number of  $\alpha$  particles per unit area and the resulting density could be represented by an exponential curve of the form  $D = D_0 (1 - e^{cN})$ . The calibration extended over ranges of density from 0.01 to 2.2. At the latter density the slope of the curve was still about two-thirds of its initial value. For some plates the times of exposure varied by a factor of 180, the source remaining constant to 5 per cent. It follows, therefore, that the Schwarzschild factor  $p$  must be approximately unity, and the exponential form of the law seems to indicate a simple relationship between density and exposure for  $\alpha$  rays, namely, that the rate of increase of density is proportional to the number of  $\alpha$  rays falling on the plate at any instant multiplied by the number of grains which are left unacted upon at that instant. A similar exponential law was found by Kinoshita† for other types of plates.

In the straggling experiments densities of more than 0.8 were infrequent. It is clear from the curve that only a small error is made by assuming that the density is proportional to the number of  $\alpha$  particles. In the experiments on

\* 'Z. f. Physik,' vol. 8, p. 243 (1921-22); vol. 13, p. 106 (1923).

† 'Roy. Soc. Proc.,' A, vol. 83, p. 432 (1920).

stragglings the breadth of the bands is the quantity which is required and any error due to the above assumption is quite negligible.

#### § 4. Measurement of the Distribution of Density in the Bands.

The distribution of density in the bands was measured with a micro-photometer making use of the null method of Dobson and measuring the density directly in terms of a neutral grey wedge. In this instrument a magnified image of the line is projected on a narrow slit so that at any one setting a narrow portion of the line is sorted out. The length of this portion on the photographic plate was about 1.5 mm. For the narrowest lines (0.24 mm. wide) the width of the slit was one-twelfth of the width of the image of the line. The effect of this finite width of slit will be discussed later.

A typical example of the results obtained is given in fig. 2, which shows the

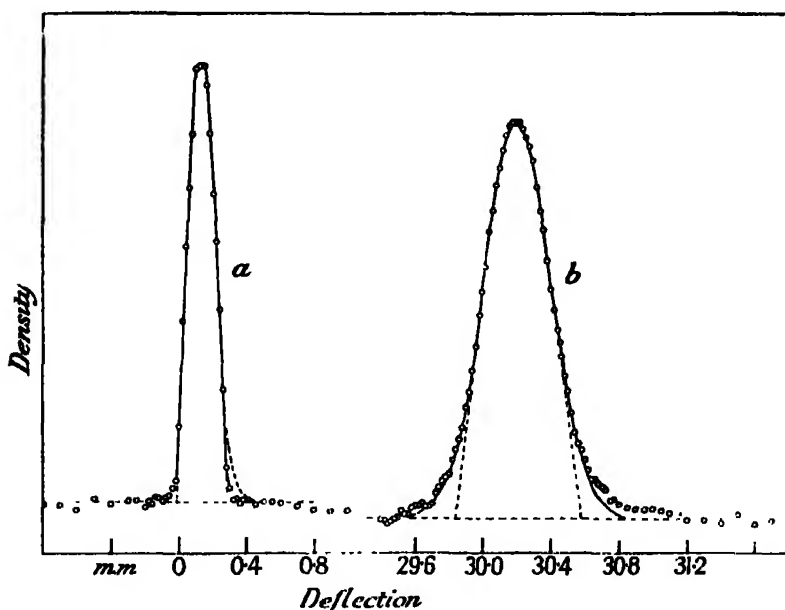


FIG. 2.— Density Curves.  $V/V_0 = 0.825$ .

*a*, Undelected Lines; *b*, Deflected Lines.

distribution of density in the undeflected and deflected lines for an exposure made with mica of 3.05 cm. air equivalent stopping power. The mean velocity was  $0.825 V_0$  and the mean deflection 29 mm. The broadening of the deflected line shows that the velocities of the  $\alpha$  particles are no longer homogeneous. For the same average deflection this broadening increased with the thickness of the

mica, while measurements of the breadth of the undeflected line from any one slit remained constant to within a few per cent.

The question whether there is any appreciable variation in the velocity of the rays when they leave the source was investigated by making exposures in the usual way but without any absorbing material. These experiments will be described in Part II. It was found that the rays from the source were not strictly homogeneous but a number difficult to estimate; probably about 5 per cent. had velocities less than the maximum by amounts up to 1.5 per cent. The general form of deflected line obtained without mica can be illustrated by modifying the undeflected line (a) of fig. 2 by the dotted line shown. This slight lack of homogeneity is probably chiefly due to some of the radium B being shot into the wire by recoil during activation, and in the deflected lines obtained with mica produces a slight lack of symmetry apparent on the low-velocity side, but only near the base. This lack of symmetry gradually disappears as the broadening gets greater with increasing thickness of mica. It is apparent in the line (b) shown in fig. 2, but the error produced by this effect in the determination of the distribution coefficient of the variation in velocity is negligible.

#### § 5 *Calculation of the Distribution of Velocities from the Experimental Data.*

The most satisfactory theory of the straggling of  $\alpha$  particles is that given by Bohr,\* which will be discussed later. This theory leads to the conclusion that the law of distribution about the mean energy of the energies of a beam of  $\alpha$  particles which have all passed through the same thickness of absorbing material is to a high degree of approximation Gaussian in form, so that if  $T$  is the mean energy of the  $\alpha$  particles and  $W(t)dt$  denotes the probability that  $T$  has a value between  $T - t$  and  $T + t + dt$ , then

$$W(t)dt = \frac{1}{\rho\sqrt{\pi}} e^{-t^2/\rho^2} dt. \quad (1)$$

[The term "distribution coefficient" will be used to denote any parameter such as  $\rho$  in an equation of this type.] Bohr further concludes that the distribution of the ranges at the end of the path is also of this form, and it can readily be proved that if the straggling is small, the distribution of velocities must be of the same form as the distribution of energies but with a different distribution coefficient.

In the present experiments a probability distribution of velocities would

\* 'Phil. Mag.,' vol. 30, p. 531 (1915).

give rise to a probability distribution of deflections if the straggling is small, for if  $D$  is the deflection and  $V$  the velocity,

$$\frac{\delta D}{\bar{D}} = -\frac{\delta V}{\bar{V}}, \quad (2)$$

if  $\delta V$  is small. If the mean velocity and mean deflection are taken as unity, the distribution coefficient of the deflections is equal to the distribution coefficient of the velocities.

If the undeflected line is narrow compared with the deflected line, and the rays are initially homogeneous, we should, therefore, expect from Bohr's theory that the distribution of density in the deflected line would be given by an expression of the form

$$y = \frac{1}{\sigma_1 \sqrt{\pi}} e^{-(x/\sigma_1)^2} dx. \quad (3)$$

A similar result would be expected, even when the broadening is small, if the density in the undeflected line happened to be distributed according to a law of the form given by equation (3). For if each element of area beneath a curve defined by  $y = \frac{1}{\sigma_1 \sqrt{\pi}} e^{-(x/\sigma_1)^2} dx$  is distributed about its centre according to

a law  $y = \frac{1}{\sigma_2 \sqrt{\pi}} e^{-(x/\sigma_2)^2} dx$ , the final result of distributing the original area is

now an area bounded by the curve  $y = \frac{1}{\sigma_3 \sqrt{\pi}} e^{-(x/\sigma_3)^2} dx$ , where

$$\sigma_3^2 = \sigma_1^2 + \sigma_2^2. \quad (4)$$

In curve *b*, fig. 2, the plotted points are the actual photometer readings and the smooth curve represents a distribution of the form given by equation (3). Allowing for the slight initial lack of homogeneity, there is no experimental evidence of any departure from a law of this form for the distribution of velocities except near the end of the range, where the relative variation in velocity is large. We take this law as a basis of calculation and have to deduce from the form of the density curves the variation in velocity which we may express by means of a distribution coefficient  $\rho_2$ , defined as follows:—If  $V$  be the velocity of an  $\alpha$  particle and  $\bar{V}$  the most probable velocity, the probability  $W(s) ds$  that  $V$  has a value between  $\bar{V}(1+s)$  and  $\bar{V}(1+s ds)$  is given by the equation

$$W(s) ds = \frac{1}{\rho_2 \sqrt{\pi}} e^{-(s/\rho_2)^2} ds, \quad (5)$$

where  $s$  gives the variation in velocity as a fraction of the mean velocity.



If tangents are drawn at the points of inflexion of the curve for equation (3), intercepting a length  $d$  on the base, then

$$d = 2\sigma\sqrt{2}, \quad (6)$$

so that if we have two such curves with coefficients  $\sigma_1$  and  $\sigma_3$ , we can deduce from equations (4) and (6) the distribution coefficient  $\sigma_2$  which transforms curve 1 into curve 3 from the relation

$$\sigma_2 = \frac{\sqrt{2}}{4} \sqrt{(d_3^2 - d_1^2)}. \quad (7)$$

Neglecting for the present the correction due to the fact that the density curves of the undeflected lines are not true probability curves, it follows that

$$\rho_2 = \frac{\sqrt{2}}{4D} \sqrt{(d_2^2 - d_1^2)}, \quad (8)$$

where  $D$  is the mean deflection of the band and  $d_1$  and  $d_2$  are the intercepts on the base of the density curves made by tangents at the points of inflexion.

This method of deducing the spreading from the intercepts on the base made by tangents at the points of inflexion of the deflected and undeflected bands has several advantages over methods based on the areas and heights of the curves, for owing to small irregularities the shapes of the curves at the top differ slightly, but the sides, like those of a true probability curve, are practically straight over a considerable distance, so that the tangents can be drawn with a high degree of accuracy. Further, since the slight initial lack of homogeneity produces no detectable increase in the intercept on the base of the deflected lines obtained with no mica, where the effect would be a maximum, it seems that this method of calculating  $\rho_2$  eliminates any error due to lack of homogeneity.

In using equation (8) corrections should be applied, since (i) the deflected line undergoes a certain amount of broadening merely on account of geometrical considerations, and (ii) the calculated value of  $\rho_2$  may require correction because the distribution of density in the undeflected line cannot be expressed by an equation of the form (2).

(i) Referring to fig. 1 it can be shown that the deflection  $d$  is given by  $d^2 - d(m + p) + n = 0$ , where

$$m = (l_1 + 2l_2) \tan \theta,$$

$$n = \frac{(l_1 l_2 + l_2^2)}{\sec^2 \theta},$$

$$p^2 = 4r^2 \cos^2 \theta - l_1^2,$$

$\theta$  is the angle between the path of the undeflected beam and the normal to the plate, and  $r$  is the radius of curvature of the deflected beam.

Hence

$$2d = m + p - \sqrt{(m + p)^2 - 4n}$$

$$= f(m, n, p).$$

Writing

$$\frac{dd}{d\theta} = \frac{\delta f}{\delta m} \frac{\delta m}{\delta \theta} + \frac{\delta f}{\delta n} \frac{\delta n}{\delta \theta} + \frac{\delta f}{\delta p} \frac{\delta p}{\delta \theta},$$

we deduce

$$\frac{dd}{d\theta} = \{1 - a(m + p)\} \left\{ \frac{m}{\sin 2\theta} - \frac{r^2 \sin 2\theta}{p} \right\} + 2an \tan \theta,$$

where

$$a = \{(m + p)^2 - 4n\}^{-\frac{1}{2}}.$$

The results of evaluating this expression for the four slits and a deflection of 30 mm. are given in the following table :—

Table I.

Slit.	Tan $\theta$ .	$dd/d\theta$ .	Percentage correction.
<i>a</i>	0.1012	-0.286	-1.36
<i>b</i>	0.0800	-0.456	-2.17
<i>c</i>	0.0564	-0.661	-3.14
<i>d</i>	0.0390	-0.850	-4.04

The negative sign means a broadening of the deflected lines, and the fourth column gives as a percentage of the width of the deflected bands the correction which must be applied on this account.

(ii) Fig. 3 shows diagrammatically a probability curve (*a*) and a typical curve for an undeflected line (*b*) drawn so that they have the same tangents at the points of inflexion. The lower curves *c*<sub>1</sub>, *c*<sub>2</sub> were obtained by subtracting ordinates. The ordinates at *C*<sub>1</sub> and *C*<sub>2</sub> divide these curves into equal areas. For the purpose of calculation we will consider that *c*<sub>1</sub> and *c*<sub>2</sub> are replaced by probability curves of the same area and base. Then choosing some suitable distribution coefficients, we calculate the resulting curves when *a*, *c*<sub>1</sub> and *c*<sub>2</sub> are distributed with this coefficient. These will be probability curves, and can readily be plotted. They are shown at *a'*, *c'* and *c*<sub>2</sub>', the distances between the centres being unchanged. By subtracting ordinates we get *b'*, which must be approximately the true curve if the area *b* had been distributed with coefficient  $\sigma$ . We may now draw in the tangents at the points of inflexion to *b* and *b'*

,  $\frac{\sqrt{2}}{(d_1 - d_2)^{\frac{1}{2}}}$  Comparing the result with  $\sigma$  we see at once

the correction which must be applied to the former to give the actual distribution coefficient  $\sigma$ . It is most convenient to express the correction as a function

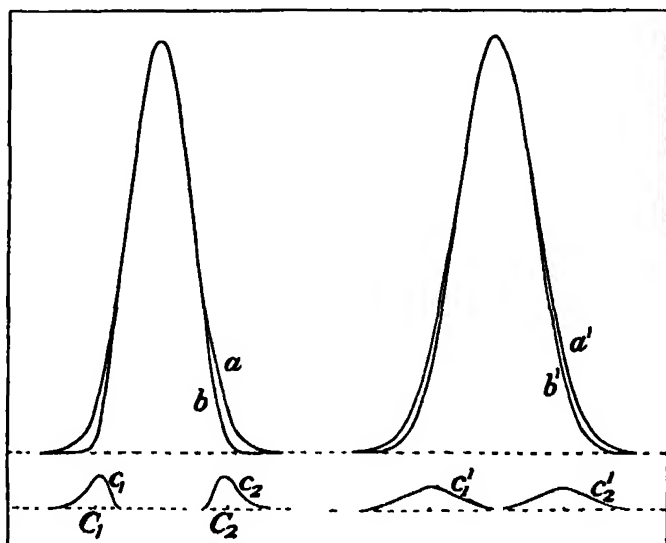


FIG. 3.—Method of Correcting Shape of Undeflected Line.

of  $d_2/d_1$ . The correction is negligible when this ratio is greater than 1.7, and this corresponds in the experiments to a thickness of mica of about 2 cm. air equivalent stopping power. The magnitude of the correction is shown in Table II.

Table II.

Ratio $d_2/d_1$ .	Correction percentage.	Ratio $d_2/d_1$ .	Correction percentage.
1.2	11.0	1.5	3.5
1.3	8.0	1.6	1.8
1.4	5.6	1.7	0.7

There will be no correction on account of the width of the slit of the photometer, since it can be shown that it is sufficiently narrow not to alter the position of the straight sides of the density curves from which the width of the line is determined. Its chief effect is to alter slightly the shape of the density curves near the base.

Details of the calculations of  $\rho_s$  from the observational data will now be given for an experiment with mica of 3.05 cm. stopping power. The photometer curves for the lines for slit  $b$  have been shown in fig. 2.

Table III.

Slit.	Width of line.		Geometrical correction	$d_2$ corrected	$(d_2^2 - d_1^2)^{\frac{1}{2}}$	Deflection.
	Undelected $d_1$ .	Deflected $d_2$ .				
	mm.	mm.	Per cent	mm.	mm.	mm.
<i>a</i>	0.244	0.686	1.4	0.677	0.632	28.99
<i>b</i>	0.298	0.748	2.2	0.723	0.669	29.08
<i>c</i>	0.245	0.708	3.1	0.686	0.641	29.18
<i>d</i>	0.290	0.748	4.0	0.718	0.659	29.35
				Mean	0.650	29.15

Ratio  $d_2/d_1 = 3$  approximately, so that there is no correction on account of the zero line not being a true probability curve. We have, then,

$$\rho_2 = \frac{\sqrt{2} \cdot 0.650}{4 \cdot 29.15} = 7.88 \times 10^{-3}.$$

#### § 6. Experiments at Low Velocities.

The arrangement of source slits and plate which has been described proved quite suitable for mica up to 4.5 cm. air equivalent. At greater thicknesses, owing to the increased width of the bands and the decrease in photographic action of the rays, the experiments were made with the distance between source and plate considerably reduced. With mica greater than 6 cm. air equivalent the straggling became so great that deflections of 1 cm. and less for slower velocities gave ample broadening.

It was found that for emergent ranges of less than 2 cm. the density curves for the deflected band showed some asymmetry. The curve (*a*) in fig. 4 is a typical example. The density curves indicated a preponderance of particles on the low-velocity side of the peak, and it was first thought that this effect might be due to scattering in the mica. For it is possible that some of the rays passing obliquely through the mica may have their direction changed by scattering so as to enable them to pass through the slit. Such rays would traverse a greater thickness of mica than those which pass through normally, and so might produce a lack of symmetry of the kind found.

To reduce any such effect the apparatus was modified by substituting a single slit instead of the set of four and placing an additional slit between the source and the main slit at a distance of 5 mm. from the source. The width of this subsidiary slit was 0.125 to 0.15 mm. The mica, instead of being close to the

source, was now placed over this slit, and the source and both slits were placed outside the poles of the magnet, only the plate being between the poles. The

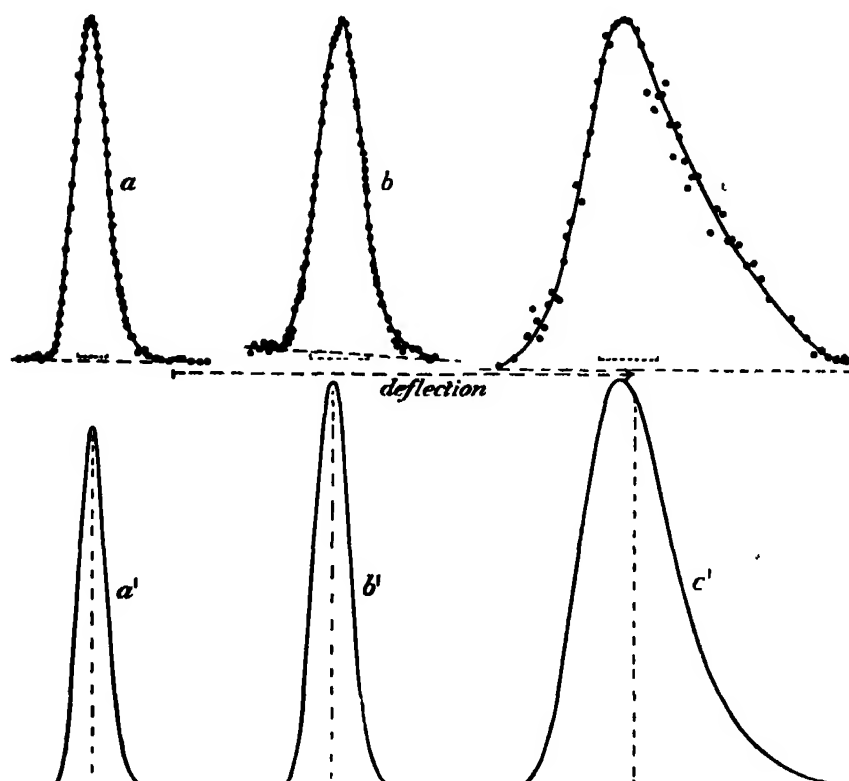


FIG. 4.

	Mica	$V/V_0$	$\rho_2$
<i>a</i>	5.50	0.56	$40.5 \times 10^{-3}$
<i>b</i>	5.87	0.49	48.4
<i>c</i>	6.45	0.30	155.0

additional slit cut out nearly all rays scattered through angles greater than  $2^\circ$ ; it does not eliminate rays scattered laterally, but these will be a small fraction of the total number scattered. For angles of scattering less than  $4^\circ$  the increase in path is unimportant.

The effect to be expected from scattering in the mica can be seen from the following table. The range of the  $\alpha$  particles has been divided into intervals and a mean velocity taken for each. The values in the third column are the fraction of the  $\alpha$  particles, which, on the theory of single scattering, should experience deflections of more than  $4^\circ$  in traversing the given interval. The results have been calculated for mica, assuming a mean atomic number 12.

Table IV.

Length of interval.	Mean value of $V/V_0$ .	Per cent.	Length of interval.	Mean value of $V/V_0$ .	Per cent.
cm.			cm.		
1	0.98	0.3	0.25	0.53	0.9
1	0.90	0.5	0.25	0.47	1.5
1	0.85	0.6	0.25	0.41	2.6
1	0.80	0.7	0.25	0.33	6.2
1	0.7	1.2	0.20	0.23	21.0
0.5	0.6	1.2			

This is sufficient to show that the effect of scattering should be negligible in these measurements at the higher velocities, and may become appreciable for velocities less than  $0.5 V_0$ , increasing rapidly towards the end of the range. For these lower velocities the additional slit will almost eliminate the effect of scattering, except, perhaps, for velocities less than  $0.25 V_0$ .

To determine  $V/V_0$  the same method as before was used to obtain on the plate a line due to particles which had not passed through the mica. Since for the slow rays the effective width of the source was now the width of the additional slit, the widths of the undeflected band for the two sets of rays would differ. It was therefore advisable that these swifter rays should not fall on the plate during the exposure for the undeflected band. For this purpose a small shutter was arranged to cover the gap left at the edge of the mica.

It was now found that with the additional slit the values of  $\rho_2$  for mica thicker than 4.5 cm. were smaller than before, the decrease becoming greater with the thickness of the mica and amounting to about 5 or 6 per cent. for mica of 6 cm. air equivalent. There is little doubt that with velocities less than  $0.6 V_0$  scattering makes the emergent beam in an apparatus with only one slit more heterogeneous than it would be owing to straggling alone. The additional slit did not eliminate the asymmetry, which became very marked at lower velocities. For example, curves *b* and *c*, fig. 4, were obtained with the modified apparatus and with mica of 5.87 and 6.45 cm. air equivalent respectively. The three curves in fig. 4 have all been reduced to the same mean deflection and show the rapid increase in the breadth of the deflected line, which takes place towards the end of the range.

Further consideration shows that some such asymmetry is to be expected on theoretical grounds. For if the energy losses of particles which have all passed through the same thickness of absorbing material are distributed approximately according to a Gauss error law, then, as was pointed out previously,

the velocities will be distributed by a law of this same type when the average departure from the mean is small compared with the average energy. Towards the end of the range, when this condition does not hold, a Gaussian distribution of energy losses will lead to an asymmetric distribution of velocities and a still more asymmetric distribution of density on the photographic plate. The curves  $a'$ ,  $b'$  and  $c'$ , fig. 4, show the theoretical shape of density curves calculated by assuming an infinitely narrow undeflected line and a Gaussian distribution of energies with distribution coefficients equal to those deduced from the curves  $a$ ,  $b$  and  $c$  respectively. It is seen that there is an increasing asymmetry in both the theoretical and observed curves, and that the latter are not inconsistent with a Gaussian distribution of energies. The two sets of curves are not exactly comparable on account of the finite width (indicated by dotted lines) of the undeflected bands. Strictly, then, we are not justified in speaking of a distribution coefficient of the velocities or deflections near the end of the range, since neither can be represented by a Gauss probability curve. Practically, however, it was convenient to continue to determine the quantity  $\rho_2$  by drawing tangents to the curves at the points of inflexion, as described in § 5. By drawing tangents to theoretical curves such as  $a'$ ,  $b'$  and  $c'$  in fig. 4 and comparing the result with the coefficients used to calculate these curves, it was found that the values of the straggling coefficients of the energies deduced from curves when there is asymmetry of this type are too small by an amount which increases from zero when the velocity is  $0.5 V_0$  to 2.5 per cent. at  $0.36 V_0$  and 10 per cent. at  $0.22 V_0$ .

The band due to the singly charged  $\alpha$  particles was not observed on the plates for velocities greater than  $0.83 V_0$ , but at  $0.7 V_0$  it was sufficiently well defined to allow measurements of the straggling to be made on it. These agreed to within the limits of experimental error with those obtained from the double-charged band. For slightly smaller velocities the broadening was so great that the two bands began to overlap and at  $0.22 V_0$  the  $\text{He}_{++}$  was so feeble as to be useless for measurements. These rapid changes in the widths and intensities of the two bands have been noted by Henderson\* and by Rutherford.† Some measurements of the ratio of the intensities found by the present photographic method will be described in Part II. At the low velocities long exposures with large sources were necessary and the fogging of the plates by  $\gamma$  rays was serious. The experiments were not carried beyond  $0.22 V_0$ . At velocities but little less than this an appreciable number of the particles do not emerge from the mica, and the method of experiment obviously fails.

\* Henderson, *loc. cit.*

† Rutherford, *loc. cit.*

## § 7. Results.

Reproductions of some of the photographs are shown in Plate 26.

The observed values of the straggling are given in Table V. The stopping power of the mica was measured by the scintillation method and the results which are expressed as the air equivalent at 15° C. and 760 mm. are probably correct to 0.01 mm. Column 2 gives  $\rho_2$ , the distribution coefficient of the velocities expressed as a fraction of the mean velocity of the particles at that point in the range. These results are shown graphically in fig. 5. The values obtained with the single slit apparatus for mica thicker than 4.5 cm. air equivalent are shown in brackets in the table and by crosses in the diagram. Column 3 gives  $\rho_1$ , the distribution coefficient of the energies defined in § 5.  $\rho_1$  is calculated from  $\rho_2$  by means of the relation

$$\rho_1 = \rho_2 MV^2, \quad (9)$$

where  $M$  is the mass of the  $\alpha$  particle and  $V$  is the mean velocity on emergence from the mica.

Table V.

Air equivalent of mica.	$\rho_2$ .	$\rho_1$ .	Air equivalent of mica.	$\rho_2$ .	$\rho_1$ .
cm.	ergs.	ergs	cm.	ergs.	ergs
0.315	1.53 $\times 10^{-8}$	3.63 $\times 10^{-8}$	5.089	(28.6)	(27.8)
0.551	2.12	4.94	5.106	(31.3)	(30.2)
1.026	3.06	6.80	5.432	35.0	28.3
2.113	5.08	9.83	5.432	36.6	29.4
2.409	5.86	10.9	5.499	(40.5)	(31.8)
3.053	7.88	13.2	5.661	40.9	29.0
3.066	7.64	12.7	5.866	48.4	28.1
3.487	9.23	14.2	6.066	(70.1)	(33.2)
3.490	9.56	14.6	6.066	(72.6)	(34.5)
4.092	12.6	16.9	6.067	67.3	31.8
4.098	12.0	16.4	6.296	92.4	29.5
4.492	17.0	20.2	6.445	161	32.9
5.533	(17.6)	(20.7)	6.501	207	32.6
5.008	(27.9)	(28.0)	6.659	276	32.5
5.056	26.3	25.6			

The accuracy of the determination of  $\rho_2$  is greatest between 3 and 5 cm., for here the various corrections are negligible and there was no difficulty in obtaining good plates. The probable error in  $\rho_2$  is here about 2 to 3 per cent. The probable error increases towards the end of the range, and in the last three results it is about 10 to 15 per cent. This is illustrated by the irregularity in the values of  $\rho_1$  towards the end of the range. Theoretically  $\rho_1$  cannot anywhere



show a decrease with increasing thickness of absorbing material such as occurs in the results given.

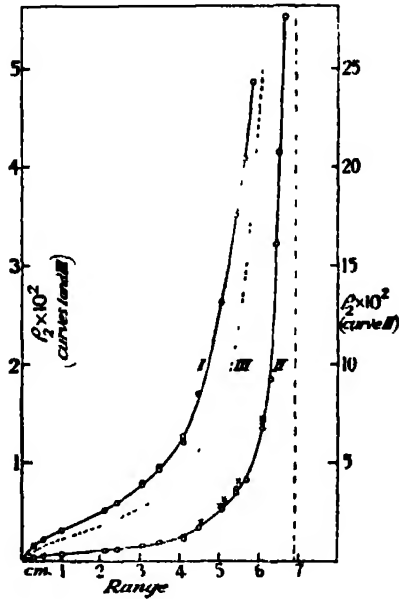


FIG. 5.—I and II observed, III calculated on Bohr's theory.

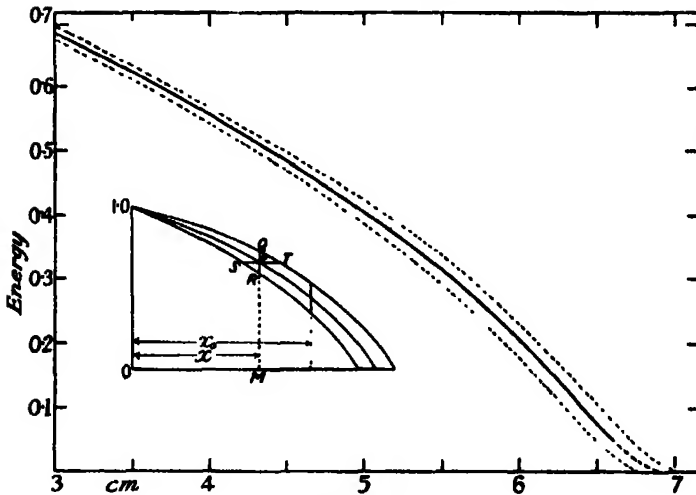


FIG. 6.

The variation in energy is illustrated in fig. 6 for the last 4 cm. of the range. The central curve gives the mean energy of the  $\alpha$  particles and the outer curves are drawn so that at any point P

$$PQ = PR = \rho_1.$$

1

2

3

4

5

Nos. 1 to 5. Obtained with the four-slit apparatus. Four undeflected lines to the left and the four corresponding  $\text{He}_+$  lines to the right. The no mica lines are just visible on each plate a little to the left of the  $\text{He}_+$  lines in No. 1, and at successively increasing distances in the other plates. The  $\text{He}_+$  line appeared in No. 4. The thicknesses of the mica (air equivalent) were 0.32, 0.55, 1.03, 3.05 and 3.49 cm.

6

7

8

9

10

11

12

The sequence of the lines from left to right is given below and the thickness of the mica for each plate.

No. 6. Undeflected,  $\text{He}_+$ , no-mica,  $\text{He}_+$ , 4.5 cm

No. 7 — " "  $\text{He}_+$ ,  $\text{He}_+$ , 4.5 cm

No. 8.—Broad band due to  $\beta$  rays deflected to the left in the residual field during exposure for undeflected line also evident in 7 and 11. Undeflected,  $\text{He}_+$ , no-mica,  $\text{He}_+$ , 4.8 cm.

No. 9. Undeflected,  $\text{He}_+$ , no-mica,  $\text{He}_+$ , 5.0 cm

No. 10. — " " " " 5.4 cm.

No. 11.— $\beta$  rays, undeflected, no-mica,  $\text{He}_+$ ,  $\text{He}_+$ , 6.0 cm.

No. 12. Undeflected, no-mica,  $\text{He}_+$ ,  $\text{He}_+$ , 6.4 cm.

The direction of the deflection is from left to right. The main deflected band and the band singly charged  $\alpha$  particles are referred to as  $\text{He}_+$  and  $\text{He}_+$ . The line used for determining  $V/V_0$ , which was due to  $\alpha$  particles which did not pass through the mica, is here called the "no-mica" line.



From tables of the error integral it follows that 84 per cent. of the particles have energies lying between the outer curves.

The distribution of the energies at any point leads at once to the straggling of the ranges. For in the diagram PT represents the distribution coefficient of the distances traversed by particles which have all been reduced to an energy PM. If we write  $PT = \rho_3 OM$ , then  $\rho_3$  is the distribution coefficient of the ranges expressed as a fraction of the mean distance traversed OM and

$$\rho_3 x = \rho_1 (dT/dx)^{-1}. \quad (10)$$

Table VI gives  $\rho_3$ , and  $\rho_3 x$  which is the straggling of the ranges in centimetres, when the mean distance traversed is that given in column 1.

Table VI.

Stopping power of mica.	$\rho_3$ observed.	$\rho_3 x$ observed.	$\rho_3 x$ calculated on Bohr's theory	$\rho_3$ , $\frac{\text{observed}}{\text{calculated}}$
cm.		cm.	cm.	
0.5	7.78 $10^{-2}$	$3.89 \times 10^{-2}$	$2.83 \times 10^{-2}$	1.37
1.0	5.44	5.44	3.96	1.37
1.5	4.31	6.16	4.78	1.35
2.0	3.63	7.26	5.45	1.33
2.5	3.25	8.12	6.00	1.35
3.0	2.90	8.87	6.48	1.37
3.5	2.77	9.70	6.88	1.41
4.0	2.53	10.12	7.22	1.40
4.5	2.43	10.87	7.48	1.45
5.0	2.42	12.13	7.69	1.58
5.5	2.17	11.92	7.84	1.52
6.0	1.86	11.17	7.94	1.41
6.5	1.77	11.48	8.01	1.43

Strictly we cannot have in general both PQ equal to PR and PT equal to PS. It can be shown from an argument which will be given in § 8 that the straggling of the ranges will be represented exactly by a Gauss probability curve, so that we should have in fig. 6  $SP = ST$ , and PQ not necessarily equal to PR. The assumption which was made earlier that the variation in energy can be represented by a Gauss error curve is, therefore, not strictly correct. However, in the first 6.6 cm. of the range the greatest departure is at about 5.5 cm., when PR is about 3 per cent. greater than PQ. This asymmetry is altogether too small to be detected experimentally. We may then continue to assume that in the whole range investigated that both the straggling of the ranges and energies can be represented by Gauss error curves.

§ 8. *The Theory of Straggling.*

Theories of the straggling of  $\alpha$  particles have been given by Flamm\* and Bohr.† In both theories it is assumed that the phenomenon is due to probability variations in the energy losses of the  $\alpha$  particle and that these losses may be calculated on classical grounds, assuming the electrons to be at rest.

The two theories give substantially the same result for the straggling due to transfers of energy to the electrons. The small difference in the calculated values is due to the fact that Flamm assumes the law  $R = kV^3$ , while Bohr deduces the rate of loss of energy from his own theory of stopping power. Values of  $\rho$ , the total straggling of the ranges, *i.e.*, the value of  $\rho_s$  when  $x = R$  in the notation used in § 7, calculated on the two theories, are given in Table VII.

Table VII.

Theoretical values of  $\rho$  for an

Bohr.	Flamm.			
	Electrons.	Electrons corrected.	Electrons + nuclei	Electrons + nuclei corrected
Radium C $1.16 \times 10^{-2}$	$0.985 \times 10^{-2}$	$1.09 \times 10^{-2}$	$1.114 \times 10^{-2}$	$1.240 \times 10^{-2}$
Polonium 1.20	1.080	1.213	1.234	1.375

The correction applied above to the value given by Flamm is necessary, since he used  $e = 4.65 \times 10^{-10}$  e.s.u. and  $V = 2.06 \times 10^9$  cm., and the fourth power of the ratio of these quantities enters into the formula.

Flamm concluded that transfers of energy to the nucleus will produce an appreciable straggling—roughly one-third of the total—but as Bohr has pointed out, any effect due to the nucleus will not be Gaussian in form. It is clear that a small number of  $\alpha$  particles will experience a considerable reduction in range on account of close nuclear collisions such as give rise to the phenomenon of single scattering. If we recalculate Flamm's nuclear straggling, neglecting all collisions for which the angle of scattering is greater than (i)  $5^\circ$ , (ii)  $20^\circ$ , the result is reduced to (i) 0.6 per cent., (ii) 14 per cent. of the original value. We may therefore safely neglect any straggling due to the nucleus at least in the first 6 cm. of the range and shall compare our experimental results with

\* 'Wien. Ber.,' vol. 123, p. 1393 (1914).

† *Loc. cit.*

values deduced from Bohr's theory from which the straggling of the energies and velocities may be readily deduced.

Bohr shows that, if  $\Delta_0 T$  be the average loss of energy in the distance  $dx$  and  $\Delta T$  the actual loss of any particular particle, then the probability  $W(\Delta T)dT$  that  $\Delta T$  has a value between  $\Delta T$  and  $\Delta T + dT$  ( $dT$  being small compared with  $\Delta T$ ) is given by the equation

$$W(\Delta T) dT = \frac{1}{\sqrt{\pi}} \frac{1}{(2P \frac{\Delta_0 T}{dx})^{\frac{1}{2}}} e^{-\frac{(\Delta T - \Delta_0 T)^2}{2P \frac{\Delta_0 T}{dx}}} dT, \quad (11)$$

where

$$P dx = \int Q^2 dA, \quad (12)$$

$dA$  being the number of collisions for which the loss of energy is  $Q$ . One important feature of this work is that the expression  $\int Q^2 dA$  for the parameter  $Pdx$  which defines the distribution of the energies after traversing a small distance  $dx$  is deduced on quite general grounds, no assumptions as to the amount of energy transferred at a collision being necessary.

Bohr shows that the distribution of the ranges expressed as a fraction of the total range is given by a distribution coefficient  $\rho$  where

$$\rho^2 = \frac{1}{R_0^2} \int_0^1 2P \left( \frac{dT}{dx} \right)^{-3} dT, \quad (13)$$

$T$  being the energy of the particle and  $R_0$  the mean range. Bohr calculates  $P$  on the assumption that the electrons are at rest in the atom and finds that  $P$  is independent of the velocity of the  $\alpha$  particles and of the binding forces of the electron; the value is given by

$$P = 16\pi e^4 N n, \quad (14)$$

where  $N$  = number of atoms per cubic centimetre.

and  $n$  = number of electrons in one atom.

We may now calculate in terms of  $P$  the theoretical distribution of the energies and velocities of a beam of particles which have all traversed a given distance  $x$ . Let us first consider a beam of particles which as a result of straggling have their energies on reaching a point  $P$  (see fig. 6) distributed over the range  $QR$ . Let us suppose that these particles proceed to the end of their range without any further probability variations occurring. The paths described in the diagram by the particles will then be such that the distance between them measured parallel to the base will be constant. If we examine the

distribution of energies when they have gone a total distance  $x_0$ , we find that the energy differences are greater than before in the ratio  $\frac{dT}{dx_0} / \frac{dT}{dx}$ , i.e., in the ratio of the average slope of the curves at  $x_0$  and at  $x$ .

This magnification of the energy variation due to change in  $dT/dx$  gives the answer to the question whether on theoretical grounds the straggling of the energies or the ranges will be exactly Gaussian. For we must assume that the behaviour of an  $\alpha$  particle is a function of its energy only, so that if at any stage we have a Gaussian distribution of the distances travelled by particles which have all lost the same amount of energy, there is an equal probability for each particle that for a given energy loss it will go a given distance and so the Gaussian form of the distribution will be conserved. But if we begin with a Gaussian distribution of energies, there is not an equal probability that in a given distance there will be a given energy loss, since the average value of  $dT/dx$  is not the same for all the particles. Hence in this case the Gaussian form cannot be conserved.

To calculate the straggling of the energies in terms of  $P$  we consider a small homogeneous group of particles in a beam which has traversed a distance  $x$ . In going a further element of distance  $dx$ ,  $2P dx$  is the square of the distribution coefficient resulting from variations in energy losses in  $dx$ . When this group reaches a point  $x_0$ , the above contribution to the total straggling of the group is increased to  $2P dx \left( \frac{dT}{dx_0} \right)^2 / \left( \frac{dT}{dx} \right)^2$ . To find the total variation in energy of the whole beam when it reaches  $x_0$ , we have to apply the well-known additive law for the squares of the distribution coefficients. Hence we have

$$\rho_1^2 = \int_0^{x_0} 2P \left( \frac{dT}{dx_0} \right)^2 / \left( \frac{dT}{dx} \right)^2 dx,$$

i.e.,

$$\rho_1^2 \left( \frac{dT}{dx_0} \right)^{-2} = \int_0^{x_0} 2P \left( \frac{dT}{dx} \right)^{-2} dx. \quad (15)$$

This result also follows at once from equation (10), § 7, and Bohr's equation for the straggling of the ranges. The method given above possibly emphasises the mechanism of the action more clearly, and shows that part of the observed variation in energy and velocity at a point in the range is not due directly to the fundamental probability variations, but to a quasi-magnification due to the change in slope of the energy distance curve. We may summarise the relations at any point  $x_0$  in the path between the straggling of the energies and ranges and  $P$  as follows

$$\rho_1^2 \cdot \left( \frac{dT}{dx_0} \right)^{-2} = \rho_3^2 x_0^2 = \int_0^{x_0} 2P \left( \frac{dT}{dx} \right)^{-2} dx. \quad (16)$$

For comparison with theory it would be most useful if we could deduce from the experiments the value of  $P$  at any point in the range, for then we should have  $\int Q^2 dA$  at any point from the straggling experiments as well as  $\int Q dA$ , which is equal to  $dT/dx$  and is known from stopping-power experiments, and is also closely related to the Bragg ionisation curve. However, the experimental error does not allow one to do more than give an average value for  $P$  and to see whether any marked change takes place in  $P$  along the range. For when put in terms of the quantities which are directly measured

$$\rho_1^2 \cdot \left( \frac{dT}{dx} \right)^{-2} = V^2 \rho_2^2 \left( \frac{dV}{dx} \right)^{-2},$$

so that the total error is likely to be considerable, particularly near the end of the range. To detect variations in  $P$  along the range we would have to be able to measure changes in the gradient of the curve for the above quantity.

### § 9. Comparison of Experimental and Theoretical Results.

From equation (16) it can be seen that a comparison of experimental and theoretical results can be readily made by calculating the straggling of the ranges, *i.e.*, by comparing values of  $\rho_3 x$  deduced from Bohr's equation

$$\rho_3^2 x^2 = \int_0^x 2P (dT/dx)^{-2} dx,$$

with values obtained from the relation

$$\rho_3 x = \rho_2 M V^2 (dT/dx)^{-1},$$

$\rho_2$ ,  $V$  and  $dT/dx$  being read off from the experimental curves.

The value of  $P$  has been calculated for air at 15° C. and 760 mm. from Bohr's formula

$$P = 16\pi e^4 N n,$$

with the following values of the constants—

$$e = 4.774 \times 10^{-10} \text{ e.s.u.},$$

$$N = 2.705 \times \frac{273}{288} \times 10^{19},$$

$$n \text{ (average number of electrons per atom)} = 14.39,$$

and so for air

$$P = 9.64 \times 10^{-16}.$$

In calculating the value of  $P$  for mica the composition of mica was taken as  $K_2O \cdot 3Al_2O_3 \cdot 6SiO_2 \cdot 2H_2O$ , and the average conversion factor of mica to



air at 15° C. and 760 mm. was determined experimentally to be 1.46 milligrammes per square centimetre. With these values we obtain for mica

$$P = 11.39 \times 10^{-16},$$

and hence the theoretical value of  $\rho_3^2 x^2$  for mica will be  $11.39/9.64 = 1.18$ , times the value calculated for air, the thickness of the mica being expressed in equivalent centimetres of air.

In fig. 7,  $2P(dT/dx)^{-2}$  is plotted using the above value of  $P$  for air. We have used the experimental values of  $dT/dx$  determined from the measurements which will be described in Part II instead of values calculated from Bohr's theory of the stopping of  $\alpha$  particles. Since these latter are in good agreement with experiment, this change only alters the result by a few per cent. It is preferable in general to use values of  $dT/dx$  which have been directly determined, since modifications of Bohr's theory of stopping power such as that of Henderson and Fowler reduce  $dT/dx$  to about one-half, but leave the calculated value of  $P$  almost unaltered. Bohr's theory of straggling is thus to a large extent independent of his theory of stopping power in so far as the latter necessitates the fixing of a limit, beyond which transfers of energy cannot take place, and the position of this limit, while very important in the calculation of stopping power, is unimportant in straggling phenomena. For values of  $x$  greater than 6.6 cm.,  $dT/dx$  has been deduced from the law

$$V^{1.5} = k(R - x).$$

It is of interest here to give values of  $\rho$  which have been deduced for various  $\alpha$  rays, using the above value of  $P$  and values of  $dT/dx$  obtained in various ways. The figures given in the first line for thorium C and C' are taken from the paper of Meitner and Freitag,\* and the values of  $dT/dx$  for the first 2 cm. of the range for thorium C' have been obtained from the Geiger law.

Table VIII.

Theoretical values of  $\rho \times 10^4$ .

$dT/dx$ deduced from	Polonium.	Thorium C.	Radium C'		Thorium C'.
			Air.	Mica.	
Bohr's theory	1.20	1.16	1.16	—	1.07
Geiger's cube law	1.21	1.17	1.09	1.18	1.05
Experimental	1.15	1.12	1.08	1.17	1.04

\* *Loc. cit.*

In fig. 7 the ordinate at any point is proportional to the rate of increase of the straggling of the ranges at that point, and the area under the curve summed up to any ordinate  $x$  gives the value for air of  $\rho_3^2 x^2$  for that value of  $x$ . The corresponding value when mica is the absorbing material is obtained by multiplying by 1.18.

The theoretical values of  $\rho_3 x$  for mica obtained in this way have been tabulated in Table VI, column 4, and in column 5 the ratio of the observed to calculated values is given. It will be seen that the observed values are roughly 1.4 times greater than the calculated, the ratio increasing somewhat towards the end of the range. Owing to the possibility of systematic errors, particularly at the beginning and end of the range, it is impossible to say definitely whether this increase is real or not.

Since in all straggling phenomena the composition of effects due to each element of length is by the addition of squares the experimentally determined values of  $\rho_3^2 x^2$  have been plotted in fig. 8 and the curve has been extrapolated in order

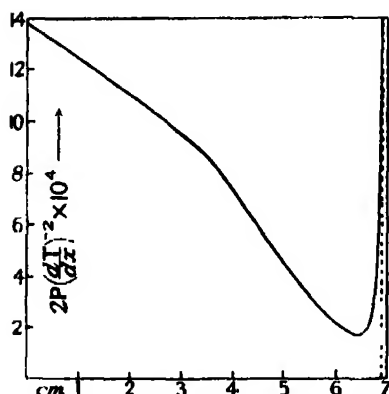


FIG. 7.—The Rate of Increase of the Straggling of the Ranges on Bohr's Theory.

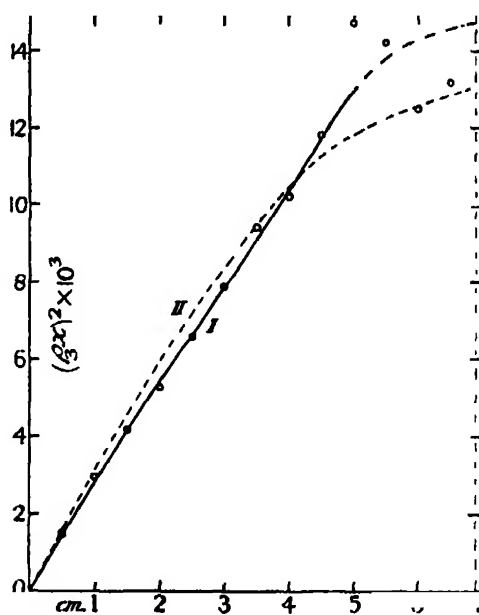


FIG. 8.—I.— $(\rho_3 x)^2$  observed. II.—Twice  $(\rho_3 x)^2$  calculated on Bohr's Theory.

to determine the straggling of the ranges at the end of the path. The mean range of the particles from radium C in air at 15° C. and 760 mm., calculated by a method which will be described in Part II, has been found to be 6.90 cm.

Assuming this value for  $R$  and denoting the value of  $\rho_s$  at the end of the path by  $\rho$ , we find for radium C in mica

$$\begin{aligned}\rho R &= 0.119 \text{ cm.}, \\ \rho &= 1.73 \times 10^{-2}.\end{aligned}$$

The probable error is about 4 per cent.

In fig. 8 the broken curve has been obtained by assuming a value of  $P$  twice that given for mica by Bohr's theory. The two curves are seen to be in fair agreement. The experiments are therefore consistent with the idea that  $P$  is approximately constant, but they require a value for  $P$  roughly twice that given by Bohr's theory. The discrepancy between theory and experiment would be explained if it could be shown that the large transfers of energy from the  $\alpha$  particle to the electrons which account for nearly all the straggling occur twice as frequently as predicted by Bohr's theory of the stopping of  $\alpha$  particles.

#### § 10. *Comparison with the Results of other Observers.*

The straggling of the ranges in polonium has been measured by I. Curie, who found

$$\rho = 1.66 \times 10^{-2}.$$

*i.e.*, a value considerably greater than that given by Bohr's theory.

If we sum the area under the curve in fig. 7 over the appropriate range for polonium, we find as the value for the straggling for polonium in air according to Bohr's theory, but with experimental values of  $dT/dx$ ,

$$\rho = 1.15 \times 10^{-2}.$$

Applying the assumption made in the previous section that the true value of  $P$  is approximately twice as great as that given by Bohr, we find a value  $\sqrt{2}$  times as great. *i.e.*,

$$\rho = 1.63 \times 10^{-2}.$$

The agreement with I. Curie's result is much better than could be expected considering the probable error in the two determinations, but it is satisfactory, since one would expect the electrons of the atoms in mica to behave on the whole in very much the same way in producing straggling as those of the atoms in air. I. Curie's results are thus completely consistent with the idea that the true value of  $P$  is approximately twice as great as that given by Bohr more recently. However, I. Curie and Mercier\* have measured the straggling of the  $\alpha$  particles of radium A and radium C by the Wilson cloud method, and obtained results which are in good agreement with Bohr's theory. They conclude that

\* *Loc. cit.*

I. Curie's value for polonium is too high. These conclusions are, however, based on experiments in which the number of tracks counted varied from 61 to 241, three counts being made for radium A and three for radium C. When the number of tracks counted is so small, considerable errors are probable, for 80 per cent. of the particles have ranges very close to the mean range and are of little use in determining the distribution. These writers note in several curves an excess of short or of long ranges. These may simply be probability variations, as would be expected with such small numbers of tracks.

Meitner and Freitag\* have also measured the straggling of  $\alpha$  rays from thorium C and C' by the Wilson cloud method, and have obtained results from 1 to 16 per cent. greater than the theoretical. These departures from the theoretical values are regarded as within the limit of experimental error. In their experiments there is a considerable variation in pressure while the rays are entering the chamber, and a correction amounting in some cases to 35 per cent. has been applied on this account.

These authors have recently informed me that a more rigorous calculation of this correction, which will shortly be published, gives for oxygen  $\rho = 1.55 - 1.60 \times 10^{-2}$ , a value quite consistent with that found here for mica. For argon, however, the value found is about  $1.30 \times 10^{-2}$ , which is only 10 per cent. greater than calculated from Bohr's theory using values of  $dT/dx$ , also calculated by Bohr's theory of stopping power. However, the velocity curve for heavy elements differs from that for the light elements in such a manner that the value of  $\rho$  for argon, using the value of  $P$  calculated from Bohr's theory and experimental values of  $dT/dx$ , would probably be less than the experimental result, and more consistent with the other results.

Although the results of the present experiments do not give quantitative agreement with the conclusions of Bohr's theory, we see from figs. 5 and 8 that the general process of straggling takes place in very much the way predicted by this theory. For example, we see that the straggling of the ranges is proceeding at a maximum rate near the beginning, and half the total straggling (i.e., half of  $\rho_0^2 x^2$ , since the phenomenon is only additive by squares) takes place in the first 2.4 cm. in the present experiments and in the first 2.2 cm. on Bohr's theory. The last centimetre contributes very little to the straggling. The physical reason underlying this is that at the beginning of the range the rate of loss of energy with distance is small, so that there must be a correspondingly large variation in distance travelled for a given variation in energy loss, and

\* *Loc. cit.*

conversely where the rate of loss of energy is a maximum (that is, at about 6.5 cm.), the rate of increase of the straggling of the ranges will be a minimum.

Henderson's conclusion that in addition to the straggling predicted by Bohr there is in air a further large straggling which arises in the last few centimetres appears to be extremely unlikely. The quantity measured by Henderson, namely, the projection of the final straight portion of the ionisation curve, cannot be taken as a measure of straggling, for I. Curie has shown that the ionisation curve for a single average  $\alpha$  particle differs but little from that of a group of  $\alpha$  particles.

### § 11. *The Straggling on the Henderson-Fowler Theory of Stopping Power.*

Henderson\* has suggested that no transfer of energy between the  $\alpha$  particles and the electron is possible if the energy which could be transferred, calculated on classical laws, is insufficient to remove the electron entirely from the atom or to transfer it to a vacant orbit. Fowler† has shown that this modification reduces the theoretical stopping power of air at the beginning of the range to 0.56 of that observed. Bohr's original theory gave values very close to those determined experimentally.

The straggling on the Henderson-Fowler theory can be calculated as follows :—

From Bohr's theory

$$P = \frac{4\pi e^4 E^4 N n}{m^2 V^4} \sum_1^n \left( \frac{1}{a^2} - \frac{1}{p_r^2 + a^2} \right),$$

where

$$a = eE(M + m)/MmV^2,$$

and  $p_r$  = value of  $p$  beyond which no transfer of energy is possible. We replace  $p_r$  by  $p_t$ , the value of  $p$  for which the energy transfer is equal to the first transference potential.

Now

$$\frac{a^2}{p^2 + a^2} = \frac{\tau_n}{4W},$$

where

$\tau_n$  = first transference potential of a particular electron in volts,

$W = \frac{1}{2} mV^2$  expressed in electron volts.

i.e.,

$$P = \frac{4\pi e^4 E^4 N}{m^2 V^4 a^2} \sum_1^n \left( \frac{\tau_n}{1 - 4W} \right).$$

Values deduced from this expression for mica and air, using the ionisation

\* 'Phil. Mag.', vol. 44, p. 680 (1922).

† 'Proc. Camb. Phil. Soc.', vol. 21, p. 521 (1922-23).

potentials given by Fowler, are shown in the following table in the form of a percentage reduction of Bohr's P at various points of the range :—

Distance from beginning of range.	Mica.	Air.
cm.	Per cent.	Per cent.
0	7.7	3.5
4	10.5	
6	15.4	
6.5	17	

The reason why the change in the straggling is so small compared with that produced in the stopping power is that the large values of Q are hardly altered by this correction, and it is just these values which contribute most to the straggling.

The existence of some such lower limit to the amount of energy which can be transferred appears to be necessary from quantum considerations, but its introduction reduces the calculated stopping power from a value in good agreement with theory to one giving only about half the measured stopping power. If we assume that transfers of energy take place twice as frequently as is calculated from the classical theory and retain the Henderson limit for the least amount of energy which can be transferred, we obtain a theoretical stopping power in good agreement with experimental results. The same assumptions also lead to a theoretical straggling approximately equal to that found in these experiments. Sir Ernest Rutherford has pointed out to me that, using the latest data on the average energy required to produce an ion in different gases, only half of the energy loss of the  $\alpha$  particle can be accounted for. This conclusion is in accord with the assumption that the present theories under-estimate the number of effective collisions with the electrons.\*

## § 12. *Summary.*

The straggling of the  $\alpha$  particles from radium C was investigated by measuring by the magnetic deflection method the variation in velocity when the rays had passed through various thicknesses of mica. The deflected and undeflected bands produced on a photographic plate were analysed with a micro-photometer and results are given for emergent velocities from  $0.98 V_0$  to  $0.22 V_0$ . The

\* We have not referred in this discussion to the effect of capture and loss of electrons by the  $\alpha$  particle. It is easy to show that this capture and loss can only produce a small effect compared with that calculated on the ordinary theories.

distribution of energies on emergence was very approximately Gaussian in form, as the theory of the phenomenon given by Bohr indicates. From the data for the energy distribution it was shown that the straggling of the ranges could be calculated at any point in the region investigated, and it was found that the straggling of the ranges is taking place most rapidly near the beginning of the range, half the total occurring in the first 2.4 cm. The straggling was everywhere found to be about 1.4 times that predicted by Bohr's theory. This indicates that for a small element of path,  $\Sigma Q^2$ , where  $Q$  is the energy transferred to an electron, is approximately twice as great as in Bohr's theory.

It is suggested that the simplest explanation which accounts for these results, and results for the stopping power and ionisation of  $\alpha$  particles, is that transfers of energy from the  $\alpha$  particle to the electrons occur twice as frequently as is accounted for by present theories.

The possibility of an experimental investigation of the straggling of  $\alpha$  particles by the method described here was first noted by Sir Ernest Rutherford in his experiments on the capture and loss of electrons by  $\alpha$  particles, and it is a pleasure to acknowledge my indebtedness to him for suggesting this work and for criticism and advice during its progress. Dr. J. Chadwick I wish to thank for advice in many difficulties. I wish also to acknowledge the help of my wife in some of the rather tedious experimental work and to thank Mr. G. R. Crowe for the preparation of the radioactive sources.

---

*The Decrease in Velocity of  $\alpha$  Particles from Radium C.*

By G. H. BRIGGS, Ph.D., Lecturer in Physics in the University of Sydney.

(Communicated by Sir Ernest Rutherford, Pres R.S.—Received January 19, 1927.)

§ 1. *Introduction.*

The early measurements of the decrease of velocity of  $\alpha$  particles in passing through matter were made by Rutherford\* and Geiger,† using the magnetic deflection method and observing by means of a zinc sulphide screen. The lowest velocities recorded were  $0.43 V_0$  by Rutherford and  $0.2 V_0$  by Geiger. Later Marsden and Taylor,‡ using the same method, made measurements with air, mica and metal foils as the absorbing materials. It appeared from their experiments that something abnormal happened when the velocity had been reduced to about  $0.415 V_0$ , for as the thickness of absorbing material was increased beyond this point, the observed velocity remained unaltered. The simplest explanation of this is that these early experiments were probably carried out with a residual gas pressure high enough for the exchange  $\text{He}_{++} \rightleftharpoons \text{He}_+$  to be frequent. Under these conditions it can readily be shown from the data given by Rutherford§ for capture and loss of electrons by  $\alpha$  particles that when the velocity lies between  $0.4 V_0$  and  $0.3 V_0$  the deflection in a magnetic field remains practically constant and equal to that of  $\text{He}_{++}$  with a velocity of  $0.4 V_0$ .

The problem of the true shape of the velocity curve towards the end of the range has been attacked in a number of ways. Kapitza|| measured the energy of a beam of  $\alpha$  particles at points along the range by the heating effect. He has also¶ examined by the Wilson cloud method the curvature of  $\alpha$  ray tracks in very strong magnetic fields. From this data, by calculating the average charge on the  $\alpha$  particle from Rutherford's experiments mentioned above, he deduced the velocity curve for the region between 5 and 20 mm. from the end of the range in air. I. Curie\*\* has assumed that the rate of loss of energy for a single  $\alpha$  particle is proportional to the number of ions produced per unit

\* 'Phil. Mag.,' vol. 12, p. 134 (1906).

† 'Roy. Soc. Proc.,' A, vol. 83, p. 505 (1909).

‡ 'Roy. Soc. Proc.,' A, vol. 88, p. 443 (1913).

§ 'Phil. Mag.,' vol. 47, p. 277 (1924).

|| 'Roy. Soc. Proc.,' A, vol. 102, p. 48 (1924).

¶ 'Roy. Soc. Proc.,' A, vol. 106, p. 602 (1924).

\*\* 'Ann. de Physique,' vol. 3, p. 299 (1925).



length of the path, and from her measurements of the ionisation or Bragg curve for a beam of rays and measurements of the straggling, she has deduced the form of the Bragg curve for a single average  $\alpha$  particle. From this she has calculated on the above assumption the form of the velocity curve over the whole range. Blackett\* has also deduced the form of the velocity curve near the end of the range from the scattering observed by the Wilson cloud method.

## § 2. *Experimental Method.*

In a previous paper, which will be referred to here as Part I, the writer has given an account of an investigation of the straggling of  $\alpha$  rays in mica by the magnetic deflection method. It was pointed out that it was possible at the same time to obtain on the photographic plates data from which the mean value of  $V/V_0$  for the beam of  $\alpha$  particles could be calculated. In order to do this it is only necessary to arrange that the mica does not completely cover the source, so that for each slit an additional line is produced with a deflection corresponding to  $V_0$ . This method was found to be quite practicable over the whole range of velocities for which the straggling was measured, *i.e.*, from  $0.98 V_0$  to  $0.22 V_0$ .

The ratio of the deflections does not give  $V/V_0$  accurately, as the deflection is not exactly proportional to  $1/r$ ,  $r$  being the radius of curvature of the path. The values of  $V/V_0$  have been deduced from values of  $r/r_0$ , which were calculated from the appropriate formula for the deflection in terms of  $r$  and the dimensions of the apparatus.

The measurements of the straggling indicate that to a high degree of approximation the energies of the  $\alpha$  particles are symmetrically distributed about a mean, so that the average  $\alpha$  particle is that corresponding to the mean energy. Near the end of the range the deflected bands are asymmetrical. But if the photographic action were independent of the velocity, the ordinate which divides the density curve of the deflected band into two equal areas would correspond to the average particle. The results given correspond to this mean deflection. Near the end of the range, where the variation in velocity is large the values may be somewhat too high owing to the difference in photographic action of the fast and slow particles in the band.

\* 'Roy. Soc. Proc.,' A, vol. 102, p. 294 (1922).

§ 3. *Measurement of the Air Equivalent of the Mica.*

There are considerable discrepancies between the values found by various observers\* for the mass of mica per square centimetre equivalent in stopping power to 1 cm. of air at various parts of the range. It may be that variations in the composition of mica account for some of these discrepancies.

In the present experiments the mass per unit area was determined by weighing uniform pieces from 50 to 100 sq. cm. in area, and the air equivalent of the actual pieces of mica used in the deflection experiments was measured by the scintillation method. The source of  $\alpha$  rays was a brass disc 2 mm. in diameter activated with radium C and placed about 0.05 mm. below the mica.

Table I shows the stopping power of the mica used expressed in dry air at 15° C. and 760 mm. Column 3 gives the observed conversion factor for mica to air at 15° C. and 760 mm. expressed in milligrams per square centimetre. The results in this column show a steady increase: the effect of experimental error is also apparent. The probable error in the determinations is about 0.1 mm.

Table I.

Mass per square centimetre.	Observed stopping power.	Ratio of mass to stopping power.
grams.	cm.	
2.083 $\times 10^{-3}$	1.440	$1.446 \times 10^{-3}$
2.995	2.056	1.456
4.381	2.982	1.469
4.968	3.392	1.464
5.781	3.903	1.459
6.474	4.492	1.442
7.274	4.959	1.467
7.386	5.056	1.461
7.903	5.432	1.455
8.352	5.661	1.474
8.837	5.986	1.477
8.915	6.067	1.469
9.255	6.296	1.471
9.469	6.445	1.469
9.630	6.501	1.481
9.832	6.659	1.477
9.871	6.712	1.471

Except for the experiments at low velocities, in which the source was outside the magnetic field, the  $\alpha$  rays did not pass normally through the mica, but their path made an angle with the normal which could be calculated from the

\* Marsden and Richardson, 'Phil. Mag.', vol. 25, p. 184 (1913); Marsden and Taylor, 'Roy. Soc. Proc.', A, vol. 88, p. 443 (1913); Lawson, 'Wien. Ber.', vol. 127, p. 943 (1918).

dimensions of the apparatus and the radius of curvature of the path of the particles.

#### § 4. Results.

The equivalent air stopping powers of the mica determined by the scintillation method and the effective stopping power found after correcting for the angle at which the rays passed through the mica are given in columns 1 and 2 of Table II. For the lower velocities both the  $\text{He}_+$  and  $\text{He}_{+1}$  bands were used to give  $V/V_0$ , and the difference in the corrections for effective thickness of the mica is so small that mean values are given except in the experiment for mica of 5.986 cm. stopping power, where the deflection was unusually large. Here the two values are tabulated. The table also contains the results (indicated by an asterisk) of some experiments in which the mica completely covered the source so that no deflected band was obtained corresponding to the velocity  $V_0$ . These results depend on the accuracy with which the magnetic field can be reproduced. Their agreement with direct determinations seems to justify their inclusion. The residual field of the magnet was between 1/500 and 1/600 of the maximum field, so that the correction on this account does not amount to 1 in 500 until the velocity is less than  $0.5 V_0$ .

Table II.

Air equivalent of mica.	Effective air equivalent.	$V/V_0$ .	$V/V_0$ calculated from $V^3$ law	
			$R = 6.96,$	$R = 6.90,$
cm.	cm.			
0.308	0.315	0.984	0.9847	0.9845
0.540	0.554	0.975*	0.9727	0.9725
1.004	1.026	0.951	0.9482	0.9477
1.004	1.032	0.947*	0.9477	0.9475
1.004	1.037	0.945*	0.9475	0.9471
1.440	1.480	0.924*	0.9234	0.9228
2.056	2.113	0.888*	0.8863	0.8853
2.982	3.053	0.825	0.8249	0.8230
3.392	3.487	0.792	0.7930	0.7909
3.972	4.098	0.746*	0.7435	0.7406
4.492	4.492	0.695	0.7078	0.7041
5.056	5.089	0.629	0.645	0.640
5.432	5.432	0.572	0.603	0.597
5.664	5.664	0.537*	0.571	0.564
5.986	6.008	0.446	0.515	0.506
	6.066	0.440	0.504	0.494
6.296	6.296	0.359	0.457	0.444
6.445	6.445	0.289	0.420	0.404
6.501	6.501	0.272	0.404	0.387
6.659	6.659	0.219	0.351	0.327

Table II also shows the values calculated from the law proposed by Geiger

$$V^3 = k(R - x),$$

using  $R = 6.96$  the extrapolated range and also for  $R = 6.90$  cm. the mean range deduced in the following paragraph. It will be seen that to velocities of  $0.75 V_0$  the experimental results agree with this law, using either value of  $R$  to within less than 1 per cent. The velocity curve is shown in fig. 1 together with Marsden and Taylor's\* curve and the  $V^3$  law for  $R = 6.96$ .

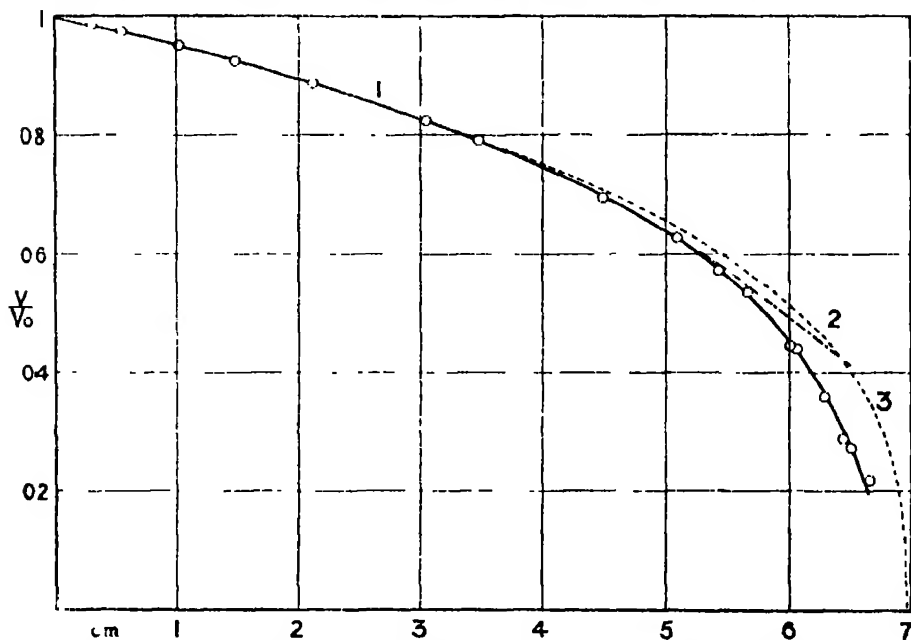


FIG. 1.—The Velocity Curve for Radium C in Air at 15° C. and 760 mm.

1, Briggs; 2, Marsden and Taylor; 3,  $V^3 = k(R - x)$ .

### § 5. The Mean Range.

The various methods which have been used to determine the ranges of  $\alpha$  particles do not measure the same quantity. The "extrapolated range" deduced from the ionisation curve can be determined most accurately. By the Wilson cloud method the mean range can be determined directly as well as another extrapolated range, namely, that obtained by producing the straight part of the number-distance curve to cut the axis.

The present writer has attempted to calculate the mean range for radium C by assuming the curve 1 given by I. Curie\* for the ionisation of a single  $\alpha$  particle

\* *Loc. cit.*

from polonium and taking a value of  $\rho = 1.6 \times 10^{-2}$  for the straggling of the ranges for radium C in air. From this data the last portion of the ionisation curve for radium C can be calculated by summing a series of curves of the type assumed from I. Curie's work, whose end-points are distributed about the mean range with a Gaussian distribution defined by  $\rho$ . The resultant curve approximates closely to the ionisation curve for radium C and shows the same long straight slope which can be produced to cut the base and so give the extrapolated range. This was found to be 0.06 cm. greater than the mean range. Taking the extrapolation range as 6.96 cm., this gives 6.90 cm. as the mean range for the  $\alpha$  particles from radium C in air at 15° C. and 760 mm.

By the Wilson cloud method I. Curie and Mercier\* have recently obtained for the mean range for radium C the value 6.92 cm. at 15° C. and 760 mm., uncorrected for the pressure of water vapour. The correction for the latter would probably bring the two results into much better agreement than could be expected from the order of accuracy of the determinations.

#### § 6. *Comparison with Results of other Observers at Low Velocities.*

In the present experiments the measurements have been made from the beginning of the range. It is important to be able to connect up results obtained in this way with experiments in which the measurements of range are made from the end of the paths, as may be done, for example, in the Wilson cloud method. If we consider two tracks obtained by this latter method, which as a result of straggling are of different length, the experiments described in Part I show that probably only 5 per cent. of this straggling occurs in the last 2 cm., so that in this part of the range the velocities will differ but little at equal distances from the end of the tracks, and will be approximately equal to that of an average  $\alpha$  particle. They may therefore be compared with measurements, such as those described in this paper, made from the beginning of the range if in the former the range taken is the mean range, which has been shown to be about 6.90 cm. The velocity is given in terms of the distance from the beginning and the mean end of the range in Table III.

In fig. 2 the writer's results near the end of the range are compared with those of other observers, the end of the range in the present experiments being taken as 6.90 cm. In Kapitza's† experiments on  $\alpha$  ray tracks in strong magnetic

\* 'J. de Physique,' vol. 7, p. 289 (1926).

† *Loc. cit.*

Table III.—Values of  $V/V_0$  in Air at 15° C. and 760 mm.

Distance traversed in air at 15° C. and 760 mm.	Distance from mean end of range.	$V/V_0$ .
0	6.9	1.000
0.5	6.4	0.977
1.0	5.9	0.951
1.5	5.4	0.923
2.0	4.9	0.894
2.5	4.4	0.863
3.0	3.9	0.828
3.5	3.4	0.790
4.0	2.9	0.746
4.5	2.4	0.696
5.0	1.9	0.638
5.5	1.4	0.563
5.7	1.2	0.525
5.8	1.1	0.504
5.9	1.0	0.481
6.0	0.9	0.455
6.1	0.8	0.427
6.2	0.7	0.396
6.3	0.6	0.361
6.4	0.5	0.322
6.5	0.4	0.278
6.6	0.3	0.222

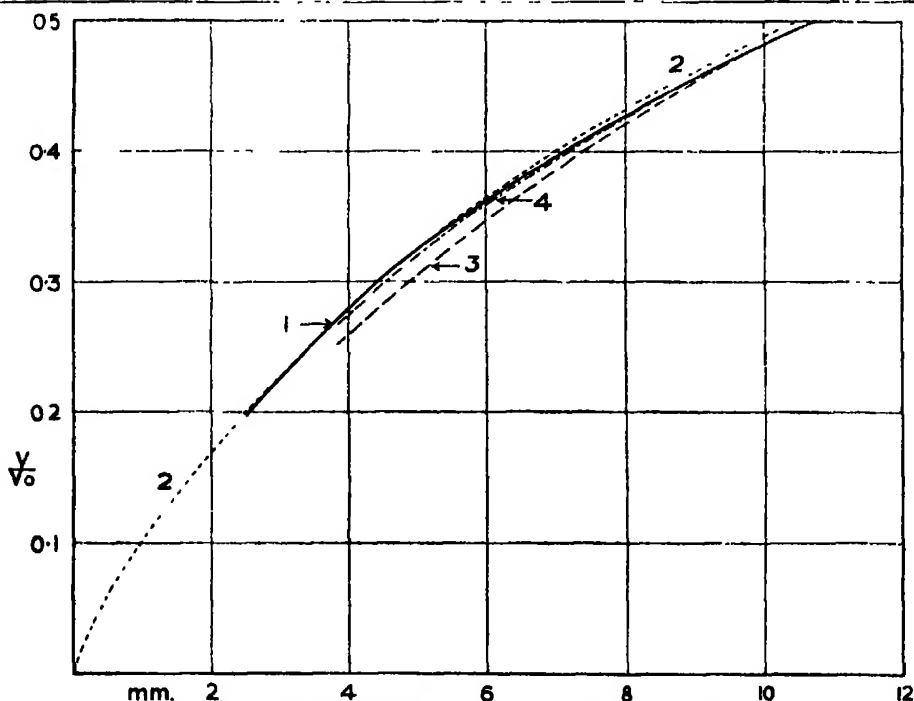


FIG. 2.—Emergent Mean Range in Air at 15° C. and 760 mm.

1, Briggs ; 2, Curie ; 3, Kapitzka,  $\alpha$  ray tracks ; 4, Kapitzka,  $\alpha$  ray tracks corrected.

fields the quantity directly measured was the ratio of the average charge to the velocity. The velocity was deduced from this data using the law

$$\frac{\lambda_1}{\lambda_2} \propto V^{4.3}$$

found by Rutherford,\* where  $\lambda_1$ ,  $\lambda_2$  are the mean free paths for capture and loss respectively. Some measurements made in the present experiments and described in the following section seem to indicate that an index 4.3 is probably more correct. In fig. 2 a curve has been drawn, deduced from Kapitza's data, using this value. It is seen that the agreement is much improved.

### § 7. *The Ratio of Singly to Double Charged $\alpha$ Particles.*

The ratio of the number of singly to doubly charged  $\alpha$  particles is given by the ratio of the areas of the density curves of the corresponding bands, for the calibration of the plates described in Part I showed that over the range of densities occurring in the deflection experiments the number of  $\alpha$  particles could be taken as proportional to the density. The ratio  $\lambda_2/\lambda_1$  is given in the following table:—

Table IV.

$V/V_0$ .	$\lambda_2/\lambda_1$ .	
	Observed.	Calculated.
0.825	0.014	0.012
0.695	0.025	0.025
0.693	0.025	0.025
0.624	0.038	0.040
0.572	0.064	0.059
0.564	0.069	0.062
0.537	0.087	0.077
0.487	0.091	0.117
0.443	0.171	0.176
0.437	0.227	0.186
0.289	0.94	1.10
0.272	1.35	1.35

From these results, together with those found by Rutherford by counting scintillations, it is deduced that

$$\frac{\lambda_2}{\lambda_1} = 5.3 \times 10^{-3} V^{-4.3}.$$

\* 'Phil. Mag.,' vol. 47, p. 277 (1924).

The index is probably correct to  $\pm 0.1$ . Henderson,\* using an electrical method of measuring, recently found  $4.3 \pm 0.3$  for the value of the index.

The calculated values given in Table III are obtained using the index 4.3.

### § 8. Comparison with Ionisation Curve.

It is of interest to compare the rate of loss of energy of the  $\alpha$  particle with the ionisation produced by it in each element of its path. In fig. 3  $dT/dx$  has been

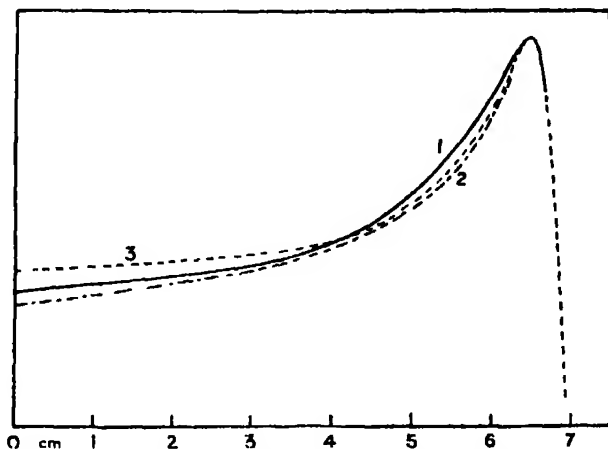


FIG. 3.—1, Rate of Loss of Energy (Briggs). 2, Ionisation Curve in Air (Henderson). 3, Ionisation Curve in Air (Curie and Béhounek).

plotted, where  $T$  is the energy of the  $\alpha$  particle. It is seen that the shape of the curve is similar to that of the ionisation curve, and the difference is probably less than the experimental error. The agreement is of interest since it is known that, except in the rare gases, only about 50 per cent. of the energy of the  $\alpha$  particle can be accounted for as ionisation.

### § 9. Experiments on the Homogeneity of the Initial Velocities of the $\alpha$ Particles from Radium C.

The homogeneity of the initial velocities of the  $\alpha$  particles was also investigated with the apparatus described in Part I, exposures being made as for the measurement of straggling but without any absorbing material. In a similar investigation for the  $\alpha$  rays from polonium, I. Curie† has indicated some of the difficulties which arise on account of the finite width of the undeflected line. The analysis of the lines with a microphotometer has many advantages over

\* 'Roy. Soc. Proc.,' A, vol. 109, p. 157 (1925).

† *Loc. cit.*



a microscopic examination, for if there is any variation in velocity in which the distribution of the velocities is symmetrical about a mean, the width  $d_2$  of the deflected line, found by producing the straight sides of the density curves to cut the base, as described in Part I, will be greater than  $d_1$ , the corresponding width of the undeflected line. The variation in velocity can also be investigated by measuring the widths of the two density curves at various distances from the base. The broadening to be expected for a given small distribution coefficient  $\rho$  of the velocities increases from zero at half the height of the curves to about  $1.6\rho$  at  $0.025$  of the height.

The first experiments were made with wires of  $0.125$  mm. diameter activated by exposure to radium emanation. Here a certain lack of homogeneity is to be expected for two reasons. In the first place, a certain amount of the radium C will be embedded in the platinum by the recoil of radium B from radium A, and, secondly, some of the  $\alpha$  rays reaching the photographic plate will be shot through the platinum from the back of the wire. It is probable that about 60 per cent. of the radium C is on the surface of the wire and the remainder is distributed uniformly through a layer of platinum about  $10^{-6}$  cm. thick. An atom of radium C which is embedded  $10^{-6}$  cm. below the surface of the wire will give rise to an  $\alpha$  particle, which, if shot out perpendicular to the radius, will have its range reduced by  $6 \times 10^{-3}$  cm. of air. About 5 per cent.

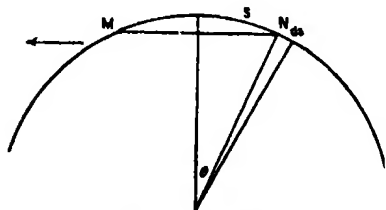


FIG. 4.—Diagram of Wire Source.

of the rays will be stopped by more than  $0.7$  mm., an amount which causes a change of deflection of about  $0.1$  mm. on the plate.

It appears that  $\alpha$  particles which come from radium C on the surface of the wire and are shot through the metal will not produce any lack of homogeneity which is measurable with a microphotometer.

If  $D_0$  and  $D$  are the deflections of the unretarded and retarded  $\alpha$  particles,  $R$  the range in platinum, we have from fig. 4 for small values of  $\theta$ , if  $MN = x$ ,

$$x = 2S \text{ approximately.}$$

$$\frac{\delta D}{D_0} = -\frac{\delta V}{V_0} = \frac{1}{3} \frac{\delta x}{R}.$$

Hence

$$D - D_0 = \frac{2}{3} \frac{S}{R},$$

so that the increase in the deflection will be proportional to  $S$  and the photographic density due to retarded particles will be constant for small values of  $S$ . Hence the  $\alpha$  particles shot through the wire give rise in the density curves to two long tails of constant height, one from the upper and one from the lower surface of the wire. These tails stretch away from the deflected band on the low-velocity side and further calculation shows that the combined density of the two is about 0.006 of that of the maximum of the main band. A similar argument shows that neglecting scattering the slits will produce similar tails whose density is 0.001 that of the main band. Scattering will, however, deflect nearly all particles which pass through the copper of which the slits are constructed completely out of either the deflected or undeflected band.

These experiments with wire sources indicated a small variation in the initial velocity which appeared to be explainable from the fact that some of the radium C was embedded in the platinum. Experiments were now begun to see whether this lack of homogeneity would be eliminated if radium B and radium C or radium C alone were deposited from solution by electrolysis on a flat surface. The sources were made by coating a piece of platinum 8 by 3 by 0.15 mm. with enamel and then grinding one of the longer edges bare and polishing it. It was found possible to get sufficient activity on such a surface without the slightest trace of tarnish. This type of source, however, gave deflected lines which showed nearly as much non-homogeneity as those obtained with the wire sources exposed to radium emanation. The same result was obtained with radium C deposited from solution on flat nickel sources. Some experiments were also made in which the slits were made of aluminium wire of about 1 mm. diameter, but with the same result.

#### § 10. *Results of the Experiments on the Initial Homogeneity.*

Fig. 3 shows the lower portion of a typical pair of density curves obtained with a flat source. The lines obtained with wire sources gave density curves of practically the same form. The area on the deflected curve attributable to slow rays varied from 3.5 per cent. to 5 per cent. in different experiments. Allowing for the geometrical broadening discussed in Part I, the widths of the deflected and undeflected curves, beyond one-quarter of the height, were the same to within experimental error.

The reason for the lack of homogeneity using flat sources prepared electrolytically is not apparent. It behaves in every way as if it were a spurious effect. Most of the evidence goes to show that on a metal such as platinum the layer of adsorbed gas is unlikely to be more than one or two molecules thick, which

is quite insufficient to account for the effect. Nor is the diffusion of the deposit into the platinum likely to be appreciable in an interval of one hour. It is

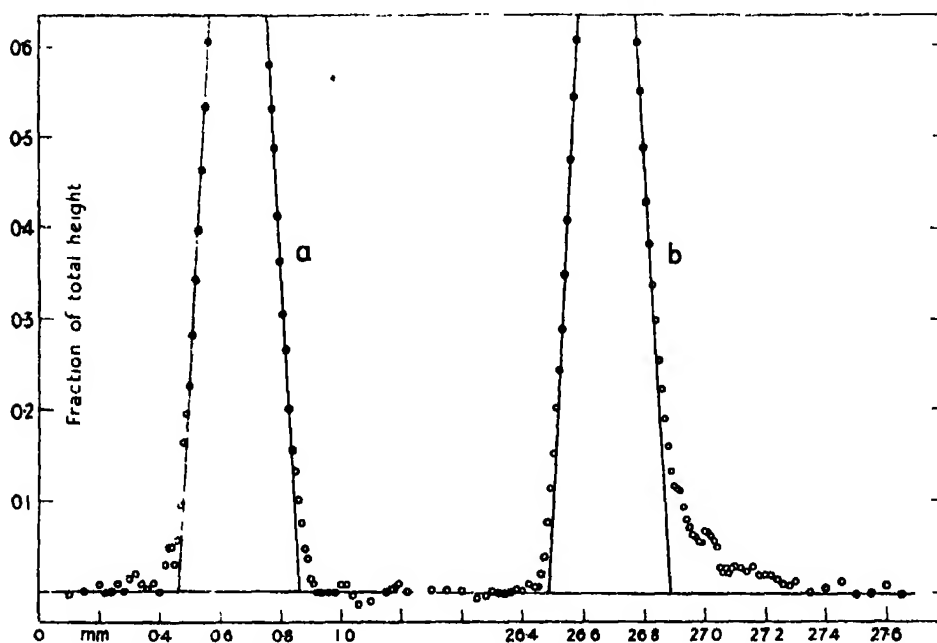


FIG 5.—Density Curves. *a*, Undelected line; *b*, deflected line.

possible that the enamel may not have protected the edges of the source sufficiently well, and activity may have penetrated a short distance along the sides of the platinum.

Comparisons of the high-velocity side of the lines made by producing the straight portion of the curves to meet the base indicate that there is no detectable alteration in the shape of the curve on this side. Any distribution of velocities involving velocities greater than the average would cause a rounding off of the curve at the base, and can be estimated by comparing distances between the curve and the line obtained by producing the straight side of the curve. Here measurements can be made as low as  $1/40$  of the height and a broadening of 0.01 mm. would be detectable. At this small fraction of the total height any broadening would be about 1.6 times greater than the average broadening of an infinitely narrow zero line. As the deflection was generally about 26 mm., one can say that if there is any variation in velocity involving a symmetrical distribution about the mean, three-quarters of the rays have velocities which differ by less than 1 in 3,000.

In some of the earlier experiments where the density of the line did not exceed

1/6 unit no lack of homogeneity was detected, and the difference between the deflected and undeflected lines was so small that one would have felt justified in estimating the degree of homogeneity as more than 1 in 500. When the density of the lines was increased by using stronger sources the lack of homogeneity was quite evident, and on re-examining the curves mentioned above the lack of homogeneity could just be detected. The reason for this is that slight variations in the background and in the grain of the plate produced fluctuations which nearly masked the asymmetry.

I. Curie in her experiments on the straggling of the  $\alpha$  particles from polonium found that about 1/8 of the particles did not conform to a probability distribution of ranges of the form indicated by theory, but had ranges which were too short. In deflection experiments with polonium similar to those described here, the measurements being made with a microscope, she found no evidence of a broadening of the deflected bands and concluded that the rays were homogeneous to within 0.3 per cent. Owing to the difficulty of obtaining strong polonium sources, the lines she obtained were feeble and the limit of the density observable was 1/8 or 1/10 of the maximum. The lack of homogeneity found in the present experiment was barely detectable at this height. It would be accounted for if about 5 per cent. of the rays have velocities less than the maximum by amounts up to 1.5 per cent.

The problem has to be left in the unsatisfactory state that whereas a definite lack of homogeneity was always observed, its behaviour was so much like a spurious effect that it is felt that improved methods of preparation of the sources would probably eliminate it.

### § 11. *Summary.*

The velocity curve for  $\alpha$  particles from radium C has been determined over a range of velocity from  $0.98 V_0$  to  $0.22 V_0$ . For velocities less than  $0.55 V_0$  the decrease in velocity was much more rapid than was found by Marsden and Taylor, but near the end of the range was in satisfactory agreement with the results found by indirect methods by Kapitza and by I. Curie.

Some results are given for the ratio of the number of singly to doubly charged  $\alpha$  particles at various velocities, which indicate that the ratio varies as  $V^{-4.3}$ .

Experiments are also described in which the variations in the initial velocity of the  $\alpha$  particle were investigated. No evidence was found of velocities greater than the average by more than 1 in 3,000. Velocities less than the maximum were present, due probably to absorption in the source.

The results given in this paper were obtained during the course of experiments on the straggling of  $\alpha$  particles described in a previous paper. It gives me great pleasure to acknowledge my indebtedness to Sir Ernest Rutherford for his interest and advice. I wish also to thank Mr. H. J. J. Braddick, B.A., for his help in the measurement of the stopping power of the mica, and Mr. G. R. Crowe for the preparation of the wire sources.

---

### *The Thermal Conductivity of Carbon Dioxide.*

By HAMAR GREGORY, Ph.D., A.R.C.S., D.I.C., Assistant Professor of Physics, Royal College of Science, and SYBIL MARSHALL, B.Sc., A.R.C.S., D.I.C.

(Communicated by H. L. Callendar, F.R.S.—Received December 11, 1926.)

#### *Introduction.*

Of the many experimental determinations of the thermal conductivity of  $\text{CO}_2$  which have been made, the absolute values given by the various observers vary from  $3.07 \times 10^{-5}$  cal. sec.<sup>-1</sup> cm.<sup>-1</sup> deg.<sup>-1</sup> (Winkelman, 1), to  $3.39 \times 10^{-5}$  cal. sec.<sup>-1</sup> cm.<sup>-1</sup> deg.<sup>-1</sup> (Weber, 2), and generally speaking the experiments were modifications of two principal methods, namely, the electrically heated wire of Schleimacher (3) and the cooling thermometer method. In both of these methods convection losses were present to a degree depending on the dimensions and disposition of the apparatus, and on the pressure of the gas; therefore, in the author's opinion, the discrepancies amongst various observers are due to the practice of attempting to eliminate these convective losses by diminishing the pressure.

Such a procedure is justifiable only if the reduction of pressure is not carried beyond the point at which the mean free path of the molecules becomes comparable with the dimensions of the containing vessel. This is a critical point in the determination of the conductivity of a gas, as the authors' experiments on  $\text{CO}_2$  indicate that the convection becomes negligible only at pressures for which the mean Free Path Effect is such that the significance imposed on the conductivity by Fourier's law loses its meaning, and below this critical pressure the conductivity varies with the pressure in a manner depending on the dimensions of the vessel containing the gas. In the experiments of Gregory and Archer (4), on the thermal conductivities of air and hydrogen, the use of a double

system of electrically-heated wires enabled the authors accurately to identify the critical pressure at which convective losses became negligible. This is an extremely important point in all applications of the hot-wire method to the absolute determination of the conductivities of gases, and alone justifies the procedure of lowering the pressure to eliminate convective losses. Above this critical pressure it is necessary to disentangle the conduction and convection losses, and below, the meaning of conduction loses its ordinary significance.

*Apparatus.*

The following investigation was carried out on the lines described in Gregory and Archer's paper on the thermal conductivities of air and hydrogen, but in

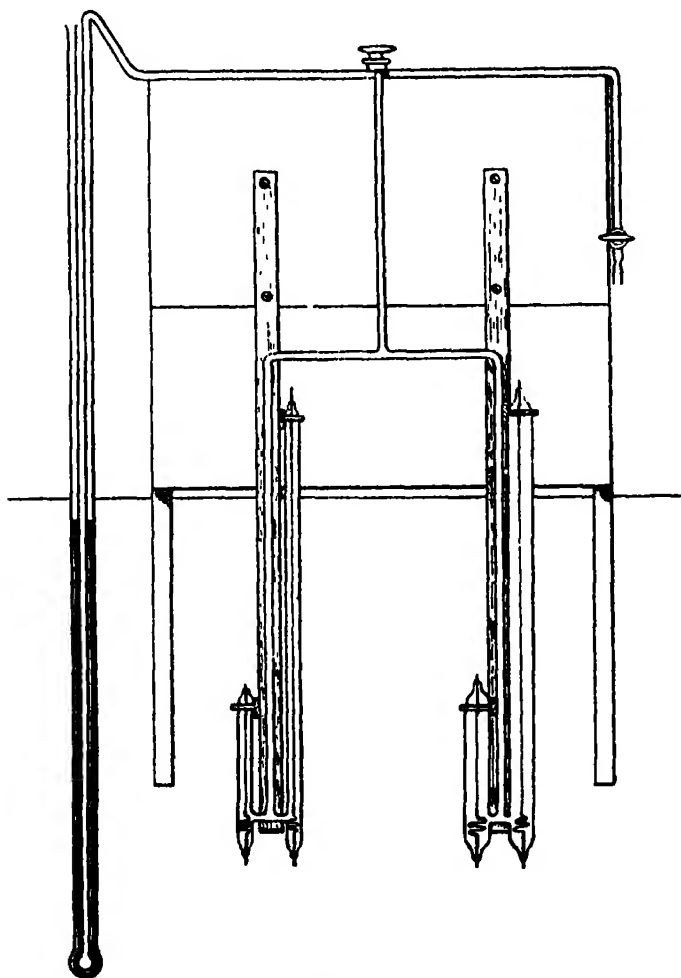


FIG. 1.

this case a vertical, instead of a horizontal, system of tubes, as shown in fig. 1, was used in order to reduce as much as possible the large convective heat loss that one would expect in a triatomic gas such as carbon dioxide. The inlets and the connections between the main tubes and their compensators were placed at the lower ends of the tubes, well below the level of the heated wire, so that there was no convective passage of gas from one part of the system to another. The tubes were made by Muller, of Parton Street, Holborn, from two pieces of thin walled lead glass tubing, of about 1 cm. and 3 cm. diameter, respectively, which had been selected, on account of their uniformity of bore, from 10 carefully calibrated pieces of each type, these 20 pieces, each about 4 feet long, having been specially selected at the Whitefriars lead glass factory at Wealdstone.

The mean radii of the tubes used were as follows :—

Wide tubes—

Internal radius	..	..	..	..	..	1.402 cm.
External radius	..	..	..	..	..	1.456 cm.

Narrow tubes—

Internal radius	..	..	..	..	..	0.5874 cm.
External radius	..	..	..	..	..	0.6439 cm.

The mean radius of the fine platinum wire was obtained by weighing three measured lengths of about a metre cut from the same wire. It was found to be 0.0050596 cm. This wire was then cut into two lengths of 30 cm. each for the main tubes and 10 cm. for the compensators, mounted on platinum springs, and stretched axially along the tubes. The object of using such fine wire was partly to cut down the radiation heat loss, which was calculated from Gregory and Archer's figures (4), taking into account the difference in diameter of the wires used in the two sets of experiments, and partly to lengthen the flat part of the temperature distribution curve along the wire, as this improves compensation.

Before the gas was admitted the tubes were placed in steam and connected to a pump, while a charcoal pocket in gaseous connection with the tubes was surrounded by an electric furnace. The tap between the tubes and the pump was then closed, and liquid air was substituted for the electric furnace surrounding the charcoal. Thus any residual gases and vapours were absorbed by the charcoal, which was then isolated from the tubes while it was still in the liquid air bath.

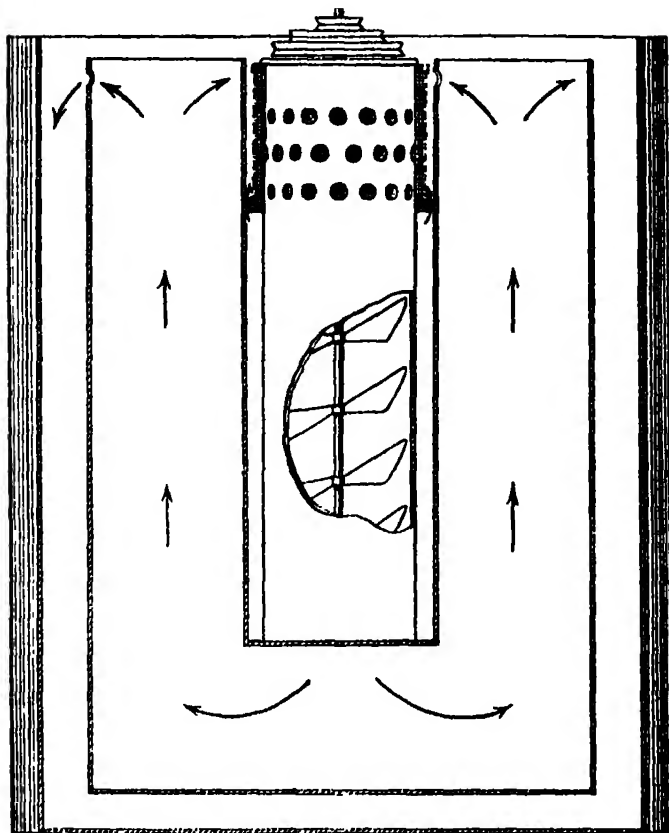


FIG. 2.

*Thermostat.*

The maintenance of the outer walls of the tubes at a constant temperature is one of extreme importance, especially when the temperature gradients of the order of  $5^{\circ}\text{C.}$  are employed. Any inefficiency in the thermostatic arrangement leads to a gradual heating of the outer walls, and a variation of their temperature of even a thousandth of a degree is detected by the sensitive bridge system employed. This difficulty was overcome by using a specially constructed motor driven cooler. This consisted of three brass tubes, joined at their lower ends, two of which surrounded the wide and narrow systems of the apparatus, the third containing several vanes arranged vertically over one another and driven by an electric motor. The brass tubes were surrounded by a mixture of ground ice and water, so that ice-cold water was drawn in through holes at the top of the tube containing the vanes, circulated past the apparatus, and issued from holes at the tops of the brass pockets.



*Preparation of Carbon Dioxide.*

The carbon dioxide was prepared in a Kipp's apparatus from pure air-free calcite and an air-free solution of pure hydrochloric acid in an equal volume of distilled water. The atmosphere above the acid in the Kipp was carbon dioxide, obtained from a subsidiary generator, to avoid solution of air during the experiment. The issuing gas was passed in turn through previously boiled distilled water and a solution of sodium bicarbonate, to absorb any hydrochloric acid fumes, through concentrated sulphuric acid and over pure phosphorus pentoxide (prepared in the Chemical Technology Department), to dry it, and finally through a dust tube before entering the apparatus.

Mr. H. D. Murray, B.A., of the Chemistry Department, very kindly analysed a sample of the carbon dioxide obtained by this method, which he found to be 99.82 per cent. pure. He states that the slight trace of impurity found was probably due to the chemicals used in the analysis, so that the purity of the gas is even greater than the above percentage, whereas cylinder gas is only 96.7 per cent. pure.

*Experimental Procedure.*

The fundamental intervals of the wide and narrow systems were obtained, and from these the bridges could be set so that the temperatures of the wires in the wide and narrow tubes were equal. The temperature of the wires thus being fixed, starting from atmospheric pressure, the pressure of the gas was lowered in small steps and the bridge was rebalanced for each different pressure by altering the current in the battery circuit, the current in each system being measured by means of a potentiometer across the terminals of a standard ohm in series with each main wire (4). Six different settings of the bridges were used corresponding to six wire temperatures.

*Results.*—The following is a key to the symbols used in the tabulation of the results :—

- P = pressure of  $\text{CO}_2$  within the tubes in centimetres mercury.  
 $\theta$  = temperature of wires above  $0^\circ \text{C.}$ , the bath temperature.  
 $\psi$  = radiation heat loss per unit length at temperature  $\theta$  in cal. sec. $^{-1}$ .  
 C = current in amperes in the hot wire.  
 $R_\theta/l$  = resistance per unit length of the wire at temperature  $\theta$ . This was found by noting the resistances in steam and in ice of a measured length, of about a metre, cut from the same wire, and assuming a linear law. A compensating wire was used in the apparatus for determining this fundamental interval.  
 J = mechanical equivalent of heat.

$C^2R_\theta/Jl$  = total heat loss per unit length at temperature  $\theta$  in cal. sec.<sup>-1</sup>.

$\theta_1$  = temperature drop across tube wall, calculated from the total heat loss, the internal and external radii of the wall, and the thermal conductivity of lead glass (4) and

for the wide tubes,  $\theta_1 = C^2R_\theta/Jl \times 3.63$  ;

for the narrow tubes,  $\theta_1 = C^2R_\theta/Jl \times 8.82$ .

$\theta'$  =  $\theta - \theta_1$  = temperature drop across the gas.

$K_a$  = apparent conductivity, consisting of conduction and convection, in calories, cm.<sup>-1</sup> sec.<sup>-1</sup> deg.<sup>-1</sup>

$$= \frac{\{C^2R_\theta/Jl - \psi\} \log \exp. (r_2/r_1)}{2\pi\theta'}$$

$r_1$  = radius of platinum wire in cms.

$r_2$  = internal radius of narrow tubes in cms.

$r_3$  = internal radius of wide tubes in cms.

Convection ceases for each system at the pressure for which the apparent conductivity is the absolute conductivity,  $K$ .

$C_N$  = current in narrow system at the above pressure.

$C_W$  = current in wide system at the above pressure.

Therefore

$$\frac{\{C_N^2R_\theta/Jl - \psi\} \log \exp. (r_2/r_1)}{2\pi\theta'} = K = \frac{\{C_W^2R_\theta/Jl - \psi\} \log \exp. (r_3/r_1)}{2\pi\theta'}$$

Therefore

$$\frac{\log \exp. (r_3/r_1)}{\log \exp. (r_2/r_1)} = \frac{C_N^2R_\theta/Jl - \psi}{C_W^2R_\theta/Jl - \psi}$$

$$\alpha_c = \frac{\log \exp. (r_3/r_1)}{\log \exp. (r_2/r_1)} = 1.183.$$

$$\alpha_0 = \frac{C_N^2R_\theta/Jl - \psi}{C_W^2R_\theta/Jl - \psi}$$

Thus, when we have two equal values for the apparent conductivity in the two systems corresponding to a different pressure for each system, and the equation  $\alpha_c = \alpha_0$  is satisfied, this value of the apparent conductivity is the absolute conductivity of the gas at the mean temperature between the hot wire and the outer wall (4).

## Curves I.

0 = 9.032° pt. = 8.908° C. Therefore mean temp. of gas = 4.45° C.

$\psi = 0.0000017$

$R_g/l = 0.13028$

P.	Wide tubes				Narrow tubes			
	$\theta_1$	0.001	$\theta'$	8.907° C.	$\theta_1$	0.004	$\theta'$	8.904° C.
	C.	$C^2R_g/Jl$	$C^2R_g/Jl - \psi$	$K_a$	C.	$C^2R_g/Jl$	$C^2R_g/Jl - \psi$	$K_a$
76.80	0.1124	0.0003934	0.0003911	0.00003031	0.1180	0.0004335	0.0004318	0.00003690
13.32	0.1108	3830	3813	3832	0.1179	4328	4311	3664
53.17	0.1100	3767	3750	3769	0.11775	4317	4300	3654
17.76	0.1097	3748	3731	3750	0.1177	4314	4297	3652
12.89	0.10946	3731	3714	3734	0.11765	4310	4293	3648*
10.55	0.10935	3724	3707	3726	0.1176	4306	4289	3645
19.01	0.1093	3720	3703	3721	0.11755	4303	4286	3642
16.97	0.10925	3717	3700	3718	0.11755	4303	4286	3642
14.79	0.10915	3710	3693	3711	0.1175	4299	4282	3639
12.48	0.1091	3706	3689	3707	0.11745	4295	4278	3636
17.73	0.10895	3697	3680	3698	0.1174	4292	4275	3633
20.02	0.1089	3693	3676	3694	0.1174	4292	4275	3633
23.61	0.10885	3690	3673	3691	0.11735	4288	4271	3630
22.96	0.1088	3686	3669	3687	0.11735	4288	4271	3630
19.93	0.10875	3683	3666	3684	0.1173	4284	4267	3626
16.68	0.10865	3676	3659	3677	0.11725	4281	4264	3624
14.40	0.10855	3669	3652	3670	0.1172	4277	4260	3620
12.44	0.10845	3662	3645	3663	0.11715	4273	4256	3617
10.41	0.10835	3655	3638	3656	0.11715	4273	4256	3617
8.50	0.10825	3649	3632	3650	0.11705	4266	4249	3611
6.81	0.10815	3642	3625	3643*	0.1169	4255	4238	3602
4.32	0.1080	36315	36145	3633	0.1167	4250	4233	3597
1.90	0.1074	3591	3674	3592	0.1161	4197	4180	3552
$\theta_1 = 0.003$ and $\theta' = 8.905^\circ$ C.								
0.29	0.10185	3229	3212	3228	0.1087	3686	3669	3118

$\alpha_g = 1.183$ , absolute thermal conductivity = 0.00003648 cal. cm.<sup>-1</sup> sec.<sup>-1</sup> deg.<sup>-1</sup>.

## Curves II.

$\theta = 13.132^\circ \text{ pt.} - 12.961^\circ \text{ C.}$  Therefore mean temp. of gas =  $6.48^\circ \text{ C.}$

$\psi = 0.0000035$

$R_\theta/l = 0.13202$

P.	Wide tubes.				Narrow tubes.			
	$\theta_1 = 0.002.$	$\theta' = 12.950^\circ \text{ C.}$			$\theta_1 = 0.006.$	$\theta' = 12.955^\circ \text{ C.}$		
	C.	${}^{\circ}\text{R}_\theta/\text{Jl.}$	${}^{\circ}\text{R}_\theta/\text{Jl} - \psi$	$K_a$	C.	${}^{\circ}\text{R}_\theta/\text{Jl}$	${}^{\circ}\text{R}_\theta/\text{Jl} - \psi$	$K_a$
79.41	0.1359	0.0005826	0.0005791	0.00004000	0.1119	0.0006353	0.0006318	0.00003690
68.70	0.1348	5731	5699	3936	0.1418	6344	6309	3685
59.83	0.1335	5624	5589	3860	0.1416	6326	6291	3675
53.78	0.1320	5498	5463	3773	0.1416	6326	6291	3675
45.20	0.13125	5435	5400	3730	0.1415	6317	6282	3669
39.01	0.1308	5387	5352	3697	0.1414	6304	6269	3662*
35.74	0.13055	5377	5342	3690	0.1413	6299	6264	3659
33.29	0.1304	5365	5330	3682	0.1412	6291	6256	3655
31.22	0.1303	5357	5322	3676	0.1412	6291	6256	3655
29.31	0.1302	5349	5314	3671	0.14115	6286	6251	3651
27.30	0.13015	5345	5310	3668	0.1411	6282	6247	3649
25.70	0.13005	5337	5302	3662*	0.1411	6282	6247	3649
23.35	0.1300	5332	5297	3659	0.1410	6273	6238	3644
21.81	0.1299	5326	5291	3655	0.1410	6273	6238	3644
19.94	0.1298	5317	5282	3649	0.14095	6268	6233	3641
18.61	0.1298	5317	5282	3649	0.14095	6268	6233	3641
16.58	0.1297	5309	5274	3643	0.1409	6263	6228	3638
14.70	0.12965	5304	5269	3640	0.14085	6263	6228	3638
12.58	0.12955	5296	5261	3634	0.14075	6247	6212	3628
10.69	0.12945	5288	5253	3628	0.14065	6241	6206	3625
7.91	0.1293	5276	5241	3620	0.14055	6232	6197	3620
$\theta_1 = 0.005 \text{ and } \theta' = 12.956^\circ \text{ C}$								
5.00	0.12905	5255	5220	3606	0.14030	6213	6178	3608
2.33	0.1285	5210	5175	3575	0.13970	6159	6124	3577
0.43	0.1223	4719	4684	3235	0.13100	5415	5380	3142

$\alpha_0 = 1.183,$  absolute thermal conductivity =  $0.00003664 \text{ cal. cm.}^{-1} \text{ sec.}^{-1} \text{ deg.}^{-1}.$

## Curves III.

 $\theta = 15.172^\circ \text{ pt.} = 14.979^\circ \text{ C.}$  Therefore mean temp. of gas  $= 7.49^\circ \text{ C.}$ 
 $\psi = 0.0000043$ 
 $R_g/l = 0.13292$ 

P.	Wide tubes.				Narrow tubes.			
	$\theta_1 = 0.002.$		$\theta' = 14.977^\circ \text{ C.}$		$\theta_1 = 0.006.$		$\theta' = 14.973^\circ \text{ C.}$	
	C.	$(^{\circ}\text{R}_g/l).$	$(^{\circ}\text{R}_g/l) - \psi.$	$K_a.$	C.	$(^{\circ}\text{R}_g/l).$	$(^{\circ}\text{R}_g/l) - \psi.$	$K_a.$
77.62	0.1462	0.0006790	0.0006747	0.00004033	0.1523	0.0007368	0.0007325	0.00003702
64.80	0.14465	6647	6604	3647	0.1521	7349	7306	3692
55.08	0.1431	6505	6462	3662	0.15205	7344	7301	3690
46.35	0.14135	6347	6304	3768	0.15195	7331	7291	3685
39.99	0.14065	6283	6240	3730	0.15185	7325	7282	3680
36.40	0.1403	6253	6210	3712	0.15175	7315	7272	3675
33.66	0.1400	6226	6183	3695	0.15175	7315	7272	3675'
31.03	0.13995	6223	6180	3694	0.15175	7315	7272	3675'
29.23	0.13985	6214	6171	3688	0.15165	7305	7262	3670
27.64	0.13975	6205	6162	3683	0.1516	7301	7258	3668
25.59	0.1397	6200	6157	3680	0.1516	7301	7258	3668
23.79	0.1396	6192	6149	3675*	0.1516	7301	7258	3668
22.32	0.1395	6182	6139	3669	0.1516	7301	7258	3668
20.34	0.1394	6173	6130	3664	0.1515	7291	7248	3663
18.20	0.1393	6165	6122	3659	0.1514	7281	7238	3658
15.21	0.13915	6151	6108	3651	0.15135	7277	7234	3658
12.71	0.1390	6138	6095	3644	0.1513	7272	7229	3656
9.75	0.13885	6125	6082	3635	0.15115	7258	7215	3646
7.13	0.13865	6109	6066	3617	0.1510	7243	7200	3639
3.95	0.1383	6075	6033	3606	0.1506	7204	7161	3619
2.18	0.1378	6032	5989	3579	0.1500	7148	7105	3591
0.49	0.1312	5468	5425	3242	0.1409	6305	6262	3165

\*  $\alpha_0 = 1.183$ , absolute thermal conductivity  $= 0.00003675 \text{ cal. cm.}^{-1} \text{ sec.}^{-1} \text{ deg.}^{-1}$ .

## Curves IV.

0 = 17.232° pt. = 17.018° C. Therefore mean temp. of gas = 8.56° C.

$\psi$  = 0.0000053

$R_0/l$  = 0.13382

P.	Wide tubes.				Narrow tubes.			
	$\theta_1 = 0.003, \quad \theta' = 17.015^\circ \text{ C.}$				$\theta_1 = 0.007, \quad \theta' = 17.011^\circ \text{ C.}$			
	C.	$C^2R_0/Jl.$	$C^2R_0/Jl - \psi.$	$K_a.$	C.	$C^2R_0/Jl.$	$C^2R_0/Jl - \psi.$	$K_a.$
78.03	0.1503	0.0007813	0.0007760	0.00004082	0.1620	0.0008393	0.0008340	0.00003710
68.29	0.1549	7675	7622	4010	0.1619	8382	8329	3705
59.13	0.1536	7516	7493	3942	0.1618	8372	8319	3701
48.35	0.1514	7331	7278	3829	0.1617	8362	8309	3696
43.04	0.1504	7234	7181	3778	0.1616	8352	8299	3692
41.55	0.1500	7196	7143	3758	0.1615	8341	8288	3687*
37.01	0.1496	7159	7106	3738	0.1615	8341	8288	3687*
34.54	0.1492	7120	7067	3718	0.1615	8341	8288	3687*
29.82	0.1489	7091	7038	3703	0.1615	8341	8288	3687*
25.69	0.1486	7063	7010	3688*	0.1615	8341	8288	3687*
22.41	0.1484	7043	6990	3677	0.1615	8341	8288	3687*
19.84	0.1483	7034	6981	3673	0.1611	8331	8278	3682
17.83	0.1482	7024	6971	3667	0.1613	8321	8268	3678
15.72	0.14805	7010	6957	3660	0.16105	8295	8242	3666
13.32	0.1479	6996	6943	3653	0.1609	8278	8225	3659
10.60	0.1479	6996	6943	3653	0.1609	8278	8225	3659
9.52	0.1477	6977	6924	3643	0.16075	8362	8209	3652
7.13	0.1475	6958	6905	3633	0.1606	8348	8195	3645
5.02	0.1473	6939	6886	3622	0.1604	8328	8175	3637
$\theta_1 = 0.002 \text{ and } \theta' = 17.016^\circ \text{ C.}$								
2.51	0.1468	6735	6682	3515	0.15975	8215	8072	3591
$\theta_1 = 0.006 \text{ and } \theta' = 17.012^\circ \text{ C.}$								
0.37	0.1326	5623	5570	2930	0.14085	6344	6291	2798

\*  $a_0 = 1.182$ , absolute thermal conductivity  $= 0.00003688 \text{ cal. cm.}^{-1} \text{ sec.}^{-1} \text{ deg.}^{-1}$

## Curves V.

$\theta = 21.331^\circ \text{ pt.} = 21.079^\circ \text{ C.}$  Therefore mean temp. of gas  $= 10.54^\circ \text{ C.}$

$\psi = 0.0000070$

$R_0/l = 0.13562$

P.	Wide tubes.				Narrow tubes.			
	$\theta_1 = 0.004.$		$\theta' = 21.075^\circ \text{ C.}$		$\theta_1 = 0.009.$		$\theta' = 21.070^\circ \text{ C.}$	
	C.	$C^2R_0/Jl.$	$C^2R_0/Jl - \psi.$	$K_{\infty}.$	C.	$C^2R_0/Jl.$	$C^2R_0/Jl - \psi.$	$K_{\infty}.$
77.13	0.17455	0.0009920	0.0009850	0.0004184	0.17995	0.0010497	0.0010427	0.00003745
65.90	0.1726	9656	9586	1072	0.1798	10180	10410	3730
	$\theta_1 = 0.003 \text{ and } \theta' = 21.076^\circ \text{ C.}$							
56.15	0.1711	9489	9419	4000	0.1796	10456	10386	3730
46.33	0.16885	9242	9172	3895	0.17945	10438	10368	3724
40.20	0.1670	9040	8970	3810	0.17935	10427	10357	3720
32.19	0.1658	8909	8839	3754	0.1792	10409	10339	3713
27.38	0.1653	8876	8806	3740	0.1791	10397	10327	3709
23.47	0.1650	8824	8754	3718	0.17895	10380	10310	3703
20.76	0.1648	8804	8734	3709	0.17895	10380	10310	3703
17.78	0.1646	8782	8712	3700*	0.17885	10368	10298	3699
15.22	0.1645	8771	8701	3690	0.17875	10357	10287	3695
13.19	0.1643	8750	8680	3687	0.1787	10350	10280	3692
10.57	0.1642	8739	8669	3682	0.1786	10337	10267	3687
7.90	0.16395	8713	8643	3671	0.1784	10316	10246	3680
5.16	0.1636	8676	8606	3655	0.17815	10280	10210	3667
2.44	0.16295	8606	8536	3625	0.1773	10189	10119	3630
	$\theta_1 = 0.008 \text{ and } \theta' = 21.071^\circ \text{ C.}$							
0.46	0.1564	7928	7858	3337	0.1668	0.0009018	0.0008948	3214

$\rho = 1.183,$  absolute thermal conductivity  $= 0.00003703 \text{ cal. cm.}^{-1} \text{ sec.}^{-1} \text{ deg.}^{-1}.$

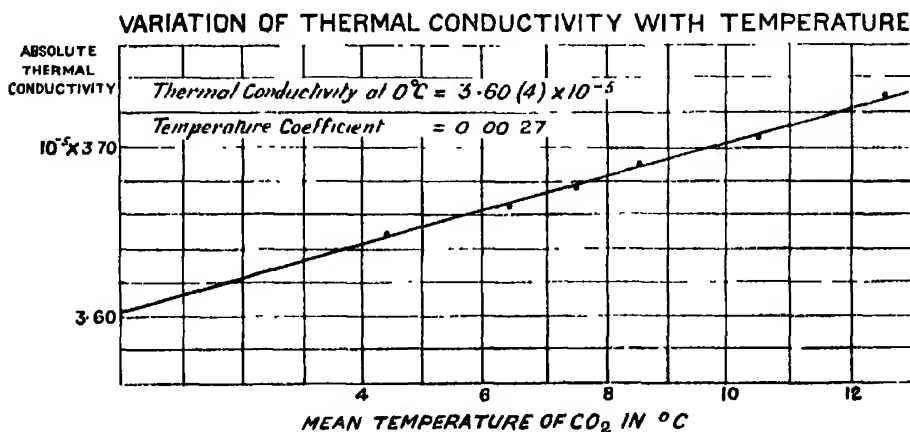


FIG. 3.

## Curves VI.

$\theta = 25.431^\circ \text{ pt. } 25.147^\circ \text{ C. Therefore mean temp. of gas} = 12.57^\circ \text{ C.}$

$\psi = 0.0000088$

$R_0/l = 0.13740$

P.	Wide tubes.				Narrow tubes.			
	$\theta_1 = 0.004,$	$\theta' = 21.143^\circ \text{ C.}$			$\theta_1 = 0.011,$	$\theta' = 25.136^\circ \text{ C.}$		
	C.	$C^2R_0/l$	$C^2R_0/l - \psi.$	$K_a.$	C.	$C^2R_0/l$	$C^2R_0/l - \psi.$	$K_a.$
78.76	0.19145	0.0012031	0.0011916	0.00001253	0.1960	0.0012616	0.0012528	0.00003771
69.58	0.1900	11855	11767	1189	0.1959	12601	12513	3767
50.80	0.18785	11588	11500	1091	0.1950	12563	12475	3756
17.73	0.1801	11373	11285	1018	0.19545	12511	12456	3750
37.90	0.1829	10985	10897	3880	0.1953	12525	12437	3744
27.90	0.1809	10745	10657	3791	—	—	—	—
18.99	0.18005	10617	10559	1759	0.1950	12487	12399	3733
14.29	0.17975	10616	10528	3748	0.19485	12466	12378	3720*
9.01	0.1793	10557	10469	3727*	0.1945	12426	12338	3714
7.09	0.1791	10533	10445	3719	0.1943	12398	12310	3706
4.38	0.17885	10505	10417	3709	0.1942	12385	12297	3702
3.55	0.1785	10403	10375	3691	0.19375	12329	12241	3785
1.73	0.1775	10349	10258	3652	0.1925	12169	12081	3735
$\theta_1 = 0.010 \text{ and } \theta' = 25.137^\circ \text{ C}$								
0.41	0.1715	0.0009659	0.0009571	3407	0.1844	0.0011166	0.0011078	3335

\*  $\alpha_0 = 1.182,$  absolute thermal conductivity  $= 0.00003726 \text{ cal. cm.}^{-1} \text{ sec.}^{-1} \text{ deg.}^{-1}.$

These values of the absolute thermal conductivity were plotted against the mean gas temperature to which they corresponded, and a straight line was drawn through the points meeting the absolute thermal conductivity axis at the point  $3.604 \times 10^{-5} \text{ cal. cm.}^{-1} \text{ sec.}^{-1} \text{ deg.}^{-1}$ ; this being the thermal conductivity of carbon dioxide at  $0^\circ \text{ C.}$  The temperature coefficient of thermal conductivity in this region, deduced from the slope of this line, is 0.0027.

The results can be applied, in conjunction with the values for the viscosity and the specific heat at constant volume of carbon dioxide, to the determination of the function  $f$  in the equation

$$K_0 = f\eta_0 C_v,$$

in which  $f$  depends on the force operating in molecular collision.



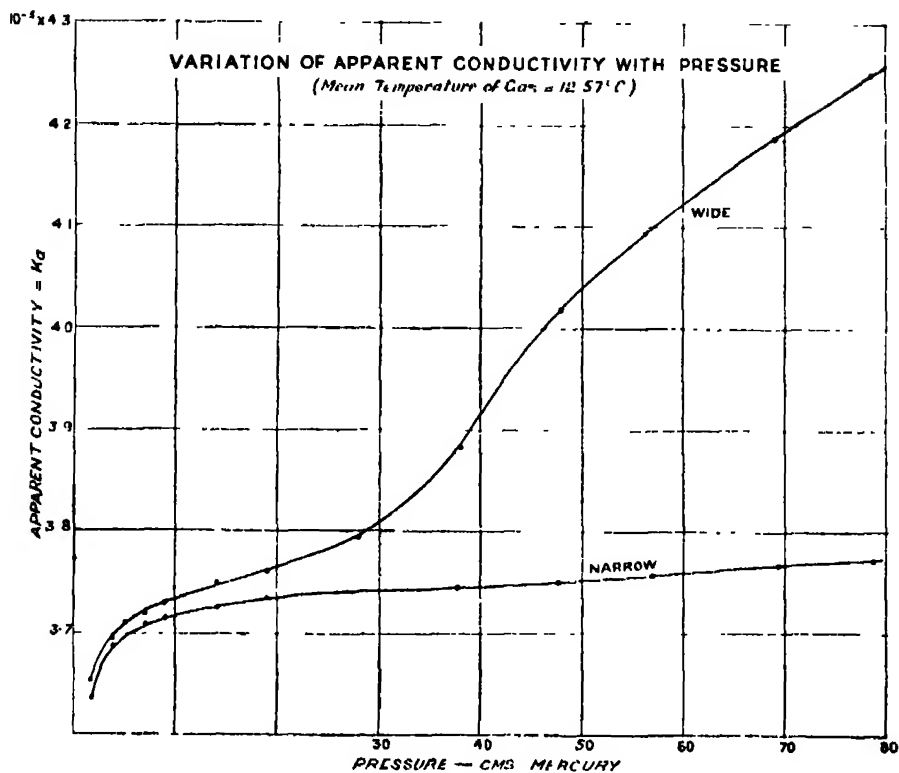


Fig. 4.

Where  $K_0 = 3.604 \times 10^{-5}$  cal. cm.<sup>-1</sup> sec.<sup>-1</sup> deg.<sup>-1</sup>

$\eta_0 = 1.428 \times 10^{-4}$

$C_v = 0.160$

Therefore  $f = K_0/\eta_0 C_v = 1.58$

#### REFERENCES.

- (1) 'Pogg. Ann.,' vol. 156, p. 497 (1875); 'Wied. Ann.,' vol. 29, p. 68 (1886); 'Wied. Ann.,' vol. 44, p. 177 (1891); 'Wied. Ann.,' vol. 48, p. 180 (1893).
- (2) 'Ann. d. Physik,' vol. 4, 54, p. 342 (1917).
- (3) 'Wied. Ann.,' vol. 34, p. 623 (1888).
- (4) 'Roy. Soc. Proc.,' A, vol. 110, p. 91 (1926).

*The Intensity of the Radiation from a Source of Electric Waves when the Electric Constants of the Medium in the Neighbourhood of the Source are different from the Electric Constants at a Distance from it.*

By H. M. MACDONALD, F.R.S.

(Received December 2, 1926.)

If a simple oscillator is close to a perfectly conducting plane, with its axis perpendicular to the plane, the magnetic force at the point  $(r, \theta)$ , where  $r$  is the distance of the point from the oscillator, and  $\theta$  is its angular distance from the axis of the oscillator, is the real part of

$$2Ae^{\frac{3\pi i}{4} + i\kappa V t} r^{-\frac{1}{2}} K_1(i\kappa r) \sin \theta,$$

and the real part of

$$Ae^{\frac{3\pi i}{4} + i\kappa V t} r^{-\frac{1}{2}} K_1(i\kappa r) \sin \theta$$

is the magnetic force due to the oscillator alone. The rate of transfer of energy across the surface of a sphere enclosing the oscillator is  $2\pi A^2/3K\kappa V$ , and the rate of transfer of energy from an oscillator  $A_1$ , when there is no conducting plane, is  $\pi A_1^2/3K\kappa V$ , and therefore, if the energy supplied is the same in both cases,  $A_1^2 = 2A^2$ , that is, the effect of the conducting plane is to increase the amplitude of the waves at any point in the ratio  $\sqrt{2}$  to 1, or to double the intensity.

The object of the following is to investigate the corresponding problem when the electric constants of the medium are not the same everywhere, and it will be shown that, if  $K, \mu$  are the electric constants of the interior space containing the oscillator, and  $K', \mu'$  are the electric constants of the space external to this, the amplitude of the oscillations is to the amplitude of the oscillations when  $K' = K, \mu' = \mu$ , in a ratio which lies between  $(\sigma/\sigma')^{\frac{1}{2}}$  and  $(\sigma'/\sigma)^{\frac{1}{2}}$ , where  $\sigma = (K/\mu)^{\frac{1}{2}}$ ,  $\sigma' = (K'/\mu')^{\frac{1}{2}}$ , and the wave-length of the oscillations is small compared with the linear dimensions of the internal space, and the oscillator is not near the boundary of the two spaces. When  $\sigma' = \sigma$ , the amplitude of the oscillations is sensibly the same as if the electric constants were not different in the two spaces, a result which is to be expected. Taking the case of a simple oscillator, where the electric constants throughout the space bounded by the sphere of radius  $r_0$ , whose centre is at the oscillator, are  $K, \mu$ , and the electric constants of the space outside this sphere are  $K', \mu'$ , let  $E_r, E_\theta, E_\phi$  be the

components of the electric force, and  $H_r$ ,  $H_\theta$ ,  $H_\phi$  the components of the magnetic force in the space  $r < r_0$ ; and let  $E_r'$ ,  $E_\theta'$ ,  $E_\phi'$ ,  $H_r'$ ,  $H_\theta'$ ,  $H_\phi'$  be the components of the electric and magnetic forces in the space  $r > r_0$ , where  $r$ ,  $\theta$ ,  $\phi$  are polar co-ordinates with the oscillator at the origin and the axis of the oscillator along the line  $\theta = 0$ ; then if the magnetic force due to the oscillator alone is the real part of

$$Ae^{\frac{3\pi i}{4} + i\kappa Vt} r^{-\frac{1}{2}} K_1(\kappa r) \sin \theta,$$

the components of the magnetic force may be written

$$H_r = 0, \quad H_\theta = 0, \quad H_\phi r \sin \theta = Ae^{\frac{3\pi i}{4} + i\kappa Vt} r^{\frac{1}{2}} K_1(\kappa r) \sin^2 \theta + Be^{i\kappa Vt} r^{\frac{1}{2}} J_1(\kappa r) \sin^2 \theta, \\ r < r_0,$$

$$H_r' = 0, \quad H_\theta' = 0, \quad H_\phi' r \sin \theta = Ce^{\frac{3\pi i}{4} + i\kappa Vt} r^{\frac{1}{2}} K_1(\kappa' r), \quad r > r_0,$$

where  $K\mu V^2 = 1$ ,  $\kappa'^2 = \kappa^2 K' \mu' V^2$ , and the real parts of the right-hand sides of these relations are taken. Again,

$$K \frac{\partial E_r}{\partial t} = \frac{1}{r^2 \sin \theta} \frac{\partial}{\partial \theta} (H_\phi r \sin \theta), \quad K \frac{\partial E_\theta}{\partial t} = -\frac{1}{r \sin \theta} \frac{\partial}{\partial r} (H_\phi r \sin \theta), \quad E_\phi = 0, \\ r < r_0,$$

and

$$K' \frac{\partial E_r'}{\partial t} = \frac{1}{r^2 \sin \theta} \frac{\partial}{\partial \theta} (H_\phi' r \sin \theta), \quad K' \frac{\partial E_\theta'}{\partial t} = -\frac{1}{r \sin \theta} \frac{\partial}{\partial r} (H_\phi' r \sin \theta), \\ E_\phi' = 0, \quad r > r_0;$$

therefore, since the tangential components of the electric and magnetic forces are continuous at the boundary  $r = r_0$ ,

$$Ae^{\frac{3\pi i}{4}} r_0^{\frac{1}{2}} K_1(\kappa r_0) + Br_0^{\frac{1}{2}} J_1(\kappa r_0) = Ce^{\frac{3\pi i}{4}} r_0^{\frac{1}{2}} K_1(\kappa' r_0),$$

$$K^{-1} Ae^{\frac{3\pi i}{4}} \frac{\partial}{\partial r_0} \{r_0^{\frac{1}{2}} K_1(\kappa r_0)\} + K^{-1} B \frac{\partial}{\partial r_0} \{r_0^{\frac{1}{2}} J_1(\kappa r_0)\} = K'^{-1} Ce^{\frac{3\pi i}{4}} \frac{\partial}{\partial r_0} \{r_0^{\frac{1}{2}} K_1(\kappa' r_0)\},$$

whence

$$A \left[ r_0^{\frac{1}{2}} K_1(\kappa r_0) \frac{\partial}{\partial r_0} \{r_0^{\frac{1}{2}} J_1(\kappa r_0)\} - r_0^{\frac{1}{2}} J_1(\kappa r_0) \frac{\partial}{\partial r_0} \{r_0^{\frac{1}{2}} K_1(\kappa r_0)\} \right] \\ = \left[ r_0^{\frac{1}{2}} K_1(\kappa' r_0) \frac{\partial}{\partial r_0} \{r_0^{\frac{1}{2}} J_1(\kappa r_0)\} - \frac{K}{K'} r_0^{\frac{1}{2}} J_1(\kappa r_0) \frac{\partial}{\partial r_0} \{r_0^{\frac{1}{2}} K_1(\kappa' r_0)\} \right].$$

$$\begin{aligned} \text{or } A \left[ r_0^4 J_{-1}(\kappa r_0) \frac{\partial}{\partial r_0} \{r_0^4 J_1(\kappa r_0)\} - r_0^4 J_1(\kappa r_0) \frac{\partial}{\partial r_0} \{r_0^4 J_{-1}(\kappa r_0)\} \right] \\ - C \left[ r_0^4 J_{-1}(\kappa' r) \frac{\partial}{\partial r_0} \{r_0^4 J_1(\kappa r_0)\} - \frac{K}{K'} r_0^4 J_1(\kappa r_0) \frac{\partial}{\partial r_0} \{r_0^4 J_{-1}(\kappa' r_0)\} \right. \\ \left. + i \{r_0^4 J_1(\kappa' r_0) \frac{\partial}{\partial r_0} \{r_0^4 J_1(\kappa r_0)\} - \frac{K}{K'} r_0^4 J_1(\kappa r_0) \frac{\partial}{\partial r_0} \{r_0^4 J_1(\kappa' r_0)\} \} \right], \end{aligned}$$

that is,

$$-2\pi^{-1}A = CLe^{\chi},$$

where

$$L \cos \chi = r_0^4 J_{-1}(\kappa' r_0) \frac{\partial}{\partial r_0} \{r_0^4 J_1(\kappa r_0)\} - \frac{K}{K'} r_0^4 J_1(\kappa r_0) \frac{\partial}{\partial r_0} \{r_0^4 J_{-1}(\kappa' r_0)\},$$

$$L \sin \chi = r_0^4 J_1(\kappa' r_0) \frac{\partial}{\partial r_0} \{r_0^4 J_1(\kappa r_0)\} - \frac{K}{K'} r_0^4 J_1(\kappa r_0) \frac{\partial}{\partial r_0} \{r_0^4 J_1(\kappa' r_0)\},$$

and

$$\begin{aligned} L^2 = \frac{2}{\pi \kappa^2} \left[ \left( 1 + \frac{1}{\kappa'^2 r_0^2} \right) \left| \frac{\partial}{\partial r_0} \{r_0^4 J_1(\kappa r_0)\} \right|^2 \right. \\ \left. + \frac{2K}{K'} \cdot \frac{1}{\kappa'^2 r_0^2} r_0^4 J_1(\kappa r_0) \frac{\partial}{\partial r_0} \{r_0^4 J_1(\kappa r_0)\} \right. \\ \left. + \frac{K^2}{K'^2} \left( \kappa'^2 - \frac{1}{r_0^2} + \frac{1}{\kappa'^2 r_0^4} \right) r_0^4 J_1^2(\kappa r_0) \right]. \end{aligned}$$

It follows that  $r > r_0$ ,  $H_\phi' r \sin \theta$  is the real part of

$$- \frac{2A}{\pi L} e^{\frac{3\pi}{4} + i\kappa Vt - i\chi} r^4 K_1(i\kappa' r) \sin^2 \theta,$$

that is,

$$H_\phi' r \sin \theta = \frac{A}{L} [r^4 J_{-1}(\kappa' r) \cos(\kappa Vt - \chi) - r^4 J_1(\kappa' r) \sin(\kappa Vt - \chi)] \sin^2 \theta,$$

whence

$$\begin{aligned} K' \frac{\partial E_\theta'}{\partial t} = - \frac{A}{r \sin \theta L} \left[ \frac{\partial}{\partial r} \{r^4 J_{-1}(\kappa' r)\} \cos(\kappa Vt - \chi) \right. \\ \left. - \frac{\partial}{\partial r} \{r^4 J_1(\kappa' r)\} \sin(\kappa Vt - \chi) \right] \sin^2 \theta, \end{aligned}$$

or

$$\begin{aligned} E_\theta' = - \frac{A}{K' \kappa V L r} \left[ \frac{\partial}{\partial r} \{r^4 J_{-1}(\kappa' r)\} \sin(\kappa Vt - \chi) \right. \\ \left. + \frac{\partial}{\partial r} \{r^4 J_1(\kappa' r)\} \cos(\kappa Vt - \chi) \right] \sin \theta. \end{aligned}$$

Now the rate of transfer of energy outwards across the surface of a sphere, whose centre is at the origin, and whose radius is  $r$ , is

$$\frac{1}{8\pi} \iint \left( M_\theta' \frac{\partial H_\phi'}{\partial t} - H_\phi' \frac{\partial M_\theta'}{\partial t} \right) r^2 \sin \theta d\theta d\phi,$$

where

$$\frac{\partial M_\theta}{\partial t} = -E_\theta',$$

and this expression is equal to

$$\begin{aligned} & \frac{1}{8\pi} \iint \left[ \frac{\Lambda \sin \theta}{K' \kappa^2 V L r} \left\{ \frac{\partial}{\partial r} \{r^{\frac{1}{2}} J_{-\frac{1}{2}}(\kappa' r)\} \cos(\kappa V t - \chi) - \frac{\partial}{\partial r} \{r^{\frac{1}{2}} J_{\frac{1}{2}}(\kappa' r)\} \sin(\kappa V t - \chi) \right\} \right. \\ & \quad + \frac{\Lambda \kappa V \sin \theta}{L r} \{r^{\frac{1}{2}} J_{-\frac{1}{2}}(\kappa' r) \sin(\kappa V t - \chi) + r^{\frac{1}{2}} J_{\frac{1}{2}}(\kappa' r) \cos(\kappa V t - \chi)\} \\ & \quad + \frac{\Lambda \sin \theta}{L r} \{r^{\frac{1}{2}} J_{-\frac{1}{2}}(\kappa' r) \cos(\kappa V t - \chi) + r^{\frac{1}{2}} J_{\frac{1}{2}}(\kappa' r) \sin(\kappa V t - \chi)\} \\ & \quad + \frac{\Lambda \sin \theta}{K' \kappa V L r} \left\{ \frac{\partial}{\partial r} \{r^{\frac{1}{2}} J_{\frac{1}{2}}(\kappa' r)\} \sin(\kappa V t - \chi) \right. \\ & \quad \left. \left. + \frac{\partial}{\partial r} \{r^{\frac{1}{2}} J_{-\frac{1}{2}}(\kappa' r)\} \cos(\kappa V t - \chi) \right\} \right] \sin^2 \theta \, d\theta \, d\phi, \end{aligned}$$

that is,

$$= \frac{\Lambda^2}{4K' \kappa V L^2} \int_0^\pi \left[ r^{\frac{1}{2}} J_{-\frac{1}{2}}(\kappa' r) \frac{\partial}{\partial r} \{r^{\frac{1}{2}} J_{\frac{1}{2}}(\kappa' r)\} - r^{\frac{1}{2}} J_{\frac{1}{2}}(\kappa' r) \frac{\partial}{\partial r} \{r^{\frac{1}{2}} J_{-\frac{1}{2}}(\kappa' r)\} \right] \sin^3 \theta \, d\theta,$$

which is

$$2\Lambda^2/3\pi K' \kappa V L^2.$$

Again, if a simple oscillator is in a medium where  $K$ ,  $\mu$  have the same values everywhere throughout the medium, and the magnetic force due to this oscillator is given by the real part of  $A_1 e^{\frac{3\pi i}{4} + i\kappa V t - i\chi}$ ,  $K_1(\kappa r) \sin \theta$ , the rate of transfer of energy from it is given by  $\pi \Lambda_1^2/3K\kappa V$ , hence, if the energy transmitted from the oscillator is the same in both cases

$$\Lambda^2 = \pi^2 K' A_1^2 L^2/4K,$$

that is,

$$\begin{aligned} (\Lambda/A_1)^2 &= \frac{\pi}{2\kappa'} \left[ \frac{K'}{K} \left( 1 + \frac{1}{\kappa'^2 r_0^2} \right) \left| \frac{\partial}{\partial r_0} \{r_0^{\frac{1}{2}} J_{\frac{1}{2}}(\kappa r_0)\} \right|^2 \right. \\ & \quad \left. + \frac{2}{\kappa'^2 r_0^3} r_0^{\frac{1}{2}} J_{\frac{1}{2}}(\kappa r_0) \frac{\partial}{\partial r_0} \{r_0^{\frac{1}{2}} J_{-\frac{1}{2}}(\kappa r_0)\} + \frac{K'}{K} \left( \kappa'^2 - \frac{1}{r_0^2} + \frac{1}{\kappa'^2 r_0^4} \right) r_0^{\frac{1}{2}} J_{-\frac{1}{2}}(\kappa r_0) \right], \end{aligned}$$

or

$$\begin{aligned} (\Lambda/A_1)^2 &= \frac{K'}{K\kappa'} \left( 1 + \frac{1}{\kappa'^2 r_0^2} \right) \left( \sin \kappa r_0 + \frac{\cos \kappa r_0}{\kappa r_0} - \frac{\sin \kappa r_0}{\kappa^2 r_0^2} \right)^2 \\ & \quad - \frac{2}{\kappa'^2 r_0^3} \left( \sin \kappa r_0 + \frac{\cos \kappa r_0}{\kappa r_0} - \frac{\sin \kappa r_0}{\kappa^2 r_0^2} \right) \left( \cos \kappa r_0 - \frac{\sin \kappa r_0}{\kappa r_0} \right) \\ & \quad + \frac{K\kappa'}{K'\kappa} \left( \cos \kappa r_0 - \frac{\sin \kappa r_0}{\kappa r_0} \right)^2; \end{aligned}$$

and, when the wave-length is small compared with  $r_0$ , this becomes

$$(A/A_1)^2 = \frac{K'\kappa}{K\kappa'} \sin^2 \kappa r_0 + \frac{K\kappa'}{K'\kappa} \cos^2 \kappa r_0,$$

that is, writing

$$(K/\mu)^{\frac{1}{2}} = \sigma, \quad (K'/\mu')^{\frac{1}{2}} = \sigma',$$

$$(A/A_1)^2 = (\sigma'/\sigma) \sin^2 \kappa r_0 + (\sigma/\sigma') \cos^2 \kappa r_0,$$

and therefore the value of  $(A/A_1)^2$  lies between  $\sigma'/\sigma$  and  $\sigma/\sigma'$ , that is, the ratio of the amplitudes of the oscillations in the two cases lies between  $(\sigma'/\sigma)^{\frac{1}{2}}$  and  $(\sigma/\sigma')^{\frac{1}{2}}$ ; if  $\sigma' = \sigma$  the amplitudes are the same.

If the oscillator is at the point  $r = r_1$ ,  $\theta = 0$ , with its axis along the line  $\theta = 0$ , the magnetic force due to the oscillator is proportional to the real part of  $\rho R^{-\frac{1}{2}} K_1(\kappa R) e^{i\kappa R}$ , where  $\rho = R \sin \theta$ ,

$$R^2 = r^2 + r_1^2 - 2rr_1 \cos \theta,$$

and the expression for the value of  $H_\phi r \sin \theta$  due to the oscillator is the real part of  $(r > r_1)$

$$\pi e^{i\kappa R} A \sum_{n=1}^{\infty} \frac{n + \frac{1}{2}}{\cos n\pi} \{r^{\frac{1}{2}} J_{-n-\frac{1}{2}}(\kappa r) - e^{(n+\frac{1}{2})\pi i} r^{\frac{1}{2}} J_{n+\frac{1}{2}}(\kappa r)\} r_1^{-\frac{1}{2}} J_{n+\frac{1}{2}}(\kappa r_1) \sin \theta \frac{dP_n}{d\theta}.$$

Therefore

$$\begin{aligned} H_\phi r \sin \theta &= \pi e^{i\kappa R} \sum_{n=1}^{\infty} \frac{n + \frac{1}{2}}{\cos n\pi} \{r^{\frac{1}{2}} J_{-n-\frac{1}{2}}(\kappa r) - e^{(n+\frac{1}{2})\pi i} r^{\frac{1}{2}} J_{n+\frac{1}{2}}(\kappa r)\} r_1^{-\frac{1}{2}} J_{n+\frac{1}{2}}(\kappa r_1) \sin \theta \frac{dP_n}{d\theta} \\ &\quad + \pi e^{i\kappa R} \sum_{n=1}^{\infty} \frac{n + \frac{1}{2}}{\cos n\pi} B_n r^{\frac{1}{2}} J_{n+\frac{1}{2}}(\kappa r) \sin \theta \frac{dP_n}{d\theta}, \end{aligned}$$

when  $r_0 > r > r_1$ , and

$$H_\phi r \sin \theta = \pi e^{i\kappa R} \sum_{n=1}^{\infty} \frac{n + \frac{1}{2}}{\cos n\pi} C_n \{r^{\frac{1}{2}} J_{-n-\frac{1}{2}}(\kappa' r) - e^{(n+\frac{1}{2})\pi i} r^{\frac{1}{2}} J_{n+\frac{1}{2}}(\kappa' r)\} \sin \theta \frac{dP_n}{d\theta},$$

when  $r > r_0$ , and the real parts of the right-hand sides of these relations are taken, where, when  $r = r_0$ ,

$$H_\phi = H_\phi', \quad \frac{1}{K} \frac{\partial}{\partial r} (H_\phi r \sin \theta) = \frac{1}{K'} \frac{\partial}{\partial r} (H_\phi' r \sin \theta);$$

whence

$$\begin{aligned} A \{r_0^{\frac{1}{2}} J_{-n-\frac{1}{2}}(\kappa r_0) - e^{(n+\frac{1}{2})\pi i} r_0^{\frac{1}{2}} J_{n+\frac{1}{2}}(\kappa r_0)\} r_1^{-\frac{1}{2}} J_{n+\frac{1}{2}}(\kappa r_1) &+ B_n r_0^{\frac{1}{2}} J_{n+\frac{1}{2}}(\kappa r_0) \\ &= C_n \{r_0^{\frac{1}{2}} J_{-n-\frac{1}{2}}(\kappa' r_0) - e^{(n+\frac{1}{2})\pi i} r_0^{\frac{1}{2}} J_{n+\frac{1}{2}}(\kappa' r_0)\}, \end{aligned}$$

$$\begin{aligned} A \left[ \frac{\partial}{\partial r_0} \{r_0^{\frac{1}{2}} J_{-n-\frac{1}{2}}(\kappa r_0)\} - e^{(n+\frac{1}{2})\pi i} \frac{\partial}{\partial r_0} \{r_0^{\frac{1}{2}} J_{n+\frac{1}{2}}(\kappa r_0)\} \right] r_1^{-\frac{1}{2}} J_{n+\frac{1}{2}}(\kappa r_1) \\ + B_n \frac{\partial}{\partial r_0} \{r_0^{\frac{1}{2}} J_{n+\frac{1}{2}}(\kappa r_0)\} = \frac{K}{K'} C_n \frac{\partial}{\partial r_0} [r_0^{\frac{1}{2}} J_{-n-\frac{1}{2}}(\kappa' r_0) - e^{(n+\frac{1}{2})\pi i} r_0^{\frac{1}{2}} J_{n+\frac{1}{2}}(\kappa' r_0)], \end{aligned}$$

and

$$\begin{aligned} C_n \left[ \left\{ r_0^{\frac{1}{2}} J_{-n-\frac{1}{2}}(\kappa' r_0) \frac{\partial}{\partial r_0} (r_0^{\frac{1}{2}} J_{n+\frac{1}{2}}(\kappa r_0)) - \frac{K}{K'} r_0^{\frac{1}{2}} J_{n+\frac{1}{2}}(\kappa r_0) \frac{\partial}{\partial r_0} (r_0^{\frac{1}{2}} J_{-n-\frac{1}{2}}(\kappa' r_0)) \right\} \right. \\ \left. - e^{(n+\frac{1}{2})\pi i} \left\{ r_0^{\frac{1}{2}} J_{n+\frac{1}{2}}(\kappa' r_0) \frac{\partial}{\partial r_0} (r_0^{\frac{1}{2}} J_{n+\frac{1}{2}}(\kappa r_0)) - \frac{K}{K'} r_0^{\frac{1}{2}} J_{n+\frac{1}{2}}(\kappa r_0) \frac{\partial}{\partial r_0} (r_0^{\frac{1}{2}} J_{n+\frac{1}{2}}(\kappa' r_0)) \right\} \right] \\ = A r_1^{-\frac{1}{2}} J_{n+\frac{1}{2}}(\kappa r_1) \left[ r_0^{\frac{1}{2}} J_{-n-\frac{1}{2}}(\kappa r_0) \frac{\partial}{\partial r_0} \{ r_0^{\frac{1}{2}} J_{n+\frac{1}{2}}(\kappa r_0) \} \right. \\ \left. - r_0^{\frac{1}{2}} J_{n+\frac{1}{2}}(\kappa r_0) \frac{\partial}{\partial r_0} \{ r_0^{\frac{1}{2}} J_{-n-\frac{1}{2}}(\kappa r_0) \} \right], \end{aligned}$$

that is,

$$C_n L_n e^{-i\chi_n} = 2A\pi^{-\frac{1}{2}} \cos n\pi r_1^{-\frac{1}{2}} J_{n+\frac{1}{2}}(\kappa r_1),$$

where

$$\begin{aligned} L_n \cos \chi_n &= r_0^{\frac{1}{2}} J_{-n-\frac{1}{2}}(\kappa' r_0) \frac{\partial}{\partial r_0} \{ r_0^{\frac{1}{2}} J_{n+\frac{1}{2}}(\kappa r_0) \} \\ &\quad - \frac{K}{K'} r_0^{\frac{1}{2}} J_{n+\frac{1}{2}}(\kappa r_0) \frac{\partial}{\partial r_0} \{ r_0^{\frac{1}{2}} J_{-n-\frac{1}{2}}(\kappa' r_0) \}, \\ L_n \sin \chi_n &= \left[ r_0^{\frac{1}{2}} J_{n+\frac{1}{2}}(\kappa' r_0) \frac{\partial}{\partial r_0} \{ r_0^{\frac{1}{2}} J_{n+\frac{1}{2}}(\kappa r_0) \} \right. \\ &\quad \left. - \frac{K}{K'} r_0^{\frac{1}{2}} J_{n+\frac{1}{2}}(\kappa r_0) \frac{\partial}{\partial r_0} \{ r_0^{\frac{1}{2}} J_{n+\frac{1}{2}}(\kappa' r_0) \} \right] \times \cos n\pi. \end{aligned}$$

Hence, taking the real parts of the expressions,

$$\begin{aligned} H_\phi' r \sin \theta &= 2A \sum_1^\infty \frac{n+\frac{1}{2}}{L_n} r_1^{-\frac{1}{2}} J_{n+\frac{1}{2}}(\kappa r_1) \{ r^{\frac{1}{2}} J_{-n-\frac{1}{2}}(\kappa' r) \cos(\kappa Vt + \chi_n) \\ &\quad + \cos n\pi r^{\frac{1}{2}} J_{n+\frac{1}{2}}(\kappa' r) \sin(\kappa Vt + \chi_n) \} \sin \theta \frac{dP_n}{d\theta}. \end{aligned}$$

Now

$$K' \frac{\partial E'}{\partial t} = - \frac{1}{r \sin \theta} \frac{\partial}{\partial r} (H_\phi' r \sin \theta),$$

whence

$$\begin{aligned} E_\phi' &= \frac{2A}{K' \kappa V r \sin \theta} \sum_1^\infty \frac{n+\frac{1}{2}}{L_n} r_1^{-\frac{1}{2}} J_{n+\frac{1}{2}}(\kappa r_1) \left[ - \frac{\partial}{\partial r} \{ r^{\frac{1}{2}} J_{-n-\frac{1}{2}}(\kappa' r) \} \sin(\kappa Vt + \chi_n) \right. \\ &\quad \left. + \cos n\pi \frac{\partial}{\partial r} \{ r^{\frac{1}{2}} J_{n+\frac{1}{2}}(\kappa' r) \} \cos(\kappa Vt + \chi_n) \right] \sin \theta \frac{dP_n}{d\theta}, \\ M_\theta' &= \frac{2A}{K' \kappa^2 V^2 r \sin \theta} \sum_1^\infty \frac{n+\frac{1}{2}}{L_n} r_1^{-\frac{1}{2}} J_{n+\frac{1}{2}}(\kappa r_1) \left[ - \frac{\partial}{\partial r} \{ r^{\frac{1}{2}} J_{-n-\frac{1}{2}}(\kappa' r) \} \cos(\kappa Vt + \chi_n) \right. \\ &\quad \left. - \cos n\pi \frac{\partial}{\partial r} \{ r^{\frac{1}{2}} J_{n+\frac{1}{2}}(\kappa' r) \} \sin(\kappa Vt + \chi_n) \right] \sin \theta \frac{dP_n}{d\theta}. \end{aligned}$$

Again, the rate of transfer of energy across the surface of the sphere, whose centre is at the origin, and whose radius is  $r > r_0$ , is

$$\frac{1}{8\pi} \int \left( M_\theta' \frac{\partial H_\phi'}{\partial t} - H_\phi' \frac{\partial M_\theta'}{\partial t} \right) r^2 \sin \theta \, d\theta \, d\phi,$$

that is,

$$\frac{1}{4} \int_0^\pi \left( M_\theta' \frac{\partial H_\phi'}{\partial t} - H_\phi' \frac{\partial M_\theta'}{\partial t} \right) r^2 \sin \theta \, d\theta,$$

and

$$\begin{aligned} M_\theta' \frac{\partial H_\phi'}{\partial t} - H_\phi' \frac{\partial M_\theta'}{\partial t} &= \frac{4A^2}{K' \kappa V r^2 \sin^2 \theta} \left[ \sum_1^\infty \frac{n+1}{L_n} r_1^{-1} J_{n+1}(\kappa r_1) \left\{ -\frac{\partial}{\partial r} \{r^1 J_{n-1}(\kappa' r)\} \cos(\kappa V t + \chi_n) \right. \right. \\ &\quad \left. \left. - \cos n\pi \frac{\partial}{\partial r} \{r^1 J_{n+1}(\kappa' r)\} \sin(\kappa V t + \chi_n) \right\} \sin \theta \frac{\partial P_n}{\partial \theta} \times \sum_1^\infty \frac{n+1}{L_n} r_1^{-1} J_{n+1}(\kappa r_1) \right. \\ &\quad \left. \{ -r^1 J_{n-1}(\kappa' r) \sin(\kappa V t + \chi_n) + \cos n\pi r^1 J_{n+1}(\kappa' r) \cos(\kappa V t + \chi_n) \} \sin \theta \frac{\partial P_n}{\partial \theta} \right. \\ &\quad \left. + \sum_1^\infty \frac{n+1}{L_n} r_1^{-1} J_{n+1}(\kappa r_1) \{r^1 J_{n-1}(\kappa' r) \cos(\kappa V t + \chi_n) \right. \\ &\quad \left. + \cos n\pi r^1 J_{n+1}(\kappa' r) \sin(\kappa V t + \chi_n) \} \sin \theta \frac{\partial P_n}{\partial \theta} \right. \\ &\quad \left. \times \sum_1^\infty \frac{n+1}{L_n} r_1^{-1} J_{n+1}(\kappa r_1) \left\{ -\frac{\partial}{\partial r} \{r^1 J_{n-1}(\kappa' r)\} \sin(\kappa V t + \chi_n) \right. \right. \\ &\quad \left. \left. + \cos n\pi \frac{\partial}{\partial r} \{r^1 J_{n+1}(\kappa' r)\} \cos(\kappa V t + \chi_n) \right\} \sin \theta \frac{\partial P_n}{\partial \theta} \right]. \end{aligned}$$

Hence, since

$$\int_0^\pi \frac{\partial P_n}{\partial \theta} \frac{\partial P_m}{\partial \theta} \sin \theta \, d\theta = 0, \quad \int_0^\pi \left( \frac{\partial P_n}{\partial \theta} \right)^2 \sin \theta \, d\theta = \frac{2n(n+1)}{2n+1},$$

the rate of transfer of energy is

$$\begin{aligned} \frac{A^2}{K' \kappa V} \sum_1^\infty \frac{(n+1)^2}{L_n^2} r_1^{-1} \{J_{n+1}(\kappa r_1)\}^2 &\left[ r^1 J_{n-1}(\kappa' r) \frac{\partial}{\partial r} \{r^1 J_{n+1}(\kappa' r)\} \right. \\ &\quad \left. - r^1 J_{n+1}(\kappa' r) \frac{\partial}{\partial r} \{r^1 J_{n-1}(\kappa' r)\} \right] \cos n\pi \frac{2n(n+1)}{2n+1}, \end{aligned}$$

that is,

$$\frac{A^2}{\pi K' \kappa V} \sum_1^\infty \frac{n(n+1)(2n+1)}{L_n^2} r_1^{-1} \{J_{n+1}(\kappa r_1)\}^2,$$

where

$$\begin{aligned} L_n^2 &= \left[ r_0^1 J_{n-1}(\kappa' r_0) \frac{\partial}{\partial r_0} \{r_0^1 J_{n+1}(\kappa r_0)\} - \frac{K}{K'} r_0^1 J_{n+1}(\kappa r_0) \frac{\partial}{\partial r_0} \{r_0^1 J_{n-1}(\kappa' r_0)\} \right]^2 \\ &\quad + \left[ r_0^1 J_{n+1}(\kappa' r_0) \frac{\partial}{\partial r_0} \{r_0^1 J_{n+1}(\kappa r_0)\} - \frac{K}{K'} r_0^1 J_{n+1}(\kappa r_0) \frac{\partial}{\partial r_0} \{r_0^1 J_{n+1}(\kappa' r_0)\} \right]^2. \end{aligned}$$



Now, when  $n + \frac{1}{2} - \kappa r_1$  is of higher order than  $(\kappa r_1)^{\frac{1}{2}}$ ,  $J_{n+\frac{1}{2}}(\kappa r_1)$  is small and diminishes rapidly exponentially as  $n$  increases; hence, if  $\kappa r_1 - \kappa r_0$  is not of lower order than  $(\kappa r_0)^{\frac{1}{2}}$ , the terms of the series for the rate of transfer of energy for which  $n + \frac{1}{2}$  is greater than  $\kappa r_0$  can be neglected in comparison with the first part of the series, as  $L_n^2$  does not vanish or become small for any value of  $n$ . Therefore the rate of transfer of energy is given by

$$A^2/(\pi K' \kappa V) \sum_1^{n_0} n(n+1)(2n+1) L_n^{-2} r_1^{-3} \{J_{n+\frac{1}{2}}(\kappa r_1)\}^2,$$

where  $n_0$  is less than  $\kappa r_0$ . Writing

$$\begin{aligned} (\kappa r_0)^{\frac{1}{2}} J_{n+\frac{1}{2}}(\kappa r_0) &= (2/\pi)^{\frac{1}{2}} R_n^{\frac{1}{2}} \sin \phi_n, \\ (\kappa r_0)^{\frac{1}{2}} J_{n-\frac{1}{2}}(\kappa r_0) &= (2/\pi)^{\frac{1}{2}} R_n^{\frac{1}{2}} \cos \phi_n \cos n\pi, \\ (\kappa' r_0)^{\frac{1}{2}} J_{n+\frac{1}{2}}(\kappa' r_0) &= (2/\pi)^{\frac{1}{2}} R_n'^{\frac{1}{2}} \sin \phi_n', \\ (\kappa' r_0)^{\frac{1}{2}} J_{n-\frac{1}{2}}(\kappa' r_0) &= (2/\pi)^{\frac{1}{2}} R_n'^{\frac{1}{2}} \cos \phi_n' \cos n\pi, \\ \tan \chi_n &= -\frac{1}{2\kappa} \frac{dR_n}{dr_0}, \quad \tan \chi_n' = -\frac{1}{2\kappa'} \frac{\partial R_n'}{\partial r_0}, \end{aligned}$$

since

$$\begin{aligned} \frac{1}{\kappa} \frac{\partial \phi_n}{\partial r_0} &= \frac{1}{R_n}, \quad \frac{1}{\kappa'} \frac{\partial \phi_n'}{\partial r_0} = \frac{1}{R_n'}, \\ \frac{1}{\kappa} \frac{\partial}{\partial r_0} \{r_0^{\frac{1}{2}} J_{n+\frac{1}{2}}(\kappa r_0)\} &= (2/\pi)^{\frac{1}{2}} R_n^{-\frac{1}{2}} \cos(\phi_n + \chi_n) \sec \chi_n, \\ \frac{1}{\kappa} \frac{\partial}{\partial r_0} \{r_0^{\frac{1}{2}} J_{n-\frac{1}{2}}(\kappa r_0)\} &= -(2/\pi)^{\frac{1}{2}} R_n^{-\frac{1}{2}} \sin(\phi_n + \chi_n) \sec \chi_n; \end{aligned}$$

whence

$$\begin{aligned} L_n^2 &= 4\pi^{-2} [(\kappa R_n'/\kappa' R_n)^{\frac{1}{2}} \cos \phi_n' \cos(\phi_n + \chi_n) \sec \chi_n + (\kappa' R_n/\kappa R_n')^{\frac{1}{2}} (K/K')] \\ &\quad \times \sin \phi_n \sin(\phi_n' + \chi_n') \sec \chi_n']^2 + 4\pi^{-2} [(\kappa R_n'/\kappa R_n)^{\frac{1}{2}} \sin \phi_n' \cos(\phi_n + \chi_n) \sec \chi_n \\ &\quad - (\kappa' R_n/\kappa R_n')^{\frac{1}{2}} (K/K') \sin \phi_n \cos(\phi_n' + \chi_n') \sec \chi_n']^2, \end{aligned}$$

that is,

$$\begin{aligned} L_n^2 &= 4\pi^{-2} [(\kappa R_n'/\kappa' R_n) \cos^2(\phi_n + \chi_n) \sec^2 \chi_n \\ &\quad + 2(K/K') \sin \phi_n \sin \chi_n' \cos(\phi_n + \chi_n) \sec \chi_n \sec \chi_n' \\ &\quad + (\kappa' R_n K^2/\kappa R_n' K'^2) \sin^2 \phi_n \sec^2 \chi_n']. \end{aligned}$$

If  $n + \frac{1}{2} = r_0 \sin \alpha_n$ , the value of  $\phi_n$  is given by

$$\phi_n = \kappa r_0 \cos \alpha_n - n\pi/2 + (n + \frac{1}{2}) \alpha_n,$$

and

$$R_n = \sec \alpha_n, \quad \tan \chi_n = \frac{1}{2} \sin^2 \alpha_n / \kappa r_0 \cos^3 \alpha_n,$$

therefore, retaining the most important parts only,  $\chi_n = 0$ ,  $\chi_n' = 0$ , and

$$L_n^2 = 4\pi^{-2} [(R_n \kappa'/\kappa R_n) \cos^2 \phi_n + (\kappa' R_n K^2/\kappa R_n' K'^2) \sin^2 \phi_n].$$

It follows that  $I_n^2 = \pi^2 K' / 4K +$  a series of cosines of multiples of  $2\phi_n$ , and since the rate of oscillation of a series of terms, whose oscillating factors are  $e^{+2i\phi_n} + 2\phi_n''$ , or  $e^{1+i\phi_n}$ , where

$$(\kappa r_1)^{\frac{1}{2}} J_{n+1}(\kappa r_1) = (2/\pi)^{\frac{1}{2}} R_n''^{\frac{1}{2}} \sin \phi_n'',$$

does not vanish for any value of  $n$ ,\* the sums of these terms for values of  $n$ , which are not small compared with  $\kappa r_0$ , can be neglected in comparison with the sum of the terms which are independent of  $\phi_n$ . Hence for values of  $n$  which are not small compared with  $\kappa r_0$ ,  $I_n^2$  can be replaced by  $\pi^2 K' / 4K$ , and the corresponding terms of the series for the rate of transfer of energy is the same as when  $K' = K$ ,  $\mu' = \mu$ , being

$$(\pi V^2 / 4K \kappa V) n(n+1)(2n+1) r_1^{-1} \{J_{n+1}(\kappa r_1)\}^2.$$

For values of  $n$  which are small compared with  $\kappa r_0$ ,  $\alpha_n$  can be replaced by zero, and then

$$I_n^2 = 4\pi^{-2} [(\kappa/\kappa') \cos^2(\kappa r_0 - n\pi/2) + (\kappa' K^2 / \kappa K'^2) \sin^2(\kappa r_0 - n\pi/2)],$$

that is,

$$I_n^2 = (4K/\pi^2 K') [(\sigma'/\sigma) \cos^2(\kappa r_0 - n\pi/2) + (\sigma/\sigma') \sin^2(\kappa r_0 - n\pi/2)],$$

therefore the ratio of the corresponding terms for  $n$  small compared with  $\kappa r_0$  in the series for the rate of transfer of energy, when  $K' = K$ ,  $\mu' = \mu$ , and when they are different is

$$(\sigma'/\sigma) \cos^2(\kappa r_0 - n\pi/2) + (\sigma/\sigma') \sin^2(\kappa r_0 - n\pi/2),$$

hence the ratio of the sums of the two series lies between

$$(\sigma'/\sigma) \cos^2 \kappa r_0 + (\sigma/\sigma') \sin^2 \kappa r_0 \quad \text{and} \quad (\sigma'/\sigma) \sin^2 \kappa r_0 + (\sigma/\sigma') \cos^2 \kappa r_0,$$

and the ratio of the rates of transfer of energy lies between  $\sigma'/\sigma$  and  $\sigma/\sigma'$ , that is, the ratio of the amplitudes of the oscillations in the two cases lies between  $(\sigma'/\sigma)^{\frac{1}{2}}$  and  $(\sigma/\sigma')^{\frac{1}{2}}$ , the same result as above. It may, therefore, be inferred that for any distribution of oscillators inside a closed surface separating two different media the ratio of the amplitude of the oscillations to the amplitude when the media are the same lies between  $(\sigma'/\sigma)^{\frac{1}{2}}$  and  $(\sigma/\sigma')^{\frac{1}{2}}$ , if none of the oscillators are close to the surface separating the two media. This includes the case where there is a conducting body in the interior space, as its effect can be represented by a distribution of oscillators throughout its volume or on its surface; hence it follows that in wireless telegraphy the amplitude of the oscillations is practically unaffected by differences in the electric constants of the atmosphere at a distance from the earth's surface.

\* Lorenz, 'Œuvres Scientifiques,' t. 1, p. 421.

*The Mechanism of a Thunderstorm.*

By G. C. SIMPSON, F.R.S.

(Received February 3, 1927.)

*Introduction.*

In 1909 I described a theory of the origin of the electricity in thunderstorms based on the observation that when a drop of water is broken up in the air the water obtains a positive charge while the corresponding negative charge is given to the air.\* Little attempt was then made to work out the details of the processes involved in a thunderstorm; only the most general consideration was given to the quantities involved and no description of the nature of the lightning discharges was attempted. This was mainly because very little was then known of the air currents in a thunderstorm and still less of the associated electrical fields.

Recently a number of papers have been published recording the electrical fields associated with thunderstorms and the sudden changes in the field which accompany lightning discharges.† The authors of these papers have expressed the opinion that their observations of changes in field-strength do not agree with what is to be expected according to the theory which I have propounded. This opinion is most strongly expressed in the paper by Schonland and Craib, where it is stated (p. 242): "Such a predominance of the positive type suggests that Simpson's theory of the production of the charge by the breaking up of large water-drops in an ascending air current, which would produce a cloud of negative polarity, must either be rejected or radically altered." On the other hand, the data on which these criticisms are based, together with the further knowledge of the meteorological conditions in thunderstorms which has recently been attained, provide the means of completing the details of the theory which were lacking in 1909, and it is now possible to describe the complete mechanism of a thunderstorm both qualitatively and quantitatively. This is the object of the present paper, in which I hope to be able to show that the criticisms are in error and that the theory completely explains all the observations at present available.

\* 'Phil. Trans.,' A, vol. 209, p. 379 (1909).

† C. T. R. Wilson, 'Phil. Trans.,' A, vol. 222, p. 73 (1920); Appleton, Watt and Herd, 'Roy. Soc. Proc.,' A, vol. 111, p. 615 (1926); Schonland and Craib, 'Roy. Soc. Proc.,' A, vol. 114, p. 229 (1927).

*General Meteorological Conditions in a Thunderstorm.*

Thunderstorms are of two types--(a) "heat" thunderstorms, and (b) "cold-front" thunderstorms. Both are due to instability in the atmosphere; but in the former the instability is produced through the heating of the surface air layers by intense insolation, while the instability in the latter is caused by the coming together of air currents having different thermal conditions. The more violent storms and most of those of tropical regions are of the "heat" type, and as the processes in this type are simpler and more easily described, I shall limit my detailed discussion to them; but as the main processes in all thunderstorms are similar, the conclusions reached can be applied to the "cold-front" thunderstorms without any difficulty.

Fig. 1 shows in diagrammatic form, but roughly to scale, the meteorological

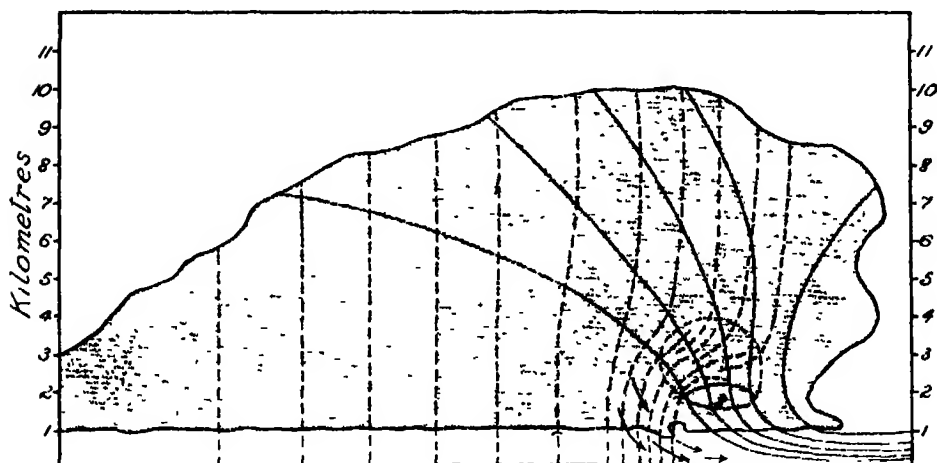


FIG. 1.

conditions in a thunderstorm of the heat type, after it has become fully developed. The thin unbroken lines represent stream lines of the air, so that they show the direction of air motion at each point, and their distance apart is inversely proportional to the wind velocity. The air enters the storm from the right, passes under the forward end of the cloud, where it takes an upward direction. We are concerned mainly with the vertical component of the velocity, and it will be noticed that although the actual velocity decreases along the stream lines, the vertical component increases as the air passes into the storm and reaches a maximum in the lower half of the cloud. The oval marked 8 indicates where the vertical component is 8 metres a second; within the oval the vertical component is more than 8 metres a second, and outside less. No water can pass

downwards through this region, because the relative velocity between air and a drop having a diameter of 0.5 cm. is 8 metres a second, and larger drops cannot exist, for they are unstable.

In the diagram the broken lines represent the paths of rain drops. On the extreme left the drops fall practically vertically, in the right half of the storm the falling drops are deflected to the left by the air stream. The magnitude of the deflection from the vertical will obviously depend on the size of the drops. Drops of the largest size will be little deflected, while the smallest drops -- cloud particles -- will travel practically along the stream lines. It is clear from the diagram without any further description that above the region of maximum vertical velocity there will be an accumulation of water. Only large drops will be able to penetrate into the lower part of this region, to just above the surface where the vertical velocity is 8 metres a second. These drops will be broken and the parts blown upwards. The small drops blown upwards will recombine and fall back again, and so the process will be continued.

The region in which this process of drop breaking and re-combining is large is indicated in the diagram by a dotted curve which starts from the surface where the vertical velocity is 8 metres a second and is shown to extend to a height of about 4 kilometres. All the time the water is within this region it is being transferred to the left, where the vertical currents are smaller, and finally it is able to escape and fall to the ground to the left of the region of maximum activity. The more violent the vertical currents the higher the region within the dotted curve extends in the atmosphere, and with very violent storms part of it extends above the altitude where the temperature reaches the freezing point. In these conditions hail is formed, and each excursion of the hailstone is recorded as a shell of clear or translucent ice. I do not wish to complicate this discussion by consideration of hail formation, so I will simply point out that so long as the surface where the vertical velocity falls to 8 metres a second is not above the 0° C. isothermal surface, water will accumulate and there will be breaking of drops.

#### *General Electrical Conditions.*

The distribution of electrical charge which will result from the conditions represented in fig. 1 are shown diagrammatically in fig. 2.

In the region where the vertical velocity exceeds 8 metres a second there can be no accumulation of electricity. Above this region where the breaking and re-combining of water drops take place—the region marked B in fig. 2— here, every time a drop breaks, the water of which the drop is composed receives a positive charge. The corresponding negative charge is given to the air and is

immediately absorbed by the cloud particles, which are carried away with the full velocity of the air current (neglecting the effect of the electrical field in

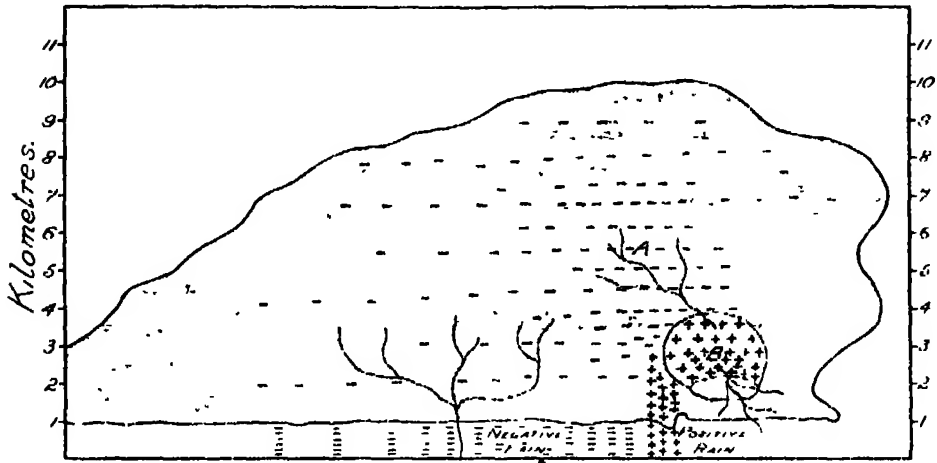


FIG. 2.

resisting separation). The positively charged water, however, does not so easily pass out of the region B, for the small drops rapidly re-combine and fall back again, only to be broken once more and to receive an additional positive charge. In this way the accumulated water in B becomes highly charged with positive electricity, and this is indicated by the plus signs in the diagram. The air with its negative charge passes out of B into the main cloud, so that the latter receives a negative charge. In what follows the region B will be described as the region of separation, for here the negative electricity is separated from the positive electricity. The density of negative charge will obviously be greatest just outside the region of separation, and this is indicated in fig. 2 by the more numerous negative signs entered in the region around A.

It should be noticed that it is not necessary for the air to have passed through the region where the vertical velocity exceeds 8 metres a second for electricity to be separated and for the air to receive a negative charge and the rain a positive charge. Breaking of drops takes place in all parts of the air stream where rain is falling, and the relative velocity between the downward moving rain and upward moving air always produces a separation of the positive and negative electricity. Thus the positive charge in the region of separation and the negative charge in the main cloud is not confined to the region between the stream lines which pass through the region where the velocity exceeds 8 metres a second. Similarly electrical effects would be produced as those indicated in

fig. 2, even if there were no vertical velocities exceeding 8 metres a second ; but in that case there would be no large accumulation of water, and it would be unlikely, but not impossible, that a sufficiently high electrical field would be produced to give rise to lightning.\*

The rain which falls out of the region of separation will obviously be positively charged, so one would expect the heavy rain near the centre of a storm to be positively charged. On the other hand, as one moves away from the region of ascending currents, one would expect the rain to be negatively charged, for it has fallen entirely out of the negatively charged cloud. This is indicated in the diagram.

With regard to the lightning, one would expect the main discharges to start in the region where the positive electricity accumulates on the rain held up in the cloud—the region of separation—and to branch upwards towards the negative charge in the main cloud and downwards towards the ground. An intense field may also be set up between the negatively charged cloud and the ground, especially if light rain has concentrated the charge in the lower part of the cloud. As a lightning discharge cannot start at a negatively charged cloud, any discharge between the ground and this part of the cloud must start on the ground and branch upwards. A more detailed description of the form of the lightning in the different parts of the storm will be given later. The chief characteristics of the lightning which are to be expected according to the theory have been indicated on fig. 2.

The above description of the meteorological and electrical conditions in a thunderstorm, according to the breaking-drop theory, gives for the first time an account of a thunderstorm in which the actual air motions, the rainfall and the distribution of electricity are combined together in a complete picture. It is now necessary to test the theory to see whether the electrical and meteorological quantities involved are of the right order of magnitude, whether the observed changes in the electrical field could be produced by the discharges which are supposed to occur, and, finally, whether the phenomenon as a whole is in accord with the observations.

#### *The Magnitude and Distribution of the Electrical Charges.*

Meteorological considerations impose certain limits on the extent of the regions in which positive and negative electricity can accumulate according to the theory. In the first place, the vertical extent of the cloud is limited by the height of the stratosphere. In Europe the height of the stratosphere is

\* 'Phil. Mag.,' vol. 30, p. 1 (1915).

approximately 10 km., in South Africa, where Schonland and Craib made their observations (latitude  $33^{\circ}$  S.), it will probably be about 15 km., while in tropical regions it may reach as high as 20 km. or more. Figs. 1 and 2 have been drawn for European conditions. The top of the cloud is shown at 10 km. and the base of the cloud 1 km. In South Africa the top of the cloud would probably be at 15 km. and the height of the other regions proportionally increased.

No actual data are available to enable one to draw the stream lines, but there can be little doubt that the lines drawn in fig. 1 are approximately correct. In the same way the position and extent of the region of maximum vertical velocity and of the region of accumulation of positively charged rain have been drawn from general principles, chief of which are that the former must be some little distance within the cloud, and the latter should be below the region where the temperature falls to the freezing point. There can be little doubt that fig. 1 represents conditions which from a meteorological point of view are possible, and that is all that is necessary in our present discussion. In any case, no reasonable redrawing of fig. 1 could alter the order of magnitude of the dimension of the various regions.

Given these regions, it is necessary to calculate the electrical fields which would be set up by various distributions of electricity within them. To do this we must simplify the problem, for it is impossible to calculate the field produced by an irregular distribution of electricity. A satisfactory method of doing this which allows of easy calculation is represented in fig. 3, A. Here the region B of fig. 2 is represented by a sphere having its centre 3 km. above the ground and a radius of 1 km.; in this sphere all the positive electricity is supposed to be confined. The region A of fig. 2 is represented as a sphere with its centre 7 km. above the ground and having a radius of 3 km.: thus this sphere, which contains the negative electricity, touches the region of positive electricity at its lowest point and the top of the cloud at its highest point. The volumes of the spheres A and B of fig. 3 are approximately the same as the volumes of the regions A and B of fig. 2.

We have now to distribute the electricity over these spheres, for it is clear that the volume distribution is not uniform. This is done in each case by dividing the main sphere into four spheres having radii  $\frac{1}{4}R$ ,  $\frac{1}{2}R$ ,  $\frac{3}{4}R$  and  $R$ , in which  $R$  is the radius of the outer sphere. We can now give to each of these spheres an appropriate volume charge spread uniformly over the sphere, and so obtain a simple method of calculating the electrical field at any point outside the sphere by assuming the charge concentrated at the centre. If  $q_1'$ ,  $q_2'$ ,  $q_3'$ , and



$q_4'$  are the uniform volume charges used for calculation, and  $q_1, q_2, q_3$  and  $q_4$  the actual volume charges in the regions 1, 2, 3, and 4 respectively, we have  $q_1 = q_1'$ ,  $q_2 = q_1' + q_2'$ ,  $q_3 = q_1' + q_2' + q_3'$ , and  $q_4 = q_1' + q_2' + q_3' + q_4'$ .

We have now to decide the order of magnitude of the total positive and negative charges and then distribute them between the spheres. Wilson\* has shown that the amount of electricity which passes in an average lightning discharge probably varies between 10 and 50 coulombs. But a lightning discharge does not neutralise all the electricity in a charged cloud, so these figures only give a minimum value of the total charge. We will, therefore, take the order of magnitude of the charge to be 100 coulombs, and distribute 100 coulombs of negative electricity in the A spheres and 100 coulombs of positive electricity in the B spheres. It is more difficult to decide how this total charge should be distributed between the spheres. In reality there is practically no limit to the possible ways in which the density may vary over the charged region, and any distribution from infinity to zero is possible, if not likely. All that we need do here is to take a distribution which is not obviously impossible. I have therefore taken the actual volume charges in the four subdivisions of the spheres to increase in steps of powers of five, that is, the actual densities in passing from sphere to sphere are taken to be  $q, 5q, 5^2q$  and  $5^3q$ . Thus the density within the inner sphere is 125 times the density in the outer sphere, but it is only 18 times the mean density in the region as a whole.

We have now to consider what changes in the positions of these spheres of varying density are likely to occur, for the field produced at points on the circumference of the outer sphere varies greatly according to the position of the various charges within the sphere. Considering the B spheres first, we may assume that the greatest density in this region, the region of separation, is at some more or less constant distance above the surface where the vertical currents fall to 8 metres per second. Therefore as the velocity of the vertical currents increase and decrease, the position of the region of maximum density will rise and fall above and below a mean position. The extreme cases are shown in figs. 3b and 3c.

The distribution of charge in the region of negative electricity, the A spheres, is not likely to undergo any large changes. The maximum density is likely to be quite near to the region where the electrical separation takes place and to decrease as one recedes from this position. The general distribution in the A spheres represented in fig. 3a is therefore likely to remain unchanged by the fluctuations in the intensity of the vertical currents.

\* *Loc. cit.*, p. 91.

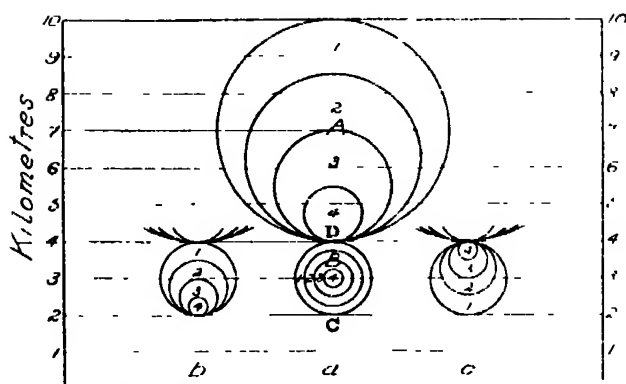


FIG. 3.

Applying the above values to the situation represented in fig. 3, we obtain the following quantities : --

*Negative Charge—*

Total quantity	= --100 coulombs.
Density in $A_1$	= $-0.130$ coulombs per $\text{km}^3$ .
Density in $A_4$	= $-16.3$ coulombs per $\text{km}^3$ .
Field at D due to negative charge	= $-0.59 \times 10^6$ volts per metre.
Field at C due to negative charge	= $-0.09 \times 10^6$ volts per metre.
Field at ground due to negative charge	= $-5.7 \times 10^4$ volts per metre.

*Positive Charge -*

Total quantity	= +100 coulombs.
Density in $B_1$	= $+3.49$ coulombs per $\text{km}^3$ .
Density in $B_4$	= $+436$ coulombs per $\text{km}^3$ .

	Distribution as in fig. 3b.	Distribution as in fig. 3a.	Distribution as in fig. 3c.
	V/M.	V/M.	V/M.
Field at D due to positive charge .....	$-0.51 \times 10^6$	$-0.88 \times 10^6$	$-5.13 \times 10^6$
Field at C .....	$+5.17 \times 10^6$	$+0.94 \times 10^6$	$+0.52 \times 10^6$
Field at ground .....	$+28 \times 10^4$	$+20 \times 10^4$	$+16 \times 10^4$

*Combined Field due to Positive and Negative Charges—*

	Distribution as in fig. 3b.	Distribution as in fig. 3a.	Distribution as in fig. 3c.
	V/M.	V/M.	V/M.
Field at D .....	$-1.10 \times 10^6$	$-1.47 \times 10^6$	$-5.72 \times 10^6$
Field at C .....	$+5.07 \times 10^6$	$+0.85 \times 10^6$	$+0.43 \times 10^6$
Potential gradient at ground	$+22.00 \times 10^4$	$+14.00 \times 10^4$	$10.00 \times 10^4$
Potential gradient at ground 15 km. away .....		-900	

The potential gradient changes sign at 5.8 km. from the storm.

Fig. 4 shows the variation of the electrical force at different heights above the ground with the three distributions of positive charge. The curves have not been calculated except at C and D, but they have been drawn to show the main features of the field and are sufficiently correct for that purpose.

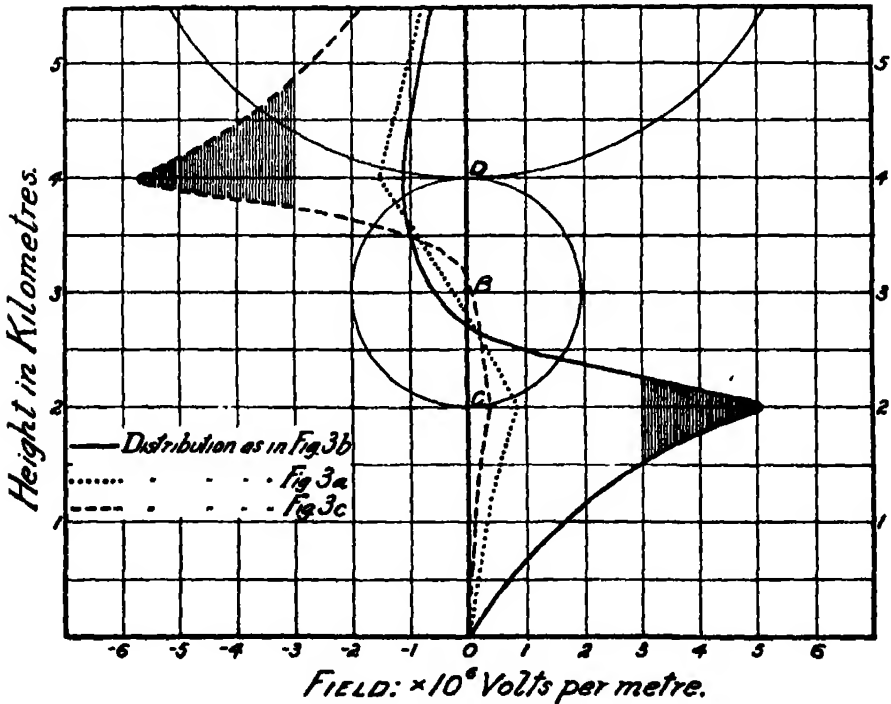


FIG. 4.

*March 3, 1927.*

SIR ERNEST RUTHERFORD, O.M., President, in the Chair.

The following papers were read :—

- I. "An Investigation of the Rate of Growth of Crystals in Different Directions." By M. BENTIVOGLIO. Communicated by Sir HENRY MIERS, F.R.S. (Revised and read by H. L. BOWMAN)
- II. "Doppler Effects and Intensities of Lines in the Molecular Spectrum of Hydrogen Positive Rays." By M. C. JOHNSON. Communicated by S. W. J. SMITH, F.R.S.
- III. "A Vector Loci Method of Treating Coupled Circuits." By E. MALLETT. Communicated by T. MATHER, F.R.S.
- IV. "The Thermal Conductivity of Carbon Dioxide." By H. GREGORY and H. MARSHALL. Communicated by H. L. CALLENDAR, F.R.S.
- V. "Bands in the Secondary Spectrum of Hydrogen." By H. S. ALLEN and I. SANDEMAN. Communicated by O. W. RICHARDSON, F.R.S.
- VI. "The Constants of the Magnetic Dispersion of Light " By C. G. DARWIN, F.R.S. and W. H. WATSON.

*March 10, 1927.*

SIR ERNEST RUTHERFORD, O.M., President, in the Chair.

The following papers were read :—

- I. "The Viscous Elastic Properties of Muscle." By A. LEVIN and J. WYMAN. Communicated by A. V. HILL, F.R.S.
- II. "Changes in the Ovary of the Mouse following Exposure to X-Rays." By F. W. R. BRAMBELL and A. S. PARKES. Communicated by J. P. HILL, F.R.S.
- III. "Ovarian Regeneration in the Mouse after Complete Double Ovariectomy." By A. S. PARKES, U. FIELDING and F. W. R. BRAMBELL. Communicated by J. P. HILL, F.R.S.
- IV. "The Relation between 'Density' of Sperm-Suspension and Fertility as determined by Artificial Insemination of Rabbits." By A. WALTON. Communicated by F. H. A. MARSHALL, F.R.S.
- V. "The Action of Glucosone on Normal Animals (Mice) and its Possible Significance in Metabolism." By A. HYND. Communicated by Sir JAMES IRVINE, F.R.S.

March 17, 1927.

SIR ERNEST RUTHERFORD, O.M., President, in the Chair.

The following papers were read :—

- I. "The Structure of Certain Silicates." By W. L. BRAGG, F.R.S., and J. WEST.
- II "The Analysis of Beams of Moving Charged Particles by a Magnetic Field." By W. A. WOOSTER. Communicated by Sir ERNEST RUTHERFORD, P R.S.
- III. "The Magnetic Susceptibility of some Binary Alloys." By J. F. SPENCER and E. M. JOHN. Communicated by W. WILSON, F.R.S.
- IV. "The Refractive Indices of Nicotine." By J. W. GIFFORD and T. M. LOWRY, F.R.S.
- V. "A Contribution to Modern Ideas on the Quantum Theory." By H. T. FLINT and J. W. FISHER. Communicated by O. W. RICHARDSON, F.R.S.

March 24, 1927.

SIR ERNEST RUTHERFORD, O.M , President, in the Chair.

The following papers were read :—

- I. "Interaction between Ipsilateral Spinal Reflexes acting on the Flexor Muscles of the Hind-limb." By S. COOPER, D. E. DENNY-BROWN and Sir CHARLES SHERRINGTON, F.R.S.
- II. "The Development and Morphology of the Gonads of the Mouse." Part I. By F. W. R. BRAMBELL. Communicated by J. P. HILL, F.R.S.
- III. "The Golgi Apparatus in the Cells of Tissue Cultures." By R. J. LUDFORD. Communicated by J. A. MURRAY, F.R.S.
- IV. "The Nature of Golgi Bodies and other Cytoplasmic Structures appearing in Fixed Material." By C. E. WALKER and M. ALLEN. Communicated by Sir JOHN FARMER, F.R.S.
- V. "The Development of Chinese *Leishmania* in *Phlebotomus Major* var. *Chinensis* and *P. Sergenti* var." By W. S. PATTON and E. HINDLE. Communicated by H. H. DALE, Sec. R.S.
- VI. "The Giant Cells in the Placenta of the Rabbit." By G. S. SANSOME. Communicated by J. P. HILL, F.R.S.

Taking first the curve for the symmetrical distribution of the positive charge about the centre of the charged region, as in fig. 3a, it will be seen that there is a maximum negative field at D and a maximum positive field at C, but in neither case does the field rise to  $3 \times 10^6$  V/M, which is the field necessary to initiate a lightning discharge. Thus with the 100 coulombs distributed in this way there would be no discharge.

In the case of the distribution in which the positive charge is concentrated in the lower half of the charged region, as indicated in fig. 3b, there is a flat maximum of negative field at D, but it does not reach  $3 \times 10^6$  V/M; therefore no discharge can take place there. At C, however, the positive field rises to  $5.1 \times 10^6$  V/M. This field is two-thirds more than that required to start a discharge at C; therefore with this distribution a charge much less than 100 coulombs would be sufficient to start a discharge, or if the 100 coulombs is retained, the concentration in the lower half of the region need not be so marked as in the example shown.

In the case of the distribution represented by fig. 3c, in which the positive electricity is concentrated in the upper half of the sphere, the field at C is naturally small and the maximum field occurs at D where the force is  $-5.7 \times 10^6$  V/M. This is nearly twice the field required for a lightning discharge; hence with this distribution, 50 coulombs of positive electricity would be sufficient to initiate a discharge between the region of positive and negative electricity.

We thus see that with 100 coulombs of positive electricity distributed in a sphere of 1 km. radius and 100 coulombs of negative electricity distributed in a sphere of 3 km. radius directly above it, it is only necessary to concentrate part of the charge in quite a natural way to obtain lightning discharges either downwards towards the ground or upwards towards the negatively charged cloud. It might be worth while to mention here that with no negative charge above the positive charge 58 coulombs of positive electricity distributed as represented in fig. 3b is sufficient to initiate a downward discharge from C. With the distribution of positive electricity shown in fig. 3c, a discharge would be initiated from the upper point of the sphere, at D, with a positive charge of 59 coulombs and no negative charge; but in this case the discharge would not be a true upward discharge, for it would travel along a line of force towards the ground just outside the charged region.

Having now demonstrated that charges of electricity of the order known to occur in thunderstorms and distributed as required by the breaking-drop theory can produce lightning discharge both upwards and downwards from the region in which the separation of electricity occurs, it is necessary to proceed one step

farther and to show that sufficient breaking of drops can occur to produce the required separation of electricity.

*The Accumulation of Water and the Number of Drops broken.*

It is quite impossible to calculate the amount of water which accumulates in the region of separation by direct meteorological methods ; but a fair estimate can be obtained from consideration of the amount of electricity carried down by the positively charged rain.

The measurements of the electricity of rain which I made in Simla and which have been confirmed by other observers give the charge per cubic centimetre of positively charged rain as varying between 0 and 7 electrostatic units. We may therefore take the order of magnitude of the positive charge on the water in the region of separation as 1 electrostatic unit per cubic centimetre. The whole region contains 100 coulombs, therefore the total amount of water in the region is  $100 \times 3 \times 10^9 = 3 \times 10^{11}$  grams. This amount of water, if spread uniformly over the cross section of the region in which it is contained, gives a layer of water 10 cm. deep. This is certainly not an impossible amount of water from a meteorological point of view. It is interesting and important to form an estimate of the time necessary for the water to accumulate to this amount.

In fig. 5 the two lines *abc* and *a'b'c'* represent the two stream lines enclosing the greater part of the region of separation. The air is supposed to have at the ground a temperature of 30° C. and a relative humidity of about 60 per cent.

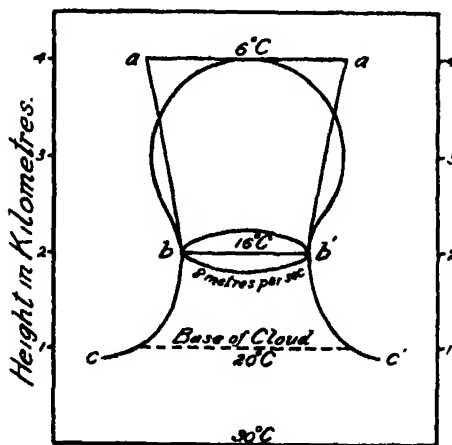


FIG. 5.

As the air ascends it reaches its dew point at a height of 1 km., where its temperature is 20° C. : this is the base of the cloud. It continues to ascend with increasing

vertical velocity until it passes into the region where the vertical velocity reaches 8 metres per second. It leaves this region at a height of about 2 km., indicated in the diagram by the line  $bb'$  and enters the region of accumulating water. By hypothesis it passes out of this region at a height of 4 km. - line  $aa'$ . As we only require the order of magnitude we may consider that the cross-sections of the current at  $aa'$  and  $bb'$  are the same and equal to the cross section of the sphere. We may also neglect the changes in the volume of air due to changes in pressure. The upward velocity of the air at  $bb'$  is 8 metres per second, therefore the volume of air entering and leaving the region of separation is  $\pi \times 10^6 \times 8 = 25 \times 10^6$  cubic metres. Now this air carries with it all the water vapour which it contained at the surface, namely, 17 grams per cubic metre. The total amount of water entering the region of separation is therefore  $25 \times 17 \times 10^6 = 425 \times 10^6$  grams per second. As the region of separation of electricity is practically the same as that of the accumulation of liquid water, the upper boundary of the region under consideration is the surface where the amount of liquid water carried out by the air current is equal to the amount which falls back under gravity in the form of rain. Thus the only water which leaves by the upper boundary is that in vapour form. The temperature here is  $6^\circ \text{C}$ . and a cubic metre of air at this temperature contains 7 grams of water vapour, so the loss of water across the upper surface is  $25 \times 7 \times 10^6 = 175 \times 10^6$  grams per second. The accumulation of water within the region of separation is therefore  $(425 - 175) 10^6 = 250 \times 10^6$  grams per second. It would therefore take

$$\frac{3 \times 10^{11}}{2.5 \times 10^8} = 10^3 \text{ seconds} = 17 \text{ minutes}$$

for the water required to accumulate. This is quite a reasonable period and is a short time for the birth of a thunderstorm.

We have now to consider the extent to which drops would be broken with this accumulation of water. As we are again dealing only with the order of magnitude, we may safely assume that half the water at any one time is in drops large enough to be broken up in the air current. A drop breaks up when its radius is 0.25 cm., therefore its volume is then 0.067 c.c. Thus the number of drops available for breaking is

$$\frac{3 \times 10^{11}}{2 \times 6.7 \times 10^{-2}} = 2.2 \times 10^{12}.$$

According to my experiments in Simla the breaking of a drop of water of



the size of a rain drop produces  $5 \times 10^{-3}$  electrostatic units of electricity. Therefore, if every drop available for breaking broke at the same time,

$$\frac{2.2 \times 5 \times 10^7}{3 \times 10^7} = 3.5 \text{ coulombs}$$

of positive electricity would be produced. Thus the drops would only have to break 10 times to produce 35 coulombs, which is the average amount required for a lightning flash. This again seems a reasonable result, and there is no reason to believe that this amount of breaking of drops could not be reached with quite moderate ascending currents.

From the above discussion it would appear that the theory under consideration is in conformity with the known facts of the air currents in a thunderstorm; that the quantities of electricity concerned, if suitably distributed within a thunderstorm cloud, are capable of producing upward and downward lightning discharges; that the accumulation of water necessary is not beyond what might be expected to occur with extensive upward currents; and that the frequency with which the accumulated water would have to be broken up from large into small drops is not excessive. It now remains to examine the records of actual thunderstorms to see whether the observations of lightning discharge and of the changes of field accompanying them agree with what would be expected according to the theory.

#### *Detailed Comparison of the Theory with Observations.*

*Rain.*—According to the scheme depicted in figs. 1 and 2, the heavy rain in the neighbourhood of the chief centre of activity of the storm has originated in two regions of the cloud. First there is the rain from the region of separation, which will be positively charged, and, secondly, the rain from the upper negatively charged cloud, which will carry a negative charge with it. Thus one would expect the rain here to be a mixture of positively and negatively charged drops, but that, on the whole, the positively charged rain should predominate. This is what is found by all observers. In my measurements in Simla the heavy rain was predominantly positive; but often, with little change in the rate of rainfall, the electricity collected in consecutive 2-minute intervals would change in amount and would not infrequently change sign. When the individual drops are investigated, as has been done by Schwend,\* this is even more clearly shown, for his observations exhibit a marked mixing of drops having positive and negative charges. In this region there is no reason why there should be

\* 'Jahresbericht der Kantonalen Lehranstalt in Samen' (1921-22).

any relationship between the size of the drops and the size of the charge carried. As one proceeds farther away from the region of the ascending currents, the charge carried by the rain is derived more and more from the negative charge carried by the cloud, until at considerable distances one would expect to find mainly negatively charged rain, although the occasional occurrence of positively charged rain is not excluded. Rain from this part of the cloud will be relatively light and uniform. The charge carried by a given quantity of water may here be very large, for the surface of the drops for a given amount of water increases greatly the smaller the drops, and the smaller the drop the slower it falls through the charged cloud, so giving more time for the accumulation of charge. This is entirely in agreement with the Simla observations, which showed that the negatively charged rain was relatively the more frequent and the more highly charged the less the intensity of the rainfall. The most highly charged rain observed in the Simla series was light rain which carried a negative charge and fell in exactly these conditions (May 13, 1908).

*Lightning.*—In a recent paper\* I discussed the physics of lightning discharges, and certain conclusions reached then are of great importance in this investigation. In that paper it was shown that after the sparking potential has been reached in any part of the atmosphere, a discharge starts at that point and progresses along a channel which constantly extends away from the seat of the positive charge. This channel generally branches and the branches are again directed away from the region of positive charge and spread out far into regions where the initial field was much below the sparking potential. It was also pointed out that the discharge drains negative electricity from the region through which it passes, and this electricity, passing along the channel towards the positively charged cloud, is frequently sufficient to neutralise the positive charge in the cloud long before the discharge has reached the negative charge towards which it is directed. We should, therefore, expect the discharges which originate at the positive electricity in the region of separation to branch upwards or downwards, but a certain number of the latter would fail to reach the ground. They may even fail to reach the bottom of the cloud, in which case it is impossible to say from visual observation whether a discharge has taken place between the two poles of the cloud or from the lower pole *towards* the ground.

Wilson† makes the following statement, which is repeated in substance by Schonland and Craib‡ :—

\* 'Roy. Soc. Proc.,' A, vol. 111, p. 56 (1926).

† *Loc. cit.*, p. 92.

‡ *Loc. cit.*

“ Discharges may be expected to occur (1) between the ground and the lower part of a thunder-cloud, (2) between the upper and lower parts of the cloud; (3) between the upper part of the cloud and the ground; and (4) upwards from the top of the cloud.”

Nothing is said about a discharge downwards from the cloud *towards* the ground but failing to reach it; although, in reality, this is the most frequent discharge of all. It is the omission of this form of discharge which has given rise to the chief objection made against the breaking-drop theory.

The majority of lightning discharges may be expected to be of the character of those just described, that is, upward and downward discharges from the positively charged regions of separation over the main ascending currents. But as the negative electricity gets carried into the remainder of the cloud, large accumulations may occur too far away from the main flashes to be discharged by them. In these circumstances strong field may be set up between the ground and the negative charge. But, as has already been remarked, a discharge cannot start on a negatively charged cloud and move towards the ground, the discharge must start on the induced positive charge on the ground, move upwards and then branch upwards and outwards within the cloud. A discharge of this type is indicated in fig. 2, and a photograph of such a lightning flash is reproduced in the paper on lightning to which reference has already been made.

We have therefore to do with three types of discharges: (a) upward discharges from the positive charge at the head of the ascending air currents, we will refer to these as of type (U); (b) downward discharges from the same region (type D); and (c) discharges from the ground to the negatively charged cloud (type N). The characteristics of discharges of types U and D are similar, but those of type N are different in many respects. Discharges of types U and D are similar in that they are relatively thin, much branched and can follow one another as fast as sufficient electricity is separated in the air currents.

Practically all discharges of type U are hidden by the cloud; but if they could be seen they would be found to be branched upwards. Some discharges of type D are completely hidden by the cloud, but some pass out of the cloud and some reach the ground; they are branched downwards. Discharges of type N are the most characteristic. They start on the ground and therefore can always be seen, they are thick and intense and do not as a rule branch until they have entered the cloud, when they branch upwards and outwards, illuminating the whole cloud with great brilliancy. After a cloud has been discharged by an N flash another discharge cannot take place for some time,

because the intense field has to be established again right to the surface of the earth. This means a large charge of negative electricity, which will take some time to accumulate.

Flashes of types U and D will occur in the part of the thunderstorm where the ascending air currents are developed and where the heavy rain occurs. On the other hand, flashes of type N will be confined almost entirely to regions under the relatively quiescent cloud mass removed from the ascending current, and where the rain, if any, is light and negatively charged.

The investigation of the frequency with which different types of lightning discharges are recorded on photographs, which I made in connection with my paper on lightning, led to results completely in accordance with the above description. Flashes of type U obviously were not represented, as they take place completely within the cloud; but the majority of flashes photographed were of type D and the branching showed clearly that they originated in a positively charged region near the bottom of the cloud. Only one photograph showed unmistakable discharges of type N; but this is a beautiful example. Other discharges of the same type may have been represented in the discharges which showed no branching, for the branching of a discharge of this type is mainly within the cloud, where it cannot be seen.

*Field of Electrical Force associated with Thunderstorms.* -The discussion of the electrical field associated with thunderstorms, especially of the changes of field due to lightning discharges, is made difficult by the fact that a given distribution of electricity may produce fields of opposite sign according to the distance of the place of observation from the seat of the electrical charges. To simplify and shorten the present discussion I do not propose to consider the actual field at any place or time, for whatever it may be we can always account for it by making a suitable distribution of charge. The sign of the field at a single observing point is no criterion even of the polarity of the cloud: we may have positive or negative fields at all distances with a cloud of the same polarity but of different pole strength. Also the actual field at the observing point is greatly affected by near charges which may have nothing to do with the discharges which cause the field-changes. It will also shorten our discussion if we consider that any change in the distribution of the electricity is brought about by movements of positive electricity alone. This is mathematically legitimate, and as lightning discharges always start where there is an excess of positive electricity and move towards the region of negative electricity, it is in accordance with what appears to take place, although the current is always carried by electrons moving in the opposite direction to that of the discharge.

If we have a charge  $Q$  coulombs concentrated at a point  $H$  km. above the earth's surface, the field at a point  $L$  km. distant along the ground from the point directly under the cloud is given by

$$F = 1.8 \frac{Q \cdot H}{(H^2 + L^2)^{3/2}} \times 10^4 \text{ V/M.}$$

A family of curves showing this relationship is given in fig. 6, in which the abscissa are volts per metre and the ordinates height in kilometres. A series of curves is drawn for  $Q = 1$  coulomb and  $L = 2, 3, 4, 5, 8, 10$  and  $15$  km. Taking a typical curve, say, that for  $3$  km., we see that a charge of  $1$  coulomb at  $6$  km.

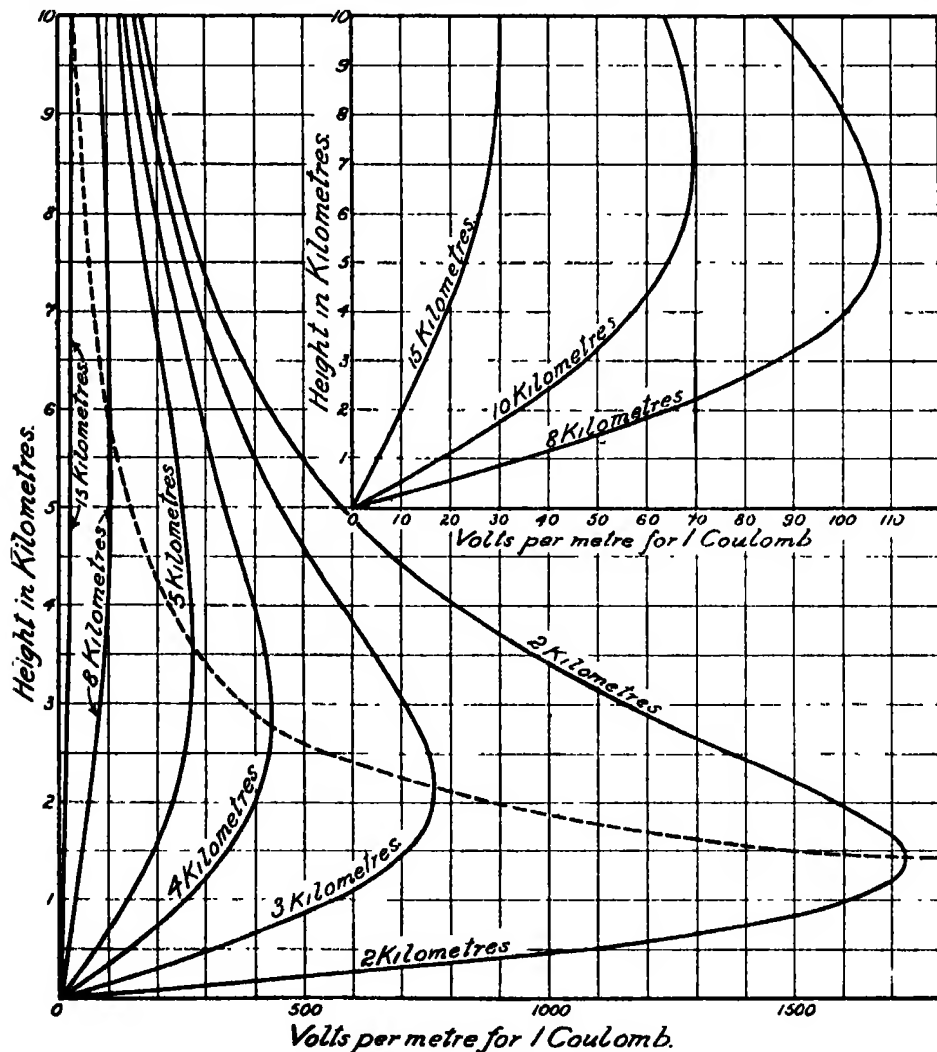


FIG. 6.

above the ground produces a potential gradient of 360 V/M at a point, P, 3 km. away. As the charge is lowered in the atmosphere the field at P increases until a maximum of 771 V/M is reached when the charge is 2 km. above the ground. As the charge is lowered still farther the field at P decreases rapidly and disappears when the charge reaches the ground. All the curves have naturally the same characteristics; the field is zero when  $H = 0$ , it reaches a maximum at a certain height and then decreases indefinitely as the charge reaches greater heights. By the aid of these curves we will examine the sign of the changes in field-strength which discharges of the three types U, D and N will produce at different distances.

Taking first discharges of type U, *i.e.*, discharges which start from the positive charge in the region of separation and move towards the negative electricity in the upper regions of the cloud. We will assume that the discharge starts at 4 km. and ends at 6 km. By this is meant that the discharge draws positive electricity from a region around a point 4 km. above the ground and distributes it over a region around a point 6 km. above ground; the actual length of the discharge channel will be longer than this and the branching may distribute the charge over quite a large region. When the storm is 15 km. away the change of field for each coulomb discharged will be from 19 V/M to 26 V/M., *i.e.*, a positive change. At 8 km. the change will still be positive from 101 V/M to 108 V/M. At 5 km., however, the change will be from 270 V/M to 230 V/M, that is, a negative change, and as the storm comes nearer the change will be increasingly negative. Thus the sign of the field-change produced by discharges of type U will always change from positive to negative as the storm approaches.

Discharges of type D must be divided into two sub-types  $D_1$  and  $D_2$  according as to whether the discharge reaches the ground or not. It is at once apparent that as the field due to a charge disappears when the charge reaches the ground all discharges of type  $D_1$  must give a negative change of field no matter how near or how distant the discharge may be. On the other hand, discharges of type  $D_2$ , *i.e.*, downward discharges which do not reach the ground, may produce either positive or negative change even without change of distance. For example, a  $D_2$  discharge 3 km. away will produce a positive change of field if it takes place from a height of 4 km. to 3 km. and a negative change if it takes place from 2 km. to 1 km. At great distances D discharges, whether they reach the ground or not, produce negative changes.

Discharges of type N always produce positive changes of the field.

It will be noticed that the ambiguity of sign occurs when a part, or the whole,

of a discharge may be above or below the point of inflexion of the curves on fig. 6. If the point of inflexion were always above the region in which the discharge takes place, there would be no ambiguity. Now all the phenomena of thunderstorms take place in the troposphere, *i.e.*, all lightning discharges start and end below 10 km. Also, the height of the point of inflexion is given by the relationship  $H = \frac{L}{\sqrt{2}}$ ; that is, whenever  $L$  is greater than 15 km.,  $H$  is greater

than 10 km. Therefore, all discharges which are more than 15 km. away produce no ambiguity in the sign of the field-changes; the relationship is then simple, a positive field-change is a clear indication that positive electricity has moved upwards, and a negative field-change that positive electricity has moved downwards. Also, if the region under the cloud can be seen, we can say at once that a positive change accompanying a discharge which can be seen to pass between the ground and the cloud indicates a discharge of type N; while if the discharge is wholly within the cloud, a positive field-change indicates a discharge of type U. Similarly a negative field-change at this distance can only be caused by a discharge of type D, and whether the discharge reaches the ground or not can only be determined by visual observation.

These considerations can be best exemplified and the theory tested by examining the observations of field-strength made by Schonland and Craib in South Africa. The typical storm shown diagrammatically in figs. 1 and 2 was prepared for the latitude of the British Isles. In South Africa the cloud would be able to extend much higher as the troposphere there extends to about 15 km. Also the high temperature allows the region of separation to be much higher than 3 km. without passing completely into the region where the temperature is below the freezing point. For these reasons amongst others we can safely assume that the discharges of the U and D type in this series of observations start at 5 km. and extend upwards and downwards from this height.

Schonland and Craib divide the storms they investigated into two classes according as to whether they were nearer than 6 km. or farther away than 8 km. In the latter class there were 18 storms, all but a few of which were more than 15 km. away. These storms, therefore, were sufficiently far away for the field-changes to be unambiguous. These distant storms gave 798 field-changes, of which 132 were positive and 666 negative. By far the large majority of the flashes were observed to occur within the cloud. In the whole series, so far as can be seen from the text, only 21 of the field-changes were associated with flashes which could be seen below the cloud, and of these 20 were positive; thus, of the 21 discharges seen, 20 were definitely of type N, *i.e.*, discharge from

the ground to the negatively charged cloud. This fits in very well with the theory according to which the majority of the discharges should be of the U and D types with an occasional discharge of the N type. As practically none of the downward discharges passed out of the cloud, we may assume that they did not extend much below 2 km. above the ground. Thus, we conclude that the average length of the D flashes was between 2 km. and 3 km., and this would probably be true also of the U flashes.

From the observations of these distant storms we are thus led to conclude that, except for an occasional discharge from the ground to the negatively charged part of the cloud, all the discharges were of the D and U types and occurred well within the cloud. Also we may conclude that there were on the average five downward discharges (negative field-changes) to one upward discharge (positive field-changes). This rate becomes 6 to 1 if we omit the 20 discharges known to be of type N.

All the six storms included by Schonland and Craib in their near class were the continuation of storms which had been observed when distant. These storms gave 48 observed field-changes, of which 39 were positive and 9 negative. This is exactly what one would have expected; for at distances nearer than 6 km. (see fig. 6) discharges starting at heights of 5 km. and passing downwards to 3 km. or 2 km. would now give positive field-changes instead of negative field-changes, while discharges passing upwards from 5 km. to any height would give negative field-changes. As the character of the discharges does not change as the storms come nearer, we should expect the ratio of upward to downward discharges to be the same in the two sets of near and far storms, and that is practically what is found, for, although there has been a complete reversal of sign, the ratio remains practically the same, being 5 or 6 to 1 for distant storms and more than 4 to 1 for the near storms.

The same agreement is found between observation and theory when the description of the individual storms given by Schonland and Craib are considered, but it is impossible to go into further detail here.

The observation that the majority of field-changes for distant storms are negative, an observation confirmed by the work of Appleton and Watson Watt, is an unambiguous indication that the majority of the discharges are from a positively charged region downwards, and is in good accord with the breaking-drop theory. There can be little doubt that the main accumulation of positively charged water will tend to be in the lower half of the region of separation rather than in the upper half. Thus the distribution of positive electricity in this region is more likely to be that shown in fig. 3 B than that shown in fig. 3 A.



This means that the sparking potential will more often be reached at the lower margin of the region of separation than at the upper, so giving rise to more discharges directed towards the ground than are directed to the cloud above.

We can get a rough independent check on the assumption that in this series of storms the downward discharges started at 5 km. and ended at 3 km. by considering what quantity of electricity would have to be discharged between these limits in order to produce the observed field-changes. Unfortunately Schonland and Craib do not give many data for the distance and field-change of individual discharges, but approximate values can be found in three cases. (a) In the description of storm 12 it is stated that when the storm was between 5 km. and 2 km. distant the field-changes were 2000 V/M. (b) Three discharges of the storm on May 1, 1926, are stated to have given field-changes of -384, -574, and -512 V/M when the distance of the discharges were 17.2 km., 13.5 km. and 15.5 km. (c) In the description of their fig. 6 it is stated that one of the field-changes of 10,000 V/M was caused by a discharge 3.10 km. away.

These data give us the widely different numerical values entered in the first two columns of the following tables, yet by assuming that the discharges were all downward discharges from a height of 5 km. to a height of 3 km., the quantity of electricity discharged in each case is found to be very similar, as will be seen from the values entered in the last column of the table. The quantities of electricity are remarkably near to one another and are of the order of magnitude we should expect, for they were all large outstanding discharges.

Field-change. V/M.	Distance. Kms.	Q. Coulombs.
2,000	4	22
- 500	15	62
10,000	3	40

It is possible to explain the observations of Wilson\* and Appleton, Watt and Herd† along the same lines, although the storms in the British Isles are less simple than those in lower latitudes, due to the fact that the region of separation is much nearer the ground in England than it is in warmer and drier regions, and therefore more of the discharges of type D reach the ground and so produce ambiguity of signs when near. It may, however, be pointed out that the description given by Watt‡ of the storms at Centre C observed by him at Khartoum is in excellent agreement with the theory. As in South Africa, the region

\* *Loc. cit.*

† *Loc. cit.*

‡ *Loc. cit.*, p. 657.

of separation in this storm appears to have been high up within the cloud. The negative electricity does not appear to have accumulated over the positive electricity, but to the side, as is shown in fig. 2. In consequence all the discharges from the region of separation were downward; but they did not leave the cloud. Each of these discharges, of which there were 181, gave, as is to be expected, a negative field-change at the observing station more than 30 km. away. There were only six positive field-changes, and five of these were seen to be the result of discharges from the earth to the cloud, and must, therefore, have been discharges of type N. It is also to be noticed that the average field-change for these six upward discharges from the ground was three times as great as the average field-change of the 181 discharges which, while striking downward, did not pass out of the cloud.

*Characteristic Recovery Curves.*—The method by which the field is renewed after each discharge is a complicated problem, and the number of published records showing different types of recovery curves is not sufficient to allow of a detailed discussion. The beautiful records obtained by Wilson, supplemented by the three published in Schonland and Craib's paper, indicate, however, that as a general rule the field after a discharge tends to return to its original state along a logarithmic curve. There are two main processes tending to counteract the separation of electricity which results from the breaking of drops: (a) the electrical field set up retards the removal of the negative charge from the positive charge, and (b) the rain from the cloud carries down negative electricity and the rain which escapes from the region of separation carries down positive electricity. In the absence of discharges a balance would be reached between these various factors, and this balance would remain so long as there was no change in the air currents supplying the storm. After such a balance has been reached each discharge temporarily destroys the balance, but it is regained more or less quickly according as to which of the factors is predominant in determining the state of balance. Thus, in spite of the fact that the force tending to separate the electricity is always acting in the same direction, the recovery curve will be positive or negative according to whether the preceding discharge was negative or positive.

#### *Some General Remarks.*

In order to simplify the problem the discharges in the preceding discussion have always been considered to pass vertically upwards or downwards. We know from observations, especially from photographs of lightning discharges, that in reality the discharges often travel along paths inclined at large angles

to the vertical, so that the lower end of a discharge may be far from vertically under the upper end. This will modify the resulting change in field-strength and may even reverse the sign according as to whether the discharge approaches or recedes from the point of observation. This is clearly seen from the curve of fig. 6. For example, if a discharge starts from a height of 4 km. at a distance of 4 km. and reaches a height of 2 km., there will be no change of field if the discharge goes vertically downwards, but there will be a large negative change if the lower end is 5 km. from the observing station and a much larger positive change if it ends only 3 km. away. This consideration must always be borne in mind when interpreting the field-changes, for it is as important for distant flashes as for near flashes, as will be seen by comparing the curves for 8 km., 10 km. and 15 km. in the upper part of fig. 6.

Another word of warning may not be out of place. The description of a thunderstorm on which this discussion is based is of an idealised storm. It will seldom occur that the course of an actual storm will follow this plan except in general outline. Large variations are possible. The ascending currents may be more local or more diffuse, they may ascend much higher or not reach as high. The region of negative electricity may be entirely over the region of separation or it may be even more to the side than is shown in figs. 1 and 2. The air currents may carry positively charged rain far from the region of separation and negatively charged rain may fall where positively charged rain is shown. It must not, therefore, be expected that observations from individual storms will fit in easily with the idealised scheme, and this applies both to the meteorological and electrical sides of the problem. The scheme will, however, be found to fit in with the average results from a large number of storms, and only in this way can it be tested. Also, it should be noticed that conclusions drawn from this study of thunderstorms cannot be directly applied to the electricity of non-thunderstorm rain. The conditions in the latter case have been discussed elsewhere.\*

It is a well-known fact that damage through lightning is much less in tropical countries than it is in Europe in spite of the greater frequency of thunderstorms in the tropics. This fact receives a simple explanation on the theory here set out, for the region of separation is much higher in the tropics than it is in higher latitudes. There are several factors tending in this direction. In the first place, the air in the tropics contains so much more water vapour that the energy available to drive the currents upwards is much greater and so they reach to greater heights. Secondly, the height at which the freezing point is

\* 'Phil. Mag.,' vol. 30, p. 1 (1915).

reached is much greater, and finally the stratosphere is so much higher that there is more vertical room in which the storm can develop. It is clear from the physics of lightning discharges that the longer the discharge path the more chance there is of the discharge ending in the atmosphere without reaching the ground. This comes out very clearly when photographs of lightning taken in tropical countries are compared with photographs taken in this country; the former show many meandering flashes which pass from cloud to cloud, while the latter often show many flashes passing straight from the cloud to the ground, often with excessive branching. Thus for the same amount of electrical display more discharges reach the ground, where they do damage, in Europe than in the tropics.

In this paper the question of thunderstorms in conditions in which drops cannot form because the temperature is below the freezing point has not been considered. That thunder and lightning do occasionally accompany snowstorms is a well-known fact; but there is some doubt as to the conditions in which such thunderstorms occur. I discussed this question in 1915\* and expressed the opinion that thunder and lightning do not occur in snowstorms unless the snow is accompanied by soft hail. This opinion has been supported by Gockel, who has independently reached the same conclusion.† In the same paper I suggested as the result of observations made in the Antarctic that the impact of ice on ice produces a separation of electricity in a manner analogous to that which occurs when a raindrop breaks.‡ If this is so, and Shaw's§ experiments indicate that it is, the collision of ice particles in these conditions takes the place of the more usual breaking of drops. The presence of the soft hail indicates violent ascending currents, in which there must be much contact between the soft hail and snow crystals in circumstances suitable for applicable separation of electricity. In fact, there are reasons to believe that the impact between ice and ice is even more effective in the separation of electricity than is the breaking of drops. But when the atmosphere is cold,

\* 'Phil. Mag.,' vol. 30, p. 1 (1915).

† 'Met. Zeit.,' vol. 40, p. 87 (1923).

‡ I should like to take this opportunity of drawing attention to an error in the paper referred to. It is there stated that impact of ice on ice leaves the ice with a positive charge, the negative charge going into the air. Later work on the Antarctic observations, however, showed that this was a wrong conclusion, for the observations can best be explained by assuming that the ice becomes negatively charged and the air positively charged; see Simpson, 'British Antarctic Expedition, 1910-13,' "Meteorology," vol. 1, pp. 309-311.

§ 'Nature,' vol. 118, p. 650 (1926).

there is little energy available for the development of thunderstorms, and, further, the separation of the positive from the negative charge is more difficult in a snowstorm than in a rainstorm because there is less relative velocity between ice crystals and air than between raindrops and air. I do not wish to develop this aspect of the problem here; I simply add these remarks for the information of those who might consider the breaking-drop theory invalidated by the occurrence of thunderstorms in conditions when drops of water cannot form and therefore cannot be broken up.

It is not my intention to make this paper controversial and to combat other people's ideas; the best way to support a theory is to show that it agrees with the observed facts, and that is what I have attempted to do in the above description. At the same time, it may facilitate further discussion if I point out the weakness in the chief objection which has been raised against the theory. The breaking-drop theory necessitates that the negative charge in a thunderstorm should be carried upwards and therefore a thunder cloud should be of negative polarity. Schonland and Craib and others have concluded that their observations of field-changes can only be explained if the polarity of a thunder cloud is positive, that is, with the positive charge above the negative charge. I have already shown that they are mistaken in this conclusion for all their observations fit in with a cloud of negative polarity when it is realised that a discharge may start downwards from the lower, or positive, pole without reaching the ground. On the other hand, if the cloud is of positive polarity, all the discharges, when the storm is distant, must produce negative changes of field-strength except discharges from the ground to the lower negative pole. This can be seen as follows:—No discharge can start from the negative pole, for I have shown in the paper on lightning mentioned above that all lightning discharges extend only *towards* the seat of the negative charge. Thus every discharge to the negative pole of a cloud must start either on the ground or at the positive pole. If the latter is above the negative pole, it can only discharge downwards, for the negative electricity towards which the discharge moves is always below it either as a volume charge in the lower pole or as an induced charge on the ground. If, therefore, a thunder cloud is of positive polarity and it is observed that all the discharges are within the cloud, these discharges can only produce negative field-changes at a distant point. If in such circumstances both positive and negative field-changes are observed this is clear proof that the polarity of the cloud is not positive. As several of the storms observed by Schonland and Craib are stated to have produced flashes only within the cloud, some associated with positive field-changes and some with negative field-changes,

it is clear that in these storms at least the polarity must have been negative, as required by the breaking-drop theory.

In conclusion, I would like to add one or two words about future investigations. Measurements of field-change alone are extremely ambiguous. This ambiguity can be removed to some extent in two ways. The branching of a lightning flash is a sure indication of the direction of the current in the discharge ; for the branches are always directed away from the region of positive electricity and towards the region of negative electricity. It is therefore to be hoped that future observers will use every endeavour to describe the appearance of the flashes associated with the individual field-changes which they record. The ambiguity can be removed to some extent, but not entirely, by simultaneous observations at two stations at some considerable distance apart. If possible, therefore, pairs of stations should be occupied and records of the same flashes obtained at each. Three stations would, of course, be even better.

#### *Summary.*

A detailed description is given of the mechanism of a thunderstorm according to the theory in which the separation of electricity is brought about by the breaking of raindrops. The orders of magnitude of the meteorological and electrical quantities involved are investigated and shown to be in accordance with observations. The observations made by Schonland and Craib in South Africa of changes of electrical field-strength produced by lightning discharges are examined in the light of the theory and found to be in complete accord.

*The Initial Stages of Gaseous Explosions. Part I—Flame Speeds during the Initial "Uniform Movement."*

By WILLIAM A. BONE, D.Sc., F.R.S., R. P. FRASER, A.R.C.S., D.I.C., and  
D. A. WINTER, B.Sc., A.R.C.S., D.I.C.

(Received January 24, 1927.)

[PLATES 27-29.]

*Introduction.*

Our knowledge of the initial stages of gaseous explosions principally rests upon foundations laid by Mallard and Le Chatelier in their classical 'Recherches Expérimentales et Théoriques sur la Combustion des Mélanges Gazeux Explosifs' published in the year 1883.\* They showed that, in general, gaseous explosions pass through certain well-defined stages, commencing with a comparatively slow flame propagation, which is soon accelerated, and culminating in the phase of maximum speed and intensity known as "detonation," as had been discovered independently by Berthelot and Vieille two years previously.†

Mallard and Le Chatelier devised new experimental methods, chiefly photographic and electrical, for investigating flame movements during the initial phases of explosions. Of these, they much preferred the photographic method, which consisted essentially in recording the movement of the flame along a horizontal glass tube on a sensitised plate moving vertically at a known velocity; thus, to quote the original memoir, "on obtiendra une courbe dont chaque point aura pour abscisse le chemin parcouru par la flamme dans la tube, et pour ordonnée le temps écoulé depuis l'origine de la combustion."

As the plates which they used were not sufficiently sensitive to record satisfactorily the movement of flames of such low actinic power as are developed in most explosive mixtures, Mallard and Le Chatelier chiefly employed mixtures of carbon disulphide with either oxygen or nitric oxide, which yield highly actinic flames, on the supposition that they might be regarded as typical of "oxygen" or of "air" mixtures, respectively.

The behaviour of such mixtures was found to differ according to whether they were ignited at or near (*a*) the *open* or (*b*) the *closed* end of a tube. In the case of (*a*)—the *open tube* method—it was always observed that the flame

\* 'Ann. Mines,' vol. 8, pp. 274 and 618 (1883).

† 'Ann. Chim. Phys.,' vol. 28, p. 289 (1881).

proceeded for a certain distance along the tube at a practically uniform slow velocity (the initial "uniform movement") which they considered as truly representing "le mode de propagation par conductibilité." With the  $\text{CS}_2$ -nitric oxide mixtures, this initial "uniform" movement was succeeded by an "oscillatory" or "vibratory" period, the flame swinging backwards and forwards with increasing amplitudes, finally, *either* dying out altogether, *or* giving rise to "detonation," according to circumstances. With the  $\text{CS}_2$ -oxygen mixtures on the other hand, the initial period of "uniform movement" was shorter, and appeared to be succeeded abruptly by "detonation," without passing through any intermediate "oscillatory" phase.

When, however, any mixture was ignited near the *closed* end of the tube, the forward movement of the flame was continuously accelerated until, finally, "detonation" was set up.

*The Initial "Uniform" Movement.*—Mallard and Le Chatelier paid great attention to the initial "uniform movement" of flame, concluding that "c'est que lorsqu'on allume un mélange gazeux explosible avec une flamme, l'inflammation commence toujours au début par se propager d'un mouvement uniforme. La vitesse de ce mouvement uniforme, qui se prolonge pendant un temps plus ou moins long suivant le cas, est constant pour un même mélange gazeux brûlant dans les mêmes conditions; elle est toujours modérée et certainement inférieure à 30 metres par seconde par tous les mélanges étudiés jusqu'à présent."

The admirable experimental investigations on the subject carried out since 1914 by R. V. Wheeler and collaborators under the auspices of the Safety of Mines Committee, have considerably extended in several directions our knowledge of "flame speeds" during the initial phase of gaseous explosions. They corrected certain errors in Mallard and Le Chatelier's uniform "flame-speed curves" for methane-air mixtures, and showed that such speeds are not so independent of the tube diameter as Mallard and Le Chatelier had supposed. Indeed, in 1920 Wheeler and Mason expressed the opinion that if the original conception of the "uniform movement" as being "le mode de propagation par conductibilité" be accepted, "it is a strictly limited phenomenon obtainable only in tubes within a certain range of diameter, large enough to prevent appreciable cooling by the walls, but narrow enough to suppress the influence of convection currents" . . . or, alternatively, that it "should be regarded simply as a particular phase in the propagation of flame that occurs when ignition is effected (in a quiescent mixture) at the open end of a straight horizontal tube (of any diameter) closed at the other end, and not as resulting from



a particular mode of heat transference"\* adding that "the latter is the preferable, if not the only correct way of regarding the uniform movement."

We were led to undertake the present research some three years ago because of our desire to test experimentally the validity of a supposed new "law of flame speeds" which W. Payman and R. V. Wheeler had propounded in the year 1922,† and for which they have since claimed general applicability to all conditions of flame propagation.‡ We had not proceeded very far with such intention, however, before we discovered features of the initial flame propagation through explosive mixtures which seemed to put matters in a rather new light. Therefore, without departing from our original intention, we decided to widen its scope. In the present paper, we propose dealing with some of the more general aspects of the problem, leaving the supposed "law of flame speeds" to be discussed in our next one.

Most of the existing data concerning flame speeds during the initial "uniform movement" after ignition refer to mixtures of combustible gases with air in various proportions. For the purposes of our enquiry, however, it was deemed necessary first of all to make a systematic study of certain oxygen mixtures concerning whose behaviour comparatively little is known. Mallard and Le Chatelier attempted to measure the initial speed of uniform flame propagation through various explosive mixtures of hydrogen and oxygen when ignited at the open end of a 1 cm. diameter glass tube, with the following results:

Percentage of		Speed in metres per second.
H <sub>2</sub> .	O <sub>2</sub> .	
33	67	10
50	50	17
77	23	18
84	16	13
89	11	8

They considered such speeds to be too high for the true "uniform" propagation "*car la propagation de la flamme a toujours été accompagnée des mouvements vibratoires.*"

We have principally studied the behaviours of undiluted mixtures of oxygen with various proportions of hydrogen, ethylene or acetylene, respectively,

\* 'Trans. Chem. Soc.,' vol. 117, p. 1228 (1920).

† 'Trans. Chem. Soc.,' vol. 121, p. 363 (1922).

‡ 'Trans. Faraday Soc.,' vol. 22, p. 301 (1926).

many of which are fast burning. For this purpose, one or other of two methods, namely, (i) photographic, and (ii) electrical, were employed. A detailed description of these will now be given.

#### EXPERIMENTAL.

##### (A) *The Methods employed for Measuring Flame Speeds.*

(i) *The Photographic Method.*—There can be no doubt that, whenever the actinic qualities of the flame permit, a photographic method on the lines employed by Mallard and Le Chatelier is preferable to any other, because it enables not only flame speeds to be measured with reasonable accuracy but also the whole flame movement to be studied visually. The problem was to devise an apparatus which would give good records of flame movements through such fast burning mixtures as we proposed to study, some of which were not highly actinic.

The apparatus employed, some details of which are shown in fig. 1, comprised a revolving metal drum A, 6 inches in diameter, fixed horizontally on its axis within a light tight camera box BB, carrying a 2 mm. horizontal slit C, running the width of the drum, in front of which is a suitable wide-angle lens L. The drum could be revolved by means of a special shunt-wound constant-speed electric motor M, through special gearings, at any constant speed between 20 and 3,000 r.p.m., the last named corresponding to a peripheral speed of 2,400 cm. per second past the camera slit. The exact drum speed in any given experiment was registered by a Jaeger time-speedometer\* X registering every half-second, the reading being taken at the instant of firing.

One of two lenses was employed in the camera according to circumstances, namely: (i) whenever the flame luminosity permitted, a Zeiss lens of 7 cm. focal length,  $f/1.4$ , focussed on fast bromide paper or film  $4\frac{1}{2}$  inches wide, or (ii) a quartz lens of 6 cm. focal length,  $f/1.8$ , focussed on a film 2 inches wide of maximum sensitivity obtainable.

Glass or quartz explosion tubes of 2.5 cm. internal diameter were used throughout the experiments, one and the same tube being employed throughout each series. In an experiment the tube EE was firmly clamped at  $K_1$  and  $K_2$  to a massive bridge DD erected over the table, but independent of it, so as to avoid the tube being affected by any slight camera vibration. Strips of black paper

\* The accuracy of the speedometer was checked at the outset by a direct tuning-fork method; it being found to read 1.6 per cent. too low, a suitable correction was always applied to the readings obtained by it.

$r_1$ ,  $r_2$  and  $r_3$  serving as reference marks were gummed on the tube at distances of 2 cm., 12 cm. and 22 cm., respectively, from its flanged mouth  $F_1$ . This

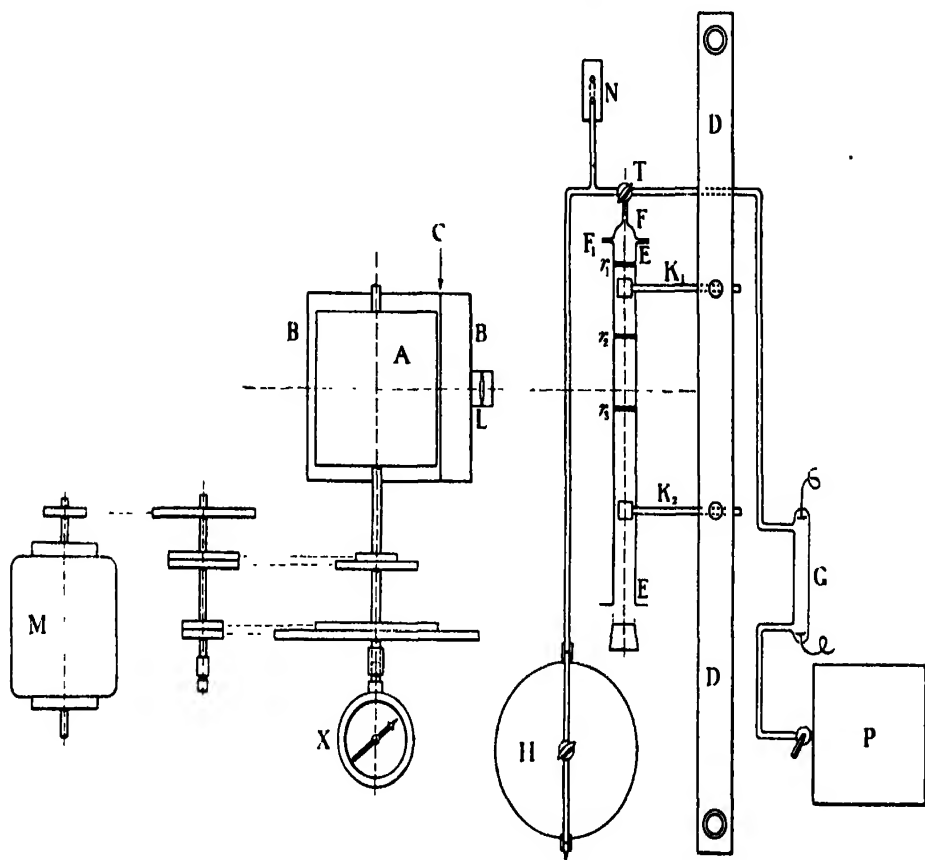


FIG. 1.

flanged mouth was closed by a movable piece  $F$  carrying a three-way tap  $T$  (2 mm. bore), one branch of which was connected by a glass tube through an 8-inch discharge tube  $G$  to a large capacity vacuum pump  $P$ , capable of evacuating the whole system down to  $1/10$ th mm. pressure within a minute. The other branch of  $T$  was connected through a T-piece to (a) the mercury manometer  $N$ , and (b) the 10-litre mercury gas holder  $H$  containing the explosive mixture under investigation. The other end of the explosion tube  $EE$  was always closed by a rubber bung.

In making an experiment the explosion tube was first of all evacuated down to below  $1/10$ th mm. as indicated by the note of the pump and the appearance of the tube  $G$  under the discharge. The explosion mixture was then carefully

admitted from the holder, until the manometer N indicated a slight pressure (2 mm. or so) above that of the atmosphere. The image of the first 40 cm. of the explosion tube was focussed along the horizontal slit in the camera, and the drum was then set revolving at such a speed as would subsequently ensure a flame-graph angle somewhere between  $25^\circ$  and  $40^\circ$  with the horizontal. The explosive mixture in EE was then ignited by gently sliding off the flanged mouth-piece F and immediately applying a 2-cm. high coal gas flame to the quiescent explosive mixture.

It should be noted that the arrangements were such that the first 22 cm. of the explosion tube (*i.e.*, up to the second reference mark) was focussed in the centre of the field; the lens was always stopped down (often to  $f_6$ ) as far as the luminosity of the flame permitted. The photographic paper or film, as the case might be, was subsequently developed and dried very evenly so as to avoid buckling or uneven contraction; and in finally making the angular measurements on the flame speed graph the image of the reference marks on the explosion tube gave a means of drawing a truly horizontal base line, and of measuring the ratio of length of object to image. From such angular measurements the true flame speed was calculated in each particular case by means of the usual formula.

It was found possible to apply the method to all the hydrocarbon-oxygen (or air) explosive mixtures, as well as to hydrogen-oxygen mixtures with initial flame speeds exceeding 1,000 cm. per second approximately.

According to our experience, the probable experimental error in measuring flame speeds by this method may be put down as less than 2.5 per cent. We doubt whether any other method yet devised is capable of greater accuracy.

(ii) *The Electrical Method.* -The method employed for measuring flame speeds in cases of mixtures where the flames were insufficiently actinic to give good photographic records is based upon the fact that when a flame passes a gap in a high tension electric circuit too wide for the current to jump in an atmosphere of cold unburnt mixture, the ionisation produced permits of its doing so. By arranging a number of such gaps, each in an independent circuit, at known intervals along the inside of an explosion tube, together with supplementary narrow gaps outside the tube in series with each circuit, such outside gaps being suitably placed in the vicinity of a narrow revolving photographic film, means are obtained of measuring both the flame speed and the time during which the combustion products behind the flame remain ionised.

The apparatus, shown in plan in fig. 2, consisted principally of three parts, namely, (i) as a convenient source of high voltage, three induction coils  $C_1$ ,  $C_2$ ,



C<sub>3</sub>, with high speed make and break mechanisms, (ii) the explosion tube EE with gaps G<sub>1</sub>, G<sub>2</sub>, G<sub>3</sub>, and (iii) a recorder RR.

The three similarly constructed induction coils were connected in parallel, each with its own tube spark gap G, and outside gap g, and the current to each primary was so adjusted as just to allow a sufficient discharge across the gaps G when the flame front reached them. The make and break mechanism employed gave 200 interruptions per second, but the insertion of a small capacity condenser (c<sub>1</sub>, c<sub>2</sub> and c<sub>3</sub>) in the secondary circuit of each coil, which remained charged during the 1/200th of a second between successive interruptions, ensured that a spark would pass across a particular gap at the instant of the flame front meeting it, thus eliminating any errors which might arise through the make and break arrangement.

Into the glass explosion tube EE (internal diameter = 2.5 cm., and usually 120 cm. to 150 cm. long) were fitted at regular intervals, 20 cm. apart, three pairs of brass ball electrodes, each ball 3/16ths inch diameter, forming the spark gaps G<sub>1</sub>, G<sub>2</sub>, G<sub>3</sub>. The first of these was situated 7 cm. from the flanged mouth-piece of the tube. These electrodes were introduced through small side tubes sealed at right angles into the main tube; sealing wax fillings were used to render all the side joints gas-tight, and each was carefully shaped on the inside so as to avoid any distortion of the circular section of the explosion tube.

The three supplementary outside spark gaps g<sub>1</sub>, g<sub>2</sub>, g<sub>3</sub> respectively, each in circuit with its corresponding inside gap G<sub>1</sub>, G<sub>2</sub>, G<sub>3</sub> respectively, were arranged in an ebonite mounting as three pointers within 0.25 mm. to 1 mm. of an earthed or negatively charged brass plate K, through which three conical holes (h<sub>1</sub>, h<sub>2</sub>, h<sub>3</sub>, each 1/100th inch diameter) were bored. By such means the sparks were photographed as minute dots upon a photographic film (1½ inches wide) fastened to the circumference of the revolving wheel (8 inches diameter) of the recorder R. Timing was effected by means of a tuning fork T interrupting a beam of light from L through a hole in a plate B adjacent to the revolving film. The arrangements for evacuating the explosion tube by means of the oil pump P, filling it with the particular mixture under investigation from the mercury gas holder H, and subsequently igniting the latter by means of a 2 cm. high coal gas flame at the open end, were similar to those employed in connection with the photographic method, and therefore need not be detailed.

It was always necessary in measuring the speeds of the initial uniform movement in any given case to make sure that the time intervals occupied by the flames in travelling the successive distances between gaps G<sub>1</sub> to G<sub>2</sub>, and G<sub>2</sub>

to  $G_3$  were substantially equal, for otherwise the uniformity of the movement might be doubtful. The substantial equality of the said two time intervals was regarded as a reasonable criterion of the uniform movement having existed at least throughout the 20 cm. distance between gaps  $G_1$  and  $G_2$ .

Our experience has shown that this method may be used for measuring flame speeds certainly up to 300 cm., and in some cases up to 600 cm. per second, with reasonable accuracy. And as it is principally in such low speed ranges that the photographic method may fail with mixtures where flames are feebly actinic, the electrical one is a most valuable adjunct to it.

#### *Comparison of the two Methods.*

On carefully comparing the two methods by using them simultaneously for speed determinations on a series of carbonic oxide oxygen mixtures, in each case saturated with moisture at  $12.5^\circ \text{C}$ ., the following results were obtained :—

Percentage CO in $\text{CO/O}_2$ mixture.	Speed in cms. per sec. of initial uniform flame movement as determined by	
	Photographic method.	Electrical method
50.0	147	144
60.0	163	167
80.0	191	195
92.5	51	51

Also in another simultaneous test with a  $52.9\text{CH}_4/47.1\text{O}_2$  mixture, the photographic method gave 126, and the electrical method 122 cm. per second as the speed of initial uniform movement. Therefore, it may be taken for granted that when used with the same mixture the two methods give results within about 2.5 per cent. of each other, *i.e.*, within what we estimate to be the usual experimental error in such determinations.

#### *(B)—Some General Observations upon the Initial Movement of Flame through Mixtures of Oxygen with Hydrogen, Ethylene, and Acetylene respectively.*

The experimental methods having been thoroughly tested we proceeded to the next stage of the investigation, namely, the determination of the speed of initial "uniform" flame movement through stagnant mixtures of oxygen with hydrogen, ethylene, or acetylene, respectively, when ignited at  $15$  to  $18^\circ \text{C}$ . and atmospheric pressure at the open end of a 2.5 cm. diameter tube (closed

at the other end) by means of a 2 cm. high coal gas flame. And it may be assumed that unless otherwise stated all the flame speeds given in this paper refer to such conditions. The experiments had to be carried out with exceptional care because many of the mixtures concerned were so sensitive that it was only by scrupulous attention to details that reliable results could be obtained.

Needless to say, every possible precaution was taken to ensure the purity of the various single gases (hydrogen, acetylene, ethylene and oxygen) used in making up the various experimental mixtures, special care being taken to reduce the amounts of adventitious nitrogen in them to the smallest dimensions; it may be assumed that the amount of it present in the experimental mixtures never exceeded, and was often less than, 1 per cent.\* The experimental mixtures were always made and stored under pressure in special 10-litre gas holders over mercury, and their compositions were always checked by chemical analysis. The windows of the laboratory in which all the operations including the flame speed determinations were carried out had dark blinds always kept drawn so as to exclude daylight. The room temperature remained between about 15 and 18° C. throughout the experiments.

Before detailing the flame-speed results, we think it desirable to say something about certain general features which seem to have an important bearing upon the proper interpretation of what has been termed hitherto "the initial uniform flame movement."

In the first place, with reference to the mixtures examined, we have found that, whilst all these initially propagating flame under the stated conditions at speeds up to about 4,000 cm. per second showed a well-defined initial "uniform movement," the speed of which was substantially the same in successive determinations, those propagating at higher initial speeds behaved differently.

Thus, for example, with ethylene-oxygen or acetylene-oxygen mixtures initially propagating flame at speeds exceeding the aforesaid limit, no initial uniform movement at all was observable. On the contrary, the flame speed was continuously accelerated from the beginning, as though ignition had taken place near a closed, instead of at the open, end of the tube. Many photographic records showing the striking contrast between the initial movements of flame through what may be termed "slow" and "fast" mixtures, respectively, of

\* For convenience of recording, the nitrogen content has been disregarded in the text; hence readers will understand that, for example, when a 50 C<sub>2</sub>H<sub>4</sub> /50 O<sub>2</sub> mixture is referred to, it means that whereas the ethylene content was exactly as stated, the oxygen would include any small proportion of nitrogen which might be present.



the same gas with oxygen were obtained during the research ; but for purposes of illustration we need only reproduce those shown in Plate 27, in which :—

A = a typical record for a  $50\text{C}_2\text{H}_4/50\text{O}_2$  mixture initially propagating flame at the comparatively slow speed of 200 cm. per second. The explosion tube in this case (as well as in B and C) was 50 cm. long and 2.5 cm. internal diameter, ignition being at the open end. It will be observed that the initial speed remained perfectly uniform as far as the flame was photographed (15 cm.).

B and C = typical records for  $20\text{C}_2\text{H}_4/80\text{O}_2$  and  $35\text{C}_2\text{H}_4/65\text{O}_2$  mixtures, respectively, initially propagating flame at speeds exceeding 4,000 cm. per second. In neither case was any uniform movement observable, on the contrary, the flame was continuously accelerated *ab initio*, detonation being set up near the far end of the tube (which was covered in the experiment) as shown by the “retonation” wave thrown back through the still burning mixture in each case.

With hydrogen-oxygen mixtures a somewhat different, though equally well-marked, change took place when the aforesaid initial speed limit was exceeded. Instead of the initial flame movement losing its uniformity, as was the case with the acetylene- or ethylene-oxygen mixtures, it showed a marked tendency to develop quite different uniform speeds in successive experiments.

As a typical example of such happenings, we reproduce in Plate 28, A, a print from a film upon which the results of three successive speed determinations with a  $63.9\text{H}_2/36.1\text{O}_2$  mixture were photographically recorded, the drum speed remaining practically constant throughout the series. The peripheral film speeds were actually 1778, 1810, and 1812 cm. per second, respectively, in the three successive experiments. It will be seen that, although in each case the initial flame movement was quite uniform, three different angles (namely,  $41^\circ 30'$ ,  $30^\circ$  and  $45^\circ$ ) corresponding with speeds of 5220, 3460 and 6000 cm. per second, respectively, were traced by the flames in successive determinations. Hence it appears as though there are mixtures so highly sensitive as to be capable of initially propagating flame at quite different uniform speeds when ignited at the open end of a tube under, as near as could be judged, the same conditions.

We have found that all hydrogen-oxygen mixtures examined containing between about 55 and 75 per cent. of the combustible gas exhibited such a tendency. It seems difficult to say in any given case which of two or more observable speeds should be regarded as the normal one, although, may be, one

speed (or near to it) may be observed more frequently than others. Hence, the *dotted* part of the hydrogen-oxygen speed-curve shown in fig. 3 should be considered as provisional only.

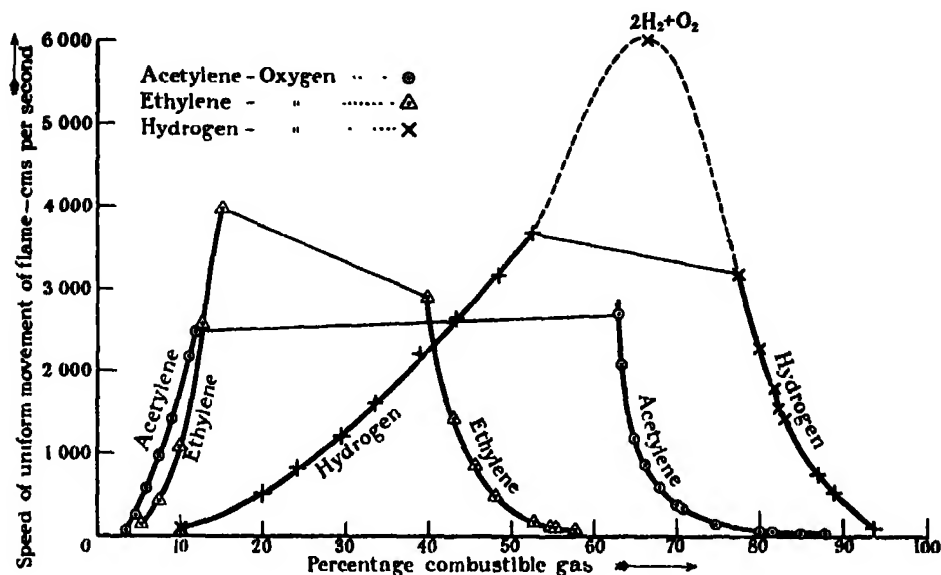


FIG. 3.

A good deal of evidence has also been accumulated during the research suggesting that, even with much slower-burning oxygen mixtures than those referred to in the preceding paragraphs, the speed of the initial uniform movement on ignition at the open end of a 2.5 cm. diameter tube, under the stated conditions, is not always quite so invariable as sometimes is supposed. Indeed, not infrequently in a series of successive speed determinations with one and the same mixture, under (so far as could be judged) the same experimental conditions, differences of the order of 10 to 20 per cent. between the recorded speeds have been observed, which certainly could not be attributed to any experimental error. Sometimes even, in one and the same experiment, after a certain run an initial quite uniform flame speed has changed over abruptly and quite unaccountably to another.

Illustrations of such occasional happenings are shown in the two photographic records reproduced in Plate 28, B and C, in which

B shows how, in two successive experiments, with a 9C<sub>2</sub>H<sub>2</sub>/91-air mixture two different uniform speeds of 434 and 364 cm. per second, respectively, were recorded. The angles actually traced by the flame on the record

were  $18^{\circ} 30'$  and  $15^{\circ} 10'$ , respectively, although the film speed remained the same in the two experiments. Such a large difference clearly lies outside "experimental error."

C is the record (negative) obtained in an experiment with a  $52.4\text{C}_2\text{H}_4/47.6\text{O}_2$  mixture, which, on ignition under the stated conditions, initially propagated flame for a certain distance with a uniform speed of 89 cm. per second, the angle initially traced by the flame on the record being  $15^{\circ} 30'$ ; after travelling a certain distance, however, the flame abruptly changed to another uniform speed of 126 cm. per second, now tracing an angle of  $21^{\circ} 30'$  on the record.

If need be, other similar instances could be reproduced from the scores of photographic records obtained during the investigations; but they are available, and may be inspected by anyone who cares to call at our laboratories for the purpose.

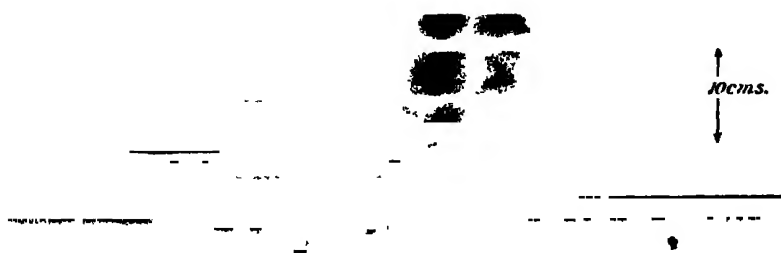
We think it would be premature at this stage of the investigation, to attempt any explanation of such facts; at present our main business is to place them on record for future consideration. It is possible, however, that further investigation may show that what we have found is not unconnected with some interesting observations recently made by C. Campbell and D. W. Woodhead\* during their investigation of the ignition of gases by an explosion wave. For these authors have found that, during the period immediately preceding detonation, one or more separate regions of inflammation may appear in the unburnt gases in front of a flame, which when photographed, appears serrated. Some of our unpublished photographs rather suggest this, and we are studying the matter further.

Such evidence as the foregoing has led us to doubt whether it is possible any longer rigidly to maintain *either* (i) that all quiescent explosive mixtures necessarily develop an initial *uniform* flame movement on ignition by means of a flame at the *open* end of a horizontal tube, or (ii) that, even when a "uniform movement" is initially set up in such circumstances, its velocity is necessarily quite the same for the same tube diameter. In the latter case, doubtless it *most frequently* happens that the observed initial uniform velocity for a given explosive mixture, and with one and the same tube diameter, will not differ very much from a certain mean value, which therefore may be regarded as having some significance relative *both* to the properties of the gaseous medium *and* to its environment. But it seems impossible to regard such *mean* uniform

\* 'Trans. Chem. Soc.,' pp. 310 to 321 (1926).



A.  $C_2H_4$  50 per cent,  $O_2$  50 per cent Uniform Speed 200 cm./sec.



B.  $C_2H_4$  20·5 per cent,  $O_2$  79·5 per cent. Average Speed = 8320 cm./sec.



C.  $C_2H_4$  35 per cent.,  $O_2$  65 per cent. Average speed = 6250 cm./sec.

(Facing p. 414.)





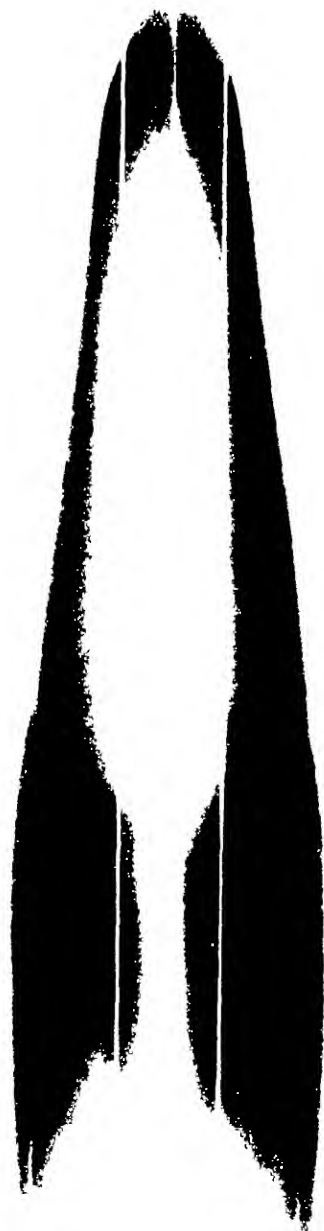
D.  $\text{H}_2$  63.9 per cent,  $\text{O}_2$  36.1 per cent. Angles,  $41^\circ 30'$ ,  $30^\circ$ ,  $45^\circ$ . Speeds, 5220, 3460, 6000.



E.  $\text{C}_2\text{H}_2$  9 per cent., Ar 91 per cent. Angles,  $18^\circ 30'$ ,  $15^\circ 10'$ . Speeds, 434, 364



F.  $\text{C}_2\text{H}_4$  52.4 per cent.,  $\text{O}_2$  47.6 per cent. 1st Phase,  $15^\circ 30'$  and  $89^\circ$ .  
2nd Phase,  $21^\circ 30'$  and  $126^\circ$ .



speed as a physical constant of the mixture in the same sense as we regard its "rate of detonation."

Lastly, we have found it possible under suitable conditions to have a slow "uniform flame movement" developed in an explosive medium *after* a period of continuous acceleration, showing that such "uniformity" is not necessarily restricted to the initial phase of flame movement. To illustrate this, we reproduce in Plate 29 a beautiful photographic record obtained on a film, which was rotated on a drum at a constant speed at right angles to the direction of the flame, when a mixture of carbonic oxide and oxygen in their combining proportions (dried by a three-hours' contact with pure redistilled phosphoric anhydride) was ignited at atmospheric temperature and pressure by a condenser discharge (3.75 m.f. at 1000 volts) passed between platinum electrodes fixed half way along a horizontal glass explosion tube (length = 35 cm., internal diameter = 2 cm.) *closed at both ends*.

The flame started at the middle of the tube and travelled symmetrically along it in opposite directions towards each of the closed ends. It will be seen (i) that after an initial period of accelerated flame velocity, extending about 5 cm. in each direction along the tube, a marked deceleration set in, culminating in a much slower "uniform movement" which lasted until the flame had nearly reached the closed end of the tube, (ii) that immediately afterwards the whole contents of the tube suddenly burst into an intense luminosity, which continued for some time as though the main combustion only occurred after the flame had reached the ends, and (iii) that, although the gaseous medium in the middle portion of the tube initially developed luminosity when the flame originally traversed it, soon afterwards it became dark again, and remained so until after the final burst of luminosity set in.

We are thus led to conclude that, so far from a condition of "slow uniform flame movement" *necessarily* arising when a quiescent explosive mixture is ignited at the *open* end of a tube, or from its being peculiar to such conditions, it may be set up in quite other circumstances. Also that, besides the composition of the given mixture and the diameter of the tube in which it is ignited, other factors are concerned in determining the speed of such "uniform flame movement" in any particular case.

Pending the results of further investigation we would refrain from expressing any decided opinion as to what governs such slow uniform movement in any given case; but at present we are inclined to attribute it to a certain balancing of the conditions as a whole rather than to any specific set of them. It seems reasonable to suppose that in any given circumstances its speed would depend



*partly* on the chemical and thermal properties of the explosive mixture itself, and *partly* on the environment. Clearly it cannot be regarded as either necessarily caused by, or dependent upon, any particular mode of ignition or flame propagation; nor does its speed in any given case appear to be a physical constant of the mixture concerned.

(C)—*Initial Uniform Flame Speeds in a 2.5 cm. diameter Horizontal Tube.\**

(a) *With Hydrogen-Oxygen Mixtures.*—According to our experiments, the “range of inflammability” of hydrogen-oxygen mixtures for horizontal flame propagation in a 2.5 cm. diameter glass tube at room temperature and pressure, lies between 10 and 94 per cent. hydrogen-content approximately. With any given mixture containing either between 10 and 55 per cent., or between 75 and 94 per cent. of hydrogen, a fairly constant initial uniform flame speed was observed; but with a given mixture containing between about 55 and 75 per cent. of hydrogen, the initial speed, though always uniform, was apt to differ in successive experiments as already explained. The speeds actually observed with the different mixtures were as follows:—

Per cent. hydrogen in mixture.	Speeds determined, Cm per second	Mean.
(1) Speeds both “uniform” and fairly constant for each mixture { 10 20 24.2 29.5 33.8 39.2 48.5 52.6	  64 512 880 790 860 1250 1150 1640 1650 1570 2200 2240 3220 3100 3670 3690	  64 512 845 1200 1620 2220 3150 3680
(2) Speeds, though always uniform in each experiment varied in successive experiments with each mixture { 63.9 69.7 71.2	 5220 6000 3460 5250 6050 6100 5150 3570	 — — —
(3) Same as in (1) { 77.5 80.0 81.6 82.9 87.5 89.4 93.5 94.4	 3220 3130 2290 2270 1980 1880 1920 1470 1410 730 530 76.5 76.5 would not ignite	 3170 2280 1930 1440 730 530 76.5 —

\* All the flame-speeds given in this section of the paper refer to the initial “uniform movement” in a 2.5 cm. diameter horizontal glass tube, filled with the explosive mixture at 15° to 18° C. and atmospheric pressure, ignition being effected by the gentle application of a 2 cm. high coal-gas flame at the *open* end, the other end being closed.

(b) *With Acetylene-Oxygen Mixtures.*—Initial uniform flame speeds were always observed with mixtures containing either between 3·5 and 11·9 per cent., or between 63·5 and 87·5 per cent. of acetylene, and in most cases there was not much difference between the speeds observed in successive experiments with one and the same mixture. With mixtures containing between about 15 and 60 per cent. of acetylene, however, there was no initial uniform flame movement, the flame being in each case continuously accelerated from the first until detonation was set up. The range of inflammability of the mixtures under the stated experimental conditions, comprises all those containing between about 3·5 and 88 per cent. (or possibly rather more) of acetylene. The following are the mean speeds of the initial uniform movement observed with the various mixtures under the experimental conditions.

*Acetylene-Oxygen C<sub>2</sub>H<sub>2</sub>/O<sub>2</sub>*

Per cent	Speeds			Mean
3·5	44·5	44·0		44·2
4·7	222	222	222	222
6·1	595	595	595	595
7·4	970	970		970
9·1	1540	1450	1400	1463
10·9	1975	2300	2280	2185
11·9	2480	2500	2450	2480
15·0	No uniformity observed between these percentages.			
60·0				
63·5	2060	2080		2070
64·5	1462	1450	1408	1440
65·0	1162	1213		1190
66·0		880		880
70·0	390	400		395
70·5	380	330	330	350
74·5	114	130		122
80·0		72·0		72·0
81·4		46·0		46·0
85·0	30·9	34·3		32·0
87·9		22·5		22·5

(c) *Ethylene-Oxygen Mixtures.* Similar remarks apply also to ethylene-oxygen mixtures; initial uniform flame speeds were always observed with mixtures containing either between about 5 and 15 per cent. or between 40 and 58 per cent. of ethylene. Mixtures within the intermediate range (15 to 40 per cent., or thereabouts, of ethylene) usually showed no initial uniform movement at all, the flame being continuously accelerated *ab initio*. So far

as could be judged, the range of inflammability of these mixtures, under the stated experimental conditions, probably comprises all containing between about 4.5 and 60 per cent. of ethylene approximately.

Ethylene-Oxygen  $C_2H_4/O_2$ .

Per cent	Speeds.			Mean.
5.3	142.8	103.5	129.5	130
7.5		607	665	635
10.0		1080	1050	1065
12.4		2600	2515	2560
15.4			3980	3980
<div style="display: flex; justify-content: space-between;"> <span>^</span> <span>No uniformity observed between these percentages.</span> <span>^</span> </div>				
<div style="display: flex; justify-content: space-between;"> <span>v</span> <span></span> <span>v</span> </div>				
40		2900		2900
43.2		1465	1395	1430
45.6	870	830	861	854
48.0		413	453	430
53.1			116.0	116.0
55.45	75.0	78.0	76.4	76.0
57.9		52.6	54.5	53.0

*Flame Speed Curves for the Initial "Uniform Movement."*

The foregoing results (a) to (c) inclusive are all plotted on the flame speed curves shown in fig. 3. For convenience sake, the two portions of the acetylene-oxygen and ethylene-oxygen curves, respectively, are in each case connected by a thin straight line.

For reasons already explained, the dotted upper portion of the hydrogen-oxygen curve should be considered as provisional; although we think that for electrolytic gas a speed of about 6000 cm. per second may be accepted as fairly accurate.

So far as they go, all the curves show much the same general features as the lower portions of similar curves for the corresponding air mixtures, except of course that the speed is generally much higher, and the range of inflammability much wider than in the latter.

The "lower limit" of inflammability of a gas does not seem to be much affected by the substitution of air by oxygen in the explosive mixture; but as might be expected, the "upper limit" is much higher with oxygen than with air. In this connection it may be recalled that, in 1920, E. Terres determined the following limits of inflammability for downward flame propagation, of

hydrogen, ethylene, and acetylene, respectively, in admixture with air and oxygen respectively.\*

Gas.	Percentage of combustible gas in "limit" mixtures with			
	Air		Oxygen.	
	Lower.	Upper	Lower	Upper
Hydrogen	9.5	65.2	9.2	91.6
Ethylene	4.0	14.0	4.1	61.8
Acetylene	3.5	52.3	3.5	89.4

And, although we have not primarily concerned ourselves with the exact determination of limits of inflammability, our results are substantially in agreement with those of Terres in this particular, having regard to the fact that, whereas his referred to "downward," ours refer to "horizontal" flame propagation.

In conclusion we desire to acknowledge that two of us (R. P. F. and D. A. W.) have carried out this investigation as holders of the Gas Research Fellowships maintained at the Imperial College of Science and Technology, London, by Radiation, Ltd., and the Gas Light and Coke Co., of London, to whose generosity in supporting this work our united thanks are tendered. Part of the preliminary work, in connection with the methods employed, was done during 1925-6, when one of us (D. A. W.) was helped by a maintenance grant from the Department of Scientific and Industrial Research.

\* 'Journ. Gasbeleucht,' vol. 63, pp. 785, 805, 820, 836 (1920).

*The Initial Stages of Gaseous Explosions—Part II. An Examination of the supposed Law of Flame Speeds.*

By WILLIAM A. BONE, D.Sc., F.R.S., R. P. FRASER, A.R.C.S., D.I.C., and  
D. A. WINTER, B.Sc., A.R.C.S., D.I.C.

[PLATES 30-32.]

*Introduction.*

In the year 1922 W. Payman and R. V. Wheeler published a paper entitled "The Combustion of Complex Gaseous Mixtures"\* in which, after stating that "in general, if a limit mixture with air of one gas is mixed, in any proportions, with a limit mixture with air of another gas, the speed of propagation of flame in both mixtures being, as it is, approximately the same under the same conditions of experiment, the speed of propagation of flame in the resultant complex mixture (which is also a limit mixture) is unchanged," they proceeded to say that the same thing holds good for the propagation of flame "not only in limit mixtures, but in all mixtures of inflammable gases with air (or oxygen), provided that the mixtures of the individual gases are of the same type, all containing excess of oxygen or all containing excess of combustible gas." And, finally, they promulgated a new "law of flame speeds" which ran as follows: "Given two or more mixtures of air or oxygen with different individual gases, in each of which the speed of propagation of flame is the same, all combinations of the mixtures of the same type† propagate flame at the same speeds, under the same conditions of experiment."

Since its original publication, they have continued to press this "law" upon the attention of other workers in the field, using it as a basis for interpreting results from other laboratories than their own, even to the extent of claiming that it governs the division of oxygen between two combustible gases present in excess. Indeed they contend that "so far as the propagation of flame is concerned, a mixture of a number of different combustible gases with air (for example) can be regarded as the summation of mixtures of each individual gas with air, the proportions of combustible gas and air in each being such that the speed of flame in it, if the mixture were burning alone, would be the same as in the complex mixture." Moreover, in the well-known case (investigated by one of us) of the explosion of mixtures of the type  $\text{CH}_4 + \text{O}_2 + x\text{H}_2$ , where the

\* 'Trans. Chem. Soc.,' vol. 121, p. 363 (1922).

† i.e., "all containing excess of oxygen or all containing excess of combustible gas."

oxygen has the chance of combining with either of the two combustible gases, they claim that the methane gets the lion's share of it, not because of its greater affinity for oxygen, but "because the methane-oxygen association that is required to yield the same speed of flame as the hydrogen-oxygen association is the richer in oxygen."

In a paper upon "the Interpretation of the Law of Speed," published by W. Payman in 1923,\* two important passages occur which ought to be quoted here as showing how he meant the "law" to be regarded. The first ran as follows: "It will be seen that the law of speeds can be explained on the assumption that any addition of incombustible gas, inflammable gas, or oxygen to a mixture of inflammable gas and oxygen in combining proportions has a retarding effect upon the speed of the uniform movement of flame proportional to its specific heat" (*loc. cit.*, p. 414), which seems to imply, what many will doubt, (i) that in the "uniform movement" combustion is complete *in the flame front*, and (ii) *either* that "dissociation" (not even of carbon dioxide) has no influence at all upon the flame speed *or* that the degree of it is unaffected by dilution with an inert gas or excess of one of the reactants.

The second passage implied a qualification, as follows: "The law of speeds as applied to the uniform movement during the propagation of flame can therefore be explained on the assumption that the variations in the speed of flame as determined under standard conditions with mixtures of different compositions depends on the rate of reaction between the inflammable gases and oxygen in the flame front. The law of speeds would hold exactly if this rate of reaction was dependent solely on the temperature, so that excess of either inflammable gas, oxygen, or of incombustible gas could be regarded as behaving simply as diluting gas, lowering the reaction temperature, but taking no part in the reaction. The fact that the rate of reaction must also depend on the concentrations of the reacting gases results in small divergencies from the law when the oxygen is in deficit. The correction necessary to allow for this cannot be correctly estimated, but the general effect of this factor is to make the speeds of the uniform movement of flame in complex mixtures rather slower than the speeds calculated from the law of speeds" (*loc. cit.*, p. 420). We are thus led to expect incalculable "small divergencies" when oxygen is in deficit, which tend to make the flame speeds "rather slower" than the "law" would require, a vague sort of qualification, capable of being variously interpreted according to each individual's idea of what margin is allowable as a "small divergence" from a supposed natural law without impugning its validity.

\* 'Trans. Chem. Soc.,' vol. 123, p. 412 (1923).

In a paper which Payman and Wheeler contributed to the discussion on "Explosive Reactions in Gaseous Media," held in London on June 14, 1926, under the auspices of the Faraday Society,\* they emphasised the operation of their supposed "law," claiming it to be applicable to *all* conditions of flame propagation; for they said: "there is a considerable amount of evidence available that the relative speeds of the uniform movement of flame obtained under the specified experimental conditions are directly proportional to the speeds under other conditions, except during the detonation wave" (*loc. cit.* p. 305).† Also, they claimed "that the law of speeds applies to the rate of development of pressure in mixtures of complex gas mixtures with air." The last-named statement seems to involve another questionable rule laid down and applied by them in 1923, namely, that, in gaseous explosions generally, "the time taken for the pressure within a spherical vessel to attain its maximum . . . (ignition being at the centre) . . . coincides with the time taken for flame to reach the boundary of the vessel; except with very slowly moving flames."‡

In a written contribution to the said discussion, one of us (W. A. B.) expressed doubts as to the general validity of the supposed "law," saying that for some time past experiments had been in progress in his laboratories with a view to testing it from the point of view of the behaviour of complex mixtures of certain hydrocarbons, hydrogen and oxygen, containing an excess of combustible gases, and that he hoped to be able soon to publish a detailed account of them.

The basis of the experimental test to which we have subjected the supposed "law" is one which the authors of it themselves have supplied. For in their recent paper at the Faraday Society they repeated that their "law" states (i) "that if a complex mixture is made by blending a number of mixtures of air with simple combustible gases all of which have the same speed of uniform movement of flame, then this complex mixture will also have the same speed of flame provided that all mixtures are of the same type, all containing excess of oxygen or all containing excess of inflammable gas," and again that (ii) "an important deduction from the law of speeds is that during the propagation of flame in a complex mixture of combustible gas and air mixtures of the type we have just considered (all with the same speed of uniform movement of flame), the combustion can be regarded as involving the simultaneous but inde-

\* 'Trans. Faraday Soc.,' vol. 22, p. 301.

† In course of the discussion, however, they said that "the statement that the Law of Speeds is not applicable to the rates of detonation in gaseous mixtures is incorrect."

‡ 'Trans. Chem. Soc.,' vol. 123, p. 1257 (1923).

pendent burning of a number of simple mixtures of the individual gases with air, in which the proportions of inflammable gas and air are such that each mixture, if burning alone, would propagate flame with the same speed as does the complex mixture." They also reported having found experimentally that complex mixtures of methane, hydrogen and air, containing insufficient oxygen for complete combustion, obey the law. As will be shown, however, in the concluding portion of our paper, such is not our experience.

It may be observed that up to now Payman and Wheeler have chiefly relied on experimental evidence in support of their "law" derived from the study of comparatively slow-burning complex gas-air mixtures, when the "diluent" (if it can properly be so called) may exercise a considerable influence. Thus, in proof of the "law" they showed experimentally in 1922 (I) that (A) a 7.35 methane/92.65 air and (B) a 1.98 pentane/98.02 air mixture each of which, on ignition at the open end of a 2.5 cm. diameter horizontal glass tube, initially propagated flame at a uniform speed of 40 cm. per second—could be blended in any proportions without altering the initial flame speed, and (II) that the same holds goods for (A) 11.0 methane/89.0 air and (B) 3.54 pentane/96.46 air mixtures, both of which initially propagate flame, in said circumstances, with an initial speed of 60 cm. per second. We think, however, that such evidence lacks cogency as regards proving a general law because (i) the mixtures in question are all comparatively *slow* burning, (ii) they would all contain somewhere between about 70 and 82 per cent. of "diluent" (chiefly nitrogen), (iii) the two combustible gases concerned are homologous hydrocarbons, presumably with similar modes of combustion. (iv) in the case of (I), where oxygen was always in excess, presumably the flame speed would be chiefly governed by some relationship between the heat of combustion and the heat capacity of the products, which calculation shows would not alter very much in the various blendings, and (v) in the case of (II), in which the two primary mixtures both contained excess of combustible gas, the percentage of oxygen in the various blended mixtures between 100A/0B and 0A/100B would all lie between 18.7 and 20.2 per cent., which (according to our experience) would be too close for a really valid test of the matter.

It has always seemed to us necessary that before any final opinion can be expressed concerning its validity, the "law" should be thoroughly tested out in regard to complex "oxygen" mixtures containing two combustible gases as dissimilar as are, say, hydrocarbons and hydrogen in their modes of burning. Accordingly, during the past two years, we have essayed to do this, with results as recorded herein, which seem to us to be decisive against it. We will now



proceed to submit our evidence as succinctly as possible, leaving the reader to form his own judgment upon it.

#### EXPERIMENTAL.

In all that follows, it should be understood :—

- (i) That the various experimental mixtures were all made up in gas-holders over mercury from highly purified gases, and that their compositions were all checked by analysis.
- (ii) That, for convenience sake, they are usually recorded as  $x$  gas/ $y$  oxygen mixtures,  $x$  being the exact percentage of combustible gas present, and  $y$  that of the oxygen *plus* (usually less than 1 per cent. of) adventitious nitrogen.
- (iii) That, *unless otherwise expressly stated*, all "flame speeds" recorded refer to the initial uniform movement on ignition of the quiescent mixtures in question at about 15 to 18° C. and atmospheric pressure by the gentle application of a 2 cm. high coal-gas flame at the *open* end of a horizontal glass tube of uniform bore, 2.5 cm. in diameter. For brevity, such will always be referred to as "the standard conditions."
- (iv) That the letters (*p.m.*) or (*e.m.*) in brackets are used to indicate which of the two experimental methods (photographic or electrical) described in Part I hereof was employed for the flame speed measurement in any particular case.

(A) *Evidence derived from the Explosion of (a)  $C_2H_4 + H_2 + O_2$  and*

*(b)  $C_2H_2 + 2H_2 + O_2$  Mixtures.*

When the law was first promulgated, it called to mind two significant experiments made more than twenty years ago by W. A. Bone and J. Drugman during their researches upon the explosive combustion of hydrocarbons, to which we would now particularly direct attention.\* It was found that when *either* an ethylene-hydrogen-oxygen mixture of the composition  $C_2H_4 + H_2 + O_2$ , or an acetylene-hydrogen-oxygen mixture of the composition  $C_2H_2 + 2H_2 + O_2$ , is exploded in a glass bulb (60 c.c. capacity), not a trace of carbon separates, nor does any steam condense on cooling. Indeed with the  $C_2H_2 + 2H_2 + O_2$  mixture no appreciable steam is produced at all, and with the  $C_2H_4 + H_2 + O_2$  mixture the amount formed is insufficient to saturate the cold products if at the outset

\* 'Trans. Chem. Soc.,' vol. 80, p. 669 (1906).

they are practically dry. The results of two such typical experiments are shown in Table I where :—

$p_1$  = initial pressure of the dry combustible mixtures when fired  
 $p_2$  = final pressure of the dry products

} both at 15° C

Table I.

Original mixture		$C_2H_4 + H_2 + O_2$			$C_2H_2 + 2H_2 + O_2$		
$p_1$		mm			mm.		
$p_2$		503			531		
$p_2/p_1$		750			653		
		1.49			1.22		
Percentage composition of gaseous products.	$CO_2$	0.35			0.2		
	$CO$	39.60			39.8		
	$C_2H_2 + C_2H_4$	1.25			Nil		
	$CH_4$	3.65			0.2		
	$H_2$	55.15			59.8		
Units of		C	H	O	C	H	O
{ Original gases		311	505	168	267	400	133
{ Gaseous products		346	478	151	262	394	131
Difference		—	27	17	—	—	—

These remarkable experiments, which were shown at the Royal Institution in 1908, and have since been repeated many times, seem incompatible with the supposed "law," except on the very unlikely supposition that even the *slowest* burning ethylene-oxygen or acetylene-oxygen mixture propagates flame faster than the *fastest* burning hydrogen-oxygen mixture. A glance at the flame-speed curves shown in Part I, fig. 3, hereof will show how untenable is any such supposition.

It is worth while considering the matter a little further, however, and in a somewhat different way. According to the supposed "law," whenever either of the two complex mixtures referred to is exploded, the oxygen (being in defect) must be divided between the two combustible gases concerned in such proportions as would give rise to *two* primary (hydrocarbon-oxygen and hydrogen-oxygen) mixtures propagating flame with the same speed as does the original complex mixture itself. But such prediction is falsified by the event, as the following typical experimental results obtained with the  $C_2H_4 + H_2 + O_2$  mixture showed.

(a) *The  $C_2H_4+H_2+O_2$  mixture.*

- (i) First of all, a moist mixture containing -

$C_2H_4 = 34.0$ ,  $H_2 = 33.6$ , and  $O_2 = 32.4$  per cent.

was carefully made up in a holder over mercury, and, after its composition had been determined by analysis, three successive measurements were made (*p.m.*) of its flame speed when ignited under the standard conditions. The photographic records showed that in all cases the initial flame movement had been quite uniform, and the observed speeds of it were : -

*Observed speeds* 83.0, 77.2, and 75.2 cm. per second.

*Mean* — 78.5 cm. per second.

- (ii) From the flame-speed curves shown in Part I (fig. 3) hereof (*q.v.*) it was seen that a speed of 78.5 cm. per second should be given by a primary  $55.5C_2H_4/44.5O_2$  mixture. Accordingly this was carefully made up in a holder over mercury, and four successive measurements of its initial uniform flame speed were subsequently made (*p.m.*) under the standard conditions, as follows :—

*Observed speeds* 70.4, 75.0, 76.4, and 78.0 cm. per second.

*Mean* - - 75 cm. per second.

Within the limits of experimental error, this substantially confirmed the speed predicted from our curve.

- (iii) By calculation, it was deduced that the only hydrogen-oxygen mixture which could be added in any proportion to the aforesaid  $55.5C_2H_4/44.5O_2$  mixture in order to produce the aforesaid complex  $C_2H_4+H_2+O_2$  mixture would be a  $86.75H_2/13.25O_2$  mixture. But, according to our hydrogen-oxygen flame speed curve shown in Part I (fig. 3) hereof, the initial flame speed of such a mixture, on ignition under stated conditions, would be as high as 790 cm. per second, or about 10 times that required by the supposed law.
- (iv) Moreover, our said hydrogen-oxygen flame speed curve predicted that an initial speed of 75 cm. per second should be given by a  $93.45H_2/6.55O_2$  mixture. Accordingly, this was made up over mercury and its flame speed determined (*e.m.*) on igniting under the standard conditions with the following results :—

*Observed speeds* 76.5, 76.5, 77.4 cm. per second.

*Mean* = 76.8 cm. per second.

Thus confirming again the so predicted speed ; but, by no possible blending of this mixture with the aforesaid  $55.5C_2H_4/45.5O_2$  mixture

referred to in (ii) could the original  $34\cdot0\text{C}_2\text{H}_4 + 33\cdot6\text{H}_2 + 32\cdot4\text{O}_2$  complex-mixtures referred to in (i) be obtained.

From the foregoing, it would appear that the behaviour of a  $\text{C}_2\text{H}_4 + \text{H}_2 + \text{O}_2$  mixture does not harmonise with the supposed "law."

(b) *The  $\text{C}_2\text{H}_2 + 2\text{H}_2 + \text{O}_2$  mixture.*

Further evidence as to the behaviour of this complex-mixture will be submitted in the next section hereof.

(B) *Evidence derived from blending tests.*

Undoubtedly the simplest and most direct test of the validity or otherwise of the "law" is that propounded by its authors, namely, "that if a complex mixture is made by blending a number of mixtures of air with simple combustible gases all of which have the same speed of uniform movement of flame, then this complex mixture will also have the same speed of flame provided that all mixtures are of the same type, all containing excess of oxygen or all containing excess of inflammable gas." Accordingly, as will hereinafter be outlined, we have applied such a "blending test" to a number of complex "oxygen"-mixtures (both *fast* and *slow*) as well as to one complex "air"-mixture. In all our experiments, one of the two primary mixtures employed has always been a hydrogen-oxygen (-air) mixture, and the other a hydrocarbon-oxygen (-air) mixture, the hydrocarbon used being either acetylene, ethylene or methane.

*The Experimental Procedure.*

It should be explained that the experimental procedure adopted by us in carrying out such blending tests was briefly somewhat as follows:—

- (i) At the commencement of each series of experiments, with the help of the flame-speed curves shown in Part I (fig. 3) hereof, about 10 litres of each of two *primary* mixtures were made up in a gas-holder over mercury, namely: (A) of a hydrocarbon-oxygen (-air) mixture, and (B) of a hydrogen-oxygen (-air) mixture, respectively, each of the same type (*i.e.*, each containing either excess of combustible gas or excess of air), and each having as nearly as possible the same initial speed of uniform flame movement, when ignited under the standard conditions.
- (ii) Successive measurements were then made of the initial flame speeds of each of the said two primary mixtures, and if the *mean* results agreed within (say) 5 per cent., the mixtures were deemed suitable for the

subsequent "blending tests." The exact composition of each primary mixture was then ascertained by careful analysis, and until the subsequent "blending tests" were completed, each was kept stored over mercury at a pressure greater than that of the atmosphere, so as to minimise any chance inleakage of air.

- (iii) The desired proportions of each of the said two primary mixtures A and B were next separately measured out, as accurately as possible, over mercury in a 1000 c.c. graduated cylindrical gas-burette, and successively transferred under pressure to another gas-holder over mercury, where they were thoroughly blended so as to produce the desired "complex mixture" C, whose exact composition was afterwards determined by analysis. As a rule, a series of such complex mixtures was so made up by blending different proportions of the two primary mixtures (75A/25B, 50A/50B, 25A/75B, etc.) for subsequent examination. The usual order of such blending was, first of all, 50/50, and afterwards (as far as possible) alternately on either side of it.
- (iv) Successive flame-speed measurements under the standard conditions were then made with each said complex-mixture so prepared, using, in most cases, and whenever possible, the photographic method.
- (v) Finally, after all the said flame-speed measurements had been completed, those of each of the two primary mixtures A and B were repeated, so as to ensure that they had undergone no alteration during the time covered by all the foregoing operations.

#### *Purity of the Gases.*

Throughout all the experiments, the utmost care was taken to ensure the purity of all the gases employed, including their practical freedom from adventitious nitrogen. Each of the hydrocarbons (acetylene, ethylene or methane) used was purified, not only by chemical methods, but also finally by liquefaction and fractionation of the liquid. The hydrogen used was prepared by the action of pure dilute sulphuric acid upon Mond's "Crescent" electrolytic zinc (99.98 per cent. purity), and was subsequently washed by passage through a train of "worms" containing a hot alkaline solution of potassium permanganate. The oxygen used was prepared by gently heating recrystallised potassium permanganate, and was washed by passage through a strong solution of caustic potash. Special attention was paid to minimising "adventitious" nitrogen, both in preparing the original gases, and in subsequently making up the various experimental mixtures from them. Indeed,

the arrangement of all the "generating" and "mixing" apparatus was such as easily allowed both the complete evacuation of all vessels and connections before or during each preparation, etc., and, in the mixing operations, the complete filling beforehand of all vessels and connections with mercury. By such means, we often succeeded in reducing the "adventitious" nitrogen in the experimental mixtures to less than 0.5 per cent., and in nearly all other cases to within 1 per cent.; it never exceeded 1.5 per cent. The accuracy of the mixing arrangements employed may be judged by the always close correspondence (as shown in the tabulated experimental results) between the "found" and "calculated" composition of the various complex-mixtures employed.

#### *Tabulation of Results.*

In most cases, the verdict of the various blending tests upon the matter at issue can be seen at a glance from the tabulated results, which in each case show:—

- (i) The composition of each of the two primary mixtures A and B, respectively, employed.
- (ii) The observed "flame-speeds," under the standard conditions, for each primary mixture A and B respectively, both *before* and *after* the blending tests.
- (iii) The proportions in which the two primary mixtures A and B were blended to produce each of the complex mixtures C examined.
- (iv) The observed flame speeds, on ignition under the standard conditions, for each complex mixture C examined.
- (v) The composition of each complex mixture examined.

(a) *Complex Acetylene-Hydrogen-Oxygen Mixtures.*—It was ascertained by reference to the flame-speed curves shown in Part I (fig. 3) hereof, supplemented by actual trial, that two primary mixtures (A)  $64.5\text{C}_2\text{H}_2/35.5\text{O}_2$  and (B)  $83\text{H}_2/17\text{O}_2$ , each containing excess of combustible gas, should give the same initial uniform flame speed, when ignited under the standard conditions. And, as it was calculated that, on blending them in the proportions 38.3A/61.7B, a complex mixture very nearly of the composition  $\text{C}_2\text{H}_2 + 2\text{H}_2 + \text{O}_2$  would result, it was decided to employ them in these tests. They both propagated flame under the standard conditions at a high initial speed, which was found to be uniform for a sufficient distance to enable reliable speed measurements to be made. The mixtures were, however, rather "sensitive"; so, to make things reasonably sure, two separate series of blending tests were carried out at different times with fresh mixtures in each case.

Table IIA.—First Series of Experiments with Complex  $C_2H_2-H_2-O_2$  Mixtures.

Percentage composition of primary mixtures A and B.	A.	$C_2H_2$ 64.4	$O_2$ 35.4	$N_2$ 0.2.		
	B.	$H_2$ 83.1	$O_2$ 15.4	$N_2$ 1.5.		
Observed flame speeds (cm. per second) for A and B before and after the blending experiments		Before		After	Mean	
	A.	1435	1420	1380	1410	
	B.	1390	1380	1410	1390	
Proportions of A and B blended to form C.	Observed flame speed for the complex mixture C.		Percentage composition of C. (i) Found and (ii) Calculated.			
A.	B.	cm. per second.		$C_2H_2$ .	$H_2$ .	$O_2+N_2$ .
75	25	1170		{ (i) 48.0 (ii) 48.3	21.0 20.8	31.0 30.9
50	50	1220	1190	{ (i) 32.4 (ii) 32.2	41.3 41.6	26.3 26.2
38.3	61.7	1190	1200	{ (i) 24.8 (ii) 24.75	50.7 51.25	24.5 24.0
25	75	1220	1240	{ (i) 16.2 (ii) 16.1	61.8 62.3	22.0 21.6
12.5	87.5	1375		{ (i) 7.9 (ii) 8.0	72.9 72.7	19.2 19.3

N.B.—All flame speeds measured photographically.

It will be seen that in neither series did the experimental results, which are set forth in Tables II (A) and (B) agree with the "law." For, in the first series, the effect of blending the two primary mixtures A and B was, in most cases, to depress their original flame speeds from about 1400 to about 1200 cm. per second, or by nearly 15 per cent. In the second series, the speed-depression was, in some cases, even greater, namely, from about 1380 to about 1050 cm. per second, or by nearly 25 per cent. Because of the sensitiveness of these mixtures, we do not stress any particular figure; but the general implication of the results as a whole is, we think, unmistakable.

In two respects, however, the divergencies of these mixtures from the "law" differed from that of any of the other complex hydrocarbon-hydrogen-oxygen mixtures, studied, in that (i) it was much less marked and (ii) apparently reached a maximum at a region somewhere between 50A/50B and 38.3A/61.7B, instead of progressively increasing with the proportion of B in the various blendings.

This last-named peculiarity seemed to synchronise with an interesting

100A, 0B. Angle,  $30^\circ$ . Speed, 1435.



50A, 50B. Angle,  $25^\circ 48'$ . Speed, 1190.



25A, 75B. Angle,  $26^\circ 30'$ . Speed, 1240.



12·5A, 87·5B. Angle, variable. Speed uncertain.

(Facing p. 439)





*A.*  $C_2H_4$  19 per cent.,  $(2H_2 + O_2)$  81 per cent.

*B.*  $C_2H_2$  22 per cent.,  $(2H_2 + O_2)$  78 per cent.



100A, 0B. Angle,  $28^{\circ} 10'$ . Speed, 177.7.



90A, 10B. Angle,  $22^{\circ} 40'$ . Speed, 141.



80A, 20B. Angle,  $17^{\circ} 20'$ . Speed, 119.7.



40A, 60B. Angle,  $15^{\circ}$ . Speed, 82.1.

Table II B.—Second Series of Experiments with Complex  $C_2H_2-H_2-O_2$  Mixtures.

Percentage composition of primary mixtures A and B	A.	$C_2H_2$ 64.6	$O_2$ 35.2	$N_2$ 0.2	
	B.	$H_2$ 83.0	$O_2$ 15.5	$N_2$ 1.5	
Observed flame speeds (cms. per second)		Before	After	Mean	
	A.	1380	1330	1355	
	B.	1440	1380	1410	
Proportions of A and B blended to form C.	Observed flame speeds for complex mixture C.		Percentage composition of C.		
	A.	B.	cms. per second.	$C_2H_2$ .	$H_2$ .
90	10	1315	58.15	8.30	33.55
75	25	1200 1170	51.45	20.75	27.8
50	50	1070 1045	34.3	41.5	24.2
38.3	61.7	1060 1020	24.74	51.12	24.14
25	75	1235 1190	17.15	62.2	20.65
12.5	87.5	1280	8.05	72.5	19.45

N.B.—All flame speeds were measured photographically.

feature observed in the corresponding photographic records, some of which (from the first series of experiments) are reproduced in Plate 30. It will be seen that, whilst both the 100A/0B, and the 50A/50B mixtures (the same also held good for the 38.3A/61.7B mixture) exhibited a well-defined "uniform" flame movement, which, in course of time, was succeeded by a peculiar kind of vibratory period; in the case of the 25A/75B mixture, the flame movement was not quite uniform from the first, and in the case of the 12.5A/87.5B mixture never at all. The peripheral speed of the drum to which the photographic films were attached being constant (within 1 per cent.) throughout the series, visual evidence of the divergencies of these mixtures from the "law" is offered by the very different angles traced by the flame during the initial uniform movement in the case of the 100A/0B and the 50A/50B mixtures, namely,  $30^\circ$  in the first and only  $25^\circ 48'$  in the second case. In the 0A/100B photographic record, which showed a quite uniform initial flame movement, the angle traced was  $29^\circ 48'$ .

Incidentally it may be mentioned that, in another connection, we have recently discovered that successive additions of acetylene to electrolytic gas, so as to produce a series of complex mixtures  $x C_2H_2/100-x (2H_2+O_2)$ , have

a peculiar disturbing influence upon the uniform character of the initial flame movement. Such influence reaches a maximum when  $x =$  about 20, after which it subsides and eventually disappears, so that with  $x = 30$  it is hardly appreciable. This feature is well brought out in the two beautiful photographic records (*p.m.*) reproduced in Plate 31 of which A was given by a  $19 \text{ C}_2\text{H}_2/81 (2\text{H}_2+\text{O}_2)$ , and B by a  $22 \text{ C}_2\text{H}_2/78 (2\text{H}_2+\text{O}_2)$  mixture, when ignited under the standard conditions. Attention is directed to the non-uniformity of the flame movement, more marked in A than B, as well as to the "feathery" character of the pictures, the cause of which we desire to reserve for further investigation. The mean "flame speed" in A was nearly 4000 cm. per second, and in B between 2200 and 2500 cm. per second. It seems possible that the peculiarities referred to in this and the two preceding paragraphs may be in some way connected with the endothermic character of acetylene; but, however that may be, we think that in all probability they may be referred to some common cause.

(b) *Complex Ethylene-Hydrogen-Oxygen Mixtures.*—Complex ethylene-hydrogen-oxygen mixtures seemed well-suited for testing the validity of the supposed "law" because of the heat of formation of the hydrocarbon being only  $-2.7$  K.C.U. per gram-molecule, as compared with  $-47.8$  for acetylene and  $+21.7$  for methane. That used in our experiment was generated by Newth's method, and finally liquefied, and the liquid fractionated, the first and last portions being rejected. Analyses showed the final product to be very pure and practically nitrogen-free.

In order to make the subsequent blending tests as complete as possible three different series were carried out, namely, two in which the primary mixtures employed both contained excess of combustible gas, and the third in which they both contained excess of oxygen. The primary mixtures used in the tests, and their "flame speeds," when ignited under the standard conditions, were as follows:—

Series.	Composition of the primary mixture.		Flame speeds cm. per second.	
	A.	B.	A.	B.
I	$\text{C}_2\text{H}_4/\text{O}_2$ 55.45/45.55	$\text{H}_2/\text{O}_2$ 93.45/6.55	75	77
II	49.9/50.1	92.5/7.5	177	181
III	12.35/87.65	38.7/61.3	2195	2190

In most cases the photographic method was employed for the flame speed measurements; and in all cases, without exception, throughout the three series the initial flame movement was quite uniform. The results of the tests, which speak for themselves, are shown in Tables IIIA, B, C, inclusive.

Table IIIA.—First Series of Experiments with Complex  $C_2H_4-H_2-O_2$  Mixtures.

Percentage composition of primary mixtures A and B.	A.	$C_2H_4$ 55.45	$O_2$ 44.35	$N_2$ 0.2.			
	B.	$H_2$ 93.45	$O_2$ 6.45	$N_2$ 0.1.			
Observed flame speeds (cm. per second) for A and B before and after the blending experiments	Before		After	Mean			
	A.	$\begin{array}{cc} 70.4 & 75.0 \\ 76.4 & 78.0 \end{array}$	75.7	75.1			
	B.	$\begin{array}{cc} 76.5 & 76.5 \\ 77.4 & \end{array}$	80.0	77.6			
Proportions of A and B blended to form C.	Observed flame speed for complex mixture C.		Percentage composition of C (i) Found and (ii) Calculated.				
A.	B.	cm. per second.		$C_2H_4$ .	$H_2$ .	$O_2+N_2$ .	
90	10	68.4	65.5	$\left\{ \begin{array}{l} (i) \\ (ii) \end{array} \right.$	$\begin{array}{l} 50.1 \\ 49.9 \end{array}$	$\begin{array}{l} 9.3 \\ 9.35 \end{array}$	$\begin{array}{l} 40.6 \\ 40.75 \end{array}$
75	25	47.5	50.0	$\left\{ \begin{array}{l} (i) \\ (ii) \end{array} \right.$	$\begin{array}{l} 41.5 \\ 41.6 \end{array}$	$\begin{array}{l} 23.5 \\ 23.35 \end{array}$	$\begin{array}{l} 35.0 \\ 35.05 \end{array}$
50	50	43.1	42.9	$\left\{ \begin{array}{l} (i) \\ (ii) \end{array} \right.$	$\begin{array}{l} 27.6 \\ 27.7 \end{array}$	$\begin{array}{l} 46.8 \\ 46.7 \end{array}$	$\begin{array}{l} 25.6 \\ 25.6 \end{array}$
35	65	25.7		$\left\{ \begin{array}{l} (i) \\ (ii) \end{array} \right.$	$\begin{array}{l} 19.25 \\ 19.4 \end{array}$	$\begin{array}{l} 62.15 \\ 61.8 \end{array}$	$\begin{array}{l} 18.6 \\ 18.8 \end{array}$
25	75	22.3	22.3	$\left\{ \begin{array}{l} (i) \\ (ii) \end{array} \right.$	$\begin{array}{l} 13.6 \\ 13.85 \end{array}$	$\begin{array}{l} 71.1 \\ 71.1 \end{array}$	$\begin{array}{l} 15.3 \\ 15.05 \end{array}$
15	85	Did not fire					
5	95						
1	99						

Table IIIB.—Second Series of Experiments with Complex  $C_2H_4-H_2-O_2$  Mixtures.

Percentage composition of primary mixtures A and B.	A.	$C_2H_4$ 49.9	$O_2$ 49.9	$N_2$ 0.2.		
	B.	$H_2$ 92.5	$O_2$ 7.4	$N_2$ 0.1.		
Observed flame speed (cm. per second) for A and B <i>before</i> and <i>after</i> the blending experiments	Before		After		Mean	
	A.	177.7    177.3 176.2	186.0	187.0	180.8	
	B.	182.0    180.0	178.0	186.0	181.5	
Proportions of A and B blended to form C.	Observed flame speed for complex mixture C.		Percentage composition of C.			
A.	B.	cm. per second.		$C_2H_4$ .	$H_2$ .	$O_2+N_2$ .
90	10	141.0		44.0	9.3	45.8
80	20	119.7	135.5	39.0	18.5	41.6
47.5	52.5	89.3		23.7	48.6	27.7
20	80	60.5	43.0	10.0	74.0	16.0
15	85	37.0	37.4	7.5	78.7	13.8
1.5	98.5	Did not fire.				
1	99					
0.5	99.5					

It will be seen that in each of Series I and II, when the primary mixtures all contained excess of combustible gas, successive increases in the proportion of the B mixture used in the blendings always lowered progressively the flame speed of the resulting complex mixtures, until in each case a point was reached when the latter no longer propagated flame.\*

In Series I, when the two primary mixtures were both slow burning, being not far removed from the "higher limit," this point was reached at 20A/80B. In Series II, when the primary mixtures were faster burning, a greater

\* It may also be noted that, in a letter to 'Nature' on January 8, 1927 (vol. 119, p. 51) upon the "Supposed Law of Flame Speeds," A. G. White, after saying that it "must break down when one of the combustible gases in a complex mixture interferes with the burning of another," stated that "by mixing suitable carbon disulphide-air and (say) ether-air mixtures having the same speed of flame, mixtures can be obtained which refuse to propagate flame."

Table IIIc.—Third Series of Experiments with Complex  $C_2H_4-H_2-O_2$  Mixtures.

Percentage composition of primary mixtures A and B.	A.	$C_2H_4$ 12.35	$O_2$ 87.5	$N_2$ 0.15.
	B.	$H_2$ 38.7	$O_2$ 61.2	$N_2$ 0.1.

Observed flame speeds (cm. per second) for A and B before and after the blending experiments		Before			After	Mean
A.	2130	2212 2200	2240	2185	2190	
B.	2180	2200	—	—	2190	

Proportions of A and B blended to form C.		Observed flame speed for complex mixture C.		Percentage composition of C. (i) Found and (ii) Calculated.			
A.	B.	cm. per second.			$C_2H_4$ .	$H_2$	$O_2 + N_2$
75	25	3050	3090	{ (i) (ii)	9.3 9.25	10.05 9.65	80.65 81.1
50	50	2900 (1410)	2900 3270 (1450)	{ (i) (ii)	6.15 6.18	19.3 19.35	74.55 74.47
25	75	3600	3000	{ (i) (ii)	3.05 3.09	29.20 29.03	67.75 67.88

N.B.—All flame speeds measured photographically.

proportion of B was required in the blending to render the resulting mixture non-inflammable.

In this connection it is interesting to recall how, during his classical researches upon flame, Sir H. Davy found that both ethylene and methane (but especially the former) have a much greater power of rendering electrolytic gas non-inflammable than has a corresponding excess of either hydrogen or oxygen, a circumstance which cannot possibly be ascribed to the known differences in their molecular heat capacities. Thus for instance, he found that 1 volume of electrolytic gas could be rendered non-inflammable (by "a strong spark from a Leyden Jar") by dilution with either about 0.5 volume of olefiant gas or about 1.0 volume of marsh gas only, whereas no less than 8 volumes of hydrogen or 9 of oxygen were required. We are now investigating the matter further, because of its practical, as well as theoretical, importance, and hope soon to make a further communication to the Society upon it.

In carrying out Series I and II the eye could easily detect, without the aid of any photographic records, the progressive slowing up of the flame speeds as the proportion of B in the various blendings was increased. In order to have visual evidence of the fact, as well as of the "uniformity" of the initial flame



movements, the peripheral speed of the drum, to which the photographic paper was attached in each case, was kept constant (within 3.5 per cent.) throughout Series II. In Plate 32 are reproduced four of the actual photographic records, so that the reader may see for himself how the angle traced by the flame with the horizontal (and consequently the flame speed) diminished as the proportion of B in the blendings increased; the angles, and corresponding flame speeds, were as follows:—

Record.	Proportion of Primary mixture.		Drum speed.	Angle.	Calculated flame speed cm. per second.
	A.	B.	cm. per second.		
1	100	0	118.8	28° 10'	178
2	90	10	120.6	22° 40'	141
3	80	20	116.4	17° 20'	120
4	40	60	118.5	15° 0'	82

In Series III, where the two primary mixtures A and B both contained excess of oxygen, and were very fast-burning and sensitive, it was found that, with blendings in the proportions 75A/25B, and 25A/75B, respectively, the observed flame speeds were all between 40 and 70 per cent. higher than those of the two primary mixtures. With the 50/50 blending, however, two quite different initial flame speeds were observed in the five successive determinations which were made. Thus, in *three* of them the speed was between 32 and 50 per cent. *higher*, but in the other *two* it was about 30 per cent. *lower*, than the speed of either of the two primary mixtures blended. In this connection, the reader is referred to what was said in Part I hereof about the possibility of variability in initial flame speed in one and the same mixture, when it is very sensitive. In none of the speeds measured, however, were the requirements of the supposed "law" fulfilled.

(c) *Complex Methane-Hydrogen-Oxygen Mixtures.*—The case of these mixtures is of particular interest because of Payman and Wheeler's claim that when a complex mixture of methane, hydrogen, and oxygen, the last-named being in deficit, is inflamed, the resulting distribution of the oxygen between the two combustible gases is governed by their "law." If, however, as our results prove, such a mixture does not obey the "law," the claim in question cannot be sustained.

Highly purified gases were used, the amounts of adventitious nitrogen present

in all of them being below 0.5 per cent. The following two primary mixtures—each containing excess of combustible gas, and each propagating flame, on ignition under the standard conditions, with an initial uniform speed of about 115 cm. per second—were selected for the blending test, namely:—

Mixture.	Composition.	Mean flame speed cm. per second.
A	53.2 CH <sub>4</sub> /46.8 O <sub>2</sub>	115
B	92.0 H <sub>2</sub> /7.1 O <sub>2</sub>	113

The electrical method (*e.m.*) was used throughout for the flame speed determinations. From the results of the blending tests, which are shown in Table IV, it will be seen that, as in the case of the corresponding ethylene-hydrogen-oxygen mixture, successive increases in the proportion of mixture B used in the blendings progressively lowered the flame speed of the resulting complex mixture, until a point was reached when the latter no longer propagated flame. Thus, with a 25A/75B complex mixture, the original flame speeds of A and B were already more than halved, and a 10A/90B mixture would not propagate flame at all under the stated experimental conditions.

Table IV.—A Series of Experiments with Complex CH<sub>4</sub>—H<sub>2</sub>—O<sub>2</sub> Mixtures.

Percentage composition of primary mixtures A and B.	<div> <div>A. CH<sub>4</sub> 53.2 O<sub>2</sub> 46.5 N<sub>2</sub> 0.3.</div> <div>B. H<sub>2</sub> 92.0 O<sub>2</sub> 7.0 N<sub>2</sub> 0.1.</div> </div>				
Observed flame speeds (cm. per second) for A and B <i>before</i> and <i>after</i> the blending experiments	Before		After		Mean
	A.	110 117	117.5		114.8
	B.	112 113	113.0	116.0	112.7
		112 110			
Proportions of A and B blended to form C.	Observed flame speed for complex mixture C.	Percentage composition of C. (i) Found and (ii) Calculated.			
A. B.	cm. per second.	CH <sub>4</sub> .	H <sub>2</sub> .	O <sub>2</sub> +N <sub>2</sub> .	
72.5 27.5	94.0	{ (i) 38.1 (ii) 38.6	25.5 25.5	36.4 35.9	
45 55	72.7	{ (i) 24.3 (ii) 23.95	51.2 51.1	24.5 24.85	
25 75	50.0	{ (i) 13.4 (ii) 13.3	70.3 69.7	16.3 17.0	
10 90 2.5 97.5 }	Did not fire.				

(d) *Complex Methane-Hydrogen-Air Mixtures*.—In the paper which they contributed to the recent Faraday Society discussion (*loc. cit.*, p. 305), Payman and Wheeler said: "Two mixtures, one of methane and the other of hydrogen, with air, having the same speed of flame and containing insufficient oxygen for complete combustion, contain widely different proportions of inflammable gas and oxygen. During the propagation of flame in a complex mixture of methane, hydrogen and air made by blending these two mixtures, the combustion of the methane-air mixture is as though it were alone or as though the hydrogen-air mixture that dilutes it were a further quantity of the methane-air mixture. That is to say, during its burning in the complex mixture the methane behaves as though it were still associated with the greater proportion of the oxygen and combines with that greater proportion. This we have shown experimentally" (and there was given a reference to their original paper 'J. Chem. Soc.', 1922 (121) p. 363).

On looking at that paper, however, we are unable to find in it more than one actual blending test, giving flame speeds, with such methane-air and hydrogen-air mixtures, namely, in which (as is said, *loc. cit.*, pp. 371 to 376) two primary mixtures, (A) a 12.5 CH<sub>4</sub>/87.5-air and (B) a 70.2 H<sub>2</sub>/29.8-air mixture, both having the same flame speed of 30 cm. per second in a 2.5 cm. diameter tube, were blended so as to give a complex mixture (C) containing

CH<sub>4</sub> = 10.25, H<sub>2</sub> = 9.99, O<sub>2</sub> = 16.16, and N<sub>2</sub> = 63.6 per cent. without altering the flame speed. We would point out, however, that (i) a simple calculation will show that the complex mixture in question could not have been produced by the blending in any proportions of the two aforesaid primary mixtures, unless some inleakage of air occurred during the process, and (ii) that a speed of only 30 cm. per second for a 70.2 H<sub>2</sub>/29.8 air mixture in a tube 2.5 cm. in diameter seems difficult to reconcile with a previous statement by Payman\* that, "it was not found possible to determine accurately the speed of the uniform movement of flame in the upper limit mixture of hydrogen-air in a tube 2.5 cm. in diameter. A mixture containing 71.4 per cent. of hydrogen was found to be the richest which would propagate flame under the experimental conditions . . . but its speed, . . . was found to be approximately 50 cm. per second." We have recently found, by our electrical method, a speed of 50 cm. per second for a 72.6 H<sub>2</sub>/27.4 air mixture.

The number of possible primary methane-air, and hydrogen-air mixtures fulfilling the required conditions, *i.e.*, each containing excess of combustible and both propagating flame with the same initial uniform speed, being limited

\* 'Journ. Chem. Soc.' vol. 115, p. 1456 (1919).

to a small range, our choice of these was necessarily restricted. Eventually, after one or two trials we selected for a series of blending tests the following two primary mixtures, each of which fulfilled the required conditions

	Flame speed. cm. per second.
(A) 11.05 CH <sub>4</sub> /88.95-air* .....	64.5
(B) 71.9 H <sub>2</sub> /28.1-air* .....	64.1

The electrical method (*e.m.*) was used throughout for the flame speed determination. The results of the blending tests, which are shown in Table V, again showed that, as in the cases of the corresponding ethylene-hydrogen-

Table V.—A Series of Experiments with Complex CH<sub>4</sub>—H<sub>2</sub>—air Mixtures.

Percentage composition of primary mixtures A and B.	A.	CH <sub>4</sub> 11.05	O <sub>2</sub> 18.2	N <sub>2</sub> 70.75.			
	B	H <sub>2</sub> 71.9	O <sub>2</sub> 5.75	N <sub>2</sub> 22.35.			
Observed flame speeds (cm. per second) for A and B <i>before</i> and <i>after</i> the blending experiments		Before		After	Mean		
	A.	65.0 64.0 65.0		64.0	64.5		
	B.	63.0 63.0 64.5 61.5	64.7 64.5 63.6	63.6			
Proportions of A and B blended to form C.		Observed flame speed for complex mixture C.		Percentage composition of C. (i) Found and (ii) Calculated.			
A.	B.	cm per second.		CH <sub>4</sub> .	H <sub>2</sub> .	O <sub>2</sub> .	N <sub>2</sub> .
90	10	61.3		{ (i) 10.25	6.9	17.1	65.75
				{ (ii) 9.95	7.2	17.05	65.8
75	25	38.5		{ (i) 8.45	17.8	15.2	58.55
				{ (ii) 8.3	18.0	15.2	58.5
62.5	37.5	32.5		{ (i) 6.6	26.9	13.7	52.8
				{ (ii) 6.9	26.95	13.6	52.55
50	50	26.6 26.2		{ (i) 5.9	35.75	12.0	46.35
				{ (ii) 5.55	35.95	12.05	46.45
37.5	62.5	23.7		{ (i) 3.8	44.7	10.6	40.9
				{ (ii) 4.15	44.9	10.5	40.45
25	75	Did not fire		{ (i) 2.8	53.6	8.95	34.65
				{ (ii) 2.75	53.9	8.90	34.45

N.B.—Electrical method used throughout.

\* As the amount of adventitious nitrogen in the combustible gas used in making these mixtures was less than one per cent., the composition of the air added was not seriously altered thereby.

oxygen, and methane-hydrogen-oxygen mixtures, *successive increases in the proportion of B used in the "blendings" progressively slowed up the initial uniform flame speed of the resulting complex mixture until a point was reached when it no longer propagated flame at all.* In this case such point was nearly reached with the 37.5A/62.5B complex mixture, and had been passed with the 25A/75B complex mixture.

In a final experiment, in which were blended equal volumes of the following two primary mixtures, namely

	Flame speed cm. per second.
(A) 11.5 CH <sub>4</sub> /88.5-air .....	52
(B) 72.6 H <sub>2</sub> /27.4-air .....	51

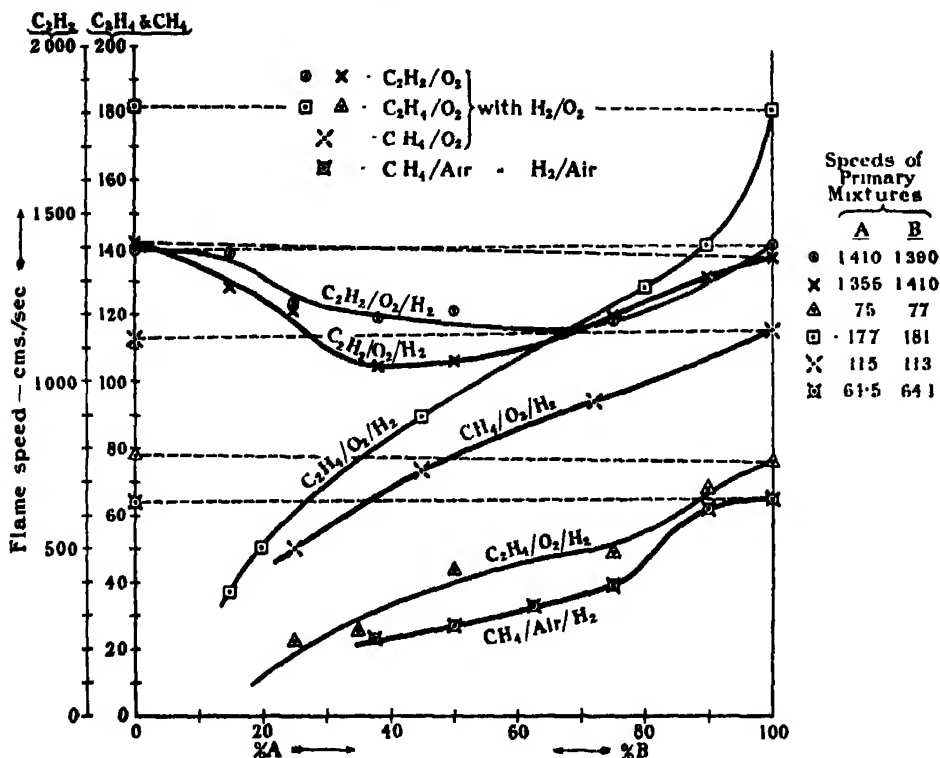
the resulting 50A/50B complex mixture propagated flame quite easily at a uniform speed of 21 cm. per second. A 35A/65B blend, however, refused to propagate flame at all.

#### Summary.

The results of most of our various "blending-tests," which have comprised a fairly wide range of complex hydrocarbon-hydrogen-oxygen (or air) mixtures, some of them initially propagating flame rather slowly, and others quite rapidly, are summed up in the accompanying diagram. The hydrocarbons used have comprised the strongly endothermic acetylene, ethylene—which is only slightly endothermic—and the exothermic methane. Most of the complex mixtures examined have contained excess of combustible gases, but in one series they contained excess of oxygen. In none of the series have the requirements of the supposed "law" been fulfilled, as a glance at the diagram will show, because had the "law" been obeyed, all the lines in it would have been horizontal straight lines.

Moreover, in all the cases which we have examined of complex ethylene-hydrogen-oxygen and methane-hydrogen-oxygen (or air) mixtures with oxygen in defect, it was found that the effect of progressively increasing the proportion of the primary hydrogen-oxygen (air) mixture B in the various blendings in any particular series was to lower the observed flame speed progressively, until a point was reached when the resulting complex mixture refused to propagate flame at all under the stated experimental conditions. Such a result is not surprising when the effect of progressively increasing the proportion of the hydrogen-oxygen (air) mixture in the various blendings upon the oxygen

content of the resulting complex mixture in any particular series is considered, but it seems fatal to the supposed "law."



It therefore follows, that whatever measure of truth there may be in Payman and Wheeler's conclusions in regard to particular instances, they are not generally applicable to gaseous explosions, and therefore cannot be vested with the authority of a natural law.

In conclusion we desire to acknowledge that two of us (R. P. F. and D. A. W.) have carried out this investigation as holders of the Gas Research Fellowships maintained at the Imperial College of Science and Technology, London, by Radiation, Ltd., and the Gas Light and Coke Co., of London, to whose generosity in supporting this work our united thanks are tendered.

*The Initial Stages of Gaseous Explosions.—Part III. The Behaviour of an Equimolecular Methane-Oxygen Mixture when fired with Sparks of Varying Intensities.*

By WILLIAM A. BONE, D.Sc., F.R.S., R. P. FRASER, A.R.C.S., D.I.C., and  
F. WITT, B.Sc., A.R.C.S., D.I.C.

(Received February 7, 1927.)

[PLATES 33–35.]

As part of the general investigation of the initial stages of gaseous explosions now being carried on by us at the Imperial College, London, we have had occasion to study photographically the behaviour of an equimolecular methane-oxygen mixture when ignited by sparks of varying intensities passed between electrodes fixed half-way along a horizontal glass tube (35 to 50 cms. long by 2 to 2.5 cms. diameter), both ends of which were *closed* in one series of experiments, but *open* in another. A few supplementary experiments were also made under other spark igniting conditions. The results of these experiments seem to be of sufficient importance, from the point of view of the interpretation of the initial stages of gaseous explosions, as to justify the separate publication of them at this juncture.

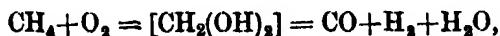
The evidence of the experiments lies so much in the photographs themselves that little need be said about them beyond indicating the precise conditions under which they were obtained. It is left to each reader to study them for himself, because, while their main features will be obvious to all, the interpretation leaves room for discussion, which it is hoped this publication will provoke.

To us they suggest such possibilities as (a) the occurrence, under ordinary sparking conditions, of what seems to be much like a definite "induction period" as a preliminary to the actual combustion; (b) an initial propagation through the medium of a "ghost-like flame" condition involving only a very partial combination of the gases; and (c) the main combustion following later as the result of the superposing of a compression wave, or the like, upon a system which during the phase (b) has already become highly sensitive to chemical changes.

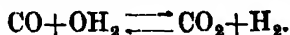
#### EXPERIMENTAL.

In all the following experiments an equimolecular mixture of methane and oxygen, made up from highly purified gases, was employed. The chemical

reactions involved in the explosive combustion of such a mixture are known to be as follows:—(i) the primary interaction of methane and oxygen producing a mixture of carbonic oxide, hydrogen and steam, probably as a result of the thermal decomposition of the incipiently formed dihydroxy-methane, thus:



and (ii) secondary interactions in the reversible system



The end products, before condensation of steam, would consist of a mixture of the oxides of carbon, hydrogen and steam in somewhat the following proportions:—

$$\text{CO}_2 = 5.0, \quad \text{CO} = 28.25, \quad \text{H}_2 = 38.5, \quad \text{H}_2\text{O} = 28.25 \text{ per cent.}$$

It should be understood that the equimolecular is one of the fastest burning of all methane-oxygen mixtures; thus, for example, its rate of detonation—2528 metres per second—exceeds that of all other such mixtures, the so-called “theoretical” mixture,  $\text{CH}_4 + 2\text{O}_2$ , having a rate of 2320 metres only.

#### FIRST SERIES.

##### *Explosion of the Mixture in a Horizontal Glass Tube closed at each End.*

In this series of experiments, a horizontal glass tube, 35 cms. long by 2 cms. internal diameter, closed at each end, and provided with platinum-balled electrodes midway along it (fig. A), was first of all thoroughly cleaned,

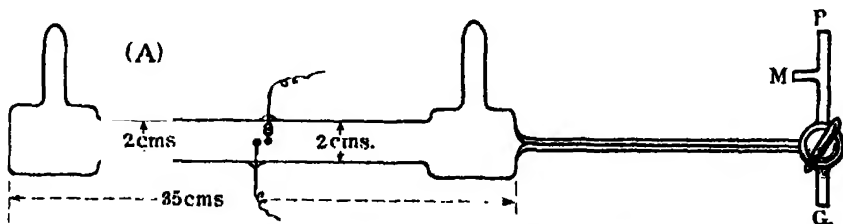


FIG. A.—Explosion Tube. G leads to gas-holder, M to manometer, P to pump.

then evacuated by means of a powerful pump, and finally filled at 20° C. and 780 mm. with the moist equimolecular methane-oxygen mixture.\* The tap in the capillary end of the tube was then shut. The contents of a number of such tubes were successively ignited by means of a spark of known intensity passed between the electrodes. The intensity of the spark was varied in different

\* The mixture would actually contain about 10 mm. of aqueous vapour.



trials, so as to discover how the subsequent explosions would be affected thereby.

The course of the resulting explosion was photographed upon a highly sensitised film fastened on a drum which was rotated about its horizontal axis at a constant speed in each experiment, by means of the mechanism already described in Part I hereof, the actual linear speed of the film past the slit behind the lens of the camera being 1540 cms. per second.

On ignition, therefore, the flame would start in the neighbourhood of the electrodes, and from thence would be propagated horizontally towards each of the closed ends of the tube. The conditions of ignition were, therefore, approximate to those of open-tube spark-ignition. The photographic record produced on the film would thus be compounded of the horizontal velocity of the flame in each direction and the vertical movement of the film. The general arrangement and working of the apparatus were the same as already described in Part I (fig. 1) hereof (*q.v.*).

In Plate 33 are reproduced four typical photographs so obtained, the only varying condition being the character and intensity of the igniting spark. The photographs are numbered in order from left to right in accordance with the increasing spark intensity.

No. 1 resulted from an experiment in which a magneto spark across a 1-mm. gap was used for igniting the explosive mixture. The passage of the spark is shown as a bright spot at the apex of the photograph. A close examination shows that for about 0.00125 sec. after the actual passage of the spark, the luminosity (if any) of the medium was insufficient to affect the film, no flame or flame movement being visible. After this short interval, which is suggestive of an "induction period," a feebly actinic ghost-like flame started, and was propagated for a distance of 10 cms. on either side of the igniting spark with a continuous acceleration, but with no appreciable increase in luminosity. The time actually taken for the flame to traverse the first 10 cms. after the commencement of visible luminosity was 0.004 sec., after which a marked deceleration of the velocity always occurred, giving rise to an approximately "uniform flame movement," which continued until the flame front reached the closed end of the tube, but without any alteration in the luminosity. At the moment, however, when this ghost-like flame front reached the end of the tube, a sudden outburst of intense luminosity occurred, as though the greater part of the actual combustion had yet to take place. The whole tube instantly became filled with an intensely luminous flame, traversed by compression-waves, a condition which lasted for at least 0.0025 sec. after the outburst.

We thus have visual evidence of three distinct phases in the explosion, namely, (a) an initial "induction period" of non-luminosity and no flame movement, lasting for about 0.00125 sec., (b) an intermediate stage of feeble luminosity, extending altogether over about 0.00425 sec., during which each of the two initial flame fronts traversed the medium and reached the closed end of the tube, and (c) a final period of intense luminosity extending over 0.0025 sec., during which, presumably, the main combustion occurred.

It should be mentioned that a close inspection of the original negative shows features of (b), rather suggesting a "composite" flame front with three closely-following feebly luminous flame-bands; but these are so difficult of reproduction that they are scarcely visible in the print. Also, behind the flame front there are "streamers" of gas distinctly more luminous than the surrounding medium, which is almost non-luminous.

No. 2 is from an experiment in which almost the minimum condenser spark discharge (0.05 microfarad at 1000 volts) was used for ignition. The phenomena associated with the resulting explosion were, in general, much the same as in No. 1. The duration of the initial "induction period" (a) was again about 0.00125, of the first flame phase (b) about 0.00425, and of the final period of intense luminosity 0.0025 sec. In fact, the two photo-records were superposable, the only observable difference between them being that in No. 2 the "composite" character of the flame front in (b) and the "streamer" effects after it were both much fainter.

No. 3 is from an experiment in which the igniting source was a condenser spark discharge of 3.75 microfarads at 1000 volts. Here quite new features are seen. In the first place, the non-luminous short "induction period" (a) previously observed is missing, visible combustion starting immediately on the passage of the spark. Next, although the general luminosity of the first flame front (b) was still much fainter than that of the final combustion (c), it was no longer so homogeneous, being marked by *striae* of enhanced luminosity, whose forward projection was reversed when the initial continuous acceleration of the first flame front was checked. These finally coalesced with the final main combustion (c), which had much the same features as the corresponding phases in Nos. 1 and 2. Also, and *quite distinct from such striae*, perfectly straight luminous tracts were discernible in the original negative, suggestive of metallic particles being shot off from the electrodes. Notwithstanding such well-marked differences, the average velocity of the first flame front during the phase (b), as well as the duration of the phase (c), were much the same as in Nos. 1 and 2.

No. 4 is from an experiment in which the igniting source was a condenser

spark discharge of 8 microfarads at 1000 volts. Here the resulting phenomena generally resembled those of No. 3, but the *striae* during the phase (b) were much more marked.

It should be pointed out that the marked difference between the appearance of the discharge spark in Nos. 3 and 4, on the one hand, and Nos. 1 and 2, on the other, is probably due to the much greater ultra-violet emission of the spark in the two first-named cases; the illumination of the walls of the tube by such an intense emission gave the spark its elongated appearance in the photographs.

There are three outstanding features common to all four experiments—namely, (i) that the *average* speed of the ghost-like flame front during the phase (b) was much the same in all, (ii) that in no case did the main combustion (c) commence until the flame front in phase (b) had reached the closed end of the tube, and (iii) that its duration was much the same in all cases.

It should be stated that analyses of the products obtained in the various experiments showed that combustion had been complete in each case.

#### SECOND SERIES.

##### *Explosion of the Mixture in a Horizontal Glass Tube open at each End.*

In this series of experiments the same mixture was ignited in a horizontal glass tube, 50 cms. long by 2.5 cms. diameter (fig. B), by a spark passed between

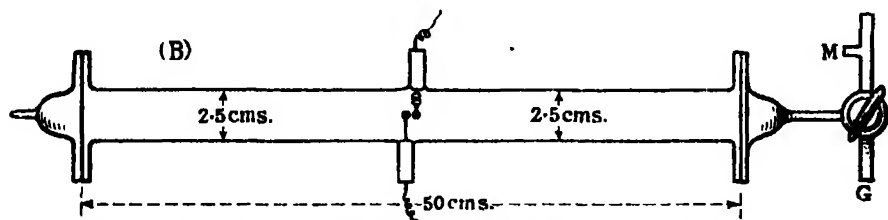
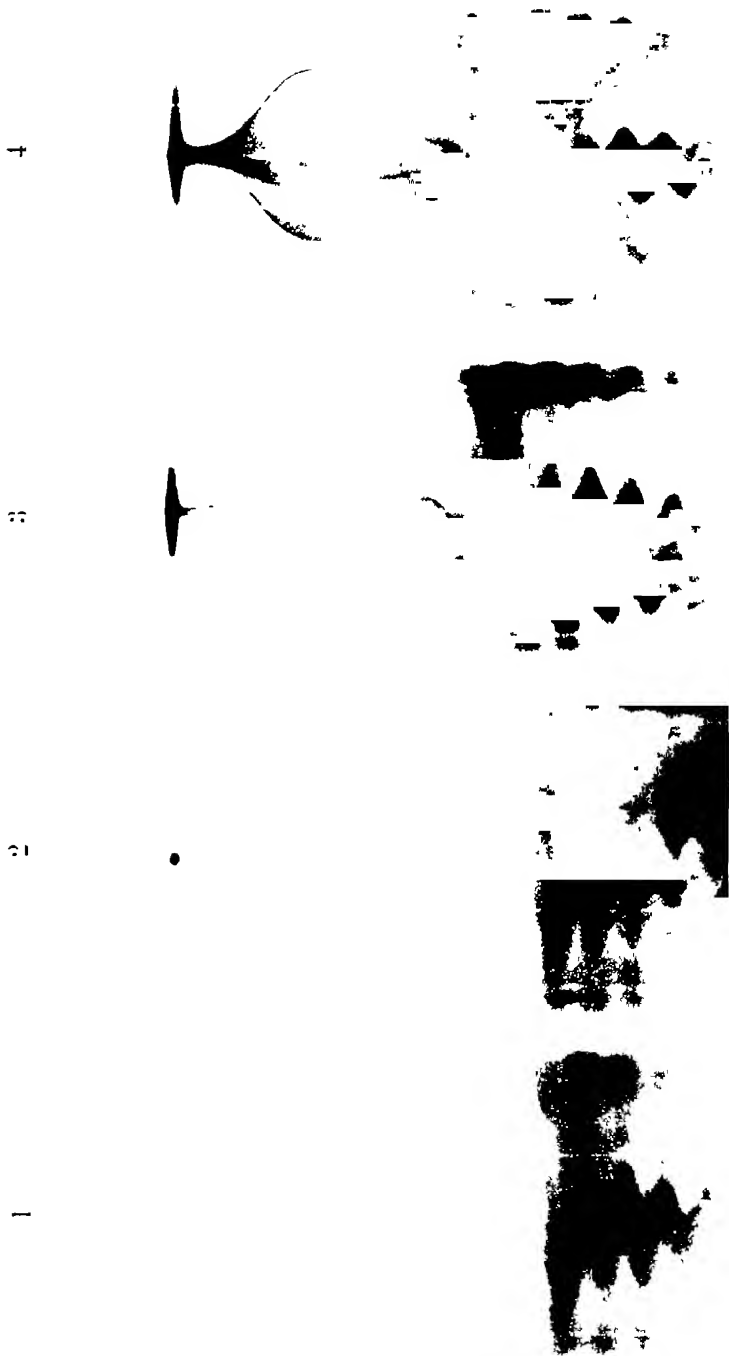
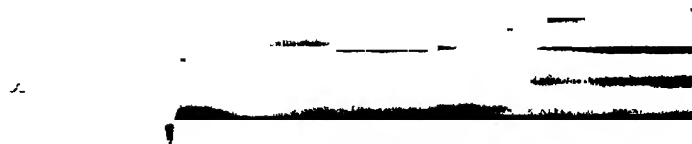


FIG. B.—Explosion Tube. G leads to gas-holder, M to manometer, and P to pump.

lead electrodes fixed midway along it. The tube had flanged ends, which, after it had been evacuated by the pump and filled with the explosive mixture, were drawn off by a gentle sliding motion immediately before the igniting spark was passed, so that the resulting explosion took place in an open tube. The linear vertical speed of the film past the slit of the camera was again constant at 1480 cms. per sec. throughout the series. Plate 34, Nos. 5 to 8, shows the results of four typical experiments in each of which the igniting spark was the same as in the corresponding experiment of Series I. Indeed, the







9

10

11

12

only differences between the conditions of the corresponding experiments in Series I and II were (i) that in II the tube was longer and rather wider than in I, and (ii) that in II both ends of it were *open* instead of being closed as in I.

*No. 5* is from an experiment in which ignition was effected by means of a magneto spark across a 1-mm. gap. Here there was a definite initial non-luminous "induction period" the duration of which was 0.0012 sec.—much the same as in the corresponding experiment (*No. 1*) in the previous series. This was succeeded by the phase (*b*), during which a ghost-like flame front was propagated through the medium with a continuous acceleration almost to the end of the tube. No *striae* were observable in the photographs, and the intensely luminous phase (*c*), always observed in Series I, was now absent.

*No. 6* is from an experiment in which the same condenser discharge spark as in *No. 2* (namely, 0.05 microfarad at 1000 volts) was used for ignition. The duration of the non-luminous "induction period," before any flame started, was precisely the same as in Series I, *No. 2*. And in most other respects, except the absence of the intensely luminous final phase (*c*), the results were generally the same as in that experiment.

*No. 7* is from an experiment in which the same condenser discharge spark as in *No. 3* (namely, 3.75 microfarads at 1000 volts) was used for ignition. Here, as also in *No. 3*, no "induction period" was observable. The initial flame movement during phase (*b*) was also much the same in both cases, but now, with the open-ended tube, no phase (*c*) supervened.

*No. 8* is from an experiment in which the same condenser discharge-spark as in *No. 4* (8 microfarads at 1000 volts) was used for ignition. Here an entirely new feature was observed, namely, that combustion immediately started with an intense luminosity in the neighbourhood (*i.e.*, in a region of about 5 cms. on either side) of the initiating spark, where it persisted (almost stationary) throughout the whole duration of the experiment. But, beyond this region, only the feebly luminous ghost-like flame movement characteristic of phase (*b*) occurred. This is a most significant result, suggestive of the intense combustion characteristic of phase (*c*) being producible by strong "ionisation" of the reacting gases in the neighbourhood of a powerful initiating spark.

### THIRD SERIES.

In Plate 35 is reproduced a series of four photographs obtained in experiments in which the same equimolecular methane-oxygen mixture was



ignited at or near the *open* end of a horizontal glass tube 50 cms. long by 2.5 cms. diameter (fig. C), the other end being closed.

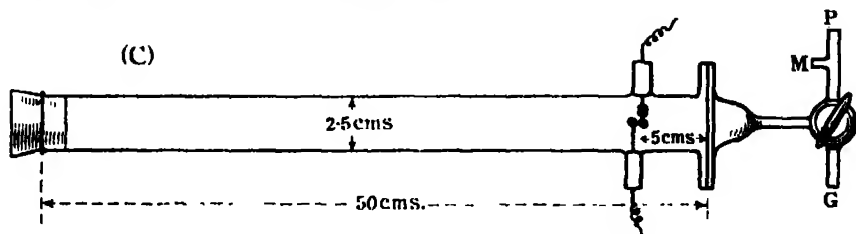


FIG. C.—Explosion Tube. G leads to gas-holder. M to manometer. P to pump.

*No. 9.* Ignition was by means of a 2-cm. high coal-gas flame applied at the open end of the tube. Here we see a long initial “uniform flame movement” (velocity = 190 cms. per sec.), followed by a well-marked oscillatory movement. The linear film speed past the slit of the camera was 550 cms. per sec.

*No. 10.* Ignition was by means of a powerful condenser-spark discharge (8 microfarads at 1000 volts) passed between brass-point electrodes at the mouth of the tube. Here there was (i) a short initial nearly uniform flame movement (velocity = 500 cms. per sec.) succeeded by (ii) an “oscillatory” movement, during which the mean forward velocity of the flame was decidedly less than in (i), although greater than that observed for the similar phase in the previous experiment with ordinary flame ignition. It should be noted that the speed of the initial uniform movement in this experiment was 500, as compared with only 190 cms. per sec. in No. 1, showing that more than one speed of initial uniform movement can be obtained for the same mixture in the same tube, according to the intensity of the igniting source. The linear speed of the film in this experiment was 220 cms. per sec.

*Nos. 11 and 12.* Ignition was by means either of a magneto (No. 3) and/or a powerful condenser spark discharge of 8 microfarads at 1000 volts (No. 4) respectively, passed between lead-balled electrodes fixed inside the tube at a distance of 5 cms. from its open end. In neither case was there any initial uniform movement, the “oscillatory” movement being set up almost from the first. The intensity of the combustion in the region of the powerful condenser spark used in No. 4 was again very marked. The linear speed of the film in each of these experiments was the same as in No. 1, namely, 550 cms. per sec.

#### CONCLUDING REMARKS.

We think that a careful study of the photographs included in this paper will convince readers that, notwithstanding all the scientific investigation of the

matter since Mallard and Le Chatelier first took it up in the year 1880, we have still much to learn about the initial stages of gaseous explosions. Indeed, a systematic re-investigation of the whole subject now seems called for, and we propose continuing our experiments in the hope of elucidating further the new features which have been disclosed so far.

Therefore, we wish it to be understood that in this paper we are merely describing, as best we can, the phenomena which we have observed, and which are recorded in the photographs. At present we are content with directing attention to their outstanding features, and indicating their significance, without attempting to explain them. We have used the terms "induction period" and "ghost-like flame" as being the best we could find to describe what the photographs show, leaving it to further investigation to discover what interpretation must be given to them. We are not yet in a position to say what proportion of the total combustion occurs during the passage through the explosive medium of the "ghost-like" flame observed in Series I and II; presumably, however, from the appearance of the photographs, it is relatively small. This, and many other points, must await further experimental investigation, which we are now undertaking.

In conclusion, we desire to state that one of us (R. P. F.) has participated in this investigation as the holder of the Gas Research Fellowship maintained by Radiation, Limited, of London, at the Imperial College of Science and Technology, London, and another (F. W.) as the holder of a maintenance grant from the Department of Scientific and Industrial Research, to both of whom our united thanks are hereby tendered.

---

*The Structure of Certain Silicates.*

By W. LAWRENCE BRAGG, F.R.S., Langworthy Professor of Physics, Manchester University, and J. WEST, John Harling Fellow, Manchester University.

(Received February 3, 1927.)

*I. Introduction.*

The structures of the silicates which occur in nature present a highly interesting series of problems for X-ray analysis. The number of crystalline forms is very large, and they have been investigated very thoroughly as regards their crystallographical and optical properties, and the way in which isomorphous replacement of one constituent by another takes place. It is generally possible to obtain well-developed crystals which are suitable for purposes of X-ray investigation. The difficulty of analysis is due to the complexity of the molecules which enter into their composition, and the low symmetry of most of the crystals; a direct attack on the problem of their structure by the usual type of X-ray examination is not easy. There are, however, certain features of these compounds which reduce the difficulties of analysis, and enable an insight into the structure to be gained even when its complete determination is not possible.

The especial feature which is discussed in the present paper is the fundamental part played by the oxygen atoms in the crystalline arrangement. The structure may be regarded as an assemblage of oxygen atoms, cemented together by silicon and by metallic atoms. In the case of most metals which are of common occurrence in the silicates, their insertion between the oxygen atoms causes only a slight distortion of the oxygen arrangement, and the relative proportion of these metals and of silicon can be varied within wide limits provided that their positive valencies neutralise the negative valencies of the oxygen atoms.

If this way of regarding the structures be right, it suggests that each series of natural silicates, classified together by the mineralogist as belonging to a mineral species although there is a wide variation in chemical composition, is based on a definite type of oxygen assemblage. A formula for the structural unit must in the first place be adjusted so as to contain the correct number of oxygen atoms although the numbers of the other atoms may vary. The importance of the oxygen atoms in determining atomic arrangement makes X-ray analysis more easy, because certain simple groupings of oxygen atoms may be recognised in much the same form in very different compounds. For

instance, a large number of the silicates discussed in the present paper are based on the cubic or hexagonal forms of close-packing of oxygen atoms, the atoms of metal and silicon being inserted into this framework. The underlying simplicity of the oxygen arrangement may be hidden by the complexity of crystal form, for the dimensions of the unit cell represent the intervals at which the complete atomic pattern repeats itself, and a complex arrangement of silicon and metal atoms leads to a pattern of low symmetry and large unit cell. Nevertheless the dimensions of the unit cell can be shown to be related to the fundamental spacings of a much simpler background of oxygen atoms, on which the complex pattern formed by the other atoms is embroidered.

## 2. Atomic Arrangement in the Silicates.

We were led in the first place to this way of regarding the silicate structures by interesting dimensional relationships between the compounds  $\text{BeO}$ ,  $\text{Al}_2\text{O}_3$ ,  $\text{BeAl}_2\text{O}_4$ ,  $\text{MgAl}_2\text{O}_4$ , and  $\text{Mg}_2\text{SiO}_4$ , and by Wasastjerna's work on the relative sizes of ionic structures. It was noticed in calculating the birefringence of corundum,  $\text{Al}_2\text{O}_3$ ,\* that the oxygen atoms are very close to the positions of hexagonal close-packing with a mean distance of 2.7 Å between atomic centres although the aluminium atoms are unequally distributed amongst them. Since Wasastjerna's figures† assign a much larger size to the oxygen ion than to the aluminium ion, this arrangement suggested that the oxygen ions were in a distorted form of closest packing with aluminium ions in the interstices of the structure, and indicated the possibility that the pseudohexagonal chrysoberyl,  $\text{BeAl}_2\text{O}_4$ , along with the very similar olivine,  $(\text{MgFe})_2\text{SiO}_4$ , might also be based on the same arrangement of oxygen atoms. This proved on trial to be the case.‡ § We were led to examine the structures where small ions might be expected to be situated in the interstices of an oxygen assemblage, and a most interesting field for this investigation is provided by the silicates.

In this paper free use is made of the conception of positive metal or silicon ions and negative oxygen ions. Although it seems justifiable to speak of atoms of magnesium, beryllium, iron, and aluminium, as positive ions bound to negative oxygen ions in crystalline structures, one is on more doubtful ground in extending the same conception to atoms of silicon. The binding forces between silicon and oxygen atoms may be of a much more complex type than the forces between distinct ionic structures of opposite charge. The only

\* W. L. Bragg, 'Roy Soc. Proc.' A, vol. 106, p. 359 (1924).

† 'Soc. Scient. Fenn. Comm.', vol. 1, p. 38 (1923), vol. 2, p. 26 (1926).

‡ W. L. Bragg and G. B. Brown, 'Roy. Soc. Proc.' A, vol. 110, p. 34 (1926).

§ W. L. Bragg and G. B. Brown, 'Z. f. Krist.', vol. 63, p. 538 (1926).

feature of silicon and oxygen arrangement which will be used here is one common to all structures containing these atoms which have as yet been analysed. It was first shown in a highly interesting way by the structure of quartz itself in the  $\beta$  form analysed by Sir William Bragg and R. E. Gibbs.\* The dimensions of the whole crystal structure were shown by these authors to depend on a tetrahedral grouping of oxygen atoms around each silicon atom, with a nearly constant distance of 2.6 Å between oxygen centres like that in the metallic oxides mentioned above. Other forms of silica, since analysed, show the same feature. Since these structures where silicon and oxygen alone are involved display this constancy of interatomic distance for oxygen atoms, it is not surprising to find it in compounds where metallic ions and silicon are present. Similar groupings of four oxygen atoms around a silicon atom are found in the orthosilicates, garnet,  $\text{Ca}_3\text{Al}_2\text{Si}_3\text{O}_{12}$ ,† zircon,  $\text{ZrSiO}_4$ ,‡§ and olivine (*loc. cit.*), and in the metasilicate Beryl,  $\text{Be}_3\text{Al}_2\text{Si}_6\text{O}_{18}$ || In all cases an interatomic distance in the neighbourhood of 2.7 Å is found for the oxygen atoms. Menzer's analysis of garnet is particularly interesting, because the atomic positions can be fixed so accurately owing to the small number of parameters (three). It was the first analysis of a complex silicate to be made, and illustrates the characteristic features of these compounds in a very striking way.

For brevity, this feature will be referred to as a "packing" of oxygen ions, with positive ions between them. Beryllium has been found to lie between four oxygen atoms ( $\text{BeO}$ ,  $\text{BeAl}_2\text{O}_4$ ,  $\text{Be}_3\text{Al}_2\text{Si}_6\text{O}_{18}$ ), aluminium to lie between six oxygen atoms ( $\text{Al}_2\text{O}_3$ ,  $\text{BeAl}_2\text{O}_4$ ,  $\text{Ca}_3\text{Al}_2\text{Si}_3\text{O}_{12}$ ,  $\text{Be}_3\text{Al}_2\text{Si}_6\text{O}_{18}$ ,  $\text{MgAl}_2\text{O}_4$ ), and silicon in each case between four oxygen atoms. The conception of the silicates as "co-ordinated" structures of ions packed together provides so convenient a way of describing structure that it will be used below, it being understood that the present enquiry is concerned with atomic position alone and not with interatomic forces. The relative dimensions of the ionic structures will now be considered.

The isomorphous replacement of an atom by another in the silicates has been discussed in a very interesting way by F. Zambonini,¶ and by E. T. Wherry.\*\*

\* 'Roy. Soc. Proc.,' A, vol. 109, p. 405 (1925).

† G. Menzer, 'Z. f. Krist.,' vol. 63, p. 157 (1926).

‡ L. Vogard, 'Phil. Mag.,' vol. 1, p. 1151 (1926).

§ W. Binks, 'Min. Mag.,' vol. 115, p. 176 (1926).

|| W. L. Bragg and J. West, 'Roy. Soc. Proc.,' A, vol. 111, p. 691 (1926).

¶ F. Zambonini, 'Rend. Accad. Lincei,' vol. 31, p. 295 (April, 1923) 1922. See also abstract by H. S. Washington, 'Amer. Min.,' vol. 8, p. 81 (1923).

\*\* 'Amer. Min.,' vol. 8, p. 1 (1923).

Their papers were published almost simultaneously and put forward very similar views. Zambonini discusses the well-known isomorphism of albite and anorthite, where there is substitution of the group  $(\frac{1}{2}\text{Al})$  for the group  $\text{NaSi}$ , with equal sums of the principal valencies. He lays stress on the relative sizes of the elements which replace each other. Aluminium can replace silicon, atom for atom, because these two atoms appear to occupy the same amount of space in the crystal edifice. The change must be accompanied by a corresponding replacement of sodium by calcium, in order that the valencies may balance, and this is possible because sodium and calcium are also ions which occupy almost identical spaces in the structure. The isomorphism of diopside,  $\text{CaMgSi}_2\text{O}_6$ , and aemite,  $\text{NaFe}^{+++}\text{Si}_2\text{O}_6$ , is a similar case. Zambonini makes the further interesting point that there is no essential difference between the rôle played by aluminium, and that played by silicon. He regards aluminium as assuming the acid function: in the present paper we refer to silicon as a positive ion like that of aluminium or the other metal constituents, and not as being the centre of an acid group, but it is immaterial to the present discussion which view is adopted. Wherry also comes to the conclusion that "the principal requisite of isomorphous replaceability is that the elements in question must possess apparently identical volumes." He cites a highly interesting series of cases, all directed to show the importance of spatial considerations in replacement. A review of the idea of "volume isomorphism" is given by L. J. Spencer in the 'Annual Reports of the Chemical Society' for 1925, in the section on Mineralogical Chemistry.

We are in absolute agreement with the views of these authors as to the importance of the sizes of the ions which replace each other. The difference between our treatment of the problem and theirs arises because it now seems necessary to adopt modified values for the sizes of the ions. We speak for convenience of the "size" or "diameter" of the ion although, of course, this is not a definite physical quantity. It is a useful expression of the empirical rule that interatomic distance is an additive property to a fair degree of approximation in these inorganic compounds. Zambonini and Wherry used values for the ionic diameters proposed by one of us in 1920.\* These values give the right estimate for the distance between positive and negative ions, but need modification in one important respect, as has been pointed out by several authors, notably by Wasastjerna.† The positive ions were originally supposed to be too large, and the negative ions too small. Wasastjerna has shown

\* W. L. Bragg, 'Phil. Mag.,' vol. 40, p. 169 (1920).

† 'Soc. Scient. Fenn. Comm.,' vol. 1, p. 38 (1923).

that an amount of about  $0.7 \text{ \AA}$  must be subtracted from the radii of the positive ions as first proposed and an equal amount added to that of the negative ions, in order that a set of empirical constants may be obtained which give a true picture of the arrangement of the ions in crystalline structures.\* This modification does not affect the striking examples of the importance of ionic size in isomorphous replacement given by Zambonini and Wherry since all the positive ions are reduced in size to the same extent. It has the effect, however, of making the negative oxygen ion the largest ion in the crystalline edifice, and therefore the most important in determining its form. The figures in the 1920 paper were unfortunately responsible for an erroneous impression of the comparative unimportance of the oxygen atom.

The relative sizes of the more common constituents of the silicates according to the modified figures are shown in fig. 1. The oxygen ion is assigned a diameter of  $2.7 \text{ \AA}$ . This must only be taken as indicating that the repulsion

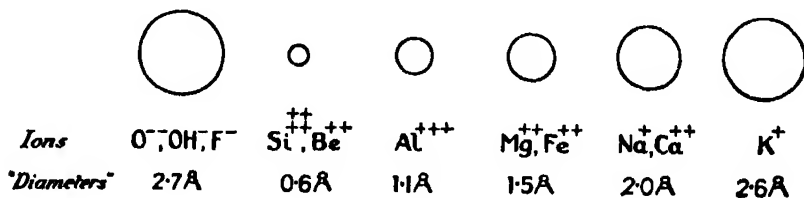


FIG. 1.

between the oxygen ions becomes sufficiently large to prevent further approach, under the influence of forces of the order operative in the crystalline structure when the centres of the ions are about  $2.7 \text{ \AA}$  apart. In structures of the type considered here, the distance is observed to vary by about  $0.2 \text{ \AA}$  in either direction. The other estimates of size are of the same nature, and it will be noticed how much larger the oxygen ion is than the majority of the other ions. The ions  $\text{OH}^-$  and  $\text{F}^-$  occupy a space comparable with that occupied by  $\text{O}^{--}$ .

It is to be inferred from these sizes that the repulsion between neighbouring oxygen ions is more important in deciding their relative positions than the repulsion between oxygen and most metals, because it sets in at so large an interatomic distance. This may be expressed by saying that these metal ions pack into the interstices of the oxygen assemblage without greatly distorting it. Very little distortion is produced by the ions,  $\text{Si}^{++}$ ,  $\text{Al}^{+++}$ ,  $\text{Be}^{++}$  and probably also  $\text{B}^{+++}$ . The ions  $\text{Fe}^{++}$ ,  $\text{Mg}^{++}$ ,  $\text{Mn}^{++}$  are rather larger, and expand the

\* Cf. "Interatomic Distances in Crystals," W. L. Bragg, 'Phil. Mag.,' vol. 2, p. 258 (1926).

structure, but may still be regarded as packed between the oxygen ions which remain at a distance of slightly more than  $2.7 \text{ \AA}$  apart. On the other hand, such ions as  $\text{Ca}^{+2}$ ,  $\text{Na}^{+1}$ ,  $\text{K}^{+1}$ ,  $\text{Ba}^{+2}$  are much too large to fit between close-packed oxygen atoms. The arrangement in the neighbourhood of these large ions is determined by the interatomic distance between metal and oxygen, not by that between oxygen and oxygen.

The crystalline edifice may then be pictured in the following way. The oxygen ions, by reason of their size and of their number, form the framework on which it is built, and they are packed together with a general distance of about  $2.7 \text{ \AA}$  between their centres. A group of ions (silicon, aluminium, beryllium, iron, magnesium) are so small in size that they will pack between the oxygen ions, cementing the structure together but having only a secondary effect on its arrangement. A second group of ions (sodium, calcium, potassium, barium) are of larger size, and play a primary part in determining the arrangement. In isomorphous replacement of atoms, the small ions are interchangeable with each other, and the large ions are interchangeable if their sizes correspond, subject to a general condition that positive and negative valencies balance each other. In most silicates, oxygen and the smaller metallic ions predominate, and it is this feature which makes it possible to regard the structure as built up on a framework of oxygen atoms.

### 3. Properties of the Close-packed Assemblage of Oxygen Atoms.

If it be correct to suppose that oxygen atoms pack together with an interatomic distance of about  $2.7 \text{ \AA}$ , unless forced apart by the insertion between them of one of the larger metallic ions, then the volume associated with each oxygen ion in any structure cannot be less than a certain limit. This limit is reached when the oxygen ions are in either the cubic or hexagonal type of closest packing, and are combined with only such ions as  $\text{Be}^{+2}$ ,  $\text{Al}^{+3}$ ,  $\text{Si}^{+4}$  which are very small. It will be supposed that the oxygen atoms are packed together in one of these ways, the distance between neighbouring atoms being everywhere  $2.7 \text{ \AA}$ . The assemblage will have certain properties.

*Cubic Type of Closest Packing.* The atoms lie on a face centred cubic lattice, with an edge  $3.82 \text{ \AA}$  in length. The volume of the unit cube is  $55.7 \text{ \AA}^3$ , and it contains four atoms each associated with a volume of  $13.9 \text{ \AA}^3$ .

*Hexagonal Type of Closest Packing.* The atoms lie on two interpenetrating hexagonal lattices, with "c" equal to  $4.41 \text{ \AA}$  and "a" equal to  $2.70 \text{ \AA}$ . The unit cell has a volume of  $27.8 \text{ \AA}^3$ , and contains two atoms each associated with a volume of  $13.9 \text{ \AA}^3$  as in the case of the cubic lattice since both are equally



closely packed. It is sometimes convenient to refer the hexagonal assemblage to orthohexagonal axes, and in order to facilitate comparison with compounds dealt with below an orthohexagonal cell containing 16 atoms will be chosen. This has a volume of  $222.8 \text{ \AA}^3$ , and the following axes:—

$$a = 4.41 \text{ \AA} \quad b = 9.36 \text{ \AA} \quad c = 5.40 \text{ \AA}.$$

In this cell, the  $a$  axis is the hexagonal axis.

A further feature of this close-packed assemblage is of interest. Molecular refractivity is an approximately additive property, and refractivities can be assigned to the ions of which a crystal is composed. Wasastjerna\* and Fajans and Joos† have given a very interesting series of figures for ionic refractivity. The refractivity of the ion  $\text{O}^{2-}$  is very large compared with that of such small ions as  $\text{Be}^{++}$ ,  $\text{Al}^{+++}$ ,  $\text{Mg}^{++}$ , and the refractivity of compounds, in which these metals of silicon occur in combination with oxygen, is almost entirely due to the oxygen atoms. The molecular refractivity does not obey an exact additive law, so no universal values can be given for the ionic refractivities. For instance, the contribution by a given ion appears to be larger when it is associated with another large ion than when it is near a small ion. In compounds of the type mentioned above, the following values enable refractive indices to be calculated with fair accuracy and give an idea of the relative importance of the different ions.

O	3.3–3.6	$\text{Mg}^{++}$	0.4
Ca	2.0	$\text{Al}^{+++}$	0.3
Na	0.7	$\text{Si}^{++}$	0.25

Taking the lower estimate of 3.3 for the refractivity of oxygen, and using the formula

$$\frac{1}{2} \cdot \frac{M}{\rho},$$

it is found that the refractive index  $n$  of the close-packed assemblage of oxygen ions, neglecting altogether the contribution of metal ions, is equal to 1.71. The refractive index of any compound in which oxygen atoms are in close packing at a distance of  $2.7 \text{ \AA}$  apart therefore must be at least 1.71.

In Table I the volumes associated with each oxygen atom and the mean refractive indices are given in the third and fourth columns. Since the atoms Be, Al, Si cause no expansion of the oxygen groups and have a very small ionic refractivity, crystals based on a close-packed arrangement of oxygen

\* 'Soc. Scient. Fenn. Comm. Phys. Math.,' vol. 1, p. 37 (1923).

† 'Z. f. Physik,' vol. 23, p. 1 (1924).

atoms will have a volume of about  $13.9 \text{ \AA}^3$  for each oxygen atom, and a refractive index in the neighbourhood of 1.71. Further, the dimensions of their unit cells will be simply related to the dimensions of the cubic or hexagonal arrangement of closest packing. The volume  $13.9 \text{ \AA}^3$  is a lower limit, and it may be increased either by the insertion into the close-packed assemblage of ions such as  $\text{Mg}^{++}$ ,  $\text{Fe}^{++}$ ,  $\text{Mn}^{++}$  (examples are the spinels, the olivine group, the chondrodite group) or by the oxygen arrangement departing altogether from the closest-packed form (examples are the forms of silica itself, and the structure of beryl). The expansion by itself decreases the refractive index since the highly refractive oxygen ions are dispersed in a larger volume, but this may be more than compensated by the introduction of an ion with high refractivity such as  $\text{Fe}^{++}$ . The table may be interpreted by these considerations and shows which structures may be expected to be based on one of the forms of closest packing.

Table I.

	Molecular volume, $\text{M}'\rho$	Volume per oxygen atom in $\text{\AA}^3$ .	Refractive index (Na).
Close-packed assemblage		13.94	.71
Beryllium oxide, $\text{BeO}$	8.26	13.62	.726
Corundum, $\text{Al}_2\text{O}_3$	25.6	14.05	.768
Chrysoberyl, $\text{BeAl}_2\text{O}_4$	34.4	14.18	.749
Cyanite, $\text{Al}_2\text{SiO}_5$	45.6	15.05	.720
Spinel, $\text{MgAl}_2\text{O}_4$	39.5	16.30	.72
Olivine ( $\text{MgFe}$ ) $_2\text{SiO}_4$	41.1	18.20	.65 ( $\text{Mg}_2\text{SiO}_4$ )
Chondrodite, $\text{H}_2\text{Mg}_2\text{Si}_2\text{O}_{10}$	109.2	18.10	.62
Humite, $\text{H}_2\text{Mg}_2\text{Si}_2\text{O}_{10}$	153.4	18.10	.60
Chinochumite, $\text{H}_2\text{Mg}_2\text{Si}_2\text{O}_{10}$	198.5	18.18	-
Monticellite, $\text{MgCaSiO}_4$	51.5	21.22	1.66
Topaz ( $\text{AlF}$ ) $_2\text{SiO}_4$	54.4	14.25*	1.61
Phenacite, $\text{Be}_2\text{SiO}_4$	37.0	15.38	.66
Diopase, $\text{H}_2\text{CuSiO}_4$	48.7	20.07	.69
Garnet, $\text{R}_3\text{R}_3'\text{Si}_3\text{O}_{12}$	112.1	15.42	.71.8
Andalusite, $\text{Al}_2\text{SiO}_5$	52.0	17.15	.636
Sillimanite, $\text{Al}_2\text{SiO}_5$	49.4	16.30	.665
Beryl, $\text{Be}_3\text{Al}_2\text{Si}_6\text{O}_{18}$	205.5	18.85	.581
Quartz, $\text{SiO}_2$	22.75	18.73	1.549

\* Fluorine and oxygen are regarded as equivalent.

#### 4. The Structure of Cyanite, $\text{Al}_2\text{SiO}_5$ .

The compounds  $\text{BeO}$ ,  $\text{Al}_2\text{O}_3$ ,  $\text{BeAl}_2\text{O}_4$ ,  $\text{Al}_2\text{SiO}_5$ ,  $\text{SiO}_2$ ,  $\text{Be}_2\text{SiO}_4$ ,  $\text{Be}_3\text{Al}_2\text{Si}_6\text{O}_{18}$  are composed of oxygen and such ions as may be regarded as inserted into the structure of an oxygen assemblage. The figures in the table show that the conditions for closest packing are obeyed by  $\text{BeO}$ ,  $\text{Al}_2\text{O}_3$ ,  $\text{BeAl}_2\text{O}_4$ , and indicate the possibility of one form of  $\text{Al}_2\text{SiO}_5$  (cyanite) being also based on closest

packing. The structures of  $\text{BeO}$ ,  $\text{Al}_2\text{O}_3$ ,  $\text{BeAl}_2\text{O}_4$  have been discussed in a previous paper.\* They are all based on the hexagonal assemblage of closest packing. In making this statement, it must be understood as referring to the general configuration of the crystal, for the oxygen atoms in  $\text{Al}_2\text{O}_3$  are displaced from the exact positions of the hexagonal arrangement by about  $0.15 \text{ \AA}$ , and probably by an amount of similar order in  $\text{BeAl}_2\text{O}_4$ . We are concerned only with the broad features of the atomic arrangement, for the finer details of exact atomic position in the complex crystals are beyond the scope of analysis in its present form.

We were led to examine cyanite because it seemed possible that it was based on closest-packing. At first sight the crystalline form seems to bear no relationship to the cubic or hexagonal assemblage. Cyanite is triclinic, and has the following axial ratios and angles † -

$$a : b : c = 0.8894 : 1 : 0.7090 \quad \alpha = 90^\circ 5\frac{1}{2}' \quad \beta = 101^\circ 2' \quad \gamma = 105^\circ 44\frac{1}{2}'.$$

The dimensions of the unit cell have been measured by Mark and Rosbaud.†† Four molecules of  $\text{Al}_2\text{SiO}_5$  are included in the unit cell, and the lengths of the axes are :—

$$a = 7.15 \text{ \AA} \quad b = 8.00 \text{ \AA} \quad c = 5.55 \text{ \AA}.$$

Rotation photographs which we have obtained give good agreement with these values.

The  $c$  axis has a length of  $5.55 \text{ \AA}$ , which is slightly more than twice the diameter of the oxygen ion,  $2.70 \text{ \AA}$ . The  $b$  axis is nearly at right angles to it, and the ratio  $b : c$  is very nearly equal to the ratio  $\sqrt{2} : 1$ . This gives the key to the structure, which is based on *cubic close packing*. The relationship is shown in fig. 2.

The  $c$  and  $b$  axes of cyanite correspond to the diagonal OC of the unit cube, and to the line OB which is twice as long as the edge of the unit cube. The  $a$  axis of cyanite makes an angle of  $105^\circ 44\frac{1}{2}'$  with the  $b$  axis, and an angle of  $101^\circ 2'$  with the  $c$  axis. If a line OA is drawn making these angles with OB and OC, it meets a point A belonging to the face centred lattice at a distance of  $7.14 \text{ \AA}$  (in cyanite  $a = 7.18 \text{ \AA}$ ). The three axes OA, OB, OC are the edges of a unit cell, which is associated with 20 points of the face-centred cubic lattice, corresponding to the unit cell of cyanite with 20 oxygen atoms (four molecules of

\* W. L. Bragg and G. B. Brown, 'Roy. Soc. Proc.,' A, vol. 110, p. 34 (1926).

† 'N. Jahrb. f. Min.,' etc., Beilageband LIV, A, p. 127 (1926).

‡ 'Z. f. Electrochemie,' vol. 7, p. 317 (1926).

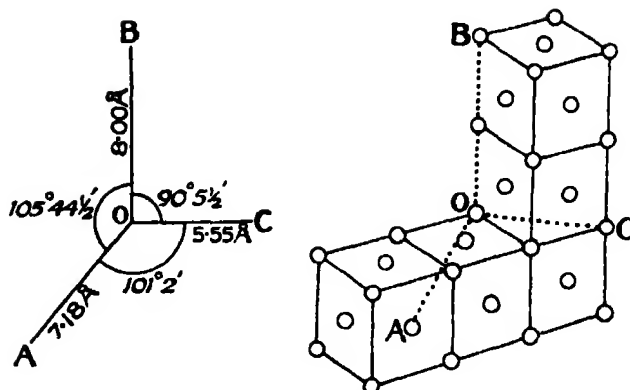


FIG. 2.—Relationship of the axes of Cyanite,  $\text{Al}_2\text{SiO}_5$ , (left), to the lines joining the points O to the points A, B, C, in a face-centred cubic lattice (right). The unit cell of which OA, OB, OC are edges contains twenty points of the cubic lattice.

$\text{Al}_2\text{SiO}_5$ ). The axes OA, OB, OC are related as follows, as is easily seen from the figure :—

$$\text{OA}^2 : \text{OB}^2 : \text{OC}^2 = 14 : 16 : 8.$$

whence  $\text{OA} \cdot \text{OB} \cdot \text{OC} = 0.935 \cdot 1 : 0.707.$

In cyanite  $a : b : c = 0.899 \cdot 1 : 0.709.$

The correspondence, which might be made still closer by increasing the average distance between oxygen atoms, is summed up in the following table :—

Cyanite, $\text{Al}_2\text{SiO}_5$			Unit cell based on face-centred cubic lattice.		
$a = 7.18 \text{ \AA}$	$\alpha = 90^\circ 5\frac{1}{2}'$		$a = 7.14 \text{ \AA}$	$\alpha = 90^\circ$	
$b = 8.00 \text{ \AA}$	$\beta = 101^\circ 2'$		$b = 7.64 \text{ \AA}$	$\beta = 100^\circ 53'$	
$c = 5.55 \text{ \AA}$	$\gamma = 105^\circ 44\frac{1}{2}'$		$c = 5.40 \text{ \AA}$	$\gamma = 105^\circ 38'$	
Twenty oxygen atoms in unit cell			Twenty points in unit cell.		

It is possible to test the correctness of this relationship without making a complete analysis of the structure. The planes of a face-centred lattice which have the largest spacings are (111), (200), (220). If the oxygen atoms in cyanite are in cubic close packing, corresponding planes of the triclinic crystal will be densely packed with oxygen atoms. Further, without knowing the positions of the aluminium and silicon atoms in the triclinic cell, there is a strong presumption that the aluminium atom lies at the centre of six oxygen atoms and the silicon atom at the centre of four such atoms. They are found in these positions in all other crystals which have been analysed. This alone is sufficient

to tell what contributions these atoms make to planes such as (111), (200), (220) of the cubic lattice.

In the following table, the first column gives the indices of each reflexion referred to the cubic lattice. The last column shows the contribution of the various atoms. The second column gives the indices of the corresponding planes in the triclinic lattice. For instance, the planes (111), ( $\bar{1}\bar{1}\bar{1}$ ), ( $\bar{1}\bar{1}1$ ), ( $\bar{1}1\bar{1}$ ) correspond to four planes of the triclinic crystal with different indices. In general, a plane ( $h\ k\ l$ ) of the cubic lattice becomes a plane ( $H\ K\ L$ ) in the triclinic lattice, where

$$H = h + \frac{3k}{2} - \frac{l}{2},$$

$$K = 2l$$

$$L = h - k.$$

This relationship will be clear from fig. 2.

Table II.

Indices referred to cubic axes.	Indices referred to triclinic axes.	Contribution from atoms
(111), ( $\bar{1}\bar{1}\bar{1}$ ), ( $\bar{1}\bar{1}1$ ), ( $\bar{1}1\bar{1}$ )	(220), ( $\bar{3}\bar{2}0$ ), ( $\bar{1}22$ ), ( $02\bar{2}$ )	O <sub>8</sub> - Al <sub>4</sub>
(200), (020), (002)	(202), ( $30\bar{2}$ ), ( $\bar{1}40$ )	O <sub>3</sub> + Al <sub>2</sub> - Si
(220), ( $\bar{2}\bar{2}0$ ), (202) ( $20\bar{2}$ ), (022), ( $02\bar{2}$ ) }	(500), ( $\bar{1}04$ ), ( $\bar{1}42$ ) ( $\bar{3}\bar{4}\bar{2}$ ), ( $24\bar{2}$ ), ( $4\bar{4}\bar{2}$ ) }	O <sub>3</sub> + Al <sub>2</sub> + Si
(222), ( $\bar{2}\bar{2}\bar{2}$ ), ( $\bar{2}\bar{2}2$ ), ( $\bar{2}2\bar{2}$ )	(440), ( $\bar{6}\bar{4}0$ ), ( $\bar{2}44$ ), ( $04\bar{4}$ )	O <sub>6</sub> + Al <sub>2</sub> - Si
(400), (040), (004)	(404), ( $\bar{6}0\bar{4}$ ), ( $\bar{2}80$ )	O <sub>3</sub> + Al <sub>2</sub> + Si

It is, of course, to be expected that distortion of the structure will modify these atomic contributions, but nevertheless planes of the type (200), (220), (222), (400) should give powerful reflexions. Planes of the type (111) will have a small reflecting power owing to the opposition of oxygen and aluminium.

This prediction is strikingly verified if rotation photographs are taken with the  $b$  axis and  $c$  axis of cyanite as axes of rotation. This corresponds to rotating the cubic lattice around its edge, or around its face-diagonal. In fig. 3 the diagram on the right is a reproduction of the rotation photograph, while that on the left shows the position of the spots due to the principal planes of the cubic lattice. The time of exposure was short and the number of spots which appear on the plates is small, but it will be seen that the most prominent reflexions are due to the simple cubic planes. A very similar case has been discussed in a

paper on chrysoberyl,\* where an orthorhombic crystal is based on a hexagonal close-packed assemblage, and the rotation photographs show strongly all the planes of the hexagonal lattice.

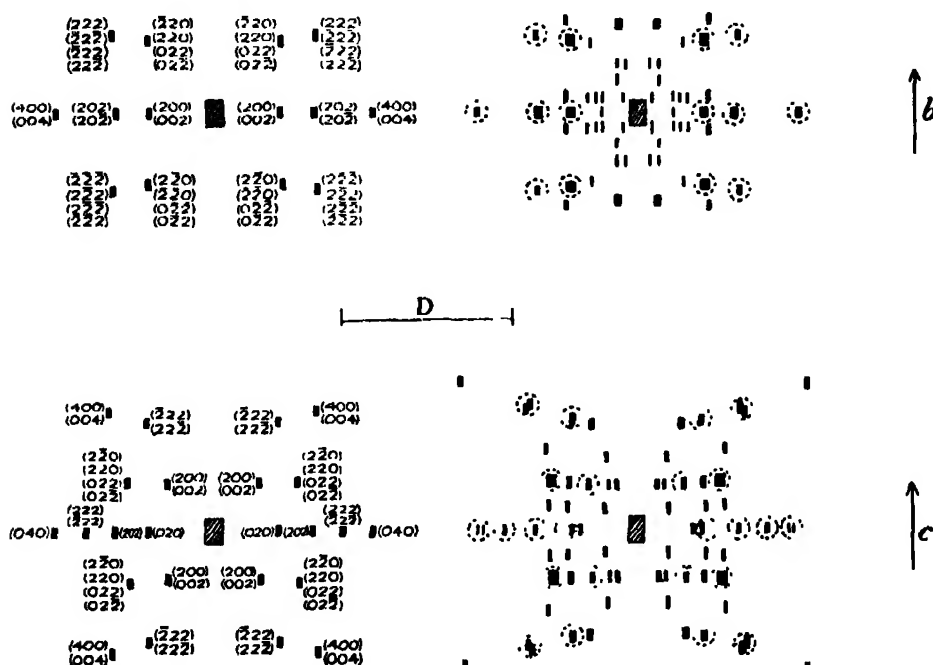


FIG. 3.—Comparison of spots from rotation photographs of Cyanite (right) with those due to principal planes of the cubic lattice (left)—cf. fig. 2. Spots in the right-hand diagram corresponding to spots in the left-hand diagram are contained in circles. The length,  $D$ , represents the distance of the axis of rotation from the photographic plate.

This evidence seems to show definitely that the triclinic crystal  $\text{Al}_2\text{SiO}_5$  is based on a simple cubic assemblage of close-packed oxygen atoms. The crystal is an example of a complex pattern formed by the aluminium and silicon atoms, based on a very simple arrangement of oxygen atoms. The unit cell appears to have so unsymmetrical a form because the number of oxygen atoms in it must be a multiple of five, owing to the formula  $\text{Al}_2\text{SiO}_5$ , and there is no simple way of outlining a cell in either assemblage of closest packing which brings in this number. The complete analysis of the crystal does not appear to be an impossible problem, although the number of parameters involved is very great indeed. For instance, in the rotation diagram the reflexions may be divided into two sets. Certain of them, as explained above, are due to the planes of the cubic lattice, and the oxygen atoms contribute largely to these reflexions.

\* *Loc. cit.*, § 2.

The remainder are not planes of the cubic lattice, and the contributions of the oxygen atoms will be very small even allowing for a slight distortion of the oxygen arrangement. By considering only these latter reflexions, the structure to be found reduces to an arrangement of aluminium and silicon atoms alone. Further, these atoms may be expected by analogy with other compounds to be very close to certain definite positions between the oxygen assemblage, and these positions are still further restricted by the consideration that the aluminium and silicon atoms will be dispersed as evenly as possible amongst the interstices. This illustrates the way in which the predominating influence of the oxygen atoms in the structure aids analysis.

### 5. Structures based on Hexagonal Close-packing of Oxygen Atoms.

In the following table a comparison is made between the structural dimensions of a series of compounds based with one possible exception on the hexagonal assemblage. An orthorhombic cell containing 16 oxygen atoms has been chosen as the unit structure in all cases.

Hexagonal close-packed assemblage	4.42	9.36	5.40	-	4	.35
BeO (Dihexagonal pyramidal)	4.38	9.32	5.38	-	4	.35
Al <sub>2</sub> O <sub>3</sub> (Rhombohedral holohedral)	4.32	9.50	5.48	-	4	.37
BeAl <sub>2</sub> O <sub>4</sub> (Orthorhombic)	4.42	9.39	5.47	-	4	.37
(Mg, Fe) <sub>2</sub> SiO <sub>4</sub> ..	4.76	10.21	5.89	-	4	.47
MgCaSiO <sub>4</sub> ..	4.815	11.08	6.37	-	4	.59
(AlF) <sub>2</sub> SiO <sub>4</sub> ..	4.64	8.79	8.38	-	6	.40

The first three compounds follow almost exactly the dimensions of the close-packed assemblage with a distance of 2.7 Å between neighbouring points. The structure is expanded by the insertion of the magnesium ions in olivine (Mg, Fe)<sub>2</sub>SiO<sub>4</sub>, and still further by magnesium and calcium ions in monticellite, MgCaSiO<sub>4</sub>.

The atoms are arranged in the same way in chrysoberyl, BeAl<sub>2</sub>O<sub>4</sub>, and in olivine,\* or in the pure magnesium silicate forsterite, Mg<sub>2</sub>SiO<sub>4</sub>. This relationship has long been surmised from the close similarity of the axial ratios. Rotation photographs of BeAl<sub>2</sub>O<sub>4</sub> and (Mg, Fe)<sub>2</sub>SiO<sub>4</sub> show only such differences as would be expected from the replacement of the light beryllium atom by the heavy silicon atom, the two magnesium atoms occupying the places of the two aluminium atoms. It has also been considered, from their similarity in crystalline form, that MgCaSiO<sub>4</sub> and Mg<sub>2</sub>SiO<sub>4</sub> have a similar structure. X-ray examina-

\* W. L. Bragg and G. B. Brown, 'Z. f. Krist.', vol. 63, p. 538 (1926).

tion has confirmed this in an interesting way. In  $\text{Mg}_2\text{SiO}_4$  the magnesium atoms are of two kinds, half being situated at centres of symmetry and half on reflexion planes of the orthorhombic space group. In  $\text{MgCaSiO}_4$  calcium atoms replace magnesium atoms of the latter type on the reflexion planes, the magnesium atoms still occupying the symmetry centres. The two compounds are strictly isomorphous, being founded on the same space group, in contrast to a pair of compounds such as calcite and dolomite where the replacement of half the calcium by magnesium lowers the symmetry.\* When so large an ion as  $\text{Ca}^{++}$

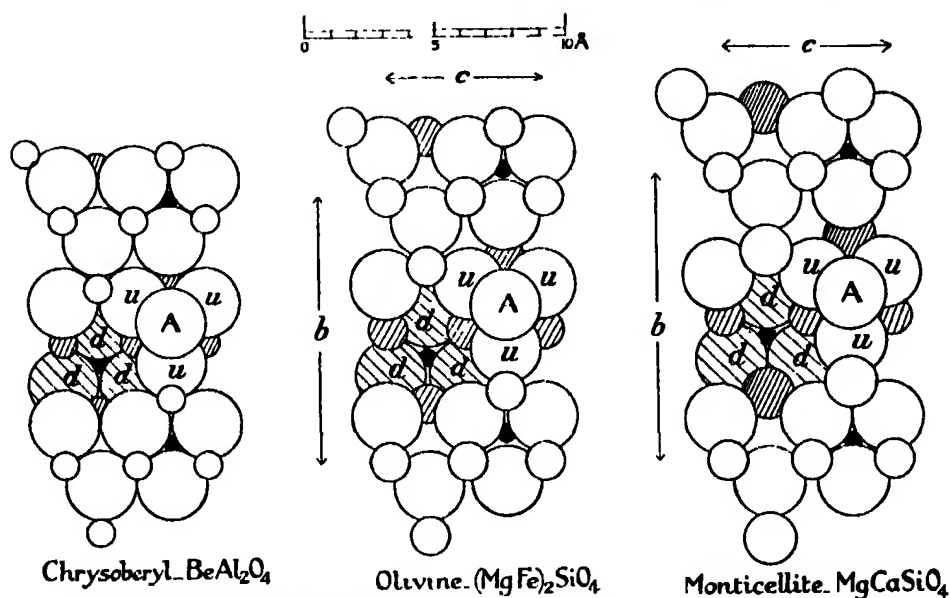
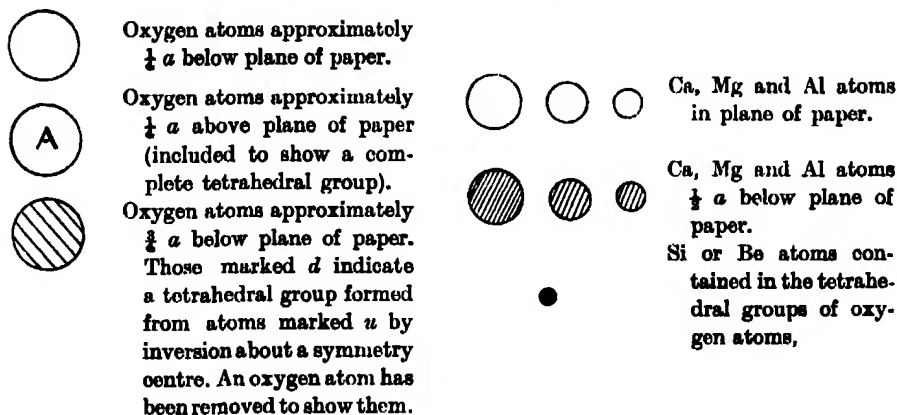


FIG. 4.—Diagram of structures viewed parallel to *a* axis.



\* R. W. G. Wyckoff and H. E. Merwin, 'Am. J. Sci.,' vol. 8, p. 447 (1924).



forms part of the structure, the oxygen atoms depart widely from a closest-packed arrangement, and the similarity in structure between  $\text{MgCaSiO}_4$  on the one hand, and  $\text{Mg}_2\text{SiO}_4$  and  $\text{BeAl}_2\text{O}_4$  on the other hand, must be considered exceptional. The structures are shown in fig. 4.

The measurements which we have made on topaz  $(\text{AlF})_2\text{SiO}_4$  are not sufficient to tell whether it may be included as an example of closest-packing. Fluorine and oxygen occupy very nearly the same space in crystalline structures. The small molecular volume for each atom, ranking fluorine with oxygen, indicates an approach to close-packing. The axial lengths are in approximate agreement with close-packing, and the sixth order reflexion from the  $c$  face of topaz is exceedingly strong. All these considerations indicate that topaz is founded on a close-packed cell whose ideal dimensions would be  $a = 4.42$ ,  $b = 9.36$ ,  $c = 8.10$ , containing six rows of atoms in the  $c$  direction, as against four in the other units. On the other hand, although the analysis of the crystal is not completed, the preliminary results show that a wide departure from close packing has taken place, and it is not certain whether it may be regarded as derived from the simple arrangement.

The spinel  $(\text{MgAl}_2\text{O}_4)$  structure may be classed with this set of crystals. The oxygen atoms in spinel are close to the positions of a cubic face-centred lattice, with magnesium atoms between four oxygen atoms and aluminium atoms between six oxygen atoms. The figures in Table I show that it occupies an intermediate position in closeness of packing between  $\text{BeAl}_2\text{O}_4$  and  $\text{Mg}_2\text{SiO}_4$ . One magnesium atom in the molecule expands the structure slightly, and two atoms expand it still more.

#### 6. The Chondrodite Group.

The minerals of the chondrodite group afford an interesting example of morphotropy. Penfield and Howe showed that the addition of the molecule  $\text{Mg}_2\text{SiO}_4$  to these compounds increases by regular steps the length of the  $c$  axis, while the other two axes remain unchanged. Further, the axial lengths are related to those of forsterite,  $\text{Mg}_2\text{SiO}_4$ . The table illustrating the relationship is taken from Groth's 'Chemische Kristallographie.'

Table III.

	$a$	$b$	$c$	$\beta$
Proectite $[\text{SiO}_4]\text{Mg}[\text{Mg}(\text{F}, \text{OH})]_2$	monoclinic	1.0803	1 : 3 × 0.6287	90° 0'
Chondrodite $[\text{SiO}_4]_2\text{Mg}_3[\text{Mg}(\text{F}, \text{OH})]_2$	monoclinic	1.0803	1 : 5 × 0.6289	90° 0'
Humite $[\text{SiO}_4]_3\text{Mg}_6[\text{Mg}(\text{F}, \text{OH})]_3$	orthorhombic	1.0802	1 : 7 × 0.6291	90° 0'
Clinohumite $[\text{SiO}_4]_4\text{Mg}_7[\text{Mg}(\text{F}, \text{OH})]_3$	monoclinic	1.0803	1 : 9 × 0.6288	90° 0'
Forsterite $[\text{SiO}_4]\text{Mg}_2$		$b$	$2a$	$2c$
	orthorhombic	1.0733	1 : 2 × 0.6297	90° 0'

This relationship has been discussed by Barlow and Pope,\* who have shown that the equivalence parameters parallel to  $a$  and  $b$  are nearly constant, and that the parameter parallel to  $c$  shows a regular progression.

X-ray measurements of chondrodite, humite and clinohumite confirm the existence of a morphotropic relationship, while showing that it is not so simple as the above table would indicate. Two axes of each crystal, which are at right angles to each other, are very nearly equal to the  $a$  and  $b$  axes of olivine  $(\text{Mg, Fe})_2\text{SiO}_4$ . For convenience, these axes have been termed " $a$ " and " $b$ " throughout the series.

Table IV.

	$a$ .	$b$ .
Olivine	4.755 Å	10.21 Å
Chondrodite	4.733 Å	10.27 Å
Humite	4.738 Å	10.23 Å
Clinohumite	4.75 Å	10.26 Å

The apparent *spacings* of the planes (001), parallel to the plane containing the  $a$  and  $b$  axes, show a regular progression. In the following table, the spacings are those corresponding to the first X-ray reflexion.

	Spacings parallel to (001).
Olivine, (002)	2.99 Å = $2 \times 1.495$ Å
Chondrodite, (001)	7.44 Å = $5 \times 1.488$ Å
Humite, (002)	10.43 Å = $7 \times 1.490$ Å
Clinohumite, (001) ?	13.43 Å = $9 \times 1.492$ Å

This is precisely similar to the relationship shown in Table III. It would hold also for the " $c$ " axes if these axes were at right angles to the " $a$ " and " $b$ " axes as is usually assumed. This is definitely not the case in the monoclinic chondrodite,† the  $c$  axis of which makes an angle of  $109^\circ 2'$  with the  $a$  axis, and may not be true for prolectite and clinohumite (we have not been able to obtain specimens of prolectite, and the measurements of clinohumite are insufficient to determine the  $c$  axis with certainty). The unit cells, projected on the (100) planes, are shown in fig. 5. Their approximate dimensions were

\* *Vide* "The Chemical Significance of Crystal Structure," W. J. Pope, 'Proc. Royal Inst.', 1910.

† Our setting of chondrodite, chosen so as to make its relationship with olivine evident, is one which makes the angle " $\alpha$ " not a right angle. Our axes should be renamed in order to follow convention and make this the angle " $\beta$ ."

obtained from rotation photographs, and determined more precisely with the spectrometer. In olivine and humite the (001) spacing is halved.

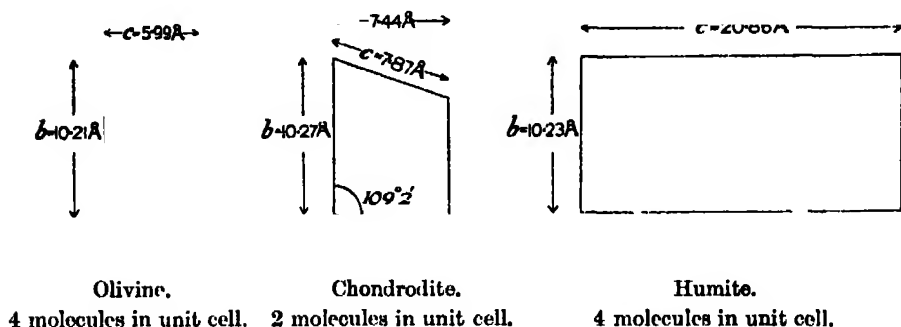


FIG. 5.

The spectra given by the (001) planes of the four compounds are shown in fig. 6. They illustrate in an interesting way the relationship between the diffraction by the underlying simple arrangement of oxygen atoms, and that by the complex arrangement of magnesium and silicon atoms. In the first place, a very strong reflexion appears in each case at an angle corresponding to a spacing of  $1.49 \text{ \AA}$ , and is repeated again at a value of  $\sin \theta$  twice as great. Obviously, planes densely packed with atoms occur in sheets parallel to (001) at intervals of  $1.49 \text{ \AA}$  in all the crystals. In the second place this strong reflexion is the second, fifth, seventh, and ninth in olivine, chondrodite, humite, and clino-humite respectively. The crystalline pattern in so far as it concerns the (001) planes therefore repeats itself at intervals  $2 \times 1.49 \text{ \AA}$ ,  $5 \times 1.49 \text{ \AA}$ ,  $7 \times 1.49 \text{ \AA}$ ,  $9 \times 1.49 \text{ \AA}$ . These results can be interpreted in a very simple way.

It has been shown that olivine is based on a hexagonal close-packed assemblage of oxygen atoms, slightly expanded by the insertion of the magnesium and iron atoms between the oxygen atoms. The relationship of olivine to the chondrodite group and the appearance of the reflexions from (001) planes are explained if it is supposed that all these structures are based on hexagonal close packing. The unit cell in olivine is a rectangular block containing 16 oxygen atoms. The cells of the other crystals contain a larger number of oxygen atoms, owing to the complexity of the molecules. The way in which these cells are related to the hexagonal close-packed assemblage is shown in fig. 7. The cell grows by the addition of layers of oxygen atoms parallel to (001). There are four such layers in olivine,\* five in chondrodite. Humite differs from chondrodite in

\* The arrows in fig. 7 measure the spacings parallel to (001) which yield the first reflexion. In olivine and humite this spacing is equal to one half the length of the c axis. The figs. 5 and 7 together will make clear the relations of the spacings to the cell dimensions.

being orthorhombic, and it is impossible that the cell should contain seven layers of oxygen atoms. A glance at the figure shows that a "c" axis, at right

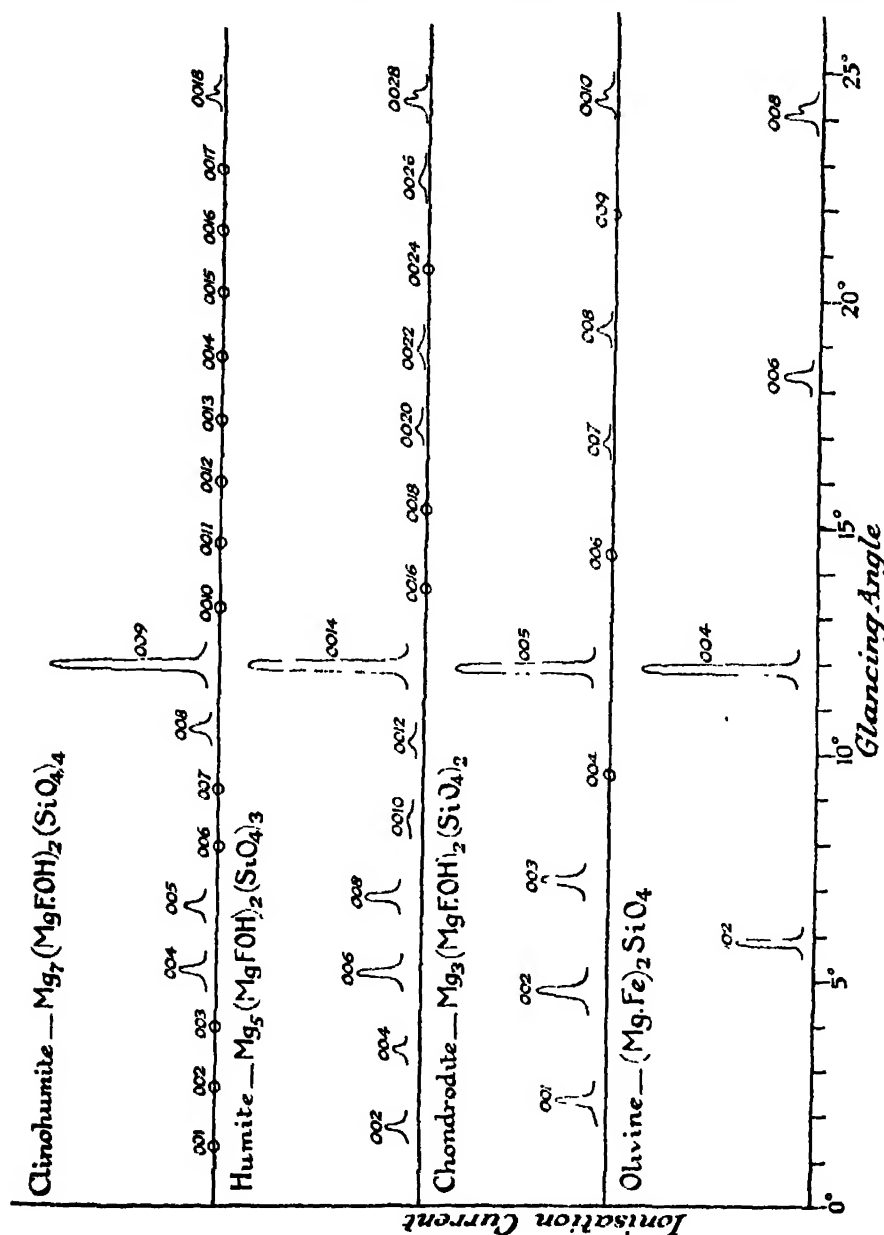


FIG. 6.—Comparison of spectra from c face of Olivine, Chondrodite, Humite and Clinohumite.

angles to "a" and "b," does not end on another oxygen atom after passing an odd number of layers, and it is necessary to double its length, making 14

layers in all, before an orthorhombic cell is possible. In the monoclinic chondrodite the "c" axis joins two oxygen atoms, five layers apart, and displaced

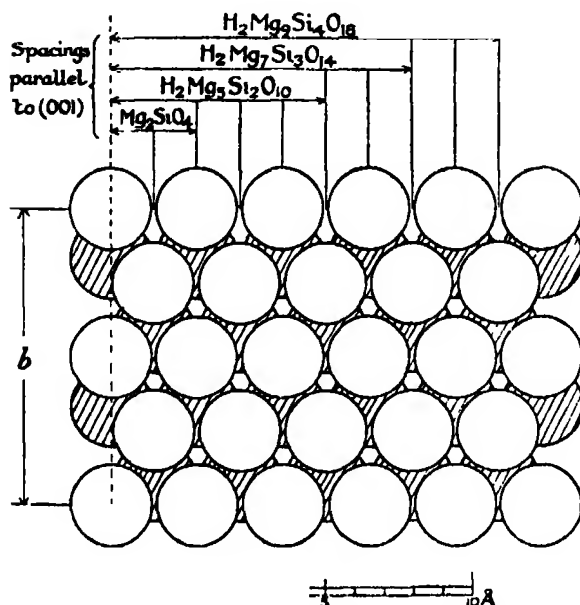


FIG. 7.--Diagram showing relations of spacings to (001) in Olivine and the members of the Chondrodite Series to the hexagonal close-packed assemblage of Oxygen ions. The layers of Oxygen ions are projected on the (100) plane. The shaded circles represent ions  $a/2$  above and below those represented by unshaded circles.

relatively to each other in the  $b$  direction. In clinohumite the number of layers is either 9 or 18.

The magnesium and silicon atoms will presumably occupy places between six and four oxygen atoms respectively in the chondrodite group as they do in olivine. Arranged in this way they lie in the layers of oxygen atoms at intervals of 1.49 Å parallel to (001), and therefore the reflexions corresponding to these spacings are very strong as shown in fig. 6.

The underlying hexagonal assemblage can be further tested by examining the reflexions of planes parallel to the  $a$  axis, and making an angle of  $60^\circ$  with (001). In olivine, for example, the reflexion (062) is strong for the same reason that (004) is strong, one plane being derived from the other by a rotation of  $60^\circ$  about the pseudohexagonal  $a$  axis, and both being densely packed with atoms. The corresponding reflexions (with complicated indices) in chondrodite and humite are also very strong. Just as in the case of cyanite, the reflexions are of two classes. The hexagonal assemblage of oxygen atoms produces a simple set

of reflexions, which are in general very strong unless it happens that these atoms are opposed by the magnesium and silicon atoms. The complex pattern of the latter atoms produces a complex series of reflexions to which the oxygen atoms make very little contribution.

### 7. Open Structures.

The arrangements of oxygen atoms in closest packing, considered above, are the simplest types of oxygen assemblage on which a structure can be based. Closest packing appears to be the exception rather than the rule, even when the atoms combined with oxygen are such as fit into the interstices of the oxygen assemblage. The figures in Table I, for instance, show that cyanite is the only one of the three forms of  $\text{Al}_2\text{SiO}_5$  which has oxygen atoms in closest packing. In the various forms of silica,  $\text{SiO}_2$ , and in beryl,  $\text{Be}_3\text{Al}_2\text{Si}_6\text{O}_{18}$ , the large volumes associated with each oxygen atom, and the low refractive indices, indicate directly that the structures are open.

Although the arrangements of the oxygen atom in these less compact structures is complicated, it would seem that the estimate of about 2.7 Å for the distance between two neighbouring oxygen atoms is of the greatest help in examining the structure. In beryl,\* for example, the structure of the dihexagonal bipyramidal crystal is determined by seven parameters. The unit cell contains 36 oxygen atoms. If an oxygen atom is placed in the general position, it is multiplied into 24 by the operations of symmetry. It can be shown that the co-ordinates of the atom in the general position are defined within very small limits by the condition that no two oxygen atoms shall be closer than 2.7 Å. If these limits are passed, the condition is violated at one place or another in the cell. These atoms being fixed, there is only one possible way in which the remaining 12 oxygen atoms can be placed, and further only one possible way in which the silicon, aluminium, and beryllium atoms can be placed in suitable interstices within the oxygen assemblage. Thus a determination of the space group, combined with the conception of oxygen-packing, leads directly to an approximate solution of the whole structure which is confirmed by the X-ray analysis. The diagram of the structure in fig. 8 shows the way in which the oxygen atoms are densely packed in certain regions, but leave open channels around the hexagonal axes which account for the large volume per oxygen atom and low refractive index of the crystal.

One of the authors has made an attempt to analyse phenacite,†  $\text{Be}_2\text{SiO}_4$ .

\* W. L. Bragg and J. West, 'Roy. Soc. Proc.' A, vol. 111, p. 691 (1926).

† 'Roy. Soc. Proc.' A, vol. 113, p. 642 (1927).

In this crystal, in contrast to  $\text{Mg}_2\text{SiO}_4$ , the oxygen atoms are not in an arrangement of closest packing, although the volume associated with each oxygen atom is not much greater than the lower limit of  $13.9 \text{ \AA}$ .

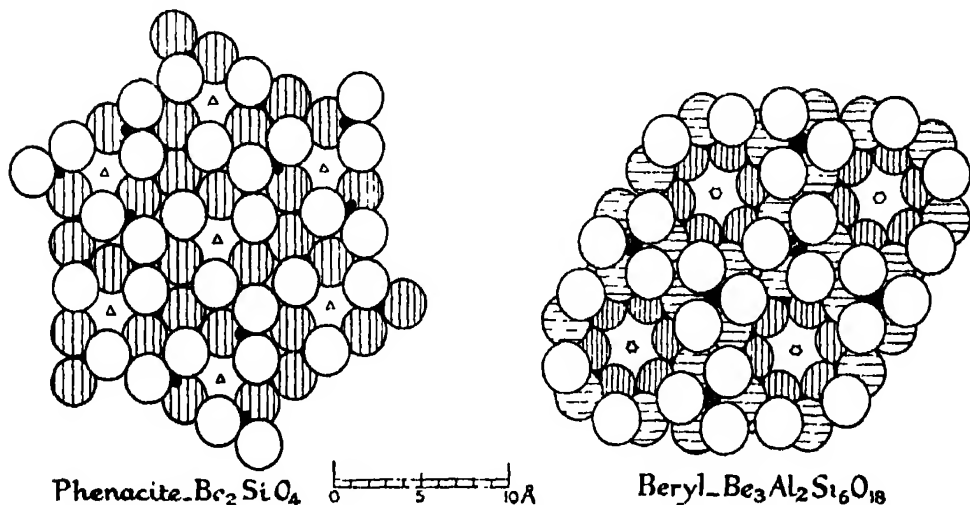


FIG. 8.

- |                                                                                                                                                                                                                                                                                                                                                                                             |                                                                                                                                                                             |
|---------------------------------------------------------------------------------------------------------------------------------------------------------------------------------------------------------------------------------------------------------------------------------------------------------------------------------------------------------------------------------------------|-----------------------------------------------------------------------------------------------------------------------------------------------------------------------------|
| <p>○ Oxygen atoms at <math>0.94 \text{ \AA}</math> above plane of paper.</p> <p>◐ Oxygen atoms at <math>0.94 \text{ \AA}</math> below plane of paper.</p> <p>◑ Oxygen atoms on reflexion plane (<math>2.29 \text{ \AA}</math> below plane of paper).</p> <p>● Silicon atoms on reflexion plane.</p> <p>● Aluminium atoms in plane of paper.</p> <p>○ Beryllium atoms in plane of paper.</p> | <p>○ Oxygen atoms <math>0.68 \text{ \AA}</math> above plane of paper.</p> <p>◐ Oxygen atoms <math>0.68 \text{ \AA}</math> below plane of paper.</p> <p>● Silicon atoms.</p> |
|---------------------------------------------------------------------------------------------------------------------------------------------------------------------------------------------------------------------------------------------------------------------------------------------------------------------------------------------------------------------------------------------|-----------------------------------------------------------------------------------------------------------------------------------------------------------------------------|

The most interesting compounds as yet analysed, and those which throw most light on the rôle played by silicon in the silicates, are the various forms of silica  $\text{SiO}_2$  itself. The structure of  $\beta$ -quartz has been determined by Sir W. H. Bragg and R. E. Gibbs,\* and by Wyckoff,† that of  $\beta$ -cristobalite by Wyckoff‡ and by Selyakoff, Strontinsky and Krasinkoff,§ and that of  $\beta$ -tridymite by

\* 'Roy. Soc. Proc.,' A, vol. 109, p. 405 (1925).

† 'Am. J. Sci.,' vol. 11, pp. 62, 101 (1926).

‡ 'Am. J. Sci.,' vol. 9, p. 448 (1925).

§ 'Z. f. Physik,' vol. 33, p. 53 (1925).

Gibbs.\* The structure of  $\alpha$ -quartz has been outlined, if not completely determined, by Gibbs.† In his paper on tridymite Gibbs reviews these various forms, which are all of the open type. The silicon atom is in every case surrounded by four oxygen atoms which are at the corners of a tetrahedron. In  $\beta$ -cristobalite this tetrahedron is regular in form, in the other crystals it is not necessarily regular but the distortion is not great. Every oxygen atom forms part of two neighbouring tetrahedral groups which are linked together in this way. The average distance between oxygen atoms in these structures is somewhat less than the value 2.7 Å of which so much use has been made in the present paper. It is about 2.52 Å in  $\beta$ -cristobalite and  $\beta$ -tridymite, and 2.58 Å in quartz.

Gibbs draws attention to the fact that this regularity in arrangement of the oxygen atoms strongly suggests a grouping of oppositely charged ions  $\text{Si}^{++}$  and  $\text{O}^{--}$ . This supposition gives a natural explanation of the high symmetry of which the groups are capable. However, if this view is accepted it seems logical to apply it not only to the group  $\text{SiO}_4^{--}$ , but also to  $\text{PO}_4^{--}$ ,  $\text{SO}_4^{--}$ ,  $\text{ClO}_4^-$ , which the  $\text{SiO}_4^{--}$  group resembles in form. This, of course, is Kossel's well-known conception of the acid radicles as oxygen ions surrounding highly-charged positive ions.

Whether the silicon atoms can be regarded as ions, or whether they are bound in some structural way to the oxygen atoms, is immaterial to the method of analysis developed in the present paper. This merely makes use of the empirical fact that an oxygen to oxygen distance of 2.6 Å to 2.7 Å is observed in all these compounds. The approximate constancy of the distance, whatever its cause, results in regular arrangements of four or six oxygen atoms around the atoms of certain metals or of silicon. The examples of structures which have been given in this paper are intended to show how useful a clue this oxygen arrangement provides for the analysis of silicates in general.

### Summary.

The silicates present a highly interesting series of problems for X-ray analysis, because the number of crystalline forms is so large, and because they have been investigated very thoroughly as regards their crystallographical and optical properties, and the way in which isomorphous replacement of one constituent by another takes place. On account of their complexity and low symmetry a direct attack on their structure is difficult. In the present paper an attempt is

\* 'Roy. Soc. Proc.,' A, vol. 113, p. 351 (1926).

† 'Roy. Soc. Proc.,' A, vol. 110, p. 443 (1926).



made to find the atomic arrangement by making use of certain characteristic features of oxygen compounds.

We owe to Wasastjerna the suggestion that the oxygen ion appears to occupy a much larger space in crystalline structures than most of the positive ions to which it is bound. One of the authors showed that in a number of oxygen compounds the form of the structure appeared to be governed almost entirely by a packing together of oxygen atoms, the other atoms being inserted into the interstices. The highly interesting form of silica investigated by W. H. Bragg, Gibbs, Wyckoff and others shows that this is true for silica as well as for the metallic atoms we studied.

In this paper we have regarded each series of silicates, classified together by the mineralogist as belonging to a mineral species although there is a wide variation in chemical composition, as based on a characteristic type of oxygen assemblage. A number of structures are based on the cubic or hexagonal arrangements of closest packing of oxygen atoms, the metal and silicon atoms being inserted into this framework. The dimensions of the unit cell are related to the fundamental spacings of this simple background of oxygen atoms, on which the complex pattern formed by the other atoms is embroidered. Closest-packing is found for an extended series of compounds, ranging from  $\text{BeO}$ ,  $\text{Al}_2\text{O}_3$ ,  $\text{BeAl}_2\text{O}_4$ , and  $\text{MgAl}_2\text{O}_4$ , to cyanite  $\text{Al}_2\text{SiO}_5$ , olivine  $(\text{MgFe})_2\text{SiO}_4$ , monticellite  $\text{MgCaSiO}_4$ , and the chondrodite  $[(\text{MgOH})_2\text{Mg}_3(\text{SiO}_4)_2]$  group.

The arrangement of oxygen atoms is in general more complex, closest-packing being an exceptionally simple case, but such compounds as have been analysed indicate that the packing of oxygen atoms remains the predominant feature of the structure. The results of X-ray analysis suggest that formulæ for the silicates should in the first place be adjusted so as to contain the correct number of oxygen atoms. The very interesting explanations of isomorphous replacement advanced amongst others by Zambonini and Wherry still hold good, but take on a new aspect when the importance of the oxygen atoms in the structure is considered.

We wish to express our gratitude to Dr. A. Hutchinson, F.R.S., for the trouble which he has taken in finding for us crystal specimens suitable for examination. Mr. W. H. Taylor has taken the rotation photographs which we have used in our calculations, and has helped with the calculations themselves and the preparation of the diagrams. Part of the apparatus used in the investigation was presented to the Laboratory by the General Electric Company of America, and part by Messrs. Metropolitan-Vickers whom we wish to thank for their generous gifts.

[*Note added March 2, 1927.*—Reference should have been made in paragraph 2 of this paper to an article by V. M. Goldschmidt, "Die Gesetze der Krystallochemie."\* This article, which is one of a series entitled "Geochemische Verteilungsgesetze der Elemente," deals with the crystalline structures of simple inorganic compounds. The author and his collaborators have extended greatly the numbers of members in the various series of structural types. Goldschmidt discusses the apparent size of the ionic or atomic "bausteine," arriving at a set of radii closely corresponding to, though more extensive than, the set proposed by Wasastjerna or the author's figures in their modified form. He gives a highly interesting review of the sets of similar structures. The review accentuates in a striking manner a feature which has become more and more evident as analysis has been extended, the feature that geometrical considerations of arrangement of the constituents appear to be of so much more importance than chemical constitution in determining crystalline form. The present paper is concerned with one particular aspect of this general feature. Goldschmidt makes a brief reference to the constitution of the silicates. The suggestions which he makes as to the constitution of the more complex forms cannot as yet be tested, but our results indicate that they may need revision in some respects.

Zachariasen† has determined the space group of one of the crystals discussed in the present paper, phenacite. He assigns to this crystal a hexagonal space lattice (space group  $C^1_{3c}$ ) whereas we base it on a rhombohedral space lattice (space group  $C^2_{3c}$ ). We have checked this point by means of a rotation photograph about an axis, which according to Zachariasen should be the "a" axis of the hexagonal lattice. The resulting photograph proves the non-existence of an identity-period corresponding to Zachariasen's "a" axis, the reflexions being on the other hand in positions explained by the rhombohedral lattice.]

\* 'Vid. Selsk. Skr. M-N. Kl.,' 1926, No. 2 (Oslo).

† W. Zachariasen, 'Norsk. geol. Tidsskr.,' vol. 9, p. 65 (1926).

---

*The Constants of the Magnetic Dispersion of Light.*

By C. G. DARWIN, F.R.S., and W. H. WATSON, Ph.D., Edinburgh University.

(Received January 20, 1927.)

1. The rotation of the plane of polarisation of light by a magnetic field provides perhaps one of the easiest approaches to a study of the spectroscopic behaviour of ordinary substances. The present work is an analysis of the available measures of the dispersion of this magnetic gyration. Several formulæ have been proposed for it, and these will be reviewed below, but it has proved most convenient to take one of them and use that; afterwards testing, to the rather limited extent possible, how far others would fit the facts. The test is made with the formula given by Becquerel\* in 1897,

$$V = \frac{e}{2mc^2} \lambda \frac{dn}{d\lambda}, \quad (1.1)$$

where  $n$  is the refractive index,  $\lambda$  the wave-length and  $V$  is Verdet's constant, the rotation of the plane of polarisation per centimetre per gauss. If this formula fits, and we shall find that it does, it should give the value of  $e/m$ . A few values were worked out by Becquerel himself on the rather meagre data available at that time, and later Siertsema obtained more accurate values for some other substances. All these gave  $e/m$  roughly of the right order of magnitude, and this fact was duly noted in the text-books and has been copied from one to another ever since, but usually without giving any numerical values at all. Since Larmor's theorem fails to hold for molecules we should hardly expect to find the ordinary value, but nevertheless it seemed useful to analyse all the experimental measures available, so as to discover if any regularity would emerge. In the physical journals there are several results of this type for particular substances, but they are very much scattered, and it should prove convenient to collect together an analysis of all the substances for which the gyration has been measured. We are not attempting any deep theory of the matter, but merely a convenient summary which may prove useful when the time comes for a proper theory of the spectroscopic behaviour of ordinary substances of the type that has been so successful for monatomic gases and vapours. It is outside the scope of the present work to discuss the behaviour of the gyration of light of frequency very close to opaque bands; this has been

\* 'C. R.,' vol. 125, p. 679 (1897).

the subject of many experiments, but they are not by any means concordant, and take us deeper into the unknown theory than it is possible at present to go.\* To avoid this trouble we have limited ourselves to transparent substances, that is, to regions of the spectrum far from the bands which cause the optical effects. The data have been extracted from Landolt and Bornstein's tables (edition 1921), in some cases supplemented from the original sources, and it has not, of course, been possible to assess the merit of each of the individual measures recorded. In a few cases there are measures of the gyration but not of the refraction; and we are greatly indebted to Dr. I. C. Somerville of the Chemical Department of the University of Edinburgh for measuring some of these refractive indices for us.

A complete analysis of gyration without prejudice would involve first of all analysis of refractive indices into dispersion formulæ. It appears that there are few substances for which this has been done, and it would involve a quite extravagant amount of labour to do it here. The great practical advantage of Becquerel's formula over the others is that it can be applied without this previous analysis. The present work will show that all the transparent substances, solid, liquid, and gas, with one exception, are fitted by Becquerel's formula satisfactorily. In a few cases the dispersion of the refractive index has been analysed into terms, and in these a test can be made between rival formulæ. The test is not very exacting, but in no case is there conclusive evidence of misfit. When the influence of the infra-red bands (which are inoperative magnetically) has been eliminated, the actual values of  $e/m$  are found to range from 50 to 100 per cent. of the ordinary value. The one exception is oxygen gas, which totally declines to fit not only Becquerel's formula, but also the most natural alternative to it. We shall discuss this in its place.

2. We must now review the theory of the dispersion of gyration. It is convenient to use, not the refractive index and Verdet constant, but the more primitive "scattering constants," which describe the waves scattered by an element of the substance under the stimulus of a given vibrating electric force. When an element of volume  $dv$  of a substance is acted on by an electric force  $E_x e^{i\omega t}$  in the presence of a magnetic field  $H$  along  $z$ , it emits waves which are those that would be given by an electric moment  $\sigma dv/4\pi E_x e^{i\omega t}$ ,  $i\rho dv/4\pi E_x e^{i\omega t}$  along  $x$  and  $y$  respectively. We call  $\sigma$  and  $\rho$  the *refraction* and *gyration* of the substance. They are, of course, functions of the frequency  $\nu$ .† It is not then hard

\* This is not intended to exclude the gyration by sodium vapour of light near the D lines; but as that is more or less completely understood we need not discuss it here.

† We shall throughout speak of frequency as the number of vibrations in  $2\pi$  sec.

to construct from  $\sigma$  and  $\rho$  the ordinary optical constants. Right- and left-handed circularly polarised waves are transmitted without change of form but with different velocities, so that their refractive indices are  $n'$  and  $n''$ , given by the positive roots of the equations

$$\frac{3(n^2 - 1)}{n^2 + 2} = \sigma \pm \rho, \quad (2.1)$$

and the rotation of the plane of polarisation in unit length is

$$\frac{v}{2c}(n' - n''). \quad (2.2)$$

When incident light has frequency not very close to any of the characteristic lines of the substance,  $\rho$  is much smaller than  $\sigma$ , and we can write  $n' - n'' = 2\rho \frac{d\sigma}{dn}$ , where  $n$  now means the refractive index for zero magnetic field. Thus

$$V.H = \frac{v}{c} \rho \frac{d\sigma}{dn}. \quad (2.3)$$

This formula does not in any way involve the assumption that the matter is rarefied, but is true for any density.

It remains to express  $\sigma$  and  $\rho$  in terms of atomic quantities, and to do so we need not go very deep into atomic theory but may make use of the general principles given in Kramer's\* theory of dispersion; there does not seem any reason to restrict these principles to the case of separated atoms. In any substance associated with an absorption line of frequency  $\omega$  there is a vector  $A$  proportional to the electric moment of the "virtual oscillator." Under electric force  $Ee^{i\omega t}$  the system acquires induced electric moment

$$\left\{ \frac{A(E\tilde{A})}{\omega - v} + \frac{\tilde{A}(EA)}{\omega + v} \right\} e^{i\omega t} \quad (2.4)$$

where  $\tilde{A}$  is the complex quantity conjugate to  $A$ . In a magnetic field  $H$  along  $z$  the line will split into components of differing frequencies. The  $\parallel$  components do not concern us here. For the  $\perp$  suppose that  $\omega$  becomes  $\omega + \epsilon$  and  $\omega - \epsilon$ . (It is probable that one line may give several  $\epsilon$ 's, but this may be disregarded, as it is easy to see that the final result will be merely a suitable average of their effects.) Associated with  $\omega + \epsilon$  we shall have a vector  $A_r$ , which gives right-hand circularly polarised light, so that  $A_r^* = -iA_r^z = A_r$ .

\* Kramer and Heisenberg, 'Z. f. Physik,' vol. 31, p. 691 (1925).

Similarly for  $\omega - \epsilon$  we have  $A_1^* = iA_1^* = A_1$ . Adding the effects of the two lines together we have (omitting a factor of proportionality)

$$\sigma = |A_r|^2 \left\{ \frac{1}{\omega + \epsilon - \nu} + \frac{1}{\omega + \epsilon + \nu} \right\} + |A_l|^2 \left\{ \frac{1}{\omega - \epsilon - \nu} + \frac{1}{\omega - \epsilon + \nu} \right\}$$

$$\rho = |A_r|^2 \left\{ \frac{1}{\omega + \epsilon - \nu} - \frac{1}{\omega + \epsilon + \nu} \right\} - |A_l|^2 \left\{ \frac{1}{\omega - \epsilon - \nu} - \frac{1}{\omega - \epsilon + \nu} \right\}. \quad (2.5)$$

We shall only consider values of  $\nu$  far from  $\omega$ , so that these expressions may be expanded writing  $\frac{1}{\omega + \epsilon - \nu} = \frac{1}{\omega - \nu} - \frac{\epsilon}{(\omega - \nu)^2}$ , etc. We must also allow that  $|A_r|^2$  will be perhaps not exactly equal to  $|A_l|^2$ ; say they are respectively  $I \pm \delta I$ . Then

$$\sigma = 2I \frac{2\omega}{\omega^2 - \nu^2} \quad \rho = 2\delta I \frac{2\nu}{\omega^2 - \nu^2} - 2I\epsilon \frac{4\nu\omega}{(\omega^2 - \nu^2)^2}. \quad (2.6)$$

This is to be summed over all the lines characteristic of the substance. If we apply the pure theory of dispersion of Lorentz, we take  $\delta I = 0$  and  $\epsilon$  equal to the Larmor rotation, and so have

$$\rho = -\epsilon \frac{d\sigma}{d\nu}. \quad (2.7)$$

Substituting this in (2.3) we get

$$V \cdot H = -\frac{\nu}{c} \epsilon \frac{dn}{d\nu}, \quad (2.8)$$

which is Becquerel's result.

3. Several formulæ have been proposed for the gyration. Translated into terms of  $\rho$  the chief ones are —

A :  $4\omega\nu/(\omega^2 - \nu^2)^2$  Lorentz, and Drude's "Hall Effect."

B :  $2\nu/(\omega^2 - \nu^2)$  Drude's "Molecular Currents."

C :  $1/(\omega^2 - \nu^2)$  Mascart and Ladenburg.

We see that theory indicates the possibility of both A and B. Drude deduced B from the idea that the motion of the electron carrying his molecular current loads the magnetic force in the light waves, in much the same way that the electric force is loaded by the motion of the electron. It is at least doubtful whether his derivation is correct, for working from the same basis one of the present writers recently obtained an A term instead.\* The discrepancy seems to lie in the fact that Drude's argument gives a Sellmeier formula for the refraction instead of the more correct formula of Lorentz, and the difference, not very

\* Darwin, 'Proc. Camb. Phil. Soc.', vol. 22, p. 817 (1925).

significant for refraction, becomes of capital importance in gyration, as this is essentially a second-order phenomenon. In spite of this doubt as to Drude's derivation, there can be no doubt that B terms are admissible.

There is some experimental evidence for the presence of B terms, but it is not very satisfactory. Among others Wood\* examined the behaviour of gyration on going through one of the absorption lines of a rare earth solution, and obtained the change of sign which a B term implies. There is, however, the theoretical difficulty that, if there is even quite a small A term present as well, it should swamp the effect of B when the incident light is near the band. So if the experimental result is accepted as implying a B term, it at the same time excludes the presence of an A. If, as seems more probable, both are present, the proper place to search for B is at a distance from the band, which is exactly the method pursued here.

When the incident frequency is far from the absorption band of the substance, we may expand in powers of  $\nu$  and have

$$A : \nu + 2 \frac{\nu^3}{\omega^2} + 3 \frac{\nu^5}{\omega^4} \quad B : \nu + \frac{\nu^3}{\omega^2} + \frac{\nu^5}{\omega^4}. \quad (3.1)$$

If the refraction has not been analysed  $\omega$  is unknown, and these only differ in the third term, usually a small quantity. It follows that the only satisfactory discrimination for a B term can be made when the refraction has been analysed so that  $\omega$  is known, and this is the case for comparatively few substances. We shall return to this later.

A term of type C would be indistinguishable from B when  $\nu$  is near  $\omega$ , but at a distance it will make the Verdet constant vary approximately as  $\nu$  instead of  $\nu^3$ . This formula was first suggested on insufficient grounds by Mascart† long ago, but has recently been revived by Ladenburg.‡ Its interest is that it seems to be required to express the gyration of oxygen. Ladenburg pointed out that in a paramagnetic substance more atoms would be pointing one way than the other, and that this would cause an unequal effect on right and left circular light. As a rough attempt he made a rather natural modification of Lorentz's development of the theory. In our notation his formula reads as

$$\frac{I + \delta I}{\omega^2 - (\nu + \epsilon)^2} - \frac{I - \delta I}{\omega^2 - (\nu - \epsilon)^2}, \quad (3.2)$$

\* Wood, R. W., 'Phil. Mag.', vol. 9, p. 725 (1905).

† Mascart, Joubert, 'Leçons sur l'électricité,' I.

‡ Ladenburg, 'Z. f. Physik,' vol. 34, p. 902 (1925).

which gives a C term and an A term. But great doubt must attach to his suggestion, for the denominator of the first term is  $(\omega + \epsilon + \nu)(\omega - \epsilon - \nu)$ , so that one factor belongs to the line  $\omega + \epsilon$  and the other to  $\omega - \epsilon$ . If we make the more natural hypothesis of writing it as  $(\omega + \epsilon)^2 - \nu^2$ , we conform to the general theory above and come back to (2.6). If it were not for the experimental values for oxygen, it would seem that a C term was inadmissible.

The theory of the line spectra of metallic vapours, etc., has reached such perfection that theoretical predictions about their gyration can be accepted with some confidence. Ladenburg's idea of paramagnetic gyration has been developed by Frenkel,\* who obtains the B term instead of the C, but makes an oversight which vitiates some of his final deductions. The matter was recently studied by one of us,† and the following are the main results:—When the temperature is so high that all the stationary states belonging to the *term*-multiplet are present to their full extent, a rather complicated compensation occurs between the  $\delta I$ 's of the separate lines of the multiplet in such a way that the B term is exactly annulled, while the A term corresponds exactly to the Larmor rotation, and this in spite of the anomalous Zeeman effect. In such a case, then, Becquerel's formula would lead to the ordinary value of  $e/m$ . At low temperatures, on the other hand, the *term*-multiplet will be incomplete and the A term will in general have an abnormal value, either too great or too small, and a B term will appear inversely proportional to the temperature.

The model from which these results come is essentially paramagnetic, and is much too specialised to suggest with any confidence what is to be expected in other cases; but we may perhaps anticipate a tendency for B terms to be paramagnetic, that is, inversely proportional to the temperature. We shall indeed see that there is practically no evidence of a B term in any of the diamagnetic substances examined. Unfortunately, most ordinary paramagnetic substances are coloured and so have not been studied here; the one exception is oxygen, and this requires not a B term but a C, and for this there is at present no theory. We shall often use the expression "paramagnetic" for a B term.

The general conclusion is that the chief effect will be an A term, and this has the advantage of lending itself to easy computation. In cases where the refraction has been analysed into terms it is possible to test for a B term, but we shall find no certain evidence of its presence in any substance. The outcome is that a single constant, the coefficient of the A term, suffices to describe the gyration

\* Frenkel 'Z. f. Physik,' vol. 30, p. 215 (1926).

† Darwin, 'Roy. Soc. Proc.,' A, vol. 112, p. 314 (1926).



of each substance. The process of analysis and a few further considerations will be given in the next section.

4. In applying Becquerel's formula we must be prepared for different magnetic effects from the different lines or bands which contribute to the refraction. Thus we may expect to have

$$\sigma = \sum_s \Lambda_s \frac{2\omega_s}{\omega_s^2 - \nu^2} \quad \rho = \frac{eH}{2mc^2} \sum_s \gamma_s \Lambda_s \frac{4\omega_s \nu}{(\omega_s^2 - \nu^2)^2}. \quad (4.1)$$

The quantity  $\gamma_s$  measures the departure of the line  $\omega_s$  from exhibiting the normal Larmor rotation. We call  $\gamma$  the *magnetic anomaly*; it is the chief object of the present work to find it for all possible substances. The anomaly is called unity for the normal case of the Larmor rotation.

If, then, we evaluate for an arbitrary frequency  $\nu$  by Becquerel's equation

$$\gamma(\nu) = V \left/ \frac{c}{2mc^2} \lambda \frac{dn}{d\lambda} \right., \quad (4.2)$$

we shall have

$$\gamma(\nu) = \sum_s \gamma_s W_s(\nu), \quad (4.3)$$

where

$$W_s(\nu) = \Lambda_s \frac{4\omega_s \nu}{(\omega_s^2 - \nu^2)^2} \left/ \sum_r \Lambda_r \frac{4\omega_r \nu}{(\omega_r^2 - \nu^2)^2} \right. \quad (4.4)$$

Thus  $\gamma(\nu)$  is a weighted average of the  $\gamma$ 's of all the lines. The nearer  $\nu$  is to any  $\omega_s$  the greater will be the associated  $W_s$ . The infra-red lines of most substances are due to atomic motions, and so have  $\gamma = 0$ . Consequently  $\gamma$  is usually low in the red and, as the influence of the infra-red bands on the refraction diminishes, rises asymptotically in the blue to a fixed value. We shall see this effect in many substances. In most cases gyration has not been measured very far into the ultra-violet, and a discrimination of the different values of  $\gamma$  for the separate lines has not ever been found possible. Sometimes dispersion formulæ are given with a constant term, say,  $A_\infty \cdot 2\omega_\infty / (\omega_\infty^2 - \nu^2)$ , with  $\omega_\infty$  infinite. When such a term is differentiated the result vanishes, so that these terms do not affect the gyration, and even if allowance is made for the finiteness of  $\omega_\infty$ , the weighting factor  $W_\infty$  will be small. We conclude that what our work really determines is the magnetic anomaly for the main group of lines in the nearest part of the ultra-violet.

The test for a B term can be applied if the  $\omega$ 's are known. Suppose that only one line is operative. Then instead of (4.1) we have

$$\rho = \frac{eH}{2mc^2} \gamma \left\{ A \frac{4\omega \nu}{(\omega^2 - \nu^2)^2} + B \frac{2\nu}{\omega^2 - \nu^2} \right\}. \quad (4.5)$$

If we calculate  $\gamma$  in the usual way, we shall get a value which is not constant with varying  $\nu$ , but involves a factor  $1 + \frac{B}{A} \frac{\omega^2 - \nu^2}{2\omega}$ , and the second term will measure the influence of the B term. Let  $\lambda_0$ ,  $\lambda$  be the wave-lengths associated with  $\omega$ ,  $\nu$ , then this term is proportional to  $1 - \frac{\lambda_0^2}{\lambda^2}$ . Taking extreme values in the red and the blue, we can see how  $\gamma$  would change if the dispersion were wholly due to a B term, and more generally can estimate what part may be due to it. The sign of the B term depends on that of  $\delta I$  in (2.6), and there is nothing to show whether it should be positive or negative.

The actual computation is very simple. It is required to find  $\lambda \frac{dn}{d\lambda}$   $\frac{dn}{d \log \lambda}$ . This was calculated by use of a three-ordinate interpolation formula connecting  $n$  with  $\log \lambda$ . A single numerical multiplier then converts the Verdet constant from minutes of arc into circular measure, the logarithm from common to natural, and introduces the factor  $e/2mc^2$  (throughout we use  $e/mc = 1.77 \times 10^7$  E.M.U.). To conform with modern practice wave-lengths are in Ångström units, instead of the units  $\mu\mu$ , ten times as large, which have often been used in work on refraction.

5. We begin with a discussion of KCl, which will illustrate several points of detail. The refraction of this substance has been fitted by Goldhammer\* with high accuracy to a formula

$$\sigma = 3 \frac{n^2 - 1}{n^2 + 2} = \frac{A_0}{\omega_0^2 - \nu^2} + \frac{A_1}{\omega_1^2 - \nu^2} + \frac{A_2}{\omega_2^2 - \nu^2} + \frac{A_\infty}{\omega_\infty^2}, \quad (5.1)$$

where  $\omega_0$ ,  $\omega_1$ ,  $\omega_2$  correspond to wave-lengths

$$510000, \quad 1575, \quad 1067,$$

while the wave-length for  $\omega_\infty$  is so short as to give a constant term. In conformity with § 4 we therefore expect that the gyration will fit the equation

$$\rho = \frac{eH}{2mc} \left\{ \gamma_1 A_1 \frac{4\omega_1 \nu}{(\omega_1^2 - \nu^2)^2} + \gamma_2 A_2 \frac{4\omega_2 \nu}{(\omega_2^2 - \nu^2)^2} \right\}, \quad (5.2)$$

with the other two terms omitted. The Verdet constant has been measured in the visible and far into the infra-red, but unfortunately not in the ultra-violet. Table I shows the results. In the third column  $V_{\text{calc.}}$  (I) is worked

\* Goldhammer, 'Dispersion u. Absorption des Lichtes,' p. 63. With  $\lambda$  in units of  $10^{-4}$  cm., he gives

$$\frac{1}{2} \sigma = 0.51416 + \frac{0.001924}{\lambda^2 - (0.10667)^2} + \frac{0.0006979}{\lambda^2 - (0.1575)^2} + \frac{605.59}{\lambda^2 - (51.009)^2}$$

out from (5.2), taking  $\gamma_1 = \gamma_2 = 1$ . The fifth column is the ratio  $V_{\text{obs.}} : V_{\text{calc.}}$  (I). It will be seen that it is remarkably constant over this very wide range. In the fourth column Becquerel's formula is applied (using the ordinary value of  $e/m$ ) without analysis of the dispersion, and in the sixth column the corresponding  $\gamma$  is  $V_{\text{obs.}} : V_{\text{calc.}}$  (II). This is the weighted mean of (4.3), and it will be seen how the influence of the infra-red line gradually disappears with shortening wave-length, so that  $\gamma$  rises asymptotically to a value identical with the constant value of the fifth column. This illustrates the process to be carried out for other substances where the dispersion has not been analysed, and it is clear that the asymptotic value of column 6 determines  $\gamma$  just as well as the constant value of column 5.

Table I.—KCl.

$\lambda_1$	$V_{\text{obs.}}$	$V_{\text{calc.}}$ (I).	$V_{\text{calc.}}$ (II)	$100\gamma$ (I).	$100\gamma$ (II)
20000	0.207	0.261	0.415	78.5	50.0
15000	0.377	0.473	0.584	79.7	64.5
10000	0.864	1.084	1.154	79.6	74.8
9000	1.051	1.349	1.40	78.1	75.1
6708	2.012	2.515	2.53	80.0	79.4
5893	2.67	3.336	3.41	79.5	78.3
5461	3.16	3.952	3.96	80.0	79.5
4807	4.60	5.845	5.90	78.9	78.1
4358	5.34	6.669	6.73	80.0	79.3
Average anomaly				79.4	78.9

It is a great pity that there are no measures of the gyration in the ultra-violet, for without them it is not possible to make any discrimination between  $\gamma_1$  and  $\gamma_2$ . The equation  $0.29\gamma_1 + 0.71\gamma_2 = 0.79$  holds with high precision, so that if both lines have the same anomaly, it is 0.79; but the weighting factors alter so slightly over the whole range of observation that little more can be said. Either  $\gamma$  could easily be as large as unity, by a suitable adjustment of the other.

We must also examine how far it would be possible for a paramagnetic term to be present. The evidence is quite strongly against it, though the absence of ultra-violet measures makes it not quite conclusive.  $1 - \frac{\lambda_1^2}{\lambda^2}$  takes the following values

$\lambda$	4358	6708	20000
$1 - \lambda_1^2/\lambda^2$	0.87	0.95	1.00

There is no sign of a progressive change in  $\gamma$  in column 5, and as the numbers there remain constant to about 1 per cent., we conclude that if there were a paramagnetic term present, it must at any rate be less than 10 per cent. of the other term. The evidence for its absence will be much stronger for those substances for which the gyration has been measured in the ultra-violet.

6. Of all work on the dispersion of gyration, the most precise is that of Sierstema\* on titanium chloride. In an exhaustive investigation he has completely accounted for the dispersion of refraction and gyration of this substance by assuming one line in the infra-red and two in the ultra-violet, one of the latter being far removed from the visible. The measurements only suffice to fix the anomaly of the nearest line, and the mean of two series of measures is

$$\text{TiCl}_4 \quad 100\gamma = -25.9$$

Most of the titanium salts are paramagnetic, and we may presume the chloride to be so also, though it does not appear to have been measured. It is therefore interesting to find that a very good fit could be made without introducing any paramagnetic term in the gyration. This is the only substance for which  $\gamma$  is negative.

In Table II are given the results of the analysis described in § 4 applied to a number of common substances that have measurements extending over very

Table II.

H <sub>2</sub> O.		NaCl.		CaF <sub>2</sub> .		SiO <sub>2</sub> *		C <sub>2</sub> H <sub>5</sub> OH.	
$\lambda$ .	100 $\gamma$	$\lambda$ .	100 $\gamma$	$\lambda$ .	100 $\gamma$ .	$\lambda$ .	100 $\gamma$ .	$\lambda$ .	100 $\gamma$ .
10000	26.4	9000	78.4	10000	41.4				
9000	33.6								
8000	47.5								
7010	59.6								
6580	63.5	6710	83.0	6710	58.2	6440	65.9		
5890	68.0	5890	84.8	5890	63.5	5890	66.7		
		5160	86.0	5160	63.8				
5180	74.2					5090	69.9		
		4920	83.4	4920	66.1	4800	73.4		
4370	77.4	4370	81.6	4370	66.1	4680	74.2	4530	62.6
4050	77.0	4050	85.1					4050	63.1
								3800	65.4
3610	78.3	3550	86.2	3650	65.5	3610	75.0	3610	66.6
2750	78.6	3100	86.5	3130	73.5			3100	66.8
2500	78.7	2600	82.5	2540	72.0	2570	74.0	2500	64.5
						2190	72.4		
	78		85		66		74		65

\* Ordinary wave.

\* L. H. Sierstema, 'Proc. Acad. Amsterdam,' vol. 18, Pt. II, p. 925 (1916).

wide ranges. The table shows  $100\gamma$  as evaluated by (4.2). The low initial value for water is, of course, due to the infra-red bands, which come quite near the visible. Table III shows the values for a few other substances that have only been measured in the visible.

Table III.

	$\text{CS}_2$	$\text{C}_6\text{H}_6$	$\text{C}_2\text{H}_5\text{I}$	$\text{C}_{10}\text{H}_7\text{Br}$	$\text{C}_6\text{H}_5\text{NO}_2$	$\text{C}_2\text{H}_5\text{C}_6\text{H}_5\text{O}_2$ *	$\text{NaClO}_2$ †
6230	40.9	56.2	56.6	53.4	27.6	57.4	31.7
5890	42.5	57.9	58.4	54.1	30.3	57.7	31.8
5530	41.9	57.4	59.2	51.7	29.1	-	-
5400	39.5	55.4	57.8	51.6	26.9	57.7	31.1
5010	39.2	55.5	54.7	50.6	25.1	57.6	31.6
4360	37.3	52.5	55.0	49.8	22.2	57.2	31.1
	40	56	57	52	25	57	31

\* Some of the wave-lengths used in these columns were different but not far from those indicated in the left-hand column

7. We next examine the gases. In the elements there are no infra-red bands and consequently  $\gamma$  should have a constant value. Table IV gives the results for hydrogen and nitrogen, using the experiments of Siertsema\* in the visible. The experimental measures have been reduced to millionths of a minute of arc per gauss centimetre at normal temperature and pressure. The refractive indices are calculated from Cuthbertson's work; they correspond to lines at 851 and 726 respectively for  $\text{H}_2$  and  $\text{N}_2$ .

Table IV.

$\lambda$ .	Hydrogen.		Nitrogen.	
	$V_{\text{obs}}$	$100\gamma$	$V_{\text{obs}}$	$100\gamma$ .
6560	4.71	97.7	4.73	63.0
6190	5.46	100.4	5.27	62.4
5890	6.04	100.2	5.96	63.7
5550	6.83	100.0	6.66	63.0
5270	7.62	100.1	7.47	63.5
5170	7.92	99.9	7.78	63.6
4860	8.95	99.0	8.86	63.6
4540	10.37	99.3	10.06	62.7
4310	11.61	99.2	11.40	63.5
4230	12.10	99.3	11.77	63.1
		99.8		63.2

\* Siertsema, 'Arch. Neerl.', vol. 2, p. 291 (1899).

More recently Sirks\* has measured hydrogen far into the ultra-violet. The results are—

$\lambda$	5780	4860	4040	3130	2650	2530	2400
$100\gamma$	100	100.3	99.0	100.0	102.3	101.3	103.0

There is thus some evidence that  $\gamma$  is rising. This might imply that the line of longest wave-length has  $\gamma$  with value greater than unity and the remoter ones with less. Havelock† has worked out several dispersion formulæ fitting the refractive index of hydrogen, but from their differences it is clear that no more exact conclusion can be drawn in this direction. We may also examine for a paramagnetic term :

$\lambda$	6560	4230	2400
$1 - \lambda_1^2/\lambda^2$	100	97.6	88.9

The inconstancy of  $\gamma$  might thus be attributed to the presence of a small negative paramagnetic term. It must, however, be remembered that at the shorter wave-lengths hydrogen is beginning to be not quite transparent, and this opacity will probably affect the value of  $\gamma$  in a way that cannot be directly calculated. We conclude that at any rate to a fairly close approximation hydrogen obeys the classical law of gyration of Lorentz with the ordinary value of  $e/m$ .

Table V.

$\text{CO}_2$		$\text{N}_2\text{O}$	
$\lambda$	$100\gamma$	$\lambda$	$100\gamma$
5780	56.6	6700	34.3
5440	57.1	6300	34.4
4860	58.2	5900	33.9
4360	58.0	5500	33.0
4050	58.1	5100	31.7
3660	56.7		
3130	57.6		
2800	56.0		
2650	55.9		
2540	56.8		
	56.1		31

\* Sirks, 'Vers. Kon. Acad. Wet. Amsterdam,' vol. 21, p. 685 (1912).

† Havelock, 'Phil. Mag.,' vol. 46, p. 560 (1923).

In the case of nitrogen the test of constancy is not so severe, as there are no ultra-violet measures. The test for a paramagnetic term gives

$$\begin{array}{ccc} \lambda & 6560 & 4230 \\ 1 - \lambda_1^2/\lambda^2 & 100 & 98.3 \end{array}$$

and the table shows no evidence of a progressive change at all.

Of the other gases we reserve oxygen for a separate discussion. Table V gives  $\text{CO}_2$  and  $\text{N}_2\text{O}$ . The latter is only known over a short range of wavelengths, but  $\text{CO}_2$  has been observed far into the ultra-violet. The results show some fluctuation, but practically no progressive change.

8. When the same method of analysis is applied to oxygen, the results are strikingly different, for  $\gamma$  is not in the least constant. There have been two experiments, those of Siertsema\* in the visible, and those of Sirks† extending into the ultra-violet, and the results are shown in Table VI. Their two curves run exactly parallel, though there is a slight difference in absolute value, no doubt due to an error in estimating some of the constants of experiment.

Table VI.—Oxygen Gas.

Siertsema.			Sirks.		
$\lambda$ .	$V_{\text{obs.}}$	$100\gamma$	$\lambda$ .	$V_{\text{obs.}}$	$100\gamma$ .
6660	4.78	54.3	4860	7.00	44.1
6300	5.07	51.3	4360	8.45	42.9
6050	5.37	50.0	3660	11.04	37.8
5780	5.71	48.3	2800	18.92	34.6
5380	6.28	45.7	2650	21.18	34.1
5050	6.84	43.6			
4770	7.46	42.2			
4450	8.28	40.3			
4230	9.09	39.7			

It is easy to attribute the behaviour of oxygen to its paramagnetism, but not at all easy to explain it by that cause, and we have not succeeded in doing so. We can here merely note various explanations that may be excluded.

(1) As the refraction shows no infra-red bands we cannot appeal to these; even if we could, the trend of  $\gamma$  is in the wrong direction. We should, however, note that liquid oxygen shows strong absorption in parts of the visible. Its gyration has been studied by Schmauss,‡ but falls outside the consideration of

\* Siertsema, *loc. cit.*

† Sirks, *loc. cit.*

‡ Schmauss, 'Ann. d. Physik,' vol. 10, p. 853 (1903).

the present paper. However, it can hardly be legitimate to impute the behaviour of oxygen gas to this cause, for the same effect ought to appear in the refraction, and of this there is no trace.

(2) It is possible that oxygen might possess two groups of lines in the ultra-violet, of which one gave negative gyration like  $\text{TiCl}_4$ . The Verdet constant would then be of the form

$$V = \frac{A_1 \lambda^2}{(\lambda^2 - \lambda_1^2)^2} - \frac{A_2 \lambda^2}{(\lambda^2 - \lambda_2^2)^2} \\ - \frac{A_1 - A_2}{\lambda^2} + 2 \cdot \frac{A_1 \lambda_1^2 - A_2 \lambda_2^2}{\lambda^4} + 3 \frac{A_1 \lambda_1^4 - A_2 \lambda_2^4}{\lambda^6} + \dots$$

Now Sirks has expanded the experimental values of  $V$  in a fairly convergent series as ( $\lambda$  in  $\text{cm.}^{-1}$ )

$$V_\lambda/V_{5780} = \frac{4.81 \times 10^{-15}}{\lambda^2} - \frac{6.16 \times 10^{-30}}{\lambda^4} + \frac{5.75 \times 10^{-45}}{\lambda^6} - \frac{1.75 \times 10^{-60}}{\lambda^8},$$

but the alternating signs will not admit of any solution corresponding to the above.

(3) We might reasonably introduce a paramagnetic term and set

$$V = A\lambda^2/(\lambda^2 - \lambda_1^2)^2 + B/(\lambda^2 - \lambda_2^2),$$

but the same alternation of signs excludes this.

There seems no escape from the fact that the experimental curve of  $V$  requires for its expression a lower power than  $v^2$  as its leading term. It can be fitted with the help of a Ladenburg term ( $v$  in  $\text{sec.}^{-1}$ ,  $V$  in radians per cm. gauss)

$$V = 4.621 \times 10^{23} v^2/(v_0^2 - v^2)^2 + 2.048 \times 10^7 \cdot v/(v_0^2 - v^2),$$

but no great value can be attached to the closeness of the fit. As we have no theory for such terms we cannot carry the matter farther.

9. The magnetic gyration of a large number of organic substances has been measured. The most recent work is that of Lowry, who has made a study of the dispersion of gyration of certain of the aliphatic series by observing at two wave-lengths, a yellow and a violet. Table VII shows the results. In a few cases the discrepancy for the two wave-lengths is considerable, and points to the influence of an infra-red band; these are marked i.r., and the value chosen is that for the violet light. It will be seen that practically every substance of this series has an anomaly very near to 60 per cent.



Table VII.

Substance.		100γ.		
		λ = 5480.	λ = 4380.	Mean.
Hexane	$C_6H_{14}$	63.0	62.4	63
Octane	$C_8H_{18}$	61.2	60.5	61
Methyl alcohol	$CH_3OH$	58.5	60.0	60
Ethyl alcohol	$C_2H_5OH$	60.3	67.6 (Table II)	65
Propyl alcohol	$C_3H_7OH$	59.7	63.4	63
Butyl alcohol	$C_4H_9OH$	61.4	58.6	60
Heptyl alcohol	$C_7H_{15}OH$	59.4	60.6	60
Glycerol	$C_3H_8(OH)_2$	57.4	59.5	59
Ether	$(C_2H_5)_2O$	52.0	63.2	63
Formic acid	$HCO_2H$	48.5	52.2	52
Acetic acid	$CH_3CO_2H$	52.0	55.4	55
Propionic acid	$C_2H_5CO_2H$	54.9	56.0	56
Butyric acid	$C_3H_7CO_2H$	55.6	54.8	55
Iso-butyric acid	$CH(CH_3)_2CO_2H$	53.7	60.8	60
Iso-valeric acid	$CH_3CH_2CH_2CO_2H$	57.9	57.0	57
Methyl acetate	$CH_3CO_2CH_3$	54.4	56.7	56
Methyl propionate	$C_2H_5CO_2CH_3$	57.2	56.0	57
Ethyl formate	$H_2CO_2C_2H_5$	57.0	56.5	57
Ethyl acetate	$CH_3CO_2C_2H_5$	56.2	59.9	59
Propyl acetate	$CH_3CO_2C_3H_7$	56.7	59.7	59
Acetone	$(CH_3)_2CO$	55.0	57.9	57
Methyl-ethyl-ketone	$CH_3CO.C_2H_5$	56.4	60.0	60
Methyl-hexyl-ketone	$CH_3CO.C_6H_{13}$	58.5	57.8	58
Diethyl ketone	$(C_2H_5)_2CO$	58.4	55.8	57
Pinacolin	$CH_3CO.C(CH_3)_3$	51.9	60.8	60
Sec. butyl alc.	$C_4H_9OH$	62.9	64.6	64
Sec. amyl alc.	$C_5H_{11}OH$	61.7	63.8	63
Di-propyl carbinol	$C_3H_7OH$	61.2	62.4	62
Methyl-hexyl-carbinol	$C_6H_{13}OH$	60.2	62.7	62

In Table VIII are collected the values of all the remaining substances given in Landolt and Bornstein's tables. They are all measured for sodium light, and so may be too low on account of infra-red bands. In some cases the same substance occurs in Table VII, and the disagreement suggests that no high accuracy can be claimed for Table VIII. There is, however, an indication that aromatic compounds have a somewhat lower anomaly than aliphatic.

At the foot of Table VIII will be seen nickel carbonyl. The value is not very good, as the refraction is not very accurately known; and it is a great pity that the gyration has not been measured for other wave-lengths, as it is quite possible that this paramagnetic substance should show the same curious behaviour as oxygen.

Table VIII.  $(\lambda = 5890)$ .

Substance.		100γ.
*Acetic acid	$\text{CH}_3\text{COOH}$	47.6
Acetoacetic acid	$\text{C}_2\text{H}_5 \cdot \text{C}_6\text{H}_5\text{O}_2$	45.5
Acetophenone	$\text{C}_6\text{H}_5\text{CO} \cdot \text{CH}_3$	37.2
Amyl nitrate	$\text{C}_5\text{H}_{11}\text{NO}_3$	40.9
Aniline	$\text{C}_6\text{H}_5\text{NH}_2$	52.8
Benzaldehyde	$\text{C}_6\text{H}_5\text{CHO}$	41.3
*Butyric acid	$\text{C}_4\text{H}_7\text{CO}_2\text{H}$	51.4
Carbon tetrachloride	$\text{CCl}_4$	51.9
Chlorobenzene	$\text{C}_6\text{H}_5\text{Cl}$	48.5
Cinnamic alcohol	$\text{C}_6\text{H}_5 \cdot \text{C}_3\text{H}_5\text{O}$	12.2
Dichloroacetic acid	$\text{CHCl}_2 \cdot \text{CO}_2\text{H}$	51.7
*Di-ethyl ether	$(\text{C}_2\text{H}_5)_2\text{O}$	55.9
Di-methyl quinol	$\text{C}_6\text{H}_4(\text{OCH}_3)_2$	54.9
Ethyl citraconate	$(\text{C}_2\text{H}_5)_2 \cdot \text{C}_6\text{H}_8\text{O}_4$	42.8
Ethyl hydrocinnamate	$\text{C}_2\text{H}_5 \cdot \text{C}_6\text{H}_5\text{O}_2$	52.6
Ethyl d-tartrate	$\text{C}_2\text{H}_5 \cdot \text{C}_6\text{H}_8\text{O}_6$	50.4
Methyl alcohol	$\text{CH}_3 \cdot \text{OH}$	58.8
Phenol	$\text{C}_6\text{H}_5\text{OH}$	52.7
Pyridine	$\text{C}_5\text{H}_5\text{N}$	53.8
Toluene	$\text{C}_6\text{H}_5\text{CH}_3$	52.5
Nickel tetracarbonyl	$\text{Ni}(\text{CO})_4$	66.2
Nitric acid	$\text{HNO}_3$	21.8
Sulphuric acid	$\text{H}_2\text{SO}_4$	44.7
†Hydrochloric acid	$\text{HCl}$	65.8
†Hydrobromic acid	$\text{HBr}$	40.9

\* See Table VII.

† Extrapolated from solutions of various strengths

Table IX.

Substance.		100γ
Hydrogen	$\text{H}_2$	100
Nitrogen	$\text{N}_2$	63.2
Carbon dioxide	$\text{CO}_2$	56.1
Nitrous oxide	$\text{N}_2\text{O}$	34
Water	$\text{H}_2\text{O}$	78
Carbon bisulphide	$\text{CS}_2$	40
Alcohol	$\text{C}_2\text{H}_5\text{OH}$	65
Titanium chloride	$\text{TiCl}_4$	25.0
Benzene	$\text{C}_6\text{H}_6$	56
Nitrobenzene	$\text{C}_6\text{H}_5\text{NO}_2$	25
Ethyl iodide	$\text{C}_2\text{H}_5\text{I}$	57
α-mono bromonaphthalene	$\text{C}_{10}\text{H}_7\text{Br}$	52
Ethyl valerate	$\text{C}_2\text{H}_5\text{C}_4\text{H}_9\text{O}_2$	57
Sylvine ...	$\text{KCl}$	79
Rocksalt ..	$\text{NaCl}$	85
Fluorite . . . .	$\text{CaF}_2$ . . .	66
Quartz (ord. wave)	$\text{SiO}_2$	74
Sodium chlorate	$\text{NaClO}_3$	31

*Summary.*

The various dispersion formulæ for the magnetic gyration of light are reviewed and tested with all the available experimental data. It is found that the gyration is adequately represented by a single constant typical of each substance. The application of Becquerel's formula (1.1) gives a value of  $e/m$  which is constant for each of those examined, and the ratio of this quantity to the ordinary value of  $e/m$ , called the anomaly and denoted by  $\gamma$ , is found for all substances for which the magnetic gyration has been measured. Oxygen (§ 8) is an exception and does not fit this or any other present theory. Tables VII and VIII give the values for a number of organic substances. The remainder, which have had a fuller discussion earlier, are summarised in Table IX. Beyond the fact that no anomaly has been found greater than unity, and that most are a good deal less (ranging round 60 per cent.), there does not seem to be any general principle governing them.

---

*Periodic Orbits of the Second Genus near the Straight-Line  
Equilibrium Points in the Problem of Three Bodies.*

By DANIEL BUCHANAN, M.A., Ph.D., F.R.S.C., Professor of Mathematics in  
the University of British Columbia.

(Communicated by J. S. Plaskett, F.R.S.—Received September 3, 1926)

1. *Introduction.*

It has been shown by Poincaré\* that periodic orbits of two genera exist in the restricted problem of three bodies. These are designated as the orbits of the First Genus and of the Second Genus. So far as the writer is aware all the periodic orbits which have been constructed up to the present time with one exception,† belong to the first genus. It is the purpose of this paper to construct orbits of the second genus.

The particular problem with which we are concerned pertains to the motion of an infinitesimal body in the vicinity of the Lagrangian straight-line equilibrium points. Various memoirs deal with the first genus orbits in the neighbour-

\* Poincaré, 'Les Méthodes Nouvelles de la Mécanique Céleste,' vol. 3, chap. 28 (1899).

† Buchanan, "Isoscoles Triangle Orbits of the Second Genus." 'Transactions of the Royal Society of Canada,' vol. 20, p. 275 (1926).

hood of these points, but we are particularly interested in only one of these, viz., the Oscillating Satellite\* as determined by Moulton. The second genus orbits with which the present paper deals are in the vicinity of the orbits of Class A of the "Osc. Sat." Reference must also be made to one of the author's papers on Asymptotic Satellites,† in which are determined the orbits that approach the periodic orbits of Class A asymptotically, as some of the results there obtained are used in the problem now under consideration.

## 2. Definition of Second Genus Orbits.

Before we proceed with the problem at hand, a brief discussion of the second genus orbits will be made.

Suppose we have a set of differential equations

$$\frac{dx_i}{dt} = X_i(x_j, \varepsilon; t), \quad (i, j = 1, \dots, n),$$

in which the  $X_i$  are analytic in the arguments, do not contain  $t$  explicitly, and are periodic with the period  $T$ . The period is, in general, a function of the parameter  $\varepsilon$ . If these equations admit the periodic solutions

$$x_i = \theta_i(\varepsilon, t)$$

having the period  $T$ , then such solutions are said to be of the first genus.

Now let

$$\varepsilon = \varepsilon_0 + \lambda,$$

$$x_i = \theta_i(\varepsilon_0; t) + y_i,$$

where  $\varepsilon_0$  is considered as a fixed constant and  $\lambda$  as a variable parameter. When these substitutions are made in the above differential equations we obtain a set in  $y_i$  in which there are no terms independent of  $y_i$  or  $\lambda$ . If this set admits the periodic solutions

$$y_i = \psi_i(\varepsilon_0, \lambda; t)$$

having the period

$$NT \text{ (1 + a power series in } \lambda),$$

$N$  being an integer, then the solutions

$$x_i = \theta_i(\varepsilon_0; t) + \psi_i(\varepsilon_0, \lambda; t)$$

\* Moulton, 'Periodic Orbits,' chap. 5. As we shall have frequent occasion to refer to this memoir it will be cited "Osc. Sat."

† Buchanan, "Asymptotic Satellites near the Straight-line Equilibrium Points in the Problem of Three Bodies," 'Amer. Journal of Math.,' vol. 41, No. 2, pp. 79-110 (1919). Frequent reference will be made to this paper and it will be cited "Asym. Sat."

are said to be of the second genus. Since the  $\psi_i$  vanish with  $\lambda$ , the second genus orbits approach those of the first as  $\lambda$  approaches zero.

### THE ORBITS OF THE FIRST GENUS.

#### 3. *The Differential Equations*

Consider the motion of an infinitesimal body which is subject to the Newtonian attraction of two finite spheres which move in circles about their centre of gravity. Let the system be referred to a set of rotating rectangular co-ordinates  $\xi\eta\zeta$  with the origin at the centre of gravity of the spheres, with the line joining their centres as the  $\xi$ -axis, and with the plane of their motion as the  $\xi\eta$ -plane. Let the  $\xi\eta$ -axes rotate about the  $\zeta$ -axis in the direction in which the spheres move and with their uniform angular velocity. The units of length, mass and time will be so chosen that the distance between the centres of the spheres, the sum of their masses, and the constant of proportionality shall each be unity. With these units thus chosen, the angular velocity will likewise be unity. The masses of the spheres will be denoted by  $1 - \mu$  and  $\mu$  where  $0 < \mu \leq 0.5$ , and it will be supposed that the mass  $\mu$  is on the positive side of the  $\eta$ -axis. Finally, if the co-ordinates of the infinitesimal body be denoted by  $\xi, \eta, \zeta$  then the differential equations defining its motion are

$$\left. \begin{aligned} \frac{d^2\xi}{dt^2} - 2\frac{d\eta}{dt} &= \frac{\partial U}{\partial \xi}, \\ \frac{d^2\eta}{dt^2} + 2\frac{d\xi}{dt} &= \frac{\partial U}{\partial \eta}, \\ \frac{d^2\zeta}{dt^2} &= \frac{\partial U}{\partial \zeta}; \\ 2U &= \xi^2 + \eta^2 + \frac{2(1-\mu)}{r_1} + \frac{2\mu}{r_2}, \\ &= (1-\mu)\left(r_1^2 + \frac{2}{r_1}\right) + \mu\left(r_2^2 + \frac{2}{r_2}\right) - \zeta^2 - \mu(1-\mu), \\ r_1 &= [(\xi + \mu)^2 + \eta^2 + \zeta^2]^{\frac{1}{2}}, \quad r_2 = [(\xi - 1 + \mu)^2 + \eta^2 + \zeta^2]^{\frac{1}{2}}. \end{aligned} \right\} \quad (1)$$

These equations admit the Jacobi integral

$$\left(\frac{d\xi}{dt}\right)^2 + \left(\frac{d\eta}{dt}\right)^2 + \left(\frac{d\zeta}{dt}\right)^2 = 2U + \text{constant}. \quad (2)$$

#### 4. The Straight-Line Equilibrium Points.

It is shown by Moulton\* and by other writers on the subject of Celestial Mechanics that the equilibrium points are obtained by solving the equations

$$\frac{\partial U}{\partial \xi} = \frac{\partial U}{\partial \eta} = \frac{\partial U}{\partial \zeta} = 0.$$

There are two sets of points satisfying these equations. One set consists of the two points which lie at the vertices of the equilateral triangles described in the  $\xi\eta$ -plane and on the line joining the centres of the finite masses as a base. The other set, the one with which we are concerned in this paper, consists of three collinear points lying along the  $\xi$ -axis. One point, designated (a), lies between  $\mu$  and  $-\infty$ ; a second point, (b), lies between  $\mu$  and  $1 - \mu$ , while the third point, (c), lies between  $1 - \mu$  and  $-\infty$ . If the co-ordinates of these points be denoted by  $(\xi_0, 0, 0)$ , then the particular values for  $\xi_0$  for the points in question are as follows:

Equilibrium Point (a)

$$\xi_0 = 1 - \mu + \left(\frac{\mu}{3}\right)^{1/3} + \frac{1}{3}\left(\frac{\mu}{3}\right)^{2/3} + \frac{1}{9}\left(\frac{\mu}{3}\right) + \dots$$

Equilibrium Point (b)

$$\xi_0 = 1 - \mu - \left(\frac{\mu}{3}\right)^{1/3} + \frac{1}{3}\left(\frac{\mu}{3}\right)^{2/3} - \frac{1}{9}\left(\frac{\mu}{3}\right) + \dots$$

Equilibrium Point (c)

$$\xi_0 = -1 - \frac{5}{12}\mu + \frac{1127}{12^4}\mu^3 + \dots$$

#### 5. The Periodic Orbits of Class A.

Let equations (1) be transformed by the substitutions

$$\xi = \xi_0 + \epsilon x, \eta = \epsilon y, \zeta = \epsilon z, t - t_0 = (1 + \delta) \tau, \quad (3)$$

where  $\epsilon$  is a parameter denoting the scale factor of the displacement from an equilibrium point;  $x, y, z$  are new dependent variables;  $\tau$  is the new independent variable;  $\delta$  is a power series in  $\epsilon$  so determined that  $x, y, z$  shall be periodic.

If derivation with respect to  $\tau$  is denoted by primes then equations (1), after  $\epsilon$  is divided out, become

$$\left. \begin{aligned} x'' - 2(1 + \delta)y' &= (1 + \delta)^2 [X_1 + X_2\epsilon + \dots + X_n\epsilon^{n-1} + \dots], \\ y'' + 2(1 + \delta)x' &= (1 + \delta)^2 [Y_1 + Y_2\epsilon + \dots + Y_n\epsilon^{n-1} + \dots], \\ z'' &= (1 + \delta)^2 [Z_1 + Z_2\epsilon + \dots + Z_n\epsilon^{n-1} + \dots], \end{aligned} \right\} \quad (4)$$

\* Moulton, 'Celestial Mechanics,' pp. 202-3. Lagrange, 'Collected Works,' vol. 6, pp. 229-324.

where  $X_n, Y_n, Z_n$  are homogeneous polynomials of degree  $n$  in  $x, y, z$ .  $X_n$  is even in both  $y$  and  $z$ ;  $Y_n$  is odd in  $y$  and even in  $z$ ; and  $Z_n$  is even in  $y$  and odd in  $z$ . The explicit values of these polynomials up to the third degree are ("Osc. Sat." § 87)

$$\begin{aligned} X_1 &= (1 + 2A)x, & X_2 &= -\frac{1}{2}B(2x^2 - y^2 - z^2), & X_3 &= 2C(2x^3 - 3xy^2 - 3xz^2), \\ Y_1 &= (1 - A)y, & Y_2 &= 3Bxy, & Y_3 &= -\frac{1}{2}C(4x^2y - y^3 - yz^2) \\ Z_1 &= -Az, & Z_2 &= 3Bxz, & Z_3 &= -\frac{3}{2}C(4x^2z - y^2z - z^3), \end{aligned}$$

$$A = \frac{1 - \mu}{r_1^{(0)^2}} + \frac{\mu}{r_2^{(0)^2}}, \quad r_1^{(0)} = +\sqrt{(\xi_0 + \mu)^2},$$

$$B = \pm \frac{1 - \mu}{r_1^{(0)^2}} \pm \frac{\mu}{r_2^{(0)^2}}, \quad r_2^{(0)} = +\sqrt{(\xi_0 - 1 + \mu)^2},$$

$$C = \frac{1}{r_1^{(0)^2}} + \frac{\mu}{r_2^{(0)^2}}.$$

The upper, middle or lower signs are to be taken in  $B$  according as the libration point is (a), (b) or (c) respectively.

The *Equations of Variation* are obtained by taking only the linear terms in (4). Their solutions are

$$\left. \begin{aligned} x &= K_1 e^{i\sigma\tau} + K_2 e^{-i\sigma\tau} + K_3 e^{p\tau} + K_4 e^{-p\tau}, \\ y &= in(K_1 e^{i\sigma\tau} - K_2 e^{-i\sigma\tau}) + m(K_3 e^{p\tau} - K_4 e^{-p\tau}), \\ z &= K_5 \cos \sqrt{A}\tau + K_6 \sin \sqrt{A}\tau, \\ n &= \frac{\sigma^2 + 1 + 2A}{2\sigma}, \quad m = \frac{\rho^2 - 1 - 2A}{2\rho}, \end{aligned} \right\} \quad (5)$$

where  $K_1, \dots, K_6$  are the constants of integration; and  $\sigma^2$  and  $\rho^2$  are the negative and positive roots, respectively, of the quadratic in  $\alpha^2$ ,

$$\alpha^4 + (2 - A)\alpha^2 + (1 - A)(1 + 2A) = 0.$$

The solutions (5) have three periods, and these give rise to three Classes of orbits, designated as A, B and C. Their periods and dimensions are as follows:

Class A

Period  $2\pi/\sqrt{A}$ , three dimensions,

Class B

Period  $2\pi/\sigma$ , two dimensions,

Class C

Period  $2j\pi/\sqrt{A} = 2k\pi/\sigma$ , three dimensions,

where  $j$  and  $k$  are integers, relatively prime, and  $\sqrt{A}$  and  $\sigma$  are commensurable.

When the higher degree terms are taken in (4) the solutions representing the orbits of Class A as found in the "Osc. Sat." are

$$\left. \begin{aligned} x &= x_1 = (a_1 + b_1 \cos 2\sqrt{A}\tau) \epsilon + (\quad) \epsilon^3 + \dots, \\ y &= y_1 = (c_1 \sin 2\sqrt{A}\tau) \epsilon + (\quad) \epsilon^3 + \dots, \\ z &= z_1 = \frac{1}{\sqrt{A}} \sin \sqrt{A}\tau + d_1 (3 \sin \sqrt{A}\tau - \sin 3\sqrt{A}\tau) \epsilon^2 + \dots \\ \delta &= \delta_2 \epsilon^2 + (\quad) \epsilon^4 + \dots, \end{aligned} \right\} \quad (6)$$

where

$$\begin{aligned} a_1 &= \frac{-3B}{4A(1+2A)}, & b_1 &= \frac{3B(1+3A)}{4A(1-7A+18A^2)}, \\ c_1 &= \frac{-3B}{\sqrt{A}(1-7A+18A^2)}, & d_1 &= \frac{3}{64A^{5/2}} \left[ \frac{3B^2(1+3A)}{1-7A+18A^2} - C \right], \\ \delta_2 &= -\frac{9}{16A^2} \left[ \frac{3B^2(1-3A+14A^2)}{(1+2A)(1-7A+18A^2)} - C \right]. \end{aligned}$$

The functions  $x_1$  and  $y_1$  are odd in  $\epsilon$  while  $z_1$  and  $\delta$  are even in  $\epsilon$ . The coefficients of the various powers of  $\epsilon$  in  $x_1, y_1, z_1$  are as follows :

$x_1$ , sums of cosines of even multiples of  $\sqrt{A}\tau$ ,

$y_1$ , sums of sines of even multiples of  $\sqrt{A}\tau$ ,

$z_1$ , sums of sines of odd multiples of  $\sqrt{A}\tau$ .

The highest multiple of  $\sqrt{A}\tau$  in the coefficient of any power of  $\epsilon$  exceeds that power by unity.

The initial values for these solutions were chosen so that  $z_1(0) = 0, z_1'(0) = 1$ .

## THE ORBITS OF THE SECOND GENUS.

### 7. The Differential Equations.

In order to obtain the orbits of the second genus, we make in (4) the substitutions

$$\left. \begin{aligned} x &= x_1 + p, & y &= y_1 + q, & z &= z_1 + r \\ t - t_0 &= (1 + \delta)(1 + \gamma)\tau, \end{aligned} \right\} \quad (7)$$

and, further, replace  $\epsilon$  by  $\epsilon + \lambda$  where  $\epsilon$  occurs explicitly on the right sides of (4). The substitutions for  $x, y, z$  are the same as those used in the "Asym.



Sat." where solutions for  $p, q, r$  were obtained so that they would approach zero as the time increases or decreases indefinitely. In the present paper  $p, q, r$  are determined as power series in  $\lambda$  having periodic coefficients, but this requires a proper determination of  $\gamma$  likewise as a power series in  $\lambda$ . These solutions for  $p, q, r$  give rise to orbits of the second genus. Their period will be discussed later in § 10.

When the above substitutions are made in (4) we obtain no terms independent of  $p, q, r, \gamma$  and  $\lambda$  since  $x_1, y_1, z_1$  are solutions of (4). The resulting substitutions give

$$\left. \begin{aligned}
 p'' - 2(1 + \delta) q' + (1 + \delta)^2 (P_{11} p + P_{12} q + P_{13} r) \\
 \quad = (1 + \delta)^2 P_1 + 2\gamma (1 + \delta) (y_1' + q') \\
 \quad + (1 + \delta)^2 (2\gamma + \gamma^2) [(1 + 2A) (x_1 + p) - \frac{1}{2}B (\epsilon + \lambda) \\
 \quad \quad \{2(x_1 + p)^2 - (y_1 + q)^2 - (z_1 + r)^2\} + (c + \lambda)^2 \{ \} + \dots] \\
 \quad + \lambda (1 + \delta)^2 [\frac{3}{2}B \{ -2(x_1 + p)^2 + (y_1 + q)^2 + (z_1 + r)^2 \\
 \quad \quad + 4\epsilon C \{ \} + \dots] \\
 \quad + \lambda^2 (1 + \delta)^2 \{2C \{ \} + \dots\} \\
 \quad + \text{higher powers in } \lambda, \\
 q'' + 2(1 + \delta) p' + (1 + \delta)^2 (Q_{11} p + Q_{12} q + Q_{13} r) \\
 \quad = (1 + \delta)^2 Q_1 - 2\gamma (1 + \delta) (x_1' + p') \\
 \quad + (1 + \delta)^2 (2\gamma + \gamma^2) [(1 - A) (y_1 + q) \\
 \quad \quad + 3B (\epsilon + \lambda) (x_1 + p) (y_1 + q) + (c + \lambda)^2 \{ \} + \dots] \\
 \quad + \lambda (1 + \delta)^2 [3B (x_1 + p) (y_1 + q) + 3\epsilon C \{ \} + \dots] \\
 \quad + \lambda^2 (1 + \delta)^2 [\frac{3}{2}C \{ \} + \dots] \\
 \quad + \text{higher powers in } \lambda, \\
 r'' + (1 + \delta)^2 (R_{11} p + R_{12} q + R_{13} r) = (1 + \delta)^2 R_1 \\
 \quad + (1 + \delta)^2 (2\gamma + \gamma^2) [-A (z_1 + r) \\
 \quad \quad + 3B (\epsilon + \lambda) (x_1 + p) (z_1 + r) + \dots] \\
 \quad + \lambda (1 + \delta)^2 [3B (x_1 + p) (z_1 + r) + 3\epsilon C \{ \} + \dots] \\
 \quad + \lambda^2 (1 + \delta)^2 [\frac{3}{2}C \{ \} + \dots] \\
 \quad + \text{higher powers in } \lambda;
 \end{aligned} \right\} \quad (8)$$

where  $P_{1j}, Q_{1j}, R_{1j}, P_j, Q_j, R_j$  ( $j = 1, 2, 3$ ) are the same as in the "Asym. Sat.," viz.,

$$\begin{aligned}
 P_{11} &= -1 - 2A + 6B\varepsilon x_1 - 6C\varepsilon^2(2x_1^2 - y_1^2 - z_1^2) + \dots \\
 P_{12} = Q_{11} &= 3B\varepsilon y_1 + 12C\varepsilon^2 x_1 y_1 + \dots \\
 P_{13} = R_{11} &= 3B\varepsilon z_1 + 12C\varepsilon^2 x_1 z_1 + \dots \\
 Q_{12} &= -1 + A - 3B\varepsilon x_1 + \frac{1}{2}C\varepsilon^2(4x_1^2 - 3y_1^2 - z_1^2) + \dots \\
 Q_{13} = R_{12} &= 3C\varepsilon^2 y_1 z_1 + \dots \\
 R_{13} = A - 3B\varepsilon x_1 + \frac{1}{2}C\varepsilon^2(4x_1^2 - y_1^2 - 3z_1^2) + \dots \\
 P_1 &= -\frac{1}{2}B\varepsilon(2p^2 - q^2 - r^2) + \varepsilon^2(\dots) + \dots \\
 Q_1 &= 3B\varepsilon pq + \dots \\
 R_1 &= 3B\varepsilon pr + \dots
 \end{aligned}$$

### 8. The Equations of Variation and their Solutions.

If we neglect the right members of equations (8) we obtain the Equations of Variation. These are the same equations of variation as those occurring in the "Asym. Sat.," equations (11). Their solutions are

$$\left. \begin{aligned}
 p &= K_1 e^{\sigma_1 \tau} u_1 + K_2 e^{-\sigma_1 \tau} u_2 + K_3 e^{\rho_1 \tau} u_3 + K_4 e^{-\rho_1 \tau} u_4 + K_5 u_5 \\
 &\quad + K_6 (u_6 + K_7 u_5), \\
 q &= i(K_1 e^{\sigma_1 \tau} v_1 - K_2 e^{-\sigma_1 \tau} v_2) + K_3 e^{\rho_1 \tau} v_3 - K_4 e^{-\rho_1 \tau} v_4 + K_5 v_5 \\
 &\quad + K_6 (v_6 + K_7 v_5), \\
 r &= i(K_1 e^{\sigma_1 \tau} w_1 - K_2 e^{-\sigma_1 \tau} w_2) + K_3 e^{\rho_1 \tau} w_3 - K_4 e^{-\rho_1 \tau} w_4 + K_5 w_5 \\
 &\quad + K_6 (w_6 + K_7 w_5),
 \end{aligned} \right\} \quad (9)$$

where  $K_1, \dots, K_6$  are the constants of integration;  $\sigma_1, \rho_1$  and  $K$  are power series in  $\varepsilon$  having constant coefficients;  $u_j, v_j, w_j$  ( $j = 1, \dots, 6$ ) are periodic functions which will be more fully characterised in the next section where a more convenient notation is introduced to handle these and similar series. So far as the computation was carried out in the "Asym. Sat.," we have

$$\begin{aligned}
 u_1 &= 1 + \varepsilon^2(\dots) + \dots, \\
 v_1 &= n + \varepsilon^2(\dots) + \dots, \\
 w_1 &= \frac{3B\varepsilon}{4A - \sigma^2} \left[ \frac{2}{\sigma} \cos \sqrt{A}\tau - \frac{i}{\sqrt{A}} \sin \sqrt{A}\tau \right] + \varepsilon^3(\dots) + \dots, \\
 u_3 &= 1 + \varepsilon^2(\dots) + \dots, \\
 v_3 &= m + \varepsilon^2(\dots) + \dots, \\
 w_3 &= -\frac{3B\varepsilon}{4A + \rho^2} \left[ \frac{2}{\rho} \cos \sqrt{A}\tau - \frac{1}{\sqrt{A}} \sin \sqrt{A}\tau \right] + \varepsilon^3(\dots) + \dots,
 \end{aligned}$$

$$u_3 = \epsilon (-2 b_1 \sin 2 \sqrt{A} \tau) + \epsilon^3 ( ) + \dots,$$

$$v_3 = \epsilon (2 c_1 \cos 2 \sqrt{A} \tau) + \epsilon^3 ( ) + \dots,$$

$$w_3 = \frac{1}{\sqrt{A}} \cos \sqrt{A} \tau + \epsilon^2 ( ) + \dots,$$

$$u_6 = 2\epsilon (a_1 + b_1 \cos 2 \sqrt{A} \tau) + \epsilon^3 ( ) + \dots,$$

$$v_6 = 2\epsilon (c_1 \sin 2 \sqrt{A} \tau) + \epsilon^3 ( ) + \dots,$$

$$w_6 = \frac{1}{\sqrt{A}} \sin \sqrt{A} \tau + \epsilon^2 ( ) + \dots,$$

$$\sigma_1 = \sigma + \epsilon^2 \left[ \frac{9B^2 \{ \sigma^2 (1 - 13A) - (3 + 7A - 22A^2) \}}{16A \sigma^3 (4A - \sigma^2)} - \delta_2 \frac{(1 - A)(1 + 2A)}{\sigma^3} \right] + \dots,$$

$$\rho_1 = \rho + \epsilon^2 ( ) + \dots,$$

$$K = - \frac{1}{1 + \delta} [2 \delta_2 \epsilon^2 + \epsilon^4 ( ) + \dots].$$

The expressions for  $a_1$ ,  $b_1$ ,  $c_1$ ,  $\delta_2$  are found under (6) ; for  $m$ ,  $n$ ,  $\sigma$ ,  $\rho$  in (5).

### 9. Notation.

As many power series in  $\epsilon$  arise having sums of sines or cosines in their coefficients, we shall designate them by the *foundation letters* S and C respectively. Two parentheses, in general, will be found in the superscripts. In the first parenthesis will be found the integers 0, 1, 2, ... followed by the letter *e* or *o*. The integer designates, in the first case, the lowest power of  $\epsilon$  in the series, and in the second case the parity in  $\epsilon$ , zero being interpreted as even. The letter *e* or *o* denotes that the arguments of the sines or cosines are even or odd multiples of  $\sqrt{A} \tau$  respectively. The integer which appears in the second parenthesis of the superscript denotes the amount by which the highest multiple of  $\sqrt{A} \tau$  in the arguments of the trigonometric terms occurring in the coefficient of any power of  $\epsilon$  exceeds that power. For example : -

$$\begin{aligned} C^{(1,0)} &\equiv (b_0^{(1)} + b_2^{(1)} \cos 2 \sqrt{A} \tau) \epsilon \\ &\quad + (b_0^{(3)} + b_2^{(3)} \cos 2 \sqrt{A} \tau + b_4^{(3)} \cos 4 \sqrt{A} \tau) \epsilon^3 \\ &\quad + \dots + \{b_0^{(2j+1)} + b_2^{(2j+1)} \cos 2 \sqrt{A} \tau \\ &\quad + \dots + b_{2j+2}^{(2j+1)} \cos (2j+2) \sqrt{A} \tau\} \epsilon^{2j+1} + \dots, \\ S^{(1)} &\equiv (b_1^{(1)} \sin \sqrt{A} \tau + b_3^{(1)} \sin 3 \sqrt{A} \tau) \epsilon + \dots \\ &\quad + \{b_1^{(2j+1)} \sin \sqrt{A} \tau + \dots + b_{2j+3}^{(2j+1)} \sin (2j+3) \sqrt{A} \tau\} \epsilon^{2j+1} + \dots, \end{aligned}$$

where the literal coefficients designate real constants.

The absence of the second parenthesis in a superscript denotes that the power of  $\epsilon$  exceeds the highest multiple of  $\sqrt{A}\tau$  which occurs in the coefficient of that power of  $\epsilon$ , but with the amount of that excess we are not concerned.

Symbols without subscripts represent a type only, while those having subscripts designate a particular series of that type. Thus two symbols having the same foundation letter represent only the same type of series if the superscripts are the same, but designate the same particular series if, in addition to the same foundation letter and superscripts, they have the same subscripts.

Many power series in  $\epsilon^2$  occur having absolute terms and constant coefficients. These will be designated by the foundation letter  $d$  with various subscripts and superscripts.

Some series have the property that the numerical coefficients of the sines or cosines of the highest multiples of  $\sqrt{A}\tau$  in the coefficients of the various powers of  $\epsilon$  in the one series are the same as, or differ only in sign from, the coefficients of the cosines or sines, respectively, of the highest multiples of  $\sqrt{A}\tau$  in the coefficients of the same powers of  $\epsilon$  in the other series. This property will be designated as the *highest-multiple-power* followed by the word *identical* or *different* according as the coefficients are the same or different, respectively.

The functions occurring in (9) when expressed in terms of the above notation are listed in Table I together with certain of their properties. The first genus solutions (6) are likewise similarly expressed.

Table I. --The Functions  $u_j, v_j, w_j$ , ( $j = 1, \dots, 6$ ) and their Properties.

Functions.	Type of Series.	Properties.
$u_1, u_2$	$C^{(0, \epsilon)}(0) \pm iS^{(0, \epsilon)}(0)$	Conjugates.
$v_1, v_2$	$C^{(0, \epsilon)}(0) \pm iS^{(0, \epsilon)}(0)$	Conjugates.
$w_1, w_2$	$C^{(1, \epsilon)}(0) \pm iS^{(1, \epsilon)}(0)$	Conjugates.
$u_3, u_4$	$C^{(0, \epsilon)}(0) \pm S^{(0, \epsilon)}(0)$	$u_3(\tau) = u_4(-\tau).$
$v_3, v_4$	$C^{(0, \epsilon)}(0) \pm S^{(0, \epsilon)}(0)$	$v_3(\tau) = v_4(-\tau).$
$w_3, w_4$	$C^{(1, \epsilon)}(0) \pm S^{(1, \epsilon)}(0)$	$w_3(\tau) = w_4(-\tau).$
$u_5$	$S^{(1, \epsilon)}(1)$	} Highest-multiple-power, different.
$v_5$	$C^{(1, \epsilon)}(1)$	
$u_6$	$C^{(1, \epsilon)}(1)$	} Highest-multiple-power, identical.
$v_6$	$S^{(1, \epsilon)}(1)$	
$w_5$	$C^{(0, \epsilon)}(1)$	} Highest-multiple-power, identical.
$w_6$	$S^{(0, \epsilon)}(1)$	
$x_1$	$C^{(1, \epsilon)}(1)$	
$y_1$	$S^{(1, \epsilon)}(1)$	
$z_1$	$S^{(0, \epsilon)}(1)$	

10. *The Period of the Orbits of the Second Genus.*

The period of the first genus orbits of Class A is  $2\pi/\sqrt{A}$  in  $\tau$  or  $T_1 = 2\pi(1+\delta)/\sqrt{A}$  in  $t$ . According to Poincaré's definition, as already stated in §2, the period of the second genus orbits must be

$$T_2 = NT_1 (1 + \text{a power series in } \lambda),$$

where  $N$  is in integer. Let us now ascertain what terms of equations (9) may be used as generating solutions which will have the period  $T_2$ . Obviously they are

$$\left. \begin{aligned} p_1 &= K_1 e^{i\sigma_1 \tau} u_1 + K_2 e^{-i\sigma_1 \tau} u_2 + K_5 u_5, \\ q_1 &= i(K_1 e^{i\sigma_1 \tau} v_1 - K_2 e^{-i\sigma_1 \tau} v_2) + K_5 v_5, \\ r_1 &= i(K_1 e^{i\sigma_1 \tau} w_1 - K_2 e^{-i\sigma_1 \tau} w_2) + K_5 w_5, \end{aligned} \right\} \quad (10)$$

provided  $\sigma_1$  and  $\sqrt{A}$  are commensurable. It has been shown in the "Osc. Sat.," §83, that  $\sigma$  and  $\sqrt{A}$  are commensurable for infinitely many values of  $\mu$  of which they are functions, and for  $\mu$  within the prescribed range  $0 < \mu \leq 5$ . Now

$$\sigma_1 = \sigma + \varepsilon^2 (\text{a power series in } \varepsilon^2),$$

and it may be possible to choose  $\varepsilon$  within the limits demanded by convergence conditions so that  $\sigma_1$  and  $\sqrt{A}$  are commensurable. Let us suppose that  $\varepsilon$  and  $\mu$  can be chosen so that  $\sqrt{A}/\sigma_1 = N/N_1$ , where  $N$  and  $N_1$  are relatively prime integers. Then the period in  $\tau$  of the solutions (10) is  $2\pi N/\sqrt{A} = 2\pi N_1/\sigma_1$ , while in  $t$  it is the prescribed period  $T_2 = NT_1 (1 + \gamma)$ .

If the generating solutions

$$p_1 = K_5 u_5, \quad q_1 = K_5 v_5, \quad r_1 = K_5 w_5$$

are used then the periodic orbits which might be obtained have the period  $2\pi/\sqrt{A}$  and are the analytic continuation of the orbits of the first genus. In order to exclude such orbits we may suppose that  $N$  is not unity.

11. *Construction of the Periodic Orbits of the Second Genus.*

We proceed now to show that equations (8) can be integrated as power series in  $\lambda$  which shall be periodic with the period  $T_2$ . Only the formal construction of these solutions is here considered as their convergence is later discussed in §18.

Let

$$p = \sum_{j=1}^{\infty} p_j \lambda^j, \quad q = \sum_{j=1}^{\infty} q_j \lambda^j, \quad r = \sum_{j=1}^{\infty} r_j \lambda^j, \quad \gamma = \sum_{j=1}^{\infty} \gamma_j \lambda^j, \quad (11)$$

be substituted in (8) and let the resulting equations be cited as (8'). On equating the coefficients of the various powers of  $\lambda$  in (8') we obtain sets of differential equations which define  $p_j, q_j, r_j$ . It will be shown that these equations can be integrated and that  $\gamma_j$  and the constants of integration at the various steps can be so determined that each  $p_j, q_j, r_j$  shall be periodic with the assigned period. One constant of integration remains arbitrary at each step and we may therefore impose one condition upon the solutions (11). Let us suppose that  $p(0)$  may have an arbitrary value. Then it follows that

$$\left. \begin{aligned} p_1(0) &= \text{arbitrary,} \\ p_j(0) &= 0, (j=2, 3, \dots \infty). \end{aligned} \right\} \quad (12)$$

Since  $p_1$  carries the factor  $\lambda$  and since  $\lambda$  remains arbitrary we may merge with  $\lambda$  the arbitrary constant associated with  $p_1$ .

In the construction which follows we confine our attention to the symmetric orbits. The first genus orbits are all symmetric, that is, the infinitesimal body crosses the  $\xi_1$ -plane at the initial time along, and perpendicular to, the  $\xi_1$ -axis. If the second genus orbits are to be symmetric they must satisfy the conditions

$$p'(0) = q(0) = r(0) = 0, \quad (13)$$

or, as a consequence of (11)

$$p_j'(0) = q_j(0) = r_j(0) = 0, \quad (j=1, 2, \dots \infty). \quad (14)$$

## 12. The First Step: Coefficients of $\lambda$ .

On equating the coefficients of  $\lambda$  in (8') we obtain

$$\left. \begin{aligned} p_1'' &+ 2(1+\delta)q_1' + (1+\delta)^2(P_{11}p_1 + P_{12}q_1 + P_{13}r_1) = P^{(1)} \\ q_1'' &+ 2(1+\delta)p_1' + (1+\delta)^2(Q_{11}p_1 + Q_{12}q_1 + Q_{13}r_1) = Q^{(1)} \\ r_1'' &+ (1+\delta)^2(R_{11}p_1 + R_{12}q_1 + R_{13}r_1) = R^{(1)} \end{aligned} \right\} \quad (15)$$

where

$$\begin{aligned} P^{(1)} &= \gamma_1 C^{(1,0)(1)} + C^{(0,0)(2)}, \\ Q^{(1)} &= \gamma_1 S^{(1,0)(1)} + S^{(2,0)(2)}, \\ R^{(1)} &= \gamma_1 S^{(0,0)(1)} + S^{(1,0)(2)}. \end{aligned}$$

The undetermined constant  $\gamma_1$  enters the right members only as indicated. The complementary functions of the above equations are the same as (9), but let the arbitrary constants be denoted by  $k_1^{(1)}, \dots, k_6^{(1)}$ .

In order to obtain the particular integrals we employ the method of the

variation of parameters and consider  $k_1^{(1)} \dots k_6^{(1)}$  not as constants but as functions of  $\tau$ . Proceeding according to this well-known method we obtain

$$\left. \begin{aligned} \Delta k_1^{(1)'} &= -e^{-i\sigma_1\tau} (M_{12} P^{(1)} + M_{14} Q^{(1)} + M_{16} R^{(1)}) \\ \Delta k_2^{(1)'} &= e^{i\sigma_1\tau} (M_{22} P^{(1)} + M_{24} Q^{(1)} + M_{26} R^{(1)}) \\ \Delta k_3^{(1)'} &= -e^{-\rho_1\tau} (M_{32} P^{(1)} + M_{34} Q^{(1)} + M_{36} R^{(1)}) \\ \Delta k_4^{(1)'} &= e^{\rho_1\tau} (M_{42} P^{(1)} + M_{44} Q^{(1)} + M_{46} R^{(1)}) \\ \Delta k_5^{(1)'} &= - (M_{52} P^{(1)} + M_{54} Q^{(1)} + M_{56} R^{(1)}) \\ \Delta k_6^{(1)'} &= (M_{62} P^{(1)} + M_{64} Q^{(1)} + M_{66} R^{(1)}) \end{aligned} \right\} \quad (16)$$

where  $\Delta$  is the determinant

$$\begin{vmatrix} e^{i\sigma_1\tau} u_1, & e^{-i\sigma_1\tau} u_2, & e^{\rho_1\tau} u_3, & e^{-\rho_1\tau} u_4, & u_5, & u_6 + K\tau u_5 \\ e^{i\sigma_1\tau} (i\sigma_1 u_1 + u_1'), & e^{-i\sigma_1\tau} (-i\sigma_1 u_2 + u_2'), & e^{\rho_1\tau} (\rho_1 u_3 + u_3'), & e^{-\rho_1\tau} (-\rho_1 u_4 + u_4'), & u_5', & u_6' + K(\tau u_5' + u_5) \\ e^{i\sigma_1\tau} i v_1, & e^{-i\sigma_1\tau} (-i v_2), & e^{\rho_1\tau} v_3, & e^{-\rho_1\tau} (-v_4), & v_5, & v_6 + K\tau v_5 \\ e^{i\sigma_1\tau} (-\sigma_1 v_1 + i v_1'), & e^{-i\sigma_1\tau} (-\sigma_1 v_2 - i v_2'), & e^{\rho_1\tau} (\rho_1 v_3 + v_3'), & e^{-\rho_1\tau} (-\rho_1 v_4 - v_4'), & v_5', & v_6' + K(\tau v_5' + v_5) \\ e^{i\sigma_1\tau} i w_1, & e^{-i\sigma_1\tau} (-i w_2), & e^{\rho_1\tau} w_3, & e^{-\rho_1\tau} (-w_4), & w_5, & w_6 + K\tau w_5 \\ e^{i\sigma_1\tau} (-\sigma_1 w_1 + i w_1'), & e^{-i\sigma_1\tau} (-\sigma_1 w_2 - i w_2'), & e^{\rho_1\tau} (\rho_1 w_3 + w_3'), & e^{-\rho_1\tau} (-\rho_1 w_4 - w_4'), & w_5', & w_6' + K(\tau w_5' + w_5) \end{vmatrix}$$

This determinant is a constant\* and its value can be determined with the least difficulty by putting  $\tau = 0$ . Thus we obtain

$$\Delta = 4i(m\rho + n\sigma)(m\sigma - n\rho) + \varepsilon^2(\dots) + \dots$$

It is shown in the "Osc. Sat.," equations (36), that  $m\rho + n\sigma$  and  $m\sigma - n\rho$  are different from zero. Hence  $\Delta$  does not vanish for  $\varepsilon = 0$  and therefore remains different from zero provided  $|\varepsilon|$  is sufficiently small. The fact that  $\Delta$  is different from zero shows that the solutions (9) constitute a fundamental set.

The  $M_{jk}$  ( $j = 1, \dots, 6$ ;  $k = 2, 4, 6$ ) are the co-factors of the elements  $jk$  in the determinant  $\Delta$ ,  $j$  referring to the column and  $k$  to the row. The forms of these co-factors in terms of the notation adopted together with their properties are given in the following table.

\* Moulton, 'Periodic Orbits,' § 18.

Table II.—The Co-factors and their Properties.

Co-factors.	Type of series.	Properties.
$M_{12}, M_{22}$	$C(0, e)(0) \pm iS(0, e)(0)$	Conjugates
$M_{14}, M_{24}$	$S(0, e)(0) \pm iC(0, e)(0)$	Conjugates.
$M_{16}, M_{26}$	$S(1, e)(0) \pm iC(1, e)(0)$	Conjugates
$M_{28}, M_{42}$	$i(C(0, e)(0) \pm S(0, e)(0))$	$M_{22}(\tau) \quad M_{42}(-\tau).$
$M_{24}, M_{44}$	$i(C(0, e)(0) \pm S(0, e)(0))$	$M_{21}(\tau) \quad M_{44}(-\tau)$
$M_{26}, M_{46}$	$i(C(1, e)(0) \pm S(1, e)(0))$	$M_{26}(\tau) \quad M_{46}(-\tau).$
$M_{52}$	$i(C(1, e)(1) \pm \tau S_{52}^{(3, e)})$	Highest multiple-power, different
$M_{54}$	$i K S_{52}^{(3, e)}$	
$M_{56}$	$i(S(1, e)(1) + \tau C_{54}^{(3, e)})$	Highest-multiple-power, identical.
$M_{64}$	$i K C_{54}^{(3, e)}$	
$M_{66}$	$i(S(0, e)(1) + \tau C_{56}^{(2, e)})$	Highest-multiple-power, identical.
$M_{68}$	$i K C_{56}^{(2, e)}$	

Equations (16) will now be considered in pairs. Beginning with the first two equations we find when these are expressed in our notation that

$$\Delta k_1^{(1)'} = -e^{-i\sigma_1\tau} \{ \gamma_1 (C(1, e)(1) + iS(1, e)(1)) + C(0, e)(2) + iS(0, e)(2) \},$$

$$\Delta k_2^{(1)'} = e^{i\sigma_1\tau} \{ \gamma_1 C(1, e)(1) - iS(1, e)(1) + C(0, e)(2) - iS(0, e)(2) \}.$$

When  $\sigma_1$  is not an even multiple of  $\sqrt{A}$  the integration of the above equations yields

$$k_1^{(1)} = e^{-i\sigma_1\tau} \{ \gamma_1 (C(1, e)(1) + iS(1, e)(1)) + C(0, e)(2) + iS(0, e)(2) \},$$

$$k_2^{(1)} = e^{i\sigma_1\tau} \{ \gamma_1 C(1, e)(1) - iS(1, e)(1) + C(0, e)(2) - iS(0, e)(2) \},$$

and, on substituting these expressions in the complementary functions, the particular integrals

$$\left. \begin{aligned} p_1 &= \gamma_1 C(1, e)(1) + C(0, e)(2), \\ q_1 &= \gamma_1 S(1, e)(1) + S(0, e)(2), \\ r_1 &= \gamma_1 S(2, e)(1) + S(1, e)(2) \end{aligned} \right\} \quad (17)$$

follow.

If  $\sigma_1$  were an even multiple of  $\sqrt{A}$  then certain non-periodic terms containing  $\tau$  explicitly would arise which it would be impossible to annul with the arbitrary constants at our disposal. But  $\sigma$  was shown in § 83 of the "Osc. Sat." to be different from an even multiple of  $\sqrt{A}$  and since

$$\sigma_1 = \sigma + \epsilon^2 \text{ (a power series in } \epsilon^2),$$



then  $\sigma_1$  will differ only slightly from  $\sigma$  and we may assume that  $\sigma_1$  is not an even multiple of  $\sqrt{A}$ . Otherwise we must exclude such values of  $\varepsilon$  as would make  $\sigma_1$  an even multiple of  $\sqrt{A}$ .

If the second pair of equations of (16) were considered in detail it would be seen that no peculiarities would arise. They yield particular integrals of the same type as (17).

The integration of the last pair of equations in (16) proceeds differently since no exponential factors are present. When expressed in our notation these equations give

$$\begin{aligned} k_5^{(1)} &= -[\gamma_1 d_1^{(1)} + \varepsilon d_2^{(1)} + \gamma_1 C_5^{(1,0,1)(2)} + C_5^{(1,1)(3)} + \tau(\gamma_1 S_5^{(2,1)} + S_5^{(3,1)})], \\ k_6^{(1)} &= \frac{1}{K}(\gamma_1 S_6^{(2,1)} + S_6^{(3,1)}), \end{aligned}$$

where  $C_5^{(1,0,1)(2)}$  and  $\frac{1}{K} S_5^{(2,1)}$  have the highest-multiple-power relation, differing only in sign. The series  $C_5^{(1,1)(3)}$  and  $\frac{1}{K} S_5^{(3,1)}$  have also the same property. The integration of the above terms yields

$$\begin{aligned} k_5^{(1)} &= -(\gamma_1 d_1^{(1)} + \varepsilon d_2^{(1)}) \tau - \gamma_1 S_6^{(0,1)(2)} - S_6^{(1,1)(3)} + \tau(\gamma_1 C_6^{(2,1)} + C_6^{(3,1)}), \\ k_6^{(1)} &= -\frac{1}{K}(\gamma_1 C_6^{(2,1)} + C_6^{(3,1)}), \end{aligned}$$

where  $S_6^{(0,1)(2)}$  and  $\frac{1}{K} C_6^{(2,1)}$ , and also  $S_6^{(1,1)(3)}$  and  $\frac{1}{K} C_6^{(3,1)}$  have the same signs in their highest-multiple-power relation. When these values of  $k_5^{(1)}$  and  $k_6^{(1)}$  are substituted in the complementary functions it will be observed that the terms in  $\tau(\gamma_1 C_6^{(2,1)} + C_6^{(3,1)})$  cancel off. The particular integrals then becomes

$$\begin{aligned} p_1 &= (\gamma_1 d_1^{(1)} + \varepsilon d_2^{(1)}) \tau u_5 + \gamma_1 C_5^{(1,1)(3)} + C_5^{(2,1)(2)}, \\ q_1 &= -(\gamma_1 d_1^{(1)} + \varepsilon d_2^{(1)}) \tau v_5 + \gamma_1 S_5^{(1,1)(3)} + S_5^{(2,1)(2)}, \\ r_1 &= -(\gamma_1 d_1^{(1)} + \varepsilon d_2^{(1)}) \tau w_5 + \gamma_1 S_6^{(0,1)(2)} + S_6^{(1,1)(3)}. \end{aligned}$$

If the highest-multiple-power relation did not exist in the functions as stated above, then the integers in the second parentheses of the superscripts of these particular integrals would be 3 and 4 instead of 1 and 2 respectively as designated.

This completes the work for finding the particular integrals. Combining now the complementary functions with these particular integrals we obtain for the complete solutions at this step

$$\begin{aligned} p_1 &= K_1^{(1)} e^{\sigma_1 \tau} u_1 + K_2^{(1)} e^{-\sigma_1 \tau} u_2 + K_3^{(1)} e^{\rho_1 \tau} u_3 + K_4^{(1)} e^{-\rho_1 \tau} u_4 \\ &\quad + K_5^{(1)} u_5 + K_6^{(1)} (u_6 + K \tau u_5) - (\gamma_1 d_1^{(1)} + \varepsilon d_2^{(1)}) \tau u_4 \\ &\quad + \gamma_1 C_5^{(1,1)(3)} + C_5^{(2,1)(2)}, \end{aligned}$$

$$\begin{aligned} q_1 = & i(K_1^{(1)} e^{i\sigma_1\tau} v_1 - K_2^{(1)} e^{-i\sigma_1\tau} v_2) + K_3^{(1)} e^{i\sigma_1\tau} v_3 - K_4^{(1)} e^{-i\sigma_1\tau} v_4 \\ & + K_5^{(1)} v_5 + K_6^{(1)} (v_6 + K\tau v_7) - (\gamma_1 d_1^{(1)} + \varepsilon d_2^{(1)}) \tau v_5 \\ & + \gamma_1 S^{(1,0)}(1) + C^{(0,0)}(2), \end{aligned}$$

$$\begin{aligned} r_1 = & i(K_1^{(1)} e^{i\sigma_1\tau} w_1 - K_2^{(1)} e^{-i\sigma_1\tau} w_2) + K_3^{(1)} e^{i\sigma_1\tau} w_3 - K_4^{(1)} e^{-i\sigma_1\tau} w_4 \\ & + K_5^{(1)} w_5 + K_6^{(1)} (w_6 + K\tau w_7) - (\gamma_1 d_1^{(1)} + \varepsilon d_2^{(1)}) \tau w_5 \\ & + \gamma_1 S^{(1,0)}(1) - S^{(1,0)}(2), \end{aligned}$$

where  $K_1^{(1)}, \dots, K_6^{(1)}$  are the constants of integration. These solutions can be made periodic with the period  $T_2$  by putting  $K_3^{(1)} = K_4^{(1)} = 0$  and imposing the relation

$$KK_6^{(1)} - d_1^{(1)}\gamma_1 = \varepsilon d_2^{(1)}. \quad (18)$$

When the symmetric conditions  $p_1'(0) = q_1(0) = r_1(0) = 0$  are imposed upon the remaining terms it is found that  $K_1^{(1)} = K_2^{(1)}, K_5^{(1)} = 0$ . Hence the symmetric periodic solutions at the first step are

$$\left. \begin{aligned} p_1 = & K_1^{(1)} (e^{i\sigma_1\tau} u_1 + e^{-i\sigma_1\tau} u_2) + K_6^{(1)} u_6 + \gamma_1 C^{(1,0)}(1) + C^{(0,0)}(2), \\ q_1 = & iK_1^{(1)} (e^{i\sigma_1\tau} v_1 - e^{-i\sigma_1\tau} v_2) + K_6^{(1)} v_6 + \gamma_1 S^{(1,0)}(1) + S^{(0,0)}(2), \\ r_1 = & iK_1^{(1)} (e^{i\sigma_1\tau} w_1 - e^{-i\sigma_1\tau} w_2) + K_6^{(1)} w_6 + \gamma_1 S^{(1,0)}(1) + S^{(0,0)}(2). \end{aligned} \right\} \quad (19)$$

The constant  $K_1^{(1)}$  remains arbitrary, but since  $p_1$  carries the factor  $\lambda$  we may put  $K_1^{(1)} = 1$  without loss of generality. We shall keep  $K_1^{(1)}$  in evidence, however, until the integration at the second step has been completed.

### 13. The Second Step: Coefficients of $\lambda^2$ .

At the second step of the integration another relation between  $K_6^{(1)}$  and  $\gamma_1$ , similar to the one obtained in the last section, will arise from the periodicity conditions, and the solutions of these two equations will uniquely determine these constants. There will also arise at this step a relation between  $\gamma_2$  and  $K_6^{(2)}$ , a constant of integration corresponding to  $K_6^{(1)}$ .

The differential equations at the second step are the same as (15) except that the dependent variables are  $p_2, q_2, r_2$  and the right members are  $P^{(2)}, Q^{(2)}, R^{(2)}$ . The complementary functions are the same as (9), the arbitraries being denoted by  $k_1^{(2)}, \dots, k_6^{(2)}$ .

We shall consider first only those parts of  $P^{(2)}, Q^{(2)}, R^{(2)}$  which enter into the determination of  $K_6^{(1)}$  and  $\gamma_1$ . When these constants have been determined the solutions for  $p_1, q_1, r_1$  at the previous step will be simplified, and consequently so will  $P^{(2)}, Q^{(2)}, R^{(2)}$ . The only terms with which we are now concerned

are those that carry the factor  $e^{i\sigma_1\tau}$  or  $e^{-i\sigma_1\tau}$ . These terms are listed in the following table.

Table III. - Certain Terms in  $P^{(2)}$ ,  $Q^{(2)}$ ,  $R^{(2)}$ .

Right Member.	Coefficients of $e^{i\sigma_1\tau}$ .	Coefficients of $e^{-i\sigma_1\tau}$ .
$P^{(2)}$	${}^e K_1^{(1)} K_0^{(1)} (C^{(1,1)}(1) + iS^{(1,1)}(1))$ $+ K_1^{(1)} \gamma_1 (C^{(0,e)}(0) + iS^{(0,e)}(0))$ $+ K_1^{(1)} (C^{(1,e)}(1) + iS^{(1,e)}(1))$	Conjugate
$Q^{(2)}$	${}^e K_1^{(1)} K_0^{(1)} (C^{(1,e)}(1) + iS^{(1,e)}(1))$ $+ iK_1^{(1)} \gamma_1 (C^{(0,0)}(0) + iS^{(0,0)}(0))$ $+ iK_1^{(1)} (C^{(1,e)}(1) + iS^{(1,e)}(1))$	Conjugate
$R^{(2)}$	${}^e K_1^{(1)} K_0^{(1)} (C^{(0,e)}(1) + iS^{(0,e)}(1))$ $+ iK_1^{(1)} \gamma_1 (C^{(0,0)}(1) + iS^{(0,0)}(1))$ $+ iK_1^{(1)} (C^{(2,e)}(1) + iS^{(2,e)}(1))$	Conjugate

On varying the parameters  $k_1^{(2)}$ , ..  $k_6^{(2)}$  we obtain

$$\left. \begin{aligned} \Delta k_1^{(2)'} &= -e^{-i\sigma_1\tau} (M_{12} P^{(2)} + M_{11} Q^{(2)} + M_{16} R^{(2)}), \\ \Delta k_2^{(2)'} &= e^{i\sigma_1\tau} (M_{22} P^{(2)} + M_{24} Q^{(2)} + M_{26} R^{(2)}), \\ \Delta k_3^{(2)'} &= -e^{-i\sigma_1\tau} (M_{32} P^{(2)} + M_{34} Q^{(2)} + M_{36} R^{(2)}), \\ \Delta k_4^{(2)'} &= e^{i\sigma_1\tau} (M_{42} P^{(2)} + M_{44} Q^{(2)} + M_{46} R^{(2)}), \\ \Delta k_5^{(2)'} &= - (M_{52} P^{(2)} + M_{54} Q^{(2)} + M_{56} R^{(2)}), \\ \Delta k_6^{(2)'} &= (M_{62} P^{(2)} + M_{64} Q^{(2)} + M_{66} R^{(2)}). \end{aligned} \right\} \quad (20)$$

Consider first the equations in  $k_1^{(2)'}$  and  $k_2^{(2)'}$ . When the right members in Table III are substituted in these equations, the exponentials cancel off and constant terms arise from the resulting products of the co-factors and right members. These constant terms are

$$\left. \begin{aligned} i k_1^{(2)'} &= K_1^{(1)} (\epsilon^2 d_1^{(2)} K_0^{(1)} + d_2^{(2)} \gamma_1 + \epsilon d_3^{(2)}), \\ -i k_2^{(2)'} &= K_1^{(1)} (\epsilon^2 d_1^{(2)} K_0^{(1)} + d_2^{(2)} \gamma_1 + \epsilon d_3^{(2)}), \end{aligned} \right\} \quad (21)$$

and their integration will yield terms in  $\tau$  explicitly which, in turn, will render  $p_2$ ,  $q_2$ ,  $r_2$  non-periodic. Hence in order that the solutions at the second step may be periodic we must have

$$K_1^{(1)} (\epsilon^2 d_1^{(2)} K_0^{(1)} + d_2^{(2)} \gamma_1 + \epsilon d_3^{(2)}) = 0. \quad (22)$$

Now  $K_1^{(1)}$  must be different from zero, otherwise the construction now being carried out would give orbits of the first genus. Hence the second factor must

vanish. Combining this equation with the one in  $K_6^{(1)}$  and  $\gamma_1$ , (18), obtained in the previous section, we get

$$\begin{aligned} KK_6^{(1)} - d_1^{(1)} \gamma_1 &= \varepsilon d_2^{(1)}, \\ \varepsilon^2 d_1^{(2)} K_6^{(1)} + d_2^{(2)} \gamma_1 &= -\varepsilon d_3^{(2)}. \end{aligned}$$

A detailed examination\* of the functional determinant of these equations, viz.,

$$K(d_2^{(2)} + \varepsilon^2 d_1^{(1)} d_1^{(2)}), \quad (23)$$

shows that it does not vanish for  $\varepsilon \neq 0$  but sufficiently small numerically. Hence the above equations in  $K_6^{(1)}$  and  $\gamma_1$  may be solved, the solutions being

$$K_6^{(1)} = (1/\varepsilon) d_3^{(1)}, \quad \gamma_1 = \varepsilon d_4^{(1)}. \quad (24)$$

Before proceeding further with the integration of equations (16) we may simplify the solutions for  $p_1$ ,  $q_1$ ,  $r_1$  in (19) and likewise the right members  $P^{(2)}$ ,  $Q^{(2)}$ ,  $R^{(2)}$  by substituting the above values for  $K_6^{(1)}$  and  $\gamma_1$ . We therefore obtain

$$\begin{aligned} p_1 &= K_1^{(1)}(e^{i\sigma_1\tau} u_1 + e^{-i\sigma_1\tau} u_2) + (i^{(0,e)} S^{(2)}), \\ q_1 &= iK_1^{(1)}(e^{i\sigma_1\tau} v_1 - e^{-i\sigma_1\tau} v_2) + S^{(0,e)} S^{(2)}, \\ r_1 &= iK_1^{(1)}(e^{i\sigma_1\tau} w_1 - e^{-i\sigma_1\tau} w_2) + (1/\varepsilon) S^{(0,e)} S^{(1)}. \end{aligned}$$

and when these values have been substituted in  $P^{(2)}$ ,  $Q^{(2)}$ ,  $R^{(2)}$  these right members become

$$\begin{aligned} P^{(2)} &= \varepsilon K_1^{(1)*} [e^{2i\sigma_1\tau} (C^{(0,e)} S^{(0)} + iS^{(0,e)} S^{(0)}) + e^{-2i\sigma_1\tau} (\text{conjugate})] \\ &\quad + \varepsilon K_1^{(1)} [e^{i\sigma_1\tau} (C^{(0,e)} S^{(2)} + iS^{(0,e)} S^{(2)}) + e^{-i\sigma_1\tau} (\text{conjugate})] \\ &\quad + \varepsilon K_1^{(1)*} (C^{(0,e)} S^{(0)} + (1/\varepsilon) (C^{(0,e)} S^{(2)} + \varepsilon \gamma_2 S^{(0,e)} S^{(2)}), \\ Q^{(2)} &= i\varepsilon K_1^{(1)*} [e^{2i\sigma_1\tau} (C^{(0,e)} S^{(0)} + iS^{(0,e)} S^{(0)}) - e^{-2i\sigma_1\tau} (\text{conjugate})] \\ &\quad + i\varepsilon K_1^{(1)} [e^{i\sigma_1\tau} (C^{(0,e)} S^{(2)} + iS^{(0,e)} S^{(2)}) - e^{-i\sigma_1\tau} (\text{conjugate})] \\ &\quad + \varepsilon K_1^{(1)*} S^{(0,e)} S^{(0)} + \varepsilon S^{(0,e)} S^{(4)} + \varepsilon \gamma_2 S^{(0,e)} S^{(2)}, \\ R^{(2)} &= i\varepsilon K_1^{(1)*} [e^{2i\sigma_1\tau} (C^{(1,e)} S^{(0)} + iS^{(1,e)} S^{(0)}) - e^{-2i\sigma_1\tau} (\text{conjugate})] \\ &\quad + i\varepsilon K_1^{(1)} [e^{i\sigma_1\tau} (C^{(0,e)} S^{(1)} + iS^{(0,e)} S^{(1)}) - e^{-i\sigma_1\tau} (\text{conjugate})] \\ &\quad + \varepsilon K_1^{(1)*} S^{(1,e)} S^{(0)} + S^{(0,e)} S^{(3)} + \gamma_2 S^{(0,e)} S^{(1)}. \end{aligned}$$

In the above expressions the word "conjugate" designates the conjugate of the function in the parenthesis immediately preceding.

\* The somewhat complicated algebraic work for the construction of the first two steps of the integration for the second genus orbits was carried out by Mr. Walter H. Gage in his thesis submitted for the degree of M.A. in the Department of Mathematics in the University of British Columbia, April, 1926. The computation for the numerical example in § 19 and the drawing of the graphs were also made by Mr. Gage. The author wishes to herobly express his indebtedness to Mr. Gage for his splendid work in this connection.

Let us now return to equations (16) and consider their integration in pairs. When the necessary substitutions are made the first pair of equations becomes

$$\left. \begin{aligned} ik_1^{(2)'} &= \varepsilon K_1^{(1)'} [e^{i\sigma_1\tau} (C_{21}^{(0,e)(0)} + iS_{21}^{(0,e)(0)}) + e^{-3i\sigma_1\tau} (C_{22}^{(0,e)(0)} + iS_{22}^{(0,e)(0)})] \\ &\quad + \varepsilon K_1^{(1)} [(C_{23}^{(0,e)(2)} + iS_{23}^{(0,e)(2)} + e^{-2i\sigma_1\tau} (C_{24}^{(0,e)(2)} + iS_{24}^{(0,e)(2)})) \\ &\quad + e^{-i\sigma_1\tau} [\varepsilon K_1^{(1)'} (C_{25}^{(0,e)(0)} + iS_{25}^{(0,e)(0)}) + (1/\varepsilon) (C_{26}^{(0,e)(2)} + iS_{26}^{(0,e)(2)}) \\ &\quad \quad \quad + \varepsilon\gamma_2 (C_{27}^{(0,e)(2)} + iS_{27}^{(0,e)(2)})], \\ ik_2^{(2)'} &= \varepsilon K_1^{(1)'} [e^{3i\sigma_1\tau} (C_{22}^{(0,e)(0)} - iS_{22}^{(0,e)(0)}) + e^{-i\sigma_1\tau} (C_{21}^{(0,e)(0)} - iS_{21}^{(0,e)(0)})] \\ &\quad + \varepsilon K_1^{(1)} [(e^{2i\sigma_1\tau} (C_{24}^{(0,e)(2)} - iS_{24}^{(0,e)(2)} + C_{23}^{(0,e)(2)} - iS_{23}^{(0,e)(2)}) \\ &\quad + e^{i\sigma_1\tau} [\varepsilon K_1^{(1)'} (C_{25}^{(0,e)(0)} - iS_{25}^{(0,e)(0)}) + (1/\varepsilon) (C_{26}^{(0,e)(2)} - iS_{26}^{(0,e)(2)}) \\ &\quad \quad \quad + \varepsilon\gamma_2 (C_{27}^{(0,e)(2)} - iS_{27}^{(0,e)(2)})]. \end{aligned} \right\} \quad (25)$$

It will be observed that the coefficients in the first equation are the conjugates of the corresponding coefficients in the second equation. On integrating we find that  $k_1^{(2)}$  and  $k_2^{(2)}$  have the same form as  $ik_1^{(2)'}$  and  $-ik_2^{(2)'}$ , respectively, provided the terms in  $\tau$  already considered in this section are excluded, and with the further proviso, which will be considered in detail later, that  $\sigma_1$  is not an odd multiple of  $\sqrt{A}$ , and  $3\sigma_1$  is not an even multiple of  $\sqrt{A}$ . With these restrictions, the particular integrals obtained by substituting the above values of  $k_1^{(2)}$  and  $k_2^{(2)}$  in the complementary functions are found to be

$$\left. \begin{aligned} p_2 &= \varepsilon K_1^{(1)'} [e^{2i\sigma_1\tau} (C^{(0,e)(0)} + iS^{(0,e)(0)}) + e^{-2i\sigma_1\tau} (\text{conjugate})] \\ &\quad + \varepsilon K_1^{(1)} [e^{i\sigma_1\tau} (C^{(0,e)(2)} + iS^{(0,e)(2)}) + e^{-i\sigma_1\tau} (\text{conjugate})] \\ &\quad + \varepsilon K_1^{(1)'} C^{(0,e)(0)} + (1/\varepsilon) C^{(0,e)(2)} + \varepsilon\gamma_2 C^{(0,e)(2)}, \\ q_2 &= i\varepsilon K_1^{(1)'} [e^{2i\sigma_1\tau} (C^{(0,e)(0)} + iS^{(0,e)(0)}) - e^{-2i\sigma_1\tau} (\text{conjugate})] \\ &\quad + i\varepsilon K_1^{(1)} [e^{i\sigma_1\tau} (C^{(0,e)(2)} + iS^{(0,e)(2)}) - e^{-i\sigma_1\tau} (\text{conjugate})] \\ &\quad + \varepsilon K_1^{(1)'} S^{(0,e)(0)} + (1/\varepsilon) S^{(0,e)(2)} + \varepsilon\gamma_2 S^{(0,e)(2)}, \\ r_2 &= i\varepsilon K_1^{(1)'} [e^{2i\sigma_1\tau} (C^{(1,o)(0)} + iS^{(1,o)(0)}) - e^{-2i\sigma_1\tau} (\text{conjugate})] \\ &\quad + i\varepsilon K_1^{(1)} [e^{i\sigma_1\tau} (C^{(1,o)(2)} + iS^{(1,o)(2)}) - e^{-i\sigma_1\tau} (\text{conjugate})] \\ &\quad + \varepsilon K_1^{(1)'} S^{(1,o)(0)} + (1/\varepsilon) S^{(1,o)(2)} + \varepsilon\gamma_2 S^{(1,o)(2)}. \end{aligned} \right\} \quad (26)$$

A consideration of the third and fourth equations in (16) will give particular integrals similar to the above. No non-periodic terms will occur since the factor  $e^{-\rho_1\tau}$  or  $e^{\rho_1\tau}$  enters,  $\rho_1$  being real.

The last two equations of (16) must be considered in detail as the integrations differ from those for  $k_1^{(2)}$  and  $k_2^{(2)}$ . It will not be necessary to consider the parts of  $P^{(2)}$ ,  $Q^{(2)}$ ,  $R^{(2)}$  carrying the exponentials as factors, since the particular

integrals arising from these terms are similar to the exponential terms of  $p_2$ ,  $q_2$ ,  $r_2$  already obtained. The remaining terms of  $P^{(2)}$ ,  $Q^{(2)}$ ,  $R^{(2)}$  give

$$\left. \begin{aligned} k_5^{(2)'} &= \varepsilon K_1^{(1)'} (U^{(1, e) (1)} + \tau S_{51}^{(3, e)}) \\ &\quad - (1/\varepsilon) ((U^{(1, e) (3)} + \tau S_{52}^{(3, e)}) - \gamma_2 ((U^{(0, e) (2)} + \tau S_{53}^{(2, e)})), \\ k_6^{(2)'} &= \frac{\varepsilon K_1^{(1)'}}{K} S_{51}^{(1, e)} + \frac{1}{\varepsilon K} S_{52}^{(3, e)} + \frac{\gamma_2}{K} S_{53}^{(2, e)}. \end{aligned} \right\} \quad (27)$$

The pairs of functions  $(U^{(1, e) (1)}, \frac{1}{K} S_{51}^{(3, e)})$ ,  $(U^{(1, e) (3)}, \frac{1}{K} S_{52}^{(3, e)})$ , and  $(U^{(0, e) (2)}, \frac{1}{K} S_{53}^{(2, e)})$  have the highest-multiple-power relationship, differing only in sign. As the functions  $(U^{(1, e) (1)}, U^{(1, e) (3)}, U^{(0, e) (2)})$  contain constant terms, the integration of these terms will yield in  $k^{(2)}$  the non-periodic term

$$- (\varepsilon^2 K_1^{(1)'} d_4^{(2)} + d_4^{(2)} + \gamma_2 d_6^{(2)}) \tau. \quad (28)$$

Other terms containing  $\tau$  explicitly will arise from  $k^{(2)}$ , but when the values for  $k_5^{(2)}$  and  $k_6^{(2)}$  are substituted in the complementary functions these terms will cancel off as at the corresponding place of the first step of the integration. The remaining terms for  $k^{(2)}$  and  $k_6^{(2)}$  will yield particular integrals of types already included in (26).

On combining now the particular integrals with the complementary functions, the constants of integration being denoted by  $K_1^{(2)}, \dots, K_6^{(2)}$ , the superscripts denoting the step of the integration, the complete solutions will be found to contain non-periodic terms of two types: first, there are the terms of the complementary functions in  $e^{\sigma_1 \tau}$  or  $e^{-\sigma_1 \tau}$ , but these may be annulled by putting  $K_3^{(2)} = K_4^{(2)} = 0$ ; second, terms in  $\tau u_5$ ,  $\tau v_5$ ,  $\tau w_5$  appear, but they all contain the same factor

$$KK_6^{(2)} - d_6^{(2)} \gamma_2 - d_5^{(2)} - \varepsilon^2 K_1^{(1)'} d_4^{(2)}$$

and may be annulled by imposing the condition upon  $K_6^{(2)}$  and  $\gamma_2$  that this factor shall vanish, i.e.,

$$KK_6^{(2)} - d_6^{(2)} \gamma_2 - d_5^{(2)} - \varepsilon^2 K_1^{(1)'} d_4^{(2)} = 0. \quad (29)$$

The remaining terms of the complete solutions will be periodic and will have the form

$$p_2 = K_1^{(2)} e^{\sigma_1 \tau} u_1 + K_2^{(2)} e^{-\sigma_1 \tau} u_2 + K_5^{(2)} u_6 + K_6^{(2)} u_6 \\ + \text{the particular integral for } p_2 \text{ in (26),}$$

$$q_2 = i (K_1^{(2)} e^{\sigma_1 \tau} v_1 - K_2^{(2)} e^{-\sigma_1 \tau} v_2) + K_5^{(2)} v_5 + K_6^{(2)} v_6 \\ + \text{the particular integral for } q_2 \text{ in (26),}$$

$$r_2 = i (K_1^{(2)} e^{\sigma_1 \tau} w_1 - K_2^{(2)} e^{-\sigma_1 \tau} w_2) + K_5^{(2)} w_5 + K_6^{(2)} w_6 \\ + \text{the particular integral for } r_2 \text{ in (26).}$$

When the symmetric conditions are imposed upon these solutions, we get  $K_1^{(2)} = K_2^{(2)}$ ,  $K_3^{(2)} = 0$  as at the first step. From the initial condition,  $p_2(0) = 0$  (14), we find that  $K_1^{(2)}$  is uniquely determined in terms of  $\epsilon$ ,  $K_1^{(1)}$ ,  $K_0^{(2)}$ ,  $\gamma_2$ . But the last two constants, as will be shown presently, are themselves functions of  $\epsilon$  and  $K_1^{(1)}$ . Hence all the arbitrary constants, except  $K_1^{(1)}$ , are uniquely determined by the periodic, symmetric and initial conditions.

Before giving the general form of the solutions at this step, let us anticipate a result which will be found at the third step, viz., a second relation between  $K_0^{(2)}$  and  $\gamma_2$  similar to (29). The functional determinant of these two equations in  $K_0^{(2)}$  and  $\gamma_2$  is the same as at the first step (23) and therefore their solutions will be

$$K_0^{(2)} = \frac{1}{\epsilon^2} d_7^{(2)}, \quad \gamma_2 = d_8^{(2)}.$$

Thus when the expressions for the various arbitrary constants have been substituted and  $K_1^{(1)}$  put equal to unity, the desired solutions at the second step become

$$\begin{aligned} p_2 &= \sum_{j=1}^2 (e^{j\sigma_1\tau} U_{j1}^{(2)} + e^{j\sigma_1\tau} U_{j2}^{(2)}) + (1/\epsilon) C^{(0, \sigma)}(2), \\ q_2 &= i \sum_{j=1}^2 (e^{j\sigma_1\tau} V_{j1}^{(2)} - e^{-j\sigma_1\tau} V_{j2}^{(2)}) + (1/\epsilon) S^{(0, \sigma)}(2), \\ r_2 &= i \sum_{j=1}^2 (e^{j\sigma_1\tau} W_{j1}^{(2)} - e^{-j\sigma_1\tau} W_{j2}^{(2)}) + (1/\epsilon^2) S^{(0, \sigma)}(1), \end{aligned}$$

where the functions having the foundation letters U, V, W are similar to  $u_1$ ,  $v_1$ ,  $w_1$ , respectively, except that in the former functions the highest multiples of  $\sqrt{A}\tau$  occurring in the coefficients of  $\epsilon^j$  may exceed  $j$ . Further, the functions which differ only in their second subscripts are conjugates.

14. *The Second Step when  $\sigma_1$  is an odd multiple of  $\sqrt{A}$  or when  $3\sigma_1$  is an even multiple of  $\sqrt{A}$ .*

*Case I.*  $\sigma_1 = (2j+1)\sqrt{A}$ ,  $j$  an integer.—In this case constant terms arise in  $k_1^{(2)'} \text{ and } k_2^{(2)'}$  in addition to those already considered in (21). The terms in (25)

$$\begin{aligned} ik_1^{(2)'} &= \epsilon K_1^{(1)} e^{-2i\sigma_1\tau} (C_{24}^{(0, \sigma)}(2) + i S_{24}^{(0, \sigma)}(2)), \\ -ik_2^{(2)'} &= \epsilon K_1^{(1)} e^{2i\sigma_1\tau} (C_{24}^{(0, \sigma)}(2) - i S_{24}^{(0, \sigma)}(2)), \end{aligned}$$

when we put

$$e^{\pm 2i\sigma_1\tau} = \cos 2\sigma_1\tau \pm i \sin 2\sigma_1\tau,$$

yield the constants

$$\begin{aligned} ik_1^{(2)'} &= K_1^{(1)} \epsilon^{4j+1} d_9^{(2)} \\ -ik_2^{(2)'} &= K_1^{(1)} \epsilon^{4j+1} d_{10}^{(2)} \end{aligned}$$

and when these are taken with (21) we obtain, instead of (22), the equation

$$K_1^{(1)} (\varepsilon^2 d_1^{(2)} K_0^{(1)} + d_2^{(2)} \gamma_1 + \varepsilon d_3^{(2)} + \varepsilon^{2j+1} d_0^{(2)}) = 0.$$

This equation is of the same form as (22) and consequently the expressions for  $K_0^{(1)}$  and  $\gamma_1$  will be the same as (24).

No constant terms arise in the solutions of (16) for  $k_3^{(2)'}$  and  $k_4^{(2)'}$  so these equations need not be considered. There are certain new terms, however, arising in  $k_5^{(2)'}$  and with these we shall now deal.

In solving (16) for  $k_5^{(2)'}$  we obtain from the terms in  $P^{(2)}$ ,  $Q^{(2)}$ ,  $R^{(2)}$  carrying the exponentials  $e^{\pm 2i\sigma_1\tau}$  the expression

$$k_5^{(2)'} = -\varepsilon K_1^{(1)*} [C^{(1,0)} + \tau S^{(3,0)}] [e^{2i\sigma_1\tau} (C^{(0,0)} + iS^{(0,0)}) + e^{-2i\sigma_1\tau} (\text{conjugate})],$$

from which arises the constant

$$k_5^{(2)'} = -K_1^{(1)*} \varepsilon^{4j+1} d_{10}^{(2)}.$$

The expression corresponding to (28) then becomes

$$-(\varepsilon^2 K_1^{(1)*} d_4^{(2)} + d_5^{(2)} + d_6^{(2)} \gamma_2 + K_1^{(1)*} \varepsilon^{4j+1} d_{10}^{(2)}) \tau,$$

but this has the same form as (28), and therefore does not change the form of the relation (29) in  $K_0^{(2)}$  and  $\gamma_2$ .

Hence when  $\sigma_1 = (2j+1)\sqrt{A}$ , only slight modifications of the preceding integration are needed, and the periodic solutions for  $p_2$ ,  $q_2$ ,  $r_2$  will not be altered in form.

*Case II.*  $3\sigma_1 = 2j\sqrt{A}$ , where  $j$  is an integer.—If  $j$  is a multiple of 3, then  $\sigma_1$  equals an even multiple of  $\sqrt{A}$  and this case was excluded in § 12.

When  $3\sigma_1$  is an even multiple of  $\sqrt{A}$ , then the parts of equations (25)

$$\begin{aligned} ik_1^{(2)'} &= \varepsilon k_1^{(1)*} e^{3i\sigma_1\tau} (C_{22}^{(0,0)} + iS_{22}^{(0,0)}) \\ -ik_2^{(2)'} &= \varepsilon K_1^{(1)*} e^{3i\sigma_1\tau} (C_{22}^{(0,0)} - iS_{22}^{(0,0)}) \end{aligned}$$

give rise to the constants

$$\begin{aligned} ik_1^{(2)'} &= K_1^{(1)*} \varepsilon^{2j+1} d_{12}^{(2)}, \\ -ik_2^{(2)'} &= K_1^{(1)*} \varepsilon^{2j+1} d_{13}^{(2)}, \end{aligned}$$

which were not previously considered, and therefore the relation corresponding to (22) becomes

$$K_1^{(1)} (\varepsilon^2 d_1^{(2)} K_0^{(1)} + d_2^{(2)} \gamma_1 + \varepsilon d_3^{(2)} + K_1^{(1)} \varepsilon^{2j+1} d_{12}^{(2)}) = 0,$$

but this equation when solved with (18) gives values for  $K_0^{(1)}$  and  $\gamma_1$  of the same form as those previously obtained in (24).

No additional non-periodic terms appear in the solutions for  $k_5^{(2)}$  and  $k_6^{(2)}$  since the exponentials  $e^{\pm i\sigma_1\tau}$  do not occur in the expressions for these parameters.



Hence in the case under consideration the solutions for  $p_2$ ,  $q_2$ ,  $r_2$  can be made periodic, and they will be of the same form as those already obtained.

### 15. *The General Step.*

The restrictions of space prevent a detailed discussion of the induction to the general term, but the integrations have been carried out sufficiently far to enable us to see how the solutions proceed.

At any step  $\nu$  all the constants of integration, except  $K_6^{(\nu)}$ , and all the  $\gamma_1$ , ...,  $\gamma_{\nu-1}$  are determined by the periodic, symmetric and initial conditions. At this step, also, a linear equation in  $K_6^{(\nu)}$  and  $\gamma_\nu$  is obtained by annulling the coefficients of  $\tau u_5$ ,  $\tau v_5$ ,  $\tau w_5$  as at the first and second steps. At the next step of the integration a second relation between  $K_6^{(\nu)}$  and  $\gamma_\nu$  will be obtained when the condition is imposed that  $k_1^{\nu+1}$  and  $k_2^{\nu+1}$  shall be periodic. The functional determinant of these two equations is the same as (23), and their solutions give

$$K_6^{(\nu)} = (1/\epsilon^\nu) d_1^{(\nu)}, \quad \gamma_\nu = (1/\epsilon^{\nu-2}) d_2^{(\nu)}. \quad (30)$$

Then at the general step the desired solutions have the form

$$\left. \begin{aligned} p_\nu &= \sum_{j=1}^{\nu} (e^{j\sigma_1\tau} U_{j1}^{(\nu)} + e^{-j\sigma_1\tau} U_{j2}^{(\nu)} + (1/\epsilon^{\nu-1}) C^{(0,\sigma)}(2), \\ q_\nu &= i \sum_{j=1}^{\nu} (e^{j\sigma_1\tau} V_{j1}^{(\nu)} - e^{-j\sigma_1\tau} V_{j2}^{(\nu)}) + (1/\epsilon^{\nu-1}) S^{(0,\sigma)}(2), \\ r_\nu &= i \sum_{j=1}^{\nu} (e^{j\sigma_1\tau} W_{j1}^{(\nu)} - e^{-j\sigma_1\tau} W_{j2}^{(\nu)}) + (1/\epsilon^\nu) S^{(0,\sigma)}(1), \end{aligned} \right\} \quad (31)$$

where the functions in the foundation letters U, V, W are similar to those at the second step.

When  $\sigma_1$  and  $\sqrt{A}$  are commensurable, but  $\sigma_1 \neq 2j\sqrt{A}$ ,  $j$  an integer, the non-periodic terms which appear are similar to those treated in the preceding section.

### 16. *The Final Form of the Equations for the Second Genus Orbits.*

In terms of the original co-ordinates ( $\xi$ ,  $\eta$ ,  $\zeta$ ) the solutions for the second genus orbits are

$$\begin{aligned} \xi &= \xi_0 + \epsilon \left( x_1 + \sum_{\nu=1}^{\infty} p_\nu \lambda^\nu \right), \\ \eta &= 0 + \epsilon \left( y_1 + \sum_{\nu=1}^{\infty} q_\nu \lambda^\nu \right), \\ \zeta &= 0 + \epsilon \left( z_1 + \sum_{\nu=1}^{\infty} r_\nu \lambda^\nu \right), \end{aligned}$$

where  $(\xi_0, 0, 0)$  are the co-ordinates of the equilibrium points (a), (b), (c), obtained in § 4;  $x_1, y_1, z_1$  are the periodic solutions (6); and  $p, q, r$ , are the expansions (31).

The equation connecting  $t$  and  $\tau$  is

$$t - t_0 = (1 + \delta) \left( 1 + \sum_{\nu=1}^{\infty} \gamma_{\nu} \lambda^{\nu} \right) \tau,$$

where  $\delta$  is defined in (6) and  $\gamma_{\nu}$  in (30).

The period in  $t$  of the first genus is

$$T_1 = (1 + \delta) 2\pi/\sqrt{A},$$

and of the second genus it is

$$T_2 = N T_1 \left( 1 + \sum_{\nu=1}^{\infty} \gamma_{\nu} \lambda^{\nu} \right),$$

where  $\varepsilon$  and  $\mu$  are chosen, if possible, so that  $\sqrt{A}/\sigma_1 = N/N_1$ ,  $N$  and  $N_1$  being relatively prime integers.

### 17. Non-Symmetric Orbits.

The second genus orbits which have been constructed cross the  $\xi\eta$ -plane many times before they re-enter, but only at the beginning (or end) of the period, and, if  $N_1$  is even, at the half period, do they cross symmetrically. The question then arises as to whether all the periodic orbits are symmetric or not.

Let us suppose the symmetric conditions  $p'(0) = q(0) = 0$  are no longer imposed. Since the infinitesimal body must cross the  $\xi\eta$ -plane in order that its motion shall be periodic, we may choose, without loss of generality, the initial time so that  $z(0) = 0$ . Now  $z = z_1 + r$  and since  $z_1(0) = 0$  it follows that  $r(0) = 0$ . Suppose we endeavour now to construct periodic orbits imposing only the condition  $r(0) = 0$ . So far as the earlier steps of the integration are concerned we have found it possible (the details are omitted, however) to construct orbits which do not have the property  $p'(0) = q(0) = 0$ . Such orbits are *apparently* non-symmetric, but, on the other hand, we have no assurance that we have not merely shifted the origin of time from a symmetric to a non-symmetric crossing and in this case these orbits might be *really* symmetric orbits. The question then as to the existence of non-symmetric periodic orbits must be left open.

### 18. The Convergence of the Solutions.

So far only the formal construction of the solutions has been made and we must now consider their convergence. The usual method of establishing the convergence of such solutions is by an existence proof in which Poincaré's

extension\* to Cauchy's theorem is used. But such a proof is long and cumbersome and generally more difficult than the actual construction of the solutions. In 1911, however, MacMillan proved a remarkable theorem† in which he showed that, if the constants of integration in a system of differential equations to which (8) are reducible can be determined so as to make the solutions formally periodic, then such solutions will converge for all finite values of the time provided a parameter corresponding to  $\lambda$  is sufficiently small numerically. By means of this theorem, therefore, we are assured of the convergence of the solutions which have been constructed.

### 19. An Illustrative Orbit.

In the computation carried out by Mr. Gage, to which reference has already been made, the value assigned to  $\mu$  was  $1/11$ . This gives the ratio of the finite masses as  $10:1$ , being that used by Darwin,‡ by Moulton in the "Osc. Sat.," and by the author in the "Asym. Sat." The scale factors  $\epsilon$  and  $\lambda$  are assigned the values  $\epsilon = 0.1$ ,  $\lambda = 0.01$ . For these values of  $\mu$ ,  $\epsilon$ ,  $\lambda$  it is found that  $\sigma_1$  and  $\sqrt{A}$  are very nearly commensurable, the ratio  $\sigma_1/\sqrt{A}$  being approximately  $31/28$ .

The numerical values of certain constants entering into the solutions, together with the equations in which these constants first arise, are listed in Table IV. The values of the constants in the first column are taken from the "Asym. Sat." The computation in this Table as well as that in Tables V and VI are for the equilibrium point (a) only.

Table IV.—Numerical Values of Certain Constants Equilibrium Point (a).

Constant.	Equation in which constant first appears.	Numerical Value.	Constant.	Equation in which constant first appears.	Numerical Value.
A	(4)	2.548	$d_1$	(6)	-0.037
B	(4)	6.548	$d_2$	(6)	0.184
C	(4)	18.283	$\sigma_1$	(9)	1.787
$\sigma^2$	(5)	-2.811	$\rho_1$	(9)	1.830
$\rho^2$	(5)	3.359	$d_1^{(2)}$	(21)	-260.723
$n$	(5)	2.657	$d_2^{(2)}$	(21)	-131.070
$\pi$	(5)	-0.747	$d_3^{(2)}$	(21)	129.467
$a$	(6)	-0.316	$\gamma_1$	(15)	0.849e
$b_1$	(6)	0.151	$K_6^{(1)}$	(18)	0.924/e
$c_1$	(6)	-0.112			

\* Poincaré, *loc. cit.*, vol. 1, § 27.

† MacMillan, 'Trans. Amer. Math. Soc.,' vol. 13, No. 2, pp. 146-158.

‡ Sir George H. Darwin, 'Acta Mathematica,' vol. 21, p. 99 (1897).

Table V contains the values of the first genus periodic solutions  $x_1, y_1, z_1$ , when multiplied by  $\varepsilon$ , for certain assigned values of  $\tau$ . Table VI gives the amount of displacement from the equilibrium point ( $a$ ) in the second genus orbits for the listed values of  $\tau$ . The displacements at the end of this table are those near the close of the period.

Table V. First Genus Solutions. Equilibrium Point ( $a$ ).

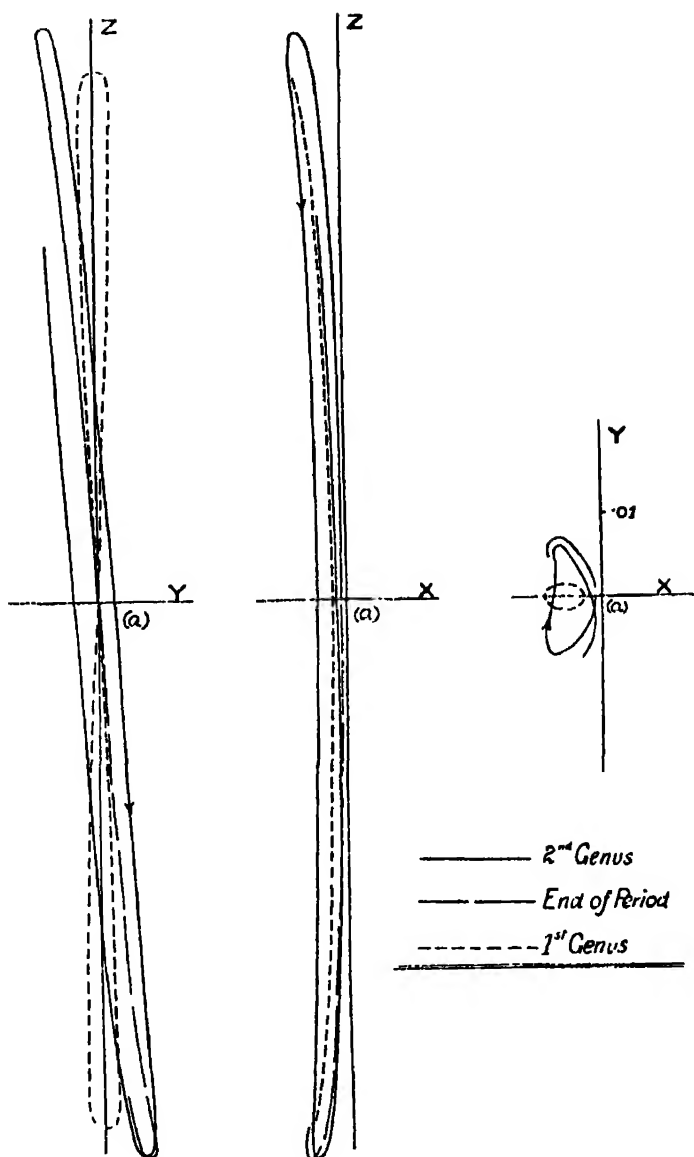
$\tau$	$\varepsilon x_1$	$\varepsilon y_1$	$\varepsilon z_1$	$\tau$	$\varepsilon x_1$	$\varepsilon y_1$	$\varepsilon z_1$
0 0	0 00165	0 00000	0 00000	1 6	0 00258	0 00103	0 0347
0 1	-0 00173	-0 00035	0 00995	1 8	0 00186	0 00057	0 0166
0 2	0 00195	-0 00067	0 01962	2 0	-0 00166	-0 00011	-0 0032
0 3	-0 00229	0 00092	0 02881	2 4	-0 00287	0 00110	0 0398
0 4	0 00272	-0 00107	0 0373	2 8	0 00419	-0 00052	-0 0607
0 5	0 00320	0 00112	0 0448	3 2	0 00122	0 00080	0 0577
0 6	-0 00367	-0 00105	0 0511	3 4	-0 00337	0 00111	0 0473
0 7	-0 00409	0 00088	0 0563	3 6	0 00244	0 00099	0 0320
0 8	-0 00442	0 00062	0 0599	3 8	-0 00179	0 00047	0 0136
0 9	-0 00462	-0 00030	0 0620	4 0	-0 00168	0 00029	0 0063
1 0	0 00467	0 00006	0 0625	4 2	-0 00215	0 00083	0 0255
1 2	-0 00433	0 00071	0 0589	4 4	-0 00302	-0 00112	0 0121
1 4	0 00352	0 00109	0 0493				

Table VI. - Second Genus Orbits. Displacements from Equilibrium Point ( $a$ ).

$$\varepsilon = 0.1, \lambda = 0.01, \sigma_1/\sqrt{A} = 31/28.$$

$\tau$	$\varepsilon(x_1 + p)$	$\varepsilon(y_1 + q)$	$\varepsilon(z_1 + r)$	$\tau$	$\varepsilon(x_1 + p)$	$\varepsilon(y_1 + q)$	$\varepsilon(z_1 + r)$
0 0	-0 00031	0 00000	0 00000	2 8	-0 00393	0 00514	0 0666
0 1	0 00040	-0 00095	0 0109	3 2	-0 00258	0 00318	-0 0632
0 2	-0 00066	-0 00189	0 0214	3 4	-0 00165	0 00152	0 0519
0 3	-0 00106	-0 00275	0 0314	3 6	-0 00090	-0 00034	-0 0353
0 4	0 00158	-0 00352	0 0407	3 8	-0 00060	0 00219	0 0152
0 5	-0 00218	0 00418	0 0488	4 0	-0 00092	-0 00376	0 0065
0 6	-0 00282	-0 00470	0 0558	4 2	0 00184	0 00487	0 0275
0 7	0 00345	-0 00508	0 0613	4 4	-0 00316	-0 00537	0 0457
0 8	-0 00403	-0 00529	0 0653				
0 9	0 00453	-0 00533	0 0676				
1 0	-0 00492	0 00520	0 0682	109 6	0 00304	0 00486	0 0576
1 2	-0 00532	-0 00449	0 0614	109 8	-0 00178	0 00378	-0 0133
1 4	-0 00525	-0 00322	0 0539	110 0	-0 00077	0 00221	-0 0246
1 6	-0 00490	-0 00158	0 0380	110 2	-0 00032	0 00036	-0 0033
1 8	-0 00446	0 00021	0 0181	110 4	-0 00055	-0 00155	0 0182
2 0	0 00417	0 00203	-0 0037				
2 4	-0 00412	0 00466	-0 0439				

The diagram is self-explanatory.



*The Phenomena arising from the Addition of Hydrogen Peroxide  
to the Sol of Silicic Acid.*

By H. A. FELLOWS, B.Sc., A.I.C., and J. B. FIRTH, D.Sc., F.I.C.

(Communicated by F. S. Kipping, F.R.S.—Received December 7, 1926.)

(PLATE 36.)

The formation of gas bubbles in silicic acid gel (or, in fact, any gel) has been described by Hatschek,\* and he expresses the view that "such bubbles, which can be produced by a variety of means, are always lenticular, while gas bubbles in a liquid at rest—however viscous—are, of course, spherical. It is possible to produce such bubbles during the transformation, and to note an *abrupt*† change from the spherical to the lenticular shape, which, as stated, cannot be explained by a mere increase in viscosity."

EXPERIMENTAL.

*Preliminary Experiment.*

Bubbles were caused to form in the gel of silicic acid in the following manner:—

A mixture of equal volumes of sodium silicate solution (1) - 1.15) and hydrochloric acid (3N) was prepared in the usual manner‡ (by using solutions of such concentrations as would cause gelation in 1 to 2 hours). After the mixture had cooled down to room temperature, 2 c.c. of twenty-volume hydrogen peroxide solution were added and the resulting mixture allowed to stand. The experiment was carried out in a small rectangular vessel to facilitate observation.

On the addition of the hydrogen peroxide to the sol mixture, there was no apparent change. The mixture behaved like a normal gel mixture until a few minutes before setting. When the mixture has assumed such a viscosity, as could be readily observed by slightly moving the container, streams of tiny bubbles appeared from many points.

In a few minutes the bubbles ceased to pass upwards and became fixed, the viscosity of the gel having become sufficient to prevent their movement. When

\* 'Koll. Zeit.,' vol. 15, p. 226 (1914); Introduction to 'Physics and Chemistry of Colloids,' p. 78.

† The present authors' italics.

‡ Vide 'J. Phys. Chem.,' vol. 29, p. 241 (1925).

this stage had been reached, the bubbles were quite small, and spherical, but soon began to increase in size. In the course of time the bubbles changed their shape, becoming first slightly elongated, and then truly lenticular. These bubbles, in the course of seven or more days, became so lenticular as to appear flat, and when viewed from the side, appeared only as a line. These disc-like bubbles then became distorted, bending in many planes, but still retaining their minimum thickness; subsequently many of the bubbles merged into one another, causing the gel to become broken up into smaller pieces. During this series of changes, the gel naturally distended, and in some cases was pushed outside the containing vessel.

The phenomena were then examined in detail, and experiments were designed to determine the instant of the decomposition of the hydrogen peroxide, and to trace the formation and development of the bubbles.

*The Determination of the Instant and Subsequent Rate of the Decomposition of the Hydrogen Peroxide, and the Bubble Formation associated therewith.*

1. In order to take advantage of the change in volume of the gel containing the bubbles, an apparatus was used which would respond readily to any change in pressure, and simultaneously record such change of pressure on a revolving drum.

The gel mixture containing the hydrogen peroxide was placed in a narrow glass vessel, to the top of which was attached by a capillary tube a small metal capsule, closed by a tightly stretched membrane of thin rubber.\* The rubber membrane or diaphragm responded very readily to any change of pressure in the apparatus. A carefully balanced aluminium lever was suspended over this diaphragm in such a manner that a fine glass pointer, fixed to the underside of one end of the lever, just rested on the top and in the centre of the diaphragm. The other end of the lever carried a slender glass rod which rested on the surface of an upright cylinder, which was caused to revolve by a suitably geared clock-work motor. Round the cylinder was fixed a glazed paper, blackened over with soot. Thus any change of pressure inside the gel container was recorded automatically on the blackened paper, leaving a white line. The records so obtained were made permanent by dipping them into a special varnish.

It will be observed from the record (fig. 1) that the change in volume inside the container takes place at a particular stage in the gel formation, point X. While the mixture is still in the sol form, there is *no* decomposition of the hydrogen peroxide as shown by the line AX, but it was observed that the rise

\* Cf. Hedges and Myers, 'J. Chem. Soc.,' vol. 125, p. 607 (1924).

in the curve was coincident with formation of the gel. Of course, no particular instant of gelation could be observed, but its formation was signalled by the

FIG. 1.

sudden appearance of the bubbles, and this is recorded on the curve as the first upward movement, which was maintained for several hours, XB.

2. A second method of observing this phenomenon was by determining the rate of evolution of gas in a Hempel gas burette, which was attached to the vessel containing the gel mixture. The liquid in the burette was water, and, to prevent any solution of gases, the water surface was covered with a thin oil film.

The same results were obtained by this method as by the former, the preliminary stationary period during which no decomposition of hydrogen peroxide took place being clearly shown, and the gradual change of volume after the decomposition had started being also evident. These stages also agreed for the same conditions with those observed by the first method.

It was shown incidentally that the gases collected were oxygen and a certain amount of chlorine. The results of a typical experiment are given in Table I., in which 50 c.c. of water-glass solution and 50 c.c. of hydrochloric acid were mixed together, and 2 c.c. of the hydrogen peroxide added. The time at the end of the mixing was recorded, and subsequent readings of the volume of the gas above the gel taken at definite intervals for each experiment.

Table I.

Time in hours	0	1	2	3	4	5	6	7	8
Vol. of gas in cubic centimetres ...	10.15	10.15	10.15	11.2	13.26	15.32	17.27	18.78	19.40

The results show clearly the initial lag and the starting of the decomposition of the hydrogen peroxide, followed by a continuous change. It is obvious from the results of both these experiments that the hydrogen peroxide is not



decomposed until a viscosity is reached in the sol mixture approaching very closely to the formation of a firm gel.

### *The Change in Shape of the Bubbles.*

The change in shape of the bubbles from spherical to lenticular has already been mentioned, and is shown quite clearly in the photographs (Plate 36).

The photographs show the gradual development of the lenticular from the initial spherical bubbles. This development is remarkably symmetrical; further, the mode of development is general throughout the gel, and it would appear to be a characteristic feature. This change in the shape of the bubbles is indicative of a two-phase system, and the symmetrical development seems to indicate a perfectly definite orientation of the gel itself.

The salient point of this observation is that the bubbles are not suddenly changed to the lenticular form, but pass quite gradually from the spherical to the lenticular.

There are two possible explanations of the sudden appearance of the bubbles.

1. After mixing the solutions of water-glass and acid, the water present begins to be definitely associated with the molecules of silica, as indicated by the rise in the viscosity of the mixture. The viscosity continues to rise gradually to a point at which the gel sets. At this stage the internal structure becomes more rigid, in the manner previously outlined. Definite surfaces are formed within the gel which are capable of functioning catalytically, and so, when the setting point is reached, decomposition of the hydrogen peroxide takes place.

Although this simple explanation may appear possible from the point of view of simple surface action, it does not adequately account for all the phenomena, and therefore the following view is considered more probable :—

2. The liability for the silica particles to attract and unite with the water does not preclude the same primary attraction causing the silica particles to unite with the hydrogen peroxide. The union with hydrogen peroxide will thus cause the formation of a compound other than a hydrated silica.

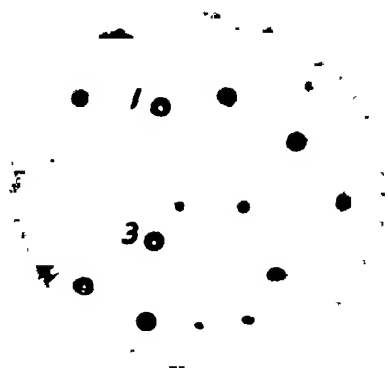
Komarovsky\* prepared a compound by the action of 30 per cent. hydrogen peroxide on silicic acid gel, which, from its analysis and chemical reactions, was shown to be a persilicic acid, or perhydrogel, and having a formula  $\text{H}_2\text{SiO}_3 \cdot \text{H}_2\text{O}_2 \cdot \frac{1}{2}\text{H}_2\text{O}$ . He states that this compound, which could be obtained in a hard powdery condition, gave a constant supply of oxygen and ozone when allowed to stand in air.

It is therefore possible for silica and hydrogen peroxide to unite together to

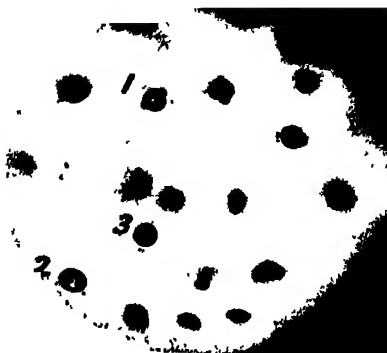
\* 'Chem. Z.,' vol. 38, p. 121 (1914).



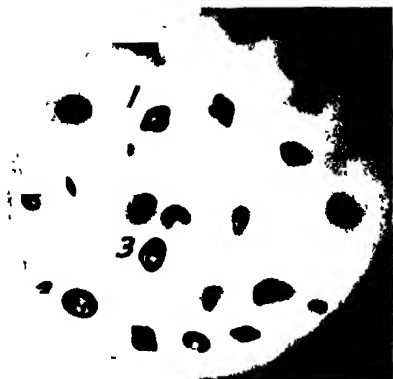
1.



2.



3.



4.



5.

(Facing p. 520.)



form a compound. The compound formed, however, by adding a small quantity of hydrogen peroxide to silicic acid sol is more probably in the first place of the nature  $\text{SiO}_2 \cdot x\text{H}_2\text{O}_2 \cdot y\text{H}_2\text{O}$ .

In the ageing process, which is really a dehydrating process, these separate molecules become connected, which tends towards the development of an internal network. The forces holding the hydrogen peroxide to the silica will not be so strong as those holding the water to the silica, owing to the additional atom of oxygen in the molecule of hydrogen peroxide. Therefore, as soon as the dehydrating action commences, *i.e.*, at the moment the gel begins to assume rigid form, the tendency will be for the hydrogen peroxide to be detached first. After this point, the decomposition of the hydrogen peroxide takes place continuously with the agency of the gel, and the shape of the bubbles will be controlled by the internal structure of the gel.

The conception of this primary fixation of the hydrogen peroxide affords a better explanation for its stability prior to gelation than does the first theory.

---

### *Measurements of the Amount of Ozone in the Earth's Atmosphere and its Relation to other Geophysical Conditions. —Part II.*

By G. M. B. DOBSON, M.A., D.Sc., Lecturer in Meteorology, University of Oxford, D. N. HARRISON, M.A., D. Phil., and J. LAWRENCE, S.J., B.A.

(Communicated by F. A. Lindemann, F.R.S.—Received January 25, 1927.)

#### *§1. Introduction.*

In a previous paper\* we have described in detail the method of measuring the total quantity of ozone in the earth's atmosphere above any locality. Results of measurements made on about 200 days at Oxford in 1925 were also discussed, and it was shown that there was a marked connection between the amount of ozone and the general type of atmospheric pressure distribution, the amount being larger in cyclonic, and smaller in anticyclonic, conditions. As there is evidence that the ozone is entirely in the upper atmosphere, it was obviously desirable to investigate this connection further, and to see if it would throw any light on these meteorological phenomena.

\* 'Roy. Soc. Proc.,' A, vol. 110, p. 660.

By the aid of a grant from the Royal Society it was possible to purchase the optical parts, etc., for five new spectrographic outfits for the measurements of ozone, and five complete spectrographs were built and calibrated here during the winter of 1925-26. The Smithsonian Institution also kindly made a grant for the building of a sixth spectrograph, which was also adjusted and calibrated here. By the kindness and co-operation of many meteorologists the five instruments have been distributed over western Europe, so that, with the original instrument still at Oxford, one might obtain a general idea of the simultaneous variations of the amount of ozone over that region. Further, the Smithsonian Institution's instrument has been sent to Montezuma, near Calama, Chile, a place where the weather conditions are exceedingly constant, and where daily observations could be made throughout the year. The location of the instruments in Europe was as follows: (1) Oxford, (2) Valencia (S.W. Ireland), (3) Lerwick (Shetland Isles), (4) Abisko (N. Scandinavia), (5) Lindenberg (Berlin), (6) Arosa (S.E. Switzerland). When possible, exposures were made three times daily at these stations, and the plates returned to Oxford, where they were developed and measured, and the amounts of ozone calculated.

Unfortunately, owing to various causes, observations were not generally begun until July, 1926. As the sun's altitude is too small at most stations between October and February, the delay in starting greatly reduced the number of observations. A fairly complete set of observations has, however, been made at four stations extending over four months in 1926, and it seems desirable to state briefly the results of the observations so far made. It is hoped that a continuous series of observations from all seven instruments may be secured from February to October, 1927. Before discussing the results obtained, it may be well to comment briefly on the accuracy of the observations.

## § 2. *Accuracy of Measurements.*

(a) *Wedge Constant.*—Great difficulty has been found in obtaining an accurate value of the wedge-constant. In the spring of 1926 six spectrographs were available, and one was used to check the constancy of the sunlight, while the wedge-constants of the others were being determined. In this way much better accuracy was obtained than in 1925, and a modification of the values used previously was found to be necessary. We are still not entirely satisfied with the final results.

(b) *Intensity of Sunlight outside the Atmosphere.*—( $I_0$ ). In the short method

of measuring the amount of ozone\* it is assumed that the ratio of the energies of two wave-lengths about 200 Å apart ( $I_0$  and  $I_0'$ ) as received outside the earth's atmosphere, remains constant. Various workers† have shown that there are large variations in the ultra-violet light emitted by the sun, so that there is a strong probability of some change in this ratio, and for this reason the wave-lengths used are chosen as close together as possible, so that any solar changes may as far as possible affect the two nearly equally. We have recently changed the method of finding this ratio, and both at Oxford and Arosa photographs are taken each day when it is possible, (1) in the early morning, (2) at noon, (3) in the evening, so that there is a large difference of the sun's zenith distance for (1) or (3) and for (2). Thus the observations can be used to obtain the values of  $\log I_0/I_0'$ . Being obtained from only two points, individual values will be less accurate than those obtained from a long series of observations on a given day as described in Part I. On the other hand, with this method the results from a very large number of days can be used, and the final value obtained is found to be more reliable. It has also the advantage of showing if there are any slow progressive or periodic changes in  $\log I_0/I_0'$  which might be due either to variations in the sun or to instrumental or photographic changes.

The values of  $\log I_0/I_0'$  obtained in this way during August and September, 1926, show no evidence of variations of any appreciable magnitude. While the value of  $\log I_0/I_0'$  obtained on any one day has very little weight owing to possible atmospheric variations and to instrumental errors, the constancy of these values obtained in the clear atmosphere at Arosa indicates that the variations are certainly small. Table I shows the values of  $\log I_0/I_0'$  for  $\lambda\lambda$  3264 and 3022, and for  $\lambda\lambda$  3232 and 3052, for all days when the conditions were satisfactory. The ozone values given later are calculated from these two pairs of wave-lengths, and the values agree well together.

Again, any changes in the sun causing variations of  $\log I_0/I_0'$  must affect equally the ozone values obtained at the different stations. Examination of

\* See Part I, pp. 668 and 678. *Note*.—By a slip it was stated in § 5 (b) (iv) that a change of 500° C. in the temperature of the sun, if considered as a black body radiator, would result in a change of 0.04 in  $\log I_0/I_0'$  for the wave-lengths 3232 and 3052 Å. This should be 0.016, which would only cause an error in ozone of about 0.004 cm. Actually, of course, the sun does not radiate as a black-body in the ultra-violet region, and the changes of intensity with temperature will be larger than for a black-body. To allow for this we assumed a much greater variation (500° C.) in the effective temperature than is actually indicated by variations of the solar constant.

† C. G. Abbot, 'Smithsonian Misc. Coll.,' vol. 77, No. 5; 'Edison Pettit, Publ. Astron. Soc. Pacific' (February, 1925); G. M. B. Dobson, 'Roy. Soc. Proc.,' A, vol. 104, p. 254.

Table I.—Values of  $\log I_0/I_0'$  from Arosa Observations.

Date.	Atmospheric conditions.	$\lambda\lambda \begin{cases} 3264 \\ 3022 \end{cases}$	Deviation from mean.	$\lambda\lambda \begin{cases} 3232 \\ 3052 \end{cases}$	Deviation from mean.
Sept. 8	Hazy to clear	1.44	0	1.25	-0.02
" 8	Clear to slight haze	1.43	-0.01	1.25	-0.02
" 11	Hazy	1.40	-0.04	1.26	-0.01
" 15	"	1.45	+0.01	-	-
" 17	Clear	1.45	+0.01	1.28	+0.01
" 17	Clear to slight haze	1.43	-0.01	1.25	-0.02
" 18	Very clear	1.45	+0.01	1.29	+0.02
" 19	Clear	1.42	-0.02	1.28	+0.01
" 19	"	1.43	-0.01	1.30	+0.03
" 20	Hazy	1.47	+0.03	1.28	+0.01
" 20	"	1.50	+0.06	1.25	-0.02
" 21	Hazy to clear	1.43	0.01	1.31	+0.04
	Mean	1.44		1.27	

the results shows no evidence of such similar variations, which are not associated with general cyclonic or anticyclonic conditions.

Finally, for several consecutive days on different occasions the pressure has been nearly constant at Arosa, and the constancy of the ozone-values found at these times (*e.g.*, August 12-18 and September 3-16) is strong evidence of the accuracy of the results.

### § 3. Geophysical Results.

(a) *Ozone Values.*—Table II gives the results of all measurements made in 1926 to the end of October. As pointed out in § 2, the values of the constants used in 1925 for the instrument at Oxford were found to be somewhat in error. In order to make the 1925 values previously published, comparable with the figures given here, they should be increased by approximately 0.015 cm. There is still some slight doubt about the values of the constants. It is hoped that true values will be accurately determined during the course of next year's work, and as further small adjustments may be necessary, the figures given in Table II should be taken as provisional. Any such adjustments will affect the absolute values only, and not the relative changes from day to day.

Table II.—Provisional Ozone Values.

At Oxford.

Unit 0·001 cm. of pure gas at N.T.P. Times of observation to nearest hour.

1926 :	February.		March.		April.		May.		June.	
	O <sub>3</sub> .	G.M.T.	O <sub>3</sub> .	G.M.T.	O <sub>3</sub> .	G.M.T.	O <sub>3</sub> .	G.M.T.	O <sub>3</sub> .	G.M.T.
1	—	—	280	11	265	10	—	—	30	8
2	—	—	248	12, 16	{ 275 256 }	{ 12 16 }	—	—	—	—
3	—	—	282	14	—	—	204	14	352	10
4	—	—	358	10	276	10	297	10	325	8
5	—	—	312?	11, 15	{ 243 231 }	{ 11 14 }	—	—	301	12
6	—	—	278	13, 15	235	14	314	8	323	10, 14
7	—	—	255	13	298	13	319	11	307	8, 17
8	—	—	234	15	—	—	328	8	278	13
9	—	—	296	12, 13	300	9, 14	312	8	291	8
10	—	—	280	10, 15	279	9	—	—	315	8, 10, 15
11	—	—	—	—	289	13, 15	310	11, 13	314?	8, 18
12	—	—	224	10, 15	293	10, 15	310	9, 14	303	12, 16
13	305	13	233	11, 12, 15	297	9, 15	305	10, 15	312	9, 17
14	—	—	—	—	272	10, 12	376	16	312?	10
15	253	13	—	—	—	—	371	12, 15	{ 313 302 }	{ 9 14 }
16	250	11, 13	—	—	—	—	{ 374 342 }	{ 9 13 }	306	8, 16
17	—	—	297	11, 15	342	9, 15	335	9	—	—
18	278	11, 12	309	16	318	9, 10	323	11	309	8, 15
19	—	—	—	—	328	8, 16	304	11, 14	{ 283 269 }	{ 9 18 }
20	—	—	302	9, 15	316	8	303	11	253	11
21	282	12	301	11, 14	337	10	301	10, 16	275	8, 17
22	275	12	320	10, 15	339	9	309	8, 13	239	8
23	—	—	306	14	—	—	288	11	300	8
24	252	15	288	10, 14	350	9	282	8	{ 308 333 }	{ 9 17 }
25	280	12	326	11	311	10	252	13	306	9
26	274	11	340	12, 15	—	—	280	8, 14	290	8, 17
27	—	—	330	12	—	—	288	8, 15	299	8, 14
28	301	11, 14	—	—	—	—	297	8, 11, 15	275	8, 16
29	—	—	296	11, 15	332	10, 12	309	8, 14	272	8
30	—	—	279	9, 15	—	—	282	12, 17	276	9, 16
31	—	—	269	10	—	—	{ 305 324 }	{ 8 16 }	—	—



Table II.—Provisional Ozone Values—continued.

Unit 0.001 cm. of pure gas at N.T.P. Times of observation to the nearest hour.

July, 1926.	Oxford.		Lerwick.		Arosa.		Landenberg.		Abisko.	
	O <sub>3</sub>	G.M.T.	O <sub>3</sub>	G.M.T.	O <sub>3</sub>	G.M.T.	O <sub>3</sub>	G.M.T.	O <sub>3</sub>	G.M.T.
1	285	10, 16	{ 295 284 287	{ 9 16 10, 11, 16	—	—	—	—	—	—
2	271	8	287	10, 11, 16	—	—	—	—	—	—
3	{ 250 267	{ 12 16	267	11, 16	—	—	239	14, 15	—	—
4	261	8	273	14	—	—	{ 238 248 252	{ 10 16 8	—	—
5	—	—	—	—	—	—	—	—	—	—
6	—	—	266	12, 13, 17	—	—	—	—	—	—
7	275	11, 16	267	8, 9, 16	—	—	257	9, 16	—	—
8	259	9, 14	268	12, 17	—	—	255	8, 16	—	—
9	{ 290 302	{ 12 16	—	—	—	—	261	15	—	—
10	264	9	—	—	—	—	—	—	—	—
11	239	9, 16	—	—	—	—	310	13	—	—
12	248	8, 17	245	9	—	—	266	9, 16	—	—
13	252	8, 15	250	9, 11, 17	—	—	252	8, 17	—	—
14	268	9, 17	259	13, 16	—	—	252	8, 15	—	—
15	—	—	{ 274 259	{ 14 17	—	—	{ 265 279	{ 8 16	—	—
16	264	9, 17	—	—	—	—	272?	8	—	—
17	270	9, 16	264	10, 13, 16	—	—	264?	8	—	—
18	250	12	268	15, 17	—	—	265	9	—	—
19	267	14	—	—	—	—	247	8	—	—
20	262	14, 17	269	10	—	—	—	—	—	—
21	278	15, 17	—	—	—	—	—	—	{ 249 250 259	{ 7 15 7, 15
22	257	9	—	—	—	—	—	—	254	7, 15
23	254	11	—	—	247	11, 16	266	8	—	—
24	—	—	304	9	250	7	267	7, 16	—	—
25	273	9, 17	{ 316 297	{ 13 16	247	11	279	14	254	7, 15
26	—	—	283	10, 15	244	7, 8, 16	280	11, 16	244	7, 15
27	289	9, 15	287	9, 16	—	—	274	7	241	7, 15
28	—	—	270	14, 16	—	—	286	6	237	7, 15
29	268	10, 17	—	—	—	—	—	—	229	7
30	{ 260 271	{ 9 17	261	10, 16	—	—	276	8	—	—
31	262	8	250	9, 15	271	13	262	7, 16	—	—

Table II.—Provisional Ozone Values—continued.  
Times of observation are given to the nearest hour.

August, 1926.	Oxford.		Lerwick.		Arosa.		Lindenberg.	
	O <sub>3</sub>	G. M. T.	O <sub>1</sub>	G. M. T.	O <sub>3</sub>	G. M. T.	O <sub>3</sub>	G. M. T.
1	267	9, 16	253	10, 11, 17	260	7, 8, 14	266	10
2	268	9, 11			254	8, 9	280?	7, 14
3	286	9, 11	---		259	7, 16	277	7, 16
4	268	8, 16	200	15, 17	---		269	8, 14
5	282	8			268	11	---	
6	282	16			280	14, 16	286?	8, 15
7	277	8, 13	279	11, 17			272	8, 15
	287	16						
8	264	8	278	9				
	255	16	291	17				
9	247	13			256	7, 16		
	267	17						
10	295	17			250	7, 15		
11	294	9			260	11, 13		
	280	15, 16						
12	251	9, 13, 16	287	13, 16	245	13, 14	288?	9
13	---		252	9, 10	243	8, 10	266?	10
14	258	8, 12, 17			244	8, 11, 15		
15	243	12	255	15	243	8, 11, 13	253	9, 15
16	243	16, 17	245	10	242	8, 11		
17	260	9, 12, 16	---		238	7	251	7, 13
18	244	8, 14	---		238	7, 11	263	12
	259	17						
19	---		264	10, 16	243	7, 12, 15	273?	10, 15
20	---		270	10	250	10, 12	282	13, 15
21	254	15, 16	273	13	231	8, 11, 16		
22	252	8, 13, 16			224	7, 12, 16	256	8, 16
23	218	12	255	9	231	7, 11, 17	283	9
24	230	10, 16	249	13	215	7, 12, 16	233	9
25	219	11, 12	290	11, 15	224	9, 11, 16		
	236	17						
26	242	8, 13, 16	278	10, 14	231	7, 11, 16	245	11
							260	15
27	243	8, 12, 16			241	8, 12, 15	275	9
							250	15
28	244	8, 12, 16	243	11	231	7, 8	262	7
							251	14
29	236	8, 12, 13			239	9, 11, 15	244	9, 14
30	230	9, 12, 16			226	11	243	8, 16
31	---		252	10	224	7, 11, 15	244?	8, 15

Table II.—Provisional Ozone Values—continued.

Times of observation to the nearest hour.

Sept., 1926.	Oxford.		Lerwick.		Valencia.		Arosa		Landenberg.	
	O <sub>3</sub> .	G.M.T.	O <sub>3</sub> .	G.M.T.	O <sub>3</sub> .	G.M.T.	O <sub>3</sub> .	G.M.T.	O <sub>3</sub> .	G.M.T.
1	--		243	10			224	7, 11, 15	240?	8, 15
2			239	9, 15			224	8, 11	232?	8
3	--						237	12, 15	244	8
4	223	10, 17					235	9, 12, 16		
5	221	9	260	10, 15			229	8		
6	224	15, 16	270	11, 16			234	7, 13	242	8, 15
7	--		267	10			224	9, 14, 15		
8	218	10	253	12, 15			231	7, 11, 15	234	9
9	230	12, 14	242	13, 14, 15			229	7, 8	238	8
10	233	10, 12, 15	229	15			232	9, 13		
11	231	13, 15	--				228	7, 12, 15	240?	8, 14
12	239	10, 14	255	12, 15			225	12, 16	246	8, 9
13	227	8, 12	252	10, 15			227	8	252?	8
14	222	8, 14	244	10, 15			229	7, 12, 16		
15	225	14	--		210	14	227	8, 11, 15	239?	8
16	213	9					228	9, 12, 16	239?	9, 10
17	214	9, 10	214	10			214	8, 11, 15	220?	12, 15
18	217	8, 12, 16	228	9, 10, 14	229	14	208	11, 14, 15	219?	9, 14
19	217	9, 12, 13	241	10			209	7, 11, 15	220?	9, 14
20	218	13, 15	--		239	10, 15	218	8, 11, 15		
21	214	14	248?	10	230	10, 14	215	7, 11, 15		
22	227	9, 12, 15	--		240?	10, 15	222	8, 11, 15		
23	241	9					224?	11, 14, 15	244?	12
24	245	11					232?	8, 11		
	{ 262 275 }	{ 9 15 }			236?	10, 11, 15	234	11	242?	9
26	--						232	8, 9	272?	11
27	254	12								
28	240	9, 10, 14					252	12, 13	278?	9
29	--				206	12, 14			280?	10, 13
30	197	10, 13, 15								

Table II.—Provisional Ozone Values—continued.

Times of observation to the nearest hour.

October, 1926.	Oxford.		Valencia.		Atosa.		Landenberg	
	O <sub>3</sub> .	G.M.T.	O <sub>3</sub> .	G.M.T.	O <sub>3</sub> .	G. M.T.	O <sub>3</sub> .	G.M.T.
1	{ 185 172	{ 9 14	-	-	242	8	-	-
2	174	9, 13	-	-	198	8, 10, 12	-	-
3	211	13	216?	11	179	9, 10, 13	-	-
4	211	12, 15	-	-	192	9, 10, 12	-	-
5	-	-	-	-	200	8, 12, 14	207	9, 14
6	236	13, 14	-	-	207	9, 10	203	14
7	238	11, 15	-	-	206	8, 10, 12	224	8, 14
8	250	12, 13, 15	-	-	212	9	236	11
9	242	10, 11, 15	-	-	215	9	255	11
10	252	10, 12, 14	-	-	-	-	-	-
11	-	-	-	-	223	9, 10, 13	266	9, 14
12	208?	11	-	-	218	11	250	11, 13
13	217	10, 11	-	-	203	9, 10, 14	232	12
14	221	10	-	-	208	10, 13, 14	-	-
15	-	-	-	-	202	9, 11	-	-
16	234	13	-	-	203	10, 11, 14	-	-
17	237	10	-	-	208	10, 11, 12	-	-
18	248	10, 14	238?	11, 15	224	12	251	11
19	237	10	-	-	232	10, 11, 13	-	-
20	244	13	-	-	206	9, 13	-	-
21	-	-	-	-	-	-	-	-
22	-	-	-	-	217	10	-	-
23	278	11, 13	269	13	214	10	-	-
24	-	-	-	-	-	-	-	-
25	265	11, 12, 14	-	-	229	10, 12	257	10
26	249	11, 12, 13	-	-	269	8	-	-
27	231?	12, 13	-	-	233	12, 13	-	-
28	-	-	-	-	228	11	-	-
29	-	-	255?	14	-	-	-	-
30	236	12, 13	249	12	-	-	-	-
31	-	-	217	12	-	-	-	-

(b) *Annual Variation.*—Table III shows the monthly means of the ozone values at Oxford during 1925 and 1926. It will be seen that the general annual variation is very similar in the two years. The value for February, 1925, depends on seven days only, during which the pressure was well below the normal, so that the ozone value for that month is abnormally high.

The dates of maximum and minimum, viz., about April and October, are not in the least what one would have expected, and we have, so far, no indication of the reason for this type of annual variation. There seems no doubt that it is not an abnormal result, since the measurements of the sun's extreme ultra-violet radiation as received at the earth's surface made by Dr. Götz, Prof. Dorno and others, indicate similar variations in previous years.

Table III.—Monthly Mean Ozone Values at Oxford.  
(Unit = 0.001 of pure ozone at N.T.P.)

	1925.	1926.
	Ozone.	Ozone
February	340	278
March	304	290
April	340	299
May	321	313
June	296	301
July	289	266
August	273	258
September	266	228
October	239	232

(c) *Relation with Terrestrial Magnetism.* Dr. C. Chree,\* showed that there was probably a connection between the magnetic character of any day at Kew and the ozone value found at Oxford. Since one might expect the ozone value to be associated with the ionisation of the upper atmosphere— if, for example, both are due to ultra-violet radiation from the sun or the ionisation is due to ionised ozone†—it seemed probable that the ozone value would be more closely connected with the diurnal range, say, of the horizontal magnetic force (H), than with the magnetic character, particularly as the H range is most closely related to sunspots.

The values of the daily range of H at Abinger magnetic station for 1925 and 1926 were most kindly supplied by the Astronomer Royal, and have been dealt with in the following way.

The days of each month were divided into three groups according to the magnitude of the “H” range, the three groups, high, medium and low, containing about equal numbers of days (10 per month). Then calling any individual high day  $n$ , the difference of the Oxford ozone value from its monthly mean was written down for days  $n-4$ ,  $n-2$ ,  $n$ ,  $n+2$  and  $n+4$ . All the days of high H range in a month were treated thus, and the means found for the  $n-4$  days, for the  $n-2$  days, and so on. The medium and low days were similarly treated. The number of days in each column is not exactly equal owing to the ozone values being missing on some days.

\* ‘Roy. Soc. Proc.’ A, vol. 110, p. 693.

† S. Chapman, ‘Q. Journ. Roy. Met. Soc.’ vol. 52, No. 219, July, 1926.



It will be seen from Table V that in all months except three, the departure of the amount of ozone from its monthly mean is greater for days of high H range, than for days of low H range, and this is also true for the mean of each year. Table IV shows that, on the whole, the effect seems to be greatest on the  $n$  days, *i.e.*, that there is no large lag on the part of either the ozone or the H range.

The 1925 figures were next divided into two classes, those belonging to days of high and low magnetic character, the high days being those to which an International magnetic character of 1.0 or more had been assigned, and the low days those of magnetic character less than 1.0.\* These two classes were then treated separately in the way just described, and the following result obtained (Table VI).

Table VI.—Ozone (departure from monthly mean) for days of high, medium and low "H" range.

	High.					Medium.					Low.				
	$n-4$	$n-2$	$n$	$n+2$	$n+4$	$n-4$	$n-2$	$n$	$n+2$	$n+4$	$n-4$	$n-2$	$n$	$n+2$	$n+4$
Days of high magnetic character.															
No. of days	33	32	37	34	30	6	4	7	7	5	3	2	2	1	2
Mean	+ 5	- 1	+ 5	+ 4	+ 1	- 5	10	+ 5	- 8	- 7	17	- 5	+ 7	- 32	+ 10
	Mean + 3					+					- 10				
Days of low magnetic character.															
No. of days	22	23	23	21	28	48	54	46	54	53	56	54	54	54	52
Mean	+ 5	+ 5	- 5	- 6	- 5	- 1	1	- 5	- 1	- 2	- 4	- 4	- 5	6	- 5
	Mean - 2					- 2					- 5				

It will be seen that from the figures available, the apparent connection between the amount of ozone and the "H" range is much more marked on days of high magnetic character, the days of low character showing little differentiation between the amounts of ozone corresponding to high and low "H" range. It must, however, be noticed that the number of days contributing to some of the columns is very small, as there are few days of high magnetic character which have a low "H" range. It will also be noticed that the connection with the "H" range is less marked than that found by Dr. Chree with magnetic character.

(d) *Connection between Ozone and Sunspots.* The sunspot numbers have been

\* See 'Met. Zeitschr.,' August, 1926, p. 307.

dealt with in a similar manner to that employed with the magnetic range. The figures used were Wolfer's provisional values published in the 'Meteorologische Zeitschrift.' For 1925 a decided tendency was found for the Oxford ozone values to be higher on days of low sunspot number than on days of high sunspot number, and this was the case for each period of the year separately. Nevertheless, the apparent connection broke down at the end of the year, and for 1926 the opposite effect has so far been found (see Table VII).

Table VII.- Deviation of  $O_3$  from monthly mean on days of high, medium and low sunspot numbers.

	High						Medium.						Low													
	n	4	n	2	n	n	2	n	4	n	2	n	n	2	n	4	n	2	n	n	2	n	4			
1925 (February to October).																										
No. of days	15	11	48	48	48	56	61	53	60	58	51	49	53	52	48											
Mean	- 9	- 9	-12	- 9	- 6	- 3	- 1	4	- 2	0	4	7	7	6	3											
	10						2						7													
1926 (February to September).																										
No. of days	47	48	49	53	54	67	78	73	69	69	48	41	44	16	45											
Mean	17	-14	-13	11	11	19	21	-19	-24	-24	-20	-21	-25	-22	-22											
	13						21						22													

We have also compared the values of eleven day means of both sunspot numbers and ozone values, but the only result appearing from them is similar to that shown in Table VII.

MM. Cabannes and Dufay have calculated the average annual amount of ozone from its absorption band in the visible region, using the Smithsonian observations at Mt. Wilson. While the variations are not large, there are indications of a maximum about 1913 when the solar activity was at a minimum.

Now that observations of ozone have been begun at Montezuma, Chile, we may hope soon to have much more definite information on these points, since the ozone values there should not be disturbed, as in temperate regions, by the changes in the meteorological conditions.

(c) *Relation to Atmospheric Pressure Distribution.*—By far the most marked relation between the ozone and any other quantity is that with the general pressure distribution. Almost without exception the ozone value is high in marked cyclonic systems and low in anticyclonic systems. The ozone values at the various observing stations have been plotted on the appropriate weather



maps so that the general distribution can be easily seen. Figs. 1 and 2 show two typical maps. While the ozone value is generally uniformly low over the

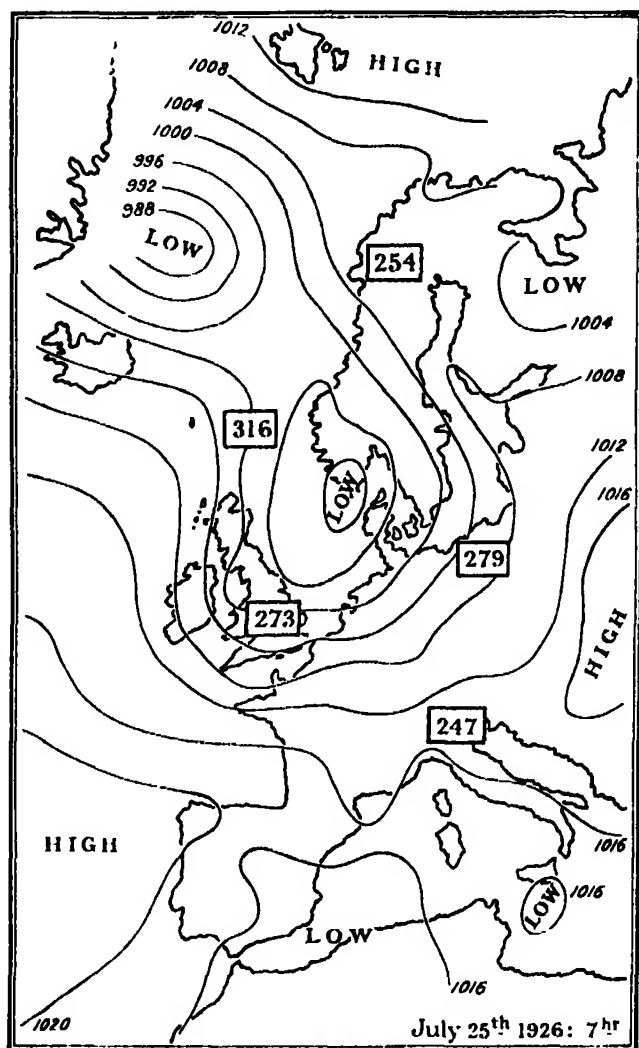


FIG. 1.

whole of an anticyclone, it is markedly higher in the rear than in the front of a cyclone, as if the origin of the air current had a large effect. At times the ozone value rises in certain regions in anticyclones but this seems generally to be due to a neighbouring cyclone.

As found in Part I, the relation is closer with the pressure in the stratosphere

than with that at the surface. We have tried to find which upper-air quantity is most closely associated with the ozone, and below is given a table of the

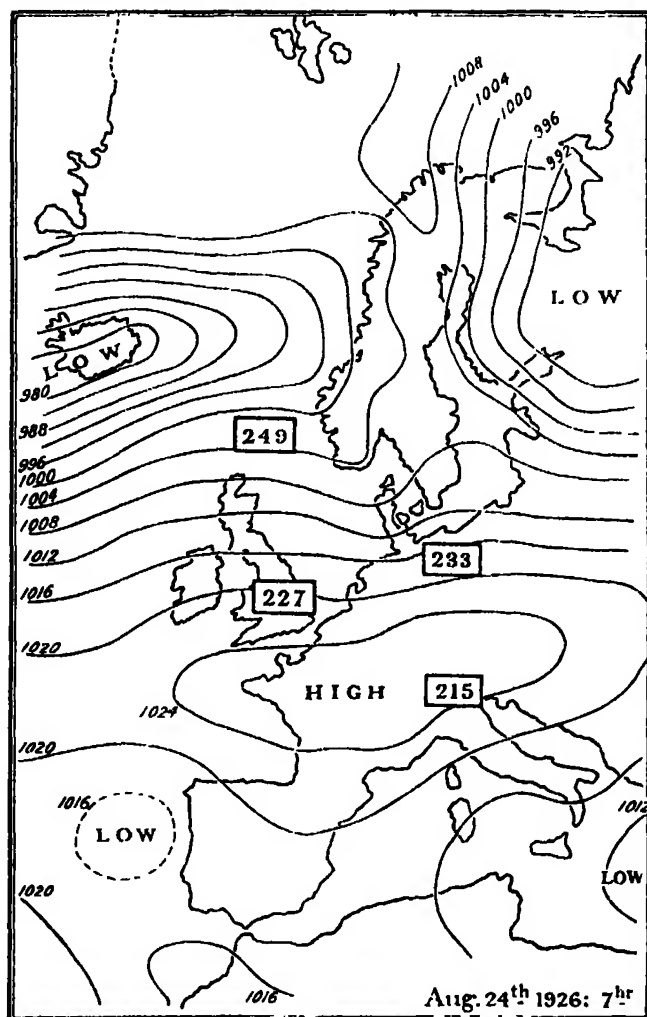


FIG. 2.

correlation coefficients between the ozone values at Oxford and the following quantities :—

Pressure at the earth's surface	=	$P_s$	mbs.
.. 9 km. height	=	$P_9$	..
.. 12 ..	=	$P_{12}$	..
.. 14 ..	=	$P_{14}$	..
.. base of stratosphere	=	$P_r$	..
Height of .. ..	=	$H_c$	km.

Mean of temperature at 1 and 2 km.  $= \frac{T_1 + T_2}{2} ^\circ \text{C}.$

.. 2 and 3 ..  $= \frac{T_2 + T_3}{2} ^\circ \text{C}.$

, 4 to 8 km.  $= \frac{T_4 + T_5 + T_6 + T_7 + T_8}{5} T_m ^\circ \text{C}.$

Temperature at 14 km.  $= T_{14} ^\circ \text{C}.$

The standard deviations are also given.

With the exception of  $P_0$ , the figures were obtained from ballon-sonde ascents, and were supplied by the kindness of the Director of the Meteorological Office and Mr. L. H. G. Dines. In order to allow for known errors of observation, and for those due to the difference in time and place between the ozone and upper air measurements, the standard deviations have been corrected, using for the ozone a standard error of measurement of 0.005 which we know to be about right, and for the upper air data a standard error estimated by Mr. L. H. G. Dines, and based on the standard error of measurement and an estimated standard error due to the difference of time and place. The number of days used was 26. The process has also been carried out after eliminating the annual variations of the various quantities. Only the values where the annual variations have been eliminated have much significance, as the others are increased or decreased by the annual variations according to the time of year under review.

Table VIII.

		Standard deviations.				Correlation with ozone.				
		Not corrected for errors.		Standard error of observation.	Corrected for errors.		Not corrected for errors.		Corrected for errors.	
		Ann. var included.	Ann. var. eliminated.		Ann. var. included.	Ann. var. eliminated.	Ann. var included.	Ann. var. eliminated.	Ann. var. included.	Ann. var. eliminated.
Ozone	10 <sup>-3</sup> cms.	29.8	19.0	5.0	29.4	19.3	-	-	-	-
P <sub>1</sub>	mb.	8.23	8.23	0	8.23	8.23	-0.55	-0.46	-	-
P <sub>2</sub>	mb.	10.6	8.0	2.5	10.35	7.60	-0.85	-0.72	-0.88	0.78
P <sub>11</sub>	mb.	7.15	4.97	2.0	6.87	4.55	-0.83	-0.60	-0.88	0.68
P <sub>12</sub>	mb.	4.85	2.98	2.0	4.41	2.21	0.82	0.56	-0.92	-0.78
P <sub>14</sub>	mb.	45.7	42.3	4.0	45.6	42.1	+0.72	+0.57	+0.73	+0.59
H <sub>c</sub>	km.	1.35	1.16	0.2	1.34	1.15	-0.80	-0.68	-0.81	-0.72
T <sub>1</sub>	°C.	3.96	3.82	1.0	3.84	3.69	+0.57	+0.51	+0.60	+0.54
T <sub>1</sub> -T <sub>2</sub>	°C.	5.57	3.77	1.0	5.48	3.63	-0.75	-0.67	0.78	0.72
T <sub>2</sub> -T <sub>3</sub>	°C.	6.74	4.75	1.0	6.66	4.65	-0.80	-0.67	-0.82	0.70
T <sub>4</sub> -T <sub>5</sub>	°C.	7.51	5.61	1.0	7.45	5.52	-0.83	-0.64	-0.85	-0.67

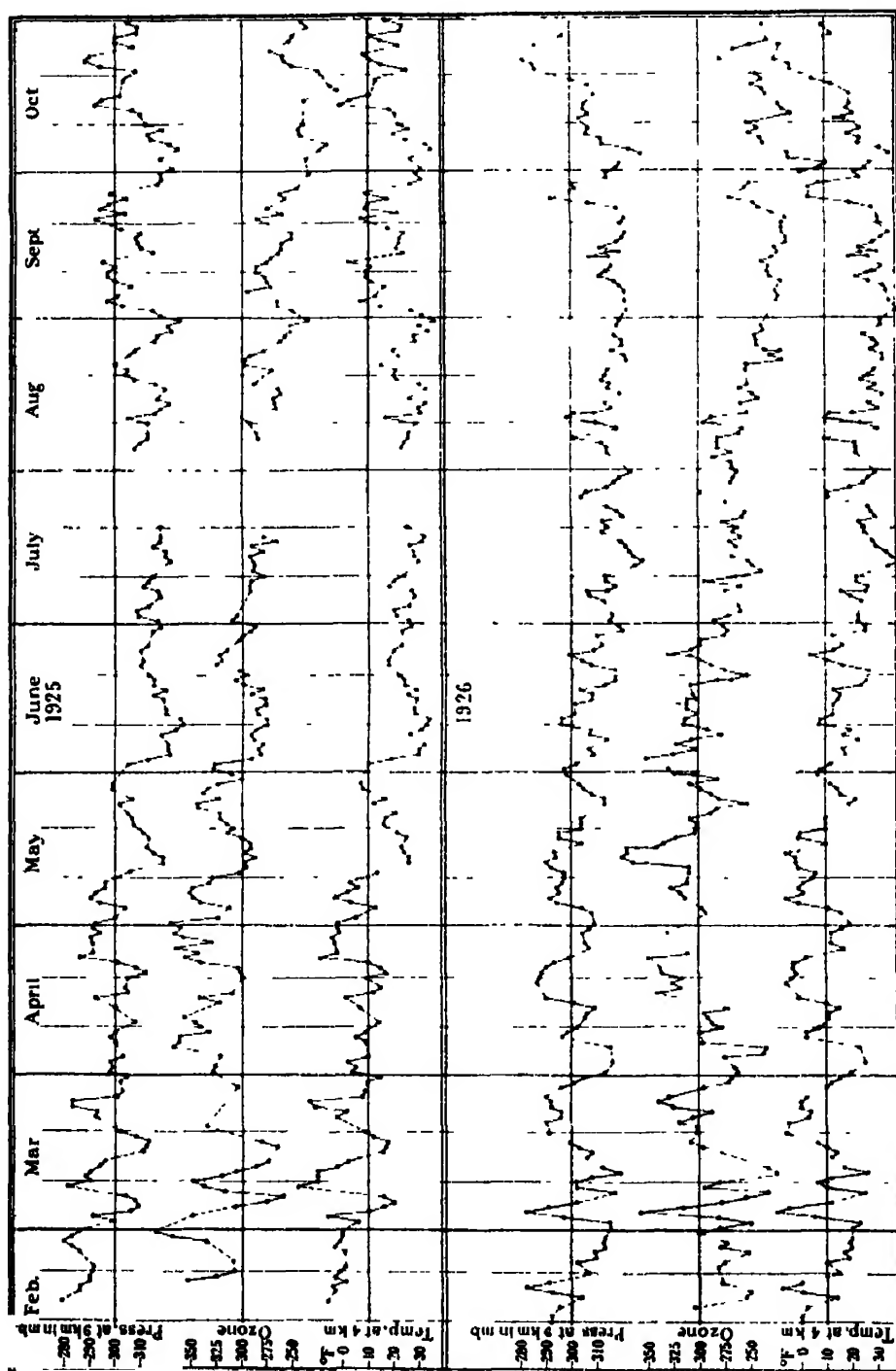
The high correlation both with  $T_m$  and the pressures from 9 to 14 km. suggested that it would be interesting to separate the two effects, and discover if one could be regarded as the true or primary effect, and the other as secondary. Accordingly the partial correlation coefficients of ozone with  $T_m$  and  $P_{12}$  were calculated, but it was found that owing to the very high correlation between  $T_m$  and  $P_{12}$  (0.95 for the figures here used) it was impossible to say that the ozone is more intimately related with one than with the other. Owing to the small number of observations, the standard errors involved were too large for any importance to be attached to the results obtained.

In order to study further this relation on as many days as possible, we have taken the air temperature at 4 km. as measured by aeroplanes, generally at Duxford, Cambridgeshire. We have also made an estimate of the pressure at 9 km. by means of the surface pressure and the aeroplane temperatures. These results are plotted in fig. 3, together with the ozone values at Oxford. The pressures at 9 km. are not strictly accurate since we have not the temperatures of the whole of the lower 9 km. Also occasionally there are marked differences of temperature between results from ascents at Duxford and, say, at Farnborough, or at Lympne, so that one must expect similar differences between these stations and Oxford. It will be seen that there is a remarkably close relation with the ozone values. Eliminating the annual variation, the correlation coefficients between ozone and the calculated  $P_9$  for the first and second halves of the years 1925 and 1926 are -0.60, -0.62, -0.81, -0.55. Again, as stated above, it is not possible to say whether the troposphere temperature or stratosphere pressure shows the closest relation with ozone values, since these two are themselves so closely related. It will be noticed that there are a few cases where definite differences are shown between the ozone and both of the above quantities, *e.g.*, April 6 to 8, 1925, and May 13 to 16, 1926. Fig. 4 shows the results, for the period March to October, 1926, in the form of a dot diagram, the values plotted being deviations from the monthly means, so that annual variations are eliminated.

(f) *Nature of the Relation between Ozone and Pressure Distribution.*—MM. Cabannes and Dufay\* and MM. Lambert, Déjardin and Chalonge† have estimated the height of the ozone layer by making measurements of the intensity of sunlight with very low sun. They find a height of 45 to 50 km., which is also about the height where one would expect the most rapid formation of ozone from oxygen under the influence of the sun's ultra-violet radiation.

\* 'Comptes Rendus,' vol. 181, p. 302 (1925).

† 'Comptes Rendus,' vol. 183, p. 800 (1926).



The question immediately arises whether the variations in the amount of ozone which we have found to be associated with cyclones and anticyclones take

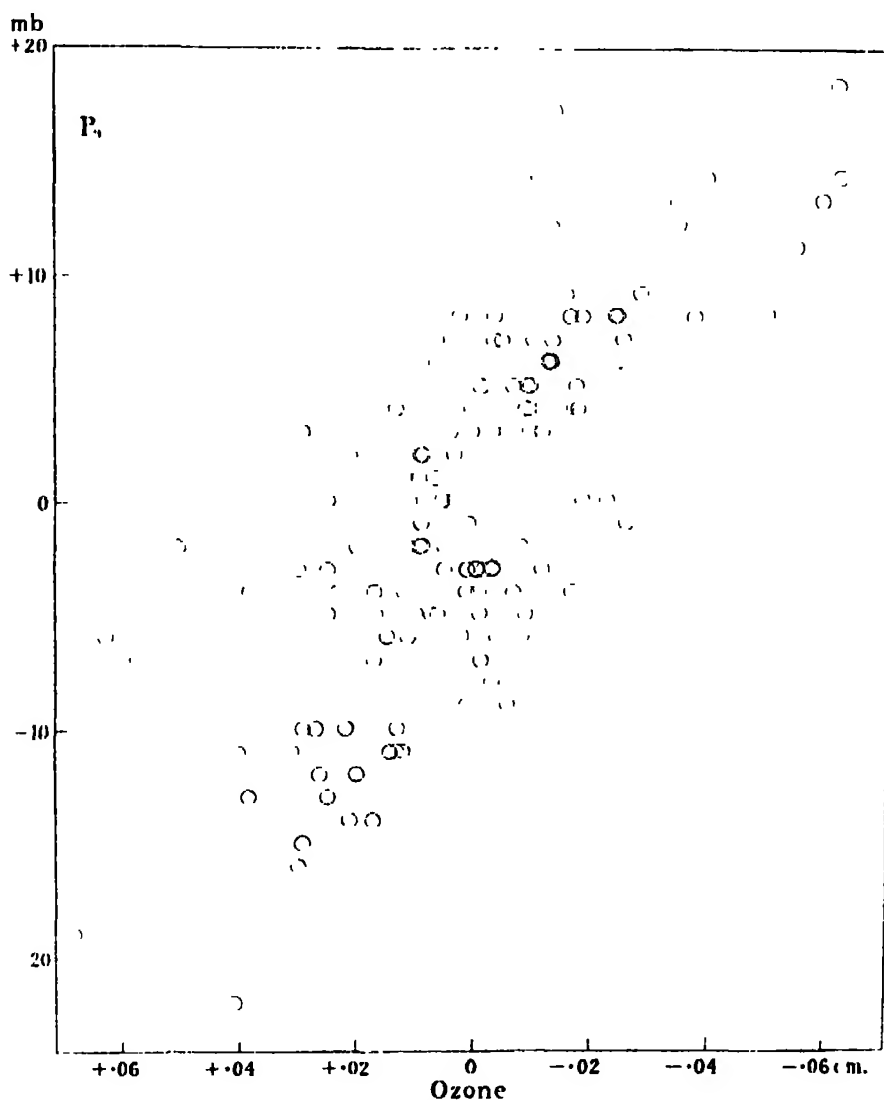


FIG. 4.

place in the ozone at this very high level. Such a result, if true, would be most surprising. As mentioned in Part I, both Lord Rayleigh and Dr. Götz have found no evidence of ozone in the lower atmosphere, and it seems unlikely that it could exist for any length of time in the presence of the dust and organic matter in the lower air. It is possible, however, that during cyclonic weather,

at any rate, there is a moderate amount of ozone in the lower part of the stratosphere. We might suppose that there were two main heights where the ozone concentration was high, the first about 50 km. where it is formed and from which it slowly sinks down, the proportion of ozone to other gases at the lower heights remaining roughly constant, so that we shall find a second maximum of the absolute amount of ozone near the bottom of the stratosphere. We might suppose that the upper layer showed the variations associated with solar or magnetic conditions, and probably also the annual variation, while the lower layer possibly at 10 to 20 km. showed variations associated with cyclones and anticyclones. The measurements of height of the ozone layer could be reconciled with such a view if one supposed that at the time the measurements were made the amount of ozone in the lower layer was small. Since the highest ozone values in cyclones and the lowest values in anticyclones at any one time of the year have a ratio of at least 3 to 2, there must be at least  $1/3$  of the total amount of ozone in the supposed lower layer in cyclonic conditions.

It has been suggested by many people that the origin of the air-current, polar or equatorial, is the chief factor in controlling the amount of ozone. Capt. C. K. M. Douglas has kindly sent us estimates of the amounts of ozone to be expected on this basis. The agreement with the actual results is generally very close. Naturally Capt. Douglas's estimates follow very closely the changes of temperature in the troposphere, and at present it is not possible to say whether (1) the origin of the air current, (2) the temperature in the troposphere, or (3) the pressure at about 10 to 15 km. has the closest connection with the ozone values. Against the view that the origin of the air current is the controlling factor it may be urged that there is no evidence for a higher average ozone value at Lerwick ( $\lambda 60^\circ$  N.) than at Arosa ( $\lambda 47^\circ$  N.). (The slightly higher values at Lerwick in July to August are quite explained by the more cyclonic weather at Lerwick.)\*

It seems most desirable to have further measurements of the height of the ozone layer made as soon as possible both in cyclonic and in anticyclonic weather, for until more definite information about its height is available it will probably be impossible to advance much further even after a continuous series of observations have been made at a number of stations, such as we hope to obtain in 1927.

As pointed out in Part I, it is very difficult to obtain any evidence of a diurnal variation of the amount of ozone by means of observations on the sun, and it

\* The first results from Chile give ozone values of about 0.21 cm. in November, but the character of the annual variation is as yet not known.

should be noted that a decrease in the amount of ozone near sunset, or an increase near sunrise will make the height of the ozone layer appear too great. The only way in which it seems possible to find evidence of a diurnal variation of the amount of ozone would be by means of spectrograms of the brighter stars taken at different times through the night. It is to be hoped that some observatory with suitable equipment may take up this question.

In conclusion we wish to thank all our numerous friends who have taken much trouble to help us in this work. To Prof. Lindemann, F.R.S., and the Clarendon Laboratory our thanks are especially due for continual help and material assistance in innumerable ways. The Director of the Meteorological Office has also given us great assistance both in arranging for the work at foreign stations and by having observations made for us at Lerwick and Valencia, while the following have most kindly undertaken the actual work of carrying out the observations, viz., Dr. F. W. P. Götz, at Arosa ; Dr. Hergesell and Dr. Duckert, at Lindenberg ; Dr. Wallén and Dr. Aurén, in Sweden, together with Mr. Lee at Lerwick and Mr. Stewart at Valencia. Our thanks are also due to the Royal Society for a grant for the instrumental equipment, and to the Department of Scientific and Industrial Research for a personal grant to one of us while engaged on this work, without which grants this work could not have been carried out.

#### *Summary.*

A method of measuring the amount of ozone in the upper atmosphere having been described in a previous paper, results of simultaneous measurements made at various places in N.W. Europe are given. As previously found, there is a marked connection between the amount of ozone and the meteorological upper-air conditions. The possible reasons for this connection are briefly discussed. Connections with terrestrial magnetism and possibly with sunspots are also indicated.

---



## *An X-Ray Investigation of Certain Long-Chain Compounds.*

By ALEX MÜLLER.

(Communicated by Sir William Bragg, F.R.S.—Received January 27, 1927.)

[PLATES 37-40.]

### *1. Introduction.*

The substances which are investigated in this paper have the following chemical formula:  $\text{CH}_3 \cdot (\text{CH}_2)_n \text{A}$  or  $\text{CH}_3(\text{CH}_2)_n \text{CH} : \text{CH}(\text{CH}_2)_p \text{A}$ . These molecules consist of two parts. One which is called the chain or hydrocarbon-chain contains a relatively large number of  $\text{CH}_2$  groups. All these groups are chemically identical (*n*-compounds) except those near the unsaturated bond or near the ends of the chain. The other part "A" is a comparatively small radical such as  $-\text{CH}_3$  or  $-\text{COOH}$  or  $-\text{CH} \cdot \text{Br} \cdot \text{COOH}$  and is called the end group.

Substances with hydrocarbon chains occur very frequently in the organic world. An X-ray investigation of a few typical representatives is likely to supply the key for the crystal structure of a large number of chemically similar substances. Such an investigation is not only interesting from the point of view of stereo-chemistry but also in connection with monomolecular films. Considerable work has been done in recent years on very thin films which these long-chain compounds form on a water surface. Langmuir (1) and later Adam (2) have measured the area occupied by a single molecule in such a film. A corresponding area has been obtained from measurements on a solid crystal by means of X-rays. A comparison of the two data leads to several interesting conclusions.

This work was started more than three years ago. It is far from being complete now, but it has reached a stage where a publication does not seem to be premature.

### *2. Summary of Previous Results.*

A series of papers dealing with X-ray analysis of long-chain compounds have been published already. Most of them appeared in the 'Journal of the Chemical Society' (see references on p. 561). In order to conserve the unity of this paper some of the more important results will be repeated here. In the first publication on fatty acids the writer (3) made the following statement:

An X-ray investigation of a series of normal fatty acids with carbon contents

ranging from 10 to 22 revealed the existence of three characteristic spacings. A long spacing  $d_1$  which, in a first approximation, showed a linear increase with the number of carbon atoms, and two side spacings  $d_2$  and  $d_3$  which were independent of the carbon content of the substance.  $d_1$  ranged from 23.2 to 47.8 ÅU.  $d_2 = 4.08$  and  $d_3 = 3.67$  ÅU.

This suggested: The unit cell is a long prism, the length of which depends upon the number of carbon atoms in the substance. The cross-section of this prism is the same for all the crystals in the series. Taking now the number of C atoms as given by the chemical formula and the diameter of the C atom as 1.54 ÅU (diamond) it follows that a straight chain of carbon atoms touching each other is not long enough to account for the length of  $d_1$ . The right length can be obtained by putting two molecules with a spiral or zig-zag carbon chain together.

A large number of similar substances have been investigated since (refs. 1 to 8). They all showed the same type of spacings. Dr. Shearer (10) found an explanation for the peculiar intensity distribution among the various orders of the long spacing. His argument was as follows: Once the existence of a chain-like structure is established it is easy to find an approximate mass-distribution between the long-spacing planes. From a given distribution the relative intensities of the various orders of the long spacing reflections can be calculated from first principles. In doing this, Dr. Shearer was able to account at least in a first approximation for the observed intensity distribution among the various orders of the long spacing.\*

These were the results which were available when the present investigation started. All this more or less preliminary X-ray work was done on substances in powder form. It was very difficult to go any further without the use of well-developed crystals.

### *3. General Description of the Materials and Methods of Crystallisation.*

Unless special precautions are taken, all these substances crystallise in the form of fine grained flaky powders. The single grain is as a rule built up of a large number of very thin and distorted flakes. It is sometimes possible to isolate from such a powder a crystal big enough to be used on the X-ray spectrometer. These crystals are, however, not very satisfactory for a first investigation. Owing to their minute size they require very long exposures and there is a great danger of missing the weaker reflections. A study of the cleavage is impracticable without the use of very special apparatus.

\* For further development of this problem see ref. (12).

Attempts were, therefore, made to grow larger crystals. Very soon it became obvious that this was not an easy problem. Mr. W. B. Saville had the extreme kindness not only to prepare and to purify the substances, but also to find conditions—other than the well-known slow evaporation of the solvent—under which large crystals could be produced. The result of his long and patient efforts can be summed up as follows :-

(1) It is practically impossible to establish detailed rules for producing large crystals. Even substances belonging to the same series seem to require what one might term a key-solvent.

(2) The use of a solvent of high specific gravity facilitates the growth of large crystals.

Mr. Saville supplied the writer with well-developed crystals of stearic, Br-stearic, stearolic and behenolic acid. The first two belong to the *n*-saturated series, the others are of the *n*-unsaturated type. A more detailed description of the habit and cleavage will be given later on.

#### 4. *X-Ray Technique and the Setting of the Crystals.*

The X-ray reflections from the crystals were recorded on photographic films and on plates. A small spectrometer with a cylindrical camera of 2.8 cm. radius was first used for a general survey. More accurate measurements were obtained with a larger instrument, quarter plates being used (Plates 38 and 39).

All the crystals were thin plates  $2/10$  to  $3/10$  of a mm. thick. They had two parallel faces which gave optically good reflections. To avoid handling the crystals more than was necessary they were attached to thin glass fibres by means of a trace of shellac. The free end of the fibre was easily fixed on the goniometer head.

Preliminary photographs had shown that two of the principal crystallographic axes were lying in the large face of the crystal. The setting of the crystal on the spectrometer with regard to these axes was easily done. The crystal surface was first set at right angles to the collimator axis by optical methods. In order to bring one of these principal axes into coincidence with the spectrometer axis, the crystal had to be rotated round a normal to its surface. This was done with the aid of the goniometer. The angle of rotation was obtained from a Laue photograph. Iron radiation was used for the rotation photographs and a molybdenum anticathode for the Laue diagrams.

### 5. General Results.

All the four crystals are monoclinic prismatic. The symmetry plane is perpendicular to the large face. Laue photographs taken with the incident beam at right angles to this face show the symmetry plane very distinctly. Plate 37, a determination of the density of stearic acid gives 1.04. The calculation shows that there are four molecules in the unit cell. It can be fairly assumed that this holds for the other three substances. No general halvings are found, the lattice belongs to the simple  $\Gamma$  type. A careful examination of the photographs shows that the  $h0l$  planes are halved when  $h$  is odd. All reflections which gave rise to any doubt were checked by the oscillation method.

The four crystals have to be assigned to the space-group  $C_{2h}$ . See Astbury and Yardley, 'Phil. Trans., Roy. Soc.,' A, vol. 224, pp. 221-257 (1924).

A source of error which is common to all investigations of this type is the failure to detect very weak reflections. This source of error can, of course, never be completely eliminated but it can be minimised by prolonged exposures.

No trace of intermediate layer lines could be found on any of the photographs obtained by long exposures and by using the small camera; nor were any signs of intermediate spots on the lemniscates which are produced by the reflection of the white radiation from the stronger planes. The following tables gives the numerical data. The agreement between observed and calculated values is as good as could be expected.

Table I.—Stearic Acid  $\text{CH}_3(\text{CH}_2)_{16}\text{COOH}$ .Monoclinic prismatic; 4 molecules in unit cell;  $h0l$  plane halved if  $h$  odd; $\Gamma$  lattice; space group  $\text{C}_{2h}$ ;  $a = 5.546$ ;  $b = 7.381$ ;  $c = 48.84$  AU; $\beta = 63^\circ 38'$ ;  $c \sin \beta = 43.76$  AU.

$$1/d^2 = 0.040496 \times h^2 + 0.018355 \times k^2 + 0.0005222 \times l^2 - 0.0040847 \times hl.$$

Indices.	Intensity obs.	Spacing obs.	Spacing calc.	$d - d$ obs. calc.	Remarks.
$h k l$					
1 1 2	Weak	4.404	4.352	+0.052	
1 1 1	Strong	4.255	4.252	+0.003	
1 1 0	"	4.122	4.122	0.000	
1 1 1	"	3.965	3.970	-0.005	
1 1 2	Weak	3.789	3.804	-0.015	
1 1 3	"	3.625	3.632	0.007	
1 1 4	"	3.474	3.459	+0.015	
1 1 5	"	3.298	3.291	+0.007	
1 1 6	"	3.110	3.129	-0.019	
1 2 2	Medium	3.069	3.046	+0.023	
1 2 1	"	3.016	3.010	+0.006	
1 2 0	"	2.903	2.963	-0.060	
1 2 1	"	2.899	2.905	-0.006	
1 2 2	"	2.833	2.837	-0.004	
1 2 3	"	2.762	2.764	-0.002	
1 2 4	Weak	2.687	2.680	+0.007	
1 2 5	"	2.598	2.605	-0.007	
0 2 0	Strong	3.689	3.690	-0.001	
2 0 1	Medium	2.422	2.420	+0.002	
0 0 3	Weak	14.55	14.55	0.00	
0 0 5	"	8.693	8.752	-0.059	
0 0 7	"	6.223	6.251	-0.028	
0 0 9	V. weak	4.810	4.862	-0.052	
0 0 10	"	4.322	4.376	-0.054	
0 0 12	Weak	3.648	3.647	+0.001	
0 0 14	"	3.116	3.126	-0.010	
0 0 16	"	2.740	2.735	+0.005	
2 0 1	M. weak	2.53	2.545	-0.015	Film.
2 0 0	"	2.50	2.484	+0.02	"
2 0 19	Medium	1.41	1.406	0.00	"
2 0 38	"	1.28	1.285	-0.005	"
0 1 20	"	2.13	2.098	+0.03	"
0 2 19	Weak	1.91	1.954	-0.04	"
0 3 19	"	1.68	1.681	0.00	"
0 0 18	Medium	2.45	2.431	+0.02	"
0 0 20	"	2.22	2.188	+0.03	"
2 2 2	"	2.13	2.126	0.00	"
2 2 0	"	2.05	2.061	-0.01	"
2 2 2	Weak	1.97	1.985	-0.015	"
3 1 0	"	1.62	1.616	0.00	"

Table II.—Bromo-Stearic Acid  $\text{CH}_3(\text{CH}_2)_{15}\text{CHBrCOOH}$ .

Monoclinic prismatic; 4 molecules in unit cell;  $h0l$  plane halved if  $h$  odd;

 $\Gamma$  lattice; space group  $\text{C}_{2h}$ ;  $a = 11.039$ ;  $b = 4.904$ ;  $c = 52.84$  AU;

 $\beta = 43^\circ 17'$ ;  $c \sin \beta = 36.23$  AU.

 $1/d^2 = 0.017458 \times h^2 + 0.041582 \times k^2 + 0.00076183 \times l^2 - 0.0053098 \times hl$ .

Indices.	Intensity obs.	Spacing obs.	Spacing calc.	$d$ -- $d$ obs. calc.	Remarks.
$h\ k\ l$					
1 1 3	Medium	4.168	4.173	- 0.005	
1 1 2	V. weak	4.41	4.408	0.00	
1 1 1	Strong	4.289	4.285	+ 0.004	
1 1 0	Weak	4.112	4.115	- 0.003	
1 1 1	M strong	3.922	3.919	+ 0.003	
1 1 2	V. weak	3.68	3.709	- 0.03	
1 1 3	Medium	3.501	3.496	+ 0.005	
1 1 4	"	3.278	3.289	- 0.011	
1 1 5	Weak	3.096	3.091	+ 0.005	
1 1 6	"	2.904	2.907	- 0.003	
1 1 7	"	2.743	2.736	+ 0.007	
2 0 6	M. weak	5.462	5.461	+ 0.001	
2 0 5	Weak	5.257	5.286	- 0.029	
2 0 4	"	5.008	5.029	- 0.021	
2 0 0	Strong	3.777	3.784	- 0.007	
2 0 1	Medium	3.501	3.510	- 0.009	
2 0 2	"	3.245	3.260	- 0.015	
2 0 3	Weak	2.825	2.834	- 0.009	
2 0 5	Medium	2.644	2.654	- 0.010	
2 1 5	V. weak	3.62	3.596	+ 0.03	
2 1 3	Medium	3.394	3.402	- 0.008	
2 1 1	Weak	3.137	3.138	- 0.001	
2 1 0	"	2.997	3.003	- 0.006	
2 1 1	"	2.831	2.854	- 0.023	
1 2 2	Medium	2.385	2.382	+ 0.003	
3 1 8	"	2.894	2.897	+ 0.007	
3 1 7	"	2.825	2.834	- 0.009	
3 1 6	"	2.752	2.768	- 0.016	
3 1 5	"	2.684	2.691	- 0.007	
3 1 4	"	2.595	2.606	- 0.011	
3 1 3	"	2.516	2.517	- 0.001	
0 0 2	M. weak	18.10	18.115	- 0.015	
0 0 3	"	12.007	12.076	- 0.069	
0 0 6	"	6.036	6.038	- 0.002	
0 0 7	"	5.178	5.176	+ 0.002	
0 0 8	"	4.531	4.529	+ 0.002	
0 0 9	"	4.029	4.026	+ 0.003	
0 0 10	"	3.625	3.623	+ 0.002	
0 0 11	"	3.307	3.294	+ 0.013	
0 0 12	"	3.021	3.019	+ 0.002	

Table III.—Stearolic Acid  $\text{CH}_3(\text{CH}_2)_7\text{C} : \text{C}(\text{CH}_2)_7\text{COOH}$ .Monoclinic prismatic; 4 molecules in unit cell;  $h0l$  plane halved if  $h$  odd; $\Gamma$  lattice; space group  $\text{C}_{2h}$ ;  $a = 9.551$ ;  $b = 4.686$ ;  $c = 49.15$  ÅU; $\beta = 53^\circ 4'$ ;  $c \sin \beta = 39.28$  ÅU.

$$1/d^2 = 0.017158 \times h^2 + 0.045541 \times k^2 + 0.00064813 \times l^2 - 0.0040076 \times hl.$$

Indices.	Intensity obs.	Spacing obs.	Spacing calc.	$d$ — $d$ obs. calc.	Remarks.
$h k l$					
0 1 2	Strong	4.558	4.558	0.000	
0 1 4	V. weak	4.22	4.229	-0.01	
0 1 6	M. weak	3.815	3.811	+0.004	
1 1 0	Strong	3.990	3.993	-0.003	
2 1 5	Weak	3.334	3.327	+0.007	
2 1 2	Strong	3.147	3.142	+0.005	
2 1 1	V. weak	3.061	3.060	+0.001	
2 1 0	"	2.966	2.959	+0.007	
2 1 1	"	2.854	2.854	0.000	
2 1 2	"	2.747	2.738	+0.009	
2 0 4	M. weak	4.04	4.615	+0.025	Diffuse spot.
2 0 0	Strong	3.817	3.817	0.000	
2 0 1	M. weak	3.596	3.596	0.000	
0 0 3	"	13.093	13.01	+0.08	
0 0 5	"	7.840	7.856	-0.016	
0 0 7	"	5.613	5.611	+0.002	

Table IV.—Behenolic Acid  $\text{CH}_3(\text{CH}_2)_7\text{C} : \text{C}(\text{CH}_2)_{11}\text{COOH}$ .Monoclinic prismatic; 4 molecules in unit cell;  $h0l$  plane halved if  $h$  odd; $\Gamma$  lattice; space group  $\text{C}_{2h}$ ;  $a = 9.551$ ;  $b = 4.686$ ;  $c = 59.10$  ÅU; $\beta = 53^\circ 30'$ ;  $c \sin \beta = 47.51$  ÅU.

$$1/d^2 = 0.016964 \times h^2 + 0.045541 \times k^2 + 0.00044302 \times l^2 - 0.0032614 \times hl.$$

Indices.	Intensity obs.	Spacing obs.	Spacing calc.	$d$ — $d$ obs. calc.	Remarks.
$h k l$					
2 0 5	Weak . .	4.629	4.646	-0.017	Diffuse on one plate.
2 0 4	" . .	4.547	4.525	+0.022	
2 0 1	V. weak . .	4.015	4.023	-0.008	
2 0 0	Strong .	3.814	3.839	-0.002	
2 0 1	V. weak .	3.645	3.656	-0.011	
2 0 3	" . .	3.316	3.308	+0.008	
2 0 4	" . .	3.157	3.147	+0.010	
0 1 2	Strong .	4.590	4.597	-0.007	
0 1 3	Medium .	4.482	4.492	-0.010	
0 1 4	" . .	4.370	4.359	+0.011	
0 1 5	Weak . .	4.207	4.203	+0.004	
1 1 0	Strong .	4.003	4.000	+0.003	
2 1 2	" . .	3.127	3.129	-0.002	
2 1 1	Weak . .	3.044	3.048	-0.004	
0 0 3	M. weak .	15.76	15.84	-0.08	
0 0 5	" . .	9.553	9.502	+0.05	
0 0 7	" . .	6.797	6.787	+0.01	

6. The Unit Cell and Calculation of  $\beta$ .

The experimental data show that the unit cell of all the substances is a very elongated prism. This is generally speaking in agreement with the conclusions drawn from previous experiments on powders. The symmetry axis " $b$ " and another crystallographic axis " $a$ " lie in the large face of the crystal. (Basal plane)  $\beta$  is the angle between the " $c$ " axis and the basal plane. This angle has as it stands no physical meaning, and is to a certain extent arbitrary. The following figure will illustrate this.

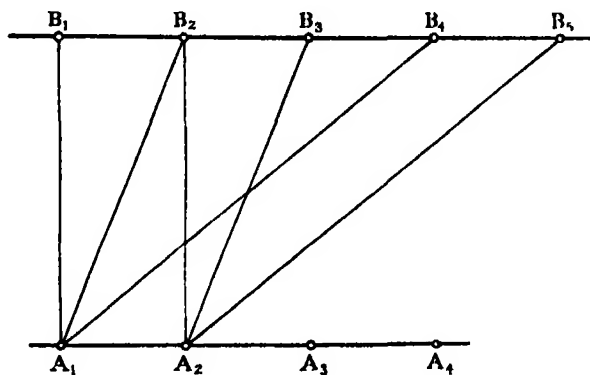


FIG. 1.

$A_1A_2A_3 \dots$  and  $B_1B_2B_3 \dots B_n$  are equivalent points in the symmetry plane of the crystal lattice. A cell with its corners in  $A_1A_2B_1B_2$  has the same symmetry properties as another  $A_1A_2B_2B_3 \dots$  and so on.  $\beta$  can be any of the angles  $\widehat{B_nA_1A_2}$  and is therefore arbitrary to a certain extent.

The question now arises: Has  $\beta$  a physical meaning, and if so, is there a rule by which it can be chosen in an unequivocal way from the series of possible values? Crystallographers have the following well-known rule:  $\beta$  is calculated such as to give the lowest possible indices to the observed faces on the crystal. Most of the specimens which are treated here show only one strongly developed face. Other faces can be observed but they are small and often not well defined. A calculation of  $\beta$  from the habit of the crystal is very inaccurate if not impossible.

A far better method for calculating  $\beta$  can be evolved from a study of the intensity distribution on the photographs. All these photographs show only a few very strong reflections, the majority of the spots being relatively faint. The strong spots are either isolated or closely grouped together (see Plate 38).

It is found that  $\beta$  can be chosen such as to give small indices to all the strongly



reflecting planes. This holds for all the four substances without a single exception, and is one of the most significant facts in this work. The following table gives  $\beta$  and the indices.

Table V.

Substance.	$\beta$	Indices of strong planes.
Stearic acid	$63^{\circ} 38'$	1 1 1; 1 1 0; 1 1 1; 0 2 0
Br-stearic acid	$43^{\circ} 17'$	1 1 1; 1 1 1; 2 0 0
Stearolic acid	$53^{\circ} 4'$	0 1 2; 2 1 2; 2 0 0; 1 1 0
Behenolic acid	$53^{\circ} 30'$	0 1 2; 2 1 2; 2 0 0; 1 1 0

### 7. *Outlines of the Structure.*

An attempt will now be made to give an explanation for this peculiar intensity distribution and for the physical meaning of  $\beta$ . The results obtained from earlier measurements suggest an arrangement of the carbon atoms in sets of equidistant layers, the distances between these layers being considerably smaller than the diameter of the carbon atom. Fig. 2 shows the distribution of these layers in the normal fatty acid series.

$A_1A_2B_1B_2$  are the projections of the corners of the unit cell on to the

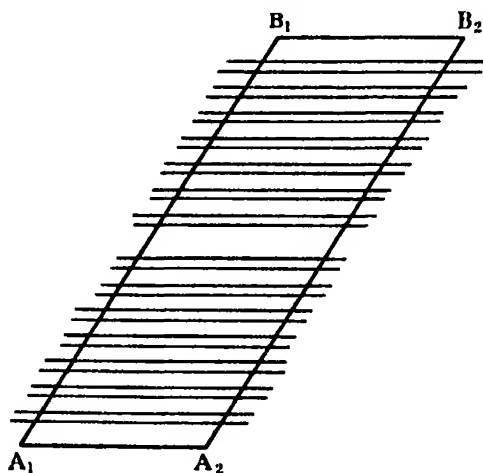


FIG. 2.

symmetry plane (plane of the paper). The parallel lines are the traces of the two sets of equidistant layers. The co-ordinates of the atomic centres in these layers cannot be deduced from the earlier measurements.

The problem now arises to design a model which has this layer structure and

which explains the facts laid down in Table V. A structure which has these properties is one where long straight chains are loosely packed with their chain axes all parallel. The atoms are placed in equidistant sets along the chain axis and touch each other.

In this model the strong reflecting planes can only be found among those which contain the chain axis or are at least close to it. From a comparison with Table V it follows that the monoclinic angle  $\beta$  is the angle between the chain axis and the basal plane of the crystal (9). There is, however, one point which has to be considered. If these chains were tightly packed, such as to touch each other sideways, the chain character of the structure vanishes, and with it the peculiar intensity distribution. The explanation is, therefore, not valid unless it is found that the crystals have an open structure. The following figures show that the structure is open.

The volume of the unit cell of stearic acid as calculated from Table I is  $1792 \times 10^{-24}$  c.c. A cubic packing of the carbons and oxygens of the four molecules gives approximately  $272 \times 10^{-24}$  c.c. The actual space occupied by these atoms is therefore only about 1/6 to 1/7 of the volume of the cell. The same holds for the other three substances.

Some of the chain models have been discussed in an earlier paper (5). One type of chain is found to fit the structure of all the four crystals investigated here. The numerical data are given later. The following is a summary of this section :—

(1) Chains of carbon atoms exist in all of the four crystals. The carbon atoms are arranged in sets which are equally spaced along straight (or nearly straight) lines (chain axes).

(2) These chains are packed in the crystal with their axes parallel or nearly parallel to each other.

(3) The distance between two successive carbon atoms in the chain is considerably smaller than the distance between one chain and its neighbours. In other words, the mass density along a chain axis is higher than the density along any other straight line in the crystal.

(4) The monoclinic angle  $\beta$  is a measure of the tilt of these chains relative to the basal plane of the crystal.

(5) The crystal molecule has a chain of carbon atoms. Their number is equal to the one in the chemical molecule.

## 8. The Structure Factor of Stearic Acid.

The statements in the foregoing section can be put in a mathematical form, the detailed analysis of which will be given in a paper on the structure of stearic acid. The present paper will confine itself to a discussion only. The structure factor of stearic acid or similar substances can be written in the following form

$$S_1 = 8 \times \cos 2\pi \frac{b_0}{b} k \times \cos \pi (A_2 - A_1) \times \frac{\cos \pi (A_1 + A_2 + (n-1)B_0) \times \sin \pi n B_0}{\sin \pi B_0}$$

if  $h + k$  even.

$$S_2 = 8 \times \sin 2\pi \frac{b_0}{b} k \times \sin \pi (A_2 - A_1) \times \frac{\sin \pi (A_1 + A_2 + (n-1)B_0) \times \sin \pi n B_0}{\sin \pi B_0}$$

if  $h + k$  odd.

$A_1 A_2$  and  $B_0$  are defined by the following equations

$$A_1 = \frac{a_0}{a} \cdot h + \frac{c_0}{c} \cdot l,$$

$$A_2 = \left( \frac{a_0}{a} - \frac{s}{2a} \cdot \frac{\sin(\alpha + \Delta\beta)}{\sin \beta \cdot \cos \alpha} \right) \times h + \left( \frac{c_0}{c} + \frac{s}{2c} \cdot \frac{\sin(\beta + \alpha + \Delta\beta)}{\sin \beta \cdot \cos \alpha} \right) \times l,$$

$$B_0 = -\frac{s}{a} \times \frac{\sin \Delta\beta}{\sin \beta} \times h + \frac{s}{c} \times \frac{\sin(\beta + \Delta\beta)}{\sin \beta} \times l,$$

$2n$  = number of carbon atoms in the molecule.

The meaning of the constants  $a_0$ ;  $b_0$ ;  $c_0$ ;  $s$ ;  $\alpha$ ;  $\Delta\beta$  are shown in fig. 3.

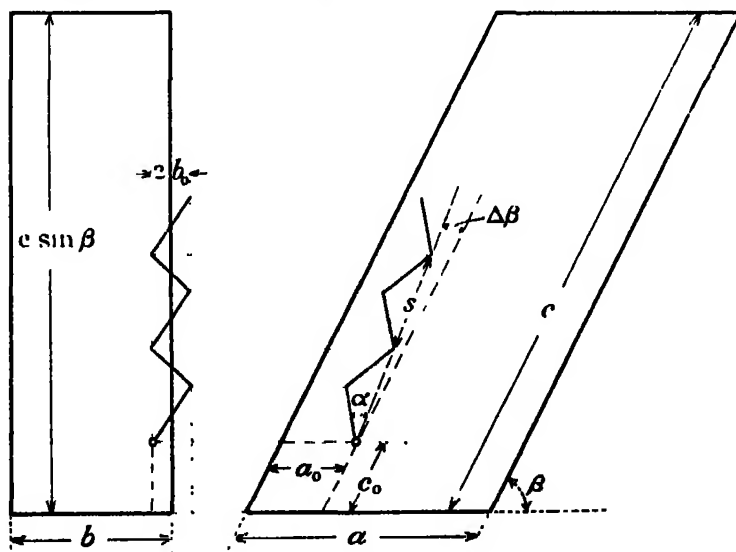


FIG. 3.

Several restrictions have been made with regard to the positions of the molecules in the cell.\* The features of the model are nevertheless sufficiently general to account for some of the more subtle details in the intensity distribution. The chain axes are supposed to lie in the symmetry plane. This is a restriction which will most likely not hold for stearolic and behenolic acid.

The contribution of the end group and of the hydrogens to the total intensity have not been taken into account in the above formula. In stearic acid where the end group consists of two oxygens only, such a neglect is not affecting the results seriously. As long as the discussion is confined to relative intensities, the same will hold for the hydrogen scattering.

The structure factor can be written in the following form

$$S = 8 \times S_c \times S_p,$$

$S_c = \frac{\sin \pi n B_0}{\sin \pi B_0}$  will be called the "chain factor."  $S_p$  is the product of the

three remaining cosines or sines and will be referred to as the "phase factor." The absolute numerical values of these two factors are now discussed below.

$S_p$  can be any figure between zero and one.  $S_c$  reaches its maximum for  $B_0 = 0; 1; 2; 3; \dots$ . The maximal value of  $S_c$  is equal to  $n$ .  $S_c$  can therefore assume any value between zero and  $n$ . Both  $S_c$  and  $S_p$  are functions of the indices.

It is well known that the observed intensities depend upon other factors as well as the structure factor. It is nevertheless possible to predict certain general features of the intensity distribution from the structure factor alone. Owing to the fact that  $n$  is large compared with one, this factor shows well marked maxima. Certain isolated groups of spots should therefore be present on the photographs. This prediction is found to be true. It does not follow that all the maximal values of  $S_c$  should show. There is the possibility of the phase factor becoming simultaneously very small. This is, however, found to be an exception.

A discussion of the numerical value of the phase factor will be given in the paper already announced at the beginning of this section. The following will deal with the chain factor which is the most important of the two.

First of all a further restriction is made with regard to the position of the

\* One pair of molecules—molecule 1 and its rotation molecule 2—has its centre of symmetry in one corner of the unit cell, the second pair—molecules 3 and 4—has its centre in the middle of the base of the cell.

chain axis in the unit cell. It is assumed that this axis is parallel to the "c" axis, *i.e.*,  $\Delta\beta = 0$ .  $B_0$  is in this case only a function of the index  $l$ .

$$B_0 = \frac{s}{c} \times l.$$

The diameter of the carbon atom is 1.54 ÅU and  $\alpha = 35^\circ 15'$ . This gives  $s = 2.51$  ÅU and

$$\pi B_0 = 9.27^\circ \times l; \pi n B_0 = 83.4^\circ \times l$$

in degrees of arc. The following table gives the numerical values of  $S_c$  in function of the index  $l$ .

Table VI.

$l$ .	$S_c$ .	$l$ .	$S_c$ .
0	9.00	34	0.97
1	6.17	35	1.11
2	0.71	36	1.88
3	2.02	37	1.55
4	0.73	38	0.98
5	1.16	39	8.88
17	0.97	40	5.29
18	3.88	41	0.03
19	8.46	42	2.03
20	7.97	43	0.35
21	2.93		

A very considerable increase of  $S_c$  is noticeable for those values of  $l$  which are near to 0;  $\pm 19$ ;  $\pm 39$  ... If all the assumptions are correct then the photographs should show very definite maxima of the reflections from the planes  $hk0$ ;  $hk19$ ;  $hk\bar{1}9$ ;  $hk39$  ... The following table gives the indices of some of these isolated reflections which are actually observed.

Table VII.

Indices of isolated spots observed.	Spacings observed.
0 0 18	2.45
0 0 20	2.22
0 1 20	2.13
0 2 0	3.69
0 2 19	1.91
0 3 19	1.68
1 1 0	4.12
2 0 1	2.42
2 0 18	1.41
2 0 38	1.28
1 1 19	1.75

Most of the high-index reflections have been checked by the oscillation method.

The chain theory receives a very strong support by these observations; wherever a maximum of intensity is observed it is also predicted by the formula.

### 9. *The Habit and Cleavage of the Crystals.*

The crystals of stearic acid were obtained in the following way. The very pure substance (melting point over  $73^{\circ}\text{C.}$ ) was dissolved in  $\text{CS}_2$ . The solvent was allowed to evaporate very slowly and crystallisation took place in the saturated solution.

The crystals are thin flakes (thickness up to  $2/10$  of a mm.). The smaller specimens are very often rhomb-shaped, fig. 4.

The basal plane of the crystal is found to lie in the flake surface. The bisectrix of the acute angle  $\psi$  coincides with the "b" axis. The edges of the flake are parallel to the II direction in the basal plane. A calculation of  $\psi$  from "a" and "b" gives  $73^{\circ} 50'$ , which is in sufficiently good agreement with a series of goniometric measurements where  $\psi = 74^{\circ} 26' \pm 24'$  is found.

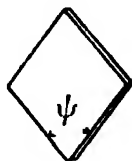


FIG. 4.

The crystals show very good cleavage parallel to the basal plane. Indistinct cleavage can be observed along other lines lying between the 13 and 25 direction.

Stearolic-, behenolic- and bromo-stearic acid were obtained by slow crystallisation from alcoholic solutions.

These crystals have a different habit from stearic acid. They grow in rectangular thin plates (fig. 5).

Their "a" and "b" axes coincide with the edges of the rectangle. Good cleavage is observed parallel to the basal plane and also along the "a" and "b" axes.

Other cleavage planes than the 001 were found when examining some of the thicker crystals of stearolic acid. The following angles between these planes and the basal plane were measured:—

"a" zone, approx.  $90^{\circ}$ .

"b" zone, angles ranging from  $52^{\circ}$  to  $69^{\circ}$ .



FIG. 5.

An X-ray examination showed that the cleavage planes in the "b" zone were close to the 100 plane.

These goniometric measurements are very inaccurate, but they speak nevertheless in favour of a chain theory.

10. *Imperfect Crystallisation.*

Certain difficulties arose during the progress of this work through the tendency of these substances to form pseudo-crystals. A discussion of these difficulties has little bearing on the main subject, but they had to be taken into consideration in order to avoid a wrong conception of the crystal structure.

One typical example of a pseudo-crystal was found among a batch of crystals of behenolic acid. These crystals were apparently perfectly normal. They were transparent and showed a habit as described in the previous section. A revolving crystal photograph was taken, the "b" axis being parallel to the axis of rotation. The spots on the photograph were well defined, the only conspicuous thing was the extreme faintness of the long-spacing reflections. A second photograph was made, the crystal being rotated round a random axis. All the spots were drawn out in circles (see Plate 39) which showed that the sample was not a true crystal. Similar phenomena were later observed with crystals of stearolic acid (see also ref. 11).

An explanation is easily found. The apparent crystal is built up of smaller aggregates which all have the "b" axis in common but have a random orientation round this axis.

An apparently well-developed crystal of stearic acid which Mr. H. S. Piper, of Bristol University, was kind enough to give me, was found to be a very peculiar type of a pseudo-crystal. This particular sample was crystallised from an ether solution. Its habit was exactly the same as described previously. The acute angle of the rhomb was  $74^{\circ} 29'$ .  $a = 5.59$ ,  $b = 7.35$ ,  $c \sin \beta = 43.8$  AU.

The spots on the revolving crystal photographs were not so well defined as usual. The long-spacing reflections showed very strongly. A Laue photograph made with the incident beam perpendicular to the flake surface gave a picture which suggested two planes of symmetry in the crystal. The spots were drawn out into a large number of streaks (Plate 40).

It seems that here again the apparent crystal is composed of smaller units which have their "b" axes in common. Instead of being oriented at random round this axis they are placed symmetrically to a normal to the basal plane and in such a way that their "a" axes are very nearly in a common plane. The following figure which represents a projection of two of these units on to the symmetry plane will illustrate this.

The fact that these substances tend to form imperfect crystals suggests that the cohesive forces are small compared with those in many other crystals; a

slight disturbance will upset the process of crystallisation. It has been observed that changes in their crystal structure occur when the temperature is slightly

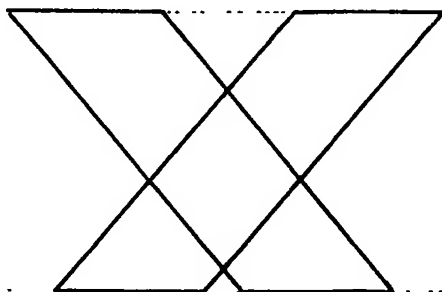


FIG. 6.

altered. A recent investigation of Piper, Malkin and Austin (13) shows how different structures result from different crystallisation methods (see also ref. 14).

This instability of the structure makes an investigation rather difficult, but it suggests an interesting field for a study of the forces which control the process of crystallisation.

### 11. *Final Conclusions.*

The following table contains the data of all the substances and of a number of constants derived from these figures by calculation.

Table VIII.

	<i>a.</i>	<i>b.</i>	$\beta$	$a \sin \beta.$	<i>a b</i>
Stearic acid	5.546	7.381	63° 16'	4.953	40.94
Br-stearic acid	11.039	4.904	43° 15'	7.565	54.13
Stearolic acid	9.551	4.686	53° 4'	7.634	44.76
Behenolic acid	9.551	4.686	53° 30'	7.678	44.76
Octadecane	5.00	7.56	90°	5.00	37.8
	$a b \sin \beta.$	$c \sin \beta.$	<i>c.</i>	length calc.	<i>c.</i>
Stearic acid	36.56	43.76	48.84	46.1	0.671
Br-stearic acid	37.10	36.23	52.88	46.1	0.648
Stearolic acid	35.77	39.28	49.14	46.1	0.614
Behenolic acid	35.98	47.51	59.10	56.3	0.612
Octadecane	37.8	25.6	25.6	22.8	0.662

The last line of the table gives the corresponding numerical values for a hydrocarbon (octadecane). These data have been published in one of the earlier



papers (8) and were obtained from a series of powder photographs. A Laue photograph from an imperfect hydrocarbon crystal gave a value for the ratio  $a/b$  which suggested that  $\beta$  is in the neighbourhood of  $90^\circ$  for this particular substance.

Column 5 shows the calculated data for the area of the base, column 6 the area of the cross section of the unit cell measured in a plane perpendicular to the "c" axis. The next column gives the length of this axis and the following the calculated length of a chain of carbon atoms of the following type.

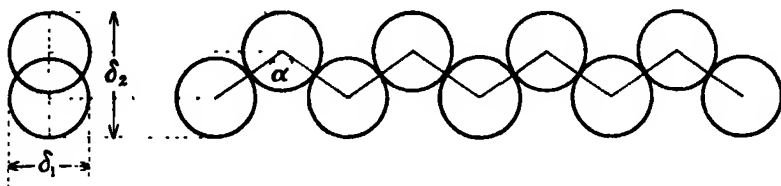


FIG. 7.

$$\sigma = 180 - 2\alpha = 109^\circ 30' \text{ tetrahedral angle.}$$

$$\delta_1 = 1.54 \text{ AU diameter of the carbon atom.}$$

In drawing conclusions from this table emphasis is laid upon the fact that the cross sections (column 6) are very nearly the same for all the substances. In addition to this there is a striking similarity between the geometrical proportions of these cross sections. This section is a rectangle the sides of which are "b" and  $a \sin \beta$  respectively. The ratio  $\epsilon = \text{short side/long side}$  is given in the last column of Table VIII. It is very nearly the same for all the substances (average 0.64).

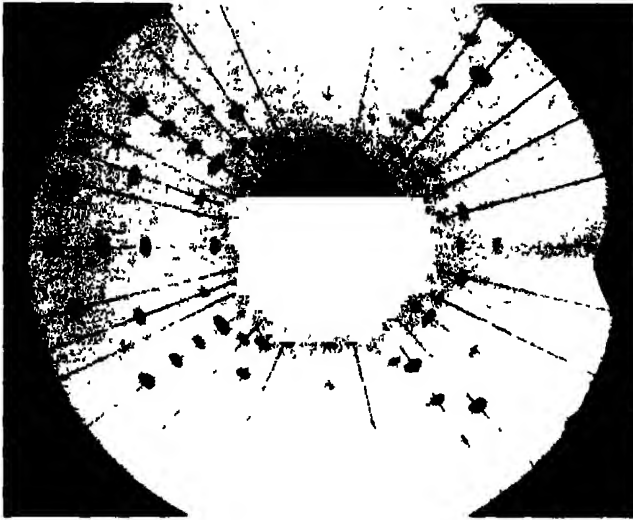
It is interesting to compare  $\epsilon$  with another ratio which can be calculated from the model of the chain (fig. 7).  $\delta_1 \delta_2$  is found to be 0.63, i.e., very nearly equal to  $\epsilon$ .

The following conclusions can be drawn with regard to the general structure of the substances.

The chain can be represented as a rod of elliptical cross section. The axial ratio of the ellipse is approximately 0.64. In the crystal these rods are packed in parallel or nearly parallel bundles and in such a way that they occupy an average cross section of  $18.3 \times 10^{16}$  sq. cm.

These conclusions are additional to those already drawn in section 7.

Considering now the calculated lengths of the carbon chains, it will be seen from Table VIII that they are shorter than the corresponding "c" axes. This difference has to be accounted for by the space occupied by the end groups.

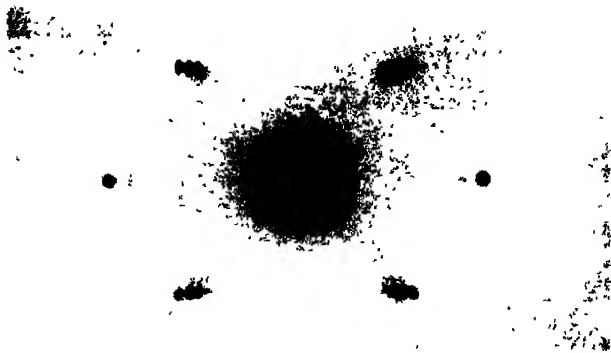


Stearic Acid.

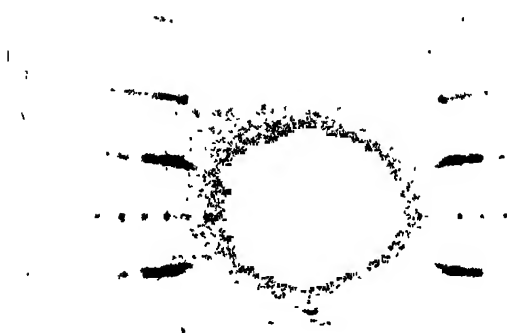


Stearolic Acid.

*Laue Photographs.*



Stearic Acid

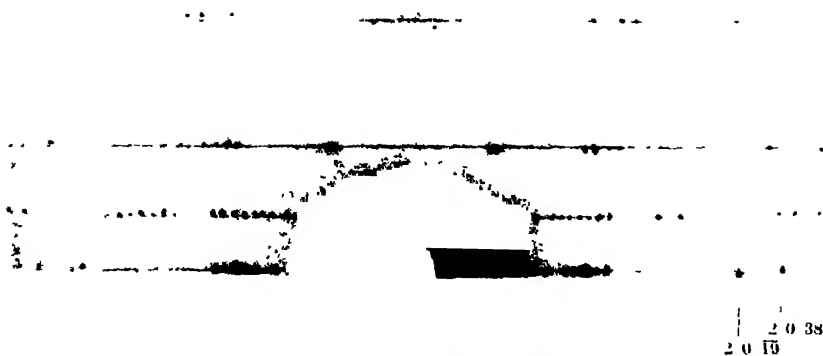


Bromo-Stearic Acid.

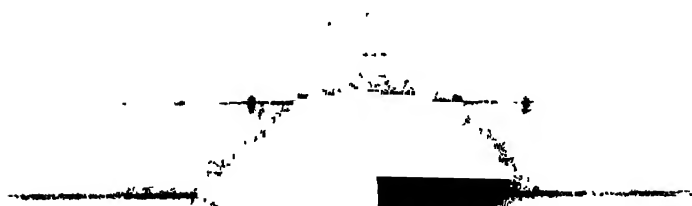


Stearolic Acid.

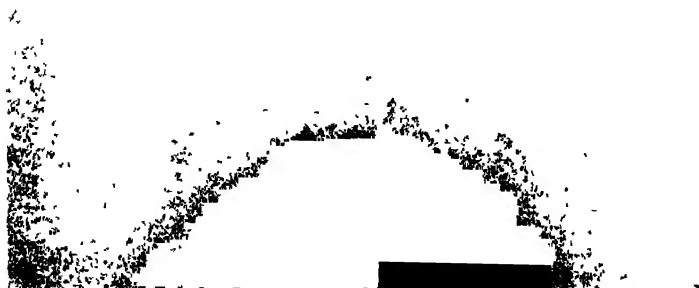
*Rotation Photographs (a Axis).*



Stearic Acid. *Rotation Photograph (b Axis).*



Behenolic Acid. *Rotation Photograph (b Axis).*



Behenolic Acid. *Rotation Photograph (random setting).*



Stearic Acid.

Imperfect Crystallisation. *Lane Photograph.*

It is the same for the hydrocarbon and the stearic acid, although there are two molecules along the *c* axis in stearic acid and only one molecule in the hydrocarbon. This suggests that the carboxyl group occupies a smaller space along the *c* axis than the  $\text{CH}_3$  group. It seems not unlikely that there is a certain concentration of carbon atoms round the carboxyl group. If all the assumptions are correct it would follow that the length of the  $\text{CH}_3$  group in the "*c*" direction is approximately 1.4 ÅU. It has to be borne in mind, however, that the calculation of the length of the end group depends upon the assumed structure of the carbon chain. A slight deviation from the tetrahedral angle in this structure produces a big effect upon the calculated length of the end group.

In the introduction it was pointed out that this paper is not meant to give the finer details of the structure of these long-chain compounds. This has to be done by studying each substance individually. It is certain that most of these substances have more than one crystalline form. The long spacing of stearic acid which is given in Table I is approximately 10 per cent. larger than the one observed in the earlier measurements on powders. Similar differences have been noticed by Piper, Malkin and Austin and other observers (13) (14). There is no doubt about differences existing between the structures of the various modifications. It seems unlikely, however, that they should be fundamentally different from the one given in this paper.

I. Langmuir (1) and later N. K. Adam (2) have measured the molecular cross sections of a large number of long-chain compounds when these substances were in a state of a compressed film on the surface of water. Adam gives  $21.0 \times 10^{-16}$  sq. cm. cross section per molecule for the stearic acid series and  $27.2 \times 10^{-16}$  sq. cm. per molecule for br-stearic acid.

$a \cdot b/2$ , which is the area per one molecule (this area is measured in the basal plane and not in a plane perpendicular to the *c* axis!), is  $20.5 \times 10^{-16}$  sq. cms. for stearic acid, and  $27.6 \times 10^{-16}$  sq. cm. for br-stearic acid. Adam's figures and these are identical within the limits of experimental error. He interprets his figures as being the cross sections of the chains, whereas in this paper the figures refer to the area of the base of the crystallographic cell, which can be described as the area of the end group or the "heads" of the molecules in Adam's terminology. The cross sections of the "heads" which Adam gives are considerably larger ( $25.1 \times 10^{-16}$  sq. cm. for stearic acid).

In plotting areas of his films against pressures Adam obtains a curve of the following type:—

He calls  $\text{OA}'$  the area of the chains,  $\text{OB}'$  the area of the "heads." In the

part CA of the surface/pressure curve, the surface is practically independent of the pressure. The interpretation which he gives for the value OA' as being

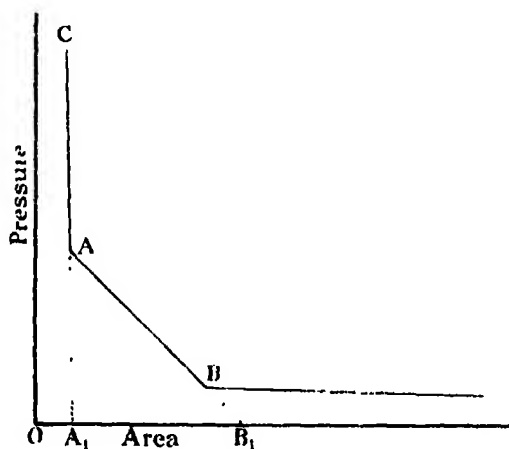


FIG. 8.

a characteristic surface is perfectly legitimate; it becomes rather doubtful when applied to OB'. There seems to be no theoretical reason for the very high compressibility of the film in a region where the molecules come in actual contact with each other.

The pressure per unit area which can be applied to a surface film is extremely high, and it seems not unreasonable to assume that the density of the compressed film is the same as it is for the solid. Assuming that this view is correct and taking into account that Adam's determination of the area of the "heads" is somewhat doubtful, it seems as if the cross section of what Adam calls the "chain" is actually the area  $a \cdot b/2$ , i.e., equal to the cross section of the end group.

If, therefore, the structures of both the film and the crystal are the same, it would follow that the chains are tilted instead of being perpendicular to the water surface. Without further investigations it is impossible to decide whether this hypothesis is correct or not.

In conclusion, the author wishes to express his sincere thanks to Sir William Bragg for his encouragement and interest in the progress of this work, also to Mr. W. B. Saville, without those incessant efforts this investigation could not have been carried out. He also wishes to acknowledge the support given to him by the Department of Scientific and Industrial Research.

REFERENCES.

(This list of references is not intended to be complete.)

- (1) I. Langmuir, 'Trans. Faraday Soc.,' vol. 15 (1920).
- (2) N. K. Adam, 'Roy. Soc. Proc.,' vol. 101, p. 452, Pt. II. (1922).
- (3) A. Müller, 'J. Chem. Soc.,' vol. 123, p. 2043 (1923).
- (4) G. Shearer, 'J. Chem. Soc.,' vol. 123, p. 3152 (1923).
- (5) A. Müller and G. Shearer, 'J. Chem. Soc.,' vol. 123, p. 3156 (1923).
- (6) R. Gibbs, 'J. Chem. Soc.,' vol. 125, p. 2622 (1924).
- (7) W. B. Saville and G. Shearer, 'J. Chem. Soc.,' vol. 127, p. 591 (1925).
- (8) A. Müller and W. B. Saville, 'J. Chem. Soc.,' vol. 127, p. 599 (1925).
- (9) A. Müller, 'Nature,' vol. 116, p. 45, July (1925).
- (10) G. Shearer, 'Roy. Soc. Proc.,' A, vol. 108, p. 655 (1925).
- (11) A. Müller, 'Nature,' May (1926).
- (12) J. A. Prins and D. Coster, 'Nature,' July (1926).
- (13) S. H. Piper, T. Malkin, and H. E. Austin, 'J. Chem. Soc.,' 1926, p. 2310.
- (14) G. M. de Boer, 'Nature,' vol. 119, January (1927).

*On the Capture of Electrons by Swiftly Moving Electrified Particles.*

By I. H. THOMAS, Trinity College, Cambridge.

(Communicated by R. H. Fowler, F.R.S. --Received January 27, 1927.)

When an  $\alpha$ -particle passes through matter it may capture an electron and continue on its way as a singly ionised helium atom. It is of interest to calculate the chance of such a capture on a classical basis and compare the results with the experimental data of Rutherford, Henderson, and Jacobsen.\* Fowler† has calculated this chance by applying equilibrium statistical theory although the conditions do not very closely resemble equilibrium conditions. In the following paper the process of capture is considered in detail, and two cases are treated in which the three-body collision which is involved can be broken up into two successive two-body collisions.

\* Rutherford, 'Phil. Mag.,' vol. 47, p. 276; Henderson, 'Roy. Soc. Proc.,' vol. 109, p. 157 (1925); Jacobsen, 'Nature,' June 19, 1926, p. 858.

† R. H. Fowler, 'Phil. Mag.,' vol. 47, p. 257; 'Proc. Camb. Phil. Soc.,' vol. 22, p. 253.



I.—On the Capture of Electrons from Light Atoms by very Swift Particles.

Suppose a particle of charge  $E$  moves with velocity  $V$  through matter containing  $N$  atoms per unit volume, each atom consisting of a nucleus of charge  $Z$  surrounded by electrons of charge  $e$  and mass  $m$  at distances  $r$ , and that  $V$  is large compared with the velocities of the electrons. The sequence of events in a capture must be like that indicated in diagram 1; corresponding numbers on the two paths represent simultaneous positions of the particle and the electron. First there is a close "collision" of the particle and the electron at

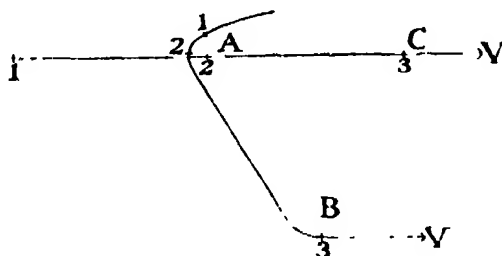


DIAGRAM 1.

A, in which the electron has its small velocity altered nearly to  $V$  and so must go off at nearly  $60^\circ$  to the direction of motion of the particle; then the electron must pass near the nucleus at B and be deflected through nearly  $60^\circ$  to bring its direction of motion nearly parallel to that of the particle: at the same time the particle will have reached C, where ABC is nearly enough an equilateral triangle.

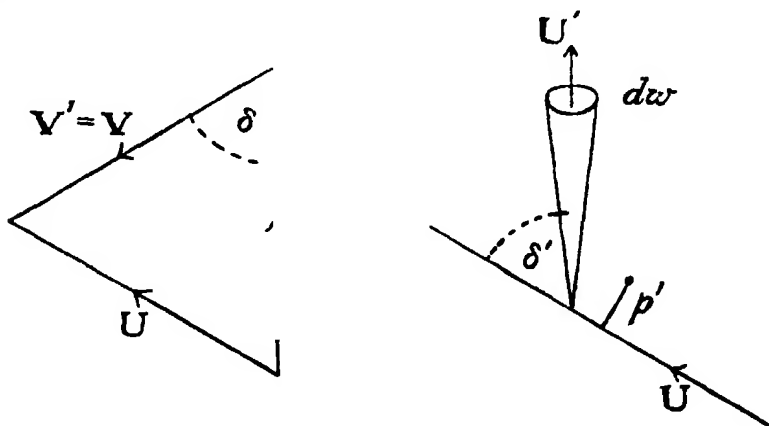


DIAGRAM 2.

In travelling distance  $dl$  the particle has a chance

$$dW_1 = 2\pi p dp N dl$$

of passing an electron, at distance  $r$  from a nucleus, at a distance between  $p$  and  $p + dp$ , when the velocity of the electron relative to the particle will be deflected through angle  $\delta$  given by

$$\cot \frac{1}{2} \delta = mV^2 p / eE. * \quad (1.0)$$

If  $U$  is the velocity of the electron afterwards,  $U = 2V \sin \frac{1}{2} \delta$  (diagram 2) so

$$p \, dp = \frac{1}{2} \operatorname{cosec}^3 \frac{1}{2} \delta \cdot e^2 E^2 / m^2 V^5 \cdot dU.$$

In order that  $U \approx V$ ,  $\frac{1}{2} \delta \approx \frac{1}{2} \pi$  and  $\operatorname{cosec} \frac{1}{2} \delta \approx 2$ , so that

$$dW_1 = 2\pi N \, dl \cdot 4e^2 E^2 / m^2 V^5 \cdot dU.$$

The chance that the electron, initially at distance  $r$  from the nucleus, will now pass it at a distance between  $p'$  and  $p' + dp'$  and be deflected through angle  $\delta'$  so as afterwards to move in a direction within a cone of angle  $d\omega$  is (diagram 2)

$$dW_2 = p' \, dp' \, d\phi / 4\pi r^2 \left( = \frac{\text{target area}}{\text{area of whole sphere}} \right),$$

where

$$d\omega = \sin \delta' \, d\delta' \, d\phi, \cot \frac{1}{2} \delta' = p' m U^2 / eZ,$$

so that

$$p' \, dp' = e^2 Z^2 / m^2 U^4 \cdot \frac{1}{2} \cot \frac{1}{2} \delta' \operatorname{cosec}^2 \frac{1}{2} \delta' \, d\delta'.$$

In order that the electron may afterwards travel in the direction of the particle,  $\delta' \approx \frac{1}{2} \pi$  and  $\frac{1}{2} \cot \frac{1}{2} \delta' \operatorname{cosec}^2 \frac{1}{2} \delta' \approx 4 \sin \delta'$  while  $U \approx V$ , so that

$$dW_2 = \frac{4e^2 Z^2}{m^2 V^4} \frac{d\omega}{4\pi r^2}.$$

Further, if  $U'$  is the final velocity of the electron,  $U' = U$  and  $dU' = dU$ , so that the chance of both collisions is

$$\begin{aligned} dW &= dW_1 \, dW_2 \\ &= 2\pi N \, dl \cdot \frac{4e^2 E^2}{m^2 V^5} \, dU' \cdot \frac{4e^2 Z^2}{m^2 V^4} \frac{d\omega}{4\pi r^2}. \end{aligned}$$

Just after this the electron is at distance  $r$  from the particle, moving in nearly the same direction and with nearly the same velocity as the particle; in order that it should be captured, that is, should afterwards revolve about the particle, its velocity relative to the particle must be less than  $u$ , where

$$\frac{1}{2} m u^2 = eE/r,$$

i.e.,

$$u = (2eE/mr)^{\frac{1}{2}}.$$

\* Cf. J. J. Thomson, 'Conduction of Electricity through Gases,' 2nd Ed., p. 376.

† In this paper the symbol " $\approx$ " is used to mean "is approximately equal to."

Thus the extremity of the vector  $U'$  must lie within a sphere of radius  $u$  about the extremity of  $V$ ,

$$\text{i.e.,} \quad U'^2 dU' d\omega = \frac{1}{3}\pi (2eE/mr)^3.$$

Hence the chance of a capture in path-distance  $dl$  of the particle

$$\begin{aligned} W &= 2\pi N dl \frac{4e^2 E^2}{m^2 V^5} \frac{4e^2 Z^2}{m^2 V^4} \frac{1}{4\pi r^2} \frac{1}{V^2} \frac{1}{3}\pi \left(\frac{2eE}{mr}\right)^3 \\ &\approx \frac{64\sqrt{2}}{3} \pi a^2 N dl \left(\frac{Z}{e}\right)^2 \left(\frac{E}{e}\right)^3 \left(\frac{a}{r}\right)^3 \left(\frac{v}{V}\right)^{11}, \end{aligned} \quad (1.1)$$

where  $av^2 = e^2/m$ , say

$a = 5.3 \cdot 10^{-9}$  cm. the "radius of the normal orbit of a hydrogen atom."

$v = 2.19 \cdot 10^8$  cm./sec., the "velocity" of the electron in that orbit. (1.11)

This formula gives the chance of capture of an electron in the above way by a very fast particle. If the matter is gaseous, it should be summed over each electron together with each nucleus in a molecule; if solid, over each electron in an atom together with each neighbouring nucleus. It is really only applicable to  $\alpha$ -particles moving in hydrogen or helium, and gives a very small chance of capture at the lowest speeds, say,  $V = 4v = 8.5 \cdot 10^8$  cm./sec. at which it could be expected to hold. The experimental evidence, however, does not require that the chance should be any larger at these high velocities of the particle.\*

*Note.*—The expression corresponding to (1.1) when the second collision is with another electron is

$$\frac{1}{3}\pi a^2 N dl (E/e)^3 (a/r)^3 (v/V)^{11}, \quad (1.2)$$

and there is then also an equal chance of capturing the second electron. This can be found in the same way as (1.1), noting that the deflections of relative velocity in both collisions must now be approximately  $\frac{1}{2}\pi$ .

## II.—On the Capture of Electrons from Heavy Atoms by Swift Particles.

A result was obtained in Part I by splitting up the three-body collision into two two-body collisions. This could be done because the speed of the particle was large compared with the initial speed of the electron. If the potential of the atomic field at the electron is large compared with the potential

\* Rutherford, Jacobsen, *loc. cit.* Jacobsen has shown that this chance is much smaller in hydrogen than in air.

due to the particle at the same distance, this splitting up is possible even when the electronic speed is not small. Then also the particle must first pass close to the electron, compared with the latter's distance from the nucleus, to give the electron sufficient energy to escape from the nuclear field with speed near that of the particle; immediately after this close encounter, the relative velocity of the particle and the electron is large, and, since the atomic field is large compared with that of the particle, the effect of the particle on the motion of the electron may be neglected till both have left the neighbourhood of the nucleus.

An exact procedure would then be to use atomic fields and orbits such as those obtained by Hartree,\* and to calculate on the above basis the chance of capturing each of the electrons in the atom for various velocities of the particle. For any particular electron, the chance would be small for a very swiftly moving particle, would increase as the particle's speed approached that of the electron, and would finally decrease when the particle's speed was so small that it could only with difficulty detach the electron from the atom at all. Thus, as the speed of the particle decreased, electrons would chiefly be captured from levels of lower and lower ionisation potential.

The calculation suggested would be little altered in result by replacing the discontinuous distribution of electrons in velocity, position, and ionisation potential, by a continuous distribution. An examination of Hartree's fields shows that the atomic fields are nearly inverse cube fields in the region relevant to the capture of electrons by  $\alpha$ -particles of speed between  $2 \cdot 10^9$  and  $4 \cdot 10^9$  cm./sec. The correct distribution of electrons is two for each  $h^3$  of volume of six-dimensional phase-space, for that part of phase-space with energy insufficient to carry the electron out of the atom.† This distribution does not correspond with reality at the outside of the atom, but the calculation in Part I shows that there the chance of capture is very small, and closer to the nucleus, where the field is no longer an inverse cube field, there are few electrons that can even be removed.

For comparison with experiment the chance of losing a captured electron is also required. It will appear that most electrons are not captured into closely bound orbits, and the time during which they remain with the particle is so short that they can hardly be supposed to fall into more closely bound orbits. Whether the electrons in the atoms must be regarded as having separate effects

\* D. R. Hartree, 'Proc. Camb. Phil. Soc.' vol 21, p. 625. I am indebted to Mr. Hartree for the use of some unpublished fields.

† Cf. 'Proc. Camb. Phil. Soc.', vol. 23, p. 542.

in detaching the captured electron from the particle, or whether the atoms can be supposed to act as wholes, will appear during the calculation.

Suppose a particle of charge  $E$  moves with velocity  $V$  through matter containing  $N$  atoms per unit volume. Each atom is represented by a central field in which an electron of charge  $e$  and mass  $m$  at distance  $r$  has potential energy  $m\lambda/r^2$ . The chance that there is an electron in volume  $d\tau$  of the phase-space of that central field is  $2d\tau/h^3$ , where  $h$  is Planck's constant, so that the chance of an electron at distance between  $r$  and  $r + dr$  and with velocity between  $v_2$  and  $v_2 + dv_2$  is

$$2 \cdot 16 \pi^2 \frac{m^3}{h^3} r^2 dr v_2^2 dv_2, \quad (2.1)$$

provided that

$$v_2^2 < 2\lambda/r^2, \quad (2.11)$$

i.e., the electron is not in an orbit that leaves the atom. All directions for  $v_2$  and  $r$  are independently equally likely.

When the particle has captured an electron, suppose it moves through matter containing  $M$  centres per unit volume, each centre being a field in which an electron has potential energy  $m\nu/r^n$  at distance  $r$ ;  $n = 2$ ,  $\nu = \lambda$ ,  $M = N$ , or  $n = 1$ ,  $\nu = e^2/m$ ,  $M$  some multiple of  $N$ , are to be taken according as the whole atom or separate electrons have a dominating effect, or possibly a combination of both.

Let  $eE/m = \mu$ , so that an electron at distance  $r$  from a particle has potential energy  $m\mu/r$ .

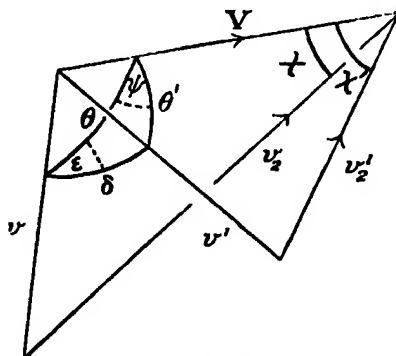


DIAGRAM 3.

Suppose a particle collides with an electron of the group (2.1). All directions for  $v_2$  are equally likely. and,  $v_2$  fixed, the nucleus is equally likely to lie in any direction from the point of collision. Thus the chance that the angle  $\hat{v}_2 V$  lies in a range  $d\chi$  about  $\chi$  is  $\frac{1}{2} d\cos \chi$  and the orientation of the  $(v_2 V)$ -plane about  $V$

makes no difference.  $\chi$ ,  $v_2$ , and  $V$  determine the relative velocity  $v$  of the particle and electron before the collision and the angle  $\hat{V}v$  ( $= 0$ ). The relative orbit is then determined by the orientation of its plane about  $v$ , which may be measured from the  $(Vv)$ -plane and by the initial distance of the particle from the line of relative motion of the electron. If these lie in ranges  $d\epsilon$  and  $dp$  about  $\epsilon$  and  $p$  respectively, the number of such collisions (diagram 3) in time  $dt$  will be

$$2.16\pi^2 \frac{m^3}{h^3} r^2 dr v_2^2 dv_2 \frac{1}{2} d\cos \chi Np dp d\epsilon v dt. * \quad (2.2)$$

If  $u$  is the critical velocity of escape from the nucleus at distance  $r$ ,

$$u^2 = 2\lambda/r^2, \quad (2.21)$$

and

$$r^2 dr = (2\lambda)^{\frac{1}{2}} u^{-4} du,$$

further

$$dt = dl/V,$$

where  $dl$  is distance travelled by the particle, so (2.2) becomes

$$2.16\pi^2 \frac{m^3}{h^3} (2\lambda)^{\frac{1}{2}} \frac{du}{u^4} r_2^2 dv_2 \frac{1}{2} d\cos \chi Np dp d\epsilon \frac{v}{V} dl. \quad (2.3)$$

The relative velocity after the collision,  $v'$ , has the same magnitude as  $v$  but is deflected through angle  $\delta$  given by

$$1 + p^2 v^4 / \mu^2 = 2 / (1 - \cos \delta) \quad (\text{cf. (1.1)}) \quad (2.31)$$

in the plane making angle  $\epsilon$  with the  $(Vv)$ -plane. Then the angle  $\hat{V}v'$  ( $= \theta'$ ), the angle between the  $(Vv)$  and  $(Vv')$ -planes ( $= \psi$ ), the velocity of the electron after the collision  $v_2'$ , and the angle  $\hat{v}_2'V$  ( $= \chi'$ ) are all determined. The independent variables  $p$ ,  $\chi$  and  $\epsilon$  in (2.3) can be replaced by  $v_2'$ ,  $\chi'$  and  $\psi$ .

$$p dp = \frac{\mu^2}{v^4} \frac{d \cos \delta}{(1 - \cos \delta)^2}. \quad \text{from (2.31)}$$

Since  $\theta$ ,  $\delta$ ,  $\theta'$  form a spherical triangle with  $\epsilon$ ,  $\psi$  as angles opposite  $\theta'$  and  $\delta$  respectively, for fixed  $\chi$ , i.e., fixed  $\theta$ ,  $v$ , and  $v'$ ,

$$\begin{aligned} d \cos \delta d\epsilon &= d \cos \theta' d\psi \\ &= \frac{v_2'}{vV} dv_2' d\psi \quad (\text{since } v_2'^2 = v^2 + V^2 - 2vV \cos \theta'). \end{aligned}$$

Then for fixed  $v_2'$  and  $\psi$ , since  $v^2 = v_2'^2 + V^2 - 2v_2' V \cos \chi$  :  $v'^2 = v_2'^2 + V^2 - 2v_2' V \cos \chi'$ ,

$$d \cos \chi = \frac{v_2'}{v_2} d \cos \chi'.$$

\* Cf. Jeans, 'Dynamical Theory of Gases,' p. 209.

Substituting these expressions, (2.3) becomes

$$2 \cdot 16\pi^2 \frac{m^3}{h^3} (2\lambda)^{\frac{1}{2}} \frac{du}{u^4} v_2^2 dv_2 \frac{v_2'}{2v_2} d\cos\chi' \frac{N\mu^2}{v^4} \frac{d\psi}{(1-\cos\delta)^2} \frac{v_2' dv_2'}{vV} \frac{v}{V} dl. \quad (2.4)$$

For fixed  $u$ ,  $v_2$ ,  $\chi'$ , and  $v_2'$ ,  $\psi$  may have any value from 0 to  $2\pi$ . For fixed  $u$ ,  $v_2'$ , and  $\chi'$ , and therefore fixed  $v$ ,  $v_2$  must satisfy the conditions

$$v - V < v_2 < v + V$$

$$0 < v_2 < u, \quad \text{from (2.11) and (2.21)}$$

If (2.4) is integrated over these values of  $\psi$  and  $v_2$  the result will be the number of electrons that, in length  $dl$  of its path, a particle starts with velocity in range  $dv_2'$  about  $v_2'$  at an angle in range  $d\chi'$  about  $\chi'$  with the direction of motion of the particle at distances from nuclei corresponding to velocities of escape in range  $du$  about  $u$ . The nucleus is still equally likely to lie in any direction.

$$1 - \cos\delta = 1 - \cos\theta \cos\theta' - \sin\theta \sin\theta' \cos\psi,$$

so

$$\int_0^{2\pi} \frac{d\psi}{(1-\cos\delta)^2} = \frac{2\pi(1-\cos\theta \cos\theta')}{|\cos\theta - \cos\theta'|^3} \\ = 2\pi \left\{ 1 - \frac{(v^2 + V^2 - v_2'^2)(v^2 + V^2 - v_2'^2)}{2Vv} \right\} / \left| \frac{v_2'^2 - v_2'^2}{2Vv} \right|^3.$$

In order that capture may finally take place,

$$v_2'^2 \leq V^2 + u^2 \quad (2.41)$$

so

$$u < v_2' < v + V,$$

and the range of  $v_2^2$  is  $(v - V)^2 < v_2^2 < u^2$ .

Replacing  $u^2$  by  $v_2'^2 - V^2$ ,

$$\int_{|v-V|}^u \int_0^{2\pi} \frac{d\psi}{(1-\cos\delta)^2} v_2' dv_2 \\ = \pi \int_{(v-V)^2}^{v_2'^2-V^2} \left[ \left\{ 1 - \frac{(v^2 + V^2 - x)(v^2 + V^2 - v_2'^2)}{2Vv} \right\} / \left( \frac{v_2'^2 - x}{2Vv} \right)^3 \right] dx \\ = \pi \frac{v}{V^3} [4V^2(v_2'^2 - V^2) - (v_2'^2 - v^2)^2].$$

The number of electrons so started is therefore

$$2 \cdot 16\pi^2 \frac{m^3}{h^3} (2\lambda)^{\frac{1}{2}} \frac{du}{u^4} N\mu^2 \frac{d\cos\chi'}{2} v_2'^2 dv_2' dl \frac{1}{v^3 V^3} [4V^2(v_2'^2 - V^2) - (v_2'^2 - v^2)^2] \quad (2.5)$$

where

$$v^2 = V^2 + v_2'^2 - 2Vv_2' \cos\chi',$$

provided that

$$u^2 = v_2'^2 - V^2 > (v - V)^2.$$

The orbit of the electron starting with velocity  $v_2'$  at distance  $r$  from the nucleus is determined by the direction in which the nucleus lies. The number of

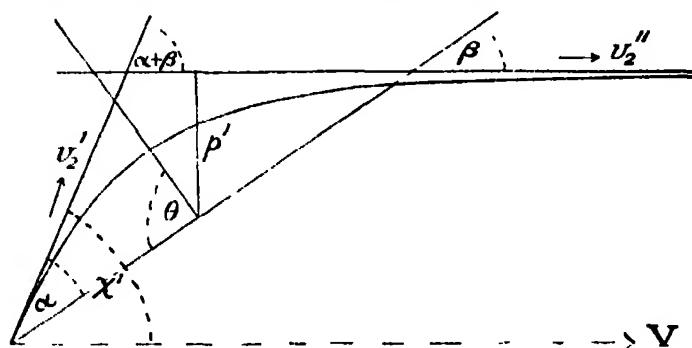


DIAGRAM 4

electrons moving in orbits for which the angle  $\widehat{rv_2'}$  lies in range  $d\alpha$  about  $\alpha$ , and the  $(rv_2')$ -plane makes angle in range  $d\phi$  about  $\phi$  with the  $(v_2'V)$ -plane is obtained by multiplying (2.5) by

$$\frac{1}{4\pi} d\cos\alpha d\phi. \quad (2.51)$$

Let the angle between  $r$  and the asymptotic velocity of the electron,  $v_2''$ , say, be  $\beta$  (diagram 4). Then for fixed  $v_2'$  and  $\alpha$ ,  $\beta$  is fixed, and, varying  $\chi'$  and  $\phi$ , the solid angle traced out by the direction of  $v_2''$  is

$$\sin(\alpha + \beta) d\phi \cos\phi d\chi'. \quad (2.52)$$

Now

$$v_2''^2 = v_2'^2 - u^2,$$

so, varying  $v_2'$ ,

$$v_2'' dv_2' = v_2' dv_2'. \quad (2.53)$$

Combining (2.52) and (2.53), for varying  $v_2'$ ,  $\phi$ , and  $\chi'$  the extremity of the vector  $v_2''$  traces out volume

$$\sin(\alpha + \beta) d\phi \cos\phi d\chi' v_2'' v_2' dv_2'.$$

Let the final velocity of the electron relative to the particle have direction in solid angle  $d\omega$  and magnitude in range  $dw$  about  $w$ . Changing independent variables from  $v_2'$ ,  $\phi$ , and  $\chi'$  to  $w$  and the direction of  $w$ ,

$$\sin(\alpha + \beta) d\phi \cos\phi d\chi' v_2'' v_2' dv_2' = w^2 dw d\omega. \quad (2.54)$$

In order that the electron may be captured,  $v_2''$  must be nearly the same as  $V$  in magnitude and direction, i.e.,

$$\begin{aligned} v_2'' &\approx V \\ \alpha + \beta &\approx \chi' \\ \phi &\approx 0. \end{aligned}$$



Using these approximations, from (2.5), (2.51) and (2.54), the number of electrons started where the velocity of escape is in range  $du$  about  $u$  in a direction making angle in range  $d\alpha$  about  $\alpha$  with the direction of the nucleus so as finally to have velocity relative to the particle in solid angle  $d\omega$  and range  $dw$  about  $w$  is, for path length  $dl$  of the particle,

$$4\pi^2 \frac{m^3}{h^3} (2\lambda)^{\frac{1}{2}} \frac{du}{u^4} N \mu^2 d \cos \alpha \frac{v_2' dl}{v^3 V^2} [4V^2 (v_2'^2 - V^2) - (v_2'^2 - v^2)^2] w^2 dw d\omega, \quad (2.6)$$

provided that

$$u^2 > (v - V)^2.$$

If  $x$  is the distance between the electron and the particle after leaving the nuclear field, the condition of capture is

$$w^2 < 2\mu/x,$$

so the last part of (2.6) integrated for all captured electrons gives

$$\int w^2 dw d\omega = \frac{4}{3} \pi \left( \frac{2\mu}{x} \right)^{\frac{3}{2}}. \quad (2.61)$$

$x$  and  $\chi'$  must now be expressed in terms of  $\alpha$ . If  $\rho, \theta$  are polar co-ordinates in the orbit of the electron past the nucleus,  $\theta$  measured from the apse, and  $p'$  is the distance of the asymptote from the nucleus,

$$\rho^2 \theta = p' \dot{V} = r v_2' \sin \alpha$$

$$\rho^2 \theta^2 + \dot{\rho}^2 = 2\lambda/\rho^2 + V^2,$$

so

$$\begin{aligned} 0 &= \int \left\{ \frac{1}{p'^2} - \frac{1}{\rho^2} \left( 1 - \frac{2\lambda}{p'^2 V^2} \right) \right\}^{-\frac{1}{2}} \frac{d\rho}{\rho^2} \\ &= \left( 1 - \frac{2\lambda}{p'^2 V^2} \right)^{-\frac{1}{2}} \cos^{-1} \frac{p'}{\rho} \left( 1 - \frac{2\lambda}{p'^2 V^2} \right)^{\frac{1}{2}} \\ t &= \int \left\{ V^2 - \frac{1}{\rho^2} (p'^2 V^2 - 2\lambda) \right\}^{-\frac{1}{2}} d\rho \end{aligned}$$

and

$$Vt = \left\{ \rho^2 - \left[ p' \left( 1 - \frac{2\lambda}{p'^2 V^2} \right)^{\frac{1}{2}} \right]^2 \right\}^{\frac{1}{2}}. \quad (2.62)$$

Thus

$$\pi + \beta = \left( 1 - \frac{2\lambda}{p'^2 V^2} \right)^{-\frac{1}{2}} \sin^{-1} \frac{p'}{\rho} \left( 1 - \frac{2\lambda}{p'^2 V^2} \right)^{\frac{1}{2}} \quad (2.63)$$

where on the right-hand side the inverse sine is greater than  $\frac{1}{2}\pi$  for  $\alpha$  less than  $\frac{1}{2}\pi$  and *vice versa*.

From (2.62)

$$Vt = \rho + O\left(\frac{1}{\rho}\right) \quad \text{as } \rho \rightarrow \infty,$$

so that

$$\begin{aligned} x^2 &= (p' + r \sin \beta)^2 + \{v^2 - p'^2(1 - 2\lambda/p'^2V^2)\}^2 - r \cos \beta)^2 \\ &= p'^2 + r^2 \sin^2 \beta + 2p'r \sin \beta + r^2 \cos^2 \beta + r^2 - p'^2 + 2\lambda/V^2 \\ &\quad - 2 \cos \beta r (r^2 + 2\lambda/V^2 - p'^2)^{1/2} \\ &= 2r^2 + 2\lambda/V^2 + 2p'r \sin \beta - 2r^2v_2'/V \cdot (1 - p'^2V^2/r^2v_2'^2)^{1/2} \cos \beta \\ &= 2r^2 + 2\lambda/V^2 + 2r^2v_2'/V \cdot \sin \beta \sin \alpha - 2r^2v_2'/V \cdot \cos \beta \cos \alpha \\ &= r^2/V^2 \cdot [2V^2 + 2\lambda/r^2 - 2Vv_2' \cos \chi] \\ &= r^2/V^2 \cdot v^2 \end{aligned}$$

and

$$x = \frac{r}{V} v = \frac{v}{V} \frac{\sqrt{2\lambda}}{u}. \quad (2.64)$$

Using (2.64) in (2.61) and the result in (2.6), the number of electrons captured by the particle in path distance  $dl$  is

$$dl \int_0^\infty \int_{(\omega)} \frac{16}{3} \pi^3 \frac{m^3}{h^3} N \mu^2 (2\mu)^{1/2} (2\lambda)^{1/2} \frac{(u^2 + V^2)^{1/2}}{u^2 v^2 V^2} [4V^2 u^2 - (u^2 + V^2 - v^2)^2] d \cos \alpha du, \quad (2.7)$$

where

$$\begin{aligned} v^2 &= 2V^2 + u^2 - 2V(V^2 + u^2)^{1/2} \cos(\alpha + \beta) \\ \pi + \beta &= \left(1 - \frac{2\lambda}{p'^2 V^2}\right)^{-1} \sin^{-1} \left\{ \left[ \frac{p'^2 u^2}{2\lambda} \left(1 - \frac{2\lambda}{p'^2 V^2}\right) \right]^{1/2} \right\} \\ p'^2 V^2 &= 2\lambda/u^2 \cdot (u^2 + V^2) \sin^2 \alpha, \end{aligned}$$

and the integration with respect to  $\alpha$  is over values of  $\alpha$  between 0 and  $\pi$  for which  $v$  is real and  $u^2$  less than  $(v - V)^2$ .

The number of electrons captured per unit path length is, therefore,

$$C^{1/2} \pi^3 m^3 / h^3 \cdot N (2\mu)^{1/2} (2\lambda)^{1/2} V^{-1/2}, \quad (2.8)$$

where  $C$  is a numerical constant.

$$C = \int_0^\infty \int_{(\alpha)} \frac{(b^2 + 1)^{1/2}}{b^2 e^2} [b^2 - \frac{1}{4}(b^2 + 1 - e^2)^2] d \cos \alpha db, \quad (2.81)$$

where

$$e^2 = b^2 + 2 - 2\sqrt{b^2 + 1} \cos(\alpha + \beta)$$

$$\pi + \beta = (1 - f^2)^{-1/2} [\pi/2 \pm \cos^{-1} \{b\sqrt{1 - f^2}/f\}]$$

and

$$f = b \operatorname{cosec} \alpha / \sqrt{1 + b^2},$$

the positive sign is to be taken for  $\alpha$  less than  $\pi/2$ , the negative sign for  $\alpha$  greater than  $\pi/2$ . The integration with respect to  $\alpha$  is for such values of  $\alpha$  between 0

and  $\pi$  that the integrand is real (i.e.,  $a\sqrt{1-f^2}/f < 1$ ) and positive (i.e.,  $(e-1)^2 < a^2$ ).

The chance the particle loses an electron depends on how closely it has captured it. The proportion of the length a particle travels that it retains a captured electron is the same as the proportion of particles that have electrons at any moment. So long as this is small it can be obtained by integrating the product of (2.6) and the mean distance a particle retains an electron of speed  $w$  at distance  $x$ .

The deflection of an electron moving at speed  $V$  at distance  $p$  from a centre of force  $mnv/r^{n+1}$  is

$$2 \int_{r_0}^{\infty} \left\{ \frac{1}{p^2} + \frac{2}{p^2 V^2} \frac{v}{r^n} - \frac{1}{r^2} \right\}^{\frac{1}{2}} \frac{dr}{r^2} = \pi,$$

where  $r_0$  is the root of the quantity underneath the radical.\*

For large  $V$  this deflection is asymptotically

$$\frac{2v}{V^2 p^n} \frac{\Gamma(\frac{1}{2}n + \frac{1}{2}) \Gamma(\frac{1}{2})}{\Gamma(\frac{1}{2}n)} \quad n > 1,$$

so that the mean energy, referred to the particle, gained by the electron on passing at distance  $p$  from a centre is

$$\frac{1}{2} m V^2 \left\{ \frac{2v}{V^2 p^n} \frac{\Gamma(\frac{1}{2}n + \frac{1}{2}) \Gamma(\frac{1}{2})}{\Gamma(\frac{1}{2}n)} \right\}^2.$$

The particle loses the electron if this is greater than

$$\frac{1}{2} m \{2\mu/x - w^2\}.$$

i.e., if

$$p < \left\{ \frac{2v}{V} \frac{\Gamma(\frac{1}{2}n + \frac{1}{2}) \Gamma(\frac{1}{2})}{\Gamma(\frac{1}{2}n)} \right\}^{\frac{1}{n}} \left/ \left( \frac{2\mu}{x} - w^2 \right)^{\frac{1}{n}} \right\}. \quad (2.85)$$

The mean distance the particle retains its electron is then

$$y = \left( \frac{2\mu}{x} - w^2 \right)^{\frac{1}{n}} \left/ \pi M \left\{ \frac{2v}{V} \frac{\Gamma(\frac{1}{2}n + \frac{1}{2}) \Gamma(\frac{1}{2})}{\Gamma(\frac{1}{2}n)} \right\}^{\frac{2}{n}} \right\}.$$

When (2.6) is multiplied by this the integration with regard to  $w$  takes the form,

$$\int_0^{\left(\frac{2\mu}{x}\right)^{\frac{1}{2}}} y w^2 dw = \frac{1}{\pi M} \left( \frac{2\mu}{x} \right)^{\frac{3}{2} + \frac{1}{n}} \frac{1}{2} \left( \frac{V \Gamma(\frac{1}{2}n)}{2v \Gamma(\frac{1}{2}n + \frac{1}{2}) \Gamma(\frac{1}{2})} \right)^{\frac{2}{n}} \frac{\Gamma(\frac{3}{2}) \Gamma(1 + \frac{1}{n})}{\Gamma(\frac{5}{2} + \frac{1}{n})}. \quad (2.86)$$

If  $V = 2 \cdot 10^9$  cm./sec., and  $(2\mu/x) - w^2 = (2 \cdot 10^8$  cm./sec.)<sup>2</sup>.

\* Cf. J. J. Thomson, 'Conduction of Electricity through Gases,' 2nd Ed., p. 371.

then for an electron ( $n = 1$ ,  $v = e^2/m$ ) the maximum value of  $p$  in (2.85) is  $1.27 \cdot 10^{-9}$  cm., while for a fairly heavy atom ( $n = 2$ ,  $v = 10 a e^2/m$ ), it is  $1.08 \cdot 10^{-8}$  cm. Thus for  $V = 2 \cdot 10^9$ , the atom as a whole will dominate the loss of electrons. For lower speeds of the particle, separate atomic electrons will have appreciable effects.

Using the same effective field as for capture ( $n = 2$ ,  $v = \lambda \cdot M = N$ ) in (2.86),

$$\int_0^{\left(\frac{2\mu}{x}\right)^2} y w^2 dw = \frac{1}{\pi N} \left(\frac{2\mu}{x}\right)^2 \frac{V}{16\lambda}.$$

Substituting in (2.6), replacing  $x$  by  $v\sqrt{2\lambda}/Vu$ , and reducing as before, the proportion of particles that at any moment have electrons is

$$C' 2\pi^2 m^3 / h^3 \cdot (2\mu)^4 (2\lambda)^{-1} V^{-1}, \quad (2.9)$$

where  $C'$  is a numerical constant.

$$C' = \int_0^\infty \int_{(\alpha)} \frac{(b^2 + 1)^{1/2}}{b^2 e^b} [b^2 - \frac{1}{4}(b^2 + 1 - e^2)^2] |d \cos \alpha| db \quad (2.91)$$

over the same range in  $\alpha$  as for  $C$  above.

Now let  $a$  be the "radius of the normal orbit of a hydrogen atom,"  $v$  the "velocity" of the electron in that orbit, as in (1.11), so that

$$h = 2\pi e m^{\frac{1}{2}} a^{\frac{1}{2}}$$

$$v = e/m^{\frac{1}{2}} a^{\frac{1}{2}}.$$

Let

$$\lambda = \gamma a e^2/m,$$

so that  $\gamma$  is the ratio of the potential at distance  $a$  in the atomic field to that at distance  $a$  in a hydrogen atom. Then, since, as defined,  $\mu = eE/m$ , the results (2.8), (2.9) may be expressed as follows.

A particle of charge  $E$  moves with velocity  $V$  through matter containing  $N$  atoms per unit volume. The potential in the effective field of an atom at distance  $r$  is  $\gamma a e/r^2$ , and there are two electrons for each  $h^3$  of volume in the phase-space of the motion of an electron in that field.

Then the chance that in distance  $dl$  the particle captures an electron is

$$C \frac{1}{4\pi} (2E/e)^4 (2\gamma)^{-1} (V/v)^{-4} N a^2 dl, \quad (3.1)$$

while the proportion of particles which at any moment have an electron is

$$C' \frac{1}{4\pi} (2E/e)^4 (2\gamma)^{-1} (V/v)^{-4}, \quad (3.2)$$

where  $C \approx 3.4$ ,  $C' \approx 4.6$ .

The values of  $C$  and  $C'$  were found by a rough numerical integration. The inner integral, with respect to  $\alpha$ , took the following values :

$b$	0.5	0.7	0.75	1	2
$c$	0.35	5.84	11.28	3.52	0.02
$c'$	0.45	7.08	15.25	4.55	0.02

in both cases there is a sharp maximum for  $b = 0.734$ , where the condition limiting  $\alpha$  changes its form.

Now

$$b = \frac{u}{V} = \sqrt{2\gamma} \frac{a}{r} \frac{v}{V},$$

so that for  $2\gamma = 9$ , say, and  $V/v$  varying from 10 to 3 the important part of the range of  $r/a$  is from 0.2 to 1.2. By comparison with Hartree's fields, the assumption as to the field is roughly justified, and for Na, K, Rb, Cs,  $2\gamma$  has the values 6.2, 8.6, 10.6, 14.6.

The above formulæ agree with experiment as well as can be expected from the roughness of the assumptions on which they are based. The experimental data for these high-speed  $\alpha$ -particles are roughly as follows. Rutherford found that the proportion of particles with an electron after passing through mica was  $1/200$  for  $V = 1.81 \cdot 10^9$  cm./sec. and varied roughly as  $V^{-4.6}$ . Replacing mica by other solids made little difference. He measured also the rate of loss in air (and other gases). Assuming that the proportion is the same for air as for mica, the chance of capture in air (at N.T.P.) was  $4.6 dl$  for  $V = 1.81 \cdot 10^9$  cm./sec. and varied roughly as  $V^{-5.6}$ . Henderson found that for many solids ranging from mica to gold the proportion of particles was nearly the same and varied with velocity as  $V^{-n}$  where  $n$  decreased from 4.3 to 3.4 as  $V$  increased from  $1.0 \cdot 10^9$  to  $1.35 \cdot 10^9$  cm./sec. His actual value agrees with Rutherford's for about  $V = 1.5 \cdot 10^9$  cm./sec.

Expression (3.2) makes the proportion of particles with an electron vary as  $V^{-4}$  and from substance to substance as  $(2\gamma)^{-1}$ , i.e., very little. For  $V = 1.81 \cdot 10^9$  cm./sec., taking  $2\gamma = 8.6$ ,  $E = 2e$ , the proportion calculated is 0.0064, Rutherford's observed value being 0.005.

Expression (3.1) makes the chance of capture vary as  $V^{-5.5}$ . Taking  $V = 1.807 \cdot 10^9$  and  $2v = 8.6$ , as above, and  $N = 2.2 \cdot 705 \cdot 10^{19}$ , the chance of capture in, say, air at N.T.P. calculated is  $20.2 dl$ , about four times as large as Rutherford's observed value. However, air is already so light that the assumptions are not very accurate.

*Note.*—The forms of results (1.1) (3.1) can be obtained, except for the numerical factor, by a dimensional argument, in the more general case of an atom attracting as an inverse  $n$ th power field.

A.—The chance  $W$  that an  $\alpha$ -particle with velocity  $V$  attracting electrons with acceleration  $\mu/r^2$  will in distance  $dl$  capture an electron from atoms  $N$  per unit volume consisting of electrons at distance  $R$  from centres attracting with acceleration  $\lambda/r^n$  must be, by an argument similar to that given above, as a limiting form for large  $V$ ,

$$W = \text{const. } N\mu^{\frac{1}{2}} dl R^{-1} \lambda^{-s} V^{-t},$$

where

$$[N] = L^{-3}$$

$$[\lambda] = L^{n+1} T^{-2}$$

$$[\mu] = L^3 T^{-2}$$

i.e.,

$$s = -\frac{2}{n-1},$$

$$t = 7 + \frac{4}{n-1}.$$

B.—If instead of electrons at distance  $R$  from the atomic centres there are electrons distributed at  $\rho$  per unit phase-space (mass of electron = unit mass),

$$W = \text{const. } N\mu^{\frac{1}{2}} dl \rho \lambda^{-s} V^{-t}$$

where

$$[\rho] = T^3 L^{-6}$$

so

$$s = -3/2(n-1),$$

$$t = 4 + 3/(n-1).$$

These results require for their validity that the conditions (magnitude of  $V$ , etc.) should allow the three-body collision to be split up into two two-body collisions as above, thus enabling the form of dependence of  $W$  on  $\mu$  and  $R$  to be determined.

Finally I wish to express my appreciation of the encouragement and help of Prof. Bohr and Prof. Kramers while I was doing this work.

### Summary.

The chance that a fast  $\alpha$ -particle will capture an electron is calculated in two cases; for particles with velocity greater than  $8 \cdot 10^8$  cm./sec. moving

through hydrogen or helium, and for particles with velocity between  $4 \cdot 10^8$  and  $2 \cdot 10^9$  cm./sec. moving through heavy matter. The method is to split up the process into a close collision of the particle with an electron and a close collision of this electron with an atomic nucleus. The results obtained are compared with the available experimental results and the agreement is satisfactory.

---

*A further Contribution to the Study of the Phenomena  
of Intertraction.*

By SIR ALMROTH E. WRIGHT, M.D., F.R.S.

(Received January 13, 1927.)

[PLATES 41, 42.]

Seeing that a phenomenon of lateral streaming which I recently described and put forward as convincing evidence of *horizontal intertraction* is construed otherwise by N. K. Adam,\* I have, with a view to testing his interpretation of the phenomenon, made some further quite simple investigations. It will not be amiss, as a preliminary to detailing these, to place the real issue in debate—the issue as to whether there is such a *vis operans* as intertraction—before us in its proper perspective. I would propose to do this by recounting what led up to the investigation of intertraction.

The study of this *vis operans* began with observations on the effect of applying to furuncles requiring evacuation a plaster consisting of soap and sugar which is used in folk-medicine for “drawing” such boils. It was found that soap and sugar applied to open boils did, in point of fact, induce a copious welling up of lymph from the subjacent tissues. In pondering this effect it suggested itself that the sugar constituent of the plaster might be attracting, or to use the household word, “drawing,” fluid from the open lymph spaces; and that the soap constituent might be decalcifying and preventing the coagulation of the out-flowing lymph by staving off the sealing of the wound by scab.

Acting upon this idea—and, of course, mindful of the fact that Heidenhain had found that sodium chloride and other crystalline substances introduced into the blood call forth an increased lymph flow—I substituted sodium chloride for the sugar, and citrate of soda for the soap; and proceeded to treat

\* ‘Roy. Soc. Proc.,’ A, vol. 113, p. 478 (1926).

wounds which required "drawing" with a 5 per cent. solution of sodium chloride combined with 0.5 per cent. of citrate of soda. This was found to be a very effective "drawing agent."

Later when I realised how voluminous was the outflow of lymph achieved, and recognised that this of itself would prevent the wound becoming lymph-bound, I omitted the citrate of soda, and employed as a "drawing agent," or if the term is preferred, as a "local lymphagogue," a simple hypertonic (2.5 to 5 per cent.) sodium chloride solution.

It is, I think, widely known that the simple hypertonic salt solution which had thus been arrived at was very extensively and effectively employed in the war in the treatment of those putrid lymph-bound conditions which result whenever surgical treatment of lacerated wounds is postponed.

Hand-in-hand with the therapeutic application of the hypertonic salt solution, its effect was studied both in the wards and in the laboratory. The ward experiments consisted in measuring the volume and the time relations of the induced lymph flow. In the case where scooped-out cavities in bone presented themselves, these were turned to use as collecting cisterns,\* and where only flat superficial wounds were available artificial cisterns were made by strapping down upon the wound the upper ends of test tubes which had been cut across in the middle (we called these lymph-cups). In each case it was found that the filling-in of hypertonic salt solution into these cisterns produced an immediate in-draught of lymph, and that the in-draught diminished and finally stanchd as the salt solution became more and more attenuated. These happenings in the wound correspond, as we shall presently see, with those witnessed when hypertonic salt solutions are brought in contact with serum *in vitro*.

Concurrently with the aforesaid *in vivo* experiments, laboratory experiments were made to find out whether the (let us call it now) *tractor action* of salt solutions was exerted upon water as such, or upon albuminous solutions as such. The experiments in question (they are fully set out in the second edition of my Treatise on the Technique of the Teat and Capillary Tube†) brought out two things. The first was that when two receptacles which contain the one a strong salt solution, and the other water, are connected up in such a way that the water can pass, while the passage of salt is even by the lightest differential barrier impeded, then the level of the fluid gradually rises in the

\* Fleming, 'Brit. Jour. Exper. Surgery,' vol. 7, p. 999 (1919).

† Wright and Colebrook, "Technique of the Teat and Capillary Tube," 2nd edition (1921), Constable, London, pp. 327-342.



receptacle which contains the salt solution. This shows that the salt, provided it be ever so lightly confined, can draw up water against the opposition of gravity. The second fact brought out was: that where, instead of water, an albuminous fluid and a confining barrier which is permeable to albumen are employed, there is obtained a much more rapid and voluminous in-draught of fluid into the salt solution.

It will be noted that in the experiments which have just been summarised, cognisance was taken only of tractor forces exerted by the salt solution.

As a next step in the study of the *vis operans*, steps were taken to render visible the movements which occur upon the frontier when a lighter albuminous fluid is imposed upon a heavier salt solution. And here, inasmuch as traction exerted in a particular direction by an element A upon an element B must have as its counterpart traction exerted in the opposite direction by the element B upon the element A, the experiments were so planned as to render manifest not only a down draught of the lighter albuminous fluid into the heavier salt solution, but also an updraught of the heavier salt solution into the lighter albuminous fluid. To this end, first the one, and then the other, of the solutions was artificially coloured. The experiments here in question are those which were described by me in my first communication on intertraction.\* These were put forward as demonstrating the operations of intertraction, and they furnish what is, in my judgment, conclusive proof of the existence of such a *vis operans*. For ordinary convection movements are here definitely ruled out, and diffusion can furnish no explanation of the configuration I have called "*pseudopodial invagination*" or of the rapidity of the movements of interpenetration.

But none the less, in bringing forward the experiments in question as ocular demonstration of the operations of intertraction, I did not fail to point out that there are in the experiment (let us call it for the sake of brevity the experiment of vertical intertraction) superposed upon the effects of intertraction also effects of other derivation.

In the first place, we have here effects due to changes in specific gravity which affect the invading serum and salt solution respectively, after they have interpenetrated deeply. What would seem to happen is that the invading serum, becoming condensed by loss of water, becomes heavier than the "intracting" saline solution and so falls to the bottom of the vessel. And contrariwise,

\* 'Roy. Soc. Proc.,' B, vol. 92, p. 118, figs. 1 and 2 (a and b) (1921). *Vide also Plate 41, figs. 1 and 2 infra.*

the invading saline solution having parted with some of its salt content, becomes lighter than the "intracting" serum, and so ascends to the surface.

Superadded to the gravitational movements just indicated, there is also a diffusion effect. Diffusion (co-operating with intertraction) finally brings about an equable dispersal of the salt and albumen and establishes uniformity between the subjacent and superjacent fluids.

These acknowledged (but I should have thought quite minor) blemishes in the vertical intertraction experiment have furnished Dr. Jessop\* and Mr. N. K. Adam with the majority of the arguments by which they jointly, and the latter author also separately, have sought to make good that the phenomenon of "pseudopodial invagination" wherever obtained can be explained with any invoking of the concept of intertraction. With respect to that residue of arguments which those authors draw from their own experiments (I speak here only of those experiments which relate to salt and serum), these I must perforce (the reasons for this will appear later) ascribe to insufficiently thoughtful consideration.

To return to what is directly material to the subject matter in discussion, it was clearly of import for the general acceptance of intertraction as a *vis operativa* that an experiment should be devised which would display intertraction effects uncomplicated by effects due to alterations of specific gravity in the intertracting fluids. It was to this end that I planned the experiment (described and figured in 'Roy. Soc. Proc.,' A, vol. 124 (1926)), in which a paper disc impregnated with coloured serum and affixed to a cover-glass is floated face downwards upon the surface of a heavier salt solution. The radial streamers obtained in this experiment are essentially the same as those shown in Plate 42, fig. 7, *infra*.

This experiment also has been censured by Mr. N. K. Adam as non-probative—the gravamen of his criticism being that, just as in the experiment on vertical intertraction, so here, those parcels of the saline solution which come in contact with the albumen would by the disbursal of salt to it, become specifically lighter, with the result that they would ascend through the serum and be deflected by the under surface of the coverglass in such a way as to produce the horizontal streamers which come out radially from the margin of the filter paper.

With respect to the interpretation of the radial streamers I submit that it is inconceivable that rising currents, even if they started at separate foci, as Mr. Adam's theory would require, should, after passing through the texture

\* 'Roy. Soc. Proc.,' A, vol. 108, p. 324 (1925).

of the filter paper, emerge from it in the form of discrete and sharply-outlined streamers. The very utmost that an upstreaming of salt solution (and it would be a general upstreaming) could be expected to effect would be an expulsion of coloured albumen in the configuration of a halo surrounding the disc.

Again *a priori* principles, and also direct inference from what is seen in the vertical intertraction experiment, combine to teach that ascending uncoloured streams of salt solution would be correlated with descending streams of coloured albumen. Now a distinctive feature of the experiment on horizontal intertraction in question is that there is here absolutely no visible downstreaming. Instead of that there can, under favourable circumstances, be discerned just within the periphery of the coloured paper disc a system of paler coloured centripetal striæ—striæ which would, of course, be the natural counterpart of the coloured centrifugal streamers.

But in point of fact, the issue as to whether the horizontal centrifugal streaming is produced by ascending currents impinging upon the filter paper disc is one which can very easily be set at rest by direct experiment. The following—for example—are elucidating experiments :—

(1) To begin with we can, instead of floating our albumen impregnated disc upon the surface of a heavier salt solution, take some three or four of such discs, lay them down one upon the other, dispose them between two glass slides, and then immerse the slides, after they have been firmly clamped together, into a vessel filled with saline solution. Here, in spite of the fact that ascending currents cannot come into operation, horizontal streamers exactly similar to those developed when the disc is afloat on the salt solution, come out from the periphery of the paper. (These are very delicate and difficult to photograph satisfactorily.)

(2) Again, we can, taking an albumen impregnated paper disc, paint its upper and lower surfaces except only the periphery with paraffin wax, and then set the disc afloat upon the saline solution. Here again, despite of upward currents being shut off, the familiar pattern of horizontal streamers is developed.

(3) Further, abandoning for the moment the paper disc, we can make a mixture of equal parts of coloured serum and of a 1 per cent. melted water agar, and then transfer a drop of this jelly to the surface of a slide upon either extremity on which we have placed thin slabs of glass as supports. We now bring down a covering slide upon our jelly in such a way as to flatten it out into a disc, and then we fill in all round it our saline solution. Here, again, despite the fact that no up-streaming currents can impinge upon the surface of the disc, horizontal streamers come out from its periphery (Plate 41, fig. 5).

(4) We take a square coverglass and paint paraffin wax upon its upper surface, leaving bare only a narrow strip along one edge. We then take a *very little* coloured serum, dispose it along the length of this ledge, and then float the coverglass, paraffined side uppermost, upon a 5, or, better, upon a 7.5 per cent. solution of salt, taking care in setting it afloat to bring down the margin that carries the serum last, and as gently as possible upon the salt solution. From the launching raft thus provided the serum is automatically drawn off by the salt solution, and is, as the photograph shows, now dispersed over the surface of the salt solution in the form of a palisade of horizontal streams (Plate 42, fig. 6). Here again it is clear—for the serum is reposing upon a ledge protected from below—that the horizontal streaming cannot be caused by any impact of ascending currents.

(5) Another also very simple experiment is the following—which was specially devised to dispose of Mr. Adam's general criticism that the water employed as a solvent for the salt will, as soon as it has been sufficiently lightened by the disbursal of its solute, ascend through the superincumbent serum. This potential source of fallacy will be removed if we substitute in our paper disc experiment for the solution of salt in water a solution of salt in serum. When having made that modification we set a serum impregnated disc afloat upon a salted serum, we bring out, just as in previous experiments, horizontal centrifugal streamers (Plate 42, fig. 7). Those now obtained differ, however, in two respects from those obtained with the watery saline solution. In the first place, they develop much more slowly; and again they are much less rapidly dispersed by diffusion. The slower development is no doubt correlated with the greater viscosity of the serum, and the slower dispersal with the fact that here diffusion is limited to a diffusion of salt out of one albuminous fluid into another sample of the same albuminous fluid, whereas where albumen is superposed upon a watery salt solution, three several elements—to wit, albumen, water and salt—are transporting themselves by diffusion the one into the other.

Reflexion having now placed at disposal for use in intertractional experiments a saline fluid which does not lie open to the imputation of being convertible into a fluid lighter than the superincumbent serum, the next thing that required doing was to substitute in the vertical intertraction experiment, as had just been done in the disc experiment, salted serum for the plain saline solution. For clearly there was now prospect of converting by this device that combined, intertractional, gravitational and diffusional experiment into one that should be purely intertractional.

A comparison of figs. 1 and 2 which are photographs of down-traction exerted by watery saline solution upon serum, and up-traction by serum upon watery salt solution, with figs. 3 and 4 which are photographs of down-traction exercised by salt serum upon serum and up-traction by serum upon salted serum, will show that the anticipation in question is in point of fact realised.

In figs. 1 and 2 we have intertraction complicated (we may deal with this first) by gravitational phenomena due to alterations which supervene in the down or up-going streamers as soon as these have invaginated themselves sufficiently deeply into the invaded fluids. The bulbous tips of the streamers are, doubtless, the results of downward and upward convectional movements occurring in the streamers when the invading fluid becomes, as the case may be, denser or lighter—the solid ends of the downward directed bulbs being perhaps comparable to what is seen when soap solution gravitates to the bottom of soap bubbles. Further all over the field, in figs. 1 and 2, we have conspicuous evidence of dispersion produced by diffusion.

In figs. 3 and 4, on the contrary, we have practically uncomplicated intertraction. That the disturbing influences of gravity and diffusion have been eliminated is seen in the undistorted shapes of both the down- and up-going streamers and in the definiteness of their outlines. Further—but this point is not brought to cognisance in the photographs—the invading streamers, in lieu of going rapidly to the bottom or, as the case may be, ascending rapidly to the surface, remain for a long time, as it were, suspended in mid-air. It is a case here of the tractor forces of the salted serum being impotent to draw the now salt satisfied, intracted serum any further down hill; and of the tractor action of the unsalted serum being impotent to draw the salt impoverished intracted serum any further up hill.

A few words may now be said upon the technique of bringing into view intertraction figures. Reflexion will show that in every case two conditions must be satisfied. The *first* is that all direct mechanical commingling of the fluids employed must be avoided. These must be disposed accurately the one on the one side, and the other on the other side, of a sharply-defined frontier. *Secondly*, when we want to witness intertraction movements across a particular frontier, we must arrange for the mechanical forces which oppose such transgressional movements to be less powerful than those that oppose intertraction along the frontier. In other words, we must, when minded to witness intertraction in the vertical plane take care that our intention is not defeated by our fluids intertracting horizontally. And similarly, when minded to witness

horizontal incursion we must put impediments in the way of vertical interpenetration.

Both these conditions are satisfied in all the experiments described above, and also in those which still await description. In the case where serum is imposed upon salt solution in a plane walled vertical cell, the required frontier is provided by the lighter serum taking up a position superficial to the heavier salt solution ; while the second requirement is satisfied by the fact that both fluids occupy the entire breadth of the cell, with the result that neither fluid can get round the flanks of the other to set up horizontal intertraction. In short, the circumstances are such that in the vertical intertraction experiment there is bound to be either vertical intertraction or none.

Again, in the experiment in which a serum impregnated paper disc is floated upon the surface of salt solution, the required frontier is obtained by the device of confining (that is the reason why we blot off all excess) our serum within the texture of the filter paper : Further in the same experiment the required obstacle to vertical intertraction is provided by our employing a salt solution of greater specific gravity than the serum. As soon as we grasp the principle that intertraction is bound to follow the line of least resistance, we appreciate why when we float an albumen impregnated disc on an appreciably heavier salt solution we are bound to get horizontal intertraction.

In the further experiments—that in which paper discs are clamped between two glass slides ; that in which we employ a disc or serum agar applied to an upper and a lower slide ; that in which we employ a paraffin-coated disc ; that where we place our serum upon the ledge of a cover glass ; and, lastly, that in which we impose our serum impregnated disc upon salted serum ; we again in each case establish a definite frontier between the serum and salt solution, and we employ also in each case a definite mechanical obstacle to block out vertical, and so compel horizontal, intertraction.

The following experiments further illustrate the principles formulated above :

*Experiment 1.*—We take two shallow glass vessels with vertical walls—such, for example, as the doublets which constitute a Petri dish—and we coat the inner face of the walls of the one dish with paraffin wax—leaving the walls of the other uncoated. We then, having filled into each dish a saturated salt solution three or four times diluted, draw up some coloured serum into a pipette, and transport a small quantum of this first to the one and then to the other dish—letting the serum in each case run down perfectly quietly from the vertical wall of the vessel on to the surface of the salt solution.

In the dish with unparaffined walls the serum will, as soon as it has run

down on to the salt solution, be thrust up against the wall by capillary attraction, and will consequently instead of running off into the centre of the vessel run round its periphery in the form of a coloured crescent. There will now all along the horns of this crescent be a display of vertical intertraction; but, in as much as capillary attraction is here pressing the serum up against the walls, there will be no horizontal intertraction. At the same time, if it so happens that the serum runs down from the wall into the salt solution more rapidly than it can be absorbed into the meniscus, there will in the sinus of the crescent come into view also horizontal intertraction. Here radial streamers will pass off from the walls.

In the vessel with paraffined walls—and the same will, of course, happen in any vessel which is filled brimful with salt solution—there will, for the reason that there will be here no thrusting up of serum against the walls, be no vertical intertraction contiguous to these. Instead of that the serum will flow off from the walls either in the form of diverging horizontal streamers, or, when an excess of serum has been employed, in the form of a superficial pellicle from which afterwards horizontal streamers will flow off in all directions. But here, also, vertical intertraction may come into view—descending streams coming off the under surface of any pellicle that has appreciable depth, and also from the under surface of any derivative streamers which may be heavy enough to indent the surface of the salt solution.

In summary, if we employ in these experiments only very minute quantities of serum there will come into view in the vessel with unparaffined walls only vertical, and in the vessel with paraffined walls only horizontal, intertraction. If, on the other hand, we employ somewhat larger quanta of serum there will be superadded, in the one case, to the vertical, horizontal, and, in the other case, to the horizontal, vertical intertraction.

*Experiment 2.*—We take, again, a vessel with vertical walls, and fill it, let us say, half full with our 4 to 5 times diluted saturated saline solution, and tilt it so that its walls may make on the upper side, an acute, and on the lower side an obtuse angle with the surface of the contained fluid. We now, taking up into a pipette two equal portions of coloured serum, let the one run down very gently from the upper, and the other in a similar manner from the lower wall upon the surface of the saline solution.

The first of these quanta will give only vertical intertraction—for here the circumstance that the free margin of the meniscus descends steeply to the surface of the salt solution constitutes an obstacle to horizontal intertraction.

The quantum of serum which has been expelled upon the lower wall of the

vessel will, on the contrary, in conformity with the fact that the free border of its meniscus slopes off very gradually into the general plane of the surface of the salt solution, give horizontal intertraction. This portion of serum will, of course, in addition to furnishing horizontal streamers from its free border, furnish also descending streamers from its inner margin which is applied to the walls of the vessel.

*Experiment 3.*—We roll out a pellet of plasticine into a very thin cylinder, flatten this out, and then lay down two strips of it transversely upon an ordinary microscopic slide, disposing them at such distance that the interval can be spanned by a coverglass. We now press a coverglass firmly down upon these supports until only a narrow chink is left between our glass surfaces. Into the cell thus formed we fill in a saline solution which is only just heavier than our coloured serum. Then—turning up our slide so that it shall lie in the vertical plane—we run in midway along the upper border of the coverglass a drop of our coloured serum. This will, of course, float upon the salt solution, but will hang down in it in the form of a plano-convex figure with its convexity downwards. The conditions will here be comparable to those which present themselves when dealing with superficial streamers which are heavy enough to indent the surface of the salt solution. Descending streamers will now come off from the under surface of the serum, and at the same time the serum will be carried out right and left in a thin line along the surface, until arrested by the lateral confines of the cell.

When, filling in the cell now with a somewhat lighter salt solution, we introduce a drop of serum midway along the lower border of the cover-glass, that drop, after first disposing itself in the form of a plano-convex figure with convexity uppermost, flattens itself down under the influence of gravity, disposing itself as a layer at the bottom of the cell. No sooner is this gravitational movement completed than intertraction phenomena begin to manifest themselves. Inasmuch as horizontal intertraction is barred by the fact that the serum cannot go any further right or left, we have here an upward streaming. Further, it may be noted that the upstreaming begins first in the median line of the cell, where the serum is still a little indented upwards—thus illustrating the general principle that eminently favourable conditions for the occurrence of intertraction are provided when the one fluid is lying in a sulcus provided by the other.

*Experiment 4.*—We get ready a shallow dish containing a fourfold diluted saturated salt solution, and then make an implanting spatula by taking a square coverglass and coating it with paraffin wax front and back, except for



a narrow strip left upon one side along one margin. We then take any kind of a rod to serve as a handle, and fix it with plasticine to the edge of the cover-glass which lies opposite to that upon which we have formed the implanting ledge. We now spread a small drop of coloured serum upon a microscopic slide; and having done so, charge our spatula by carrying it, with its ledge down-turned, along the face of that slide. Then, holding the cover-glass perpendicular and steadying our hand, we touch off the serum upon the surface of the salt solution and withdraw the spatula. This operation, if accurately carried out, gives us a narrow longitudinal implantation; and from this we obtain—inasmuch as our implantation has appreciable depth as well as length—uncomplicated vertical intertraction. It takes the form of a very picturesque palisade of descending streamers. If, on the other hand, our technique has been imperfect, and we have (*a*) either taken up too much serum upon our spatula, or (*b*) have dipped too deeply, or (*c*) have in implanting not held the coverglass absolutely perpendicular, we get in addition to vertical intertraction a certain amount of horizontal dispersion, and, again, from this there may be developed horizontal intertraction figures.

As a second procedure, we take as our spatula a coverglass of which one surface only has been coated with paraffin and the other moistened with water. We place a charge of coloured serum upon the moistened face of the cover-glass and then bring this down at an obtuse angle upon the surface of the salt solution. The serum will now, in conformity with the fact that we have formed a convex meniscus, stream off upon the salt solution in the form of a delicate pellicle, and this will, if we hold our hand perfectly steady, give intertraction figures such as are obtained with a launching raft.

We now, with a view to furnishing ourselves with a vertical receiving screen which we can set up in our salt solution, take a coverglass and set it upright in a pellet of plasticine—flattened out so as to provide a stand or foot.

When this has been put into position in the salt solution, we recharge the bare face of our coverglass with coloured serum, and, sloping this spatula as before, bring it down very gently upon the salt solution a little distance in front of our vertical receiving screen. The serum will now, as before, stream off upon the surface of the salt solution, will impinge upon the coverglass, will pack itself up against this, and will then descend along this obstacle in a palisade of streamers.

A final word now requires to be said in justification of the position taken up by me above with respect to Dr. Jessop and Mr. Adam's discountenancing of intertraction, and their impugning of its claim to rank as a *vis operans* which

brings about the commixture of certain pairs of fluids. I have ventured to say that all the arguments which were newly adduced in their paper were deductions from experiments which were insufficiently thought out.

The first in order of these arguments is Dr. Jessop and Mr. Adam's joint contention that no intertraction streamers appear when shallow pools of fluid are placed side by side upon a glass slide. Photographs 8 and 9 show that all that is required for the bringing into view intertraction figures, in the case of fluids disposed side by side in shallow pools, is to exercise care to prevent any preliminary commingling of the fluids.

The intertraction figures depicted in Photo. 8 were obtained by laying down four superposed narrow strips of filter paper transversely upon a microscopic slide, clamping down another slide firmly upon these, and then filling in on one side coloured serum, and then, as soon as a frontier had been established by the inhibition of the filter paper with serum, filling in the other cell with saline solution.

In the experiment depicted in Photograph 9 another quite simple device was employed. Here a non-tapering capillary tube was coated with paraffin, and then this was scraped off upon one side in such a way as to form a longitudinal groove. This done the paraffined capillary tube was inserted (with the longitudinal groove directed laterally) between two slides which were supported at their ends upon thin glass slabs. Communication between the two sides of the slide having been in this manner cut off, coloured serum was filled into one compartment, and salt solution into the other. And finally when the fluids were in position the capillary tube was rotated in such a manner as to bring the groove aforementioned into the vertical plane, and so open up a narrow channel of communication between the fluids. The opening of this tap is immediately followed by the development of horizontal streamers.

I pass now from the consideration of Dr. Jessop and Mr. Adam's experiment with shallow pools to Mr. Adam's experiments with albumen impregnated discs.

These have furnished three observations which he brings forward as discountenancing the theory of intertraction. The *first* is that when an albumen impregnated disc which is floating upon a heavier salt solution is tilted, the streamers instead of coming out all round, come out only from the upper edge of the disc. The *second* is that radial streamers fail to make their appearance when the disc is placed *in* (the italics are mine) a shallow pool of salt solution. The *third* is that when a disc soaked in coloured salt solution is floated upon a heavier albuminous solution "the colour is washed out in descending instead of in radial streamers."

To the animadversions founded upon the two first of these observations perfectly obvious replies can be given.

With regard to the *first*, it has been shown above that intertraction always follows the lines of least resistance. When, therefore, gravity is brought in operation differentially by tilting the disc it is only to be expected that upward streaming should (since it will be reinforced by gravity) continue (and be increased); and that downward streaming, since it would be opposed by gravity, should be suppressed.

With regard to the objection that horizontal streamers fail to appear when the albumen impregnated disc is immersed (for I take it that the descriptive term *immersion* denotes immersion), it will be plain that, for as much as the entire upturned face provides a much wider portal of outlet than the edge of this disc, and since up-traction through this face would be aided by gravity, it is to be expected that vertical should in the circumstances replace horizontal intertraction.

I come now to Mr. Adam's third animadversion—that founded upon the observation that a disc of filter paper soaked in coloured salt solution gives, when floated upon a heavier albuminous solution, descending instead of radial streamers. I had neglected to make this experiment, but have now verified Mr. Adam's finding.

Mr. Adam's point, however, has, as will be appreciated, lost all serious theoretical importance by its having been demonstrated above that intertraction is a *vera causa* of radial streaming.

There would, despite of that, be a blot upon the theory of intertraction, if a lighter salt solution floated upon a heavier albuminous solution did not give a radial streaming.

I therefore, going over in my mind the principles of the technique for obtaining intertraction figures as set out above, took counsel with myself after the following fashion: "It must be possible to obtain radial streamers from the salt solution impregnated disc, if by compressing the disc between two sheets of glass, I block all exit of salt solution from the upper and lower faces of the disc."

When this is done typical radial streamers are obtained, but the streamers are too delicate to give a satisfactory photograph.

"Again," so I reflected, "it should be possible to get horizontal intertraction figures by taking a slab of salted and coloured agar, and interposing this between two slides, and then surrounding it with an albuminous fluid."

Photograph 10 shows that we can in this manner obtain very good intertraction figures.

"Lastly," so I reasoned further, "the obtaining of radial streamers

from a disc of any lighter fluid, floated upon any heavier fluid, must depend upon there being between the fluids a difference of specific gravity which shall be sufficient to offer effective opposition to vertical intertraction."

Giving effect to this reflection I took a particular albuminous fluid upon which a disc soaked in 3 per cent. coloured salt solution had given notable downward streaming, and inspissated it by evaporating it down in an incubator to three-fourths of its original volume. When that had been done, and again a disc soaked in 3 per cent. coloured salt solution was superimposed, the tardily developed horizontal intertraction figures which are shown in Photograph 11 were obtained.

Further points with regard to the orientation of intertraction now suggested themselves. In the first place it became evident that, whether we float a disc impregnated with salt solution upon an albuminous fluid, or a disc impregnated with albuminous fluid upon salt solution, there is bound to be at one end of the scale a difference of specific gravity such as will give only horizontal intertraction, and at the other end of the scale a difference which will give only vertical intertraction, and somewhere in the middle of the scale a difference of specific gravity which will give either vertical and horizontal intertraction (the second supervening upon the first) or else diagonal intertraction. In point of fact all these orientations and varieties of intertraction can be obtained. For example when a disc soaked in 3 per cent. coloured salt solution was imposed, instead of upon the inspissated albuminous fluid before spoken of, upon the uninspissated fluid, there was developed, instead of purely horizontal intertraction, vertical intertraction, followed (after ten or more minutes when, no doubt, the hydrocele fluid had become denser by inflow of salt) by definite horizontal intertraction. And again while a disc of filter paper impregnated with human serum (the coloured human serum employed had a specific gravity corresponding to that of a 3 to 3.5 per cent. salt solution) was imposed upon a salt solution of 3 per cent. or over gives in every case only horizontal intertraction; such a disc imposed upon 2 per cent. salt solution gives vertical followed by horizontal intertraction; or according to circumstances "*diagonal intertraction*"—the streamers descending at an angle of perhaps  $45^\circ$  to the vertical, producing a figure very similar to that of a wicker hen coop.

Finally, the consideration of the facts just detailed suggests that in flotation experiments such as are here in question, factors other than differences in specific gravity may influence the results. It would seem probable—regarding for example the fact that 3 per cent. salt solution offers adequate resistance to the

downward streaming of serum from a filter paper disc—that the adhesion of the serum to the filter paper, and, in correlation with that, the closer or looser texture of the filter paper may, when the orientation of intertraction hangs in the balance, determine its direction. And in view of the fact that there is not an exact parallelism between the results obtained when a serum impregnated disc is floated upon salt solution, and those obtained when a salt impregnated disc is floated upon serum, it may perhaps be suggested that while a loosely textured filter paper may give a sufficiently close frontier for serum, a more closely textured filter paper may be required for salt solution.

In conclusion I beg to express my gratitude to Mr. R. M. Fry for valuable help in my experiments and for the photographs which illustrate this paper.

*[Postscript with additional figure (fig. 12) added March 9th, 1927.—*In the course of proof correction it suggested itself to me that a pattern of centripetal streamers would infallibly be developed if a crystallising dish or similar vessel was filled with saturated salt solution, and a meniscus of coloured serum was then run round its periphery. Further it suggested itself that if a cylindrical pillar was set up in the centre and was ringed round with coloured serum there would be obtained from the meniscus a pattern of centrifugal streaming. And finally, consideration indicated that a pattern of combined centripetal and centrifugal streaming would be obtained if there were placed upon the floor of the dish a glass ring (such a glass ring as is used for the construction of a live-cell), and saturated salt solution were then poured without and within nearly up to the top of the ring, and then coloured serum was painted on each side with a small camel's hair brush.

In all the three variants of the experiment here outlined singularly beautiful horizontal and perfectly regular intertraction figures are obtained:—the pink (eosin-coloured) centripetal streams in variants 1 and 3 of the experiment reminding one remotely of the Japanese flag; while the centrifugal streams obtained in variants 1 and 3 call to mind quite vividly the corona of tentacles coming off from the disc of a fully expanded sea-anemone.

The photograph (fig. 12) exhibits the pattern of combined centripetal and centrifugal horizontal intertraction obtained in the third variant of the experiment. It is inadequate in the respect that it does not bring out the fact that there is upon the walls of the central pillary also a little vertical intertraction.]



1



2a



2b



3a



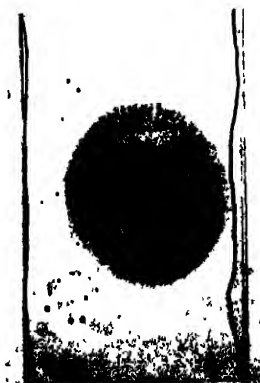
3b



4a



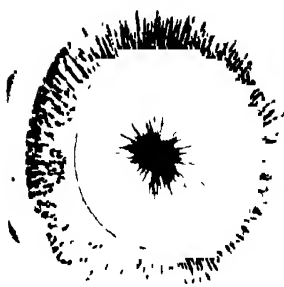
4b



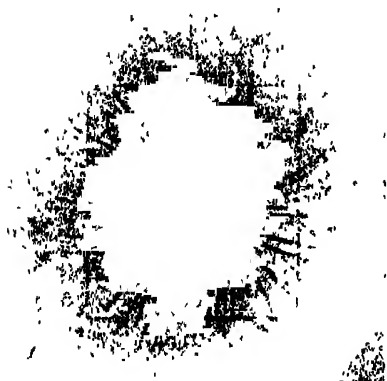
5



6



12



7



8



9



10

11



EXPLANATION OF PLATES.

PLATE 41.

- FIG. 1.—*Downward Traction*.—Coloured serum imposed upon uncoloured 5 per cent. salt solution.
- FIG. 2 (a) and (b).—*Upward Traction*.—Uncoloured serum imposed upon coloured 10 per cent. salt solution.
- FIG. 3 (a) and (b).—*Downward Traction*.—Coloured serum imposed upon uncoloured 2.5 per cent. salted serum.
- FIG. 4 (a) and (b).—*Upward Traction*.—Uncoloured serum imposed upon coloured 3 per cent. salted serum.
- FIG. 5.—*Horizontal Traction*.—A disc of agar impregnated with coloured serum has been interposed between two slides, and the cell thus made has been filled in with 5 per cent. salt solution.

PLATE 42.

- FIG. 6.—*Horizontal Traction*.—Coverglasses which have been coated with paraffin except for a bare ledge on the right-hand margin have been charged with coloured serum along this ledge, and have been set afloat upon 5 per cent. salt solution.
- FIG. 7.—*Horizontal Traction*.—A disc of filter paper which has been impregnated with coloured serum has been set afloat upon an uncoloured serum containing 5 per cent. of salt.
- FIG. 8.—*Horizontal Traction*.—A cell formed of two superposed slides has been divided into two compartments by clamping the slides together upon a number of superposed strips of filter paper. Coloured serum was now filled into the left-hand compartment, and when this had soaked into the filter paper barrier, uncoloured 5 per cent. salted serum into the right-hand compartment.
- FIG. 9.—*Horizontal Traction*.—The arrangement is the same as in fig. 8, except that here the cell was divided into two compartments by a capillary tube coated with paraffin except along a narrow longitudinal groove, which furnished a narrow channel of communication.
- FIG. 10.—*Horizontal Traction*.—Here a coloured slab of agar, which had a salt content equivalent to 2.5 per cent. salt solution, was interposed between two slides and was then surrounded by an uncoloured hydrocele fluid.
- FIG. 11.—*Horizontal Traction*.—A disc of filter paper soaked in 3 per cent. coloured salt solution was floated upon an uncoloured inspissated hydrocele fluid.
- FIG. 12.—*Horizontal Centrifugal and Centripetal Intertraction* proceeding from a twin meniscus disposed on either side of a glass ring standing in saturated salt solution.



### *The Refractive Indices of Nicotine.*

By Colonel J. W. GIFFORD, F.R.A.S., and Prof. T. M. LOWRY, F.R.S.

(Received January 17, 1927.)

Measurements of the refractive indices of nicotine have been made by Gladstone and Dale and by Brühl. Their numbers are lower throughout than those now submitted. The instruments and hollow quartz prism used were the same that were employed for the measurement of the refractive indices of water,\* and had more recently been used for measuring the refractive indices of benzene and cyclo-hexane.†

At the outset a difficulty was encountered. When the hollow quartz prism was filled with water, its sides having previously been held in position by rubber bands, all air bubbles got rid of and the stopper sealed with mercury, the sides were held firmly in position by atmospheric pressure alone and there was no further trouble. But with benzene and cyclo-hexane this was not the case. and rubber bands of any kind were quickly attacked and made useless. It was, therefore, necessary to attach the sides to the body of the prism by some sort of aqueous cement. The glycerine jelly used by microscopists for mounting was found to meet all requirements. But it was soon found that nicotine was a solvent of all the gelatines, gums, rubber, wax and paraffins of different melting points that were tried, and that any cements made of them were quickly attacked. The only thing remaining seemed to be to complete the polishing of the body of the prism, which had until now been left in the grey, and to place the sides in optical contact with it, a somewhat risky and delicate operation, which was successfully carried out by Messrs. A. Hilger, Ltd. Some rather troublesome reflections from the newly-polished surfaces had to be masked out and then further trouble from the prism was at an end.

*Material.*—The nicotine had been purified through the zinc chloride compound by the method of Ratz ('*Monatshefte*,' vol. 26, p. 1241, 1905), and was distilled in a current of hydrogen under reduced pressure until a colourless distillate was obtained. In this way the optical rotatory power of the sample was raised to  $\alpha_{D_{461}}^{20} = -205^\circ$  in a 1-dm. tube, as compared with the ideal value of  $206^\circ$ , which is the highest that we have been able to reach by this method of purification.

\* '*Roy. Soc. Proc., A*, vol. 78, p. 406 (1907).

† '*Roy. Soc. Proc., A*, vol. 104, p. 430 (1924).

*Method of observation.*—This was that by which all three sides of the prisms were brought into use, and the mean of the three deviations taken as described in an earlier paper.\*

*Temperature and pressure.*—These were determined before and after each series of group measurements and corrections were made as already described.†

*Temperature refraction coefficient.*—For this purpose several complete measurements of the iron line 5270 Å.U. (line E of the solar spectrum) at different temperatures were made. The mean result gave a coefficient of  $-0.0004027$  for  $1^{\circ}$  C.

*Range of the spectrum.*—Absorption of all rays took place beyond the hydrogen line 4341 Å.U. (generally known as G'), the mercury arc line at 4041 being already too faint for measurement. There was, therefore, no ultra-violet, even though the brownish tint which the material took on later had at this time not yet appeared.

Refractive Indices of Nicotine at  $15^{\circ}$  C.

Wave-length.	Refractive index.	Wave-length.	Refractive index.
A'. 7685 K <sub>2</sub>	1.52061 <sub>6</sub>	E 5270 Fe	1.53514 <sub>8</sub>
B'. 7065 H <sub>2</sub>	1.52294 <sub>9</sub>	F. 4861 H <sub>2</sub>	1.54035 <sub>9</sub>
6708 Li	1.52452 <sub>7</sub>	♠ 4678 Cd	1.54317 <sub>8</sub>
C. 6563 H <sub>2</sub>	1.52520 <sub>6</sub>	4471 He	1.54699 <sub>9</sub>
D. 5893 Na	1.52939 <sub>9</sub>	4413 Cd <sub>7</sub>	1.54808 <sub>9</sub>
A. 5608 Pb	1.53177 <sub>9</sub>	G. 4341 H <sub>γ</sub>	1.54935 <sub>9</sub>
5461 H <sub>2</sub>	1.53291 <sub>7</sub>		

These indices have been carried to seven figures, but greater accuracy than an error of 1 or 2 units in the sixth is not claimed.

\* 'Roy. Soc. Proc.,' A, vol. 70, p. 329 (1902).

† 'Roy. Soc. Proc.,' A, vol. 100, p. 621 (1922).

*The Stability of an Infinite System of Circular Vortices.*

By Prof. H. LEVY, M.A., D.Sc., and A. G. FORSDYKE, A.R.C.Sc., B.Sc.

(Communicated by S. Chapman, F.R.S.—Received December 10, 1926—Revised February 12, 1927.)

A system of equal circular vortex filaments have their centres evenly spaced along a straight line, and their planes at right angles to this line. The present investigation is concerned with the stability or instability of such an arrangement. The corresponding problem in two dimensions has been dealt with by Kármán\* who considered the case of two infinite trails of parallel rectilinear vortices, with the object of applying his results to the resistance of an infinite cylinder moving in a fluid and to the state of motion in the rear of the cylinder. The infinite system of circular vortex filaments, on the other hand, may be supposed, in certain circumstances to be discussed in a later paper, to be generated in the rear of a three-dimensional body in motion in a fluid. The present investigation may therefore be regarded as a first step towards an examination of the three-dimensional problem analogous to that treated by Kármán for two dimensions.

A special difficulty arises in an investigation of this type from the fact that the system of vortex rings, possessing an infinite number of degrees of freedom, are capable of adopting an infinite number of possible configurations about the position of equilibrium.

The method followed here is to seek for possible normal modes of vibration of the system. These may be separated into two kinds:—

- (a) Those which involve an oscillatory motion of each ring as a whole along the axis of symmetry with corresponding oscillations in the radius of each ring.
- (b) Those which involve a periodic oscillation of the central filament of the ring about the steady circular position.

For the purpose of the present paper it will suffice to deal with (a).

MOTION OF THE UNDISTURBED SYSTEM.

§ 1. The vortex rings being infinite in number, any one of them may be regarded as the central ring with respect to which the system is symmetrical; and so

\* 'Phys. Zeit.', XIII (1912).

the equations of motion found for any particular ring will apply to each of the others. It follows that the radius of each ring remains constant; also that each ring, and therefore the whole system, moves forward in the direction of its axis with a definite axial velocity, which for convenience of treatment is considered in two parts, viz. :-

- (a) A velocity  $U$ , equal to the axial velocity of a single vortex ring due to its own influence only.
- (b) A velocity  $V$  due to the influence of the remaining rings of the system.

Denote the radius of the vortex rings by  $b$  and the strength by  $\kappa$ . Suppose their centres spaced at equal intervals  $a$  along the common axis of the rings. The section of each vortex is considered to be circular in form and of radius  $\epsilon$ , which is small compared with  $a$  and  $b$ . Then

$$U = \frac{\kappa}{4\pi b} \left\{ \log \frac{8b}{\epsilon} - \frac{1}{2} \right\}. \quad (1)$$

To find  $V$ , take a system of rectangular axes  $xyz$  with origin at the centre of the central vortex ring and the  $y$  axis in the positive direction of the axis of the rings. Let  $A$  be the point where the  $x$  axis meets the central vortex ring. On the ring " $na$ ,"  $n$  being any integer and this ring having its centre at the point  $(0, na, 0)$ , let  $B$  be a point whose azimuth, measured from the direction of the  $x$  axis, is  $\phi$ . We consider the motion at  $A$  due to an element of vortex  $ds$  at  $B$ . The whole velocity at  $A$  is obtained by integrating this element of velocity round the ring " $na$ " and summing for all the rings of the system.

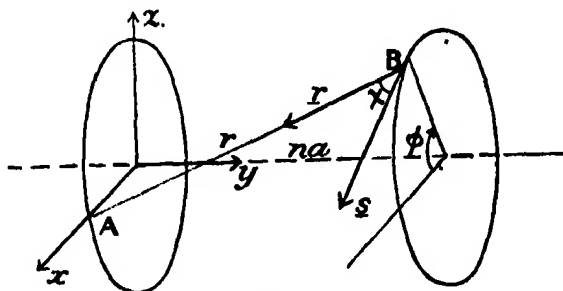


FIG. 1.

Denote by  $\mathbf{s}$  the unit vector in the direction of the vorticity at  $B$ , and by  $\mathbf{r}$  the unit vector along  $BA$ , the length of  $BA$  being  $r$ . The element of velocity at  $A$  is then in the direction  $[\mathbf{s}, \mathbf{r}]$ , which has direction cosine

$$\frac{1}{\sin \chi} \{s_y r_z - s_z r_y\}, \quad \frac{1}{\sin \chi} \{s_z r_x - s_x r_z\}, \quad \frac{1}{\sin \chi} \{s_x r_y - s_y r_x\},$$

where  $\chi$  is the angle between  $r$  and  $s$  and  $r_x, r_y, r_z, s_x, s_y, s_z$  are the direction cosines of  $r$  and  $s$  respectively.

Further, the magnitude of the element of velocity at A is  $\frac{\kappa}{4\pi} \frac{\sin \chi \cdot ds}{r^2}$ , so that the axial component of this is

$$\delta V = \frac{\kappa}{4\pi} \cdot \frac{ds}{r^2} \{s_x r_x - s_z r_z\}. \quad (2)$$

Now co-ordinates of A =  $b, 0, 0$ ,

co-ordinates of B =  $b \cos \phi, na, b \sin \phi$ ,

$$s_x, s_y, s_z = \sin \phi, 0, -\cos \phi,$$

$$r_x, r_y, r_z = \frac{1}{r} \{b(1 - \cos \phi), -na, -b \sin \phi\}.$$

Therefore

$$\delta V = \frac{\kappa}{4\pi} \frac{b^2 d\phi}{r^3} (1 - \cos \phi),$$

so that

$$V = \frac{\kappa b^2}{4\pi} \sum'_{n=-\infty}^{+\infty} \int_0^{2\pi} \frac{(1 - \cos \phi) d\phi}{\{2b^2(1 - \cos \phi) + n^2 a^2\}^{3/2}},$$

the  $\Sigma'$  indicating that the value  $n = 0$  is to be excluded from the summation.

This gives

$$V = \frac{\kappa b^2}{2\pi} \sum_{n=1}^{\infty} \int_0^{2\pi} \frac{(1 - \cos \phi) d\phi}{\{2b^2(1 - \cos \phi) + n^2 a^2\}^{3/2}}. \quad (3)$$

This series is convergent, behaving at infinity like  $\Sigma 1/n^3$ .

### MOTION OF THE DISTURBED SYSTEM.

§ 2. Consider a disturbance in which the rings retain their circular form, the ring at " $na$ " undergoing a small axial displacement  $\alpha_n$  and a small radial increment  $\beta_n$ , subject to the relations

$$\begin{aligned} \alpha_n &= (-1)^n \alpha_0. \\ \beta_n &= \beta_0 \text{ if } n \text{ is even.} \\ \beta_n &= \beta_1 \text{ if } n \text{ is odd.} \end{aligned}$$

This includes the possibility of displacements  $\alpha_n$  in opposite directions along the axis, causing different increases in the respective radii of the rings.

Referring to the diagram, we now have

Co-ordinates of A =  $b + \beta_0, \alpha_0, 0$ .

Co-ordinates of B =  $(b + \beta_n) \cos \phi, na + \alpha_n, (b + \beta_n) \sin \phi$ .

$$\begin{aligned}
 \text{Therefore } r^2 &= \{(b + \beta_0) - (b + \beta_n) \cos \phi\}^2 + \{\alpha_0 - (na + \alpha_n)\}^2 \\
 &\quad + (b + \beta_n)^2 \sin^2 \phi \\
 &= 2b^2 (1 - \cos \phi) + 2b (1 - \cos \phi) (\beta_0 + \beta_n) + n^2 a^2 \\
 &\quad + 2na (\alpha_n - \alpha_0) \text{ to first order,} \\
 &= J + \gamma, \text{ where} \\
 J &= \{2b^2 (1 - \cos \phi) + n^2 a^2\} \\
 \gamma &= \{2b (1 - \cos \phi) (\beta_0 + \beta_n) + 2na (\alpha_n - \alpha_0)\}.
 \end{aligned}$$

Hence  $1/r^3 = J^{-3/2} - \frac{3}{2} J^{-5/2} \cdot \gamma$  to first order.

$$\begin{aligned}
 \text{Again } r_x, r_y, r_z &= 1/r \{(b + \beta_0) - (b + \beta_n) \cos \phi, \alpha_0 - (na + \alpha_n), \\
 &\quad - (b + \beta_n) \sin \phi\} \\
 s_x, s_y, s_z &= \sin \phi, \quad 0, \quad -\cos \phi.
 \end{aligned}$$

The radial component of the element of velocity at A is therefore

$$\begin{aligned}
 &\frac{\kappa}{4\pi} \frac{ds}{r^3} \{s_y r_z - s_z r_y\} \\
 &= \frac{\kappa}{4\pi} \cdot \frac{\cos \phi \cdot d\phi}{r^3} \{-nab + b(\alpha_0 - \alpha_n) - na\beta_n\} \text{ to first order,} \\
 &= \frac{\kappa}{4\pi} \cos \phi \cdot d\phi [-nab \{J^{-3/2} - \frac{3}{2} J^{-5/2} \gamma\} + \{b(\alpha_0 - \alpha_n) - na\beta_n\} J^{-3/2}].
 \end{aligned}$$

We therefore obtain for the radial velocity at A

$$\begin{aligned}
 \frac{\kappa}{4\pi} \sum_{n=-\infty}^{\infty} \int_0^{2\pi} &\left[ \frac{-nab \cos \phi}{\{2b^2 (1 - \cos \phi) + n^2 a^2\}^{3/2}} \right. \\
 &+ \frac{nab \cos \phi \{2b (1 - \cos \phi) (\beta_0 + \beta_n) + 2na (\alpha_n - \alpha_0)\}}{\{2b^2 (1 - \cos \phi) + n^2 a^2\}^{5/2}} \\
 &\left. + \frac{b \cos \phi (\alpha_0 - \alpha_n)}{\{2b^2 (1 - \cos \phi) + n^2 a^2\}^{3/2}} - \frac{na\beta_n \cos \phi}{\{2b^2 (1 - \cos \phi) + n^2 a^2\}^{3/2}} \right] d\phi.
 \end{aligned}$$

The first term, representing the radial velocity in the undisturbed state, vanishes on summation, as also do the terms involving  $\beta_0, \beta_n$ , since  $\beta_n = \beta_{-n}$ .

Thus

$$\begin{aligned}
 \frac{d\beta_0}{dt} &= \frac{\kappa}{2\pi} \sum_{n=1}^{\infty} \{3n^2 a^2 b \int_0^{2\pi} \frac{\cos \phi (\alpha_n - \alpha_0) d\phi}{\{2b^2 (1 - \cos \phi) + n^2 a^2\}^{5/2}} \\
 &\quad + b \int_0^{2\pi} \frac{\cos \phi (\alpha_0 - \alpha_n) d\phi}{\{2b^2 (1 - \cos \phi) + n^2 a^2\}^{3/2}}.
 \end{aligned}$$

This vanishes for  $n$  even, and when  $n$  is odd  $\alpha_n = -\alpha_0$ , so it becomes

$$\frac{d\beta_0}{dt} = \sum_{n=1}^{\infty} \frac{\kappa \alpha_0}{2\pi} \left[ 2b \int_0^{2\pi} \frac{\cos \phi \cdot d\phi}{\{2b^2(1-\cos \phi) + n^2 a^2\}^{3/2}} - 6n^2 a^2 b \int_0^{2\pi} \frac{\cos \phi \cdot d\phi}{\{2b^2(1-\cos \phi) + n^2 a^2\}^{5/2}} \right], \quad (4)$$

where  $\Sigma_0$  indicates that only the odd values of  $n$  are to be included in the summation.

To investigate the axial motion, consider first only that part of the velocity of the central ring due to itself. We have from (1)

$$U = \frac{\kappa}{4\pi b} \left\{ \log \frac{8b}{\epsilon} - \frac{1}{4} \right\}.$$

The change in this consequent upon a small radial increment  $\beta_0$  is

$$\begin{aligned} & \beta_0 \frac{\kappa}{4\pi} \frac{d}{db} \left\{ \frac{1}{b} \log \frac{8b}{\epsilon} - \frac{1}{4b} \right\} \\ &= \beta_0 \frac{\kappa}{4\pi b^2} \left\{ \frac{5}{4} - \log \frac{8b}{\epsilon} \right\} \\ &= H\beta_0 \quad (\text{say}). \end{aligned} \quad (5)$$

Secondly, considering the axial velocity of the central ring due to the remaining rings of the system, we have for the element of velocity due to  $ds$  at B

$$\begin{aligned} & \frac{\kappa}{4\pi} \frac{ds}{r^2} \{s_z r_x - s_x r_z\} \\ &= \frac{\kappa}{4\pi} d\phi [b^2(1-\cos \phi) \{J^{-3/2} - \frac{3}{2} J^{-5/2} \gamma\} + \{2b\beta_n - b\cos \phi(\beta_0 + \beta_n)\} J^{-3/2}]. \end{aligned}$$

This gives for the whole axial velocity

$$\begin{aligned} & \frac{\kappa}{4\pi} \sum_{n=-\infty}^{\infty} \left[ \int_0^{2\pi} \frac{b^2(1-\cos \phi) d\phi}{\{2b^2(1-\cos \phi) + n^2 a^2\}^{3/2}} \right. \\ & \quad - \frac{3}{2} \int_0^{2\pi} \frac{b^2(1-\cos \phi) \{2b(1-\cos \phi)(\beta_0 + \beta_n) + 2na(\alpha_n - \alpha_0)\} d\phi}{\{2b^2(1-\cos \phi) + n^2 a^2\}^{5/2}} \\ & \quad + 2b\beta_n \int_0^{2\pi} \frac{d\phi}{\{2b^2(1-\cos \phi) + n^2 a^2\}^{3/2}} \\ & \quad \left. + b(\beta_0 + \beta_n) \int_0^{2\pi} \frac{\cos \phi \cdot d\phi}{\{2b^2(1-\cos \phi) + n^2 a^2\}^{3/2}} \right]. \end{aligned}$$

The first term we neglect, since, being the corresponding part of the general velocity of advance  $V$ , it is independent of the disturbance. Further, the terms involving  $\alpha_0, \alpha_n$  vanish on summation, leaving

$$\begin{aligned} \frac{\kappa}{2\pi} \sum_{n=1}^{\infty} \left\{ -3b^3 (\beta_0 + \beta_n) \int_0^{2\pi} \frac{(1 - \cos \phi)^2 \cdot d\phi}{\{2b^2(1 - \cos \phi) + n^2 a^2\}^{5/2}} \right. \\ \left. + 2b\beta_n \int_0^{2\pi} \frac{d\phi}{\{2b^2(1 - \cos \phi) + n^2 a^2\}^{3/2}} \right. \\ \left. - b(\beta_0 + \beta_n) \int_0^{2\pi} \frac{\cos \phi \cdot d\phi}{\{2b^2(1 - \cos \phi) + n^2 a^2\}^{3/2}} \right\}. \end{aligned}$$

§ 3. We have now to reduce the integrals occurring in (4) and (6) to standard forms. By putting  $\theta = \phi/2$  and  $c = na/2b$  we obtain

$$\begin{aligned} \int_0^{2\pi} \frac{\cos \phi \cdot d\phi}{\{2b^2(1 - \cos \phi) + n^2 a^2\}^{3/2}} &= \frac{1}{8b^3} \int_0^{\pi} \frac{(1 - 2 \sin^2 \theta) d\theta}{(\sin^2 \theta + c^2)^{3/2}} \\ &= \frac{1}{2b^3} \left\{ \int_0^{\pi/2} \frac{-2 \cdot d\theta}{(\sin^2 \theta + c^2)^{3/2}} + \int_0^{\pi/2} \frac{(1 + 2c^2) d\theta}{(\sin^2 \theta + c^2)^{3/2}} \right\}. \end{aligned} \quad (7)$$

$$\int_0^{2\pi} \frac{\cos \phi \cdot d\phi}{\{2b^2(1 - \cos \phi) + n^2 a^2\}^{5/2}} = \frac{1}{8b^5} \left\{ \int_0^{\pi/2} \frac{-2d\theta}{(\sin^2 \theta + c^2)^{5/2}} + \int_0^{\pi/2} \frac{(1 + 2c^2) d\theta}{(\sin^2 \theta + c^2)^{5/2}} \right\}. \quad (8)$$

$$\int_0^{2\pi} \frac{(1 - \cos \phi)^2 d\phi}{\{2b^2(1 - \cos \phi) + n^2 a^2\}^{5/2}} = \frac{1}{2b^5} \int_0^{\pi/2} \frac{\sin^4 \theta \cdot d\theta}{(\sin^2 \theta + c^2)^{5/2}}. \quad (9)$$

$$\int_0^{2\pi} \frac{d\phi}{\{2b^2(1 - \cos \phi) + n^2 a^2\}^{5/2}} = \frac{1}{2b^5} \int_0^{\pi/2} \frac{d\theta}{(\sin^2 \theta + c^2)^{5/2}}. \quad (10)$$

Now  $\int_0^{\pi/2} \frac{d\theta}{(\sin^2 \theta + c^2)^{1/2}}$  is immediately reducible to a complete elliptic integral. The other integrals (7) ... (10) require further reduction before this is possible.

$$(a) \quad \int_0^{\pi/2} \frac{d\theta}{(\sin^2 \theta + c^2)^{3/2}}.$$

Consider

$$\Theta_1 = \frac{d}{d\theta} \left\{ \frac{\frac{1}{2} \sin 2\theta}{(\sin^2 \theta + c^2)^{1/2}} \right\} = \frac{1 - 2 \sin^2 \theta}{(\sin^2 \theta + c^2)^{1/2}} + \frac{\sin^4 \theta - \sin^2 \theta}{(\sin^2 \theta + c^2)^{3/2}}.$$



Now by writing  $1 - 2 \sin^2 \theta = \lambda (\sin^2 \theta + c^2) + \mu$  and equating coefficients of the powers of  $\sin \theta$ , we find

$$\frac{1 - 2 \sin^2 \theta}{(\sin^2 \theta + c^2)^{1/2}} = -2 (\sin^2 \theta + c^2)^{1/2} + (1 + 2c^2) (\sin^2 \theta + c^2)^{-1/2}.$$

Similarly

$$\frac{\sin^4 \theta - \sin^2 \theta}{(\sin^2 \theta + c^2)^{3/2}} = (\sin^2 \theta + c^2)^{1/2} - \frac{1 + 2c^2}{(\sin^2 \theta + c^2)^{1/2}} + \frac{(c^2 + c^4)}{(\sin^2 \theta + c^2)^{3/2}}.$$

Therefore

$$\Theta_1 = -(\sin^2 \theta + c^2)^{1/2} + \frac{c^2 + c^4}{(\sin^2 \theta + c^2)^{3/2}}.$$

Integrating from 0 to  $\pi/2$ , the integral  $\Theta_1$  vanishes at both limits and so

$$\int_0^{\pi/2} \frac{d\theta}{(\sin^2 \theta + c^2)^{3/2}} = \frac{1}{(c^2 + c^4)} \int_0^{\pi/2} (\sin^2 \theta + c^2)^{1/2} \cdot d\theta \quad (11)$$

(b) By considering in a similar way  $\Theta_2 = \frac{d}{d\theta} \left\{ \frac{\frac{1}{2} \sin 2\theta}{(\sin^2 \theta + c^2)^{3/2}} \right\}$  and using (11),

we find

$$\begin{aligned} \int_0^{\pi/2} \frac{d\theta}{(\sin^2 \theta + c^2)^{5/2}} &= \frac{2(1 + 2c^2)}{3(c^2 + c^4)^2} \int_0^{\pi/2} (\sin^2 \theta + c^2)^{1/2} \cdot d\theta \\ &\quad - \frac{1}{3(c^2 + c^4)} \cdot \int_0^{\pi/2} \frac{d\theta}{(\sin^2 \theta + c^2)^{1/2}} \end{aligned} \quad (12)$$

(c) By using (11) and (12) we find

$$\begin{aligned} \int_0^{\pi/2} \frac{\sin^4 \theta \cdot d\theta}{(\sin^2 \theta + c^2)^{5/2}} &= \frac{2c^2 + 3}{3(c^2 + 1)} \int_0^{\pi/2} \frac{d\theta}{(\sin^2 \theta + c^2)^{1/2}} \\ &\quad - \frac{(2c^2 + 4)}{3(c^2 + 1)^2} \int_0^{\pi/2} (\sin^2 \theta + c^2)^{1/2} d\theta. \end{aligned} \quad (13)$$

Finally the integrals

$$\left. \begin{aligned} \int_0^{\pi/2} \frac{d\theta}{(\sin^2 \theta + c^2)^{1/2}} \quad \text{and} \quad \int_0^{\pi/2} (\sin^2 \theta + c^2)^{1/2} \cdot d\theta \\ \text{reduce to} \\ \frac{1}{\sqrt{c^2 + 1}} F_1 \left( \frac{1}{\sqrt{c^2 + 1}} \right) \quad \text{and} \quad \sqrt{c^2 + 1} E_1 \frac{1}{\sqrt{c^2 + 1}} \text{ respectively} \end{aligned} \right\} \cdot (14)$$

Throughout the remainder of the paper these complete elliptic integrals will be denoted by  $F_1$  and  $E_1$  respectively.

§ 4. Formulæ (7) ... (14) enable us now to express (4) and (6) in complete elliptic functions to the modulus  $\frac{1}{\sqrt{c^2+1}}$ .

By (8), (11), (12) and (14)

$$\int_0^{2\pi} \frac{\cos \phi d\phi}{\{2b^2(1 - \cos \phi) + n^2a^2\}^{5/2}} = \frac{1}{8b^5} \left\{ \frac{2c^4 + 2c^2 + 2}{3c^4(c^2 + 1)^{3/2}} E_1 - \frac{1 + 2c^2}{3c^2(c^2 + 1)^{3/2}} F_1 \right\}. \quad (15)$$

By (9), (13) and (14)

$$\int_0^{2\pi} \frac{(1 - \cos \phi)^2 \cdot d\phi}{\{2b^2(1 - \cos \phi) + n^2a^2\}^{5/2}} = \frac{1}{2b^5} \left\{ \frac{2c^2 + 3}{3(c^2 + 1)^{3/2}} F_1 - \frac{2c^2 + 1}{3(c^2 + 1)^{3/2}} E_1 \right\}. \quad (16)$$

By (7), (11) and (14)

$$\int_0^{2\pi} \frac{\cos \phi \cdot d\phi}{\{2b^2(1 - \cos \phi) + n^2a^2\}^{3/2}} = \frac{1}{2b^3} \left\{ \frac{1 + 2c^2}{c^2 \sqrt{c^2 + 1}} E_1 - \frac{2}{\sqrt{c^2 + 1}} F_1 \right\}. \quad (17)$$

By (10) and (14)

$$\int_0^{2\pi} \frac{d\phi}{\{2b^2(1 - \cos \phi) + n^2a^2\}^{3/2}} = \frac{1}{2b^3} \frac{1}{c^2 \sqrt{c^2 + 1}} E_1. \quad (18)$$

§ 5. Substituting in (4) we have

$$\begin{aligned} \frac{d\beta_0}{dt} &= \sum_1^{\infty} \frac{\kappa\alpha_0}{2\pi b^2} \left[ \frac{1}{b^2} \left\{ \frac{1 + 2c^2}{c^2 \sqrt{c^2 + 1}} E_1 - \frac{2}{\sqrt{c^2 + 1}} F_1 \right\} \right. \\ &\quad \left. - \frac{2n^2a^2}{8b^2b^3} \left\{ \frac{2c^4 + 2c^2 + 2}{c^4(c^2 + 1)^{3/2}} E_1 - \frac{1 + 2c^2}{c^2(c^2 + 1)^{3/2}} F_1 \right\} \right] \\ &= \sum_1^{\infty} \frac{\kappa\alpha_0}{2\pi b^2} \left[ \frac{E_1 - F_1}{(c^2 + 1)^{3/2}} - E_1 \frac{1}{c^2(c^2 + 1)^{3/2}} \right] \\ &= C\alpha_0, \end{aligned} \quad (19)$$

C being negative for all values of c since  $E_1 < F_1$ .

Since any of the vortex rings may be regarded as the central one of the system, the same equation will hold for any other ring of the row. Consequently  $d\beta_1/dt = C\alpha_1$ .

Again, substituting from (15) ... (18) in (6) and having regard to (5) we find

$$\begin{aligned} \frac{d\alpha_0}{dt} &= H\beta_0 + \frac{\kappa}{2\pi} \sum_1^{\infty} \left[ -\frac{b^3(\beta_0 + \beta_n)}{2b^5} \left\{ \frac{2c^2 + 3}{(c^2 + 1)^{3/2}} F_1 - \frac{2c^2 + 1}{(c^2 + 1)^{3/2}} E_1 \right\} \right. \\ &\quad \left. + \frac{b\beta_n}{b^3} \frac{E_1}{c^2 \sqrt{c^2 + 1}} - \frac{b(\beta_0 + \beta_n)}{2b^3} \left\{ \frac{1 + 2c^2}{c^2 \sqrt{c^2 + 1}} E_1 - \frac{2}{\sqrt{c^2 + 1}} F_1 \right\} \right]. \end{aligned}$$

Now  $\beta_n = \beta_0$  if  $n$  is even and  $\beta_n = \beta_1$  if  $n$  is odd. Hence

$$\begin{aligned}
 \frac{d\alpha_0}{dt} &= H\beta_0 \\
 &+ \frac{\kappa}{2\pi b^2} \sum_2 \left[ -\beta_0 \left\{ \frac{2c^2+3}{(c^2+1)^{3/2}} F_1 - \frac{2c^2+4}{(c^2+1)^{3/2}} E_1 \right\} + \frac{\beta_0 E_1}{c^2 \sqrt{c^2+1}} \right. \\
 &\quad \left. - \beta_0 \left\{ \frac{1+2c^2}{c^2 \sqrt{c^2+1}} E_1 - \frac{2}{\sqrt{c^2+1}} F_1 \right\} \right] \\
 &+ \frac{\kappa}{2\pi b^2} \sum_1 \left[ -\frac{\beta_0}{2} \left\{ \frac{2c^2+3}{(c^2+1)^{3/2}} F_1 - \frac{2c^2+4}{(c^2+1)^{3/2}} E_1 \right\} \right. \\
 &\quad \left. - \frac{\beta_0}{2} \left\{ \frac{1+2c^2}{c^2 \sqrt{c^2+1}} E_1 - \frac{2}{\sqrt{c^2+1}} F_1 \right\} \right] \\
 &+ \frac{\kappa}{2\pi b^2} \sum_1 \left[ -\frac{\beta_1}{2} \left\{ \frac{2c^2+3}{(c^2+1)^{3/2}} F_1 - \frac{2c^2+4}{(c^2+1)^{3/2}} E_1 \right\} \right. \\
 &\quad \left. + \frac{\beta_1 E_1}{c^2 \sqrt{c^2+1}} - \frac{\beta_1}{2} \left\{ \frac{1+2c^2}{c^2 \sqrt{c^2+1}} E_1 - \frac{2}{\sqrt{c^2+1}} F_1 \right\} \right] \\
 &= H\beta_0 \\
 &+ \frac{\kappa\beta_0}{2\pi b^2} \sum_2 \left\{ \frac{2}{(c^2+1)^{3/2}} E_1 - \frac{1}{(c^2+1)^{3/2}} F_1 \right\} \\
 &+ \frac{\kappa\beta_0}{2\pi b^2} \sum_1 \left\{ \frac{c^2-1}{2c^2(c^2+1)^{3/2}} E_1 - \frac{1}{2(c^2+1)^{3/2}} F_1 \right\} \\
 &+ \frac{\kappa\beta_1}{2\pi b^2} \sum_1 \left\{ \frac{3c^2+1}{3c^2(c^2+1)^{3/2}} E_1 - \frac{1}{2(c^2+1)^{3/2}} F_1 \right\} \quad (20) \\
 &= H\beta_0 + G\beta_0 + B\beta_1 \quad (\text{say}).
 \end{aligned}$$

It follows that  $d\alpha_1/dt = H\beta_1 + G\beta_1 + B\beta_0$ .

Write  $A = H + G$ .

§ 6. We then have the system of linear equations

$$\left. \begin{aligned}
 \frac{d\alpha_0}{dt} - A\beta_0 - B\beta_1 &= 0 \\
 \frac{d\alpha_1}{dt} - B\beta_0 - A\beta_1 &= 0 \\
 -C\alpha_0 + \frac{d\beta_0}{dt} &= 0 \\
 -C\alpha_1 + \frac{d\beta_1}{dt} &= 0
 \end{aligned} \right\} \quad (21)$$

of which the solution is given by

$$\begin{vmatrix} D & 0 & -A & -B \\ 0 & D & -B & -A \\ -C & 0 & D & 0 \\ 0 & -C & 0 & D \end{vmatrix} 0 = 0, \quad (22)$$

where 0 represents any one of the four variables  $\alpha_0, \alpha_1, \beta_0, \beta_1$  and D denotes the operator  $d/dt$ .

Expanding the determinant

$$\{D^2 - C(A - B)\} \{D^2 - C(A + B)\} 0 = 0,$$

which has its solution of the form  $\sum_{r=1}^4 A_r e^{\lambda_r t}$ .

Since C is essentially negative, it follows that if either  $(A + B)$  or  $(A - B)$  is negative, at least two of the quantities  $\lambda_r$  will have real values, equal and opposite in sign, and the arrangement will therefore be unstable.

Consider  $A - B = H + G - B$ .

Now from (20) it follows that there is an upper limit to the value of  $(G - B)$ , since the series for G and B behave at infinity like  $\sum 1/n^3$  and are therefore convergent.

Moreover, since H is equal to  $\log \epsilon$ , by taking  $\epsilon$  sufficiently small,  $|H|$  may be made as large as we please, the sign of H being negative. For an indefinitely thin vortex, therefore,  $H + G - B$  will certainly be negative and the arrangement therefore unstable.

Now although the equations of motion determined by this method are only applicable when  $\epsilon$  is small in comparison with  $a$  and  $b$ , it might happen that the upper limit for values of  $\epsilon$  which make this analysis valid is such as to make  $|H|$  less than the value of  $G - B$ . This being so, the stability would depend upon  $\epsilon$ , although  $\epsilon$  were subject to the restriction mentioned. Accordingly, we investigate the behaviour of the quantity  $G - B$  irrespective of H.

From (20), omitting the factor  $\kappa/2\pi b^2$ , we find

$$\begin{aligned} G - B &= \sum_2^\infty \left\{ \frac{E_1 - F_1}{(c^2 + 1)^{3/2}} + \frac{1}{(c^2 + 1)^{3/2}} E_1 \right\} + \sum_1^\infty \frac{-2c^2 - 2}{2c^2 (c^2 + 1)^{3/2}} E_1 \\ &= \sum_2^\infty \left\{ \frac{E_1 - F_1}{(c^2 + 1)^{3/2}} + \frac{E_1}{(c^2 + 1)^{3/2}} \right\} - \sum_1^\infty \frac{E_1}{(c^2 + 1)^{3/2}} - \sum_1^\infty \frac{E_1}{c^2 (c^2 + 1)^{3/2}}. \end{aligned} \quad (23)$$

## 604 *Stability of an Infinite System of Circular Vortices.*

Consider the first three terms of (23). The first is negative for all values of  $c$  and so if

$$\sum_1^{\infty} \frac{E_1}{(c^2 + 1)^{3/2}} > \sum_2^{\infty} \frac{E_1}{(c^2 + 1)^{3/2}},$$

the whole expression is negative. This is so if

$$f(c) \equiv \frac{E_1}{(c^2 + 1)^{3/2}}$$

is a steadily decreasing function of  $c$ .

The graph of  $f(c)$  is of the form shown and values of  $f(c)$  are given for small values of  $c$ .

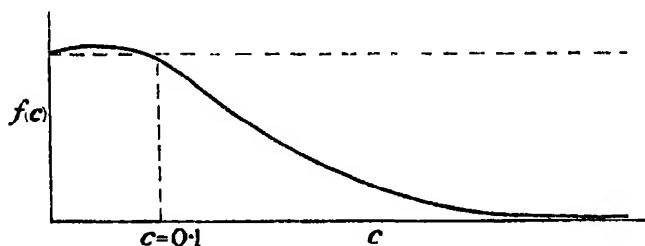


FIG. 2.

$c = 0$	0.017	0.035	0.052	0.070	0.0875	0.105
$f(c) = 1$	1.00023	1.00075	1.00087	1.00129	1.00102	0.999

$f(c)$  is therefore a steadily decreasing function of  $c$  if  $c > 0.1$  and  $G - B$  is therefore negative for such values of  $c$ . For values of  $c > 0.1$  we see from (23) that the most important term in  $G - B$  is  $-\frac{E_1}{c^2(c^2 + 1)^{3/2}}$ , again negative.  $G - B$  is therefore negative for all values of  $c$ .

We conclude, therefore, that the arrangement is definitely unstable for all values of the ratio of the distances apart of the rings to their radii.

### *The L Emission Spectra of Lead and Bismuth.*

By C. E. EDDY, M.Sc., Fred Knight and University Research Scholar, and  
A. H. TURNER, B.Sc., Natural Philosophy Laboratory, University of  
Melbourne.

(Communicated by Sir Ernest Rutherford, P.R.S. - Received January 31, 1927.)

#### *Introduction.*

In a previous paper published by the authors\* which dealt with the L emission series of mercury, the wave-lengths of four lines were given the  $\nu/R$  values of which corresponded with transitions between energy levels disallowed by the Bohr Selection Principle. In a further investigation, to discover if corresponding lines could be found in the L spectra of elements close to mercury in the Periodic Classification, the spectra of lead and bismuth were examined. In each case the corresponding four lines were found, and in addition several other "non-diagram" lines. The present paper gives a brief account of the results obtained.

Several other investigators have found lines which correspond with transitions contrary to the Selection Principle. Dauvillier† found many such in the L emission series of the heavy elements from ytterbium to gold, and Rogers‡ in the spectra of tungsten and platinum. Crofutt also found several for tungsten, and the existence of a tungsten line  $\gamma_{11}$  ( $L_3N_4$ ) has been confirmed by Dershem and by Overn.

That the lines found are due to impurities in the metals used seems highly improbable, as none of the wave-lengths for these lines correspond with those of any other element either in the K, L or M series or in the second or higher orders spectra. Also the voltage employed throughout this investigation, as determined by a careful sphere gap calibration, was at no time greater than 25 kilovolt, that is, was insufficient to excite the second degree spectrum of the elements lead and bismuth.

#### *Apparatus and Experiment.*

The metal X-ray tube and spectrometer which have been previously described were again used. The lead spectrum was obtained from a copper target coated

\* 'Roy. Soc. Proc.,' A, vol. 111, p. 117 (1926).

† 'J. de Physique,' vol. 3, p. 221 (1922).

‡ 'Proc. Camb. Phil. Soc.,' vol. 21, p. 430 (1922-3).

with an alloy of lead and solder, containing a high percentage of lead. The bismuth lines were at first produced from a target surface consisting of a lead and bismuth alloy. Both spectra were thus obtained at the one exposure. Since, however, some of the fainter bismuth lines lay in close proximity to strong lead lines, later a pure bismuth surface was prepared by casting a bismuth button in a cavity in the copper surface. The wave-lengths of the strong lead lines ( $\alpha_2$ ,  $\alpha_1$ ,  $\beta_1$ ,  $\beta_2$  and  $\gamma_1$ ) were determined relative to the same lines of tungsten photographed on the one film. The tungsten lines were readily obtained from the deposition of that element upon the target surface from the filament. The weaker lead lines, and all the bismuth lines, were then determined relative to the strong lead lines.

The tube was excited by a potential of about 23 kilovolt, with currents of about 15 milliamperes, and exposures of about  $2\frac{1}{2}$  hours were required to photograph the whole spectrum. "Superspeed" Kodak Duplitised X-ray film was used with a rear intensifying screen. The slit width was less than 0.075 mm. for the stronger lines, and about 0.1 mm. when the very weak lines were being photographed. The crystal was of calcite, and was rotated continuously during an exposure by means of a small motor.

The films were measured by means of the projection method previously described. The values assumed as standards for the tungsten lines were the means of those obtained by Siegbahn and Dolejsek\* and by Duane and Patterson.† Two measurements of each film were made, and their means taken. The probable errors in the wave-lengths for the stronger lines are shown in the tables. For the weak lines the error should in no case exceed 0.6 XU.

### *Results and Discussion.*

The values obtained for the stronger lead lines, which were taken as standards for our further measurements, are shown in detail in Table I. The lines  $\beta_1$  and  $\beta_2$  are given as being coincident; even the use of a very narrow slit gave no indication of a doublet. The values obtained by Coster, using an absolute method, are shown underneath for comparison.

\* 'Z. f. Physik,' vol. 10, p. 159 (1922).

† 'Phys. Rev.,' vol. 16, p. 525 (1920).

Table I.—Lead Strong Lines.

Film.	$\alpha_2$ .	$\alpha_1$ .	$\beta_1, \beta_2$ .	$\gamma_1$ .
3	11.16.3	11.9.10	9.18.27	7.56.58
5	11.16.4	11.9.9	9.18.31	7.56.53
6	11.16.1	11.9.14	9.18.29	7.56.55
7	11.15.59	11.9.14	9.18.31	7.56.51
8	11.16.3	11.9.14	9.18.30	7.56.52
Means	11.16.2 $\pm 1.4$	11.9.12 $\pm 1.9$	9.18.30 $\pm 1.2$	7.56.54 $\pm 1.0$
XU.	1183.60 $\pm 0.04$	1171.85 $\pm 0.06$	979.88 $\pm 0.03$	837.71 $\pm 0.06$
Coster				
	11.15.54	11.9.14	9.18.30	7.56.35
	11.16.0	11.9.18	9.18.31	7.56.42
Means	11.15.57	11.9.16	9.18.31	7.56.39
XU.	1183.52	1171.02	979.90	837.08

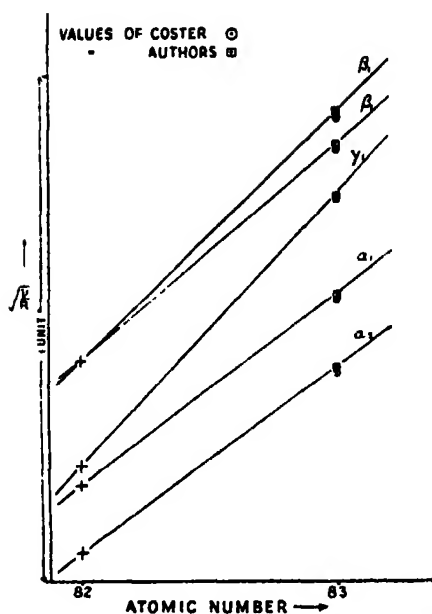
In Table II are shown the results for the stronger bismuth lines. The results of Coster are shown underneath. In this case the disagreement for each of the lines is much greater than the sum of the probable errors, and is difficult to account for. Although Coster obtained his values from measurements of at most 2 films, very good agreement exists between his individual readings. Since Coster determined these 5 lines by an absolute method, and then the fainter lines relative to these, the disagreement persists for all the bismuth results. From the graph of  $\sqrt{v/R}$  against  $N$  (see figure) it appears that our values lie nearer to the Moseley curve than do those of Coster.

Table II.—Bismuth Strong Lines.

Film.	$\alpha_2$ .	$\alpha_1$ .	$\beta_2$ .	$\beta_1$ .	$\gamma_1$ .
4	10.57.51	10.50.59	9.2.32	9.0.31	7.41.31
9	10.57.50	10.51.1	9.2.38	9.0.37	7.41.37
10	10.57.48	10.51.3	9.2.33	9.0.36	7.41.34
11	10.57.54	10.51.6	9.2.34	9.0.35	7.41.30
12	10.57.52	10.51.5	9.2.34	9.0.34	7.41.30
13	10.57.53	10.51.2	9.2.33	9.0.36	7.41.34
Means	10.57.51 $\pm 1.6$	10.51.3 $\pm 1.9$	9.2.34 $\pm 1.4$	9.0.35 $\pm 1.5$	7.41.33 $\pm 2.0$
XU.	1152.22 $\pm 0.06$	1140.45 $\pm 0.06$	952.16 $\pm 0.04$	948.70 $\pm 0.04$	810.91 $\pm 0.07$
Coster					
	10.58.27	10.51.27	9.3.0	9.0.59	7.41.25
		10.51.28	9.3.1	9.0.51	7.41.23
Means	10.58.27	10.51.28	9.3.0	9.0.55	7.41.24
XU.	1153.3	1141.15	952.93	949.30	810.65

Table III contains the results of all the lines found for both lead and bismuth. The first column in each case shows the wave-lengths, calculated from measure-





Moseley Diagram for Bismuth Strong Lines.

ments of at least 3 films. The fainter lines, wherein errors of more than 0.1 XU may occur, are given only to the first decimal place. In some cases where two lines were believed to coincide, or where a faint line lay so close to a strong line that it was masked by the lateral spreading of the latter on the film, the two lines are bracketed together. Coster's values of the wave-lengths are given in the second column, while the third column in each case contains the values of  $\nu/R$  as calculated from our results.

The existence of the four unnamed non-diagram lines tentatively allotted by the writers to the mercury spectrum has been confirmed. Two of these lines were found to correspond to the lines  $\gamma_7$  and  $\gamma_9$  of Dauvillier. In addition, several other lines noted by Dauvillier have been measured and are included under the symbols used by him. The line  $\alpha_3$ , which was measured by both Dauvillier and Rogers, was searched for, but no line corresponding to such a transition could be found. Dauvillier has denoted this line as possessing an intensity of the same order as  $\alpha_2$ , but a line of this intensity, if present, could readily be recognised. In addition, three lines— $\beta_5'$ ,  $\beta_5''$  and  $\beta_2''$ —were not obtained for either element. Dauvillier found  $\beta_5'$  for two elements, and  $\beta_5''$  for only one; Rogers did not obtain either for platinum or tungsten. The line  $\beta_2''$  occurred in Dauvillier's results for 9 elements, in Rogers's for 2; in

Table III.

Line.			Lead.			Bismuth.		
			Wave-length in XU.		$\sqrt{\nu/R}$ .	Wave-length in XU.		$\sqrt{\nu/R}$ .
			Authors.	Coster.		Authors.	Coster.	
<i>l</i>	L <sub>III</sub>	M <sub>I</sub>	1346.46	1346.62	26.015	1312.98	1312.95	26.345
—	L <sub>III</sub>	M <sub>II</sub>	1328.8		26.187	1269.3		26.794
<i>a</i> <sub>2</sub>	L <sub>III</sub>	M <sub>IV</sub>	1183.66	1183.52	27.747	1152.22	1153.3	28.122
<i>a</i> <sub>1</sub>	L <sub>III</sub>	M <sub>V</sub>	1171.85	1172.02	27.886	1140.45	1141.15	28.267
<i>γ</i>	L <sub>II</sub>	M <sub>I</sub>	1089.38	1090.2	28.922	1055.40	1057	29.383
<i>β</i> <sub>8</sub>	L <sub>III</sub>	N <sub>I</sub>	1019.6	1018.8	29.895	990.64	991.6	30.331
<i>β</i> <sub>4</sub>	L <sub>I</sub>	M <sub>II</sub>	1005.76	1004.69	30.101	973.50	975.4	30.595
<i>β</i> <sub>3</sub>	L <sub>III</sub>	N <sub>V</sub>	981.0		30.465			
<i>β</i> <sub>2</sub>	L <sub>II</sub>	M <sub>IV</sub>	979.80	979.90	30.496	952.16	952.93	30.936
<i>β</i> <sub>1</sub>	L <sub>III</sub>	N <sub>V</sub>				948.70	947.30	30.992
<i>β</i> <sub>11</sub>	L <sub>II</sub>	M <sub>IV</sub>	977.9		30.526			
<i>β</i> <sub>6</sub>	L <sub>II</sub>	M <sub>V</sub>	974.5	973.5	30.580	952.16	952.93	30.936
<i>β</i> <sub>5</sub>	L <sub>I</sub>	M <sub>III</sub>	966.13	966.02	30.712	935.88	935.7	31.204
<i>β</i> <sub>7</sub>	L <sub>III</sub>	N <sub>VI VII</sub>	958.8		30.829			
<i>β</i> <sub>7</sub>	L <sub>III</sub>	O <sub>I</sub>	958.0	959.0	30.842	931.9		31.270
<i>β</i> <sub>8</sub>	L <sub>III</sub>	O <sub>V</sub>	948.76	949.52	30.992	922.47	922.3	31.434
<i>β</i> <sub>10</sub>	L <sub>I</sub>	M <sub>IV</sub>	936.3		31.197	913.4		31.660
<i>β</i> <sub>9</sub>	L <sub>I</sub>	M <sub>V</sub>	922.2		31.435			
<i>γ</i> <sub>5</sub>	L <sub>II</sub>	N <sub>I</sub>	865.7	863.9	32.443	837.8	837.8	32.980
—	L <sub>II</sub>	N <sub>III</sub>	849.1		32.761	821.7		33.302
<i>γ</i> <sub>1</sub>	L <sub>II</sub>	N <sub>IV</sub>	837.71	837.08	32.982	810.91	810.65	33.526
<i>γ</i> <sub>10</sub>	L <sub>II</sub>	N <sub>V</sub>	833.2		33.072	806.2		33.620
<i>γ</i> <sub>7</sub>	L <sub>I</sub>	N <sub>I</sub>	825.2		33.230	802.0		33.709
<i>γ</i> <sub>6</sub>	L <sub>I</sub>	N <sub>II</sub>	818.56	818.2	33.366	793.47	792.9	33.889
<i>γ</i> <sub>8</sub>	L <sub>I</sub>	P	810.8		33.402	791.3		33.936
<i>γ</i> <sub>5</sub>	L <sub>I</sub>	N <sub>III</sub>	812.92	813.70	33.481	787.59	787.4	34.015
<i>γ</i> <sub>6</sub>	L <sub>II</sub>	O <sub>IV</sub>						
<i>γ</i> <sub>9</sub>	L <sub>I</sub>	P <sub>II</sub>	801.2		33.726	777.1		34.245
<i>γ</i> <sub>4</sub>	L <sub>I</sub>	O <sub>II</sub>	784.0	783.6	34.094	760.0	761	34.628
<i>γ</i> <sub>8</sub>	L <sub>II</sub>	O <sub>I</sub>	779.3		34.214	756.2		34.715

the case of lead this line would be nearly coincident with  $\beta_8$ , and for bismuth it would be very close to the strong  $\beta_1$  line.

In Table IV, the  $\nu/R$  units obtained from the observed wave-lengths of the lines are compared with the difference between the  $\nu/R$  values of the levels associated with each. The latter values were obtained from the table compiled by Bohr and Coster. The first column shows the levels concerned in the transition, the second and fourth respectively contain the value of  $\nu/R$  calculated from our wave-length determinations for lead and bismuth respectively, and the third and fifth columns show the value of  $\nu/R$  calculated from the energy level data of Bohr and Coster. In most cases very fair agreement exists between the two values.

Table IV.

Line.	Levels concerned in transition.	Lead.		Bismuth.		Mercury.	
		Obs.	Calc.	Obs.	Calc.	Obs.	Calc.
—	$L_{III} \quad M_{II}$	699.3	698.6	717.9	716.4	660.0	661.7
$\beta_2'$	$L_{III} \quad N_V$	928.2	930.0				
$\beta_{11}$	$L_{II} \quad M_{IV}$	931.8	931.4	960.5	960.0		
$\beta_7'$	$L_{III} \quad N_{VI, VII}$	950.4	950.0	Probably close to another line			
—	$L_{II} \quad N_{III}$	1073.4	1072.6	1109.0	1109.1	1004.0	1003.7
$\gamma_{10}$	$L_{II} \quad N_{IV}$	1093.8	1091.4	1130.3	1125.7		
$\gamma_7'$	$L_I \quad N_I$	1104.3	1103.3	1136.3	1136.9	1032.1	1030.9
$\gamma_2'$	$L_{II} \quad P$	1115.7	1121.9	1161.6	1159.4		
$\gamma_9$	$L_I \quad N_{IV}$	1137.4	1137.1	1172.7	1178.4	1064.1	1064.0
$\gamma_8$	$L_I \quad P_{IV, V}$	1169.4	1169.3	1205.1	1207.9		

Two lines  $\beta_2'$  and  $\beta_7'$ , which were measured for lead, were not obtained for bismuth; the former line lies very close to  $\beta_2$ , the latter to  $\beta_3$ ; since both  $\beta_2$  and  $\beta_3$  are strong lines, the two faint lines may have been screened by them.

In conclusion, we wish to express our gratitude to Prof. T. H. Laby for his helpful interest in this investigation and for his assistance in writing this report.

*The Transverse Magneto-Resistance Effect in Single Crystals  
of Iron.*

By W. L. WEBSTER, Ph.D., Cavendish Laboratory, Cambridge. (Senior 1851  
Student.)

(Communicated by Sir Ernest Rutherford, P.R.S.—Received February 15, 1927.)

1. *Introduction.*

The experiments to be described in this paper, deal with the change of resistance of single crystals of iron caused by a magnetic field perpendicular to the direction of the current. In two earlier papers, it has been shown that both the phenomena of magneto-striction\* and change of resistance in a longitudinal magnetic field† were very different when measured in different directions in the crystal. And the results led to the conclusion that the change of resistance in the latter case was due to the change of orientation of the atoms accompanying magnetization, any direct influence of the field on the resistance being negligible. With these results in mind it seemed important to determine how the change of resistance in a transverse magnetic field depended on the crystal structure, and whether this more complicated effect, dealing with two directions in the crystal instead of one, would fit in with the results previously obtained.

Many measurements of this phenomenon have been made for soft iron, and it has generally been accepted‡ that there is only a decrease of resistance, slow at first, then rapid, finally approaching a saturation value. Occasionally an initial increase has been found, but this has not been considered genuine, being accounted for by the presence of a longitudinal component of magnetization due to imperfect orientation of the rod in the magnetic field.

The present experiments have confirmed the importance of the crystal structure in these phenomena. It is found that altering either the direction of the magnetic field or of the current produces a very marked change in the results observed, but it may be noted that the change is gradual and continuous. Below 5,000 gauss and above 12,000 gauss, there is always a gradual decrease in resistance which is approximately proportional to the magnetic field. In between, there takes place a rapid change in resistance, which may

\* 'Roy. Soc. Proc.,' A, vol. 109, p. 570 (1925).

† 'Roy. Soc. Proc.,' A, vol. 113, p. 196 (1926).

‡ Campbell, 'Galvanomagnetic and Thermomagnetic Effects,' p. 188.

have either sign according to the direction of the current and whose magnitude depends on the direction of the field, being in some cases entirely absent.

It seems possible to explain these results by assuming a double origin of the phenomenon. The initial and final gradual decreases are probably due to some direct action of the magnetic field on the conducting electrons; and it is natural to connect the intermediate rapid change, which is very similar to the longitudinal resistance effect, with the change of orientation of the atoms, which was used to account for that effect.

## 2. *Measurements.*

The measurements were made on rods cut from single crystals of iron with their axes parallel to a (100), (110), or (111) crystal axis. Several examples of each type were measured, in some cases, for the rods used in the previous work. The rods were about 1.8 cms. in length, and had an approximately square cross-section with a side of about 1 mm. The rod was held with its axis perpendicular to the direction of the magnetic field, and a steady current of about 1.5 amps. per sq. mm. passed through it. The magnetic field was applied and the resulting change of resistance measured. By rotating the rod about its axis, the direction of the field could be changed relative to the crystal structure, and so the change of resistance could be measured as a function of the field, with the field in a series of positions in the crystal.

The change of resistance was measured by a differential method. The potential drop along about 1.2 mm. of the crystal rod was tapped off by two hard-copper knife edges pressed firmly against the rod, and was balanced against a fixed external potential of  $1.4 \times 10^{-3}$  volts. The balance was obtained by adjusting the current in the rod by means of a carbon resistance in series with the iron rod, and was made in the absence of the magnetic field. The deflexion of the galvanometer used to record the balance, when the magnetic field was applied, gave a direct measure of the change of resistance, calibration being effected by changing the balancing voltage by a known amount. The Gambrell low-resistance galvanometer used previously was again employed; it would record changes in resistance of one part in  $5 \times 10^4$ .

For each point, nine readings of the galvanometer were taken with the field successively off and on, and with the direction of the field reversed, the mean of the successive differences being used. The variation of the value of  $dR/R$  obtained in this way was about  $5 \times 10^{-5}$ . As in the case of the longitudinal effect, the change of resistance was not quite independent of the direction of the field and current, but systematically showed a change of about 5 per cent.

if either were reversed. This was probably due to the iron-copper contacts and was ignored throughout. The rod was shielded from air currents, and there was practically no change of resistance due to change of temperature except over long periods, probably on account of the proximity of the heavy pole pieces of the magnet.

The magnetic field was obtained with a large electro-magnet and was calibrated by the Gauss method. The pole faces were about 2.5 cms. in diameter and 0.4 cms. apart and with a magnetizing current of 5 amps. a field strength of 27,000 gauss could be reached. As it was not possible to make the leads from the knife-edges quite non-inductive, it was necessary, in order to prevent large induced deflexions of the galvanometer at the make and brake of the field, to introduce between the poles a small compensating coil connected in series with these leads, by adjustment of which this disturbance could be eliminated.

It may be pointed out here that as the rods were not round, the magnetization could not be really uniform except with very large fields. Several attempts were made to cut circular rods, but in each case the crystal structure was disturbed, and the attempt was abandoned. The errors introduced do not appear to have been very serious. Comparison of the results for rods with the crystal axes in different positions relative to the normals to the sides of the rod, gave quite similar results; and measurements on a (111) rod before and after the edges had been rounded off by grinding with fine emery, were almost identical except for an increased sharpness in the bends in the curves. Certainly in the highest fields used, about 15,000 gauss above that giving magnetic saturation, there should be very little error due to this cause.

To find the correct position of the rod in the magnetic field, it was arranged that the rod could be moved through about five degrees about an axis perpendicular to its own axis and to the direction of the field. With a constant magnetic field, generally 5,000 gauss, the change of resistance was determined for a series of positions  $\frac{1}{2}^\circ$  apart, and the rod finally set in the position giving the largest decrease in resistance. As the longitudinal magnetization produces an increase in resistance, it must then have been practically eliminated.

The position of the field relative to the normal to one of the faces of the rod was measured by a small circular scale, graduated in  $10^\circ$  divisions, attached to the rod; and as the position of the crystal axes were known relative to this normal, the position of the field, in the crystal, could at any time be determined.

## 3. Results.

As has been mentioned above, the effect was measured in rods cut parallel to a (100), (110), or (111) crystal axis, in several examples of each type. As the results for any one type were quite similar, curves are given for only one of each.

For a (100) rod where the current is along a cubic axis, the results are shown in figs. 1 and 2. In fig. 1, the change of resistance is shown as a function

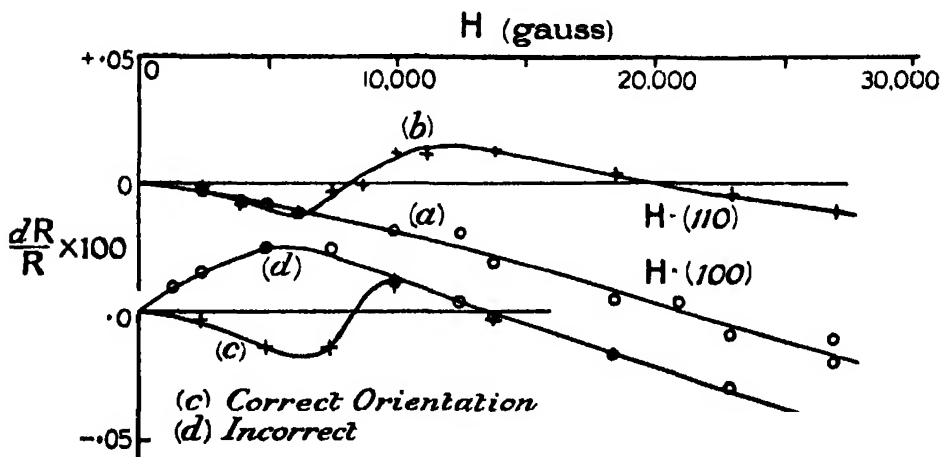


FIG. 1.

of the magnetic field in the two extreme cases: (a) where the field is along a (100) axis, and (b) along a (110) axis. For the former,  $dR/R$  is negative and roughly proportional to the magnetic field; for the latter, this relation holds, below 6,000 gauss and above 12,000 gauss, but in between there occurs a rapid positive change in resistance, which is sufficient to cause a net increase in resistance. That this is not due to bad orientation of the rod can be seen by comparison with the curves (c) and (d) where the effect of an error of orientation of  $2^\circ$  is shown such an error gives rise to an increase of resistance quite different in nature. In fig. 2, curves (a) and (b) give the variation in  $dR/R$  as the position of the magnetic field is altered for fields of 12,500 and 27,500 gauss respectively; the value of  $dR/R$  at 6,000 gauss is almost constant. These curves really measure the variation in the magnitude of the intermediate rapid increase in resistance, and would be parallel were it not that there is a variation in the final slope of the  $(dR/R - H)$  curves, shown in curve (c). The position of the field when parallel to a (100) or (110) axis are indicated, and it is important to notice

that the curves show the symmetry associated with the cubic axis along which the current flows.

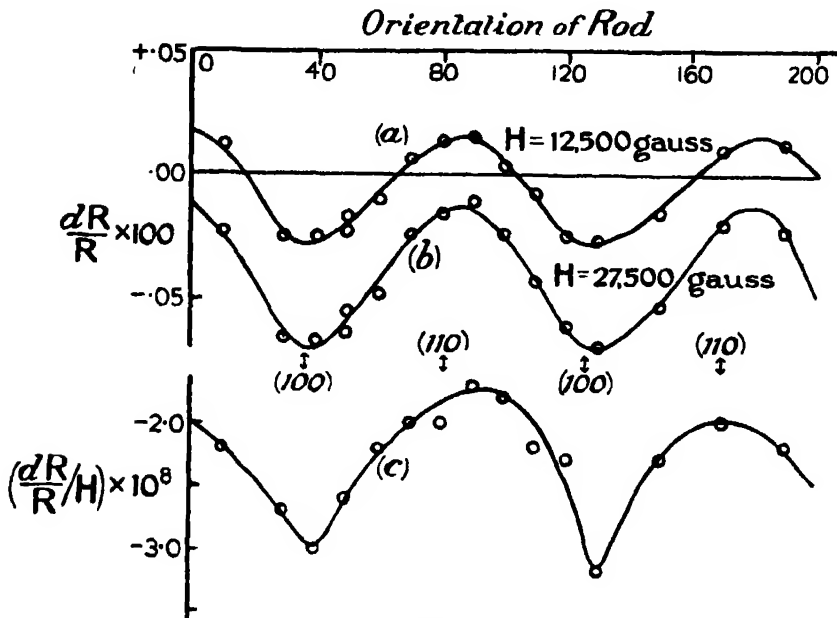


FIG. 2.

The results for a (110) rod are shown in figs. 3 and 4. In fig. 3, (a) is the case with the field parallel to a (100) axis, and, as in the corresponding case for the (100) rod, shows a gradual negative change in  $dR/R$  roughly proportional to the field; for (b), the field is parallel to a (110) axis, and shows a gradual decrease in resistance below 5,000 and above 14,000 gauss, but in the intermediate region there is now a negative change of resistance which is much larger than the corresponding positive change for the (100) rod. The curves in fig. 4 again show the symmetry associated with the direction of the current.

For the (111) rod the results were not so satisfactory. Curve (c) of fig. 3 is one of the curves obtained for a rod more or less rounded; it shows the initial and final negative change proportional to the field, and in between a rapid decrease in resistance of the same order as that occurring with the (110) rod. The curves of fig. 5, however, give only slight indications of the appropriate symmetry. It may be pointed out that in this case the variation is comparatively small, so that the influence of the errors due to strains in the crystal, small inclusions not properly orientated, and inhomogeneous magnetization may be rather important.



Curve (d) of fig. 3 gives the result for a soft iron rod. As might be expected it is roughly a mean of the curves for the single crystals; that there is no

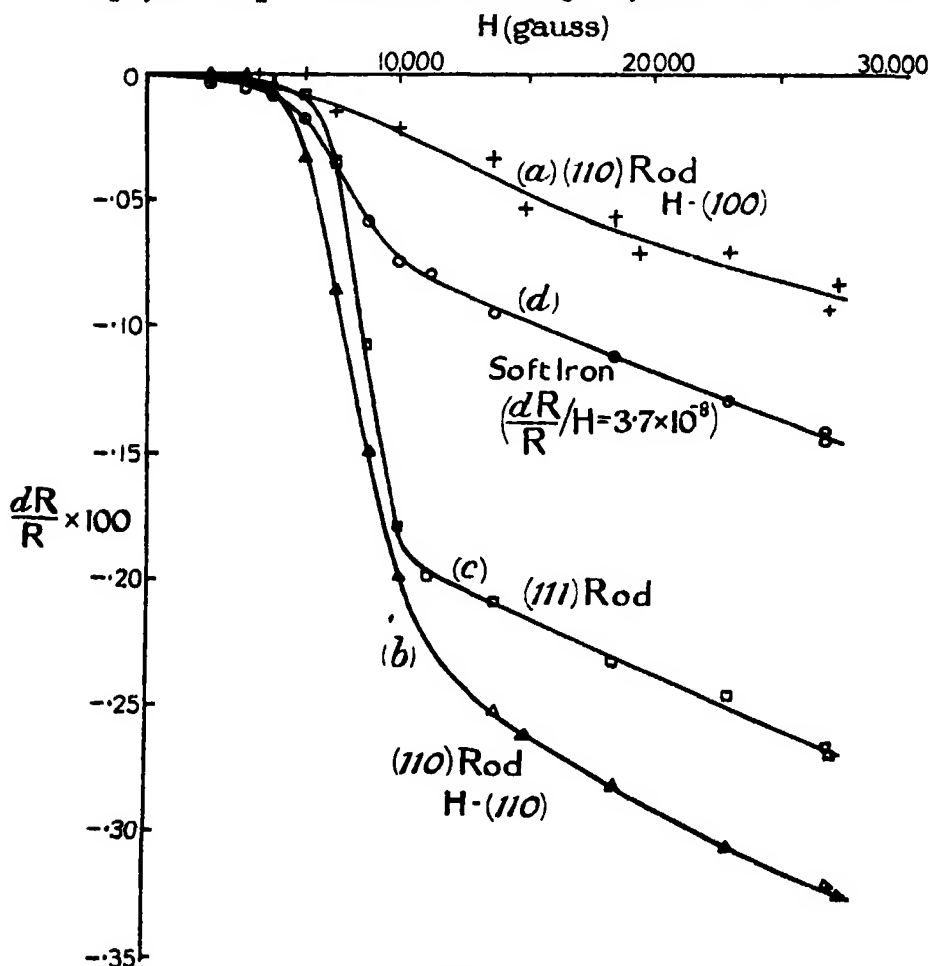


FIG. 3.

sign of the positive change of resistance is due to the comparative smallness of this effect.

It may be pointed out that in general there is a marked parallelism between the variation in the final slope of the  $(\frac{dR}{R} - H)$  curves and the variation in the magnitude and sign of the rapid intermediate change of resistance. The slope becomes smaller when the change of resistance is positive, and increases when the change is negative.

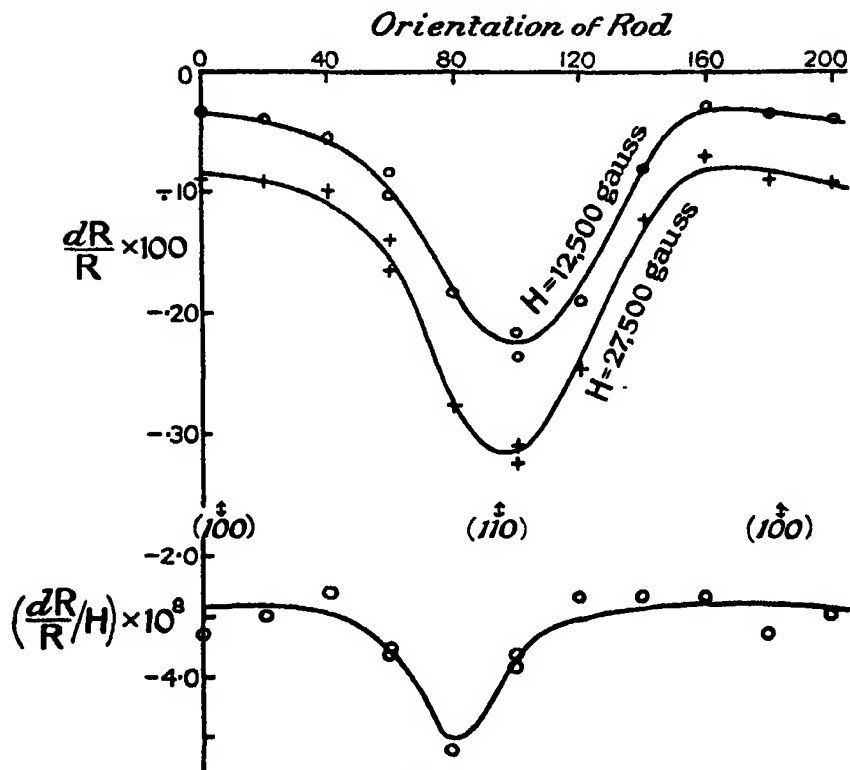


FIG. 4.

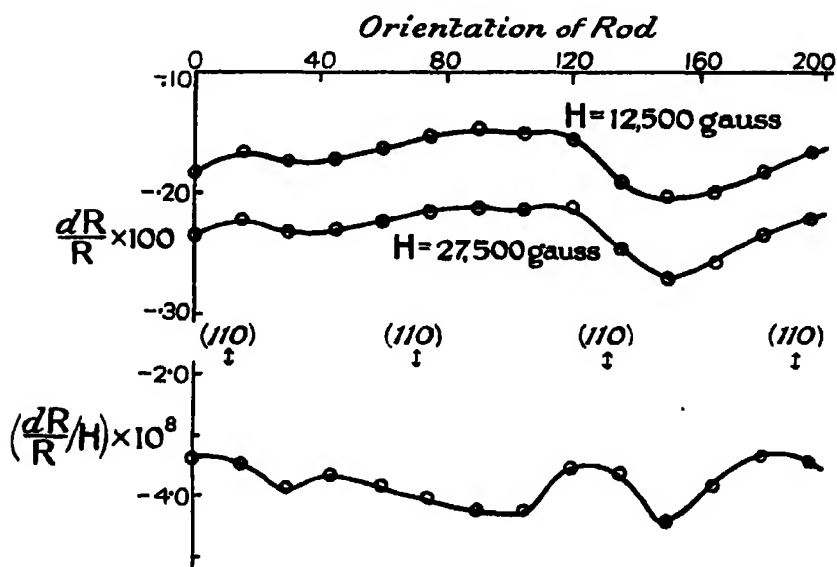


FIG. 5.

#### 4. Discussion.

These results suggest at once that there are two effects superimposed on one another, causing the resistance to change. One of these gives rise to initial and final gradual decrease in resistance which is present to much the same degree for all directions of the field and current; and since the change of resistance in this case seems to be roughly proportional to the field, it seems natural to suppose that this effect is due to some direct action of the field on the conducting electron.

The other effect gives rise to the intermediate rapid change of resistance which may have either sign, depending on the direction of the current, and whose magnitude varies with the direction of the magnetic field. The demagnetizing coefficient ( $=2\pi$ , for a circular rod) shows that this effect occurs between an intensity of magnetization of about 800 c.g.s. units and magnetic saturation. This fact, and that it vanishes entirely for magnetization parallel to a cubic axis, indicates that it is of the same nature as the change of resistance occurring with a longitudinal magnetization, and is therefore to be ascribed to the change of orientation of the atoms accompanying magnetization.

Concerning the actual mechanism of the resistance change it is impossible to say anything very definite. In the previous paper following the ideas of Fraenkel and others, it was assumed that the conducting electron must be considered always bound to some atom, but that it may pass from one atom to another, the resistance being due to the difficulty of this transition. A change of orientation of the atom must affect this transition, and so must change the resistance. Such an explanation seems to be applicable to the present case as well as to the longitudinal effect, as there seems to be no a priori objection to a change of either sign from this cause.

As to the effect of the field, although it might be expected that the interaction between it and the conducting electron would take place during the transition between two neighbouring atoms when it was not actually bound to either, the time during which the electron may be considered "free" must be too small to allow any appreciable effect; moreover such a treatment would probably lead to an increase of resistance in place of a decrease. It seems more probable that the origin of the field effect lies in a modification of the orbit of the conducting electron about the atom. The field might be supposed to produce, in effect, a weakening in the bond between the electron and the atom, consequently an increase in the probability of transition, and a decrease in resistance. Then a change of orientation of the atom, which, by reducing the contact between

the orbits in neighbouring atoms, causes a positive change of resistance of the orientation type, must also reduce the efficiency of the field in altering the resistance, and vice versa. A marked parallelism between the efficiency of the field, indicated by the final slope of the  $(dR/R-H)$  curves, and the magnitude of the orientation effect should therefore be, and in fact is, observed.

### 5. *Summary.*

The change of resistance in a transverse magnetic field has been measured in single crystals of iron with the current along a (100), (110), or (111) crystal axis, and with the magnetic field in a series of positions in the planes normal to these directions. Below 5,000 gauss and above 12,000 gauss there is always a gradual decrease in resistance which is approximately proportional to the field strength. In the region between, there occurs a rapid change of resistance which is positive when the current is along a cubic axis and negative for the other two directions; and whose magnitude depends on the direction of the magnetic field, vanishing when the field is along a cubic axis.

It is suggested that the phenomenon is of a double nature; that the gradual change of resistance is to be ascribed to some direct action of the field on the conducting electrons; and that the intermediate rapid change is due to the change of orientation of the atoms accompanying magnetization.

In conclusion, I should like to thank Sir Ernest Rutherford for his interest in this work, Dr. Kapitza for helpful discussion, and especially Miss Elam who very kindly re-examined the rods used, to determine the direction of the crystal axes in the plane normal to the axis of the rod.

---

*Studies on the Mercury Band-Spectrum of Long Duration.*

By LORD RAYLEIGH, F.R.S.

(Received March 11, 1927.)

[PLATES 43 and 44.]

§ 1. *Introduction.*

In a former paper\* I described a method of observing the band spectrum in luminous mercury vapour distilled away from the arc. The vapour immediately on leaving the arc shows line spectrum exclusively, but as it matures the band spectrum gradually becomes predominant. It was shown by special experiments that the band spectrum derives its energy from the source which maintains the line spectrum.

It is also possible, as originally shown by Phillips working in my laboratory at the Imperial College, to excite the band spectrum by exposure of the vapour initially to the right of the resonance line 2537, and to carry it away from the place of excitation with the mercury vapour when the latter is caused to distil. Neither of these methods is very convenient, however, for obtaining a bright spectrum, and an alternative one has been developed which works much better. This is to use a discharge from a Wehnelt cathode to excite the vapour. Under suitable conditions a comparatively bright band spectrum may be obtained initially, with a minimum intensity of line spectrum mixed with it.† The vapour distilling from such a discharge shows initially at least the same type of spectrum as the discharge itself. If line spectrum predominates in the discharge it will predominate in the vapour which passes away from it, though, as in the case of the arc above mentioned, it ultimately turns to band spectrum. But if the band spectrum predominate initially, it does so throughout.

Free and rapid distillation of the vapour is important. In the experiments with the arc (*loc. cit.*) enough evaporation occurred from the mercury cathode under the heat of the discharge. In the present work, where no mercury electrodes are used, and where the energy dissipated in the discharge is small, the vapour is supplied from an independent boiler below. The tube above the discharge is with advantage kept straight, or, if a bend is necessary, it should preferably be an obtuse one. The condenser is kept exhausted by an air pump, and the condensed liquid returns to the boiler as in the condensing steam engine.

\* 'Roy. Soc. Proc.,' A, vol. 108, p. 262 (1925).

† Cf. Grottrian, 'Z. f. Physik,' vol. 5, p. 148 (1921).

§ 2. *Experimental Arrangement.*

This is shown in fig. 1.

The vapour rises from mercury in a silica flask A. The flask is heated in an electrical oven (not shown) which maintains a constant rate of evaporation. The vapour stream passes the hot cathode B and the anode C. Here it becomes

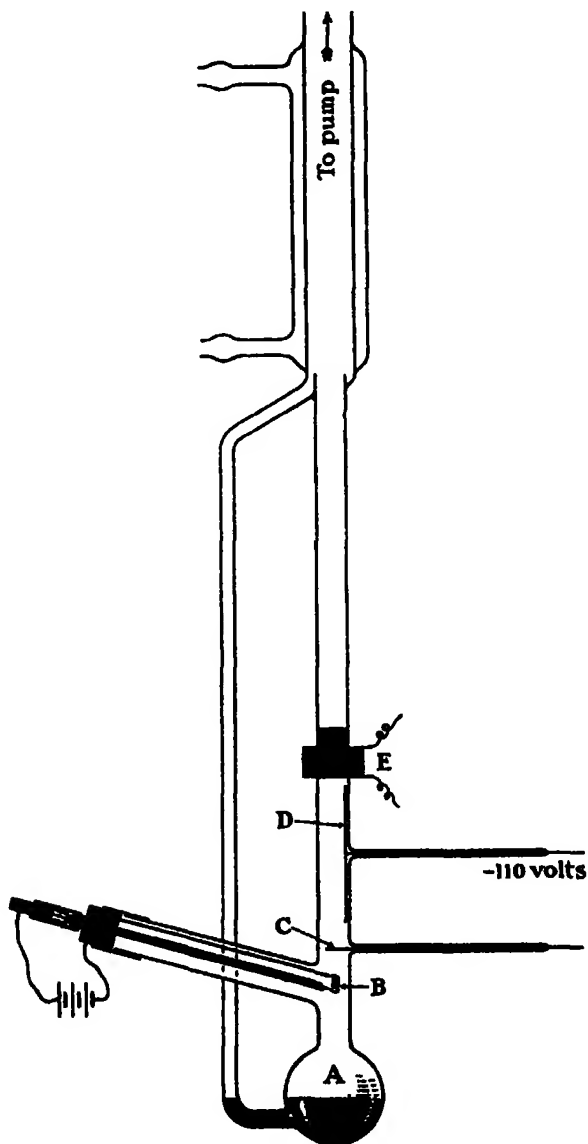


FIG. 1.—(One-quarter actual size.)

luminous, and the luminosity is carried up outside the region of excitation. D is a supplementary plate electrode measuring 1 by 7 cm.; its purpose will be mentioned presently. The vertical part of the tube is kept hot enough, by suitable electric heaters, to prevent the mercury from condensing. The tube with the heater is in a box with a front opening wide enough to allow of observation. The condenser for the mercury is constructed as shown, with an annular gutter to catch the liquid, and a side tube to return it to the boiling flask. The water jacket is made in one piece with the main apparatus. E is a coil for strongly heating the tube locally. It will be further referred to later on. The apparatus is exhausted from the top. A large glass balloon connected to it serves as a vacuum reservoir, and avoids the necessity of keeping the pump going continuously during long exposures. Any small leakage through the rubber joints could be taken up by pumping from time to time.

The source of current used was, as a rule, the 110-volt supply, controlled by high resistances extending to the discharge tube. Much more stable regulation was got in this way than by controlling the filament current.

The filament temperature necessary depends upon the amount of lime upon it, and increases as the lime coating flakes off or volatilises by long use at too high a temperature. Without lime the filament has to be made nearly as hot as it will bear, and it is necessary to add to the usual voltage of 110 volts to get the discharge to pass steadily. With a filament freshly coated with lime, a dull red heat is enough.

The distance between anode and cathode has usually been between 1.5 and 2 cm. The discharge will pass whether the moving stream of vapour passes from cathode to anode or *vice versa*. But the effects are steadier and more certain in the former position. This was shown by a special experiment with two similar anodes, one above and the other below the cathode filament; they could be used alternatively by means of a two-way switch, with the result just mentioned. The anode should not be restricted to a mere point, for in that case a patch of glow strong in line spectrum is apt to develop upon it. A wire of not less than 1.5 mm. diameter, stretching across a diameter of the discharge tube, is adequate, and does not seriously obstruct the flow of vapour.

### § 3. *Line and Band Spectrum. Conditions of Excitation. The Band Spectrum and the Resonance Lines.*

Let us suppose the distillation to be started, and a current passed between the electrode. The luminous vapour passes up from them into the region above, and persists, though with diminishing intensity, up to the condenser.

The character of luminosity (line spectrum or band spectrum) depends on the strength of the electric current, and on the density of the vapour stream. Rapid evaporation, and therefore a dense vapour stream, is favourable to the band spectrum. Maintaining the current at about 3 milliamperes, it is possible to pass from nearly pure line spectrum to nearly pure band spectrum by increasing the evaporation. Usually, however, the rate of evaporation has been maintained constant, and attention concentrated on the effect of varying the other conditions. Of these the most important is the current strength. Using a suitable rate of evaporation, small currents (say 1 milliampere or less) give a predominant band spectrum. Larger currents give an increasing predominance of line spectrum, both in the discharge and in the vapour which moves away from it. With currents of, say, 30 milliamperes or more, the conditions approximate to those when an arc from a mercury cathode is used, as in the earlier experiments.\* Little can then be seen of the band spectrum, though it appears as the vapour matures by travelling a long distance. The low current excitation, however, gives the band spectrum initially, as does optical excitation by the light of  $\lambda$  2537. But the electrical excitation of the band spectrum can be got much brighter.

To illustrate the transition from line to band spectrum, the resistances in the external circuit may be arranged so that by use of a switch we can pass from a current of, say, 30 milliamperes to 1 or 0.1 milliampere. It might be expected, perhaps, that this would lead to a great diminution of brightness in the excited vapour; but, strangely enough, this is not the case, and if the conditions are right, the small exciting current actually makes the rising vapour much brighter than the large exciting current. This is doubtless connected in part with the greater duration of the band spectrum luminosity which, it will be shown later, lasts for more than 1/100th of a second, and could perhaps be made to survive perceptibly for 1/10th second. Incidentally, the experiment proves that the band spectrum is *actually* less with large currents, and is not merely made inconspicuous by contrast with strong line-spectrum luminosity.

So far as my experience goes, the line spectrum cannot be wholly got rid of by reducing the current, even to values so small as 1/100th of a milliampere. The lines (other than 2537 which is inherently associated with the band spectrum, see below) still appear faintly even with these small currents in the discharge, and, faintly, in the excited vapour, though in the latter they are very faint. Under these conditions the band spectrum, though overwhelmingly predominant, is actually rather faint, and most of the experiments have been made with a

\* 'Roy. Soc. Proc.,' *loc. cit.*



current of 1/10th milliampere, which gives the band spectrum in fair purity and brightness. As in the case of the arc discharge,\* residual line spectrum can be removed by passing the excited vapour close to an electrode which is at a negative potential relative to the anode. In the present case the iron plate D, fig. 1, at -110 volts, serves this purpose.†

As shown in the earlier paper‡ a portion of the intensity of the line 2537 is associated with the band spectrum, and in contrast with the portion which is associated with the complete line spectrum it cannot be removed by the electric field.

This conclusion has been criticised by Miss Hayner,§ who has suggested that what was observed to survive was the band 2539 (sometimes described as 2540) which (she supposes) was not sufficiently distinguished from the adjacent line. I had, however, satisfied myself that this was not the explanation before writing the paper, using a small size Hilger quartz spectrograph to photograph the residual light.|| I have now at command a medium size Hilger spectrograph capable of showing it more clearly still. The arrangement was nearly as in fig. 1. The current was large enough to allow of an appreciable amount of ordinary line spectrum to come up, and the visual lines each tapered down to a sharp point as before described.¶ The height of this sharp point was not so easily kept steady with the hot cathode discharge as with the arc formerly used, but it could be regulated by the current strength. Several different exposures with the larger spectrograph showed that at a point well above the sharp points of the visual lines 2537 could be photographed, and with adequate exposure 2540 came up as well in subordinate intensity. (Plate 44, No. 9.)

In none of these experiments has the line 2537 failed to show up in great intensity compared with all the other features of the band spectrum. Indeed, the only case I know of where it fails to do so is when the band spectrum is excited by fluorescence under the aluminium, and possibly certain other sparks.\*\* The great intensity of the feature (b) in the prismatic camera photo-

\* 'Roy. Soc. Proc.,' *loc. cit.*

† Some traces of line spectrum still remain and are detected by long exposure, but they are of a different order of intensity, and are further referred to in § 7.

‡ 'Roy. Soc. Proc.,' *loc. cit.*

§ 'Z. f. Physik,' vol. 35, p. 385 (1926).

|| I find that I did not expressly mention this. In some other kindred experiments a low resolving power was used, and it was not sufficiently explained that the conclusion had been established independently.

¶ *Loc. cit.*

\*\* 'Roy. Soc. Proc.,' A, vol. 111, p. 456 (1926).

graph to be presently described (Plate 43, Nos. 1 to 4) would alone be enough to suggest that it consists in the main of line spectrum; and in all cases examined, closer analysis with the large slit spectrograph shows that this is the case. After thorough purging from the positive ions which are associated with the complete line spectrum this line remains in great intensity, though, as explained before, a part of its intensity is removed with the positive ions. One or two other much fainter lines are perhaps in the same case with the line 2537. This and certain other complications, not here discussed, will, perhaps, be treated in a future paper.

The question naturally suggests itself whether the other important resonance line  $1^1S_0 - 1^1P_1$  1850 appears with the band spectrum. It was carefully looked for, with a bright spectrum and long exposure, using the small quartz spectrograph and a plate coated with oil, after the method of Duclaux and Jeantet. No trace of it was found, though the whole band spectrum on the less refrangible side of 2537 was over-exposed. (Plate 44, No. 7.)

#### § 4. *A Series of Flutings forming part of the Band Spectrum.*

In one of these long exposure photographs signs were noticed of a fluted structure in the region between 2650 and 3200. The structure in question is very indistinct owing to lack of contrast between the maxima and the intervening minima. This is no doubt the reason why it has not been noticed in the afterglow before. The maxima were very difficult to locate accurately by eye on the original negative. The best method of investigating them would be by means of a registering microphotometer, but I have not so far been able to get access to one of these instruments. It is hoped to do so before long. In the meantime I had resort to a special process of photographic intensification. This is in principle the same as one described by my father,\* but with some modifications of detail which have been found advantageous.

His method was to take a number of somewhat weak positives on glass, and to superpose them so as to increase the contrast. The difficulty of doing this is due to the parallax between the successive pictures which is introduced by the thickness of the glass. He overcame it by means of a system of lenses arranged to ensure that the rays used should traverse the assemblage as a parallel beam.

It is, however, more convenient to diminish the parallax by using celluloid films instead of glass plates. The films are, of course, much thinner, and allow the actual pictures to be placed in fairly close contact. Films have the further

\* Rayleigh, 'Phil. Mag.,' vol. 22, p. 734 (1911); 'Scientific Papers,' vol. 6, p. 65.

advantage that they lend themselves well to a simple mechanical device for bringing the pictures into register. My procedure is to throw an image of the original negative on to the wall, from which project two needle points somewhat further apart than the length of the projected spectrum. A strip of celluloid "process" film is fastened on the wall by pressing it home on to these needle points by means of a flat piece of cork. A short exposure is given, and then another strip of film is substituted, which is exposed in turn, and so on, up to, say, about five separate strips. The strips are then developed with a contrast developer, and after drying can be assembled by putting two needles through the original holes. When assembled, the ends are trimmed off to uniform length, and united with sealing wax applied over them. The needles are then removed. To keep the assemblage of films flat, they are conveniently held between glass plates, with india-rubber bands. The cemented ends are allowed to project beyond the glass.

The photograph (Plate 43, No. 5) was made by enlargement from an assemblage of films. It is therefore reproduced in negative, which for the present purpose is quite suitable.

The measurements given below were made on a paper print intensified in this way. They were interpolated between the mercury lines, and must be considered as provisional only. The bands doubtless extend further in both directions, but they become more and more difficult to make out. In this respect and in general aspect they are very similar to the ozone bands investigated by Prof. Fowler and myself.\* The wave-lengths have been given exactly as measured. It is hoped that the error does not exceed  $\pm 1 \text{ \AA}$ . It would be possible to readjust them slightly without doing any violence to observed facts, so as to reduce irregularities in the successive differences, but I have thought it best to leave it to any future investigator who makes use of the results to do this for himself if he thinks it desirable. The wave-lengths in brackets are interpolated. The corresponding bands are masked by mercury lines, which prevent their being satisfactorily measured.

The bands in this list do not show any heads, or any definite direction of shading. It is therefore very difficult to bring them into relation with the quantum theory of band spectra. There seems, however, to be some indication of convergence to a definite limit, as for example in the fluorescence spectrum of iodine. In the latter case important theoretical conclusions have been drawn by Franck from the position of the limit. There can be no doubt of the impor-

\* 'Roy. Soc. Proc.,' A, vol. 94, p. 522 (1917).

Wave-length.	Difference.	Wave-length.	Difference.
2697	5	2833	13
2702	7	2846	13
2709	5	2859	12
2714	7	2871	13
2721	6	2884	11
2727	8	[2895]	12
2735	7	2907	11
2742	7	2918	14
2749	0	2932	14
2758	8	2946	13
2766	9	2959	17
2775	8	2976	18
2783	10	2994	19
2793	9	3013	21
[2802]	10	[3034]	21
2812	11	3055	
2823	10		

tance of determining it in the present case, though the problem is technically very difficult. A further attempt will be made.

Stark\* has given a list of bands which he obtained in dense mercury vapour in the positive column of an ordinary discharge tube with a current of 10 to 30 milliamperes. His list includes some which are doubtless to be identified with certain of the above, though the agreement of wave-length is not very satisfactory. On the other hand many of the bands in Stark's list are quite extraneous to the spectrum which is under discussion here, and possibly belong to the ionised molecule. In particular, the group of bands given by Stark, as 3448, 3437, 3415, 3405, 3396, may be referred to. I have myself obtained them strongly under conditions similar to those used by Stark. They are then far more conspicuous than the group here tabulated, being much narrower and more intense. But a direct comparison of the negatives shows them to be absent in

\* 'Phys. Z.,' vol. 14, p. 564 (1913).

the spectra of the excited vapour obtained with the hot cathode and low current intensity. In the latter I have been unable to detect the slightest trace of structure in the region of the broad maxima near 3300 and 4400.

§ 5. *The Salient Features of the Band Spectrum, similarity in Rate of Decay.*

Many of the features of the band spectrum can be separated by the use of very small resolving power. Almost any resolving power, however small, is adequate to separate from one another—

- (a) The rather narrow band at 2345.
- (b) The complex, consisting of the resonance line 2537 and the features near it.
- (c) The maximum at about 2650, which seems to be associated with the series of flutings described in § 4.
- (d) The broad maximum at about 3300.
- (e) The green visual band, having a visual maximum about 4850, and a photographic maximum on ordinary plates about 4550.

To save circumlocution, the letters used in this list will be used in referring to the various features.

Satisfactorily to separate the items under (b), viz., the resonance line 2537·52, the band 2540 and the continuous band beginning at 2535·9 in which both are immersed,\* requires a spectrograph of fair resolving power. Leaving this on one side for the moment, and limiting the problem to the separation of (a), (b), (c), (d) and (e) from one another, it was found convenient to use a quartz prismatic camera with a quartz-fluorite achromat to photograph the spectrum of the glow at one exposure along the whole course of the tube. This simple method gives the wide field of view necessary in the vertical direction along the length of the tube, though, of course, the images of the bands show considerable curvature, introduced by the prism. The method is moreover economical of light, and gives the minimum of trouble in adjustment. The quartz-fluorite achromat is of 16 cm. focal length, and the quartz prism of 60° angle. The camera was placed 1 metre from the apparatus. Immediately in front of the tube was a slit 6 mm. wide, extending over the whole length which it was desired to examine.

The photograph No. 1, Plate 43, shows the spectrum of the vapour rising in the tube, as photographed with these arrangements. The bands are not labelled on this particular photograph, but can readily be identified from

\* See 'Roy. Soc. Proc.,' A, vol. 111, p. 456 (1926).

the neighbouring photographs, 2 and 4, which show the same features. The interruption in the middle is due to the heating coil, which was not in use in this particular experiment, but could not readily be removed. The actual distances in centimetres up the tube are shown on the scale on the left, which applies to all the photographs 1 to 4. The level marked zero on this scale is the level of the anode, and the whole distance above this is *outside the region of electrical excitation*. Little can be made out of the line spectrum. The band spectrum is very bright at the lower levels, and gradually fades out, but can be traced 25 cm. on these photographs. I have no doubt that if there were any particular object in doing so, an experiment could be arranged to show the glow several metres away from the region of discharge.

For some observations the loss of intensity as the vapour rises causes inconvenience, and it is desirable to compensate it by means of a suitable rotating sector. It was found that under the experimental conditions the visual intensity fell eight-fold in a distance of 14 cm. The sector was cut from black card, the angular aperture of the opening increasing rapidly with radial distance. This aperture was contained between a radius on one side and a logarithmic spiral curve on the other. At a certain radius it was  $360^\circ/8$  or 45 degrees, and increased progressively to the full  $360^\circ$  at the edge of the disc, 14 cm. out from the position last mentioned. The sector was placed immediately in front of the tube and rotated by a small electric motor. It compensated the loss of intensity very satisfactorily, making the luminosity appear quite uniform over a distance of about 16 cm. It was used in observing the part of the tube above the heating coil.

No. 2, Plate 43, shows a photograph of the spectrum of this part of the tube taken with the sector in use.

The visual band (e) is, of course, of uniform intensity on the photograph 1 over the length of 16 cm. which was covered by the sector; for the sector had been shaped so as to secure this result. But it is seen *in addition* that the ultra-violet members (a), (b), (c), (d) of the above list are also of uniform apparent intensity over this range. The sector reduces the intensity more than eight times as between its maximum and minimum transmission, and it follows therefore that over a full eight-fold range of real intensity, all these parts of the spectrum decay sensibly *pari passu*. It seems probable that if these rates of decay were not really the same, the inequality would have been conspicuous in this experiment. There seems no special probability that if such a difference existed it would be small, or that more than an eight-fold decay would be needed to bring it into evidence.

This experiment is at first sight difficult to reconcile with the results of Houtermans.\* His published photographs of the fluorescence of mercury vapour stimulated by the 2537 light of the mercury arc, show clearly a great difference of relative intensity between the various members at two different levels in the tube.

His method of experimenting differed from mine in that separate photographs were taken of the initial and of the final point of the range examined, instead of one photograph covering the whole range. This is, of course, a detail of technique, but it may conceal an essential point. In seeking a reconciliation, I should be inclined in the first instance to direct attention to the fact that his initial photographs were taken in the region where excitation is occurring, whereas photograph No. 2, Plate 43, refers entirely to the behaviour of the vapour after it has left the region of excitation. But it is useless to speculate on the matter, further experiment is required.

The above observations seem to show that the rates of decay of the various members of the band spectrum are nearly or quite the same. It is not certain that this rate of decay is independent of other conditions such as the density of the vapour stream; but the actual time required to decay to half intensity was determined under the experimental conditions used. For this purpose we require the velocity of the vapour by which distances along the tube can be converted into time intervals.

The discharge current was interrupted periodically by means of a rapidly vibrating contact breaker of known period. The tube was viewed in a cubical rotating mirror mounted on an axis that was vertical, and therefore parallel to the vapour stream. The appearance was as in fig. 2. In this diagram

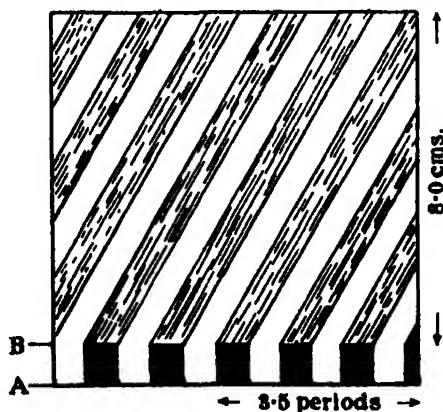


FIG. 2.

\* 'Z. f. Physik,' vol. 41, p. 140 (1927).

vertical heights are on a reduced scale, the level of the cathode being at A and that of the anode at B. Between these stretches the intermittent discharge, which is seen in the mirror broken up into vertical bands of light. Above the level of the top electrode we find these bands prolonged; they are still straight, but are inclined at an angle to their former vertical direction. The value of this angle depends, of course, on the angular velocity of the mirror.

To interpret this, we may regard the pattern seen as a graphical representation of events, distances being measured along the vertical axis, and times along the horizontal axis.

As regards the short stretch between the electrodes, every part of this is bright during discharge and comparatively dark in the intervals. The cycle of light and darkness is therefore in the same phase at every level, and the luminous bands appear vertical.

Suppose now that we follow up a vertical axis, beyond the level of the electrode we encounter regular alternations of light and darkness, corresponding to the successive pulses of luminosity which are in fact moving up the tube but would be seen stationary at an instantaneous view. Following a horizontal line, we find the alternations of light and darkness which correspond to the succession in time of the pulses which pass a given level. Finally, following along one of the inclined bright bands, we follow the career of a given pulse, as it occupies successive positions at successive times.

The slope of one of these bright bands gives the velocity. The vertical intercept is measured directly in centimetres, the horizontal intercept in periods of the interrupter which are counted by the bright discharges. We thus get the velocity directly in centimetres per period. By a knowledge of the period it can be translated into centimetres per second.

The interrupter used was one which has been in my possession many years. It was from a design by Mr. W. Spottiswoode, P.R.S., and is the same in principle as the ordinary vibrating hammer of an induction coil, with substitution of a comparatively stiff rod of 70 mm. long and 5 mm. diameter for the usual flat strip. It was used either to work a small induction coil, or alternatively to interrupt the 110 volt supply. In the latter case a resistance of 100 ohms was used in series, and the discharge electrodes connected across this resistance.

Owing to the appreciable vertical distance between the electrodes, the thickness of a luminous pulse is larger than might be desired, and the pulses tend to encroach on one another. Thus the dark spaces between them are less distinct than if the vertical dimension of the discharge had been less. It would be well



to use electrodes on the same level, with the electric current perpendicular to the vapour stream.

Under the actual conditions, and with the rate of distillation which was used when the photographs (Plate 43, Nos. 1 to 4) were being taken, it was found that for a distance of 8 cm. traversed, the time was  $3.5 \pm 0.5$  periods.\*

The rate of vibration of the contact breaker was independently determined as 1120 complete periods per second.

Thus the velocity of the vapour-stream is 2560 cm. per second, and an interval of  $10^{-3}$  seconds is represented by 2.56 cm. On the reduced scale of the photographs it is, of course, less. The time scale marked on the right of Plate 43 is based on this determination.

We have seen that the intensity of the band spectrum is reduced to one-eighth of its initial value in 14 cm. distance, equivalent to a time interval of  $5.47 \times 10^{-3}$  seconds.

Thus the time in which it would decay to half its initial value is  $1.82 \times 10^{-3}$  seconds.

#### § 6. *Effect of Heat on the Excited Vapour, Showing Band Spectrum.*

Interesting and significant results have been obtained under this head. It was observed by R. W. Wood† that the green fluorescence of mercury vapour under the aluminium spark was extinguished by local intense heating of the silica bulb in which the fluorescence was observed. So far as I am aware, nothing further has been done in this direction. I was anxious to discover what would be the effect in the ultra-violet region. The anticipation was that the whole of the band spectrum would disappear, and that the resonance line 2537 would alone survive, but this proved very wide of the mark. It was desired also to determine whether the effect of heat would be permanent, or whether, in the absence of a fresh stimulus, the vapour would recover as it moved away from the hot part of the tube. As will be seen the methods of experiment used are well adapted to an attack on this question. The arrangement was as in the previous section, but the heating coil above mentioned was now brought into use.

It consisted of about 2 metres of nichrome wire, wound in several layers, which were insulated from one another with asbestos paper. The whole was well lagged with asbestos. The current was regulated so as to heat the tube

\* Since writing the above I have seen a description of what is practically the same method which has just appeared, cf. M. Asterblum, 'Zeits. f. Phys.', vol. 41, p. 294 (February, 1927).

† 'Phil. Mag.', vol. 18, p. 247 (1909).

to a pretty bright red heat, but the temperature attained was not measured. The coil itself enveloped a length of about 2 cm., but an additional screen covered about 2 cm. of the tube above the coil, so that in all 4 cm. were concealed from view. This additional screen was to suppress the light from the red hot tube, which otherwise complicated the experimental spectra.

The photograph (Plate 43, No. 3) was taken without the use of the revolving sector. It shows a very remarkable difference of behaviour between the green visual band (*e*) and the other features (*a*), (*b*), (*c*), (*d*). The heat quenches the band (*e*) altogether, while it has little or no perceptible effect on (*b*) and (*d*). The effect on (*a*) and (*c*) is intermediate, but much slighter than the effect on the visual band (*e*).

This photograph shows the remarkable fact (verified also by visual observation) that the visual green band (*e*) after quenching by the heat recovers intensity as it passes up the cooler part of the tube. This recovery is not only relative to the other features of the spectrum, but the intensity actually recovers, though not to anything like its original value. The changes of intensity due to the change of temperature appear to be superposed on the decay of intensity which would occur at the lower temperature. The visual band (*e*) loses so much intensity on heating that the recovery on cooling is rapid enough to positively gain on the normal decay, and an actual recovery results. In the case of (*a*) and (*c*) the temperature effects are not large enough to prevail over the normal decay, at any rate under the actual experimental conditions.

As in the previous case (§ 5) it is convenient to compensate the normal effect of decay, in order to examine more easily what relative changes of intensity occur among the various components of the spectrum as the changes of temperature develop. The sector used before was originally adjusted to make the visual band (*e*) appear uniform along the tube at constant temperature. As we have seen, it was found to equalise the other features (*a*), (*b*), (*c*), (*d*) as well. The same sector was again applied to the part of the tube above the heating coil, and gave the result shown in Plate 43, No. 4. The features (*b*) and (*d*), which are little affected by the heat, are still equalised by the sector, as might be expected. The gain of the visual band (*e*) relative to them is now much accentuated; and it becomes apparent that (*a*) and (*c*) which were affected to some extent by the heat, show some relative recovery, though it is less marked than for the visual band. So far as can be judged by a qualitative examination, it seems that after the vapour has passed up 14 cm. from the heated region, the various components of the spectrum have made some progress towards recovering their initial relative intensities, which were disturbed by the change of

temperature. But the visual maximum is still far inferior to the maximum at 3300, to which, in the absence of any temperature disturbance, it was comparable.

The experiments on the heating effect described so far were made with small spectroscopic resolving power, which allowed many points to be examined very advantageously.

I now pass to experiments in which a much more complete analysis of the spectrum was made, by means of a Hilger slit spectrograph of medium size. The use of this instrument entailed limitations in other directions, and the work was confined to making exposures to the excited vapour showing band spectrum (1) at the lowest temperature which would keep the vapour from condensing; (2) with the tube kept at a dull red heat throughout the course of the vapour stream, with the exception of the discharge space and a short distance above it.

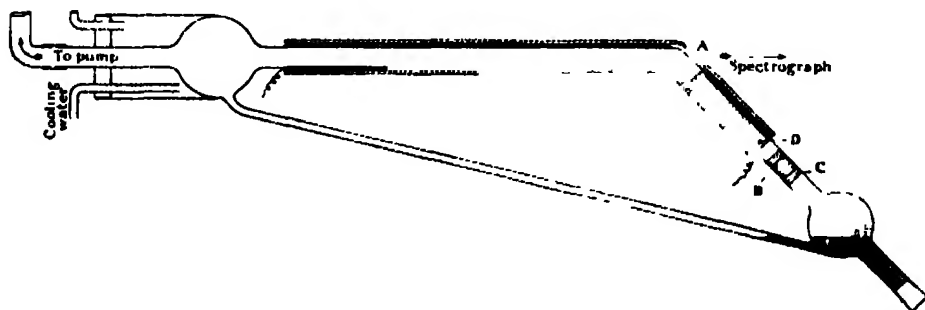


FIG. 3.—(One-sixth actual size.)

The tube used is shown in fig. 3. Its design is similar to fig. 1 so far as the distillation and return of the mercury are concerned, but the greater part of the length is arranged horizontally for an end-on view at A. The exciting discharge is perpendicular to the vapour stream, and to the plane of the diagram, the anode being an iron plate C placed against the wall of the tube, and the cathode (not shown) a hot oxide coated platinum wire placed opposite to it. The circle B represents the junction of the side tube carrying the cathode, which is of similar design to that shown in fig. 1. D is an auxiliary plate electrode which is at  $-110$  volts relative to the anode, and is used to clear off line spectrum, corresponding in all respects to the electrode marked D in fig. 1. The tube is covered with a heating coil of nichrome wire, asbestos lagged. There is a small window at A for spectroscopy. The condenser is of bulb form, and half of it is surrounded by a water jacket made of large rubber tubing, cut from a motor tyre tube.

The temperature was regulated by a rheostat in the circuit of the heating coil. The heater for evaporation was independent, and is not shown. The rubber cork at the bottom could be removed for assembling or cleaning out. The exposures were made at a current of 1/10 milliampere, and it was necessary to continue them in some cases for 24 hours. A graduated series made at the lower temperature was matched against a single exposure made at the higher temperature. Intensities were taken with sufficient accuracy as being in the inverse ratio to the exposure times required to get a given effect.

In this way the various features of the-spectrum were found to be diminished by the heat, in the following ratios :-

	Intensity ratio cold/hot.
(a) Band 2345	4
(b) { Resonance Line 2537	1
Band 2540	1
Continuous region from 2540 to about 2600	1
(c) Maximum at 2650 and flutings apparently associated with this maximum and reaching to about 3100	4
(d) Broad maximum at 3300	2
(e) Broad maximum at 4550, as recorded on ordinary photographic plates, but extending visually far into the green	>320

It will be seen that these more quantitative results confirm generally the qualitative data from the prismatic camera photographs Nos. 3 and 4, Plate 43.

The maximum (e) in the visual region was not visible at all on the high temperature photograph taken with a narrow slit, nor would the green light be seen by direct visual examination of the tube, though the competing dull red luminosity of the tube was unfavourable to the visual test. To make the photographic test more severe the spectrograph slit was opened from the standard width of 0.05 mm., used in taking the photographs above mentioned, to 1 mm., a factor of 20 times, and a 24-hour exposure was given. The resolving power remains enough to deal with the broad maxima, though not, of course, with the more delicate features.

There was a slight impression about the neighbourhood of the green band. It did not agree very well with the green band as regards its limits, and I am not certain that it was genuine and independent of diffuse light from the apparatus, and other accidental causes. But whatever the source, it was not more intense than the green band at the lower temperature as obtained with 1½-hour exposure, and 0.05 mm. slit width. From this is deduced the intensity ratio > 320, given above, which may be regarded as conservative.

The data given of course apply only to the actual experimental conditions. In particular the ratios found would doubtless depend upon the temperature. The particular temperature used was adjusted to the disappearance of the visual

green. If the tube were made hotter the ultra-violet bands would be more affected. Indeed, in some earlier and cruder experiments, which I do not describe, this was the case. But it has not been attempted to go further into the matter.

The pair of photographs, No. 6, Plate 44, are illustrative of this part of the work, though, of course, the reproduction cannot give as much information as a graduated series of original negatives. The upper photograph is taken at the lower temperature, the lower one at the higher temperature. The bands are marked above with the same letters as are used to designate them in Plate 43, and a few wave-lengths are added below, some of them belonging to stray traces of ordinary line spectrum. No. 8 shows an enlargement of 6 in the region near the resonance line, allowing the various features included in (*b*) to be distinguished. It is clear from this experiment in which the green glow is extinguished by continued heating (Plate 44, No. 6) that the radiations of energy in this region is not only delayed but finally prevented by the high temperature. Evidently the energy which would normally follow this course must be ultimately degraded in some other way. There is no evidence that the radiation at other wave-lengths is increased, on the contrary it appears to be diminished likewise, except in the case of the resonance line 2537 and the bands in its immediate neighbourhood, which are not perceptibly affected. Quantitatively, however, the behaviour of the green visual band is unique, its temperature sensitivity being of a different order of magnitude from that of any of the other bands.

The phenomenon of recovery on cooling, if the heating is not too much prolonged, is significant, and seems difficult to reconcile with the idea that dissociation of the excited molecules can be the cause of disappearance of the green light, for such a dissociation of excited molecules could hardly be reversible under the conditions.

#### § 7. *Relations of the Band Spectrum to the $1^3P$ states of the Atom. Occurrence of forbidden lines with the Band Spectrum.*

As is well known, the arc spectrum of mercury consists of triplets and singlets. The resonance line 2537·52, which has so often been mentioned, interconnects these two series, and represents a transition of the atom from the  $1^3P_1$  excited state to the  $1^1S_0$  normal state.

There are two other states  $1^3P_0$  and  $1^3P_2$  on either side of  $1^3P_1$ , which complete the triplet of states, but the lines corresponding to the transitions from these states to the normal state are not met with in the spectroscopic tables. That they are not readily observed is, of course, primarily a fact of observation, but

it is embodied in, and, to some extent, explained by, the selection principle which requires that in a change of state the inner quantum number should change by  $\pm 1$ , or by 0, with prohibition of the special case  $0 \rightarrow 0$ .

The ideal position of these lines can, however, be obtained by applying to the frequency of the resonance line the frequency intervals which occur in, *e.g.*, the triplets of the sharp series. In this way we deduce for the wave-length of the "forbidden" lines  $2655\cdot60$  and  $2269\cdot80$ .

The connection of the  $1^3P_1$  state of the atom with the band spectrum is very definite. To begin with, we have the overwhelming intensity of the resonance line  $1^1S_0 - 1^3P_1$  (2537) itself, associated with the band spectrum. Secondly it was shown\* that the band emission sets in sharply at a wave-length only  $0\cdot5 \text{ \AA}$  less than the centre of the resonance line. Thirdly, it is possible to excite the whole of the band spectrum on the side of longer wave-length by stimulation with the light of the resonance line.

Next, we come to the  $1^3P_2$  state of the atom, which would be represented by the "forbidden" line  $1^1S_0 - 1^3P_2$  (2270). This line is known from the work of Hansen, Takamine and Werner,† and Takamine and Fukuda.† It was best obtained from a "branched arc" in which a small fraction of the current of a mercury vacuum arc was taken off from a supplementary anode. The line was very faint compared with the resonance line or the other strong lines of the mercury spectrum.

Prof. Takamine noticed that the conditions favourable for the excitation of this forbidden line also tended to bring out the band 2345, called (*a*) in § 5 above, and he wrote to me (November 25, 1925) suggesting that on account of the presence of this band on my negatives of the excited vapour, I should look for the line 2270. I was unable to find any trace of it on the negatives made up till then, and replied to that effect.

Later, I repeated Takamine's experiments with the branched arc, and observed the line 2270 with the band 2345 and one or two of its companion bands 2338, 2334, etc., which are considerably fainter. 2345, however, was not more intense than I had often got it in the stream of excited vapour, and the broad maximum 3300 referred to as (*d*) in § 5 was present in fair intensity, which seemed to make the result less distinctive. Moreover, 2345 is strong in the absorption spectrum of unexcited mercury vapour, while no trace has ever been detected of 2270 in absorption. I was, therefore, somewhat discouraged in the attempt to trace any connection.

\* 'Roy. Soc. Proc.,' A, vol. 111, p. 457 (1926).

† For references see Takamine, 'Z. f. Physik,' vol. 37, p. 76 (1926).

The strong exposure with 1 mm. slit, see above, p. 635, gave suggestive indications which reopened the question. A 72-hours' exposure was then made with a slit width of 0.25 mm. and a current of 1/10 milliampere, and this gave very definite results.

The "forbidden" line 2270 came up well, and associated with it a band spectrum beginning abruptly at the line 2270, and extending in the direction of long waves as far as the band 2345. Four of the weaker bands known to be associated with 2345, namely, 2338, 2334, 2329, 2325, are visible and traces of more, but proceeding in the direction of short waves this structure became less distinct, and the spectrum becomes apparently continuous and of diminishing intensity up to 2270, when it abruptly stops. With the wide slit used, the limit was seen to agree with the line with an uncertainty of  $\pm 1.5 \text{ \AA}$ . See Plate 44, No. 10.\* A second exposure of 144 hours thoroughly confirmed these results. The continuous region on the long wave side of the forbidden line 2270 is distinguished from that on the long wave side of the resonance line, because the former initially increases in intensity as we go away from the line, whereas the latter initially diminishes.

The absolute intensity of 2270 is very small compared with Prof. Takamine's source, but its intensity relative to the neighbouring mercury lines (belonging for the most part to the diffuse triplet series) is much greater. Thus in an excellent photograph which he sent with his letter above mentioned, 2270 is decidedly inferior to 2259, and much inferior to 2378 and 2379. On my photographs it is much superior to all of these.† On the other hand the lines which on Takamine's photograph are about as intense as 2270 are altogether invisible on mine.

Finally, we come to the  $1^3P_0$  state of the atom. Franck‡ has sought to connect the band spectrum luminosity of long duration with a state of the molecule corresponding closely to this state of the atom, and Houtermans,§ developing Franck's ideas, has pointed out that the weak maximum about 2650 is not far from the calculated position of the "forbidden" line 2656.

It must, I think, be admitted that as a matter of observation there is nothing very crucial in the assumed connection of this maximum with the wave-length

\* The photographic manipulation was directed to bring out the limit of the continuous spectrum at 2270 and the band structure 2345, 2338, &c., visible on the negative had to be sacrificed, owing to the limited range of gradation available.

† 2378 and 2379 are not resolved with the wide slit used, but 2270 is much superior even to the blend.

‡ 'Trans. Faraday Soc.,' vol. 21, p. 530 (1926).

§ *Loc. cit.*

2656. For the intensity maximum is very broad and ill-defined (see *e.g.*, No. 6, Plate 44). If there were a sudden increase in the intensity of band spectrum setting in at the position of the line, as in the case of 2537 and 2270, the case would be altogether different. But this is not so. The maximum is a flat one, and 2656 is in the middle of it.

After detecting the presence of 2270 it was natural to look for 2656 as well.

As already mentioned, the photographs taken were not absolutely free of ordinary line spectrum. This spectrum when bright is apparently removed completely by the electric field. The photographs in the former paper\* afford convincing evidence of this. The auxiliary electric field was employed in the present case, but the initial brightness of the line spectrum was not great in the discharge itself, and in the excited vapour the visual lines cannot be seen at all. If present they are masked by the relatively bright background of band spectrum. Nevertheless, some lines come out on long exposure photographs, see *e.g.*, No. 6, Plate 44, of the present paper, when some of the lines are marked by their wave-lengths. In general, these lines are the strongest lines of the arc spectrum, but there are some striking exceptions not yet investigated. I do not know how it is that they escape quenching by the auxiliary electric field. It may be that they are merely due to stray light of the discharge itself, but in any case they represent a small residual effect only. To appreciate this fully they should be compared with 2537 on such photographs as No. 6, Plate 44. It is to be remembered that in the ordinary arc spectrum their intensity is comparable with 2537.

Now among these lines there is one whose approximate position is the same as the arc line  $2655.13 \text{ } ^3\text{P}_1 - ^3\text{D}_2$ . Near this position are the lines 2653.68 and 2652.04, of which it is enough to mention that they belong to the diffuse triplet series. The three lines together have the appearance of a close triplet in the arc spectrum, but this, of course, is spurious.

It was at first casually supposed that the line near 2655 *was* the arc line mentioned. But when the question of the "forbidden" line had been raised, it was noticed that this line was too strong to make such an attribution altogether satisfactory. Comparing various negatives available, it was found that as the current strength of the exciting discharge was lowered this line became relatively stronger, until at 1/100th milliampere it was the only line visible on the plate without the use of a magnifier, always excepting the resonance line 2537. Suspicion then became very strong, and a comparison spectrum was taken with the ordinary vacuum arc. The current used to excite the vapour was

\* 'Roy. Soc. Proc.,' 1925, *loc. cit.* Plate 5, Nos. 5, 6, 7, etc.



1/10th milliampere. It became apparent that the line in question was not present in the arc spectrum, and thus not coincident with 2655·13, but of slightly longer wave-length. See Plate 44, No. 11, which shows the displacement (excited vapour in the middle). A measurement—not the most accurate that could be made—gave the wave-length as 2655·73 which satisfactorily identifies it with the “forbidden” line at a computed wave-length of 2655·60.\*

The presence of the “forbidden” lines 2270 and 2656 in the excited vapour is of interest altogether apart from their association with the band spectrum. For they are here emitted in the absence of a magnetic field or an electric field, even the weak field required to produce discharge. It would seem that the theoretical views held hitherto about the conditions for their emission require some reconsideration. I do not wish, of course, to minimise the great difference in ease of excitation between these lines and the permitted line 2537, which has already been emphasised by Foote, Takamine and Chenault, in connection with their own experiments.

By taking short exposure photographs for intensity comparison with the long exposures, the relative exposure times required to bring up these lines to the same intensity were roughly estimated. They were as follows:—

Line.	Wave-length.	Time.	Reciprocal of time.
$1^1S_0 - 1^3P_0$	2656	100	0·01
$1^1S_0 - 1^3P_1$	2537	1	1·00
$1^1S_0 - 1^3P_1$	2270	17,000	0·00006

The intensity ratios thus approximately indicated may be compared with those of an ordinary series triplet. The triplets of the sharp or the diffuse series for example have intensity ratios 5 : 3 : 1.

It is worth noting that the “forbidden” line 2655·60 has not come under observation before, though it is here obtained about 170 times brighter than the line 2269·80 which *has* been observed. The probable reason is that it is usually masked by the mercury line 2655·13, which is shown in comparison with it in photograph No. 11, Plate 44.

### § 8. Conclusion and Summary.

In this paper not much is said about the ultimate interpretation of the data. The facts are undoubtedly complex, and as yet far from being adequately

\* A better negative gave 2655·78. This is not very close to the value 2655·60 calculated on p. 637, but it is close to the value 2655·81 calculated from the term values adopted in Fowler's Report. There is some internal discrepancy in the published series scheme.

explored. I have tried to elucidate those points which seemed likely to be most instructive, but in the course of the work many other questions have suggested themselves, the answer to which should contribute to the ultimate solution. The present contribution has not been made without effort. I have been efficiently helped throughout by my assistant Mr. R. Thompson.

### Summary.

An improved method is worked out for obtaining the mercury band spectrum of long duration. The stream of vapour is excited by a current of less than a milliampere, using a hot cathode. It is then observed spectroscopically after leaving the region of discharge.

As in previous investigations, the resonance line 2537 is associated with the band spectrum, but the resonance line 1850 is absent.

The important divisions of the band spectrum are : -

- (a) The band at 2345, with attendant bands of shorter wave-length.
- (b) The resonance line 2537, with bands within a few Ångströms of it.
- (c) The fainter maximum at 2650, and a series of flutings which are made out with difficulty but seem to be associated with it. Approximate wave-lengths of these bands are given.
- (d) The broad maximum at 3300.
- (e) The broad visual maximum.

It is found that when the vapour is examined *after excitation* all these features decay *pari passu*. The actual time taken to decay to half intensity under the conditions is measured as  $1.82 \times 10^{-3}$  second.

If the excited stream of vapour is passed through a tube locally heated to redness, the band (e) is extinguished, (a) and (c) are slightly weakened, but (b) and (d) are almost unaffected.

As the vapour passes on to the cold part of the tube the visual light (e) reappears to some extent, and (a) and (c) tend to regain their intensity relative to (b) and (d).

The "forbidden" line  $2270\ 1^1S_0 - 1^3P_2$  is present in the spectrum, and can be brought out by long exposure. It is evidently connected intimately with the band spectrum, since a reach of apparently continuous spectrum begins at this point, and extends with increasing intensity to the band group 2345, 2338, etc. On the short wave-length side of the forbidden line 2270 the background of the spectrum is quite dark, and also between 2345 and the resonance line 2537. From the resonance line 2537 onwards to the visual the whole background is more or less bright, as emphasised in earlier papers.

The other "forbidden" line 2656,  $1^1S_0 - 1^3P_0$ , is likewise present with the band spectrum, and in far greater intensity than 2270. It is believed that this line has not previously come under observation. There is apparently no sudden change in the intensity of the band spectrum at this point in contrast with 2537 and 2270.

#### DESCRIPTION OF PLATES 43 AND 44.

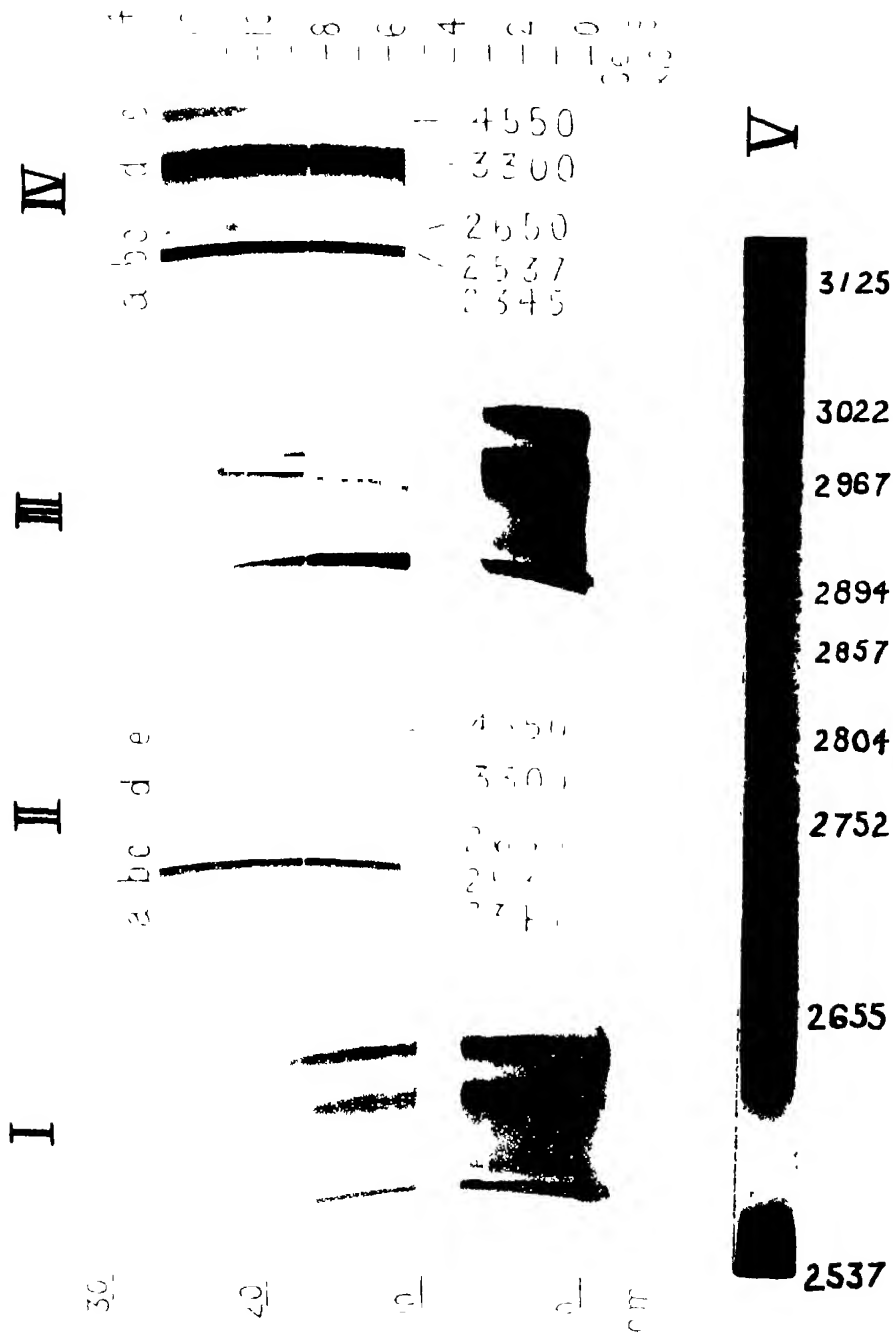
(The order of photographs is not the same as their order of description in the text.)

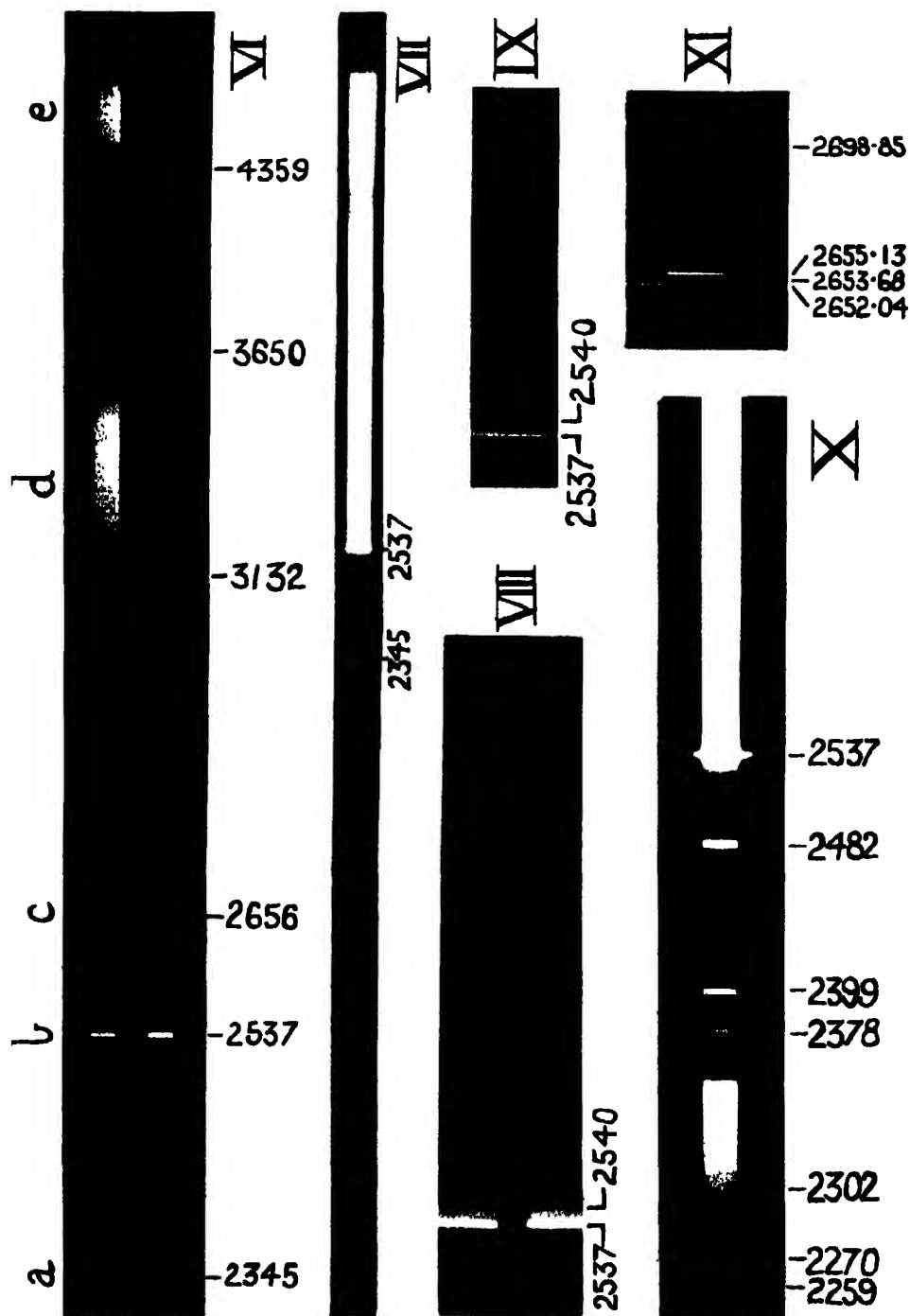
##### PLATE 43.

- No. 1.—Prismatic camera spectrum of excited mercury vapour. Wave-lengths as in 2. Zero of scale on the left shows limit of the region of excitation (anode level). Scale on the right shows times. These scales apply to Nos. 1 to 4 inclusive.
- No. 2.—The same spectrum. Decay of intensity equalized by a revolving sector. Shows that all features of the spectrum decay at the same rate after excitation is over.
- No. 3.—The same spectrum. Vapour strongly heated as it passes through the region at 10 cm. up. Note the disappearance of the visual band 4550 (called *e*). Note also that this band recovers as the vapour cools, reaching a maximum at 18 cm. and then finally decaying.
- No. 4.—Same as 3 but with revolving sector in use. Note that 2345 (*a*), 2650 (*c*), 4550 (*e*) all recover intensity relative to 2537 (*b*) and 3300 (*d*).
- No. 5.—Slit spectrogram of excited vapour. Specially intensified to bring out a series of flutings which seem to be associated with the maximum 2655 (*c*). Wave-lengths of superposed line spectrum are marked. Reproduced in negative.

##### PLATE 44.

- No. 6.—Slit spectrogram of excited vapour. Low temperature below. High temperature above. Features lettered as under 4. Note that the visual band is extinguished, and all others diminished, except the resonance line 2537 and the band near it (see 8).
  - No. 7.—Slit spectrogram of excited vapour. Region to right of 2537 over-exposed. Range extends to 1850 but no trace of the resonance line at this point is seen.
  - No. 8.—Enlargement of a portion of 6.
  - No. 9.—The resonance line 2537 with the band 2540 to show that the former is not removed by passing the excited vapour through an electric field.
  - No. 10.—Long exposure photographs of the excited vapour, taken with wide slit. Note the "forbidden" line 2270  $1^1S_0 - 1^1P_1$ . Note also the band spectrum connecting this line with the band 2345 (*e*). Note that the background of the spectrum is dark on either side of this stretch of band spectrum.
  - No. 11.—"Forbidden" line 2656  $1^1S_0 - 1^3P_0$ , in the excited vapour. Comparison top and bottom is the ordinary mercury vacuum arc. Wave-lengths marked apply to the latter only.
-





*Note on a Connection between the Visible and Ultra-Violet  
Bands of Hydrogen.*

By O. W. RICHARDSON, F.R.S., Yarrow Research Professor of the Royal  
Society.

(Received February 25, 1927.)

The many lined spectrum of hydrogen on the short wave length side of  $\lambda 1675 \text{ \AA}$  was discovered by Schumann, and measured and extended by Lyman who published a list of wave-lengths of the lines in his book.\*

A considerable number of the lines between 1025 and 1240  $\text{\AA}$  have been carefully measured recently by Werner† who succeeded in arranging them into bands. Another system of bands in this region was discovered by Lyman\* in the spectrum of a discharge in argon which contained a trace of hydrogen. These bands, which it is convenient to call the Lyman bands, have recently been arranged by Witmer‡ who has also measured up and reclassified some of Werner's bands.

Still more recently Dieke and Hopfield§ have succeeded in obtaining the *absorption* spectrum of  $\text{H}_2$ , and by studying this in connection with the emission spectra have been able to extend very considerably the system of bands of which the Lyman bands and Werner bands form a part. They were able to show that each of these sets of vibration bands have the same final electronic state A, but different initial electronic states B (Lyman bands) and C (Werner bands). The difference of the levels is in wave numbers  $B - A = 91562$  and  $C - A = 99986$ . The constant  $w_0$  which measures the vibration frequency at infinitesimal amplitude and the constant  $xw_0$  which determines the deviation from simple harmonic motion have for the three states the values :—

State.	A.	B.	C.
$w_0$	4362	1355	2444
$xw_0$	114.5	18	67

It is not clear exactly how these numbers have been calculated but such details cannot affect their values very much.

\* 'Spectroscopy of the Extreme Ultra-violet' (1914).

† 'Roy. Soc. Proc.,' A, vol. 113, p. 107 (1926).

‡ 'Proc. Nat. Acad., U.S.A.,' vol. 12, p. 238 (1926); 'Phys. Rev.,' vol. 28, p. 1223 (1926).

§ 'Z. f. Physik,' vol. 40, p. 299 (1926).

It is evident from the magnitude of  $B - A$  and of  $C - A$  and the data in 'Structure,' Part V\* (cf. for example Table XI, p. 399), that A must be a state of total quantum number 1. It is probable that the B and C states are both states with total quantum number 2, and it is natural to enquire whether they may be identified with any of the 2 states which have been found to be final states for the bands in the visible. There is no state in the visible as yet discovered which corresponds to the B state, but both the states  $2\sigma = 29330.30$  and  $2\pi = 29502.82$  in 'Structure,' Part V,\* are very close to the C state. The ionisation potential of  $\text{H}_2$  is known to be very close to 15.9 volts† or 128800 wave number. Subtracting 99986 from this we get 28814, which would agree with either  $2\pi$  or  $2\sigma$  as nearly as the accuracy of the ionisation potential demands.

To distinguish between the claims of  $2\pi$  and  $2\sigma$  or to ascertain their adequacy we can examine the values of the vibration term constants  $w_0$  and  $xw_0$ . Unfortunately the values given by Dieke and Hopfield lie between the values given for  $2\sigma$  and those extrapolated for  $2\pi$  from the  $3\pi$ ,  $4\pi$  and higher states. To obtain a better judgment on the matter I have recalculated these quantities using Werner's measurements of the *lines* treated on the classification basis of Dieke and Hopfield, and following methods of treatment as similar as possible to those used in 'Structure,' Part V. From the  $m = 1, 2, \dots 6$  lines of Werner's B and E bands I get  $2w_0(1 - 2x + \dots)$ , from F and G  $w_0(1 - x + \dots)$ , and hence a preliminary value of  $w_0x$ . From I and L I get  $w_0(1 - 3x + \dots)$  and take the means of these and the values of the same quantities got from B, E, F, and G. I then get a new set of values of  $w_0x$  by subtracting the mean of  $w_0(1 - x + \dots)$ , got from E, B and F, G from the mean  $w_0(1 - 3x + \dots)$ . These are then averaged with the former  $w_0x$  and 3 independent values of  $w_0$  are then got from  $w_0(1 - 2x + \dots)$  from B and E, from  $w_0(1 - x + \dots)$  from F and G, and from the mean  $w_0(1 - 3x + \dots)$  from G, F, E, B and I, L. These are finally averaged with the result shown in the second and third rows of the following table:—

$m \rightarrow$	1.	3.	4.	5.	6.
(1) Mean $w_0$	2384.6	2385.1	2372.5	2369.3	2361.7
(1) Mean $w_0x$	76.9	73.8	70	73.8	75
(2) Mean $w_0$	2352.1	2389.6	2368.3	2374.6	2362
(2) Mean $w_0x$	58.3	75.4	67	75.0	64

\* O. W. Richardson, 'Roy. Soc. Proc.,' A, vol. 113, p. 399 (1926).

† *Loc. cit.*, p. 412.

The fourth and fifth rows give the corresponding quantities got when Witmer's measures of the lines are used in the same way. They are in reasonable agreement with the first though not so regular. It must be remembered that an error of 0.1 Å makes a change of nearly 10 in the wave number in this region of the spectrum.

These numbers would seem definitely to rule out  $2\sigma$  for which  $w_0 = 2593.82$  and  $xw_0 = 68.41$ . They are, however, not incompatible with  $2\pi$  for which the values extrapolated from the terms with higher electron total quantum numbers are approximately  $w_0 = 2350$  and  $xw_0 = 63$ .

This means that none of the  $Q(m)$  lines in 'Structure,' Part V, have a final 2 state which is the same as the initial 2 state of any of the known ultra-violet bands. The same applies to the  $P(m)$  and  $R(m)$  lines given in 'Structure,' Part IV,\* as associated with some of these  $Q$  branches. In the notation of the notes on p. 400 of Part V all these lines have final  $2\sigma$  states.

It remains to enquire whether there is any evidence in the spectrum of the existence of final  $2\pi$  states which would agree with the C states. For some time I have held the opinion that the bands designated  $AP'Q'R'(m) \dots EP'Q'R'(m)$  in 'Structure,' Part IV, must be the  $0 \rightarrow 0$ ,  $1 \rightarrow 1$ ,  $2 \rightarrow 2$ ,  $3 \rightarrow 3$  and  $4 \rightarrow 4$  vibration bands of  $2\pi - 3\sigma$ .† There is substantial evidence in favour of this view which I propose to produce in detail in a later paper. I may, however, mention that, together with the  $2\sigma - 3\pi$  lines and 11 lines in the yellow arranged by Curtis, lines from this group make up all the lines with any strength in the First Type discharge between  $H_\alpha$  and  $\lambda = 5000$  Å.U. (see Part IV, fig. 2, p. 716). Furthermore, the A ( $0 \rightarrow 0$ ) band is associated with bands in and beyond the blue of which the  $Q(1)$  lines form a Rydberg Ritz sequence, and the lines of these bands enter into combinations with others in a manner which accords with this hypothesis. Admitting that  $2\sigma - 3\pi$ ,  $1 \rightarrow 1$ ,  $Q(1)$  is  $\lambda 6093.83 = \nu 16405.52$  we can calculate  $2\sigma - 3\pi$ ,  $1 \rightarrow 0$ ,  $Q(1)$  approximately either by using a value of 2, 1, 1 — 2, 0, 1 extrapolated from the values for  $n\sigma$ , where  $n = 3, 4, 5$  and 6 in Table XIII of Part V (p. 406) or by using the values of  $w_0(1 - x)$  got from the ultra-violet bands. With regard to these it is not certain whether the line numbered 0 or that numbered 2 by Werner (these lines are numbered 1 and 3 respectively by Witmer) should be taken as the  $Q(1)$  line. We thus get for the  $1 \rightarrow 0$   $Q(1)$  line the following alternatives: (1) by the extrapolation 18690 (2)

\* O. W. Richardson, 'Roy. Soc. Proc.,' A, vol. 111, p. 714 (1926).

† This is in accordance with the view that the electronic structure of the  $H_\alpha$  spectrum is closely similar to that of the He line spectrum. For a brief outline and the notation here used see 'Structure,' Part V, p. 400 (footnotes).



Werner's  $m = 0$ , 18713.22 (3),  $m = 2$ , 18716.82 (4), Witmer's  $m = 1$ , 18699.3, and (5)  $m = 3$ , 18719.7. With a possible alternative for the second line which was afterwards thrown out by the combinations, the only reasonable arrangement of lines to form a Q branch in this region is that designated as  $3\sigma, 1, m - 2\pi, 0, m$  in the following table:—

 $3\sigma, 1, m - 2\pi, 0, m.$ 

$m.$	Properties.								Wave-length in air (Int.).	Wave- number.	1st Diff.	2nd Diff.
1	(1)	(2)	(3)	(4)	(5)	(6)	(7)	(8) (a)	5340.84 (1)	18718.46	12.01 20.14 34.41	14 13 8.27
2				++				$1\alpha_0Q$ (5) (a)	5344.82 (-)	18706.45		
3								(a)	5351.75 (0)	18680.31		
4				++				$1\alpha_0Q$ (6) (a)	5361.63 (-)	18645.90		

 $3\sigma, 2, m - 2\pi, 1, m.$ 

1								(?)	5462.99 (0)	18299.94	11.68 22.89 31.27	11.21 8.38
2								(a)	5466.47 (0)	18288.26		
3								T (a)	5473.32 (p)	18265.37		
4								D (a)	5482.71 (rd <sup>2</sup> )	18234.10		

 $3\sigma, 3, m - 2\pi, 2, m.$ 

1								D (a)	5585.52 (r)	17898.46	14.46 24.25	9.79
2								T (a)	5590.04 (g)	17884.00		
3		++	+					(3)	5597.63 (4)	17859.75		

Having got the  $3\sigma, 1, m - 2\pi, 0, m$ , the  $3\sigma, 0, m - 2\pi, 0, m$ , the  $3\sigma, 1, m - 2\pi, 1, m$  and the  $3\sigma, 2, m - 2\pi, 2, m$  bands the  $3\sigma, 2, m - 2\pi, 1, m$  and the  $3\sigma, 3, m - 2\pi, 2, m$  bands were found by assuming that these bands would be interrelated in a similar manner to the corresponding  $3\pi - 2\sigma$  bands described in Part V. There is a possible weak alternative to the strong line 5597.63 (4) attributed to  $3\sigma, 3, 3 - 2\pi, 2, 3$ , but I am inclined to think that this strength is a genuine abnormality. Of these lines the only one observed on a typical first type plate was  $3\sigma, 3, 3 - 2\pi, 2, 3$ . The line  $3\sigma, 2, 1 - 2\pi, 1, 1$  was doubtful, being possibly mixed up with another line. It was not to be expected that these lines would be strong in the first type otherwise they would probably have been

picked out already. The fact that the line  $3\sigma, 1, 1 - 2\pi, 0, 1$  is recorded by Merton and Barratt as depressed in the condensed discharge is very satisfactory, this being a very common feature of the low rotation quantum number lines in this spectrum (see the various tables in Parts IV and V). The fact that the only line recorded as enhanced by the condensed discharge is the low pressure line  $3\sigma, 3, 3 - 2\pi, 2, 3$  also points in the same direction. The  $\text{He}++$  character of  $3\sigma, 1, 4 - 2\pi, 0, 4$  is also satisfactory as it will be remembered that the higher rotation quantum number lines of the following bands, each of which is the band of lowest vibration number in the sequence of bands to which it belongs, are brought up by helium, viz.,  $3\pi, 0, m - 2\sigma, 0, m$ ;  $3\pi, 1, m - 2\sigma, 0, m$ ;  $4\pi, 0, m - 2\sigma, 2, m$ ;  $4\pi, 0, m - 2\sigma, 0, m$ ; and  $3\sigma, 0, m - 2\pi, 0, m$ . We should therefore expect  $3\sigma, 1, m - 2\pi, 0, m$  to have the same property. This argument is unfortunately weakened by the fact that the positions of  $3\sigma, 1, 2 - 2\pi, 0, 2$  and  $3\sigma, 1, 4 - 2\pi, 0, 4$  are respectively practically indistinguishable from those of  $3\pi, 1, 5 - 2\sigma, 0, 5$  and  $3\pi, 1, 6 - 2\sigma, 0, 6$  which should also be very weak lines brought up by helium.

From  $3\sigma, 1, m - 2\pi, 0, m$ ;  $3\sigma, 1, m - 2\pi, 1, m$ ;  $3\sigma, 2, m - 2\pi, 1, m$  and  $3\sigma, 2, m - 2\pi, 2, m$  we can calculate the values of  $w_0$  and  $xw_0$ . The result is shown in the second and fourth rows of the following table:—

$m \rightarrow$	1.	2.	3.	4.
(3) $w_0$	2385.57	2378.96	2367.62	2356. --
(1) $w_0$	2385.1	2372.5	2369.3	2361.7
(3) $xw_0$	72.63	72.30	70.71	70. --
(1) $xw_0$	73.8	70	73.8	73

The third and fifth rows give the corresponding values got from the ultra-violet lines (C states) on the basis of the classification of Dieke and Hopfield using Werner's measures of the wave-numbers and changing the rotation numbers of his lines from 2, 3, 4 and 5 to 1, 2, 3 and 4 respectively. The agreement is quite as good as the ultra-violet measurements warrant but it requires this change in the numbering. This evidently supports the view, which Werner himself also considers probable, that the lines numbered 2 in the ultra-violet bands are the Q (1) lines, the lines numbered 0 and 1 probably being R or R' lines.

This agreement would seem to establish the identity of the C states in the ultra-violet spectrum and the  $2\pi$  states in the visible spectrum if the  $3\sigma, 1, m - 2\pi, 0, m$ ;  $3\sigma, 2, m - 2\pi, 1, m$  and  $3\sigma, 3, m - 2\pi, 2, m$  Q branches are real.

There is in existence further evidence of such reality. In addition to the  $0 \rightarrow 0$ ,  $1 \rightarrow 1$ ,  $2 \rightarrow 2$ ,  $3 \rightarrow 3$  and  $4 \rightarrow 4$  bands of the  $3\sigma - 2\pi$  transition I have a list of the lines of the Q branches of the following bands belonging to the next electron transition  $4\sigma - 2\pi$ , viz.,  $4\sigma, 0, m - 2\pi, 2, m$ ;  $4\sigma, 0, m - 2\pi, 1, m$ ;  $4\sigma, 1, m - 2\pi, 2, m$ ;  $4\sigma, 0, m - 2\pi, 0, m$ ;  $4\sigma, 1, m - 2\pi, 1, m$ ;  $4\sigma, 2, m - 2\pi, 2, m$ ;  $4\sigma, 1, m - 2\pi, 0, m$ ; and  $4\sigma, 2, m - 2\pi, 1, m$ . These combine with each other and also with the appropriate lines of the  $3\sigma \rightarrow 2\pi$  bands. Furthermore in these bands just as in the  $3\sigma \rightarrow 2\pi$  bands the  $0 \rightarrow 0$ ,  $1 \rightarrow 1$  and  $2 \rightarrow 2$  bands are the strongest and their leading lines come up in the first type discharge. The other bands are weaker and also react to the first type discharge in about the same way as the other  $3\sigma \rightarrow 2\pi$  bands.

If these conclusions are right it is possible to calculate the moment of inertia of the normal hydrogen molecule with more certainty than has hitherto been the case, as well as that of the molecule in the  $2\pi$  state. The latter is the final state of the  $AP'Q'R'$  ( $m$ ), etc., bands, and from Table XXI of Part IV we have  $4b = R'(2) - P'(3) - [R'(1) - P'(2)] = 142$  at the  $n = 0 \rightarrow 0$   $m = 1 \rightarrow 1$  end of the bands. This gives

$$J_0 = 7.81 \times 10^{-41}, \quad r_0 = 1.005 \times 10^{-8} \text{ cm.}$$

for the moment of inertia and the distance between the nuclei for  $H_2$  in the  $2\pi$  state. We can check this by calculating data like those of Table XVI of Part V (p. 409) from the Q branches of the  $3\sigma - 2\pi$  bands. The method is inaccurate on account of irregularities in the lines and the meagreness of the data. By the method used in getting Table XVI of Part V, I find  $\frac{3}{2}w_0u^2(1 + 2b) = 1.01$ , whereas the method which depends on getting the difference of the second differences of the lines of Q branches of bands with the same ( $0 \rightarrow 0$ ) initial vibration states, but with the final vibration states differing by unity comes out to be 2.68. This agreement is not satisfactory but the divergence is almost inevitable from the character of the data. Anyhow the mean of these values 1.85 is close to the value got by extrapolating from the values of the corresponding quantity given in Table XVI for the  $3\pi$ ,  $4\pi$ ,  $5\pi$  and  $6\pi$  states, and so is hardly likely to be far wrong. This value using  $w_0 = 2385.57$  and  $xw_0 = 72.63$  leads to  $uw_0 = 55.9$  and  $J_0 = 9.93 \times 10^{-41}$  which may be regarded as a confirmation of the more accurate value  $7.81 \times 10^{-41}$  given above. It is satisfactory to have this confirmation even if it is only rough because it throws out alternative interpretations of the spectrum which otherwise might have to be considered.\*

\* [Note added March 30, 1927.—It is interesting to observe that this estimate of  $J_0$  for the  $2\pi$  state is not very different from that found for the  $2\sigma$  state in Part V. The  $2\pi$  and

For the normal state of  $H_2$  using the ultra-violet bands and applying the formula  $2(B_1 - B_2)(m + \frac{1}{2})^2$  to Werner's measurements of the wave-numbers of the lines (as numbered above) for the band A (3) C (0),  $2(B_1 - B_2) = -41.5$ , for A (2) C (0),  $2(B_1 - B_2) = -45.6$ , and for A (1) C (0),  $2(B_1 - B_2) = -48.3$ . These values extrapolate to  $2(B_1 - B_2) = -51.7$  for A (0) C (0). Combining this with the value  $2B_1 = 71$  got from the P. R branches of the  $3\sigma - 2\pi$  bands we get  $2B_2 = 71 + 51.7$ , whence

$$J_0 = 4.52 \times 10^{-41} \text{ and } r_0 = 0.765 \times 10^{-8} \text{ cm.}$$

for normal  $H_2$ . The other method which is unreliable on account of the large errors of measurement in the ultra-violet bands, when used as a check leads to  $J_0 = 7.9 \times 10^{-41}$ . All that I am inclined to conclude from this value is that it lends no support for a value under  $4.52 \times 10^{-41}$ . This is higher than almost all the values which it has been found possible to reconcile with the specific heats of hydrogen at different temperatures.\*

It is necessary to say a little about the heats of dissociation and so on in Table XVIII of Part V (p. 415). The value 125000 of  $R_m M_\infty$  for  $m = 1$  estimated on p. 414 must now be replaced by the value of the ionisation potential 128800 since it appears that this agrees with the spectroscopic data. This has the effect of changing the successive values of  $DM_m$  from 34050, 20721, 18170, 17850, 17644 and 17598 to 34050, about 17000, 15554, 15234, 15128 and 15082. At the same time the value of  $D'M_m$  for  $m = 2$  should be changed from the value 26900 for the  $2\sigma$  state to the value about 21000 for the  $2\pi$  state to be compatible with the others. This makes all the  $DM_m$  from  $m = 2$  to  $m = 6$  not vary so much as before and the same is true of the corresponding  $D'M_m$ , but now the  $DM_m$  run about 5000 below the  $D'M_m$ . I am inclined to think that this is due to the linear extrapolation, which is used in getting the  $D'M_m$ , breaking down.

the  $2\sigma$  states each have very similar values for the electronic and vibrational terms. The estimate of  $J_0$  for the  $2\sigma$  state is surer than that for the  $2\pi$  state, being supported by three independent methods, viz. :—(1) from the  $P_1R$  branches of Part IV which are more securely established than the  $P'R'$  branches; (2) from quite good values of  $xw_0$  and of  $\frac{1}{2}w_0w^2(1 + 2b)$  and finally (this is not mentioned in Part V) (3) from the application of Kratzer's fourth power term  $4 \left\{ \frac{B_2^3}{w_{01}^3} - \frac{B_1^3}{w_{01}^3} \right\} (m + \frac{1}{2})^4$  to the small decrement in the second differences with increasing  $m$  in the  $_{\infty} \alpha_n Q$  branches. If  $2B_1 = 53.55$  and  $2B_2 = 60.88$  the calculated value of  $8 \left\{ \frac{B_2^3}{w_{01}^3} - \frac{B_1^3}{w_{01}^3} \right\}$  is found to be 0.0048 as compared with 0.0057 got from the third differences of the  $Q$  lines.

\* See Van Vleck, 'Phys. Rev.,' vol. 28, p. 980; Hutchinson, *ibid.*, p. 1022 (1926).

It will be observed that the  $D'M_m$  converge at  $m = \infty$  to the value 15018. This is not in agreement with a result of Alexandrow\* who finds by a calculation based on the "wave-mechanics" that the ionisation potential of the ion  $H_2^+$  is exactly equal to that of the neutral hydrogen atom, viz.,  $Rh = 13.5$  volts. This would require that  $DM_m$  should converge to the value zero at  $m = \infty$ . However, Alexandrow's result is in contradiction with the experimental value of the ionisation potential of  $H_2$  although he is under the impression that this is not the case, being misled, as I think, by a wrong value of the heat of dissociation of  $H_2$ .

*Absorption of Radiation in the Extreme Ultra-Violet by the  
Inert Gases.*

By CLIVE CUTHBERTSON, O.B.E., F.R.S.

(Received December 8, 1926.)

[PLATES 45, 46.]

In 1910 I published† a set of determinations of the refraction and dispersion of the five inert gases for eight wave lengths in the visible region, together with values of the constants  $C$  and  $n_0^2$  in the expression

$$\mu - 1 = \frac{C}{n_0^2 - n^2}.$$

If Drude's form of the dispersion equation is substituted,

$$1 = \sum \frac{Ne^2}{\pi m (n_0^2 - n^2)},$$

where  $N$  is the number of electrons per cubic centimetre, and  $n_0$  the free frequency of the electrons, and it is assumed that there is only one free frequency in the molecule, it is possible to deduce from this equation the number, or apparent number, of electrons per molecule which affect dispersion and their free frequency.

If  $N$ , in Drude's expression,  $= N'q$ , where  $N'$  is the number of molecules in unit volume and  $q$  the number of "dispersion" electrons per molecule, and if

\* 'Ann. d. Physik,' vol. 81, p. 603 (1926).

† C. and M. Cuthbertson, 'Roy. Soc. Proc.,' vol. 84, p. 13.

$N' = 2.705 \times 10^{19}$ ;  $e = 4.774 \times 10^{-10}$  e.s.u.;  $e/m = 5.301 \times 10^{17}$  e.s.u., the experimental results for the inert gases lead to the following figures—

Table I.—Constants in the expression  $\mu - 1 = \frac{N'qe^2}{2\pi m (n_0^2 - n^2)}$ .

Element.	$q$ .	$n_0^2 \times 10^{-27}$ .	$\lambda_0 \cdot 10^8$ (A.U.).
Helium	1 21238	34992	507
Neon	2.59826	38916	481
Argon	4.71632	17009	726
Krypton	5.3446	12768	840
Xenon	6.1209	8978	1001

During the last few years the region in which the calculated free frequencies lie has been brought, by the work of Lyman and others, within the bounds of experimental examination, and this paper gives an account of an attempt to test whether absorption bands do, in fact, exist in the neighbourhood of the points where the simple theory predicts the existence of free frequencies.

The plan at first adopted was to endeavour to produce a continuous spectrum of radiation, extending from about  $\lambda$  2500 to the region of X-rays, by means of a concave grating in a vacuum spectrograph, and, by admitting gas between the source of radiation and the photographic film, to block out that region in which absorption might occur. The apparatus consisted of a concave grating  $5 \times 3.8$  cm., ruled for the extreme ultra-violet at the National Physical Laboratory with the Blythswood engine. The grating had a focal length of 48.5 cm. and was mounted in a tube similar in many respects to those used by Lyman, Millikan and Simeon, but made as small as possible, to economise the rare gases krypton and xenon which were to be used. Some dimensions of the apparatus are given at the end of the paper.

At first, attempts were made to produce a continuous spectrum by bombarding a plate attached to one side of the slit by slow electrons produced by heating to its melting point a tungsten wire about 0.1 cm. distant, but no effect could be detected on the Schumann film. This method was, therefore, abandoned, and it was decided to use the carbon arc *in vacuo* as a source of radiation, and to deduce the position of the absorption band from the wave-lengths of the bright lines blocked out by the gas. The use of carbon has several advantages. It has a spectrum of many lines in this region which have been carefully mapped by Millikan\* and Simeon. It is comparatively easy to keep running in a high

\* R. A. Millikan, 'Astrophys. J.,' vol. 52, p. 47, and vol. 53, p. 150; F. Simeon, 'Roy. Soc. Proc.,' vol. 102, p. 484, and vol. 104, p. 368.

vacuum, and it does not destroy the grating by sputtering as metallic electrodes are apt to do.

Its principal disadvantage is due to the fact that, when heated, it gives off gases which themselves absorb the radiation and tend to mask the effect produced by the gas under examination. So powerful is the absorption in this region that the pressure of gas necessary to obliterate the spectrum is of the order of 0.02 mm. over a path of 102 cm., equivalent to a layer of gas only 0.025 mm. thick at normal temperature and pressure. The volume of the spectrograph, arc chamber and Langmuir pump together was about 6000 c.c., and this pressure was produced by 0.15 c.c. of gas, so that the gas given off by the electrodes could easily become a serious source of error. To avoid this it was necessary to run the arc for about 10 minutes at 8 amperes in a high vacuum with the pumps in continual action before the film was exposed. After this treatment gas ceased to come off; but it frequently happened that, when the gas under examination was introduced and the arc restarted, a further small quantity of gas was released. I do not feel sure that the final results are free from error due to this cause. The behaviour of the electrodes is different for different gases and very puzzling (see below).

Attempts were made to avoid this difficulty by following Holweck's method of using a thin film between the arc chamber and the spectrograph; but the difficulty of the technique and the complications introduced by the absorption of the film led to the abandonment of this device.

The general result of the research was to show that absorption bands exist in the ultra-violet near the predicted places, but only in the case of krypton and xenon was it possible to locate the point of maximum absorption with any degree of confidence. With argon and helium the beginning of the absorption band, about  $\lambda$  800, is easily recognised, and with neon beyond  $\lambda$  595; but the absorption does not diminish on the short wave side of the band within the limits imposed by the gratings. Two of these were used. With the first the line  $\lambda$  386 A.U. was once visible; but with the second it was never possible, with the exposure given, to see any lines beyond  $\lambda$  459.2, so that estimates of absorption in this region were not of much value. In order to locate these bands it will be necessary to find a better form of background than the carbon arc spectrum, and one which extends further into the gap between the ultra-violet and X-ray regions.

## RESULTS.

*Xenon.*

Of xenon 20 c.c. were obtained from M. Lepape, of the Collège de France, Paris. The gas was prepared by a process which has been patented and has not been published in scientific journals. Its purity is said to be at least 99.9 per cent. On fractionation the spectra of the lightest and heaviest fractions were identical.

Plate 45, A, B, C, D, and E show the results obtained when small quantities of the gas were interposed between the source of light and the photographic film.\*

A shows a reproduction, twice the natural size, of a photograph of the carbon spectrum in a vacuum between the strong line at  $\lambda$  1277 and the central image. The exposure given was not long (3 minutes) and many of the faint lines registered by Millikan and Simeon are absent; but the following lines are seen with the estimated intensities noted opposite them. Simeon's values of the wave lengths are used.

Principal lines visible in carbon arc spectrum.

$\lambda$ (A.U.).	Intensity.	$\lambda$ (A.U.).	Intensity.
1277	20	858.2	10
1247	5	809.6	5
1176	20	806.2	
1151	2	799.6	
1068	2	687.1	10
1036	20	651.3	4
1010	15	641.8	2
976.7	20	594.9	3
945.0	5	558	3
903.7	20	459.5	2

The important point to notice in this table is the relative intensity of  $\lambda$  858 and the  $\lambda\lambda$  809.6–799.6 group compared with the further lines on the short wave side.

Plate 45, B, C, D, E and F show the same spectrum when the spectrograph contains xenon at pressures of approximately 0.01 mm., 0.038 mm., 0.14 mm. and 0.545 mm. In F, at the highest pressure used (0.545 mm., equivalent at normal temperature and pressure to a layer of gas 0.69 mm. thick) the last

\* I regret that, owing to the effects of scattered light, chemical fog and scratches the photographs are so disappointing. But it was thought better to reproduce them without retouching.

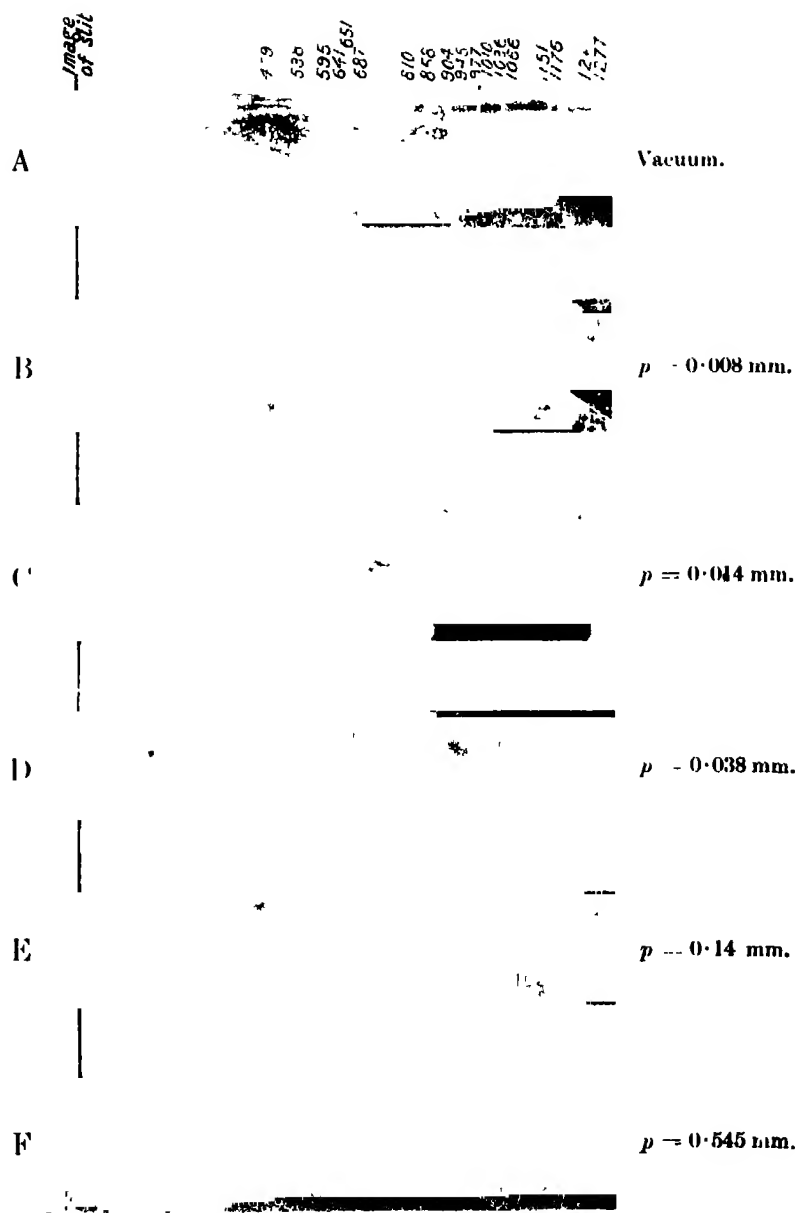


visible line is  $\lambda$  1036, and the very strong neighbouring lines  $\lambda$  1010 and  $\lambda$  977 are completely absorbed, showing that the absorption increases rapidly at this point. In E, taken at a pressure of 0.14 mm. (equivalent layer 0.178 mm.), the limit is still the same. D, taken at 0.038 mm. pressure shows all lines to  $\lambda$  1036. The slightly weaker line  $\lambda$  1010 is gone, but  $\lambda$  977 is faintly visible.  $\lambda$  945 is still fainter, and the very strong line  $\lambda$  903.7 is almost gone. C, taken at 0.014 shows  $\lambda$  903.7 faintly.  $\lambda$  858 and  $\lambda$  809, 806 and 799.6 are completely absorbed, but now  $\lambda$  687 and  $\lambda$  651 are visible and even  $\lambda$  459 appears. B, taken at 0.008–0.015 mm. definitely extends the long wave side of the spectrum to  $\lambda$  903.7. Again,  $\lambda$  858 and  $\lambda$  809–799.6 are invisible, but the lines beyond again appear.  $\lambda$  687 is a strong line, but  $\lambda$  651 and  $\lambda$  641 are weak, and the appearance of these lines, coupled with the absence of  $\lambda$  858 and  $\lambda$  810–799.9, is taken to indicate that the point of maximum absorption lies between  $\lambda$  687 and  $\lambda$  903.7 and probably not far from  $\lambda$  858.

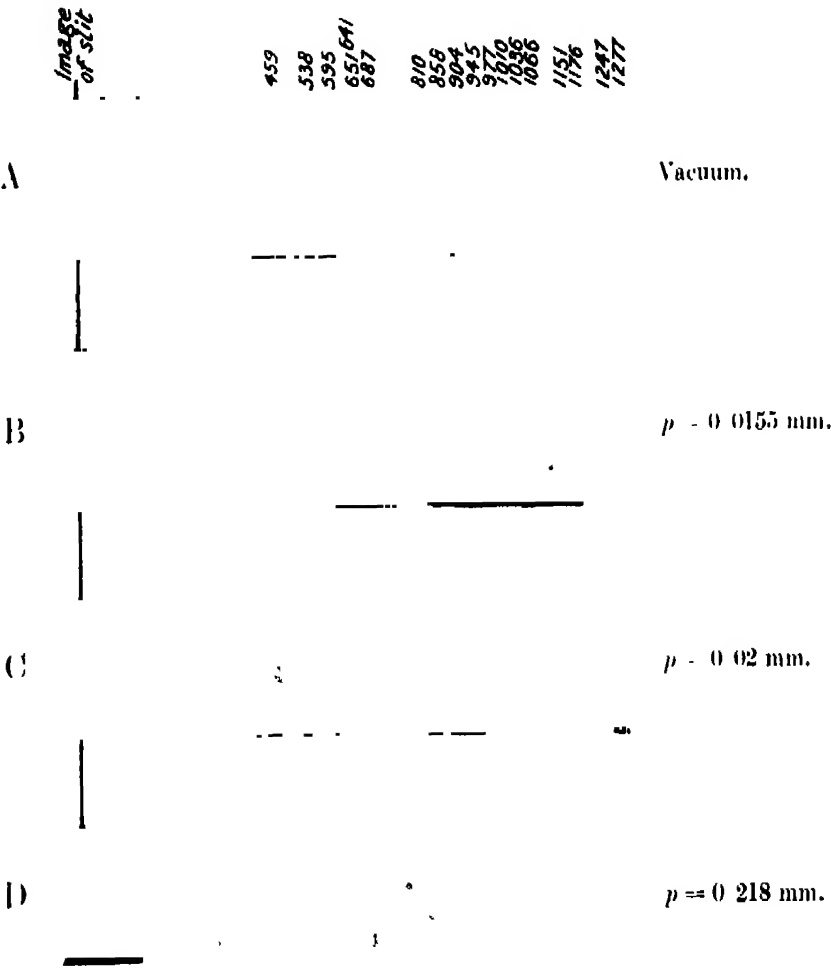
It would be misleading to attempt to draw any conclusion more definite than this from the experimental results. The lines registered depend on the intensity of the radiation which falls on the grating, and this is an uncertain quantity. The electrodes were about 6 cm. from the slit, and the arc *in vacuo* did not maintain a steady position for more than a few seconds at a time. As the electrodes burned away the source of light was displaced and the intensity of illumination changed so that no two photographs were identical in this respect. Further uncertainty arose in developing the films. The directions for the use of Schumann films recommended development for about 30 seconds at 15° C. But it was found difficult to obtain consistent results in this way owing to the rapidity with which chemical fog sets in; and the best results were obtained by developing for 1½ to 2½ minutes in an ice bath at about 1° C. This procedure is recommended by Lyman. But even when precautions are taken it is difficult to obtain two exactly similar negatives.

In photographs with xenon several lines were seen between  $\lambda$  1176 and 1036 which do not belong to the carbon spectrum, and may, therefore, probably be ascribed to xenon. Their approximate wave-lengths and intensities were as follows:—

$\lambda$ (A.U.).		Intensity.	$\lambda$ (A.U.).		Intensity.
1159	..	Faint.	1068	..	Faint ? 1066 C.
1152	..	Very faint.	1050	..	? Triple, faint.
1100	..	Strong.	1029	..	Faint.
1075	..	Strong.			



Carbon Arc Spectrum, photographed through Xenon. ( $\times 2$ .)



Carbon Arc Spectrum, photographed through Krypton. ( $\times 2$ .)

*Krypton.*

20 c.c. of this gas also were supplied by M. Lepape, and were of a similar standard of purity except for a trace of argon shown in the spectrum of the lightest fraction. Plate 46 shows a series of photographs similar to those given for xenon in Plate 45.

D shows that, at the highest pressure employed, 0.218 mm., no lines are visible beyond  $\lambda$  903.7 except a faint line at  $\lambda$  884.

C, at  $p = 0.02$  mm. does not show any extension of the limit of visibility.

B, at  $p = 0.0155$  mm. shows  $\lambda$  687 faintly and  $\lambda$  650 and  $\lambda$  595 still weaker; but, as in the case of xenon,  $\lambda$  857 and  $\lambda$  810 are absent.

It is concluded from these results that the absorption of krypton in the ultra-violet begins at  $\lambda$  903.7, about 132 A.U. beyond that of xenon, and that the maximum is probably on the long wave side of  $\lambda$  687.

*Argon.*

Argon was obtained from the British Oxygen Company and was believed to contain 99 per cent. argon and 1 per cent. oxygen. The latter was removed by passing the gas over red hot copper.

Table II gives the results of two series of experiments arranged in order of decreasing pressure.

Table II. —Ultra-violet absorption of argon.

Date of Experiment.	Pressure. mm.	Last lines visible.
November 20, 1925	5.57	Nothing beyond $\lambda$ 903.7.
" 20, 1925	2.56	" $\lambda$ 858.
" 20, 1925	1.12	" $\lambda$ 858.
" 23, 1925	0.5	" $\lambda$ 858.
" 25, 1925	0.236	$\lambda$ 809 just visible.
July 19, 1926	0.06	$\lambda$ 858 and $\lambda$ 809 group distinct.
" 19, 1926	0.038	Nothing beyond $\lambda$ 858.
" 19, 1926	0.025	All lines to $\lambda$ 687 visible.
August 30, 1926	0.02	All lines to $\lambda$ 687 plain; nothing beyond.
" 30, 1926	0.02	$\lambda$ 687 just visible.
November 20, 1926	0.007	$\lambda\lambda$ 687, 651, 641, 595 just visible.

The progressive transparency of argon with decreasing pressure is as consistent as could be expected in view of the difficulties noted above. At 5.57 mm. (a pressure much higher than that used for xenon and krypton)  $\lambda$  858 is obscured. At half that pressure (2.56 mm.)  $\lambda$  858 becomes visible, but remains the last visible line till the pressure is reduced to about a tenth ( $= 0.236$  mm.) when  $\lambda$  810 is seen. Not till we reach 0.025 mm. is  $\lambda$  687 seen, and below this pressure

the further spectrum slowly comes into view. Comparing the results with those of xenon and krypton at similar pressures we find :—

Element.	Pressure. mm.	Last line visible(A.U.).
Xenon . . .	0.114	1036
Krypton ....	0.218	904
Argon .	0.236	810

There is a special difficulty in the case of argon due to the fact that at low pressure it tends to disappear during the arcing and has to be renewed. The pressure recorded should not be higher than the final pressure of each run.

On the whole argon behaves as if the centre of the absorption band were on the short wave side of  $\lambda$  687 and probably beyond  $\lambda$  595, but how far beyond it would not be safe to conjecture.

#### *Helium.*

A specimen of Canadian helium was used and purified with liquid air. Table III shows the results of a series of experiments.

Table III.

Date of Experiment.	Pressure. mm.	Last lines visible (A.U.).
November 19, 1926	0.25	858 faint
June 17, 1926	0.185	809 "
November 24, 1926	0.1	809 very faint
June 21, 1926	0.035	687
November 18, 1926	0.014	651
November 19, 1926	0.01	651 and 595

These experiments cannot be described as more than preliminary ; but they show that, at a pressure so low as 0.25 mm., there is an absorption beginning between  $\lambda$  858 and  $\lambda$  809. The latter line only appears when the pressure is reduced to 0.01 mm., and its faintness at even lower pressures suggests that the band begins here. With decreasing pressure the gas becomes more transparent, and at 0.01 mm. the line  $\lambda$  595 is seen. A pressure of 0.01 mm. over a path of 102 cm. at 17° C. is equivalent to a layer of gas at n.t.p. only 0.013 mm. thick.

Helium shares with argon the peculiarity of disappearing during the running of the arc.

*Neon.*

Limitations of time prevented the completion of more than one set of observations on neon, but the photographs were remarkably successful.

The gas was obtained from the British Oxygen Company and contained .98 per cent. neon and 2 per cent. helium. Three photographs were taken at pressures of 0.55 mm., 0.1 mm. and 0.018 mm. The results are shown below.

Table IV.

Date of experiment.	Pressure. mm.	Last lines visible (A.U.).
November 29, 1926	0.55	595
„ 29, 1926	0.10	595
„ 29, 1926	0.018	459

A comparison of these figures with those given for helium shows that of all the five inert gases neon is the most transparent. The lines in the extreme ultra-violet were not only visible, but almost as strong as in a vacuum.

It has been remarked above that argon and helium both disappear when the arc is running, and it was therefore to be expected that neon would behave in the same way. But, contrary to expectation, the gas did not disappear, the pressure remaining as constant during an experiment as in the case of krypton and xenon.

In the photograph taken with the highest pressure of neon (0.55 mm.) there is a pair of lines ( $\lambda\lambda$  742.9 and 735.7 approximately) which do not appear in the carbon arc spectrum. In that taken at 0.1 mm. only the stronger appears; while at 0.018 mm. neither is present. It is, therefore, probable that the lines are due to neon, and are those recorded by Hertz as having the wave lengths 735.7 and 743.5 A.U. ('*Zeitschrift für Physik*,' vol. 32, p. 933, 1925) and by Lyman and Saunders ('*Physical Review*,' vol. 25, p. 86, 1925).

Under the conditions of the present work the line of longer wave length was much the stronger. Lyman records that this is not always the case ('*Nature*,' Sept. 5, 1925).

*Remarks.*

The broad result of the work described above is to confirm, though somewhat roughly, the predictions of the simplest form of the theory of dispersion in the case of the five inert gases.

In xenon Table I shows that, on the assumptions there made, the calculated

free frequency is at  $\lambda 1001$ . The absorption band now found begins near  $\lambda 1036$  at a pressure of 0.545 mm., and probably culminates between  $\lambda 903.7$  and  $\lambda 687$ .

In krypton the calculated free frequency is  $\lambda 840$ : the absorption begins near  $\lambda 904$  at a pressure of 0.218 mm., and probably culminates somewhere on the long wave side of  $\lambda 687$ .

In argon the calculated free frequency is at  $\lambda 726$ . The absorption at 0.5 mm. begins between  $\lambda 858$  and the group  $\lambda\lambda 809, 806, 799$ . The maximum cannot be located.

In helium the calculated free frequency is at  $\lambda 507$ . The absorption begins about  $\lambda 858$  and seems to increase more slowly than in the case of the heavier gases. It is more transparent than argon.

In neon the calculated free frequency is at  $\lambda 481$  and the gas is the most transparent of all. At 0.5 mm. lines are visible to  $\lambda 595$  and at 0.02 mm.  $\lambda 459$  is clearly visible.

In all five cases the maximum of absorption is on the short wave side of the free frequency calculated from observations on the dispersion by means of a one-term formula of Drude's type.

I have pleasure in expressing my thanks to Sir William Bragg for the privilege of admission to the Davy-Faraday Research Laboratory, and to the staff of the Laboratory for much valuable help. My thanks are also due to Mr. R. W. Paul for the design and execution of the grating carrier, to Mr. W. R. Bullimore, of Messrs. A. C. Cossor & Co., for the loan of apparatus and for advice and help, and to Messrs. A. Hilger & Co. for much assistance.

Finally my thanks are due to the Government Grant Committee of the Royal Society for grants in aid of the research.

#### *Dimensions of apparatus, etc.*

*Grating.*—Ruled area  $5 \times 3.8$  cm. Mean grating interval 0.00017632 cm. Focal distance 48.5 cm. Scale of photograph, 1000 A.U. = 2.756 cm. approximately.

*Vacuum Spectrograph.*—Length 56.6 cm. Diameter 9.6 cm. Breadth of slit 0.1 mm.

*Pump System.*—Langmuir, backed by Gaede and Fleuss; Töpler in parallel to collect rare gases. A vacuum of 0.0001 mm. obtainable in about one hour.

*Pressures* were measured with a McLeod gauge, sensitive to 0.0001 mm.

*On a Relation between the Refractive and Dispersive Constants of the Inert Gases.*

By CLIVE CUTHBERTSON, O.B.E., F.R.S.

(Received December 8, 1926.)

In 1911 I published in the 'Philosophical Magazine' \* a paper on new determinations of some constants of the inert gases, and drew attention to the remarkable empirical relations which subsist between (1) the calculated numbers of "dispersion" electrons in the atoms of these five elements, (2) their "viscosity diameters" as determined by Prof. A. O. Rankine, and (3) their critical temperatures.

Since that time the figures used have undergone revision. The accurate determination of the value of  $\epsilon$  by Millikan has enabled us to give absolute, instead of relative, values to the apparent numbers of dispersion electrons ( $q$ , see Table I). Chapman† has recalculated the viscosity diameters, and Rankine‡ has revised Chapman's values, in the light of corrections to be made in his own values of Sutherland's constants for argon, krypton and xenon. But these alterations have not affected the validity of the relations then published.

There were, however, two weak points in the paper in question. (I) The linear relations shown were not so exact as to preclude the possibility that they might be portions of curves, and (II) the legitimacy of using the figures given depended on the assumption that a single term in Drude's dispersion formula is sufficient to give the dominant free frequency of the electrons, at any rate to a first approximation. The investigation, described in the preceding paper, of the actual position of the absorption bands has shown that, certainly in the case of xenon and krypton, and probably in the case of the other three gases, strong absorption bands do exist not far from the positions predicted by the simple formula; and, if the evidence is accepted, it becomes possible to use the values of  $q$  in speculations on the constitution of the atom with some confidence that the  $q$ 's represent, in some way, the average or effective number of dispersion electrons in the atom.

I have recently found a new relation between the experimental values of

\* "New Determinations of some Constants of the Inert Gases," vol. 21, p. 69 (1911).

† S. Chapman, 'Phil. Trans.,' A, vol. 216, p. 279 (see p. 347).

‡ A. O. Rankine and C. J. Smith, 'Phil. Mag.,' vol. 42, p. 601 (1921).



the refractivities and the values of  $q$  for all five gases which appears to be sufficiently exact to invite explanation.

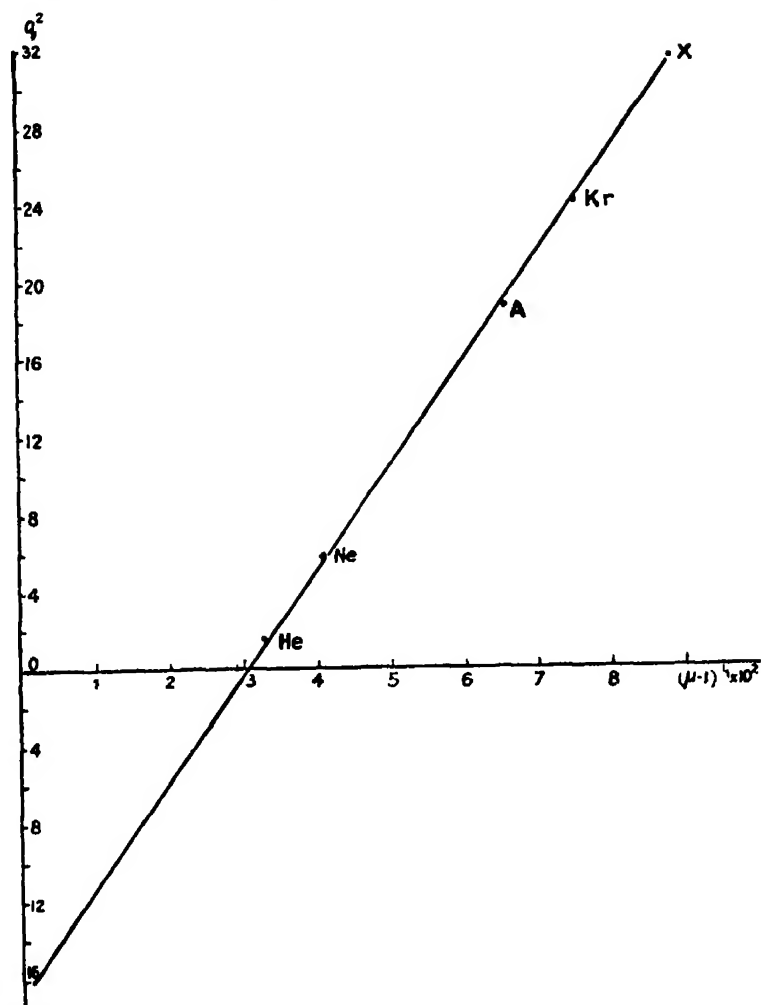


Table I.

Element.	$(\mu_{\infty}-1)10^3$	$(\mu_{\infty}-1)^{1/2} \times 10^3$	$(\mu_{\infty}-1)^{1/2} \times 10^3$ calculated.	$(\mu_{\infty}-1)^{1/2} \times 10^3$ obs. - calc.	$q$ .	$q^2$ .	$n_0^2 \times 10^{-30}$
Helium	34.65	3.260	3.273	-0.013	1.113	1.24	34.992
Neon	66.75	4.056	4.083	-0.026	2.385	5.69	38.916
Argon	277.3	6.522	6.466	+0.056	4.330	18.75	17.009
Krypton	418.6	7.480	7.436	+0.044	4.906	24.07	12.768
Xenon	682.2	8.802	—	—	5.619	31.57	8.978

If the cube roots of the refractivities of the inert gases for long waves are plotted against  $q^2$ , the squares of the apparent numbers of dispersion electrons derived from dispersion measurements by the use of the expression

$$\mu - 1 = \frac{N' q \epsilon^2}{2\pi m (n_0^2 - n^2)}$$

the points lie on a straight line with such accuracy that the hypothesis of chance seems to be excluded. The figures used are collected below for convenience.

The equation to the line is

$$A + q^2 = B (\mu_\infty - 1)^{1/3}$$

where A and B are constant for all five gases. Taking the position of xenon as a point on the line and  $A = 16.7$  we obtain  $B = 5.483 \times 10^2$ . Column 4, Table I, shows the values of  $(\mu_\infty - 1)^{1/3} \times 10^2$  calculated from these figures, and column 5 the difference between the observed and calculated values for the other points. In no case does the discrepancy reach 1 per cent. of the observed value.

If, ignoring the modern theory of dispersion, we go back to the Clausius-Mosotti formula that

$$g = \frac{2}{3} (\mu_\infty - 1) = \frac{N' 4\pi\sigma^3}{3}$$

where  $g$  is the fraction of unit volume which is occupied by the atoms (assumed to be conducting spheres) and  $\sigma$  is the radius of the sphere,

$$\sigma = \left( \frac{\mu_\infty - 1}{2\pi N'} \right)^{1/3}$$

so that the cube roots of the refractivities would be proportional to the radii of the atoms. In this case the interpretation of the figure would seem to be that the radius of the atom is proportional to  $q^2$  plus a constant. If, in place of the obsolete Clausius-Mosotti hypothesis, we take the theory which regards the atom as built up of electrons arranged round positive centres, and assume that the configuration of the outer layers of the electrons in these gases would be similar, it would appear that  $K - 1$ , or  $\mu_\infty - 1$ , would be proportional to the cube of the linear dimensions; so that, in this case also, the result is the same.

If  $\mu_\infty - 1$  is proportional to  $(A + q^2)^3$  it follows that  $n_0^2$  is of the form  $C \cdot q / (A + q^2)^3$  where C is a constant for all five gases. This expression has a maximum dependent on the constants. If we choose them so as to give the values of  $n_0^2$  shown in the table for helium and xenon ( $34,992 \times 10^{27}$  and  $8,978 \times 10^{27}$  respectively) we find that the maximum is  $38,400 \times 10^{27}$ , which is very nearly the value of  $n_0^2$  for neon ( $38,916 \times 10^{27}$ ). The value of A is taken as 16.7.

## *The Spectrum of Ionised Nitrogen (N II).*

By A. FOWLER, F.R.S., Yarrow Research Professor of the Royal Society, and  
L. J. FREEMAN, B.Sc., D.I.C., Imperial College of Science and Technology,  
South Kensington.

(Received March 23, 1927.)

[PLATES 47, 48.]

### *Introductory.*

In a previous communication\* it was shown that many of the lines in the spectrum of singly-ionised nitrogen (N II) in the region  $\lambda$  6000 to  $\lambda$  3000 were accounted for by triplet and singlet terms, in agreement with theoretical expectation. The observational data have since been extended over a much greater range, and the purpose of the present paper is to give the results of a more complete analysis of the spectrum, together with a list of all the lines which are considered to be due to N II.

The further analysis of the spectrum has been facilitated by the recent developments of the theory of spectra which we owe to Pauli, Heisenberg and Hund.† The theory enables the types of spectroscopic terms associated with any specified configuration of the electrons to be predicted, besides indicating the terms which may, or may not, combine with each other, and terms which may be properly associated in the same Rydberg sequence. Thus, as pointed out by Laporte,‡ although the two terms of “*p*” type indicated in the previous paper belong to a Rydberg sequence, one of them is theoretically the deepest possible term of this type, so that extrapolation for the evaluation of a deeper term of the same sequence is not permissible; on the other hand, the theory indicates that the deepest term of the spectrum, in the notation of the previous paper, is of the *p*’ type, and the extrapolated value from the observed term of this type appeared to be in general agreement with that deduced from astrophysical considerations. It thus appears that the approximate value of 70,000 previously assigned to the first *p* term should have been assigned to the *p*’ term, and that all the term values were consequently too low by about 20,000 units of wave-number.

The majority of the brighter lines, and many of the fainter ones, have now

\* A. Fowler, ‘Roy. Soc. Proc.’ A, vol. 107, p. 31 (1924).

† ‘Z. f. Physik,’ vol. 33, p. 345 (1925). See also R. H. Fowler and D. R. Hartree, ‘Roy. Soc. Proc.’ A, vol. 111, p. 83 (1926), and McLennan, McLay & Smith, ‘Roy. Soc. Proc.’ A, vol. 112, p. 76 (1926).

‡ ‘Jour. Opt. Soc., America,’ vol. 13, p. 13 (1926).

been classified, and most of them have been found to be derived from terms predicted for transitions of a single electron. There are, however, a few definite groups of lines which are not accounted for by this set of terms, and it would seem that these must arise from simultaneous transitions of two of the valence electrons.

#### *Observational Data.*

The spectrum has been investigated mainly by the use of condensed discharges in vacuum tubes containing nitrogen at various pressures. Under these conditions, the spectrum of neutral atoms of nitrogen (N I) is represented only by the two well-known pairs of lines in the Schumann region at wave-lengths 1745.3, 1742.7, 1494.8, 1492.8, from which it may be inferred that most of the nitrogen molecules break down directly into ionised atoms. With discharges of moderate intensity, the N II spectrum thus appears almost alone, but stronger discharges result in the appearance of lines of N III, N IV, and even of N V.\* From a comparison of the spectra obtained with different discharges and pressures, it was not difficult to separate lines of N II from those representing higher stages of ionisation, even in the region of short wave-lengths beyond the transmission of fluorite. An attempt has been made to record all the lines of N II, faint as well as strong, in the region extending from  $\lambda$  6850 in the red to  $\lambda$  830, which appears to be the limit of action of the vacuum spectrograph, at present available. Lines of nitrogen of still shorter wave-lengths, however, have been recorded in the "hot spark" spectrum by Millikan and his colleagues.

The positions of many of the brighter lines from  $\lambda$  5045 to  $\lambda$  3919 have been determined in the third order of a 10-ft. concave grating, and are distinguished in the general catalogue (Table I) by their being stated to three decimal places. The remaining lines, except the fainter ones in the green, yellow and red, were measured on photographs taken in the first order of the grating (5.6 Å per mm.), or with glass and quartz spectrographs of the same order of dispersion, or greater, and are not expected to be in error by more than two or three hundredths of an Ångström. As mentioned in the previous paper, however, there are some lines which are subject to displacements at higher pressures of the gas in vacuum tubes, and although photographs of the spectrum at low pressures have been chiefly measured, it is not certain that such displacements have been altogether eliminated. Wave-lengths between  $\lambda$  1850 and  $\lambda$  1215 were

\* The pair of lines at  $\lambda\lambda$  1242.93, 1238.94, attributed to N V by Millikan and Bowen, has been obtained strongly in the vacuum discharge, and also with less intensity in the condensed spark in nitrogen at atmospheric pressure.

measured on photographs taken in the first order of the Hilger vacuum spectrograph, having a concave grating of 1 metre radius and giving a dispersion of about 17 Å per millimetre; from  $\lambda$  1215 to  $\lambda$  830 the second order was used. Carbon sparks in nitrogen at atmospheric pressure, with varying amounts of self-induction, provided a useful additional source within the range of transmission of a fluorite window. Good standards for wave-length determinations are now provided by Lang and Smith's very accurate measures of carbon lines,\* and by measures of carbon, oxygen and nitrogen lines which have been made by Bowen and Ingram.†

The intensities of the lines are indicated throughout by numbers in brackets following the wave-lengths or wave-numbers. Such estimates give a fair indication of the relative intensities over a short range of the spectrum, and especially in individual multiplets, but do not necessarily show the relative intensities of lines in widely separated regions. Wave-numbers have been calculated from the wave-lengths with the aid of the convenient tables published by Kayser.‡

Details of the wave-lengths, intensities, wave-numbers and classification of the N II lines are collected in Table I. Wave-lengths greater than  $\lambda$  1850 are the values *in air*, while shorter wave-lengths are *in vacuo*,  $\lambda$  1850 being near the limit for quartz spectrographs.

Table I.—N II Lines,  $\lambda$  6850 —  $\lambda$  915.

$\lambda$ , Intensity.	$\nu$ .	Classification.	$\lambda$ , Intensity.	$\nu$ .	Classification.
6836.2 (1)	14624.0	$1^1P_1''' - 2^3S_1'$	6284.30 (3)	15908.28	$1^1P_1 - 1^1P_1'''$
6812.26 (2)	14675.4	$1^1P_2''' - 2^3S_1'$	6242.52 (5)	16014.75	
6830.5 (2)	15077.7		6173.40 (3)	16194.06	$1^3F_3' - 2^3D_3'$
6610.58 (6)	15123.06		6170.16 (1)	16202.56	$1^3F_2' - 2^3D_1'$
[6554.7]	[15252]	$1^3D_2 - 2^3D_1'$	6107.82 (4)	16208.71	$1^3F_2' - 2^3D_3'$
6545.2 (0)	15274.2	$\begin{cases} 1^3D_3 - 2^3D_2' \\ 1^3D_1 - 2^3D_1' \end{cases}$	6150.9 (0)	16253.3	$1^3F_3' - 2^3D_3'$
6533.0 (1)	15302.7	$1^3D_2 - 2^3D_2'$	6136.0 (0)	16290.4	$1^3F_3' - 2^3D_3'$
6522.3 (0)	15327.8	$1^3D_1 - 2^3D_1'$	6114.6 (0)	16349.8	$1^3F_3' - 2^3D_3'$
6515.2 (0)	15344.5				
6504.9 (2)	15368.8	$1^3D_2 - 2^3D_2'$	6065.5 (0)	16484.8	
6492.0 (0)	15399.3	$1^3D_1 - 2^3D_1'$			
6482.07 (8)	15422.92	$1^1P_1' - 2^1D_2'$	5960.93 (0)	16771.27	$2^3P_2 - 1^3D_1$
6379.63 (5)	15670.57	$1^1P_1' - 2^1D_2'$	5952.39 (3)	16795.33	$2^3P_2 - 1^3D_1$
6365.7 (0)	15704.9		5941.67 (8)	16825.63	$2^3P_2 - 1^3D_3$
6357.0 (3)	15726.4		5940.25 (2)	16829.66	$2^3P_1 - 1^3D_1$
6347.1 (1)	15750.9		5931.79 (7)	16853.66	$2^3P_1 - 1^3D_3$
6340.67 (4)	15766.85		5927.82 (4)	16864.95	$2^3P_2 - 1^3D_1$
6328.6 (1)	15796.9				

\* 'Phys. Rev.,' vol. 28, p. 36 (1926).

† 'Phys. Rev.,' vol. 28, p. 444 (1926).

‡ 'Tabelle der Schwingungszahlen,' Leipzig (1925).

Table I—(continued).

$\lambda$ , Intensity.	$\nu$ .	Classification.	$\lambda$ , Intensity.	$\nu$ .	Classification.
5767.43 (3)	17333.95	$1^1P_1' - 1^1D_1'$	5016.387 (5)	19929.12	$1^1D_2' - 1^1F_3'$
5747.29 (4)	17394.69	$1^1P_1' - 1^1D_2'$	5012.026 (2)	19916.46	
5730.67 (2)	17445.14	$1^1P_2' - 1^1D_1'$	5010.620 (6)	19952.06	$1^1P_1' - 1^1S_1'$
5710.76 (6)	17505.96	$1^1P_2' - 1^1D_2'$	5007.316 (7)	19965.22	$1^1S_1' - 1^1P_2'''$
5696.21 (6)	17581.54	$1^1P_1' - 1^1D_1'$	5005.140 (10)	19973.90	$1^1D_2' - 1^1F_4'$
5679.56 (10)	17602.12	$1^1P_2' - 1^1D_2'$	5002.692 (2)	19983.68	$1^1P_0' - 1^1S_1'$
5676.02 (6)	17613.10	$1^1P_0' - 1^1D_1'$	5001.460 (8)	19988.67	$1^1D_2' - 1^1F_3'$
5666.64 (8)	17642.26	$1^1P_1' - 1^1D_2'$	5001.128 (7)	19989.92	$1^1D_1' - 1^1F_3'$
			4997.23 (0)	20005.62	
5565.30 (0)	17963.51	$a^1P_2' - a^1D_1'$	4994.358 (6)	20017.02	$1^1S_1' - 1^1P_1'''$
5551.95 (3)	18006.70	$a^1P_2' - a^1D_2'$	4991.22 (2)	20029.61	
5543.49 (3)	18034.18	$a^1P_1' - a^1D_1'$	4987.377 (4)	20045.04	$1^1S_1' - 1^1P_0'''$
5540.16 (1)	18045.02		4957.94 (0)	20164.1	
5535.39 (5)	18060.67	$a^1P_2' - a^1D_1'$			
5530.27 (4)	18077.29	$a^1P_2' - a^1D_2'$	4895.20 (4)	20122.49	
5526.26 (2)	18090.41	$a^1P_0' - a^1D_1'$	4860.35 (2)	20568.92	
5495.70 (5)	18191.00	$2^1P_2' - 1^1P_2'''$	4810.286 (2)	20783.00	$1^1D_2' - 1^1D_1$
5480.10 (3)	18242.79	$2^1P_2' - 1^1P_1'''$	4806.00 (0)	20801.53	
5478.13 (2)	18249.35	$2^1P_1' - 1^1P_1'''$	4803.272 (6)	20813.34	$1^1D_2' - 1^1D_2$
5462.62 (3)	18301.16	$2^1P_1' - 1^1P_2'''$	4793.656 (2)	20855.09	$1^1D_2' - 1^1D_1$
5454.26 (2)	18329.21	$2^1P_1' - 1^1P_0'''$	4788.126 (5)	20879.18	$1^1D_2' - 1^1D_2$
5452.12 (2)	18336.41	$2^1P_0' - 1^1P_1'''$	4781.168 (2)	20909.56	$1^1D_2' - 1^1D_2$
			4779.710 (4)	20915.94	$1^1D_1' - 1^1D_1$
			1774.222 (2)	20939.98	$1^1D_1' - 1^1D_1$
5411.65 (00)	18473.5		4765.0 (00)	20980	
5383.82 (0)	18569.0	$1^1S_1' - 1^1D_2$ [18569.34]	4755.5 (00)	21022	
5372.35 (00)	18608.7		4751.5 (00)	21040	
5351.21 (3)	18682.18		4735.8 (0)	21110	
5340.15 (1)	18720.87		4726.9 (00)	21150	
5338.77 (2)	18725.71		4721.59 (0)	21173.40	
5320.75 (4)	18789.13		4718.43 (2)	21187.58	
5314.17 (0)	18812.4		4712.13 (0)	21215.91	
5313.47 (1)	18814.87		4709.45 (1)	21227.98	$1^1S_1' - 1^1P_1'''$
5298.74 (0)	18867.2		4706.41 (0)	21241.70	
5281.45 (0)	18928.9		4704.33 (0)	21251.09	
5272.49 (00)	18961.1		4702.57 (0)	21259.04	
5260.60 (0)	19004.0		4700.12 (0)	21270.12	
5228.14 (0)	19122.0		4695.91 (1)	21289.19	
5206.63 (0)	19200.95		4694.55 (3n)	21295.36	
5190.53 (00)	19227.17	$a^1D_2' - a^1F_3'$	4677.93 (3n)	21371.01	
5190.42 (2)	19260.91	$a^1D_2' - a^1F_4'$			
5184.97 (2)	19281.16	$a^1D_2' - a^1F_3'$	4674.98 (2)	21384.50	$1^1P_1' - 2^1P_0$
5183.21 (2)	19287.71		4670.0 (0)	21407	
5179.50 (5)	19301.52	$a^1D_2' - a^1F_4'$	4667.28 (2)	21419.78	$1^1P_1' - 2^1P_1$
5175.89 (3)	19314.98	$a^1D_2' - a^1F_3'$	4654.57 (2)	21478.27	$1^1P_1' - 2^1P_2$
5174.46 (1)	19320.32		4651.84 (00)	21490.8	
5173.37 (2)	19324.30	$a^1D_1' - a^1F_3'$			
5172.32 (1)	19328.32				
5171.46 (1)	19331.63		4643.106 (8)	21531.30	$1^1P_2' - 2^1P_1$
5170.08 (1)	19336.61		4630.551 (10)	21589.67	$1^1P_2' - 2^1P_2$
5168.24 (1)	19343.57		4621.405 (7)	21632.41	$1^1P_1' - 2^1P_0$
			4613.884 (6)	21667.66	$1^1P_1' - 2^1P_1$
			4609.60 (0)	21687.8	
5104.45 (2)	19585.30	$2^1S_0' - 2^1P_1'$	4607.167 (7)	21699.26	$1^1P_0' - 2^1P_1$
5078.50 (0)	19693.14		4601.490 (8)	21726.03	$1^1P_1' - 2^1P_2$
5073.60 (3)	19704.39	$1^1P_1' - 1^1S_1'$			
5045.098 (8)	19815.71	$1^1P_2' - 1^1S_1'$			
5040.76 (0)	19832.76	$1^1D_2' - 1^1F_3'$	4564.78 (1)	21900.71	$2^1D_2' - 1^1F_3'$
5025.665 (6)	19892.33	$1^1D_2' - 1^1F_3'$	4552.50 (4)	21959.82	$2^1D_2' - 1^1F_3'$
5023.11 (2)	19902.45		4530.37 (5)	22067.08	$2^1D_2' - 1^1F_3'$

Table I—(continued).

$\lambda$ , Intensity.	$\nu$ .	Classification.	$\lambda$ , Intensity.	$\nu$ .	Classification.
4507.58 (3)	22178.65	$1^3D_2'-1^3P_2'''$	3994.995 (10)	25024.27	$1^1P_1'-1^1P_1$
4488.15 (0)	22274.89	$1^3D_2'-1^3P_2'''$	3955.851 (6)	25271.88	$1^3P_1'-1^1P_1$
4477.74 (2)	22326.46	$1^3D_2'-1^3P_1'''$	3919.003 (6)	25509.50	$2^1D_2'-1^1P_1''$
[4476.0]	[22335.5]	$1^3D_2'-1^3P_1'''$			
4465.54 (0)	22387.44	$1^3D_1'-1^3P_1'''$	3856.07 (3)	25925.81	$2^3P_1'-2^3P_1'$
4459.96 (1)	22415.44	$1^3D_1'-1^3P_0'''$	3855.08 (2)	25932.48	$2^3P_1'-2^3P_0'$
4447.035 (10)	22480.00	$2^1D_2'-1^1D_2 ?$	3847.38 (3)	25984.37	$2^3P_1'-2^3P_1'$
4441.99 (3n)	22506.13		3842.20 (3)	26019.40	$2^3P_1'-2^3P_1'$
4433.48 (2n)	22549.33		3838.39 (5)	26045.23	$2^3P_1'-2^3P_1'$
4432.71 (6n)	22553.25		3829.80 (3)	26103.65	$2^3P_1'-2^3P_1'$
4431.82 (0)	22557.78				
4427.97 (2)	22577.39		3615.88 (1)	27647.94	$1^3S_1'-2^3P_0'$
4427.21 (2)	22581.27		3609.00 (2)	27690.93	$1^3S_1'-2^3P_1'$
4426.05 (0)	22587.10		3593.00 (3)	27819.34	$1^3S_1'-2^3P_1'$
4402.5 (0n)	22708	Very diffuse	3437.162 (6)	29085.46	$1^1P_1'-2^1S_0'$
4375.00 (0)	22850.74	$2^1D_2'-1^1D_2$	3408.136 (3)	29333.17	$1^3P_1'-2^1S_0'$
4241.80 (8n)	23568.28		3331.32 (3)	30009.52	$1^3D_2'-2^3P_1'$
4236.98 (6n)	23595.09		3330.30 (2)	30018.70	$1^3D_1'-2^3P_0'$
4227.83 (3n)	23646.16	$1^1P_1'-2^1P_1'$	3328.79 (4)	30032.34	$1^3D_2'-2^3P_1'$
			3324.58 (2)	30070.37	$1^3D_1'-2^3P_1'$
4215.72 (0)	23714.1	N III ?	3318.14 (2)	30128.72	$1^3D_2'-2^3P_1'$
4208.12 (00n)	23756.9		[3311.5]	[30189.4]	$1^3D_1'-2^3P_1'$
4207.51 (1n)	23760.4				
4206.57 (0n)	23765.7		3023.80 (2)	33061.34	
4206.35 (00n)	23766.9		3006.86 (7)	33247.67	$2^1D_2'-2^1P_1'$
4181.17 (0n)	23910.0		2992.81 (0)	33403.71	
4180.89 (0)	23911.6				
4179.68 (1n)	23918.6		2897.49 (3n)	34502.5	A*
4176.17 (3n)	23938.7		2892.86 (4n)	34557.8	A
4173.75 (0n)	23952.6		2891.05 (1n)	34579.4	
4173.51 (0n)	23953.0		2885.25 (6n)	34648.9	A
4172.04 (00)	23962.4		2884.25 (2n)	34660.9	A
4171.63 (2n)	23964.7		2879.73 (4n)	34715.3	A
4167.50 (0)	23988.5		2877.66 (2n)	34740.3	A
4160.8 (0nn)	24027				
4156.8 (0nn)	24050		2830.5 (0nn)	35319	Very diffuse
4155.0 (00n)	24061		2823.67 (4)	35404.51	
			2799.20 (4)	35713.99	
4145.759 (3)	24114.26	$a^3P_1'-a^3S_1'$	2735.0 (1n)	36652.3	
4133.654 (2)	24184.87	$a^3P_1'-a^3S_1'$	2709.82 (6)	36891.9	$2^1S_0'-3^1P_1'$
4124.10 (1)	24240.90	$a^3P_0'-a^3S_1'$			
4110.00 (0n)	24324.0		2590.91 (4)	38584.0	
4092.65 (0n)	24427.2		2526.93 (0)	39561.8	
4087.35 (0n)	24458.8				
4082.85 (00)	24485.8		[2526.2]	[39572.7]	$2^3P_1'-2^3D_1$
4082.28 (2n)	24489.2		2524.55 (1)	39599.1	$2^3P_1'-2^3D_2$
4076.83 (0n)	24522.0		2522.51 (1)	39631.1	$2^3P_1'-2^3D_1$
4073.04 (2n)	24544.8		2522.27 (4)	39634.9	$2^3P_1'-2^3D_2$
4057.00 (1)	24641.8	B*	2520.85 (3)	39657.8	$2^3P_1'-2^3D_2$
4044.75 (1)	24716.45		2520.27 (2)	39666.4	$2^3P_0'-2^3D_1$
4043.54 (3n)	24723.85	B			
4041.325 (5n)	24737.39	B	2496.88 (4)	40038.0	$2^3P_1'-2^3P_1'''$
4035.090 (4n)	24775.62	B	2494.02 (1)	40083.8	$2^3P_1'-2^3P_1'''$
4026.087 (3n)	24831.02	B	2493.22 (0)	40096.7	$2^3P_1'-2^3P_1'''$
			2490.37 (2)	40142.6	$2^3P_1'-2^3P_1'''$
			2488.82 (1)	40167.6	$2^3P_1'-2^3P_1'''$
			2488.21 (0)	40177.4	$2^3P_0'-2^3P_1'''$

\* See Table V.

Table I—(continued).

$\lambda$ , Intensity.	$\nu$ .	Classification.	$\lambda$ , Intensity.	$\nu$ .	Classification.
2461.30 (3)	40616.6	$1^1P_1-3^1P_1'$	*2096.79 (3)	47676.7	$1^3D_1'-3^3P_1'$
2424.00 (0)	41241.6		2096.16 (2)	47691.0	$1^3D_1'-3^3P_2'$
2418.87 (0n)	41329.0		2095.47 (6)	47706.8	$1^3D_2'-3^3P_2'$
2415.79 (0)	41381.7		2094.12 (2)	47737.4	$1^3D_1'-3^3P_1'$
2411.13 (0)	41461.7		2091.20 (3)	47804.2	$1^3D_2'-3^3P_2'$
2402.45 (0)	41611.5		[2088.5]	[47864.4]	$1^3D_1'-3^3P_1'$
2400.13 (0)	41651.7		1886.82 (4)	52981.5	
2398.75 (0)	41675.7		1877.97 (2)	53231.1	
2397.10 (0)	41704.4		1868.50 (1)	53500.8	
2395.67 (00)	41729.3		1867.58 (0)	53527.2	
2394.99 (0)	41741.1		[1863.7]	[53637.6]	$1^3P_2'-2^3D_1'$
2390.90 (2)	41812.5	$1^3S_1'-2^3P_1'''$	1861.94 (2)	53689.2	$1^3P_2'-2^3D_2'$
2388.24 (1)	41859.0	$1^3S_1'-2^3P_1'''$	[1859.0]	[53774.0]	$1^3P_1'-2^3D_1'$
2386.80 (0)	41884.8	$1^3S_1'-2^3P_0'''$	1858.50 (5)	53786.0	$1^3P_2'-2^3D_1'$
2317.01 (3)	43145.0		1857.84 (2)	53807.7	$1^3P_0'-2^3D_1'$
2316.66 (1)	43152.4		1857.14 (3)	53826.4	$1^3P_1'-2^3D_1'$
2316.46 (2)	43156.1		$\lambda$ , Vac.		
2314.54 (1n)	43191.8		1836.36 (1)	54455.5	$1^3P_2'-2^3S_1'$
2311.00 (1)	43246.8		1831.78 (0)	54591.7	$1^3P_1'-2^3S_1'$
2310.61 (1)	43265.3		1830.71 (00)	54623.6	$1^3P_0'-2^3S_1'$
2308.90 (5)	43297.3		1766.08 (1)	56022.6	
2308.75 (5)	43303.9		1765.13 (1)	56653.0	
2300.69 (0)	43451.9		1763.63 (2)	56701.2	
2298.97 (0)	43484.3		†1751.75 (10)	57085.7	? N I
2293.40 (2)	43589.9	$\begin{cases} 2^3P_2-3^3P_1'; \\ 1^3D_2'-2^3D_2 \end{cases}$	†1747.865 (7)	57213.0	$1^1S_0'-1^3P_1'$
2292.72 (1)	43602.8	$\begin{cases} 2^3P_1-3^3P_0'; \\ 1^3D_2'-2^3D_2 \end{cases}$	1743.22 (2)	57365.1	$\beta^3P_{112}-1^3D_1'$
2291.67 (2)	43622.8	$\begin{cases} 1^3D_2'-2^3D_2 \\ 2^3P_1-3^3P_1'; \\ 1^3D_2'-2^3D_2 \end{cases}$	†1740.315 (5)	57460.9	$1^1S_0'-1^1P_1'$
2290.31 (1)	43648.7	$\begin{cases} 2^3P_1-3^3P_1'; \\ 1^3D_2'-2^3D_2 \end{cases}$	1075.83 (5)	59671.9	$\beta^3P_{012}-1^3S_1'$
[2289.9]	[43656.5]	$\begin{cases} 1^3D_2'-2^3D_1 \\ 2^3P_0-3^3P_1'; \\ 1^3D_2'-2^3D_2 \end{cases}$	1029.86 (0)	61355.0	$\beta^3P_{112}-2^3P_0$
2288.47 (3)	43683.8	$\begin{cases} 2^3P_2-3^3P_1'; \\ 1^3D_2'-2^3D_2 \end{cases}$	1029.02 (1)	61386.6	$\beta^3P_{012}-2^3P_1$
2286.73 (4)	43717.0	$\begin{cases} 2^3P_2-3^3P_1'; \\ 1^3D_2'-2^3D_2; \\ 1^3D_4'-2^3D_1 \end{cases}$	1027.42 (1)	61447.0	$\beta^3P_{112}-2^3P_1$
[2285.3]	[43743.8]	$1^3D_1'-2^3D_2$	1616.06 (1n)	61876.9	
2283.70 (2)	43775.0	$2^3P_1-3^3P_2'$	1590.25 (2n)	62883.2	
2238.91 (2)	44650.8		1574.28 (1n)	63521.1	
2237.21 (0n)	44684.8		1573.21 (1n)	63564.3	
2236.78 (0n)	44693.3		1411.90 (4)	70822.0	
2235.18 (1)	44725.3		1346.41 (0)	74271.6	$\beta^3D_{112}-1^3D_1'$
2231.65 (0)	44796.0		1345.29 (1)	74332.9	$\beta^3D_{112}-1^3D_1'$
2219.58 (0)	45039.6		1343.37 (2)	74439.7	$\beta^3D_2'-1^3D_2'$
2206.10 (3)	45314.7	$1^3S_1'-3^3P_1'$ (in part)	1330.80 (00)	75142.8	
2203.72 (1)	45363.6	$1^3S_1'-3^3P_1'$	1320.43 (0)	75220.2	
2197.58 (2)	45489.9	$1^3S_1'-3^3P_2'$	1328.01 (1)	75300.6	
			1326.67 (2)	75376.7	
			1319.85 (5)	75766.2	
			1319.10 (2)	75809.3	
			1310.89 (5n)	76282.9	} ? N I

\* The following lines in this group have been omitted as probably being due to N III: 2099.87 (47006.8), 2097.74 (47655.2), 2097.25 (47687.3), 2091.95 (47787.0).

† There is a carbon line at  $\lambda$  1751.33.

‡  $\lambda\lambda$  by Bowen and Ingram. Assigned to N II by authors from experimental behaviour.



Table I—(continued).

$\lambda$ , Vac.	$\nu$ .	Classification.	$\lambda$ , Vac.	$\nu$ .	Classification.
		Bowen.			
*1276.74 (1)	78324.5	$\left\{ \begin{array}{l} \beta^3 D_1 - 2^3 P_0; \\ \quad \beta D_{12} - 3mP_0 \end{array} \right.$	*916.698 (8)	109087.2	$a P_2 - b P_{12}$
*1276.18 (2)	78358.9	$\left\{ \begin{array}{l} \beta^3 D_2 - 2^3 P_1; \\ \quad \beta D_{12} - 3mP_1 \end{array} \right.$	*916.018 (6)	109168.2	$a P_1 - b P_{12}$
*1275.06 (3)	78427.7	$\left\{ \begin{array}{l} \beta^3 D_3 - 2^3 P_2; \\ \quad \beta D_3 - 3mP_2 \end{array} \right.$	*915.963 (6)	109174.7	$a P_1 - b P_0$
1258.75 (3)	79444		*915.603 (6)	109217.6	$a P_0 - b P_1$
1243.14 (7)	80442	} ? N I	*672.026 (2)	148803.8	$\left\{ \begin{array}{l} 1^3 P_2 - 1^3 P_1'; \\ \quad a P_2 - 3 k P_1 \end{array} \right.$
1242.67 (4)	80472		*671.780 (2)	148858.3	$\left\{ \begin{array}{l} 1^3 P_1 - 1^3 P_0'; \\ \quad a P_1 - 3 k P_0 \end{array} \right.$
1229.7 (4 $\pi$ )	81321		*671.650 (1)	148887.1	$\left\{ \begin{array}{l} 1^3 P_1 - 1^3 P_1'; \\ \quad a P_1 - 3 k P_1 \end{array} \right.$
1226.4 (4 $\pi$ )	81539		*671.397 (3)	148943.2	$\left\{ \begin{array}{l} 1^3 P_{02} - 1^3 P_{12}; \\ \quad a P_{02} - 3 k P_{12} \end{array} \right.$
1224.2 (3)	81686		*671.027 (2)	149025.3	$\left\{ \begin{array}{l} 1^3 P_1 - 1^3 P_1'; \\ \quad a P_1 - 3 k P_2 \end{array} \right.$
†1200.681 (1)	83288.1	} Nebulous group, probably more complex. N II ?	*045.180 (5)	154995.5	$\left\{ \begin{array}{l} 1^3 P_2 - \beta^3 S_1; \\ \quad a P_2 - b S \end{array} \right.$
†1200.200 (2)	83319.4		*044.836 (5)	155078.2	$\left\{ \begin{array}{l} 1^3 P_1 - \beta^3 S_1; \\ \quad a P_1 - b S \end{array} \right.$
†1199.633 (3)	83365.8		*644.633 (4)	155127.0	$\left\{ \begin{array}{l} 1^3 P_0 - \beta^3 S_1; \\ \quad a P_0 - b S \end{array} \right.$
†1134.987 (3)	88106.7				
†1134.420 (3)	88150.8				
†1134.180 (2)	88169.4				
		Bowen.			
*1085.701 (8)	92106.4	$\left\{ \begin{array}{l} 1^3 P_2 - \beta^3 D_1; \\ \quad a P_2 - b D_2 \end{array} \right.$	*533.71 (3)	187368	$\left\{ \begin{array}{l} 1^3 P_2 - 1^3 D_1; \\ \quad a P_2 - 3 n D_{12} \end{array} \right.$
*1085.540 (3)	92120.1	$\left\{ \begin{array}{l} 1^3 P_2 - \beta^3 D_{12}; \\ \quad a P_2 - b D_{12} \end{array} \right.$	*533.53 (3)	187431	$\left\{ \begin{array}{l} 1^3 P_{01} - 1^3 D_{12}; \\ \quad a P_{01} - 3 n D_{12} \end{array} \right.$
*1084.506 (7)	92202.8	$\left\{ \begin{array}{l} 1^3 P_1 - \beta^3 D_{12}; \\ \quad a P_1 - b D_{12} \end{array} \right.$			
*1083.983 (6)	92252.4	$\left\{ \begin{array}{l} 1^3 P_0 - \beta^3 D_1; \\ \quad a P_0 - b D_1 \end{array} \right.$			

\*  $\lambda\lambda$  and classification by Bowen ('Phys. Rev.', vol. 29, p. 231, Feb., 1927).†  $\lambda\lambda$  by Bowen and Ingram. Assigned to N II by authors from experimental behaviour.*Term Notation.*

Pending a more general agreement as to the notation and numeration of spectroscopic terms, it is necessary to explain the procedure which is followed in the present communication. A spectrum like that of N II, which is derived from singlet and triplet terms, could be effectively described by the use of the earlier notation, in which capital letters (S, P, D, etc.) were used for singlet, and small letters (*s*, *p*, *d*, etc.) for triplet terms. There is, however, a strong tendency towards the description of all spectra by the same generalised notation, and to use capital letters exclusively for the representation of term types.\*

In this notation, which is adopted in the present paper, the multiplicity of the system to which a term belongs is indicated by an index number on the upper left of the term symbol, and the inner quantum number by a suffix on

\* This is the more necessary now as small letters, *s*, *p*, *d*, etc., are used by some authors to indicate the *k* values of electron orbits.

the lower right. Thus, the P terms of a triplet system are represented by  $^3P_2$ ,  $^3P_1$ ,  $^3P_0$ . So far, there will probably be general agreement, but the designation of individual terms or groups of terms is more debatable. In the spectra of atoms having more than a single valence electron, the occurrence of two or more sets of terms of the same type, which was revealed especially by the work of Russell and Saunders on the alkaline earths,\* is emphasised by the recent theoretical developments. Thus, as is now well known, we may find numerous terms of each of the types S, P, D ..., which may be recognised as such by their respective contributions to Zeeman patterns, but not all of which have the same combining properties. Each class of terms is divisible into two groups, distinguished by the use of dashes, as S, S'; P, P'; D, D', and so on; the S, P, D... terms combine among themselves in accordance with the older selection rules, as do also the S', P', D' terms. The two classes of terms, however, intercombine in accordance with the modified selection rule  $\Delta l = 0, \dagger$  as for example P P', D D'; other previously unexpected combinations, such as P F', are also possible. Each group of terms may sometimes be further subdivided so as to indicate Rydberg sequences; thus, one set of P terms constitutes the P sequence and another the P'' sequence, while the P' terms may similarly be divided into P' and P''' sequences. According to the new theory, there is no difference at all between such P, P'', P' or P''' terms, and the notation merely expresses properties which are more fundamentally indicated by electron configurations.

The new theory indicates that in general the structure of the spectrum of an element does not depend solely upon a single electron, as in the earlier theory applicable to the alkali metals, but represents the resultant effect of *all* the electrons; or, since the resultant of the underlying electrons which belong to completed  $n_k$  groups or "shells" is zero, the terms, or energy levels, are determined by all the electrons which form parts of uncompleted shells. In the general case, a given configuration of electrons gives rise to a group of terms, differing in energy value among themselves (but not greatly), these differences being accounted for by the different orientations of the corresponding orbits. In the case of *N II*, the two electrons which are concerned in the production of at least the greater part of the spectrum are normally in  $2_s$  orbits, and the corresponding theoretical terms are  $^3P_{012}$ ,  $^1D_2$ ,  $^1S_0$ , which are completely specified by writing  $(2_s 2_s) ^3P_{012}$ ,  $(2_s 2_s) ^1D_2$ ,  $(2_s 2_s) ^1S_0$ . The next set of terms,  $^3P_{012}$ ,  $^1P_1$ , arise when one of the electrons occupies a  $3_s$  orbit while the other remains

\* 'Astrophys. J.', vol. 61, p. 38 (1925).

†  $l$  indicates the term type, being 1 for S, 2 for P, 3 for D, and so on. It is related to the vector sum of the  $k$  values of all the electrons which contribute to the spectrum.

in  $2_2$ , and these may be similarly represented by  $(2_2 3_1) {}^3P_{012}$ ,  $(2_2 3_1) {}^1P_1$ . Transitions between the two sets of levels give rise to spectrum lines which may be represented by writing, for example,  $(2_2 2_2) {}^3P_2 - (2_2 3_1) {}^1P_1$ . In this notation there is no necessity to "dash" any of the terms, as the possibility of combinations is already indicated by selection rules applicable to the electron transitions. These rules are as follows:—

- (1) Not more than two electrons make simultaneous transitions from one  $n_k$  orbit to another.
- (2) The transitions are restricted to those for which  $\Delta k = \pm 1$  for one of the electrons and  $\Delta k = 0$ , or  $\pm 2$  for the other.
- (3) All combinations are further subject to the inner quantum selection rule,  $\Delta j = 0, \pm 1$ , with  $j = 0 \rightarrow j = 0$  forbidden.

Rydberg sequences would be formed from successive terms such as  $(2_2 2_2)$ ,  $(2_2 3_2)$ ,  $(2_2 4_2)$ , and so on.

While this notation undoubtedly conveys all necessary information with regard to the electron configurations, term types, possible Rydberg sequences and combination possibilities, it is very doubtful whether it is the most convenient for general descriptive purposes. It seems to the writers to be unnecessarily cumbersome for writing and printing,\* and to be less convenient for use in the actual analysis of a spectrum than the system mentioned above, in which the combination properties of the various terms are more readily perceived. In the present paper, the older notation has accordingly been adopted, but it will be a simple matter to convert this to the electronic designations, if desired.

As regards the numeration of terms, the deepest term of each class has been numbered 1, the next deepest 2, and so on, in the case of terms which arise when only one electron is displaced from its normal orbit; terms which originate in the simultaneous displacement of both of the  $2_2$  electrons are distinguished by the similar use of  $a, b, c$  for a sequence of terms of the same class,  $a$  being the deepest.

The selection rules applicable to the adopted system of notation, as deduced from those which serve for the electron transitions, are as follows:—

- (1) Within one class of terms (i.e., "dashed" or "undashed")  $\Delta l = \pm 1$  or  $\pm 3$ , the latter usually yielding only faint lines.

\* The existence of quintet terms, as discovered in the analogous spectrum of O III by Mihul ('Comptes Rendus,' vol. 184, p. 89 (1927)), would still further complicate the electronic notation.

- (2) Between the two classes  $\Delta l = 0$ , or  $\pm 2$ , lines due to the latter transitions usually being faint.
- (3)  $\Delta j = 0, \pm 1$ , with  $j = 0 \rightarrow j = 0$  forbidden.

### *Predicted Terms of N II.*

For transitions of a single electron the terms predicted by theory are indicated in Table II. They have been deduced by the application of Hund's rules, supplemented by data given by Laporte.\* The unexcited atom of singly-ionised nitrogen has a structure similar to that of neutral carbon (atomic number = 6), and as shown in Table II, two electrons are in the K, or 1, group and four in the L group; two of the latter are in  $2_1$  orbits, and two in  $2_2$  orbits. The first four thus occur in completed groups [the number required to complete a group being  $2(2k - 1)$ ] and only the electrons in  $2_2$  orbits need at present be considered.

In the first instance (Table II), one of the two outer electrons is supposed to remain in its  $2_2$  orbit (*i.e.*,  $\Delta k = 0$  for this electron), and the table shows the different groups of terms which arise as the other electron occupies successively larger orbits. Usually, the deepest term of the group arising from a given configuration is that having the largest multiplicity and the largest  $l$  value, but this rule is not always followed in the case of *N II*, and other exceptions have been recorded.

The predicted terms are named so as to indicate the combining properties in accordance with the notation already described, and are also arranged to show the various Rydberg sequences. Terms which have actually been identified are printed in heavy type.

The predictions have aided in the analysis of the spectrum beyond that noted in the previous paper by indicating in the first instance the character of the deepest terms, and next by giving approximate values of unidentified terms and thence some idea of the location of multiplets arising from their combinations with terms already known. It will be observed that there is excellent agreement between observation and theory, so far as the comparison can at present be made.

The "core" of the atom of *N II* is the normal state of the atom of *N III* and is similar in structure to the neutral atom of boron, having two  $1_1$ , two  $2_1$ , and one  $2_2$  electrons. The terms corresponding to this configuration are  $^3P_1$  and  $^2P_2$ , of which the former is the deeper. All the terms given in Table II are based upon these two states of the core, and from Hund's rules it may be

determined which of the various sequences are based upon  $^3P_1$  and which upon  $^3P_2$ . Thus:—

Based upon  $^3P_2$  state of core :

$$^3S'_1 \quad ^3P_2 \quad ^3P'_2 \quad ^3P'''_{012} \quad ^3D_3 \quad ^3D'_3 \quad ^3D'''_{123} \quad ^3F_4 \quad ^3F'_4 \quad ^3G'_5$$

Based upon  $^3P_1$  state of core :

$$^3P_{01} \quad ^3P'_{01} \quad ^3D_{12} \quad ^3D'_{12} \quad ^3F_{23} \quad ^3F'_{23} \quad ^3G'_{34}$$

All singlets are based upon the  $^3P_2$  state of the core.

It should be noted that the dashed and undashed terms of the previous paper have been interchanged, in order to make the probable deepest term of the

Table II.—Predicted and

K	L	M	N	O	Triplet Terms.			
1 <sub>1</sub>	2 <sub>1</sub> 2 <sub>2</sub>	3 <sub>1</sub> 3 <sub>2</sub> 3 <sub>3</sub>	4 <sub>1</sub> 4 <sub>2</sub> 4 <sub>3</sub> 4 <sub>4</sub>	5 <sub>1</sub>				
2	2 2			2 <sub>1</sub> 2 <sub>2</sub>				$1^3P$
2	2 1	1		2 <sub>1</sub> 3 <sub>1</sub>				$1^3P'$
2	2 1	1		2 <sub>1</sub> 3 <sub>2</sub>	$1^3D'$	$2^3P$	$1^3S'_1$	
2	2 1	1		2 <sub>1</sub> 3 <sub>3</sub>	$1^3F'$	$1^3D$	$1^3P'''$	
2	2 1		1	2 <sub>1</sub> 4 <sub>1</sub>				$2^3P'$
2	2 1		1	2 <sub>1</sub> 4 <sub>2</sub>	$2^3D'$	$3^3P$	$2^3S'_1$	
2	2 1		1	2 <sub>1</sub> 4 <sub>3</sub>	$2^3F'$	$2^3D$	$2^3P'''$	
2	2 1		1	2 <sub>1</sub> 4 <sub>4</sub>	$1^3G'$	$1^3F$	$1^3D'''$	
2	2 1			1 2 <sub>1</sub> 5 <sub>1</sub>				$3^3P'$

$^3P_2 = 238840$	$1^3P'_2 = 89937.33$	$1^3P'''_2 = 49908.75$	$1^3D'_1 = 72324.22$
50	31.60	—28.06	60.78
$1^3P_1 = 238799$	$1^3P'_1 = 89905.73$	$1^3P'''_1 = 49936.81$	$1^3D'_2 = 72263.44$
84	136.36	—51.80	96.19
$1^3P_2 = 238715$	$1^3P'_2 = 89769.37$	$1^3P'''_2 = 49988.61$	$1^3D'_3 = 72167.25$

$2^3P_2 = 68273.32$	$2^3P'_2 = 42305.61$	$2^3P'''_2 = 28079.7$	$2^3D'_1 = 36131.76$
35.26	51.79	—25.5	50.92
$2^3P_1 = 68238.07$	$2^3P'_1 = 42253.82$	$2^3P'''_1 = 28095.2$	$2^3D'_2 = 36080.84$
58.37	119.29	—46.1	96.20
$2^3P_2 = 68179.70$	$2^3P'_2 = 42134.53$	$2^3P'''_2 = 28141.3$	$2^3D'_3 = 35984.64$

$3^3P_1 = [35075]$	$3^3P'_1 = 24634.3$	$3^3P'''_1 = [17968]$	$3^3D'_1 = [21620]$
	45.8		
	$3^3P'_1 = 24588.5$		
	127.1		
	$3^3P'_1 = 24461.4$		
	$4^3P'_1 = [15980]$		

\* Identified by Bowen (see Addendum).

undashed type, in accordance with the conventional procedure. The older suffixes have also been replaced by inner quantum numbers, so that, including singlet terms, the relation of the earlier to the present notation is as follows:—

$$\begin{array}{lll}
 p_3 = 1^3P_0' & p_3' = 2^3P_0 & d_3' = 1^3D_1 \\
 p_2 = 1^3P_1' & p_2' = 2^3P_1 & d_2' = 1^3D_2 \\
 p_1 = 1^3P_2' & p_1' = 2^3P_2 & d_1' = 1^3D_3 \\
 p_3^2 = 2^3P_0' & d_3 = 1^3D_1' & s = 1^3S_1' \\
 p_2^2 = 2^3P_1' & d_2 = 1^3D_2' & P = 1^1P_1' \\
 p_1^2 = 2^3P_2' & d_1 = 1^3D_3' & S = 1^1P_1 \\
 & & S^2 = 2^1S_0'
 \end{array}$$

Observed Terms of *N II*.

Singlet Terms.				Term Values.
	$1^1D_1'$		$1^1S_0'$	238849—147119
			$1^1P_1'$	89937— 89658
	$2^1D_1'$	$1^1P_1$	$2^1S_0'$	74235— 00572
$1^1F_1$		$1^1D_1$	$1^1P_1'''$	52334— 48725
			$2^1P_1$	42305— 40987
	$3^1D_1$	$2^1P_1$	$3^1S_0'$	36132
$2^1F_3'$		$2^1D_1$	$2^1P_1'''$	28607
$1^1G_4$	$1^1F_3$	$1^1D_1'''$		
			$3^1P_1'$	24634

$1^3D_1 = 51408.36$	$1^3F_4' = 52334.32$	$1^1P_1' = 89657.96$	$1^1D_1' = > 210000$
$1^3D_2 = 51384.32$	$1^3F_3' = 52274.90$	$2^1P_1' = 40987.42$	$2^1D_1' = 74235.10$
$1^3D_3 = 51353.98$	$1^3F_4' = 52193.35$	$3^1P_1' = 24018.7$	$3^1D_1' = [37270]$
$2^3D_1 = 28606.9$	$2^3F_4' = [28855]$	$1^1P_1 = 64633.77$	$1^1S_0' = 147118.8$
$2^3D_2 = 28580.4$		$2^1P_1 = [33753]$	$2^1S_0' = 00572.53$
$2^3D_3 = 28544.8$			$3^1S_0' = [32407]$
	$1^3S_1' = 69953.66$		
$3^3D_2 = [18130]$	$2^3S_1' = 35313.9$	$1^1F_3' = 52148.02 ?$	
	$3^3S_1' = [21570]$		
		$1^1D_1 = 51754.50 ?$	
		$1^1P_1''' = 48725.55$	

*Triplet Term Values.*

Although no long sequences of terms occur in the spectrum of N II, it is possible to determine the absolute values of the terms with considerable accuracy because of the identification of three  $^3P^3P'$  multiplets which form a Rydberg sequence. Thus, we find

$$2\ ^3P_2 - 1\ ^3P_2' = -21589.67$$

$$2\ ^3P_2 - 2\ ^3P_2' = 26045.23$$

$$2\ ^3P_2 - 3\ ^3P_2' = 43717.0$$

Taking 109678.3 as the value of the series constant,  $R$ , these lines are represented by the formula

$$\nu = 68179.70 - 4R/[m + 0.259020 - 0.096678/m]^2$$

giving

$$1\ ^3P_2' = 89769.37$$

$$2\ ^3P_2 = 68179.70.$$

The remaining term values are then derived in the usual way from the combinations in which they appear, with the results shown in the lower part of Table II.\*

It should be noted that two successive Rydberg terms have been identified for  $^3S_1$ ,  $^3P'''$ ,  $^3D'$ , and  $^3D$ . Formulæ for these terms may accordingly be computed for purposes of extrapolation. Thus, we find

$$m\ ^3S_1' = 4R/[m + 0.465402 + 0.177780/m]^2$$

$$m\ ^3P_2''' = 4R/[m + 0.918807 + 0.087336/m]^2$$

$$m\ ^3D_3' = 4R/[m + 0.543799 - 0.156426/m]^2$$

$$m\ ^3D_3 = 4R/[m + 0.915447 + 0.014760/m]^2$$

The correcting terms in these formulæ are quite small, and if this be also true of the sequences of which only one term has been identified, roughly approximate values of additional terms may be derived by the calculation of simple Rydberg formulæ. Thus

$$m\ ^3P = 4R/[m + 0.536663]^2$$

$$m\ F_4' = 4R/[m + 0.899230]^2$$

Terms which have been calculated from the formulæ are included in Table II, where they are enclosed in square brackets. Combinations involving such computed terms, however, have not been traced, and it is evident that they must either be absent or very faint.

The formula for  $m\ ^3P$  is of particular interest because the deepest of all the

\* If  $R_\infty$  (=109737) be preferred to  $R_H$  (=109678.3) all the term values should be increased by about 4 units.

terms is expected to be of this type. The formula gives for the first term of this sequence ( $m = 1$ ) the value 185,780, as first pointed out by Laporte. This suggests the occurrence of a multiplet  $1^3P_{012} - 1^3P'_{012}$  in the neighbourhood of  $\nu$  96,000 and a triplet  $1^3P_{012} - 1^1P'_1$  in close proximity, since  $1^1P'$  and  $1^3P'$  are but slightly different in value (see later). Bowen and Millikan\* have already assigned a triplet to N II, on the ground of its separations and position in the spectrum, namely, according to the more recent measures of Bowen and Ingram :—

$\lambda$	$\nu$	$\Delta\nu$
916.690 (4)	109088.1	83.9
915.986 (4)	109172.0	46.6
915.595 (3)	109218.6	

If this be taken as  $1^3P_{012} - 1^1P'_1$ , the value of  $1^3P_0$  would be 198,876, and the corresponding ionisation potential would be 24.5 volts, in close agreement with the 24 volts estimated from stellar spectra.†

There are, however, no indications in the published lists of nitrogen lines in this region, or in our own plates, of such an adjacent multiplet as would be expected. The photographs of this region given by Hopfield and Leifson‡ also give no indications of such a multiplet. The above identification of the  $1^3P_{012} - 1^1P'$  triplet is consequently very doubtful; the multiplet would, indeed, be expected to be more intense than the triplet, as in the case of the multiplet  $1^3P'_{012} - 2^3P_{012}$  and the adjacent triplet  $1^1P' - 2^3P_{012}$  (near  $\lambda$  4640). It is, in fact, very doubtful whether there is actually a *triplet* of N II in the position given by Millikan and Bowen. Our own plates of vacuum tube spectra, both with strong and weak discharges, show only two lines, apparently agreeing in position with the two more refrangible members of the supposed triplet. Further, Hopfield and Leifson, who also used vacuum tubes, have similarly tabulated only these two lines [ $\lambda$  916.03 (2), 915.59 (3)]. It may be, therefore, that the  $\lambda$  916.69 component of the supposed triplet is really a line special to the "hot spark" conditions under which Millikan and Bowen's photographs were taken.

Further investigations of the spectrum in the region beyond  $\lambda$  830 ( $\nu$  120480) thus appear to be necessary before final conclusions can be reached with regard to the deepest terms. From the available evidence, it would seem that the

\* 'Phys. Rev.,' vol. 24, p. 221 (1924).

† R. H. Fowler and E. A. Milne, 'Monthly Notices R.A.S.,' vol. 84, p. 499 (1924).

‡ 'Astrophys. Journ.,' vol. 58, p. 59 (1923).



$1^3P - 1^1P'$  and  $1^3P - 1^3P'$  lines lie beyond this limit and that the value of  $1^3P$  is greater than 210420 ( $=120480 + 89940$ ); that is, the ionisation potential must be greater than 26 volts.\*

### Triplet Combinations.

The combinations arising from terms of the triplet system due to the changing orbits of a single electron are shown in Table III. The table includes the combinations noted in the previous paper, but some of the wave-lengths have been revised, and repetition is also necessary on account of the amended notation.

The terms are uniformly arranged in increasing order from left to right, and in decreasing order downwards in each group of similar type. Wave-numbers enclosed in brackets are computed values. Inverted terms are indicated by the negative signs of  $\Delta\nu$ .

On account of experimental difficulties, arising partly from the long exposures required for vacuum tubes with instruments of large dispersion, and partly from the instability of some of the wave-lengths, there are slight differences in the values of the same terms derived from different combinations. The values deduced from the sets of measures judged to be the most trustworthy

Table III.—Triplet Combinations.

Term Values.	$1^3P_1'$ 80769.37	$136.36$	$1^3P_1'$ 89905.73	$31.60$	$1^3P_0'$ 89937.33	Combinations.
$2^3P_0 = 68273.32$ $35.25$			$21632.41$ (7)			
$2^3P_1 = 68238.07$ $58.37$	$21531.30$ (8)	$136.36$	$21667.66$ (6)	$31.60$	$21699.26$ (7)	$1^3P' - 2^3P$
$2^3P_2 = 68179.70$	$21589.67$ (10)	$136.36$	$21726.03$ (8)			
$1^3D_1' = 72324.22$ $60.78$	$17445.14$ (2)	$136.40$	$17581.54$ (6)	$31.50$	$17613.10$ (6)	
$1^3D_1' = 72263.44$ $96.19$	$17505.98$ (6)	$136.30$	$17642.26$ (8)			$1^3P' - 1^3D'$
$1^3D_2' = 72167.25$	$17602.12$ (10)					
$2^3D_1'^* = 36131.76$ $50.92$	[53637.0]		[53774.0]		$53807.7$ (3)	
$2^3D_1' = 36080.84$ $96.20$	$53689.2$ (2)	$137.1$	$53826.3$ (3)			$1^3P' - 2^3D'$
$2^3D_2' = 35984.64$	$53786.0$ (5)					
$1^3S_1' = 69953.66$	$19815.91$ (8)	$136.35$	$19952.06$ (6)	$31.62$	$19983.68$ (2)	$1^3P' - 1^3S'$
$2^3S_1' = 35313.9$	$54455.5$ (1)	$136.2$	$54591.7$ (0)	$31.9$	$54623.6$ (00)	$1^3P' - 2^3S'$

\* Term values adopted from  $1^3F' - 2^3D'$ .

\* See Addendum.

Table III—(continued).

Term Values.	$1^3D_1'$ 72167.25	96.19	$1^3D_2'$ 72263.44	60.78	$1^3D_3'$ 72324.22	Combinations.
$1^3D_1 = 51408.32$ 24.07			20855.09 (2) 24.09	60.85	20915.94 (4) 24.04	$1^3D' - 1^3D$
$1^3D_2 = 51384.25$ 30.35	20783.00 (2) 30.24	96.18	20879.18 (5) 30.38	60.80	20930.98 (2)	
$1^3D_3 = 51353.90$	20813.34 (6)	96.22	20909.56 (2)			
$2^3D_1^* = 28606.95$ 26.52			[43656.5]		†43717.0 (4)	$1^3D' - 2^3D$
$2^3D_2 = 28580.43$ 35.63	†43589.9 (2)		†43683.8 (3)		[43743.8]	
$2^3D_3 = 28544.80$	43622.8 (2)		†43717.0 (4)			
$2^3P_0' = 42305.52$ 51.63					30018.70 (2) 51.67	$1^3D' - 2^3P'$
$2^3P_1' = 42253.80$ 119.07			30009.52 (3) 119.20	60.85	30070.37 (2)	
$2^3P_2' = 42134.82$	30032.34 (4)	96.38	30128.72 (2)		[30189.4]	
$3^3P_0' = 24633.2$ 45.9					47601.0 (2) 46.4	$1^3D' - 3^3P'$
$3^3P_1' = 24587.3$ 127.5			47676.7 (3) 127.5	60.7	47737.4 (2)	
$3^3P_2' = 24459.8$	47706.8 (6)	97.4	47804.2 (3)		[47864.4]	
$1^3F_1' = 52334.32$ 59.42	19832.76 (0) 59.57	96.36	19929.12 (5) 59.45	60.80	19989.92 (7)	$1^3D' - 1^3F'$
$1^3F_2' = 52274.90$ 81.55	19892.33 (6) 81.57	96.24	19988.57 (8)			
$1^3F_4' = 52193.35$	19973.90 (10)					
$1^3P_2''' = 49988.67$ —51.79	22178.65 (3)	96.04	22274.69 (0) 51.77		[22335.55]	$1^3D' - 1^3P'''$
$1^3P_1''' = 49936.88$ —28.10			22326.46 (2)	60.98	22387.44 (0) 28.00	
$1^3P_0''' = 49908.78$					22415.44 (1)	

\* Term values adopted from  $2^3P - 2^3D$ .† Superposed on lines of  $2^3P - 3^3P'$ .

Table III—(continued).

Term Values.	$2^1P_2$ 68179.70	58.37	$2^1P_1$ 68238.07	35.25	$2^1P_0$ 68273.32	Combinations.
$1^1D_1 = 51408.40$ 24.01	16771.27 (0)	58.39	16829.66 (2)	35.29	16864.95 (4)	$2^1P - 1^1D$
$1^1D_1 = 51384.39$ 30.32	16795.33 (3)	58.33	16853.66 (7)			
$1^1D_2 = 51354.07$	16825.63 (8)					
$2^1D_1 = 28606.9$ 26.5	[39572.7]		39631.1 (1)	35.3	39666.4 (2)	$2^1P - 2^1D$
$2^1D_1 = 28580.4$ 35.6	39599.1 (1)	58.7	39657.8 (3)			
$2^1D_1 = 28544.8$	39634.9 (4)					
$2^1P_0' = 42305.59$ 51.75			25932.48 (2)			$2^1P - 2^1P'$
$2^1P_1' = 42253.84$ 119.40	25925.81 (3)	58.56	25984.37 (3)	35.03	26019.40 (3)	
$2^1P_2' = 42134.44$	26045.23 (5)	58.42	26103.65 (3)			
$3^1P_0' = 24035.3$ 45.7			43602.8 (1)			$2^1P - 3^1P'$
$3^1P_1' = 24589.6$ 126.7	43589.9 (2)	58.8	43648.7 (1)	35.1	43683.8 (3)	
$3^1P_2' = 24402.9$	43717.0 (4)	58.0	43775.0 (2)			
$1^1P_2''' = 49988.71$ —51.80	18191.00 (5)	58.35	18249.35 (2)			$2^1P - 1^1P'''$
$1^1P_1''' = 49936.91$ —28.05	18242.79 (3)	58.37	18301.16 (3)	35.25	18336.41 (2)	
$1^1P_0''' = 49908.86$			18329.21 (2)			
$2^1P_2''' = 28141.53$ —45.77	40038.0 (4)	58.7	40096.7 (0)			$2^1P - 2^1P'''$
$2^1P_1''' = 28095.76$ —25.29	40083.8 (1)	58.8	40142.6 (2)	34.8	40177.4 (0)	
$2^1P_0''' = 28070.47$			40167.6 (1)			
Term Values.	$1^1F_4'$ 52193.35	81.55	$1^1F_3'$ 52274.90	59.42	$1^1F_2'$ 52334.32	Combinations.
$2^1D_1' = 36131.76$ 50.92					16202.56 (1)	$1^1F' - 2^1D'$
$2^1D_2' = 36080.84$ 96.20			16194.06 (3)	59.2	16253.3 (0)	
$2^1D_3' = 35984.64$	16208.71 (4)	81.7	16290.4 (0)		[16349.8]	

Table III--(continued).

Term Values.	$1^3D_3$		$1^3D_2$		$1^3D_1$		Combinations.
	51353.08	30.24	51384.32	24.04	51408.36		
$2^3D_1' = 36131.76$ 50.92			[15252]		*15274.2 (0)		$1^3D - 2^3D'$
$2^3D_2' = 36080.84$ 96.20	*15274.2 (0)		15302.7 (1)		15327.8 (0)		
$2^3D_3' = 35984.64$	15368.8 (2)		15399.3 (0)				

\* Used twice.

 $^3S' \ ^3P'$  Combinations.

$$(1 \ ^3S_1' = 69953.66; 2 \ ^3S_1' = 35313.9.)$$

$1^3P_2' - 1^3S_1' = 19815.71$ (8)		$1^3S_1' - 1^3P_1''' = 19965.22$ (7)	
	136.35		-51.80
$1^3P_1' - 1^3S_1' = 19952.06$ (6)		$1^3S_1' - 1^3P_1''' = 20017.02$ (6)	
	31.62		-28.02
$1^3P_0' - 1^3S_1' = 19983.08$ (2)		$1^3S_1' - 1^3P_0''' = 20045.04$ (4)	
$1^3P_2' - 2^3S_1' = 54455.5$ (1)			
$1^3P_1' - 2^3S_1' = 54591.7$ (0)			
$1^3P_0' - 2^3S_1' = 54623.6$ (00)			
$1^3S_1' - 2^3P_0' = 27647.94$ (1)		$1^3S_1' - 2^3P_1''' = 41812.5$ (2)	
	51.99		-46.5
$1^3S_1' - 2^3P_1' = 27699.93$ (2)		$1^3S_1' - 2^3P_1''' = 41850.0$ (1)	
	119.41		-25.8
$1^3S_1' - 2^3P_2' = 27819.34$ (3)		$1^3S_1' - 2^3P_0''' = 41884.8$ (0)	
$1^3S_1' - 3^3P_0' = [ \quad ]$			
$1^3S_1' - 3^3P_1' = 45363.6$ (1)		$1^3S_1' - 1^3D_2 = 18569.0$ (0)	
	126.3		
$1^3S_1' - 3^3P_2' = 45489.9$ (2)			

\* Masked by a line at 45314.7 (3).

have usually been adopted, but, other things being equal, the means of the different values have been taken. Thus, in Table III the adopted values of the terms are given at the top and on the left for each combination, while the observed values are given for the corresponding lines. The agreement between the observed and calculated values is, in general, very satisfactory, except for some of the fainter lines in the far ultra-violet, where special difficulties are met with in the choice of standards, and errors of measurement are greatly magnified in conversion to wave-numbers.

*Singlet Terms.*

Although there are several strong lines which evidently do not form part of multiplets, the identification of the singlet terms is much more difficult and uncertain than that of the triplets, for which indications are furnished by the recurrence of separations. The expected  $1^1P_1'$  term, however, appears to be certainly indicated by its combinations with  $1^3D_{12}'$ ,  $2^3P_{012}$  and  $1^3S_1'$  to which attention was directed in the previous paper, namely

$$\begin{array}{rcl}
 1^1P_1' - 1^3D_1' = 17333.95 \text{ (3)} & & 1^1P_1' = 89658.18 \\
 & 60.74 & \\
 1^1P_1' - 1^3D_2' = 17394.69 \text{ (4)} & & 1^1P_1' = 89658.13 \\
 & & \\
 1^1P_1' - 2^3P_0 = 21384.50 \text{ (2)} & & 1^1P_1' = 89657.82 \\
 & 35.28 & \\
 1^1P_1' - 2^3P_1 = 21419.78 \text{ (2)} & & 1^1P_1' = 89657.85 \\
 & 58.49 & \\
 1^1P_1' - 2^3P_2 = 21478.27 \text{ (2)} & & 1^1P_1' = 89657.82 \\
 & & \\
 1^1P_1' - 1^3S_1' = 19704.39 \text{ (3)} & & 1^1P_1' = 89657.82 \\
 & & \hline
 \text{Mean} \quad 1^1P_1' = 89657.96 & & \hline
 \end{array}$$

The value thus deduced for  $1^1P_1'$  is of the expected order of magnitude (that is, not very different from  $1^3P$ ), and no other term would be appropriate to all the combinations observed.

Other singlet terms are indicated by the occurrence of certain strong pairs of lines having the separation  $1^3P_1' - 1^1P_1'$ ; that is  $\Delta\nu = 89905.73 - 89657.96 = 247.77$ . In association with two of these pairs there are other lines showing a separation of 237.7 from the second members of the pairs. Particulars of these lines, with the suggested singlet terms which give rise to them, are as follows:—

$$\begin{array}{rcl}
 (1^3P_1' = 89905.73) & & 1^1P_1' = 89657.96 \\
 15422.92 \text{ (8)} & \left. \begin{array}{l} = 1^1P_1' - 2^1D_2' \\ = 1^3P_1' - 2^1D_2' \end{array} \right\} & 2^1D_2' = 74235.10 \\
 15670.57 \text{ (5)} & \left. \begin{array}{l} 247.65 \\ 237.71 \end{array} \right\} & \\
 15908.28 \text{ (3)} & = 1^1P_1 - 1^1P_1''' & \\
 & & \\
 25024.27 \text{ (10)} & \left. \begin{array}{l} = 1^1P_1' - 1^1P_1 \\ = 1^3P_1' - 1^1P_1 \end{array} \right\} & 1^1P_1 = 64633.77 \\
 25271.88 \text{ (6)} & \left. \begin{array}{l} 247.61 \\ 237.62 \end{array} \right\} & \\
 25509.50 \text{ (6)} & = 2^1D_2' - 1^1P_1''' & 1^1P_1''' = 48725.55
 \end{array}$$

$$\begin{array}{rcl}
 29085.46 \text{ (6)} & = 1^1P_1' - 2^1S_0' & \\
 & \quad \quad \quad 247.71 & \\
 29333.17 \text{ (3)} & = 1^3P_1' - 2^1S_0' & \left. \vphantom{\begin{array}{l} 29085.46 \\ 29333.17 \end{array}} \right\} 2^1S_0' = 60572.53 \\
 \\
 *57213.0 \text{ (8)} & = 1^1S_0' - 1^3P_1' & \\
 & \quad \quad \quad 247.9 & \\
 *57460.9 \text{ (5)} & = 1^1S_0' - 1^1P_1' & \left. \vphantom{\begin{array}{l} *57213.0 \\ *57460.9 \end{array}} \right\} 1^1S_0' = 147118.8
 \end{array}$$

While this assignment of terms should perhaps be regarded as provisional, the correlation with the corresponding theoretical terms may be considered satisfactory. The identification of the  $1^1P_1'$  term seems to be beyond question, and evidence in favour of the suggested identification of  $2^1D_2'$  is afforded by its combinations with  $1^3F'$  and  $1^3D$ . Thus

$2^1D_2' = 74235.10$	$2^1D_2' = 74235.10$	$2^1D_2' = 74235.10$
$1^3F_3' = 52274.90$	$1^3F_2' = 52334.32$	$1^3D_2 = 51384.32$
<hr/>		
Calcd. 21960.20	21900.78	22850.78
Obsd. 21959.82 (5n)	21900.74 (1n)	22850.74 (0)
<hr/>		

These combinations would not be appropriate to either  $1^1P_1$  or  $2^1S_0'$ , which belong to the same group of levels arising from the electron configuration ( $2s^2 3s$ ). It will be observed that the suggested  $2^1D_2'$  term is larger than either of the  $1^3D'$  or  $2^3P$  terms of the same group, and would accordingly not follow the more general rule that a term of greatest multiplicity is the deepest of a group. Extrapolation by a Rydberg table gives  $1^1D_2'$  about 214,000, while the extrapolated value of  $1^3P$  is considerably smaller. There are, however, theoretical reasons for supposing that  $1^3P$  must be the deepest term of the spectrum, and it is probable that these simple extrapolations do not lead to the correct relative values of the deepest terms. A small negative correcting term (say,  $0.012/m$ ) in the formula for  $1^1D_2'$ , and a somewhat larger negative term (say,  $0.236/m$ ) in that for  $3P$ , would suffice to make both  $1^3P$  and  $1^1D_2'$  larger than 214000, with  $1^3P > 1^3D'$ . There would be nothing unusual in such correcting terms, but, as already pointed out, the question as to which is actually the deepest term of the spectrum cannot be settled until more detailed observations have been made in the region beyond  $\lambda$  830.

In the assignment of the  $1^1P_1$  and  $2^1S_0'$  terms, Hund's rule for the deeper

\* From Bowen and Ingram's measures.

term was applied in the first instance. Adopting  $2\ ^1S_0' = 60572.5$ , a simple Rydberg extrapolation gives  $1\ ^1S_0' = 146060$ , which at once indicates the strong pair of lines at  $57213.0$ ,  $57460.9$  as  $1\ ^1S_0' - 1\ ^3P_1'$  and  $1\ ^1S_0' - 1\ ^1P_1'$  respectively. The  $1\ ^1S_0'$  terms may accordingly be represented by the formula

$$m\ ^1S_0' = 4R/[m + 0.655626 + 0.071230/m]^2$$

which is again remarkable for the small value of the correcting term. Extrapolation by this formula gives  $3\ ^1S_0' = 32406.6$ , but the corresponding combinations with  $1\ ^1P_1'$  and  $1\ ^3P_1'$  have not been found.

So far as the above observed combinations are involved,  $2\ ^1S_0'$  might have been interchanged with  $1\ ^1P_1'$ . But if  $1\ ^1P_1'$  ( $-64634$ ) were to be taken as  $2\ ^1S_0'$ , the extrapolated value of the deepest term of this type would be about  $170000$ , and a pair of lines with separation  $247.7$  would have been expected in the region about  $\nu\ 80000$ . The fact that no such lines have been observed, although well within the range of observation, is strong evidence that the  $2\ ^1S_0'$  and  $1\ ^1P_1'$  terms have been correctly allocated.

The  $1\ ^1P'''$  term indicated above has been chosen as such in consideration of its appropriate magnitude.

Attention should be directed to the fact that in the above scheme, some of the combinations which are possible according to the familiar selection rules do not appear in the spectrum. Thus, there are no indications of  $1\ ^3P_2' - 2\ ^1D_2'$ , or of  $1\ ^3P_0' - 1\ ^1P_1'$ ,  $1\ ^3P_2' - 1\ ^1P_1'$ . Corresponding lines in the analogous spectrum of SiI are also weak or missing. While this may throw some doubt on the identification of the singlet terms in question, there is apparently no other evidence of the existence of such terms as theory indicates.

Other combinations involving singlet terms already mentioned are as follows :

$$1\ ^3S_1' - 1\ ^1P_1''' = 21227.98\ (1)$$

$$1\ ^1P_1 - 1\ ^1P_1''' = 15908.28\ (3)$$

Additional combinations were identified by trial of extrapolated values, namely

$$\left. \begin{aligned} 2\ ^1S_0' - 2\ ^1P_1' &= 19585.30\ (2) \\ 2\ ^1D_2' - 2\ ^1P_1' &= 33247.67\ (7) \\ 1\ ^1P_1 - 2\ ^1P_1' &= 23646.16\ (3) \end{aligned} \right\} 2\ ^1P_1' = 40987.42$$

Two other possible combinations, suggested by a consideration of the probable magnitudes of the  $1\ ^1F_3'$  and  $1\ ^1D_2$  terms are as follows :—

$$\begin{aligned} 2\ ^1D_2' - 1\ ^1F_3' &= 22067.08\ (5) & 1\ ^1F_3' &= 52168.02\ ? \\ 2\ ^1D_2' - 1\ ^1D_2 &= 22480.60\ (10) & 1\ ^1D_2 &= 51754.50\ ? \end{aligned}$$

Numerous singlets remain unidentified.

*Double Electron Transitions.*

Groups of lines, or multiplets, have been found in which the separations have nothing in common with those of the terms already considered. It does not seem possible that these can form part of the theoretical scheme of terms due to the changing orbit of a single electron, and it is probable that they are to be attributed to simultaneous transitions of two electrons. The theoretical predictions for some of the terms which may arise in this way are shown in Table IV.

Table IV.—Predicted Terms for Double Transitions.

K 1 <sub>1</sub>	L 2 <sub>1</sub> 2 <sub>2</sub>	M 3 <sub>1</sub> 3 <sub>2</sub> 3 <sub>3</sub>	N 4 <sub>1</sub>		Terms.	Estimated relative values.
2	2	2		(3 <sub>1</sub> 3 <sub>1</sub> )	<i>a</i> <sup>1</sup> S'	0
2	2	1 1		(3 <sub>1</sub> 3 <sub>2</sub> )	<i>a</i> <sup>3</sup> P', <i>a</i> <sup>1</sup> P'	— 20000
2	2	1 1		(3 <sub>1</sub> 3 <sub>3</sub> )	<i>a</i> <sup>3</sup> D', <i>a</i> <sup>1</sup> D'	— 42000
2	2	1	1	(3 <sub>1</sub> 4 <sub>1</sub> )	<i>b</i> <sup>1</sup> S', <i>a</i> <sup>3</sup> S'	— 30000
2	2	2		(3 <sub>1</sub> 3 <sub>2</sub> )	<i>a</i> <sup>3</sup> P, <i>a</i> <sup>1</sup> D''', <i>a</i> <sup>1</sup> S'''	— 42000
2	2	1 1		(3 <sub>1</sub> 3 <sub>3</sub> )	<i>a</i> <sup>3</sup> F', <i>a</i> <sup>3</sup> D, <i>a</i> <sup>3</sup> P''', <i>a</i> <sup>1</sup> F', <i>a</i> <sup>1</sup> D, <i>a</i> <sup>1</sup> P'''	— 64000
2	2	2		(3 <sub>1</sub> 3 <sub>3</sub> )	<i>a</i> <sup>3</sup> F, <i>a</i> <sup>3</sup> P'', <i>a</i> <sup>1</sup> G', <i>a</i> <sup>1</sup> D''''', <i>a</i> <sup>1</sup> S'''''	— 80000

The terms are dashed or undashed so as to conform with the selection rules for possible combinations with the terms of Table II. The first term of each class is indicated by the prefix *a* and the second by *b*. *a* <sup>1</sup>S', *a* <sup>1</sup>S''' and *a* <sup>1</sup>S''''', for example, are the first of three different sequences of <sup>1</sup>S' terms, while *a* <sup>1</sup>S', *b* <sup>1</sup>S' are successive members of the same sequence.

As no intercombinations with the previous set of terms have been found, the values of the above terms cannot yet be stated with any precision. Roughly approximate estimates of the differences between the different groups, however, may possibly be deduced from the values of the terms already known, and such estimates may be of use in indicating the parts of the spectrum in which combination groups of lines may be expected. For example, as shown in Table II, the configuration 2<sub>2</sub> 3<sub>3</sub> gives the 1 <sup>3</sup>D' group of terms, while 2<sub>2</sub> 3<sub>2</sub> gives the group beginning with 1 <sup>3</sup>F'; so that, taking rough means, the work required to convert the 3<sub>2</sub> electron to 3<sub>3</sub> is represented by 70,000 — 50,000 = 20,000. Similarly, referring to Table IV, the configurations 3<sub>1</sub> 3<sub>2</sub> and 3<sub>1</sub> 3<sub>3</sub> give the *a* <sup>3</sup>P' and *a* <sup>3</sup>D' groups respectively, and if the work required for the change from 3<sub>2</sub> to 3<sub>3</sub>



were the same as in the previous case, we should have  $a^3P' - a^3D'$  of the order of 20000. On account of the reduced screening effect of the  $3_1$  electron as compared with the  $2_3$ , however, this difference would be increased, say to 22000. Other differences for the term groups have been estimated in a similar manner.

In view of the uncertainty with regard to the  $1^3P$  term, no attempt has been made to estimate the actual values of the double-transition terms. The estimated *relative* values given in the last column of Table IV are accordingly referred to  $a^1S'$  taken as zero. These will serve equally well in attempts to correlate observed multiplets with the theoretical terms. [Bowen's value for  $1^3P$  (see Addendum) suggests that  $a^1S'$  may be of the order of  $-80000$ .]

Three multiplets which are inter-related are shown in Table V, with the types of terms suggested by the above considerations. Besides these, there is a fairly strong isolated multiplet of rather nebulous lines beginning at  $\lambda$  2897 ( $\nu = 34502$ ), and probably another beginning at  $\lambda$  4073 ( $\nu = 24544$ ); these have been named *A* and *B* respectively for convenience of reference.

Table V.—Double Transition Multiplets.

	$a^3P_0'$ -25759.10	56.23	$a^3P_1'$ -25815.13	70.63	$a^3P_2'$ -25885.74
$a^1S' = -50000.00^*$	24240.00 (1)	56.03	24184.87 (2)	70.61	24114.26 (3)
* Assumed relative value.					
	$a^3D_3'$ -43946.53	53.89	$a^3D_2'$ -43892.64	43.13	$a^3D_1'$ -43849.51
$a^3P_0' = -25759.10$ 56.23					18090.41 (2) 56.23
$a^3P_1' = -25815.13$ 70.63			18077.29 (4) 70.59	43.11	18034.18 (3) 70.67
$a^3P_2' = -25885.74$	18060.57 (5)	53.87	18006.70 (3)	43.19	17983.51 (0)
$a^3F_3' = -63173.80$ 33.73	19227.17 (00) 33.74	53.99	19281.16 (2) 33.82	43.23	19324.39 (2)
$a^3F_2' = -63207.53$ 40.52	19260.91 (2) 40.61	54.07	19314.98 (3)		
$a^3F_1' = -63248.05$	19301.52 (5)				

*Multiplet A.*

34648.9 (6)				
91.1				
34557.8 (4)	157.5	34715.3 (4)		
55.3		54.4		
34502.5 (3)	158.4	34660.9 (2)	79.4	34740.3 (2)

Table V—(continued).

## Multiplet B.

24737.39 (5)					
192.59					
24544.80 (2)	230.82	24775.62 (4)			
		51.77			
		24723.85 (3)	107.17	24831.03 (3)	

## ADDENDUM.

Since the foregoing account of our work was completed, an important paper on the extreme ultra-violet spectra of carbon, nitrogen, oxygen, and fluorine has been published by S. I. Bowen, of Prof. Millikan's Laboratory, at Pasadena.\* The work of Dr. Bowen is remarkable for the high resolution and precision of wave-lengths which have been attained in this difficult region, and for the classification of many of the lines of the elements in question at different stages of ionisation. In the case of *N II*, Dr. Bowen has amended the values of the  $1^3P'$  terms ( $3kP$  in his notation), and thence of some of the remaining terms, in the manner already explained in the present communication, and has identified the deep  $1^3P$  ( $\alpha P$ ) terms through their combination with  $1^3P'$ . Thus, adopting the values of  $1^3P'$  from Table II, in place of 93000 assigned to  $1^3P_2$  by Bowen, the multiplet  $1^3P - 1^3P'$  is as follows:—

Bowen's $\alpha P \rightarrow$		$1^3P_2$ 238716	84	$1^3P_1$ 238800	50	$1^3P_0$ 238850
Bowen's $3kP$	$1^3P'_0 = 89037.3$			148858 (2)		
	31.6			29		
	$1^3P'_1 = 89905.7$	148804 (2)	83	148887 (1)		*148943 (3)
	136.3	139		138		
	$1^3P'_2 = 89769.4$	*148943 (3)		149025 (2)		

\* Used twice.

The term  $1^3P$  is thus shown to be greater than 210000, as we had anticipated, and although somewhat greater than expected, there can be little doubt that the term has been correctly identified. As already pointed out, the triplet  $1^3P - 1^3P'$  would also be expected near the above multiplet, but this does not appear in Bowen's list, which, however, only includes lines classified by him.

In the discussion of his observations, Bowen has shown the importance of a group of terms which arises when one of the  $2_1$  electrons is displaced to a  $2_2$  orbit; that is (omitting the K electrons), from the configuration  $(2_1)(2_2)^2$ , or

\* 'Phys. Rev.', vol. 29, p. 231 (Feb. 1927).

$sp^3$  in the notation adopted by Bowen. For this configuration the theoretical terms, distinguished by the prefix  $b$ , are

$$^1P, ^1D, ^3S, ^3P, ^3D, ^5S,$$

or, in the notation of the present paper,

$$^1P_1', ^1D, ^3S, ^3P', ^3D, ^5S.$$

To avoid confusion, the prefix  $b$  of Bowen will be replaced by  $\beta$ .

In addition to the combinations given by Bowen, a few others have been noted among the lines occurring in our list (Table I). One of them provides an interesting check on the values of the  $\beta^3D$  terms, and thence of  $1^3P$ . One of Bowen's multiplets may be constructed as follows, wave-numbers in square brackets being calculated from the known separations of the  $2^3P$  terms of Table II:—

Bowen's $b\ D \rightarrow$		$\beta^3D_1$ 146597.8	$\beta^3D_2$ 146597.0	$-10.4$	$\beta^3D_3$ 146607.4
Bowen's $3\ m\ P$	$2^3P_0 = 68273.3$	78324.5 (2)			
	$35.2$	[35.2]			
	$2^3P_1 = 68238.1$	[78359.7]	[0.8]	78358.9 (3)	
	$58.4$	[58.4]		[58.4]	
	$2^3P_2 = 68179.7$	[78418.1]	[0.8]	[78417.3]	[−10.4]
					78427.7 (4)

An additional multiplet from our own list of lines, taking values of  $1^3D'$  from Table II, may similarly be represented as follows:—

	$\beta^3D_1$ 146595.8	$-0.5$	$\beta^3D_2$ 146596.3	$-10.6$	$\beta^3D_3$ 146606.9
$1^3D_1' = 72324.2$	74271.6 (1)	[−0.5]	[74272.1]		
$60.8$	[60.8]		[60.8]		
$1^3D_2' = 72263.4$	[74332.4]	[−0.5]	74332.9 (2)	[−10.6]	[74343.5]
$96.2$			[96.2]		[96.2]
$1^3D_3' = 72167.2$			[74429.1]	[−10.6]	74439.7 (3)

It will be seen that there is a close agreement between the two sets of values of  $\beta^3D$ , and the mean values may accordingly be adopted, namely:—

$$\left. \begin{aligned} \beta^3D_1 &= 146596.8 \\ \beta^3D_2 &= 146596.7 \end{aligned} \right\} \text{Not resolved} \\ -10.5 \\ \beta^3D_3 = 146607.2$$

These terms may next be used to obtain another set of values of  $1^3P_{012}$

through the combination  $1^3P - \beta^3D$ . Using Bowen's wave-numbers, with which our measures are in good agreement, the multiplet is as follows:—

Bowen's $b D \rightarrow$		$\beta^3D_1$		$\beta^3D_2$		$\beta^3D_3$
		146596.7	0	146596.7	-10.5	146607.2
Bowen's $a P$	$1^3P_0 = 238849.1$	92252.4 (6)				
	49.6	[49.6]				
	$1^3P_1 = 238799.5$	[92202.8]		92202.8 (7)		
	84.3	[84.3]		82.7		
	$1^3P_2 = 238715.2$	[92120.1]		92120.1 (3)	-13.7	92106.4 (8)

The values of  $1^3P$  thus obtained are in striking agreement with those derived directly from  $1^3P - 1^3P'$  and clearly indicate the great accuracy of Bowen's measures.

Other combinations given by Bowen, using mean values for  $1^3P$ , are as follows:—

Bowen's $a P \rightarrow$		$1^3P_0$		$1^3P_1$		$1^3P_2$
		238715.6	84.1	238799.7	49.8	238849.5
Bowen's $b S; \beta^3S_1 - 83721.4$		154905.5 (5)	82.7	155078.2 (5)	48.8	155127.0 (4)
Bowen's $3 n D$	$1^3D_1 = 51408.4$	[187307.2]		[187391.3]		[187441.1]
	$1^3D_2 = 51384.3$	[187331.3]		[187415.4]		
	$1^3D_3 = 51354.0$	[187361.6]				
	Observed	187368 (3)			187431 (3)	

The agreement between the calculated and observed values of  $1^3P - 1^3D$  is as good as can be expected in this part of the spectrum, where 1 Ångström unit represents about 360 units of wave-number.

Another multiplet indicated by Bowen represents the combination  $1^3P - \beta^3P'$ . This involves the group of lines about  $\lambda$  916, in which our own photographs of the *N II* spectrum fail to show Bowen's line at  $\lambda$  916.698 (8) ( $\nu = 109087.2$ ). Bowen's classification of this group may be represented as follows:

Bowen's $a P \rightarrow$		$1^3P_0$		$1^3P_1$		$1^3P_2$
		238715.6	84.1	238799.7	49.8	238849.5
Bowen's $b P$	$\beta^3P'_0 = 129625.0$	109174.7 (6)				
	-5.6	6.5				
	$\beta^3P'_{11} = 129630.6$	109087.2 (8)	81.0	109168.2 (6)	49.4	109217.6 (6)

The absence of the line 109087 from our N II spectrum throws considerable doubt on this identification of the  $\beta^3P'$  terms, but some support is afforded by other combinations apparently involving  $\beta^3P'$  which are not included in Bowen's list, namely :—

	$\beta^3P'_1$ 129625.0	—5.6	$\beta^3P'_{1s}$ 129630.6
$2^3P_0 = 68273.3$			[61357.3] 61355.0 (0) [61392.5]
$2^3P_1 = 68238.1$	[61386.9]		
	61386.6 (1)		
$2^3P_2 = 68179.7$			[61450.9] 61447.0 (1)
$1^3S_1 = 69953.7$	[59671.3]		[59676.9]
	59671.9 (5)		
$1^3D_1 = 72324.2$	[57300.8]*		[57306.4]*
$1^3D_2 = 72263.4$			[57367.2] 57365.1 (2) [57463.3]†
$1^3D_3 = 72167.3$			

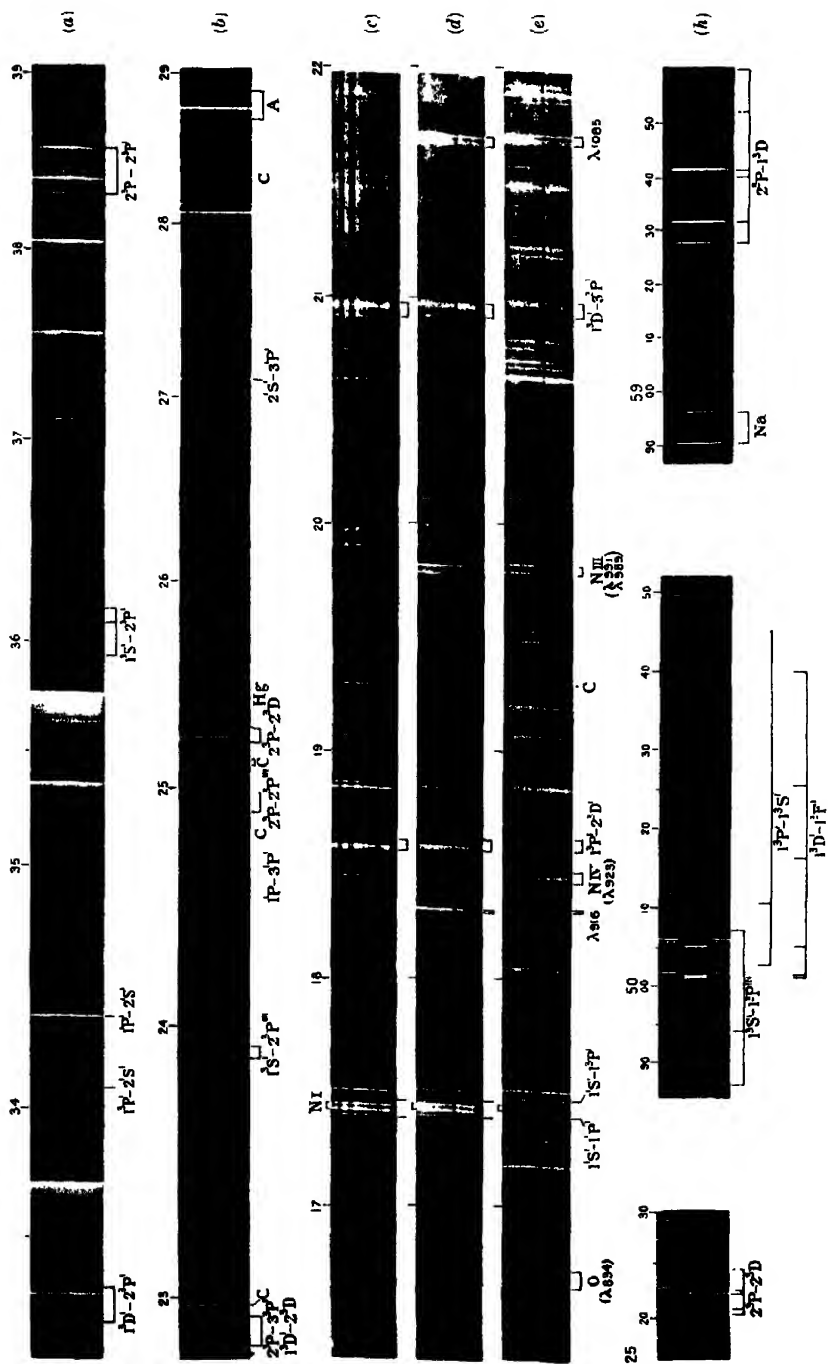
\* Masked by N I 57298.1.

† Masked by N II 57460.9.

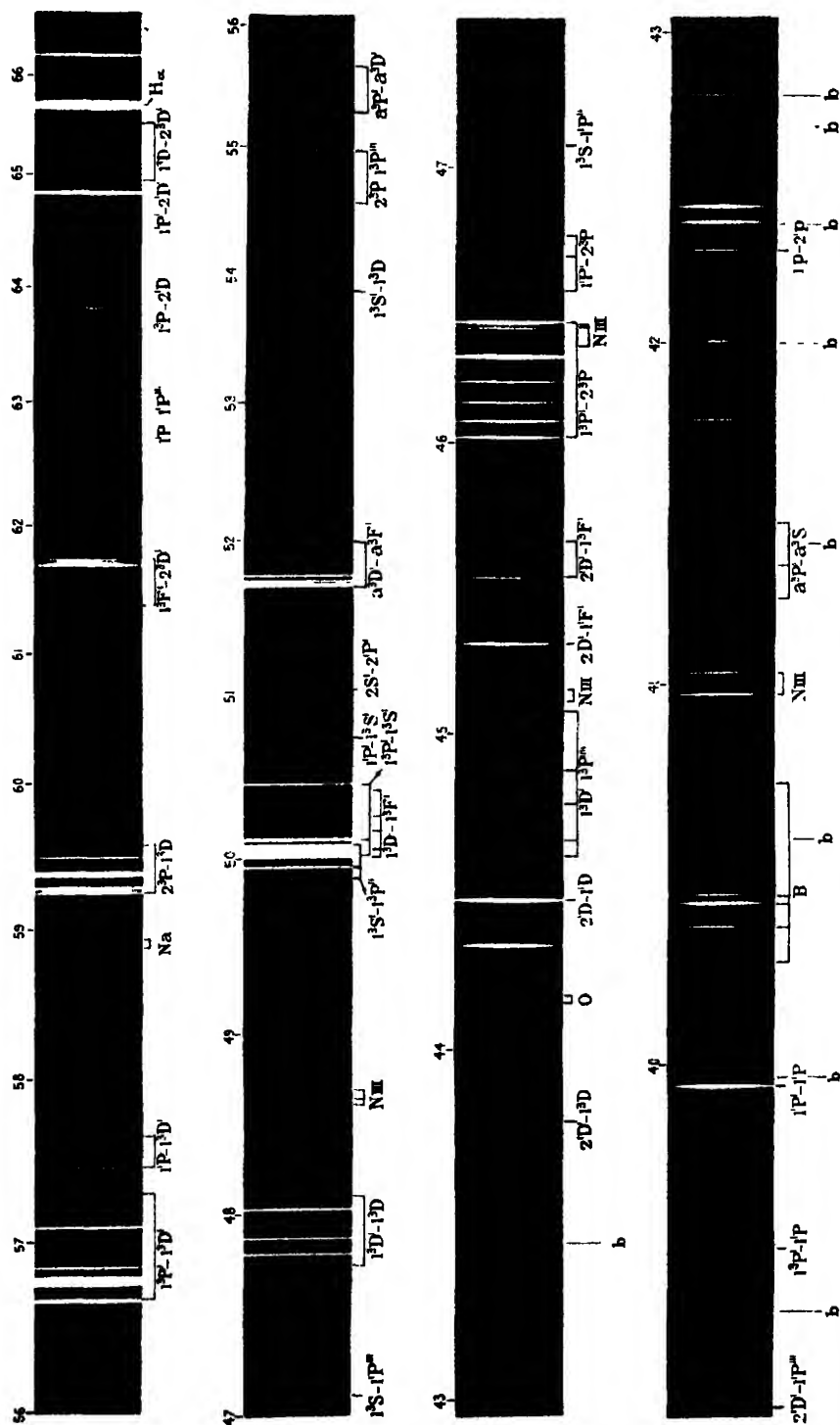
The calculated wave-numbers of possible lines are enclosed in square brackets, and it will be seen that there is a fair agreement with the observed values. It should be noted, however, that a singlet term, which might be  $\beta^1P'_1$ , would represent the observations almost equally well. Observations of these lines in higher orders of the grating will probably throw further light on the characters of the above multiplets.

In continuation of a previous investigation of the spectrum of ionised nitrogen (N II), observations have been made over the range  $\lambda$  6836 to  $\lambda$  830. Of 340 lines recorded in this region, about one-half have now been classified; and of the remaining lines more than 100 are very faint. The spectrum is built up from triplet and singlet terms, the absolute values of which have been determined with the aid of a sequence of three  $^3P' - ^3P$  multiplets.

The scheme of terms deduced from the Heisenberg-Hund theory of complex spectra has greatly facilitated the analysis of the spectrum, and the results are in excellent agreement with the theory. Of the 19 deepest terms predicted by the theory for transitions of a single electron, complex terms being counted



Spectra of Nitrogen.



## Spectra of Nitrogen

as one, all but one have been identified. The term  $1^3P_0$  recently identified by Bowen from a multiplet at  $\lambda$  671, is probably the deepest, its value being 238850, corresponding to an ionisation potential of 29.5 volts.

A few multiplets which appear in the spectrum are attributed to double electron transitions.

The authors are indebted to Mr. E. W. H. Selwyn for some excellent photographs taken with the vacuum spectrograph, and to Mr. R. H. Fowler and Mr. D. R. Hartree for valuable guidance on certain theoretical questions.

#### DESCRIPTION OF PLATES 47 and 48.

**PLATE 47.**—This is intended to give a general view of the spectrum of *N II* between  $\lambda$  6600 and  $\lambda$  3900. The photographs were taken with a glass spectrograph of moderate dispersion. It should be noted that the short lines at the bottom of the first strip represent a comparison spectrum of iron. Lines due to *N III* or to a slight impurity of oxygen are indicated, as are also the weak bands due to nitrogen (*b*).

**PLATE 48.**—(*a*, *b*) Nitrogen vacuum tube, quartz spectrograph,  $\lambda$  3900— $\lambda$  2300. Weak discharge, favouring development of *N II*. (*c*) Nitrogen tube, vacuum spectrograph,  $\lambda$  2200— $\lambda$  1650; 1st order only. Shows some lines of *N III* in addition to the lines of *N II*. (*d*) Nitrogen tube,  $\lambda$  2200— $\lambda$  1650 in 1st order, and  $\lambda$  1100— $\lambda$  825 in 2nd order. (*e*) Same as (*d*), but with stronger discharge. (*f*) Enlargement of  $2^3P - 2^3D$  group  $\lambda$  2520— $\lambda$  2524. (*g*) Group at  $\lambda$  5007, 3rd order 10-feet concave grating, showing resolution of  $\lambda$  5001. (*h*) Enlargement of  $2^3P - 1^3D$  group,  $\lambda$  5928— $\lambda$  5961, 1st order 10-feet grating.

---



*The Rigidity of Solid Unimolecular Films.*

By H. MOUQUIN and E. K. RIDEAL.

(Communicated by G. I. Taylor, F.R.S.—Received December 8, 1926.)

1. *Introduction.*

On evaporation at low temperatures of a benzene solution of palmitic or stearic acid on the surface of water an apparently solid film is left. The experiments of I. Langmuir and N. K. Adam have shown that these films are unimolecular in character, and inasmuch that they possess a fairly well defined melting point, although this varies with the acidity of the underlying solution, we may regard these films as unimolecular sheets of orientated solid acid. Anyone who examines these films even superficially cannot fail to notice their exceptional strength, all the more extraordinary when we consider their extreme thinness. Whilst the compressibility of such films, a property which can be readily determined by examination of the slope of the force area curve obtained with the well-known Langmuir trough apparatus, does not present any unusual features, being of the order anticipated for a hydrocarbon, yet we may expect that the coefficient of rigidity will be unexpectedly high. It seemed a matter of some importance to attempt to measure the rigidity of such films, by applying a suitable torque and determining the displacements effected, a method suggested to us by Prof. G. I. Taylor.

In our preliminary experiments we endeavoured to employ a simple static method of placing a disc at the centre of a large circular film and applying torsion by means of a torsion head and wire on the disc to which a mirror is attached. We have to express our thanks to Prof. G. I. Taylor for the loan of an excellent and finely-calibrated head for this purpose. After numerous attempts with various modifications of the method we were reluctantly compelled to abandon it. The results were invariably the same; on applying a small torque to the disc no motion was visible on the image of the mirror attached to the disc. If the torque be increased the film is ruptured and the disc breaks loose and slips, generally forcing itself entirely from attachment to the film. Even with discs coated with wax or corrugated and milled on the circular edge no better results were obtained. Evidently the grip on the disc being only of one molecule thick is not sufficient to hold the slightest movement on the part of the shearing disc.

*2. Experimental Method.*

The following method was then devised which enabled us to apply indirectly a tangential force to each point on the whole surface of the film. It consisted essentially of rotating a disc immediately under the surface of the film, thereby exerting a drag on it through the intermediary of the viscosity of the water.

Two experimental difficulties in this experiment had to be overcome. It was found advisable to rotate the disc by means of a rotating spindle through the centre, as any superfluous mechanism in the body of the water greatly increases the risk of contamination of the water surface. The disc with its spindle being of solid brass was easily kept clean, and the introduction of the spindle produced no appreciable error in the results. To eliminate any direct drag that might be caused by the spindle it was coated with a thin coating of a high boiling point non-spreading paraffin oil, and as an added precaution a small wire was passed round it in order to form a ring of free surface around the spindle, and thus to prevent any possible chance of sticking before each experiment. The other problem was to fasten the edge of the film securely to the edge of the round porcelain dish employed. This adhesion could be effected in one of two ways. A satisfactory union was obtained by coating the sides of the dish with solid paraffin freed from capillary active impurities, and introducing the film forming solid in the form of a benzene solution. The slight excess of benzene on the surface partially dissolves some of the solid paraffin on the edge of the vessel, and on evaporation firmly attaches to it the main area of the unimolecular film. This method presented a serious difficulty in that it took an extremely long time for the film to acquire its maximum rigidity, constant values could only be obtained in some cases at the end of the second day after evaporation of the benzene. It appears probable that the elimination of the last traces of benzene from the underlying water and from the interstices between the orientated hydrocarbon chains by evaporation is in reality a very slow process. The method finally adopted was the more simple one of raising the temperature of the water above the melting point of the fatty acid used, which was present as a small crystal on the water surface and allowing it to solidify after it had formed the unimolecular film whilst in the liquid state. The experimental arrangement is depicted in fig. 1.

The apparatus consisted essentially of a porcelain glazed circular beaker 14 cm. in diameter provided with lagging, a small glass enclosed regulator controlled heating coil and constant level arrangement. The rotating disc 10 cm. in diameter provided with a stout 1-cm. spindle was rotated underneath the surface of the liquid in the beaker at a constant speed. The drive was

effected by means of a geared down electric motor running under conditions of controlled power consumption.

The distance between the water surface and the revolving disc is measured

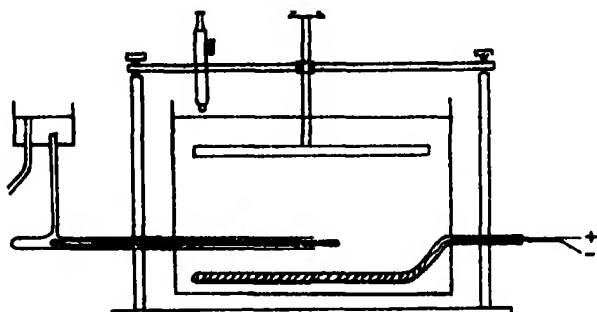


FIG. 1.

by means of a spherometer, the disc being levelled with the aid of glass floats on the water surface and suitable levelling screws. In the experiments it was found convenient to separate the surface of the water on which the film is spread from the revolving disc by about 1.5 mm. The method of conducting an experiment is as follows. After thorough cleansing of all the apparatus the dish is filled with N/1000 hydrochloric acid prepared from grease-free and freshly boiled\* distilled water. The rotating disc is lowered underneath the free surface of the water on which is now placed a small crystal of the acid under investigation. The crystal is allowed to melt by raising the temperature of the water, and on cooling a rigid unimolecular film of the acid is formed on the free surface of the water and is found to be frozen firmly to the sides of the vessel. Care is taken not to have too great an excess of the fatty acid present as the numerous islands thus formed materially increase the rigidity of the whole layer. As has already been indicated in order to obtain reliable results it is necessary to ensure a free spindle, a continuous adhesion of the film on to the edge of the vessel and finally a uniform unbroken and uncontaminated film.

The speed of the rotating disc and the depth of immersion are governed by the necessity of ensuring a sufficiently slow speed not to cause excessive turbulence at the edges or create a parabolic depression of the water surface, and at the same time to obtain a reasonable displacement which is well within the elastic limits of the film, that is, it returns to zero after stopping the shearing force. Displacements were measured by observing small dust particles on the surface of the film through a microscope provided with an eye-piece containing

\* If unboiled water be employed bubbles of gas disengaged during the subsequent elevation of the temperature readily fracture the films.

a graduated scale of 1 division = 0.10 mm. When the disc is stopped the particle under observation springs back to its initial position when the elastic limit has not been exceeded. These displacements must be observed within a reasonable period, otherwise there is a slight permanent distortion finally produced. In fact, wrinkling and actual fracture of the film can be observed if the speed of the disc be too great for any length of time.

### 3. Calculation of Displacements.

The formal relationship between the angular velocity of the disc,  $\Omega$ , the viscosity of the water,  $\eta$ , the depth of immersion of the rotating disc,  $h$ , of radius,  $a$ , and the displacement of the particle,  $\delta$ , at a distance,  $r$ , from the axis of the spindle can be obtained in the following manner.

If the speed of the disc be so slow that there exists no outward pressure gradient in the plane of the film itself the traction  $F$  exerted on a point of the film at a distance,  $r$ , from the centre due to the rotation of the disc will be

$$F = \frac{\Omega \eta r}{h}.$$

This yields a torque

$$\frac{2\pi\Omega\eta}{h} r^3 dr,$$

on a ring of radius,  $r$ , and breadth,  $dr$ , and a total torque

$$\frac{2\pi\Omega\eta}{h} \int_0^a r^3 dr = \frac{\pi\Omega\eta a^4}{2h}.$$

If the film is to remain fixed there must be an equal and opposite torque applied to it, either concentrated at the centre or spread uniformly over the edge. In either case it is clear that the strain is a simple shear expressed by

$$r \frac{d}{dr} \left( \frac{\delta}{r} \right),$$

where  $\delta$  is the displacement. The corresponding strain component is

$$\mu r \frac{d}{dr} \left( \frac{\delta}{r} \right),$$

where  $\mu$  is the coefficient of rigidity.

If  $\rho_{r,\theta}$  is the stress per unit length in a tangential direction at a point  $r$ ,  $\theta$  the equilibrium of the ring of radius  $r$  and breadth requires

$$-\frac{d}{dr} (2\pi r^2 \rho_{r,\theta}) dr = \frac{2\pi\Omega\eta}{h} r^3 dr$$

or

$$2\pi r^2 \rho_{r,\theta} = -\frac{2\pi\Omega\eta}{h} \frac{r^4}{4} + \text{constant}.$$

When the restraining torque is distributed over the edge, as in our apparatus, the constant must be zero, since  $\rho_{r,0}$  must be finite at the centre,

$$\rho_{r,0} = \mu r \frac{d}{dr} \left( \frac{\delta}{r} \right) = - \frac{\Omega \eta}{h} \frac{r^2}{4},$$

hence

$$\frac{d}{dr} \left( \frac{\delta}{r} \right) = - \frac{\Omega \eta}{4h\mu} r,$$

and

$$\frac{\delta}{r} = - \frac{\Omega \eta}{8h\mu} r^2 + \text{constant},$$

whence

$$\delta = - \frac{\Omega \eta}{8\mu h} r^3 + Cr,$$

when  $r = a$ ,  $\delta = 0$  hence

$$\delta = - \frac{\Omega \eta}{8\mu h} (r^3 - a^3 r). \quad (1)$$

It may be observed that  $\delta$  is a maximum when  $a^2 = 3r^2$  or  $r = 0.58$ .

#### Experimental Results.

In the following tables are given the values of  $\mu$  for palmitic and stearic acids both determined at 293° K. calculated with the aid of equation (1).

Palmitic acid. $\eta = 0.0101 \quad a = 5.0 \text{ cm.}$					Stearic acid. $\eta = 0.0101 \quad a = 5.0 \text{ cm.}$				
$\frac{2\pi}{\Omega} \text{ secs.}$	$h \text{ cm.}$	$r \text{ cm.}$	$\delta \text{ cm.}$	$\mu \text{ dynes/cm.}$	$\frac{2\pi}{\Omega} \text{ secs.}$	$h \text{ cm.}$	$r \text{ cm.}$	$\delta \text{ cm.}$	$\mu \text{ dynes/cm.}$
12	0.12	4	0.02	9.75	16	0.15	4	0.011	10.7
8	0.12	4	0.032	9.7	20	0.15	4	0.009	10.3
6	0.12	4	0.041	9.6	11	0.20	4	0.012	10.4
18	0.19	4	0.008	10.3	16	0.20	4	0.009	10.0
12	0.19	4	0.012	10.2	22	0.20	4	0.007	9.2
7	0.19	4	0.020	10.6	12	0.21	3.6	0.012	11.0
11	0.15	4	0.015	11.3					
8	0.15	4	0.024	10.0				Mean	10.27
10	0.184	3.4	0.016	9.7					
7	0.184	3.4	0.024	9.6					
8	0.184	3.4	0.026	9.2					
11	0.10	3.5	0.042	8.0					
15	0.10	3.5	0.023	10.0					
			Mean	9.8					

\* Owing to the fact that there is a hole in the middle of the film of radius  $\epsilon$  through which the spindle passes a small correction term is necessary in this equation, the complete form of which is

$$\delta = \frac{\Omega \eta}{8\mu h} \left( a^2 r - r^3 + \frac{1}{2} \epsilon^2 \frac{r}{a^2} - \frac{1}{2} \frac{\epsilon^4}{r} \right).$$

Since  $\epsilon$  is only 0.5 cm. the correction lies within the experimental errors of the method.

The variation in the displacement  $\delta$  with the distance  $r$  from the centre of the disc is shown on the adjoined curve where also the theoretical curve obtained with the aid of equation (1) is shown for comparison.

Evidently all the conditions required by equation (1) are not quite satisfied

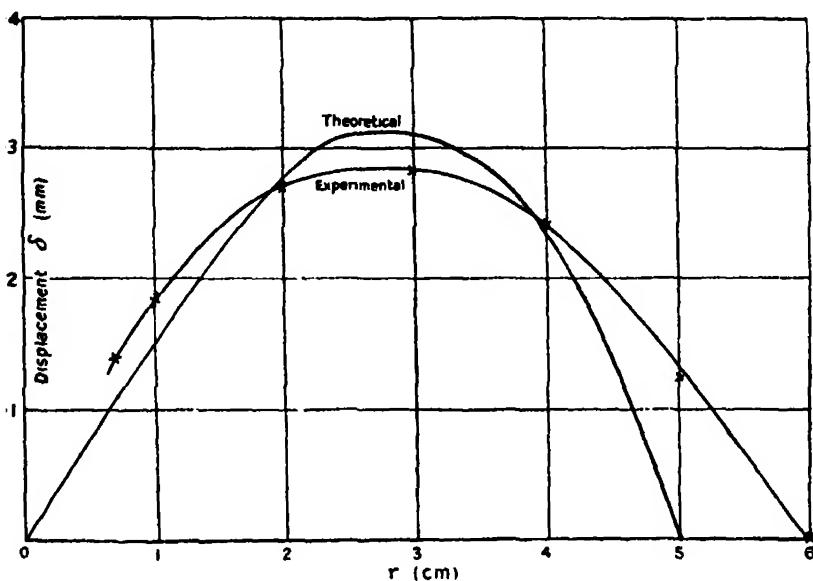


FIG. 2.

in the experiments for the experimental curve is not quite a cubic. The main factors causing these divergences are the small size of the disc which makes it difficult to observe small variations of displacement in the region of the maximum, and also the fact that the radius of the dish is 2 cm. greater than that of the rotating disc. This last divergence was intentional because it was shown by experiment that this space is necessary to neutralise the inevitable stray currents formed on the edge of the disc and along the sides of the dish, the effects of which are not readily calculated. It was found that some slight displacements were observable past the edge of the disc but these ceased within 1 cm. from the periphery. A smaller dish, even 1 cm. larger than the disc was found to be unsuitable since crinkling of the film due to some abnormal current along the sides of the dish immediately broke the adhesion of the film to the sides of the dish rendering observations impossible.

The variations in the coefficients of rigidity  $\mu$  for stearic and palmitic acids with the temperature are shown in fig. 3.

The temperature coefficients are those anticipated for a waxy substance in

that the rigidity decreases rapidly with increase of temperature when approaching the melting point. The films, however, appear to remain in the state of

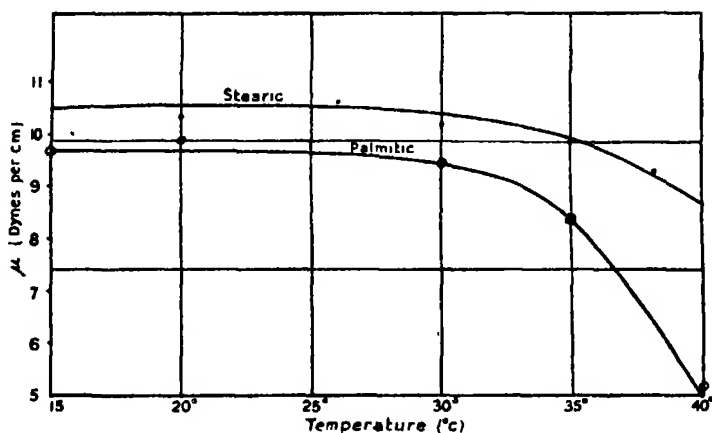


FIG. 3.

plastic solids right up to the melting point at which temperature they break up sharply and begin to rotate with the disc.

The rigidity constant  $\mu$  obtained with the aid of equation (1) might be considered as related to the coefficient of rigidity  $n$  of a solid and the film thickness; if this constant  $\mu$  expressed in dynes per centimetre be divided by the film thickness  $x$  in centimetres we obtain the true constant of rigidity  $\mu/x = n$  in dynes/cm.<sup>2</sup>.

The lengths of the acids in their orientated posture as derived by I. Langmuir in his experiments are 24 Å and 25 Å respectively for palmitic and stearic acids. From these values the length of the carboxyl groups which are immersed in and solvated with the water, and thus do not contribute to the rigidity, have to be subtracted. The actual length of the head is unknown, but on the assumption that it is regular in shape we may take the length equal to the breadth of ca. 4 Å, giving a total length of hydrocarbon chain in adhesion of 20 Å for palmitic and 21 Å for stearic acid.

We thus obtain for the rigidity of the two acids,

$$\text{for palmitic acid} \quad n = \frac{9.84}{20 \cdot 10^{-8}} = 4.9 \cdot 10^7 \text{ dynes per cm.}^2,$$

$$\text{for stearic acid} \quad n = \frac{10.27}{21 \cdot 10^{-8}} = 4.9 \cdot 10^7 \text{ dynes per cm.}^2,$$

these values, practically identical for the two acids, may be compared with 8,000 kgm. wt./mm.<sup>2</sup> or  $7.6 \cdot 10^{11}$  dynes per cm.<sup>2</sup> for iron, and an approximate

value of  $1.6 \cdot 10^7$  dynes per cm.<sup>2</sup> for rubber. We may likewise observe that the ratio of the coefficient of compressibility to that of rigidity for these unimolecular solid films is from N. K. Adam's measurements for the former quantity equal to  $\frac{2}{10^9}$  or 80 : 1.

*Summary.*

The rigidity of unimolecular films of palmitic and stearic acids on water have been determined. It is shown that the rigidity constants are almost identical for the two acids and equal to  $4.9 \cdot 10^7$  dynes per cm.<sup>2</sup> at 20° C. The temperature coefficients of the rigidities have been measured and shown to be of a character anticipated for waxy solids.

*Doppler Effects and Intensities of Lines in the Molecular Spectrum of Hydrogen Positive Rays.*

By M. C. JOHNSON, M.A., M.Sc., Assistant Lecturer in Physics, University of Birmingham.

(Communicated by S. W. J. Smith, F.R.S.—Received February 9, 1927.)

1. *Introduction.*

It is known from the work of Fulcher, Merton, Richardson, and others, that definite groups of lines in the secondary spectrum of hydrogen are strengthened in certain types of discharge. The interpretation of these phenomena in terms of specific molecular excitations has been begun by Richardson,\* on the basis of his classification of associated groups into bands.

In the present paper the grouping of lines in the secondary spectrum is studied by longitudinal observation of positive rays in hydrogen. The optical spectrum of positive rays may be used in the following ways to contribute to the elucidation of the mechanisms of this spectrum. Firstly, the grouping of lines when excited by the impact of positive ions falling through a potential of several thousand volts can be examined. This can be compared with the grouping due to the impact of electrons at low voltages comparable with the ionisation potentials, and with the grouping in the Geissler tube spectrum. Secondly, a large Doppler effect appears in the Balmer lines when the positive

\* 'Roy. Soc. Proc.,' A, vol. 111, p. 751 (1926).



rays are photographed longitudinally. From this can be determined what proportion of the atomic spectrum is carried by neutralised positive rays, and what proportion is excited in the stationary gas by the impact of positive ions. Further, it is possible to decide in some cases which of the Balmer line carriers have been free atoms in the positive rays stream, and which are recently dissociated molecular positive rays. These proportions are found to vary along the Balmer series. They can thus be related to the intensity grouping of the adjacent regions of the molecular spectrum. Thirdly, previous investigators of the secondary hydrogen spectrum in positive rays have, with one exception, agreed there is no Doppler effect in that spectrum. The exception is Rau, who by an ingenious indirect method showed eight extremely faint components.\* In the present work some further Doppler components have been found, and the intensity indicated below which any other components must lie. Evidence is thus obtained as to which of the lines in the secondary spectrum are mainly due to the excitation of stationary molecules, and which are carried by neutralised positive rays. This can be compared with the phenomena of the Richardson electron discharges, for which other evidence is available as to the mode of excitation.†

## 2. *Experimental.*

The luminosity behind the perforated cathode of a positive ray tube is very faint compared with the usual sources of light in spectroscopy. Hence the positive ray photography of the 1200 lines in Merton and Barratt's list‡ is quite out of the question. The 150 or so lines here discussed were obtained by exposing up to 19 hours with a form of positive ray apparatus developed for other work. This apparatus and its technique have been described in detail in previous papers.§ The cylindrical positive ray tube of the Wien type was found to show a comparatively strong secondary spectrum after gassing and pumping for about two weeks. During this time the only admissions were through a hot palladium tube. The apparatus would stand 20 hour exposures under perfectly constant conditions when run at an optimum pressure corresponding to a dark space of about 7 cm., a current of about 1 milliampere, and a fall of potential in the dark space of about 4000 volts. Larger currents or higher voltages invariably caused unsteadiness, leading to collapse, even though both electrodes were water-cooled.

\* 'Ann. d. Physik,' vol. 73, p. 270 (1924).

† *Loc. cit.* and 'Roy. Soc. Proc.,' A, vol. 106, p. 662 (1924).

‡ 'Phil. Trans.,' vol. 222, p. 369 (1922).

§ M. C. Johnson, 'Proc. Phys. Soc.,' vol. 38, p. 324, and vol. 39, p. 26 (1926).

A six-prism Evershed solar spectrograph was used, being of great light economy, and the whole apparatus was built up in a thermostatic chamber. Many spectrograms were taken on plates of different types suited to the different regions of the spectrum. Measurements were made with a Watson micrometer microscope, on those plates for which electrical and gas conditions had remained constant throughout the exposure. In each case comparison photographs of a Geissler hydrogen tube were secured above and below the positive ray spectrum.

Although the intensity grouping is very different in the positive rays from that of a Geissler tube, about 60 lines could be recognised at sight. With these, dispersion curves were drawn for each plate from Merton and Barratt's list. The curves were on a large enough scale to measure all fainter lines and possible Doppler components, generally to within  $1/4$  or  $1/2$  A.U. Identification was then made from Merton and Barratt, supplemented by the lists of Tanaka,\* Allibone,† and Deodhar.‡ Possible ambiguity in the case of components was checked by impurity lists.

### 3. Measurements.

The measurements are tabulated as follows. The first column gives the wave-length of the positive ray line in air, in I.A.U. from the standard tables, the next the estimated positive ray intensity, and the third the intensity in Merton and Barratt's Geissler tube. The fourth column gives the Richardson classification where a line belongs to the Q branch of his associated bands.§ The letters F, L, H, C indicate Fulcher and low and high pressure and condensed discharge characteristics from Merton and Barratt. The other standard characteristics were examined but not found to bear any relation to the positive ray grouping. The remaining columns give corresponding data for those lines whose absence from the positive rays is conspicuous. Only those marked as of intensity 4 and upwards are reproduced, as many fainter lines would not be expected in the very faint positive ray light, and their absence could not be taken as significant. For the blue region fainter Merton and Barratt lines are also included, as no strong lines appear. Lines marked T, A, D are from the lists of Tanaka, Allibone, and Deodhar respectively, and are not in Merton and Barratt. Lines whose Q denomination is in brackets are those included by Richardson as possibly covering band lines.

\* 'Roy. Soc. Proc.,' A, vol. 108, p. 592 (1925).

† 'Roy. Soc. Proc.,' A, vol. 112, p. 196 (1926).

‡ 'Roy. Soc. Proc.,' A, vol. 113, p. 420 (1926).

§ 'Roy. Soc. Proc.,' A, vol. 113, p. 368 (1926).

Present. λ I. A.U. in air.	Positive ray intensity.	M. and B. intensity.	Remarks.	Absent. λ I. A.U. in air.	M. and B. intensity.	Remarks.
6589.05	8	A, D	with component			
6532.62	7	1	5 α 5 Q 2 C			
Line covered by component of 6533			with component			
6428.10	2	5	4 α 4 Q 1 F	6527.35	4	5 α 5 Q 1 F
6399.45	4	6	L	6517.69	4	H
6362.48	2	5		6380.11	4	H
6340.57	2	6	3 α 3 Q 3 F, L	6332.46	5	3 α 3 Q 2 F, L
6327.07	9	8	3 α 3 Q 1 F, L	6329.60	6	C
6299.42	5	7	F, L			
6285.37	3	—	F, H	6274.86	5	H, C
6271.31	1	3	L	6262.49	4	2 α 22 Q 5 L
6238.39	3	8	2 α 22 Q 3 F, L	6232.99	4	
6230.23	1	7	2 α 22 Q 2 F, L	6221.73	4	H
6224.81	9	9	2 α 22 Q 1 F, L	6199.38	8	F, L
6201.15	6	5	F, L	6197.05	5	F, H
6182.98	5	8	F, L	6174.03	6	H
				6169.63	5	L, C
				6161.59	7	H
				6159.58	4	C
				6155.61	5	
				6151.47	4	C
6135.34	5	8	1 α 1 Q 3 H	6134.27	4	H, C
6127.40	2	9	1 α 1 Q 2 F, L	6098.23	6	F, L
6121.76	10	10	1 α 1 Q 1 F, L	6090.92	7	H, C
6095.96	6	8	F, L	6074.39	4	H, C
6080.78	6	9	F, L	6070.00	7	H
6067.70	3	5	H	6066.64	4	L
6063.28	1	6	H	6056.10	5	0 α 0 Q 5 L
				6053.27	4	H, C
				6052.34	5	H, C
				6047.85	5	H, C
				6042.70	5	0 α 0 Q 4 H
				6041.01	4	H, C
6031.80	5	10	0 α 0 Q 3 F, L	6027.98	8	H
				6023.74	7	0 α 0 Q 2 H, C
				6021.28	7	
6018.29	10	10	0 α 0 Q 1 F, L			
6004.92	1	2	C	5994.05	6	F, L
6002.81	3	7	H, C	5990.51	4	H
				5989.22	5	F, H, C

Present. $\lambda$ I. Å.U. in air.	Positive ray intensity.	M. and B. intensity.	Remarks.	Absent. $\lambda$ I. Å.U. in air.	M. and B. intensity.	Remarks.
5982.54	1	8	H, C			
5975.43	7	10	F, L			
				5967.31	6	H, C
				5963.46	5	H, C
5959.70	3	8	H, C			
5949.90	4	9	L			
				5947.27	6	L
5938.60	3	9	H, C			
				5936.02	4	
5931.33	3	8	H			
5924.82	2	7	L, C			
5920.65	2	6	(6 $\alpha$ 5 Q 5) L			
				5916.24	6	H, C
5889.96	4	3	6 $\alpha$ 5 Q 1			
				5888.14	6	H, C
5884.66	2	5	C			
				5883.88	6	H, C
5878.43	4	5	L, C			
5871.81	5	4	L, C			
				5869.18	4	H, C
				5864.47	5	H, C
5859.79	1	3	L			
5851.67	1	3	C			
				5849.31	6	H, C
5835.98	6	9	L, C			
				5832.89	5	C
5822.80	4	5	L, C			
5815.00	4	6	H, C			
				5812.56	9	H, C
				5806.09	5	C
				5794.65	4	C
				5791.74	6	H, C
				5788.25	4	C
5785.81	5	7	L, C			
				5778.96	4	H, C
5774.98	4	7	L, C			
5760.37	2	4	H, C			
				5759.51	4	H, C
5736.88	4	8	C			
5730.26	2	0				
				5728.54	7	H, C
				5713.30	4	L, C
5689.19	2	7	H, C			
5684.09	1	4	C			
5655.75	1	5	4 $\alpha$ 3 Q 1 F, L			
				5612.53	4	L
5597.63	2	4	L, C			
5552.52	1	4	3 $\alpha$ 2 Q 3 F, C			
5543.41	1	2	3 $\alpha$ 2 Q 2 F, L, C			
5537.45	4	7	3 $\alpha$ 2 Q 1 F, L			
5518.48	1	2	L			
5505.51	2	4	L			
5481.08	2	4	L			
5461.50	2	1	2 $\alpha$ 1 Q 5 C			
				5434.83	5	2 $\alpha$ 1 Q 3 F
5425.96	1	3	2 $\alpha$ 1 Q 2 F			
5419.90	3	6	2 $\alpha$ 1 Q 1 F, L			
5401.06	1	1	L			

Present. $\lambda$ I. Å.U. in air.	Positive ray intensity.	M. and B. intensity.	Remarks.	Absent. $\lambda$ I. Å.U. in air.	M. and B. intensity.	Remarks.
5388.21	2	8		5365.91	6	H
				5355.92	4	L
				5336.52	6	
				5317.90	5	1 $\alpha$ 0 Q 3 F, H
				5309.03	4	1 $\alpha$ 0 Q 2 F
5303.15	1	8	1 $\alpha$ 0 Q 1 F	5291.59	5	
				5284.50	4	
				5272.29	5	
				5266.04	6	
				5261.18	4	H
				5256.61	5	H
				5196.38	4	C
5180.50	6	4	H			
5174.71	6	3	H, C	5146.35	4	L
				5113.17	5	L
				5084.83	5	L
5081.96	1	2				
5067.47	1	2	(0 $\beta$ 1 Q 2)	5063.84	4	0 $\beta$ 1, Q 1
5055.08	1	6	L			
5039.83	1	4	L			
5030.37	1	4				
5015.12	2	4	H	5013.05	7	
5011.19	5	3		5003.40	4	L
				4973.27	6	L
4971.76	2	0	L			
4966.85	2	4				
4955.74	1	3				
4939.57	2	2	L			
4934.29	8	4	(3 $\alpha$ 1 Q 5)			
4928.62	6	10		4875.92	4	
4874.28	2	1	L	4873.05	6	
Line covered by component of H $\beta$				4856.54	5	
				4849.34	6	
				4838.25	4	
4829.66	1	D				
4822.96	1	3	L			
4817.51	1	1	L			
4811.67	1	0	(2 $\alpha$ 0 Q 5)			
4804.06	1	0	L	4797.76	4	
4793.95	1	3	L			
4786.04	1	2	H			
4780.94	1	4	H	4763.82	4	L
4762.28	1	T				
4752.67	7	T				
4748.57	3	T				
4742.75	3	3	4 $\beta$ 4 Q 1 L			
4735.48	2	T				
4734.55	2					
4727.75	3	0	H	4723.01	5	

Present. $\lambda$ I. Å.U. in air.	Positive ray intensity.	M. and B. intensity.	Remarks.	Absent. $\lambda$ I. Å.U. in air.	M. and B. intensity.	Remarks.
4721.56	2	1		4719.02	6	
4716.04 } 4716.03 } 4710.05 }	2 2 2	D { 2	Broad. Probably both present	1709.32	4	1 $\beta$ 3 Q 3
4705.24	2	0		4683.79	5	3 $\beta$ 3 Q 2 L
4699.92	4	T		4662.79	5	L
4686.79	2	2	L	4661.39	4	L
4679.11	2	3	H	4653.04	5	
4670.68	1	0	L	4631.89	10	
4665.58	10	3	L	4625.39	4	2 $\beta$ 2 Q 3 H
4654.01	1	1	H	4582.58	4	
4649.47	1	0				
4633.95	7	9				
4627.96	10	5				
4620.72	3	1	2 $\beta$ 2 Q 2 L			
4613.10	4	0	L			
4598.48	2	2	3 $\gamma$ 4 Q 4 H			
4580.04	1	5	L			
4572.73	6	4	H			
4568.10	7	6	L			
4561.13	6	0	2 $\gamma$ 3 Q 3. Displaced L			
4554.13	5	4	1 $\beta$ 1 Q 1 L			
4547.93	4	1	L			
4541.12	1	1	H			
4538.28	2	1	H			
4534.56 } 4534.17 }	5 { 5	3 3				
4531.14	5	0	L			
4517.47	6	1	With component. L			
4510.91	1	2	H			
4504.90	1	--	L	4498.10	6	
				4490.45	5	0 $\beta$ 0 Q 1 L
4486.05	10	3				
4481.28	5	0	0 $\gamma$ 1 Q 2			
4474.24	5	2	H			
4468.23	1	T				
4460.96	1	5				
4456.77	8	2		4447.56	4	
				4445.24	3	
4438.26	1	--				
4420.29	3	1	Displaced L	4417.32	3	
				4414.22	2	
				4412.26	4	
				4410.57	2	
4404.57	1	0	L			
4398.19	2	1	H			

Present. $\lambda$ I. Å.U. in air.	Positive ray intensity.	M. and B. intensity.	Remarks.	Absent. $\lambda$ I. Å.U. in air.	M. and B. intensity.	Remarks.
4391.88	2	1		4390.89	2	
4387.33	6	T				
4379.38	2	2				
4374.34	4	T				
4366.77	4	0				
4361.90	1	0				
4358.48	2	T				
4356.96	3	0				
4347.71	2	T				
4327.95	1	1	L.			
4320.64	1	T				
4311.72	1	0				
4303.40	3	1	L.			
4284.08	1	T				
4233.60	2	1	3 $\beta$ 2 Q 1 4 $\gamma$ 4 Q 1 L	4243.27	2	2 $\beta$ 2 Q 3 L.

#### 4. The Doppler Effect in the Molecular Spectrum.

The following lines are recorded by Rau as having very faint Doppler components detectable by his method.

4723

4634

4573

4568

He also records four lines in the violet beyond the limit of the present photographs. This limit was set by the increasing complexity of the intensities in the violet, compared with the standard lines.

In the present work careful examination was made of the limiting intensity below which any components must fall, if existent. The faintest lines detectable are of intensity 1. The preceding table indicates that, *e.g.*, for 4573 there is no component down to one-sixth of the undisplaced intensity, which cannot be identified in the comparison lists. For 4634 no component down to one-seventh is possible. Rau's 4723 is one of the strong Merton and Barratt lines listed here as absent from the positive rays.

4568, on the other hand, appears at first sight to have a component of strength 6. Check exposures repeatedly made of this region make it necessary to suggest that this is not a violet component of 4568, but a red component of 4561. In these check exposures the accelerating potential was varied over as wide a range as the limits mentioned in para. 2 would allow. The position of the line was found to vary, the higher voltage driving it further from 4561 towards the red. This renders impossible the more familiar alternative of a violet

component to 4568, as recorded by Rau. The following quantitative data are taken from two plates. The velocities are calculated for an  $H_2$  molecule with a single charge.

Volts.	$v = \sqrt{2eV/m}$ cm./sec.	$v = cd\lambda/\lambda$ cm./sec.
3900	$6.16 \times 10^7$	$1.65 \times 10^7$
2600	$5.02 \times 10^7$	$1.32 \times 10^7$
	Ratio 1.23	
	Ratio 1.25	

The accuracy is not high on these faint plates, but the rough agreement in the ratios adds plausibility to the unusual suggestion of a red component in a spectrum whose other Doppler effects are to the violet. The difference between observed and calculated velocities indicates that a larger molecule than  $H_2$  might be concerned. No theory of this difference can be attempted in the absence of any knowledge of the electron capture and loss conditions for molecules. Large differences in the corresponding atomic velocities are discussed in a previous paper.\*

It should be noted that instead of 4561 the source of this component might possibly be the faint 4560.20 or 4558.50 which are in the region over which it might move. 4561 is the most probable since it alone appears in the comparison spectrum. The comparison tube was chosen for its closer resemblance to the positive rays than other Geissler tubes.

This displaced line is broader than the undisplaced line, which is hardly seen except in the comparison spectrum. Possibly it represents some unknown perturbation varying in this manner with the potential. If not, there are two alternatives. (a) The line is carried by a neutral molecule which had temporarily captured an additional electron in the cathode slit. This would be the  $H^-$  of the parabola analysis of positive rays. (b) The line is carried by an ionised molecule which had gained its positive charge behind the cathode, and was hence attracted back towards the entrance to the discharge tube. The latter explanation is unlikely, as so many ionised molecules are moving from the discharge tube that a corresponding, but stronger, violet displacement should also be seen.

Four other probable Doppler components were observed in the secondary spectrum.

ii. The line 4420 is displaced to the violet of its comparison spectrum. The displacement is of the order of 2 A.U., and might mean that the faint 4418.67 was present and 4420.29 absent in the positive rays, and *vice versa* in the comparison spectrum. But in the clearest plate the displacement is broadened

\* 'Proc. Phys. Soc.,' vol. 39, p. 26 (1926).



up to 4 A.U. from 4420, which makes the Doppler explanation more probable. If this is correct, the undisplaced line is extremely faint compared with its strength in the comparison spectrum.

iii. The line 4517 has a faint haze to the violet, beginning at 3 A.U. and ending beyond 7 A.U. from 4517 in the clearest plate. In this case the undisplaced line itself is visible and is about twice the intensity of the component. The indefinite ending of the haze makes it impossible to say more than that it probably extends beyond the limit imposed by the velocity which  $H_\beta$  could acquire.

iv. and v. Very much clearer are two other Doppler components in the red region. In each case there is a strong line agreeing with the comparison spectrum, together with a broad displaced component to the violet, covering several A.U. The intensities and displacements are as follows. The line beyond  $H\alpha$  is taken from Allibone and is also in Deodhar, being beyond the range of Merton and Barratt's list. The Doppler velocity is calculated at the furthest extension of the displaced line and at the point of its maximum intensity.

Wave-length.	Intensity.	$cd\lambda/\lambda$ (furthest).	$cd\lambda/\lambda$ (max. intensity).
6589.05	8		
Component	10	$5.0 \times 10^7$ cm./sec.	$3.2 \times 10^7$ cm./sec.
6532.62	7		
Component	10	$4.1 \times 10^7$ cm./sec.	$3.3 \times 10^7$ cm./sec.

$H\alpha$  has so strong a component that the image is over-exposed, and comparison with it cannot be accurately made. For  $H\beta$  on a plate taken at 3900 volts the furthest extension is clearer, and it is found that

$$cd\lambda/\lambda = 6.3 \times 10^7 \text{ cm./sec.}$$

The maximum possible velocity is calculated for lines on these two plates by the formula

$$v = \sqrt{2eV/m}.$$

$H_1$  at 3550 volts  $8.31 \times 10^7$  cm./sec. ; at 3900 volts  $8.72 \times 10^7$  cm./sec.

$H_2$  „  $5.87 \times 10^7$  „ „  $6.16 \times 10^7$  „

$H_3$  „  $4.80 \times 10^7$  „ „  $5.04 \times 10^7$  „

From these data it is probable that the Balmer moving series is carried by neutralised atoms which were already free atoms, and had not been incorporated in molecules, when accelerated in the dark space. Blackett and Franck\* have discussed the formation of Balmer lines from free atoms, and

\* 'Z. f. Physik,' vol. 34, p. 389 (1925).

from molecules by simultaneous dissociation and atomic excitation. The latter process is prevalent in the "white" hydrogen discharge, and is probably common in most Geissler tubes. In the present work the value of calculated and observed positive ray velocities shows that the former, and not the latter, is the source of the displaced Balmer line.

The carriers of 6589 were accelerated as  $H_2$ , but the carriers of 6533 would, if the ratio of observed to calculated maximum velocity is governed by the same laws as in the other lines, be  $H_3$ .

#### 5. *Relation of the Character of the Molecular Spectrum to the Doppler Effect in the Atomic Spectrum.*

Analysis of the table of lines present and absent in the positive ray spectrum shows definite kinship with the type of discharge which favours the development of the Fulcher and Richardson bands and low pressure lines.

	Present.	Absent.
Richardson Q lines . . . . .	32	14
Fulcher lines . . . . .	24	9
Merton low pressure lines . . . . .	63	22
Merton high pressure lines . . . . .	27	38
Merton condensed discharge lines . . . . .	25	33
Fulcher lines at high pressure (rare) . . . . .	1	3

Together with this tendency to enhanced features of the Fulcher type, the positive rays show a very rapid decrease of intensity along the Balmer series. Both these phenomena characterise Richardson's First Type discharge, though the positive ray intensity of the first Balmer lines is relatively greater than in the Richardson spectrum. Thus the spectrum produced by the impact of high potential positive ions is more akin to that of the lowest potential electron impact than to that of the high potential Geissler discharge. It may also be compared with the excitation referred to by Richardson as the Third Type, which occurs at high potentials and low pressures and is probably radiative.

In the blue region the greatest departure of the positive ray from the Merton and Barratt spectrum is due to the enhancing of lines not seen by them but listed by Tanaka. Now Tanaka used plates taken with a current density at least 25 times that in Merton and Barratt's experiments. Current density is an expression which conceals any ultimate mechanism, as is suggested by the fact that the positive ray enhancement of Tanaka's lines occurred with a current of 1 milliampere in a tube of several centimetres diameter. It must also be

noticed, in comparing conditions, that the positive ray tube was at a far lower pressure than that at which either thermionic or Geissler tubes are normally worked.

The positive ray spectrum can be subdivided into three regions: (a) from  $H\alpha$  to the gap in the Q lines beginning at 5880; (b) from the end of the gap at 5660 to  $H\beta$ ; (c) from  $H\beta$  to the violet. It is then found that the presence and absence of Q lines shows a certain variation along the spectrum.

	Present.	Absent.
Region (a) .....	14	5
„ (b) .....	10	4
„ (c) .....	8	5

This table may be compared with the relative intensity of undisplaced and displaced lines of the Balmer series. In strong lines this is difficult to estimate accurately. Approximate values are as follows:—

	Undisplaced intensity.	Displaced intensity.
$H\alpha$ .....	50	50
$H\beta$ ... ..	20	12
$H\gamma$ .....	6	1

This suggests that conditions growing less favourable to the First Type discharge are associated here with conditions growing less favourable to the production of Balmer lines by neutralisation of moving positive atoms. It may be noted that in Richardson's Second Type discharge\* the formation of Balmer lines by neutralisation is associated with great intensity for the higher quantum numbers.

### 6. *The Carriers of the Spectra.*

The intensities tabulated for the positive ray lines show that, with the five exceptions discussed, the moving components in the secondary spectrum are invisible, and must be of intensity below  $1/n$  of the intensity of the undisplaced lines.  $n$  varies up to 10 in the various lines. We conclude that, with those exceptions, the secondary spectrum in the positive rays is due mainly to molecules which had not recently been positively charged. The spectrum is known to be emitted by neutral molecules, but these might have been positive in front of the cathode. Such molecules would, after neutralisation, still show traces of their acceleration in the dark space. They would give rise to components

\* Richardson and Tanaka, 'Roy. Soc. Proc.,' A, vol. 106, p. 662 (1924).

of intensity comparable with that of the undisplaced lines, as in the Balmer series. The principal source of the molecular spectrum in this particular discharge is hence either the absorption of radiation, or the impact of positive ions on stationary neutral molecules.

The strength of the Fulcher and associated spectra in the positive rays is interesting on this account, as it is an example of their excitation under conditions different from those discussed by Richardson. In the low potential electron discharge Richardson gives strong evidence in favour of their excitation from molecules which have been ionised and recombined again.

In regard to the problem of discriminating between  $H_2$  and  $H_3$  in the secondary spectrum, a recent work\* puts forward evidence for the association of  $H_3$  with strength of Fulcher lines, though Richardson's evidence points rather to  $H_2$ . The strongest positive ray line possessing a Doppler component is 6589. This is shown in the present work to be carried by a molecule accelerated as  $H_2$ . The next strongest is 6533, and is shown to be more probably due to  $H_3$ . But the great intensity of their Doppler effects dissociates these two from the majority of the lines in the spectrum, and their carriers and excitation mechanisms are not to be connected with those of the other lines. It may be noticed, however, that the first of these is not a Q line, and is not included by Allibone in his red extension of the Fulcher spectrum. 6533, on the other hand, is a Q line.

The present experiments point to  $H_2$  rather than  $H_3$  for the lines with no strong Doppler effect. It is difficult to conceive a process of formation of  $H_3$  in the stationary gas which gives the spectrum. The only visible reaction of this gas is to be struck by positive ions behind the cathode. It does not take part in the discharge at all, and it is in the discharge presumably that the formation of unstable molecules can take place.

In conclusion, the evidence as to carriers in the positive ray discharge may be summed up as follows. With five exceptions the secondary spectrum is due to stationary diatomic molecules which have not been recently ionised. The Balmer spectrum is partly due to excitation of free atoms and partly due to neutralisation of positively charged atoms which were already dissociated when in the dark space. The ratio of the former to the latter increases along the Balmer series. With this increase is associated a decrease of the Fulcher characteristics in the secondary spectrum.

These conclusions indicate the contrast between the excitation processes in the positive rays and excitation processes in the two low voltage electron

\* Smyth and Brasefield, 'Proc. Nat. Acad. Sci.,' vol. 12, p. 443 (1926)

discharges elucidated by Richardson. In spite of these differences, the main aspect of the intensity grouping in the secondary spectrum of the positive ray stream is closer in appearance to that of the lowest voltage electron discharge than to other mechanisms in which the hydrogen spectrum is shown.

I am very grateful to Prof. S. W. J. Smith, F.R.S., for encouraging these experiments and allowing time and equipment for carrying them out. For instrument construction I am indebted to Mr. G. O. Harrison.

### *The Quantum Theory of Dispersion.*

By P. A. M. DIRAC, St. John's College, Cambridge; Institute for Theoretical Physics, Göttingen.

(Communicated by R. H. Fowler, F.R.S.—Received April 4, 1927.)

#### § 1. *Introduction and Summary.*

The new quantum mechanics could at first be used to answer questions concerning radiation only through analogies with the classical theory. In Heisenberg's original matrix theory, for instance, it is assumed that the matrix elements of the polarisation of an atom determine the emission and absorption of radiation analogously to the Fourier components in the classical theory. In more recent theories\* a certain expression for the electric density obtained from the quantum mechanics is used to determine the emitted radiation by the same formulæ as in the classical theory. These methods give satisfactory results in many cases, but cannot even be applied to problems where the classical analogies are obscure or non-existent, such as resonance radiation and the breadths of spectral lines.

A theory of radiation has been given by the author which rests on a more definite basis.† It appears that one can treat a field of radiation as a dynamical system, whose interaction with an ordinary atomic system may be described by a Hamiltonian function. The dynamical variables specifying the field are the energies and phases of its various harmonic components, each of which

\* E. Schrödinger, 'Ann. d. Physik,' vol. 81, p. 109 (1926); W. Gordon, 'Z. f. Physik,' vol. 40, p. 117 (1926); O. Klein, 'Z. f. Physik,' vol. 41, p. 407 (1927).

† 'Roy. Soc. Proc.,' A, vol. 114, p. 243 (1927). This is referred to later by *loc. cit.*

is effectively a simple harmonic oscillator. One must, of course, in the quantum theory take these variables to be  $q$ -numbers satisfying the proper quantum conditions. One finds then that the Hamiltonian for the interaction of the field with an atom is of the same form as that for the interaction of an assembly of light-quanta with the atom. There is thus a complete formal reconciliation between the wave and light-quantum points of view.

In applying the theory to the practical working out of radiation problems one must use a perturbation method, as one cannot solve the Schrödinger equation directly. One can assume that the term ( $V$  say) in the Hamiltonian due to the interaction of the radiation and the atom is small compared with that representing their proper energy, and then use  $V$  as the perturbing energy. Physically the assumption is that the mean life time of the atom in any state is large compared with its periods of vibration. In the present paper we shall apply the theory to determine the radiation scattered by the atom, considering also the case when the frequency of the incident radiation coincides with that of a spectral line of the atom. The method used will be that in which one finds a solution of the Schrödinger equation that satisfies certain initial conditions, corresponding to a given initial state for the atom and field. In general terms it may be described as follows:—

If  $V_{mn}$  are the matrix elements of the perturbing energy  $V$ , where each suffix  $m$  or  $n$  refers to a stationary state of the whole system of atom plus field the stationary state of the atom being specified by its action variables,  $J$  say, and that of the field by a given distribution of energy among its harmonic components, or by a given distribution of light-quanta), then each  $V_{mn}$  gives rise to transitions from state  $n$  to state  $m^*$ ; more accurately, it causes the eigenfunction representing state  $m$  to grow if that representing state  $n$  is already excited, the general formula for the rate of change of the amplitude  $a_n$  of an eigenfunction being†

$$i\hbar/2\pi \cdot \dot{a}_m = \sum_n V_{mn} a_n = \sum_n v_{mn} a_n e^{2\pi i(W_n - W_m)t/\hbar}, \quad (1)$$

where  $v_{mn}$  is the constant amplitude of the matrix element  $V_{mn}$ , and  $W_n$  is the

\* In *loc. cit.*, § 6, it was in error assumed that  $V_{mn}$  caused transitions from state  $m$  to state  $n$ , and consequently the information there obtained about an absorption (or emission) process in terms of the number of light-quanta existing before the process should really apply to an emission (or absorption) process in terms of the number of light-quanta in existence after the process. This change, of course, does not affect the results (namely the proof of Einstein's laws) which can depend on  $|V_{mn}|^2 = |V_{nm}|^2$ .

† *Loc. cit.*, equation (4). In the present paper  $\hbar$  is taken to mean just Planck's constant [instead of  $(2\pi)^{-1}$  times this quantity as in *loc. cit.*] which is preferable when one has to deal much with quanta  $h\nu$  of radiation.

total proper energy of the state  $m$ . To solve these equations one obtains a first approximation by substituting for the  $a$ 's on the right-hand side their initial values, a second approximation by substituting for these  $a$ 's their values given by the first approximation, and so on. One or two such approximations will usually be sufficient to give a solution that is fairly accurate for times that are small compared with the life time, but may all the same be large compared with the periods of the atom. From the first approximation, namely,

$$a_m = a_{m0} + \sum_n v_{mn} a_{n0} (1 - e^{2\pi i (W_n - W_m) t/h}) / (W_m - W_n), \quad (2)$$

where  $a_{n0}$  denotes the initial value of  $a_n$ , one sees readily that when two states  $m$  and  $n$  have appreciably different proper energies, the amplitude  $a_m$  gets changed only by a small extent, varying periodically with the time, on account of transitions from state  $n$ . Only when two states,  $m$  and  $m'$  say, have the same energy does the amplitude  $a_m$  of one of them grow continually at the expense of that of the other, as is necessary for physically recognisable transitions to occur, and the rate of growth is then proportional to  $v_{mm'}$ .

The interaction term of the Hamiltonian function obtained in *loc. cit.* [equation (30)] does not give rise to any direct scattering processes, in which a light-quantum jumps from one state to another of the same frequency but different direction of motion (i.e., the corresponding matrix element  $v_{mm'} = 0$ ). All the same, radiation that has apparently been scattered can appear by a double process in which a third state,  $n$  say, with different proper energy from  $m$  and  $m'$ , plays a part. If initially all the  $a$ 's vanish except  $a_{m'}$ , then  $a_n$  gets excited on account of transitions from state  $m'$  by an amount proportional to  $v_{nm'}$ , and although it must itself always remain small, a calculation shows that it will cause  $a_m$  to grow continually with the time at a rate proportional to  $v_{mn}v_{nm'}$ . The scattered radiation thus appears as the result of the two processes  $m' \rightarrow n$  and  $n \rightarrow m$ , one of which must be an absorption and the other an emission, in neither of which is the total proper energy even approximately conserved.

The more accurate expression for the interaction energy obtained in § 3 of the present paper does give rise to direct scattering processes, whose effect is of the same order of magnitude as that of the double processes, and must be added to it. The sum of the two will be found to give just Kramers' and Heisenberg's dispersion formula\* when the incident frequency does not coincide with that of an absorption or emission line of the atom. If, however, the incident frequency coincides with that of, say, an absorption line, one of the

\* Kramers and Heisenberg, 'Z. f. Physik,' vol. 31, p. 681 (1925).

terms in the Kramers-Heisenberg formula becomes infinite. The present theory shows that in this case the scattered radiation consists of two parts, of which the amount of one increases proportionally to the time since the interaction commenced, and that of the other proportionally to the square of this time. The first part arises from those terms in the Kramers-Heisenberg formula that remain finite, with perhaps a contribution from the infinite term, while the second, which is much larger, is just what one would get from transitions of the atom to the upper state and down again governed by Einstein's laws of absorption and emission.

A difficulty that appears in the present treatment of radiation problems should be here pointed out. If one tries to calculate, for instance, the total probability of a light-quantum having been emitted by a given time, one obtains as result a sum or integral with respect to the frequency of the emitted light-quantum that does not converge in the high frequencies. This difficulty is not due to any fundamental mistake in the theory, but comes from the fact that the atom has, for the purpose of its interaction with the field, been counted simply as a varying electric dipole, and the field produced by a dipole, when resolved into its Fourier components, has an infinite amount of energy in the short wave-lengths, owing to the infinite field in its immediate neighbourhood. If one does not make the approximation of regarding the atom as a dipole, but uses the exact expression for the interaction energy, then the fact that the singularity in the field is of a lower order of magnitude and remains constant is sufficient to make the series or integral converge. The exact interaction energy is too complicated to be used as a basis for radiation theory at present, and we shall here use only the dipole energy, which will mean that divergent series are always liable to appear in the calculation. The best method to adopt under such circumstances is first to work out the general theory of any effect using arbitrary coefficients  $v_{mn}$ , and then to substitute for these coefficients in the final result their values given by the dipole interaction energy. If one then finds that the series all converge, one can assume that the result is a correct first approximation; if, however, any of them do not converge, one must conclude that a dipole theory is inadequate for the treatment of that particular effect. We shall find that for the phenomena of dispersion and resonance radiation dealt with in the present paper, there are no divergent series in the first approximation, so that the dipole theory is sufficient. If, however, one tries to calculate the breadth of a spectral line, one meets with a divergent series, so that a dipole theory of the atom is presumably inadequate for the correct treatment of this question.



§ 2. *Preliminary Formulæ.*

We consider the electromagnetic field to be resolved into its components of plane, plane-polarised, progressive waves, each component  $r$  having a definite frequency, direction of motion and state of polarisation, and being associated with a certain type of light-quanta. (To save writing we shall in future suppose the words "direction of motion" applied to a light-quantum or a component of the field to imply also its state of polarisation, and a sum or integral taken over all directions of motion to imply also the summation over both states of polarisation for each direction of motion. This is convenient because the two variables, direction of motion and state of polarisation, are always treated mathematically in the same way.) For an electromagnetic field of infinite extent there will be a continuous three-dimensional range of these components. As this would be inconvenient to deal with mathematically, we suppose it to be replaced by a large number of discrete components. If there are  $\sigma_r$  components per unit solid angle of direction of motion per unit frequency range, we can keep  $\sigma_r$  an arbitrary function of the frequency and direction of motion of the component  $r$ , provided it is large and reasonably continuous, and shall find that it always cancels from the final results of a calculation, which fact appears to justify our replacement of the continuous range by the discrete set.

We can express  $\sigma_r$  in the form  $\sigma_r = (\Delta\nu_r \Delta\omega_r)^{-1}$ , where  $\Delta\nu_r$  can be regarded as the frequency interval between successive components in the neighbourhood of the component  $r$ , and  $\Delta\omega_r$  is in the same way the solid angle of direction of motion to be associated with this component. The quantities  $\Delta\nu_r$ ,  $\Delta\omega_r$  enable one to pass directly from sums to integrals. Thus if  $f_r$  is any function of the frequency and direction of motion of the component  $r$  that varies only slightly from one component to a neighbouring one, the sum of  $f_r \Delta\nu_r$  for all components having a specified direction of motion is

$$\sum_r f_r \Delta\nu_r = \int f_r d\nu_r, \quad (3)$$

and the sum of  $f_r \Delta\omega_r$  for all components having a specified frequency is

$$\sum_r f_r \Delta\omega_r = \int f_r d\omega_r. \quad (3')$$

Also the sum of  $f_r (\sigma_r)^{-1}$  for all components is

$$\sum_r f_r (\sigma_r)^{-1} = \sum_r f_r \Delta\nu_r \Delta\omega_r = \int f_r d\nu_r d\omega_r. \quad (3'')$$

If the number\*  $N_s$  of quanta of energy of the component  $s$  varies only slightly from one component to a neighbouring one, one can give a meaning to the intensity of the radiation per unit frequency range. By supposing the discreteness in the number of components to arise from the radiation being confined in an enclosure (which would imply stationary waves and a special function  $\sigma_s$ ) one obtains† for the rate of flow of energy per unit area per unit solid angle per unit frequency range

$$I_{\nu\omega} = N_s h \nu_s^3 / c^2, \quad (4)$$

a result which may be taken to hold generally for arbitrary  $\sigma_s$  and progressive waves.‡ If only those components with a specified direction of motion are excited, we have instead that the rate of flow of energy per unit area per unit frequency range is

$$I_{\nu} = N_s h \nu_s^3 / c^2 \cdot \Delta\omega_s; \quad (5)$$

while if only a single component  $s$  is excited, we have that the rate of flow of energy per unit area is

$$I = N_s h \nu_s^3 / c^2 \cdot \Delta\omega_s \Delta\nu_s = N_s h \nu_s^3 / c^2 \sigma_s. \quad (6)$$

In this last case the amplitude of the electric force has the value  $E$  given by

$$E^2 = 8\pi I / c = 8\pi N_s h \nu_s^3 / c^3 \sigma_s, \quad (7)$$

and the amplitude  $a$  of the magnetic vector potential, when chosen so that the electric potential is zero, is

$$a = cE / 2\pi\nu_s = 2 (h\nu_s^2 / 2\pi c \sigma_s)^{1/2} N_s^{1/2}. \quad (8)$$

### § 3. The Hamiltonian Function.

We shall now determine the Hamiltonian function that describes the interaction of the field with an atom more accurately than in *loc. cit.* We consider the atom to consist of a single electron moving in an electrostatic field of potential  $\phi$ . According to the classical theory its relativity Hamiltonian equation when undisturbed is

$$p_x^2 + p_y^2 + p_z^2 - (W + e\phi)^2 / c^2 + m^2 c^2 = 0,$$

so that its Hamiltonian function is

$$H = W = c \{ m^2 c^2 + p_x^2 + p_y^2 + p_z^2 \}^{1/2} - e\phi. \quad (9)$$

\* The rule given in *loc. cit.* that symbols representing c-number values for q-number variables should be primed need not always be observed if no confusion thus arises, as in the present case.

† *Loc. cit.*, § 6, equation (28).

‡ This is justified by the fact that one can obtain the result by an alternative method that does not require a finite enclosure, namely by using a quantum-mechanical argument similar to that of *loc. cit.* (lower part of p. 259), applied to the case of discrete momentum values.

If now there is a perturbing field of radiation, given by the magnetic vector potential  $\kappa_x, \kappa_y, \kappa_z$  chosen so that the electric scalar potential is zero, the Hamiltonian equation for the perturbed system will be

$$\left(p_x + \frac{e}{c}\kappa_x\right)^2 + \left(p_y + \frac{e}{c}\kappa_y\right)^2 + \left(p_z + \frac{e}{c}\kappa_z\right)^2 - \frac{(W + e\phi)^2}{c^2} + m^2c^2 = 0,$$

which gives for the Hamiltonian function

$$\begin{aligned} H = W &= c \left\{ m^2c^2 + \left(p_x + \frac{e}{c}\kappa_x\right)^2 + \left(p_y + \frac{e}{c}\kappa_y\right)^2 + \left(p_z + \frac{e}{c}\kappa_z\right)^2 \right\}^{\frac{1}{2}} - e\phi \\ &= c \{ [m^2c^2 + p_x^2 + p_y^2 + p_z^2] + [2e/c \cdot (p_x\kappa_x + p_y\kappa_y + p_z\kappa_z) \\ &\quad + e^2/c^2 \cdot (\kappa_x^2 + \kappa_y^2 + \kappa_z^2)] \}^{\frac{1}{2}} - e\phi. \end{aligned}$$

By expanding the square root, counting the second term in square brackets [ ] as small, and then neglecting relativity corrections for this term, one finds approximately

$$\begin{aligned} H &= c[m^2c^2 + p_x^2 + p_y^2 + p_z^2]^{\frac{1}{2}} - e\phi + e/c \cdot (i\kappa_x + j\kappa_y + k\kappa_z) \\ &\quad + e^2/2mc^2 \cdot (\kappa_x^2 + \kappa_y^2 + \kappa_z^2) \\ &= H_0 + e/c \cdot (i\kappa_x + j\kappa_y + k\kappa_z) + e^2/2mc^2 \cdot (\kappa_x^2 + \kappa_y^2 + \kappa_z^2), \end{aligned} \quad (10)$$

where  $H_0$  is the Hamiltonian for the unperturbed system given by (9). When one counts the radiation field as a dynamical system, one must add on its proper energy  $\Sigma N_r \hbar \nu_r$  to the Hamiltonian (10).

According to the classical theory, the magnetic vector potential for any component  $r$  of the radiation is

$$\kappa_r = a_r \cos 2\pi\theta_r/\hbar = 2(\hbar\nu_r/2\pi c\tau_r)^{\frac{1}{2}} N_r^{\frac{1}{2}} \cos 2\pi\theta_r/\hbar \quad (11)$$

from (8), where  $\theta_r$  increases uniformly with the time such that  $\theta_r = \hbar\nu_r$ , and is the variable that must be taken to be the canonical conjugate of  $N_r$  when the radiation field is treated as a dynamical system. The direction of this vector potential is that of the electric vector of the component of radiation. Hence the total value of the component of the vector potential in any direction, say that of the  $x$ -axis, is

$$\kappa_x = \Sigma_r \kappa_r \cos \alpha_{xr} = 2(\hbar/2\pi c)^{\frac{1}{2}} \Sigma_r \cos \alpha_{xr} (\nu_r/\sigma_r)^{\frac{1}{2}} N_r^{\frac{1}{2}} \cos 2\pi\theta_r/\hbar, \quad (12)$$

where  $\alpha_{xr}$  is the angle between the electric vector of the component  $r$  and the  $x$ -axis. In the quantum theory, where the variables  $N_r, \theta_r$  are  $q$ -numbers, the expression  $2N_r^{\frac{1}{2}} \cos 2\pi\theta_r/\hbar$  must be replaced by the real  $q$ -number  $N_r^{\frac{1}{2}} e^{2\pi i\theta_r/\hbar} + (N_r + 1)^{\frac{1}{2}} e^{-2\pi i\theta_r/\hbar}$ . With this change one can take over the

Hamiltonian (10) into the quantum theory, which gives, when one includes the term  $\Sigma N_r \hbar \nu_r$ ,

$$H = H_0 + \Sigma N_r \hbar \nu_r + e \hbar^{\frac{1}{2}} / (2\pi)^{\frac{1}{2}} c^{\frac{1}{2}} \cdot \Sigma_r x_r (\nu_r / \sigma_r)^{\frac{1}{2}} [N_r^{\frac{1}{2}} e^{2\pi i \theta_r / \hbar} + (N_r + 1)^{\frac{1}{2}} e^{-2\pi i \theta_r / \hbar}] \\ + e^2 \hbar / 4\pi m c^3 \cdot \Sigma_{r,s} \cos \alpha_{rs} (\nu_r \nu_s / \sigma_r \sigma_s)^{\frac{1}{2}} [N_r^{\frac{1}{2}} e^{2\pi i \theta_r / \hbar} + (N_r + 1)^{\frac{1}{2}} e^{-2\pi i \theta_r / \hbar}] \\ \times [N_s^{\frac{1}{2}} e^{2\pi i \theta_s / \hbar} + (N_s + 1)^{\frac{1}{2}} e^{-2\pi i \theta_s / \hbar}] \quad (13)$$

where  $x_r$  denotes the component of the vector  $(x, y, z)$  in the direction of the electric vector of the component  $r$ , i.e.,

$$x_r = x \cos \alpha_{xr} + y \cos \alpha_{yr} + z \cos \alpha_{zr},$$

and  $\alpha_{rs}$  denotes the angle between the electric vectors of the components  $r$  and  $s$ , i.e.,

$$\cos \alpha_{rs} = \cos \alpha_{rr} \cos \alpha_{rs} + \cos \alpha_{rr} \cos \alpha_{rs} + \cos \alpha_{rr} \cos \alpha_{rs}.$$

The terms in the first line of (13) are just those obtained in *loc. cit.*, equation (30), and give rise only to emission and absorption processes. The remaining terms (i.e., those in the double summation) were neglected in *loc. cit.* These terms may be divided into three sets:—

(i) Those terms that are independent of the  $\theta$ 's, which can be added to the proper energy  $H_0 + \Sigma N_r \hbar \nu_r$ . The sum of all such terms, which can arise only when  $r = s$ , is

$$e^2 \hbar / 4\pi m c^3 \cdot \Sigma_r \nu_r / \sigma_r \cdot [N_r^{\frac{1}{2}} e^{2\pi i \theta_r / \hbar} (N_r + 1)^{\frac{1}{2}} e^{-2\pi i \theta_r / \hbar} \\ + (N_r + 1)^{\frac{1}{2}} e^{-2\pi i \theta_r / \hbar} N_r^{\frac{1}{2}} e^{2\pi i \theta_r / \hbar}] \\ = e^2 \hbar / 4\pi m c^3 \cdot \Sigma_r \nu_r / \sigma_r \cdot (2N_r + 1).$$

The terms  $e^2 \hbar / 4\pi m c^3 \cdot \Sigma \nu_r / \sigma_r \cdot 2N_r$  are negligible compared with  $\Sigma N_r \hbar \nu_r$ , owing to the very large quantity  $\sigma_r$  in the denominator, while the terms  $e^2 \hbar / 4\pi m c^3 \cdot \Sigma \nu_r / \sigma_r$  may be ignored since they do not involve any of the dynamical variables, in spite of the fact that the sum  $\Sigma \nu_r / \sigma_r$ , equal to  $\int \nu_r d\nu_r d\omega_r$  from (3''), does not converge for the high frequencies.

(ii) The terms containing a factor of the form  $e^{2\pi i (\theta_r - \theta_s) / \hbar}$  ( $r \neq s$ ), whose sum is

$$e^2 \hbar / 4\pi m c^3 \Sigma_r \Sigma_{s \neq r} \cos \alpha_{rs} (\nu_r \nu_s / \sigma_r \sigma_s)^{\frac{1}{2}} [N_r^{\frac{1}{2}} (N_s + 1)^{\frac{1}{2}} e^{2\pi i (\theta_r - \theta_s) / \hbar} \\ + (N_r + 1)^{\frac{1}{2}} N_s^{\frac{1}{2}} e^{-2\pi i (\theta_r - \theta_s) / \hbar}] \\ = e^2 \hbar / 2\pi m c^3 \Sigma_r \Sigma_{s \neq r} \cos \alpha_{rs} (\nu_r \nu_s / \sigma_r \sigma_s)^{\frac{1}{2}} N_r^{\frac{1}{2}} (N_s + 1)^{\frac{1}{2}} e^{2\pi i (\theta_r - \theta_s) / \hbar}. \quad (14)$$

These terms, which are the only important ones in the three sets, give rise to transitions in which a light-quantum jumps directly from a state  $s$  to a state  $r$ .

Such transitions may be called true scattering processes, to distinguish them from the double scattering processes described in § 1.

(iii) The remaining terms, each of which involves a factor of one or other of the forms  $e^{\pm 4\pi i \theta_r \cdot \hbar}$ ,  $e^{\pm 2\pi i (\theta_r + \theta_s) \cdot \hbar}$ . These terms correspond to processes in which two light-quanta are emitted or absorbed simultaneously, and cannot arise in a light-quantum theory in which there are no forces between the light quanta. The effects of these terms will be found to be negligible, so that the disagreement with the light-quantum theory is not serious.

#### § 4. Discussion of the Emission and True Scattering Processes.

We shall consider now the simple emission processes, in order to discuss the divergent integral that arises in this question. Suppose a light-quantum to be emitted in state  $r$ , with a simultaneous jump of the atom from the state  $J = J'$  to the state  $J = J''$ . If we label the final state of the whole system of atom plus field  $m$  and the initial state  $k$ , the value at time  $t$  of the amplitude  $a_m$  of the eigenfunction of the final state will be in the first approximation

$$a_m = v_{mk} (1 - e^{2\pi i (W_m - W_k)t/\hbar}) / (W_m - W_k), \quad (15)$$

obtained by putting  $a_{k_0} = 1$ ,  $a_{n_0} = 0$  ( $n \neq k$ ) in equation (2). The only term in the Hamiltonian (13) that can contribute anything to the matrix element  $v_{mk}$  is the one involving  $e^{2\pi i \theta_r \cdot \hbar}$ , whose  $(J'', N_1', N_2' \dots N_r' + 1 \dots; J', N_1', N_2' \dots N_r' \dots)$  matrix element is  $e\hbar^{\frac{1}{2}}/(2\pi)^{\frac{1}{2}} c^{\frac{1}{2}} \cdot \dot{x}_r(J''J') (v_r/\sigma_r)^{\frac{1}{2}} (N_r' + 1)^{\frac{1}{2}}$ , where  $\dot{x}_r(J''J')$  is the ordinary  $(J''J')$  matrix element of  $\dot{x}_r$ . If there is no incident radiation we must take all the  $N$ 's zero, which gives

$$v_{mk} = e\hbar^{\frac{1}{2}}/(2\pi)^{\frac{1}{2}} c^{\frac{1}{2}} \cdot \dot{x}_r(J''J') (v_r/\sigma_r)^{\frac{1}{2}},$$

and also

$$W_k = H_0(J') \quad W_m = H_0(J'') + h\nu_r.$$

Thus

$$W_m - W_k = H_0(J'') + h\nu_r - H_0(J') = h[\nu_r - \nu(J'J'')]$$

where  $\nu(J'J'') = [H_0(J') - H_0(J'')]/h$  is the transition frequency between states  $J'$  and  $J''$ , if one assumes  $J'$  to be the higher one. Hence from (15)

$$|a_m|^2 = \frac{e^2}{\pi\hbar c^3} |\dot{x}_r(J'J'')|^2 \frac{\nu_r}{\sigma_r} \frac{1 - \cos 2\pi[\nu_r - \nu(J'J'')]t}{[\nu_r - \nu(J'J'')]^2}.$$

To obtain the total probability of any light-quantum being emitted within the solid angle  $\delta\omega$  about the direction of motion of a given light-quantum  $r$  with this jump of the atom, we must multiply  $|a_m|^2$  by  $\delta\omega/\Delta\omega$ , and sum for all frequencies. This gives, with the help of (3)

$$\delta\omega \sum_r \frac{|a_m|^2}{\Delta\omega_r} = \delta\omega \frac{e^2}{\pi\hbar c^3} |\dot{x}_r(J'J'')|^2 \int_0^\infty \nu_r d\nu_r \frac{1 - \cos 2\pi[\nu_r - \nu(J'J'')]t}{[\nu_r - \nu(J'J'')]^2}. \quad (16)$$

The integral does not converge for the high frequencies. This is due, as mentioned in § 1, to the non-legitimacy of taking only the dipole action of the atom into account, which is what one does when one substitutes for the magnetic potential in (10) its value given by (12), which is its value at some fixed point such as the nucleus instead of its value where the electron is momentarily situated. To obtain the interaction energy exactly, one should put  $\cos 2\pi [\theta_r/\hbar - \nu_r \xi_r/c]$  instead of  $\cos 2\pi \theta_r/\hbar$  in (11), where  $\xi_r$  is the component of the vector  $(x, y, z)$  in the direction of motion of the component  $r$  of radiation. This will make no appreciable change for low frequencies  $\nu_r$ , but will cause a new factor  $\cos 2\pi \nu_r \xi_r/c$  or  $\sin 2\pi \nu_r \xi_r/c$ , whose matrix elements tend to zero as  $\nu_r$  tends to infinity, to appear in the coefficients of (13). This will presumably cause the integral in (16) to converge when corrected, as its divergence when uncorrected is only logarithmic.

Assuming that the integrand in (16) has been suitably modified in the high frequencies, one sees that for values of  $t$  large compared with the periods of the atom (but small compared with the life time in order that the approximations may be valid) practically the whole of the integral is contributed by values of  $\nu_r$  close to  $\nu(J'J'')$ , which means physically that only radiation close to a transition frequency can be spontaneously emitted. One finds readily for the total probability of the emission, by performing the integration,

$$\delta \omega c^2/\pi \hbar c^3 \cdot |\dot{x}_r(J'J'')|^2 \cdot 2\pi^2 t \nu(J'J''),$$

which leads to the correct value for Einstein's A coefficient per unit solid angle, namely,

$$2\pi e^2/\hbar c^3 \cdot |\dot{x}_r(J'J'')|^2 \nu(J'J'') = 8\pi^3 e^2/\hbar c^3 \cdot |x_r(J'J'')|^2 \nu^3(J'J'').$$

We shall now determine the rate at which true scattering processes occur, caused by the terms (14) in the Hamiltonian. We see at once that the frequency of occurrence of these processes is independent of the nature of the atom, and is thus the same for a bound as for a free electron. The true scattering is the only kind of scattering that can occur for a free electron, so that we should expect the terms (14) to lead to the correct formula for the scattering of radiation by a free electron, with neglect of relativity mechanics and thus of the Compton effect.

Suppose that initially the atom is in the state  $J'$  and all the  $N$ 's vanish except one of them,  $N_s$ , say, which has the value  $N_s'$ . We label this state for the whole system by  $k$ , and the state for which  $J = J'$  and  $N_s = N_s' - 1$ ,  $N_r = 1$  with

all the other  $N$ 's zero by  $m$ . In the first approximation  $a_m$  is again given by (15), where we now have

$$v_{mk} = e^2 \hbar / 2\pi m c^3 \cdot \cos \alpha_{rs} (\nu_r \nu_s / \sigma_r \sigma_s)^{1/2} N_s^{1/2}, \quad (17)$$

$$W_k = H_0(J') + N_s' \hbar \nu_s, \quad W_m = H_0(J') + (N_s' - 1) \hbar \nu_s + \hbar \nu_r. \quad (18)$$

Thus

$$W_m - W_k = \hbar (\nu_r - \nu_s), \quad (19)$$

and hence

$$|a_m|^2 = \frac{e^4}{2\pi^2 m^2 c^6} \cos^2 \alpha_{rs} \frac{\nu_r \nu_s}{\sigma_r \sigma_s} N_s' \frac{1 - \cos 2\pi (\nu_r - \nu_s) t}{(\nu_r - \nu_s)^2}.$$

To obtain the total probability of a scattered light-quantum being in the solid angle  $\delta\omega$  we must, as before, multiply  $|a_m|^2$  by  $\delta\omega/\Delta\omega_r$  and sum for all frequencies  $\nu_r$ , which gives\*

$$\delta\omega \Sigma_r \frac{|a_m|^2}{\Delta\omega_r} = \delta\omega \frac{e^4}{2\pi^2 m^2 c^6} \cos^2 \alpha_{rs} \frac{\nu_s}{\sigma_s} N_s' \int \nu_r d\nu_r \frac{1 - \cos 2\pi (\nu_r - \nu_s) t}{(\nu_r - \nu_s)^2}. \quad (20)$$

We again obtain a divergent integral, of the same form as before, which we may assume becomes convergent in the more exact theory. We now have that practically the whole of the integral is contributed by values of  $\nu_r$  close to  $\nu_s$  and the total probability for the scattering process is

$$\delta\omega \frac{e^4}{2\pi^2 m^2 c^6} \cos^2 \alpha_{rs} \frac{\nu_s}{\sigma_s} N_s' \cdot 2\pi^2 t \nu_s, \quad \delta\omega \frac{e^4}{\hbar m^2 c^4 \nu_s} \cos^2 \alpha_{rs} \cdot t I$$

from (6), where  $I$  is the rate of flow of incident energy per unit area. The rate of emission of scattered energy per unit solid angle is thus

$$e^4 / m^2 c^4 \cdot \cos^2 \alpha_{rs} I,$$

where  $\alpha_{rs}$  is the angle between the electric vectors of the incident and scattered radiation, which is the correct classical formula.

\* The reason why there is a small probability for the scattered frequency  $\nu$ , differing by a finite amount from the incident frequency  $\nu_s$  is because we are considering the scattered radiation, after the scattering process has been acting for only a finite time  $t$ , resolved into its Fourier components. One sees from the formula (20) that as the time  $t$  gets greater, the scattered radiation gets more and more nearly monochromatic with the frequency  $\nu_s$ . If one obtained a periodic solution of the Schrödinger equation corresponding to permanent physical conditions, one would then find that the scattered frequency was exactly equal to the incident frequency.

§ 5. Theory of Dispersion.

We shall now work out the second approximation to the solution of equations (1), taking the case when the system is initially in the state  $k$ , so that the first approximation, given by (2) with  $a_{na} = \delta_{nk}$ , reduces to

$$a_m = \delta_{mk} + v_{mk} (1 - e^{2\pi i (W_m - W_k)t/h}) / (W_m - W_k).$$

When one substitutes these values for the  $a_n$ 's in the right-hand side of (1), one obtains

$$\begin{aligned} i\hbar/2\pi \cdot \dot{a}_m &= v_{mk} e^{2\pi i (W_m - W_k)t/h} \\ &+ \sum_n v_{mn} v_{nk} (1 - e^{2\pi i (W_n - W_k)t/h}) e^{2\pi i (W_m - W_n)t/h} / (W_n - W_k) \\ &= (v_{mk} - \sum_n \frac{v_{mn} v_{nk}}{W_n - W_k}) e^{2\pi i (W_m - W_k)t/h} + \sum_n \frac{v_{mn} v_{nk}}{W_n - W_k} e^{2\pi i (W_m - W_n)t/h}, \end{aligned}$$

and hence when  $m \neq k$

$$\begin{aligned} a_m &= (v_{mk} - \sum_n \frac{v_{mn} v_{nk}}{W_n - W_k}) \frac{1 - e^{2\pi i (W_m - W_k)t/h}}{W_m - W_k} \\ &+ \sum_n \frac{v_{mn} v_{nk}}{W_n - W_k} \frac{1 - e^{2\pi i (W_m - W_n)t/h}}{W_m - W_n}. \quad (21) \end{aligned}$$

We may suppose the diagonal elements  $v_{nn}$  of the perturbing energy to be zero, since if they were not zero they could be included with the proper energy  $W_n$ . There will then be no terms in (21) with vanishing denominators, provided all the energy levels are different.

Suppose now that the proper energy of the state  $m$  is equal to that of the initial state  $k$ . Then the first term on the right-hand side of (21) ceases to be periodic in the time, and becomes

$$\{v_{mk} - \sum_n v_{mn} v_{nk} / (W_n - W_k)\} 2\pi t / i\hbar,$$

which increases linearly with the time. The rate of increase consists of a part, proportional to  $v_{mk}$ , that is due to direct transitions from state  $k$ , together with a sum of parts, each of which is proportional to a  $v_{mn} v_{nk}$ , and is due to transitions first from  $k$  to  $n$  and then from  $n$  to  $m$ , although the amplitude  $a_n$  of the eigenfunction of the intermediate state always remains small.

When one applies the theory to the scattering of radiation one must consider not a single final state with exactly the same proper energy as the initial state, but a set of final states with proper energies lying close together in a range that contains the initial proper energy, corresponding to all the possible scattered light-quanta with different frequencies but the same direction of motion that



may appear. One must now determine the total probability of the system lying in any one of these final states, which is

$$\Sigma |a_m|^2 = \int (\Delta W_m)^{-1} |a_m|^2 dW_m,$$

where  $\Delta W_m$  is the interval between the energy levels. The second term in the expression (21) for  $a_m$  may be neglected since it always remains small (except in the case of resonance which will be considered later) and hence

$$\Sigma |a_m|^2 = \int \left| v_{mk} - \Sigma_n \frac{v_{mn} v_{nk}}{W_n - W_k} \right|^2 \frac{2[1 - \cos 2\pi(W_m - W_k)t/\hbar]}{\Delta W_m \cdot (W_m - W_k)^2} dW_m.$$

If one assumes that the integral converges, so that for large values of  $t$  practically the whole of it is contributed by values of  $W_m$  close to  $W_k$ , one obtains

$$\Sigma |a_m|^2 = \frac{4\pi^2 t}{\hbar \Delta W_m} \left| v_{mk} - \Sigma_n \frac{v_{mn} v_{nk}}{W_n - W_k} \right|^2, \quad (22)$$

where the quantities on the right refer to that final state that has exactly the initial proper energy.

We take the states  $k$  and  $m$  to be the same as for the true scattering process considered in the preceding section, so that equations (17), (18) and (19) still hold, and  $\Delta W_m = \hbar \Delta \nu_r = \hbar/\sigma_r \Delta \omega_r$ . We can now take the state  $n$  to be either the state  $J = J''$ ,  $N_s = N_s' - 1$ ,  $N_t = 0$  ( $t \neq s$ ) for any  $J''$ , which would make the process  $k \rightarrow n$  an absorption of an  $s$ -quantum and  $n \rightarrow m$  an emission of an  $r$ -quantum, or the state  $J = J''$ ,  $N_s = N_s'$ ,  $N_r = 1$ ,  $N_t = 0$  ( $t \neq s, r$ ), which would make  $k \rightarrow n$  the emission and  $n \rightarrow m$  the absorption. In the first case we should have

$$v_{nk} = \frac{e}{c} \left( \frac{\hbar \nu_s}{2\pi c \sigma_s} \right)^{\frac{1}{2}} \dot{x}_s(J''J') N_s'^{\frac{1}{2}} \quad v_{mn} = \frac{e}{c} \left( \frac{\hbar \nu_r}{2\pi c \sigma_r} \right)^{\frac{1}{2}} \dot{x}_r(J'J''),$$

and

$$W_n = H_0(J'') + (N_s' - 1) \hbar \nu_s, \quad W_n - W_k = \hbar[\nu(J''J') - \nu_s]^*,$$

and in the second

$$v_{nk} = \frac{e}{c} \left( \frac{\hbar \nu_r}{2\pi c \sigma_r} \right)^{\frac{1}{2}} \dot{x}_r(J''J') \quad v_{mn} = \frac{e}{c} \left( \frac{\hbar \nu_s}{2\pi c \sigma_s} \right)^{\frac{1}{2}} \dot{x}_s(J'J'') N_s'^{\frac{1}{2}},$$

and

$$W_n = H_0(J'') + N_s' \hbar \nu_s + \hbar \nu_r, \quad W_n - W_k = \hbar[\nu(J''J') + \nu_r].$$

We shall neglect the other possible states  $n$ , namely those for which the matrix elements  $v_{mn}$ ,  $v_{nk}$  come from terms in the double summation in the Hamiltonian

\* The frequency  $\nu(J''J')$  is not necessarily positive.

(13), as we are working only to the first order in these terms. (We are working to the second order only in the emission and absorption terms, which, as we shall find, is the same as the first order in the terms of the double summation.) We now obtain for the right-hand side of (22) in which we must take  $\nu_r = \nu_s$ ,

$$N_s' t \Delta \omega_r \frac{e^4 \nu_s^2}{\hbar^2 c^3 \sigma_s} \left| \frac{\hbar}{m} \cos \alpha_{rs} - \sum_{J''} \left\{ \frac{\dot{x}_r(J'J'') \dot{x}_s(J''J')}{\nu(J''J') - \nu_s} + \frac{\dot{x}_s(J'J'') \dot{x}_r(J''J')}{\nu(J''J') + \nu_s} \right\} \right|^2 \quad (23)$$

The most convenient way of expressing this result is to find the amplitude  $P$  (a vector) of the electric moment of that vibrating dipole of frequency  $\nu_s$  that would, according to the classical theory, emit the same distribution of radiation as that actually scattered by the atom. The number of light-quanta of the type  $r$  (with  $\nu_r = \nu_s$ ) emitted by the dipole  $P$  in time  $t$  per unit solid angle is

$$2\pi^3 \nu_s^4 / \hbar c^3 \cdot P_r^2 t,$$

where  $P_r$  is the component of  $P$  in the direction of the electric vector of the light-quanta  $r$ . Comparing this with (23) (which must first be divided by  $\Delta \omega_r$  to change it to the probability of a light quantum being scattered per unit solid angle) one finds for  $P_r$ ,

$$\begin{aligned} P_r &= \left( \frac{8\pi N_s'}{\hbar c^3 \nu_s \sigma_s} \right)^{1/2} \frac{e^2}{4\pi^2} \left| \frac{\hbar}{m} \cos \alpha_{rs} - \sum_{J''} \left\{ \frac{\dot{x}_r(J'J'') \dot{x}_s(J''J')}{\nu(J''J') - \nu_s} + \frac{\dot{x}_s(J'J'') \dot{x}_r(J''J')}{\nu(J''J') + \nu_s} \right\} \right| \\ &= E \frac{e^2}{\hbar} \frac{1}{\nu_s^2} \left| \frac{\hbar}{4\pi^2 m} \cos \alpha_{rs} - \sum_{J''} [\nu(J''J')]^2 \left\{ \frac{x_r(J'J'') x_s(J''J')}{\nu(J''J') - \nu_s} \right. \right. \\ &\quad \left. \left. + \frac{x_s(J'J'') x_r(J''J')}{\nu(J''J') + \nu_s} \right\} \right|, \quad (24) \end{aligned}$$

using (7), where  $E$  is the amplitude of the electric vector of the incident radiation.

We can put this result in a different form by using the following relations, which follow from the quantum conditions,

$$\sum_{J''} [x_r(J'J'') x_s(J''J') - x_s(J'J'') x_r(J''J')] = [x_r x_s - x_s x_r](J'J') = 0 \quad (25)$$

and

$$\begin{aligned} \sum_{J''} [x_r(J'J'') \dot{x}_s(J''J') - \dot{x}_s(J'J'') x_r(J''J')] &= [x_r \dot{x}_s - \dot{x}_s x_r](J'J') \\ &= i\hbar / 2\pi m \cdot \cos \alpha_{rs}, \quad (26) \end{aligned}$$

which gives

$$\begin{aligned} \sum_{J''} [x_r(J'J'') x_s(J''J') \nu(J''J') + x_s(J'J'') x_r(J''J') \nu(J''J')] \\ = \hbar / 4\pi^2 m \cdot \cos \alpha_{rs}. \quad (27) \end{aligned}$$

Multiplying (25) by  $v_s$  and adding to (27), we obtain

$$\Sigma_{J''} [x_r (J' J'') x_s (J'' J') \{v (J'' J') + v_s\} + x_s (J' J'') x_r (J'' J') \{v (J'' J') - v_s\}] = \hbar/4\pi^2 m \cdot \cos \alpha_{rs}. \quad (28)$$

With the help of this equation, (24) reduces to

$$P_r = E \frac{e^2}{\hbar} \left| \Sigma_{J''} \left\{ \frac{x_r (J' J'') x_s (J'' J')}{v (J'' J') - v_s} + \frac{x_s (J' J'') x_r (J'' J')}{v (J'' J') + v_s} \right\} \right|,$$

so that the vector  $P$  is equal to

$$P = E \frac{e^2}{\hbar} \left| \Sigma_{J''} \left\{ \frac{x (J' J'') x_s (J'' J')}{v (J'' J') - v_s} + \frac{x_s (J' J'') x (J'' J')}{v (J'' J') + v_s} \right\} \right|, \quad (29)$$

where  $x$  without a suffix means the vector  $(x, y, z)$ . This is identical with Kramers' and Heisenberg's result.\*

In applying the formula (22), instead of taking the final state  $m$  of the system to be one for which the atom is again in its initial state  $J = J'$ , we can take a new final state for the atom,  $J = J'''$  say. The frequency  $v_r$  for the scattered radiation that gives no change of total proper energy is now

$$v_r = v_s - v (J''' J') = v_s + v (J'' J''') - v (J'' J'), \quad (30)$$

which differs from the incident frequency  $v_s$ , so that we obtain in this way the non-coherent scattered radiation. (We assume that this  $v_r$  is positive as otherwise there would be no non-coherent scattered radiation associated with the final state  $J = J'''$  of the atom.) In the present case we have  $v_{mk} = 0$ , corresponding to the fact that the true scattering process does not contribute to the non-coherent radiation. We now obtain for  $P_r$ , after a similar and almost identical calculation to that leading to equation (24),

$$P_r = E \frac{e^2}{\hbar} \frac{1}{v_r v_s} \left| \Sigma_{J''} v (J'' J') v (J'' J''') \left\{ \frac{x_r (J''' J'') x_s (J'' J')}{v (J'' J') - v_s} + \frac{x_s (J''' J'') x_r (J'' J')}{v (J'' J') + v_r} \right\} \right| \quad (31)$$

This result can be put in the form corresponding to (29) with the help of equations analogous to (25) and (26) referring to the non-diagonal  $(J''' J')$  matrix elements of  $[x, x_s - x_s x_r]$  and  $[x, \dot{x}_s - \dot{x}_s x_r]$ . These equations give, corresponding to (28),

$$\Sigma_{J''} [x_r (J''' J'') x_s (J'' J') \{v (J'' J') - v_r\} + x_s (J''' J'') x_r (J'' J') \{v (J'' J''') - v_r\}] = 0.$$

\* Kramers and Heisenberg, *loc. cit.*, equation (18). For previous quantum-theoretical deductions of the dispersion formula see Born, Heisenberg and Jordan, 'Z. f. Physik,' vol. 35, p. 557, Kap. 1, equation (40) (1926); Schrödinger, *loc. cit.*, § 2, equation (23); and Klein, *loc. cit.*, § 5, equation (82).

When the left-hand side of this equation is subtracted from the summation in (31) one obtains, on account of the relations

$$\begin{aligned} \nu(J''J') \nu(J''J''') &= \nu(J''J') [\nu(J''J') + \nu_r - \nu_s] \\ &= [\nu(J''J') - \nu_s] [\nu(J''J') + \nu_r] + \nu_r \nu_s, \end{aligned}$$

and

$$\nu(J''J') \nu(J''J''') = [\nu(J''J''') - \nu_r] [\nu(J''J') + \nu_r] + \nu_r \nu_s$$

which follow from (30), the result

$$P_r = E \frac{e^2}{h} \sum_{J''} \left\{ \frac{x_r(J''J''') x_s(J''J')}{\nu(J''J') - \nu_s} + \frac{x_s(J''J''') x_r(J''J')}{\nu(J''J') + \nu_r} \right\}$$

again in agreement with Kramers and Heisenberg.

### § 6. The Case of Resonance.

The dispersion formulæ obtained in the preceding section can no longer hold when the frequency of the incident radiation coincides with that of an absorption or emission line of the atom, on account of a vanishing denominator. One easily sees where a modification must be made in the deduction of the formulæ. Since one of the intermediate states  $n$  now has the same energy as the initial state  $k$ , the term in the second summation in (21) referring to this  $n$  becomes large and can no longer be neglected.

In investigating this case of resonance one must, for generality, suppose the incident radiation to consist of a distribution of light-quanta over a range of frequencies including the resonance frequency, instead of entirely of light-quanta of a single frequency, as the results will depend very considerably on how nearly monochromatic the incident radiation is. Thus one must take the initial state  $k$  of the system to be given by  $J = J'$  and  $N_s = N_s'$ , where  $N_s'$  is zero except for light-quanta of a specified direction, and is for these light-quanta (roughly speaking) a continuous function of the frequency, so that the rate of flow of incident energy per unit area per unit frequency range is given by (5). The final state  $m$  for a process of coherent scattering is one for which  $J = J'$  again, and a light-quantum  $s$  has been absorbed and one  $r$  of approximately the same frequency emitted. Thus we have

$$W_m - W_k = h(\nu_r - \nu_s). \quad (32)$$

As before, the intermediate states  $n$  will be those for which  $J = J''$  (arbitrary) and either the  $s$ -quantum has already been absorbed or the  $r$ -quantum has already been emitted. If we take for definiteness the case when the range of incident frequencies includes only one resonance frequency, and this is an

absorption frequency to the state of the atom  $J = J^l$ , say, then that intermediate state of the system for which  $J = J^l$  and for which the  $s$ -quantum has already been absorbed will have very nearly the same proper energy as the initial state. Calling this intermediate state  $l$  we have

$$W_l - W_k = h(\nu_0 - \nu_s) \quad W_m - W_l = h(\nu_r - \nu_0) \quad (33)$$

where  $\nu_0$  is the resonance frequency, equal to  $[H(J^l) - H(J')]/h$ .

In equation (21) we can now neglect only those terms of the second summation for which  $n \neq l$ . This gives

$$a_m = \left( v_{mk} - \sum_{n \neq l} \frac{v_{mn} v_{nk}}{W_n - W_k} \right) \frac{1 - e^{2\pi i (W_m - W_k) t/h}}{W_m - W_k} \\ + \frac{v_{ml} v_{lk}}{W_l - W_k} \left\{ \frac{1 - e^{2\pi i (W_m - W_l) t/h}}{W_m - W_l} - \frac{1 - e^{2\pi i (W_m - W_k) t/h}}{W_m - W_k} \right\},$$

which, with the help of (32) and (33), may be written

$$a_m = \left( v_{mk} - \sum_{n \neq l} \frac{v_{mn} v_{nk}}{W_n - W_k} \right) \frac{1 - e^{2\pi i (\nu_r - \nu_s) t}}{h(\nu_r - \nu_s)} \\ + \frac{v_{ml} v_{lk}}{h^2(\nu_0 - \nu_s)} \left\{ \frac{1 - e^{2\pi i (\nu_r - \nu_0) t}}{\nu_r - \nu_0} - \frac{1 - e^{2\pi i (\nu_r - \nu_s) t}}{\nu_r - \nu_s} \right\}.$$

We must now determine the total probability of a specified light-quantum  $r$  being emitted with the absorption of any one of the incident light-quanta  $s$ , which is given by  $\sum_s |a_m|^2$ , equal to  $\int (\Delta\nu_s)^{-1} |a_m|^2 d\nu_s$ . To evaluate this we require the following integrals

$$\int_0^\infty \frac{|1 - e^{2\pi i (\nu_r - \nu_s) t}|^2}{(\nu_r - \nu_s)^2} d\nu_s = 4\pi^2 t \\ \int_0^\infty \frac{1}{(\nu_0 - \nu_s)^2} \left| \frac{1 - e^{2\pi i (\nu_r - \nu_0) t}}{\nu_r - \nu_0} - \frac{1 - e^{2\pi i (\nu_r - \nu_s) t}}{\nu_r - \nu_s} \right|^2 d\nu_s \\ = 4\pi \frac{2\pi (\nu_r - \nu_0) t - \sin 2\pi (\nu_r - \nu_0) t}{(\nu_r - \nu_0)^3} \\ \int_0^\infty \frac{1 - e^{2\pi i (\nu_r - \nu_s) t}}{(\nu_r - \nu_s)(\nu_0 - \nu_s)} \left\{ \frac{1 - e^{-2\pi i (\nu_r - \nu_0) t}}{\nu_r - \nu_0} - \frac{1 - e^{-2\pi i (\nu_r - \nu_s) t}}{\nu_r - \nu_s} \right\} d\nu_s \\ = 2\pi \left\{ \frac{2\pi (\nu_r - \nu_0) t - \sin 2\pi (\nu_r - \nu_0) t}{(\nu_r - \nu_0)^2} + i \frac{1 - \cos 2\pi (\nu_r - \nu_0) t}{(\nu_r - \nu_0)^2} \right\},$$

for large  $t$ , and with their help obtain,

$$\begin{aligned} \sum_r |a_m|^2 = & \left| v_{mk} - \sum_{n \neq k} \frac{v_{mn} v_{nk}}{W_n - W_k} \right|^2 \frac{4\pi^2 t}{h^2 \Delta v_s} \\ & + \frac{|v_{mi} v_{ik}|^2}{h^4} \frac{4\pi}{\Delta v_s} \frac{2\pi (v_r - v_0) t - \sin 2\pi (v_r - v_0) t}{(v_r - v_0)^3} \\ & + 2R \left( v_{mk} - \sum_{n \neq k} \frac{v_{mn} v_{nk}}{W_n - W_k} \right) \frac{v_{ki} v_{im}}{h^3 \Delta v_i} \frac{2\pi}{\Delta v_s} \left\{ \frac{2\pi (v_r - v_0) t - \sin 2\pi (v_r - v_0) t}{(v_r - v_0)^2} \right. \\ & \left. + i \frac{1 - \cos 2\pi (v_r - v_0) t}{(v_r - v_0)^2} \right\} \quad (34) \end{aligned}$$

where the quantities on the right now refer to that incident light-quantum  $s$  for which  $v_s = v_r$ , and  $R$  means the real part of all that occurs in the term after it.

The first of these three terms is just the contribution of those terms of the dispersion formula (22) that remain finite, the second is that which replaces the contribution of the infinite term,\* and the third gives the interference between the first two, and replaces the cross terms obtained when one squares the dispersion electric moment. One can see the meaning of the second term more clearly if one sums it for all frequencies  $v_r$  of the scattered radiation in a small frequency range  $v_0 - \alpha'$  to  $v_0 + \alpha''$  about the resonance frequency  $v_0$  (which frequency range must be large compared with the theoretical breadth of the spectral line in order that the approximations may be valid). This is equivalent to multiplying the term by  $(\Delta v_r)^{-1}$  and integrating through the frequency range. If, for brevity, one denotes the quantity  $4\pi |v_{mi} v_{ik}|^2 / h^4 \Delta v_r \Delta v_s$  by  $f(v_r)$ , the result is, neglecting terms that do not increase indefinitely with  $t$  or that tend to zero as the  $\alpha$ 's tend to zero,

$$\begin{aligned} & \int_{v_0 - \alpha'}^{v_0 + \alpha''} f(v_r) \frac{2\pi (v_r - v_0) t - \sin 2\pi (v_r - v_0) t}{(v_r - v_0)^3} dv_r \\ & = f(v_0) \int_{v_0 - \alpha'}^{v_0 + \alpha''} \frac{2\pi (v_r - v_0) t - \sin 2\pi (v_r - v_0) t}{(v_r - v_0)^3} dv_r \\ & \quad + f'(v_0) \int_{v_0 - \alpha'}^{v_0 + \alpha''} \frac{2\pi (v_r - v_0) t - \sin 2\pi (v_r - v_0) t}{(v_r - v_0)^2} dv_r \\ & = f(v_0) (2\pi t)^2 \left[ \frac{1}{2} \pi - \frac{1}{2\pi t \alpha''} - \frac{1}{2\pi t \alpha'} \right] + f'(v_0) 2\pi t \log \alpha'' / \alpha'. \end{aligned}$$

\* It should be noticed that this second term does not reduce to the square of the  $l$  term in the summation (22) when  $v_r$  is not a resonance frequency, but to double this amount. This difference is due to the fact that processes involving a change of proper energy are not entirely negligible for the initial conditions used in the present paper, and one such scattering process, which was neglected in § 5, becomes in the resonance case a process with no change of proper energy and is included in the calculation

Thus the contribution of the second term in (34) to the small frequency range  $\nu_0 - \alpha'$  to  $\nu_0 + \alpha''$  consists of two parts, one of which increases proportionally to  $t^2$  and the other proportionally to  $t$ . The part that increases proportionally to  $t^2$ , namely,

$$\frac{1}{2}\pi f(\nu_0)(2\pi t)^2 = \frac{1}{2}(2\pi)^4 |v_{mi}v_{ik}|^2 / h^4 \Delta\nu_r \Delta\nu_s \cdot t^2,$$

is just that which would arise from actual transitions to the higher state of the atom and down again governed by Einstein's laws, since the probability that the atom has been raised to the higher state by the time  $\tau$  is\*  $(2\pi)^2 |v_{ik}|^2 / h^2 \Delta\nu_s \cdot \tau$ , and when it is in the higher state the probability per unit time of its jumping down again with emission of a light-quantum in the required direction is  $(2\pi)^2 |v_{mi}|^2 / h^2 \Delta\nu_r$ , so that the total probability of the two transitions taking place within a time  $t$  is

$$\frac{(2\pi)^2 |v_{ik}|^2}{h^2 \Delta\nu_s} \cdot \frac{(2\pi)^2 |v_{mi}|^2}{h^2 \Delta\nu_r} \int_0^t \tau d\tau = \frac{(2\pi)^4 |v_{mi}v_{ik}|^2}{h^4 \Delta\nu_r \Delta\nu_s} \frac{1}{2} t^2.$$

The part that increases linearly with the time may be added to the contributions of the first and third terms, which also increase according to this law. For values of  $t$  large compared with the periods of the atom, the terms proportional to  $t$  will be negligible compared with those proportional to  $t^2$ , and hence the resonance scattered radiation is due practically entirely to absorptions and emissions according to Einstein's laws.

---

\* This result and the one for the emission follow at once from formula (32) of *loc. cit.*

*The Analysis of Beams of Moving Charged Particles by a  
Magnetic Field.*

By W. A. WOOSTER, B.A., Charles Abercrombie Smith Student of Peterhouse, Cambridge.

(Communicated by Sir Ernest Rutherford, P.R.S. —Received February 28, 1927.)

§ 1. INTRODUCTION.

The practice of analysing beams of charged particles moving with different velocities by means of the magnetic field is now well established. Among the many important physical quantities which have been determined in this way must be included the value of  $e/m$ , the velocities, intensities and charge carried by the homogeneous  $\beta$ -ray groups of radioactive elements, the masses of isotopes, and, recently,\* it has been applied to the analysis of very slow electrons. In most of this work it has only been necessary to find the energies of the various groups of charged particles, and for this purpose no detailed consideration of the focussing action of the magnetic field was necessary. Problems relating to the relative numbers of particles in the homogeneous groups cannot, however, be solved without more accurate knowledge of the action of the magnetic field, and it was in connection with the relative intensities of the  $\beta$ -ray groups of radium B and radium C that the work here described was started.

In carrying out these calculations, it soon became evident that they had a much wider application than simply to the problem to which they owed their origin. In addition to furnishing a method of obtaining the structure of the line produced by the focussing action of the magnetic field for any kind of source of charged particles, these calculations indicate the best design for the apparatus containing the source of charged particles. Further, when applied to particles which have traversed thin layers of stopping material, the analysis leads to a knowledge of the velocity distribution of the retarded particles. Up to the present no method has been devised of finding this velocity distribution experimentally, and although the results obtained are only approximate, yet they show definitely that the method indicated here is quite practicable.

There are two ways in which the analysis of a heterogeneous beam may be carried out. In one the particles, projected at right angles to the field, are deviated through small angles and appear as bands on a photographic plate ;

\* K. Cole, 'Phys. Rev.', vol. 28, p. 781 (1926).



whilst in the other, which is alone considered here. the tracks of the particles are semicircles, converging to a narrow line CE on a photographic plate P, placed relative to the source of the particles S as indicated in fig. 1.

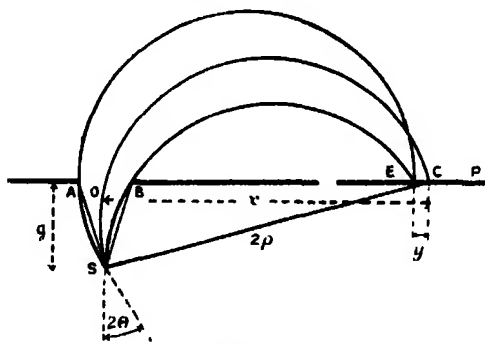


FIG. 1.

It will be observed, on referring to the figure, that the circle which passes through O, the foot of the perpendicular from S on the plane ABP, attains the farthest distance along the plate from S, all other circles, whether passing through AB to the right or left of O, striking the plate nearer to the source than C. There is thus, no matter how wide the slit AB, a definite limit to the line CE on the side opposite the source, and further, owing to a fortunate property of the geometry of the circle, most of the rays are concentrated into this edge. The side C of the line CE is thus sharply defined, and since the momentum of a given group of particles is proportional to the diameter of the track SC, the sharpness of the edge C enables the momentum to be accurately determined, no matter how diffuse may be the other side of the line. The well-defined limit C is due to the fact that in a magnetic field the moving charged particles describe circles and are not influenced by the mechanical construction of the apparatus—a fact which explains the possibility of obtaining quite accurate results without elaborate apparatus. So long as attention is confined to the energies, momenta or masses of the particles, measurements from the source to the sharp edge of the line are sufficient; but, when it becomes desirable to obtain the intensities of the lines, then consideration must be given to their structure and the influence on it of the components of the apparatus. It is the solution of the problem of the structure of the line under various conditions which is undertaken in the present paper, and it will be seen how a knowledge of the dependence of this structure on the disposition and size of the source, limiting slit and photographic plate, enables us to find the best arrangement of them.

It is obvious that there is a close analogy between this apparatus, which

by means of a magnetic field separates out into a velocity spectrum, particles of the same mass and charge, and the prism or grating spectrometer, which analyses light into its constituents. The dispersing agent in the present case is the magnetic field, which therefore plays the same rôle in this instrument as does the prism or diffraction grating in optical spectrometers. It is very desirable, for simplicity of reference, to give some name to the apparatus indicated in fig. 1, and it would appear appropriate, in view of the above, to term it a "magnetic spectrometer." In the present paper this term will be applied to the apparatus whatever may be the nature of the particles deflected by the magnetic field or the means of registering their presence. The photographic plate is largely used for this purpose as, in addition to providing a permanent record, it registers an extended portion of spectrum for a given value of the magnetic field. It is, however, often replaced by an ionisation chamber which is fixed relative to the source, and to investigate the number of particles of different speeds or masses the magnetic field is varied so as to bring successive portions of the spectrum over the entrance to the ionisation chamber. Whether a photographic plate or an ionisation chamber be employed, it is necessary when anything more than the energy of the particles is required to determine the structure of the line into which they are focussed. Unlike the form of the line obtained with a prism or grating spectrometer, that produced by their magnetic analogue is very complex, and it has not been possible to find any comprehensive formula expressing its structure under all conditions. Instead, however, a method has been devised by which the structure may readily be obtained in any given case and also the method of obtaining the best experimental conditions.

## § 2. THE "MAGNETIC SPECTROMETER" USING A PHOTOGRAPHIC PLATE.

It will be evident from what has been said above that the key to the solution of the various problems associated with intensities in the magnetic spectrum is the structure of the line produced on the photographic plate. In general, the line is too complex to find a general analytical expression which gives its form for all sizes of source, limiting slit and radius of track of the particles. It is possible, however, to find such an expression if the source be supposed infinitely narrow. The effect produced by a source of finite size may then be obtained by suitably superposing the effects of a large number of such infinitely narrow sources placed parallel to one another and to the length of the actual source. The first step in the analysis is therefore to find the form of the line due to the very narrow source, and this we now proceed to do.

*(a) Structure of Line due to an Infinitely Narrow Source.*

It may be shown by purely geometrical considerations for a track such as SAE (fig. 1), the tangent to which at the source makes an angle  $\theta$  with the corresponding tangent to the track SOC, that the distance  $y$  between the points where SAE and SOC strike the plate is given by the equation

$$y = \frac{4\rho^2}{x+s}(1 - \cos \theta),$$

where  $x$  = distance from the centre of the limiting slit to the head of the line and  $2s$  = AB = slit-width.

Since  $\theta$  and  $2s$  are not usually greater than  $10^\circ$  and 0.5 cm. respectively nor  $x$  less than 6.0 cm., this equation may be written

$$y = \frac{2\rho^2}{x} \theta^2, \quad (1)$$

the possible error being not more than about 4 per cent. As the maximum error arises for particles which contribute only to the tail of the line, the equation (1) is sufficient for our purposes.

This equation relates to particles which are fired out at right angles to the magnetic field; there are, of course, with a source of finite length, many that arrive at any one point in the plane CP having traversed paths making at every point angles slightly less than  $\pi/2$  with the magnetic field, say  $(\pi/2 - \alpha)$  (see fig. 2). The velocity of the particles in the direction of the magnetic field is  $v \cdot \sin \alpha$ , and it may be shown that the distance  $l$  moved parallel to this direction whilst describing the semicircular track is given by the equation

$$l = \pi\rho\alpha. \quad (2)$$

The velocity of the particle in the plane at right angles to the field is  $v \cdot \cos \alpha$  and the radius of the track projected on to this plane is  $\rho \cdot \cos \alpha$ . These particles do not therefore attain as great a distance from the source when they strike the plate as those for which  $\alpha = 0$ , as is indicated in fig. 2. If  $\phi_1$  is this

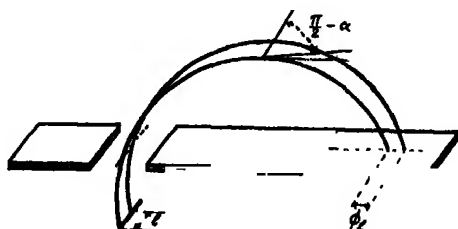


FIG. 2.

displacement backwards from the head of the line, then by purely geometrical considerations it may be shown that

$$\phi_t = \frac{2\rho^2}{x} \alpha^2. \quad (3)$$

This equation holds for all values of  $\theta$ , within the same limits as before, and has about the same accuracy as equation (1).

Suppose a plane drawn through the mid-point of the source at right angles to the magnetic field. This plane will be called the central plane, and the line in which it intersects the photographic plate the central line. Consider now an element of the spectrum line of length  $dy$  (fig. 3) and breadth  $dl$ , lying sym-

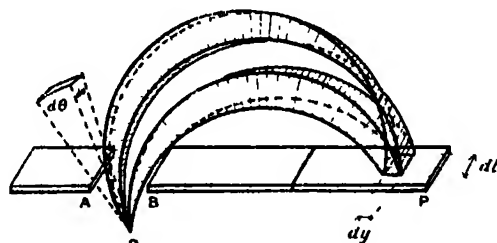


FIG. 3.

metrically with respect to the central line. The particles entering this element from a point at the middle of the source are contained within two "pyramids," the corresponding tangents to which at the source make equal angles with the normal to the plane ABP. These "pyramids" are further defined by equal angular elements  $d\theta$ ,  $dx$ , the values of which may be obtained from equations (1) and (2), thus

$$d\theta = \sqrt{\frac{x}{2\rho^2}} \frac{1}{2\sqrt{y}} dy, \quad dx = \frac{dl}{\pi\rho}.$$

The solid angle of the two beams of particles entering this element is thus

$$\frac{d\theta \cdot dx}{2\pi} = \frac{1}{4\pi^2} \sqrt{\frac{x}{2\rho^4}} \frac{1}{\sqrt{y}} dy \cdot dl.$$

The intensity of the line at the centre of the element ( $dy \cdot dl$ ) is equal to the ratio of the number of particles entering the element to the area they affect, i.e.,

$$I = \frac{d\theta \cdot dx}{2\pi} \bigg/ dy \cdot dl = \frac{1}{4\pi^2} \sqrt{\frac{x}{2\rho^4}} \cdot \frac{1}{\sqrt{y}}. \quad (4)$$

Equation (4) gives the number of particles which, starting from the mid-point of the source, strike unit area of the plate at any point along the central line. These particles are, of course, but a small fraction of the total number which arrive at this point from all portions of the source. Consider, therefore, a point on the source distant  $l$  from the central plane; by equation (2), we know that particles from this point for which  $\theta = 0^\circ$  strikes the plate at a distance from the head of the line equal to  $\phi_l$ , and those for which  $\theta = \theta_1$  arrive at a point distant  $y_1 + \phi_l$  from the head of the line, where  $y_1$  and  $\theta_1$  are connected by equation (1). Thus, if these particles for which  $\alpha$  is not equal to zero are to arrive in the same element ( $dy$ ,  $dl$ ) as was considered above, they must strike the plate at the same distance  $y$  from the head of the line. We may therefore write

$$y = y_1 + \phi_l.$$

For these obliquely directed particles we must substitute  $y_1$  for  $y$  in equation (4). Thus

$$I = \frac{1}{4\pi^2} \sqrt{\frac{x}{2\rho^3}} \frac{1}{\sqrt{y - \phi_l}}.$$

The total intensity due to the whole source is equal to  $2 \int_0^L I dl$ , where  $2L =$  length of the source.

By combining equations (2) and (3), we find that

$$\phi_l = \frac{2l^2}{\pi^2 x}, \quad (5)$$

and therefore, on reduction,

$$2 \int_0^L I dl = \frac{x}{4\pi\rho^2} \sin^{-1} \sqrt{\frac{2L^2}{\pi^2 xy}}. \quad (6)$$

This equation gives the intensity at any point distant  $y$  from the head of the line along the central line of the plate, due to a source of length  $2L$ , but infinitely narrow, and is the starting point for all calculations on sources of finite width.

It is clear that  $y$  cannot be  $< \frac{2L^2}{\pi^2 x}$  for equation (6) to be true, and since the value of  $\phi_L$  is  $\frac{2L^2}{\pi^2 x}$ , this is equivalent to saying that  $y \geq \phi_L$ . Now from equation (5) we know that

$$\phi_l = \frac{2l^2}{\pi^2 x},$$

and, hence, as  $y$  decreases so must the value of  $l$ , i.e., less and less of the source becomes effective as we approach very near to the head of the line. However, the amount of the source which is effective will always be such that

$$y = \frac{2l^2}{\pi^2 x},$$

and therefore the total intensity as obtained from equation (6) for points lying between the limits  $y = \phi_L$  and  $y = 0$  will be constant. With the dimensions of the apparatus in general use, the value of  $y$  at which the equation gives a constant intensity lies between 0.008 and 0.001 cm.

Curves are given in fig. 4 showing how the intensity due to infinitely narrow

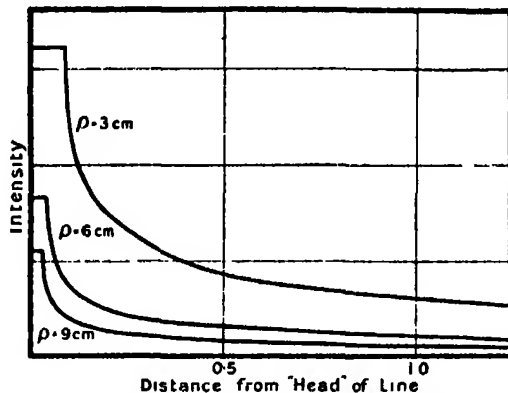


FIG. 4.—Intensity Curves for Infinitely Narrow Sources.

Distance of source from slit = 1.5 cm.; length of source = 1 cm. Distances from head of line in mm.

sources of finite length vary with radius of curvature. It will be observed that the length of the curve over which the intensity is uniform becomes greater the smaller the radius of curvature—due to the corresponding increase in  $\alpha$  and hence also of  $\phi_L$ ; further, the intensity of the straight portions of the curves vary approximately inversely as  $\rho$ , which is to be expected from equation (6), since  $x$  is practically equal to  $2\rho$ .

#### (b) The Structure of Lines due to Sources of Finite Breadth.

(a) *Flat Sources.*—The form of the line given by an infinitely narrow source being ascertained, we may now proceed to find the form of lines due to sources of finite size by supposing them made up of a number of infinitely narrow sources placed side by side and parallel to the magnetic field. Consider first

the case of a flat source the plane of which is parallel to the plane of the slit and photographic plate. Here we shall have a uniform distribution of the narrow sources, and by integrating between appropriate limits, the area of that curve in fig. 4 which corresponds to the particular radius of curvature of the rays, we obtain a new curve due to the flat source (see fig. 5(c)). In general, a flat source is not used with its plane horizontal, but its normal is arranged to make an angle ranging from  $30^\circ$  to  $10^\circ$  with the plane of the slit and photographic plate and to point upwards and towards the latter. To find the structure of the lines due to such a source we cannot integrate the appropriate curve of fig. 4 between ordinates separated by the breadth of the source projected on the plane AP, because one side of the source is nearer to this plane than the other. The distance  $x$  of the head of the line from the centre of the slit AB is connected with the distance of the source from the slit,  $g$  (fig. 1), by the equation

$$x^2 = 4g^2 - g^2.$$

and hence

$$2x dx = -2g dg.$$

If the breadth of the source is  $\xi$  and the normal to the plane of the source makes the angle  $\eta$  with the plane of slit and plate,

$$dg = \xi \cos \eta$$

and

$$dx = -\frac{g\xi}{x} \cos \eta.$$

The intensity of emission of the particles is uniform over the surface of the source, and hence we may again obtain the form of the line by integrating the appropriate curve of fig. 4 between limits which are separated by the width of the source projected on a horizontal plane, less  $dx$ ,

$$\text{i.e.,} \quad \xi \sin \eta - \frac{g\xi}{x} \cos \eta.$$

In this way the curves (a) and (b) of fig. 5 were constructed.

(b) *Cylindrical Sources*.—Cylindrical sources are placed with their axes parallel to the magnetic field, and as in the case of flat sources they may be regarded as a number of infinitely narrow sources placed side by side. We cannot, however, obtain the intensity distribution in the line due to a cylindrical source by integrating the appropriate curve of fig. 4 between fixed limits, because  $g$  does not change uniformly as we pass from right to left over the source (see fig. 6). If we consider the points  $\eta_1, \eta_2, \eta_3$ , etc., on the surface of

the source, we observe that each is a certain horizontal distance  $dy$  from the vertical line, through the middle of the source and also a distance  $dg$  vertically

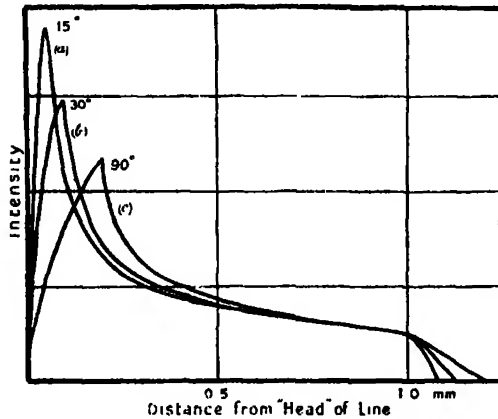


FIG. 5.—Intensity Curves for Flat Sources.

Distance of source from slit = 1.5 cm.; length of source = 1 cm. Angles made by normal to [flat source with plane of photographic plate = 15°, 30°, 90°.  $\rho = 6$  cm. Slit width = 0.4 cm.

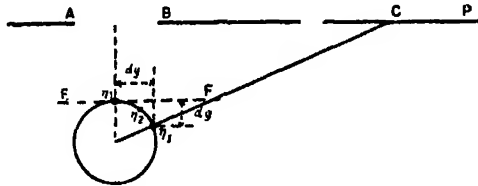


FIG. 6.

below the point  $\eta_3$ , in which the plane EF, parallel to AP, intersects the surface of the source. If we suppose the cylindrical source to be replaced by a flat one parallel to plane AP and passing through  $\eta_3$ , we should then dispose the points  $\eta_1'$ ,  $\eta_2'$ , etc., on this source at a distance

$$dy = \frac{g}{x} dg$$

from the point  $\eta_3$ . The cylindrical source is thus equivalent to a flat one with a non-uniform emissivity of charged particle, there being more from the edges than the middle. The relative position of the curves due to infinitely narrow sources placed at  $\eta_1$ ,  $\eta_2$ ,  $\eta_3$  on the surface of the cylinder are, of course, the same as those of  $\eta_1'$ ,  $\eta_2'$ ,  $\eta_3'$  on the plane EF, and the resulting intensity is readily obtained by a summation of the ordinates of the superposed curves due to infinitely narrow sources at these points. This process was carried out for



particles of different radii of curvature and sources of different diameters. The results are given in figs. 7 and 8.

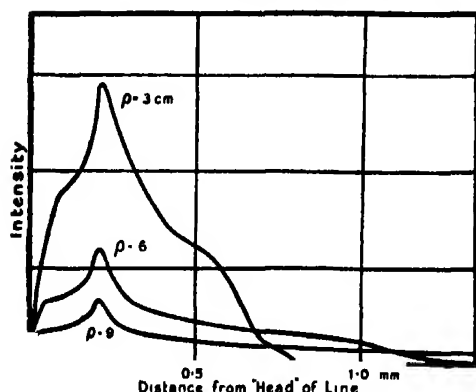


FIG. 7.

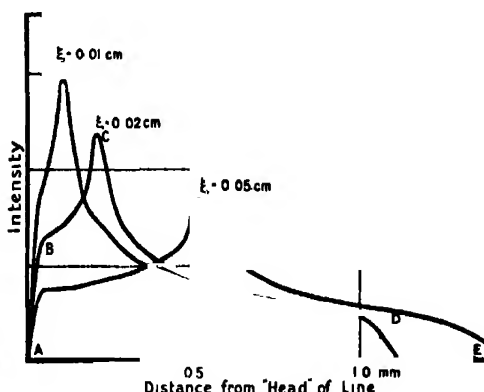


FIG. 8.

Intensity Curves for Cylindrical Sources.

Distance of source from slit = 1.5 cm.; length of source = 1 cm.  $\rho = 6$  cm. Slit width = 0.4 cm.  
 $\xi$  = diameter of source (in fig. 7,  $\xi = 0.02$ ).

The structure of the line produced by a circular source is made up of four distinct parts AB, BC, CD, DE (fig. 8), and it is interesting to trace their origin. The rise AB is produced by the side of the source nearer the plate, and is steep because, as we pass from the first effective portion toward the top of the source, the displacement away from the photographic plate is compensated by a diminution in the distance of the source from the slit. After the point B is passed, the intensity continues to rise to the maximum C, the first point to which the rays from the far side of the source are able to attain. The distance of the peak from the head of the line is thus very nearly equal to the diameter of the source. After the point C is passed the intensity decreases because the rays which pass through the centre of the slit are no longer able to affect the plate. At D the edges of the slit begin to cut off the remaining rays, and at E this process is complete. The distance from the head of the line A to the tail E is given approximately by

$$y = \frac{2\rho^2}{x} \theta^2,$$

where  $2\theta$  is the linear angle subtended at the source by the slit AB. It is interesting to note that though the form of the line given by flat and cylindrical sources is so complex, each of the distinct parts has a special significance. It has been pointed out that the sharp edge of the line enables the energy and momentum of the particles to be accurately determined, and it is easy to see

that this sharp edge may be identified with the portion AB of the curves. The total number of particles entering the line is measured by the area under the curve, but as this is somewhat difficult to measure photometrically, owing to the presence in many cases of a continuous background, the height of the peak is generally taken as a measure of the intensity. In the work by Dr. C. D. Ellis and the author on the "Relative Intensities of the  $\beta$ -Ray Lines of Radium B and Radium C,"\* the heights of the peaks were measured photometrically, and by means of the results of these calculations they were corrected for the variation of the intensity of peak with radius of curvature of the electron path. The manner in which the curve falls off along CDE is also of importance, as it indicates the extent of the homogeneity of the particles or whether small satellites to the line exist on the side of low velocity. Thus, summarising, we may say that the head of the line determines the energy and momentum, the peak the intensity, and the tail the homogeneity of the beam.

### § 3. "MAGNETIC SPECTROMETER" USING THE IONISATION CHAMBER.

It has been seen how the form of the line which is obtained on the photographic plate may be calculated, and we now proceed to solve the similar problem which arises when the photographic plate is replaced by an ionisation chamber. For any given value, lying between certain limits, of the radius of curvature imposed upon a homogeneous group of particles, a certain number may enter the ionisation chamber. As the magnetic field is varied the number which can enter will also vary, and the problem consists in determining how the number of particles entering the chamber depends on the radius of curvature and the slit widths above the source and chamber.† The homogeneous particles will in this case, as in the one considered above, be distributed according to the appropriate curve of figs. 5, 7, 8, which in fig. 9 is represented by EF.

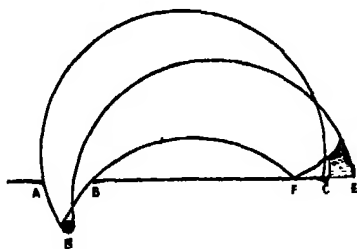


FIG. 9.

\* Ellis and Wooster, 'Roy. Soc. Proc.,' A, vol. 114, p. 276 (1927).

† The slit AB is often placed midway between source and chamber, instead of just above the source, but this has a negligible influence on the form of the line obtained at the window of the chamber.

For the radius of curvature corresponding to EF, the number of particles entering the chamber is proportional to the shaded area of the line. If this area be found for all values of  $\rho$  between the limits set by the slit of the ionisation chamber, and the areas be plotted against the corresponding value of  $\rho$ , we obtain curve (1) of fig. 10.

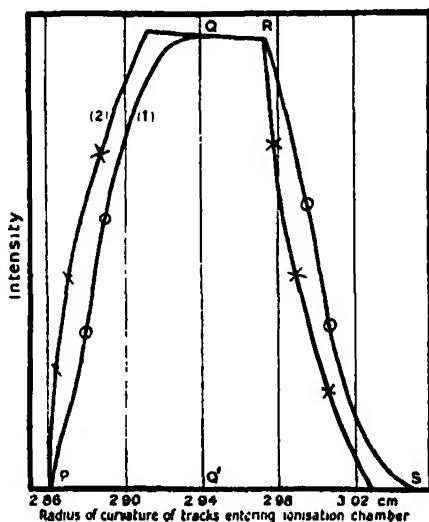


FIG. 10.

×, source infinitely narrow; O, source of 0.05 cm. diameter.

This curve will be seen to be made up of three parts PQ, QR, RS which occur in the following way:—As the radius increases so that E moves from C toward D, the area under the spectrum line and the vertical ordinate through C increases until, when the tail of the line F has reached C, the shaded area is a maximum and we have arrived at the point Q of fig. 10. The whole line EF is now entering the chamber, but as E moves still farther toward D, the intensity of the line EF decreases, being, as we saw in the previous section, inversely proportional to  $\rho$ . This accounts for the slight drop from Q to R. The point R corresponds to the case when E has reached D. As the radius increases E passes beyond D and less of the spectrum line enters the chamber, until the point S is attained, which corresponds to F being coincident with D. A treatment of this problem has been given by Gurney,\* which only applies when the source is supposed of finite length, but infinitely narrow. In this case the spectrum line is much shorter, and the resulting curve obtained with a Faraday cylinder as the field is varied is shown by curve (2) of fig. 10. It will be

\* Gurney, 'Roy. Soc. Proc.,' A, vol. 109, p. 540 (1925).

observed that there is a considerable divergence between the form of the curves obtained in the two cases. This, however, does not affect the value obtained by Gurney for the total number of  $\beta$ -particles emitted during the disintegration of one atom each of radium B and radium C, since this is independent of the form of the spectrum line, provided the magnetic field be changed, after each count of the numbers of particles in the ratio SC/SD (fig. 9), as has been done by the above author.

The area under the curve PQRS represents the number of electrons entering the ionisation chamber, and it is important to see how this varies with size of slits AB and CD and the diameter of the source. An increase in the limiting slit AB merely augments the tail of the line, and this makes the straight portion QR shorter and at the same time a little higher. The distance PQ', which is equal to the distance between head and tail of line is determined, in general, both by the value of AB and the diameter of the source, though if AB were made very small, PQ' would still be equal to the diameter of the source. The same is true of the third portion of the curve RS. If CD is decreased, the portion QR becomes smaller without decreasing its height, and when CD is equal to the width of the line, there is no straight portion, as Q coincides with R. Further reduction of CD sharpens the peak but diminishes the intensity of the rays entering the chamber, and finally, when CD is very small, the curve PQRS becomes identical with the spectrum line. The most generally useful value for CD is that of the length of the spectrum line EF, for then a good intensity is obtained together with a fairly high resolution. The length of the line is given by equation (1), which, when AB is adjusted to its best value, is equal to twice the diameter of the source. Thus, in general, the value of CD should be about twice the diameter of the source.

#### DISCUSSION.

In the preceding paragraphs we have seen how the form of line obtained with a "magnetic spectrometer" may be found under various conditions, and it remains to indicate how this information affects the experimental procedure in general use. It is always desirable to be able to obtain values of the energies and momenta of the charged particles which are as accurate as possible, and for this, narrow well-defined lines are necessary. The resolving power depends on the width of the line and on the radius of curvature. The former is constant for all radii of curvature, being approximately equal to the width of the source projected on a plane parallel to the plate, and we may therefore say that the resolving power is inversely proportional to the width of the

source. The lines given by flat sources tipped at appropriate angles are much narrower than those produced by cylindrical sources of the same width, as may be seen by reference to figs. 5, 7, 8. It is not possible, however, even with a very narrow flat source tipped at the most favourable angle, to obtain very narrow lines on a photographic plate when the charged particles are appreciably scattered in the emulsion of the plate. As an example of this we may take the case of one homogeneous group of  $\beta$ -rays in the spectrum of radium B having an energy of one-quarter million volts. Using Ilford X-ray plates, the scattering of the particles in the film is such that a line which would otherwise be infinitely narrow becomes 0.2 mm. wide, and for particles of higher energy the scattering would, of course, be still greater. In the case of positive rays, no such scattering occurs, and here the narrowest lines would be obtained with flat-tipped sources. It has been shown earlier that the dispersion is proportional to  $\rho$ , and since the width of the line is practically constant for all values of  $\rho$ , the resolving power is also proportional to  $\rho$ .

In many experiments using beams of charged particles, there is present a continuous spectrum which fogs the plate and renders it difficult to locate very faint lines. This difficulty may, to a certain extent, be removed by suitably adjusting the limiting slit. The intensity of the continuous spectrum at any point is proportional to the total area under the line corresponding to a homogeneous group of particles striking the plate at that point, whilst the intensity of a homogeneous group is measured by the intensity at the peak of the line. Thus to increase the line at the expense of the background, it is necessary progressively to cut off the tail until the intensity at the peak begins to be diminished. This can be done by decreasing the slit width AB to a value which will now be derived. The head of the line occurs at a point on the plate distant  $2\rho$  from the side of the source nearer the plate and the peak at the same distance from the other side of the source. Now all portions of the source contribute to the peak, the rays from the side of the source nearer the plate starting off at angles  $\pm \theta$  with the central ray, whilst those from the other side of the source pass through the centre of the slit (see fig. 9). Thus if AB be decreased until the limiting angles are  $\pm \theta$ , the peak will be in no way affected. The value of  $\theta$  required for this can be obtained from equation (1) when the diameter of the source is substituted for  $y$ . A table of values for the optimum slit width is given below, in which the distance from source to slit is taken as 1.5 cm.

Table of Values of Optimum Slit Width.

$\rho$ cm.	Diameter of source.		
	0.01 cm.	0.02 cm.	0.05 cm.
	cm.	cm.	cm.
3	0.170	0.241	0.381
6	0.122	0.173	0.273
9	0.100	0.141	0.223

It has been assumed in the calculations of the form of the lines that the sources send out charged particles of homogeneous velocities. This is not always the case in actual experimental work, owing to some retarding film or potential causing the velocities which would otherwise be discrete to have a probability distribution about some mean value. If the retardation is produced by a film of matter of known thickness and disposition with regard to the source, the method given in the first section may be extended to find the form of the line. The source is supposed divided into a number of infinitely narrow sources placed parallel to one another, and the lines given by each of these are superposed, giving, on addition of the ordinates, the resultant line due to the whole source. This process has been carried out for a source of electrons consisting of a very thin glass tube ( $\alpha$ -ray tube) filled with radium emanation. The  $\beta$ -particles arise from the active material deposited on the inner walls of the tube, and are retarded to various extents by the glass walls. The thickness of the latter at several points round the tube was found by measuring the residual range of the  $\alpha$ -particles shot out along the corresponding diameters. Allowance was made for the variation in radial thickness of the walls and also for the fact that when taking a  $\beta$ -ray photograph with this tube, the particles from the edges of the tube have to traverse a much greater thickness of stopping material than those from the middle. The form of line obtained by calculating in this way could be made to agree with that found experimentally if a certain velocity distribution was assumed for the particles emerging from the top of the tube. These particles had traversed approximately the same thickness and, in agreement with theoretical work by Bohr,\* the velocity distribution curve was found to follow a probability law, although the numerical values of the exponent did not agree. This was not surprising, since the particles producing the  $\beta$ -ray line could have been

\* Bohr, 'Phil. Mag.,' vol. 30, p. 581 (1915).

scattered through quite large angles in passing through the glass walls of the emanation tube, and in Bohr's deduction only particles which had been scattered through small angles were considered. The experimental intensity curves used for this calculation were obtained originally for another purpose, and the results obtained from them in this connection could only be approximate. However, it was quite evident from the analysis that this method of obtaining the velocity distribution is quite practicable and is important because it is the only method which has up to the present been suggested.

Finally, it will be seen that the main purpose of this paper is to point out a method by means of which the "magnetic spectrometer" may be used to the best advantage. This method consists in first finding the structure of the line produced by the apparatus for certain given conditions of size of source, slit, etc., and then modifying them to give the particular form of line required. The structure of the line in any given case can be obtained approximately from the curves of figs. 5, 7, 8, and for a more accurate determination the method given in § 2 can be employed.

#### SUMMARY.

(1) The intensity distribution in the line produced by a magnetic field acting on a beam of homogeneous particles is determined

- (a) for a source of particles which is infinitely narrow ;
- (b) for sources of various finite widths.

(2) The conditions under which the analysis of moving charged particles is most favourably carried out are derived from this structure of the lines.

(3) The application of this analytical method to the determination of the velocity distribution of particles passing through thin sheets of matter is pointed out.

In conclusion, I wish to express my sincere thanks to Prof. Sir Ernest Rutherford for his interest in this work and to Dr. C. D. Ellis for much helpful criticism.

## INDEX to VOL. CXIV. (A)

- Allen (H. S.) and Sandeman (I.) Bands in the Secondary Spectrum of Hydrogen, 293.  
 Alpha-particles from Radium C (Briggs), 313, 341.  
 Atom, oriented hydrogen, its effective cross section (Fraser), 212.  
 Atoms and ions, many-electron, theoretical prediction of their physical properties (Pauling), 181.  
 Auroral green line (McLennan, McLeod and McQuarrie), 1.  
 Barnes (H. T.) Some Physical Properties of Icebergs and a Method for their Destruction, 161.  
 Beckett (H. E.) *See* George and Beckett.  
 Beta-rays, photographic action (Ellis and Wooster), 266.  
 Bismuth and lead, L-emission spectra (Eddy and Turner), 605.  
 Bone (W. A.) and Forshaw (A.) Studies upon Catalytic Combustion, V, 169.  
 Bone (W. A.), Fraser (R. P.) and Winter (D. A.) The Initial Stages of Gaseous Explosions, I, 402. II, 420.  
 Bone (W. A.), Fraser (R. P.) and Witt (F.) The Initial Stages of Gaseous Explosions, III, 442.  
 Bragg (W. L.) and West (J.) The Structure of Certain Silicates, 450.  
 Briggs (G. H.) The Straggling of  $\alpha$ -Particles from Radium C, 313. The Decrease in Velocity of  $\alpha$ -Particles from Radium C, 341.  
 Buchanan (D.) Periodic Orbits of the Second Genus, 490.  
 Burgers (W. G.) An X-Ray Investigation of Optically Anomalous Crystals of Racemic Potassium Chlorosulphoacetate, 222.  
 Carbon dioxide, thermal conductivity (Gregory and Marshall), 354.  
 Catalytic Combustion, V (Bone and Forshaw), 169.  
 Consonants, voiced and unvoiced, their nature and artificial production (Paget), 98.  
 Craib (J.) *See* Schonland and Craib.  
 Crystals, optical anomalous, of racemic potassium chlorosulphoacetate (Burgers), 222.  
 Cuthbertson (C.) Absorption of Radiation in the Extreme Ultra-Violet by the Inert Gases, 650; On a Relation between the Refractive and Dispersive Constants of the Inert Gases, 659.  
 Darwin (C. G.) and Watson (W. H.) The Constants of the Magnetic Dispersion of Light, 474.  
 Detonation of gaseous mixtures (Egerton and Gates), 137, 152.  
 Dirac (P. A. M.) The Quantum Theory of the Emission and Absorption of Radiation, 243; The Quantum Theory of Dispersion, 710.  
 Dispersion of light, magnetic, constants (Darwin and Watson), 474.  
 Dispersion, quantum theory (Dirac), 710.  
 Dobson (G. M. B.), Harrison (D. N.) and Lawrence (J.) Measurements of the Amount of Ozone in the Earth's Atmosphere, II, 521.  
 Doppler effects in molecular spectrum of hydrogen (Johnson), 697.  
 Doublets, mutual potential energy of a plane network (Topping), 67.



- Eddy (C. E.) and Turner (A. H.) The L-Emission Spectra of Lead and Bismuth, 605.
- Egerton (A.) and Gates (S. F.) On Detonation of Gaseous Mixtures of Acetylene and of Pentane, 137; On Detonation in Gaseous Mixtures at High Initial Pressures and Temperatures, 152.
- Electromagnetic field, analysis into moving elements (Milner), 23.
- Electrons, capture by electrified particles (Thomas), 561.
- Ellis (C. D.) and Wooster (W. A.) The Photographic Action of  $\beta$ -Rays, 266; The Relative Intensities of the Groups in the Magnetic  $\beta$ -Ray Spectra of Radium B and C, 276.
- Fells (H. A.) and Firth (J. B.) The Phenomena arising from the Addition of Hydrogen Peroxide to the Sol of Silicic Acid, 517.
- Films, solid unimolecular, rigidity of (Mouquin and Rideal), 690.
- Firth (J. B.) *See* Fells and Firth.
- Forsdyke (A. G.) *See* Levy and Forsdyke.
- Forshaw (A.) *See* Bone and Forshaw.
- Foster (J. S.) Stark Patterns observed in Helium, 47.
- Fowler (A.) and Freeman (L. J.) The Spectrum of Ionised Nitrogen, 602.
- Fraser (R. G. J.) The Effective Cross Section of the Oriented Hydrogen Atom, 212.
- Fraser (R. P.) *See* Bone, Fraser and Winter and Bone, Fraser and Witt.
- Freeman (L. J.) *See* Fowler and Freeman.
- Garrett (M. W.) Experiments to Test the Possibility of Transmutation by Electronic Bombardment, 289.
- Gaseous explosions, initial stages (Bone and others), 402, 420, 442.
- Gaseous mixtures, detonation (Egerton and Gates), 137, 152.
- Gates (S. F.) *See* Egerton and Gates.
- George (W. H.) and Beckett (H. E.) The Energy of the Struck String, I, 111.
- Gifford (J. W.) and Lowry (T. M.) The Refractive Indices of Nicotine, 592.
- Gregory (H.) and Marshall (S.) The Thermal Conductivity of Carbon Dioxide, 354.
- Harrison (D. N.) *See* Dobson, Harrison and Lawrence.
- Hinshelwood (C. N.) Quasi-Unimolecular Reactions. The Decomposition of Diethyl Ether in the Gaseous State, 84.
- Hydrogen, bands in the secondary spectrum (Allen and Sandeman), 293.
- Hydrogen, connection between visible and ultra-violet bands (Richardson), 643.
- Hydrogen positive rays, spectrum, Doppler effects and intensities of lines (Johnson), 697.
- Icebergs, some physical properties and a method for destruction (Barnes), 161.
- Inert gases, absorption of radiation in the extreme ultra-violet (Cuthbertson), 650.
- Inert gases, relation between refractive and dispersive constants (Cuthbertson), 659.
- Intensity of radiation from a source of electric waves (Macdonald), 367.
- Intertraction (Wright), 576.
- Ions and atoms, many-electron, theoretical prediction of their physical properties (Pauling), 181.
- Johnson (M. C.) Doppler Effects and Intensities of Lines in the Molecular Spectrum of Hydrogen Positive Rays, 697.
- Lawrence (J.) *See* Dobson, Harrison and Lawrence.
- Lead and bismuth, L-emission spectra (Eddy and Turner), 605.
- Levy (H.) and Forsdyke (A. G.) The Stability of an Infinite System of Circular Vortices, 594.

- Long-Chain compounds, X-ray investigation (Müller), 542.
- Lowry (T. M.) *See* Gifford and Lowry.
- Macdonald (H. M.) The Intensity of Radiation from a Source of Electric Waves, 367.
- McLennan (J. C.), McLeod (J. H.) and McQuarrie (W. C.) An Investigation into the Nature and Occurrence of the Auroral Green Line, 1.
- McLeod (J. H.) *See* McLennan, McLeod and McQuarrie.
- McQuarrie (W. C.) *See* McLennan, McLeod and McQuarrie.
- Magnetic dispersion of light (Darwin and Watson), 474.
- Magnetic field, analysis of beams of moving charged particles by (Wooster), 729.
- Magneto-resistance effect, transverse in single crystals of iron (Webster), 611.
- Marshall (S.) *See* Gregory and Marshall.
- Mercury band-spectrum of long duration (Rayleigh), 620.
- Milner (S. R.) An Analysis of the Electromagnetic Field into Moving Elements, 23.
- Mouquin (H.) and Rideal (E. K.) The Rigidity of Solid Unimolecular Films, 690.
- Muller (A.) An X-Ray Investigation of Certain Long-Chain Compounds, 542.
- Newbery (E.) Anodic Overvoltage Measurements with the Cathode Ray Oscillograph, 103.
- Nicotine, refractive indices (Gifford and Lowry), 592.
- Nitrogen, ionised, spectrum (Fowler and Freeman), 662.
- Orbits, periodic, of the second genus (Buchanan), 490.
- Overvoltage measurements with oscillograph (Newbery), 103.
- Ozone in the Earth's Atmosphere (Dobson, Harrison and Lawrence), 521.
- Paget (Sir Richard) The Nature and Artificial Production of the (so-called) Voiced and Unvoiced Consonants, 98.
- Pauling (L.) The Theoretical Prediction of the Physical Properties of Many-Electron Atoms and Ions. Mole Refraction, Diamagnetic Susceptibility and Extension in Space, 181.
- Quantum theory of dispersion (Dirac), 710.
- Quantum theory of the emission and absorption of radiation (Dirac), 243.
- Quasi-unimolecular reactions (Hinshelwood), 84.
- Radiation from a source of electric waves (Macdonald), 367.
- Radiation, quantum theory of emission and absorption (Dirac), 243.
- Radium B and C, relative intensities of the groups in the magnetic  $\beta$ -ray spectra (Ellis and Wooster), 276.
- Radium C,  $\alpha$ -particles from (Briggs), 313, 341.
- Rayleigh (Lord) Studies on the Mercury Band-Spectrum of Long Duration, 620.
- Richardson (O. W.) Note on a Connection between the Visible and Ultra-Violet Bands of Hydrogen, 643.
- Rideal (E. K.) *See* Mouquin and Rideal.
- Sandeman (I.) *See* Allen and Sandeman.
- Schonland (B. F. J.) and Craib (J.) The Electric Fields of South African Thunderstorms,
- Silicates, structure (Bragg and West), 450.
- Silicic acid, addition of  $H_2O_2$  to the sol (Fells and Firth), 517.
- Simpson (G. C.) The Mechanism of a Thunderstorm, 376.
- Sparkling potentials of discharge tubes (Taylor), 73.

- Spectra, L-emission of lead and bismuth (Eddy and Turner), 605.  
 Spectra of radium, magnetic  $\beta$ -ray (Ellis and Wooster), 276.  
 Spectra, ultra-violet, of the inert gases (Cuthbertson), 650.  
 Spectrum—auroral green line (McLennan, McLeod and McQuarrie), 1.  
 Spectrum, band, of mercury (Rayleigh), 620.  
 Spectrum of hydrogen, visible and ultra-violet bands (Richardson), 643.  
 Spectrum of ionised nitrogen (Fowler and Freeman), 662.  
 Spectrum, secondary, of hydrogen, bands (Allen and Sandeman), 293.  
 Stark patterns observed in helium (Foster), 47.
- Taylor (J.) On the Sparking Potentials of Discharge Tubes containing carefully Purified Electrodes, 73.  
 Thomas (L. H.) On the Capture of Electrons by Swiftly Moving Electrified Particles, 561.  
 Thunderstorm, mechanism (Simpson), 376.  
 Thunderstorms, electric fields (Schonland and Craib), 229.  
 Topping (J.) On the Mutual Potential Energy of a Plane Network of Doublets, 67.  
 Transmutation by electronic bombardment (Garrett), 289.  
 Turner (A. H.) *See* Eddy and Turner.
- Vortices, circular, stability of an infinite system (Levy and Foradyke), 594.
- Watson (W. H.) *See* Darwin and Watson.  
 Webster (W. L.) The Transverse Magneto-Resistance Effect in Single Crystals of Iron, 611.  
 West (J.) *See* Bragg and West.  
 Winter (D. A.) *See* Bone, Fraser and Winter.  
 Witt (F.) *See* Bone, Fraser and Witt.  
 Wooster (W. A.) The Analysis of Beams of Moving Charged Particles by a Magnetic Field, 729.  
 Wooster (W. A.) *See also* Ellis and Wooster.  
 Wright (Sir Almroth) A further Contribution to the Study of the Phenomena of Interaction, 576.





**I. A. R. I. 75.**

IMPERIAL AGRICULTURAL RESEARCH  
INSTITUTE LIBRARY  
NEW DELHI.

Date of issue.	Date of issue.	Date of issue.
25.12.48		
25.12.48	1999	